ELECTROMAGNETIC
WAVE THEORY

ELECTROMAGNETIC WAVE THEORY

JIN AU KONG

PREFACE

This book presents a unified macroscopic theory of electromagnetic waves in accordance with the principle of special relativity from the point of view of the form invariance of the Maxwell equations and the constitutive relations. Great emphasis is placed on the fundamental importance of the $\overline{k}$ vector in electromagnetic wave theory. We introduce a fundamental unit $K_o = 2\pi$ meter^{-1} for the spatial frequency, which is cycle per meter in spatial variation. This is similar to the fundamental unit for temporal frequency Hz, which is cycle per second in time variation. The unit K_o is directly proportional to the unit Hz; one K_o in spatial frequency corresponds to 300 MHz in temporal frequency.

This is a textbook on electromagnetic wave theory, and topics essential to the understanding of electromagnetic waves are selected and presented. Chapter 1 presents fundamental laws and equations for electromagnetic theory. Chapter 2 is devoted to the treatment of transmission line theory. Electromagnetic waves in media are studied in Chapter 3 with the kDB system developed to study waves in anisotropic and bianisotropic media. Chapter 4 presents a detailed treatment of reflection, transmission, guidance, and resonance of electromagnetic waves. Starting with Čerenkov radiation, we study radiation and antenna theory in Chapter 5. Chapter 6 then elaborates on the various theorems and limiting cases of Maxwell's theory important to the study of electromagnetic wave behavior. Scattering by spheres, cylinders, rough surfaces, and volume inhomogeneities are treated in Chapter 7. In Chapter 8, we present Maxwell's theory from the point of view of Lorentz covariance in accordance with the principle of special relativity. The problem section at the end of each section provides useful exercise and applications.

The various topics in the book can be taught independently, and the material is organized in the order of increasing complexity in mathematical techniques and conceptual abstraction and sophistication. This book has been used in several undergraduate and graduate courses that I have been teaching at the Massachusetts Institute of Technology.

The first version of the book was published in 1975 by Wiley Interscience, New York, entitled *Theory of Electromagnetic Waves,* which was based on my 1968 Ph.D. thesis, where the concept of bianisotropic media was introduced. The book was expanded and published in 1986 with the present title and its second edition appeared in 1990. Since 1998, it has been published by EMW Publishing Company, Massachusetts. The development of the various concepts in the book relies heavily on published work. I have not attempted the task of referring to all relevant publications. The list of books and journal articles in the Reference Section at the end of the book is at best representative and by no means exhaustive. Some of the results contained in the book are taken from many of my research projects, which have been supported by grants and contracts from the National Science Foundation, the National Aeronautics and Space Administration, the Office of Naval Research, the Army Research Office, the Jet Propulsion Laboratory of the California Institute of Technology, the MIT Lincoln Laboratory, the Schlumberger-Doll Research Center, the Digital Equipment Corporation, the IBM Corporation, and the funding support associated with the award of the S. T. Li prize for the year 2000.

During the writing and preparation of the book, many people helped. In particular, I would like to acknowledge Chi On Ao for formulating the TeX macros, and Zhen Wu for editing the text and constructing the index. Over the years, many of my teaching and research assistants provided useful suggestions and proofreading, notably Leung Tsang, Michael Zuniga, Weng Chew, Tarek Habashy, Robert Shin, Shun-Lien Chuang, Jay Kyoon Lee, Apo Sezginer, Soon Yun Poh, Eric Yang, Michael Tsuk, Hsiu Chi Han, Yan Zhang, Henning Braunisch, Bae-Ian Wu, Xudong Chen, and Baile Zhang. I would like to express my gratitude to them and to the students whose enthusiastic response and feedback continuously give me joy and satisfaction in teaching.

J. A. Kong

Cambridge, Massachusetts
December 2007

CONTENTS

1

FUNDAMENTALS

1.1 Maxwell's Theory

A. Maxwell's Equations

B. Vector Analysis

1.2 Electromagnetic Waves

A. Wave Equation and Wave Solution

B. Unit for Spatial Frequency k

C. Polarization

1.3 Force, Power, and Energy

A. Lorentz Force Law

B. Lenz' Law and Electromotive Force (EMF)

C. Poynting's Theorem and Poynting Vector

1.4 Hertzian Waves

A. Hertzian Dipole

B. Electric and Magnetic Fields

C. Electric Field Pattern

1.5 Constitutive Relations

A. Isotropic Media

B. Anisotropic Media

C. Bianisotropic Media

D. Biisotropic Media

E. Constitutive Matrices

1.6 Boundary Conditions

A. Continuity of Electric and Magnetic Field Components

B. Surface Charge and Current Densities

C. Boundary Conditions

1.7 Reflection and Guidance

A. Wave Vector $\overline{k}$

B. Reflection and Transmission of TE Waves

C. Reflection and Transmission of TM Waves

D. Brewster Angle and Zero Reflection

E. Guidance by Conducting Parallel Plates

Answers

1.1 Maxwell's Theory

A. Maxwell's Equations

The laws of electricity and magnetism were established in 1873 by James Clerk Maxwell (1831–1879). In three-dimensional vector notation, the Maxwell equations are

$$\nabla \times \overline{H} = \frac{\partial}{\partial t} \overline{D} + \overline{J} \qquad (1.1.1)$$

$$\nabla \times \overline{E} = -\frac{\partial}{\partial t} \overline{B} \qquad (1.1.2)$$

$$\nabla \cdot \overline{D} = \rho \qquad (1.1.3)$$

$$\nabla \cdot \overline{B} = 0 \qquad (1.1.4)$$

where $\overline{E}, \overline{B}, \overline{H}, \overline{D}, \overline{J}$, and ρ are real functions of position and time.

$\overline{E}$ = electric field strength   (volts/m)

$\overline{B}$ = magnetic flux density   (webers/m^2)

$\overline{H}$ = magnetic field strength   (amperes/m)

$\overline{D}$ = electric displacement   (coulombs/m^2)

$\overline{J}$ = electric current density   (amperes/m^2)

ρ = electric charge density   (coulombs/m^3)

Equation (1.1.1) is Ampère's law or the generalized Ampère circuit law. Equation (1.1.2) is Faraday's law or Faraday's magnetic induction law. Equation (1.1.3) is Coulomb's law or Gauss' law for electric fields. Equation (1.1.4) is Gauss' law or Gauss' law for magnetic fields. We generally refer to $\overline{E}$ and $\overline{D}$ as electric fields, and $\overline{H}$ and $\overline{B}$ as magnetic fields.

Maxwell's contribution to the laws of electricity and magnetism is the term $\partial \overline{D}/\partial t$, which is called the displacement current. The addition of the displacement current to the electric current density $\overline{J}(\overline{r}, t)$ in the original Ampère's law has at least three major consequences. First, in a capacitor which is an open circuit for direct current, the displacement current insures the continuity of alternating currents in electric circuits. Secondly, the continuity law

$$\nabla \cdot \overline{J} = -\frac{\partial}{\partial t} \rho \qquad (1.1.5)$$

follows from (1.1.1) and (1.1.3) by making use of the vector identity $\nabla \cdot (\nabla \times \overline{H}) = 0$. It is the displacement term that guarantees the conservation of electric current and charge densities. Eq. (1.1.5) states that the electric current and charge densities are conserved at all time. Thirdly, Faraday's law in (1.1.2) states that surrounding a time-varying magnetic field, electric fields are produced, and are also time-varying. With the displacement term in (1.1.1), Ampère's law states that around time-varying electric fields, time-varying magnetic fields are produced. This interrelationship between the time-varying electric and magnetic fields constitutes the foundation of electromagnetic wave theory and led Maxwell to the prediction of electromagnetic waves.

In developing his theory for the electromagnetic fields in space and time, Maxwell conceived of a substance filling the whole space called aether. In the aether, the electric fields $\overline{D}$ and $\overline{E}$ are related by a dielectric permittivity ϵ_o, and the magnetic fields $\overline{B}$ and $\overline{H}$ are related by a magnetic permeability μ_o.

$$\overline{D} = \epsilon_o \overline{E} \tag{1.1.6a}$$
$$\overline{B} = \mu_o \overline{H} \tag{1.1.6b}$$

where

$$\epsilon_o \approx 8.85 \times 10^{-12} \qquad \text{farad/meter}$$
$$\mu_o = 4\pi \times 10^{-7} \qquad \text{henry/meter}$$

where the numerical values for ϵ_o and μ_o are expressed in MKS units. We now call (1.1.6) the constitutive relations for free space.

With Equations (1.1.1)–(1.1.6), Maxwell's theory of electromagnetic fields is completely expressed. Originally written in Cartesian component form, Maxwell's equations were cast in the current vector form by Oliver Heaviside (1850–1925). In 1888, Heinrich Rudolf Hertz (1857–1894) demonstrated the generation of radio waves and experimentally verified Maxwell's theory. Since then, electromagnetic theory has played a central role in the development of radio, television, wireless communications, radar, microwave heating, remote sensing, and numerous other practical applications. The special theory of relativity developed by Albert Einstein (1879–1955) in 1905 further asserted the rigorousness and elegance of Maxwell's theory. As a well-established scientific discipline, this sophisticated theoretical structure embodies many principles and concepts which serve as fundamental rules of nature and vital links for all scientific disciplines.

James Clerk Maxwell (13 June 1831 – 5 November 1879)

James Clerk Maxwell attended University of Edinburgh (1847–1850), and studied under William Hopkins at Cambridge University (1850–1854). He was a fellow of Trinity (1855–1856), Professor of Natural Philosophy at Marischal College of the University of Aberdeen (1856–1860), and at King's College (1860–1865). He was the first Cavendish Professor of Experimental Physics at Cambridge University to build and direct the Cavendish Laboratory (1871–1879). He published four books and about 100 papers starting at age 14, including 'On Faraday's Lines of Forces' in 1855, 'On Physical Lines of Force' in 1861, and 'A Dynamical Theory of the Electromagnetic Field' in 1864. In 1865, at age 33, he retired to his country home estate to write his monumental book *A Treatise of Electricity and Magnetism* (Constable and Company, London, 1873; Dover Publications, New York, 1006 pages, 1954).

Michael Faraday (22 September 1791 – 25 August 1867)

Faraday became an assistant to Sir Humphry Davy at the Royal Institution on 1 March 1813. In September 1821, his experimentation demonstrated electro-magnetic rotation, initiated the concept of electric motor. In August 1831, he discovered electro-magnetic induction, and that magnetism produced electricity through movement, the principle behind the electric transformer and generator. He became professor of chemistry in 1833. Faraday published many of his results in the three-volume *Experimental Researches in Electricity* (1839–1855).

Johann Carl Friedrich Gauss (30 April 1777 – 23 February 1855)

Gauss studied mathematics at the University of Göttingen from 1795 to 1798, and received his doctoral degree from the University of Helmstedt in 1799. In 1807 he took the position of director of the Göttingen Observatory. In 1832 he presented a systematic use of absolute units (length, mass, time) to measure nonmechanical quantities. From 1831 to 1837 he worked closely with Wilhelm Eduard Weber (24 October 1804 – 23 June 1891) on terrestrial magnetism and organized a system of stations for systematic observations.

André-Marie Ampère (20 January 1775 – 10 June 1836)

Ampère was appointed professor at Bourg Ecole Centrale in 1802, at the Ecole Polytechnique in 1809, and at Université de France in 1826. In September 1820, Ampère showed that two parallel conductors attract each other if they carry currents that flow in the same direction and repel if the currents flow in opposite directions. In 1823–1826, he completed his memoir on the 'Mathematical Theory of Electrodynamic Phenomena, Uniquely Deduced from Experience'.

Charles-Augustin de Coulomb (14 June 1736 – 23 August 1806)

Coulomb worked in the Corps du Génie until he retired in 1791. In 1777 he invented the torsion balance, which enabled him to establish the fundamental laws of electricity by measuring the force between two small spheres charged with electricity. Between 1785 and 1791, he published seven treatises on electricity and magnetism.

B. Vector Analysis

A vector $\overline{A}$ has a magnitude and a direction, which can be represented graphically by a straight-line element of length proportional to the magnitude of $\overline{A}$ and with an arrow pointing in the direction of $\overline{A}$. In a Cartesian coordinate system (also called the rectangular coordinate system), we write in terms of the three Cartesian components A_x, A_y, and A_z [Fig. 1.1.1].
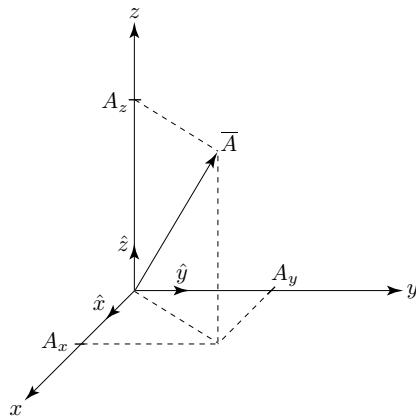
Figure 1.1.1 Projection of $\overline{A}$ in rectangular coordinate system.

$$\overline{A} = \hat{x}A_x + \hat{y}A_y + \hat{z}A_z$$

where A_x, A_y, A_z are the projections of $\overline{A}$ onto the x, y, z axes. We denote the directions of the x, y, z axes with $\hat{x}, \hat{y}, \hat{z}$ each of them has unit magnitude with the scalar product $\hat{x} \cdot \hat{x} = \hat{y} \cdot \hat{y} = \hat{z} \cdot \hat{z} = 1$. They are called the unit vectors. Furthermore $\hat{x} \cdot \hat{y} = \hat{y} \cdot \hat{z} = \hat{z} \cdot \hat{x} = 0$. We use a hat instead of an overbar to represent the vector with unit magnitude.

Rene Descartes (31 March 1596 – 11 February 1650)

   Rene Descartes originated the Cartesian coordinates and founded analytic geometry. His philosophy is called Cartesianism (from Cartesius, the Latin form of his name), with the famous statement 'I think, therefore I am.' He preached universal doubt; only one thing cannot be doubted: doubt itself.

Vector Addition and Subtraction

Two vectors $\overline{A}$ and $\overline{B}$, when they are not in the same direction or in opposite directions, determine a plane. In Cartesian components, we write

$$\overline{A} = \hat{x}A_x + \hat{y}A_y + \hat{z}A_z$$
$$\overline{B} = \hat{x}B_x + \hat{y}B_y + \hat{z}B_z$$

It follows that

$$\overline{A} \pm \overline{B} = \hat{x}(A_x \pm B_x) + \hat{y}(A_y \pm B_y) + \hat{z}(A_z \pm B_z)$$

Scalar Dot Product

The scalar or dot product of two vectors $\overline{A}$ and $\overline{B}$, denoted by $\overline{A} \cdot \overline{B}$, is a scalar number,

$$\overline{A} \cdot \overline{B} = A_x B_x + A_y B_y + A_z B_z$$

Vector Cross Product

The vector or cross product of two vectors $\overline{A}$ and $\overline{B}$, denoted by $\overline{A} \times \overline{B}$, is a vector. In terms of their Cartesian components,

$$\overline{A} \times \overline{B} = \hat{x}(A_y B_z - A_z B_y) + \hat{y}(A_z B_x - A_x B_z) + \hat{z}(A_x B_y - A_y B_x)$$
$$= \begin{vmatrix} \hat{x} & \hat{y} & \hat{z} \\ A_x & A_y & A_z \\ B_x & B_y & B_z \end{vmatrix}$$

For the three orthogonal unit vectors $\hat{x}$, $\hat{y}$, and $\hat{z}$ it is seen that $\hat{x} = \hat{y} \times \hat{z}$, $\hat{y} = \hat{z} \times \hat{x}$, $\hat{z} = \hat{x} \times \hat{y}$.

The direction of $\overline{A} \times \overline{B}$ follows the right-hand rule, i.e., when the fingers of the right hand rotate from $\overline{A}$ to $\overline{B}$, the thumb of the right hand points in the direction of $\overline{A} \times \overline{B}$. Thus the vector $\overline{A} \times \overline{B}$ is perpendicular to both $\overline{A}$ and $\overline{B}$ and the plane containing $\overline{A}$ and $\overline{B}$. It is seen that for $\overline{A} = \hat{x}A_x + \hat{y}A_y$ and $\overline{B} = \hat{x}B_x + \hat{y}B_y$ both in the xy-plane, $\overline{A} \times \overline{B} = \hat{z}(A_x B_y - A_y B_x)$ is in the $\hat{z}$ direction perpendicular to both $\overline{A}$ and $\overline{B}$.

Division by a vector is not defined; thus $\overline{B}/\overline{A}$ and $1/\overline{A}$ are meaningless expressions. If none of the operations of addition, subtraction, dot product, or cross product is imposed on $\overline{A}$ and $\overline{B}$, the entity $\overline{A}\,\overline{B}$ is called a dyad. In the language of tensor analysis, a dyad is a tensor of second rank, while all vectors are tensors of first rank.

Operation of Three Vectors

For three vectors $\overline{A}$, $\overline{B}$, and $\overline{C}$, we have

$$\overline{C}\cdot(\overline{A}\times\overline{B}) = \overline{A}\cdot(\overline{B}\times\overline{C}) = \overline{B}\cdot(\overline{C}\times\overline{A}) \tag{1.1.7}$$

$$= \begin{vmatrix} C_x & C_y & C_z \\ A_x & A_y & A_z \\ B_x & B_y & B_z \end{vmatrix} = \begin{vmatrix} A_x & A_y & A_z \\ B_x & B_y & B_z \\ C_x & C_y & C_z \end{vmatrix} = \begin{vmatrix} B_x & B_y & B_z \\ C_x & C_y & C_z \\ A_x & A_y & A_z \end{vmatrix}$$

$$\overline{C}\times(\overline{A}\times\overline{B}) = \hat{x}\left[C_y\,(A_xB_y - A_yB_x) - C_z(A_zB_x - A_xB_z)\right]$$
$$+\,\hat{y}\left[C_z(A_yB_z - A_zB_y) - C_x(A_xB_y - A_zB_y)\right]$$
$$+\,\hat{z}\left[C_x(A_zB_x - A_xB_z) - C_y(A_xB_y - A_yB_x)\right]$$

$$= (\hat{x}A_x + \hat{y}A_y + \hat{z}A_z)(C_xB_x + C_yB_y + C_zB_z)$$
$$-\,(C_xA_x + C_yA_y + C_zA_z)(\hat{x}B_x + \hat{y}B_y + \hat{z}B_z)$$

$$= \overline{A}(\overline{C}\cdot\overline{B}) - (\overline{C}\cdot\overline{A})\overline{B} \tag{1.1.8}$$

Notice that the vector $\overline{C}\times(\overline{A}\times\overline{B})$ is perpendicular to $\overline{C}$ and lies in the plane determined by $\overline{A}$ and $\overline{B}$.

Operation with the del Operator

The del operator ∇ is a vector differential operator written as

$$\nabla = \hat{x}\frac{\partial}{\partial x} + \hat{y}\frac{\partial}{\partial y} + \hat{z}\frac{\partial}{\partial z}$$

The following can be proved in Cartesian coordinates or in vector form:

$$\nabla\cdot(\overline{E}\times\overline{H}) = \overline{H}\cdot(\nabla\times\overline{E}) - \overline{E}\cdot(\nabla\times\overline{H}) \tag{1.1.9}$$

$$\nabla\cdot(\nabla\times\overline{A}) = 0 \tag{1.1.10}$$

$$\nabla\times(\nabla\Phi) = 0 \tag{1.1.11}$$

$$\nabla\times(\nabla\times\overline{E}) = \nabla(\nabla\cdot\overline{E}) - \nabla^2\overline{E} \tag{1.1.12}$$

where

$$\nabla^2 = \nabla\cdot\nabla = \frac{\partial^2}{\partial x^2} + \frac{\partial^2}{\partial y^2} + \frac{\partial^2}{\partial z^2} \tag{1.1.13}$$

is the Laplacian operator in the rectangular coordinate system.

Pierre-Simon Laplace (28 March 1749 – 5 March 1827)

Pierre-Simon Laplace was appointed to a chair of mathematics at the École Militaire in Paris at the age of 19. During the French Revolution he helped to establish the metric system. The Laplace equation $\nabla^2\cdot\Phi = 0$ was published in 1813.

Gradient of a Scalar

When the del operator operates on a scalar function $\Phi(x, y, z)$, the result is a vector

$$\nabla\Phi = \hat{x}\frac{\partial}{\partial x}\Phi + \hat{y}\frac{\partial}{\partial y}\Phi + \hat{z}\frac{\partial}{\partial z}\Phi \tag{1.1.14}$$

called the gradient of $\Phi(x, y, z)$. The differential form of the gradient of Φ as defined states that

$$\begin{aligned}
\nabla\Phi = {} & \hat{x}\lim_{\Delta x \to 0}\frac{\Delta\Phi}{\Delta x} + \hat{y}\lim_{\Delta y \to 0}\frac{\Delta\Phi}{\Delta y} + \hat{z}\lim_{\Delta z \to 0}\frac{\Delta\Phi}{\Delta z} \\
= {} & \hat{x}\lim_{\Delta x \to 0}\frac{1}{\Delta x}\left[\left(\Phi(x + \frac{\Delta x}{2}, y, z) - \Phi(x - \frac{\Delta x}{2}, y, z)\right)\right] \\
& + \hat{y}\lim_{\Delta y \to 0}\frac{1}{\Delta y}\left[\left(\Phi(x, y + \frac{\Delta y}{2}, z) - \Phi(x, y - \frac{\Delta y}{2}, z)\right)\right] \\
& + \hat{z}\lim_{\Delta z \to 0}\frac{1}{\Delta z}\left[\left(\Phi(x, y, z + \frac{\Delta z}{2}) - \Phi(x, y, z - \frac{\Delta z}{2})\right)\right] \tag{1.1.15}
\end{aligned}$$

When $\Phi(x, y, z) = \Phi(x)$ is a function of x only, $\nabla\Phi(x)$ is a vector pointing in the direction of increasing x with the magnitude equal to the slope of the function at x.

EXAMPLE 1.1.1   Electric field vector as gradient of a potential function.

When there is no time variation, we may write the electric field vector $\overline{E}$ as

$$\overline{E} = -\nabla\Phi \tag{E1.1.1.1}$$

and call Φ a potential function. As the gradient $\nabla\Phi$ points in the direction of increasing potential Φ, the electric field $\overline{E}$ points from high potential towards low potential, similar to water flowing from a high altitude to lower ground.

Giving the potential of a point charge Q is

$$\Phi = \frac{Q}{4\pi r}$$

the electric field is

$$\overline{E} = -\frac{\partial}{\partial r}\Phi = \frac{Q}{4\pi r^2}$$

Thus the electric field points from high potential to low potential.

— END OF EXAMPLE 1.1.1 —

Divergence of a Vector

The divergence of a vector function is a scalar, defined as

$$\nabla \cdot \overline{D} = \left(\hat{x}\frac{\partial}{\partial x} + \hat{y}\frac{\partial}{\partial y} + \hat{z}\frac{\partial}{\partial z} \right) \cdot (\hat{x}D_x + \hat{y}D_y + \hat{z}D_z)$$

$$= \frac{\partial}{\partial x}D_x + \frac{\partial}{\partial y}D_y + \frac{\partial}{\partial z}D_z \qquad (1.1.16)$$
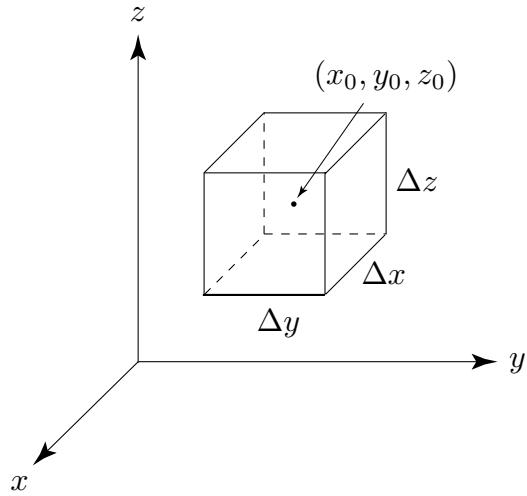
Figure 1.1.2 Differential volume $\Delta x \Delta y \Delta z$.

Consider a differential volume with sides $\Delta x, \Delta y, \Delta z$ centered around a point (x_0, y_0, z_0) [Fig. 1.1.2]. The divergence as defined states that

$$\nabla \cdot \overline{D} = \lim_{\substack{\Delta x \to 0 \\ \Delta y \to 0 \\ \Delta z \to 0}} \frac{1}{\Delta x \Delta y \Delta z} \left\{ \Delta y \Delta z \left[D_x(x_0 + \frac{\Delta x}{2}, y_0, z_0) - D_x(x_0 - \frac{\Delta x}{2}, y_0, z_0) \right] \right.$$

$$+ \Delta z \Delta x \left[D_y(x_0, y_0 + \frac{\Delta y}{z}, z_0) - D_y (x_0, y_0 - \frac{\Delta y}{z}, z_0) \right]$$

$$\left. + \Delta x \Delta y \left[D_z(x_0, y_0, z_0 + \frac{\Delta z}{2}) - D_z(x_0, y_0, z_0 - \frac{\Delta z}{2}) \right] \right\}$$

$$(1.1.17)$$

Gauss Theorem or Divergence Theorem

The first term in the braces is equal to the field component D_x at the surface at $x = x_0 + \frac{\Delta x}{2}$ multiplied by the surface area $\Delta y \Delta z$. We define a surface normal vector $d\overline{S}$ pointing outward of the volume such that at the surface at $x = x_0 + \frac{\Delta x}{2}$, $d\overline{S} = \hat{x} \Delta y \Delta z$ and at the surface at $x = x_0 - \frac{\Delta x}{2}$, $d\overline{S} = -\hat{x} \Delta y \Delta z$. Then the negative sign in the second term is due to $\overline{D}$ dot multiplied by $d\overline{S}$. All six terms account for the six differential areas bounding the differential volume $\Delta V = \Delta x \Delta y \Delta z$ with a surface normal $d\overline{S}$. We thus express the divergence of $\overline{D}$ as

$$\nabla \cdot \overline{D} = \lim_{\Delta V \to 0} \frac{1}{\Delta V} \oiint d\overline{S} \cdot \overline{D} \qquad (1.1.18)$$

Applying (1.1.18) to a large volume V containing an infinite number of such infinitesimal differential volumes [Fig. 1.1.3], we note that integrating the divergence over the volume surfaces shared by adjacent differential volumes will have no contribution because the surface normals point in opposite directions and thus cancel. The result is the divergence theorem or Gauss theorem
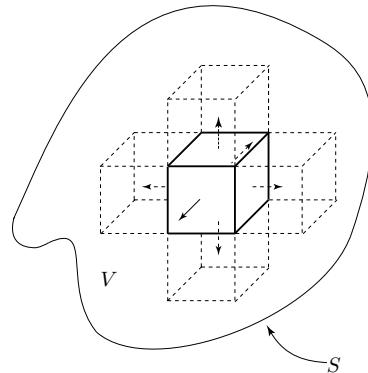
Figure 1.1.3 Derivation of divergence theorem.

$$\iiint_V dV \, \nabla \cdot \overline{D} = \oiint_S d\overline{S} \cdot \overline{D} \qquad (1.1.19)$$

The divergence theorem states that the volume integral of the divergence of the vector field $\overline{D}$ is equal to the total outward flux $\overline{D}$ through the surface S enclosing the volume.

Curl of a Vector

The curl of a vector field $\overline{H}$ is a vector defined as

$$\nabla \times \overline{H} = \left(\hat{x}\frac{\partial}{\partial x} + \hat{y}\frac{\partial}{\partial y} + \hat{z}\frac{\partial}{\partial z} \right) \times \overline{H} = \begin{vmatrix} \hat{x} & \hat{y} & \hat{z} \\ \frac{\partial}{\partial x} & \frac{\partial}{\partial y} & \frac{\partial}{\partial z} \\ H_x & H_y & H_z \end{vmatrix}$$

$$= \hat{x}\left(\frac{\partial}{\partial y}H_z - \frac{\partial}{\partial z}H_y \right) + \hat{y}\left(\frac{\partial}{\partial z}H_x - \frac{\partial}{\partial x}H_z \right) + \hat{z}\left(\frac{\partial}{\partial x}H_y - \frac{\partial}{\partial y}H_x \right)$$

$$(1.1.20)$$

Consider a differential volume of sides $\Delta x, \Delta y, \Delta z$ centered around a point (x_0, y_0, z_0). In the Cartesian coordinate system, the differential form of the curl of $\overline{H}$ as defined states that

$$\nabla \times \overline{H} = \lim_{\substack{\Delta x \to 0 \\ \Delta y \to 0 \\ \Delta z \to 0}} \left\{ \frac{1}{\Delta x}\left[\hat{x} \times \left(\overline{H}(x_0 + \frac{\Delta x}{2}, y_0, z_0) - \overline{H}(x_0 - \frac{\Delta x}{2}, y_0, z_0) \right) \right] \right.$$

$$+ \frac{1}{\Delta y}\left[\hat{y} \times \left(\overline{H}(x_0, y_0 + \frac{\Delta y}{2}, z_0) - \overline{H}(x_0, y_0 - \frac{\Delta y}{2}, z_0) \right) \right]$$

$$\left. + \frac{1}{\Delta z}\left[\hat{z} \times \left(\overline{H}(x_0, y_0, z_0 + \frac{\Delta z}{2}) - \overline{H}(x_0, y_0, z_0 - \frac{\Delta z}{2}) \right) \right] \right\}$$

$$= \lim_{\substack{\Delta x \to 0 \\ \Delta y \to 0 \\ \Delta z \to 0}} \frac{1}{\Delta x \Delta y \Delta z} \times$$

$$\left\{ \hat{x}\left[\Delta x \Delta z \left(H_z(x_0, y_0 + \frac{\Delta y}{2}, z_0) - H_z(x_0, y_0 - \frac{\Delta y}{2}, z_0) \right) \right. \right.$$

$$\left. - \Delta x \Delta y \left(H_y(x_0, y_0, z_0 + \frac{\Delta z}{2}) - H_y(x_0, y_0, z_0 - \frac{\Delta z}{2}) \right) \right]$$

$$+ \hat{y}\left[\Delta x \Delta y \left(H_x(x_0, y_0, z_0 + \frac{\Delta z}{2}) - H_x(x_0, y_0, z_0 - \frac{\Delta z}{2}) \right) \right.$$

$$\left. - \Delta y \Delta z \left(H_z(x_0 + \frac{\Delta x}{2}, y_0, z_0) - H_z(x_0 - \frac{\Delta x}{2}, y_0, z_0) \right) \right]$$

$$+ \hat{z}\left[\Delta y \Delta z \left(H_y(x_0 + \frac{\Delta x}{2}, y_0, z_0) - H_y(x_0 - \frac{\Delta x}{2}, y_0, z_0) \right) \right.$$

$$\left. \left. - \Delta x \Delta z \left(H_x(x_0, y_0 + \frac{\Delta y}{2}, z_0) - H_x(x_0, y_0 - \frac{\Delta y}{2}, z_0) \right) \right] \right\}$$

$$(1.1.21)$$

Stokes Theorem

The $\hat{z}$ component of (1.1.21) is

$$\hat{z} \cdot (\nabla \times \overline{H}) = (\nabla \times \overline{H})_z = \frac{\partial}{\partial x} H_y - \frac{\partial}{\partial y} H_x$$

$$= \lim_{\substack{\Delta x \to 0 \\ \Delta y \to 0}} \frac{1}{\Delta x \Delta y} \left\{ \Delta y \left[H_y(x_0 + \frac{\Delta x}{2}, y_0, z_0) - H_y(x_0 - \frac{\Delta x}{2}, y_0, z_0) \right] \right.$$

$$\left. - \Delta x \left[H_x(x_0, y_0 + \frac{\Delta y}{2}, z_0) - H_x(x_0, y_0 - \frac{\Delta y}{2}, z_0) \right] \right\}$$

The first term in the bracket is equal to the component H_y at $x = x_0 + \frac{\Delta x}{2}$ multiplied by the differential length Δy. We define a vector differential length $d\overline{l}$ [Fig. 1.1.4] such that for the side Δy at $x = x_0 + \frac{\Delta x}{2}$, $d\overline{l} = \hat{y} dy$; for the side Δx at $y_0 + \frac{\Delta y}{2}$, $d\overline{l} = -\hat{x} dx$; for the side Δy at $x = x_0 - \frac{\Delta x}{2}$, $d\overline{l} = -\hat{y} dy$; and for the side Δx at $y = y_0 - \frac{\Delta y}{2}$, $d\overline{l} = \hat{x} dx$. If we use the fingers of the right hand to trace the direction of $d\overline{l}$ along the loop, the right-hand thumb points in the surface normal direction $\hat{z}$. Thus
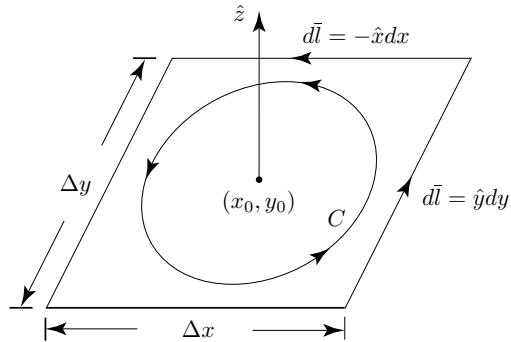
Figure 1.1.4 Derivation of $\hat{z}$-component of the curl of a vector field.

$$\hat{z} \cdot (\nabla \times \overline{H}) = \lim_{\substack{\Delta x \to 0 \\ \Delta y \to 0}} \frac{1}{\Delta S} \oint_C d\overline{l} \cdot \overline{H} \qquad (1.1.22)$$

where C denotes the contour circulating the area $\Delta S = \Delta x \Delta y$. Similar results are derivable for the $\hat{x}$ and $\hat{y}$ components of $\nabla \times \overline{H}$. For a differential area ΔS with a surface normal in the direction of $\hat{s}$, we have

$$\hat{s} \cdot (\nabla \times \overline{H}) = \lim_{\Delta S \to 0} \frac{1}{\Delta S} \oint_C d\overline{l} \cdot \overline{H} \qquad (1.1.23)$$

We now apply (1.1.21) to an open surface S, subdivide into N differential areas [Fig. 1.1.5]. For a differential area ΔS_j bounded by a contour C_j and with a surface normal $\hat{s}_j$, we have $\Delta \overline{S}_j = \hat{s}_j \Delta S_j$ and

$$\Delta \overline{S}_j \cdot (\nabla \times \overline{H})_j = \oint_{C_j} d\bar{l} \cdot \overline{H}$$

Adding the contributions of all N differential areas [Fig. 1.1.5], we find

$$\lim_{\substack{\Delta S_j \to 0 \\ N \to \infty}} \sum_{j=1}^{N} \Delta \overline{S}_j \cdot (\nabla \times \overline{H})_j = \oint_{C} d\bar{l} \cdot \overline{H}$$
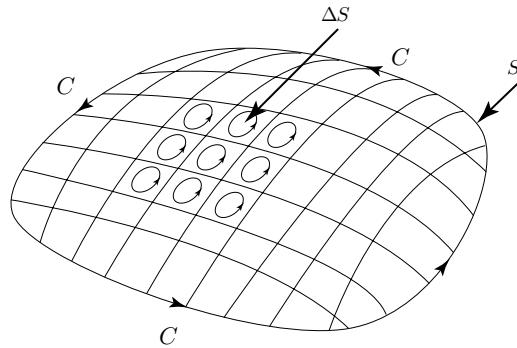
Figure 1.1.5   Derivation of Stokes' theorem.

Since the common part of the contours in two adjacent elements is traversed in opposite directions by the two contours, the net contribution of all the common parts in the interior sums to zero and only the contribution from the external contour C bounding the open surface S remains in the line integral on the right-hand side. The left-hand side becomes a surface integral, and the result is Stokes' theorem:

$$\iint d\overline{S} \cdot (\nabla \times \overline{H}) = \oint_{C} d\bar{l} \cdot \overline{H} \qquad (1.1.24)$$

Stokes' theorem states that the surface integral of the curl of the vector field $\overline{H}$ over an open surface S is equal to the closed line integral of the vector along the contour enclosing the open surface.

George Gabriel Stokes (13 August 1819 – 1 February 1903) was appointed Lucasian Professor of Mathematics at Cambridge University in 1849. His mathematical and physical papers were published in 5 volumes, the first 3 of which Stokes edited himself in 1880, 1883 and 1891. The last 2 were edited by Joseph Larmor in 1887 and 1891.

Maxwell Equations in Integral Form

Applying Stokes theorem to the Ampére's law and Faraday's law and applying the divergence theorem to Gauss' and continuity laws, we find

$$\oint_C d\bar{l} \cdot \overline{H} = \iint d\overline{S} \cdot \overline{J} + \iint d\overline{S} \cdot \frac{\partial}{\partial t} \overline{D} \tag{1.1.25}$$

$$\oint_C d\bar{l} \cdot \overline{E} = -\iint d\overline{S} \cdot \frac{\partial}{\partial t} \overline{B} \tag{1.1.26}$$

$$\oiint_S d\overline{S} \cdot \overline{D} = \iiint_V dV \, \nabla \cdot \overline{D} = \iiint_V dV \, \rho \tag{1.1.27}$$

$$\oiint_S d\overline{S} \cdot \overline{B} = \iiint_V dV \, \nabla \cdot \overline{B} = 0 \tag{1.1.28}$$

$$\oiint_S d\overline{S} \cdot \overline{J} = -\iiint_V dV \frac{\partial}{\partial t} \rho \tag{1.1.29}$$

These are the integral form of Maxwell equations.

Oliver Heaviside (18 May 1850 – 3 February 1925)

The year after the publication of Maxwell's *Treatise of Electricity and Magnetism* in 1873, Heaviside resigned from his job at age 24 and devoted all his time to the study of Maxwell's theory. Despite of the criticism from all the disbelievers, he remained the faithful decipher and declared himself a Maxwellian. He refuted the quaternion notation initiated by Hamilton and Tait and developed the vector notation to cast Maxwell's equation into the form as we show in this book.

Cylindrical and Spherical Coordinate Systems

In addition to the rectangular coordinates with unit vectors $\hat{x}, \hat{y}, \hat{z}$, the cylindrical coordinate system with unit vectors $\hat{\rho}, \hat{\phi}, \hat{z}$, and the spherical coordinate system with unit vectors $\hat{\rho}, \hat{\theta}, \hat{\phi}$ are often used in this book.

In a general orthogonal coordinate system, we use $\hat{u}_i$ $(i = 1, 2, 3)$ to denote the three basis vectors, $dl_i = h_i du_i$ to denote a differential length, where h_i is called a metric coefficient. The basis vectors are perpendicular to one another $\hat{u}_i \cdot \hat{u}_j = 0$ for $i \neq j$ but they are not necessarily of unit length. In Table 1.1.1 we summarize the basis vectors and the metric coefficients for the rectangular (or Cartesian), cylindrical, and spherical coordinate systems.

Orthogonal Coordinate System	Rectangular Coordinates (x, y, z)	Cylindrical Coordinates (ρ, ϕ, z)	Spherical Coordinates (r, θ, ϕ)
Base Vectors $(\hat{u}_1, \hat{u}_2, \hat{u}_3)$	$\hat{x}, \hat{y}, \hat{z}$	$\hat{\rho}, \hat{\phi}, \hat{z}$	$\hat{r}, \hat{\theta}, \hat{\phi}$
Metric Coefficients (h_1, h_2, h_3)	$1, 1, 1$	$1, \rho, 1$	$1, r, r \sin \theta$
Differential Volume $(h_1 h_2 h_3 du_1 du_2 du_3)$	$dx\,dy\,dz$	$\rho\,d\rho\,d\phi\,dz$	$r^2 \sin \theta\, dr\,d\theta\,d\phi$

Table 1.1.1 Orthogonal coordinate systems.

In terms of the general orthogonal coordinate system, the gradient, the divergence, the curl, and the Laplacian operators are defined as

$$\nabla \Phi = \hat{u}_1 \frac{\partial \Phi}{h_1 \partial u_1} + \hat{u}_2 \frac{\partial \Phi}{h_2 \partial u_2} + \hat{u}_3 \frac{\partial \Phi}{h_3 \partial u_3}$$

$$\nabla \cdot \overline{D} = \frac{1}{h_1 h_2 h_3} \left[\frac{\partial}{\partial u_1} (h_2 h_3 D_1) + \frac{\partial}{\partial u_2} (h_3 h_1 D_2) + \frac{\partial}{\partial u_3} (h_1 h_2 D_3) \right]$$

$$\nabla \times \overline{H} = \frac{1}{h_1 h_2 h_3} \begin{vmatrix} h_1 \hat{u}_1 & h_2 \hat{u}_2 & h_3 \hat{u}_3 \\ \frac{\partial}{\partial u_1} & \frac{\partial}{\partial u_2} & \frac{\partial}{\partial u_3} \\ h_1 H_1 & h_2 H_2 & h_3 H_3 \end{vmatrix}$$

$$\nabla^2 \Phi = \nabla \cdot \nabla \Phi$$

$$= \frac{1}{h_1 h_2 h_3} \left[\frac{\partial}{\partial u_1} h_2 h_3 \frac{\partial \Phi}{h_1 \partial u_1} + \frac{\partial}{\partial u_2} h_3 h_1 \frac{\partial \Phi}{h_2 \partial u_2} + \frac{\partial}{\partial u_3} h_1 h_2 \frac{\partial \Phi}{h_3 \partial u_3} \right]$$

Identifying the metrics h_1, h_2, h_3 with those as listed in Table 1.1.1, we readily obtain the expressions in cylindrical and spherical coordinates. In the cylindrical coordinate system [Fig. 1.1.6],

$$\text{Vector differential length} \quad d\bar{l} = \hat{\rho}\,d\rho + \hat{\phi}\rho\,d\phi + \hat{z}\,dz$$

$$\text{Differential area} \quad d\overline{S} = \hat{\rho}\rho\,d\phi\,dz + \hat{\phi}\,d\rho\,dz + \hat{z}\rho\,d\rho\,d\phi$$

$$\text{Differential volume} \quad dV = \rho\,d\rho\,d\phi\,dz$$
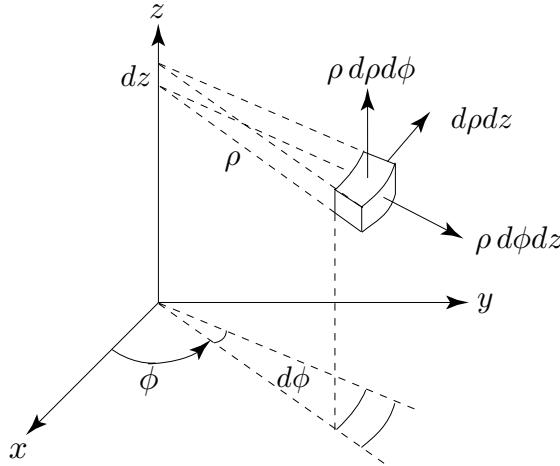
Figure 1.1.6 Cylindrical coordinate system.

$$\nabla\Phi = \hat{\rho}\frac{\partial\Phi}{\partial\rho} + \hat{\phi}\frac{1}{\rho}\frac{\partial\Phi}{\partial\phi} + \hat{z}\frac{\partial\Phi}{\partial z}$$

$$\nabla\cdot\overline{D} = \frac{1}{\rho}\frac{\partial}{\partial\rho}(\rho D_\rho) + \frac{1}{\rho}\frac{\partial}{\partial\phi}D_\phi + \frac{\partial}{\partial z}D_z$$

$$\nabla\times\overline{H} = \frac{1}{\rho}\begin{vmatrix} \hat{\rho} & \rho\hat{\phi} & \hat{z} \\ \dfrac{\partial}{\partial\rho} & \dfrac{\partial}{\partial\phi} & \dfrac{\partial}{\partial z} \\ H_\rho & \rho H_\phi & H_z \end{vmatrix}$$

$$\nabla^2\Phi = \nabla\cdot\nabla\Phi$$

$$= \frac{1}{\rho}\frac{\partial}{\partial\rho}\left[\rho\frac{\partial\Phi}{\partial\rho}\right] + \frac{1}{\rho^2}\frac{\partial^2\Phi}{\partial\phi^2} + \frac{\partial^2\Phi}{\partial z^2}$$

In the spherical coordinate system [Fig. 1.1.7],

Vector differential length $d\bar{l} = \hat{r}dr + \hat{\theta}rd\theta + \hat{\phi}r\sin\theta d\phi$

Differential area $d\overline{S} = \hat{r}r^2\sin\theta d\theta d\phi + \hat{\theta}r\sin\theta dr d\phi + \hat{\phi}r dr d\theta$

Differential volume $dV = r^2\sin\theta dr d\theta d\phi$
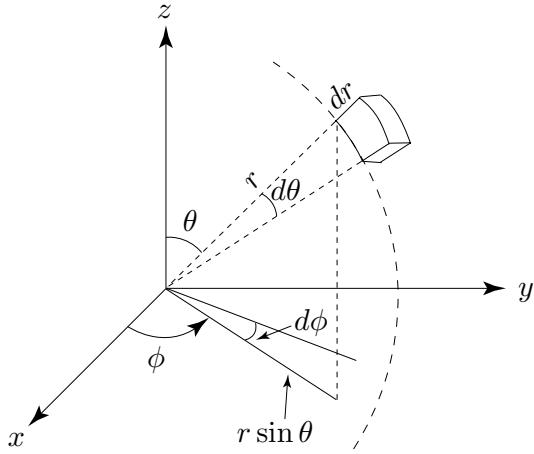
Figure 1.1.7 Spherical coordinate system.

$$\nabla \Phi = \hat{r}\frac{\partial \Phi}{\partial r} + \hat{\theta}\frac{1}{r}\frac{\partial \Phi}{\partial \theta} + \hat{\phi}\frac{1}{r\sin\theta}\frac{\partial \Phi}{\partial \phi}$$

$$\nabla \cdot \overline{D} = \frac{1}{r^2}\frac{\partial}{\partial r}(r^2 D_r) + \frac{1}{r\sin\theta}\frac{\partial}{\partial \theta}(\sin\theta D_\theta) + \frac{1}{r\sin\theta}\frac{\partial}{\partial \phi}D_\phi$$

$$\nabla \times \overline{H} = \frac{1}{r^2\sin\theta}\begin{vmatrix} \hat{r} & r\hat{\theta} & r\sin\theta\hat{\phi} \\ \dfrac{\partial}{\partial r} & \dfrac{\partial}{\partial \theta} & \dfrac{\partial}{\partial \phi} \\ H_r & rH_\theta & r\sin\theta H_\phi \end{vmatrix}$$

$$\nabla^2 \Phi = \nabla \cdot \nabla \Phi$$

$$= \frac{1}{r^2}\frac{\partial}{\partial r}\left[r^2\frac{\partial \Phi}{\partial r}\right] + \frac{1}{r^2\sin\theta}\frac{\partial}{\partial \theta}\left[\sin\theta\frac{\partial \Phi}{\partial \theta}\right] + \frac{1}{r^2\sin^2\theta}\frac{\partial^2 \Phi}{\partial \phi^2}$$

$$= \frac{1}{r}\frac{\partial^2}{\partial r^2}\left[r\Phi\right] + \frac{1}{r^2\sin\theta}\frac{\partial}{\partial \theta}\left[\sin\theta\frac{\partial \Phi}{\partial \theta}\right] + \frac{1}{r^2\sin^2\theta}\frac{\partial^2 \Phi}{\partial \phi^2}$$

Index Notation

A vector in the Cartesian coordinate system can be represented by its three components. Thus, A_j with $j = 1, 2, 3$ represents A_1, A_2, A_3 of the vector $\overline{A}$. The dot product $\overline{A} \cdot \overline{B}$ is written as $A_j B_j$ where the repeated index j implies summation over j from 1 to 3:

$$A_j B_j = \sum_{j=1}^{3} A_j B_j = A_1 B_1 + A_2 B_2 + A_3 B_3$$

To express cross products in index notation we need to define a Levi-Cevita symbol ε_{ijk} where i, j, k take values from 1 to 3. When any of the two indices are equal the Levi-Cevita symbol is zero. Otherwise, ε_{ijk} is either $+1$ or -1. It is $+1$ if ijk is an even permutation of 1,2,3; -1 if ijk is an odd permutation of 1,2,3. Thus $\varepsilon_{123} = \varepsilon_{231} = \varepsilon_{312} = 1$ and $\varepsilon_{213} = \varepsilon_{132} = \varepsilon_{321} = -1$ and all others equal to 0. Let $\overline{C} = \overline{A} \times \overline{B}$. In index notation, we write $C_i = \varepsilon_{ijk} A_j B_k$. Thus, $C_1 = \varepsilon_{123} A_2 B_3 + \varepsilon_{132} A_3 B_2 = A_2 B_3 - A_3 B_2$. The dyad $\overline{A}\,\overline{B}$ is $A_j B_k$, no summation implied because no index is repeated. The identities (1.1.7) and (1.1.8) are

$$C_i \varepsilon_{ijk} A_j B_k = A_j \varepsilon_{jki} B_k C_i = B_k \varepsilon_{kij} C_i A_j$$

$$\varepsilon_{ijk} C_j \varepsilon_{klm} A_l B_m = (\varepsilon_{ijk} \varepsilon_{klm}) C_j A_l B_m = (\delta_{il}\delta_{jm} - \delta_{im}\delta_{lj}) C_j A_l B_m$$
$$= A_i C_m B_m - C_l A_l B_i$$

where $\delta_{ij} = 1$ when $i = j$ and $\delta_{ij} = 0$ when $i \neq j$.

In index notation, divergence of D_j, $\nabla \cdot D_j$, is $\partial_j D_j$.

In index notation, ∇ is represented by ∂_i and $\nabla\phi$ by $\partial_i \phi$.

In index notation, curl of H_i, $\nabla \times H_i$, is written as $\varepsilon_{ijk}\partial_j H_k$.

The identities (1.1.9)–(1.1.12) are, in index notation

$$\partial_i(\varepsilon_{ijk} E_j H_k) = \varepsilon_{ijk} H_k \partial_i E_j + \varepsilon_{ijk} E_j \partial_i H_k = H_k \varepsilon_{kij} \partial_i E_j - E_j \varepsilon_{jik} \partial_i H_k$$

$$\partial_i \varepsilon_{ijk} \partial_j A_k = -\varepsilon_{jik} \partial_i \partial_j A_k = 0$$

$$\varepsilon_{ijk} \partial_j \partial_k \phi = -\varepsilon_{ikj} \partial_j \partial_k \phi = -\varepsilon_{ikj} \partial_k \partial_j \phi = 0$$

$$\varepsilon_{ijk} \partial_j \varepsilon_{klm} \partial_l E_m = (\delta_{il}\delta_{jm} - \delta_{im}\delta_{jl})\partial_j \partial_l E_m = \partial_m \partial_i E_m - \partial_j \partial_j E_i$$

Maxwell equations, when written in index notation, take the form:

$$\varepsilon_{ijk} \partial_j H_k = \partial_t D_i + J_i$$
$$\varepsilon_{ijk} \partial_j E_k = \partial_t B_i$$
$$\partial_j D_j = \rho$$
$$\partial_j B_j = -\partial_t \rho$$

where ∂_t denotes partial derivative with respect to time.

EXAMPLE 1.1.2   Poisson equation and Laplace equation.

In (E1.1.1.1), we wrote the electric field vector as the gradient of a potential function Φ:

$$\overline{E} = -\nabla\Phi \qquad\qquad (E1.1.2.1)$$

By virtue of (1.1.11), we see that $\nabla \times \overline{E} = 0$. Thus the above definition for the electric field is true only when the term $\partial\overline{B}/\partial t$ in Faraday's law can be

neglected, i.e., when there is no time variation. We may refer to the above electric field as the static electric field. Derive an equation for Φ.

SOLUTION:

Coulomb's law (or Gauss' law for electricity) in free space is

$$\nabla \cdot \overline{E} = \rho/\epsilon_o$$

In terms of the potential function, we obtain the Poisson equation

$$\nabla^2\Phi = -\rho/\epsilon_o \qquad\qquad (\text{E1.1.2.2})$$

In places where there is no charge density, $\rho = 0$, we have the Laplace equation $\nabla^2\Phi = 0$.

<div align="right">— END OF EXAMPLE 1.1.2 —</div>

Siméon Denis Poisson (21 June 1781 – 25 April 1840) studied mathematics at the Ecole Polytechnique and was student of Pierre-Simon Laplace and Joseph-Louis Lagrange. His memoir on finite differences was written at age 18. His well-known contributions include Poisson's equation in potential theory was developed in 1829–1835.

EXAMPLE 1.1.3

The voltage V_{ab} is defined as the integration of $\overline{E}$ along a line segment of $\overline{\ell}$ from point a to point b.

$$V_{ab} = \int_a^b d\overline{\ell} \cdot \overline{E} \qquad\qquad (\text{E1.1.3.1})$$

Thus V_{ab} is the potential difference between points a and b. For positive V_{ab}, the electric field vector points from a to b. Point a is at a higher potential Φ_a than Φ_b at point b, $\Phi_b < \Phi_a$ and $V_{ab} = \Phi_a - \Phi_b$.

<div align="right">— END OF EXAMPLE 1.1.3 —</div>

EXAMPLE 1.1.4

Maxwell's equations were originally written in the form of scalar partial differential equations. Written in terms of all field components, we find that for Ampère's law,

$$\frac{\partial}{\partial y}H_z - \frac{\partial}{\partial z}H_y = \frac{\partial}{\partial t}D_x + J_x \qquad\qquad (\text{E1.1.4.1}a)$$

$$\frac{\partial}{\partial z}H_x - \frac{\partial}{\partial x}H_z = \frac{\partial}{\partial t}D_y + J_y \qquad\qquad (\text{E1.1.4.1}b)$$

$$\frac{\partial}{\partial x}H_y - \frac{\partial}{\partial y}H_x = \frac{\partial}{\partial t}D_z + J_z \qquad\qquad (\text{E1.1.4.1}c)$$

for Faraday's law,

$$\frac{\partial}{\partial y}E_z - \frac{\partial}{\partial z}E_y = -\frac{\partial}{\partial t}B_x \qquad (\text{E1.1.4.2}a)$$

$$\frac{\partial}{\partial z}E_x - \frac{\partial}{\partial x}E_z = -\frac{\partial}{\partial t}B_y \qquad (\text{E1.1.4.2}b)$$

$$\frac{\partial}{\partial x}E_y - \frac{\partial}{\partial y}E_x = -\frac{\partial}{\partial t}B_z \qquad (\text{E1.1.4.2}c)$$

for Coulomb's law

$$\frac{\partial}{\partial x}D_x + \frac{\partial}{\partial y}D_y + \frac{\partial}{\partial z}D_z = \rho \qquad (\text{E1.1.4.3})$$

and for Gauss' law

$$\frac{\partial}{\partial x}B_x + \frac{\partial}{\partial y}B_y + \frac{\partial}{\partial z}B_z = 0 \qquad (\text{E1.1.4.4})$$

Taking the sum of $\partial(\text{E1.1.4.1}a)/\partial x$, $\partial(\text{E1.1.4.1}b)/\partial y$, $\partial(\text{E1.1.4.1}c)/\partial z$, and making use of (E1.1.4.3), we obtain

$$\frac{\partial}{\partial x}J_x + \frac{\partial}{\partial y}J_y + \frac{\partial}{\partial z}J_z = -\frac{\partial}{\partial t}\rho \qquad (\text{E1.1.4.5})$$

which is the continuity law. Given (E1.1.4.5), Coulomb's law can be derived from Ampère's law. Likewise, Gauss' law can be derived from Faraday's law, $\nabla \cdot \overline{B} = Const$, noticing that no static magnetic monopole is found to exist and that $Const = 0$. Thus (E1.1.4.3) and (E1.1.4.4) are not independent scalar equations, they can be derived from (E1.1.4.1) and (E1.1.4.2).

— End of Example 1.1.4 —

Problems

P1.1.1

Three vectors $\overline{A}$, $\overline{B}$, and $\overline{C}$ drawn in a head-to-tail fashion form the three sides of a triangle. What is $\overline{A} + \overline{B} + \overline{C}$ and what is $\overline{A} + \overline{B} - \overline{C}$?

P1.1.2

Prove $|\overline{A} \times \overline{B}|^2 = A^2 B^2 - (\overline{A} \cdot \overline{B})^2$ by using $\overline{C} \times (\overline{A} \times \overline{B}) = \overline{A}(\overline{C} \cdot \overline{B}) - (\overline{C} \cdot \overline{A})\overline{B}$.

P1.1.3

A position vector $\overline{r} = \hat{x}\sqrt{2} + \hat{y}\sqrt{2} + \hat{z}2$. Determine its spherical components r, θ, ϕ and its cylindrical components ρ, ϕ, z.

P1.1.4

Find a unit vector $\hat{c}$ that is perpendicular to both $\overline{A} = \hat{x}4 + \hat{y}5 - \hat{z}3$ and $\overline{B} = \hat{x}2 - \hat{y}7 - \hat{z}1.5$.

P1.1.5

Let $\overline{A} = \hat{x}A$, and the projection of another vector $\overline{B}$ on $\overline{A}$ be $B_x = B\cos\theta_{AB}$. What is $\overline{A} \cdot \overline{B}$ in terms of the angle θ_{AB} between $\overline{A}$ and $\overline{B}$?

P1.1.6

Assume $A > B$ and draw a line projecting $\overline{B}$ on $\overline{A}$. The line length $h = B\sin\theta_{AB}$, which is also related to A from $h^2 = |\overline{A} - \overline{B}|^2 - (A - B\cos\theta_{AB})^2$ by the cosine law in geometry. Show that $\overline{A} \cdot \overline{B} = AB\cos\theta_{AB}$

P1.1.7

The direction of $\overline{A} \times \overline{B}$ follows the right-hand rule, i.e., when the fingers of the right hand rotate from $\overline{A}$ to $\overline{B}$, the thumb of the right hand points in the direction of $\overline{A} \times \overline{B}$. Thus the vector $\overline{A} \times \overline{B}$ is perpendicular to both $\overline{A}$ and $\overline{B}$ and the plane containing $\overline{A}$ and $\overline{B}$. Let $\overline{A} = \hat{x}A_x + \hat{y}A_y$ and $\overline{B} = \hat{x}B_x + \hat{y}B_y$ both in the xy-plane, find $\overline{A} \times \overline{B}$.

P1.1.8

Using $\cos\theta_{AB} = \overline{A} \cdot \overline{B}/AB$, show that $|\overline{A} \times \overline{B}| = |AB\sin\theta_{AB}|$.

P1.1.9

For $\Phi(x) = x^2$, and $\Phi(x) = -x^3$, what are their gradients?

P1.1.10

The function $\Phi = x^2 + 2y^2$ describes a family of ellipses. Find its gradient and show that $\nabla\Phi$ is normal to the ellipse and pointing in the directions of an expanding ellipse.

P1.1.11

Consider the function $\Phi = x + y$. Find the gradient of the function.

P1.1.12

Prove the following identities:

$$\nabla \cdot (\overline{E} \times \overline{H}) = \overline{H} \cdot (\nabla \times \overline{E}) - \overline{E} \cdot (\nabla \times \overline{H}) \qquad (1.1.9)$$

$$\nabla \cdot (\nabla \times \overline{A}) = 0 \qquad (1.1.10)$$

$$\nabla \times (\nabla\Phi) = 0 \qquad (1.1.11)$$

$$\nabla \times (\nabla \times \overline{E}) = \nabla(\nabla \cdot \overline{E}) - \nabla^2\overline{E} \qquad (1.1.12)$$

P1.1.13

The six terms in (1.1.21) are associated with the six differential surfaces bounding (x_0, y_0, z_0). For the first term, the surface normal is in the $\hat{x}$ direction; we write $d\overline{S} = \hat{x}\Delta y\Delta z$. For the second term $d\overline{S} = -\hat{x}\Delta y\Delta z$. For the third term $d\overline{S} = \hat{y}\Delta z\Delta x$, etc. Derive a curl theorem by integrating over the volume similar to the divergence theorem.

P1.1.14

What is the result if the surface integral of $\nabla \times \overline{H}$ is carried out over a closed surface? Compare with Stokes Theorem in (1.1.24) and the curl theorem in P1.1.13 for the curl integrated over a volume V enclosed by a surface S.

P1.1.15

For the vector $\overline{A} = \hat{\rho}\rho^2 + \hat{z}2z$, verify the divergence theorem for the circular cylindrical region enclosed by $\rho = 5, z = 0$, and $z = 3$.

P1.1.16

Prove that $[\overline{A} \times (\nabla \times \overline{B})]_i = A_j \partial_i B_j - [(\overline{A} \cdot \nabla)\overline{B}]_i$.

P1.1.17

Prove that $\nabla(\overline{A} \cdot \overline{B}) = (\overline{A} \cdot \nabla)\overline{B} + (\overline{B} \cdot \nabla)\overline{A} + \overline{A} \times (\nabla \times \overline{B}) + \overline{B} \times (\nabla \times \overline{A})$.

P1.1.18

Show that $\nabla(\overline{A} \cdot \overline{A}) = 2(\overline{A} \cdot \nabla)\overline{A} + 2\overline{A} \times (\nabla \times \overline{A})$.

P1.1.19

Express static electric field vector as the gradient of a potential function

$$\Phi = \frac{C}{\sqrt{x^2 + y^2 + z^2}}$$

and find the electric field of a charge q from Maxwell equations.

1.2   Electromagnetic Waves

A. Wave Equation and Wave Solution

The Maxwell equations in differential form are valid at all times for every point in space. First we shall investigate solutions to the Maxwell equations in regions devoid of source, namely in regions where $\overline{J} = 0$ and $\rho = 0$. This of course does not mean that there is no source anywhere in all space. Sources must exist outside the regions of interest in order to produce fields in these regions. Thus in source-free regions in free space, the Maxwell equations become

$$\nabla \times \overline{H} = \epsilon_o \frac{\partial}{\partial t} \overline{E} \qquad (1.2.1)$$

$$\nabla \times \overline{E} = -\mu_o \frac{\partial}{\partial t} \overline{H} \qquad (1.2.2)$$

$$\nabla \cdot \overline{E} = 0 \qquad (1.2.3)$$

$$\nabla \cdot \overline{H} = 0 \qquad (1.2.4)$$

To derive an equation for the vector field $\overline{E}$, we take curl of (1.2.2), substitute (1.2.1)

$$\nabla \times \nabla \times \overline{E} = -\mu_o \frac{\partial}{\partial t} \nabla \times \overline{H} = -\mu_o \epsilon_o \frac{\partial^2}{\partial t^2} \overline{E} \qquad (1.2.5)$$

and make use of the vector identity $\nabla \times \nabla \times \overline{E} = \nabla \nabla \cdot \overline{E} - \nabla^2 \overline{E}$. Noticing from (1.2.3) that $\nabla \cdot \overline{E} = 0$, we have

$$\boxed{\nabla^2 \overline{E} - \mu_o \epsilon_o \frac{\partial^2}{\partial t^2} \overline{E} = 0} \qquad (1.2.6)$$

This is known as the Helmholtz wave equation. Solutions to the wave equation (1.2.6) that satisfy all Maxwell equations are electromagnetic waves.

Hermann Ludwig Ferdinand von Helmholtz (31 August 1821 – 8 September 1894) was a professor of anatomy and physiology at the University of Bonn in 1858, then became a professor of physics at the University of Berlin in 1871, and the first director of the Physico-Technical Institute of Berlin in 1888. His 3-volume Handbook of Physiological Optics appeared between 1856 and 1867.

Wave Solution

We shall now study a solution to (1.2.6) assuming $E_y = E_z = 0$. Let E_x be a function only of z and t and independent of x and y. The electric field vector can be written as

$$\overline{E} = \hat{x} E_x(z,t)$$

The wave equation it satisfies follows from (1.2.6) which becomes

$$\frac{\partial^2}{\partial z^2} E_x - \mu_o \epsilon_o \frac{\partial^2}{\partial t^2} E_x = 0 \qquad (1.2.7)$$

The simplest solution to (1.2.7) takes the form

$$\overline{E} = \hat{x} E_x(z,t) = \hat{x} E_0 \cos(kz - \omega t) \qquad (1.2.8)$$

Substituting (1.2.8) in (1.2.7) we find that the following equation, called the dispersion relation, must be satisfied:

$$\boxed{k^2 = \omega^2 \mu_o \epsilon_o} \qquad (1.2.9)$$

The dispersion relation provides an important connection between the spatial frequency k and the temporal frequency ω.

There are two points of view useful in the study of a space-time varying quantity such as $E_x(z,t)$. The temporal view point is to examine the time variation at fixed points in space. The spatial view point is to examine spatial variation at fixed times, a process that amounts to taking a series of pictures.

From the temporal view point, we first fix our attention on one particular point in space, say $z = 0$. We then have the electric field $E_x(z = 0, t) = E_0 \cos \omega t$. Plotted as a function of time in Fig. 1.2.1, we find that the waveform repeats itself in time as $\omega t = 2m\pi$ for any integer m. The period is defined as the time T for which $\omega T = 2\pi$. The number of periods in a time of one second is the frequency f defined as $f = 1/T$, which gives

$$f = \frac{\omega}{2\pi} \qquad (1.2.10)$$
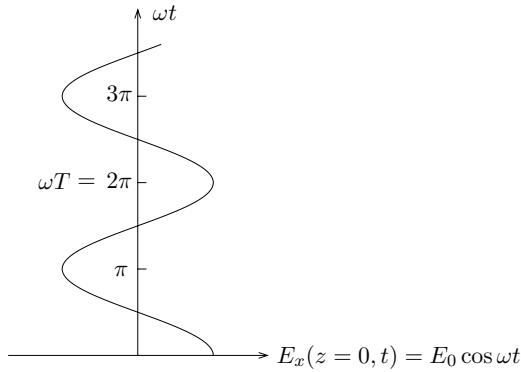
Figure 1.2.1 Electric field strength as a function of ωt **at** $z = 0$.
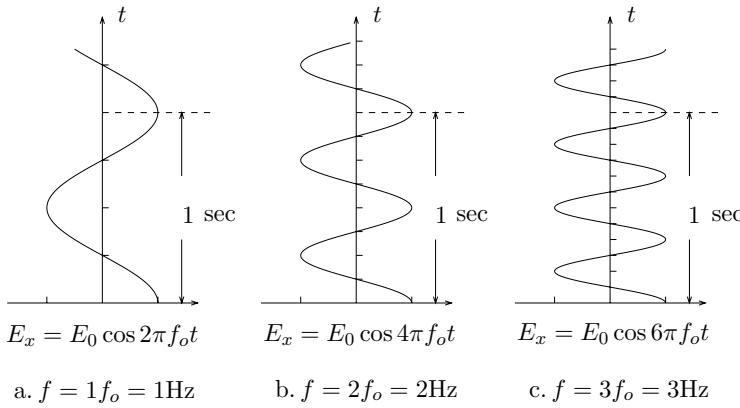
Figure 1.2.2 Electric field strength vs. t **for different frequencies** ω.

The unit for frequency f is Hertz (Hz) with $1\ \text{Hz} = 1\ \text{s}^{-1}$, which is equal to the number of cycles per second. Since $\omega = 2\pi f$, ω is the angular frequency of the wave.

In this book, we often refer to ω as the frequency, simply because ω is more commonly encountered than f. The temporal frequency ω characterizes the variation of the wave in time. We plot in Fig. 1.2.2a $E_x(z = 0, t)$ as a function of t instead of ωt. Let there be one period within the time interval of 1 second. Thus, $f = f_o = 1\ \text{Hz}$, and we let $\omega = \omega_o = 2\pi\ \text{rad/s}$. In Fig. 1.2.2b, we plot $\omega = 2\omega_o$; there are two periods in a time interval of one second and the period in time is 0.5 seconds. In Fig. 1.2.2c, $\omega = 3\omega_o$ and there are three periods in one second.

B. Unit for Spatial Frequency k

To examine wave behavior from the spatial view point, let $\omega t = 0$. The electric field becomes

$$E_x(z, t = 0) = E_0 \cos kz \qquad (1.2.11)$$

The electric field thus varies periodically in space. We plot $E_x(z, t = 0)$ as a function of kz in Fig. 1.2.3. The waveform repeats itself periodically in space when $kz = 2m\pi$ for integer values of m. The period of one spatial variation is the wavelength λ defined as the distance for which $k\lambda = 2\pi$. The number of spatial variations per unit distance is
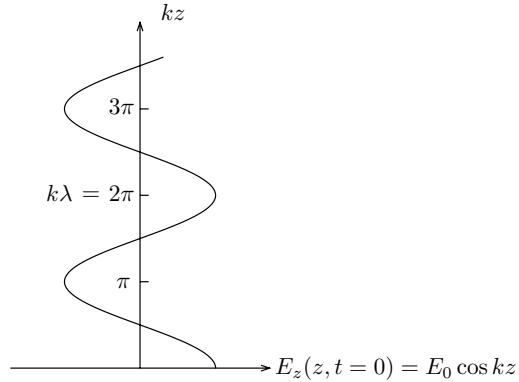
Figure 1.2.3 Electric field strength as a function of kz at $t = 0$.
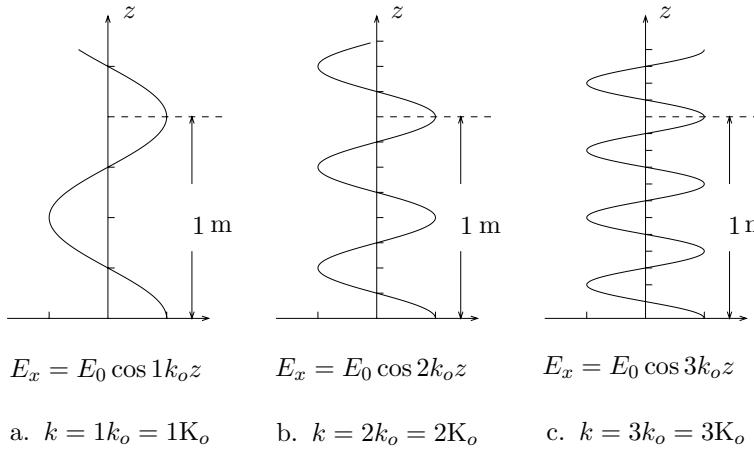
$$k = \frac{2\pi}{\lambda} \qquad (1.2.12)$$

We call k the spatial frequency, which characterizes the spatial variations of the field strength, similar to the temporal frequency which characterized the temporal variations of the field strength. The spatial frequency is also called the wavenumber as it is equal to the number of wavelengths in a distance of 2π and has the dimension of inverse length.

Let me define for the spatial frequency k a fundamental unit K_o:

$$\boxed{1\,\text{K}_o = 2\pi \ \text{rad/m}} \qquad (1.2.13)$$

Similar to the unit Hz which is cycles per second in temporal variation, K_o is cycles per meter in spatial variation. For a wave that has a spatial

$$E_x = E_0 \cos 1k_o z \qquad E_x = E_0 \cos 2k_o z \qquad E_x = E_0 \cos 3k_o z$$

a. $k = 1k_o = 1\mathrm{K}_o$ b. $k = 2k_o = 2\mathrm{K}_o$ c. $k = 3k_o = 3\mathrm{K}_o$

Figure 1.2.4 Electric field strength vs. distance z with different spatial frequency k.

frequency of one period of spatial variation in one meter distance, we have $k = 1\,\mathrm{K}_o$. An electromagnetic wave in free space with $k = 3\,\mathrm{K}_o$ has three spatial variations in a distance of one meter.

We plot in Fig. 1.2.4a $E_x(z, t = 0)$ as a function of z instead of kz. There is one cycle of spatial variation within the wavelength of 1 meter. Since $\mathrm{K}_o = 2\pi\ \mathrm{rad/m}$, we have $k = 1\,\mathrm{K}_o = 2\pi\ \mathrm{rad/m}$. In Fig. 1.2.4b, we plot $k = 2\,\mathrm{K}_o$; there are two variations in a spatial distance of one meter and the wavelength is 0.5 meters. In Fig. 1.2.4c, $k = 3\,\mathrm{K}_o$ and there are three variations in one meter.

From the dispersion relation for electromagnetic waves (1.2.9), we see that the spatial frequency and the temporal frequency are related by the velocity of light. Thus for a spatial frequency of $1\,\mathrm{K}_o$, the corresponding temporal frequency is $f = 300\,\mathrm{MHz}$. With k expressed in unit K_o, we find

$$\boxed{f = 3 \times 10^8\ k \quad \mathrm{Hz}\ ; \quad \lambda = 1/k \quad \mathrm{m}} \qquad (1.2.14)$$

Within the spatial frequency range of $0.01\,\mathrm{K}_o$ to $100\,\mathrm{K}_o$ electromagnetic waves are used for microwave heating, radar, navigation, and carrying signals from radio, television, and satellite communications. The visible light has a spatial frequency band between $1.4 \times 10^6 \sim 2.6 \times 10^6\,\mathrm{K}_o$. In Fig. 1.2.5 we illustrate the electromagnetic wave spectrum according to the spatial frequency in K_o and corresponding wavelength in meters, frequency in Hz, and energy in electron-volts (eV).

$$K_o = 2\pi \, \text{m}^{-1}$$
$$k = A \, K_o$$
$$\lambda = 1/A \, \text{m}$$
$$f = 300A \, \text{MHz}$$
$$\hbar\omega = 1.24 \times 10^{-6} A \, \text{eV}$$

Ultraviolet

Visible $(1.4 \sim 2.6 \, \text{MK}_o; 417 \sim 789 \, \text{THz})$
Near Infrared $(0.77 \sim 1.4 \, \text{MK}_o; 231 \sim 417 \, \text{THz})$
Thermal Infrared $(0.067 \sim 0.14 \, \text{MK}_o; 20 \sim 43 \, \text{THz})$

Millimeter Wave

EHF

SHF Radar C, X, K_u, K bands $(13.3 \sim 90 \, \text{K}_o; 4 \sim 27 \, \text{GHz})$

UHF Microwave Oven $(8.17 \, \text{K}_o; 2.45 \, \text{GHz})$
      Television $(1.57 \sim 2.97 \, \text{K}_o; 470 \sim 890 \, \text{MHz})$

VHF Television $(.18 \sim .72 \, \text{K}_o; 54 \sim 216 \, \text{MHz})$
      FM Radio $(.29 \sim .36 \, \text{K}_o; 88 \sim 108 \, \text{MHz})$

HF   Short Wave Radio $(.01 \sim .001 \, \text{K}_o; 3 \sim 30 \, \text{MHz})$

MF   AM Radio $(.00178 \sim .00535 \, \text{K}_o \quad 535 \sim 1605 \, \text{kHz})$

LF $(10^{-4} \sim 10^{-3} \, \text{K}_o; 30 \sim 300 \, \text{kHz})$

VLF $(10^{-5} \sim 10^{-4} \, \text{K}_o; 3 \sim 30 \, \text{kHz})$

ULF $(10^{-6} \sim 10^{-5} \, \text{K}_o; 0.3 \sim 3 \, \text{kHz})$

SLF $(10^{-7} \sim 10^{-6} \, \text{K}_o; 30 \sim 300 \, \text{Hz})$

ELF $(10^{-8} \sim 10^{-7} \, \text{K}_o; 3 \sim 30 \, \text{Hz})$

$\text{K}_o \left(\begin{smallmatrix} \text{Spatial} \\ \text{Frequency} \end{smallmatrix}\right)$

$\left(\begin{smallmatrix} \text{Temporal} \\ \text{Frequency} \end{smallmatrix}\right) \text{Hz}$

Figure 1.2.5 Electromagnetic wave spectrum.

In this book I shall place great emphasis on the use of k, which is of more fundamental importance in electromagnetic wave theory than both of the more popular concepts of wavelength λ and frequency f. The corresponding values of wavelength λ and frequency f are, for $k = A\,\mathrm{K}_o$,

$$\lambda = 2\pi/k = 2\pi/(A\mathrm{K}_o) = \frac{1}{A}\,\mathrm{m}; \quad f = ck/2\pi = cA\mathrm{K}_o/2\pi = 3\times10^8 A\,\mathrm{Hz}$$

The photon energy in electron-volts (eV) is calculated from

$$\hbar\omega = (\hbar cA\mathrm{K}_o/q)\,\mathrm{eV} \approx 1.24 \times 10^{-6}A\,\mathrm{eV} = \hbar ck/q \ \mathrm{eV}$$

where $q = 1.6 \times 10^{-19}$ coulombs is the electron charge, and $\hbar = 1.05 \times 10^{-34}$ Joule-second is Planck's constant $h = 6.626 \times 10^{-34}$ J-sec divided by 2π.

Max Karl Ernst Ludwig Planck (23 April 1858 – 4 October 1947)
     Max Planck entered the University of Munich in 1874. He taught at the University of Munich in 1880–1885, Kiel 1885–1889. After the death of Kirchhoff in 1887, Planck succeeded his chair of theoretical physics at the University of Berlin in 1889 until his retirement in 1927. In 1900 he announced a formula now known as Planck's radiation formula and introduced the quanta of energy.

EXAMPLE 1.2.1   Operating frequencies of common devices:

Device	Temporal frequency (Hz)	Spatial frequency (K_o)
AM Radio	$535 - 1605$ kHz	$0.00178 - 0.00535$ K_o
Shortwave Radio	$3 - 30$ MHz	$0.01 - 0.1$ K_o
FM Radio	$88 - 108$ MHz	$0.293 - 0.36$ K_o
Airport ILS	$108 - 112$ MHz	$0.35 - 0.373$ K_o
Commercial Television		
Channels 2-4	$54 - 72$ MHz	$0.18 - 0.24$ K_o
Channels 5-6	$76 - 88$ MHz	$0.253 - 0.293$ K_o
Channels 7-13	$174 - 216$ MHz	$0.58 - 0.72$ K_o
Channels 14-83	$470 - 890$ MHz	$1.57 - 2.97$ K_o
Microwave Oven	2.45 GHz	8.17 K_o
Communication Satellite		
Downlink	$3.70 - 4.20$ GHz	$12.3 - 14$ K_o
Uplink	$5.925 - 6.425$ GHz	$19.75 - 21.4$ K_o
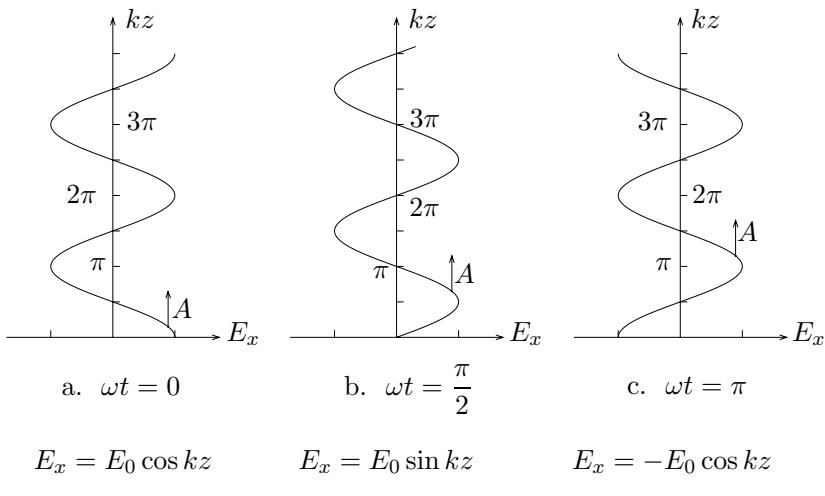
— END OF EXAMPLE 1.2.1 —

Phase Velocity and Phase Delay

In Figs. 1.2.6b and 1.2.6c we plot $E_x(z, t)$ at two progressive times $\omega t = \pi/2$ and $\omega t = \pi$. We observe that the electric field vector at A appears to be propagating along the $\hat{z}$ direction as time progresses. The velocity of propagation V_p is determined from $kz - \omega t = \text{constant}$ which gives

$$V_p = \frac{dz}{dt} = \frac{\omega}{k} \tag{1.2.15}$$

We call V_p the phase velocity. By virtue of the dispersion relation (1.2.9), we see that $V_p = (\mu_o \epsilon_o)^{-1/2}$, which is equal to the velocity of light in free space c.

$$E_x = E_0 \cos kz \qquad E_x = E_0 \sin kz \qquad E_x = -E_0 \cos kz$$

Figure 1.2.6 Electric field strength vs. kz at different times.

The spatial frequency k is, according to the dispersion relation, directly related to the temporal frequency ω by the phase delay

$$\Lambda_p = \frac{k}{\omega} = \sqrt{\mu_o \epsilon_o} \tag{1.2.16}$$

which determines how much time it takes for the wave to propagate a unit distance. In free space $\Lambda_p = 10^{-8}/3$ s/m or it takes 3.33 nanoseconds for an electromagnetic wave to travel the distance of one meter.

EXAMPLE 1.2.2 Electric field vector $\overline{E}$ and magnetic field vector $\overline{H}$.

A wave equation similar to (1.2.6) can be derived for the magnetic field vector $\overline{H}$. Wave solutions for $\overline{E}$ and $\overline{H}$ can be written as

$$\overline{E} = \hat{x}E_x(z,t) = \hat{x}E_0\cos(kz - \omega t) \qquad (E1.2.2.1)$$

$$\overline{H} = \hat{y}H_y(z,t) = \hat{y}H_0\cos(kz - \omega t) \qquad (E1.2.2.2)$$

It is seen that $\overline{E}$ and $\overline{H}$ satisfy (1.2.3) and (1.2.4). From (1.2.1), we find

$$\nabla \times \overline{H} = \begin{vmatrix} \hat{x} & \hat{y} & \hat{z} \\ \dfrac{\partial}{\partial x} & \dfrac{\partial}{\partial y} & \dfrac{\partial}{\partial z} \\ 0 & H_y & 0 \end{vmatrix} = \hat{x}\; kH_0\sin(kz - \omega t)$$

$$= \epsilon_o\frac{\partial}{\partial t}\overline{E} = \hat{x}\;\omega\epsilon_o E_0\sin(kz - \omega t)$$
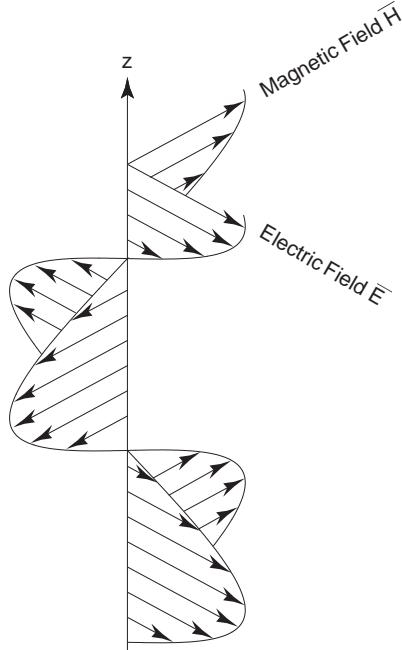
Figure E1.2.2.1 Electric and magnetic fields of an electromagnetic wave.

The magnitudes E_0 and H_0 are related by $E_0/H_0 = k/\omega\epsilon_o = \sqrt{\mu_o/\epsilon_o} = \eta$, where $\eta = \sqrt{\mu_o/\epsilon_o}$ is called the free-space impedance. The same result is obtained by substituting (E1.2.2.1) and (E1.2.2.2) into (1.2.2). The electromagnetic wave is propagating in the positive $\hat{z}$ direction. The field vectors of the electromagnetic wave are transversal to the direction of propagation and lie in the xy-plane, on which the phase $kz - \omega t$ of the wave is a constant. Since the phase front of the wave is the xy-plane, we call the electromagnetic wave as represented by (E1.2.2.1) and (E1.2.2.2) a plane wave.

— END OF EXAMPLE 1.2.2 —

C. Polarization

The polarization of a wave is conventionally defined by the time variation of the tip of the electric field vector $\overline{E}$ at a fixed point in space. If the tip moves along a straight line, the wave is linearly polarized. When the locus of the tip is a circle, the wave is circularly polarized. For an elliptically polarized wave, the tip of $\overline{E}$ describes an ellipse. If the right-hand thumb points in the direction of propagation while the fingers point in the direction of the tip motion, the wave is defined as right-hand polarized. The wave is left-hand polarized when it is described by the left-hand thumb and fingers.

Consider the following wave solution:

$$\begin{aligned}
\overline{E}(z,t) &= \hat{x}E_x + \hat{y}E_y \\
&= \hat{x}\cos(kz - \omega t) + \hat{y}A\cos(kz - \omega t + \psi) \quad (1.2.17)
\end{aligned}$$

with $A > 0$. The wave propagates in the $+\hat{z}$ direction. From the temporal view point,

$$\overline{E}(t) = \hat{x}\cos(\omega t) + \hat{y}A\cos(\omega t - \psi)$$

We now study polarization for the following special cases:

Case 1) $\psi = 2m\pi$, where $m = 0, 1, 2, \ldots$ is an integer. We have

$$\overline{E}(t) = \hat{x}\cos(\omega t) + \hat{y}A\cos(\omega t)$$

The tip of the electric field vector moves along a line as shown in Fig. 1.2.7a. The wave is linearly polarized.

Case 2) $\psi = (2m + 1)\pi$, we have

$$\overline{E}(t) = \hat{x}\cos(\omega t) - \hat{y}A\cos(\omega t)$$

The tip of the electric field vector moves along a line as shown in Fig. 1.2.7b. The wave is linearly polarized.

Case 3) $\psi = \pi/2$ and $A = 1$, we have

$$\overline{E}(t) = \hat{x}\cos(\omega t) + \hat{y}\sin(\omega t) \quad (1.2.18)$$

It can be seen that while the x component is at its maximum the y component is zero. As time progresses, the y component increases and the x component decreases. The tip of $\overline{E}$ rotates from the positive E_x

a. Linear polarization

b. Linear polarization

c. Right-hand
   circular polarization

d. Left-hand
   circular polarization

e. Right-hand
   elliptical polarization

f. Left-hand
   elliptical polarization
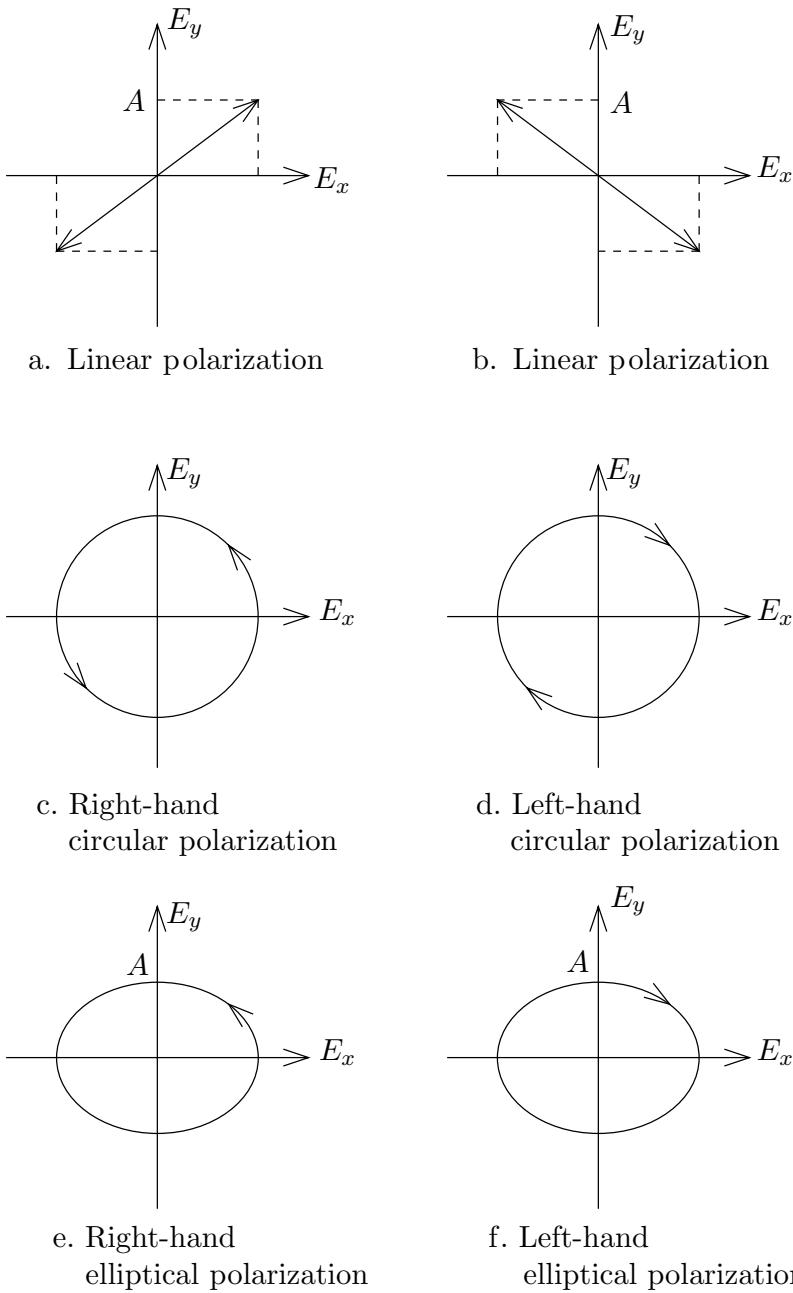
Figure 1.2.7 Polarizations.

axis to the positive E_y axis [Fig. 1.2.7c]. Elimination of t from the x and y components in (1.2.18) yields a circle of radius 1, $E_x^2 + E_y^2 = 1$. Thus the wave is right-hand circularly polarized.

Case 4) $\psi = -\pi/2$ and $A = 1$, we have

$$\overline{E}(t) = \hat{x}\cos(\omega t) - \hat{y}\sin(\omega t) \qquad (1.2.19)$$

As time progresses, the y component increases and the x component decreases. The tip of $\overline{E}$ rotates from the positive E_x axis to the negative E_y axis. Thus the wave is left-hand circularly polarized [Fig. 1.2.7d].

Case 5) $\psi = \pm\pi/2$, we have

$$\overline{E}(t) = \hat{x}\cos(\omega t) \pm \hat{y}A\sin(\omega t) \qquad (1.2.20)$$

The wave is right-hand elliptically polarized for $\psi = \pi/2$ [Fig. 1.2.7e] and left-hand elliptically polarized for $\psi = -\pi/2$ [Fig. 1.2.7f].
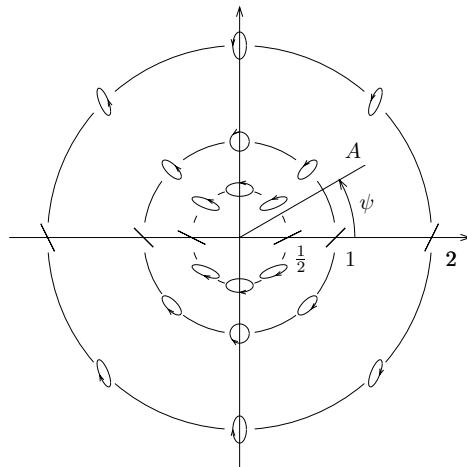
Figure 1.2.8 Polarizations for various values of ψ and A.

The above discussion can be summarized in Fig. 1.2.8 where we illustrate the polarization for different values of A and ψ. On the horizontal axis, $\psi = 0$, or π, the wave is linearly polarized. If $A = 1$ and $\psi = \pi/2$, the wave is right-hand circularly polarized. For $A = 1$ and $\psi = -\pi/2$, the wave is left-hand circularly polarized. Otherwise the wave is elliptically polarized. The polarization is right-handed if the phase difference is between zero and π, and left-handed if ψ is between π and 2π.
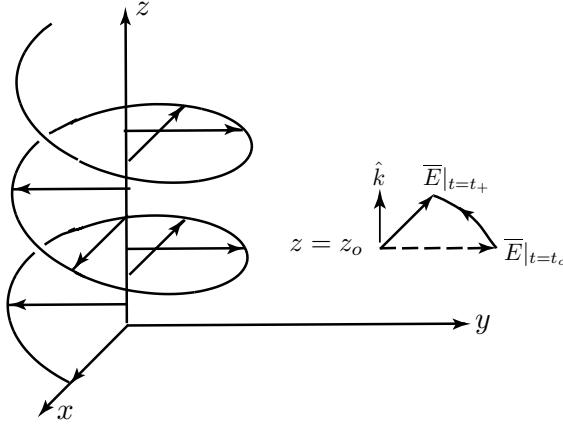
SMALL CAPS EXAMPLE 1.2.3   Polarization from the spatial view point.
      Wave polarization can be viewed by either taking a series of still pictures
at several fixed times, called the spatial view point or by making observations
at a fixed point in space, called the temporal view point. The definition of
polarization so far has been discussed from the temporal view point. Let us
now look at polarization from the spatial view point.

Figure E1.2.3.1 Spatial view of polarization.

      Consider the right-hand circularly polarized wave with $\psi = \pi/2$ and
$A = 1$ in case 3), setting $t = 0$ in wave solution (1.2.17), we have

$$\overline{E}(z, t = 0) = \hat{x} \cos(kz) - \hat{y} \sin(kz) = \hat{x} E_x(z) - \hat{y} E_y(z)$$

This is a left-handed helix as shown below.

$$E_x = E_0 \cos\left(\frac{2\pi}{\lambda} z\right) \qquad E_y = E_0 \sin\left(\frac{2\pi}{\lambda} z\right)$$

The parametric equation of a helix is

$$x = R \cos\left(\frac{2\pi}{p} z\right) \qquad y = R \sin\left(\frac{2\pi}{p} z\right) r$$

where p is the pitch of the helix. Thus, the locus of the tip point of the electric
field vector measured along the z axis is a left-handed helix with the pitch
$p = \lambda$. The helix advances along $+\hat{z}$ without rotating. At $z = z_0 = 3\lambda/4$,
electric field vector is at $\overline{E}|_{t=t_o}$ when $t_o = 0$, it is shown as $\overline{E}|_{t=t_+}$ when
$t_+ = \pi/4\omega$.

                                        — END OF EXAMPLE 1.2.3 —

Poincaré Sphere and Stokes Parameters

We now use the ellipse as shown in Fig. 1.2.9 to illustrate all polarization states by introducing two parameters: polarization angle α and orientation angle β. We let the major axis of the ellipse be e_1 and the minor axis $e_2 \leq e_1$. The shape of the ellipse can be specified by the ellipticity angle α defined as

$$\tan \alpha = \pm \frac{e_2}{e_1} \tag{1.2.21}$$

where the plus sign corresponds to right-hand polarization for which $0 \leq \alpha \leq \pi/4$ and the negative sign to left-hand polarization for which $-\pi/4 \leq \alpha \leq 0$. We see that for linearly polarized wave $\alpha = 0$. For as is evident from the defining equation for Fig. 1.2.9.
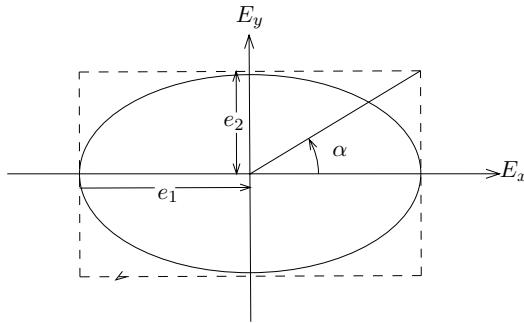
Figure 1.2.9 Elliptical polarization.

$$\overline{E}(t) = \hat{x} \cos \omega t + \hat{y} A \sin \omega t \tag{1.2.22}$$

For right-hand circularly polarized waves, $\alpha = -\pi/4$ and $e_2 = e_1$, for left-hand circularly polarized waves, $\alpha = -\pi/4$ and $e_2 = e_1$. For right-hand polarization, $\alpha \geq 0$, for left-hand polarization, $\alpha \leq 0$.

The orientation angle β is introduced with Fig. 1.2.10 by rotating the ellipse in Fig. 1.2.9. The major axis of the ellipse is rotated and makes the angle β with the E_x axis with $0 \leq \beta \leq \pi$. Thus for a linearly polarized wave along the E_y- axis, $\beta = \pi/2$.

Instead of the planar representation of polarization states as shown in Fig. 1.2.8, we shall now discuss representation of polarization states with a sphere called Poincaré sphere as shown in Fig. 1.2.11. The radius
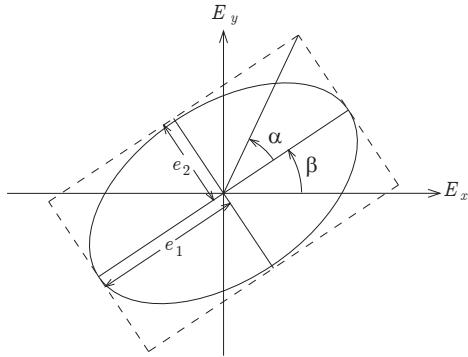
Figure 1.2.10 Elliptical polarization.

of the sphere is I, and the three axes are Q, U, V as shown below:

$$Q = I \cos 2\alpha \cos 2\beta$$
$$U = I \cos 2\alpha \sin 2\beta$$
$$V = I \sin 2\alpha$$
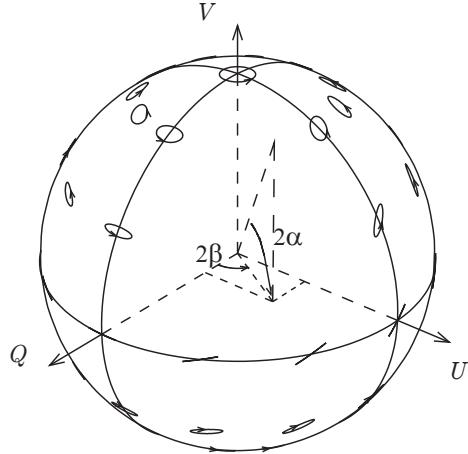
Figure 1.2.11 Poincare sphere.

We see that $I^2 = Q^2 + U^2 + V^2$. When the wave is right-hand circularly polarized $Q = U = 0$, $V = I$, as $\alpha = \pi/4$. When the wave is left-hand circularly polarized, $Q = U = 0$, $V = -I$, as $\alpha = -\pi/4$. When the wave is linearly polarized, $V = 0$, as $\alpha = 0$. With a

rigorous mathematical derivation, I, Q, U, V can be derived from e_x and e_y, and they are called Stokes parameters, which are useful in characterizing polarized as well as unpolarized electromagnetic waves.

Jules Henri Poincaré (29 April 1854 – 17 July 1912)

Henri Poincaré entered the Ecole Polytechnique in 1873, graduating in 1875, and received his doctorate in mathematics from the University of Paris in 1879. In 1886 he was appointed to a chair of mathematical physics and probability at the Sorbonne and also at the Ecole Polytechnique. In 1894, he published the first of his six papers on algebraic topology.

EXAMPLE 1.2.4

To facilitate a mathematical discussion of polarization, we decompose the $\overline{E}$ vector of a wave into two components perpendicular to the direction of propagation. For a specific point in space, we write

$$\overline{E}(t) = \hat{x}E_x + \hat{y}E_y = \hat{x}e_x\cos(\omega t - \psi_x) + \hat{y}e_y\cos(\omega t - \psi_y) \qquad \text{(E1.2.4.1)}$$

where $\hat{x}$, $\hat{y}$, and the direction of propagation are mutually perpendicular and thus form an orthogonal system. We assume the amplitudes e_y and e_x are both positive. The locus of the tip $\overline{E}(t)$ is determined by eliminating the time t dependence between the two components E_x and E_y.

In general, a polarized wave has elliptical polarization; that is, when time is eliminated from the two components of $\overline{E}$, the resultant equation describes an ellipse. Consider the case $\psi_x = \psi_0$, $\psi_y - \psi_x = \pm\pi/2$ in (E1.2.4.1) and let $e_x = e_1 > e_2 = e_y$. We have

$$\overline{E}'(t) = \hat{x}'E'_x + \hat{y}'E'_y = \hat{x}'e_1\cos(\omega t - \psi_0) + \hat{y}'e_2\sin(\omega t - \psi_0) \quad \text{(E1.2.4.2)}$$

with e_1 denoting the major axis and e_2 the minor axis, we write

$$\tan\alpha = \frac{e_2}{e_1} \qquad \text{(E1.2.4.3)}$$

where $-\pi/4 \le \alpha \le \pi/4$.

The general polarization states are more popularly described with the Poincaré sphere as discussed below. Consider the elliptical polarization as given by (E1.2.4.1), which describes a tilted ellipse as plotted in Fig. 1.2.10. The major axis of the ellipse described in (E1.2.4.2) is rotated and makes the angle β with the E_h axis with $0 \le \beta \le \pi$. We call β the orientation angle.

In view of (E1.2.4.2) and Fig. 1.2.9, we have from coordinate transformation

$$E'_x = E_x\cos\beta + E_y\sin\beta$$
$$E'_y = -E_x\sin\beta + E_y\cos\beta$$

leading to

$$e_1 \cos(\omega t - \psi_0) = E_x \cos\beta + E_y \sin\beta \qquad \text{(E1.2.4.4}a\text{)}$$
$$e_2 \sin(\omega t - \psi_0) = -E_x \sin\beta + E_y \cos\beta \qquad \text{(E1.2.4.4}b\text{)}$$

Substituting the components E_h and E_v of (E1.2.4.1) in (E1.2.4.4) and comparing the coefficients of $\cos\omega t$ and $\sin\omega t$, we obtain

$$e_1 \cos\psi_0 = e_x \cos\psi_x \cos\beta + e_y \cos\psi_y \sin\beta \qquad \text{(E1.2.4.5}a\text{)}$$
$$e_1 \sin\psi_0 = e_x \sin\psi_x \cos\beta + e_y \sin\psi_y \sin\beta \qquad \text{(E1.2.4.5}b\text{)}$$
$$e_2 \cos\psi_0 = -e_x \sin\psi_x \sin\beta + e_y \sin\psi_y \cos\beta \qquad \text{(E1.2.4.5}c\text{)}$$
$$e_2 \sin\psi_0 = e_x \cos\psi_x \sin\beta - e_y \cos\psi_y \cos\beta \qquad \text{(E1.2.4.5}d\text{)}$$

Eliminating ψ_0 from (E1.2.4.5a) and (E1.2.4.5b), we find

$$e_1^2 = e_x^2 \cos^2\beta + e_y^2 \sin^2\beta + e_x e_y \sin 2\beta \cos\psi \qquad \text{(E1.2.4.6}a\text{)}$$

Similarly from (E1.2.4.5c) and (E1.2.4.5d), we have

$$e_2^2 = e_x^2 \sin^2\beta + e_y^2 \cos^2\beta - e_h e_v \sin 2\beta \cos\psi \qquad \text{(E1.2.4.6}b\text{)}$$

Multiplying (E1.2.4.5a) by (E1.2.4.5c), (E1.2.4.5b) by (E1.2.4.5d) and then adding, we again eliminate ψ_0 and obtain

$$e_1 e_2 = e_x e_y \sin\psi \qquad \text{(E1.2.4.6}c\text{)}$$

Finally we multiply (E1.2.4.5a) by (E1.2.4.5d) and subtract from the product of (E1.2.4.5b) and (E1.2.4.5c), which yields

$$2 e_x e_y \cos\psi = (e_x^2 - e_y^2) \tan 2\beta \qquad \text{(E1.2.4.6}d\text{)}$$

Equation (E1.2.4.6) will be used in the following discussion on Stokes parameters and the Poincaré sphere.

    To facilitate the discussion of various polarization states of electromagnetic waves, the four Stokes parameters pertaining to $\overline{E}(t)$ given in (E1.2.4.1) are defined as follows :

$$I = \frac{1}{\eta}\left(e_x^2 + e_y^2\right) \qquad \text{(E1.2.4.7}a\text{)}$$

$$Q = \frac{1}{\eta}\left(e_x^2 - e_y^2\right) \qquad \text{(E1.2.4.7}b\text{)}$$

$$U = \frac{2}{\eta}e_x e_y \cos\psi \qquad \text{(E1.2.4.7}c\text{)}$$

$$V = \frac{2}{\eta}e_x e_y \sin\psi \qquad \text{(E1.2.4.7}d\text{)}$$

Notice that $I^2 = Q^2 + U^2 + V^2$.

Adding (E1.2.4.6a) and (E1.2.4.6b) yields $e_1^2 + e_2^2 = e_x^2 + e_y^2 = \eta I$. Making use of (E1.2.4.3), we have

$$e_1^2 = \eta I \cos^2 \alpha \qquad \text{(E1.2.4.8)}$$

Subtracting (E1.2.4.6b) from (E1.2.4.6a) and making use of (E1.2.4.6d), we find $e_1^2 - e_2^2 = (e_x^2 - e_y^2)/\cos 2\beta$. Making use of (E1.2.4.3) and (E1.2.4.8), we find

$$Q = \frac{1}{\eta}(e_x^2 - e_y^2) = I \cos 2\alpha \cos 2\beta \qquad \text{(E1.2.4.9a)}$$

In terms of I, we find from (E1.2.4.7c), (E1.2.4.6d) and (E1.2.4.9a)

$$U = I \cos 2\alpha \sin 2\beta \qquad \text{(E1.2.4.9b)}$$

and from (E1.2.4.7d), (E1.2.4.6c) and (E1.2.4.8)

$$V = I \sin 2\alpha \qquad \text{(E1.2.4.9c)}$$

Equation (E1.2.4.9) suggests a simple geometrical representation of all states of polarization by recognizing that Q, U, and V can be regarded as the rectangular components of a point on a sphere with radius I, known as the Poincaré sphere. We define, in the spherical coordinate system, $\theta = \pi/2 - 2\alpha$ and $\phi = 2\beta$. As seen from (E1.2.4.3), positive α is for right-hand polarization which is represented by points on the upper hemisphere. On the lower hemisphere, the points correspond to left-hand polarization. The north pole represents right-hand circular polarization and the south pole represents left-hand circular polarization. The sphere is called the *Poincaré sphere*. Fig. 1.2.8 is seen to be a planar projection of the Poincaré sphere with the plane and the sphere touching each other at $Q = I$. The equator is mapped into the horizontal axis.

— End of Example 1.2.4 —

Example 1.2.5   Partial polarization.

Radiation from many natural and man-made sources consists of field components that fluctuate with time. We write

$$E_h = e_h(t) \cos\left(\omega t - \psi_h(t)\right)$$

$$E_v = e_v(t) \cos\left(\omega t - \psi_v(t)\right)$$

The wave is quasi-monochromatic when $e_h(t)$, $e_v(t)$, $\psi_h(t)$, and $\psi_v(t)$ are slowly varying compared with $\cos \omega t$. The Stokes parameters are defined by

a time-average procedure over a large time interval T, denoted with the brackets $<>$:

$$< E_h^2(t) >= \frac{1}{T} \int_0^T dt \, [E_h(t)]^2$$

The Stokes parameters are

$$I = I_h + I_v = \frac{1}{\eta} \left(<E_h^2> + <E_v^2> \right)$$

$$Q = I_h - I_v = \frac{1}{\eta} \left(<E_h^2> - <E_v^2> \right) = I < \cos 2\alpha \cos 2\beta >$$

$$U = \frac{2}{\eta} < E_h E_v \cos \psi >= I < \cos 2\alpha \sin 2\beta >$$

$$V = \frac{2}{\eta} < E_h E_v \sin \psi >= I < \sin 2\alpha >$$

For completely unpolarized waves, E_h and E_v are uncorrelated and we have $I =$ total Poynting power and $Q = U = V = 0$. For completely polarized waves we have $I^2 = Q^2 + U^2 + V^2$. For partially polarized waves it can be shown that $I^2 \geq Q^2 + U^2 + V^2$ [Example 1.2A.2]. With the Poincaré sphere of radius I, the partially polarized waves correspond to points inside the sphere.

In concluding this section on wave polarization, we remark that the polarization is defined according to the time variations of the $\overline{E}$ vector. As we shall see in Chapter 3, it is imperative that we define polarization in terms of $\overline{D}$ when anisotropic and bianisotropic media are involved. This is because in isotropic media $\overline{E}$ is perpendicular to $\overline{k}$, $\overline{k} \cdot \overline{E} = 0$, while in non-isotropic media $\overline{k} \cdot \overline{D} = 0$. This also suggests that wave polarization can be defined in terms of the field vector $\overline{B}$.

— END OF EXAMPLE 1.2.5 —

Problems

P1.2.1

Electromagnetic waves satisfy all of the Maxwell equations. Consider, in free space, the following electric field vectors:

$$\overline{E}_1 = \hat{x} \cos(\omega t - kz)$$

$$\overline{E}_2 = \hat{z} \cos(\omega t - kz)$$

$$\overline{E}_3 = (\hat{x} + \hat{z}) \cos(\omega t + ky)$$

$$\overline{E}_4 = (\hat{x} + \hat{z}) \cos \left(\omega t + k|x + z|/\sqrt{2} \right)$$

Do these electric field vectors satisfy the wave equation and all Maxwell equations? Which of the four fields qualify as electromagnetic waves? For those not qualified as electromagnetic waves, state which of the Maxwell equations are violated.

P1.2.2

The electric field vector

$$\overline{E} = \hat{x} E_0 \cos(kz - \omega t)$$

represents an electromagnetic wave propagating in the $+\hat{z}$ direction. What is the expression if the wave is propagating in the $-\hat{z}$ direction?

P1.2.3

An electromagnetic wave has spatial frequency $k_o = 100 \, \text{K}_o$. Determine the wavelength in meters and the temporal frequency in GHz.

Determine the spatial frequency in unit of K_o for a laser light at wavelength $\lambda = 0.6328 \, \mu\text{m}$.

Determine the spatial frequency in unit of K_o for a microwave oven at frequency 2.4 GHz.

P1.2.4

The known spectrum of electromagnetic waves covers a wide range of frequencies. Electromagnetic phenomena are all described by Maxwell's equations and, by convention, are generally classified according to wavelengths or frequencies. Radio waves, television signals, radar beams, visible light, X rays, and gamma rays are examples of electromagnetic waves.

(a) Give in meters the wavelengths corresponding to the following frequencies:
   (i) 60 Hz
   (ii) AM radio (535–1605 kHz)
   (iii) FM radio (88–108 MHz)
   (iv) Visible light ($\sim 10^{14}$ Hz)
   (v) X-rays ($\sim 10^{18}$ Hz)
(b) Give in Hertz the temporal frequencies corresponding to the wavelengths:
   (i) 1 km, (ii) 1 m, (iii) 1 mm, (iv) $1 \, \mu\text{m}$, (v) 1 Å.
(c) Give in K_o the spatial frequencies corresponding to the wavelengths in (b).
(d) Give in eV the spatial frequencies corresponding to the wavelengths in (b).

P1.2.5

Consider the electric field amplitude

$$E_x(z, t) = E_0 \cos(kz - \omega t)$$

Find the phase velocity $v_p = \omega/k$ and the group velocity $v_g = d\omega/dk$.

P1.2.6

Consider an electromagnetic wave propagating in the $\hat{z}$-direction with

$$\overline{E} = \hat{x}e_x \cos(kz - \omega t + \psi_x) + \hat{y}e_y \cos(kz - \omega t + \psi_y)$$

where e_x, e_y, ψ_x, and ψ_y are all real numbers.

(a) Let $e_x = 2$, $e_y = 1$, $\psi_x = \pi/2$, $\psi_y = \pi/4$. What is the polarization?
(b) Let $e_x = 1$, $e_y = \psi_x = 0$. This is a linearly polarized wave. Prove that it can be expressed as the superposition of a right-hand circularly polarized wave and a left-hand circularly polarized wave.
(c) Let $e_x = 1$, $\psi_x = \pi/4$, $\psi_y = -\pi/4$, $e_y = 1$. This is a circularly polarized wave. Prove that it can be decomposed into two linearly polarized waves.

P1.2.7

Wave polarization can be viewed by either taking a series of still pictures at several fixed times, called the spatial view point or by making observations at a fixed point in space, called the temporal view point. We define polarization from the temporal view point. Let us now look at polarization from the spatial view point.

Consider an electromagnetic wave with $k = 100 \, \mathrm{K}_o$ propagating in the $\hat{z}$ direction.

$$\overline{E}(\overline{r}, t) = E_0[\hat{x} \cos(kz - \omega t) - \hat{y} \sin(kz - \omega t)]$$

What are the wavelength and the polarization of this wave?

From the spatial point of view, by taking a picture at $t = 0$, the tips of the electric field vectors form a helix. Is the helix right-handed or left-handed? What is the pitch of this helix?

Observing at a fixed point in space, show that the tip of the electric field describes the same polarization as in the temporal view point when the helix advances without turning.

P1.2.8

For polarized waves

$$I = I_h + I_v$$
$$Q = I_h - I_v = I \cos 2\alpha \cos 2\beta$$
$$U = I \cos 2\alpha \sin 2\beta$$
$$V = I \sin 2\alpha$$

Show that when the wave is right-handed circularly polarized $Q = U = 0$ and $V = I$, when it is left-hand circularly polarized, $Q = U = 0$ and $V = -I$, and when the wave is linearly polarized, $V = 0$.

1.3 Force, Power, and Energy

A. Lorentz Force Law

The interaction of the electric and magnetic fields with the current and charge densities are governed by the Lorentz force law

$$\overline{f} = \rho\overline{E} + \overline{J} \times \overline{B} \qquad (1.3.1)$$

where $\overline{f}$ is the force density (with unit $\mathrm{N/m^3}$). The Lorentz force law relates electromagnetism to mechanics. The manifestation of the electric field vector $\overline{E}$ and the magnetic field vector $\overline{B}$ can be demonstrated with the forces exerted on the charge density ρ and the current density $\overline{J}$. It can thus be used to define the fields $\overline{E}$ and $\overline{B}$.

Hendrik Antoon Lorentz (18 July 1853 – 4 February 1928)
Hendrik Lorentz entered the University of Leyden in 1870, obtained his B.Sc. degree in 1871, and in 1875, his doctor's degree for his thesis on the reflection and refraction of light. Three years later he was appointed to the Professor of Physics at Leyden. In 1904 he developed the Lorentz transformation formula that form the basis for the special theory of relativity .

EXAMPLE 1.3.1   Coulomb's law.
For static electric fields in the absence of magnetic fields, the Lorentz force law becomes $\overline{f} = \rho\overline{E}$. Acting on a charged particle q, the total force is $\overline{F} = q\overline{E}$. Assuming that the electric field $\overline{E}$ is generated by another charged particle Q situated at the origin, we have

$$\overline{E} = \hat{r}\frac{Q}{4\pi\epsilon_o r^2}$$

Thus the total force acting on the charged particle q is

$$\overline{F} = \hat{r}\frac{qQ}{4\pi\epsilon_o r^2}$$

which is proportional to the squared inverse distance. This is the well-known Coulomb's law.

— END OF EXAMPLE 1.3.1 —

Issac Newton (25 December 1642 – 20 March 1727)
Newton attended Cambridge University at the age of 19 and entered Trinity College in 1661. After receiving his B.A. degree in 1664, he returned to his birth place Woolsthorpe, England. In the next two years, he extended the binomial theorem, invented calculus, discovered the law of universal gravitation, and experimentally proved that white light is composed of all colors, all these great accomplishments in scientific history before his 25th birthday.

EXAMPLE 1.3.2   Cyclotron frequency.

Consider a particle with charge q and mass m moving with velocity $\overline{v}$ in a uniform static magnetic field in the $-\hat{z}$ direction, $\overline{B} = -\hat{z}B_0$. In the absence of electric fields, if the velocity v has no component in the $\hat{z}$ direction, the Lorentz force is perpendicular to the direction of the velocity and the charge particle moves in the x-y plane. Let $\overline{v} = \hat{x}v_x + \hat{y}v_y$, we have

$$\overline{F} = q\overline{v} \times \overline{B} = -\hat{x}qv_yB_0 + \hat{y}qv_xB_0$$

Equating to Newton's law

$$\overline{F} = m\frac{d\overline{v}}{dt} = \hat{x}m\frac{dv_x}{dt} + \hat{y}m\frac{dv_y}{dt}$$

we find

$$m\frac{dv_x}{dt} = -qv_yB_0 \qquad\qquad (E1.3.2.1a)$$

$$m\frac{dv_y}{dt} = qv_xB_0 \qquad\qquad (E1.3.2.1b)$$

Eliminating v_y from the above two equations, we find

$$\frac{d^2v_x}{dt^2} = -\omega_c^2 v_x$$

where

$$\omega_c = \frac{qB_0}{m} \qquad\qquad (E1.3.2.2)$$
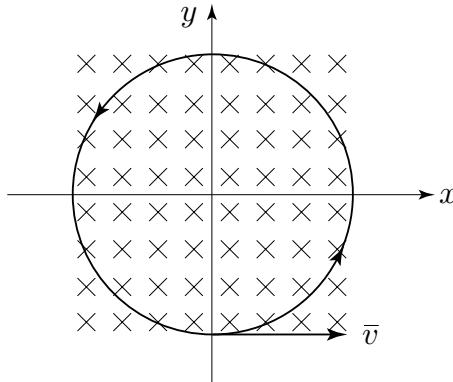
Figure E1.3.2.1   Cyclotron frequency.

is called the cyclotron frequency, which is proportional to the magnitude of the magnetic field and is independent of the velocity of the particle.

The solution to (E1.3.2.1) can be written as

$$v_x = \frac{dx}{dt} = v \cos \omega_c t \qquad (E1.3.2.3a)$$

$$v_y = \frac{dy}{dt} = v \sin \omega_c t \qquad (E1.3.2.3b)$$

To find the trajectory of the particle, we write the solution of (E1.3.2.3) as

$$x = \frac{v}{\omega_c} \sin \omega_c t = R \sin \omega_c t \qquad (E1.3.2.4a)$$

$$y = -\frac{v}{\omega_c} \cos \omega_c t = -R \cos \omega_c t \qquad (E1.3.2.4b)$$

The trajectory of the particle is thus a circle with radius

$$R = (x^2 + y^2)^{1/2} = \frac{v}{\omega_c} \qquad (E1.3.2.5)$$

In terms of the applied magnetic field, we find from (E1.3.2.2)

$$R = \frac{mv}{qB_0} \qquad (E1.3.2.6)$$

It is seen that the larger the magnetic field, the smaller the radius. If the charged particle has a velocity component in the $\hat{z}$ direction, the trajectory of the particle will follow a helical path.

— END OF EXAMPLE 1.3.2 —

EXERCISE 1.3.1   Centrifugal force.

In cylindrical coordinate system, $\overline{\rho}$ is the radial vector and $\hat{\rho}$ is in the radial direction. The force acting on the charge in the above example is

$$\begin{aligned} \overline{F} &= \hat{x}m\frac{d^2x}{dt^2} + \hat{y}m\frac{d^2y}{dt^2} = m\frac{d^2}{dt^2}\overline{\rho} \\ &= mR\omega_c^2(-\hat{x}\sin \omega_c t + \hat{y}\cos \omega_c t) = -m\omega_c^2(\hat{x}x + \hat{y}y) \\ &= -m\hat{\rho}R\omega_c^2 = -\hat{\rho}m\frac{v^2}{R} \qquad (Ex1.3.1.1) \end{aligned}$$

which is equal to the negative of the centrifugal force pointing in the $\hat{\rho}$ direction, whose magnitude is equal to the Lorentz force $\hat{\rho}qvB_o$.

— END OF EXERCISE 1.3.1 —

EXAMPLE 1.3.3   Cyclotron.

A cyclotron [Fig. E1.3.3.1] is an accelerator for charged particles. The a.c. source provides an alternating voltages at the cyclotron frequency and a charged particle is repeatedly accelerated every time it passes through the voltage drop.
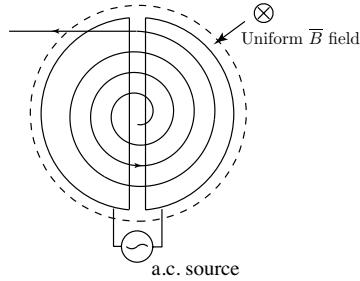
Figure E1.3.3.1   Cyclotron.

— END OF EXAMPLE 1.3.3 —

EXAMPLE 1.3.4   Isotope separation.

To separate the isotope Uranium 235 from Uranium 238, the isotopes are first vaporized and then ionized by electric discharge. Accelerated through a voltage drop V, they acquire a kinetic energy $qV = mv^2/2$. Passing through [Fig. E1.3.4.1] a uniform magnetic field, the isotopes move along circular paths of different radii.
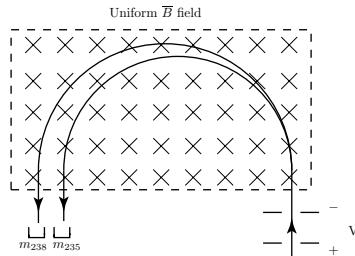
Figure E1.3.4.1   Isotope separation.

$$\frac{R_{235}}{R_{238}} = \frac{m_{235}v_{235}}{m_{238}v_{238}} = \frac{m_{235}}{m_{238}}\sqrt{\frac{m_{238}}{m_{235}}} = \sqrt{\frac{m_{235}}{m_{238}}}$$

Thus Uranium 235 can be obtained in a collector with a smaller radius.

— END OF EXAMPLE 1.3.4 —

EXAMPLE 1.3.5

The two rods attract each other when their currents are in the same direction and are repulsive when their currents are in the opposite directions.
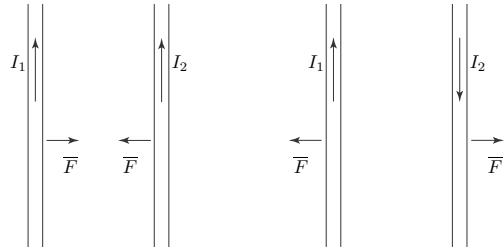
Figure E1.3.5.1 Attractive and repulsive forces.

— END OF EXAMPLE 1.3.5 —

EXAMPLE 1.3.6   Linear motor.

In Fig. E1.3.6.1, we show a sliding bar with length l moving perpendicular to a DC magnetic field $\overline{B} = \hat{z}B_0$ in the $\hat{z}$ direction. According to the Lorentz force law, a force

$$\overline{F}_m = \hat{y}Il \times \hat{z}B_0 = \hat{x}IlB_0$$

is produced that moves the sliding bar in the $\hat{x}$ direction.
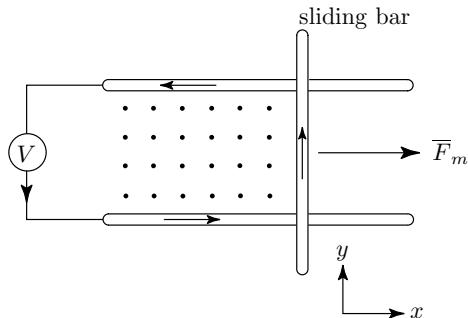
Figure E1.3.6.1 Linear motor.

If a force is applied to move the sliding bar with velocity $v = -\hat{x}$, an induced voltage $V = vlB_0$ will be generated across the resistor.

— END OF EXAMPLE 1.3.6 —

EXAMPLE 1.3.7   Magnetic moment and magnetic torque.
    A rectangular loop [Figure E1.3.7.1] carrying a static current I is placed
in a static magnetic field $\overline{B} = \hat{x}B_0$. The magnetic moment of the current
loop is $\overline{M} = \hat{m}M$. Its direction $\hat{m}$ follows from the right-hand rule: with the
fingers pointing in the direction of the current, the thumb of the right hand is
pointing in the direction of $\hat{m}$. Its magnitude M is equal to the area of the
loop A times the current I, $M = AI$. If the rectangular loop has lengths
l_x and l_y, the area of the loop is $A = l_x l_y$.
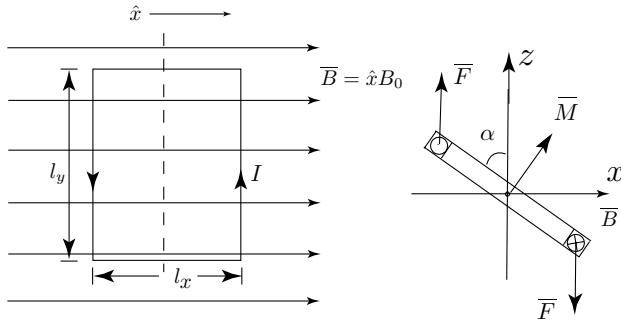
Figure E1.3.7.1   Torque on a loop.

    The loop is on the x-y plane with two sides aligned with the x-axis and
two sides aligned with the y-axis. Since the static magnetic field is in the $\hat{x}$
direction, there is no force acting on the two sides with length l_x aligned with
the x-axis. The forces acting on the two sides with length l_y aligned with the
y axis are in the positive and negative $\hat{y}$ directions. Thus the loop is rotating
around the y-axis following the right-hand rule; with the fingers pointing in
the direction of the rotation, the thumb of the right hand is pointing in the
$\hat{y}$ direction.
    The torque acting on the loop is calculated as

$$\overline{T} = \frac{1}{2}l_x\hat{x} \times (\hat{y} \times \hat{x}Il_yB_0) - \frac{1}{2}l_x\hat{x} \times (-\hat{y} \times \hat{x}Il_yB_0) = \hat{y}IAB_0$$

For the current configuration, $\overline{M} = \hat{z}IA$ and $\overline{B} = \hat{x}B_0$. In general, the
magnetic torque is

$$\overline{T} = \overline{M} \times \overline{B} \tag{E1.3.7.1}$$

Thus there is no torque acting on the component of $\overline{M}$ in the direction of
the magnetic field.

<div align="right">— END OF EXAMPLE 1.3.7 —</div>

EXAMPLE 1.3.8

A simple DC motor [Fig. E1.3.8.1] consists of a loop of area A with N turns, called an armature, which is immersed in a uniform magnetic field, either produced by a permanent magnet or an electromagnet. The armature is connected to a commutator which is a divided slip ring. A DC current I is supplied through a pair of brushes resting against the commutator such that the torque

$$T = NB_o IA \sin \alpha$$

produced by the current on the armature always acts in the same direction.
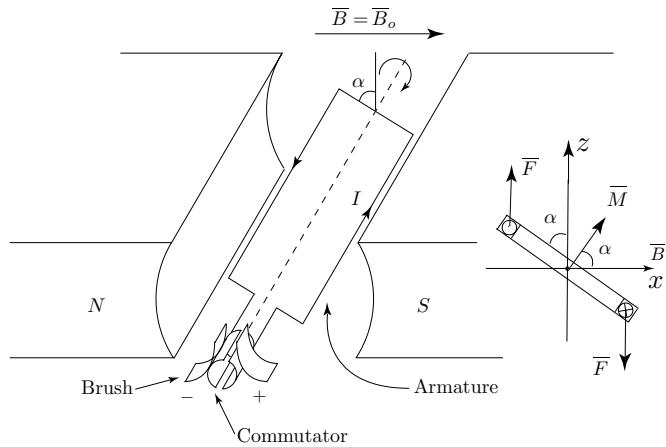
Figure E1.3.8.1a DC motor.
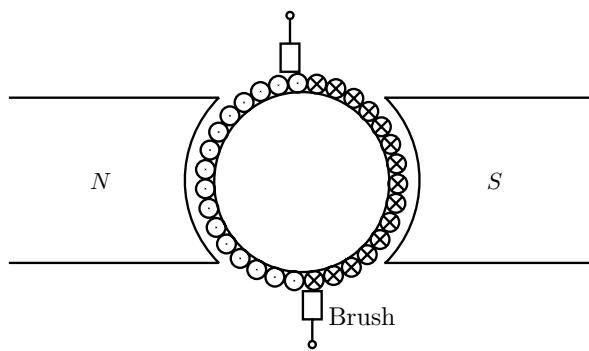
Figure E1.3.8.1b Side view of a DC motor.

— END OF EXAMPLE 1.3.8 —

Alessandro Volta (18 February 1745 – 5 March 1827)

Alessandro Volta was appointed to the chair of physics at the University of Pavia in 1775. In 1800, Volta built the first electric battery, consisting of alternating zinc and silver disks separated by layers of paper or cloth soaked in a solution of either sodium hydroxide or brine, called the 'voltaic pile'.

Hans Christian Oersted (14 August 1777 – 9 March 1851)

Oersted became a professor at the University of Copenhagen in 1806. In April 1820, during an evening lecture to a few advanced students, he discovered that a wire connecting the ends of a voltaic battery deflected a magnet in its vicinity. This discovery was published on 21 July 1820.

EXAMPLE 1.3.9

In October of 1821, Faraday demonstrated the principle of electric motor with a dish of mercury. When he connected a battery to form a circuit with the mercury pool, using a fixed wire carrying current and a dangling magnet with one end fixed and the other end moving around the surface of the pool of mercury. Let the magnet be designated as a magnetic moment $\overline{M}$ placed in a magnetic field $\overline{B}$. The torque acting on the magnet is $\overline{T} = \overline{M} \times \overline{B}$. Show that the magnet rotates around the wire in a circular trajectory.

SOLUTION:

To find the magnetic field $\overline{H}$ at the position of the loop due to the straight wire carrying current I_0 in the $\hat{z}$ direction, we use the integral form of Ampère's law,

$$\oint_C \overline{H} \cdot d\bar{l} = \int_0^{2\pi} H_\phi d\, d\phi = 2\pi d H_\phi = \int_s \overline{J} \cdot ds = I_0$$

which gives the magnetic field $\overline{B}$ at the loop's position

$$\overline{B} = \mu_0 \overline{H} = \hat{\phi} \frac{I_0 \mu_0}{2\pi d}$$

To calculate the torque, we apply,

$$\overline{T} = \overline{M} \times \overline{B} = \hat{z} \frac{M I_0 \mu_0}{2\pi d}$$

which means that the current loop will move about the z-axis in a counter-clockwise direction.

— END OF EXAMPLE 1.3.9 —

B. Lenz' Law and Electromotive Force (EMF)

We apply Stokes theorem to Faraday's law and define the line integral of $\overline{E}$ as the electromotive force (EMF):

$$\text{EMF} = \oint_C d\bar{l} \cdot \overline{E} = -\frac{\partial}{\partial t} \iint d\overline{S} \cdot \overline{B}$$
$$= -\frac{\partial}{\partial t} \Psi \tag{1.3.2}$$

where

$$\Psi = \iint_A d\overline{S} \cdot \overline{B} \tag{1.3.3}$$

is the magnetic flux linking a loop with area A bounded by a closed contour C [Fig. 1.3.1]. Equation (1.3.2) states that the EMF is equal to the negative time derivative of the magnetic flux linking the loop. Thus the EMF always produces a flux in the loop to oppose the direction of change of the flux linking the loop; if Ψ is increasing, the EMF decreases the flux, and vice versa. This is known as Lenz' law.
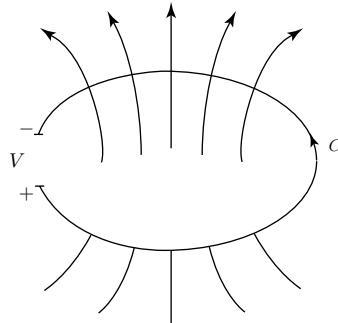
Figure 1.3.1 Flux linking a loop.

Heinrich Lenz (12 February 1804 – 10 February 1865)
    Heinrich Lenz was scientific assistant at the St. Petersburg Academy of Science, becoming full Academician in 1834. From 1835 to 1841, he served as lecturer in physics at the Naval Military School. He was dean of mathematics and physics (1840–1863) at the University of St. Petersburg. He began his investigation of electromagnetism in 1831 and in 1833 discovered Lenz' law, which is fundamental to electrical machinery.

Notice that the EMF has unit of voltage (Volt) and not unit of force. The voltage drop across the loop V is equal to the negative of the induced EMF.

$$V = -\text{EMF} = \frac{d}{dt}\Psi \qquad (1.3.4)$$

Thus in the presence of a time varying magnetic field linking a loop, a voltage is generated to oppose the time change of the magnetic field. The voltage generated across the loop V is equal to the negative of the induced EMF.

LeChatelier's Principle (Henri Louis Le Chatelier, 8 October 1850 – 17 September 1936) is the chemist's version of Lenz' law, which states that when an external stress (pressure, concentration, or temperature change) is applied to a chemical system that is in a state of equilibrium, the system will automatically respond so as to undo the stress applied externally.

In Physics, this same phenomenon is embodied in the Third Law of Motion, that is, for every action there is an equal and opposite reaction. In biology, a condition in an organism known as homeostasis means that when a stress is applied to an organism, the organism's bodily functions automatically respond so as to remove the stress.

EXAMPLE 1.3.10   Linear generator.

If a force is applied to move the sliding bar with velocity $v = -dx/dt$ as shown in Fig. E1.3.10.1, the total magnetic field $\Psi = xlB_o$ linking the loop will be decreasing at the rate of vlB_0. According to Lenz' law, a current in the bar must be produced to oppose the decreasing of the magnetic flux. Thus an induced voltage $V = vlB_0$ is generated across the resistor.
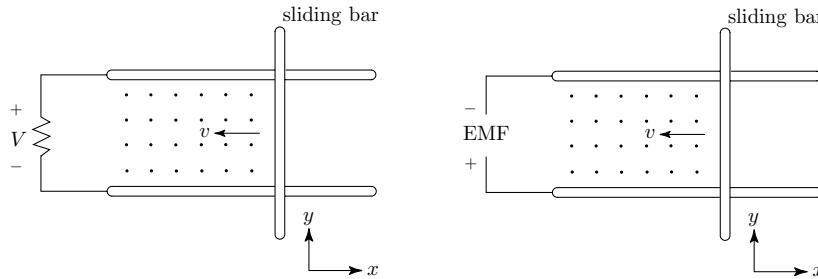
Figure E1.3.10.1 Linear generator.

— END OF EXAMPLE 1.3.10 —

EXAMPLE 1.3.11   AC generator.

An AC generator can be made of the DC motor by replacing the DC current source with a load resistance R and providing an external rotatory force on the armature. Applying a torque that makes the loop turn in the direction as shown in Fig. E1.3.11.1, a motional EMF

$$V = \int d\bar{l} \cdot \overline{E} = \int d\bar{l} \cdot \overline{F}/q = \int d\bar{l} \cdot \overline{v} \times \overline{B} = \omega AB \sin\alpha$$
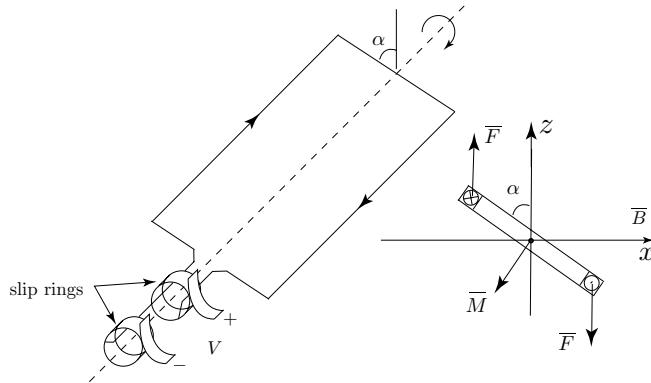
Figure E1.3.11.1   AC generator.

is produced. For the armature rotating with an angular frequency ω, we have $\overline{v} \times \overline{B} = \hat{l}\omega BA \sin\alpha$ and $\alpha = \omega t$.

The same result can be derived by using Lenz' law

$$\text{EMF} = -d\Psi/dt$$

where

$$\Psi = \iint_A d\overline{S} \cdot \overline{B} = -AB \cos\alpha \qquad (\text{E1.3.11.1})$$

We find the generated AC voltage

$$V = -EMF = \omega AB \sin\omega t$$

— END OF EXAMPLE 1.3.11 —

C. Poynting's Theorem and Poynting Vector

Energy conservation immediately follows from the Maxwell equations. Dot-multiply Faraday's law (1.1.2) by $\overline{H}$, Ampère's law (1.1.1) by $\overline{E}$ and subtract. By making use of the vector identity $\nabla \cdot (\overline{E} \times \overline{H}) = \overline{H} \cdot \nabla \times \overline{E} - \overline{E} \cdot \nabla \times \overline{H}$, we obtain Poynting's theorem

$$\nabla \cdot (\overline{E} \times \overline{H}) + \overline{H} \cdot \frac{\partial \overline{B}}{\partial t} + \overline{E} \cdot \frac{\partial \overline{D}}{\partial t} = -\overline{E} \cdot \overline{J} \qquad (1.3.5)$$

The Poynting vector

$$\overline{S} = \overline{E} \times \overline{H} \qquad (1.3.6)$$

is interpreted as the power flow density with the dimension watts/m^2, and $\overline{H} \cdot (\partial \overline{B}/\partial t) + \overline{E} \cdot (\partial \overline{D}/\partial t)$ represents the time rate of change of the stored electric and magnetic energy density. On the right-hand side of (1.3.5), $-\overline{E} \cdot \overline{J}$ is the power supplied by the current $\overline{J}$.

John Henry Poynting (9 September 1852 – 30 March 1914)
     John Henry Poynting was educated at Liverpool and Cambridge and was one of Maxwell's students. He was professor of physics at Mason Science College (later the University of Birmingham) from 1880 until his death. In 1884–1885, he established Poynting's theorem.

EXAMPLE 1.3.12
     Consider the simple wave solution

$$\overline{E} = \hat{x} E_0 \cos(kz - \omega t) \qquad (E1.3.12.1a)$$
$$\overline{H} = \hat{y} H_0 \cos(kz - \omega t) \qquad (E1.3.12.1b)$$

where $H_0 = E_0/\eta_o$ and $\eta_o = \sqrt{\mu_o/\epsilon_o}$ is called the characteristic impedance of free space. Substituting (E1.3.12.1) in (1.3.5) we see that Poynting's theorem is satisfied.
     The Poynting vector is calculated to be Poynting's vector

$$\overline{S} = \overline{E} \times \overline{H} = \hat{z} \sqrt{\frac{\epsilon_o}{\mu_o}} E_0^2 \cos^2(kz - \omega t) \qquad (E1.3.12.2)$$

In free space, we find

$$\overline{H} \cdot \frac{\partial}{\partial t}(\mu_o \overline{H}) = \frac{\partial}{\partial t}\left[\frac{1}{2}\mu_o \overline{H} \cdot \overline{H}\right] = \frac{\partial}{\partial t} W_m$$

and

$$\overline{E} \cdot \frac{\partial}{\partial t}(\epsilon_o \overline{E}) = \frac{\partial}{\partial t}\left[\frac{1}{2}\epsilon_o \overline{E} \cdot \overline{E}\right] = \frac{\partial}{\partial t}W_e$$

In the source-free region we also have $\overline{J} = 0$. Poynting's theorem becomes

$$\nabla \cdot (\overline{E} \times \overline{H}) + \frac{\partial}{\partial t}(W_e + W_m) = 0 \qquad (E1.3.12.3)$$

where

$$W_e = \frac{1}{2}\,\epsilon_o\,\left|\overline{E}\right|^2 = \frac{1}{2}\epsilon_o E_0^2 \cos^2(kz - \omega t) \qquad (E1.3.12.4)$$

is the stored electric energy density and

$$W_m = \frac{1}{2}\,\mu_o\,\left|\overline{H}\right|^2 = \frac{1}{2}\mu_o H_0^2 \cos^2(kz - \omega t) \qquad (E1.3.12.5)$$

is the stored magnetic energy density. It is seen that the stored electric energy is equal to the stored magnetic energy, $W_e = W_m$.

— END OF EXAMPLE 1.3.12 —

James Watt (19 January 1736 – 25 August 1819)

James Watt was a Scottish engineer who played an important part in the development of the steam engine as a practical power source and a key stimulus to the Industrial Revolution. Watt is the unit of power.

James Prescott Joule (24 December 1818 – 11 October 1889)

Joule attended the University of Manchester in 1835 and in 1840 he published his paper On the Production of Heat by Voltaic Electricity. He experimentally verified the law of conservation of energy in his study of the transfer of mechanical energy into heat energy. Joule is the unit of energy.

William Thomson (Lord Kelvin) (26 June 1824 – 17 December 1907)

At age 22, William Thomson became professor of physics at the University of Glasgow where he remained for 53 years until his retirement in 1899. He first defined the absolute temperature scale in 1847. In 1851 he published the paper, 'On the Dynamical Theory of Heat.' In 1866 he was Knighted by Queen Victoria. In 1892 he became Lord Kelvin of Largs. Kelvin is the unit of absolute temperature.

EXAMPLE 1.3.13   Power, energy, force, and radiation pressure.
    The time-average Poynting vector power density is given by

$$<\overline{S}> = \frac{1}{T} \int_0^T dt\, \overline{S} = \hat{z}\frac{E_0^2}{2\eta_o} = \hat{z}\frac{1}{2}\eta_o H_0^2 = \hat{z}P \qquad \text{(E1.3.13.1)}$$

where

$$P = \frac{E_0^2}{2\eta_o} = \frac{1}{2}\eta_o H_0^2$$

is the power density of the wave with unit of Watts/m^2. The total time-average electromagnetic energy density (with unit J/m^3) is equal to the sum of the electric energy density and the magnetic energy density,

$$W = <W_e> + <W_m> = \frac{1}{2}\epsilon_o E_0^2 = \frac{1}{2}\mu_o H_0^2 \qquad \text{(E1.3.13.2)}$$

We may define an energy velocity v_e equal to the ratio of power density to energy density. We find $P/W = v_e = 1/\sqrt{\mu_o\epsilon_o}$ which is the velocity of light.
    Radiation pressure is force per unit area $F = P/v_e$ (with unit N/m^2). Thus the radiation pressure of the wave is

$$F = P/v_e = W = \frac{1}{2}\epsilon_o E_0^2 = \frac{1}{2}\mu_o H_0^2 \qquad \text{(E1.3.13.3)}$$

which is equal to the time-average total energy density in the wave and acts in the direction of propagation of the wave. The radiation pressure, although generally very small, can lead to large scale effects. For example, comet tails are forced to point away from the Sun due to the radiation pressure from the Sun.

<div align="center">— END OF EXAMPLE 1.3.13 —</div>

    Applying the divergence theorem to Poynting's theorem (1.3.5), we write

$$\oiint_S d\overline{S} \cdot \overline{E} \times \overline{H} = -\frac{\partial}{\partial t}\iiint_V dV\left(\frac{1}{2}\epsilon_o E^2 + \frac{1}{2}\mu_o H^2\right) - \iiint_V dV\,\overline{E}\cdot\overline{J}$$

$$(1.3.7)$$

The left-hand side represents power flow out of the surface enclosing the volume V. The first term on the right-hand side represents the depletion of the electric energy and the magnetic energy inside the volume in order to supply the outflow of the Poynting power. The last term represents the power generated by the source J inside the volume V.

Momentum Conservation Theorem

Substituting the Maxwell equations for ρ and $\overline{J}$ in the Lorentz force law

$$\overline{f} = \rho\overline{E} + \overline{J} \times \overline{B} \tag{1.3.8}$$

we find that

$$\overline{f} = -\frac{\partial}{\partial t}(\overline{D} \times \overline{B}) - \nabla \cdot \left[\frac{1}{2}(\overline{D} \cdot \overline{E} + \overline{B} \cdot \overline{H})\overline{\overline{I}} - \overline{D}\,\overline{E} - \overline{B}\,\overline{H}\right] \tag{1.3.9}$$

where $\overline{\overline{I}}$ is a unit dyad with diagonal elements equal to 1 and all off-diagonal elements equal to zero.

The interpretation of the terms is

$$\overline{G} = \overline{D} \times \overline{B} = \text{momentum density vector} \tag{1.3.10}$$

$$\overline{\overline{T}} = \frac{1}{2}(\overline{D} \cdot \overline{E} + \overline{B} \cdot \overline{H})\overline{\overline{I}} - \overline{D}\,\overline{E} - \overline{B}\,\overline{H}$$

$$= \text{Maxwell stress tensor} \tag{1.3.11}$$

Thus we have the theorem

$$\nabla \cdot \overline{\overline{T}} + \frac{\partial \overline{G}}{\partial t} = -\overline{f} \tag{1.3.12}$$

which expresses conservation of momentum. This is in a form similar to Poynting's theorem in (1.3.5) except that it is now a vector equation. In fact, (1.3.5) and (1.3.12) combine to become a four-dimensional conservation theorem in relativity.

Problems

P1.3.1

According to the classical model of an atom as proposed by Niels Bohr (1885–1962), electrons revolve around the nucleus in quantized orbits with radii $R = n\hbar/mv$ where n is an integer, m is the electron mass and v is the electron velocity. Letting the nucleus be a positive charge of Ze, calculate R by equating the centrifugal force with the Lorentz force. Estimate the radius for a hydrogen atom with $Z = 1$.

P1.3.2

The Earth receives over all frequency bands about $1.5\,\text{kW/m}^2$ of power from the Sun.

(a) The Earth-Sun distance is 150×10^9 m . How long does it take the sunlight to reach the Earth?
(b) The Earth radius is 6400 km. What is the total power received by the Earth?
(c) The Sun radiates 10^{-20} W m^{-2} Hz^{-1} at 3 GHz. Assuming constant power level over 1 GHz bandwidth, what is the Poynting power density and the corresponding electric field amplitude?

P1.3.3

For an electromagnetic wave with electric field with $E_0 = 3 \times 10^6$ V/m (which is the breakdown electric field strength for air), find the power density and radiation pressure. What is the area required in order to supply the electric power of 2.4×10^{11} W for use by a nation?

P1.3.4

In cylindrical coordinate system, $\overline{\rho} = \hat{\rho}\rho = \hat{x}x + \overline{y}y$ is the radial vector. Show that the force acting on the charge in Example 1.3.2 is

$$\overline{F} = -\hat{\rho}m\frac{v^2}{R}$$

which is equal to the negative of the centrifugal force pointing in the $\hat{\rho}$ direction, whose magnitude is equal to the Lorentz force $\hat{\rho}qvB_o$.
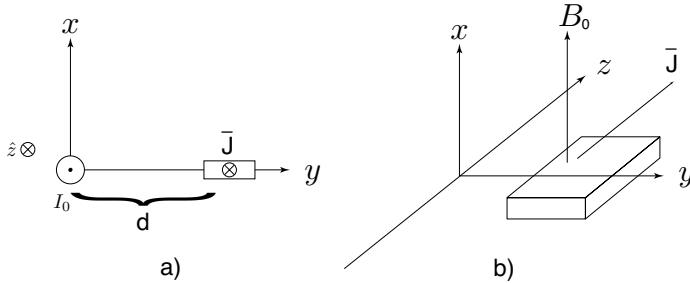
P1.3.5

Figure P1.3.5.1

(a) Consider an infinitely long wire with current I_0 flowing along the $-\hat{z}$ direction as shown in Fig. P1.3.5.1a. Find the $\overline{B}$ field at $y = d$ generated by the current.
(b) Consider a slab of semiconductor with positive charge carriers of density N so that there is a uniform current density of $\overline{J} = \hat{z}Nqv$ flowing in the $+\hat{z}$ direction as shown in Figure P1.3.5.1b. Calculate the force density $\overline{F}$ acting on the charges if a static magnetic field $\overline{B} = \hat{x}B_0$ is applied.

P1.3.6

For a charged particle q moving with velocity v in a constant magnetic field B_0 , the trajectory is a circle. Set the Lorentz force equal to the

centrifugal force and derive the cyclotron frequency and the radius of the circle.

P1.3.7

The solar wind is a high-conductivity plasma which is emitted radially from the surface of the Sun. Let us calculate the flux of electromagnetic energy in the solar wind at the orbit of the Earth.

In the plane of the Earth's orbit, the magnetic field of the Sun is approximately radial, pointing outward in certain regions and inwards in others. This field is "frozen" in the high-conductivity plasma. Since the Sun rotates (with a period of 27 days), and the plasma has a radial velocity, the lines of $\overline{B}$ are in fact Archimedes spirals ($r = a\theta$ in polar coordinates) and, at the Earth, they form an angle of about $45°$ with the Sun-Earth direction. This is the so-called garden hose effect.

At the orbit of the Earth the solar wind has a density of about 10^7 proton-masses/m^3 and a velocity of about 4×10^5 m/sec, while the magnetic field of the Sun is about 5×10^{-9}(webers/m^2).

(a) First show that, in an electrically neutral ($\rho = 0$) and nonmagnetic fluid of conductivity σ and velocity $\overline{v}$, the Maxwell equations become

$$\nabla \cdot \overline{D} = 0 \qquad \nabla \cdot \overline{B} = 0 \qquad \nabla \times \overline{E} = -\frac{\partial \overline{B}}{\partial t}$$

$$\nabla \times \overline{B} = \mu_0 \left\{ \sigma(\overline{E} + \overline{v} \times \overline{B}) + \epsilon_0 \frac{\partial \overline{E}}{\partial t} \right\}$$

the polarization currents being negligibly small compared to the conduction currents. Note that, for an infinite conductivity,

$$\overline{E} = -\overline{v} \times \overline{B}$$

This is a satisfactory approximation for the solar wind.

(b) Show that the component of $\overline{v}$ which is normal to $\overline{B}$ is $\overline{v}_n = \frac{1}{B^2}\overline{B} \times (\overline{v} \times \overline{B})$, and that the Poynting vector of the solar wind is

$$\overline{S} = \frac{B^2}{\mu_o}\overline{v}_n$$

Numerically it is approximately equal to 4×10^{-9} times the average value of the Poynting vector of the solar radiation, which is about $1.4\,\text{kW/m}^2$. The Poynting vector of the solar wind is normal to the local $\overline{B}$ and it points at an angle of $45°$ away from the Sun-Earth direction.

(c) Compare the relative magnitudes of the kinetic, electric, and magnetic energy densities. Which is the largest?

P1.3.8

   Particles excited by an electromagnetic wave may be modeled as harmonic oscillators with a characteristic frequency and damping. For electrons,

$$\frac{\partial^2 \overline{x}}{\partial t^2} + \delta \frac{\partial \overline{x}}{\partial t} + \omega_0^2 \overline{x} + \frac{q\overline{E}}{m} = 0$$

which is just an expression for momentum conservation $(F = MA)$.

(a) Assume $\delta = 0$. Show that for $\omega > \omega_0$ (ω is defined as the frequency of the $\overline{E}$-field), the electrons vibrate in phase with the E-field while for $\omega < \omega_0$, they are $180°$ out of phase. Can you explain opacity of certain substances in terms of this effect? (see Scientific American, Sept. 1968, p. 60 ff.)

(b) Derive a Poynting theorem and show that

$$\nabla \cdot \overline{S} + \frac{\partial W}{\partial t} + P_D = 0$$

$$S \equiv E \times H \quad \text{(Electromagnetic power density)}$$

   Determine W and P_D.

P1.3.9

   Consider two infinite parallel metal plates separated by a distance d along the $\hat{x}$ direction. Initially the system is at rest, and the top plate has a uniform surface charge density of σ while the bottom plate has a uniform surface charge density of $-\sigma$. At time $t = 0$ a uniformly decaying magnetic field is applied parallel to the plane of the plates, that is,

$$\overline{B}(t) = \hat{y}B_0 e^{-\gamma t}$$

(a) Calculate the Poynting vector, $\overline{S}$, for the system and the momentum density vector, $\overline{g}_f$, of the field for $t > 0$ using the relation,

$$\overline{g}_f = \mu_0 \epsilon_0 \overline{S}$$

(b) As the magnetic field begins to decay, it will induce an electric field. By the Lorentz force law, this induced field exerts a force on the two charged metal plates. Determine the strength and direction of this induced electric field and the resulting force density vector exerted on the two plates.

(c) From mechanics, the force and momentum vectors are related by

$$\overline{F} = \frac{d}{dt}\,\overline{p}.$$

   Using this relation, calculate the mechanical momentum density vector that results from the induced electric field.

(d) As the magnetic field decays, the momentum of the field is transferred to the plate in the form of mechanical momentum. Using the results of parts (a) and (c), show that for $t > 0$, the total momentum of the system is conserved.

P1.3.10

The magnetic moment of a particle with charge q at position $\bar{r}$ with velocity $\bar{v}$ is defined as

$$\overline{M} = \frac{1}{2} q \bar{r} \times \bar{v}$$

Show that the magnetic moment of a plane loop with area A carrying current I is

$$\overline{M} = \hat{m} I A$$

where $\hat{m}$ is the normal to the plane loop following the right-hand rule: with the fingers following the direction of the current, the thumb of the right hand is pointing in the direction of $\hat{n}$.

P1.3.11

In mechanics, the classical equations of motion are $\overline{T} = d\overline{L}/dt$, where $\overline{L}$ is the angular momentum. The magnetic moment $\overline{M}$ is analogous to the expression for the mechanical angular momentum $\overline{L}$ in terms of the velocity of mass distributions instead of the charge distributions. The magnetic moment of a particle with charge q at position $\bar{r}$ with velocity $\bar{v}$ is defined as

$$\overline{M} = \frac{1}{2} q \bar{r} \times \bar{v}$$

If the charged particle has mass m, the mechanical angular momentum is

$$\overline{L} = m \bar{r} \times \bar{v}$$

We set $\overline{M} = \gamma \overline{L}$ and called γ the gyromagnetic ratio. From (E1.3.7.1), we see that applying to the magnetic moment, we have $d\overline{M}/dt = \gamma d\overline{L}/dt = \gamma \overline{T} = \gamma \overline{M} \times \overline{B}$.

(a) Determine the gyromagnetic ratio γ for the charged particle.

(b) Consider a nucleus with magnetic moment $\overline{M}$ placed in a dc magnetic field in the $\hat{z}$-direction, $\overline{B} = \hat{z} B_0$. The nucleus is precessing about the $\hat{z}$ axis. Determine the frequency of precession, which is called the Larmor frequency.

(c) Place the magnetic moment $\overline{M}$ of a nucleus precesses in a static magnetic field $\overline{B} = \hat{x} x + \hat{z} B_z$. Show that $B_z = B_0 - z$ to satisfy Maxwell equations.

(d) When the nucleus is placed on the z axis where $x = 0$, $\overline{B} = \hat{z}B_z$. Determine the Larmor frequency of precession and show that it is a function of z.

(e) An induced voltage with the angular frequency ω due to $\overline{M}$ can be picked up from an RF (radio frequency) coil placed on the x-z plane. Assume that the magnetic dipoles are spinning protons of water at room temperature, with $\gamma = 2.7 \times 10^8\,\mathrm{T^{-1}s^{-1}}$. Let there be two protons precessing on the z axis with a separation of δ_z. Calculate the difference of Larmor frequency in kHz of the pick-up coil if $\delta_z = 1\,\mathrm{mm}$.

P1.3.12

Consider a loop carrying a current of I_l with normal $\hat{n} = \hat{x} - \hat{y}$ is placed a distance d above a straight wire, which is carrying a current of I_0. Calculate the magnetic moment of the current loop and the magnetic field generated by straight wire at the loop's position. Using these two values, calculate the torque vector, $\overline{T}$, of loop. In what direction does the loop move due to the torque?

P1.3.13

Joule's law, $P_d = \overline{J} \cdot \overline{E}$, determines power dissipation per volume due to Ohmic loss. Derive Joule's law by using the Lorentz force law, $\overline{f} = \rho\overline{E}$, and assuming an average constant drifting velocity $\overline{v}$ due to collision of the conduction electrons.

P1.3.14

Consider the simple wave solution

$$\overline{E} = \hat{x}E_0 \cos(kz - \omega t) \qquad\qquad \text{(P1.3.14.1}a\text{)}$$
$$\overline{H} = \hat{y}H_0 \cos(kz - \omega t) \qquad\qquad \text{(P1.3.14.1}b\text{)}$$

where $H_0 = E_0/\eta_o$ and $\eta_o = \sqrt{\mu_o/\epsilon_o}$ is the characteristic impedance of free space. Substituting (P1.3.14.1) in (1.3.5) to show that Poynting's theorem is satisfied. Derive the associated Lorentz force.

P1.3.15

Use Maxwell's equations to show that for $\overline{J} = 0$ and $\rho = 0$,

$$\frac{\partial}{\partial t}(\overline{D} \times \overline{B}) + \nabla \cdot \left(W\overline{\overline{I}} - \overline{D}\,\overline{E} - \overline{B}\,\overline{H}\right) = 0$$

where the total stored energy density $W = \left(\overline{D} \cdot \overline{E} + \overline{B} \cdot \overline{H}\right)/2$. Consider $\overline{D} = \epsilon_o\overline{E}$ and $\overline{B} = \mu_o\overline{H}$ and use index notation.

1.4 Hertzian Waves

A. Hertzian Dipole

A Hertzian dipole is made of two opposite charges $\pm q$ separated by an infinitesimally small distance ℓ. The dipole moment $p = q\ell$ has an angular frequency ω such that each point charge changes from $+q$ to $-q$ and vice versa in a period of $2\pi/\omega$. Mathematically, p is defined as the product of $\ell \to 0$ and $q \to \infty$ such that p is a constant. Assume that the two charges are situated at $z = \pm\ell/2$ on the z-axis [Fig. 1.4.1]. Hertz solved for all the electromagnetic fields with the use of a potential function known as the Hertzian potential Π

$$\Pi = \frac{q\ell}{4\pi r} \cos(kr - \omega t) \tag{1.4.1}$$
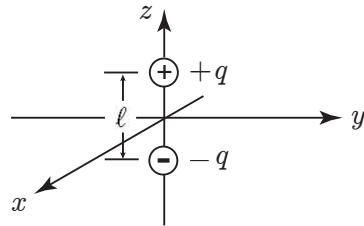
Figure 1.4.1 Hertzian dipole.

The solution to the wave equation for Π that Hertz studied for his Hertzian dipole assumes spherical symmetry. Substituting the Hertian potential Π (1.4.1) into the wave equation in spherical coordinate system, we find

$$\frac{1}{r} \frac{\partial^2}{\partial r^2}(r\Pi) - \mu_o \epsilon_o \frac{\partial^2}{\partial t^2}\Pi = 0$$

and obtain the dispersion relation $k^2 = \omega^2 \mu_o \epsilon_o$.

Heinrich Rudolf Hertz (22 February 1857 – 1 January 1894)

Heinrich Rudolf Hertz attended Dresden Polytechnic (1876), University of Munich (1877), and Berlin Academy (1878–80). He studied under Professors Hermann von Helmholtz and Gustav Kirchhoff, and his doctoral thesis was on Electromagnetic Induction in Rotating Conductors. He was employed as an Assistant to Helmholtz (1880–83) at the Berlin Academy, Privatdozent at the University of Kiel (1883–85), Professor of Physics at the Karlsruhe Technische Hochschule (1885–89), and University of Bonn (1889–94).

To derive the electromagnetic fields $\overline{E}$ and $\overline{H}$, we write $\overline{\Pi} = \hat{z}\Pi$ and define a vector potential $\overline{A}$ and a scalar potential Φ such that

$$\overline{A} = \mu_o \frac{\partial \overline{\Pi}}{\partial t} \tag{1.4.2}$$

$$\Phi = -\frac{1}{\epsilon_o} \nabla \cdot \overline{\Pi} \tag{1.4.3}$$

In terms of Φ and $\overline{A}$, the magnetic field $\overline{H}$ and the electric field $\overline{E}$ are

$$\overline{H} = \frac{1}{\mu_o} \nabla \times \overline{A} \tag{1.4.4}$$

$$\overline{E} = -\frac{\partial \overline{A}}{\partial t} - \nabla \Phi \tag{1.4.5}$$

Notice that (1.4.4) satisfies Gauss' law of $\nabla \cdot \overline{B} = 0$ and (1.4.5) follows from Faraday's law.

It is seen from (1.4.2) and (1.4.3) that

$$\nabla \cdot \overline{A} + \mu_o \epsilon_o \frac{\partial \Phi}{\partial t} = 0 \tag{1.4.6}$$

which is known as the Lorenz gauge condition relating the scalar and vector potentials. Making use of (1.4.4), (1.4.5), and (1.4.6), we can derive from Ampère's law and Gauss' law of $\nabla \cdot \overline{D} = \rho$ the following inhomogeneous Helmholtz equations:

$$\nabla^2 \overline{A} - \mu_o \epsilon_o \frac{\partial^2}{\partial t^2} \overline{A} = -\mu_o \overline{J} \tag{1.4.7}$$

$$\nabla^2 \Phi - \mu_o \epsilon_o \frac{\partial^2}{\partial t^2} \Phi = -\rho/\epsilon_o \tag{1.4.8}$$

The Hertzian potential provides a solution to the above equations.

———————————————————

Ludvig Valentin Lorenz (18 January 1829 – 9 June 1891)

Ludvig Lorenz graduated from the Technical University of Denmark and taught at the Danish Military Academy. The Lorenz gauge condition and the retarded potentials were contained in the article 'On the Identity of the Vibrations of Light with Electrical Currents', published in the Philosophical Magazine and Journal of Science in July–December 1867. In 1869, Lorenz arrived at the result of a dielectric mixing formula, which was also obtained by H. A. Lorentz in 1878, now known as the 'Lorenz-Lorentz' formula.

———————————————————

Example 1.4.1

In spherical coordinates, the unit vectors are [Fig. E1.4.1.1]

$$\hat{r} = \hat{x} \sin\theta \cos\phi + \hat{y} \sin\theta \sin\phi + \hat{z} \cos\theta$$

$$\hat{\theta} = \hat{x} \cos\theta \cos\phi + \hat{y} \cos\theta \sin\phi - \hat{z} \sin\theta$$

$$\hat{\phi} = -\hat{x} \sin\phi + \hat{y} \cos\phi$$

$$\hat{z} = \hat{r} \cos\theta - \hat{\theta} \sin\theta$$
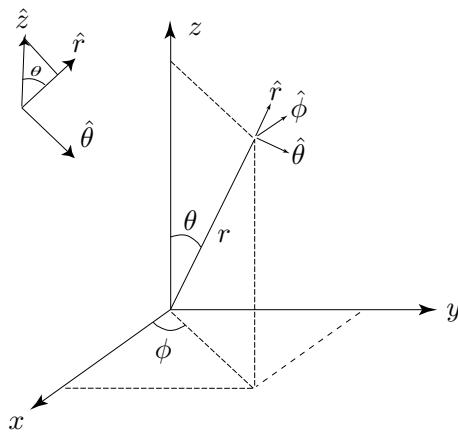
Figure E1.4.1.1   Unit vectors in spherical coordinates.

The vector del operators in spherical coordinate system are

$$\nabla\Phi = \hat{r}\frac{\partial\Phi}{\partial r} + \hat{\theta}\frac{1}{r}\frac{\partial\Phi}{\partial\theta} + \hat{\phi}\frac{1}{r\sin\theta}\frac{\partial\Phi}{\partial\phi}$$

$$\nabla \cdot \overline{A} = \frac{1}{r^2}\frac{\partial}{\partial r}(r^2 A_r) + \frac{1}{r\sin\theta}\frac{\partial}{\partial\theta}(\sin\theta A_\theta) + \frac{1}{r\sin\theta}\frac{\partial}{\partial\phi}A_\phi$$

$$\nabla \times \overline{A} = \frac{1}{r^2\sin\theta}\begin{vmatrix} \hat{r} & r\hat{\theta} & r\sin\theta\hat{\phi} \\ \dfrac{\partial}{\partial r} & \dfrac{\partial}{\partial\theta} & \dfrac{\partial}{\partial\phi} \\ A_r & rA_\theta & r\sin\theta A_\phi \end{vmatrix}$$

$$\nabla^2\Phi = \frac{1}{r}\frac{\partial^2}{\partial r^2}\left[r\Phi\right] + \frac{1}{r^2\sin\theta}\frac{\partial}{\partial\theta}\left[\sin\theta\frac{\partial\Phi}{\partial\theta}\right] + \frac{1}{r^2\sin^2\theta}\frac{\partial^2\Phi}{\partial\phi^2}$$

— End of Example 1.4.1 —

B. Electric and Magnetic Fields

The magnetic field $\overline{H}$ is obtained from (1.4.7) with

$$\overline{A} = \mu_o \frac{\partial \overline{\Pi}}{\partial t} = \hat{z} \mu_o \frac{\partial \Pi}{\partial t} = (\hat{r} \cos \theta - \hat{\theta} \sin \theta) \frac{\omega \mu_o q \ell}{4\pi r} \sin(kr - \omega t)$$

$$\overline{H} = \frac{1}{\mu_o} \nabla \times \overline{A} = \frac{1}{\mu_o r^2 \sin \theta} \begin{vmatrix} \hat{r} & r\hat{\theta} & r \sin \theta \hat{\phi} \\ \frac{\partial}{\partial r} & \frac{\partial}{\partial \theta} & \frac{\partial}{\partial \phi} \\ A_r & rA_\theta & 0 \end{vmatrix}$$

$$= \hat{\phi} \frac{1}{\mu_o r} \left[\frac{\partial}{\partial r}(r A_\theta) - \frac{\partial}{\partial \theta} A_r \right]$$

$$= \hat{\phi} \frac{\omega k q \ell}{4\pi r} \sin \theta \left[\frac{1}{kr} \sin(kr - \omega t) - \cos(kr - \omega t) \right] \qquad (1.4.9)$$

To obtain the electric field $\overline{E}$ from (1.4.8), noticing that $\partial r / \partial z = z/r = \cos \theta$. We find

$$\Phi = -\frac{1}{\epsilon_o} \frac{\partial \Pi}{\partial z} = \frac{k \, q \ell}{4\pi \epsilon_o r} \cos \theta \left[\frac{1}{kr} \cos(kr - \omega t) + \sin(kr - \omega t) \right]$$

$$\overline{E} = -\frac{\partial \overline{A}}{\partial t} - \nabla \Phi$$

$$= (\hat{r} \cos \theta - \hat{\theta} \sin \theta) \frac{\omega^2 \mu_o q \ell}{4\pi r} \cos(kr - \omega t) - \left[\hat{r} \frac{\partial \Phi}{\partial r} + \hat{\theta} \frac{1}{r} \frac{\partial \Phi}{\partial \theta} \right]$$

$$= \frac{k^2 q \ell}{4\pi \epsilon_o r} \left\{ \hat{r} 2 \cos \theta \left[\frac{1}{kr} \sin(kr - \omega t) + \frac{1}{k^2 r^2} \cos(kr - \omega t) \right] \right.$$

$$\left. + \hat{\theta} \sin \theta \left[\frac{1}{kr} \sin(kr - \omega t) + (\frac{1}{k^2 r^2} - 1) \cos(kr - \omega t) \right] \right\}$$

$$(1.4.10)$$

Consider the following special cases:

Case A) When $kr \gg 1$, we are in the far field as $r \gg \lambda/2\pi$; or at a fixed r, the frequency $\omega = ck \gg c/r$. We only keep terms of the order of $1/r$. The field vectors are

$$\overline{E} = -\hat{\theta} \frac{k^2 q \ell}{4\pi \epsilon_o r} \sin \theta \cos(kr - \omega t) \qquad (1.4.11)$$

$$\overline{H} = -\hat{\phi} \frac{\omega k q \ell}{4\pi r} \sin \theta \cos(kr - \omega t) \qquad (1.4.12)$$

It is seen that both $\overline{H}$ and $\overline{E}$ are tangent to the surface of a large sphere with radius r. The field vectors $\overline{H}$ and $\overline{E}$ are perpendicular to each other. As a function of θ, the magnitudes of both the electric and magnetic fields are proportional to $\sin\theta$. We plot the radiation field pattern in Fig. 1.4.2. The length E is proportional to the magnitude of the electric field in the direction θ.
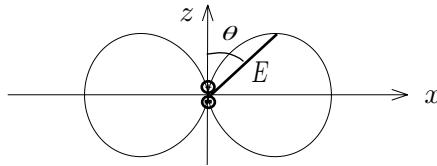
Figure 1.4.2 Radiation field pattern.

Case B) For static fields when $\omega = 0$, $k = \omega/c = 0$, we find

$$\overline{E} = \frac{q\ell}{4\pi\epsilon_o r^3}(\hat{r}2\cos\theta + \hat{\theta}\sin\theta), \qquad \overline{H} = 0 \qquad (1.4.13)$$

There is only electric field for a static dipole.

Case C) In the immediate neighborhood of the dipole, $kr \to 0$. Keeping terms of the orders $1/r^2$, the magnetic field vector is

$$\overline{H} = -\hat{\phi}\frac{\omega q\ell}{4\pi r^2}\sin\theta\sin\omega t = \hat{\phi}\frac{d(q\cos\omega t)}{dt}\frac{\ell}{4\pi r^2}\sin\theta = \hat{\phi}\frac{I\ell}{4\pi r^2}\sin\theta$$
$$(1.4.14)$$

This corresponds to the field produced by an element of length ℓ carrying current I along the z axis, and is known as the Biot-Savart law.

Jean-Baptiste Biot (21 April 1774 – 3 February 1862), professor of mathematical physics at the Collège de France since 1800, reported experiments with his assistant **Felix Savart** (30 June 1791 – 16 March 1841) following Orsted's discovery in April 1820 to the Académie des Sciences in October 1820 which led to the Bior-Savart law. Savart became Professor at the Collège de France in 1836.

EXAMPLE 1.4.2

Apply the Biot-Savart law (1.4.14) to determine the magnetic field of an infinitely long wire at a distance ρ from the wire. We place the observation point at (ρ, z), let $\ell = dz'$, and integrate (1.4.14) to obtain [Fig. E1.4.2.1]

$$\overline{H} = \hat{\phi}\frac{1}{4\pi}\int_{-\infty}^{+\infty} dz'\frac{I\sin\theta}{z'^2 + \rho^2} \qquad \text{(E1.4.2.1)}$$

The integration can be carried out with the substitution $z' = -\rho\cot\theta$. We find $dz' = \rho d\theta/\sin^2\theta$, $z'^2 + \rho^2 = \rho^2/\sin^2\theta$, and (E1.4.2.1) becomes

$$\overline{H} = \hat{\phi}\frac{1}{4\pi}\int_0^\pi d\theta\frac{I\sin\theta}{\rho} = \hat{\phi}\frac{I}{2\pi\rho}$$
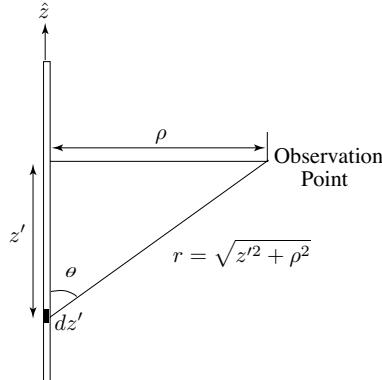
Figure E1.4.2.1 Integration of current elements in an infinitely long wire.

The above result can also be obtained by applying Stokes' theorem to Ampère's law $\nabla \times \overline{H} = \overline{J}$.

$$\oint_C d\bar{l}\cdot\overline{H} = \iint d\overline{S}\cdot\overline{J} = I$$

The integration path for the line integral is a circle of radius ρ around the line source whose area integral gives rise to the current I. The result is $2\pi\rho H_\phi = I$.

<div align="right">— END OF EXAMPLE 1.4.2 —</div>

C. Electric Field Pattern

To study and sketch the electric and magnetic field lines, Hertz introduced a parameter Q in terms of a radial distance $\rho = r\sin\theta$ in the cylindrical coordinate system. We have

$$
Q = \rho\frac{\partial\Pi}{\partial\rho} = \rho\frac{\partial r}{\partial\rho}\frac{\partial\Pi}{\partial r}
$$

$$
= r\sin^2\theta\frac{\partial}{\partial r}\left[\frac{q\ell}{4\pi r}\cos(kr - \omega t)\right]
$$

$$
= \frac{kq\ell}{4\pi}\sin^2\theta\left[-\sin(kr - \omega t) - \frac{1}{kr}\cos(kr - \omega t)\right]
$$

$$
\nabla Q = \hat{r}\frac{\partial Q}{\partial r} + \hat{\theta}\frac{1}{r}\frac{\partial Q}{\partial\theta}
$$

$$
= \hat{r}\frac{k^2 q\ell}{4\pi}\sin^2\theta\left[\frac{1}{kr}\sin(kr - \omega t) + (\frac{1}{k^2 r^2} - 1)\cos(kr - \omega t)\right]
$$

$$
+ \hat{\theta}\frac{kq\ell}{2\pi r}\sin\theta\cos\theta\left[-\sin(kr - \omega t) - \frac{1}{kr}\cos(kr - \omega t)\right]
$$

which is the product of two factors, one depends only on θ, and the other on r and t. From (1.4.9) and (1.4.10), we find

$$
\overline{H} = \hat{\phi}\frac{\omega kq\ell}{4\pi r}\sin\theta\left[\frac{1}{kr}\sin(kr - \omega t) - \cos(kr - \omega t)\right] \qquad (1.4.15)
$$

$$
\overline{E} = \frac{k^2 q\ell}{4\pi\epsilon_o r}\left\{\hat{r}2\cos\theta\left[\frac{1}{kr}\sin(kr - \omega t) + \frac{1}{k^2 r^2}\cos(kr - \omega t)\right]\right.
$$

$$
\left. + \hat{\theta}\sin\theta\left[\frac{1}{kr}\sin(kr - \omega t) + (\frac{1}{k^2 r^2} - 1)\cos(kr - \omega t)\right]\right\}(1.4.16)
$$

Thus in terms of Q,

$$
\overline{H} = -\hat{\phi}\frac{1}{\rho}\frac{\partial}{\partial t}Q
$$

$$
\overline{E} = \frac{1}{\epsilon_o\rho}\hat{\phi} \times \nabla Q
$$

The electric field lines on any ρ-z plane are seen to follow the intersection of $Q = $ constant surfaces with the ρ-z plane. In Fig. 1.4.3, we plot the electric field lines at different times.
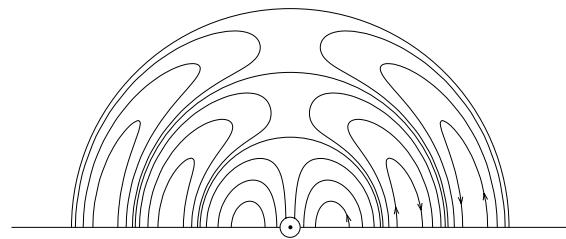
$\omega t = 0$

$\omega t = \pi/2$

$\omega t = \pi$

$\omega t = 3\pi/2$

Figure 1.4.3 Electric field patterns.

EXAMPLE 1.4.3

Consider the radiation field zone when $kr \gg 1$ and

$$Q = -\frac{kq\ell}{4\pi} \sin^2 \theta \sin(kr - \omega t)$$

Construct three constant Q surfaces at $\omega t = -\pi/2$ (or $3\pi/2$) and indicate the electric field line directions.

ANSWER: Consider

$$\sin^2 \theta \cos(kr) = c$$

We sketch the three cases of $c = 0, \frac{1}{2}, 1$ in Fig. E1.4.3.1.

$$
\begin{array}{lll}
\text{For} & c = 0, & kr = 2m\pi \pm \frac{\pi}{2} \\
\text{For} & c = \frac{1}{2}, & kr = 2m\pi \qquad \text{for } \theta = \pm\frac{\pi}{4} \\
& & kr = 2m\pi \pm \frac{\pi}{3} \quad \text{for } \theta = \frac{\pi}{2} \\
\text{For} & c = 1, & \theta = \frac{\pi}{2} \quad \text{and} \quad kr = 2m\pi.
\end{array}
$$
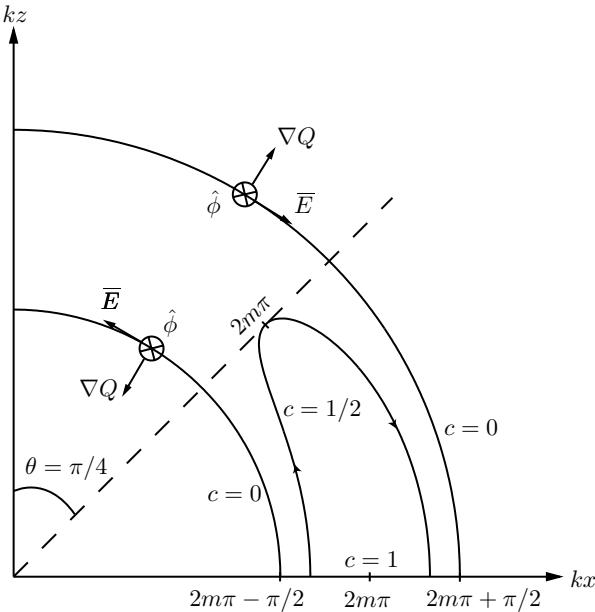
Figure E1.4.3.1 Radiation field plot.

— END OF EXAMPLE 1.4.3 —

EXAMPLE 1.4.4

In the radiation far field of a Hertzian dipole with $kr \gg 1$, the electric and magnetic fields are

$$\overline{E} = -\hat{\theta}\eta\frac{\omega q k\ell}{4\pi r}\sin\theta\cos(kr - \omega t) \tag{E1.4.4.1}$$

$$\overline{H} = -\hat{\phi}\frac{\omega q k\ell}{4\pi r}\sin\theta\cos(kr - \omega t) \tag{E1.4.4.2}$$

It is seen that both $\overline{H}$ and $\overline{E}$ are tangent to the surface of a large sphere with radius r. The field vectors $\overline{H}$ and $\overline{E}$ are perpendicular to each other and their magnitudes are related by $\eta = (\mu_o/\epsilon_o)^{1/2}$.

To investigate the power and energy issues, Hertz invoked Poynting's theorem. Poynting's power density vector $\overline{S}$ for fields for $kr \gg 1$ is

$$\overline{S} = \overline{E} \times \overline{H} = \hat{r}\eta\left(\frac{\omega q k\ell}{4\pi r}\right)^2\sin^2\theta\cos^2(kr - \omega t)$$

which is seen to be pointing in the $\hat{r}$-direction away from the large sphere. We now calculate the time-average power density

$$<\overline{S}> = \frac{1}{2\pi}\int_0^{2\pi} d(\omega t)\,\overline{E} \times \overline{H} = \hat{r}\,\frac{\eta}{2}\left(\frac{\omega q k\ell}{4\pi r}\right)^2\sin^2\theta$$

The radiation pattern is shown in Fig. E1.4.4.1. The length P is proportional to the magnitude of the radiated power in the direction θ.
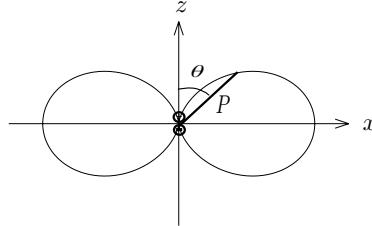
Figure E1.4.4.1 Radiation power pattern.

Integrating the $\hat{r}$ directed power over the surface of a sphere of radius r gives

$$P = \oiint dS\,\hat{r}\cdot<\overline{S}> = \frac{4\pi\eta}{3}\left(\frac{\omega q k\ell}{4\pi}\right)^2 = \frac{\eta}{12\pi}(\omega q k\ell)^2 = 10(\omega q k\ell)^2 \tag{E1.4.4.3}$$

Notice that the total time-average power leaving the dipole source can be calculated with a spherical surface of any radius r, and yields the same result.

<div align="right">— END OF EXAMPLE 1.4.4 —</div>

Poynting's Power Vector for Hertzian Waves

For a Hertzian dipole, the magnetic field $\overline{H}$ and the electric field $\overline{E}$ are

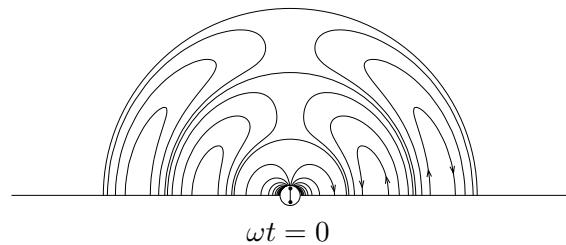$$\overline{H} = \hat{\phi}\frac{\omega kq\ell}{4\pi r}\sin\theta\left[\frac{1}{kr}\sin(kr - \omega t) - \cos(kr - \omega t)\right] \qquad (1.4.17)$$

$$\overline{E} = \eta\frac{\omega kq\ell}{4\pi r}\left\{\hat{r}2\cos\theta\left[\frac{1}{kr}\sin(kr - \omega t) + \frac{1}{k^2r^2}\cos(kr - \omega t)\right]\right.$$
$$\left. + \hat{\theta}\sin\theta\left[\frac{1}{kr}\sin(kr - \omega t) + (\frac{1}{k^2r^2} - 1)\cos(kr - \omega t)\right]\right\} \quad (1.4.18)$$

The Poynting vector power density is
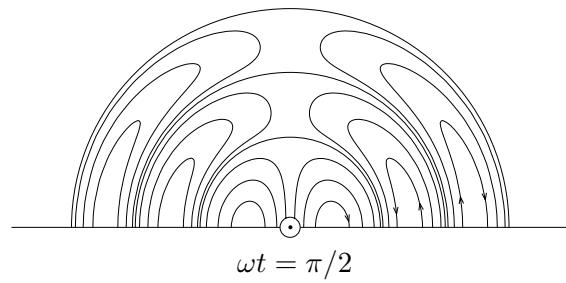
$$\overline{S} = \overline{E} \times \overline{H}$$
$$= \eta\left(\frac{\omega kq\ell}{4\pi\epsilon_o r}\right)^2\left\{-\hat{\theta}\ \sin 2\theta\left[(\frac{1}{k^3r^3} - \frac{1}{kr})\frac{1}{2}\sin 2(kr - \omega t)\right.\right.$$
$$\left. - \frac{1}{k^2r^2}\cos 2(kr - \omega t)\right]$$
$$+ \hat{r}\ \sin^2\theta\left[(\frac{1}{k^3r^3} - \frac{2}{kr})\frac{1}{2}\sin 2(kr - \omega t)\right.$$
$$\left.\left. - \frac{1}{k^2r^2}\cos 2(kr - \omega t) + \cos^2(kr - \omega t)\right]\right\} \quad (1.4.19)$$

We now calculate the time-average of $\overline{S}$. Notice that the time average of $\sin 2(kr - \omega t)$ and $2\cos(kr - \omega t)$ is zero, and the time average of either $\sin^2(kr - \omega t)$ or $\cos^2(kr - \omega t)$ is $1/2$. The above expression, after integration, is equal to the time-average power density at any point $\overline{r}$.

$$<\overline{S}> = \frac{1}{2\pi}\int_0^{2\pi} d(\omega t)\overline{E} \times \overline{H} = \hat{r}\ \frac{\eta}{2}\left(\frac{\omega qk\ell}{4\pi r}\right)^2\sin^2\theta$$

Integrating the $\hat{r}$ directed power over the surface of a sphere of radius r gives [Fig. 1.4.4]

$$P = \oiint dS\,\hat{r}\cdot <\overline{S}> = \int_0^{2\pi} d\phi \int_0^{\pi} d\theta\ r^2\sin\theta\left[\frac{\eta}{2}\left(\frac{\omega qk\ell}{4\pi r}\right)^2\sin^2\theta\right]$$
$$= \int_0^{\pi} d\theta\ 2\pi r^2\sin^3\theta\left[\frac{\omega k^3}{2\epsilon_o}\left(\frac{q\ell}{4\pi r}\right)^2\right] = \frac{4\pi\eta}{3}\left(\frac{\omega qk\ell}{4\pi}\right)^2 = \frac{\eta}{12\pi}(\omega qk\ell)^2$$
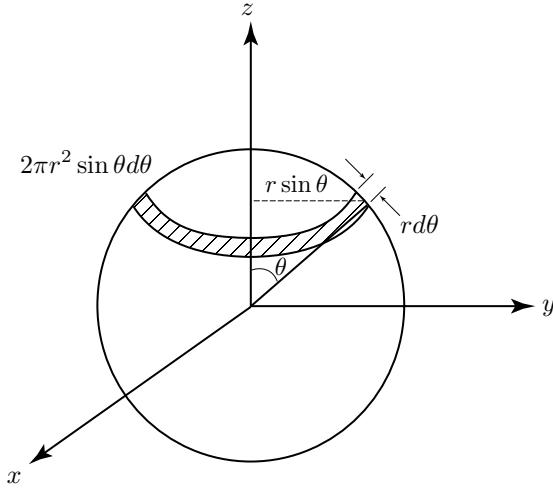
Figure 1.4.4 Integration geometry for time-average power density.

where $2\pi r^2 \sin\theta$ is the ribbon-like surface element to be integrated from $\theta = 0$ to $\theta = \pi$. Notice that the total time-average power leaving the dipole source obtained by calculating with a spherical surface with any radius r is the same.

EXAMPLE 1.4.5

For a Hertzian dipole, the time average of $\overline{E}\cdot\overline{J}$ is, with $\overline{J} = \hat{z}\omega q\ell \sin\omega t\delta(\overline{r})$, and as $r \to 0$,

$$<\overline{E}\cdot\overline{J}> = \frac{\eta k}{2}\frac{(\omega q\ell)^2}{4\pi r}\left\{2\cos^2\theta\left[-\frac{1}{kr}\cos kr + \frac{1}{k^2r^2}\sin kr\right]\right.$$

$$\left. -\sin^2\theta\left[-\frac{1}{kr}\cos kr + (\frac{1}{k^2r^2}-1)\sin kr\right]\right\}\delta(\overline{r})$$

$$=\frac{\eta k}{2}\frac{(\omega q\ell)^2}{4\pi r}\left\{\cos^2\theta\left[\frac{3}{kr}(1-\frac{k^2r^2}{2}+...)+(\frac{3}{k^2r^2}-1)(kr-\frac{k^3r^3}{6}+...)\right]\right.$$

$$\left. -\left[-\frac{1}{kr}(1-\frac{k^2r^2}{2}+...)+(\frac{1}{k^2r^2}-1)(kr-\frac{k^3r^3}{6}+...)\right]\right\}\delta(\overline{r})$$

$$=\frac{\eta k}{2}\frac{(\omega q\ell)^2}{4\pi r}\left\{\left[\frac{2kr}{3}\right]\right\}\delta(\overline{r}) = \frac{\eta}{12\pi}(\omega qk\ell)^2\delta(\overline{r})$$

where we have Talor expanded $\sin kr$ and $\cos kr$ around $r = 0$.

                                                                        — END OF EXAMPLE 1.4.5 —

EXAMPLE 1.4.6

For a dipole moment $\overline{p} = q\overline{\ell}$, the magnetic and electric fields are

$$\overline{H} = \frac{\omega k}{4\pi r}(\overline{p} \times \hat{r})\left[\frac{1}{kr}\sin(kr - \omega t) - \cos(kr - \omega t)\right] \tag{E1.4.6.1}$$

$$\overline{E} = \frac{k^2}{4\pi\epsilon_o r}\left\{[(\overline{p} \times \hat{r}) \times \hat{r} + 2\hat{r}(\hat{r} \cdot \overline{p})]\left[\frac{1}{k^2 r^2}\cos(kr - \omega t) + \frac{1}{kr}\sin(kr - \omega t)\right]\right.$$

$$\left. - [(\overline{p} \times \hat{r}) \times \hat{r}]\cos(kr - \omega t)\right\} \tag{E1.4.6.2}$$

Applying the Biot-Savart law to derive the magnetic field of an infinitely long wire, we first make use of the first term in (E1.4.6.1) with the same approximation as for (1.4.14) to obtain

$$\overline{H} \approx \frac{\omega k}{4\pi r}(\overline{p} \times \hat{r})\frac{1}{kr}\sin(-\omega t) = \frac{1}{4\pi r^2}\left[\frac{d(q\cos\omega t)}{dt}\overline{\ell} \times \hat{r}\right] = \frac{1}{4\pi r^3}(I\overline{\ell} \times \overline{r})$$

where I is the current and $\overline{\ell}$ denotes the direction and length of the current element. The vector $\overline{r} = \hat{\rho}\rho + \hat{z}z'$ points from the source element to the observation point.

— END OF EXAMPLE 1.4.6 —

EXAMPLE 1.4.7

Consider the scattering of electromagnetic waves by particles of size much smaller than a wavelength, such as sunlight by air molecules. Model the particle as a small sphere of radius a with an induced dipole moment proportional to a and the intensity of the illuminating electric field,

$$ql = 4\pi\epsilon_o a^3\left(\frac{\epsilon_a - \epsilon_o}{\epsilon_a + 2\epsilon_o}\right)E_0$$

where ϵ_a is the dielectric constant of the air molecule and E_0 is the incident electric field intensity. The total power P_s re-radiated by the particle acting as a Hertzian dipole is, by virtue of (E1.4.4.3)

$$P_s = \frac{\eta}{12\pi}(\omega q k\ell)^2 = \frac{4\pi}{3\eta}\left(\frac{\epsilon_a - \epsilon_o}{\epsilon_a + 2\epsilon_o}\right)^2 k^4 a^6 E_0^2$$

The scattering cross-section is defined as

$$\sigma_s = \frac{P_s}{E_0^2/2\eta} = \frac{8\pi}{3}\left(\frac{\epsilon_a - \epsilon_o}{\epsilon_a + 2\epsilon_o}\right)^2 k^4 a^6$$

This is known as the result of Rayleigh scattering, which has been used to explain why the sky is blue.

— END OF EXAMPLE 1.4.7 —

John William Strutt (Lord Rayleigh) (12 November 1842 – 30 June 1919) entered Trinity College, Cambridge, in 1861, and graduated in 1865. His first paper in 1865 was on Maxwell's electromagnetic theory. His theory of scattering (1871) provided the explanation of why the sky is blue. From 1879–1884 he succeeded Maxwell as the second Cavendish professor of experimental physics at Cambridge.

Problems

P1.4.1

The magnetic field $\overline{H}$ and electric field $\overline{E}$ of a Hertzian dipole at very large distances $(kr \gg 1)$ are

$$\overline{H} = -\hat{\phi} \frac{\omega k q \ell}{4\pi r} \sin\theta \cos(kr - \omega t)$$

$$\overline{E} = -\hat{\theta} \frac{k^2 q \ell}{4\pi \epsilon_o r} \sin\theta \cos(kr - \omega t)$$

(a) Find the Poynting's power density vector $\overline{S}$ as a function of time. What is the time-averaged power density vector $\langle \overline{S} \rangle$?

(b) By integrating the Poynting vector over the surface of a sphere of radius r, find the time-averaged power P radiated by the Hertzian dipole.

(c) The amplitude of the current in the Hertzian dipole is $I_o = \omega q$. By using $P = \frac{1}{2} I_o^2 R_{rad}$, find the radiation resistance R_{rad} of the Hertzian dipole.

(d) A radio station is 15 km away from a city. The transmitting antenna tower may be modeled as a Hertzian dipole antenna of dipole moment $q\ell$. To maintain the FCC standard of 25 mV/m field strength in the city, how much radiation power P must be provided?

P1.4.2

Determine the static electric field for a Hertzian dipole oriented in a general direction $\overline{p} = \hat{x} p_x + \hat{y} p_y + \hat{z} p_z$, with dipole moment $p = q\ell$.

P1.4.3

Sun navigation was first observed in 1911. It was found that some species of ants, horseshoe crabs, honeybees, etc., are sensitive to polarized light. These creatures can navigate as long as there is a small patch of blue sky. The sky polarization depends upon the angle ϕ between the sun's rays to a particular point in the sky and an observer's line of sight to the same point. The sunlight, which is unpolarized, or randomly polarized, excites air molecules which behave like small dipole antennas when irradiated by the incident electric fields of the sunlight. The scattered electric field $\overline{E}_s'$ for each excited dipole antenna is linearly polarized in planes perpendicular to the sunlight

path; and looking along the sun ray path the scattered wave is unpolarized, or randomly polarized.

At sunset, if an ant looks directly at the sun $(\phi = 0)$, what is the polarization? What is the polarization if the ant looks at the zenith $(\phi = 90°)$ perpendicular to the sun ray path? Show that the sky light appears to be partially linearly polarized when it looks at other parts of the sky [*Scientific American*, July 1955].

P1.4.4
(a) For the electromagnetic field solution of a Hertzian dipole with dipole moment $p = ql$, let $k \to 0$ and show that $\overline{H} = 0$. Determine the electric field $\overline{E}$ of a static dipole with $k = 0$.
(b) Consider the Rayleigh scattering of electromagnetic waves by particles of size much smaller than a wavelength, such as sunlight by air molecules. Model the particle when illuminated with a light wave as an induced Hertzian dipole with dipole moment p, which is proportional to the incident field amplitude E_o, and can be expressed as $p = p_o E_o$. Find the total power P_s re-radiated by the particle. Find the scattering cross-section defined by $2\eta P/E_0^2$. The above result is usually used to explain why the sky is blue.

P1.4.5
Why is sky blue (but why isn't it purple?) ?

P1.4.6
(a) Consider an optical fiber with cross section area A. The electromagnetic wave guided inside the fiber is scattered by the atoms and the molecules making up the fiber. Since the sizes of the scattering particles are much smaller than the guided light wavelength, the process can again be described by Rayleigh scattering. Assume $\epsilon = 2\epsilon_o$, show that the scattered power from each particle is $\frac{\pi}{12\eta} k^4 a^6 E_o^2$.
(b) Assume the guided light has intensity E_0, wavelength 10^{-6} m, and particle radius $a = 10^{-10}$ m. Find the guided power flow in watts and the total scattered power of a fiber with a length of 1 km in terms of the density of the particles inside the fiber N. Calculate the ratio of the scattered power to the guided power.
(c) Assume the particle density is approximately $3/4\pi a^3$ per m^3, estimate, with the numbers given above, the fiber loss per kilometer (in dB/km) due to the Rayleigh scattering.

P1.4.7
Two Hertzian dipole antennas are located at $(0,0,0)$ and $(0,d,0)$ with dipole moments $p_1 = q_1 l$ and $p_2 = q_2 l$ current densities:

$$\overline{J}_1 = \hat{z} I_1 \delta(x)\delta(y)\delta(z) \qquad \text{and} \qquad \overline{J}_2 = \hat{x} I_2 \delta(x)\delta(y-d)\delta(z)$$

as shown in Figure P1.4.7.1. The two in phase dipoles are oriented in z and x directions respectively.
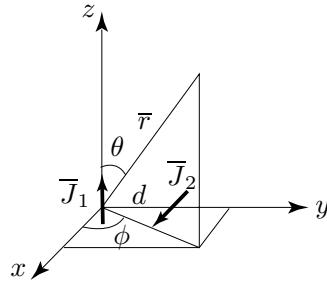
Figure P1.4.7.1

(a) For the x-oriented dipole, the far field ($r \gg 1$) expression of $\overline{E}$ on the yz-plane is:

$$\overline{E}_2 = \hat{x}\frac{k^2 q_2 \ell}{4\pi r\epsilon_0}\cos(k\sqrt{x^2 + (y-d)^2 + z^2} - \omega t)$$

Show that as $d \ll \sqrt{x^2 + y^2 + z^2} = r$

$$\overline{E}_2 = \hat{x}\frac{k^2 q_2 \ell}{4\pi r\epsilon_0}\cos(kr - kd\sin\theta - \omega t)$$

(b) Find the total far field $\overline{E}$ on the yz-plane.

(c) Let q_1 and q_2 be real and positive. On the yz-plane, if the far field $\overline{E}$ for $\theta = 45°$ is circularly polarized,

   (i) Find the minimum d in terms of λ.
   (ii) What is the ratio of q_1/q_2?
   (iii) Specify the handness of the circularly polarized field.

P1.4.8

The Biot-Savart law states that the magnetic field at (r, θ, ϕ) produced by an element of length ℓ at the origin carrying current I along the z axis is

$$\overline{B} = \hat{\phi}\frac{\mu_o I \ell}{4\pi r^2}\sin\theta$$

Consider a wire with infinite length carrying current I in the direction of z. Use the Biot-Savart law to show that the magnetic field produced by the wire is

$$\overline{B} = \hat{\phi}\frac{\mu_o I}{2\pi\rho}$$

where ρ is the distance from the wire. Apply Stokes' theorem to Ampère's law without the displacement term, find $\overline{B}$ and confirm the above result.

For a high-voltage transmission line carrying current $I = 1\,\mathrm{kA}$, find the magnetic field strength 10 meters away from the wire, and compare with the earth magnetic field strength which is approximately 5×10^{-5} Tesla.

1.5   Constitutive Relations

Maxwell's equations govern the behavior of electric field vectors $\overline{D}$ and $\overline{E}$, magnetic field vectors $\overline{B}$ and $\overline{H}$, and source fields $\overline{J}$ and ρ.

$$\nabla \times \overline{H} = \frac{\partial}{\partial t}\overline{D} + \overline{J} \tag{1.5.1}$$

$$\nabla \times \overline{E} = -\frac{\partial}{\partial t}\overline{B} \tag{1.5.2}$$

$$\nabla \cdot \overline{D} = \rho \tag{1.5.3}$$

$$\nabla \cdot \overline{B} = 0 \tag{1.5.4}$$

$$\nabla \cdot \overline{J} = -\frac{\partial}{\partial t}\rho \tag{1.5.5}$$

Equation (1.5.3) can be derived by taking the divergence of (1.5.1) and introducing (1.5.5). Similarly, Eq. (1.5.4) is derivable from divergence of (1.5.2). Giving sources $\overline{J}$ and ρ satisfying (1.5.5), we have a total of six independent scalar equations, three from (1.5.1) and three from (1.5.2), to determine 12 components of the field vectors $\overline{D}$, $\overline{E}$, $\overline{H}$, and $\overline{B}$. Thus we need six more scalar equations.These are the constitutive relations, which provide a mathematical description of the electromagnetic properties of all media.

I proposed that we call them *bianisotropic media* [Kong, 1968] when material media are characterized by the following constitutive relations:

$$\overline{D} = \overline{\overline{\epsilon}} \cdot \overline{E} + \overline{\overline{\xi}} \cdot \overline{H} \tag{1.5.6}$$

$$\overline{B} = \overline{\overline{\zeta}} \cdot \overline{E} + \overline{\overline{\mu}} \cdot \overline{H} \tag{1.5.7}$$

where $\overline{\overline{\epsilon}}$, $\overline{\overline{\mu}}$, $\overline{\overline{\xi}}$, and $\overline{\overline{\zeta}}$ are all 3×3 matrices. Their elements are called *constitutive parameters*. In its most general form, a constitutive parameter can be cast in the form of integro-differential operators. In this section, we discuss special cases of the constitutive relations.

The bianisotropic description of material has fundamental importance from the point of view of relativity. The principle of relativity requires that all physical laws of nature must be characterized by mathematical equations that are form-invariant from one observer to the other. Although the numerical values of the field quantities may vary from one observer to another, the forms of the Maxwell equations in (1.5.1) to (1.5.5) are invariant, and so are the bianisotropic form as expressed in (1.5.6) and (1.5.7) for the constitutive relations.

A. Isotropic Media

For isotropic media, $\overline{\overline{\xi}} = \overline{\overline{\zeta}} = 0$, and $\overline{\overline{\mu}} = \mu\overline{\overline{I}}$ with $\overline{\overline{I}}$ denoting the 3×3 identity matrix. The constitutive relations for an isotropic medium can be written simply as

$$\overline{D} = \epsilon\overline{E} \qquad \text{where } \epsilon = \text{permittivity} \qquad\qquad (1.5.8)$$

$$\overline{B} = \mu\overline{H} \qquad \text{where } \mu = \text{permeability} \qquad\qquad (1.5.9)$$

By isotropy we mean that the field vector $\overline{E}$ is parallel to $\overline{D}$ and the field vector $\overline{H}$ is parallel to $\overline{B}$. In free space void of any matter, $\mu = \mu_o$ and $\epsilon = \epsilon_o$,

$$\mu_o = 4\pi \times 10^{-7} \qquad \text{henry/meter}$$

$$\epsilon_o \approx 8.85 \times 10^{-12} \qquad \text{farad/meter}$$

Inside a material medium, the permittivity ϵ is determined by the electrical properties of the medium and the permeability μ by the magnetic properties of the medium.

EXAMPLE 1.5.1

A dielectric material can be described by a free-space part and a part that is due to the material alone. The material part can be characterized by a polarization vector $\overline{P}$ such that

$$\overline{D} = \epsilon\overline{E} = \epsilon_o\overline{E} + \overline{P} \qquad\qquad (E1.5.1.1)$$

The polarization $\overline{P}$ symbolizes the electric dipole moment per unit volume of the dielectric material. In the presence of an external electric field, the polarization vector may be caused by induced dipole moments, alignment of the permanent dipole moments of the medium, or migration of ionic charges.

A magnetic material can also be described by a free-space part and a part characterized by a magnetization vector $\overline{M}$ such that

$$\overline{B} = \mu\overline{H} = \mu_o\overline{H} + \mu_o\overline{M} \qquad\qquad (E1.5.1.2)$$

A medium is diamagnetic if $\mu < \mu_o$ and paramagnetic if $\mu > \mu_o$. Diamagnetism is caused by induced magnetic moments that tend to oppose the externally applied magnetic field. Paramagnetism is due to alignment of magnetic moments. When placed in an inhomogeneous magnetic field, a diamagnetic material tends to move toward regions of weaker magnetic field, and a paramagnetic material toward regions of stronger magnetic field. Ferromagnetism and antiferromagnetism are highly nonlinear effects.

— END OF EXAMPLE 1.5.1 —

B. Anisotropic Media

For anisotropic media, $\overline{\overline{\xi}} = \overline{\overline{\zeta}} = 0$, and the constitutive relations are usually written as

$$\overline{D} = \overline{\overline{\epsilon}} \cdot \overline{E} \qquad \text{where } \overline{\overline{\epsilon}} = \text{permittivity tensor} \qquad (1.5.10)$$

$$\overline{B} = \overline{\overline{\mu}} \cdot \overline{H} \qquad \text{where } \overline{\overline{\mu}} = \text{permeability tensor} \qquad (1.5.11)$$

The field vector $\overline{E}$ is no longer parallel to $\overline{D}$, and the field vector $\overline{H}$ is no longer parallel to $\overline{B}$. A medium is *electrically anisotropic* if it is described by the permittivity tensor $\overline{\overline{\epsilon}}$ and a scalar permeability μ, and *magnetically anisotropic* if it is described by the permeability tensor $\overline{\overline{\mu}}$ and a scalar permittivity ϵ. Note that a medium can be both electrically and magnetically anisotropic as described by both $\overline{\overline{\epsilon}}$ and $\overline{\overline{\mu}}$ in (1.5.10) and (1.5.11).

Crystals are described in general by symmetric permittivity tensors. There always exists a coordinate transformation that transforms a symmetric matrix into a diagonal matrix. In this coordinate system, called the *principal system,*

$$\overline{\overline{\epsilon}} = \begin{bmatrix} \epsilon_x & 0 & 0 \\ 0 & \epsilon_y & 0 \\ 0 & 0 & \epsilon_z \end{bmatrix} \qquad (1.5.12)$$

The three coordinate axes are referred to as the principal axes of the crystal. For cubic crystals, $\epsilon_x = \epsilon_y = \epsilon_z$ and they are isotropic. In tetragonal, hexagonal, and rhombohedral crystals, two of the three parameters are equal. Such crystals are *uniaxial*. Here there is a two-dimensional degeneracy; the principal axis that exhibits this anisotropy is called the *optic axis.* For a uniaxial crystal with

$$\overline{\overline{\epsilon}} = \begin{bmatrix} \epsilon & 0 & 0 \\ 0 & \epsilon & 0 \\ 0 & 0 & \epsilon_z \end{bmatrix} \qquad (1.5.13)$$

the z axis is the optic axis. The crystal is *positive uniaxial* if $\epsilon_z > \epsilon$; it is *negative uniaxial* if $\epsilon_z < \epsilon$. In orthorhombic, monoclinic, and triclinic crystals, all three crystallographic axes are unequal. We have $\epsilon_x \neq \epsilon_y \neq \epsilon_z$, and the medium is *biaxial.*

C. Bianisotropic Media

For isotropic or anisotropic media, the constitutive relations relate the two electric field vectors and the two magnetic field vectors by either a scalar or a tensor. Such media become polarized when placed in an electric field and become magnetized when placed in a magnetic field. A bianisotropic medium provides the cross-coupling between the electric and magnetic fields. When placed in an electric or a magnetic field, a bianisotropic medium becomes both polarized and magnetized. The constitutive relations for a bianisotropic medium take the form

$$\overline{D} = \overline{\overline{\epsilon}} \cdot \overline{E} + \overline{\overline{\xi}} \cdot \overline{H} \tag{1.5.14a}$$

$$\overline{B} = \overline{\overline{\zeta}} \cdot \overline{E} + \overline{\overline{\mu}} \cdot \overline{H} \tag{1.5.14b}$$

where $\overline{D}$ depends on both $\overline{E}$ and $\overline{H}$, and so does $\overline{B}$.

Magnetoelectric Media

Magnetoelectric materials, theoretically predicted by Dzyaloshinskii, and Landau and Lifshitz [1960], were observed experimentally in 1960 by Astrov [1960] in antiferromagnetic chromium oxide. The constitutive relations that Dzyaloshinskii proposed for chromium oxide have the following form:

$$\overline{D} = \begin{bmatrix} \epsilon & 0 & 0 \\ 0 & \epsilon & 0 \\ 0 & 0 & \epsilon_z \end{bmatrix} \cdot \overline{E} + \begin{bmatrix} \xi & 0 & 0 \\ 0 & \xi & 0 \\ 0 & 0 & \xi_z \end{bmatrix} \cdot \overline{H} \tag{1.5.15a}$$

$$\overline{B} = \begin{bmatrix} \xi & 0 & 0 \\ 0 & \xi & 0 \\ 0 & 0 & \xi_z \end{bmatrix} \cdot \overline{E} + \begin{bmatrix} \mu & 0 & 0 \\ 0 & \mu & 0 \\ 0 & 0 & \mu_z \end{bmatrix} \cdot \overline{H} \tag{1.5.15b}$$

It was then shown by Indenbom [1960] and by Birss [1963] that 58 magnetic crystal classes can exhibit the magnetoelectric effect. Rado [1964] proved that the effect is not restricted to antiferromagnetics; ferromagnetic gallium iron oxide is also magnetoelectric.

Moving Media

Media in motion were the first bianisotropic media to receive attention in electromagnetic theory. In 1888, Wilhelm Röentgen (1845–1923) discovered that a moving dielectric becomes magnetized when it

is placed in an electric field. In 1905, H. A. Wilson showed that a moving dielectric in a uniform magnetic field becomes electrically polarized. Almost any medium becomes bianisotropic when it is in motion.

D. Biisotropic Media

Tellegen Media

In 1948, the gyrator was introduced by B. D. H. Tellegen as a new element, in addition to the resistor, the capacitor, the inductor, and the ideal transformer, for describing a network. To realize his new network element, Tellegen conceived of a medium possessing constitutive relations of the form

$$\overline{D} = \epsilon\overline{E} + \tau\overline{H} \qquad (1.5.16a)$$

$$\overline{B} = \tau\overline{E} + \mu\overline{H} \qquad (1.5.16b)$$

where $\tau^2/\mu\epsilon$ is nearly equal to 1. Tellegen considered that the model of the medium had elements possessing permanent electric and magnetic dipoles parallel or antiparallel to each other, so that an applied electric field that aligns the electric dipoles simultaneously aligns the magnetic dipoles; and a magnetic field that aligns the magnetic dipoles simultaneously aligns the electric dipoles. Tellegen also wrote general constitutive relations (1.5.14) and examined the symmetry properties by energy conservation.

Chiral Media

Chiral media, which include many classes of sugar solutions, amino acids, DNA, and natural substances have the following constitutive relations

$$\overline{D} = \epsilon\overline{E} + \chi\frac{\partial\overline{H}}{\partial t} \qquad (1.5.17a)$$

$$\overline{B} = \mu\overline{H} - \chi\frac{\partial\overline{E}}{\partial t} \qquad (1.5.17b)$$

where χ is the chiral parameter. Media characterized by the constitutive relations (1.5.16) and (1.5.17) are biisotropic media.

E. Constitutive Matrices

Constitutive relations in the most general form can be written as

$$c\overline{D} = \overline{\overline{P}} \cdot \overline{E} + \overline{\overline{L}} \cdot c\overline{B} \tag{1.5.18a}$$

$$\overline{H} = \overline{\overline{M}} \cdot \overline{E} + \overline{\overline{Q}} \cdot c\overline{B} \tag{1.5.18b}$$

where $c = 3 \times 10^8$ m/s is the velocity of light in vacuum, and $\overline{\overline{P}}$, $\overline{\overline{Q}}$, $\overline{\overline{L}}$, and $\overline{\overline{M}}$ are all 3×3 matrices. Their elements are called *constitutive parameters*. In the definition of the constitutive relations, the constitutive matrices $\overline{\overline{L}}$ and $\overline{\overline{M}}$ relate electric and magnetic fields. When $\overline{\overline{L}}$ and $\overline{\overline{M}}$ are not identically zero, the medium is *bianisotropic*. When there is no coupling between electric and magnetic fields, $\overline{\overline{L}} = \overline{\overline{M}} = 0$ and the medium is *anisotropic*. For an anisotropic medium, if $\overline{\overline{P}} = c\epsilon\overline{\overline{I}}$ and $\overline{\overline{Q}} = (1/c\mu)\overline{\overline{I}}$ with $\overline{\overline{I}}$ denoting the 3×3 unit matrix, the medium is *isotropic*. The reason that we write constitutive relations in the present form is based on relativistic considerations. First, the fields $\overline{E}$ and $c\overline{B}$ form a single tensor in four-dimensional space, and so do $c\overline{D}$ and $\overline{H}$. Second, constitutive relations written in the form (1.5.18) are Lorentz-covariant. These aspects will be discussed in Chapter 8.

Equation (1.5.18) can be rewritten in the form

$$\begin{bmatrix} c\overline{D} \\ \overline{H} \end{bmatrix} = \overline{\overline{C}} \cdot \begin{bmatrix} \overline{E} \\ c\overline{B} \end{bmatrix} \tag{1.5.19a}$$

and $\overline{\overline{C}}$ is a 6×6 constitutive matrix:

$$\overline{\overline{C}} = \begin{bmatrix} \overline{\overline{P}} & \overline{\overline{L}} \\ \overline{\overline{M}} & \overline{\overline{Q}} \end{bmatrix} \tag{1.5.19b}$$

which has the dimension of admittance.

The constitutive matrix $\overline{\overline{C}}$ may be a function of space-time coordinates, thermodynamical and continuum-mechanical variables, or electromagnetic field strengths. According to the functional dependence of $\overline{\overline{C}}$, we can classify the various media as (i) inhomogeneous if $\overline{\overline{C}}$ is a function of space coordinates, (ii) nonstationary if $\overline{\overline{C}}$ is a function of time, (iii) time-dispersive if $\overline{\overline{C}}$ contains time derivatives, (iv) spatially dispersive if $\overline{\overline{C}}$ contains spatial derivatives, (v) nonlinear if $\overline{\overline{C}}$

depends on the electromagnetic field, and so forth. In the general case $\overline{\overline{C}}$ may be a function of integro-differential operators and coupled to fundamental equations of other physical disciplines.

We have defined constitutive relations by expressing $\overline{D}$ and $\overline{H}$ in terms of $\overline{E}$ and $\overline{B}$. We may also express constitutive relations in the form of $\overline{D}$ and $\overline{B}$ as a function of $\overline{E}$ and $\overline{H}$:

$$\left[\frac{\overline{D}}{\overline{B}} \right] = \overline{\overline{C}}_{EH} \cdot \left[\frac{\overline{E}}{\overline{H}} \right] \tag{1.5.20a}$$

where in view of (1.5.14) and (1.5.18),

$$\overline{\overline{C}}_{EH} = \left[\begin{matrix} \overline{\overline{\epsilon}} & \overline{\overline{\xi}} \\ \overline{\overline{\zeta}} & \overline{\overline{\mu}} \end{matrix} \right] = \frac{1}{c} \left[\begin{matrix} \overline{\overline{P}} - \overline{\overline{L}} \cdot \overline{\overline{Q}}^{-1} \cdot \overline{\overline{M}} & \overline{\overline{L}} \cdot \overline{\overline{Q}}^{-1} \\ -\overline{\overline{Q}}^{-1} \cdot \overline{\overline{M}} & \overline{\overline{Q}}^{-1} \end{matrix} \right] \tag{1.5.20b}$$

Here $\overline{\overline{C}}_{EH}$ is the constitutive matrix under $\overline{E}\,\overline{H}$ representation.

To express $\overline{E}$ and $\overline{H}$ in terms of $\overline{B}$ and $\overline{D}$, we write

$$\left[\frac{\overline{E}}{\overline{H}} \right] = \overline{\overline{C}}_{DB} \cdot \left[\frac{\overline{D}}{\overline{B}} \right] \tag{1.5.21a}$$

where

$$\overline{\overline{C}}_{DB} = \left[\begin{matrix} \overline{\overline{\kappa}} & \overline{\overline{\chi}} \\ \overline{\overline{\gamma}} & \overline{\overline{\nu}} \end{matrix} \right] = c \left[\begin{matrix} \overline{\overline{P}}^{-1} & -\overline{\overline{P}}^{-1} \cdot \overline{\overline{L}} \\ \overline{\overline{M}} \cdot \overline{\overline{P}}^{-1} & \overline{\overline{Q}} - \overline{\overline{M}} \cdot \overline{\overline{P}}^{-1} \cdot \overline{\overline{L}} \end{matrix} \right] \tag{1.5.21b}$$

In terms of parameters in $\overline{EH}$ representation, we find

$$\overline{\overline{\kappa}} = \left[\overline{\overline{\epsilon}} - \overline{\overline{\xi}} \cdot \overline{\overline{\mu}}^{-1} \cdot \overline{\overline{\zeta}} \right]^{-1}$$

$$\overline{\overline{\chi}} = -\overline{\overline{\kappa}} \cdot \overline{\overline{\xi}} \cdot \overline{\overline{\mu}}^{-1}$$

$$\overline{\overline{\nu}} = \left[\overline{\overline{\mu}} - \overline{\overline{\zeta}} \cdot \overline{\overline{\epsilon}}^{-1} \cdot \overline{\overline{\xi}} \right]^{-1}$$

$$\overline{\overline{\gamma}} = -\overline{\overline{\nu}} \cdot \overline{\overline{\zeta}} \cdot \overline{\overline{\epsilon}}^{-1}$$

Here $\overline{\overline{C}}_{DB}$ is the constitutive matrix under $\overline{D}\,\overline{B}$ representation. The other possible construction for expressing $\overline{E}$ and $\overline{B}$ in terms of $\overline{H}$ and $\overline{D}$ is not shown because it will not be needed in later developments.

Problems

P1.5.1

For each of the following constitutive relations, state whether the given medium is

(1) Isotropic/anisotropic/bianisotropic,
(2) Linear/nonlinear,
(3) Spatially/temporally dispersive,
(4) Homogeneous/inhomogeneous.

(a) Cholesteric liquid crystals can be modeled by a spiral structure with constitutive relations given by

$$\overline{D} = \begin{pmatrix} \epsilon(1 + \delta\cos Kz) & \epsilon\delta\sin Kz & 0 \\ \epsilon\delta\sin Kz & \epsilon(1 - \delta\cos Kz) & 0 \\ 0 & 0 & \epsilon_z \end{pmatrix} \cdot \overline{E}$$

where the spiral direction is along the z axis.

(b) In view of the optical activities in quartz crystals, the constitutive relation for a quartz crystal is phenomenologically described as

$$E_j = \kappa_{ij}D_i + \frac{1}{\mu_o\epsilon_o}G_{ij}\frac{\partial}{\partial t}B_i$$

$$H_j = \frac{1}{\mu_o}B_j - \frac{1}{\mu_o\epsilon_o}G_{ij}\frac{\partial}{\partial t}D_i$$

(c) When a magnetic field $\overline{B}_0$ is applied to a conductor carrying a current, an electric field $\overline{E}$ is developed. This is called the *Hall effect*, discovered by Edwin Herbert Hall in 1879 while he was a graduate student at the Johns Hopkins University. Assuming the conduction carrier drifts with a mean velocity $\overline{v}$ proportional to $R\sigma\overline{E}$, the constitutive relation that takes care of the Hall effect is given by

$$\overline{J} = \sigma\left(\overline{E} + R\sigma\overline{E}\times\overline{B}_0\right)$$

where σ is the conductivity and R is the Hall coefficient. For copper, $\sigma \approx 6.7\times10^7\,\mathrm{mho/m}$ and $R \approx -5.5\times10^{-11}\,\mathrm{m^3/coul}$.

(d) The phenomenon of natural optical activity can be explained with the use of the constitutive relation

$$D_i = \epsilon_{ij}E_j + \gamma_{ijk}\frac{\partial E_j}{\partial x_k}$$

where ϵ_{ij} and γ_{ijk} are functions of frequency and $\gamma_{ijk} = -\gamma_{jik}$.

(e) The phenomenon of pyroelectricity in a crystal is observed when it is heated. The constitutive relation for a *pyroelectric material* can be written as

$$\overline{D} = \overline{D}_0 + \overline{\overline{\epsilon}}\cdot\overline{E}$$

where a spontaneous term $\overline{D}_0$ exists even in the absence of an external field.

(f) The phenomenon in which dipole moments are induced in a crystal by mechanical stress is called *piezoelectricity*. A piezoelectric material is characterized by a piezoelectric tensor $\gamma_{i,kl} = \gamma_{i,lk}$ such that

$$D_i = D_{0i} + \epsilon_{ik} E_k + \gamma_{i,kl} s_{kl}$$

where s_{kl} is the stress tensor to second order in electric fields. All pyro-electric media are also piezoelectric.

(g) An isotropic dielectric can exhibit the Kerr effect when placed in an electric field. In this case the permittivity can be written as

$$\epsilon_{ij} = \epsilon \delta_{ij} + \sigma E_i E_j$$

where ϵ is the unperturbed permittivity. The principal axis of ϵ_{ij} coincides with the electric field.

(h) In an electrooptical material that exhibits Pockel's effect, the constitutive relation can be written as

$$D_i = \epsilon_{ij} E_j + \sigma_{ijk} E_j E_k$$

where $\sigma_{ijk} = \sigma_{jik}$ is a third-rank tensor symmetrical in i and j, and therefore has 18 independent elements.

P1.5.2

Similar to the expression of the constitutive relation $\overline{D} = \overline{\overline{\epsilon}} \cdot \overline{E} = \epsilon_o \overline{E} + \overline{P}$, the constitutive relation $\overline{B} = \overline{\overline{\mu}} \cdot \overline{H}$ can also be represented in terms of a "free-space" part $\mu_o \overline{H}$ and a magnetization vector $\overline{M}$ such that

$$\overline{B} = \mu_o \overline{H} + \mu_o \overline{M}$$

Notice that while $\overline{P}$ has the same dimension as $\overline{D}$, $\overline{M}$ has the same dimension as $\overline{H}$.

In the case of media possessing permanent moments, the polarization $\overline{P}$ and the magnetization $\overline{M}$ are given classically by the Langevin equation

$$L(x) = \coth x - \frac{1}{x}$$

For a paramagnetic material with magnetic moments Nm,

$$M = NmL\left(\frac{mH}{kT}\right)$$

where $k = 1.38 \times 10^{-23}$ joule/kelvin is Boltzmann's constant, and T is the absolute temperature in kelvins. Show that in the low-field limit, since $mH \ll kT$, the medium is linear.

1.6 Boundary Conditions

A. Continuity of Electric and Magnetic Field Components

Assume that there is a plane boundary surface at $z = 0$ separating Regions 1 and 2,
we can derive the boundary condition for $\overline{H}$ by using a small pill-box [Fig. 1.6.1] and
letting Δz go to zero. As across the boundary, field amplitudes may be discontinuous
while on the x-y plane they are not varying much. We thus ignore partial derivatives
with respect to x and y, and keep only partial derivatives with respect to z. We
find that

$$\nabla \times \overline{H} = \frac{\partial}{\partial z}\left\{\hat{z} \times \overline{H}\right\}$$

$$= \lim_{\Delta z \to 0} \frac{1}{\Delta z}\left\{\hat{z} \times \left[\overline{H}(x_0, y_0, z_0 + \frac{\Delta z}{2}) - \overline{H}(x_0, y_0, z_0 - \frac{\Delta z}{2})\right]\right\}$$

$$= \lim_{\Delta z \to 0} \frac{1}{\Delta z}\left\{\hat{z} \times \left[\overline{H}_1 - \overline{H}_2\right]\right\} \tag{1.6.1}$$

where $\overline{H}(x_0, y_0, z_0 + \frac{\Delta z}{2}) = \overline{H}_2$ is in region 2, and $\overline{H}(x_0, y_0, z_0 - \frac{\Delta z}{2}) = \overline{H}_1$ is in
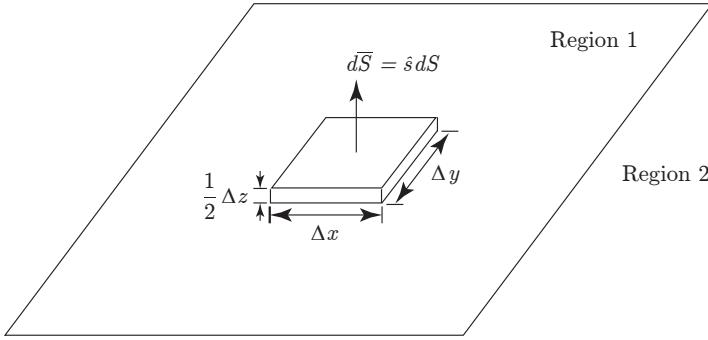region 1.

Figure 1.6.1 Small pill-box volume.

From Ampère's law, letting the surface normal $\hat{n} = \hat{z}$, we find

$$\hat{n} \times (\overline{H}_1 - \overline{H}_2) = \lim_{\Delta z \to 0} \Delta z\left\{\frac{\partial \overline{D}}{\partial t} + \overline{J}\right\} \tag{1.6.2}$$

Assume that the time derivative of $\overline{D}$, $\frac{\partial \overline{D}}{\partial t}$ and the vector current density $\overline{J}$ are both finite, we obtain from (1.6.2) $H_{1y} = H_{2y}; H_{1x} = H_{2x}$ or that

$$\boxed{\hat{n} \times (\overline{H}_1 - \overline{H}_2) = 0} \qquad (1.6.3)$$

Thus the tangential components of the magnetic field $\overline{H}$ are continuous across the boundary surface.

Similar derivations apply to the electric field components. From Faraday's law across the boundary, we conclude that

$$\boxed{\hat{n} \times (\overline{E}_1 - \overline{E}_2) = 0} \qquad (1.6.4)$$

Thus the tangential components of the electric field $\overline{E}$ are continuous across the boundary surface.

Letting Δz go to zero by using the small pill-box in [Fig. 1.6.1], we find from Gauss' law

$$\nabla \cdot \overline{D} = \lim_{\Delta z \to 0} \frac{1}{\Delta z} \left[D_z(x_0, y_0, z_0 + \frac{\Delta z}{2}) - D_z(x_0, y_0, z_0 - \frac{\Delta z}{2}) \right]$$

$$= \lim_{\Delta z \to 0} \frac{1}{\Delta z} \left[\hat{z} \cdot (\overline{D}_1 - \overline{D}_2) \right] \qquad (1.6.5)$$

where $D_z(x_0, y_0, z_0 + \frac{\Delta z}{2}) = D_{1z}$ and $D_z(x_0, y_0, z_0 - \frac{\Delta z}{2}) = D_{2z}$. We find

$$\hat{n} \cdot (\overline{D}_1 - \overline{D}_2) = \lim_{\Delta z \to 0} \rho \, \Delta z \qquad (1.6.6)$$

Assume that the charge density is finite across the boundary, we find

$$\boxed{\hat{n} \cdot (\overline{D}_1 - \overline{D}_2) = 0} \qquad (1.6.7)$$

Thus the normal components of the electric field $\overline{D}$ are continuous across the boundary surface.

Similarly from Gauss' law $\nabla \cdot \overline{B} = 0$, we find

$$\boxed{\hat{n} \cdot (\overline{B}_1 - \overline{B}_2) = 0} \qquad (1.6.8)$$

The normal component of the magnetic field $\overline{B}$ is continuous across the boundary surface. The magnetic field $\overline{H}$ is continuous.

B. Surface Charge and Current Densities

It is often convenient, in particular mathematically, to define regions where the electric and magnetic fields are zero. The media occupying such regions are called perfect conductors, which are idealizations of media where the fields inside are vanishingly small. We assume that all fields in Region 2 are zero, $\overline{E}_2 = \overline{H}_2 = \overline{B}_2 = \overline{D}_2 = 0$.

Electric charges and currents are located primarily in a very thin layer on the surface of perfect conductors. Thus on the surface of perfect conductors, we assume ρ is infinite contained in a zero thickness. We may define a surface charge density

$$\rho_s = \lim_{\Delta z \to 0} \rho \Delta z$$

which is finite and has dimension coulombs/m^2. The concept of surface charge density will have very practical usefulness. As $\overline{D}_2 = 0$, Equation (1.6.6) becomes

$$\boxed{\rho_s = \hat{n} \cdot \overline{D}_1} \qquad (1.6.9)$$

Thus the difference between the $\overline{D}$ field components normal to the boundary surface is equal to the surface charge density at the boundary surface.

On the right hand side of (1.6.2), the time derivatives $\partial D_x/\partial t$ and $\partial D_y/\partial t$ are finite but we may assume J_x and J_y to be infinite to create a surface current density $\overline{J}_s$ when $\Delta z \to 0$:

$$\overline{J}_s = \lim_{\substack{\Delta z \to 0 \\ \overline{J} \to \infty}} \overline{J} \, \Delta z \qquad (1.6.10)$$

We obtain from (1.6.1), as $\overline{H}_2 = 0$,

$$\boxed{\overline{J}_s = \hat{n} \times \overline{H}_1} \qquad (1.6.11)$$

Thus the discontinuity in the tangential components of $\overline{H}$ is equal to the surface current at the boundary surface.

The boundary conditions (1.6.8) and (1.6.4) remain unchanged,

$$\hat{n} \times \overline{E}_1 = 0$$

$$\hat{n} \cdot \overline{B}_1 = 0$$

the normal component of the magnetic field $\overline{B}$ and the tangential components of the electric field $\overline{E}$ are continuous.

C. Boundary Conditions

The Maxwell equations have been written in differential form. They must be supplemented with boundary conditions and initial conditions wherever derivatives do not exist. The boundary conditions can be derived from either the differential form or the integral form of the Maxwell equations. The field vectors $\overline{E}$, $\overline{B}$, $\overline{D}$, and $\overline{H}$ are assumed to be finite but may be discontinuous across the boundary. The volume current and charge densities $\overline{J}$ and $\overline{\rho}$, however, may be infinite, such as on the surface of a perfect conductor, where we can define the surface current density $\overline{J}_s = \delta \overline{J}$ in the limit as $\delta \to 0$ and $\overline{J} \to \infty$,

$$\overline{J}_s = \lim_{\substack{\delta \to 0 \\ \overline{J} \to \infty}} \overline{J} \, \delta \tag{1.6.12}$$

and the surface charge density $\rho_s = \delta \rho$ in the limit as $\delta \to 0$ and $\rho \to \infty$

$$\rho_s = \lim_{\substack{\delta \to 0 \\ \rho \to \infty}} \rho \, \delta \tag{1.6.13}$$

The surface current density has dimension amp/m and the surface charge density has dimension $coul/m^2$.

For a stationary boundary separating regions 1 and 2, we let the surface normal $\hat{n}$ point from region 2 to region 1. The boundary conditions are as follows:

$$\hat{n} \times (\overline{E}_1 - \overline{E}_2) = 0 \tag{1.6.14}$$

$$\hat{n} \times (\overline{H}_1 - \overline{H}_2) = \overline{J}_s \tag{1.6.15}$$

$$\hat{n} \cdot (\overline{B}_1 - \overline{B}_2) = 0 \tag{1.6.16}$$

$$\hat{n} \cdot (\overline{D}_1 - \overline{D}_2) = \rho_s \tag{1.6.17}$$

where subscripts 1 and 2 denote fields in regions 1 and 2, respectively. Essentially the boundary conditions state that the tangential components of $\overline{E}$ and the normal components of $\overline{B}$ are continuous across the boundary; the discontinuity of the tangential components of $\overline{H}$ is equal to the surface current density $\overline{J}_s$; and the discontinuity of the normal components of $\overline{D}$ is equal to the surface charge density ρ_s.

EXAMPLE 1.6.1   Derivation of boundary conditions.
     We now derive the boundary conditions by using integral formulas. First
we consider the integration of a vector field $\overline{A}$ over a volume V enclosed by
a surface S with surface normal $\hat{s}$. The following formulas are useful:
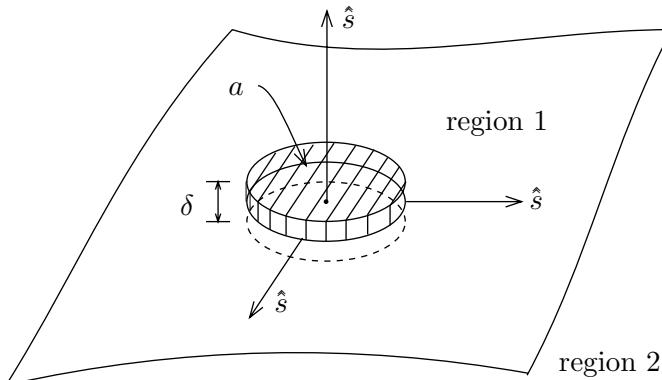
$$\iiint dV\, \nabla \cdot \overline{A} = \oiint dS\, \hat{s} \cdot \overline{A} \qquad (E1.6.1.1a)$$

$$\iiint dV\, \nabla \times \overline{A} = \oiint dS\, \hat{s} \times \overline{A} \qquad (E1.6.1.1b)$$

where $(E1.6.1.1a)$ is the familiar Gauss' theorem which relates integration
of the divergence of the vector field $\overline{A}$ over the volume V to the integra-
tion of the field over the surface S enclosing V. Equation $(E1.6.1.1b)$ is
derived from $(E1.6.1.1a)$ by noting that $\nabla \cdot (\overline{C} \times \overline{A}) = -\overline{C} \cdot \nabla \times \overline{A}$ where
$\overline{C}$ is a constant vector independent of position. Applying the Gauss' theorem
$(E1.6.1.1a)$ to $\nabla \cdot (\overline{C} \times \overline{A})$, we obtain

$$-\overline{C} \cdot \iiint dV\, \nabla \times \overline{A} = \oiint dS\, \hat{s} \cdot \overline{C} \times \overline{A} = -\overline{C} \cdot \oiint dS\, \hat{s} \times \overline{A}$$

This is seen to be $(E1.6.1.1b)$ dot-multiplied by $\overline{C}$ on both sides. Letting $\overline{C}$
be an arbitrary vector, the result is then $(E1.6.1.1b)$.

Figure E1.6.1.1 Pillbox for derivation of boundary conditions.

     Now consider an interface separating regions 1 and 2 [Fig. E1.6.1.1]. As-
sume a small pillbox volume across the interface. Integrating Maxwell equa-
tions over the volume and applying (E1.6.1.1), we obtain

$$\oiint dS\,\hat{s} \times \overline{E} = -\iiint dV \frac{\partial}{\partial t}\overline{B} \qquad\qquad \text{(E1.6.1.2)}$$

$$\oiint dS\,\hat{s} \times \overline{H} = \iiint dV \frac{\partial}{\partial t}\overline{D} + \iiint dV\,\overline{J} \qquad \text{(E1.6.1.3)}$$

$$\oiint dS\,\hat{s} \cdot \overline{B} = 0 \qquad\qquad \text{(E1.6.1.4)}$$

$$\oiint dS\,\hat{s} \cdot \overline{D} = \iiint dV\,\rho \qquad\qquad \text{(E1.6.1.5)}$$

These are the Maxwell equations in integral form, which will be used to derive boundary conditions for both stationary and moving boundaries.

If we assume that the boundary surface is not in motion, then for the terms involving partial derivatives with time, $\partial/\partial t$ can be moved to the outside of the integral. Since the integration is over the volume, the result is a function of time only, and the partial derivatives become total derivatives. Therefore, for stationary boundary surfaces, the Maxwell equations in integral form become

$$\oiint dS\,\hat{s} \times \overline{E} = -\frac{d}{dt}\iiint dV\,\overline{B} \qquad\qquad \text{(E1.6.1.6)}$$

$$\oiint dS\,\hat{s} \times \overline{H} = \frac{d}{dt}\iiint dV\,\overline{D} + \iiint dV\,\overline{J} \qquad \text{(E1.6.1.7)}$$

$$\oiint dS\,\hat{s} \cdot \overline{B} = 0 \qquad\qquad \text{(E1.6.1.8)}$$

$$\oiint dS\,\hat{s} \cdot \overline{D} = \iiint dV\,\rho \qquad\qquad \text{(E1.6.1.9)}$$

Now we let the volume of the pillbox approach zero in such a manner that the thickness of the ribbon side, δ, goes to zero before the top and bottom areas a shrink to a point. We dispose of terms of the order of δ.

We see that the terms involving time derivatives in (E1.6.1.6) and (E1.6.1.7) drop out because they are proportional to δ. We then consider the right-hand sides of (E1.6.1.7) and (E1.6.1.9) which become $\delta a\overline{J}$ and $\delta a\rho$, respectively. If $\overline{J}$ and ρ are finite, both terms will be zero because they are proportional to δ. When there are surface charges and currents at the boundary, the right-hand sides of (E1.6.1.7) and (E1.6.1.9) become $a\overline{J}_s$ and $a\rho_s$. We then see that the surface integral terms involving cross and dot products will be dropped except when $\hat{s}$ is in the directions $\hat{n}$ or $-\hat{n}$. After canceling a on both sides of the equations, we obtain from (E1.6.1.6)–(E1.6.1.9) the boundary conditions (1.6.14)–(1.6.17).

— End of Example 1.6.1 —

EXAMPLE 1.6.2

Consider an electromagnetic wave with

$$\overline{E}_i = \hat{x}E_0 \cos(kz - \omega t) \qquad\qquad (E1.6.2.1a)$$

$$\overline{H}_i = \hat{y}H_0 \cos(kz - \omega t) \qquad\qquad (E1.6.2.1b)$$

impinging upon the surface of a perfectly conducting surface [Fig. E1.6.2.1]. The boundary condition at the surface of the boundary requires that

$$\hat{n} \times (\overline{E}_1 - \overline{E}_2) = 0 \qquad\qquad (E1.6.2.2a)$$

$$\hat{n} \times (\overline{H}_1 - \overline{H}_2) = \overline{J}_s \qquad\qquad (E1.6.2.2b)$$

where $\hat{n} = -\hat{z}$ is the normal to the surface. A perfect conductor is defined to have fields zero inside, thus $\overline{E}_2 = \overline{H}_2 = 0$.
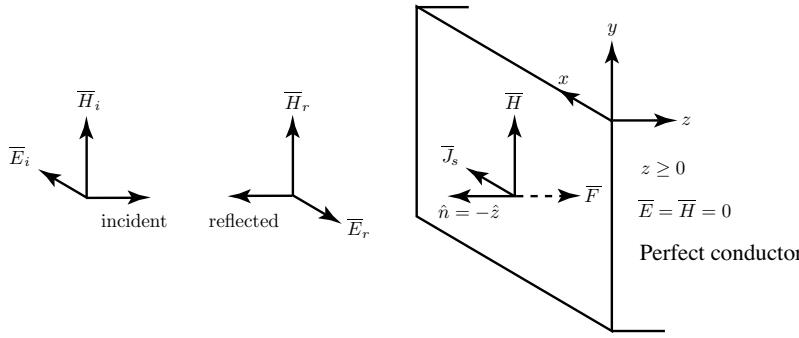

Figure E1.6.2.1 Reflection by a perfect conductor.

The reflected wave that satisfies the boundary conditions (E1.6.2.2) is

$$\overline{E}_r = -\hat{x}E_0 \cos(kz + \omega t) \qquad\qquad (E1.6.2.3a)$$

$$\overline{H}_r = \hat{y}H_0 \cos(kz + \omega t) \qquad\qquad (E1.6.2.3b)$$

which is propagating in the $-\hat{z}$ direction. The surface current $\overline{J}_s$ at $z = 0$ is found to be

$$\overline{J}_s = \hat{n} \times [(\overline{H}_i + \overline{H}_r) - 0]_{z=0} = \hat{x}2H_0 \cos \omega t$$

The magnetic field at $z = 0$ is $\overline{B} = \mu_o(\overline{H}_i + \overline{H}_r) = \hat{y}2\mu_o H_0 \cos \omega t$. From the Lorentz force law, the force density acting on $\overline{J}_s$ is

$$\overline{F} = \frac{1}{2}\overline{J}_s \times \overline{B} = \hat{z}2\mu_o H_0^2 \cos^2 \omega t$$

The factor $1/2$ is due to the fact that there is magnetic field only on one side of the current sheet. The time-average value is thus

$$F = \mu_o H_0^2$$

which is twice the value of the incident radiation pressure in Example 1.3.13. This is because the reflected wave is in the $-\hat{z}$ direction, and it exerts a recoil force on the conductor when it launches the reflected wave.

— End of Example 1.6.2 —

Problems

P1.6.1

Derive boundary conditions for $\overline{E}$ and $\overline{H}$ by applying Stokes' theorem to [P1.6.1.1].
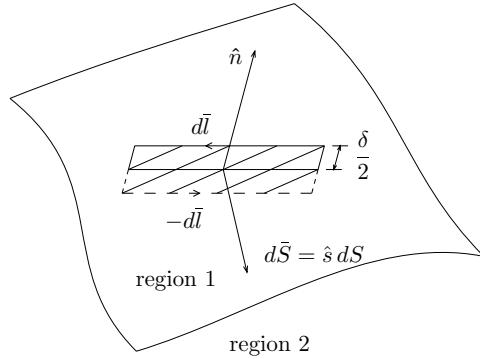
Figure P1.6.1.1   Derivation of boundary condition with Stokes' theorem.

P1.6.2

Derive the boundary conditions for $\overline{H}$ by applying the curl theorem to a small pill-box volume on the x-y plane which has an area A and an infinitesimal thickness Δz.

P1.6.3

Applying the divergence theorem (1.1.19) and integrating over the pillbox volume in Fig. E1.6.1.1 with area a and circumferential length l to find boundary condition for $\overline{D}$.

1.7   Reflection and Guidance

A. Wave Vector $\overline{k}$

The electric field $\overline{E}(\overline{r}, t)$ is governed by the Helmholtz wave equation.

$$\left(\nabla^2 - \mu\epsilon\frac{\partial^2}{\partial t^2}\right)\overline{E}(\overline{r}, t) = 0 \qquad (1.7.1)$$

with

$$\nabla^2 = \frac{\partial^2}{\partial x^2} + \frac{\partial^2}{\partial y^2} + \frac{\partial^2}{\partial z^2} \qquad (1.7.2)$$

as the Laplacian operator ∇^2 in rectangular coordinate system.

Consider the solution

$$\overline{E}(\overline{r}, t) = \overline{E}\cos\left(k_x x + k_y y + k_z z - \omega t\right) \qquad (1.7.3)$$

where $\overline{E}$ is a constant vector. The electric field vector in (1.7.3) represents a linearly polarized wave. Since a general polarization can be expressed as a combination of two linear polarizations, the following analysis applies to all polarizations.

Substituting (1.7.3) into (1.7.1), we obtain the dispersion relation

$$\boxed{k_x^2 + k_y^2 + k_z^2 = \omega^2\mu\epsilon = k^2} \qquad (1.7.4)$$

We define a vector

$$\overline{k} = \hat{x}k_x + \hat{y}k_y + \hat{z}k_z \qquad (1.7.5)$$

The vector $\overline{k}$ is called the wave vector, the propagation vector, or simply the $\overline{k}$ vector. By virtue of the dispersion relation (1.7.4), we see that the magnitude of the $\overline{k}$ vector is equal to $\omega(\mu\epsilon)^{1/2}$.

The scalar product of the wave vector $\overline{k} = \hat{x}k_x + \hat{y}k_y + \hat{z}k_z$ and the position vector $\overline{r} = \hat{x}x + \hat{y}y + \hat{z}z$ gives

$$\overline{k}\cdot\overline{r} = k_x x + k_y y + k_z z$$

A constant phase front is determined by $\overline{k}\cdot\overline{r} = \text{constant}$, which indicates that the front is a plane perpendicular to the $\overline{k}$ vector [Fig. 1.7.1]. The phase front is a plane and the amplitude of the electric field on the plane is a constant. We call the solution in (1.7.3) a uniform plane
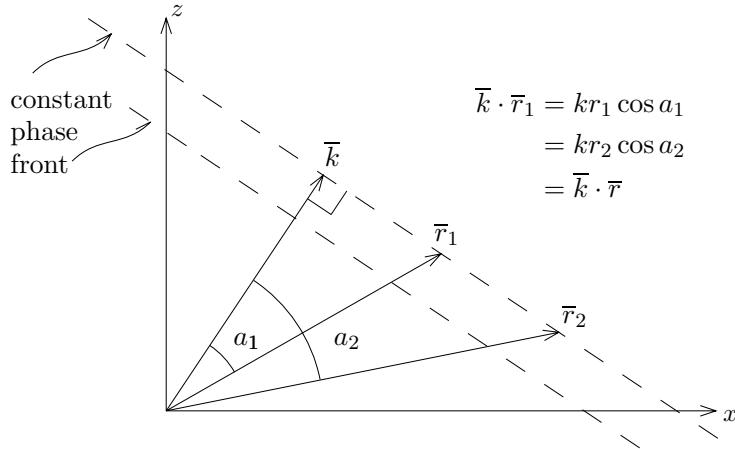
Figure 1.7.1 Constant phase fronts of a plane wave.

wave. A plane wave is non-uniform if its phase front is a plane but the amplitudes of the field are not constant. Since the constant phase front must be perpendicular to $\overline{k}$ at all times, we conclude that this phase front propagates in the direction of $\overline{k}$.

B. Reflection and Transmission of TE Waves

Consider a plane wave incident from a medium with permittivity ϵ_0 and permeability μ_0 upon a dielectric medium with permittivity ϵ_t and permeability μ_0. The boundary surface of the two media is situated at $x = 0$. Let the incident plane wave be linearly polarized with the electric field vector in the $\hat{y}$ direction [Fig. 1.7.2].

We call the x-z plane the plane of incidence, which is formally defined as the plane formed by the normal to the boundary surface and the incident wave vector $\overline{k}$. The incident electric field vector $\overline{E}_i$ is perpendicular to the plane of incidence and the magnetic field vector $\overline{H}_i$ is parallel to the plane of incidence. We call the incident wave a transverse electric (TE) wave. The TE wave is also called perpendicularly polarized, horizontally polarized, or simply the E wave or s wave.

An incident wave of general polarization can be decomposed into two linearly polarized waves; one with the electric field vector perpendicular to the plane of incidence which is the TE wave, and one with the electric field vector parallel to the plane of incidence which is called
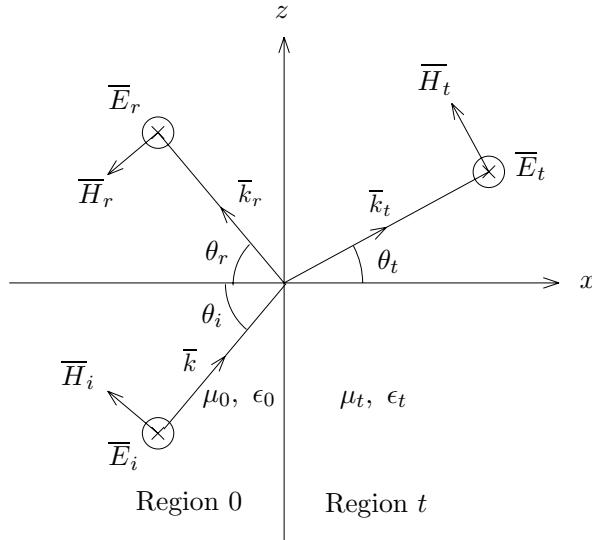
Figure 1.7.2 Reflection and transmission of TE waves at a plane boundary separating Regions 0 **and** t.

the transverse magnetic (TM) wave. The TM wave will have the magnetic field vector perpendicular to the plane of incidence and is also called parallelly polarized, vertically polarized, or simply the H wave or p wave. We shall first study the case of TE wave incidence.

The incident electric field vector is assumed to have unit amplitude and is written as

$$\overline{E}_i(\overline{r}, t) = \hat{y}\cos(\overline{k} \cdot \overline{r} - \omega t)$$
$$= \hat{y}\cos(k_x x + k_z z - \omega t) \qquad (1.7.6a)$$

with the wave vector

$$\overline{k} = \hat{x}k_x + \hat{z}k_z$$

The magnetic field vector

$$\overline{H}_i(\overline{r}, t) = \frac{1}{\omega\mu_0}(-\hat{x}k_z + \hat{z}k_x)\cos(k_x x + k_z z - \omega t) \qquad (1.7.6b)$$

The Poynting vector power density for the incident plane wave is

$$\overline{S}_i(\overline{r}, t) = \overline{E}_i(\overline{r}, t) \times \overline{H}_i(\overline{r}, t)$$
$$= \overline{k}\frac{1}{\omega\mu_0}\cos^2(k_x x + k_z z - \omega t) \qquad (1.7.6c)$$

which is in the direction of the wave vector $\overline{k}$.

The reflected fields for the incident TE wave are

$$\overline{k}_r = -\hat{x}k_{rx} + \hat{z}k_{rz} \tag{1.7.7a}$$

$$\overline{E}_r(\overline{r}, t) = \hat{y}R\cos(-k_{rx}x + k_{rz}z - \omega t) \tag{1.7.7b}$$

$$\overline{H}_r(\overline{r}, t) = -\frac{1}{\omega\mu_0}(\hat{x}k_{rz} + \hat{z}k_{rx})R\cos(k_x x + k_z z - \omega t) \tag{1.7.7c}$$

The Poynting vector power density for the reflected plane wave is

$$\overline{S}_r(\overline{r}, t) = \overline{k}_r\frac{R^2}{\omega\mu_0}\cos^2(k_{rx}x + k_{rz}z - \omega t) \tag{1.7.7d}$$

where R is the reflection coefficient for the electric field component.

The incident wave vector $\overline{k} = \hat{x}k_x + \hat{z}k_z$ and the reflected wave vector $\overline{k}_r = -\hat{x}k_{rx} + \hat{z}k_{rz}$ are governed by the dispersion relations

$$k_x^2 + k_z^2 = \omega^2\mu_0\epsilon_0 = k^2 \tag{1.7.8}$$

$$k_{rx}^2 + k_{rz}^2 = \omega^2\mu_0\epsilon_0 = k_r^2 \tag{1.7.9}$$

This is seen by substituting $(1.7.6a)$ and $(1.7.7a)$ in the Helmholtz wave equations for E_{iy} and E_{ry}.

In Region t, we write the transmitted TE wave solution in the following form

$$\overline{k}_t = \hat{x}k_{tx} + \hat{z}k_{tz} \tag{1.7.10a}$$

$$\overline{E}_t(\overline{r}, t) = \hat{y}T\cos(k_{tx}x + k_{tz}z - \omega t) \tag{1.7.10b}$$

$$\overline{H}_t(\overline{r}, t) = \frac{T}{\omega\mu_t}(-\hat{x}k_{tz} + \hat{z}k_{tx})\cos(k_{tx}x + k_{tz}z - \omega t) \tag{1.7.7c}$$

$$\overline{S}_t(\overline{r}, t) = \overline{k}_t\frac{T^2}{\omega\mu_t}\cos^2(k_x x + k_z z - \omega t) \tag{1.7.7d}$$

where T is the transmission coefficient, and the dispersion relation

$$k_{tx}^2 + k_{tz}^2 = \omega^2\mu_t\epsilon_t = k_t^2 \tag{1.7.11}$$

governs the magnitude k_t for the transmitted wave vector $\overline{k}_t = \hat{x}k_{tx} + \hat{z}k_{tz}$.

Let the boundary surface be at $x = 0$ where the tangential components of $\overline{E}$ and $\overline{H}$ are continuous for all z and t. We obtain

$$\cos(k_z z - \omega t) + R\cos(k_{rz} z - \omega t) = T\cos(k_{tz} z - \omega t) \quad (1.7.12)$$

$$\frac{k_x}{\mu_0}\cos(k_z z - \omega t) - \frac{k_{rx}}{\mu_0}R\cos(k_{rz} z - \omega t) = \frac{k_{tx}}{\mu_t}T\cos(k_{tz} z - \omega t)$$

$$(1.7.13)$$

Since (1.7.12) and (1.7.13) must hold for all z and t, it follows that

$$\boxed{k_z = k_{rz} = k_{tz}} \qquad (1.7.14)$$

This is called the phase matching condition.

From the dispersion relations (1.7.8) and (1.7.9), we find $k_{rx} = k_x$. Equations (1.7.12) and (1.7.13) then reduce to

$$1 + R = T \qquad (1.7.15)$$

$$1 - R = \frac{\mu_0 k_{tx}}{\mu_t k_x}T \qquad (1.7.16)$$

Note that the boundary conditions of normal $\overline{D}$ and normal $\overline{B}$ components continuous at $x = 0$ are satisfied since the condition of continuous normal $\overline{B}$ yields the same equation as (1.7.15) and there is no normal $\overline{D}$ component.

The reflection and transmission coefficients R and T are determined from (1.7.15) and (1.7.16), giving

$$R = R_{0t}^{TE} = \frac{1 - p_{0t}^{TE}}{1 + p_{0t}^{TE}} \qquad (1.7.17)$$

$$T = T_{0t}^{TE} = \frac{2}{1 + p_{0t}^{TE}} \qquad (1.7.18)$$

where

$$p_{0t}^{TE} = \frac{\mu_0 k_{tx}}{\mu_t k_x} \qquad (1.7.19)$$

With p_{0t}^{TE} for the TE waves defined in (1.7.19), R_{0t}^{TE} in (1.7.17) is called the Fresnel reflection coefficient for a TE wave incident from Region 0 and reflected at the boundary separating Regions 0 and t. In (1.7.18), T_{0t}^{TE} is the transmission coefficient from Region 0 to Region t.

Augustin Jean Fresnel (10 May 1788 – 14 July 1827)

Augustin Fresnel was educated at the Ecole Polytechnique and served as an engineer in various departments of France. With his mathematical analysis, he removed a number of objections to the wave theory, and used the wave theory to calculate diffraction patterns that agreed with experimental observations. He developed a system of lenses which has revolutionized lighthouse illumination throughout the world.

Equation (1.7.14), the phase matching condition, is a very important formula arising from the boundary conditions. In terms of the angle of incidence θ_i, the angle of reflection θ_r, and the angle of transmission θ_t, and the relation $k_r = k$ as seen from (1.7.8) and (1.7.9), the phase matching condition (1.7.14) gives

$$k \sin \theta_i = k_r \sin \theta_r = k_t \sin \theta_t$$

Thus the angle of reflection is equal to the angle of incidence $\theta_r = \theta_i$, and

$$\frac{\sin \theta_t}{\sin \theta_i} = \frac{k}{k_t} = \frac{\sqrt{\mu_0 \epsilon_0}}{\sqrt{\mu_t \epsilon_t}} = \frac{n_0}{n_t} \qquad (1.7.20)$$

where $n_0 = c\sqrt{\mu_0 \epsilon_0}$ is called the refractive index for Region 0 and $n_t = c\sqrt{\mu_t \epsilon_t}$ is the refractive index for Region t. Equation (1.7.20) is known as Snell's law.

Willebrord van Roijen Snell (1580 – 1626) studied at the University of Leiden and received his degree in 1607. In 1613 he succeeded his father as professor of mathematics at the University of Leiden. Snell's law for the refraction of light between two media was experimentally discovered in 1621.

Power Conservation

The time-average Poynting vectors for the incident, the reflected, and the transmitted waves are calculated to be

$$<\overline{S}_i> = \frac{1}{2\omega\mu_0}\overline{k} = \frac{1}{2\omega\mu_0}(\hat{x}k_x + \hat{z}k_z) \qquad (1.7.21)$$

$$<\overline{S}_r> = \frac{|R|^2}{2\omega\mu_0}\overline{k}_r = \frac{|R|^2}{2\omega\mu_0}(-\hat{x}k_x + \hat{z}k_z) \qquad (1.7.22)$$

$$<\overline{S}_t> = \frac{|T|^2}{2\omega\mu_t}\overline{k}_t = \frac{|T|^2}{2\omega\mu_t}(\hat{x}k_{tx} + \hat{z}k_z) \qquad (1.7.23)$$
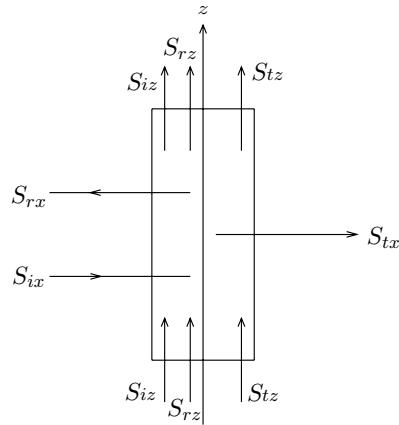
Figure 1.7.3 Power conservation at a plane boundary.

Power conservation is observed by considering a control volume across the boundary surface [Fig. 1.7.3]. We must prove that the x components of all the Poynting vectors entering and exiting the control volume are equal. We define the power reflection coefficient or the *reflectivity* to be

$$r = \frac{-\hat{x}\cdot <\overline{S}_r>}{\hat{x}\cdot <\overline{S}_i>} = |R|^2 \qquad (1.7.24)$$

and the power transmission coefficient or the *transmissivity* to be

$$t = \frac{\hat{x}\cdot <\overline{S}_t>}{\hat{x}\cdot <\overline{S}_i>} = p_{0t}\,|T|^2 \qquad (1.7.25)$$

By virtue of (1.7.17)–(1.7.18), we see that

$$r + t = 1$$

This demonstrates power conservation for reflection and transmission at a plane boundary surface.

EXERCISE 1.7.1   Notice that

$$<S_{ix}> - <S_{rx}> = <S_{tx}>$$
$$<S_{iz}> - <S_{rz}> \neq <S_{tz}>$$

— END OF EXERCISE 1.7.1 —

C. Reflection and Transmission of TM Waves

The reflection and transmission of TM waves [Fig. 1.7.4] by a plane boundary can be carried out in a manner similar to the treatment of TE waves. The incident magnetic field vector $\overline{H}_i = \hat{y}H_{iy}$ is assumed to have unit amplitude and the magnetic and electric field components are written as

$$H_{iy} = \cos(k_x x + k_z z - \omega t) \qquad (1.7.26a)$$

$$E_{ix} = \frac{k_z}{\omega\epsilon_0}\cos(k_x x + k_z z - \omega t) \qquad (1.7.26b)$$

$$E_{iz} = -\frac{k_x}{\omega\epsilon_0}\cos(k_x x + k_z z - \omega t) \qquad (1.7.26c)$$
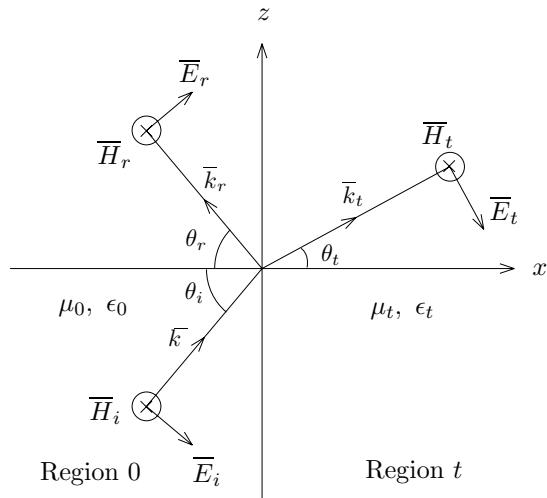

Figure 1.7.4 Reflection and transmission of TM waves.

The reflected field components for the incident TM wave are

$$H_{ry} = R^{TM}\cos(-k_{rx}x + k_{rz}z - \omega t) \qquad (1.7.27a)$$

$$E_{rx} = \frac{k_{rz}}{\omega\epsilon_0}R^{TM}\cos(-k_{rx}x + k_{rz}z - \omega t) \qquad (1.7.27b)$$

$$E_{rz} = \frac{k_{rx}}{\omega\epsilon_0}R^{TM}\cos(-k_{rx}x + k_{rz}z - \omega t) \qquad (1.7.27c)$$

where R^{TM} is the reflection coefficient for the magnetic field component H_{iy}. In Region t, the transmitted TM field components are

$$H_{ty} = T^{TM} \cos(k_{tx}x + k_{tz}z - \omega t) \tag{1.7.28a}$$

$$E_{tx} = \frac{k_{tz}}{\omega \epsilon_t} T^{TM} \cos(k_{tx}x + k_{tz}z - \omega t) \tag{1.7.28b}$$

$$E_{tz} = -\frac{k_{tx}}{\omega \epsilon_t} T^{TM} \cos(k_{tx}x + k_{tz}z - \omega t) \tag{1.7.28c}$$

where T^{TM} is the transmission coefficient for the magnetic field component H_{iy}.

The incident wave vector $\overline{k} = \hat{x}k_x + \hat{z}k_z$, the reflected wave vector $\overline{k}_r = -\hat{x}k_{rx} + \hat{z}k_{rz}$, and the transmitted wave vector satisfy the same dispersion relations (1.7.8), (1.7.9), and (1.7.11) as for the TE wave case. Matching the boundary conditions of tangential components of $\overline{E}$ and $\overline{H}$ continuous at $x = 0$, we obtain the same phase matching condition (1.7.14) and the reflection and transmission coefficients R^{TM} and T^{TM}

$$R^{TM} = R_{0t}^{TM} = \frac{1 - p_{0t}^{TM}}{1 + p_{0t}^{TM}} \tag{1.7.29}$$

and

$$T^{TM} = T_{0t}^{TM} = \frac{2}{1 + p_{0t}^{TM}} \tag{1.7.30}$$

where

$$p_{0t}^{TM} = \frac{\epsilon_0 k_{tx}}{\epsilon_t k_x} \tag{1.7.31}$$

Note that the Fresnel reflection coefficient for TM waves is now representing the ratio of the reflected and incident *magnetic* fields.

EXERCISE 1.7.2   At the surface of a perfect conductor, we may calculate the reflection coefficients by letting $\epsilon_t \to \infty$. We find that for TE waves $p_{0t}^{TE} \to \infty$ and $R_{0t}^{TE} \to -1$ while for TM waves $p_{0t}^{TM} \to 0$ and $R_{0t}^{TM} \to 1$. Thus the tangential electric field vanishes at the boundary and the tangential magnetic field doubles its strength in order to support the induced surface currents.

$-$ END OF EXERCISE 1.7.2 $-$

D. Brewster Angle and Zero Reflection

The Brewster angle θ_b is the incident angle $\theta_i = \theta_b$ at which there is no reflected power. Setting $R = 0$ or $p_{0t} = 1$ we find, from (1.7.19), for TE waves $k_{tx} = k_x$ or

$$k_t \cos \theta_t = k \cos \theta_i \qquad (1.7.32)$$

To solve for the incident angle, we make use of Snell's law

$$k_t \sin \theta_t = k \sin \theta_i \qquad (1.7.33)$$

It follows from (1.7.32) and (1.7.33) that $\theta_t = \theta_i$ and $\epsilon_t = \epsilon_0$. Thus there is zero reflection since there is no boundary.

For TM waves, we obtain from (1.7.31), $\epsilon_0 k_{tx} = \epsilon_t k_x$ or

$$\epsilon_0 k_t \cos \theta_t = \epsilon_t k \cos \theta_i \qquad (1.7.34)$$

Since $k = \omega \sqrt{\mu_0 \epsilon}$ and $k_t = \omega \sqrt{\mu_0 \epsilon_t}$, we obtain from (1.7.34)

$$k \cos \theta_t = k_t \cos \theta_i \qquad (1.7.35)$$

Multiplying (1.7.33) and (1.7.35), we obtain

$$\sin 2\theta_b = \sin 2\theta_t$$

In addition to the trivial solution $\theta_t = \theta_b$, we also obtain

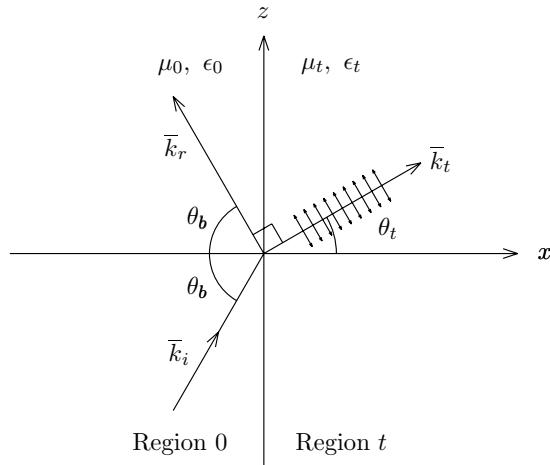$$\theta_b + \theta_t = \frac{\pi}{2} \qquad (1.7.36)$$

Figure 1.7.5 Incidence at the Brewster angle.

Since the reflected direction is perpendicular to the transmitted direction, the reflected wave vector $\overline{k}_r$ is perpendicular to the transmitted wave vector $\overline{k}_t$ [Fig. 1.7.5].

Physically we can explain this by visualizing the dielectric media as consisting of dipoles that are excited by the transmitted wave and radiating at the same frequency. Each individual dipole has a radiation pattern that is maximum in a direction perpendicular to the dipole axis and null along the dipole axis. For a TM wave excitation, all dipoles oscillate parallel to the plane of incidence along the $\overline{E}$-field lines. At the Brewster angle of incidence, the reflected $\overline{k}_r$ vector is in the same direction as the dipole oscillation in the transmitted medium. Thus, no TM wave is reflected.

Substituting (1.7.36) in (1.7.35), we obtain the Brewster angle

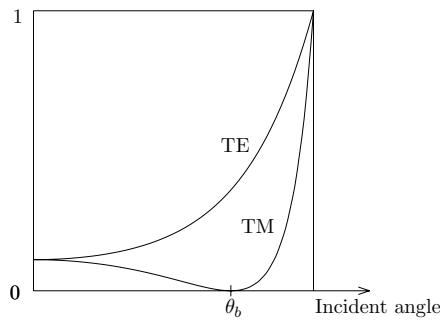$$\theta_b = \tan^{-1}\frac{k_t}{k} = \tan^{-1}\sqrt{\frac{\epsilon_t}{\epsilon_0}} \qquad (1.7.37)$$

Figure 1.7.6 Reflectivity of TE and TM waves.

In Fig. 1.7.6, we plot the reflectivities as functions of the incident angle. In general, on a solid dielectric surface, the TE waves reflect more than the TM waves. For an unpolarized incident wave, the reflected wave becomes linearly polarized perpendicular to the plane of incidence. Thus the Brewster angle is also referred to as the polarization angle.

David Brewster (11 December 1781 – 10 February 1868)

David Brewster entered the University of Edinburgh at the age of 11. He was knighted in 1831, and his Treatise on Optics was also published in 1831. He taught at St. Andrews and in 1838 was promoted to principal. In 1859, he became principal of the University of Edinburgh.

   The reflection and transmission of TM waves by a plane boundary has been carried out in a manner similar to the treatment of TE waves. We can also invoke the principle of duality and write down the answers directly. Making the replacements $\overline{E} \to \overline{H}$, $\overline{H} \to -\overline{E}$, $\mu_0 \rightleftarrows \epsilon_0$, and the boundary conditions of continuous tangential $\overline{H}$ and $\overline{E}$ at $x = 0$, we find the dual of the TE problem [Fig. 1.7.2] to be precisely the TM problem [Fig. 1.7.4]. We obtain the reflection and transmission coefficients as in (1.7.29)–(1.7.30) with p_{0t}^{TE} in (1.7.19) replaced by $p_{0t}^{TM} = \epsilon_0 k_{tx}/\epsilon_t k_x$.

EXAMPLE 1.7.1
   Consider an electromagnetic wave impinging normally upon a dielectric half space (Region 2) with permittivity ϵ_2 from a medium (Region 1) with permittivity ϵ_1.

(a) Let $\epsilon_1 = \epsilon_o$ and $\epsilon_2 = 4\epsilon_o$. What are the reflection coefficient R_{12} and the transmission coefficient T_{12}?
(b) What is the sum of Poynting power of the wave on either side of the interface? Do they conserve?
(c) What is the sum of momentum density of the wave on either side of the interface? Do they conserve?
(d) Find the radiation pressure exerted on both sides of the boundary. Do they match?
(e) Will the half space move towards the incident wave or away from it?

SOLUTION:
(a)
$$p_{0t} = \frac{\mu_0 k_{tx}}{\mu_t k_x} = \frac{\mu_0 \omega \sqrt{\mu_0 4\epsilon_0}}{\mu_0 \omega \sqrt{\mu_0 \epsilon_0}} = 2$$
$$R_{12} = \frac{1 - p_{0t}}{1 + p_{0t}} = \frac{1 - 2}{1 + 2} = -\frac{1}{3}$$
$$T_{12} = 1 + R_{12} = \frac{2}{1 + p_{0t}} = \frac{2}{3}$$

(b) Computing the time averaged Poynting power of the incident, reflected, and transmitted waves, we find

$$< \overline{S}_i > = \hat{x}\frac{E_0^2}{2\eta_1} = \hat{x}\frac{E_0^2}{2\eta_0}$$

$$< \overline{S}_r > = -\hat{x}\frac{R_{12}^2 E_0^2}{2\eta_1} = -\hat{x}\frac{R_{12}^2 E_0^2}{2\eta_0} = -\hat{x}\left(\frac{1}{9}\right)\frac{E_0^2}{2\eta_0}$$

$$< \overline{S}_t > = \hat{x}\frac{T_{12}^2 E_0^2}{2\eta_2} = \hat{x}\frac{2T_{12}^2 E_0^2}{2\eta_0} = \hat{x}\left(\frac{8}{9}\right)\frac{E_0^2}{2\eta_0}$$

and since

$$\hat{x} \cdot < \overline{S}_i >= -\hat{x} \cdot < \overline{S}_r > + \hat{x} \cdot < \overline{S}_t >$$

we see that power is conserved.

(c) The momentum density of the field is given by $\overline{g} = \mu\epsilon\overline{S}$, so that

$$< \overline{g}_i > = \hat{x}\mu_0\epsilon_0 \frac{E_0^2}{2\eta_0} = \hat{x}\frac{E_0^2}{2\eta_0 c^2}$$

$$< \overline{g}_r > = -\hat{x}\left(\frac{1}{9}\right)\frac{E_0^2}{2\eta_0 c^2} = -\hat{x}\mu_0\epsilon_0 \frac{E_0^2}{18\eta_0 c^2}$$

$$< \overline{g}_t > = \hat{x}\mu_0(4\epsilon_0)\left(\frac{8}{9}\right)\frac{E_0^2}{2\eta_0} = \hat{x}\frac{16E_0^2}{9\eta_0 c^2}$$

The total momentum density of the field is not conserved which implies there exists a mechanical momentum. Assuming that the plates are initially at rest, in order for total momentum to be conserved we need the mechanical momentum,

$$< \overline{g}_{\text{mech}} >=< \overline{g}_i > - < \overline{g}_r > - < \overline{g}_t >= -\hat{x}\frac{11E_0^2}{9\eta_0 c^2}$$

(d) The radiation pressure magnitude is given by $|\overline{F}| = \sqrt{\mu\epsilon}\,|\overline{S}|$. The direction in which the force is applied depends on whether the wave is an impinging wave (force acts in same direction as $\overline{S}$) or a launched wave (force acts in opposite direction as $\overline{S}$ due to recoil effect). For the incident, reflected, and transmitted fields we find,

$$< \overline{F}_i > = \sqrt{\mu_0\epsilon_0} < \overline{S}_i >= \hat{x}\frac{E_0^2}{2\eta_0 c}$$

$$< \overline{F}_r > = -\sqrt{\mu_0\epsilon_0} < \overline{S}_r >= \hat{x}\frac{E_0^2}{18\eta_0 c}$$

$$< \overline{F}_t > = -\sqrt{\mu_0(4\epsilon_0)} < \overline{S}_t >= -\hat{x}\frac{8E_0^2}{9\eta_0 c}$$

so that there is a net force of

$$< \overline{F}_{\text{tot}} >= -\hat{x}\frac{13E_0^2}{18\eta_0 c}$$

acting on the half space.

(e) Using the results of either part (c) or (d) we find that the half space will move towards the incident wave.

<div align="right">— E<small>ND OF</small> E<small>XAMPLE</small> 1.7.1 —</div>

E. Guidance by Conducting Parallel Plates

Consider the guidance of electromagnetic waves by a pair of perfectly conducting plates at $x = 0$ and $x = d$ [Fig. 1.7.7]. For TM waves, the Maxwell equations are

$$\left(\frac{\partial^2}{\partial x^2} + \frac{\partial^2}{\partial z^2} - \mu\epsilon\frac{\partial^2}{\partial t^2}\right)H_y = 0 \qquad (1.7.38a)$$

$$\epsilon\frac{\partial}{\partial t}E_x = -\frac{\partial}{\partial z}H_y \qquad (1.7.38b)$$

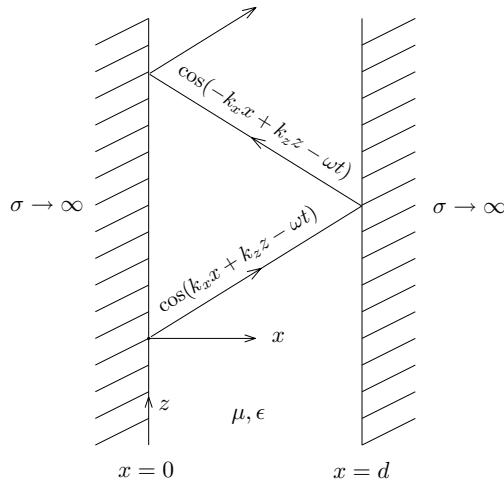$$\epsilon\frac{\partial}{\partial t}E_z = \frac{\partial}{\partial x}H_y \qquad (1.7.38c)$$

Figure 1.7.7 Parallel-plate waveguide.

In the parallel-plate waveguide, the wave is guided along the $\pm\hat{z}$ directions. The two wave solutions with wave vectors $\overline{k}$ and $\overline{k}_r$ in the guided region are

$$\overline{H}_i = \hat{y}\cos(k_x x + k_z z - \omega t) \qquad (1.7.39)$$

$$\overline{E}_i = [\hat{x}k_z - \hat{z}k_x]\frac{1}{\omega\epsilon}\cos(k_x x + k_z z - \omega t) \qquad (1.7.40)$$

$$\overline{H}_r = \hat{y}\ R\cos(-k_x x + k_z z - \omega t) \qquad (1.7.41)$$

$$\overline{E}_r = [\hat{x}k_z + \hat{z}k_x]\frac{R}{\omega\epsilon}\cos(-k_x x + k_z z - \omega t) \qquad (1.7.42)$$

The boundary conditions at the parallel plates require that the tangential electric field be zero at $x = 0$ and $x = d$.

$$- \cos(k_z z - \omega t) + R\cos(k_z z - \omega t) = 0 \qquad (1.7.43a)$$

$$- \cos(k_x d + k_z z - \omega t) + R\cos(-k_x d + k_z z - \omega t) = 0 \qquad (1.7.43b)$$

Solution to the above equations yields $R = 1$ and

$$\boxed{2k_x d = 2m\pi} \qquad (1.7.44)$$

which is known as the guidance condition. It states that in the $\hat{x}$ direction the bouncing waves must interfere constructively with $2k_x d = 2m\pi$ in order for the wave to be guided [Fig. 1.7.8].

The dispersion relation is $k_x^2 + k_y^2 = k^2$. The set of discrete k_x values admissible inside the guide is

$$\boxed{k_x = \frac{m\pi}{d} \ \mathrm{m}^{-1} = \frac{m}{2d} \ \mathrm{K}_o = k_{cm}} \qquad (1.7.45)$$

where m is any integer. We name the guided waves TM_m modes.
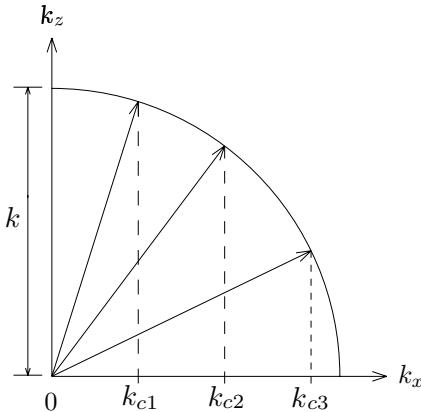

Figure 1.7.8 Interpretation of the guidance condition.

Thus as a result of the boundary condition at $x = 0$ and $x = d$, the spatial variation along the $\hat{x}$ direction of a guided wave must be an integer number in a distance of $2d$. The magnetic and electric vector fields are

$$\overline{H} = \hat{y}\cos k_x x \ \cos(k_z z - \omega t) \qquad (1.7.46)$$

$$\overline{E} = \hat{x}\frac{k_z}{\omega\epsilon}\cos k_x x \ \cos(k_z z - \omega t) + \hat{z}\frac{k_x}{\omega\epsilon}\sin k_x x \ \sin(k_z z - \omega t) \qquad (1.7.47)$$
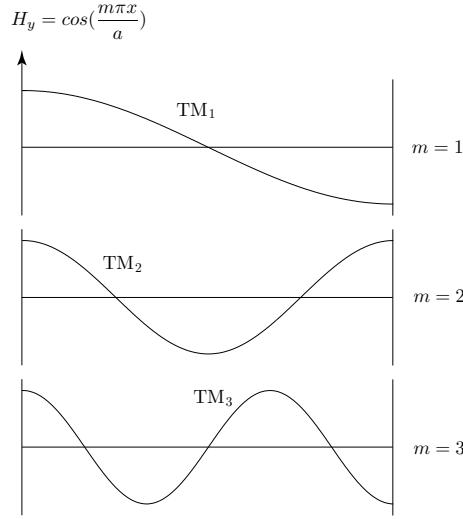
Figure 1.7.9 Field amplitudes for TM_1, TM_2, and TM_3 modes.

In Fig. 1.7.9, we plot H_y for $m = 1, 2, 3$. They are standing waves in the transversal x direction and propagate in the z direction. We see that there are more spatial variations in the waveguide with separation of d, when the x component of the spatial frequency, $k_x = (m/2d)\,\mathrm{K}_o$, is higher with larger m. The velocity of the TM_m mode in the z direction is determined from the dispersion relation

$$k_z^2 = k^2 - k_{cm}^2 \qquad (1.7.48)$$

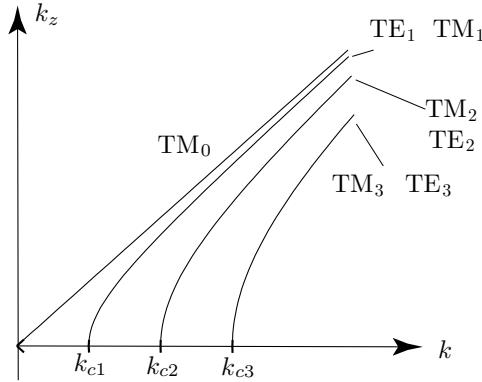Figure 1.7.10 ω–k_z diagram.

The phase and group velocities are, as $\omega = ck$ and $k_z dk_z = k dk$,

$$v_p = \omega/k_z = ck/k_z \qquad\qquad\qquad (1.7.49)$$

$$v_g = d\omega/dk_z = cdk/dk_z = ck_z/k \qquad\qquad (1.7.50)$$
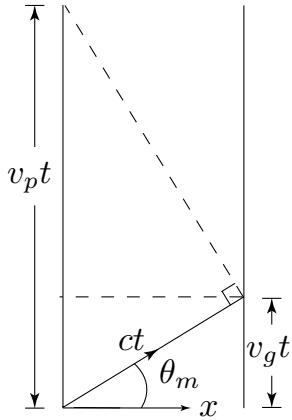
Figure 1.7.11 Distances traveled with phase and group velocities.

where $c = 1/\sqrt{\mu\epsilon}$. The phase velocity v_p is larger than c, as seen from Fig. 1.7.11. Let $\sin\theta_m = k_{cm}/k = m\pi/kd = m\lambda/2d$. We see that $v_p = c/\sin\theta_m$ and $v_g = c\sin\theta_m$, thus $v_p v_g = c^2$. In Figure 1.7.12 we show that for a propagating TM_m mode, as frequency increases, the angle θ_m increases, and the group velocity $v_g = c\Delta k/\Delta k_z$ increases.

Figure 1.7.12 Guidance with increasing frequency.

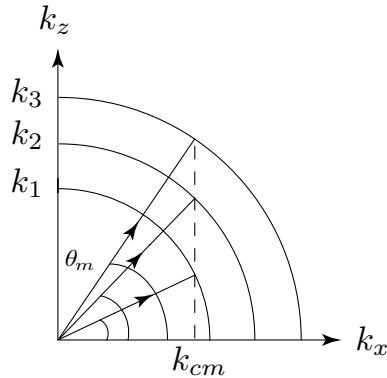It is seen from (1.7.48) that as $k < k_{cm}$, $k_z^2 = -(k_{cm}^2 - k^2) = -k_{zI}^2$, suggesting that the guided wave will attenuate in the $\hat{z}$ direction. The fields satisfying the Maxwell equations and the boundary conditions become

$$\overline{H} = \hat{y} \cos k_x x \, e^{-k_{zI} z} \cos \omega t \tag{1.7.51}$$

$$\overline{E} = \hat{x} \frac{k_{zI}}{\omega \epsilon} \cos k_x x \, e^{-k_{zI} z} \sin \omega t - \hat{z} \frac{k_x}{\omega \epsilon} \sin k_x x \, e^{-k_{zI} z} \sin \omega t \tag{1.7.52}$$

The time-average power in the $\hat{z}$ direction is zero, and the guided modes for $k < k_{cm}$ are evanescent.

The spatial frequency at which $k_z = 0$ is called the cutoff spatial frequency k_{cm}

$$k_{cm} = \frac{m}{2d} \, \mathrm{K}_o \tag{1.7.53}$$

corresponding to cutoff wavelength $\lambda_{cm} = 2d/m$. In order for the mth order TM mode to propagate, the spatial frequency k must be larger than k_{cm} or the wavelength must be smaller than λ_{cm}. Notice that if the TM_m mode is propagating, then all TM_l modes with $l < m$ can also propagate. Thus for a given spatial frequency k such that $k_{cm} < k < k_{c(m+1)}$, there will be $m+1$ TM modes admissible inside the waveguide. The lowest-order TM mode is TM_0 whose $k_{c0} = 0$.

The electric and magnetic fields for the TM_0 mode are, since $k_x = 0$ and $k_z = k$,

$$H_y = \cos(kz - \omega t) \tag{1.7.54a}$$

$$E_x = \frac{k}{\omega \epsilon} \cos(kz - \omega t) \tag{1.7.54b}$$

which is equivalent to a plane wave propagating in the $\hat{z}$ direction. The TM_0 mode is also called the fundamental mode or the TEM mode in the parallel-plate waveguide.

EXAMPLE 1.7.2   TE modes.
We write the solution for TE waves as

$$E_y = (A \cos k_x x - B \sin k_x x) \sin(k_z z - \omega t) \tag{E1.7.2.1}$$

The boundary conditions at $x = 0, d$ require $E_y = 0$ which gives $A = 0$ and the same guidance condition (1.7.45). We thus obtain the electric and

magnetic fields for TE modes

$$\overline{E} = -\hat{y}\ B \sin k_x x\ \sin(k_z z - \omega t) \qquad\qquad \text{(E1.7.2.2)}$$

$$\overline{H} = \hat{x}\ \frac{k_z}{\omega\mu} B \sin k_x x\ \sin(k_z z - \omega t)$$

$$+ \hat{z}\ \frac{k_x}{\omega\mu} B \cos k_x x\ \cos(k_z z - \omega t) \qquad\qquad \text{(E1.7.2.3)}$$

where

$$k_x = \frac{m\pi}{d}\ \ \text{m}^{-1} = \frac{m}{2d}\ \ \text{K}_o = k_{cm} \qquad\qquad \text{(E1.7.2.4)}$$

The above result can be interpreted in terms of plane waves reflecting from the conducting plates in the same way as for the TM waves. One important difference is that TE_0 does not exist and the lowest-order TE mode is TE_1.
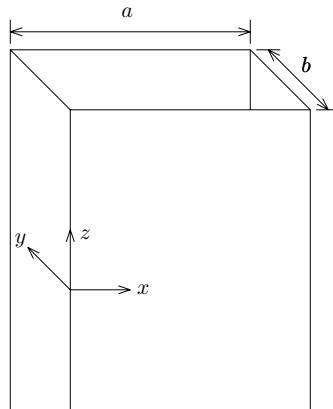

Figure E1.7.2.1 Metallic rectangular waveguide.

Consider a metallic rectangular waveguide having dimensions a along the x axis and b along the y axis [Fig. E1.7.2.1]. The TE wave fields inside the guided region can be written as (E1.7.2.2) and (E1.7.2.3). The boundary conditions at $x = 0, a$ require $E_y = E_z = 0$ and at $y = 0, b$ require $E_x = E_z = 0$ which give rise to the same guidance condition (E1.7.2.4) with d replaced by a.

Surface charges are $\rho_s = \mp B \sin k_x x\ \sin(k_z z - \omega t)$ at $y = 0, b$. Surface currents are $\overline{J}_s = \mp \hat{z} B \sin k_x x \sin(k_z z - \omega t)$ at $y = 0, b$. Since there is no variation in the $\hat{y}$ directions, the fields are for TE_{m0} modes. The fundamental mode is TE_{10} and the lowest cutoff spatial frequency is $k = k_{c1} = (1/2a)\,\text{K}_o$ corresponding to a cutoff wavelength of $\lambda_{c1} = 2a$.

— End of Example 1.7.2 —

Problems

P1.7.1

Consider an electromagnetic wave propagating in an isotropic medium with permittivity ϵ and permeability μ. It has the following electric field vector

$$\overline{E} = (\hat{x}E_x + \hat{y}E_y + \hat{z}E_z)\cos\left(k_x x + k_z z - \omega t\right)$$

where E_x, E_y, and E_z are real constants.

(a) Determine the constraints on E_x, E_y, and E_z, in terms of k_x and k_z, such that the above electric field vector represents an electromagnetic wave.

(b) Let $k_x = \sqrt{3}k/2$, $k_z = k/2$ and $E_x = E_y = E_o$. What is the polarization of the wave?

(c) Add another plane wave component to the wave shown above, so that the total electric wave is left-hand circularly polarized.

P1.7.2

When the incident k vector is normal to a plane boundary, a TE wave becomes a TEM wave; a TM wave also becomes a TEM wave. Compare the reflection and transmission coefficients for TE and TM waves at normal incidence. Do both TE and TM results reduce to the same numbers? If not, why? Do the reflectivities and transmissivities for TE and TM waves at normal incidence reduce to the same result?

P1.7.3

The gas laser depicted in Fig. P1.7.3.1 uses "Brewster angle" quartz windows on the gas discharge tube in order to minimize reflection losses. Determine the angle θ if the index of refraction for quartz at the wavelength of interest is $n = 1.46$. Because of these windows, the laser output is almost completely linearly polarized. What is the direction of polarization, i.e., is $\overline{E}$ parallel or perpendicular to the paper? Why?
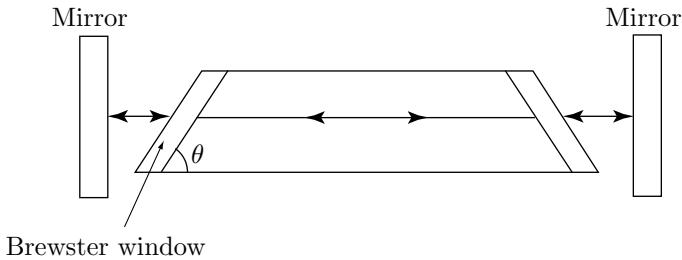

Figure P1.7.3.1 A gas laser with Brewster windows.

P1.7.4

Sun light glares caused by reflections from plane surfaces are partially linearly polarized.

(a) Determine the Brewster angle for $\epsilon_t = 9\epsilon_o$. The Brewster angle, θ_B, is also called the polarization angle because at θ_B the reflected wave is entirely TE polarized.

(b) Your polaroid glasses absorb one linear component of incident light. To minimize sun glare, what component, TE or TM, reaches your eyes after passing through the glasses? Explain why.

P1.7.5

Consider a plane wave incident on a planar boundary at $x = 0$ from a dielectric medium with $\epsilon = 9\epsilon_o$ upon another dielectric medium with μ_o and ϵ_t. The right-hand circularly polarized incident electric field is

$$\overline{E}_i = E_0(\sqrt{3}\hat{x} + \hat{z})\cos(k_x x - k_z z - \omega t) + 2\hat{y}\sin(k_x x - k_z z - \omega t)$$

where E_0 is a real constant. The reflected field is

$$\overline{E}_r = E_0\left[2R^{TE}\hat{y}\sin(k_x x + k_z z - \omega t) + R^{TM}(-\sqrt{3}\hat{x} + \hat{z})\cos(k_x x + k_z z - \omega t)\right]$$

(a) Show that the incident angle is $30°$.

(b) For $k_x = 1\,\mathrm{K}_o$, find the frequency (Hz) and wavelength (m) in region 1.

(c) Find the value of ϵ_t $(0 < \epsilon_t/\epsilon_o < \infty)$ for which the reflected wave is linearly polarized.

P1.7.6

A laser beam in free space with the polarization of electric field parallel to the paper is incident normally upon a glass surface. There is 16% power of the incident wave being reflected and the rest being transmitted. Neglect the reflection on the bottom surface. The reflection coefficients of TE and TM incident waves are given by, respectively,

$$R^{TE} = \frac{\cos\theta_i - \sqrt{n^2 - \sin^2\theta_i}}{\cos\theta_i + \sqrt{n^2 - \sin^2\theta_i}}$$

$$R^{TM} = \frac{n^2\cos\theta_i - \sqrt{n^2 - \sin^2\theta_i}}{n^2\cos\theta_i + \sqrt{n^2 - \sin^2\theta_i}}$$

where $n = \sqrt{\epsilon/\epsilon_o}$ is the refraction index and θ_i is the incident angle.

(a) What is the amplitude of the reflected electric field $\overline{E}_r$ in terms of the amplitude of the incident electric field $\overline{E}_i$?

(b) What is the refraction index $(n = \sqrt{\epsilon/\epsilon_o})$ of the glass?

(c) Let the surface of the glass rotate by $\theta = \sin^{-1}(2/3)$ about an axis perpendicular to the paper. How much of the incident power is reflected?
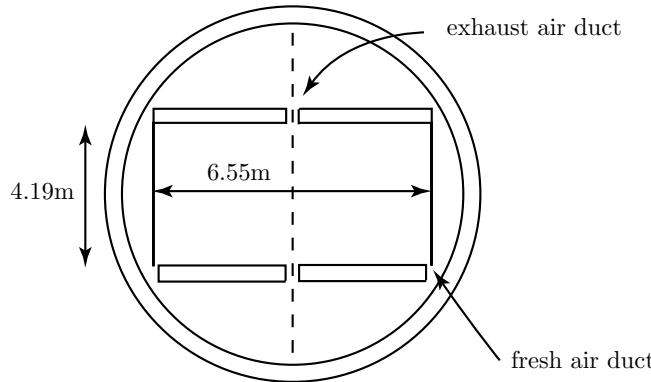
(d) Let the surface of the glass rotate by θ about an axis perpendicular to the paper, so that the laser beam is totally transmitted without reflection. What is the rotation angle θ in radians?

P1.7.7

Find the cutoff wavelength λ_{cm} and the cutoff angular frequency ω_{cm} corresponding to the cutoff spatial frequency $k_{cm} = (m/2d) \, K_o$.

P1.7.8

An AM radio in an automobile cannot receive any signal when the car is inside a tunnel. Consider, for example, the Lincoln Tunnel under the Hudson River, which was built in 1939. A cross-section of the tunnel is shown in Figure P1.7.8.1. Ignore the air ducts; assume that they are closed. Model the tunnel as a rectangular waveguide of dimension $6.55\text{m} \times 4.19\text{m}$.

Figure P1.7.8.1 Tunnel modeled as rectangular waveguide.

(a) Give the range of frequencies for which only the dominant mode, TE_{10}, may propagate.
(b) Explain why AM signals cannot be received.
(c) Can FM signals be received? Above what frequencies?

Answers

P1.1.1

$\overline{A} + \overline{B} + \overline{C} = 0$ and $\overline{A} + \overline{B} - \overline{C} = -2\overline{C}$.

P1.1.2

$|\overline{A} \times \overline{B}|^2 = (\overline{A} \times \overline{B}) \cdot (\overline{A} \times \overline{B}) = \overline{A} \cdot (\overline{B} \times (\overline{A} \times \overline{B})) = \overline{A} \cdot (\overline{A}B^2 - \overline{B}(\overline{A} \cdot \overline{B})) = A^2 B^2 - (\overline{A} \cdot \overline{B})^2$

P1.1.3

$r = \sqrt{8}, \theta = \pi/4, \phi = \pi/4$; and $\rho = 2, \phi = \pi/4, z = 2$.

P1.1.4

$\hat{c} = \hat{x}\,0.6 + \hat{z}\,0.8$.

P1.1.5

$\overline{A} \cdot \overline{B} = A_x B_x = AB_x = AB \cos\theta_{AB}$

P1.1.6

From $B^2 \sin^2\theta_{AB} = |\overline{A} - \overline{B}|^2 - (A - B\cos\theta_{AB})^2$, we find $|\overline{A} - \overline{B}|^2 = A^2 + B^2 - 2AB\cos\theta_{AB}$. It follows that $AB\cos\theta_{AB} = \frac{1}{2}[A^2 + B^2 - (\overline{A} - \overline{B}) \cdot (\overline{A} - \overline{B})] = \overline{A} \cdot \overline{B}$

P1.1.7

$\overline{A} \times \overline{B} = \hat{z}(A_x B_y - A_y B_x)$ is in the $\hat{z}$ direction perpendicular to both $\overline{A}$ and $\overline{B}$.

P1.1.8

$$|\overline{A} \times \overline{B}|^2 = (A_y B_z - A_z B_y)^2 + (A_z B_x - A_x B_z)^2 + (A_x B_y - A_y B_x)^2$$
$$= A^2 B^2 - (A_x B_x + A_y B_y + A_z B_z)^2$$
$$= A^2 B^2 - (\overline{A} \cdot \overline{B})^2 = A^2 B^2 (1 - \cos^2\theta_{AB}) = (AB\sin\theta_{AB})^2$$

P1.1.9

For $\Phi(x) = x^2$, $\nabla\Phi(x) = \hat{x}2x$. For $\Phi(x) = -x^3$, $\nabla\Phi(x) = -\hat{x}3x^2$.

P1.1.10

Its gradient is $\nabla\Phi = \hat{x}2x + \hat{y}4y$.
For the ellipse with $\Phi = x^2 + 2y^2$ equals a constant,

$$d\Phi = 2xdx + 4ydy = (\hat{x}2x + \hat{y}4y) \cdot (\hat{x}dx + \hat{y}dy) = \nabla\Phi \cdot d\overline{r} = 0$$

where $d\overline{r}$ is tangent to the ellipse. Thus the gradient $\nabla\Phi$ is normal to the ellipse and pointing in the directions of an expanding ellipse.

P1.1.11

The gradient of the function is $\nabla\Phi = \hat{x} + \hat{y}$. For $\Phi_2 = x_2 + y_2 > \Phi_1 = x_1 + y_1$, $\nabla\Phi$ is pointing in the direction of increasing Φ.

P1.1.12

$$\nabla \cdot \left(\overline{E} \times \overline{H} \right) = \nabla \cdot \begin{bmatrix} \hat{x} & \hat{y} & \hat{z} \\ E_x & E_y & E_z \\ H_x & H_y & H_z \end{bmatrix}$$

$$= \frac{\partial}{\partial x} \left(E_y H_z - E_z H_y \right) + \frac{\partial}{\partial y} \left(E_z H_x - E_x H_z \right) + \frac{\partial}{\partial z} \left(E_x H_y - E_y H_x \right)$$

$$= H_x \left(\frac{\partial}{\partial y} E_z - \frac{\partial}{\partial z} E_y \right) + H_z \left(\frac{\partial}{\partial x} E_y - \frac{\partial}{\partial y} E_x \right) + H_y \left(\frac{\partial}{\partial z} E_x - \frac{\partial}{\partial x} E_z \right)$$

$$- E_x \left(\frac{\partial}{\partial y} H_z - \frac{\partial}{\partial z} H_y \right) - E_y \left(\frac{\partial}{\partial z} H_x - \frac{\partial}{\partial x} H_z \right) - E_z \left(\frac{\partial}{\partial x} H_y - \frac{\partial}{\partial y} H_x \right)$$

$$= \overline{H} \cdot \left(\nabla \times \overline{E} \right) - \overline{E} \cdot \left(\nabla \times \overline{H} \right)$$

$$\nabla \cdot \left(\nabla \times \overline{A} \right) = \nabla \cdot \begin{bmatrix} \hat{x} & \hat{y} & \hat{z} \\ \partial/\partial x & \partial/\partial y & \partial/\partial z \\ A_x & A_y & A_z \end{bmatrix} = 0$$

$$\nabla \times \left(\nabla \phi \right) = \begin{bmatrix} \hat{x} & \hat{y} & \hat{z} \\ \partial/\partial x & \partial/\partial y & \partial/\partial z \\ \partial\phi/\partial x & \partial\phi/\partial y & \partial\phi/\partial z \end{bmatrix} = 0$$

$$\nabla \times \left(\nabla \times \overline{E} \right) = \nabla \times \begin{bmatrix} \hat{x} & \hat{y} & \hat{z} \\ \partial/\partial x & \partial/\partial y & \partial/\partial z \\ E_x & E_y & E_z \end{bmatrix}$$

$$= \begin{bmatrix} \hat{x} & \hat{y} & \hat{z} \\ \partial/\partial x & \partial/\partial y & \partial/\partial z \\ \left(\frac{\partial E_z}{\partial y} - \frac{\partial E_y}{\partial z} \right) & \left(\frac{\partial E_x}{\partial z} - \frac{\partial E_z}{\partial x} \right) & \left(\frac{\partial E_y}{\partial x} - \frac{\partial E_x}{\partial y} \right) \end{bmatrix}$$

$$= \left[\frac{\partial}{\partial x} \left(\frac{\partial E_y}{\partial y} + \frac{\partial E_x}{\partial x} + \frac{\partial E_z}{\partial z} \right) - \left(\frac{\partial^2}{\partial x^2} + \frac{\partial^2}{\partial y^2} + \frac{\partial^2}{\partial z^2} \right) E_x \right] \hat{x}$$

$$+ \left[\frac{\partial}{\partial y} \left(\frac{\partial E_y}{\partial y} + \frac{\partial E_x}{\partial y} + \frac{\partial E_z}{\partial z} \right) - \left(\frac{\partial^2}{\partial y^2} + \frac{\partial^2}{\partial y^2} + \frac{\partial^2}{\partial z^2} \right) E_y \right] \hat{y}$$

$$+ \left[\frac{\partial}{\partial z} \left(\frac{\partial E_y}{\partial y} + \frac{\partial E_x}{\partial y} + \frac{\partial E_z}{\partial z} \right) - \left(\frac{\partial^2}{\partial y^2} + \frac{\partial^2}{\partial y^2} + \frac{\partial^2}{\partial z^2} \right) E_z \right] \hat{z}$$

$$= \nabla \left(\nabla \cdot \overline{E} \right) - \nabla^2 \overline{E}$$

To prove (1.1.9), we may also write

$$\nabla \cdot (\overline{E} \times \overline{H}) = \begin{vmatrix} \frac{\partial}{\partial x} & \frac{\partial}{\partial y} & \frac{\partial}{\partial z} \\ E_x & E_y & E_z \\ H_x & H_y & H_z \end{vmatrix} = \begin{vmatrix} H_x & H_y & H_z \\ \frac{\partial}{\partial x} & \frac{\partial}{\partial y} & \frac{\partial}{\partial z} \\ E_x & E_y & E_z \end{vmatrix} - \begin{vmatrix} E_x & E_y & E_z \\ \frac{\partial}{\partial x} & \frac{\partial}{\partial y} & \frac{\partial}{\partial z} \\ H_x & H_y & H_z \end{vmatrix}$$

$$= \overline{H} \cdot (\nabla \times \overline{E}) - \overline{E} \cdot (\nabla \times \overline{H})$$

P1.1.13

We write (1.1.21) as $\nabla \times \overline{H} = \lim_{\Delta V \to 0} \oiint dS\,\hat{s} \times \overline{H}/\Delta V$

Applying the above result to a large V containing an infinite number of such differential volumes, we find the curl theorem

$$\iiint_V dV\,\nabla \times \overline{H} = \oiint_S dS\,\hat{s} \times \overline{H}$$

This is the curl theorem similar to the divergence theorem except that now the result is in vector form.

P1.1.14

If the surface integral of $\nabla \times \overline{H}$ is carried out over a closed surface, there will be no external contour enclosing the surface and the result will be zero.

$$\oiint_S d\overline{S} \cdot (\nabla \times \overline{H}) = 0 \qquad\qquad (A1.1.14.1)$$

This scalar equation should not be confused with Stokes theorem which is obtained by integrating over an open surface or the curl theorem in P1.1.13 for which we integrated over a volume V enclosed by a surface S, which is a vector relation.

P1.1.15

$\nabla \cdot \overline{A} = 3\rho + 2\,,\ \iiint dV\,\nabla \cdot \overline{A} = 6\pi \int (3\rho^2 + 2\rho) = 6\pi(5^3 + 5^2) = 900\pi$

$$\oiint_S d\overline{S} \cdot \overline{A} = 10\pi \int_0^3 dz\,5^2 + 6\pi 5^2 = 900\pi$$

P1.1.16

$[\overline{A} \times (\nabla \times \overline{B})]_i = \epsilon_{ijk}\epsilon_{klm}A_j\partial_l B_m = (\delta_{il}\delta_{jm} - \delta_{im}\delta_{jl})A_j\partial_l B_m = A_m\partial_i B_m - A_l\partial_l B_i = A_j\partial_i B_j - [(\overline{A} \cdot \nabla)\overline{B}]_i$

P1.1.17

$\partial_i(\overline{A} \cdot \overline{A}) = A_j\partial_i B_j + B_j\partial_i A_j = A_j\partial_j B_i + B_j\partial_j A_i + A_j\partial_i B_j - A_j\partial_j B_i + B_j\partial_i A_j - B_j\partial_j A_i = A_j\partial_j B_i + (\delta_{il}\delta_{jm} - \delta_{im}\delta_{jl})A_j\partial_l B_m + A_j\partial_j B_i + (\delta_{il}\delta_{jm} - \delta_{im}\delta_{jl})B_j\partial_l A_m = A_j\partial_j B_i + B_j\partial_j A_i + \epsilon_{ijk}A_j\epsilon_{klm}\partial_l A_m + \epsilon_{ijk}A_j\epsilon_{klm}\partial_l A_m = [(\overline{A} \cdot \nabla)\overline{B} + \overline{A} \times (\nabla \times \overline{B}) + (\overline{B} \cdot \nabla)\overline{A} + \overline{B} \times (\nabla \times \overline{A})]_i$

or $[(\overline{A} \cdot \nabla)\overline{B} + \overline{A} \times (\nabla \times \overline{B})]_i = [(\overline{A} \cdot \nabla)\overline{B}]_i + A_j\partial_i B_j - [(\overline{A} \cdot \nabla)\overline{B}]_i$.

P1.1.18

$\partial_i(\overline{A} \cdot \overline{A}) = 2A_j\partial_i A_j = 2A_j\partial_j A_i + 2A_j\partial_i A_j - 2A_j\partial_j A_i = 2A_j\partial_j A_i + 2(\delta_{il}\delta_{jm} - \delta_{im}\delta_{jl})A_j\partial_l A_m = 2A_j\partial_j A_i + 2\epsilon_{ijk}A_j\epsilon_{klm}\partial_l A_m = 2[(\overline{A} \cdot \nabla)\overline{A} + \overline{A} \times (\nabla \times \overline{A})]_i$

or $[(\overline{A} \cdot \nabla)\overline{A} + \overline{A} \times (\nabla \times \overline{A})]_i = [(\overline{A} \cdot \nabla)\overline{A}]_i + A_j\partial_i A_j - [(\overline{A} \cdot \nabla)\overline{A}]_i$.

P1.1.19

$$\overline{E} = -\nabla\Phi = \frac{C}{(x^2 + y^2 + z^2)^{3/2}}[\hat{x}x + \hat{y}y + \hat{z}z] = \overline{r}\frac{C}{r^3} = \hat{r}\frac{C}{r^2}$$

in terms of the position vector $\overline{r} = \hat{x}x + \hat{y}y + \hat{z}z$, and the length of the position vector $r = \sqrt{x^2 + y^2 + z^2}$, and $\hat{r}$ is pointing in the direction of $\overline{r}$ with unit length. Assuming that the electric field is due to a charged particle q situated at the origin, we can integrate Gauss' law over a small spherical volume with radius $r = \delta$ surrounding the origin to obtain

$$q = \oiint_S d\overline{S} \cdot \overline{D} = \int_0^\pi \int_0^{2\pi} d\theta \, d\phi \, \delta^2 \, \sin\theta \, \frac{\epsilon_o C}{\delta^2} = 4\pi\epsilon_o C$$

Thus the constant $C = q/4\pi\epsilon_o$ and the static electric field

$$\overline{E} = \hat{r}\frac{q}{4\pi\epsilon_o r^2}$$

P1.2.1

$\overline{E}_1$ and $\overline{E}_3$ qualify as electromagnetic waves.
$\overline{E}_2$ and $\overline{E}_4$ violate Gauss' law $\nabla \cdot \overline{E} = 0$.

P1.2.2

$\overline{E} = \hat{x}E_0 \cos(kz + \omega t)$. As time t increases, z must decrease in order for $kz + \omega t =$ constant, thus the wave is propagating in the $-\hat{z}$ direction.

P1.2.3

Wavelength $\lambda = 2\pi/k_0 = 0.01$ m.
Frequency $f = c/\lambda = 30$ GHz.
For $\lambda = 632.8$ nm, $k = 1/\lambda = 1.58 \times 10^6$ K_o.
For $f = 2.4$ GHz, $k = f/c = 2.4 \times 10^9$ Hz$/3 \times 10^8$ m/s $= 8$ K_o.

P1.2.4

(a) (i) 60 Hz: $\lambda = c/f = 5 \times 10^6$ (m)
(ii) AM radio (535–1605 kHz): $\lambda = 186.9 \sim 560.8$ (m)
(iii) FM radio (88–108 MHz): $\lambda = 2.778 \sim 3.409$ (m)
(iv) Visible light ($\sim 10^{14}$ Hz): $\lambda = \sim 3 \times 10^{-6}$ (m)
(v) X-rays ($\sim 10^{18}$ Hz): $\lambda = \sim 3 \times 10^{-10}$ (m)

(b) (i) 1 km: $f = c/\lambda = 3 \times 10^5$ (Hz)
(ii) 1 m: $f = 3 \times 10^8$ (Hz)
(iii) 1 mm: $f = 3 \times 10^{11}$ (Hz)
(iv) 1 μ m: $f = 3 \times 10^{14}$ (Hz)
(v) 1 Å: $f = 3 \times 10^{18}$ (Hz)

(c) (i) 1 km: $k = 2\pi/\lambda = K_o/\lambda = 10^{-3}$ K_o

  (ii) 1 m: $k = 1\,\mathrm{K}_o$
 (iii) 1 mm: $k = 10^3\,\mathrm{K}_o$
 (iv) 1 μ m: $k = 10^6\,\mathrm{K}_o$
  (v) 1 Å: $k = 10^{10}\,\mathrm{K}_o$

(d) (i) 1 km: $\hbar\omega = 1.24 \times 10^{-9}$ eV
   (ii) 1 m: $\hbar\omega = 1.24 \times 10^{-6}$ eV
  (iii) 1 mm: $\hbar\omega = 1.24 \times 10^{-3}$ eV
  (iv) 1 μ m: $\hbar\omega = 1.24$ eV
   (v) 1 Å: $\hbar\omega = 1.24 \times 10^4$ eV

P1.2.5

  $v_p = v_g = c$

P1.2.6

(a) At $z = z_0$, $E_x = -2\sin(kz_0 - \omega t)$, and $E_y = \frac{1}{\sqrt{2}}\cos(kz_0 - \omega t) - \frac{1}{\sqrt{2}}\sin(kz_0 - \omega t)$. Since $E_x^2/2 - \sqrt{2}E_x E_y + 2E_y^2 = 1$, the wave is elliptically polarized.

(b) $\overline{E} = \frac{1}{2}\left[\hat{x}\cos(kx - \omega t) + \hat{y}\sin(kz - \omega t)\right] + \frac{1}{2}\left[\hat{x}\cos(kx - \omega t) - \hat{y}\sin(kz - \omega t)\right]$

(c) $\overline{E} = \hat{x}\cos(kz - \omega t + \pi/4) + \hat{y}\cos(kz - \omega t - \pi/4)$. This is the superposition of two linearly polarized waves.

P1.2.7

  The wave has wavelength 1 cm, and is right-hand circularly polarized, the helix is left-handed, and its pitch is 1 cm.

P1.2.8

  For a right-handed circularly polarized wave $\alpha = \pi/4$, then

$$Q = I\cos(2\pi/4)\cos(2\beta) = 0$$
$$U = I\cos(2\pi/4)\sin(2\beta) = 0$$
$$V = I\sin(2\pi/4) = I$$

  For a left-handed circularly polarized wave $\alpha = -\pi/4$, then

$$Q = I\cos(-2\pi/4)\cos(2\beta) = 0$$
$$U = I\cos(-2\pi/4)\sin(2\beta) = 0$$
$$V = I\sin(-2\pi/4) = -I$$

  For linearly polarized wave $\alpha = 0$, then

$$V = I\sin 0 = 0$$

P1.3.1

  $mv^2/R = Ze^2/4\pi\epsilon R^2 \Rightarrow R = 4\pi\epsilon n^2\hbar^2/Zme^2 \approx 0.52\,n^2 \times 10^{-10}\,\mathrm{m}$ for $Z = 1$.

P1.3.2

(a) $T = 150 \times 10^9/c = 500\,\text{sec} = 8.33\,\text{min}$
(b) $P_r = 1.5\,\text{kW/m}^2 \times \pi \times (6.4 \times 10^6)^2\,\text{m}^2 = 1.93 \times 10^{14}\,\text{kW}$
(c) $S = P\,(\text{power density per Hz}) \times W\,(\text{bandwidth}) = 10^{-11}\,\text{Wm}^{-2}$
$E = \sqrt{2\eta S} = 8.68 \times 10^{-5}\,\text{volt/m}$

P1.3.3

The power density is $P = 1.2 \times 10^{10}\,\text{W/m}^2$. The radiation pressure is $p = 40\,\text{N/m}^2$. The area required is $20\,\text{m}^2$.

P1.3.5

(a) $\overline{B} = \hat{x} I_0 \mu_o / 2\pi d$
(b) $\overline{F} = \hat{y} N q v B_0$

P1.3.4

$$\overline{F} = \hat{x} m \frac{d^2 x}{dt^2} + \hat{y} m \frac{d^2 y}{dt^2} = -m\omega_c^2(\hat{x}x + \hat{y}y) = -m\hat{\rho}R\omega_c^2 = -\hat{\rho}mv^2/R$$

P1.3.6

The Lorentz force acting on the particle is qvB_0 and the centrifugal force acting on the particle is mv^2/R, where R is the radius of the circle. We have $qvB_0 = mv^2/R$. The time it takes the particle to complete one revolution is $2\pi R/v = 2\pi m/qB_0$. The cyclotron frequency is thus $\omega_c = v/R = qB_0/m$, and the radius is $R = mv/qB_0$.

P1.3.7

(a) Because there is a magnetic field, the effective electric field that drives conduction current is approximately

$$\overline{E}_{eff} \cong \overline{E} + \overline{v} \times \overline{B}$$

Hence $\overline{J} \cong \sigma(\overline{E} + \overline{v} \times \overline{B})$. When $\sigma \to \infty$, $\overline{E}, \overline{B}$ still remains finite, then we have to impose $\overline{E} + \overline{v} \times \overline{B} = 0$ or $\overline{E} = -\overline{v} \times \overline{B}$. This is used in approximating solar wind fields.

(b) Let $\overline{v} = \overline{v}_n + \overline{v}_\parallel$, where $\overline{v}_n$ is normal to $\overline{B}$ and $\overline{v}_\parallel$ is parallel to $\overline{B}$. Then $\overline{E} = -\overline{v} \times \overline{B} = -\overline{v}_n \times \overline{B}$. The Poynting vector

$$\overline{S} = \overline{E} \times \overline{H} = \frac{1}{\mu_0}\overline{E} \times \overline{B} = -\frac{1}{\mu_0}(\overline{v}_n \times \overline{B}) \times \overline{B} = \frac{B^2}{\mu_0}\overline{v}_n$$

$$\approx \frac{(5 \times 10^{-9})^2}{4\pi \times 10^{-7}} \times 4 \times 10^5 \times \cos 45° \approx 5.6\mu\text{W/m}^2$$

(c) Kinetic energy density $W_k = \frac{1}{2}\rho_m v^2 \approx \frac{1}{2} \times (1800 \times 9.1 \times 10^{-31} \times 10^7) \times (4 \times 10^5)^2 = 1.31 \times 10^{-9}\,\text{joule/m}^3$.
Electric energy density $W_e = \frac{1}{2}\epsilon_0 E^2 \approx \frac{1}{2} \times 8.85 \times 10^{-12} \times (4 \times 10^5 \times 5 \times 10^{-9} \times \sin 45°)^2 = 8.85 \times 10^{-18}\,\text{joule/m}^3$.

Magnetic energy density $W_m = \frac{1}{2\mu_0} B^2 \approx \frac{1}{2 \times 4\pi \times 10^{-7}} \times (5 \times 10^{-9})^2 = 9.9 \times 10^{-12}$joule/m^3 Therefore $W_k \gg W_m \gg W_e$.

Kinetic energy density is the largest.

P1.3.8

a) For $\delta = 0$ our model becomes $\frac{\partial^2 x}{\partial t^2} + \omega_0^2 x + \frac{qE}{m} = 0$. Assuming that driving and driven quantities have sinusoidal time dependency ω, we may write $\left(\omega_0^2 - \omega^2\right) \overline{x} = -\frac{qE}{m}$ or $x = \frac{qE}{m\left(\omega^2 - \omega_0^2\right)}$. For $\omega > \omega_0$ the electrons are in phase with the E-field, but for $\omega < \omega_0$ the electrons are $180°$ out of phase. In terms of current (or radiation) the oscillation is $180°$ out of phase for $\omega > \omega_0$ (for electrons or ions) thus tending to cancel the exciting field (by radiating a competing field $180°$ out of phase). This cancellation becomes complete if there are many particles participating and if their amplitudes are large enough. Thus we want $\omega > \omega_0$ (for opacity) but not so large as to render $\overline{x}$ too small and we want a high density. This condition is in fact met by $0 < \omega^2 - \omega_0^2 < \omega_p^2$ as is the case in many metals with ω in optical regime and ω_0 much smaller and ω_p in the ultraviolet regime. Thus these metals appear opaque.

b) Poynting theorem $-\nabla \cdot (\overline{E} \times \overline{H}) - \frac{\mu_0}{2} \frac{\partial}{\partial t} H^2 - \frac{\epsilon_0}{2} \frac{\partial}{\partial t} E^2 = \overline{E} \cdot \overline{J}$.

$\overline{E} = -\frac{m}{q} \left(\frac{\partial^2 \overline{x}}{\partial t^2} + \delta \frac{\partial \overline{x}}{\partial t} + \omega_0^2 \overline{x} \right)$. Assume a particle density n and velocity v, $\overline{J} = qnv = qn \frac{\partial \overline{x}}{\partial t}$. Thus

$$E \cdot J = -mn \frac{\partial \overline{x}}{\partial t} \cdot \left(\frac{\partial^2 \overline{x}}{\partial t^2} + \delta \frac{\partial \overline{x}}{\partial t} + \omega_0^2 \overline{x} \right)$$

$$= -mn \left(\frac{\partial}{\partial t} \left[\frac{1}{2} \left(\frac{\partial \overline{x}}{\partial t} \right)^2 \right] + \delta \left(\frac{\partial x}{\partial t} \right)^2 + \omega_0^2 \frac{\partial}{\partial t} \left(\frac{1}{2} x^2 \right) \right)$$

$$W \equiv \frac{\mu_0 H^2}{2} + \frac{\epsilon_0 E^2}{2} + \frac{mn}{2} \left(\frac{\partial x}{\partial t} \right)^2 + \frac{mn\omega_0^2}{2} x^2 \text{ (Energy desity)}$$

$$P_D \equiv mn\delta \left(\frac{\partial x}{\partial t} \right)^2 \text{ (Power density dissipated through collision)}$$

$\frac{\mu_0 H^2}{2} = $ magnetic energy density

$\frac{\epsilon_0 E^2}{2} = $ electric energy density

$\frac{mn}{2} \left(\frac{\partial x}{\partial t} \right)^2 = $ particle kinetic energy density

$\frac{mn\omega_0^2 x^2}{2} = $ particle potential energy density

P1.3.9

(a) Using Gauss' law, the electric field between the two plates due to the charges is given by $\overline{E} = \hat{x}\,\sigma/\epsilon_0$. The Poynting vector and the momentum density vector are given by $\overline{S} = \overline{E} \times \overline{H} = \hat{x}\frac{\sigma}{\epsilon_0} \times \hat{y}\frac{B_0}{\mu_0}e^{-\gamma t} = \hat{z}\frac{B_0\sigma}{\epsilon_0\mu_0}e^{-\gamma t}$ and $\overline{g}_f = \epsilon_0\mu_0\overline{S} = \hat{z}B_0\sigma e^{-\gamma t}$.

(b) By Faraday's law, the induced electric field will exist along the surface of the plate. Accordingly,

$$\oint_C \overline{E} \cdot d\overline{l} = -\frac{\partial}{\partial t}\int_S \overline{B} \cdot d\overline{S} \Rightarrow 2E_0 l = \gamma l dB_0 e^{-\gamma t} \Rightarrow E_0 = \frac{\gamma dB_0}{2}e^{-\gamma t}$$

By symmetry, both the E-field at the top and bottom will be equal in magnitude, however opposite in direction. The total force density along the top and bottom of the plate will be $\overline{F} = \hat{z}\,2\sigma E_0 = \hat{z}\,\gamma dB_0\sigma e^{-\gamma t}$.

(c) The mechanical momentum density vector, $\overline{g}_m$, can then be found by integrating the force density vector.

$$\overline{g}_m = \hat{z}\int_0^t \gamma B_0\sigma e^{-\gamma t'}\,dt' = \hat{z}\left[-B_0\sigma e^{-\gamma t'}\right]_0^t = \hat{z}B_0\sigma(1 - e^{-\gamma t})$$

(d) Adding the field and mechanical momentum terms, we see that the total momentum of the system is conserved, $\overline{g} = \overline{g}_f + \overline{g}_m = \hat{z}\,B_0\sigma$.

P1.3.10

For the plane current loop, we let the line charge density be ρ amp/m. The magnetic moment for the segment dl is

$$d\overline{M} = \frac{1}{2}(\rho dl)\overline{r} \times \overline{v} = \frac{1}{2}dl\overline{r} \times \overline{I} = \frac{1}{2}I\overline{r} \times d\overline{l}$$

The total magnetic moment of the loop is thus $\overline{M} = \oint d\overline{M} = \frac{1}{2}I\oint \overline{r} \times d\overline{l}$. For the plane loop $\oint \overline{r} \times d\overline{l} = 2\hat{m}A$. In the case of a circle with radius R, $\oint \overline{r} \times d\overline{l} = \hat{z}2\pi R^2$.

P1.3.11

(a) $\gamma = q/2m$. For a complicated structure of charged distributions, the gyromagnetic ratio is $\gamma = gq/2m$, where the g-factor g describes the magnetic structure.

(b) Let $\overline{M} = \hat{x}M_x + \hat{y}M_y + \hat{z}M_z$, $\frac{d\overline{M}}{dt} = \gamma\overline{M} \times \overline{B}$ gives

$\frac{dM_y}{dt} = -\gamma M_x B_0 \qquad \frac{dM_x}{dt} = \gamma M_y B_0 \qquad \frac{dM_z}{dt} = 0 \qquad$ which yield

$M_x = M_0\cos(\gamma B_0 t + \phi_0) \qquad M_y = -M_0\sin(\gamma B_0 t + \phi_0) \qquad M_z = M_{0z}$

Thus the angular Larmor frequency of precession is $\omega = \gamma B_0$. .

(c) $\nabla \cdot \overline{B} = 0$ gives $B_z = B_0 - z$

(d) The angular precession Larmor frequency is . $\omega = \gamma B_z = \gamma(B_0 - z)$.

(e) $\delta f = \delta \omega / 2\pi = \gamma \times \delta_z / 2\pi = 43\,\text{kHz}$

P1.3.12

The magnetic field, $\overline{H}$ at the position of the loop due to the straight wire carrying current I_0 is $\overline{H} = \hat{\phi} \frac{I_0}{2\pi d} = \hat{x} \frac{I_0}{2\pi d}$.

$$\overline{T} = \overline{M} \times \overline{B} = \hat{z} \frac{A_0 I_l I_0 \mu_0}{2\pi d}$$

which means that the current loop will move about the z-axis in a counter-clockwise direction.

P1.3.13

The dissipated power per unit volume is $P_d = \overline{f} \cdot \overline{v} = \rho \overline{v} \cdot \overline{E} = \overline{J} \cdot \overline{E}$.

P1.3.14

The Poynting vector is calculated to be

$$\overline{G} = \overline{D} \times \overline{B} = \hat{z} \sqrt{\frac{\epsilon_o}{\mu_o}} \, c^2 E_0^2 \cos^2(kz - \omega t)$$

The Maxwell stress tensor is

$$\overline{\overline{T}} = \frac{1}{2} \left(\mu_o H_0^2 + \epsilon_o E_0^2 \right) \cos^2(kz - \omega t) \overline{\overline{I}} - \left(\hat{x}\hat{x}\epsilon_o E_0^2 + \hat{y}\hat{y}\mu_o H_0^2 \right) \cos^2(kz - \omega t)$$

From (1.3.12) we find the force density

$$\overline{f} = -\nabla \cdot \overline{\overline{T}} - \frac{\partial \overline{G}}{\partial t} = \hat{z} k (\mu_o H_0^2 + \epsilon_o E_0^2) \sin(kz - \omega t) \cos(kz - \omega t)$$

P1.3.15

For $\partial_i = \frac{\partial}{\partial x_i}$, Maxwell's equations can be written in index notation as

$$\nabla \times \overline{H} = \frac{\partial \overline{D}}{\partial t} \qquad \Longleftrightarrow \qquad \frac{\partial D_i}{\partial t} = \varepsilon_{ijk} \partial_j H_k$$

$$\nabla \times \overline{E} = -\frac{\partial \overline{B}}{\partial t} \qquad \Longleftrightarrow \qquad \frac{\partial B_i}{\partial t} = -\varepsilon_{ijk} \partial_j E_k$$

$$\nabla \cdot \overline{D} = 0 \qquad \Longleftrightarrow \qquad \partial_i D_i = 0$$

$$\nabla \cdot \overline{B} = 0 \qquad \Longleftrightarrow \qquad \partial_i B_i = 0$$

The ith component of the time derivative of $\overline{D} \times \overline{B}$ is

$$\frac{\partial}{\partial t}(\overline{D} \times \overline{B})_i = \frac{\partial}{\partial t}(\varepsilon_{ijk} D_j B_k) = \varepsilon_{ijk} D_j \frac{\partial B_k}{\partial t} + \varepsilon_{ijk} \frac{\partial D_j}{\partial t} B_k$$

$$= -\varepsilon_{ijk}\varepsilon_{pqk} D_j (\partial_p E_q) + \varepsilon_{kij}\varepsilon_{mnj} B_k \partial_m H_n$$

$$= -(\delta_{ip}\delta_{jq} - \delta_{iq}\delta_{jp}) D_j (\partial_p E_q) + (\delta_{km}\delta_{in} - \delta_{kn}\delta_{im}) B_k (\partial_m H_n)$$

$$= D_j \partial_j E_i - D_j \partial_i E_j + B_k \partial_k H_i - B_k \partial_i H_k \qquad\qquad \text{(A1.3.15.1)}$$

where we use the identity $\varepsilon_{ijk}\varepsilon_{rsk} = \delta_{ir}\delta_{js} - \delta_{is}\delta_{jr}$. Identify the terms in the right hand side of equation (A1.3.15.1):

$$D_j\partial_i E_j = \epsilon_0 E_j \partial_i E_j = \partial_i(\frac{1}{2}\epsilon_0\overline{E}\cdot\overline{E}) = \partial_i(\frac{1}{2}\overline{D}\cdot\overline{E})$$

$$B_k\partial_i H_k = \mu_0 H_k \partial_i H_k = \partial_i(\frac{1}{2}\mu_0\overline{H}\cdot\overline{H}) = \partial_i(\frac{1}{2}\overline{B}\cdot\overline{H})$$

$$D_j\partial_j E_i = D_j\partial_j E_i + E_i\partial_j D_j = \partial_j(D_j E_i) = \nabla\cdot(\overline{D}E_i)$$

$$B_k\partial_k H_i = B_k\partial_k H_i + H_i\partial_k B_k = \partial_k(B_k H_i) = \nabla\cdot(\overline{B}H_i)$$

we find $\frac{\partial}{\partial t}(\overline{D}\times\overline{B})_i = -\partial_i(\frac{1}{2}\overline{D}\cdot\overline{E} + \frac{1}{2}\overline{B}\cdot\overline{H}) + \nabla\cdot(\overline{D}E_i + \overline{B}H_i)$, which is identical to

$$\frac{\partial}{\partial t}(\overline{D}\times\overline{B}) + \nabla\cdot\left(W\overline{\overline{I}} - \overline{DE} - \overline{BH}\right) = 0$$

P1.4.1

(a) $\langle\overline{S}\rangle = \hat{r}\frac{\omega k^3}{2\epsilon_o}\left(\frac{q\ell}{4\pi r}\right)^2\sin^2\theta$

(b) $P = \int_0^\pi d\theta 2\pi r^2\sin\theta\left[\frac{\omega k^3}{2\epsilon_o}\left(\frac{q\ell}{4\pi r}\right)^2\sin^2\theta\right] = \frac{4\pi\omega k^3}{3\epsilon_o}\left(\frac{q\ell}{4\pi}\right)^2$

(c) $R_{rad} = \frac{2P}{I_o^2} = \frac{8\pi k^3}{3\epsilon_o\omega}\left(\frac{\ell}{4\pi}\right)^2$

(d) For $\theta = \pi/2$ $E_o = -\frac{k^2 q\ell}{4\pi\epsilon_o r}$, $q\ell = -\frac{4\pi\epsilon_o r}{k^2}E_o$. Notice that the radiation field is only in the upper half space for the radio antenna, therefore
$P = \frac{2\pi}{3\eta_o}(E_o r)^2 = \frac{1}{180}\left(25\times 10^{-3}\times 15\times 10^3\right)^2 = 781.25(W)$

P1.4.2

For the p_z component, the electric field vector in the rectangular coordinate system is
$$\overline{E}_{p_z} = [\hat{r}2\cos\theta + \hat{\theta}\sin\theta]\frac{p_z}{4\pi\epsilon_o r^3}$$

$$= \frac{p_z}{4\pi\epsilon_o}\left\{\hat{x}\frac{3}{r^3}\left(\frac{xz}{r^2}\right) + \hat{y}\frac{3}{r^3}\left(\frac{yz}{r^2}\right) + \hat{z}\frac{3}{r^3}\left(\frac{z}{r}\right)^2 - \hat{z}\frac{1}{r^3}\right\}$$

The total electric field due to all three components is therefore
$$\overline{E} = [3\hat{r}(\hat{r}\cdot\overline{p}) - \overline{p}]\frac{1}{4\pi\epsilon_o r^3} = [(\overline{p}\times\hat{r})\times\hat{r} + 2\hat{r}(\hat{r}\cdot\overline{p})]\frac{1}{4\pi\epsilon_o r^3}$$

P1.4.3

Looking at $\phi = 0$, the sky is unpolarized, looking at the zenith ($\phi = 90°$) the sky is linearly polarized, looking at other parts of the sky, it is partially linearly polarized.

P1.4.4

(a) $\overline{E} = \frac{p}{4\pi\epsilon r^3}\left(\hat{\theta}\sin\theta + \hat{r}2\cos\theta\right)$

(b) The total power scattered by a Hertzian dipole with dipole moment $p_0 E_0$

$$P = \int_0^\pi d\theta \, 2\pi r^2 \sin\theta \left[\frac{\omega k^3}{2\epsilon_o}\left(\frac{p_0 E_0}{4\pi r}\right)^2 \sin^2\theta\right] = \frac{4\pi\omega k^3}{3\epsilon_o}\left(\frac{p_0 E_0}{4\pi}\right)^2 = \frac{k^4 p_0^2 E_0^2}{12\pi\eta\epsilon_0^2}$$

Scattering cross section $2\eta P_s/E_o^2 = \frac{k^4}{6\pi\epsilon_0^2}\, p_0^2$.

P1.4.5

$P_s = \frac{4\pi}{3\eta}\left(\frac{\epsilon_a - \epsilon_o}{\epsilon_a + 2\epsilon_o}\right)^2 k^4 a^6 E_0^2$. Sky is blue as blue light has a larger k and thus scatters more. It is not violet because there is less violet light reaching the lower atmosphere for scattering and the color receptors in our eyes are stimulated differently. The red and green cones are stimulated about equally and the blue cones are stimulated more strongly, resulting in perceiving a pale sky blue color.

P1.4.6

(a) $P_{\text{scatt}} = \frac{4\pi}{3\eta}\left[\frac{\epsilon_p - \epsilon_o}{\epsilon_p + 2\epsilon_o}\right]^2 k^4 a^6 E_o^2 = \frac{\pi}{12\eta}k^4 a^6 E_o^2$

(b) The total power loss of a control-volume with area A and length dl is

$$\frac{1}{P}\frac{dP}{d\ell} = \frac{2\eta}{AE_0^2} \times \frac{\pi k^4 \times 10^{-60}}{12\eta} E_0^2 \times N \times A$$

$$= \frac{\pi k^4 \times 10^{-60}}{6} N = \frac{\pi(2\pi \times 10^6)^4 \times 10^{-60}}{6} N$$

$$= \frac{8N}{3}\pi^5 \times 10^{-36} \text{ m}^{-1} = \frac{8N}{3}\pi^5 \times 10^{-33} \text{ km}^{-1}$$

which gives rise to a loss of $(300.88 - 10\log N)$ dB/km.

(c) $\frac{1}{P}\frac{dP}{d\ell} \approx 0.2 \text{ km}^{-1}$ gives rise to a loss of 6.99 dB/km.

P1.4.7

(a) $\sqrt{x^2 + (y-d)^2 + z^2} = \sqrt{x^2 + y^2 + z^2 - 2yd + d^2} \approx \sqrt{r^2 - 2yd}$
$= r\sqrt{1 - 2\frac{y}{r^2}d} \approx r(1 - \frac{1}{2} \times 2\frac{y}{r^2}d) = r - \frac{y}{r}d = r - d\sin\theta$

(b) $\overline{E}_{tot} = -\frac{k^2\ell}{4\pi r\epsilon_0}\left[\hat{\theta}q_1\cos(kr - \omega t)\sin\theta - \hat{x}q_2\cos(kr - kd\sin\theta - \omega t)\right]$

(c)

(i) $d\sin\theta = \frac{\lambda}{4}$; $d = \sqrt{2}\frac{\lambda}{4}$

(ii) $\frac{\sqrt{2}}{2}q_1 = q_2$; $q_1/q_2 = \sqrt{2}$

(iii) $\overline{E}_{tot} = -\frac{k^2\ell q_2}{4\pi r\epsilon_0}\left[\hat{\theta}\cos(\omega t - kr) - \hat{\phi}\sin(\omega t - kr)\right] \Rightarrow L.H.C.P$

P1.4.8

Writing $\ell = dz$, $r = \sqrt{\rho^2 + z^2}$, $\sin\theta = \frac{\rho}{\sqrt{\rho^2 + z^2}}$, and $z = \rho\tan\alpha$, yields

$$\overline{B} = \hat{\phi}\int_{-\infty}^{\infty} dz\frac{\mu_o\rho I}{4\pi(\rho^2 + z^2)^{3/2}} = \hat{\phi}\int_{-\pi/2}^{\pi/2}\sec^2\alpha d\alpha\frac{\mu_o\rho^2 I}{4\pi\sec^3\alpha} = \hat{\phi}\frac{\mu_o I}{2\pi\rho}.$$

The magnetic field is $\overline{B} = \hat{\phi}\frac{\mu_o I}{2\pi\rho} = \hat{\phi}\frac{4\pi \times 10^{-7} \times 10^3}{2\pi \times 10} = \hat{\phi}\, 2 \times 10^{-5}$ Tesla.

P1.5.1

(a) This constitutive relation for cholesteric liquid crystals is
  (1) *Anisotropic*
  (2) *Linear*
  (4) *Inhomogeneous*: $\overline{\overline{\epsilon}}$ depends on position.
(b) This constitutive relation for the quartz crystals is
  (1) *Bianisotropic*
  (2) *Linear*
  (3) *Temporally dispersive*
  (4) *Homogeneous*
  Another answer is

$$E_j = \kappa_{ij} D_i + c^2 G_{ij}\frac{\partial}{\partial t}B_i = \kappa_{ij}D_i - c^2 G_{ij}(\nabla \times \overline{E})_i$$

$$H_j = \frac{1}{\mu_0}B_j - c^2 G_{ij}\frac{\partial}{\partial t}D_i = \frac{1}{\mu_0}B_j - c^2 G_{ij}(\nabla \times \overline{H})_i$$

Express $\overline{D}$ and $\overline{B}$ in terms of $\overline{E}$ and $\overline{H}$.

$$D_j = \kappa_{ij}^{-1}\left[E_i + c^2 G_{ki}(\nabla \times \overline{E})_k\right]$$
$$B_j = \mu_0\left[H_j + c^2 G_{ij}(\nabla \times \overline{H})_i\right]$$

Then the constitutive relation is
  (1) *Anisotropic*
  (2) *Linear*
  (3) *Spatial dispersive*
  (4) *Homogeneous*
(c) We can write $\overline{J} \simeq \sigma(\overline{E} + R\sigma\overline{E} \times \overline{B}_0)$, in matrix form

$$\begin{bmatrix} J_x \\ J_y \\ J_z \end{bmatrix} = \begin{bmatrix} \sigma & R\sigma^2 B_{0z} & -R\sigma^2 B_{0y} \\ -R\sigma^2 B_{0z} & \sigma & R\sigma^2 B_{0x} \\ R\sigma^2 B_{0y} & -R\sigma^2 B_{0x} & \sigma \end{bmatrix}\begin{bmatrix} E_x \\ E_y \\ E_z \end{bmatrix}$$

$$\nabla \times \overline{H} = -i\omega\epsilon_0\overline{E} + \overline{J}$$

$$= -i\omega\begin{bmatrix} \epsilon_0 + i\dfrac{\sigma}{\omega} & i\dfrac{R\sigma^2}{\omega}B_{0z} & -i\dfrac{R\sigma^2}{\omega}B_{0y} \\ -i\dfrac{R\sigma^2}{\omega}B_{0z} & \epsilon_0 + i\dfrac{\sigma}{\omega} & i\dfrac{R\sigma^2}{\omega}B_{0x} \\ i\dfrac{R\sigma^2}{\omega}B_{0y} & -i\dfrac{R\sigma^2}{\omega}B_{0x} & \epsilon_0 + i\dfrac{\sigma}{\omega} \end{bmatrix} \cdot \overline{E} = -i\omega\overline{\overline{\epsilon}} \cdot \overline{E}$$

The constitutive relation is thus
  (1) *Anisotropic*

(2) *Linear*

(3) *Temporally dispersive*: Permittivity depends on ω.

(4) *Homogeneous*

(d) Consider the following dispersion relation:

$$D_i = \epsilon_{ij} E_j + \gamma_{ijk} \frac{\partial E_j}{\partial x_k}$$

A repeated index in a product implies summation over that index from 1 to 3 (e.g., $A_i B_i = A_1 B_1 + A_2 B_2 + A_3 B_3$). An equation or an inequality holds for each of the unrepeated indices.

The constitutive relation is

(1) *Anisotropic*: $\overline{D}$ and $\overline{E}$ are not related by a scalar factor.

(2) *Linear*

(3) *Spatially dispersive*: The constitutive relation involves space derivatives of $\overline{E}$.

(4) *Homogeneous*: ϵ_{ij} and γ_{ijk} do not depend on $\overline{r}$.

(e) The constitutive relation for pyroelectricity is

(1) *Anisotropic*

(2) *Linear*: Variations of $\overline{D}$ and $\overline{E}$ are linearly related. $\delta\overline{D} = \overline{\overline{\epsilon}} \cdot \delta E$.

(4) *Homogeneous*

(f) The constitutive relation for piezoelectricity is

(1) *Anisotropic*

(2) *Linear*: Variations of $\overline{D}$ and $\overline{E}$ are linearly related. $\delta\overline{D} = \overline{\overline{\epsilon}} \cdot \delta E$.

(4) *Homogeneous*

Note: S_{kl} is the mechanical stress tensor. The force acting on an imaginary surface S in a solid is

$$F_k = \int_S ds\, S_{kl} n_l$$

The dimensions of S_{kl} are Force/Area.

(g) For the Kerr effect, the constitutive relation is

(1) *Anisotropic*

(2) *Nonlinear*

(4) *Homogeneous*

(h) For the Pockel's effect, the constitutive relation is

(1) *Anisotropic*

(2) *Nonlinear*

(4) *Homogeneous*

P1.5.2

In the low-field limit, $L(x) \approx \frac{x}{3}$, and $M \approx \frac{Nm^2 H}{3kT}$, and the medium is linear.

P1.6.1

Consider a ribbon-like surface as shown in Fig. P1.6.1.1. Integrating over the surface of the ribbon area, Faraday's law and Ampère's law become

$$\oint d\bar{l} \cdot \overline{E} = -\frac{d}{dt} \iint dS\,\hat{s} \cdot \overline{B}$$

$$\oint d\bar{l} \cdot \overline{H} = \frac{d}{dt} \iint dS\,\hat{s} \cdot \overline{D} + \iint dS\,\hat{s} \cdot \overline{J}$$

Let the ribbon area approach zero in such a manner that δ goes to zero first and the terms involving δ are discarded. To relate $\overline{E}_1, \overline{H}_1$ in region 1 to $\overline{E}_2, \overline{H}_2$ in region 2, we proceed as follows.

The integral forms of Faraday's law and Ampère's law as applied to the ribbon area in Fig. P1.6.1.1 yield, as $\delta \to 0$,

$$\frac{d}{dt} \iint dS\,\hat{s} \cdot \overline{B} = 0 = \frac{d}{dt} \iint dS\,\hat{s} \cdot \overline{D}$$

because $d(\hat{s} \cdot \overline{B})/dt$ and $d(\hat{s} \cdot \overline{D})/dt$ remain finite while the ribbon area approaches zero. Therefore

$$d\bar{l} \cdot (\overline{E}_1 - \overline{E}_2) = 0$$

$$d\bar{l} \cdot (\overline{H}_1 - \overline{H}_2) = \hat{s} \cdot \overline{J}\delta\,dl$$

The electric field $\overline{E}$ in the $d\bar{l}$ direction is tangential to the surface and can be written as $d\bar{l} \cdot \overline{E} = dl\hat{s} \cdot \hat{n} \times \overline{E} = dl\hat{s} \times \hat{n} \cdot \overline{E}$ for all $dl\hat{s}$ along the interface and similarly for $\overline{H}$. We thus have

$$\hat{n} \times (\overline{E}_1 - \overline{E}_2) = 0$$

$$\hat{n} \times (\overline{H}_1 - \overline{H}_2) = \lim_{\delta \to 0} \overline{J}\delta \equiv \overline{J}_s$$

P1.6.2

We apply the curl theorem to a small pill-box volume on the x-y plane [Fig. P1.7.8.1], which has an area A and an infinitesimal thickness Δz. We let $\Delta z \to 0$ faster than $A \to 0$, such that terms involving Δz can be neglected:

$$\iiint dV\,\nabla \times \overline{H} \approx A\hat{z} \times (\overline{H}_{z>0} - \overline{H}_{z<0})$$

Such results are useful in the derivation of boundary conditions for the Maxwell equations. Integrating Ampere's law $\nabla \times H = \partial\overline{D}/\partial t + \overline{J}$ over the pill-box volume, we have $A\hat{z} \times (\overline{H}_{z>0} - \overline{H}_{z<0}) = A\Delta z \partial\overline{D}/\partial t + A\Delta z\overline{J}$. The first term on the right-hand side is neglected because physically $\partial\overline{D}/\partial t$ is finite. However if $\overline{J}$ is infinite in the pill-box then $\Delta z\overline{J} = \overline{J}_s$ is finite, where $\overline{J}_s = \hat{z} \times (\overline{H}_{z>0} - \overline{H}_{z<0})$. We call $\overline{J}_s$ surface current.

P1.6.3

Using Gauss' law of $\nabla \cdot \overline{D} = \rho$, we find $a\delta\rho = \hat{s}(a + l\delta) \cdot \left(\overline{D}_1 - \overline{D}_2\right)$. In the limit of $\delta \rightarrow 0$, $\delta\rho = \rho_s$, the last term vanishes, and we obtain (1.6.9).

P1.7.1

(a) $\nabla \cdot \overline{E} = 0$ gives $\begin{cases} E_x k_x + E_z k_z = 0 \\ E_y = \text{arbitrary} \end{cases}$

(b) $\overline{E} = \left(\hat{x} + \hat{y} - \hat{z}\sqrt{3}\right) E_o \cos\left(k_x x + k_z z - \omega t\right)$ is linearly polarized.

(c) Let $\overline{E}_{add} = \left(\hat{x}E_1 + \hat{y}E_2 + \hat{z}E_3\right) \sin\left(k_x x + k_z z - \omega t\right)$ and we require

$$\begin{cases} E_3 = -\sqrt{3}E_1 \\ \left(\hat{x}E_x + \hat{y}E_y + \hat{z}E_z\right) \cdot \left(\hat{x}E_1 + \hat{y}E_2 + \hat{z}E_3\right) = 0 \\ \left|\hat{x}E_x + \hat{y}E_y + \hat{z}E_z\right| = \left|\hat{x}E_1 + \hat{y}E_2 + \hat{z}E_3\right| \end{cases}$$

Thus $\overline{E}_{add} = \left(-\frac{1}{2}\hat{x} + 2\hat{y} + \hat{z}\frac{\sqrt{3}}{2}\right) E_o \sin\left(k_x x + k_z z - \omega t\right)$.

P1.7.2

R^{TE} and T^{TE} are for electric field vectors while R^{TM} and T^{TM} are for magnetic field vectors. They do not reduce to the same numbers.

$$R^{TE} = \frac{1 - n}{1 + n} \qquad R^{TM} = \frac{n - 1}{n + 1}$$

As for reflectivity and transmissivity, the two cases yield identical results.

P1.7.3

$\theta_B = \tan^{-1} n = \tan^{-1} 1.46 = 55.59°, \quad \theta = 90° - \theta_B = 34.41°.$

P1.7.4

(a) The Brewster angle for $\epsilon_t = 9$ is $\theta_B = \tan^{-1}\sqrt{\epsilon_t} = \tan^{-1}\sqrt{9} = 71.57°$.

(b) The dominant portion of the sun glares is TE polarized wave. The polaroid glasses absorb the TE component of the incident light, thus the TM component reaches the eyes after passing through the polaroid glasses.

P1.7.5

(a) $\overline{E}_i \cdot \overline{k}_i = 0 \Rightarrow \sqrt{3}k_x - k_z = 0 \Rightarrow \theta_i = \tan^{-1}(k_x/k_z) = \tan^{-1}(1/\sqrt{3}) = 30°$.

(b) For $k_x = 1\,(K_o)$, we get $k_z = \sqrt{3}k_x = \sqrt{3}\,(K_o)$. $\Rightarrow k = \sqrt{k_x^2 + k_z^2} = 2\,(K_o)$, and $k = \omega\sqrt{\mu_o 9\epsilon_o} = 3\omega/c$. So $f = \omega/2\pi = ck/(3 \cdot 2\pi) = 2 \times 10^8$ (Hz) and $\lambda = 2\pi/k = 0.5$ m.

(c) If the totally reflected wave is linearly polarized, the incident angle is the Brewster angle, thus $\theta_i = 30° = \tan^{-1}\sqrt{\epsilon_t/9\epsilon_o} \Rightarrow \epsilon_t = 9\epsilon_o \tan^2 30° = 3\epsilon_o$.

P1.7.6

(a) $P_r = 0.16P_i$, so $\left|\overline{E}_r\right| = \sqrt{0.16}\left|\overline{E}_i\right| = 0.4\left|\overline{E}_i\right|$.

(b) $R = (n-1)/(n+1) = 0.4$ so $n = 7/3$.

(c) This problem is the TM wave case, so $P_r/P_i = \left|R^{TM}\right|^2 = (11/38)^2$.

(d) The tilted angle is the Brewster angle, $\theta_B = \tan^{-1} n = \tan^{-1}(7/3)$.

P1.7.7

$$\lambda_{cm} = 2d/m \text{ and } \omega_{cm} = m\pi/d(\mu\epsilon)^{1/2}.$$

P1.7.8

(a) $f_{c10} = \frac{\omega_{c10}}{2\pi} = \frac{c}{2\pi}\left(\frac{\pi}{a}\right) = \frac{3\times10^8}{2\pi} \times \frac{\pi}{6.55} = 22.9\,(\text{MHz}) < f < f_{c01} = \frac{c}{2\pi}\left(\frac{\pi}{b}\right) = \frac{3\times10^8}{2\pi} \times \frac{\pi}{4.19} = 35.8\,(\text{MHz})$

(b) An AM radio operates in the range of 500 to 1600 (KHz) is below the cutoff frequency of the fundamental mode TE_{10}. Therefore, AM signals can not be received in the tunnel.

(c) FM signals operating in the range of 88.1 to 107.9 (MHz) can be received in the tunnel.

2

TRANSMISSION LINES

2.1 Transmission Line Theory

A. Transmission Line Equations

B. Circuit Theory

2.2 Time-Domain Transmission Line Theory

A. Wave Equations and Wave Solutions

B. Transients on Transmission Lines

C. Normal Modes and Natural Frequencies

D. Initial Value Problem

2.3 Sinusoidal Steady State Transmission Lines

A. Sinusoidal Steady State

B. Complex Impedance

C. Time Average Power

D. Generalized Reflection Coefficient

E. Normalized Complex Impedance (Smith Chart)

F. Transmission Line Resonators

2.4 Lumped Element Transmission Lines

A. Lumped Element Line

B. Dispersion Relations for Lumped Element Lines

C. Periodically Loaded Transmission Lines

2.5 Transmission Line Modeling

A. Modeling Reflection and Transmission

    B. Modeling Antenna Radiation

    C. Array Antennas

    D. Array Pattern Multiplication

    E. Equivalence Principle

Answers

2.1   Transmission Line Theory

A. Transmission Line Equations

Transmission line theory deals with coaxial cables, parallel-plate wave-guides, open-wire transmission lines, microstrip lines, etc, and provides a simplified model to study complicated transmission systems. Parallel-plate waveguide is a canonical example in the study of transmission line theory. In order to derive transmission line equations from the Maxwell equations, we consider two parallel plates [Fig. 2.1.1] separated by a distance d. Both plates have the same width w. For $w \gg d$, we can assume that all electromagnetic fields are confined in between the plates and there are no fringing fields outside the plate regions. An electromagnetic wave is guided along the $\hat{z}$ direction with the electric field $\overline{E}$ in the $\hat{x}$ direction and the magnetic field $\overline{H}$ in the $\hat{y}$ direction. Since both $\overline{E}$ and $\overline{H}$ are perpendicular to the direction of propagation, the guided wave is a transverse electromagnetic (TEM) wave. We write

$$\overline{E} = \hat{x} E_x(z, t) \qquad\qquad (2.1.1a)$$

$$\overline{H} = \hat{y} H_y(z, t) \qquad\qquad (2.1.1b)$$
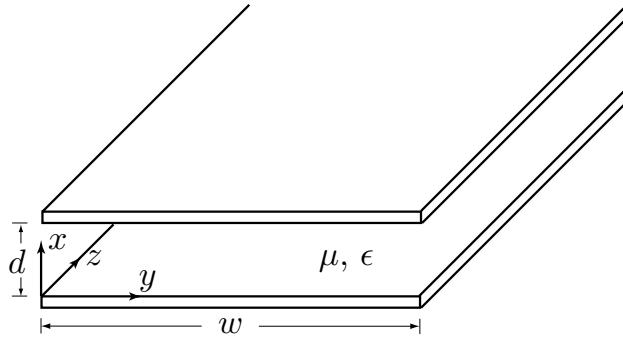
Figure 2.1.1   Parallel-plate transmission line.

For example,

$$E_x\,(z, t) = E_0 \cos(kz - \omega t) \qquad\qquad (2.1.2a)$$

$$H_y\,(z, t) = H_0 \cos(kz - \omega t) \qquad\qquad (2.1.2b)$$

where $E_0/H_0 = \sqrt{\mu/\epsilon}$.

On the plate at $x = 0$, the boundary conditions of zero tangential $\overline{E}$ and zero normal $\overline{B}$ are satisfied. The boundary condition for the normal $\overline{D}$ field gives rise to the surface charge density

$$\rho_s = \hat{x} \cdot \epsilon\overline{E} = \epsilon E_x(z,t) = \epsilon E_0 \cos(kz - \omega t)$$

The boundary condition for the tangential magnetic field gives rise to the surface current density

$$\overline{J}_s = \hat{x} \times \overline{H} = \hat{z} H_y(z,t) = \hat{z} H_0 \cos(kz - \omega t)$$
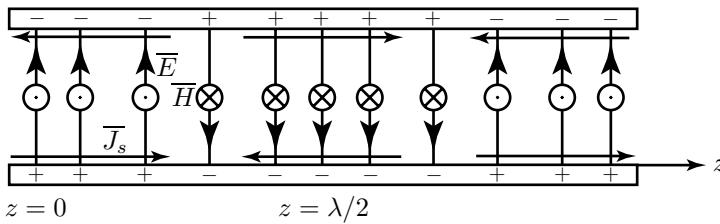
Figure 2.1.2 Surface charge and current on parallel-plate waveguide.

It is seen that

$$\nabla \cdot \overline{J}_s = -\frac{\partial}{\partial t}\rho_s$$

which guarantees conservation of charge. On the plate surface at $x = d$, the surface charge and current densities are the negatives of those on the plate surface at $x = 0$ as shown in Fig. 2.1.2 which is plotted at $t = 0$.

The Maxwell equations with the solutions in (2.1.1) reduce to the following pair of equations

$$\frac{\partial}{\partial z} E_x(z,t) = -\mu \frac{\partial}{\partial t} H_y(z,t) \qquad (2.1.3)$$

$$\frac{\partial}{\partial z} H_y(z,t) = -\epsilon \frac{\partial}{\partial t} E_x(z,t) \qquad (2.1.4)$$

A voltage $V(z,t)$ is defined as $V(z,t) = E_x(z,t)d$ and a current $I(z,t)$ is defined as $I(z,t) = H_y(z,t)\, w$.

For the parallel-plate waveguide, we further define the inductance per unit length

$$L = \mu \, \frac{d}{w} \qquad \text{(H/m)} \qquad\qquad (2.1.5)$$

and capacitance per unit length

$$C = \epsilon \, \frac{w}{d} \qquad \text{(F/m)} \qquad\qquad (2.1.6)$$

From (2.1.3) and (2.1.4), we obtain the transmission equations

$$\frac{\partial}{\partial z} V(z,t) = -L \, \frac{\partial}{\partial t} I(z,t) \qquad\qquad (2.1.7)$$

$$\frac{\partial}{\partial z} I(z,t) = -C \, \frac{\partial}{\partial t} V(z,t) \qquad\qquad (2.1.8)$$

These two equations in terms of $V(z,t)$ and $I(z,t)$ and circuit parameters L and C are known as the transmission line equations. Similar transmission line equations for coaxial lines, two-wire transmission lines, and microstrip lines can be derived for the TEM waves on such lines.

EXAMPLE 2.1.1   Poynting's theorem.
Multiplying (2.1.7) by I and (2.1.8) by V and adding, we obtain Poynting's theorem for transmission lines

$$\frac{\partial}{\partial z}(VI) = -\frac{\partial}{\partial t}\left(\frac{1}{2}LI^2 + \frac{1}{2}CV^2\right) \qquad\qquad (E2.1.1.1)$$

We identify VI as the power flow, $W_m = \frac{1}{2}LI^2$ as the magnetic energy per unit length, and $W_e = \frac{1}{2}CV^2$ as the electric energy per unit length. Thus Poynting's theorem is a statement of power conservation at all points and all times on the transmission line.

— END OF EXAMPLE 2.1.1 —

EXAMPLE 2.1.2   Coaxial transmission lines.
A coaxial transmission line consists of an inner circular conducting cylinder with radius a and an outer circular conducting sheath with radius b, where $a < b$. The electric and magnetic field vectors are

$$\overline{E} = \hat{\rho} E_\rho(z,t)/\rho \qquad\qquad (E2.1.2.1)$$
$$\overline{H} = \hat{\phi} H_\phi(z,t)/\rho \qquad\qquad (E2.1.2.2)$$

Faraday's law and Ampère's law reduce to the following pair of equations

$$\frac{\partial}{\partial z} E_\rho(z,t) = -\mu \frac{\partial}{\partial t} H_\phi(z,t) \qquad \text{(E2.1.2.3)}$$

$$\frac{\partial}{\partial z} H_\phi(z,t) = -\epsilon \frac{\partial}{\partial t} E_\rho(z,t) \qquad \text{(E2.1.2.4)}$$

A voltage $V(z,t)$ is defined as

$$V(z,t) = \int_a^b d\rho E_\rho(z,t)/\rho = \ln\left(\frac{b}{a}\right) E_\rho(z,t)$$

and a current $I(z,t)$ is defined as

$$I(z,t) = \int_0^{2\pi} d\phi \rho H_\phi(z,t)/\rho = 2\pi H_\phi(z,t)$$

Notice that the surface current density on the inner conducting surface at $\rho = a$ is $\overline{J}_s = \hat{\rho} \times \hat{\phi} H_\phi(z,t)/a = \hat{z} H_\phi(z,t)/a$ and the surface current density on the outer conducting surface at $\rho = b$ is $\overline{J}_s = -\hat{\rho} \times \hat{\phi} H_\phi(z,t)/b = -\hat{z} H_\phi(z,t)/b$. For the coaxial transmission line, we further define the inductance per unit length

$$L = \mu \frac{\ln(b/a)}{2\pi} \qquad \text{(H/m)} \qquad \text{(E2.1.2.5)}$$

and the capacitance per unit length

$$C = \epsilon \frac{2\pi}{\ln(b/a)} \qquad \text{(F/m)} \qquad \text{(E2.1.2.6)}$$

Eqs. (E2.1.2.3) and (E2.1.2.4) then become

$$\frac{\partial}{\partial z} V(z,t) = -L \frac{\partial}{\partial t} I(z,t) \qquad \text{(E2.1.2.7)}$$

$$\frac{\partial}{\partial z} I(z,t) = -C \frac{\partial}{\partial t} V(z,t) \qquad \text{(E2.1.2.8)}$$

which are of the same form as (2.1.7) and (2.1.8).

— END OF EXAMPLE 2.1.2 —

EXAMPLE 2.1.3

In the parallel-plate waveguide, the voltage is obtained as

$$V(z,t) = dE_x \ (z,t) = d\cos(kz - \omega t)$$

and the current $I(z,t)$ is obtained as

$$I(z,t) = wH_y \ (z,t) = w\cos(kz - \omega t)$$

In a coaxial transmission line, the voltage and current are obtained as

$$V(z,t) = \ln\left(\frac{b}{a}\right) E_\rho(z,t) = \ln\left(\frac{b}{a}\right)\cos(kz - \omega t)/\rho$$

and the current $I(z,t)$ is obtained as

$$I(z,t) = 2\pi H_\phi(z,t) = 2\pi \cos(kz - \omega t)/\rho$$

We see that the voltage at $z = 0$ is opposite to the voltage at $z = \lambda/2$, contrary to Kirchhoff's voltage law (KVL), which requires the two voltages to be equal. The surface current density at $z = 0$ and that at $z = \lambda/2$ are opposite in direction, also contrary to Kirchhoff's current law (KCL) which requires that current flowing into a node is equal to that flowing out.

— END OF EXAMPLE 2.1.3 —

Note: Transverse electromagnetic (TEM) waves guided by transmission lines have the electric field $\overline{E}$ perpendicular to the magnetic field $\overline{H}$ and both $\overline{E}$ and $\overline{H}$ transverse to the direction of propagation along the transmission line. A transmission line is composed of two conductors parallel to each other. The cross-sections of the transmission line at any point on the propagation path are of the same shape. A parallel-plate transmission line consists of two parallel conducting plates separated by a constant distance; the space in between the plates may be filled uniformly with dielectric material. A microstrip line usually consists of a thin narrow metal strip fabricated on top of a dielectric slab backed by a grounded conduction plane. A two-wire transmission line consists of a pair of parallel conducting wires separated by a uniform distance. A coaxial transmission line consists of an inner conductor and a coaxial outer conducting sheath separated by a dielectric medium. In addition to the TEM mode of propagation along the transmission lines, there exist many other modes, which will not be covered by the transmission line theory.

B. Circuit Theory

The Kirchhoff voltage law (KVL) states that the voltage sum over a closed loop must equal to zero. This is a static limit of Faraday's law. When there is no time varying field linking a closed loop, $\partial \overline{B}/\partial t = 0$, we have

$$\nabla \times \overline{E} = 0 \qquad (2.1.9)$$

Integrating the above equation over a closed loop, we obtain

$$\oint d\overline{\ell} \cdot \overline{E} = \sum_n V_n = 0 \qquad (2.1.10)$$

where the voltage drops are defined by $V_n = \int d\overline{\ell}_n \cdot \overline{E}$. In Figure 2.1.3, the sum of the voltage drops around the loop is equal to zero.
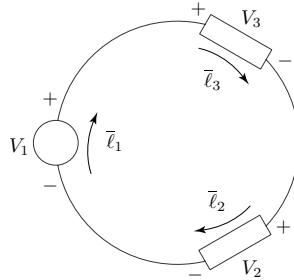
Figure 2.1.3 Kirchhoff voltage law (KVL).

The source voltage V_s may be generated by the EMF due to a time-varying magnetic field, governed by Faraday's law.

$$\nabla \times \overline{E} = -\frac{\partial}{\partial t}\overline{B} \qquad (2.1.11)$$

From Stokes theorem, we find

$$\oint d\overline{\ell} \cdot \overline{E} = \sum_n V_n = \text{EMF} \qquad (2.1.12)$$

where

$$\text{EMF} = -\frac{\partial}{\partial t}\iint d\overline{S} \cdot \overline{B} = -\frac{d\Psi}{dt} \qquad (2.1.13)$$

and $\Psi = \iint d\overline{S} \cdot \overline{B}$ is magnetic flux linking the loop. The Kirchhoff's voltage law (KVL) is thus modified with the addition of EMF in (2.1.12).

EXAMPLE 2.1.4

Consider the loop in Fig. E2.1.4.1 consisting of two resistors with resistances $R_1 = 2.5$ ohm and $R_2 = 7.5$ ohm. Let the magnetic flux linking the loop be increasing at the rate of 10 Wb/s. According to (2.1.13), an EMF of 10 V is induced to counter the increase. The direction of the induced current is as shown so as to produce a magnetic field in the opposite direction of the increasing magnetic field. The voltage across R_1 is $V_1 = 2.5$ V, which can be obtained by taking the closed loop consisting of the voltmeter and R_1 yielding $0 = 2.5 - V_1$, or by taking the loop consisting of the voltmeter and R_2 which includes the time varying magnetic field and yielding $10 = 7.5 + V_1$. Likewise, the voltage readings for the other two voltmeters are $V_2 = -7.5$ V and $V_3 = 2.5$ V.
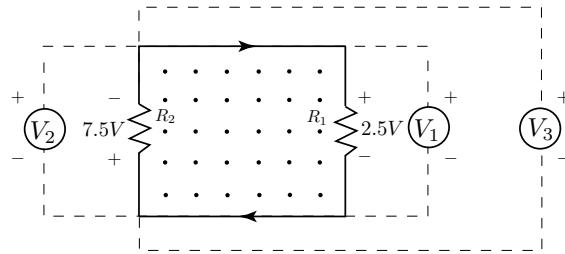
Figure E2.1.4.1 EMF of the loop is 10 volts.

It is noted that although the voltmeters for V_2 and V_3 are connected to the same two nodes, the two readings are drastically different, a clear violation of Kirchhoff's voltage law (KVL), which applies only when $\nabla \times \overline{E} = 0$.

Consider the electric circuit as shown in Fig. E2.1.4.2 where the induced counter EMF is 20 V. Following the same analysis, we find $V_1 = 5$ V, $V_2 = -15$ V, $V_3 = -5$ V, $V_4 = 10$ V, and $V_5 = 20$ V.
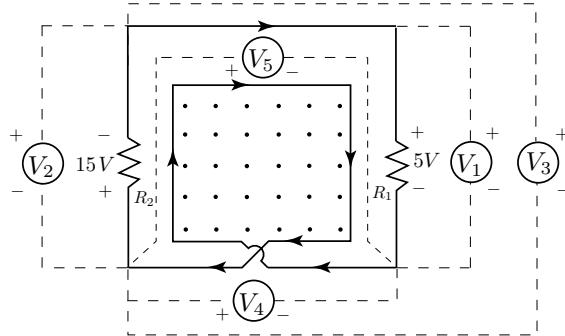
Figure E2.1.4.2 EMF of the loop is 20 volts.

— END OF EXAMPLE 2.1.4 —

Circuit Elements

The fundamental circuit elements are the resistor, the capacitor, and the inductor. The voltage V across a loop of N turns is equal to the negative of the induced EMF.

$$V = -\text{EMF} = \frac{d}{dt}\Psi = L_0 \frac{dI}{dt} \qquad (2.1.14)$$
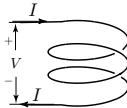
Figure 2.1.4 Inductance.

where $\Psi = \iint_A d\overline{S}\cdot\overline{B} = L_0 I$, and the loop can be viewed as an inductor with inductance L_0 such that the magnetic flux is proportional to the current I flowing in the loop.

The Kirchhoff current law (KCL) states that the currents flowing into a node must equal to those flowing out of the node. This is a result of the continuity law. When there is no charge accumulation at a point, $\partial\rho/\partial t = 0$, we have

$$\nabla \cdot \overline{J} = 0 \qquad (2.1.15)$$
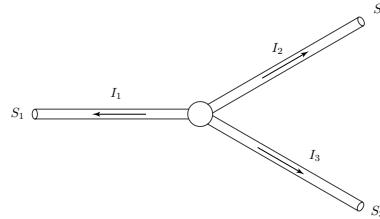
Figure 2.1.5 Kirchhoff current law (KCL).

Integrating the above equation over the surface enclosing the node, we obtain

$$\oiint_S d\overline{S} \cdot \overline{J} = \sum_n I_n = 0 \qquad (2.1.16)$$

where the currents are defined by $I_n = \iint d\overline{S}_n \cdot \overline{J}$. In Figure 2.1.5, the sum of the currents flowing out of the node is zero. Thus some of the arrows of the current directions must be reversed such that the currents flowing into the node equal the currents flowing out and the sum is zero.

Gustav Robert Kirchhoff (12 March 1824 – 17 October 1887)

Gustav Kirchhoff was a student of Gauss. In 1845 he announced Kirchhoff's laws, extending the theory of Georg Simon Ohm. He graduated from the University of Koenigsberg in 1847. In 1854 he became professor of physics at the University of Heidelberg. In 1875 he became chair of mathematical physics at the University of Berlin.

Notice that the Kirchhoff circuit laws in (2.1.16) and (2.1.10) are not dependent on either space or time. From the point of view of Faraday's law, (2.1.9) is true only when $\partial \overline{B}/\partial t = \mu_o \partial \overline{H}/\partial t = 0$ which is for static fields with no time variation, or mathematically equivalent to letting $\mu_o = 0$. Thus the speed of light can be thought of being equal to infinity in circuit theory.

Since the space coordinates do not enter the circuit theory, the spatial dimension of the layout of a circuit is theoretically zero (or the speed of light is infinite). Notice also the inconsistencies in the circuit theory. While Kirchhoff's current and voltage laws are statements of Ampère's and Faraday's laws when the time derivative is zero, the circuit elements of inductor and capacitor are defined using the time derivatives in the Faraday and Ampère laws. The circuit theory is a limiting case of the Maxwell equations when the time variation is small. In electromagnetic wave theory, this limit is equivalent to $k \approx 0$; therefore, it is applicable only when the frequency is very low or when the wavelength is very large. As the physical dimensions become comparable to the fraction of a wavelength, transmission line theory should be used in place of circuit theory.

Consider a cylindrical wire with cross-sectional area A carrying current I [Fig. 2.1.6a]. Let the cylinder be a conducting material with conductivity σ and governed by Ohm's law

$$\overline{J} = \sigma \overline{E} \tag{2.1.17}$$

Integrating Ampère's law

$$\nabla \times \overline{H} = \overline{J}$$

over the area of the cylinder A, we have from Stokes theorem

$$I = \oint_C d\overline{l} \cdot \overline{H} = JA = \frac{\sigma A}{\ell} V = GV \tag{2.1.18}$$

where $G = \sigma A/\ell$ is the conductance of the cylinder. The inverse of the conductance is resistance. Thus
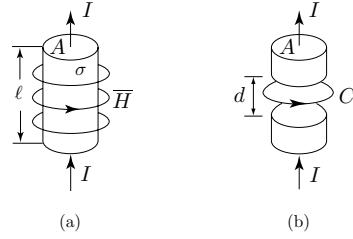
$$V = RI \qquad R = \frac{\ell}{\sigma A} \tag{2.1.19}$$

<div align="center">(a)　　　　　　　　(b)</div>

Figure 2.1.6 Displacement current.

According to Ampère's law with the displacement current $\partial \overline{D}/\partial t$

$$\nabla \times \overline{H} = \frac{\partial}{\partial t}\epsilon_o \overline{E}$$

the current flowing in a wire creates a magnetic field $\overline{H}$ circulating the wire. Now separate the wire into two pieces with a narrow gap of separation d [Fig. 2.1.6b]. There is no conduction current J across the gap. The gap area A is bounded by the closed loop C circulating along the magnetic field lines. Integrating Ampère's law over the gap area A, we have from Stokes theorem

$$I = \oint_C d\bar{l} \cdot \overline{H} = \frac{d}{dt} \iint d\overline{S} \cdot \epsilon_o \overline{E} = \frac{\epsilon_o A}{d} \frac{dV}{dt} = C_0 \frac{dV}{dt} \tag{2.1.20}$$

where $V = Ed$ is the voltage across the gap and $C_0 = \epsilon_o A/d$ is the capacitance of the gap area, which is a capacitor. The displacement current sustained by this capacitor, which accompanies a time varying voltage, assures the continuity of the current flow. Note that the capacitor is an opened circuit and direct current (dc) cannot flow, so current continuity is assured by the displacement current only for time varying fields. This represents a very practical consequence of the displacement term in Maxwell's theory, which preserves the continuity law.

Electric Conductive Circuits

According to Faraday's law, the sum of the voltage around a closed loop C is equal to the time-varying magnetic flux linking the area formed by the loop. Kirchhoff's voltage law (KVL) states that the voltage around a closed loop is equal to zero. Thus KVL is correct only when $\nabla \times \overline{E} = 0$. It is important to note that if there is magnetic field linking the loop, then KVL will be invalid.

The governing equations for electric conductive circuits are

$$\nabla \times \overline{E} = -\partial \overline{B}/\partial t \qquad (2.1.21)$$

$$\nabla \cdot \overline{J} = 0 \qquad (2.1.22)$$

$$\overline{J} = \sigma \overline{E} \qquad (2.1.23)$$

For an electric conductive circuit as shown in Fig. 2.1.7, we find

$$V_s = \frac{\ell}{\sigma A} I + \frac{d}{\sigma_o A} I = RI$$

Notice that the current density J in the conductive ring area is different from that in the gap area and

$$R = \frac{\ell}{\sigma A} + \frac{d}{\sigma_o A}$$
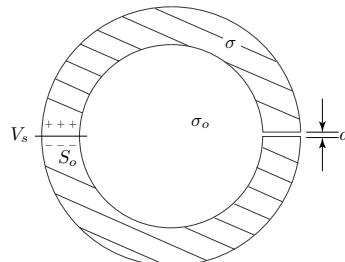
Figure 2.1.7 Electric circuit excited by voltage source.

The source voltage V_s may be generated by the EMF due to a time-varying magnetic field. The KVL in (2.1.12) is modified to read

$$\oint d\overline{\ell} \cdot \overline{E} = \sum_n V_n = \text{EMF} \qquad (2.1.24)$$

The Kirchhoff's voltage law (KVL) is modified with the addition of EMF in (2.1.24). The Kirchhoff's current law (KCL) can also be modified by restoring the term $-\partial \rho/\partial t$ in the right-hand side of (2.1.22).

Magnetic Circuits

A magnetic circuit is characterized by the following equations:

$$\nabla \times \overline{H} = \overline{J}_s \qquad\qquad (2.1.25)$$

$$\nabla \cdot \overline{B} = 0 \qquad\qquad (2.1.26)$$

$$\overline{B} = \mu \overline{H} \qquad\qquad (2.1.27)$$

where J_s includes both conduction and displacement currents. For a magnetic circuit as shown in Fig. 2.1.8, we integrate (2.1.25) along the closed contour C of the ring with permeability μ including the gap with width d, we find

$$I_s = \oint_C d\bar{\ell} \cdot \overline{H} \approx \frac{\Psi l}{\mu S_o} + \frac{\Psi d}{\mu_o S_o} = \mathcal{R}\Psi \qquad\qquad (2.1.28)$$
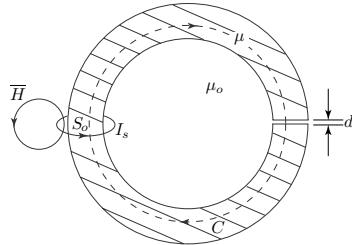
Figure 2.1.8 Magnetic circuit excited by current loop.

where $\mathcal{R}$ is known as the magnetic reluctance, which is analogous to the electric resistance in electric circuits. The loop current I_s that excites the magnetic circuit, is called the magnetomotive force (MMF), which may also be caused by the displacement current for a time-varying electric field integrated over the loop area.

We approximate the magnetic flux Ψ by

$$\Psi = \iint d\overline{S} \cdot \overline{B} \approx B S_o \qquad\qquad (2.1.29)$$

where S_o is the cross-sectional area of the ring. By virtue of (2.1.26), we see that the flux is continuous around the ring, thus in the magnetic material with permittivity μ, $\Psi = \mu H S_o$, and in the gap area $\Psi = \mu_o H S_o$. The magnetic field strength H in the magnetic material is different from that in the gap area.

Problems

P2.1.1

Capacitance is a constant relating current I to the time variation of V. Suppose the capacitor is charged to a total charge of Q. By integrating

$$I = C\frac{dV}{dt}$$

over time for the charging period, find the voltage V in terms of the total charge on the plate Q, and show that the capacitance C_0 is a measure of the ability to store electric charge.

P2.1.2

Consider a conductor of circular cross-section with radius $R = 1\,\text{mm}$ carrying a current $I = 1\,\text{Ampere}$, which is caused by movement of electric charges q. Calculate the velocity of the charge particles, assuming a charge density of $N = 8.5 \times 10^{28}$ per cubic meter.

P2.1.3

The inner conductor of a coaxial line is made of copper of diameter $2a = 0.501\,\text{cm}$ and the outer conductor is made of aluminum of diameter $2b = 1.393\,\text{cm}$. The dielectric between the inner and outer conductors is polyethylene with $\epsilon = 1.5\epsilon_o$. What is the characteristic impedance of the coaxial line? If the maximum voltage is 250 volt, what is the maximum electric field in the line?

P2.1.4

The behavior of TEM lines is characterized by their inductance per unit length L and capacitance per unit length C, and the same basic relationships $(Z_0 = \sqrt{L/C}$ and $k = \omega\sqrt{LC} = \omega\sqrt{\mu\epsilon})$ apply to all such lines.

(a) For a coaxial line, let the separation distance between the two concentric perfect conductors be d. Find the dimensions as a function of d for an air-filled coaxial line with a characteristic impedance of $50\,\Omega$.
(b) Repeat for a parallel-plate line.
(c) In designing a feeding system to drive a particular load, one finds that an essential component is a coaxial line with a characteristic impedance of $1 \times 10^4\,\Omega$. Would this be a practical design?
(d) Would it be practical to have $Z_0 = 1\,\Omega$ for an air-filled coaxial line?

P2.1.5

The behavior of TEM lines is characterized by their inductance per unit length, L, and capacitance per unit length, C, and the same basic relationships $(Z_0 = \sqrt{L/C}$ and $k = \omega\sqrt{L/C} = \omega\sqrt{\mu\epsilon})$ apply to all such lines.

The values of L and C for any arbitrary cross-section can be computed

using:

$$C = \frac{Q}{V} = \frac{\oint \epsilon \overline{E}_T \cdot (-\hat{z} \times d\bar{\ell})}{\int_1^2 \overline{E}_T \cdot d\bar{s}} \qquad L = \frac{\Psi}{I} = \frac{\int_1^2 \mu \overline{H}_T \cdot (\hat{z} \times d\bar{s})}{\oint \overline{H}_T \cdot d\bar{\ell}}$$

where $\overline{E}_T$ and $\overline{H}_T$ are the transverse field components in the x-y plane $(E_z = H_z \equiv 0)$. [Figure P2.1.5.1]
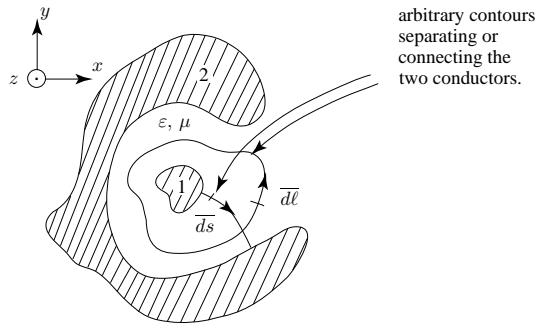

Figure P2.1.5.1

(a) Show that $LC = \mu\epsilon$.
(b) Let the separation distance between the two perfect conductors be d. Find the dimensions as a function of d for an air-filled coaxial line with a characteristic impedance of 50 ohms.
(c) Repeat for a parallel plate line.
(d) In designing a feeding system to drive a particular load, one finds that an essential component is a coaxial line with a characteristic impedance of 1×10^3 ohms. Would this be feasible design?
(e) Would it be practical to have $Z_0 = 1\,\Omega$ for an air-filled coaxial line? For a parallel plate line?

2.2   Time-Domain Transmission Line Theory

A. Wave Equations and Wave Solutions

Eliminating $I(z,t)$ or $V(z,t)$ from (2.1.7) and (2.1.8), we obtain

$$\left(\frac{\partial^2}{\partial z^2} - LC\frac{\partial^2}{\partial t^2}\right)\begin{bmatrix} V(z,t) \\ I(z,t) \end{bmatrix} = 0 \qquad (2.2.1)$$

which are the wave equations for $V(z,t)$ and $I(z,t)$.

For waves propagating in the $+\hat{z}$ direction, a solution for $V(z,t)$ is

$$V(z,t) = V_0 \cos(kz - \omega t) \qquad (2.2.2)$$

Substituting in (2.2.1) we obtain the dispersion relation

$$k^2 = \omega^2 LC \qquad (2.2.3)$$

The velocity of propagation is

$$v = \frac{\omega}{k} = \frac{1}{\sqrt{LC}} = \frac{1}{\sqrt{\mu\epsilon}} \qquad (2.2.4)$$

which is equal to the velocity of light. The relation $\sqrt{LC} = \sqrt{\mu\epsilon}$ is seen to hold for the parallel plate waveguide and the coaxial lines, which is in fact generally true for a TEM wave propagating on a general transmission line.

From (2.1.7) or (2.1.8), we find the corresponding $I(z,t)$

$$I(z,t) = \sqrt{\frac{C}{L}}\, V_0 \cos(kz - \omega t) = \frac{1}{Z_0} V(z,t) \qquad (2.2.5)$$

We define the characteristic impedance of the line Z_0 to be

$$Z_0 = \sqrt{\frac{L}{C}} \qquad (2.2.6)$$

which has the dimension of impedance and relates V and I as $V = Z_0 I$. The solutions (2.2.2) and (2.2.5) represent a sinusoidal wave propagating in the $\hat{z}$ direction because as time increases, z must also increase in order to maintain a phase $kz - \omega t = \text{constant}$.

For a voltage wave propagating in the $-\hat{z}$ direction, we write the solution as

$$V(z,t) = V_0 \cos{(kz + \omega t)}$$

The associated current wave is then

$$I(z,t) = -\sqrt{\frac{C}{L}}\, V_0 \cos{(kz + \omega t)} = -\frac{1}{Z_0}\, V(z,t) \qquad (2.2.7)$$

The negative sign in (2.2.7) can be understood by realizing that the magnetic fields in a parallel plate waveguide for the negative travelling wave is opposite to that of the positive travelling wave.

We symbolize a transmission line in general with two fat lines [Fig. 2.2.1], on which voltage and current waves propagate with the characteristic velocity (2.2.4). We use thin lines to connect the transmission line to circuit elements. On the thin lines the voltage and current waves propagate with infinite velocity, thus their length is of no concern. In general, a voltage wave of arbitrary shape propagating in the $\hat{z}$ direction can be written as

$$V_+(z,t) = f(z - vt) \qquad (2.2.8)$$
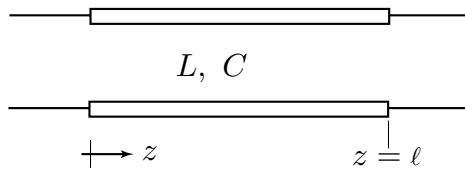
For a voltage wave propagating in the $-\hat{z}$ direction, we have

$$V_-(z,t) = f(z + vt) \qquad (2.2.9)$$

The corresponding current waves are

$$I_+(z,t) = \frac{1}{Z_0} f(z - vt) = \frac{1}{Z_0} V_+(z,t) \qquad (2.2.10)$$

$$I_-(z,t) = -\frac{1}{Z_0} f(z + vt) = -\frac{1}{Z_0} V_-(z,t) \qquad (2.2.11)$$

$$L,\ C$$

$$z \qquad\qquad z = \ell$$

Figure 2.2.1 Transmission line representation.

The transmission line equations (2.1.7) and (2.1.8) are satisfied with the above voltage and current solutions of general wave shape, and the voltage and current are related by the characteristic impedance Z_0.

EXAMPLE 2.2.1 Consider a transmission line of length ℓ that is open ended. The solutions to the wave equation (2.2.1) for the voltage and current waves are

$$V(z,t) = V_+ \cos(kz - \omega t) + V_- \cos(kz + \omega t) \qquad \text{(E2.2.1.1)}$$

$$I(z,t) = I_+ \cos(kz - \omega t) + I_- \cos(kz + \omega t) \qquad \text{(E2.2.1.2)}$$

The relations between the voltage and current waves traveling in the positive and negative $\hat{z}$ directions are given by (2.2.10) and (2.2.11):

$$I_+(z,t) = V_+(z,t)/Z_0 \qquad \text{(E2.2.1.3)}$$
$$I_-(z,t) = -V_-(z,t)/Z_0 \qquad \text{(E2.2.1.4)}$$
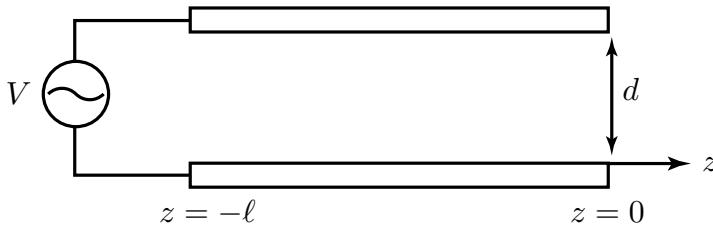
Figure E2.2.1.1 Open-circuited transmission line as capacitor.

Let the origin of the z axis be placed at the right end of the transmission line and the left end is connected to a source at $z = -\ell$. Since the current is zero at $z = 0$, we find $I_- = -I_+$. We thus have

$$V(z,t) = V_+[\cos(kz - \omega t) + \cos(kz + \omega t)] = 2V_+ \cos kz \cos \omega t$$

$$I(z,t) = I_+[\cos(kz - \omega t) - \cos(kz + \omega t)] = 2I_+ \sin kz \sin \omega t$$

A capacitance C_0 viewed from the input can be used to relate I and the time derivative of V as $I = C_0 dV/dt$. We find, in the limit when $-kz = k\ell \ll 1$,

$$C_0 = -\frac{I_+}{\omega V_+} \tan kz \approx \frac{1}{\omega Z_0} k\ell = \epsilon \frac{w\ell}{d}$$

for a parallel-plate waveguide. This corresponds to a capacitor of area $w\ell$ and separation d.

— END OF EXAMPLE 2.2.1 —

B. Transients on Transmission Lines

The transmission line equations that govern voltage $V(z,t)$ and current $I(z,t)$ on the line are

$$\frac{\partial}{\partial z} V(z,t) = -L \frac{\partial}{\partial t} I(z,t) \qquad (2.2.12)$$

$$\frac{\partial}{\partial z} I(z,t) = -C \frac{\partial}{\partial t} V(z,t) \qquad (2.2.13)$$

Wave equations for $V(z,t)$ and $I(z,t)$ can be derived from (2.2.12) and (2.2.13), which give

$$\left(\frac{\partial^2}{\partial z^2} - LC \frac{\partial^2}{\partial t^2} \right) \begin{bmatrix} V(z,t) \\ I(z,t) \end{bmatrix} = 0 \qquad (2.2.14)$$

Solutions to the second order partial differential equation (2.2.14) for $V(z,t)$ can be written as

$$V(z,t) = V_+(z - vt) + V_-(z + vt) \qquad (2.2.15)$$

where $V_+(z - vt)$ represents a voltage wave propagating in the $\hat{z}$ direction and $V_-(z + vt)$ represents a voltage wave propagating in the $-\hat{z}$ direction. Both $V_+(z - vt)$ and $V_-(z + vt)$ can assume general wave forms.

Substituting (2.2.15) in (2.2.14) yields

$$v = 1/\sqrt{LC} = 1/\sqrt{\mu\epsilon} \qquad (2.2.16)$$

which is equal to the speed of light.

We write the solution for $I(z,t)$ as

$$I(z,t) = I_+(z - vt) + I_-(z + vt) \qquad (2.2.17)$$

From the transmission line equations (2.2.12) and (2.2.13), we find the relationship between V_+ and I_+, and V_- and I_-:

$$V_+ = Z_0 I_+ \qquad (2.2.18)$$
$$V_- = -Z_0 I_- \qquad (2.2.19)$$

where

$$Z_0 = \sqrt{L/C} \qquad (2.2.20)$$

is the characteristic impedance of the transmission line. In (2.2.18) and (2.2.19) we also ignore the arguments $z - vt$ and $z + vt$ as the subscript $+$ in V and I denotes a wave traveling in the positive $\hat{z}$ direction with implied argument $z - vt$ and the subscript $-$ denotes a wave traveling in the negative $\hat{z}$ direction with implied argument $z + vt$.

From Transient to Steady State

To study transients on a transmission line, consider the transmission line with length ℓ in Fig. 2.2.2 which has a resistive termination R_L. At $z = \ell$, the total voltage V and current I must satisfy the boundary condition

$$V(z = \ell) = R_L\, I(z = \ell) \tag{2.2.21}$$

At $z = 0$ the line is connected to a dc voltage source V_0 with internal resistance R_s. The boundary condition at $z = 0$ is
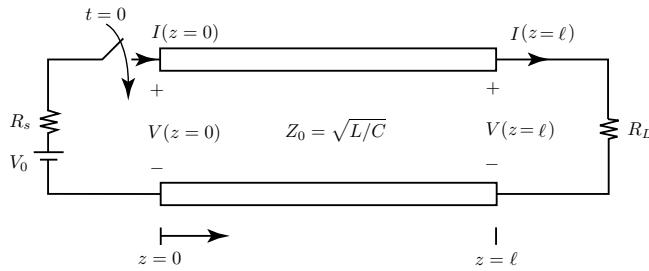
$$V_0 = V(z = 0) + R_s\, I(z = 0) \tag{2.2.22}$$

Figure 2.2.2 Transient on transmission line.

We turn on the voltage source at time $t = 0$. Thus for $t < 0$, $V = I = 0$. We also know that at steady state as $t \to \infty$, the voltage on the line is

$$V = \frac{R_L}{R_s + R_L}\, V_0$$

We now study the transient build-up of the voltage and current on the transmission line.

At $t = 0$ a forward traveling wave V_+ is generated. By the transmission line equations, the corresponding current is $I_+ = V_+/Z_0$. The boundary condition (2.2.22) gives

$$V_0 = V_+ + R_s\, I_+ = \left(1 + \frac{R_s}{Z_0}\right)V_+$$

This $\hat{z}$ directed traveling wave has a speed of $v = 1/\sqrt{LC}$ and will reach the termination R_L at $t = \ell/v$. We sketch

$$V_+ = \frac{V_0}{R_s/Z_0 + 1} = \frac{V_0}{R_{sn} + 1} \tag{2.2.23}$$
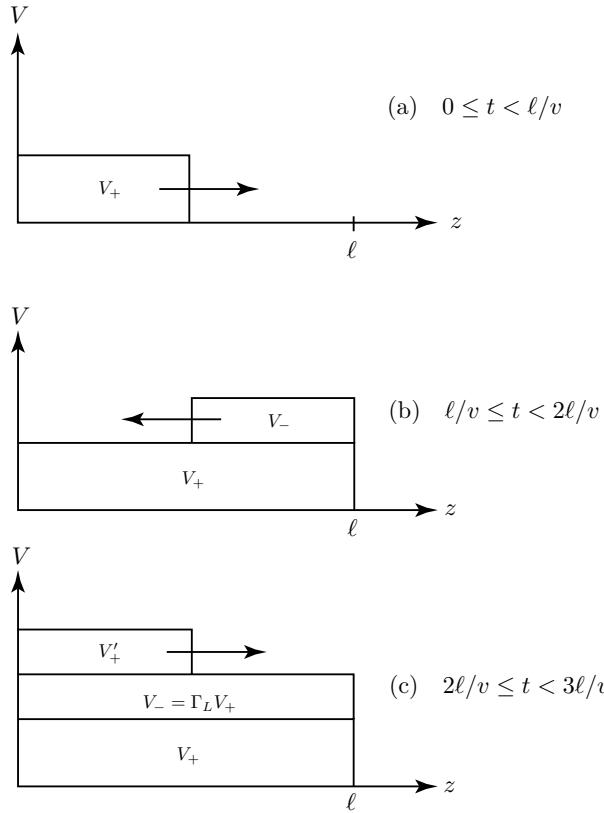
Figure 2.2.3 Transient build-up on a transmission line.

in Fig. 2.2.3a for $0 \le t < \ell/v$.

At time $t = \ell/v$, the voltage wave reaches the termination at $z = \ell$. The boundary condition (2.2.21) can only be satisfied by sending back a $-\hat{z}$ directed voltage wave V_- with the corresponding current wave $I_- = -V_-/Z_0$. The boundary condition (2.2.21) gives

$$V_+ + V_- = R_L \left(I_+ + I_-\right) = \frac{R_L}{Z_0}\left(V_+ - V_-\right) \qquad (2.2.24)$$

The backward traveling wave V_- is found to be

$$V_- = \frac{R_{Ln} - 1}{R_{Ln} + 1} V_+$$

We sketch both V_+ and V_- in Fig. 2.2.3b for $\ell/v \le t < 2\ell/v$. We

define a reflection coefficient at the load to be

$$\Gamma_L = \frac{R_{Ln} - 1}{R_{Ln} + 1} \tag{2.2.25}$$

and write

$$V_- = \Gamma_L V_+ \tag{2.2.26}$$

In the sketch, we assume $R_L > Z_0$.

At time $t = 2\ell/v$, the backward traveling wave reaches the source end at $z = 0$. A new forward traveling wave V'_+ and $I'_+ = V'_+/Z_0$ is generated. The boundary condition (2.2.22) requires that

$$V_0 = \left(V_+ + V_- + V'_+\right) + \frac{R_s}{Z_0}\left(V_+ - V_- + V'_+\right)$$

Making use of (2.2.24), we find

$$V'_+ = \frac{R_{sn} - 1}{R_{sn} + 1} V_- \tag{2.2.27}$$

We define a reflection coefficient at the source

$$\Gamma_s = \frac{R_{sn} - 1}{R_{sn} + 1} \tag{2.2.28}$$

and write

$$V'_+ = \Gamma_s V_- \tag{2.2.29}$$

The total voltage on the line for $2\ell/v \le t < 3\ell/v$ is sketched in Fig. 2.2.3c.

Repeating the process, we find the expression for the voltage on the line after an infinite number of reflections to be

$$\begin{aligned}
V &= V_+ + V_- + V'_+ + V'_- + V''_+ + V''_- + \cdots \\
&= V_+ \left(1 + \Gamma_L + \Gamma_s\Gamma_L + \Gamma_s\Gamma_L^2 + \Gamma_s^2\Gamma_L^2 + \Gamma_s^2\Gamma_L^3 \cdots\right) \\
&= V_+ \left(1 + \Gamma_L\right)\left[1 + \Gamma_s\Gamma_L + (\Gamma_s\Gamma_L)^2 + \cdots\right] \\
&= V_+ \left(1 + \Gamma_L\right)\frac{1}{1 - \Gamma_s\Gamma_L}
\end{aligned}$$

where we made use of the formula $\sum_{n=0}^{\infty} x^n = \frac{1}{1-x}$ as in our case $|x| = |\Gamma_s \Gamma_L| < 1$. It is straightforward to show that

$$V = \frac{V_0}{R_{sn} + 1} \frac{2R_{Ln}}{R_{Ln} + 1} \frac{(R_{sn} + 1)(R_{Ln} + 1)}{(R_{sn} + 1)(R_{Ln} + 1) - (R_{sn} - 1)(R_{Ln} - 1)}$$

$$= V_0 \frac{2R_{Ln}}{2(R_{sn} + R_{Ln})} = \frac{R_L}{R_s + R_L} V_0$$

which is exactly equal to the steady state value as $t \to \infty$.

We now consider the following special cases:

Case A) Open circuit

$\qquad R_L \to \infty$, matched source resistance $R_s = Z_0$.

SOLUTION: The reflection coefficients are

$$\Gamma_s = 0; \qquad \Gamma_L = \frac{R_L - Z_0}{R_L + Z_0} = \frac{1 - Z_0/R_L}{1 + Z_0/R_L} = 1$$

as $Z_0/R_L = 0$ when $R_L \to \infty$. We find

$$V_+ = \frac{1}{2} V_0, \qquad V_- = \Gamma_L V_+ = \frac{1}{2} V_0, \qquad V'_+ = 0$$

The results are sketched in Fig. 2.2.4. Steady-state is reached as $t \geq 2\ell/v$.
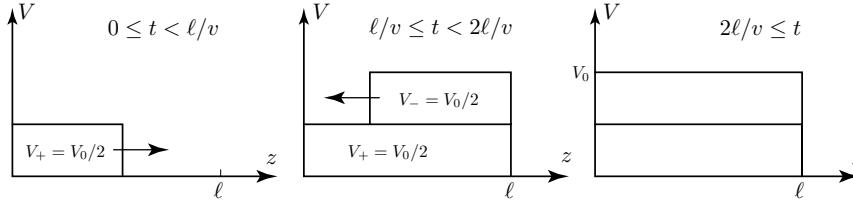
Figure 2.2.4 Transients on an open circuited line.

Case B) Short circuit

$\qquad R_L = 0$, matched source resistance $R_s = Z_0$.

SOLUTION:

$$\Gamma_s = 0 \qquad \Gamma_L = \frac{R_L - Z_0}{R_L + Z_0} = -1$$

$$V_+ = \frac{1}{2} V_0, \qquad V_- = \Gamma_L V_+ = -\frac{1}{2} V_0, \qquad V'_+ = 0$$

The results are sketched in Fig. 2.2.5.
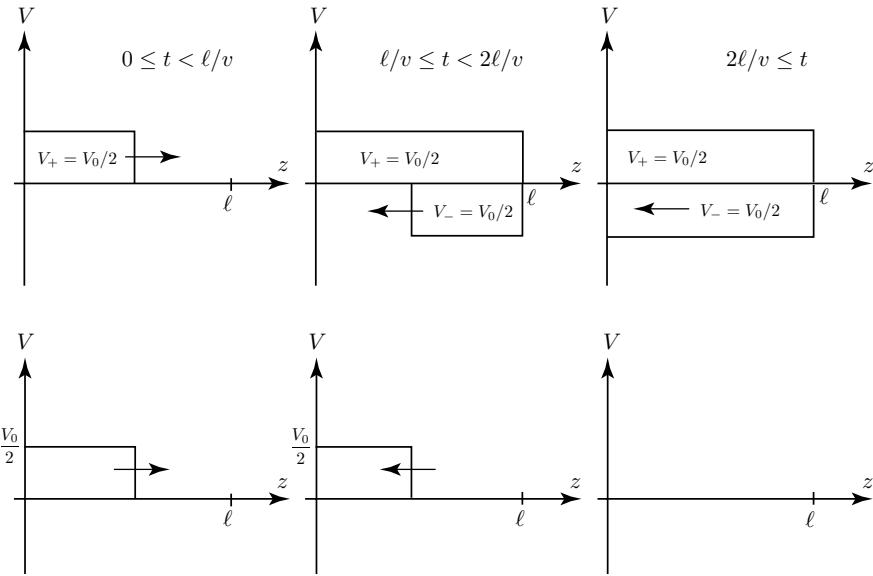
Figure 2.2.5 Transients on a shorted circuit line.

Case C) Matched load impedance $Z_L = Z_0$, and matched source impedance $Z_s = Z_0$.

SOLUTION: The reflection coefficients are $\Gamma_s = \Gamma_L = 0$. We find

$$V_+ = \frac{1}{2} V_0, \qquad V_- = 0$$

The results are sketched in Fig. 2.2.6.
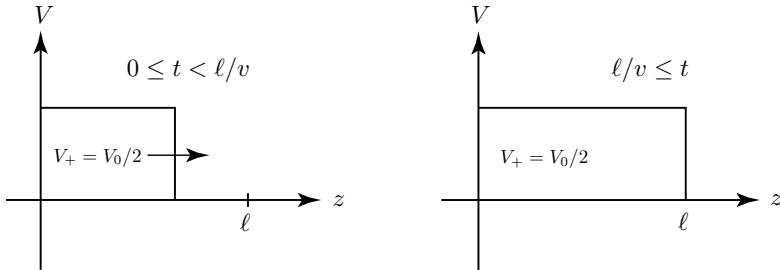
Figure 2.2.6 Transient on a matched line.

EXAMPLE 2.2.2   Capacitance terminated transmission line and matched source resistance $R_s = Z_0$, as shown in Fig. E2.2.2.1.
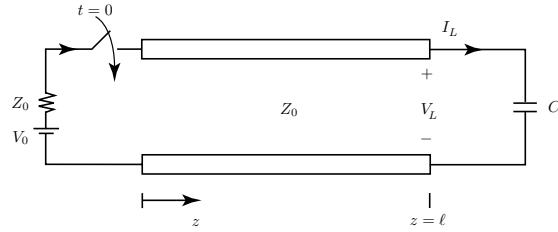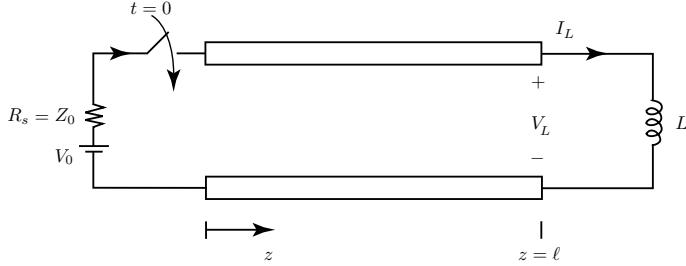

Figure E2.2.2.1 Transmission line with capacitive termination.

SOLUTION: The source reflection coefficient is $\Gamma_s = 0$. The boundary condition at $z = \ell$ with the capacitance termination is

$$I_L = C\,\frac{dV_L}{dt}$$

(a) $0 \le t < \frac{\ell}{v}$ (b) $\frac{\ell}{v} \le t < \frac{2\ell}{v}$
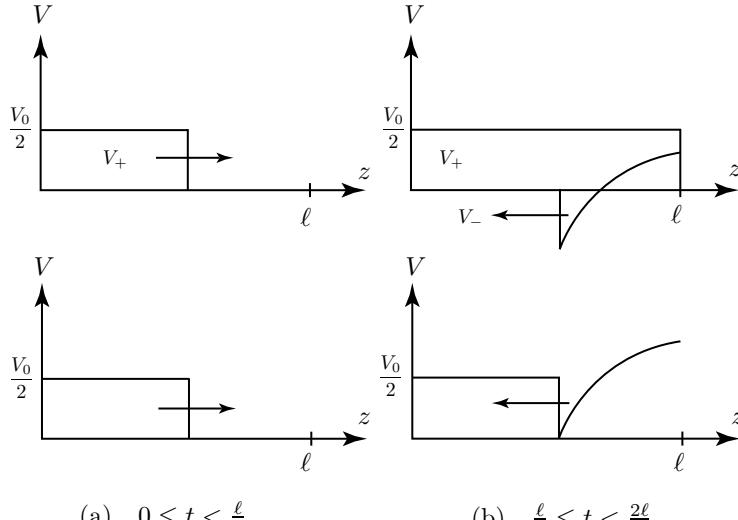
Figure E2.2.2.2 Transient on capacitor terminated line.

For $0 \le t < \ell/v$, the waveform is shown in Fig. E2.2.2.2a. At $t = \ell/v$, a backward traveling wave V_- is generated. The total load voltage is $V_L = V_+ + V_-$ and the total load current $I_L = (V_+ - V_-)/Z_0$. The boundary condition

at $z = \ell$ requires that $V_+ - V_- = Z_0 C \frac{dV_L}{dt}$ which yields a differential equation for V_L :

$$\frac{dV_L}{dt} + \frac{1}{Z_0 C} V_L = \frac{2}{Z_0 C} V_+$$

The particular solution is $V_L = 2V_+$. The homogeneous solution for $\ell/v \le t$ is $Ae^{-t/Z_0 C}$. At $t = \ell/v$, $V_L = 0$; it follows that $A = -2V_+ e^{\ell/v Z_0 C}$. We thus have

$$V_L = 2V_+ \left[1 - e^{-(t-\ell/v)/Z_0 C}\right] u(t - \ell/v)$$

where $u(t - \ell/v)$ is a step function with $u(t - \ell/v) = 1$ for $t - \ell/v \ge 0$ and $u(t - \ell/v) = 0$ for $t - \ell/v < 0$. We thus have

$$V_- = V_L - V_+ = V_0 \left[\frac{1}{2} - e^{-(t-\ell/v)/Z_0 C}\right] u(t - \ell/v)$$

The reflected wave V_- is sketched in Fig. E2.2.2.2b. It is seen that the capacitor first behaves as a short circuit and becomes open circuited when steady state is reached.
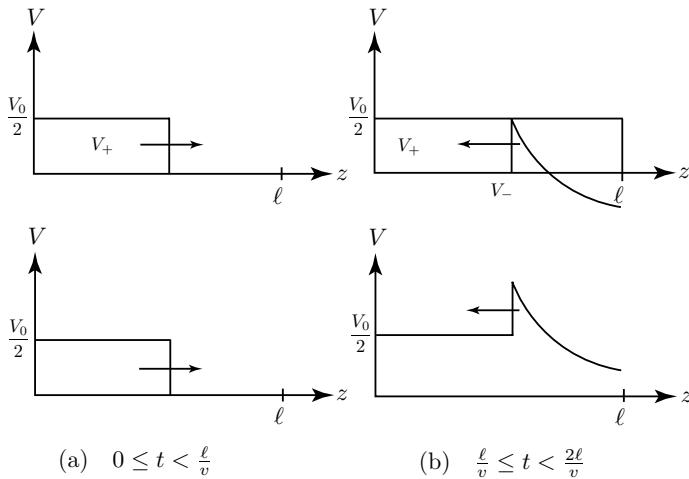
— END OF EXAMPLE 2.2.2 —

EXAMPLE 2.2.3   Inductance terminated transmission line and matched source resistance $R_s = Z_0$, as shown in Fig. E2.2.3.1.

Figure E2.2.3.1 Transmission line with inductive termination.

SOLUTION: The source reflection coefficient is $\Gamma_s = 0$. The boundary condition at $z = \ell$ with the inductor termination is

$$V_L = L \frac{dI_L}{dt}$$

For $0 \le t < \ell/v$, the waveform is sketched in Fig. E2.2.3.2a. At $t = \ell/v$, a backward traveling wave V_- is generated. The total load current is $I_L =$

$I_+ + I_-$ and the total load voltage $V_L = Z_0(I_+ - I_-)$. The boundary condition at $z = \ell$ requires that

$$Z_0(I_+ - I_-) = L\frac{dI_L}{dt}$$

which yields a differential equation for I_L:

$$\frac{dI_L}{dt} + \frac{Z_0}{L}I_L = 2\frac{Z_0}{L}I_+$$

At $t = \ell/v$, $I_L = 0$; the solution is

$$I_L = 2I_+\left[1 - e^{-Z_0(t-\ell/v)/L}\right]$$

and

$$I_- = I_L - I_+ = 2I_+\left[\frac{1}{2} - e^{-Z_0(t-\ell/v)/L}\right]$$

We thus have

$$V_- = -Z_0I_- = -V_0\left[\frac{1}{2} - e^{-Z_0(t-\ell/v)/L}\right]u(t - \ell/v)$$

The reflected wave V_- is sketched in Fig. E2.2.3.2b. It is seen that the inductor first behaves as an open circuit and becomes short circuited when steady state is reached.

(a) $0 \leq t < \frac{\ell}{v}$ (b) $\frac{\ell}{v} \leq t < \frac{2\ell}{v}$

Figure E2.2.3.2 Transient on an inductor terminated line.

— END OF EXAMPLE 2.2.3 —

EXAMPLE 2.2.4   A common method for generating short, high voltage pulses is to use a charged transmission line with a fast switch. The basic idea of such devices is illustrated in Fig. E2.2.4.1.
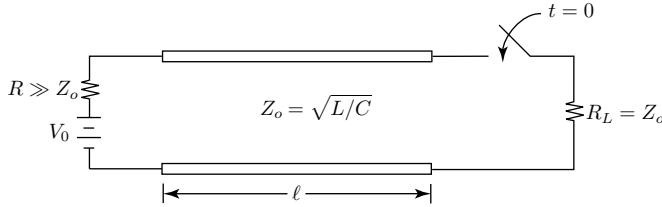
Figure E2.2.4.1

(a) The line has been charged to a voltage V_0 by a dc high voltage source with internal resistance $R \gg Z_0$. If the switch closes at $t = 0$ with the line fully charged to $V = V_0$, sketch and dimension the voltage $V_L(t)$ across the load.

(b) If the transmission line is an air-filled coaxial cable with $Z_0 = 50\,\Omega$, how long should the line be to give a voltage pulse of $0.1\,\mu$s duration? How big must the supply voltage be to deliver one joule of total pulse energy to the load R_L?

(c) To see if the above is physically reasonable, calculate the smallest possible inner radius of the air-filled $50\,\Omega$ coaxial line with $100\,\text{kV}$ charging voltage, if the breakdown electric field is taken as $3 \times 10^6\,\text{V/m}$.

SOLUTION:

(a) At $t = 0$, a backward traveling wave V_- is generated to satisfy the boundary condition at R_L,

$$V_0 + V_- = -\frac{V_-}{Z_0}R_L$$

which gives $V_- = -V_0/2$. The voltage V_L at R_L is

$$V_L = V_0 + V_- = \frac{V_0}{2}$$
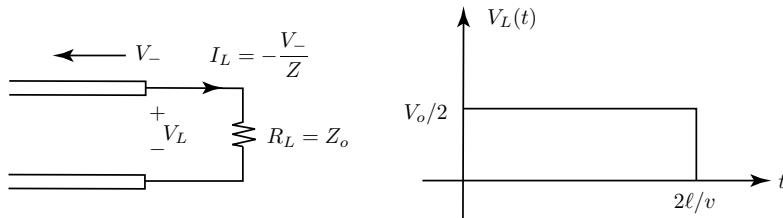
The load voltage $V_L(t)$ is shown in Fig. E2.2.4.2.

Figure E2.2.4.2

(b)

$$\frac{2\ell}{v} = 10^{-7}\,\text{s} \qquad \text{gives} \qquad \ell = 15\,\text{m}$$

$$\left(\frac{V_0}{2}\right)^2 \frac{1}{Z_0} t = 1\ \text{J} \qquad \text{gives} \qquad V_0 = 44.7\,\text{kV}$$

(c) For a coaxial line we have the following:

$$Z_0 = \eta\frac{\ln(b/a)}{2\pi} = 50\ \Omega \qquad \text{gives} \qquad \ln\left(\frac{b}{a}\right) = \frac{5}{6}$$

$$\overline{E}(\rho, z) = \hat{\rho}\frac{V(z)}{\rho\ln(b/a)} \qquad \text{gives} \qquad \frac{V_0}{a\ln(b/a)} \le 3 \times 10^6\ \text{V/m}$$

this yields $b = 2.3a$ and $a \ge 4\,\text{cm}$.

— END OF EXAMPLE 2.2.4 —

EXAMPLE 2.2.5   A modified form of the scheme in Example 2.2.4 is the Blumlein (Alan Dower Blumlein 1903–1942) line as shown in Fig. E2.2.5.1. Both lines are of length ℓ. Sketch and dimension $V_L(t)$. What is the advantage of this scheme?
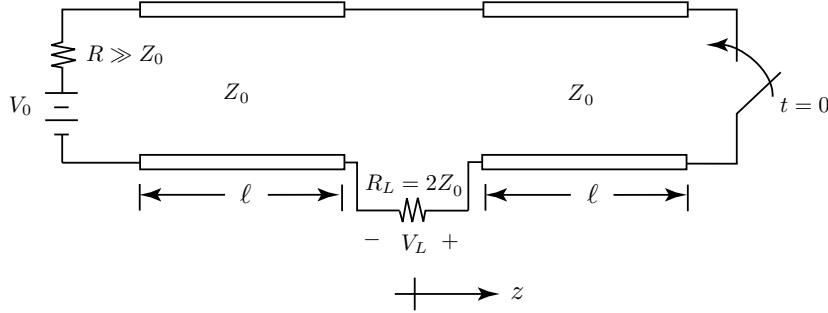
Figure E2.2.5.1 Blumlein line.

SOLUTION:

At $t = 0$, a backward traveling wave $V_- = -V_0$ is generated at $z = \ell$.

At $t = \ell/v$, V_- reaches the load $R_L = 2Z_0$ at $z = 0$. A reflected wave V'_+ is generated on the transmission line at $z = 0_+$. The equivalent circuit is shown in Fig. E2.2.5.2. The current at R_L is $I_L = I'_+ + I_- = (V'_+ - V_-)/Z_0 = V_0/2Z_0$, and the voltage at R_L is $V_L = I_L R_L = V_0$. The boundary condition

to be satisfied at $z = 0_+$ is $V_- + V'_+ = -I_L(R_L + Z_0) = (V_- - V'_+)(R_L + Z_0)/Z_0$, which gives $V'_+ = \Gamma V_-$, where the reflection coefficient is

$$\Gamma = \frac{3Z_0 - Z_0}{3Z_0 + Z_0} = \frac{1}{2}$$

Thus

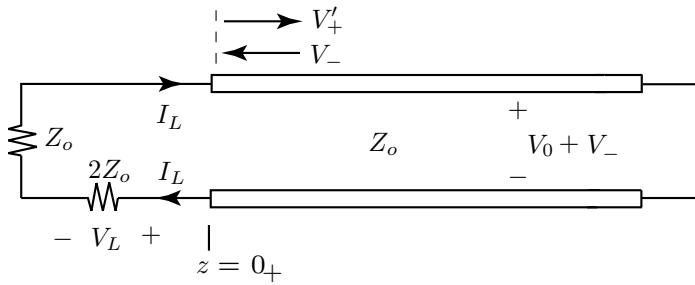$$V'_+ = \Gamma V_- = -V_0/2 \qquad \text{at} \qquad z = 0_+$$

Figure E2.2.5.2

At $z = 0_-$, a wave V'_- is generated. By KVL, $V_0 + V'_- = V_0 + V_- + V'_+ + V_L$, thus

$$V'_- = V'_+ = -V_0/2 \qquad \text{at} \qquad z = 0_-$$

At $t = 2\ell/v$, V'_- generates a reflected wave V''_+ at $z = -\ell$, which has a reflection coefficient $\Gamma = 1$. Thus

$$V''_+ = V'_- = -V_0/2 \qquad \text{at} \qquad z = -\ell$$

At the same time $t = 2\ell/v$, V'_+ generates a reflected wave V''_- at $z = \ell$, which has a reflection coefficient $\Gamma = -1$. Thus

$$V''_- = -V'_+ = V_0/2 \qquad \text{at} \qquad z = \ell$$

At $t = 3\ell/2v$, V''_+ and V''_- reach the load at $z = 0$. By KVL,

$$V_0 + V'_- + V''_+ = V_0 + V_- + V'_+ + V''_- + V_L$$

which gives $V_L = 0$. The newly generated pair of waves $V'''_+ = V'''_- = V_0/4$ will again give $V_L = 0$ at later times. Therefore, $V_L = V_0$ for the duration from $t = \ell/v$ to $t = 3\ell/v$. The advantage of the Blumlein line is that the pulse amplitude is V_0 instead of $V_0/2$ as shown in Example 2.2.4.

<div align="right">— END OF EXAMPLE 2.2.5 —</div>

C. Normal Modes and Natural Frequencies

Consider the transmission line shown in Fig. 2.2.7. The left-hand-side at $z = 0$ is short circuited and the right-hand-side at $z = \ell$ is an open circuit. The voltage and current waves on the line are governed by the transmission line equations

$$\frac{\partial}{\partial z} V(z,t) = -L\frac{\partial}{\partial t} I(z,t) \tag{2.2.30}$$

$$\frac{\partial}{\partial z} I(z,t) = -C\frac{\partial}{\partial t} V(z,t) \tag{2.2.31}$$

with the boundary conditions

$$V(z = 0) = 0 \tag{2.2.32}$$
$$I(z = \ell) = 0 \tag{2.2.33}$$
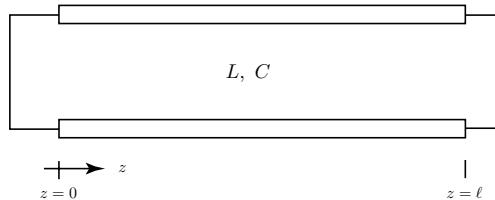
Figure 2.2.7 Transmission line with $V(z = 0) = 0$ and $I(z = \ell) = 0$.

Solutions to (2.2.30) and (2.2.31) for $V(z,t)$ and $I(z,t)$ are

$$V(z,t) = A\sin(kz - \omega t) + B\sin(kz + \omega t) \tag{2.2.34}$$

$$I(z,t) = \frac{1}{Z_0}\left[A\sin(kz - \omega t) - B\sin(kz + \omega t)\right] \tag{2.2.35}$$

with the dispersion relation $k = \omega\sqrt{LC}$. Boundary condition (2.2.32) yields $B = A$. Solutions (2.2.34) and (2.2.35) become

$$V(z,t) = V\sin kz\cos\omega t \tag{2.2.36}$$

$$I(z,t) = -\frac{V}{Z_0}\cos kz\sin\omega t \tag{2.2.37}$$

where $V = 2A$. The boundary condition (2.2.33) gives

$$\cos k\ell = 0 \tag{2.2.38}$$

From (2.2.38) we find the natural spatial frequency of the nth mode

$$k_n = \frac{n\pi}{2\ell} \qquad n: \text{ odd} \tag{2.2.39}$$

where we use subscript n to indicate that k now takes on only a discrete set of values. The corresponding natural temporal frequency of the nth mode is

$$\omega_n = \frac{n\pi}{2\ell\sqrt{LC}} = \frac{n\pi}{2}\frac{v}{\ell} \qquad n: \text{ odd} \tag{2.2.40}$$

where $v = 1/\sqrt{LC}$ is the characteristic velocity of the line.

The voltage distribution of the nth mode along the line is

$$V_n(z,t) = V_n \sin\frac{n\pi}{2}\frac{z}{\ell} \ \cos\frac{n\pi}{2}\frac{vt}{\ell} \tag{2.2.41}$$
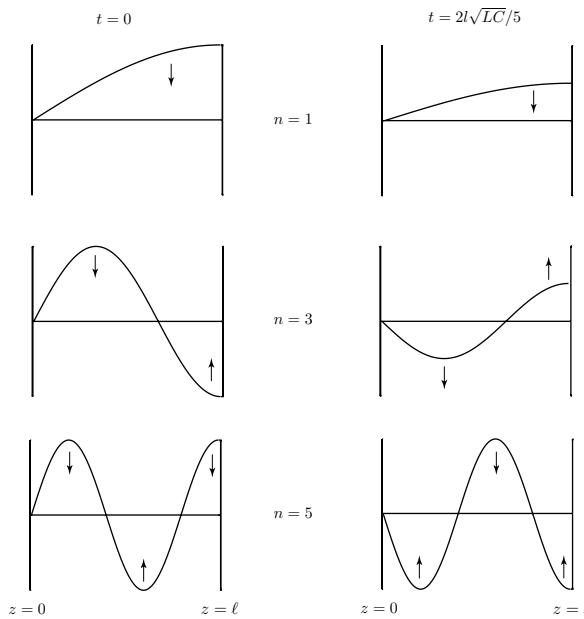
Figure 2.2.8 Normal modes V_1, V_3, V_5 **at times** $t = 0$ **and** $2\ell/5v$.

We now illustrate $V_n(z,t)$ at various times for the different modes. In Fig. 2.2.8 we plot the first three modes at times $t = 0$ and $t = 2\ell/5v$. We observe that since the z-dependence is fixed, the amplitudes of

each mode varies with time; the higher the mode number, the higher the spatial variation and the higher the temporal frequency of amplitude variation. The arrows indicate the direction of the amplitude dependence for increasing t.

D. Initial Value Problem

Consider the transmission line in Fig. 2.2.9. The line is charged to a unit voltage for $t < 0$. At $t = 0$, the left-hand-side at $z = 0$ is short circuited. We wish to investigate the waveform evolution after the switch is closed.
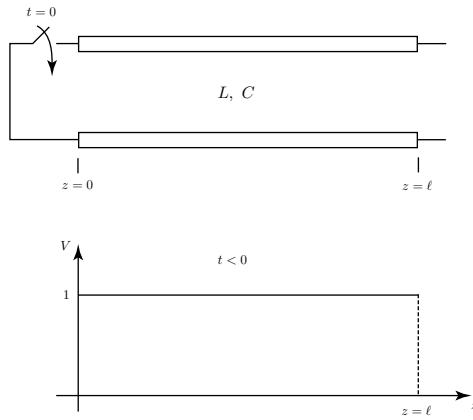

Figure 2.2.9 Initial value problem.

We have learned the normal modes of the line with a short circuit on the left at $z = 0$ and an open circuit on the right at $z = \ell$. Each mode satisfies the transmission line equations and boundary conditions. We express $V(z, t)$ as a superposition of all these modes with different mode amplitudes V_n.

$$V(z, t) = \sum_{\substack{n=1 \\ n\,\text{odd}}}^{\infty} V_n \sin \frac{n\pi}{2} \frac{z}{\ell} \cos \frac{n\pi}{2} \frac{vt}{\ell} \qquad (2.2.42)$$

The total voltage $V(z, t)$ also satisfies the transmission line equations and the boundary conditions. The mode amplitudes V_n are to be determined from the initial condition.

The initial condition is $V(z, t = 0) = 1$. Substituting in (2.2.42) we have

$$1 = \sum_{\substack{n=1 \\ n\,\mathrm{odd}}}^{\infty} V_n \sin \frac{n\pi z}{2\ell}$$

$$= V_1 \sin \frac{\pi z}{2\ell} + V_3 \sin \frac{3\pi z}{2\ell} + V_5 \sin \frac{5\pi z}{2\ell} + \cdots$$

To find V_5, for instance, we multiply both sides by $\sin \frac{5\pi z}{2\ell}$ and integrate from $z = 0$ to $z = \ell$. All terms on the right-hand-side become zero after the integration except the term $V_5 \sin \frac{5\pi z}{2\ell}$. We find

$$\int_0^\ell dz \sin \frac{5\pi z}{2\ell} = V_5 \int_0^\ell dz \sin^2 \frac{5\pi z}{2\ell} = \frac{\ell}{2} V_5$$

Thus

$$V_5 = \frac{2}{\ell} \int_0^\ell dz \sin \frac{5\pi z}{2\ell}$$

In general, we have

$$V_n = \frac{2}{\ell} \int_0^\ell dz \sin \frac{n\pi z}{2\ell} = \frac{4}{n\pi} \left[-\cos \frac{n\pi z}{2\ell} \right]_0^\ell = \frac{4}{n\pi}$$

Therefore

$$V(z, t) = \sum_{\substack{n=1 \\ n\,\mathrm{odd}}}^{\infty} \frac{4}{n\pi} \sin \frac{n\pi z}{2\ell} \cos \frac{n\pi}{2} \frac{vt}{\ell} \qquad (2.2.43)$$

is the solution for the voltage on the line for $t \geq 0$.

We now study the solution for several different times at $t = 0$, $t = \ell/2v$, $t = \ell/v$, and $t = 3\ell/2v$. In Fig. 2.2.10a–d, we sketch the sum of the first three terms.

At $t = 0$, we have

$$V(z, t = 0) = \frac{4}{\pi} \sin \frac{\pi z}{2\ell} + \frac{4}{3\pi} \sin \frac{3\pi z}{2\ell} + \frac{4}{5\pi} \sin \frac{5\pi z}{2\ell} + \cdots$$

The sum over all of the terms should give back the initial condition of $V(z, t \leq 0) = 1$.
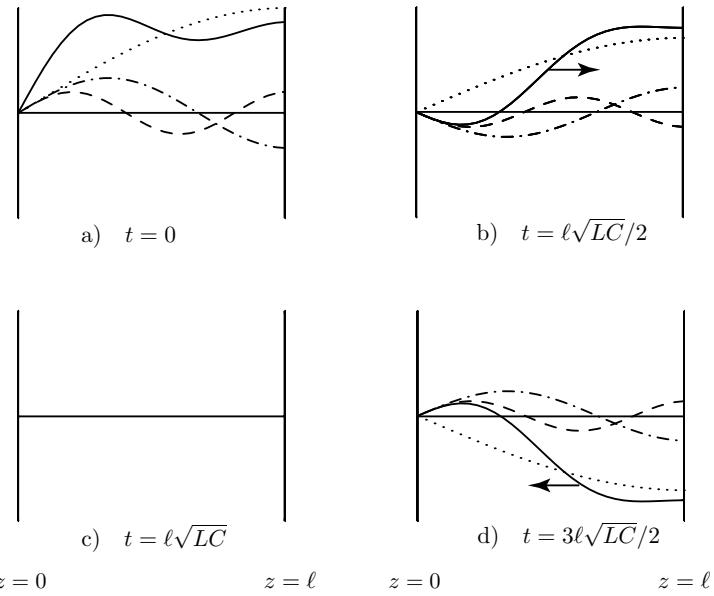
a) $t = 0$

b) $t = \ell\sqrt{LC}/2$

c) $t = \ell\sqrt{LC}$

d) $t = 3\ell\sqrt{LC}/2$

$z = 0$ $z = \ell$ $z = 0$ $z = \ell$

Figure 2.2.10 Superposition of normal modes.

At $t = \ell/2v$, we have

$$V(z, t = \ell/2v) = \frac{4}{\pi} \sin \frac{\pi z}{2\ell} \cos \frac{\pi}{4} + \frac{4}{3\pi} \sin \frac{3\pi z}{2\ell} \cos \frac{3\pi}{4}$$
$$+ \frac{4}{5\pi} \sin \frac{5\pi z}{2\ell} \cos \frac{5\pi}{4} + \cdots$$

At $t = \ell/v$, we have $V(z, t = \ell/v) = 0$.

At $t = 3\ell/2v$, we have

$$V(z, t = 3\ell/2v) = \frac{4}{\pi} \sin \frac{\pi z}{2\ell} \cos \frac{3\pi}{4} + \frac{4}{3\pi} \sin \frac{3\pi z}{2\ell} \cos \frac{9\pi}{4}$$
$$+ \frac{4}{5\pi} \sin \frac{5\pi z}{2\ell} \cos \frac{15\pi}{4} + \cdots$$

We see that the wave travels back and forth along the line.

If we add up all terms of the series for $V(z, t)$, we should obtain
the result in Fig. 2.2.11. This is seen by solving the problem in the
time-domain as illustrated in Section 4.3. At time $t = 0$ when the
switch is closed, a positive traveling wave is generated to satisfy the
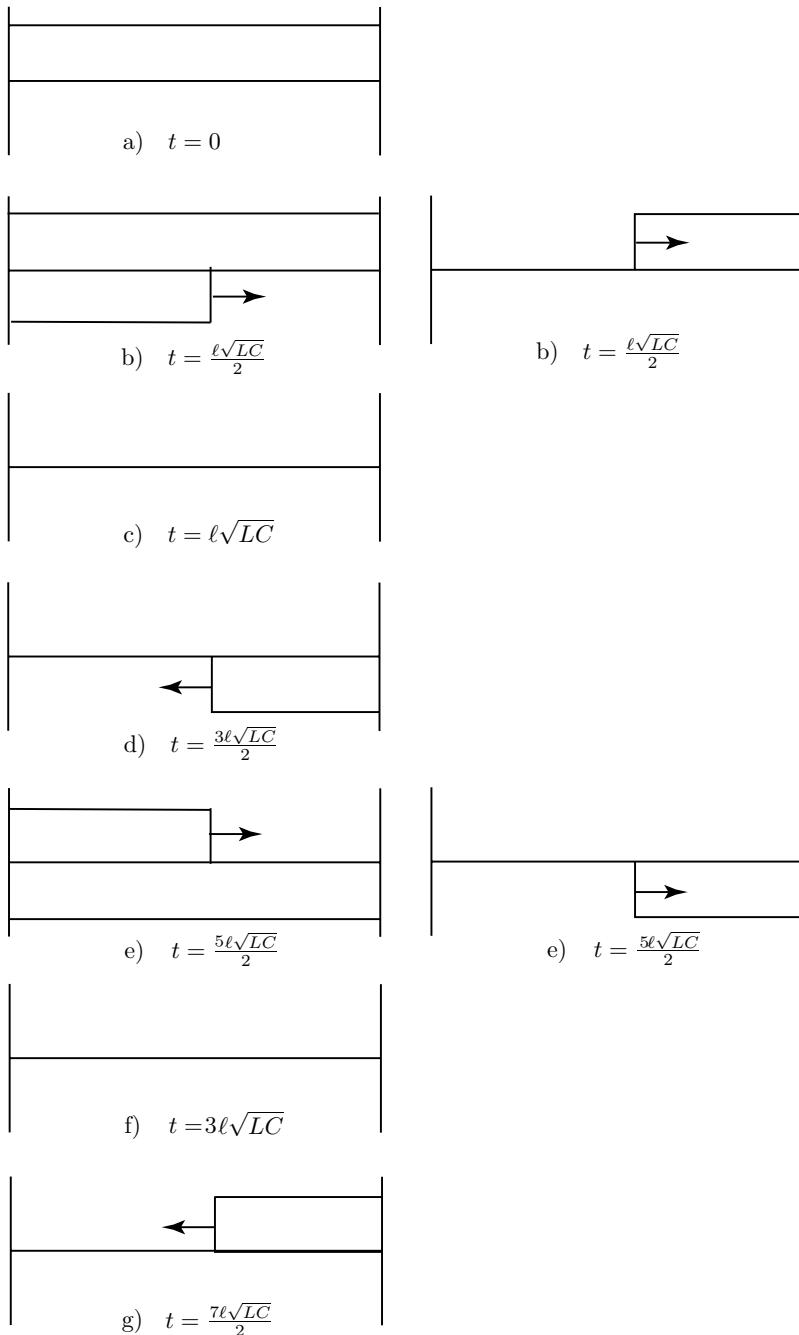
a) $t = 0$

b) $t = \frac{\ell\sqrt{LC}}{2}$

b) $t = \frac{\ell\sqrt{LC}}{2}$

c) $t = \ell\sqrt{LC}$

d) $t = \frac{3\ell\sqrt{LC}}{2}$

e) $t = \frac{5\ell\sqrt{LC}}{2}$

e) $t = \frac{5\ell\sqrt{LC}}{2}$

f) $t = 3\ell\sqrt{LC}$

g) $t = \frac{7\ell\sqrt{LC}}{2}$

Figure 2.2.11 Solution to the initial value problem.

boundary condition of $V = 1 + V_+ = 0$ at $z = 0$. This yields $V_+ = -1$ for the time period $0 \leq t < \ell/v$. The result is Fig. 2.2.11b. At $t = \ell/v$, the positive traveling wave V_+ has reached the open circuit end and the boundary condition calls for the generation of a negative traveling wave such that the total current $I = (V_+ - V_-)/Z_0 = 0$. Thus $V_- = V_+ = -1$ for the time period $\ell/v \leq t < 2\ell/v$ and the result is shown in Fig. 2.2.11d. The reflection coefficient $\Gamma = -1$ at $z = -\ell$ gives $V'_+ = 1$ for the period $2\ell/v \leq t < 3\ell/v$ and the reflection coefficient $\Gamma = -1$ at $z = 0$ gives $V'_- = 1$ for the period $3\ell/v \leq t < 4\ell/v$. The results are shown in Fig. 2.2.11e-g.

EXAMPLE 2.2.6

Consider a transmission line resonator with length l and terminated with impedances R_s and R_l as shown in Figure E2.2.6.1.
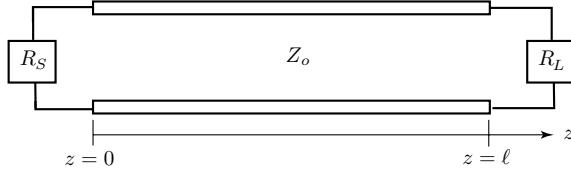

Figure E2.2.6.1 Transmission line resonator.

For open-circuited resonators, $R_S \rightarrow \infty$ and $R_L \rightarrow \infty$, we find that the resonance spatial frequencies are $k = n\pi/l$ with $n = 0, 1, 2, ...$ and the voltages and currents are

$$V(z) = V_0 \cos \frac{n\pi z}{l}$$
$$I(z) = I_0 \sin \frac{n\pi z}{l}$$

The currents are zero at $z = 0$ and $z = l$. The $n = 0$ mode has zero current and a constant voltage on the line.

For short-circuited resonators, $R_S = R_L = 0$, the resonance spatial frequencies are $k = (2n + 1)\pi/2l$ with $n = 0, 1, 2, ...$ and the voltages and currents are

$$V(z) = V_0 \cos \frac{(2n + 1)\pi z}{2l}$$
$$I(z) = I_0 \sin \frac{(2n + 1)\pi z}{2l}$$

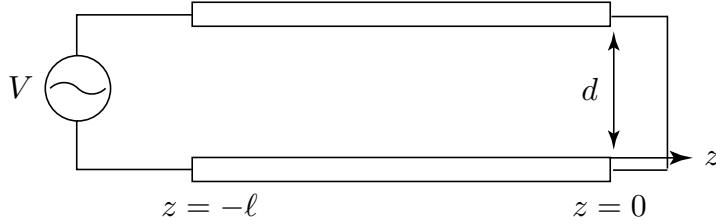The voltages are zero at $z = 0$ and $z = l$.

— END OF EXAMPLE 2.2.6 —

Problems

P2.2.1

An inductance L_0 is defined as

$$V = L_0 dI/dt$$

Consider a transmission line of length ℓ that is short circuited.

Figure P2.2.1.1 Short-circuited transmission line as inductor.

In the limit when $-kz = k\ell \ll 1$, find L_o.

P2.2.2

Model a stripline as a parallel-plate transmission line with $d = 3.16\,\text{mm}$ and $w = 3.76\,\text{mm}$, separated by dielectric with permittivity $\epsilon = 2.5\epsilon_o$. The electric and magnetic fields in the stripline are

$$E_x\,(z,t) = E_0 \cos(kz - \omega t)$$
$$H_y\,(z,t) = (E_0/\eta) \cos(kz - \omega t)$$

(a) What is the characteristic impedance of the line?
(b) What are the voltage and current on the line?
(c) What is the time-averaged power on the line?
(d) If the breakdown electric field of the dielectric field is $2 \times 10^7\,\text{V/m}$ and the maximum time-averaged power on the line is $100\,\text{kW}$, will the corresponding maximum electric field strength be below the breakdown field strength?

P2.2.3

Consider an air-filled TEM transmission line with length l as shown in Figure P2.2.3.1. The voltage of the source is V_o and the resistor at the source is $R_s = Z_0$, where Z_0 is the characteristic impedance of the line. The switch at the load is on for $t < 0$, the voltage and current on the line are stationary.

At $t = 0$, the switch at $z = 0$ is suddenly opened.

(a) Sketch the voltage on the line at $t = l/2v$, where v is the velocity of wave on the line. Indicate the value of the voltage on the line.
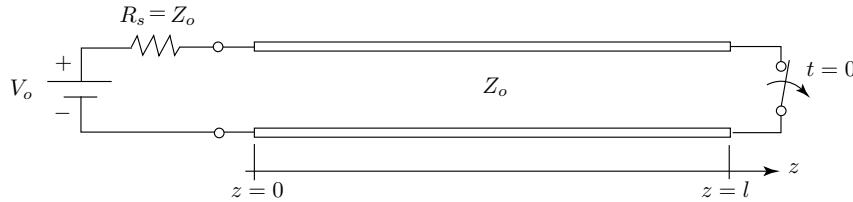
Figure P2.2.3.1

(b) Find the time $t \, (> 0)$, so that the voltage on the line becomes constant. What is the value of this constant voltage?

P2.2.4

A time-domain reflectometer (TDR) is used to detect fault on a transmission line, which could be an underground or undersea cable being damaged at a distance ℓ_f from the generator. Model the fault as a shunt resistance R_f. A unit step voltage is sent from the generator down the line at time $t = 0$. At time $t = 20 \, \mu s$, the voltage reads $V = 0.5 \, \text{V}$ instead of $V = 1 \, \text{V}$ which lasted from $t = 0$ to $t = 20 \, \mu s$. Assuming that the insulating material for the transmission line has a relative permittivity of $\epsilon = 2.25$ and its characteristic impedance is $Z_0 = 90 \, \Omega$, determine the distance of the fault from the generator ℓ_f and R_f.

P2.2.5

A break in a high-voltage DC power line occurs at $z = 0$ at time $t = 0$ (because of a falling tree) [Figure P2.2.5.1]. The line was carrying a DC voltage V_o and DC current I_o before the break occurred. The tree is non-conducting.
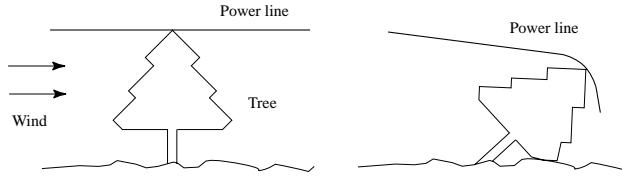

Figure P2.2.5.1 DC power line broken by a tree.

(a) Sketch I and V on the line at some time t after the break has occurred, but before any reflections from the source and load ends. The characteristic impedance of the line is Z_0.

(b) Consider a $600 \, \text{kV}$ line, carrying a power of 10^3 megawatts, with a characteristic impedance of $500 \, \Omega$ (two-wire line). What is the peak voltage on the line after the break occurs?

P2.2.6

A very long transmission line with characteristic impedance Z_0 and wave velocity $v = c$ has a shunt resistor of unknown value R_L at an unknown

location $z = \ell$. A measurement of the voltage at the input, $V_0(t)$, with a unit step generator applied to the line, yields the result shown in Fig. P2.2.6.1.
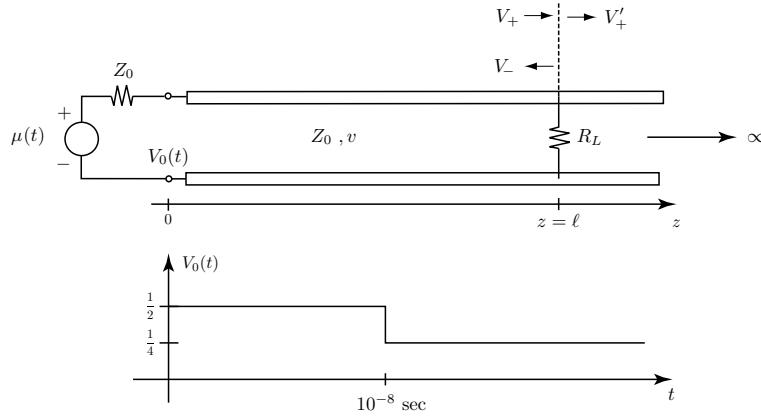

Figure P2.2.6.1

(a) What is ℓ?
(b) What is R_L?
(c) Sketch the voltage and current distribution on the line at the time $t = 1.5\ell/v$.

P2.2.7
   Consider a transmission line circuit shown in the following figure. At $t = 0$, the switch is disconnected from Position A and connected to Position B.
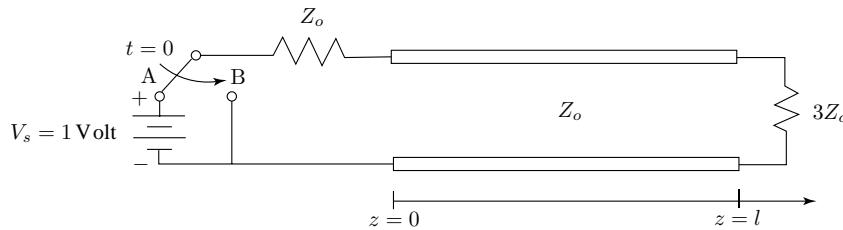

Figure P2.2.7.1

(a) Find the reflection coefficient at the load (at $z = l$).
(b) Make labelled sketches of the total voltage $V(z)$ on the line, $0 < z < l$, at
   (i) $t < 0$
   (ii) $t = l/2v$
   (iii) $t = 2l/v$
where v represents the velocity of propagation on the transmission line.

P2.2.8

A resonator is built using a section of coaxial cable as shown in Figure P2.2.8.1, where the ends are short circuits.
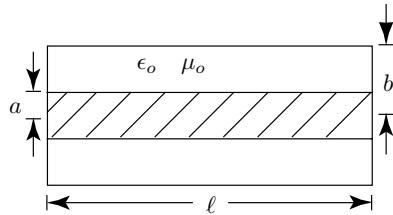

Figure P2.2.8.1

(a) Find the lowest resonant frequency ω_o of the resonator.
(b) Find the length ℓ for a resonator with a frequency of $1.5\,\text{MHz}$.
(c) Introduce a gap of d ($d \ll \ell$) at the end of the resonator as shown in Figure P2.2.8.2 and model it as a transmission line with a capacitive load, C_o. What is C_o?
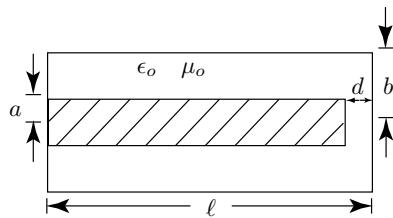

Figure P2.2.8.2

(d) Find the lowest resonant frequency ω_o of the modified resonator in terms of a, b, d and ℓ.
(e) Find the length ℓ for a resonator with a frequency of $1.5\,\text{MHz}$.

P2.2.9

(a) Consider a polyethylene ($\epsilon = 2.25\epsilon_0$) filled coaxial cable with an inner diameter of $0.81\,\text{mm}$ and an outer diameter of $2.946\,\text{mm}$. Assume the $\overline{E}$-field is $\overline{E} = \hat{\rho}E_0/r$ and the $\overline{H}$-field is $\overline{H} = \hat{\phi}E_0/\eta r$. Derive the per-unit-length capacitance and inductance of the coaxial cable and show that the impedance of the transmission line is $\frac{60}{\sqrt{\epsilon_r}}\ln\frac{b}{a}$. What is the corresponding impedance for the given parameters?
(b) The attenuation due to finite conductivity is proportional to $P_d/2P_f$, where P_d is the power dissipated and P_f is the power flow along the transmission line. Show that for coaxial cable, it is proportional to $(\frac{1}{a} + \frac{1}{b})/\ln\frac{b}{a}$. Show that for minimum loss, $x = a/b$ is determined from $xe^{x+1} = 1$, which yields $x = 0.2785$. What is the impedance?

(c) Model the coaxial cable as a parallel plate waveguide with periodic boundary and show that the cutoff frequency of the next higher-order waveguide mode above TEM is: $f_c \simeq \frac{v_{\text{TEM}}}{\pi(a+b)}$, where v_{TEM} is the velocity of the TEM waves in the medium that fills the space between the conductors. (Hint: Use the mean radius for the effective circumference). Find f_c of the given coaxial cable.

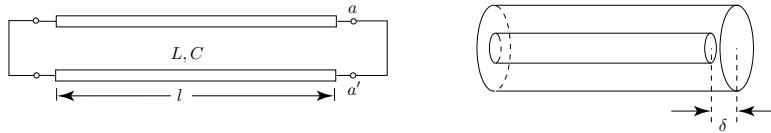(d) A section of coaxial cable is closed at both end [Figure P2.2.9.1], what is the lowest resonant frequency?

Figure P2.2.9.1

(e) A gap with distance δ is introduced at one end of the resonator [Fig. P2.2.9.1]. What is C_o ? Find the new fundamental natural frequency of the transmission line.

P2.2.10

A lossless transmission line of length ℓ is open-circuit at both ends Determine the normal mode voltage and currents on the line, normalized such that $V_n(z = 0) = 1$. What are the corresponding natural frequencies?

2.3   Sinusoidal Steady State Transmission Lines

A. Sinusoidal Steady State

At sinusoidal steady state with angular frequency ω, voltage $V(z,t)$ and current $I(z,t)$ can be written as

$$V(z,t) = \text{Re}\{V(z)e^{j\omega t}\} \qquad\qquad (2.3.1)$$

$$I(z,t) = \text{Re}\{I(z)e^{j\omega t}\} \qquad\qquad (2.3.2)$$

where $V(z) = A(z)e^{j\alpha(z)}$ and $V(z) = B(z)e^{j\beta(z)}$ are called phasors which are complex functions of z only.

The transmission line equations

$$\frac{\partial}{\partial z}V(z,t) = -L\frac{\partial}{\partial t}I(z,t) \qquad\qquad (2.3.3)$$

$$\frac{\partial}{\partial z}I(z,t) = -C\frac{\partial}{\partial t}V(z,t) \qquad\qquad (2.3.4)$$

can be cast in complex form by using (2.3.1) and (2.3.2). We find

$$\frac{\partial}{\partial z}V(z) = -j\omega L I(z) \qquad\qquad (2.3.5)$$

$$\frac{\partial}{\partial z}I(z) = -j\omega C V(z) \qquad\qquad (2.3.6)$$

where $V(z)$ and $I(z)$ are both complex.

Eliminating $V(z)$ and $I(z)$ from (2.3.5) and (2.3.6), we obtain

$$\left(\frac{\partial^2}{\partial z^2} + \omega^2 LC\right)\left\{\begin{array}{c} V(z) \\ I(z) \end{array}\right\} = 0 \qquad\qquad (2.3.7)$$

The general solutions for $V(z)$ and $I(z)$ are

$$V(z) = V_+ e^{-jkz} + V_- e^{jkz} \qquad\qquad (2.3.8)$$

$$I(z) = \frac{1}{Z_0}(V_+ e^{-jkz} - V_- e^{jkz}) \qquad\qquad (2.3.9)$$

The first term represents a wave traveling in the $+\hat{z}$ direction and the second term a wave traveling in the $-\hat{z}$ direction. Substituting (2.3.8) and (2.3.9) in (2.3.7), we find the dispersion relation

$$k^2 = \omega^2 LC \qquad\qquad (2.3.10)$$

Substituting (2.3.8) and (2.3.9) in (2.3.5) and (2.3.6), we find

$$Z_0 = \sqrt{L/C} \qquad\qquad (2.3.11)$$

as the characteristic impedance of the transmission line.

B. Complex Impedance

Impedance is defined as the ratio of voltage to current.

$$Z = \frac{V}{I} \tag{2.3.12}$$

In electric circuits, capacitance C_o is defined by the relation

$$I(t) = C_o \frac{dV(t)}{dt} \tag{2.3.13}$$

and the inductance L_o by the relation

$$V(t) = L_o \frac{dI(t)}{dt} \tag{2.3.14}$$

we write

$$V(t) = V_o \cos(\omega t + \alpha) = \mathrm{Re}\{V_o e^{j\alpha} e^{j\omega t}\} = \mathrm{Re}\{V e^{j\omega t}\} \tag{2.3.15}$$

$$I(t) = I_o \cos(\omega t + \beta) = \mathrm{Re}\{I_o e^{j\beta} e^{j\omega t}\} = \mathrm{Re}\{I e^{j\omega t}\} \tag{2.3.16}$$

Eqs. (2.3.13) and (2.3.14) become

$$\mathrm{Re}\{I e^{j\omega t}\} = C_o \mathrm{Re}\{j\omega V e^{j\omega t}\} \tag{2.3.17}$$

$$\mathrm{Re}\{V e^{j\omega t}\} = L_o \mathrm{Re}\{j\omega I e^{j\omega t}\} \tag{2.3.18}$$

which gives, omitting the time convention $e^{j\omega t}$

$$I = j\omega C_o V \tag{2.3.19}$$
$$V = j\omega L_o I \tag{2.3.20}$$

The impedances for the capacitance and the inductance are thus

$$Z = \frac{1}{j\omega C_o} \tag{2.3.21}$$
$$Z = j\omega L_o \tag{2.3.22}$$

A complex impedance is written as $Z = R + jX$. The real part R is called the resistance, and its imaginary part X is called the reactance. Thus capacitances and inductances are reactive elements. Admittance is the inverse of the impedance $Y = 1/Z = G + jB$. The real part G is called conductance and imaginary part B is called susceptance. For a resistor R, an inductor L_0, and a capacitor C_0 in series, the impedance is $Z = R + j\omega L_0 - j/\omega C_0$.

Complex Reflection Coefficient at the Load

Consider the transmission line in Fig. 2.3.1 which is terminated with a load impedance Z_L. The convention for transmission lines at sinusoidal steady state is to put the coordinate zero at the load. For a line of length ℓ, the load is at $z = 0$ and the generator is at $z = -\ell$.

We write the general solution to the transmission line equations as

$$V(z) = V_0(e^{-jkz} + \Gamma_L e^{jkz}) \qquad (2.3.23)$$

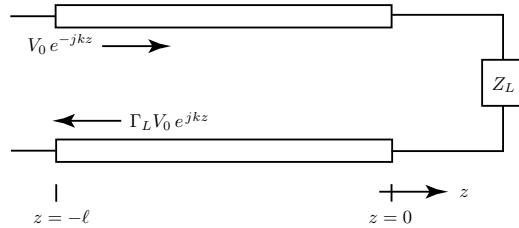$$I(z) = \frac{V_0}{Z_0}(e^{-jkz} - \Gamma_L e^{jkz}) \qquad (2.3.24)$$

$V_0\, e^{-jkz} \longrightarrow$

$\boxed{Z_L}$

$\longleftarrow \Gamma_L V_0\, e^{jkz}$

$z = -\ell \qquad\qquad\qquad z = 0 \qquad z$

Figure 2.3.1 **Transmission line with termination Z_L.**

We define a generalized impedance $Z(z)$ as

$$Z(z) = \frac{V(z)}{I(z)} = Z_0 \frac{e^{-jkz} + \Gamma_L e^{jkz}}{e^{-jkz} - \Gamma_L e^{jkz}} \qquad (2.3.25)$$

where $Z(z)$ is a complex function of z instead of a simple complex number as in circuit theory. At $z = 0$, $Z(z = 0) = Z_L$, we have

$$Z_L = \frac{V(0)}{I(0)} = Z_0 \frac{1 + \Gamma_L}{1 - \Gamma_L} \qquad (2.3.26)$$

which gives

$$\Gamma_L = \frac{Z_L - Z_0}{Z_L + Z_0} = \frac{Z_{Ln} - 1}{Z_{Ln} + 1} \qquad (2.3.27)$$

We call Γ_L the load reflection coefficient, where

$$Z_{Ln} = Z_L/Z_0 \qquad (2.3.28)$$

is the normalized load impedance.

Consider the following three cases:

Case A) For an open circuit load, $Z_L \to \infty$. We find

$$\Gamma_L = \frac{1 - 1/Z_{Ln}}{1 + 1/Z_{Ln}} = 1$$

Case B) For a short circuit load, $Z_L = 0$, and we find $\Gamma_L = -1$.

Case C) For a matched load, $Z_L = Z_0$. We have $Z_{Ln} = 1$ and $\Gamma_L = 0$.

Thus for a matched load, there is only a forward traveling wave and no reflected backward traveling wave. All the power will be delivered to the load impedance.

Complex Input Impedance

The generalized impedance $Z(z)$ in (2.3.25) as defined for every point z on the line is

$$
\begin{aligned}
Z(z) &= \frac{V(z)}{I(z)} = Z_0 \frac{e^{-jkz} + \Gamma_L e^{jkz}}{e^{-jkz} - \Gamma_L e^{jkz}} \\
&= Z_0 \frac{(Z_{Ln} + 1)e^{-jkz} + (Z_{Ln} - 1)e^{jkz}}{(Z_{Ln} + 1)e^{-jkz} - (Z_{Ln} - 1)e^{jkz}} \\
&= Z_0 \frac{2Z_{Ln} \cos kz - j2 \sin kz}{-j2Z_{Ln} \sin kz + 2 \cos kz} \\
&= Z_0 \frac{Z_{Ln} - j \tan kz}{1 - jZ_{Ln} \tan kz} \tag{2.3.29}
\end{aligned}
$$

At the load $z = 0$ and $Z(z = 0) = Z_L$ is the load impedance. At the input terminal, $z = -\ell$, $Z(z = -\ell)$ is the input impedance. We find

$$Z(-\ell) = \frac{V(-\ell)}{I(-\ell)} = Z_0 \frac{Z_{Ln} + j \tan k\ell}{1 + jZ_{Ln} \tan k\ell} \tag{2.3.30}$$

Case A) For an open circuit load $(Z_{Ln} \to \infty)$ we find the input impedance

$$Z(-\ell) = Z_0 \frac{1 + j \tan k\ell/Z_{Ln}}{1/Z_{Ln} + j \tan k\ell} = \frac{Z_0}{j \tan k\ell} \tag{2.3.31}$$
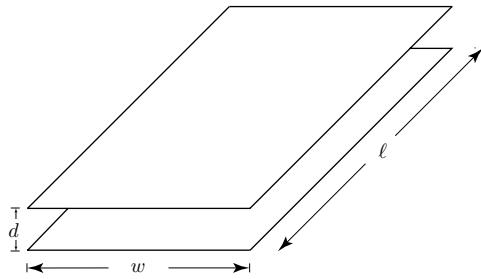
Figure 2.3.2 Parallel-plate transmission line with length ℓ.

When $k\ell \ll 1$, we can approximate $\tan k\ell \approx k\ell$. As $k\ell = 2\pi\ell/\lambda, k\ell \ll 1$ means the transmission length ℓ is very small compared to a wavelength λ. Consider the parallel-plate transmission line with length ℓ [Fig. 2.3.2]. The capacitance per unit length is $C = \epsilon\, w/d$ and the total capacitance is $C_0 = \epsilon\, w\, \ell/d$. We see that the input impedance becomes, making use of the dispersion relation $k = \omega\sqrt{LC}$, and $Z_0 = \sqrt{L/C}$,

$$Z(-\ell) = \sqrt{\frac{L}{C}}\frac{1}{j\omega\sqrt{LC}\ell} = \frac{1}{j\omega C_0}$$

This is the impedance of a capacitor in circuit theory. In general, an impedance is expressed in terms of the resistance R and the reactance X:

$$Z = R + jX$$

The impedance is capacitive if $X < 0$ and inductive if $X > 0$. For the above parallel-plate transmission line $X = -1/\omega C_0$ is smaller than zero and thus the reactance is capacitive.

As ℓ increases, we plot (2.3.31) in Fig. 2.3.3. It is observed that for $\pi/2 < k\ell < \pi$ or $\lambda/4 < \ell < \lambda/2$, the parallel plates are in fact inductive. Whether the input impedance of the parallel plates is capacitive or inductive critically depends on their length.

This is an important illustration of why ordinary circuit theory, which is a limiting case of the general theory, will not be valid at high frequencies or when $k\ell$ is not much less than one. The input impedance of a transmission line repeats itself every half wavelength, or $k\ell = n\pi$. A capacitive input impedance becomes inductive and an inductive input impedance becomes capacitive when ℓ is increased by multiples of $\pi/k = \lambda/2$.
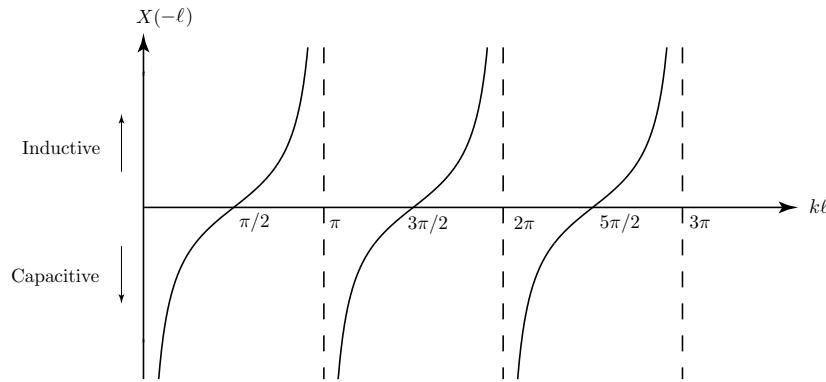
Figure 2.3.3 Reactance for open circuit transmission line.

Case B) For a short circuit load, $Z_{Ln} = 0$. We find the input impedance

$$Z(-\ell) = jZ_0 \tan k\ell$$

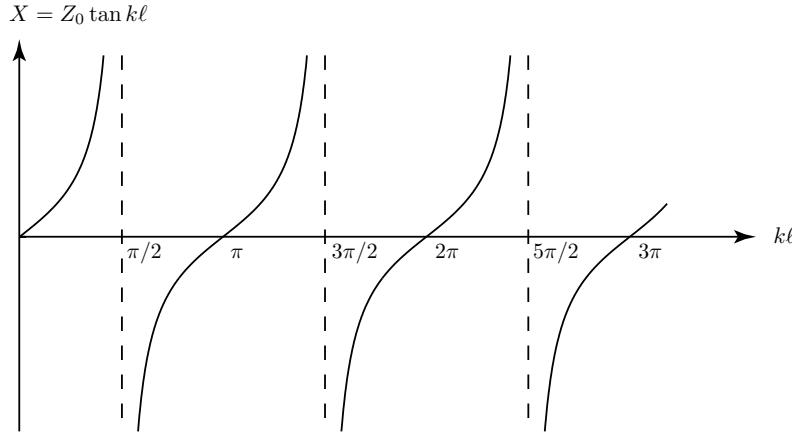The reactance $X = Z_0 \tan k\ell$ is sketched in Fig. 2.3.4.

Figure 2.3.4 Reactance for short circuit transmission line.

Case C) For a matched load, $Z_{Ln} = 1$. We find the input impedance $Z(-\ell) = Z_0$. Thus a matched line has a generalized impedance equal to the characteristic impedance at every point on the line.

C. Time Average Power

From (2.3.23) and (2.3.24)

$$V(z) = V_0(e^{-jkz} + \Gamma_L e^{jkz}) \qquad (2.3.32)$$

$$I(z) = \frac{V_0}{Z_0}(e^{-jkz} - \Gamma_L e^{jkz}) \qquad (2.3.33)$$

we assert that, assuming V_0 is real and $\Gamma_L = |\Gamma_L|e^{j\gamma}$,

$$\begin{aligned}
V(z,t) &= \mathrm{Re}\{V(z)e^{j\omega t}\} \\
&= V_0(\cos(\omega t - kz) + |\Gamma_L|\cos(\omega t - kz + \gamma)) \quad (2.3.34) \\
I(z,t) &= \mathrm{Re}\{I(z)e^{j\omega t}\} \\
&= \frac{V_0}{Z_0}(\cos(\omega t - kz) - |\Gamma_L|\cos(\omega t - kz + \gamma)) \quad (2.3.35)
\end{aligned}$$

compose of waves traveling in the $\hat{z}$ and $-\hat{z}$ directions.

The instantaneous power is

$$\begin{aligned}
P(z,t) &= V(z,t)I(z,t) \\
&= \frac{V_0^2}{Z_0}\{V_0(\cos^2(\omega t - kz) - |\Gamma_L|^2\cos^2(\omega t - kz + \gamma))\} \ (2.3.36)
\end{aligned}$$

The complex power is defined as

$$V(z)I^*(z) = \frac{V_0^2}{Z_0}\{1 - |\Gamma_L|^2 + [\Gamma_L e^{-jkz} - (\Gamma_L e^{jkz})^*]\} \ (2.3.37)$$

The time average power is

$$\begin{aligned}
<P> &= \frac{1}{2\pi}\int_0^\infty d(\omega t)P(z,t) = \frac{V_0^2}{2Z_0}\{1 - |\Gamma_L|^2\} \\
&= \frac{1}{2}\mathrm{Re}\{VI^*\} \qquad (2.3.38)
\end{aligned}$$

EXAMPLE 2.3.1   Applying (2.3.38) to (2.3.8) and (2.3.9), we find

$$\begin{aligned}
<P> &= \frac{1}{2Z_o}\mathrm{Re}\{V_+V_+^* - V_-V_-^* - (V_+V_-^*e^{j2kz} - V_-V_+^*e^{-j2kz})\} \\
&= \frac{1}{2Z_o}\mathrm{Re}\{V_+V_+^* - V_-V_-^*\}
\end{aligned}$$

as $(V_+V_-^*e^{j2kz} - V_-V_+^*e^{-j2kz})$ is purely imaginary. Thus the power at any point is equal to the difference between the forward and backward travelling waves.

<div align="right">— END OF EXAMPLE 2.3.1 —</div>

D. Generalized Reflection Coefficient

A generalized reflection coefficient $\Gamma(z)$ for every point z on the transmission line can be defined from (2.3.32)

$$V(z) = V_0 \left(e^{-jkz} + \Gamma_L e^{jkz} \right) = V_0 e^{-jkz} \left[1 + \Gamma(z) \right] \quad (2.3.39)$$

where

$$\Gamma(z) = \Gamma_L e^{j2kz} \quad (2.3.40)$$

is the generalized reflection coefficient.

The magnitude $|\Gamma_L|$ of the load reflection coefficient

$$\Gamma_L = \frac{Z_{Ln} - 1}{Z_{Ln} + 1}$$

is no greater than one, $|\Gamma_L| \leq 1$, when the characteristic impedance Z_0 is real. From (2.3.40) we also have $|\Gamma(z)| \leq 1$ for all z.
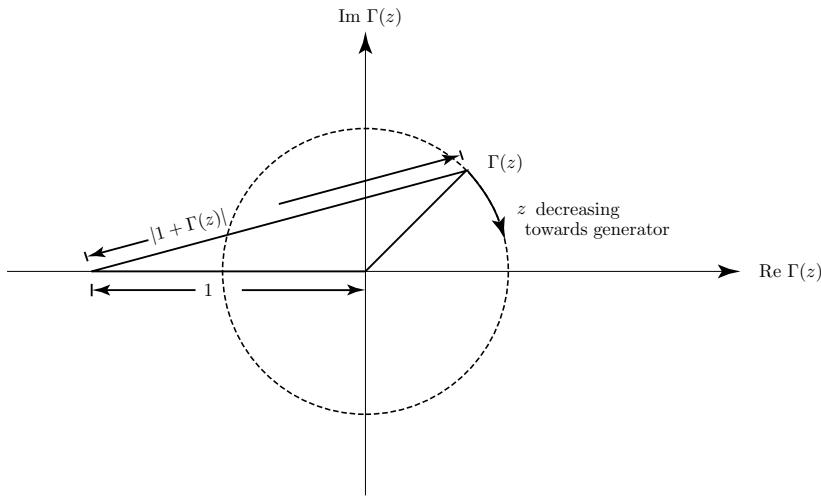

Figure 2.3.5 Motion of $\Gamma(z)$ on complex Γ-plane.

We interpret (2.3.40) by means of a complex Γ-plane plot on which we draw a line representing $\Gamma(z)$ at point z [Fig. 2.3.5]. The magnitude of the voltage is proportional to the length of the line $|1+\Gamma(z)|$. As z decreases, the point is moving towards the generator or the source,
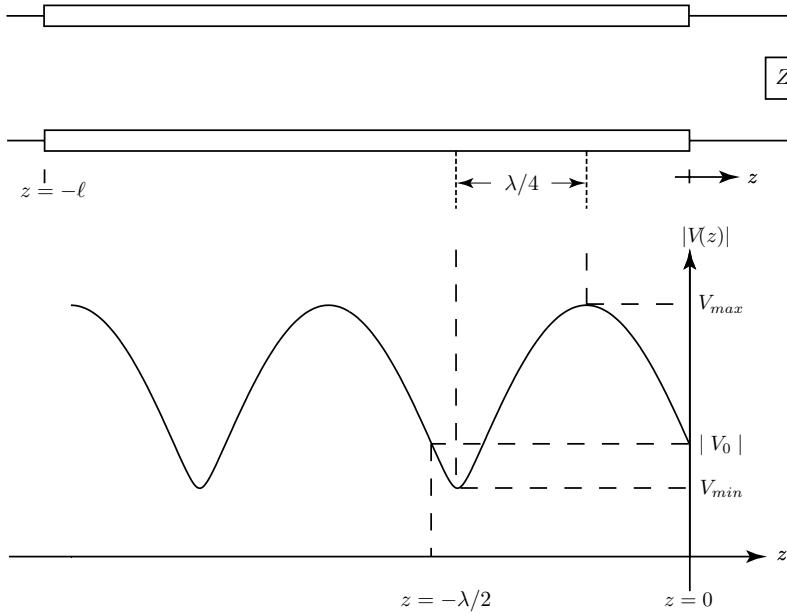
Figure 2.3.6 Plot of voltage standing wave pattern.

remembering the convention that the load is at $z = 0$ and the source or generator is at $z = -\ell$. In Fig. 2.3.6, we plot the magnitude

$$|V(z)| = |V_0||1 + \Gamma(z)|$$

The result is called a voltage standing wave pattern. Notice the pattern is periodic and repeats itself for every $2kz = 2\pi$ or a distance of $\lambda/2$. The maximum voltage amplitude occurs at points when $\Gamma(z) = |\Gamma_L|$, $|V(z)| = |V_0|(1 + |\Gamma_L|)$. The minimum voltage amplitude occurs at points when $\Gamma(z) = -|\Gamma_L|$, $|V(z)| = |V_0|(1 - |\Gamma_L|)$. We define a voltage standing wave ratio (VSWR) as

$$\text{VSWR} = \frac{V_{max}}{V_{min}} = \frac{1 + |\Gamma_L|}{1 - |\Gamma_L|} \qquad (2.3.41)$$

The distance separating V_{max} and V_{min} is $\lambda/4$. It follows that when the load is an open or short circuit, $\Gamma_L = \pm 1$ and $\text{VSWR} \to \infty$. For a matched load, $\Gamma_L = 0$ and $\text{VSWR} = 1$.

EXAMPLE 2.3.2

Consider a voltage standing wave pattern (VSWP) on a transmission line as shown in Fig. 2.3.6. Let VSWR $= 3$ and the characteristic impedance $Z_0 = 50\,\Omega$. The voltage $V_{max} = 3V_{min}$ is at $z = -\lambda/8$. Find the load impedance Z_L.

SOLUTION: From

$$\frac{V_{max}}{V_{min}} = \frac{1 + |\Gamma_L|}{1 - |\Gamma_L|} = 3$$

we find the magnitude of Γ_L, $|\Gamma_L| = 1/2$.

$$\Gamma(z) = \Gamma_L e^{2jkz} \Rightarrow \Gamma(z = -\lambda/8) = \Gamma_L e^{2j(\frac{2\pi}{\lambda})(-\lambda/8)} = \frac{1}{2} \Rightarrow \Gamma_L = \frac{1}{2}e^{j\pi/2}$$

Thus the normalized load impedance

$$Z_{Ln} = \frac{1 + \Gamma_L}{1 - \Gamma_L} = \frac{2 + j}{2 - j} = \frac{(2 + j)^2}{5} = 0.6 + j0.8.$$

The load impedance is $Z_L = 50(0.6 + j0.8)\,\Omega = (30 + j40)\,\Omega$.

The complex voltage and current at the load are

$$V_L = V_+(1 + \Gamma_L) \qquad\qquad (\text{E2.3.2.1})$$

$$I_L = \frac{V_+}{Z_0}(1 - \Gamma_L) \qquad\qquad (\text{E2.3.2.2})$$

The time-averaged power dissipated at the load Z_L is

$$P_L = \frac{1}{2}\text{Re}[V_L I_L^*]$$

The complex voltage and current at the input are

$$V(-\ell) = V_+(e^{jk\ell} + \Gamma_L e^{-jk\ell}) \qquad\qquad (\text{E2.3.2.3})$$

$$I(-\ell) = \frac{V_+}{Z_0}(e^{jk\ell} - \Gamma_L e^{-jk\ell}) \qquad\qquad (\text{E2.3.2.4})$$

The time-averaged power dissipated in the line is

$$P = \frac{1}{2}\text{Re}[V(-\ell)I^*(-\ell)] = \frac{1}{2}\text{Re}[V_L I_L^*]$$

— END OF EXAMPLE 2.3.2 —

E. Normalized Complex Impedance (Smith Chart)

The generalized reflection coefficient Γ_L has a maximum amplitude of unity. Thus the whole usable complex Γ_L plane is restricted to a circle of radius one. On this complex Γ plane we define a normalized complex impedance

$$Z_n(z) = \frac{V(z)}{Z_0 I(z)} = \frac{1 + \Gamma(z)}{1 - \Gamma(z)}$$

$$= R_n + jX_n \qquad (2.3.42)$$

At each point within the unit circle on the complex Γ plane, we assign a pair of numbers R_n and X_n according to (2.3.42). The result is called the Smith chart which was constructed by Philip H. Smith (1905–1987) in 1936 and published in 1939, originally called the reflection chart or circular chart. It serves as an analog computer reading normalized impedance for every generalized reflection coefficient representable within a unit circle on the complex Γ plane.

From (2.3.42), we can determine R_n and X_n in terms of the real and imaginary parts of $\Gamma = \Gamma_R + j\Gamma_I$. From equation (2.3.42), which is known as the bilinear transformation, we find

$$R_n + jX_n = \frac{1 + \Gamma_R + j\Gamma_I}{1 - \Gamma_R - j\Gamma_I}$$

$$= \frac{(1 + \Gamma_R + j\Gamma_I)(1 - \Gamma_R + j\Gamma_I)}{(1 - \Gamma_R)^2 + \Gamma_I^2}$$

which yields

$$R_n = \frac{1 - \Gamma_R^2 - \Gamma_I^2}{(1 - \Gamma_R)^2 + \Gamma_I^2}$$

$$X_n = \frac{2\Gamma_I}{(1 - \Gamma_R)^2 + \Gamma_I^2}$$

The above two equations can be re-arranged to give

$$\left(\Gamma_R - \frac{R_n}{1 + R_n}\right)^2 + \Gamma_I^2 = \left(\frac{1}{1 + R_n}\right)^2$$

$$(\Gamma_R - 1)^2 + \left(\Gamma_I - \frac{1}{X_n}\right)^2 = \left(\frac{1}{X_n}\right)^2$$
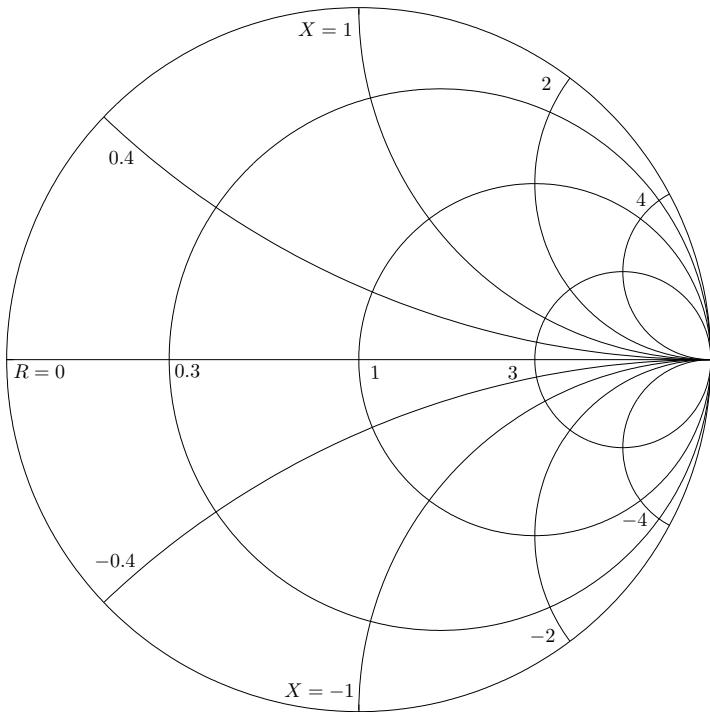
Figure 2.3.7 Smith chart.

Thus on the complex Γ-plane, each value of R_n gives rise to a circle centered at $\Gamma_R = R_n/(1+R_n)$ and $\Gamma_I = 0$ with a radius of $1/(1+R_n)$ and each value of X_n produces a circle centered at $\Gamma_R = 1$ and $\Gamma_I = 1/X_n$ with a radius of $|1/X_n|$. The loci of constant R_n and X_n are plotted within the unit circle of $|\Gamma| \leq 1$ and the result is the Smith chart [Fig. 2.3.7].

EXERCISE 2.3.1   In Example 2.3.2, we can locate on the Smith chart the position of $\Gamma = j0.5$ and find that the normalized impedance is $Z_n = 0.6 + j0.8$. It is seen that VSWR $= 3$ occurs on the real axis coincident with the $R = 3$ locus, where voltage is maximum. Thus rotating counterclockwise an angle of $\pi/2$, we obtain the location of Γ_L and read from the Smith chart the value of $Z_{Ln} = 0.6 + j0.8$.

— END OF EXERCISE 2.3.1 —

F. Transmission Line Resonators

Consider a transmission line resonator with length l and terminated with impedances Z_s and Z_L as shown in Figure 2.3.8. The transmission line equations are given by

$$V(z) = V_+ e^{-jkz} + V_- e^{jkz}$$

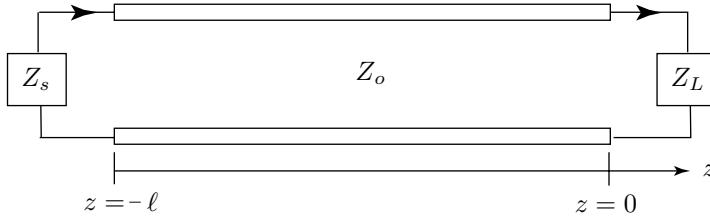$$I(z) = \frac{V_+}{Z_o} e^{-jkz} - \frac{V_-}{Z_o} e^{jkz}$$

Figure 2.3.8 Transmission line resonator.

At $z = 0$, $V(0) = Z_L I(0)$ gives

$$V_+ + V_- = Z_{Ln}(V_+ - V_-)$$

where $Z_{Ln} = Z_L/Z_0$. Thus

$$\frac{V_-}{V_+} = \frac{Z_{Ln} - 1}{Z_{Ln} + 1} = \Gamma_L \tag{2.3.43}$$

At $z = -l$, $V(-l) = -Z_S I(-l)$ gives

$$V_+ e^{jkl} + V_- e^{-jkl} = -Z_{Sn}(V_+ e^{jkl} - V_- e^{-jkl})$$

where $Z_{Sn} = Z_S/Z_0$. Thus

$$\frac{V_+ e^{jkl}}{V_- e^{-jkl}} = \frac{Z_{sn} - 1}{Z_{sn} + 1} = \Gamma_S \tag{2.3.44}$$

Multiplying (2.3.43) and (2.3.44), we find the resonance condition

$$\boxed{e^{j2kl} = \Gamma_L \Gamma_S} \tag{2.3.45}$$

For short-circuited resonators, $Z_S = Z_L = 0$, $\Gamma_S = \Gamma_L = -1$, and $V_- = -V_+$. We find that the resonance spatial frequencies are

$$k = n\pi/l$$

and the resonance frequencies are

$$\omega = n\pi/l\sqrt{LC}$$

with $n = 0, 1, 2, \ldots..$ The voltages and currents are

$$V(z) = V_+ e^{-jkz} + V_- e^{jkz} = V_0 \sin\frac{n\pi z}{l}$$

$$I(z) = \frac{V_+}{Z_o}e^{-jkz} - \frac{V_-}{Z_o}e^{jkz} = j\frac{V_0}{Z_0}\cos\frac{n\pi z}{l}$$

where $V_0 = -j2V_+$. The voltages are zero at $z = 0$ and $z = l$. For the $n = 0$ mode, $V_0 = 0$.
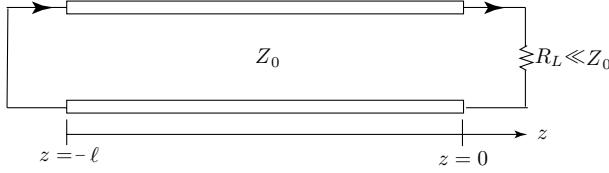

Figure 2.3.9 Transmission line resonator with small loss.

The resonator voltage and current will decay in time when there is a small loss in the resonator. In Fig 2.3.9, we assume a small load resistance $R_L \ll Z_0$. From the resonance condition in (2.3.45), we find by assuming $k = n\pi/l + jk_I$

$$e^{j2kl} = e^{-2k_I l} \approx 1 - 2k_I l + \ldots = -\Gamma_L = -\frac{Z_{Ln} - 1}{Z_{Ln} + 1} \approx 1 - 2\frac{R_L}{Z_0} + \ldots$$

It follows that $k_I l = R_L/Z_0$ and $\omega = n\pi v/l + jk_I v$ with $\omega_I = jk_I v = jR_L v/Z_0 = jR_L/L$. Thus the voltage and current attenuate in time with the factor $e^{-(R_L/L)t}$.

EXAMPLE 2.3.3
    Consider a series R, L, C circuit with $R \ll \sqrt{L/C}$ in Fig. E2.3.3.1,
KVL gives

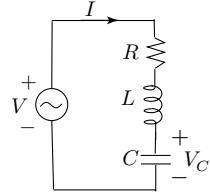$$V = RI + L\frac{dI}{dt} + V_c$$

Figure E2.3.3.1 Series R L C circuit.

where V_c is the voltage across the capacitor, which is related to I by $I = CdV_c/dt$. Thus the differential equation for the circuit is

$$\frac{dV}{dt} = R\frac{d}{dt}I + L\frac{d^2}{dt^2}I + \frac{1}{C}I$$

We let the solution be

$$V = V_s e^{st}$$
$$I = I_s e^{st}$$

The terminal voltage V_s is then related to the current I_s in the circuit by

$$V_s = (R + sL + \frac{1}{sC})I_s = \frac{s^2 + (R/L)s + 1/LC}{s/L}I_s = \frac{(s - s_+)(s - s_-)}{s/L}I_s$$

We find, for $R \ll \sqrt{L/C}$,

$$s_\pm = -\frac{R}{2L} \pm j\sqrt{\frac{1}{LC} - \left(\frac{R}{2L}\right)^2} = -\omega_I \pm j\sqrt{\omega_0^2 - \alpha_r^2} \approx -\omega_I \pm j\omega_0$$

$$I_s = \frac{s/L}{(s + \omega_I)^2 + \omega_0^2} V_s$$

where $\omega_0 = 1/\sqrt{LC}$ is the resonant frequency and

$$\omega_I = \frac{R}{2L}$$

gives the attenuation rate of the voltage and current in the circuit, $e^{-\omega_I t}$.

At $s = j\omega_0$,

$$I_s(s = j\omega_0) = \frac{V_s(\omega_0)}{R}$$

The dissipated power is

$$P_d(\omega_0) = \frac{R}{2}|I_s(s = j\omega_0)|^2 = \frac{|V_s(\omega_0)|^2}{2R}$$

The stored energy is

$$W_T = \frac{1}{2}L|I(s = j\omega_0)|^2$$

We see that

$$\omega_I = \frac{R}{2L} = \frac{\frac{1}{2}R|I|^2}{2 \cdot \frac{1}{2}L|I|^2} = \frac{P_d}{2W_T}$$

The quality factor

$$Q = \frac{\omega_0 W_T}{P_d} = \frac{\omega_0}{2\omega_I} = \frac{(R/L)}{1/\sqrt{LC}} = \frac{\sqrt{L/C}}{R}$$

At $s = j(\omega_0 \pm \omega_I)$,

$$|I(s = j(\omega_0 \pm \omega_I))| \approx \left| \frac{j\omega_0 V_s(\omega_0)/L}{(\omega_I \pm j\omega_I)(j2\omega_0 \pm j\omega_I + \omega_I)} \right| \approx \frac{|V_s(\omega_0)|}{\sqrt{2}R}$$

The dissipated power is

$$P_d(\omega_0 \pm \omega_I) = \frac{R}{2}|I(s = j(\omega_0 \pm \omega_I))|^2 = \frac{|V_s(\omega_0)|^2}{4R} = \frac{P_d(\omega_0)}{2}$$

The half-power point occurs at $\omega = \omega_0 \pm \omega_I = \omega_0 \pm \Delta\omega$. Thus the half-power point bandwidth is

$$BW = 2\omega_I$$

It is seen that the quality factor

$$Q = \frac{\omega_o}{2\omega_I} = \frac{\omega_o}{BW} = \frac{\sqrt{L/C}}{R} = \frac{\omega_o W_T}{P_d}$$

is expressible in terms of inverse attenuation rate, inverse bandwidth, resonator circuit elements, and stored energy over dissipated power.

<div align="right">— END OF EXAMPLE 2.3.3 —</div>

Problems

P2.3.1

Convert the following time domain expressions into their complex equivalents in the frequency domain, where we have defined

$$A = \mathrm{Re}\left[\underline{A}e^{j\omega t}\right]$$

$$\text{Example}: \quad A = \sin\omega t \qquad \underline{A} = -j$$

(a) Find $\underline{A}$.

    (i) $A = 3\sin\left(\omega t - \dfrac{\pi}{4}\right)$

    (ii) $A = \hat{x}\sin\omega t - \hat{y}2\cos\omega t$

    (iii) $A = \cos\phi\cos\omega t$

(b) Find A.

    (i) $\underline{A} = je^{j\pi/4}$

    (ii) $\underline{A} = \hat{x} + \hat{y}3j$

    (iii) $\underline{A} = A_0 e^{j\phi} + j$

P2.3.2

The result of a measurement of the voltage standing wave pattern on a transmission line with source impedance $Z_0 = 50\Omega$ and characteristic impedance $Z_0 = 50\Omega$ is illustrated in Figure P2.3.2.1.
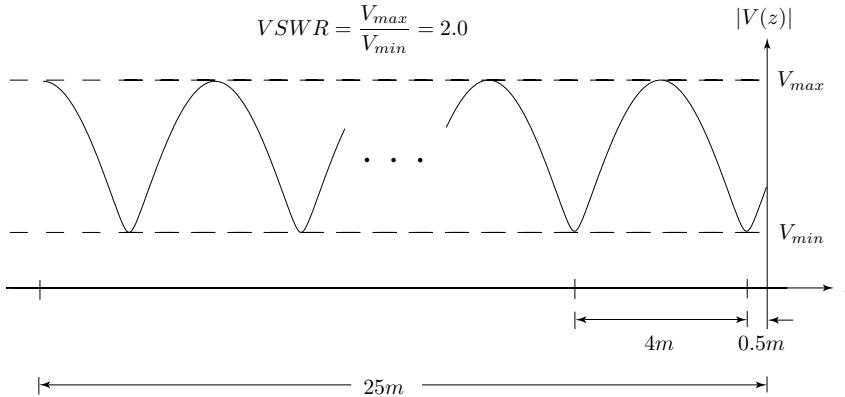

Figure P2.3.2.1 Voltage standing wave pattern.

(a) From the given data, determine the wavelength and load impedance Z_L.
(b) What is the input impedance at the source $Z(z = -25\text{ m})$?
(c) Determine the complex load voltage $V_L = V(z = 0)$ in terms of V_s.
(d) What is the time-averaged power dissipated in the load Z_L?

P2.3.3

The "current standing wave pattern" of a TEM transmission line with characteristic impedance $Z_0 = 50\,\Omega$, permeability μ_0 and permittivity $\epsilon = 4\epsilon_0$ is shown in Figure P2.3.3.1.

(a) What is the frequency of excitation $f = \omega/2\pi$?
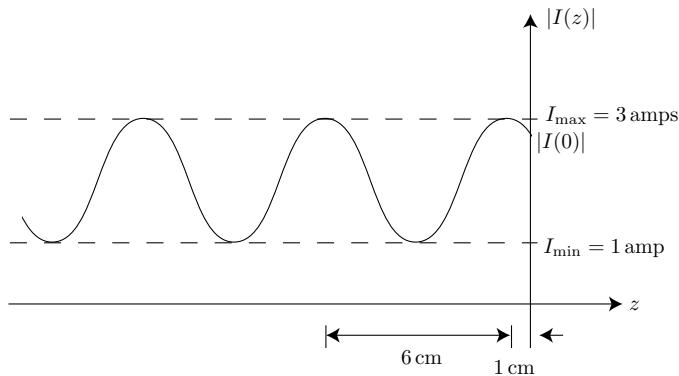(b) Calculate the reflection coefficient Γ_L.

Figure P2.3.3.1

(c) Determine the load impedance Z_L in Ω.
(d) What is the time-average power flow along the line? Give a numerical answer.

P2.3.4

Show that the VSWR$= R_n$ with $R_n \geq 1$ on the real Γ_R axis.

P2.3.5

Quarter-wave transformers are primarily used as intermediate matching sections. Consider a transmission line of characteristic impedance Z_1 connected to a pure resistive load of impedance $Z_L = R_L$ through a section of transmission line having characteristic impedance Z_2 of length ℓ. (see Figure P2.3.5.1). Show that when $\ell = \lambda/4$ and $Z_2 = \sqrt{Z_1 Z_L}$, the reflection coefficient $\Gamma = 0$.
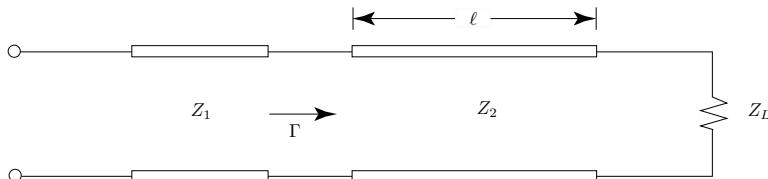

Figure P2.3.5.1

P2.3.6

Consider the TEM transmission line system connected to a sinusoidal voltage source as shown in Figure P2.3.6.1.
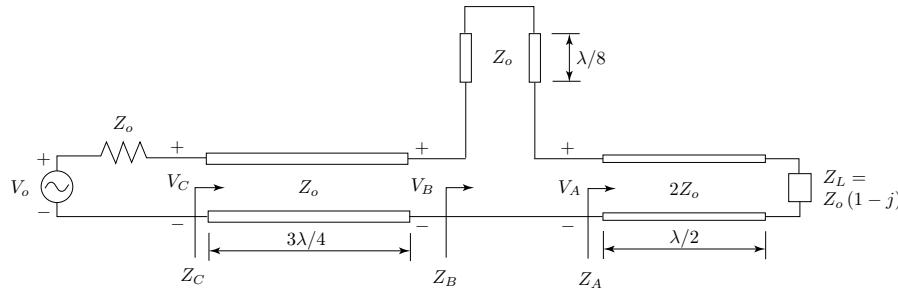
Figure P2.3.6.1

(a) Find the impedance Z_A in terms of Z_0.
(b) Find the impedance Z_B in terms of Z_0.
(c) Find the impedance Z_C in terms of Z_0.
(d) Show that the time average power dissipated in Z_C is $|V_o|^2/8Z_0$. Assume Z_0 is real.
(e) Find the voltage V_L across the load Z_L in terms of V_o and use V_L to calculate the time average power dissipated in the load Z_L in terms of V_o and Z_o. Assume Z_o is real.

P2.3.7

Consider the transmission line circuit shown below [Figure P2.3.7.1].
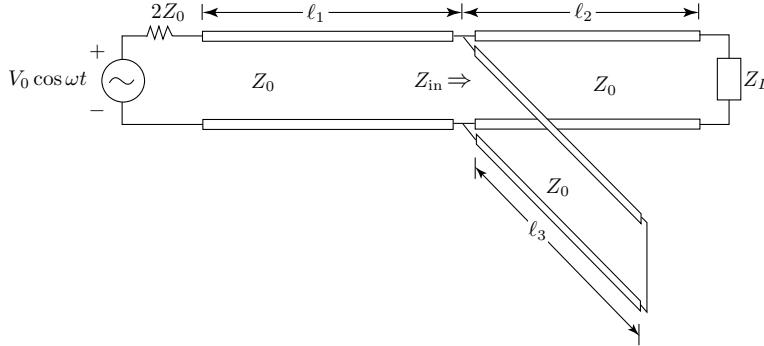
Figure P2.3.7.1

(a) Given $Z_{\rm in} = Z_0/2$, what minimum non-zero length ℓ_1, if any, will maximize power dissipated in the load Z_L. If none exists, state "none exists."
(b) Let $Z_L = (0.8 - j1.4)Z_0$. Determine the shortest distance ℓ_2 and the shortest corresponding length ℓ_3 such that $Z_{\rm in} = Z_0/2$.
(c) State the constraints, if any, on Z_L (in terms of Z_L or Γ_L) such that $Z_{\rm in}$ can be made to be $Z_0/2$. If no constraints exist, state "none exist."

P2.3.8

Consider now the TEM transmission line resonator circuit shown oper-

ating near the lowest order resonant frequency [Figure P2.3.8.1].
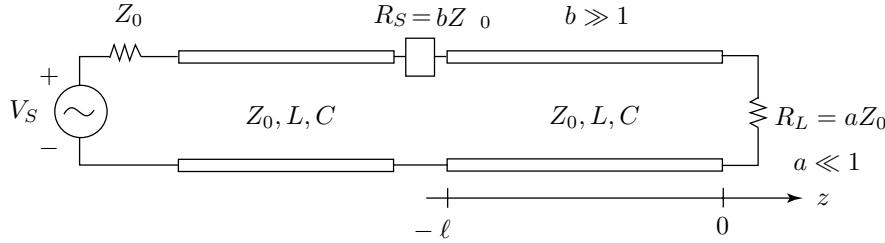
Figure P2.3.8.1 Internal and external Q.

(a) What is internal $Q_I = \omega_0 W_T / P_d$?
(b) What is external $Q_E = \omega_0 W_T / P_e$?

P2.3.9

Consider an air-filled transmission line with characteristic impedance Z_o to be connected with a capacitor C_o and inductor L_o as illustrated in Figure P2.3.9.1. The operating angular frequency of the transmission line system is ω. The transmission line equations are given by

$$V(z) = V_+ e^{-jkz} + V_- e^{jkz}, \qquad I(z) = \frac{V_+}{Z_o} e^{-jkz} - \frac{V_-}{Z_o} e^{jkz}$$

Figure P2.3.9.1

(a) Show that $\frac{V_-}{V_+} = e^{-2j\phi}$, where $\phi = \tan^{-1} \omega C_o Z_o$.
(b) Show that the natural spatial frequency k_n of the n-th order normal mode for this resonator satisfies the following equation

$$\cot(k_n \ell - \phi) = ck_n \frac{L_o}{Z_o}$$

where $c = 3 \times 10^8$ m/s is speed of light for the air-filled transmission line.

(c) Let $\ell = 1\,\mathrm{m}$. Find the natural temporal frequency f in MHz of the lowest order normal mode for

   (i) $C_o = 0$ and $L_o = 0$;
   (ii) $C_o = 0$ and $L_o = \infty$.

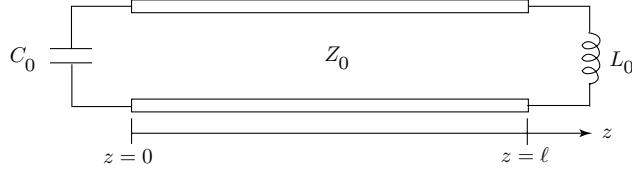(d) Let $C_o = 0$ and $\ell = 1\,\mathrm{m}$. With no restriction of L_o, find the range of possible operating frequencies (in MHz) where there can only be one normal mode existing on the line.

P2.3.10

   In the transmission line circuit shown in Fig. P2.3.10.1, the system is driven at the lowest non-zero resonant frequency (where l is equal to $\frac{\lambda}{2}$). In this problem, first use the perturbation approach to calculate the real part of the input impedance, and then compare the result with the calculation using the Smith chart.
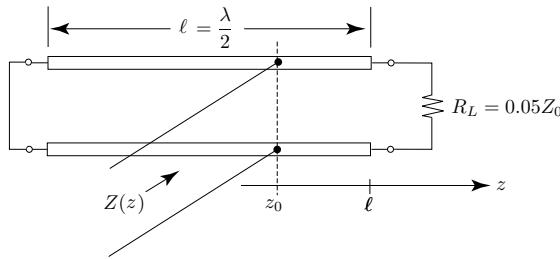
Figure P2.3.10.1

(a) Calculate the complex eigenfrequencies $\omega = \omega_R - j\omega_I$ using a perturbation approach to find ω_R. Calculate the real part of the input impedance Z at the frequency where $l = \frac{\lambda}{2}$ by assuming that only the "resonant" term need to be included in the mode expansion for Z. Evaluate $\frac{Z}{Z_0}$ numerically for $\frac{z_0}{l} = \frac{1}{6}, \frac{1}{4}, \frac{1}{3}$, and $\frac{1}{2}$.

(b) The input impedance can also be evaluated on the Smith chart. Compare the results with the approximate results in (a) for the same z_0/l.

(c) The resonator is driven by a shunt current source of amplitude I_s applied at $z = w$. The source frequency ω is varied around ω_1. Assuming small loss, write down the modal expansion and indicate the dominant term. Hence plot $|V(z = w)|$ as a function of ω and indicate how Q_s can be obtained experimentally from such plots for the loaded and unloaded resonator.

2.4   Lumped Element Transmission Lines

We have derived from Maxwell equations the transmission line equations

$$\frac{dV}{dz} = -j\omega L I \qquad\qquad (2.4.1)$$

$$\frac{dI}{dz} = -j\omega C V \qquad\qquad (2.4.2)$$

from two-conductor transmission lines, in particular from a parallel-plate transmission line. We now show that (2.4.1) and (2.4.2) can be found from a circuit model approximating that of a continuous line. Take a small section of length Δz and approximate it with a series inductor with inductance $L\Delta z$ and a shunt capacitor with capacitance $C\Delta z$ [Fig. 2.4.1].
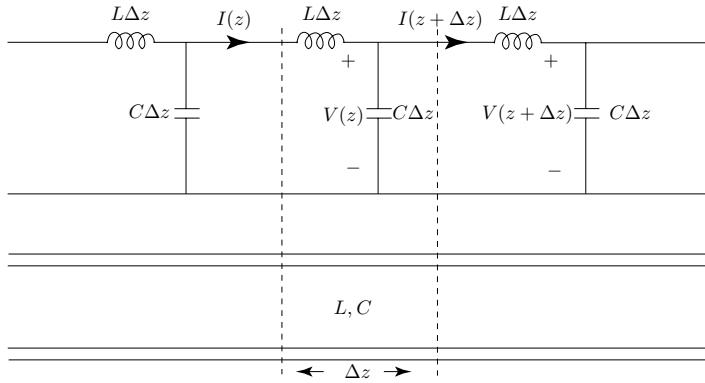
Figure 2.4.1 Lumped element approximation of transmission line.

We apply KVL (Kirchhoff voltage law) and KCL (Kirchhoff current law) to the lumped element section and obtain

$$V(z + \Delta z) - V(z) = -j\omega L\Delta z\, I(z)$$

$$I(z + \Delta z) - I(z) = -j\omega C\Delta z\, V(z)$$

Keeping the first term to order Δz by letting $\Delta z \to 0$, we find

$$\lim_{\Delta z \to 0} \frac{V(z + \Delta z) - V(z)}{\Delta z} = -j\omega L\, I(z)$$

$$\lim_{\Delta z \to 0} \frac{I(z + \Delta z) - I(z)}{\Delta z} = -j\omega C\, V(z)$$

which give rise to the transmission line equations (2.4.1) and (2.4.2).

A. Lumped Element Line

We now directly use KVL and KCL to derive and study the behavior of waves on a lumped element line as shown in Fig. 2.4.2. Each section has a physical length ℓ. Applying KVL and KCL to the nth section of the line, we have

$$V_{n+1} - V_n = -j\omega L_0 \, I_{n+1} \tag{2.4.3}$$

$$I_{n+1} - I_n = -j\omega C_0 V_n \tag{2.4.4}$$
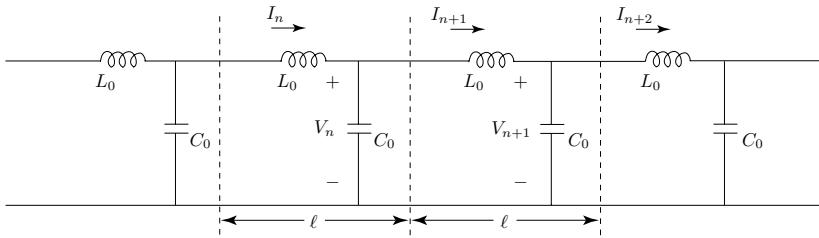
Figure 2.4.2 Lumped-element transmission line.

Consider a positive traveling wave similar to e^{-jkz} on a continuous line. Identifying $kz = kn\ell = n\theta$ with $\theta = k\ell$ as phase shift along each cell, we write

$$V_n = V_+ e^{-jn\theta} \tag{2.4.5}$$

$$I_n = I_+ e^{-jn\theta} \tag{2.4.6}$$

Substituting (2.4.5) and (2.4.6) in (2.4.3) and (2.4.4), we find

$$V_+ \left(e^{-j(n+1)\theta} - e^{-jn\theta} \right) = -j\omega L_0 \, I_+ e^{-j(n+1)\theta} \tag{2.4.7}$$

$$I_+ \left(e^{-j(n+1)\theta} - e^{-jn\theta} \right) = -j\omega C_0 \, V_+ e^{-jn\theta} \tag{2.4.8}$$

Multiplying (2.4.7) and (2.4.8) and eliminating V_+ and I_+, we obtain the dispersion relation

$$\sin^2 \frac{\theta}{2} = \frac{1}{4} \omega^2 L_0 \, C_0 = \frac{\omega^2}{\omega_0^2} \tag{2.4.9}$$

where

$$\omega_0 = \frac{2}{\sqrt{L_0 \, C_0}} \tag{2.4.10}$$
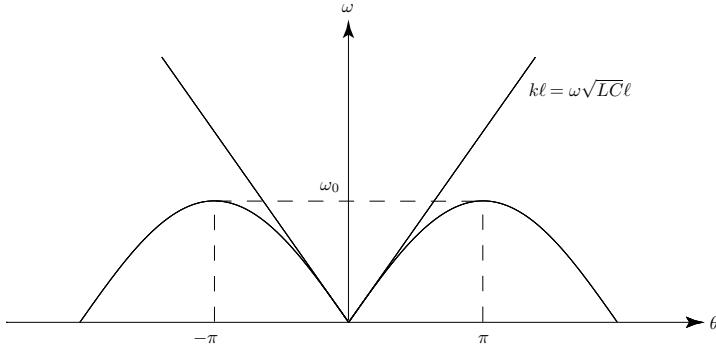
Figure 2.4.3 Dispersion relation for low-pass transmission line.

The dispersion relation (2.4.9) is plotted in Fig. 2.4.3.

In the low frequency limit $\omega \ll \omega_0$, we approximate

$$\frac{\omega}{\omega_0} = \pm \sin \frac{\theta}{2} \approx \pm \frac{\theta}{2}$$

where we use the upper sign when θ is positive, corresponding to a wave traveling in the positive direction, and the lower sign when θ is negative, corresponding to a wave traveling in the negative direction, so that ω is always positive.

Identifying $\theta = k\ell$, we find by using (2.4.10)

$$k = \frac{2\omega}{\ell\omega_0} = \omega \sqrt{\frac{L_0}{\ell} \frac{C_0}{\ell}} = \omega \sqrt{LC}$$

with $L = L_0/\ell$ and $C = C_0/\ell$ as inductance and capacitance per unit length. The lumped element line thus behaves as a continuous line in the low frequency limit.

EXAMPLE 2.4.1   Delay line using lumped element line.

The velocity of propagation on a continuous line is $v = \omega/k = 1/\sqrt{LC} = 1/\sqrt{\mu\epsilon} = 3 \times 10^8$ m/s for $\mu = \mu_o$ and $\epsilon = \epsilon_o$. For the lumped element line, assume $L_0 = 10^{-4}$ H, $C_0 = 10^{-8}$ F, and $\ell = 10^{-2}$ meter. We find the velocity $v = \ell/\sqrt{L_0 C_0} = 10^4$ m/s. Thus the lumped element line can be used as a delay line.

— END OF EXAMPLE 2.4.1 —

When $\omega > \omega_0$, the phase shift θ must be a complex number; we write

$$\theta = \theta_R - j\theta_I$$

The dispersion relation (2.4.9) becomes

$$\sin \frac{\theta_R - j\theta_I}{2} = \sin \frac{\theta_R}{2} \cosh \frac{\theta_I}{2} - j \cos \frac{\theta_R}{2} \sinh \frac{\theta_I}{2} = \frac{\omega}{\omega_0}$$

We have

$$\cos \frac{\theta_R}{2} \sinh \frac{\theta_I}{2} = 0$$

$$\sin \frac{\theta_R}{2} \cosh \frac{\theta_I}{2} = \frac{\omega}{\omega_0}$$

The above equations give the solution $\theta_R = \pi$ and $\theta_I = 2\cosh^{-1}\frac{\omega}{\omega_0}$. The voltage on the nth cell is

$$V_n = V_+ e^{-jn(\theta_R - j\theta_I)} = V_+ e^{-n\theta_I} e^{-jn\theta_R}$$

The term $e^{-jn\theta_R}$ signifies a phase shift from the nth cell to the $(n+1)$th cell, the term $e^{-n\theta_I}$ signifies there is an amplitude attenuation from cell to cell as well. Since high frequency $(\omega > \omega_0)$ waves are attenuated and low frequency $(\omega < \omega_0)$ waves pass with no attenuation, the lumped element line in Fig. 2.4.2 is a low-pass filter.

In the limit $\omega \gg \omega_0$, the dispersion relation for the low pass lumped element line gives

$$\cosh \frac{\theta_I}{2} = \frac{1}{2}\left(e^{\theta_I/2} + e^{-\theta_I/2}\right) \approx \frac{1}{2} e^{\theta_I/2} = \frac{\omega}{\omega_0} = \frac{1}{2}\omega\sqrt{L_0 C_0}$$

We thus have

$$e^{\theta_I/2} = \omega\sqrt{L_0 C_0}$$

The ratio of V_{n+1}/V_n gives

$$\frac{V_{n+1}}{V_n} = -e^{-\theta_I} = \frac{-1}{\omega^2 L_0 C_0}$$

From elementary circuit theory, considering the $(n+1)$th cell with $I_{n+2} = 0$, the voltage V_n is divided on the inductor with impedance $j\omega L_0$ and V_{n+1} across the capacitor with impedance $1/j\omega C_0$. We have

$$\frac{V_{n+1}}{V_n} = \frac{1/j\omega C_0}{j\omega L_0 + 1/j\omega C_0} \approx \frac{1/j\omega C_0}{j\omega L_0} = \frac{-1}{\omega^2 L_0 C_0}$$

Thus at very high frequencies, the inductors behave like open circuits, and the capacitors approach short circuit.

B. Dispersion Relations for Lumped Element Lines

Consider a general lumped element line shown in Figure 2.4.4. The impedance $Z_t = R_0 + X_0$ and the admittance $Y_t = G_0 + jB_0$. KVL and KCL give

$$V_{n+1} - V_n = -Z\,I_{n+1} \tag{2.4.11}$$
$$I_{n+1} - I_n = -YV_n \tag{2.4.12}$$
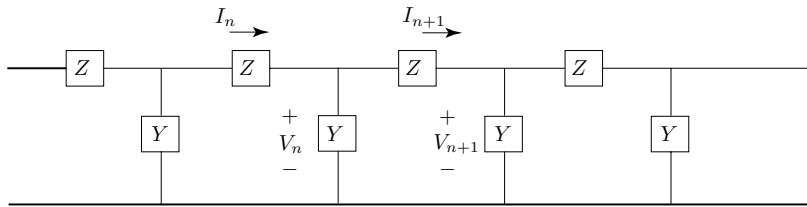
Figure 2.4.4 A general lumped element line.

With the traveling wave solution as in (2.4.5) and (2.4.6),

$$I_n = I_+ e^{-jn\theta}$$
$$V_n = V_+ e^{-jn\theta}$$

we obtain from the dispersion relation

$$\sin^2 \frac{\theta}{2} = -\frac{1}{4}\,ZY \tag{2.4.13}$$

It reduces to (2.4.9) when $Z = j\omega L_0$ and $Y = j\omega C_0$.

EXAMPLE 2.4.2
   Study the wave behavior on a lumped element line with $Z = 1/j\omega C_0$ and $Y = 1/jwL_0$ shown in Figure E2.4.2.1.

Figure E2.4.2.1 High-pass lumped element line.

Figure E2.4.2.2 Dispersion curve for high-pass lumped element line.

The dispersion relation (2.4.13) gives

$$\sin^2 \frac{\theta}{2} = \frac{1}{4\omega^2 L_0 C_0} = \frac{\omega_0^2}{\omega^2}, \qquad \omega_0 = \frac{1}{2\sqrt{L_0 C_0}} \qquad \text{(E2.4.2.1)}$$

It is seen that θ is real for $\omega > \omega_0$ and θ is complex when $\omega < \omega_0$ [Fig. E2.4.2.2]. High frequency $(\omega > \omega_0)$ passes and low frequency $(\omega < \omega_0)$ is cutoff. This is because at high frequencies, the capacitor behaves like a short circuit and inductors approach open circuit.

From the dispersion curve for the high-pass filter shown in Fig. E2.4.2.2, we see that for $\omega > \omega_0$, the group velocity is negative when the phase velocity is positive and vice versa. Thus the group velocity and the phase velocity of a traveling wave on the line are in opposite directions and the line is called a backward wave line.

$-$ End of Example 2.4.2 $-$

The effect of loss on a transmission line causes attenuation and dispersion of a propagating wave. With dispersion, different frequencies propagate with different phase veloci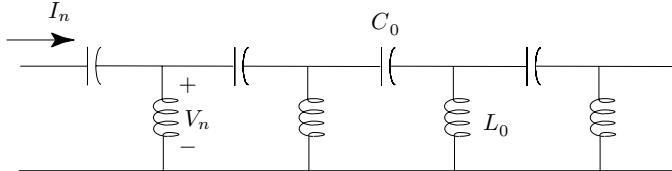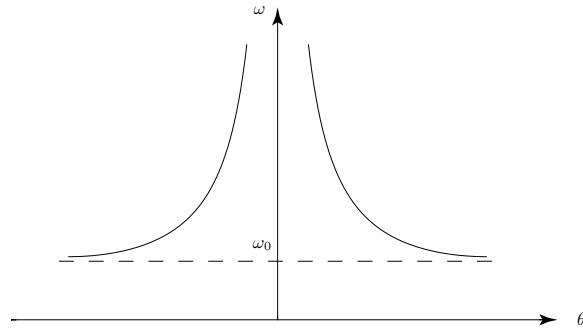ties which lead to distortion of any non-sinusoidal wave form. Both the attenuation and distortion resulting from loss in transmission lines were responsible for impeding the development of long distance communication of speech in the early days of the telephone. In 1893, Oliver Heaviside developed the transmission line theory based on Maxwell equations. Until that time, the transmission line was described by a diffusion equation, which was formulated in circuit terms, involving a distributed series R and parallel C network. Taking proper account of the inductance, Heaviside noticed that the effects of attenuation and phase distortion both decrease as inductance is increased. He thus proposed that telephone lines be loaded periodically with lumped inductors, which was experimentally verified in 1900 by Pupin of Columbia University.

Instead of a continuous transmission line loaded with Pupin coils L_p, we model the transmission line between the Pupin coils as lumped inductance and capacitance [Fig. 2.4.5]. This model is valid if the coils are much less than a wavelength apart. We have

$$Y = j\omega C_0$$
$$Z = j\omega(L_0 + L_p) + R_0$$
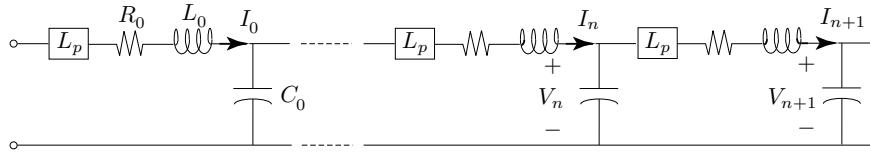
Figure 2.4.5 Transmission line loaded with Pupin coils.

We obtain from the dispersion relation (2.4.13)

$$\sin^2\frac{\theta}{2} = -\frac{1}{4}ZY = \frac{1}{4}[\omega^2(L_0 + L_p)C_0 - j\omega R_0 C_0]$$

Assuming θ is very small, $\sin^2\frac{\theta}{2} \approx \left(\frac{\theta}{2}\right)^2$. For $R_0/\omega(L_0 + L_p) \ll 1$, we find from $f(x) = (1 + x)^{1/2} = f(0) + f'(0)x + f''(0)x^2/2 + ... = 1 + x/2 - x^2/8 + ...$, with $x = -jR_0/\omega(L_0 + L_p)$,

$$\theta = \pm\,\omega\sqrt{(L_0 + L_p)C_0}\left[1 - j\frac{R_0}{\omega(L_0 + L_p)}\right]^{\frac{1}{2}}$$

$$\approx \pm\,\omega\sqrt{(L_0 + L_p)C_0}\left[1 + \frac{R_0^2}{8\omega^2(L_0 + L_p)^2}\right] \mp j\frac{R_0}{2}\sqrt{\frac{C_0}{L_0 + L_p}}$$

Thus the effect of increasing L_p is to reduce both attenuation and distortion. However the above analysis requires $|\theta| \ll 1$ which is equivalent to having the operating frequency well below cutoff. For speech communication, we are interested in the propagation of signals up to 12 kHz. Assuming $R_0 = 0$, we are requiring $12\times10^3\pi\sqrt{(L_0 + L_p)C_0} \ll 1$. This requirement imposes an upper limit on L_p.

C. Periodically Loaded Transmission Lines

First consider the two-port description of a transmission line as shown in Figure 2.4.6. The transmission line equations are written in terms of V_+ and V_- as

$$V(z) = V_+ e^{-jkz} + V_- e^{jkz}$$
$$I(z) = Y_0(V_+ e^{-jkz} - V_- e^{jkz})$$
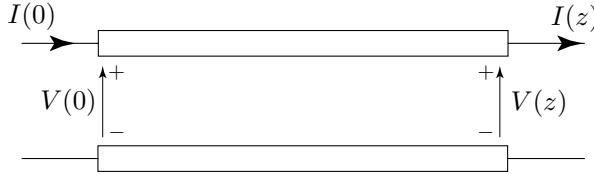
Figure 2.4.6 Two-port description of a transmission line.

At $z = 0$,
$$V(0) = V_+ + V_-$$
$$I(0) = Y_0(V_+ - V_-)$$

which can be solved for V_+ and V_- .

$$V_+ = \frac{1}{2}[V(0) + Z_0 I(0)]$$
$$V_- = \frac{1}{2}[V(0) - Z_0 I(0)]$$

and we have

$$V(z) = V(0)\cos kz - jZ_0 I(0)\sin kz$$
$$I(z) = -jY_0 V(0)\sin kz + I(0)\cos kz$$

or

$$\begin{bmatrix} V(z) \\ I(z) \end{bmatrix} = \begin{bmatrix} \cos kz & -jZ_0 \sin kz \\ -jY_0 \sin kz & \cos kz \end{bmatrix} \begin{bmatrix} V(0) \\ I(0) \end{bmatrix}$$

for the two-port transmission line.

Consider a periodically loaded transmission line as shown in Fig. 2.4.7. Treating the transmission line section of the nth cell as a two-port network, we have

$$\tilde{V}_{n+1} = V_n \cos k\ell - jZ_0 I_n \sin k\ell \qquad (2.4.14a)$$
$$\tilde{I}_{n+1} = -jY_0 V_n \sin k\ell + I_n \cos k\ell \qquad (2.4.14b)$$

where by virtue of KCL

$$\tilde{I}_{n+1} = YV_{n+1} + I_{n+1} \qquad\qquad (2.4.15a)$$

$$\tilde{V}_{n+1} = Z\tilde{I}_{n+1} + V_{n+1} = (ZY+1)V_{n+1} + ZI_{n+1} \quad (2.4.15b)$$

To obtain the dispersion relation, we notice that $V_{n+1} = V_n e^{-j\theta}$ and $I_{n+1} = I_n e^{-j\theta}$. From (2.4.14) and (2.4.15), we obtain

$$V_n\{(ZY+1)e^{-j\theta} - \cos k\ell\} = -\{Ze^{-j\theta} + jZ_0 \sin k\ell\}I_n$$

$$I_n\{e^{-j\theta} - \cos k\ell\} = -\{Ye^{-j\theta} + jY_0 \sin k\ell\}V_n$$
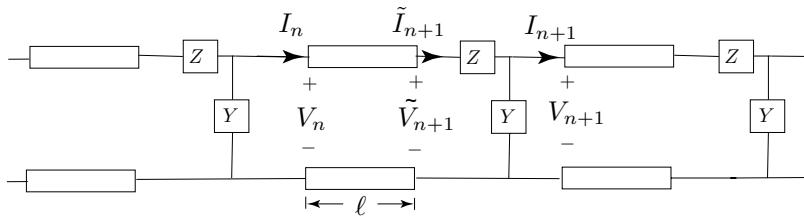
Figure 2.4.7 Periodically loaded transmission line.

Multiplying the two equations and eliminating $V_n I_n$, we find the dispersion relation

$$2\cos\theta = (ZY+2)\cos k\ell + j(ZY_o + Z_oY)\sin k\ell \qquad (2.4.16)$$

Observe that when both Z and Y are reactive, the right-hand side of (2.4.16) is real, but when the absolute value is greater than unity, θ is complex and the wave is evanescent on the line.

EXAMPLE 2.4.3

Consider a periodically loaded transmission line as shown in Fig. E2.4.3.1. We substitute into (2.4.16) $Z = 0$ and $Y = j\omega C_0$, we obtain the dispersion relation
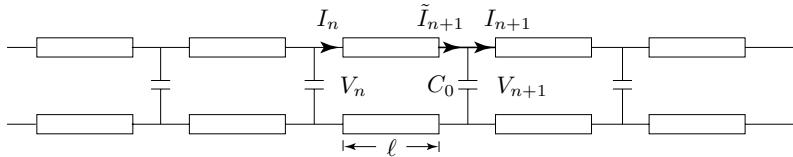
Figure E2.4.3.1 Periodically loaded transmission line.

$$\cos\theta = \cos k\ell - \frac{\omega C_0}{2Y_0}\sin k\ell \qquad\qquad (\text{E2.4.3.1})$$

Observe that when the absolute value of the right-hand-side of (E2.4.3.1) is greater than unity, θ is complex and the wave is evanescent on the line.

Case A) When $\omega C_0 \gg Y_0$, the dispersion relation (E2.4.3.1) allows a real solution for θ only when $k\ell \approx n\pi$, i.e., ℓ is close to an integer multiplier of half wavelength. Let

$$k\ell = n\pi + \delta(\theta)$$

It follows that $\cos(k\ell) \approx \cos(n\pi) = (-1)^n$ and $\sin k\ell \approx (-1)^n\delta(\theta)$. From (E2.4.3.1), we find

$$\cos\theta = \cos k\ell - \frac{k\ell C_0}{2C\ell}\sin k\ell \approx (-1)^n(1 - \frac{n\pi}{2}\frac{C_0}{C\ell})\delta(\theta)$$

For odd n, the trigonometric identity $\cos\theta = 2\cos^2\frac{\theta}{2} - 1$ yields

$$\delta(\theta) = \frac{4C\ell}{n\pi C_0}\cos^2\frac{\theta}{2}$$

For even n, the trigonometric identity $\cos\theta = 1 - 2\sin^2\frac{\theta}{2}$ yields

$$\delta(\theta) = \frac{4C\ell}{n\pi C_0}\sin^2\frac{\theta}{2}$$

Thus the maximum value of $\delta(\theta)$ is $4C\ell/n\pi C_0$.
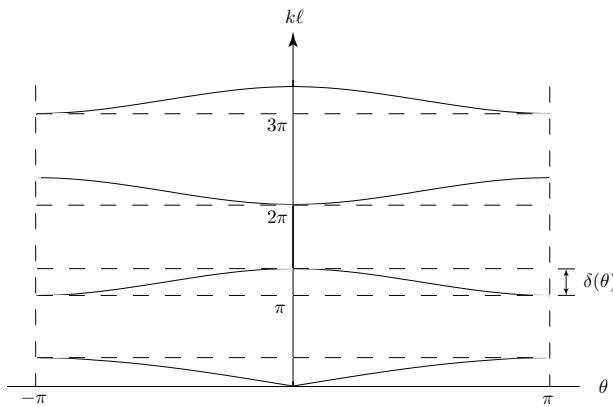
Figure E2.4.3.2 Periodically loaded transmission line as band-pass filter.

A plot of $k\ell$ versus θ is shown in Fig. E2.4.3.2. Propagation is possible only for very narrow frequency bands. We find the bandwidths

$$\frac{\triangle\omega}{\omega} \approx \frac{\delta}{n\pi} = \frac{4C\ell}{(n\pi)^2 C_0} \ll 1$$

Thus the capacitive loaded transmission line is a band-pass filter.

Case B) $\omega C_o \ll Y_o$. The dispersion relation is plotted in Figure E2.4.3.3 for $-\pi \leq \theta \leq \pi$. As $\omega C_o/Y_o = 0$, $\cos\theta = \cos k\ell$, and $k\ell = 2m\pi \pm \theta$. When the transmission line is lightly loaded with small lossless capacitive elements spaced periodically along the line, it can be used as a notch filter which rejects very narrow bands of the frequency spectrum while passing the remainder of the band.
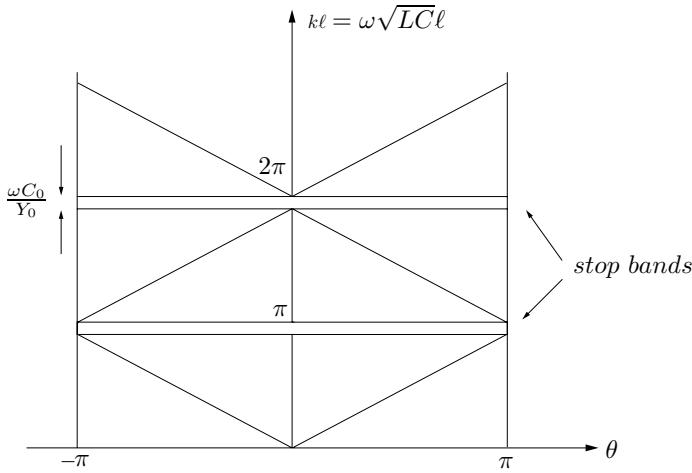
Figure E2.4.3.3 Bandpass lumped element line.

At $\theta = 0$, we let $k\ell = 2n\pi - \delta$. From (E2.4.3.1), we find

$$1 = \cos\delta + \frac{\omega C_0}{2Y_0}\sin\delta \approx 1 - \frac{1}{2}\delta^2 + \frac{\omega C_o}{2Y_o}\delta = \left[1 - \frac{1}{2}\delta\left(\delta - \frac{\omega C_o}{Y_o}\right)\right]$$

Thus $k\ell = 2m\pi$ and $k\ell = 2m\pi - \omega C_o/Y_0$.

At $\theta = \pm\pi$, we let $k\ell = (2m+1)\pi - \delta$. From (E2.4.3.1), we find

$$-1 = -\cos\delta + \frac{\omega C_0}{2Y_0}\sin\delta \approx -1 + \frac{1}{2}\delta^2 + \frac{\omega C_o}{2Y_o}\delta = \left[-1 + \frac{1}{2}\delta\left(\delta - \frac{\omega C_o}{Y_o}\right)\right]$$

Thus $k\ell = (2m+1)\pi$ and $k\ell = (2m+1)\pi - \omega C_o/Y_0$.

— End of Example 2.4.3 —

EXAMPLE 2.4.4

Let $Z = j\omega L_0$ and $Y = j\omega C_0$. We find from (2.4.16)

$$2\cos\theta = (2 - \omega^2 L_0 C_0)\cos k\ell - \omega(L_0 Y_o + C_0 Z_o)\sin k\ell$$

For $k\ell \ll 1$, we obtain

$$\sin^2\frac{\theta}{2} \approx \frac{(k\ell)^2}{4}\left(1 + \frac{C_0}{C\ell} + \frac{L_0}{L\ell} + \frac{L_o C_0}{L\ell C\ell}\right) = \frac{\omega^2}{\omega_0^2}$$

where $\omega_0 = 2/\sqrt{L\ell C\ell + C_0 L\ell + L_o C\ell + L_o C_o}$. It is seen that θ is real when $\omega \leq \omega_0$. The velocity on the line is $v = \ell/\sqrt{L\ell C\ell + C_0 L\ell + L_o C\ell + L_o C_o}$. For $\omega > \omega_0$, θ is imaginary and the wave is evanescent on the line. When the transmission line section length is very small, it is equivalent to a low-pass filter with inductance $L\ell + L_0$ and capacitance $C\ell + C_0$.

— END OF EXAMPLE 2.4.4 —

Problems

P2.4.1

The "high pass filter" type of lumped line shown in Fig. E2.4.2.1 does not support propagating waves for $\omega < \omega_0 = 1/(2\sqrt{L_0 C_0})$.

(a) With the assumed voltage dependence

$$V_{-n} = V_+ e^{-jn\theta_r} e^{-n\theta_I}$$

what are θ_r and θ_I for $\omega < \omega_0$? Sketch θ_r and θ_I as a function of ω for $\omega < \omega_0$.

(b) In the limit $\omega \ll \omega_0$, find an approximate expression for $\frac{V_{-n+1}}{V_{-n}}$ and indicate how this result can be derived from simple circuit considerations.
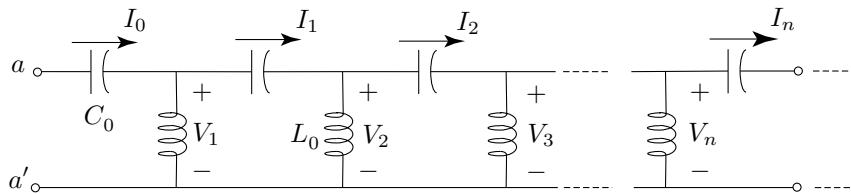
P2.4.2

Figure P2.4.2.1

(a) Determine the dispersion relation for the backward wave line shown in Fig. P2.4.2.1. That is, assume $V_n = Ae^{-jn\theta}$, $I_n = Be^{-jn\theta}$ and determine $\theta(\omega)$. Sketch $\theta(\omega)$ for $\omega > \omega_0 = \frac{1}{2\sqrt{L_0 C_0}}$.

(b) For a given $\omega > \omega_0$, the result in part (a) yields two real values of θ (excluding values which differ by $2n\pi$). Determine the impedance, $Z = \frac{V_n}{I_n}$, for each of these modes and show that the time-averaged power flow is in the direction opposite the phase velocity.

(c) A voltage source $v_s(t) = V_s \sin \omega_0 t$ is connected to terminal pair $a - a'$. Determine the steady-state $v_n(t)$.

(d) Suppose the source connected to $a - a'$ is given by

$$v_s(t) = V_s \frac{\sin \omega_1 t}{\omega_1 t} \sin \omega_0 t$$

where $\omega_1 \ll \omega_0$. Determine $v_n(t)$.

P2.4.3

Consider the backward wave line shown in Figure P2.4.3.1. Derive a expression for the characteristic impedance of this line, $z_+ = V_n/I_n$ for the mode with positive phase velocity $(\exp -jn\theta)$ and for a frequency in the propagating region $(\omega > \omega_h)$. Repeat for the mode with negative phase velocity. What is the time-average power carried by the line in each of these cases? Is the sign of the power what you would expect?
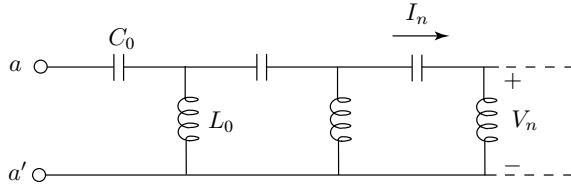
Figure P2.4.3.1

P2.4.4

(a) Determine the propagation constant $\theta(\omega)$, for the lumped transmission line shown in Figure P2.4.4.1. Show that the result can be placed in the form

$$\sin^2 \frac{\theta}{2} = \frac{\omega^2 - \omega_0{}^2}{\omega_1^2}$$

where ω_0^2 and ω_1^2 are appropriate constants.

(b) For what range of ω will the line support a propagating wave, i.e., admit real θ solutions?

P2.4.5

Consider the lumped element line shown in Figure P2.4.5.1.
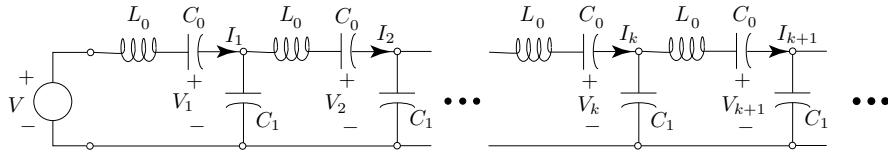
Figure P2.4.4.1
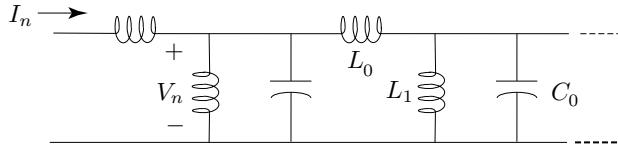
Figure P2.4.5.1

(a) Derive an expression for the propagation constant $\theta(\omega)$. Show that the result can be written in the form

$$\sin^2 \frac{\theta}{2} = \frac{\omega^2 - \omega_1^2}{\omega_0^2}$$

What are the constants ω_0 and ω_1?

(b) Over what frequency band does the line support "propagating" waves (admit real θ solutions)? Sketch θ vs. ω for $L_1 = L_0$.

P2.4.6

It is sometimes very useful to use a lumped element model for a transmission line that is actually a continuous structure. One question that arises is how finely we should subdivide the line into equivalent lumped-element sections to have a reasonably accurate model. The following problem illustrates these ideas in power system applications.

(a) Develop and plot a general chart of phase angle error of a lumped element transmission line versus the ratio of frequency to cutoff frequency. The error is defined as

$$\frac{\text{Phase shift for length of actual line} - \text{Phase shift for equivalent lumped section}}{\text{Phase shift for length of actual line}}$$

Limit the plot to frequencies less than the cutoff frequency.

(b) Model a power transmission line with $L = 1.45\,\text{mH/mile}$ and $C = 0.021\,\mu\text{F/mile}$. Given a line using 10 mile lumped sections, at what frequency will the error defined in part (a) be equal to 5%?

2.5   Transmission Line Modeling

A. Modeling Reflection and Transmission

Consider a linearly polarized wave with electric field

$$\overline{E} = \hat{y}E_y = \hat{y}E_0 e^{-jk_x x - jk_z z}$$

incident from a medium with μ and ϵ, upon a half-space medium with μ_t and ϵ_t as shown in Figure 2.5.1.
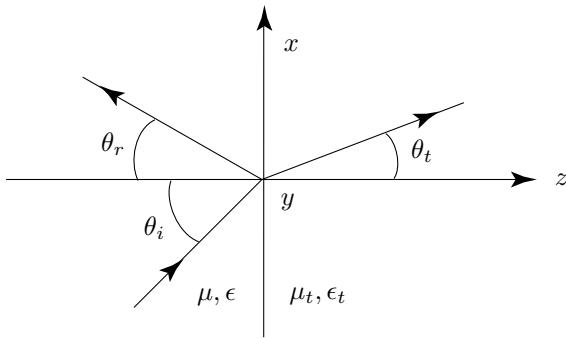
Figure 2.5.1 Reflection and transmission at a plane boundary.

The associated magnetic field $\overline{H}$ is obtained from the Maxwell equation

$$\overline{H} = \frac{1}{-j\omega\mu}\nabla \times \overline{E} = \frac{1}{j\omega\mu}\left\{\hat{x}\frac{\partial}{\partial z}E_y - \hat{z}\frac{\partial}{\partial x}E_y\right\}$$

$$= (\hat{x}\frac{-k_z}{\omega\mu} + \hat{z}\frac{k_x}{\omega\mu})E_0 e^{-jk_x x - jk_z z}$$

$$= \hat{x}H_x + \hat{z}H_z$$

The boundary condition at the interface $z = 0$ requires that the total tangential $\overline{E}$ and $\overline{H}$ be continuous for all x.

In the region $z \geq 0$ with μ_z and ϵ_t, the transmitted fields are

$$\overline{E}_t = \hat{y}E_{ty} = \hat{y}TE_0 e^{-jk_{tx} x - jk_{tz} z}$$

$$\overline{H}_t = \hat{x}H_{tx} + \hat{z}H_{tz} = (\hat{x}\frac{-k_{tz}}{\omega\mu_t} + \hat{z}\frac{k_{tx}}{\omega\mu_t})TE_0 e^{-jk_{tx} x - jk_{tz} z}$$

where T denotes transmission coefficient.

In the region $z \leq 0$ with μ and ϵ, there is also a reflected wave with

$$\overline{E}_r = \hat{y}E_{ry} = \hat{y}RE_0 e^{-jk_{rx}x+jk_{rz}z}$$

$$\overline{H}_r = \hat{x}H_{rx} + \hat{z}H_{rz} = (\hat{x}\frac{k_{rz}}{\omega\mu} + \hat{z}\frac{k_{rx}}{\omega\mu})RE_0 e^{-jk_{rx}x+jk_{rz}z}$$

where R denotes reflection coefficient.

The boundary condition at $z = 0$ requires that

$$E_y + E_{ry} = E_{ty}$$
$$H_x + H_{rx} = H_{tx}$$

which gives

$$e^{-jk_x x} + Re^{-jk_{rx}x} = Te^{-jk_{tx}x} \qquad (2.5.1)$$

$$\frac{k_z}{\omega\mu}e^{-jk_x x} - \frac{k_{rz}}{\omega\mu}Re^{-jk_{rx}x} = \frac{k_{tz}}{\omega\mu_t}Te^{-jk_{tx}x} \qquad (2.5.2)$$

Since the above equations must be satisfied for all x, we conclude that

$$k_x = k_{rx} = k_{tx}$$

This is known as the phase matching condition. Equations (2.5.1) and (2.5.2) become

$$1 + R = T$$

$$\frac{k_z}{\omega\mu} - \frac{k_{rz}}{\omega\mu}R = \frac{k_{tz}}{\omega\mu_t}T$$

we find

$$R = \frac{1 - \mu k_{tz}/\mu_t k_z}{1 + \mu k_{tz}/\mu_t k_z}$$

$$T = \frac{2}{1 + \mu k_{tz}/\mu_t k_z}$$

The reflection and transmission problem can be modeled as a transmission line with characteristic impedance $Z = \omega\mu/k_z$ connected to a transmission line with characteristic impedance $Z_t = \omega\mu_t/k_{tz}$ as shown in Figure 2.5.2.
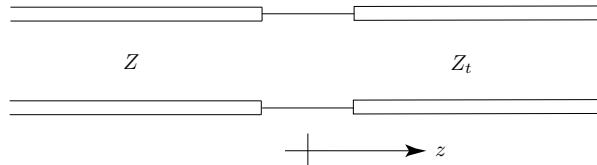
Figure 2.5.2 Transmission line modeling of reflection and transmission.

EXAMPLE 2.5.1

(a) Consider a uniform plane wave in free space normally incident upon a perfect conductor. As a function of z, plot the standing wave patterns, $|E(z)|$ and $|H(z)|$, due to the superposition of the incident and reflected waves.

(b) Now consider a slab of material of thickness d, permeability μ_1, and permittivity ϵ_1, placed $\lambda/4$ away from the perfect conductor as shown in Figure E2.5.1.1.
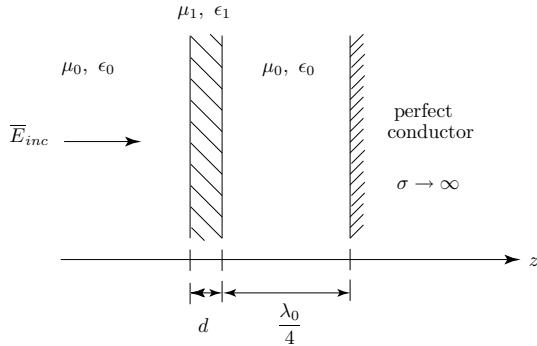
Figure E2.5.1.1

Employing the transmission line analogy [Fig. 2.5.2], the impedance as viewed from the front surface of the material $Z(z = -d - \lambda/4)$ where the wave strikes, may be expressed in terms of the terminating impedances, the thickness and propagation constant of the material [Fig. E2.5.1.2].
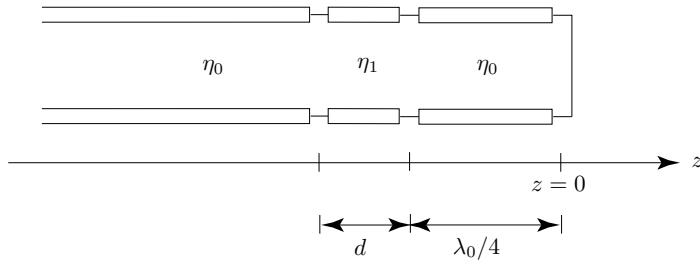
Figure E2.5.1.2

What is $Z(z = -d - \lambda/4)$? In the case of a thin film, $|k_1 d| \ll 1$, show that

$$Z(z = -d - \lambda/4) \cong -j\frac{\eta_1}{k_1 d}$$

where the characteristic impedances $\eta_0 = \sqrt{\mu/\epsilon_0}$ and $\eta_1 = \sqrt{\mu_1/\epsilon_1}$.

(c) Let the thin film be a conducting material with conductivity σ_1 and a corresponding complex dielectric constant $\epsilon_1 = \epsilon_{1R}[1 - \frac{j\sigma_1}{\omega\epsilon_{1R}}]$. In the limit of high conductivity, $\frac{\sigma_1}{\omega\epsilon_{1R}} \gg 1$, and small thickness, $|k_1 d| \ll 1$, show that

$$Z(z = -d - \lambda/4) \cong \frac{1}{\sigma_1 d} \equiv R_1$$

In transmission line terms, this corresponds to a resistance R_1 placed $\lambda_0/4$ in front of a short-circuit transmission line with characteristic impedance $\eta_0 = \sqrt{\mu/\epsilon_0}$ [Fig. E2.5.1.3].
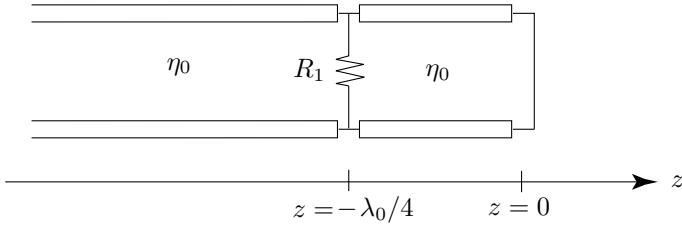
Figure E2.5.1.3

(d) For what value of R_1 is there a perfect match for a normally incident plane wave? For high-frequency applications it is often desirable to reduce or eliminate spurious reflections from metallic objects placed in the vicinity of radiating systems. Thus a thin conducting film may be utilized for this purpose if placed appropriately in front of a metallic surface.

(e) At the frequency 1 GHz, with $\mu_1 = \mu_0$, $\epsilon_{1R} = \epsilon_0$, $\sigma_1 = 5\,\text{mho/meter}$, determine the thickness d to achieve the value of R_1 of part (d). Verify that $\frac{\sigma_1}{\omega\epsilon_{1R}} \gg 1$ and $|k_1 d| \ll 1$ are satisfied.

SOLUTION:

(a) At $z = 0$: $\overline{E}_i + \overline{E}_r = 0 \rightarrow \overline{E}_r = -\overline{E}_i$

$$\begin{cases} \overline{E}_i = \hat{x}E_0 e^{-jkz} \\ \overline{H}_i = \hat{y}\frac{E_0}{\eta_0}e^{-jkz} \end{cases} \rightarrow \begin{cases} \overline{E}_r = -\hat{x}E_0 e^{jkz} \\ \overline{H}_r = \hat{y}\frac{E_0}{\eta_0}e^{jkz} \end{cases}$$

$$\overline{E} = \overline{E}_i + \overline{E}_r = -\hat{x}2jE_0 \sin kz$$

$$\overline{H} = \overline{H}_i + \overline{H}_r = \hat{y}2\frac{E_0}{\eta_0}\cos kz$$

The standing wave patterns for $|E(z)|$ and $|H(z)|$ are shown in Fig. E2.5.1.4.
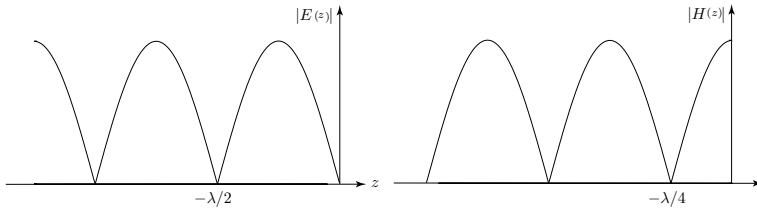
Figure E2.5.1.4

(b) In the transmission line [Figure E2.5.1.2]:

$$Z(z) = Z_0 \frac{Z_L - jZ_0 \tan kz}{Z_0 - jZ_L \tan kz}$$

$$Z(0) = 0 \quad Z(-\frac{\lambda}{4}) = \eta_0 \frac{0 + j\eta_0 \tan\left(-\frac{\pi}{2}\right)}{\eta_0} \to \infty$$

$$Z(-d - \frac{\lambda}{4}) = \eta_1 \frac{Z(-\frac{\lambda}{4}) + j\eta_1 \tan k_1 d}{\eta_1 + jZ(-\frac{\lambda}{4}) \tan k_1 d} = \frac{-j\eta_1}{\tan k_1 d}$$

$$|k_1 d| \ll 1 \quad \Rightarrow \quad Z(-d - \frac{\lambda}{4}) \simeq \frac{-j\eta_1}{k_1 d}$$

(c)

$$\epsilon = \epsilon_{1R}\left(1 - j\frac{\sigma_1}{\omega\epsilon_{1R}}\right) \simeq -j\frac{\sigma_1}{\omega} \qquad \text{for} \quad \frac{\sigma_1}{\omega\epsilon_{1R}} \gg 1$$

$$Z(-d - \frac{\lambda_0}{4}) = \frac{-j\eta_1}{k_1 d} = \frac{-j\sqrt{\mu_1/\epsilon_1}}{\omega\sqrt{\mu_1\epsilon_1}d} = \frac{-j}{\omega\epsilon_1 d} \cong \frac{1}{\sigma_1 d} \equiv R_1$$

(d)

$$\Gamma(-\frac{\lambda}{4}) = \frac{R_1 - \eta_0}{R_1 + \eta_0} = 0 \Rightarrow R_1 = \eta_0$$

(e)

$$R_1 = \frac{1}{\sigma_1 d} = 377 \quad \Rightarrow \quad d = 0.53 \text{ mm}$$

$$\frac{\sigma_1}{\omega\epsilon_{1R}} = \frac{5}{2\pi(10^9)(8.85 \times 10^{-12})} \cong 90 \gg 1$$

$$|k_1 d| = \left|\omega\sqrt{\mu_0\epsilon_0}\sqrt{1 - j\frac{\sigma_1}{\omega\epsilon_{1R}}} \cdot d\right|$$

$$\cong \left|\frac{2\pi 10^9}{3 \times 10^8}(-j\sqrt{90})(0.53 \times 10^{-3})\right| \cong 0.1 \ll 1$$

— END OF EXAMPLE 2.5.1 —

B. Modeling Antenna Radiation

The radiated electric field $\overline{E}$ and magnetic field $\overline{H}$ can be determined by using the radiation fields of a Hertzian dipole, which has been modeled as a pair of charges $\pm q$ separated by an infinitesimal distance and oscillating at angular frequency ω. Let the linear antenna be oriented along the z-axis with separation Δz. For a Hertzian dipole with dipole moment $q\Delta z \cos \omega t$ situated at the origin, we have determined the electric and magnetic fields $\overline{E}$ and $\overline{H}$ in the radiation field very far away from the dipole, $kr \gg 1$:

$$\overline{E}(\overline{r}, t) = -\hat{\theta}\eta \frac{k\omega q\Delta z}{4\pi r} \sin\theta \cos(kr - \omega t)$$

$$\overline{H}(\overline{r}, t) = -\hat{\phi}\frac{k\omega q\Delta z}{4\pi r} \sin\theta \cos(kr - \omega t)$$

Using time convention $e^{j\omega t}$, we take time derivative and obtain the current moment $d(q\Delta z \cos \omega t)/dt = -\omega q\Delta z \sin \omega t = Re\{j\omega q\Delta z e^{j\omega t}\}$. Converting the above solution to the complex phasor notation, we have

$$\overline{E}(\overline{r}) = \hat{\theta}\eta \frac{jkI\Delta z}{4\pi r} \sin\theta e^{-jkr} \tag{2.5.3}$$

$$\overline{H}(\overline{r}) = \hat{\phi}\frac{jkI\Delta z}{4\pi r} \sin\theta e^{-jkr} \tag{2.5.4}$$

where $I\Delta z = j\omega q\Delta z$ and $\eta = \sqrt{\mu_o/\epsilon_o}$ is the characteristic impedance for free space.

Linear Antennas

A linear antenna can be formed by bending an open-circuited two-wire transmission line. The commonly used linear antenna is a half-wavelength dipole. In Fig. 2.5.3 we illustrate the current distribution on a half-wavelength dipole by folding $\lambda/4$ section of each wire of a two-wire transmission line. We have

$$I(z) = I_0 \sin\left[k(\frac{\ell}{2} - \mid z \mid)\right] \tag{2.5.5}$$

where $\ell = \lambda/2$ for the half-wavelength dipole antenna. The procedure can be used to construct linear antennas of any length ℓ.
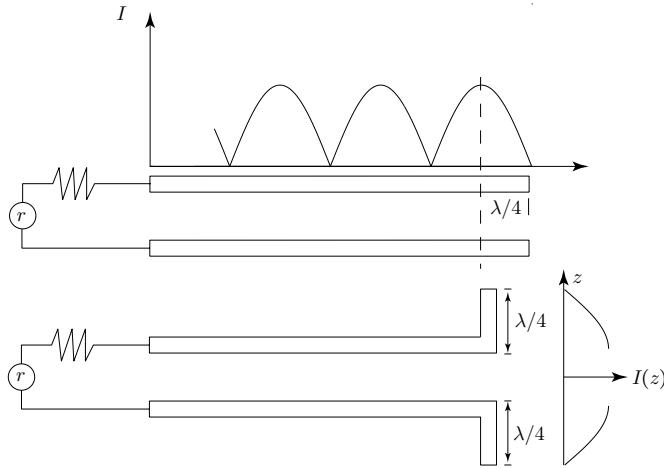
Figure 2.5.3 Current distribution on a half-wavelength dipole.

Radiation Patterns of Linear Antennas

To calculate the radiation field of a linear antenna, we divide the antenna into many infinitesimal segments as shown in Fig. 2.5.4. Since the observation point is far away, the vector $\overline{r}$ originating from the segment Δz at z is parallel to the position vector $\overline{r}$ from the origin. Furthermore, the electric field $\Delta\overline{E}$ due to the segment dipole at z is also pointing in the $\hat{\theta}$-direction. We approximate the distance R by

$$R \approx r - z\cos\theta \tag{2.5.6}$$
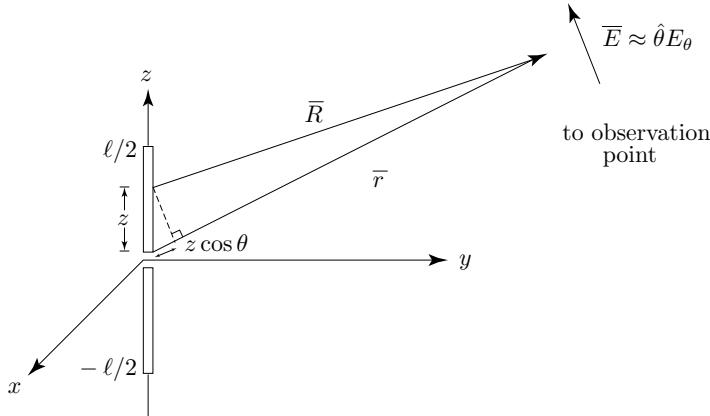
Figure 2.5.4 Calculation of radiation electric field by superposition.

The electric field ΔE due to $I(z)\Delta z$ at z is then

$$\Delta \overline{E} \approx \hat{\theta}\eta \frac{jkI\Delta z}{4\pi R} \sin\theta e^{-jkR} \approx \hat{\theta}\eta \frac{jkI\Delta z}{4\pi r} \sin\theta e^{-jkr} e^{jkz\cos\theta} \quad (2.5.7)$$

Notice that we neglected $z\cos\theta$ in the denominator but retained it in the exponential because it is important there when Δz is of the order of π, the exponential term can change from $e^{j0} = 1$ to $e^{j\pi} = -1$.

The total electric field $\overline{E}$ is obtained by superposition of contributions from all segments on the linear antenna. We integrate over the length of the antenna to obtain

$$\overline{E} = \hat{\theta}E_\theta = \hat{\theta}\eta \frac{jk\sin\theta}{4\pi r} e^{-jkr} f(\theta) \quad (2.5.8)$$

where

$$f(\theta) = \int_{-\ell/2}^{\ell/2} dz I(z) e^{jkz\cos\theta} \quad (2.5.9)$$

is called the current moment of the linear antenna. The magnetic field $\overline{H}$ is obtained in a similar manner. In terms of E_θ,

$$\overline{H} = \hat{\phi}\frac{1}{\eta}E_\theta$$

Thus, the task of the calculation of the far fields of a linear antenna is reduced to the evaluation of the current moment $f(\theta)$ in (2.5.9).

For a linear antenna with a current distribution given in (2.5.5), we find

$$f(\theta) = \int_{-\ell/2}^{\ell/2} dz I(z) e^{jkz\cos\theta} = \int_{-\ell/2}^{\ell/2} dz I_0 \sin\left[k(\frac{\ell}{2} - |z|)\right] e^{jkz\cos\theta}$$

$$= \int_0^{\ell/2} dz I_0 \sin\left[k(\frac{\ell}{2} - z)\right] e^{jkz\cos\theta} + \int_{-\ell/2}^0 dz I_0 \sin\left[k(\frac{\ell}{2} + z)\right] e^{jkz\cos\theta}$$

$$= \int_0^{\ell/2} dz \, 2I_0 \sin\left[k(\frac{\ell}{2} - z)\right] \cos\left[kz\cos\theta\right]$$

$$= \int_0^{\ell/2} dz I_0 \left\{ \sin\left[\frac{k\ell}{2} - kz(1 - \cos\theta)\right] + \sin\left[\frac{k\ell}{2} - kz(1 + \cos\theta)\right] \right\}$$

$$= I_0 \left\{ \frac{\cos\left[\frac{k\ell}{2} - kz(1 - \cos\theta)\right]}{k(1 - \cos\theta)} + \frac{\cos\left[\frac{k\ell}{2} - kz(1 + \cos\theta)\right]}{k(1 + \cos\theta)} \right\}_0^{\ell/2}$$

$$= \frac{2I_0}{k\sin^2\theta} \left\{ \cos(\frac{k\ell}{2}\cos\theta) - \cos(\frac{k\ell}{2}) \right\} \quad (2.5.10)$$

The electric field is therefore

$$E_\theta = \eta \frac{jk\sin\theta}{4\pi r} e^{-jkr} f(\theta) = \eta \frac{jI_0 e^{-jkr}}{2\pi r \sin\theta} \left\{ \cos\left(\frac{k\ell}{2}\cos\theta\right) - \cos\left(\frac{k\ell}{2}\right) \right\}$$

$$(2.5.11)$$

As $\theta \to 0$, L'Hôpital's rule gives $E_\theta = 0$. Thus there is no electric field along the direction of the linear antenna.

For a half-wavelength dipole with $\ell = \lambda/2$ and $k\ell = \pi$, (2.5.11) becomes

$$|E_\theta| = \frac{\eta I_0}{2\pi r \sin\theta} \cos\left(\frac{\pi}{2}\cos\theta\right)$$
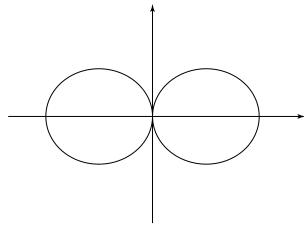
Figure 2.5.5 Radiation pattern for $\lambda/2$ linear antenna.

The radiation pattern is sketched in Figure 2.5.5. For $\ell = 3\lambda/2$, Equation (2.5.11) becomes

$$\mid E_\theta \mid = \frac{\eta I_0}{2\pi r \sin\theta} \left| \cos\left(\frac{3\pi}{2}\cos\theta\right) \right|$$

The radiation pattern is sketched in Figure 2.5.6. We see that the null angles are at $\theta = 0$, $\cos^{-1} 1/3$, and π.
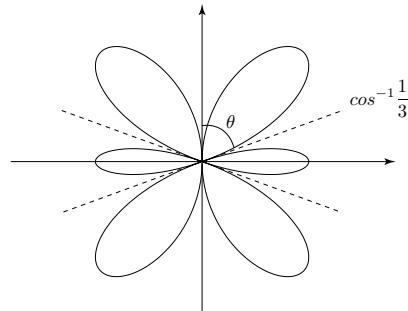
Figure 2.5.6 Radiation pattern for $3\lambda/2$ linear antenna.

EXAMPLE 2.5.2

Consider a linear antenna with current distribution $I(z)$. The radiation far fields are given by

$$\overline{E} = \hat{\theta}\eta\frac{jk\sin\theta}{4\pi r}e^{-jkr}\int_{-\ell/2}^{\ell/2}dzI(z)e^{jkz\cos\theta} = \hat{\theta}E_\theta$$

$$\overline{H} = \hat{\phi}\frac{1}{\eta}E_\theta$$

The directive gain is defined as

$$G(\theta,\phi) = \frac{\langle S \rangle}{P_r/4\pi r^2}$$

and the radiation resistance can be calculated from

$$R_r = \frac{2P_r}{I_o^2}$$

Find the total radiated power P_r, the directive gain $G(\theta,\phi)$ and radiation resistance R_r for the following current distributions

(a) Hertzian dipole, $I(z) = I_o$, $\ell \to 0$ and $I_o\ell = \text{constant}$,
(b) Triangular shape $I(z) = I_o(1 - |2z/\ell|)$ and $k\ell \ll 1$.

SOLUTION:

$$\langle \overline{S} \rangle = \frac{1}{2}\overline{E} \times \overline{H}^* = \hat{r}\frac{1}{2\eta}|E_\theta|^2 = \hat{r}\frac{\eta}{2}\left|\frac{k\sin\theta}{4\pi r}\int_{-l/2}^{l/2}dzI(z)e^{jkz\cos\theta}\right|^2$$

The total radiated power is

$$P_r = \int_0^{2\pi}d\phi\int_0^\pi r^2\sin\theta d\theta\,\langle S\rangle$$

(a) $E_\theta = \eta\frac{jk\sin\theta}{4\pi r}e^{-jkr}I_o\ell$ and $\langle S\rangle = \frac{\eta}{2}|I_ol|^2\left(\frac{k}{4\pi r}\right)^2\sin^2\theta$. Thus

$$P_r = \pi\eta|I_ol|^2\left(\frac{k}{4\pi}\right)^2\int_0^\pi\sin\theta d\theta\sin^2\theta = \frac{4\pi}{3}\eta\left(\frac{kI_ol}{4\pi}\right)^2$$

$G(\theta,\phi) = \frac{3}{2}\sin^2\theta$ and $R_r = \frac{2P_r}{I_o^2} = 20(kl)^2$. where we have used $\eta = 120\pi\,\Omega$.

(b)

$$\langle S\rangle = \frac{\eta}{2}\left|\frac{k\sin\theta}{4\pi r}\int_{-l/2}^{l/2}dzI(z)e^{jkz\cos\theta}\right|^2 \approx \frac{\eta}{8}\left|\frac{kI_ol}{4\pi r}\right|^2\sin^2\theta$$

$P_r = 40\left|\frac{kI_ol}{4}\right|^2$, $G(\theta,\phi) = \frac{3}{2}\sin^2\theta$, and $R_r = 5|kl|^2$.

                                                                        — END OF EXAMPLE 2.5.2 —

C. Array Antennas

Radiation Patterns of Array Antennas

We now calculate the radiation field of an array antenna consisting of Hertzian dipoles on the x-y plane. Assume N dipole antennas are aligned on the x-axis with separation d and all pointing in the $\hat{z}$-direction [Fig. 2.5.7]. The 0th dipole is situated at $x = a$. Let the dipoles have uniform phase shift α so that the dipole moment for the nth dipole is $I\ell e^{jn\alpha}$. Since the observation point is far away, the vector $\overline{R}$ originated from the dipole at $x = a + nd$ is parallel to the position vector $\overline{r}$ from the origin. The electric field $\Delta\overline{E}$ due to the dipole at $x = a + nd$ is pointing along the $\hat{\theta}$-direction. We approximate the distance R by

$$R = r - (a + nd)\cos\phi \qquad (2.5.12)$$

The electric field $\Delta\overline{E}$ due to $(n+1)$th dipole at $x = a + nd$ is then

$$\Delta\overline{E} \approx \hat{\theta}\eta\frac{jkI\ell e^{jn\alpha}}{4\pi R}e^{-jkR} \approx \hat{\theta}\eta\frac{jkI\ell e^{jn\alpha}}{4\pi r}e^{-jkr}e^{jk(a+nd)\cos\phi}$$
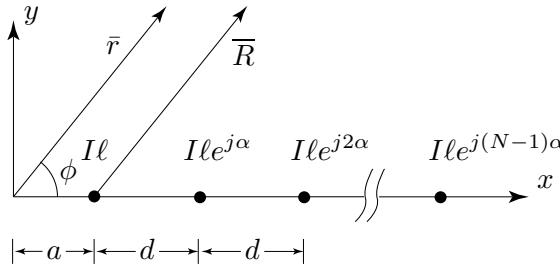
Figure 2.5.7 Dipole antenna array.

Notice that we neglected $(a+nd)\cos\phi$ in the denominator but retained it in the exponential term.

The total electric field $\overline{E}$ is obtained by superposition of the contributions from all Hertzian dipole antennas. The electric field of the antenna array is the sum from all dipoles.

$$\overline{E} = \hat{\theta}\eta\frac{jkI\ell}{4\pi r}e^{-jkr}e^{jka\cos\phi}\sum_{n=0}^{N-1}e^{jn(kd\cos\phi+\alpha)}$$

$$= \hat{\theta}\eta\frac{jkI\ell}{4\pi r}e^{-jkr}e^{jka\cos\phi}F(\phi) \qquad (2.5.13)$$

where $F(\theta, \phi)$ is known as the array factor.

$$F(\phi) = \sum_{n=0}^{N-1} e^{jn(kd\cos\phi+\alpha)} = \frac{1 - e^{jN(kd\cos\phi+\alpha)}}{1 - e^{j(kd\cos\phi+\alpha)}} \qquad (2.5.14)$$

The magnitude of the array factor is calculated to be

$$|F(\phi)| = \left| \frac{\sin\left[N(kd\cos\phi + \alpha)/2\right]}{\sin\left[(kd\cos\phi + \alpha)/2\right]} \right| \qquad (2.5.15)$$

Notice that principal maxima of $|F(\phi)|$ occur at $kd\cos\phi + \alpha = 0$ where $|F(\phi)| = N$. In the following we shall sketch radiation patterns on the xy-plane for various dipole configurations.

EXAMPLE 2.5.3

    Sketch radiation patterns in the xy-plane for the following dipole arrays:

(a) Two-dipole array with $\alpha = 0$ and $d = \lambda/2$.
(b) Two-dipole array with $\alpha = \pi$ and $d = \lambda/2$.
(c) Two-dipole array with $\alpha = 0$ and $d = \lambda$.
(d) Three-dipole array with $\alpha = 0$ and $d = \lambda/2$.
(e) Four-dipole array with $\alpha = 0$ and $d = \lambda/2$.

Solution:

(a) The radiation pattern for the two-dipole array with $\alpha = 0$ and $d = \lambda/2$ is shown in Fig. E2.5.3.1. The corresponding array factor for the two-dipole array with $\alpha = 0$ and $d = \lambda/2$ is, by virtue of (2.5.14) and (2.5.15),

$$|F(\phi)| = \left| 1 + e^{j\pi\cos\phi} \right| = \left| \frac{\sin\left[\pi\cos\phi\right]}{\sin\left[\frac{\pi}{2}\cos\phi\right]} \right|$$
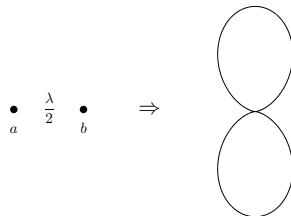
Figure E2.5.3.1 Radiation pattern of two dipoles in phase.

The principal maxima occur in the broadside direction along the y-axis, where at $\phi = \pm\pi/2$, $F(\phi = \pm\pi/2) = 2$, the two dipoles radiate in phase and constructively interfere. In the endfire direction along the $\hat{x}$-direction, where $\phi = 0$, and π, dipole a radiates 1 while dipole b gives $e^{j\pi} = -1$ due to the dipole separation of $d = \lambda/2$. We have $F(\phi) = 0$. The radiation pattern is null since the two dipoles destructively interfere.

(b) The radiation pattern for the two-dipole array with $\alpha = \pi$ and $d = \lambda/2$ is shown in Fig. E2.5.3.2. The corresponding array factor is

$$|F(\phi)| = \left| 1 - e^{j\pi \cos \phi} \right| = \left| \frac{\sin\left[\pi(\cos\phi + 1)\right]}{\sin\left[\pi(\cos\phi + 1)/2\right]} \right|$$
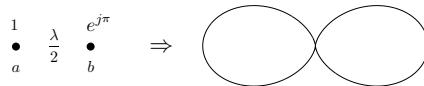
Figure E2.5.3.2 Radiation pattern of two dipoles with $\alpha = \pi$.

The radiation pattern yields a null in the broadside direction of $\phi = \pm\pi/2$ as the two dipoles destructively interfere. In the endfire direction of $\phi = 0$ and π, the radiation pattern is maximum because as dipole a radiates 1, dipole b also gives $e^{j2\pi} = 1$ due to its own phase of π and the phase of π coming from the dipole separation of $d = \lambda/2$. Thus the two dipole fields constructively interfere.

(c) The radiation pattern for the two-dipole array with $\alpha = 0$ and $d = \lambda$ is shown in Fig. E2.5.3.3. The corresponding array factor is

$$|F(\phi)| = \left| 1 + e^{j2\pi \cos \phi} \right| = \left| \frac{\sin\left[2\pi \cos \phi\right]}{\sin\left[\pi \cos \phi\right]} \right|$$
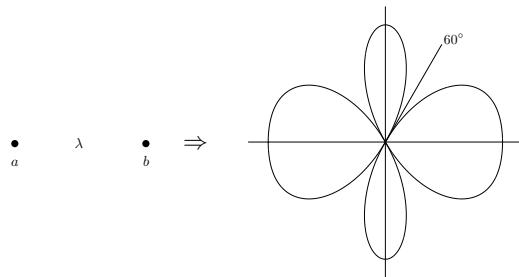
Figure E2.5.3.3 Radiation pattern of two dipoles separated by λ.

It is seen that the radiation pattern has a null in the direction of $\pi/3$. The field produced by dipole a and that produced by dipole b differ in phase equivalent to a path length of $\lambda \cos \pi/3 = \lambda/2$.

(d) The radiation pattern for the three-dipole array with $\alpha = 0$ and $d = \lambda/2$ is shown in Fig. E2.5.3.4. The corresponding array factor is

$$|F(\phi)| = \left|1 + e^{j\pi \cos \phi} + e^{j2\pi \cos \phi}\right| = \left|\frac{\sin\left[3\pi \cos \phi/2\right]}{\sin\left[\pi \cos \phi/2\right]}\right|$$
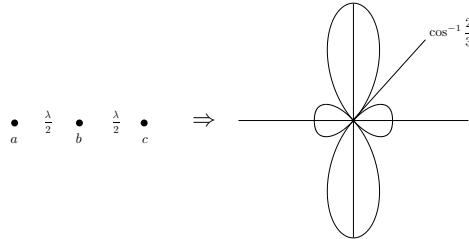
Figure E2.5.3.4   Radiation pattern of three dipoles in phase.

It is seen that there is a null in the direction of $\phi = \cos^{-1} 2/3$. In the broadside direction of $\phi = \pm\pi/2$, the three dipoles constructively interfere. In the endfire direction, the electric field amplitude is $1/3$ of the principal maximum in the broadside direction because two of the three dipoles destructively interfere.

(e) The radiation pattern for the four-dipole array with $\alpha = 0$ and $d = \lambda/2$ is shown in Fig. E2.5.3.5. The corresponding array factor is

$$|F(\phi)| = \left|1 + e^{j\pi \cos \phi} + e^{j2\pi \cos \phi} + e^{j3\pi \cos \phi}\right| = \left|\frac{\sin\left[2\pi \cos \phi\right]}{\sin\left[\frac{\pi}{2} \cos \phi\right]}\right|$$
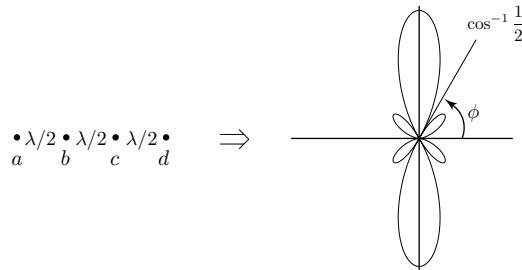
Figure E2.5.3.5   Radiation pattern of four-dipole array.

In the broadside direction, all four dipole fields constructively interfere to yield the principal maxima. The null in the endfire direction can be understood because dipoles a and b destructively interfere and dipoles c and d also destructively interfere. In the direction of $\phi = \cos^{-1} = 1/2$, dipoles a and c produce a null and so do dipoles b and d.

<div align="right">— END OF EXAMPLE 2.5.3 —</div>

D. Array Pattern Multiplication

The radiation pattern of an array of antennas may be obtained by using the technique of pattern multiplication. To illustrate the pattern multiplication method, consider four dipoles pointing in the $\hat{z}$-direction, spaced $\lambda/2$ apart with equal amplitude and phase.

We treat the two dipoles separated by $\lambda/2$ as a single unit denoted by the symbol $\odot$. The unit pattern is shown in Fig. E2.5.3.1. The four-dipole array as shown in Fig. 2.5.8 is the convolution (denoted by $\otimes$ in Fig. 2.5.8) of the unit $\odot$ and the group consisting of two elements separated by distance λ. The group pattern is shown in Fig. E2.5.3.3. The resultant radiation pattern is obtained by multiplication of the unit pattern and the group pattern as shown in Fig. 2.5.9.

Figure 2.5.8 Four-dipole array as convolution of two-dipole arrays.
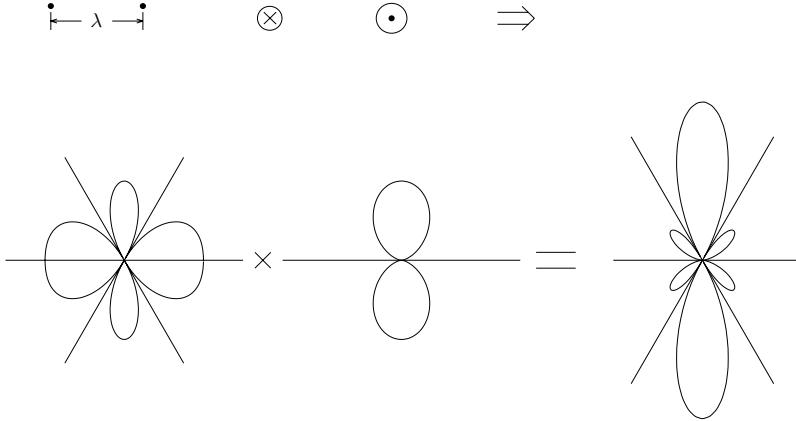
Figure 2.5.9 Multiplication of group and unit patterns.

The radiation pattern is identical to that in Fig. E2.5.3.5.

EXAMPLE 2.5.4

The following five dipole antennas are all pointing in the $\hat{z}$-direction. The amplitude of the center dipole is twice as the other four. Sketch the radiation patterns in the x-y plane.

SOLUTION: Using the pattern multiplication technique, we treat the five-dipole array as a group of two units separated by one wavelength. Each unit consists of three dipole antennas with the unit pattern as shown in Fig. E2.5.3.4. The dipole array is shown as the convolution of a group of two units in Fig. E2.5.4.1.

Figure E2.5.4.1   Five-dipole array as convolution of group of two units.
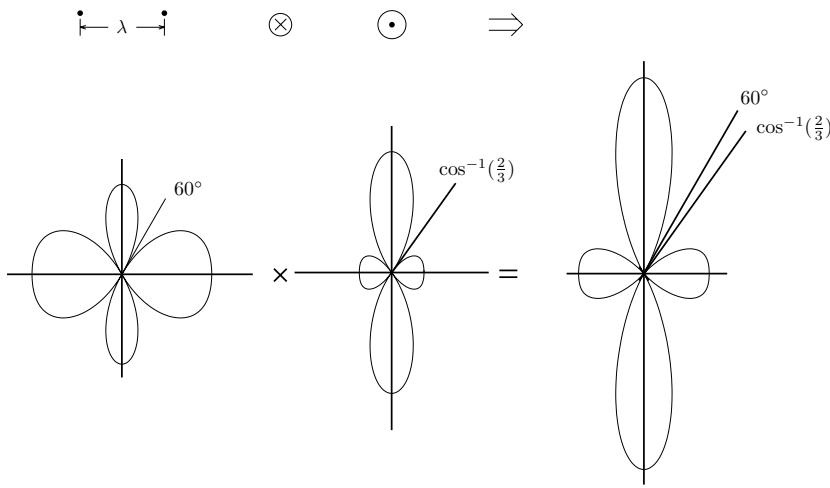
Figure E2.5.4.2   Radiation pattern of five-dipole array.

The group consists of two elements separated by a distance of λ. The group pattern is shown in Fig. E2.5.3.3. The resultant radiation pattern is the multiplication of the group pattern and the unit pattern as shown in Fig. E2.5.4.2.

— END OF EXAMPLE 2.5.4 —

EXAMPLE 2.5.5

A two-dimensional array consisting of six dipoles on the xy-plane is shown in Fig. E2.5.5.1. The three-dipole array forms a unit which convolves with a group of two-elements separated by one wavelength.
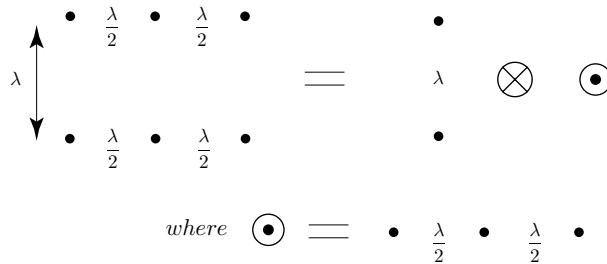
Figure E2.5.5.1 Six-dipole two-dimensional array.

The group pattern is Fig. E2.5.3.3 rotated by 90 degrees. The unit pattern is shown in Fig. E2.5.4.1. The resultant pattern is the multiplication of the group and the unit patterns as shown in Fig. E2.5.5.2.
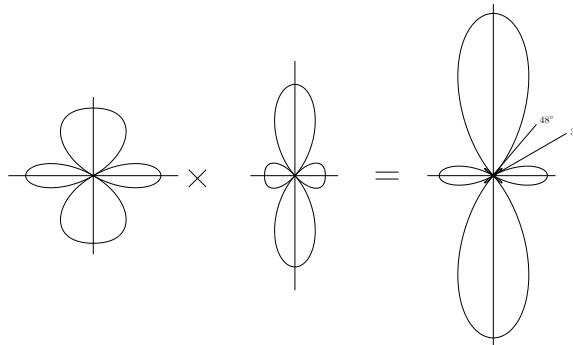
Figure E2.5.5.2 Radiation pattern of the six-dipole array.

The six-dipole two-dimensional array can also be obtained by convolution of the two-dipole pair separated by one wavelength as a unit with the group consisting of three elements. The group pattern in Fig. E2.5.5.2 becomes the unit pattern and the unit pattern becomes the group pattern. Interchanging the group and unit patterns in Fig. E2.5.5.2, the resultant pattern remains the same.
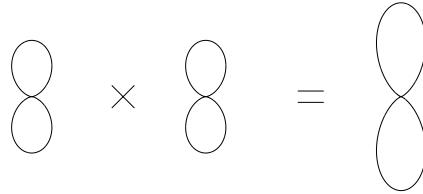
— END OF EXAMPLE 2.5.5 —

EXAMPLE 2.5.6   Binomial array.

   To construct an array antenna with no side lobes, consider the following synthesis procedure. Noticing that the radiation pattern of two dipoles separated by a half-wave-length has no side lobes, we make the two dipole array a unit separated by $\lambda/2$. The resultant pattern is shown in Fig. E2.5.6.1.
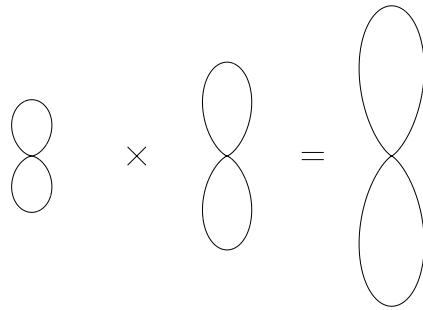
Figure E2.5.6.1 Multiplication of two two-dipole array patterns.

which corresponds to an array shown in Fig. E2.5.6.2.

Figure E2.5.6.2 Resultant array consisting of three elements.

Treat the array in Fig. E2.5.6.2 as a unit. Multiplying the unit pattern with the same group pattern of two-dipoles, the resultant pattern is shown in Fig. E2.5.6.3.

Figure E2.5.6.3 Resultant pattern of array with no sidelobes.

which corresponds to an array shown in Fig. E2.5.6.4.

Figure E2.5.6.4 Resultant array consisting of four elements.

Again repeat the process by making the above array as a unit, we obtain a resultant pattern that is more sharply peaked and the corresponding array has the amplitudes 1 4 6 4 1 . Thus, we conclude that an array antennas with binomial coefficients as amplitudes will have no sidelobes.

Mathematically, the array factor for the binomial array can be obtained in the following fashion:

$$|F(\phi)| = \left|1 + C_1^N e^{j\pi\cos\phi} + C_2^N e^{j2\pi\cos\phi} + \ldots + C_N^N e^{jN\pi\cos\phi}\right|$$

$$= \left|(1 + e^{j\pi\cos\phi})^N\right| = \left|2\cos(\frac{\pi}{2}\cos\phi)\right|^N$$

For $N = 1$, the above equation is equivalent to the expression obtained for two dipoles.

— END OF EXAMPLE 2.5.6 —

EXAMPLE 2.5.7

The total electric field $\overline{E}$ for the dipole array in Figure 2.5.7 was obtained by superposition of the contributions from all Hertzian dipole antennas.

$$\overline{E} = \hat{\theta}\eta\frac{jkI\ell}{4\pi r}e^{-jkr}e^{jka\cos\phi}\sum_{n=0}^{N-1}e^{jn(kd\cos\phi+\alpha)} \tag{E2.5.7.1}$$

The distance from the dipole to the observation point is

$$R = r - (a + nd)\cos\phi \tag{E2.5.7.2}$$

The result in (E2.5.7.1) can also be obtained from the following integral similar to (2.5.8)

$$\overline{E} = \hat{\theta}\frac{j\omega\mu}{4\pi r}e^{-jkr}\int_{-\infty}^{\infty}dxI(x)e^{jkx\cos\phi} \tag{E2.5.7.3}$$

with the source

$$I(x) = \sum_{n=0}^{N-1}\delta(x - a - nd)e^{jn\alpha}$$

We find the array factor

$$F(\phi) = \int_{-\infty}^{\infty}dxI(x)e^{jkx\cos\phi} \tag{E2.5.7.4}$$

For the four dipoles in the previous Example with $\alpha = 0$ and $d = \lambda/2$, we have

$$I(x) = \delta(x) + \delta(x - d) + \delta(x - 2d) + \delta(x - 3d) \tag{E2.5.7.5}$$

The array factor becomes

$$F(\phi) = 1 + e^{j\pi\cos\phi} + e^{j2\pi\cos\phi} + e^{j3\pi\cos\phi}$$

— END OF EXAMPLE 2.5.7 —

EXAMPLE 2.5.8

The array factor

$$F(\phi) = \int_{-\infty}^{\infty} dx I(x) e^{jkx \cos \phi} \qquad (E2.5.8.1)$$

is seen to be the Fourier transform of the current distribution $I(x)$.

For the source distribution of four dipoles with $\alpha = 0$ and $d = \lambda/2$, and

$$I(x) = I\ell \left[\delta(x) + \delta(x - d) + \delta(x - 2d) + \delta(x - 3d)\right] \qquad (E2.5.8.2)$$

we can write $I(x)$ in the form of convolution as follows:

$$I(x) = I\ell \int_{-\infty}^{\infty} dx' \left[\delta(x - x') + \delta(x - x' - 2d)\right][\delta(x') + \delta(x' - d)] \quad (E2.5.8.3)$$

which is graphically represented as

Figure E2.5.8.1

Eq. (E2.5.8.3) and the above Figure illustrates the convolution of a two-dipole array with separation one wavelength with another two-dipole array with half-wavelength separation.

The array factor (E2.5.8.3) then becomes

$$F(\phi) = \int_{-\infty}^{\infty} dx \int_{-\infty}^{\infty} dx' \left[\delta(x - x') + \delta(x - x' - 2d)\right][\delta(x') + \delta(x' - d)] e^{jkx \cos \phi}$$

$$= \int_{-\infty}^{\infty} du [\delta(x - x') + \delta(u - 2d)] e^{jku \cos \phi}$$

$$\int_{-\infty}^{\infty} dx' \left[\delta(x') + \delta(x' - d)\right] e^{jkx' \cos \phi}$$

$$= [1 + e^{j2kd \cos \phi}][1 + e^{jkd \cos \phi}]$$

where we substitute the variable $x - x' = u$. The radiation pattern as represented by $|F(\phi)|$ is illustrated in Figure 2.5.9, which is the multiplication of the radiations of the two dipole arrays. This is the result of the Fourier transform (E2.5.8.3) of the convolution in (E2.5.8.3).

— END OF EXAMPLE 2.5.8 —

E. Equivalence Principle

Equivalence principle is useful in formulating problems for finite "regions of interest" by replacing all "regions of no interest" with equivalent sources. Current sheets are important conceptual tools to be placed on the surfaces of the regions of interest to generate equivalent problems that have identical solutions to the original problem. According to the equivalence principle, we can place current sheets on the boundaries of the regions of interest, or we can place image sources in the regions of no interest. The solutions of the equivalent problems are identical in the regions of interest but in the regions of no interest, the solutions will be different and incorrect. With judicious design of an equivalence problem, many complicated problems can be reformulated to facilitate the solutions.

Radiation by Current Sheets

Consider a plane wave

$$\overline{E} = \hat{x}\eta H_0 e^{-jkz}$$
$$\overline{H} = \hat{y}H_0 e^{-jkz} \tag{2.5.16}$$

propagating in an unbounded space. We can designate $z \geq 0$ as the region of interest and formulate an equivalent problem by placing a current sheet with

$$\overline{J}_s = -\hat{x}2H_0$$
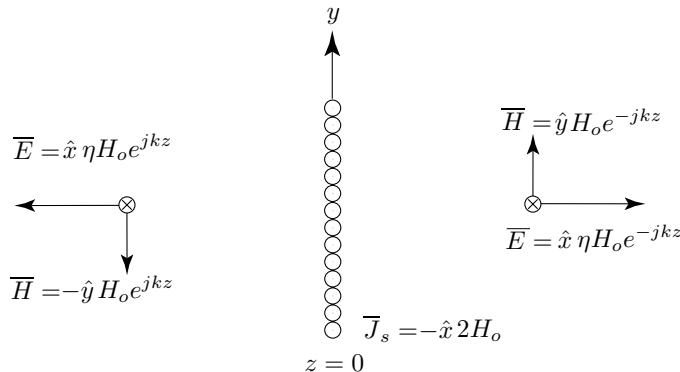
Figure 2.5.10 Current sheet for the reflected wave.

at $z = 0$. The current sheet produces the original plane wave for $z > 0$. In the half-space $z < 0$, however, the current sheet produces a plane wave

$$\overline{E} = \hat{x}\eta H_0 e^{jkz}$$
$$\overline{H} = -\hat{y}H_0 e^{jkz} \tag{2.5.17}$$

propagating in the $-\hat{z}$ direction, which is different from the original plane wave. Thus the two problems are equivalent in the region of interest but different in the region of no interest.

Image Theorem

Consider dipole antennas placed in front of a perfectly conducting half-space as shown in Fig. 2.5.11. We can replace the conducting half-space with images of the dipole antennas. For the dipole parallel to the surface, the image dipole is also parallel to the surface but in the opposite direction, such that the tangential electric field at $z = 0$ is zero. In order to have zero tangential electric field on the surface, the image of the dipole perpendicular to the surface is also perpendicular to the surface but points in the same direction.
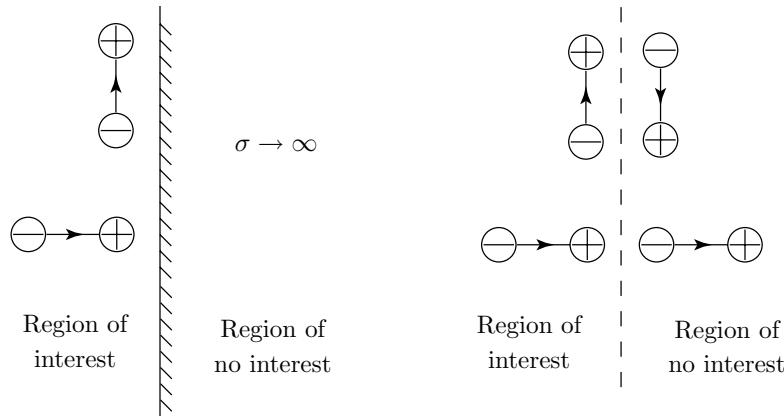
Figure 2.5.11 Image dipole antennas.

The region of interest for this case is the half-space containing the original dipole. In the region of no interest, which was occupied by the perfect conductor, now contains the image dipole. Thus the solutions to the problem of dipoles in front of the conducting half-space are only valid in the region of interest.

EXAMPLE 2.5.9

Consider a dipole antenna placed in front of a perfectly conducting half-space as shown in Fig. E2.5.9.1.
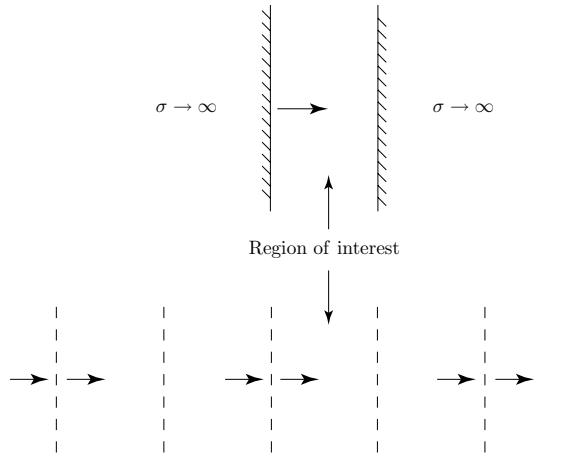
Figure E2.5.9.1 Images of a dipole in between two conductors.

In order to satisfy the boundary condition of zero tangential electric field on the surfaces of both perfect conductors, multiple images are required. It is important to note that the solution of fields due to all the dipoles is only valid in the region of interest. The region of interest is in between the conductors containing the original dipole. The region of no interest was occupied by the perfect conductors and the fields are zero there.

— END OF EXAMPLE 2.5.9 —

Fourier Optics and Diffraction

Consider a plane wave incident upon a slit of width ℓ as shown in Figure 2.5.12. The problem is to obtain the diffracted field to the right of the slit, which is designated as the region of interest. To the left of the slit for $z < 0$, the incident plane wave can be replaced by a current sheet with $\overline{J}_s = -\hat{x}2H_0$. We assume that the slit width is large enough so that the slit open region can be replaced by the current sheet of width ℓ. With the same far-field approximation as (2.5.6) and (E2.5.7.2), we find

$$R \approx r - y\sin\theta \qquad (2.5.18)$$

and write the far field electric field in terms of the current moment per

unit length in x as $F(\theta)$ such that $\overline{E} = \hat{x}AF(\theta)$ with

$$F(\theta) = \int dy J_s(y) e^{jky\sin\theta} \qquad (2.5.19)$$
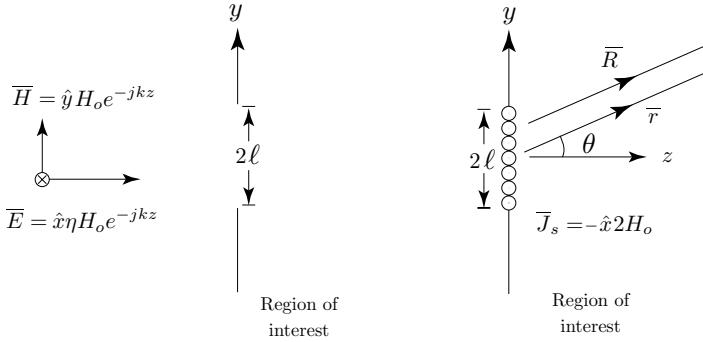
Figure 2.5.12   Diffraction by a slit.
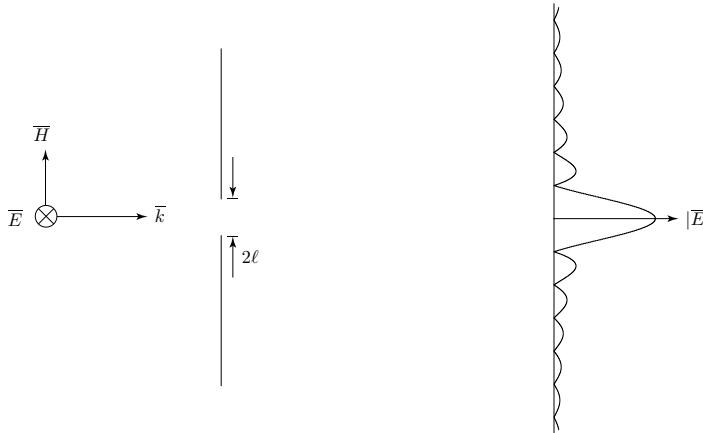
Figure 2.5.13   Diffraction pattern.

where the factor A contains e^{-jkr} and other parameters such as distance and spatial frequencies.

Equation (2.5.19) states that the electric field is a Fourier transform of J_s. This is a simple formula in Fourier optics. For the example of diffraction by a slit, we find

$$F(\theta) = \int_{-\ell}^{\ell} dy\, H_0 e^{jky\sin\theta} = 2\ell H_0 \frac{\sin[k\ell\sin\theta]}{k\ell\sin\theta} \qquad (2.5.20)$$

The diffraction pattern is plotted in Fig. 2.5.13. Far away from the slit, $y/z \ll 1$, approximate $\sin\theta \approx y/z$. We see that nulls of the diffraction pattern occur at $k\ell y/z = n\pi$. Compare the above result with that of an N-dipole array with separation d along the y-axis. In the limit of $N \to \infty$, $d \to 0$, and $Nd = 2\ell$, we find the array factor

$$|F(\theta)| = \left| \frac{\sin(\frac{N}{2}kd\sin\theta)}{\sin(\frac{1}{2}kd\sin\theta)} \right| \approx \left| \frac{N\sin[k\ell\sin\theta]}{k\ell\sin\theta} \right|$$

which is of the same form as (2.5.20).

In Figure 2.5.14, we plot the diffraction pattern for three slits.
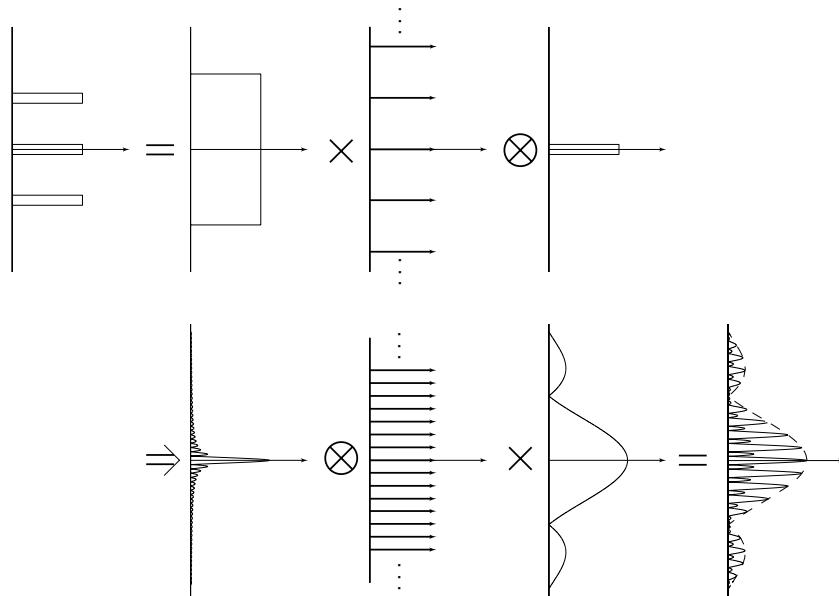
Figure 2.5.14 Diffraction by three slits.

The plot illustrates the pattern multiplication technique. First, the three slits are treated as a gate function multiplying an infinite impulse train and then convolving with one slit. The Fourier transform is then the result of the transform of the gate function convolving with the multiplication of the transforms of the infinite impulse train and one single slit.
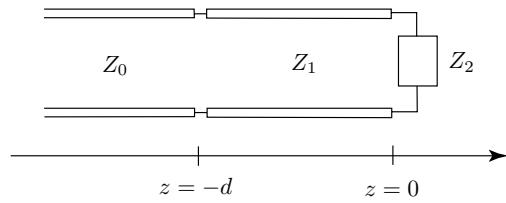
Problems

P2.5.1

Consider a material of thickness d, permittivity ϵ_1, coating a material with permittivity ϵ_2. The frequency is $f = 3 \times 10^8$ Hz.

(a) For a plane wave at normal incidence, the transmission line analogy shown in Figure P2.5.1.1 may be applied to this problem. Determine the equivalent transmission line parameters Z_0, Z_1, Z_2, where d is specified in terms of λ_1, the wavelength in region $-d < z < 0$.

Figure P2.5.1.1

A uniform plane wave is normally incident on this material with

$$\overline{E}_i = \hat{y} E_0 e^{-jk_0 z}$$

where E_0 is a real constant and $k_0 = \omega\sqrt{\mu_0 \epsilon_0}$.

(b) For $d = \frac{1}{8}$ m, give the expression for the transmitted electric field $\overline{E}_t$ and the time-average Poynting vector $\langle \overline{S}_t \rangle$ for $z > 0$ in terms of E_0, ω, μ_0, and ϵ_0.

(c) Repeat (b) for $d = \frac{1}{4}$ m.

P2.5.2

A plane wave with wavelength λ is incident from free space upon a layer of dielectric medium with permittivity $\varepsilon = 4\varepsilon_0$.

(a) When the incident angle is $\theta = 15°$, what is the transmitted angle θ_t?

(b) When the wave is at normal incident $(\theta = 0°)$, find a cascaded transmission line equivalent to the problem. What is the length of the transmission line representing the dielectric layer? What is the reflection coefficient Γ?

P2.5.3

Owing to corrosion and tarnishing problems, metallic reflectors may prove unsuitable at optical frequencies for applications requiring exposure to the atmosphere. An alternative is the use of dielectric mismatching to build up high reflectivity. A typical scheme illustrated below uses alternating layers of high dielectric material, H, and low dielectric material, L, each layer being one-quarter wavelength thick (in the dielectric).
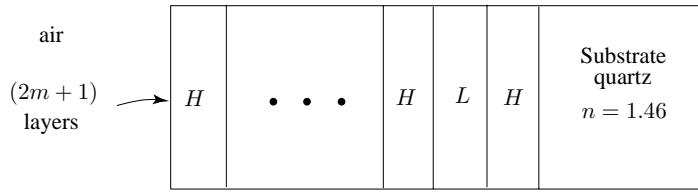
Figure P2.5.3.1

Using refractive indices $n_H = 1.6$ and $n_L = 1.2$, find the power reflection coefficients for $m = 6$, and $m = 25$. Modeling the structure by using transmission line sections [Figure P2.5.3.1].

P2.5.4

A microwave radiometer can measure thermal radiation at microwave wavelengths, the intensity being directly proportional to the average physical temperature of the radiating matched load. Such a device is to be used to measure the internal temperature of hospital patients; but is necessary to match the sensor impedance to that of the patient. The problem is modelled in Figure P2.5.4.1.
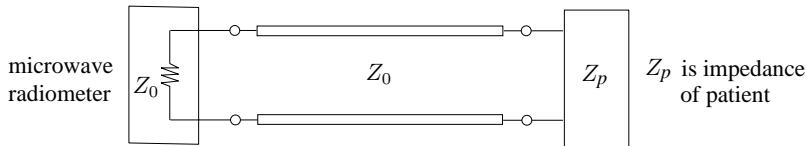
Figure P2.5.4.1

The radiometer is temporarily replaced by a signal generator at the frequency of interest. The VSWR measured in the transmission line is then 2 and the voltage standing minimum is located $\lambda/8$ from Z_p.

(a) What percentage of the signal generator power is reflected from Z_p?
(b) What is Z_p if $Z_0 = 50\,\Omega$?
(c) A single inductor L is to be placed in series with the transmission line to match the load. What is the closest distance to the patient the inductor should be placed and what value of L, if any, should be used in order to produce a match? The frequency (ω) of operation is 10^{10} rad/sec.

P2.5.5

A BALUN is a term used by antenna engineers to describe a device which transforms an unbalanced to a balanced transmission line. (An "unbalanced" coaxial line is one in which the magnitude of the total current in the outer conductor is not equal to the current in the inner conductor; that is, in which
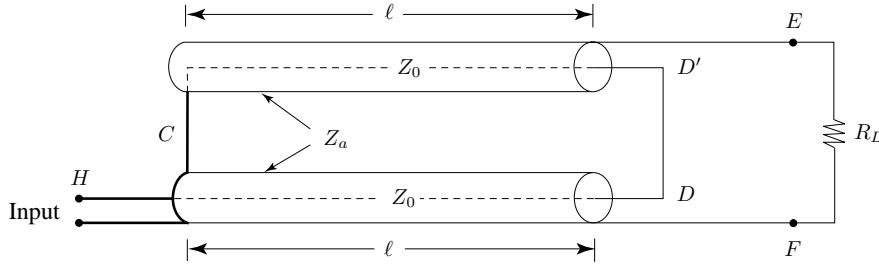
Figure P2.5.5.1

there is current flow on the outside of the outer conductor.) Figure P2.5.5.1 shows a coaxial balun proposed by W. K. Roberts in 1957.

The antenna is modelled as a resistive load R_L (equal to the "radiation resistance"). The two coaxial cables are identical and have characteristic impedance Z_0. The outer conductors of the two coaxial cables are shorted at one end and these outer conductors form a two-wire transmission line of characteristic impedance Z_a. An equivalent circuit can be drawn as shown in Figure P2.5.5.2. (Convince yourself that this circuit is equivalent to the physical arrangement above.) In answering the following questions, consider the case where $Z_a = R_L$.
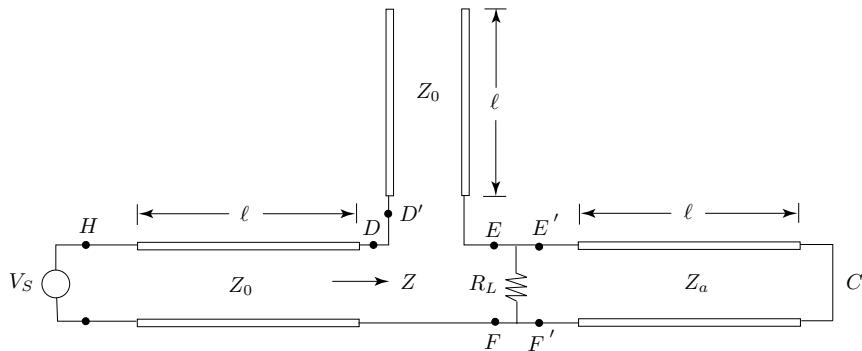
Figure P2.5.5.2

(a) Show, from the equivalent circuit, that the impedance looking into the terminals D-F is

$$Z = R_L \sin^2 k\ell + j \cot k\ell \left(R_L \sin^2 k\ell - Z_0 \right).$$

(b) The line is perfectly matched if $Z = Z_0$. Assume $Z_0 = 50\,\Omega$ and $R_L = Z_a = 70\,\Omega$; determine $k\ell$ such that the line is perfectly matched.
(c) This balun is useful for matching a balanced circuit to an unbalanced circuit of nearly the same impedance over a wide frequency range. Show,

from the above formula for Z, that the first two frequencies for a perfect match have a ratio of approximately $2:1$ for the given data in (b).

(d) Assume the coaxial cables are one quarter wavelength long, i.e., $k\ell = \pi/2$. Show that $\text{VSWR} = 1.4$ for the given data in (b).

P2.5.6

A "turnstile" antenna consists of two Hertzian dipoles oscillating at an angular frequency ω and situated at right angles to each other as shown in Fig. P2.5.6.1. The antenna have current distributions given by $\bar{I}_1 = \hat{x}I$ and $\bar{I}_2 = \hat{y}jI$, respectively.
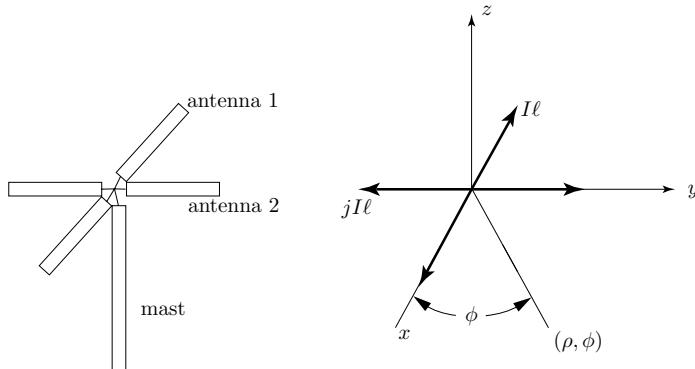
Figure P2.5.6.1

(a) Using the spherical coordinate system, show that in the far field $kr \gg 1$, $\overline{E} \simeq -j\omega[\hat{\theta}A_\theta + \hat{\phi}A_\phi]$.

(b) Find the total electric field in the far-field $(k\rho \gg 1)$ in the x-y plane with $\theta = \pi/2$. Show that the real space-time dependence of the electric field is of the form $\cos(\omega t + \phi - k\rho)$. Note that

$\hat{x} = \hat{r}\cos\phi\sin\theta - \hat{\phi}\sin\phi + \hat{\theta}\cos\phi\cos\theta$

$\hat{y} = \hat{r}\sin\phi\sin\theta + \hat{\phi}\cos\phi + \hat{\theta}\sin\phi\cos\theta$.

(c) Find the radiation power pattern in the x-y plane.

(d) Calculate the power density radiated in the $+\hat{z}$ direction in the far field.

P2.5.7

The migratory patterns of Caribou in Alaska are to be monitored by means of small attached transmitters. Periodically the transmitter radiates a coded pulse train with a total radiated power of 10 watts at 300 MHz. Assume the transmitting antenna is an isotropic radiator (with gain 1), but the receiving antenna is an array with 30 dB gain (gain in dB is $10\log_{10}$ gain). The receiver is matched to the antenna which has an impedance of $50\,\Omega$ and can detect the coded signals if the voltage across the receiver terminals is greater than $1\,\mu\text{V}$. Assuming the path is line-of-sight, at what distance can

the Caribou be tracked? Can they be tracked from a synchronous satellite at 36,000 km altitude?

P2.5.8

In the United States, broadcasting to the general public is regulated by the Federal Communications Commission (FCC), which allocates frequencies and establishes technical standards. Three general classes of broadcast stations have been established. *Standard broadcast stations* (amplitude modulation-AM) are licensed for operation on channels spaced by 10 kHz and occupying the band from 535 to 1605 kHz. *Frequency modulation* (FM) *broadcast stations* are authorized for operation on 100 allocated channels, each 200 kHz wide, extending consecutively from 201 on 88.1 MHz to channel 300 on 107.9 MHz. *Television broadcast stations* (operating with vestigial-sideband amplitude modulation of the visual carrier and frequency modulation of the aural carrier) are authorized for commercial and educational operation on designated channels 2–83, each 6 MHz wide, extending from 54–806 MHz. (See reference: *Reference Data for Radio Engineers*, Howard W. Sams & Co., ITT, 1983.)

The electromagnetic waves radiated by AM stations have the $\overline{E}$ field perpendicular to the ground and parallel to the antenna towers (vertical polarization). Most FM stations broadcast with circular polarization. For television broadcasting, the $\overline{E}$ field is parallel to the ground (horizontal polarization).

The induced current on a receiving antenna is largest when the antenna is aligned with the electric field. Given are three wire antenna configurations. For each type of broadcast, AM, FM, and TV, specify which configuration(s) gives maximum reception [Figure P2.5.8.1].
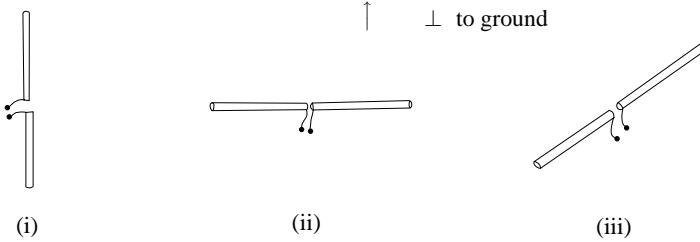
Figure P2.5.8.1

P2.5.9

Consider an elementary ground-to-air communication system with an airplane flying parallel to the ground at an altitude d. The path of the airplane is directly over the transmitting antenna (P_q). Both receiving (P_a) and transmitting antennas are short dipoles and remain parallel during the flight and perpendicular to the ground. Assume throughout that $d \gg \lambda$.

(a) Let the total time-average power radiated by the ground antenna be P. Determine the power received by the receiving antenna on the airplane,

assuming the receiving antenna is matched. Express your answer in terms of θ, d, λ, and P. For what value of θ is the received power maximized?

(b) Assume 10 kW is radiated, the receiver sensitivity is 10^{-10} watts (i.e., the minimum detectable signal is 10^{-10} watts) and the wavelength is 10 cm. How far away from the transmitter will the signal be detectable in the airplane? (Hint: For $r \gg d$, $d/\cos\theta = r \simeq x$ and $\sin\theta \simeq 1$.)

P2.5.10

(a) Find an expression for the far field electric field due to the traveling wave current distribution

$$I(z) = I_0 e^{-jkz}$$

along a terminated wire antenna of length L.

(b) Show that the magnitude of the electric field for large distances from the antenna is given by

$$|E_\theta| = \frac{30 I_0 \sin\theta}{r(1 - \cos\theta)} [2 - 2\cos(kL(1 - \cos\theta))]^{1/2}.$$

(c) Sketch the radiation pattern in the plane containing the antenna if L is equal to $3/2$ wavelengths.

P2.5.11

A radio station is located on the coast, west of a city, as shown in Figure P2.5.11.1a. The transmitting antenna tower may be modeled as a Hertzian dipole antenna of dipole moment $I_o\ell$.
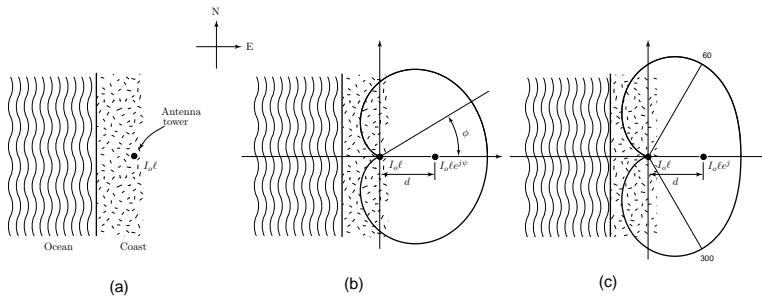
Figure P2.5.11.1

(a) The radio station was able to erect another antenna tower. Relative to the first antenna tower, at what distance d should the second tower be placed and with what phase difference ψ $(-\pi < \psi \leq \pi)$ should it be fed, so that there is a null in the radiation pattern in the direction of the ocean and no "dead" spots in the reception area as shown in Figure P2.5.11.1b?

(b) As shown in Figure P2.5.11.1c, consider another radio station which must serve two cities, sending most of the power over the land area and little power in the direction of the ocean (a null at $\phi = 180°$), with maximum radiation in the direction of the two cities $(\phi = \pm 60°)$, and no nulls, or "dead" spots, in the reception area $(|\phi| \leq 90°)$. Determine the spacing d of these two antenna towers and the relative phase difference $\psi\ (-\pi < \psi \leq \pi)$ to satisfy these requirements.

P2.5.12

Using the pattern multiplication technique, sketch the radiation pattern in the x-y plane for the dipole antenna array as shown in Figure P2.5.12.1 where all elements are excited with equal amplitudes and phases. Find the angles for the nulls and indicate them on sketches. The dipoles are all in the $\hat{z}$-direction.
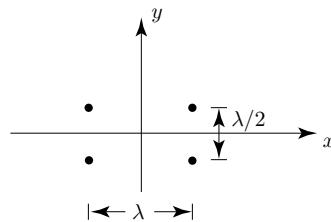
Figure P2.5.12.1

P2.5.13

(a) Construct a binomial array with 3 in-phase Hertzian dipoles along the $\hat{z}$ axis. Specify the relative amplitude of excitation for each element.

(b) Sketch the radiation pattern on the xy-plane and identify the null positions.

(c) A 2D array is created using the binomial array from part (a). The array is shown in Figure P2.5.13.1. Sketch the group pattern and the total radiation pattern for an in-phase array and identify the null positions.
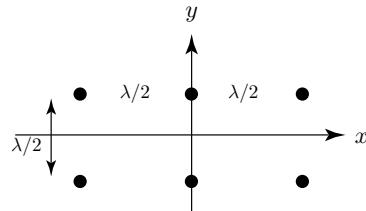
Figure P2.5.13.1

(d) Find the minimum phase shift α between the units such that there will be no side lobes.

P2.5.14

(a) An antenna system in free space radiates the following magnetic field in the far field $(kr \gg 1)$ region.

$$\overline{H} = \hat{\phi} j \frac{H_0}{r} e^{-jkr} \sin\theta \cos(2\pi \sin\theta \cos\phi) e^{-j2\pi \sin\theta \cos\phi}$$

What is the corresponding electric field in the far-field zone?

(b) The gain function for a transmitting antenna system may be written as

$$G_t(\theta, \phi) = 20 \sin^2\theta \cos^2(2\pi \sin\theta \cos\phi).$$

A matched receiver is located $1\,\text{km}$ away in the direction $\theta = 30°$, $\phi = 90°$ relative to the transmitter. The receiver has a gain of 10 in the direction of the transmitter. Find the available power received if the transmitter radiates 1 kilowatt of power at $f = 1\,\text{GHz}$.

P2.5.15

(a) Consider an eight-element linear array with dipoles pointing in the $\hat{z}$ direction and spaced $\lambda/2$ apart with equal amplitude and phase. Using pattern multiplication, sketch the resultant radiation field pattern in the x-y plane. Locate the positions of the nulls and maxima.

(b) Consider four dipoles of equal amplitude and phase on the x-y plane situated at $(x = \lambda/2, y = \lambda/4)$, $(x = \lambda/2, y = -\lambda/4)$, $(x = -\lambda/2, y = \lambda/4)$, and $(x = -\lambda/2, y = -\lambda/4)$. Using pattern multiplication, sketch the total radiation field pattern in the x-y plane. Locate the positions of the nulls and maxima.

P2.5.16

An electric dipole antenna with dipole moment $I\ell$ is oriented in the $\hat{z}$ direction and is placed at the corner of a wall as shown in Figure P2.5.16.1. The ground and the wall are considered to be perfectly conducting and their areas are assumed to be infinite.
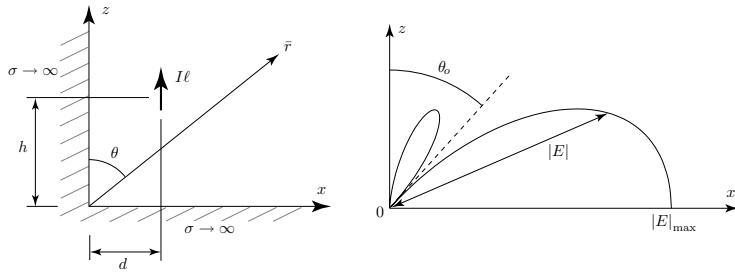
Figure P2.5.16.2

(a) Explain why the radiation field from the dipole antenna is zero everywhere if $d = 0$.

(b) Let $h = 0$. The radiation pattern of the electric field $|E|$ is shown in
   Figure P2.5.16.2, where the maximum value $|E|_{\mathrm{max}}$ appears at $\theta = 90°$,
   and the nulls appear at $\theta = 0$ and θ_o.
   (i) What is the value of θ_o?
   (ii) Find the distance d in terms of wavelength λ.
(c) Let $h = 0$. Find the value(s) of d in terms of wavelength λ such that
   the radiated power along the $\hat{x}$ axis is zero.
(d What is the field in region $z < 0$, and what is the field in region $x < 0$?

P2.5.17
   Two electrically short dipoles of effective height ℓ parallel to the z-axis
are separated by a distance λ along the x-axis. Both dipoles are driven by
currents that have the same amplitude, I_0.
   Find the expression for the far field $\overline{E}$ produced by this array in terms
of the phase ψ of the current of dipole 1 with respect to that of dipole 2.
Sketch the radiation in the x-y plane for $\psi = 0$ and $\frac{\pi}{2}$.

P2.5.18
   Two short dipoles, each having an effective length d, and spaced one
wavelength apart, form a simple array. The terminal currents are fed $180°$
out of phase.
(a) Determine the radiating electric field as a function of r, θ, and ϕ for
   $r \gg \lambda$.
(b) Find the time-averaged power density radiated as a function of r, θ, and
   ϕ. For a given θ, at what angle ϕ is the radiated power a maximum?
(c) Sketch the radiated power density as a function of ϕ in the plane $\theta = \frac{\pi}{2}$.
   What is the angle for maximum radiated power?

P2.5.19
   Consider a T.V. station operating Channel 25 at $537.25\,\mathrm{MHz}$ and radi-
ating a total power of $5 \times 10^3\,\mathrm{kW}$. The radiation pattern in the horizontal
plane is isotropic, with a gain $G_r = 3$. How much power will be received
by an antenna with a gain of 10 located one mile 1.6×10^3 meters from
the T.V. tower? (Assume that the receiving antenna is matched and has its
polarization directivity optimized).

Answers

P2.1.1

$$C_0 = Q/V$$

P2.1.2

$I = Nqv\pi R^2$ gives $v = I/Nq\pi R^2 = 1/\pi 10^{-6} \times 8.5 \times 10^{28} \times 1.6 \times 10^{-19} = 0.023 \, \text{mm/sec}.$

P2.1.3

$\eta = 308\Omega$ and $Z_0 = 50\Omega$. $V_0 \ln(b/a) = 250$, $E_{\max} = V_0/a = 1190 \, \text{v/m}$

P2.1.4

(a) For an air-filled coaxial line, $\eta = \eta_o = 120\pi \, \Omega$. From $Z_0 = \frac{\eta}{2\pi} \ln\left(\frac{b}{a}\right)$, we find, for $b = a + d$, $a = \frac{d}{e^{5/6}-1} \approx 0.77d$, and $b = 1.77d$.

(b) For a parallel-plate line filled with air, $w = \frac{12\pi}{5} d \approx 7.54 \, d$.

(c) Let $Z_0 = \frac{\eta}{2\pi} \ln\left(\frac{b}{a}\right) = 10^4 \, \Omega$. We find $\frac{b}{a} = e^{10^3/6} = 2.41 \times 10^{12}$ which is too large, and is not practical.

(d) Let $Z_0 = \frac{\eta}{2\pi} \ln\left(\frac{b}{a}\right) = 1\,\Omega$. We find $\frac{b}{a} = e^{1/60} = 1.017$. The separation d is too small, and is not practical.

P2.1.5

(a) $LC = \mu\epsilon$ as $\overline{E}_T = -\sqrt{\frac{\mu}{\epsilon}} \, \hat{z} \times \overline{H}_T$, and $\overline{H}_T = \sqrt{\frac{\epsilon}{\mu}} \, \hat{z} \times \overline{E}_T$.

(b) $Z_0 = (\eta_0/2\pi) \ln(b/a)$, where a and b are the radii of the inner and outer conductor respectively with $b = a + d$.

$$Z_0 = 50\Omega = \frac{\eta_0}{2\pi} \ln\left(1 + \frac{d}{a}\right) \Rightarrow a = \left[e^{\left(\frac{2\pi Z_0}{\eta_0}\right)} - 1\right]^{-1} d = 0.769d$$

(c) $Z_0 = 50\Omega = \frac{\eta_0 d}{w} \Rightarrow w = \frac{\eta_0}{Z_0} d = \frac{12\pi}{5} d$.

(d) In order to get $Z_0 = 1\,\text{k}\Omega$, we have, $\frac{2\pi Z_0}{\eta_0} = \frac{10^3}{60} = 16.7 \Rightarrow a = 5.78 \times 10^{-8} d$. This is not a feasible design.

(e) To get $Z_0 = 1\,\Omega$ for a coaxial line, we have $\frac{2\pi Z_0}{\eta_0} = \frac{1}{60} \Rightarrow a = 59.5d$. It is not practical. For a parallel plate line, we need $w = 377d$, which is practical.

P2.2.1

The solutions for the voltage and current waves are

$$V(z,t) = V_+[\cos(kz - \omega t) - \cos(kz + \omega t)] = 2V_+ \sin kz \sin \omega t$$

$$I(z,t) = I_+[\cos(kz - \omega t) + \cos(kz + \omega t)] = 2I_+ \cos kz \cos \omega t$$

We find, in the limit when $-kz = k\ell \ll 1$,

$$L_0 = -\frac{V_+}{\omega I_+} \tan kz \approx \frac{Z_0}{\omega} k\ell = \mu \frac{\ell d}{w}$$

for a parallel-plate transmission line.

P2.2.2

(a) $Z_0 = \frac{d}{w}\sqrt{\frac{\mu}{\epsilon}} = 200\Omega$.
(b) $V(z,t) = E_0 d\cos(kz - \omega t)$; $I(z,t) = (E_0 w/\eta)\cos(kz - \omega t)$
(c) $P = E_0^2 wd/2\eta$.
(d) $E_{\max} = 2 \times 10^6$ V/m, below the breakdown field strength.

P2.2.3

(a) At $t = 0$, a backward traveling wave $V'_- = V_0$ is generated such that $I = V_0/Z_0 - V_-/Z_0 = 0$. [Fig. A2.2.3.1]
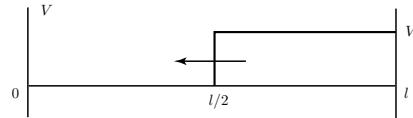
Figure A2.2.3.1

(b) For $t \geq l/v$, $V = V_o$.

P2.2.4

$l_f = vt = t/\sqrt{\mu\epsilon} = 10\,\mu s \times 2 \times 10^8\,\text{m/s} = 2000\,\text{m}$
$V = V_+(1 + \Gamma_L)$, $\Gamma_L = V/V_+ - 1 = -\frac{1}{2}$, $\Gamma_L = \frac{R_L - Z_0}{R_L + Z_0}$ gives $R_f = R_L = 30\,\Omega$

P2.2.5

(a) At the point of the break there is an open circuit $(\Gamma = 1)$ and the current is zero. To satisfy the boundary condition at the breakpoint for $t \geq 0$, two current waves, I_+ and I_- with value $-I_o$ are created. From I_+ , $V_+ = Z_0 I_+ = -Z_0 I_o$. From I_- , $V_- = -Z_0 I_- = Z_o I_o$
(b) $P_{dc} = I_o V_o = 1 \times 10^9\,\text{W} \Rightarrow I_o = \frac{1}{6} \times 10^4\,\text{A} \Rightarrow V_{\text{peak}} = V_o + Z_0 I_o = 1430\,\text{kV}$

P2.2.6

(a) $\ell = 3 \times 10^8\,\text{m}^{-1} \times \frac{1}{2} \times 10^{-8}\,\text{s} = 1.5\,\text{m}$
(b) Since $V = V_+(1 + \Gamma_L)$ and $V = 0.25V$, $V_+ = 0.5V$, we find $\Gamma_L = -\frac{1}{2} = \frac{Z_L - Z_0}{Z_L + Z_0}$. It follows that $Z_L = \frac{1}{3}Z_0$. Replace the infinite line by Z_0 which is in parallel with R_L . From $\frac{R_L Z_0}{R_L + Z_0} = \frac{Z_0}{3}$, we determine $R_L = \frac{Z_0}{2}$
(c) The voltage and current distribution on the line at time $t = 1.5\,\ell/v$ is shown in Figure A2.2.6.1

P2.2.7

(a) $\Gamma_L = \frac{3-1}{3+1} = \frac{1}{2}$
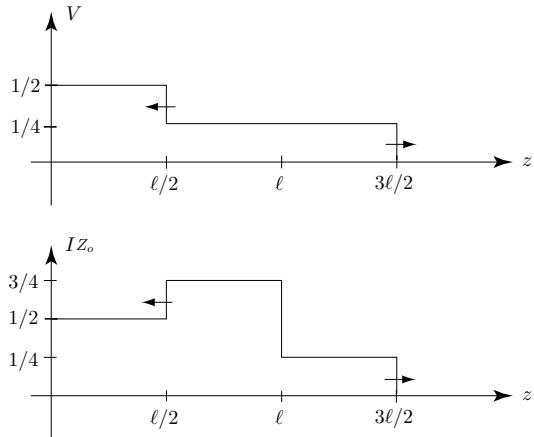
Figure A2.2.6.1

(b) For $t < 0$, $V(z) = 1 \times \frac{3Z_0}{Z_0 + 3Z_0} = \frac{3}{4}$. At $t = 2l/v$, $V(z) = 0$ along the transmission line.
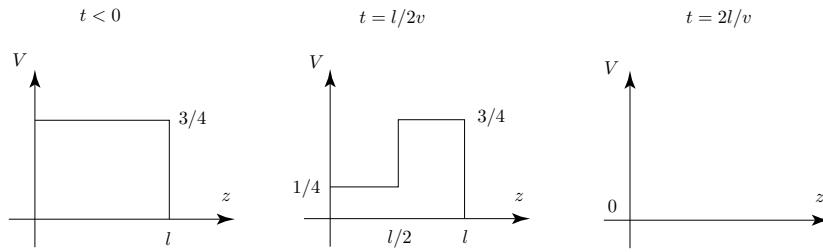
Figure A2.2.7.1

P2.2.8

(a) $\ell = \lambda/2$, $\lambda = 2\ell$; $k_o = \frac{2\pi}{2\ell} = \frac{\pi}{\ell}$; $\omega_o = k_o c = \frac{\pi c}{\ell}$

(b) $f_o = 1.5\text{MHz} \Rightarrow \omega_o \simeq 9 \times 10^6$; $\ell = \frac{\pi c}{\omega_o} = 100\text{m}$

(c) $C_o = \frac{\pi a^2 \epsilon_o}{d}$; $C_\ell = \frac{2\pi \ell \epsilon_o}{\ln(b/a)}$

(d) $\tan k\ell = \frac{C_\ell}{C_o} \frac{1}{k\ell}$

Since d is small, $k\ell \simeq \frac{C_\ell}{C_o} \frac{1}{k\ell}$ and $\omega_o^2 = \frac{c^2}{\ell} \frac{2d}{a^2 \ln(b/a)}$

(e) $\ell = \frac{c^2}{\omega_o^2} \frac{2d}{a^2 \ln(b/a)}$; $a = 3\text{mm}$, $b = 3.3\text{mm}$; $\ell \simeq 8\text{mm}$

P2.2.9

(a) $Z_0 = \sqrt{L/C} = \frac{\mu}{2\pi} \ln(b/a) / \frac{2\pi \epsilon}{\ln(b/a)} = \frac{\eta}{2\pi} \ln(b/a) r \simeq 50\,\Omega$

(b) $Z \sim 50\Omega$

(c) $f_c = 33.9\,\text{GHz}$

(d) $l = \lambda/2 \Rightarrow l = \frac{1}{2f_0\sqrt{\mu\epsilon}}$ $\omega_0 = \frac{\pi}{l\sqrt{\mu\epsilon}}$

(e) $C_0 = \frac{\pi a^2 \epsilon}{\delta}$

P2.2.10

$$V(z,t) = 2A\cos(\omega t)\cos(kz)$$

$$I(z,t) = \frac{2A}{Z_0}\sin(\omega t)\sin(kz)$$

$$k\ell = n\pi; \qquad \omega_n = \frac{n\pi}{\ell\sqrt{LC}}$$

P2.3.1

(a)

(i) $A = \mathrm{Re}\left[-3je^{j(\omega t - \pi/4)}\right] \quad \Rightarrow \quad \underline{A} = -3je^{-j\pi/4} = \frac{1}{\sqrt{2}}(-3 - 3j)$

(ii) $A = \mathrm{Re}\left[e^{j\omega t}(-j\hat{x} - 2\hat{y})\right] \quad \Rightarrow \quad \underline{A} = -j\hat{x} - 2\hat{y}$

(iii) $A = \cos\phi\cos\omega t = \mathrm{Re}\left[\cos\phi e^{j\omega t}\right] \quad \Rightarrow \quad \underline{A} = \cos\phi$

(b)

(i) $\underline{A} = je^{j\pi/4} \quad \Rightarrow \quad A = \mathrm{Re}\left(je^{j\pi/4}e^{j\omega t}\right) = \cos(\omega t + 3\pi/4)$

(ii) $\underline{A} = \hat{x} + \hat{y}3j \quad \Rightarrow \quad A = \mathrm{Re}\left[(\hat{x} + \hat{y}3j)e^{j\omega t}\right] = \hat{x}\cos\omega t - 3\hat{y}\sin\omega t$

(ii) $A = \mathrm{Re}\left[\left(A_o e^{j\phi} + j\right)e^{j\omega t}\right] = A_o\cos(\omega t + \phi) - \sin(\omega t)$

P2.3.2

(a) $\lambda = 8\,\mathrm{m}; \quad Z_L = Z_0 Z_{Ln} = 50(0.55 - j0.3),\ \Omega = (27.5 - j15)\,\Omega$

(b) $Z_n(-25) = 0.55 + j0.3 \quad Z(-25) = (27.5 + j15)\Omega$

(c) $V(-25) = V_s\frac{Z(-25)}{Z(-25)+Z_0} = V_+\left[e^{-jk(-25)} + \Gamma_L e^{jk(-25)}\right]$

$V_+ = V_s\frac{Z(-25)}{[Z(-25)+Z_0]\left[e^{-jk(-25)}+\Gamma_L e^{jk(-25)}\right]}$

$V_L = V_+(1+\Gamma_L) = V_s(0.19 - j0.35)$

(d)

$$<P> = \frac{1}{2}\Re\{V_L I_L^*\} = \frac{1}{2}\Re\left\{V_L\frac{V_L^*}{Z_L^*}\right\} = \frac{|V_L|^2}{2}\Re\left\{\frac{1}{Z_L^*}\right\}$$

$$= \frac{1}{2}|V_s(0.19 - j0.35)|^2\Re\left\{\frac{1}{27.5 + j15}\right\} = 0.0022|V_s|^2$$

Note that instead of calculating $<P>$ at the load, the same result can be obtained by calculating $<P>$ at $z = -25$ m.

$$<P> = \frac{|V(-25)|^2}{2}\Re\left\{\frac{1}{Z(-25)^*}\right\} = \frac{|V_s|^2|Z(-25)|^2}{2|Z(-25)+Z_0|^2}\cdot\frac{\Re\{Z(-25)\}}{|Z(-25)|^2}$$

$$= \frac{|V_s|^2\Re\{Z(-25)\}}{2|Z(-25)+Z_0|^2} = \frac{|V_s|^2}{2}\frac{27.5}{(50+27.5)^2 + 15^2} = 0.0022|V_s|^2$$

P2.3.3

(a) $\frac{1}{2}\lambda = 6\,\mathrm{cm},\ \lambda = 12\,\mathrm{cm},\ v = \frac{c}{\lambda} = \frac{1.5\cdot 10^8}{0.12}\,\mathrm{Hz} = 1.25\,\mathrm{GHz}$

(b) $\Gamma_L = 0.5e^{-j2/3\pi}$
(c) $Z_L = Z_{Ln}Z_0 = (18.5 - j25.5)\,\Omega$
(d) $P = \frac{1}{2} \cdot 4 \cdot 50 \cdot 0.75\,\mathrm{W} = 75\,\mathrm{W}$

P2.3.4

At voltage maximum, the normalized impedance is

$$Z_n(z) = \frac{1 + \Gamma(z)}{1 - \Gamma(z)} = \frac{1 + |\Gamma_L|}{1 - |\Gamma_L|} = R_n$$

Thus $\mathrm{VSWR} = \frac{V_{max}}{V_{min}} = \frac{1+|\Gamma_L|}{1-|\Gamma_L|} = R_n$ with $R_n \geq 1$ on the real Γ_R axis.

P2.3.5

$$Z(z = -\lambda/4) = Z_0 \frac{e^{jk\ell} + \Gamma_L e^{-jk\ell}}{e^{jk\ell} - \Gamma_L e^{-jk\ell}} = Z_2 \frac{1 - \Gamma_L}{1 + \Gamma_L}$$

$$= Z_2 \frac{(Z_L + Z_2) - (Z_L - Z_2)}{(Z_L + Z_2) + (Z_L - Z_2)} = \frac{Z_2^2}{Z_L}$$

$$\Gamma = \frac{Z(z=-\lambda/4)-Z_1}{Z(z=-\lambda/4)+Z_1} = 0 \text{ when } Z_2 = \sqrt{Z_1 Z_L}\,.$$

P2.3.6

(a) $Z_A = Z_0(1 - j)$
(b) $Z_B = Z_A + jZ_0 = Z_0(1 - j) + jZ_0 = Z_0$
(c) $Z_C = Z_0$
(d) $\langle P \rangle = \frac{1}{2}\frac{|V_o|^2}{4Z_0} = \frac{|V_o|^2}{8Z_0}$
(e) $V_C = \frac{V_o}{2},\quad V_B = jV_C = j\frac{V_o}{2},\quad V_A = j\frac{V_o}{2}\frac{Z_o(1-j)}{Z_o(1-j)+jZ_o} = \frac{V_o}{2}(1 + j)$

$\quad\quad V_L = -V_A = -\frac{V_o}{2}(1 + j),\quad \langle P \rangle = \frac{1}{2}\frac{|V_o|^2}{4Z_0}\Re\{1 - j\} = \frac{|V_o|^2}{8Z_0}$

P2.3.7

(a) When $\ell_1 = 0.25\lambda$, $Z(z = \ell_1 - \ell_2) = \dfrac{Z_0^2}{Z_{\mathrm{in}}} = 2Z_0$ will maximize power.

(b) From the Smith chart $\ell_2 = 0.125\lambda$, $\ell_3 = 0.074\lambda$ (Figure A2.3.7.1).
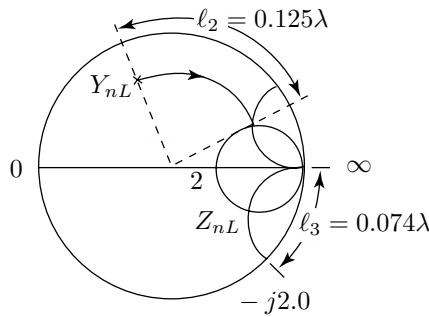
Figure A2.3.7.1

(c) Intersections with the circle $\text{Re}\{Y_n\} = 2$ give $|\Gamma_L| = \left|\dfrac{Z_L - Z_0}{Z_L + Z_0}\right| \geq \dfrac{1}{3}$.

P2.3.8

(a) $W_T = 2\langle W_e \rangle = \frac{C\ell}{4}|V_0|^2 \quad P_d = \frac{1}{2}R_L|I(z=0)|^2 = \frac{a|V_0|^2}{2Z_0}$

$\quad Q_I = \frac{\omega_0 W_T}{P_d} = \frac{\pi}{4a}$

(b) $W_T = 2\langle W_e \rangle = \frac{C\ell}{4}|V_0|^2 \quad P_e = \frac{1}{2Z_0}\left|\frac{V_0}{1+jb}\right|^2 = \frac{|V_0|^2}{2Z_0(1+b^2)}$

$\quad Q_E = \frac{\omega_0 W_T}{P_e} = \frac{\pi}{4}(1 + b^2)$

P2.3.9

(a) $\frac{V(0)}{I(0)} = \frac{V_+ + V_-}{V_+ - V_-}Z_o = \frac{1}{j\omega C_o} \Rightarrow \frac{V_-}{V_+} = \frac{1 - j\omega C_o Z_o}{1 + j\omega C_o Z_o} = e^{-2j\phi}$.

(b) $\frac{V(\ell)}{I(\ell)} = \frac{V_+ e^{-jk\ell} + V_- e^{jk\ell}}{V_+ e^{-jk\ell} - V_- e^{jk\ell}}Z_o = j\omega L_o . \ \frac{V_-}{V_+} = e^{-2j\phi} \Rightarrow \cot(k_n\ell - \phi) =$

$\quad ck_n\frac{L_o}{Z_o}$.

(c-i) $\cot\left(\omega_n\frac{\ell}{c}\right) = 0 \Rightarrow \omega_n\frac{\ell}{c} = n\pi + \frac{\pi}{2}$. $n = 0 \Rightarrow f_0 = \frac{\omega_0}{2\pi} = 75\,\text{MHz}$.

(c-ii) $\cot\left(\omega_n\frac{\ell}{c}\right) = \infty \Rightarrow \omega_n\frac{\ell}{c} = n\pi$. $n = 0 \Rightarrow f_0 = \frac{\omega_0}{2\pi} = 0$.

(d) $\cot\left(\omega\frac{\ell}{c}\right) = \frac{\omega L_o}{Z_o} \Rightarrow 0 < \omega\frac{\ell}{c} < \frac{\pi}{2}$, or $0 < f < 75\,\text{MHz}$.

P2.3.10

(a) $z_0 = \frac{1}{6}\ell; \quad \frac{Z}{Z_0} = 5 \qquad\qquad z_0 = \frac{1}{4}\ell; \quad \frac{Z}{Z_0} = 10$

$\quad z_0 = \frac{1}{3}\ell; \quad \frac{Z}{Z_0} = 15 \qquad\qquad z_0 = \frac{1}{2}\ell; \quad \frac{Z_0}{Z_0} = 20$

(b) $z_0 = \frac{1}{6}\ell; \quad \frac{Z}{Z_0} = 5 + j0.4 \qquad\qquad z_0 = \frac{1}{4}\ell; \quad \frac{Z}{Z_0} = 10 + j0.5$

$\quad z_0 = \frac{1}{3}\ell; \quad \frac{Z}{Z_0} = 15 + j0.4 \qquad\qquad z_0 = \frac{1}{2}\ell; \quad \frac{Z_0}{Z_0} = 20$

(c) The resonator is driven by a shunt current source of amplitude I_s applied at $z = w$. The source frequency ω is varied around ω_1 . Assuming small loss, write down the modal expansion and indicate the dominant term. Hence plot $|V(z = w)|$ as a function of ω and indicate how Q_s can be obtained experimentally from such plots for the loaded and unloaded resonator.

P2.4.1

(a) For $\omega < \omega_0$, $\theta_r = \pi$ and $\frac{\omega}{\omega_0} = \frac{1}{\cosh(\theta_I/2)}$.

(b) $\frac{V_{n+1}}{V_n} \simeq \frac{j\omega L_0}{j\omega L_0 + \frac{1}{j\omega C_0}} \simeq -\omega^2 L_0 C_0 \quad (\omega^2 L_0 C_0 \ll 1)$

P2.4.2

(a) $\sin^2\frac{\theta}{2} = \frac{\omega_{01}^2}{\omega^2} = \frac{1}{4\omega^2 L_0 C_0}$.

(b) $Z = \frac{V_n}{I_n} = \frac{A}{B} = -sgn\theta\sqrt{\frac{L_0}{C_0}}e^{-j\frac{\theta}{2}}$.

(c) $v_n(t) = V_s \sin\left(\omega_0 t + n\pi/2\right)$

(d) $v_n(t) = V_s \sin\left(\omega_0 t + \frac{n\pi}{2}\right) \dfrac{\sin \omega_1 \left(t - \frac{\sqrt{2}n}{\omega_{01}}\right)}{\omega_1 \left(t - \frac{\sqrt{2}n}{\omega_{01}}\right)}$

P2.4.3

$$\langle P \rangle_{\text{positive}} = \frac{1}{2} \text{Re } Z |I_+|^2 = -\frac{1}{2}|I_+|^2 \sqrt{\frac{L_0}{C_0}} \cos\frac{\theta}{2} \quad < 0$$

$$\langle P \rangle_{\text{negative}} = \frac{1}{2} \text{Re } (V_- I_-^*) = \frac{1}{2}|I_-|^2 \sqrt{\frac{L_0}{C_0}} \cos\frac{\theta}{2} \quad > 0$$

Hence power travels in opposite direction of the phase velocity.

P2.4.4

(b) $\omega_0^2 \leq \omega^2 \leq \omega_1^2 + \omega_0^2$.

P2.4.5

(a) $\omega_0 = 2/\sqrt{L_0 C_0}; \quad \omega_1 = 1/\sqrt{L_1 C_0}$.
(b) $\omega_1^2 \leq \omega^2 \leq \omega_0^2 + \omega_1^2$.

P2.4.6

(a) $\theta_a = k\ell = \omega\ell\sqrt{LC} = \omega\sqrt{L\ell C\ell} = 2\frac{\omega}{\omega_0}; \quad \theta_L = 2\sin^{-1}\frac{\omega}{\omega_0}$.
(b) $\omega \approx \omega_0/2 = 18.1 \times 10^3$ rad/sec $\Rightarrow f = 2.88$ kHz.

P2.5.1

(a) $Z_0 = 120\pi\Omega, \ Z_1 = \sqrt{\frac{\mu_0}{\epsilon_1}} = \frac{Z_0}{2} = 60\pi\Omega, \ Z_2 = \sqrt{\frac{\mu_0}{\epsilon_2}} = \frac{Z_0}{4} = 30\pi\Omega$

(b) $\overline{E}_t = \hat{y}E_0 \dfrac{2}{3} \dfrac{1}{1 + \dfrac{1}{3}} \left(e^{-\frac{\pi}{4}j}\right) e^{-j4k_0 z} = \dfrac{1 - j}{2\sqrt{2}} \hat{y}E_0 e^{-j4k_0 z}$

$$\langle \overline{S}_t \rangle = \frac{\hat{z}}{2\eta_2} \left|\overline{E}_t\right|^2 = \frac{\hat{z}}{2} \frac{4}{\eta_0} \frac{E_0^2}{4} = \frac{E_0^2}{2\eta_0} \hat{z}$$

(c) $\overline{E}_t = \hat{y}E_0 \dfrac{2}{3} \dfrac{1 - \dfrac{3}{5}}{1 - \dfrac{1}{3}} (-j)e^{-j4k_0 z} = -\dfrac{2}{5} j\hat{y}E_0 e^{-j4k_0 z}$

$$\langle \overline{S}_t \rangle = \frac{\hat{z}}{2\eta_2} \left|\overline{E}_t\right|^2 = \frac{\hat{z}}{2} \frac{4}{\eta_0} \left(\frac{2}{5}\right)^2 E_0^2 = \frac{8E_0^2}{25\eta_0} \hat{z}$$

Note that $\langle \overline{S}_t \rangle = \hat{z}\frac{E_0^2}{2\eta_0} \left[1 - |\Gamma_0|^2\right] = \hat{z} \langle \overline{S}_{inc} \rangle \left[1 - |\Gamma_0|^2\right]$

P2.5.2

(a) $\theta_t = \theta = 15°$ because the media on the two sides are the same.
(b) The layer is 1/2 wavelength thick — perfect transmission $\Gamma = 0$.

P2.5.3

Let $\mu = \mu_0$, $n = \sqrt{\epsilon/\epsilon_0}$, and $\eta = \sqrt{\mu_0/\epsilon} = \eta_0/n$, $n_S = 1.46$, and model this problem as in Figure A2.5.3.1.

Looking into the substrate, we see an impedance of η_0/n_S . From the left of the first dielectric layer, we can use the inversion properties of a quarter-
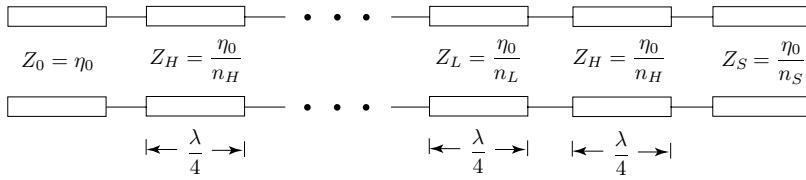
Figure A2.5.3.1

wave transmission line to give: $Z_{in} = \left(\dfrac{\eta_0}{n_H}\right)^2 \cdot \dfrac{n_S}{\eta_0}$ and, back another layer:

$Z_{in} = \left(\dfrac{n_H}{n_L}\right)^2 \dfrac{\eta_0}{n_S}$. So, after $2m$ layers, we get $Z_{in} = \left(\dfrac{n_H}{n_L}\right)^{2m} \dfrac{\eta_0}{n_S}$. And

after the last H layer: $Z_{in} = \dfrac{n_S}{n_H^2} \left(\dfrac{n_L}{n_H}\right)^{2m} \eta_0$.

The reflection coefficient, Γ, from outside the last layer is:

$$\Gamma = \frac{Z_L/Z_0 - 1}{Z_L/Z_0 + 1} = \frac{\dfrac{n_S}{n_H^2}\left(\dfrac{n_L}{n_H}\right)^{2m} - 1}{\dfrac{n_S}{n_H^2}\left(\dfrac{n_L}{n_H}\right)^{2m} + 1} = \begin{matrix} -0.9645103 \text{ for } m = 6 \\ -0.99999935 \text{ for } m = 25 \end{matrix}$$

The power reflection coefficient $|\Gamma|^2 = \begin{matrix} 0.930280 \text{ for } m = 6 \\ 0.9999987 \text{ for } m = 25 \end{matrix}$

P2.5.4

(a) $\text{VSWR} = 2 \Rightarrow |\sigma_l| = \frac{1}{3} \Rightarrow \sigma_l = -\frac{j}{3} \Rightarrow \dfrac{\text{Power reflected}}{\text{Power incident}} = |\sigma_l|^2 = \frac{1}{9}$
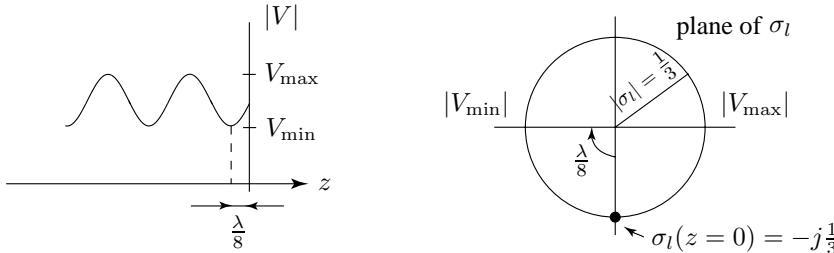
Figure A2.5.4.1

(b) $Z_p = Z_0 \dfrac{1+\sigma_l}{1-\sigma_l} = 50 \dfrac{\left(1 - j/3\right)}{\left(1 + j/3\right)} = 40 - j30$

(c) $Z_{pn} = 0.8 - j0.6$

To connect inductor in series to match the load, we need to go to the point $A_n = 1 - j0.7$ at $\omega = 10^{10} \Rightarrow \lambda = 19\,\text{cm} \quad \ell = 0.473\lambda \Rightarrow \ell = 8.9\,\text{cm}$.

To match A_n , we need to add in series an inductor of value: $X_n = +0.7$ $\Rightarrow$
$X = 0.7 \times 50 = 35\,\Omega \Rightarrow$ $L = \frac{X}{\omega} = 3.5\,\text{nH}$.

P2.5.5

(a) Z_{DF} = Impedance looking into the terminals DF
Z_{DE} = Impedance looking into the terminals DE
Z_{EF} = Impedance looking into the terminals EF
Therefore, we have $Z = Z_{DF} = Z_{DE} + Z_{EF}$
Open circuit $\Rightarrow Z_l = \infty \Rightarrow \Gamma_L = 1 \Rightarrow \Gamma(z) = e^{j2kz}$

$Z_{DE} = Z|_{z=-\ell} = Z_0 \frac{1+e^{-j2k\ell}}{1-e^{-j2k\ell}} = -jZ_0 \cot k\ell$

Short circuit $\Rightarrow Z_L = 0 \Rightarrow \Gamma_L = -1 \Rightarrow \Gamma(z) = -e^{j2kz}$

$Z_{E'F'} = Z|_{z=-\ell} = Z_a \frac{1-e^{-j2k\ell}}{1+e^{-jk\ell}} = jZ_a \tan k\ell = jR_L \tan k\ell$

$Z_{EF} = \frac{R_L \cdot Z_{E'F'}}{R_L + Z_{E'F'}} = \frac{R_L \tan^2 k\ell + jR_L \tan k\ell}{1 + \tan^2 k\ell} = R_L \sin^2 k\ell + jR_L \sin k\ell \cos k\ell$

$Z = Z_{DE} Z_{EF} = R_L \sin^2 k\ell + j \cot k\ell (R_L \sin^2 k\ell - Z_0)$

(b) $Z = Z_0 \Rightarrow Z_0 = R_L \sin^2 k\ell \Rightarrow \sin^2 k\ell = \frac{Z_0}{R_L} = \frac{50}{70} \Rightarrow \sin k\ell = 0.85 \Rightarrow$
$k\ell = \begin{cases} 1.01 + n\pi \\ 2.13 + m\pi \end{cases}$ in radians

(c) $k = \frac{\omega}{c} \Rightarrow \frac{\omega_1 \ell}{c} = 1.01$, $\frac{\omega_2 \ell}{c} = 2.13 \Rightarrow \frac{\omega_2}{\omega_1} = \frac{2.13}{1.01} = 2.11$.

(d) $k\ell = \dfrac{\pi}{2} \Rightarrow Z = R_L = 70\,\Omega \Rightarrow \Gamma_L = \dfrac{\frac{Z}{Z_0} - 1}{\frac{Z}{Z_0} + 1} = \dfrac{1.4 - 1}{1.4 + 1} = \dfrac{1}{6} \Rightarrow$

$VSWR = \dfrac{1 + |\Gamma_L|}{1 - |\Gamma_L|} = \dfrac{1 + \frac{1}{6}}{1 - \frac{1}{6}} = 1.4$

P2.5.6

(a) For far field, $\overline{E}(\bar{r}) = -j\omega\mu \frac{e^{-jkr}}{4\pi r} \left(\hat{\theta} f_\theta + \hat{\phi} f_\phi \right)$
where $\overline{f}(\theta, \phi) = \overline{I}\ell = (\hat{x} + j\hat{y})I\ell = \hat{\theta} e^{j\phi} \cos\theta I\ell + \hat{\phi} j e^{j\phi} I\ell$ so
$\overline{E}(\bar{r}) = -j\omega\mu \frac{I\ell e^{-jkr}}{4\pi r} e^{j\phi} \left(\cos\theta \cdot \hat{\theta} + j\hat{\phi} \right)$

(b) $\overline{E}(\bar{r}) = \hat{\phi}\omega\mu \frac{I\ell e^{-jk\rho}}{4\pi \rho} e^{j\phi}$
$\overline{E}(\bar{r}, t) = \text{Re}\left\{ \overline{E}(\bar{r}) e^{j\omega t} \right\} = \hat{\phi}\omega\mu \frac{I\ell}{4\pi \rho} \cos(\omega t + \phi - k\rho)$

(c) $< \overline{S} > = \frac{1}{2}\text{Re}\frac{|\overline{E}|^2}{\eta} = \frac{1}{2}\eta \left(\frac{kI\ell}{4\pi\rho} \right)^2$ which is a constant independent of the azimuthal angle ϕ .

(d) $| < \overline{S} > | = \frac{1}{2}\text{Re}\frac{|\overline{E}|^2}{\eta} = \frac{1}{2}\eta \left(\frac{kI\ell}{4\pi\rho} \right)^2$

P2.5.7

$r_{\max} = \frac{\lambda}{4\pi} \sqrt{\frac{G_r P_t}{P_{rec}}} \sim 7.96 \times 10^4\,\text{km} > 3.6 \times 10^4\,\text{km}$

P2.5.8

(a) Figure P2.5.8.1(i) gives the maximum reception for AM.
(b) Figure P2.5.8.1(ii) gives the maximum reception for TV.

(c) All three configurations gives the same reception for FM.

P2.5.9

(a) The angle of maximum power reception is $\theta = \tan^{-1}\sqrt{2}$.

(b) $r_{\max} \sim 79.6\,\mathrm{km}$

P2.5.10

(a) $I(z) = I_0 e^{-jkz}$

$\overline{E} = \hat{\theta}\eta \frac{jk\sin\theta}{4\pi r} e^{-jkr} f(\theta) = \hat{\theta}\eta \frac{jk\sin\theta}{4\pi r} e^{-jkr} \int_{-L/2}^{L/2} dz I(z) e^{jkz\cos\theta}$

(b) $|E_\theta| = \frac{jk(120\pi)\sin\theta}{4\pi r} \int_{-L/2}^{L/2} dz I_0 e^{-jkz} e^{jkz\cos\theta}$

$\quad = \frac{jk(30)\sin\theta}{jkr(\cos\theta-1)} \left[I_0 e^{jkz(\cos\theta-1)} \right]_{-L/2}^{L/2}$

$\quad = \frac{30 I_0 \sin\theta}{r(1-\cos\theta)} 2\sin\left[\frac{kL}{2}(1-\cos\theta) \right]$

$\quad = \frac{30 I_o \sin\theta}{r(1-\cos\theta)} 2\left\{ \frac{2-2\cos[kL(1-\cos\theta)]}{4} \right\}^{\frac{1}{2}}$

(c) For $L = \frac{3}{2}\lambda$ and far field
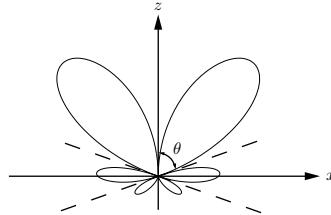
Figure A2.5.10.1 $L = \frac{3}{2}\lambda$

$$|\overline{E}(\overline{r})| \propto \frac{\sin\theta}{1-\cos\theta} \sin\left[\frac{3\pi}{2}(1-\cos\theta) \right] = \frac{\sin\left[\frac{3\pi}{2}(1-\cos\theta) \right]}{\tan\frac{\theta}{2}}$$

P2.5.11

(a) $d = \lambda/4$ and $\psi = -\pi/2$.

(b) $\psi = \frac{\pi}{3}(4m+2n+1)$, and $d = \frac{2\lambda}{3}(m-n-1/2)$. Let $m=0$ and $n=-1$, we get $\psi = -\pi/3$ and $d = \lambda/3$.

P2.5.12

Nulls at $\phi = \pm 60°, \pm 90°, \pm 120°$

P2.5.13

(a) $1:2:1$

(b) 0 and π

(c) $0,\ \pi/2,\ \pi.\ 3\pi/2$

(d) $\alpha = \pi$

P2.5.14

(a) $\overline{E} = \hat{\theta}\sqrt{\frac{\mu_0}{\varepsilon_0}} H_\phi = \hat{\theta}\sqrt{\frac{\mu_0}{\varepsilon_0}} j \frac{H_0}{r} e^{-jkr} \sin\theta \cos[2\pi \sin\theta \cos\phi] e^{-j2\pi \sin\theta \cos\phi}$

(b) $P_r = 1000 \left(\frac{0.3}{4\pi 1000}\right)^2 10 \cdot 5 = 28.5 \times 10^{-6}\,\text{W}$

P2.5.15

(a) The eight-element linear array can be generated by the convolution of the unit and the group consisting of two dipoles separated by distance 2λ. The unit is a four dipole array with separations of $\lambda/2$. The resultant radiation pattern is the product of the unit pattern and the group pattern, which has two maxima at $\psi_{max} = \pm 90°$ and fourteen nulls at $\psi = 0, \pm 41.4°, \pm 60°, \pm 75.5°, \pm 104.5°, \pm 120°, \pm 138.6°, 180°$.

(b) The unit is a two dipole array with separation of λ along x-axis. The group consists two dipoles separated by distance $\lambda/2$ and located along y-axis. The resultant pattern has two maxima at $\psi_{max} = 0, 180°$ and six nulls at $\psi = \pm 60°, \pm 90°, \pm 120°$. The sidelobes between $60°$ and $90°$, $90°$ and $120°$, $-90°$ and $-60°$, $-90°$ and $-120°$ are small.

P2.5.16

(a) When $d = 0$, the (image) dipoles cancel with each other.

(b) $E \sim \sin\theta \cdot \sin(kd\sin\theta)$. At $\theta = 90°$, $|E| = |E|_{max} \Rightarrow kd = n\pi + \frac{\pi}{2}$.

   (i) $kd\sin\theta_o = \pi \Rightarrow \theta_o = \sin^{-1}\frac{2}{2n+1} = \sin^{-1}\frac{2}{3}$ ($n = 1$).

   (ii) $n = 1 \Rightarrow kd = \frac{3\pi}{2} \Rightarrow d = \frac{3}{4}\lambda$.

(c) $kd = n\pi \Rightarrow d = \frac{n}{2}\lambda$ ($n = 0, 1, 2, \cdots$).

(d) The fields in region $z < 0$ and $x < 0$ are zero.

P2.5.17

$$\overline{E}(\overline{r}) = \hat{\theta}j\omega\mu\frac{Il}{2\pi r}e^{-jkr+j\pi\sin\theta\cos\phi+j\frac{\psi}{2}}\sin\theta\cos\left[\pi\sin\theta\cos\phi + \frac{\psi}{2}\right]$$

P2.5.18

(a) $\overline{E} = \hat{\theta}\frac{\omega\mu I_1 d}{2\pi r}e^{-jkr+j\pi\sin\theta\cos\phi}\sin\theta\sin[\pi\sin\theta\cos\phi]$

(b) $<\overline{S}> = \frac{1}{2}\text{Re}\left\{\overline{E}\times\overline{H}^*\right\} = \hat{r}\frac{1}{2}\eta\left|\frac{kI_1 d}{2\pi r}\right|^2\sin^2\theta\sin^2[\pi\sin\theta\cos\phi]$

   $\pi\sin\theta\cos\phi = \frac{\pi}{2} \qquad \Rightarrow \qquad \phi = \cos^{-1}\left(\frac{1}{2\sin\theta}\right)$

(c) $\phi = \pi/3$.

P2.5.19

$$A_{rec} = \frac{\lambda^2}{4\pi}G_{rec}, \quad (P_{rec})_{MAX} = A_{rec}S_{inc}, \quad S_{inc} = \frac{P_{rad}G_{rad}}{4\pi r^2}$$

$$P_{rec} = \frac{\lambda^2}{4\pi}G_{rec}G_{rad}\frac{P_{rad}}{4\pi r^2} = \left(\frac{3\times10^8}{537.25\times10^6}\right)^2\frac{(3\times10)(5\times10^6)}{(16)(\pi^2)(1.6\times10^3)^2} = 0.116\,\text{w}$$

3

MEDIA

3.1 Time-Harmonic Fields

    A. Continuous Monochromatic Waves

    B. Polarization of Monochromatic Waves

    C. Time-Average Poynting Power Vector

    D. Waves in Conducting Media

    E. Waves in Plasma Media

    F. Dispersive Media

    G. Field Energy in Dispersive Media

3.2 Bianisotropic Media

    A. Anisotropic Media

    B. Biisotropic Media

    C. Bianisotropic Media

    D. Symmetry Conditions for Lossless Media

    E. Reciprocity Conditions

    F. Causality Relations

3.3 kDB System for Waves in Media

    A. Wave Vector $\overline{k}$

    B. kDB System

    C. Maxwell Equations in kDB System

    D. Waves in Isotropic Media

    E. Waves in Uniaxial Media

F. Waves in Gyrotropic Media

G. Waves in Bianisotropic Media

H. Waves in Nonlinear Media

Answers

3.1   Time-Harmonic Fields

A. Continuous Monochromatic Waves

For electromagnetic waves of a particular frequency in the steady state, the fields are time-harmonic and are known as monochromatic waves or continuous waves (CW). The CW cases are important for three reasons: (i) the CW assumption can be used to eliminate the time dependence in the Maxwell equations and thus considerably simplify the mathematics; (ii) once the CW case is solved and a sound understanding is developed for the frequency-domain phenomena, Fourier theory can be applied to study the time-domain phenomena; (iii) CW representation covers the whole spectrum of electromagnetic waves. Clearly, a thorough understanding of CW or the time-harmonic case is essential in the study of all electromagnetic wave phenomena.

In general, for a time-harmonic field with angular frequency ω, we let

$$\overline{E}(\overline{r}, t) = \text{Re}\{\overline{E}(\overline{r})\, e^{-i\omega t}\} \tag{3.1.1}$$

where Re denotes the real part of a complex quantity, $\overline{E}(\overline{r})$ is a complex vector, and $e^{-i\omega t}$ is the time convention used to denote the time harmonic dependence.

The complex electric field vector $\overline{E}(\overline{r})$ is a function of position only and independent of time. In this book we do not use different symbols to distinguish real quantities such as $\overline{E}(\overline{r}, t)$ in the time domain and complex quantities such as $\overline{E}(\overline{r})$ in the frequency domain. Their meanings should be clear from the context. In case of possible ambiguity, we shall explicitly indicate the complex field quantities to be functions of $\overline{r}$ only and the real time-domain fields to be functions of both $\overline{r}$ and t.

Similar definitions apply to other field quantities with $\overline{E}$ replaced by $\overline{B}$, $\overline{D}$, $\overline{H}$, $\overline{J}$, and ρ in (3.1.1).

$$\overline{B}(\overline{r}, t) = \text{Re}\{\overline{B}(\overline{r})\, e^{-i\omega t}\} \tag{3.1.2}$$

$$\overline{D}(\overline{r}, t) = \text{Re}\{\overline{D}(\overline{r})\, e^{-i\omega t}\} \tag{3.1.3}$$

$$\overline{H}(\overline{r}, t) = \text{Re}\{\overline{H}(\overline{r})\, e^{-i\omega t}\} \tag{3.1.4}$$

$$\overline{J}(\overline{r}, t) = \text{Re}\{\overline{J}(\overline{r})\, e^{-i\omega t}\} \tag{3.1.5}$$

$$\rho(\overline{r}, t) = \text{Re}\{\rho(\overline{r})\, e^{-i\omega t}\} \tag{3.1.6}$$

Substituting $\overline{E}(\overline{r}, t)$ and $\overline{B}(\overline{r}, t)$ in Faraday's law

$$\nabla \times \overline{E}\,(\overline{r}, t) = -\frac{\partial}{\partial t}\,\overline{B}\,(\overline{r}, t) \qquad (3.1.7)$$

we obtain

$$\mathrm{Re}\left\{[\nabla \times \overline{E}(\overline{r}) - i\omega\overline{B}(\overline{r})]e^{-i\omega t}\right\} = 0 \qquad (3.1.8)$$

This equation is true *for all time t.*

Note: When the real part of the complex quantity in the square brackets multiplied by all values of $e^{-i\omega t}$ is equal to zero, the complex quantity itself must be equal to zero. Consider $\mathrm{Re}\{Ce^{-i\omega t}\} = 0$ where $C = C_R + iC_I$ denotes the complex quantity with both C_R and C_I real. Show that $C_R = 0$ by letting $\omega t = 0$, and $C_I = 0$ by letting $\omega t = \pi/2$.

We find from (3.1.8) that Faraday's law for time-harmonic fields becomes

$$\nabla \times \overline{E}(\overline{r}) - i\omega\overline{B}(\overline{r}) = 0 \qquad (3.1.9)$$

Similar arguments apply to other Maxwell equations and we find that they become, if we omit writing the argument $\overline{r}$,

$$\nabla \times \overline{E} = i\omega\overline{B} \qquad (3.1.10)$$

$$\nabla \times \overline{H} = -i\omega\overline{D} + \overline{J} \qquad (3.1.11)$$

$$\nabla \cdot \overline{B} = 0 \qquad (3.1.12)$$

$$\nabla \cdot \overline{D} = \rho \qquad (3.1.13)$$

This amounts to replacing time derivatives in all Maxwell's equations by $-i\omega t$ and treating all field quantities as complex.

We see that the Maxwell equations for time-harmonic fields no longer have time dependence, thus mathematically reduced the four independent variables x, y, z, t to x, y, z. The electromagnetic field quantities are now dependent on space only. However all field quantities are now complex. To recover the real space-time dependent field vector, we simply multiply the complex quantity by $e^{-i\omega t}$ and take its real part as shown in (3.1.1).

B. Polarization of Monochromatic Waves

Considering the time evolution of $\overline{E}(r,t)$ at $r = 0$ by letting

$$\overline{E} = \overline{E}_R + i\overline{E}_I \qquad (3.1.14)$$

The plane defined by the two vectors $\overline{E}_R$ and $\overline{E}_I$ is called the polarization plane. For the time dependent electric field vector, we find from (3.1.1)

$$\overline{E}(t) = \mathrm{Re}\{(\overline{E}_R + i\overline{E}_I)e^{-i\omega t}\} = \overline{E}_R \cos \omega t + \overline{E}_I \sin \omega t \qquad (3.1.15)$$

In Figure 3.1.1 we sketch the two vectors $\overline{E}_R$ and $\overline{E}_I$. At $t = 0$, $\overline{E}(t)$ coincides with $\overline{E}_R$. At $\omega t = \pi/2$, $\overline{E}(t)$ coincides with $\overline{E}_I$. The tip of $\overline{E}$ as a function of time traces out an ellipse. When $\overline{E}_R$ is perpendicular to $\overline{E}_I$, one represents the major axis and the other the minor axis of the ellipse.

The time derivative of $\overline{E}(t)$ gives

$$\frac{\partial \overline{E}(t)}{\partial t} = \omega[-\overline{E}_R \sin \omega t + \overline{E}_I \cos \omega t\,]$$

At $t = 0$, the time rate of change of the electric field vector is in the direction of $\overline{E}_I$. As $\omega t = \pi/2$, the time rate of change of $\overline{E}$ is in the opposite direction of $\overline{E}_R$. Thus as time increases, the vector $\overline{E}$ moves from $\overline{E}_R$ to $\overline{E}_I$.
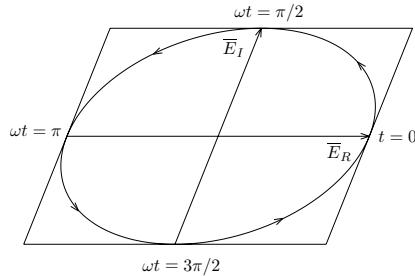
Figure 3.1.1 The polarization plane.

When $\overline{E}_R$ and $\overline{E}_I$ are parallel or anti-parallel to each other, the total electric field vector represents a linearly polarized wave. For an electromagnetic wave propagating out of the paper in the direction of the thumb, the motion of the tip of $\overline{E}(\overline{r},t)$ follows the right-hand finger. The wave is right-hand elliptically polarized. When $\overline{E}_R$ and $\overline{E}_I$ are perpendicular to each other and have the same magnitudes, the wave will be circularly polarized.

C. Time-Average Poynting Power Vector

The complex Poynting's theorem is derived by dot-multiplying (3.1.10) by $\overline{H}^*$ and subtracting the complex conjugate of (3.1.11) dot multiplied by $\overline{E}$. Making use of the identity $\overline{H}^* \cdot \nabla \times \overline{E} - \overline{E} \cdot \nabla \times \overline{H}^* = \nabla \cdot (\overline{E} \times \overline{H}^*)$, we obtain

$$\nabla \cdot (\overline{E} \times \overline{H}^*) = i\omega \left[\overline{H}^* \cdot \overline{B} - \overline{E} \cdot \overline{D}^* \right] - \overline{E} \cdot \overline{J}^* \qquad (3.1.16)$$

The complex Poynting's vector $\overline{S}$ is defined to be

$$\overline{S} = \overline{E} \times \overline{H}^* \qquad (3.1.17)$$

However, it is noted that, mathematically, $\overline{E} \times \overline{H}^*$ is not a uniquely defined quantity as far as Poynting's theorem is concerned. An arbitrary curl field $\nabla \times \overline{A}$ can be added to $\overline{E} \times \overline{H}^*$ without changing (3.1.16). Physically the complex vector $\overline{S}$ as defined in (3.1.17) has been identified as a complex power density vector.

   The term $\overline{E} \cdot \overline{J}^* = \overline{E} \cdot (\overline{J}_c^* + \overline{J}_f^*)$ in (3.1.16) consists of two parts: one part due to the ohmic current $\overline{J}_c$ and the other due to the free current $\overline{J}_f$. Equation (3.1.16) can be rearranged to read

$$-\overline{E} \cdot \overline{J}_f^* = \nabla \cdot (\overline{E} \times \overline{H}^*) + \overline{E} \cdot \overline{J}_c^* + i\omega (\overline{E} \cdot \overline{D}^* - \overline{B} \cdot \overline{H}^*) \qquad (3.1.18)$$

Consider a small volume element V. Equation (3.1.18) states that the complex power supplied to V by $\overline{J}_f$, $-\overline{E} \cdot \overline{J}_f^*$, is equal to the divergence of the complex Poynting power flow out of V, $\nabla \cdot (\overline{E} \times \overline{H}^*)$, plus the complex power dissipated in V, $\overline{E} \cdot \overline{J}_c^*$, plus the last term related to the stored complex electromagnetic energy in V.

   While the instantaneous value of the field vectors can be immediately determined from (3.1.1), the instantaneous value of the Poynting power density vector cannot be determined from the same rule; the power flow vector $\overline{S}$ involves the product of two field vectors. For more insight into this issue, we let a complex field vector be represented by two real vectors. We write

$$\overline{E}(\overline{r}) = \overline{E}_R(\overline{r}) + i\overline{E}_I(\overline{r}) \qquad (3.1.19)$$

where $\overline{E}_R$ and $\overline{E}_I$ are both real vectors representing the real and imaginary parts of the complex vector $\overline{E}$. Similarly,

$$\overline{H}(\overline{r}) = \overline{H}_R(\overline{r}) + i\overline{H}_I(\overline{r}) \qquad (3.1.20)$$

The instantaneous values for the field vectors are

$$\overline{E}(\overline{r},t) = \mathrm{Re}\{\overline{E}(\overline{r})e^{-i\omega t}\} = \overline{E}_R \cos\omega t + \overline{E}_I \sin\omega t \qquad (3.1.21)$$

and

$$\overline{H}(\overline{r},t) = \overline{H}_R \cos\omega t + \overline{H}_I \sin\omega t \qquad (3.1.22)$$

The complex Poynting's vector is

$$\overline{S} = \overline{E} \times \overline{H}^* = \overline{E}_R \times \overline{H}_R + \overline{E}_I \times \overline{H}_I + i(\overline{E}_I \times \overline{H}_R - \overline{E}_R \times \overline{H}_I) \quad (3.1.23)$$

We define the instantaneous Poynting's vector $\overline{S}(\overline{r},t)$ as

$$\overline{S}(\overline{r},t) = \overline{E}(\overline{r},t) \times \overline{H}(\overline{r},t) \qquad (3.1.24)$$

In view of (3.1.21) and (3.1.22), we have

$$\overline{S}(\overline{r},t) = \overline{E}_R \times \overline{H}_R \cos^2\omega t + \overline{E}_I \times \overline{H}_I \sin^2\omega t$$
$$+ (\overline{E}_R \times \overline{H}_I + \overline{E}_I \times \overline{H}_R)\sin\omega t \cos\omega t \quad (3.1.25)$$

Clearly (3.1.25) is not related to (3.1.23) in any way by the rule for field vectors as shown in (3.1.1). The instantaneous Poynting's vector $\overline{S}(\overline{r},t)$ is a real vector and is time-dependent. To relate $\overline{S}(\overline{r})$ to $\overline{S}(\overline{r},t)$ we must eliminate the time dependence in $\overline{S}(\overline{r},t)$. This is accomplished by a time averaging process. We find

$$<\overline{S}(\overline{r},t)> = \frac{1}{2\pi} \int_0^{2\pi} d(\omega t)\, \overline{S}(\overline{r},t)$$
$$= \frac{1}{2} \left[\overline{E}_R \times \overline{H}_R + \overline{E}_I \times \overline{H}_I \right]$$
$$= \frac{1}{2}\mathrm{Re}\left\{ \overline{S}(\overline{r}) \right\} \qquad (3.1.26)$$

where the first equality defines the time average of $\overline{S}(\overline{r},t)$, the second equality follows from (3.1.25), and the last equality follows from (3.1.23). Thus, when the complex Poynting's power vector $\overline{S} = \overline{E} \times \overline{H}^*$ is known, taking half of its real part yields the time average value of the instantaneous Poynting's vector:

$$<\overline{E}(\overline{r},t) \times \overline{H}(\overline{r},t)> = \frac{1}{2}\mathrm{Re}\left\{ \overline{E} \times \overline{H}^* \right\} \qquad (3.1.27)$$

This rule, in general, applies to the product of any two field quantities. That is, the time average of the product of two field quantities is equal to half of the real part of the product of one complex field quantity and the complex conjugate of the other complex field quantity.

D. Waves in Conducting Media

Under the time harmonic representation, constitutive elements describing material media are, in general, complex. Consider a conducting medium governed by Ohm's law

$$\overline{J}_c = \sigma \overline{E}$$

From the Maxwell equation

$$\nabla \times \overline{H} = -i\omega \overline{D} + \overline{J}_c + \overline{J}_f \qquad (3.1.28)$$

where $\overline{J}_f$ represents the source, we can absorb $\overline{J}_c$ in $\overline{D}$ by noting that $\overline{D} = \epsilon \overline{E}$. We find

$$\nabla \times \overline{H} = -i\omega \left[\epsilon + \frac{i}{\omega} \sigma \right] \overline{E} + \overline{J}_f$$

Thus we define a new permittivity

$$\epsilon_c = \epsilon + i\frac{\sigma}{\omega} \qquad (3.1.29)$$

which is complex and accounts for the conductivity of the medium. When both ϵ and σ are real, the conductivity σ then constitutes the imaginary part of a complex permittivity $\epsilon + i\sigma/\omega$.

The Maxwell equations for the conducting medium in source-free regions with $\overline{J}_f = \rho = 0$ are simply

$$\nabla \times \overline{H} = -i\omega\epsilon_c \overline{E} \qquad (3.1.30)$$

$$\nabla \times \overline{E} = i\omega\mu \overline{H} \qquad (3.1.31)$$

$$\nabla \cdot \overline{H} = 0 \qquad (3.1.32)$$

$$\nabla \cdot \overline{E} = 0 \qquad (3.1.33)$$

The wave equation for $\overline{E}$ is

$$\left(\nabla^2 + \omega^2 \mu\epsilon_c \right) \overline{E} = 0 \qquad (3.1.34)$$

Wave solution $\overline{E} = \hat{x}E_x = \hat{x}E_0 e^{ikz}$ has the dispersion relation

$$k^2 = \omega^2 \mu\epsilon_c = \omega^2 \mu \left(\epsilon + i\frac{\sigma}{\omega} \right) \qquad (3.1.35)$$

as seen from (3.1.29). The spatial frequency k is now complex, we find

$$k = \omega\sqrt{\mu\epsilon} \left[1 + i\frac{\sigma}{\omega\epsilon} \right]^{1/2} = k_R + ik_I \qquad (3.1.36)$$

The solution for a wave propagating in the $\hat{z}$ directions is

$$\overline{E} = \hat{x}E_0 e^{ikz} = \hat{x}E_0 e^{-k_I z + ik_R z} \qquad (3.1.37)$$

which attenuates exponentially in the direction of propagation.

Penetration Depth in Conducting Media

The solution of the electromagnetic fields in a conducting medium is

$$
\begin{cases}
\overline{E} = \hat{x} E_0 e^{-k_I z + i k_R z} \\[2mm]
\overline{H} = \hat{y} \dfrac{(k_R + i k_I)}{\omega \mu} E_0 e^{-k_I z + i k_R z} \\[2mm]
\overline{S} = \hat{z} \dfrac{(k_R - i k_I)}{\omega \mu} |E_0|^2 e^{-2 k_I z} \\[2mm]
< \overline{S} > = \hat{z} \dfrac{k_R}{2 \omega \mu} |E_0|^2 e^{-2 k_I z}
\end{cases}
\tag{3.1.38}
$$

The electric field in time-domain is

$$
\begin{aligned}
\overline{E}(z,t) = \hat{x} E_x(z,t) &= \mathrm{Re}[\hat{x} E_0 e^{-k_I z + i k_R z} e^{-i \omega t}] \\
&= \hat{x} E_0 e^{-k_I z} \cos(k_R z - \omega t)
\end{aligned}
\tag{3.1.39}
$$

The wave propagates and attenuates in the $\hat{z}$ direction. The spatial variation of $E_x(z,t)$ in (3.1.39) is illustrated in Fig. 3.1.2.
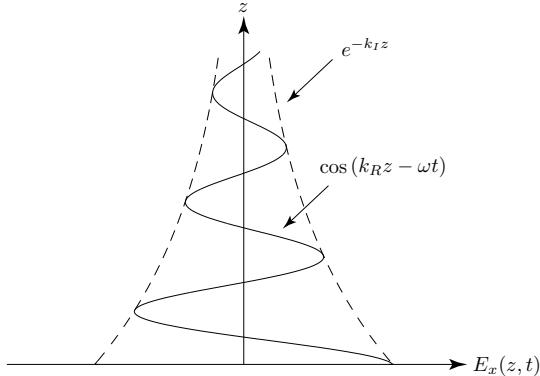
Figure 3.1.2 Wave in dissipative medium at $t = 0$.

The penetration depth is defined as

$$
d_p = \frac{1}{k_I}
\tag{3.1.40}
$$

such that the wave amplitude attenuates by a factor of e^{-1} in a distance d_p. We now consider the two limiting cases of very high conductivity and very small conductivity.

For a highly conducting medium with $1 \ll \sigma/\omega\epsilon$, we approximate

$$k = k_R + ik_I \approx \omega\sqrt{\mu\epsilon}\left[i\frac{\sigma}{\omega\epsilon}\right]^{1/2} = \sqrt{\frac{\omega\mu\sigma}{2}}(1+i) \qquad (3.1.41)$$

We find the penetration depth

$$d_p = \sqrt{\frac{2}{\omega\mu\sigma}} = \delta \qquad (3.1.42)$$

which is usually a very small number known as the *skin depth*.

For a slightly conducting medium with $\sigma/\omega\epsilon \ll 1$, we can approximate

$$k = k_R + ik_I \approx \omega\sqrt{\mu\epsilon}\left[1 + i\frac{\sigma}{2\omega\epsilon}\right] = \omega\sqrt{\mu\epsilon} + i\frac{\sigma}{2}\left(\frac{\mu}{\epsilon}\right)^{1/2} \qquad (3.1.43)$$

We find the penetration depth

$$d_p = \frac{2}{\sigma}\left(\frac{\epsilon}{\mu}\right)^{1/2} \qquad (3.1.44)$$

It is interesting to note that the penetration depth in (3.1.44) is independent of frequency. However, we have assumed a homogeneous medium here, at high frequencies there will be large attenuation due to scattering.

To find a general solution for k_R and k_I in (3.1.36), we obtain from the identity $\sqrt{1 + iA} = \sqrt{\frac{1}{2}(\sqrt{1+A^2}+1)} + i\sqrt{\frac{1}{2}(\sqrt{1+A^2}-1)}$,

$$k_R = \omega\sqrt{\mu\epsilon}\left[\frac{1}{2}\left(\sqrt{1 + \frac{\sigma^2}{\epsilon^2\omega^2}} + 1\right)\right]^{1/2} \qquad (3.1.45)$$

$$k_I = \omega\sqrt{\mu\epsilon}\left[\frac{1}{2}\left(\sqrt{1 + \frac{\sigma^2}{\epsilon^2\omega^2}} - 1\right)\right]^{1/2} \qquad (3.1.46)$$

which reduces to (3.1.41) in the case of highly conducting medium and reduces to (3.1.43) in the case of slightly conducting medium.

E. Waves in Plasma Media

Consider a plasma medium, which is a neutral ionized gas consisting of free electrons and positive ions. Since the ions are much heavier than the electrons, we assume that only the interaction between the free electrons and electromagnetic waves need be considered. Let the electron plasma comprising electrons with density N, electron mass 9.1×10^{-31} kg, and electron charge $q = -1.6 \times 10^{-19}$ coul. We can derive a constitutive relation for the plasma medium by finding the polarization vector $\overline{P} = Nq\overline{r}$ where N is the number of electrons/m^3.

Under an applied electromagnetic wave field, an electron is subject to the Lorentz force $\overline{f} = q(\overline{E} + \overline{v} \times \overline{B}) \approx q\overline{E}$. The second term is negligible for $v/c \ll 1$, as $|\overline{B}| = |\overline{E}|/c$ for a plane wave in free space, and $|\overline{v} \times \overline{B}| \approx (v/c)|\overline{E}| \ll |\overline{E}|$, although $\overline{v} \times \overline{B}$ and $\overline{E}$ are in different directions. From Newton's second law, we have

$$q\overline{E} \approx \overline{f} = \frac{d}{dt}(m\overline{v}) = m\frac{d^2}{dt^2}\overline{r} = -m\omega^2\overline{r}$$

which gives the polarization vector

$$\overline{P} = Nq\overline{r} = -\frac{Nq^2}{m\omega^2}\overline{E}$$

From the source-free Maxwell equation

$$\nabla \times \overline{H} = -i\omega\overline{D} = -i\omega(\epsilon_o\overline{E} + \overline{P}) = -i\omega\epsilon_o\left(1 - \frac{Nq^2}{m\epsilon_o\omega^2}\right)\overline{E}$$

we find the permittivity for the plasma medium

$$\epsilon_p(\omega) = \epsilon_0\left[1 - \frac{\omega_p^2}{\omega^2}\right] \tag{3.1.47}$$

and the plasma frequency ω_p is defined to be

$$\omega_p = \sqrt{\frac{Nq^2}{m\epsilon_0}} \approx 56.4\sqrt{N} \tag{3.1.48}$$

Equation (3.1.47) explicitly displays the frequency dependence of the permittivity ϵ_p. It is noted that ϵ_p is always less than ϵ_o.

The wave equation for $\overline{E}$ is

$$\left(\nabla^2 + \omega^2 \mu \epsilon_p\right) \overline{E} = 0 \qquad (3.1.49)$$

with the dispersion relation

$$k^2 = \omega^2 \mu_o \epsilon_o \left(1 - \frac{\omega_p^2}{\omega^2}\right) \qquad (3.1.50)$$

For $\omega > \omega_p$, the solution of a plane wave propagating in the $\hat{z}$ direction is

$$\begin{cases} k = \dfrac{\omega}{c}\sqrt{1 - \dfrac{\omega_p^2}{\omega^2}} \\[2ex] \overline{E} = \hat{x} E_0 e^{ikz} \\[2ex] \overline{H} = \hat{y}\dfrac{k}{\omega\mu} E_0 e^{ikz} \\[2ex] \overline{S} = \hat{z}\dfrac{k}{\omega\mu}|E_0| \\[2ex] <\overline{S}> = \hat{z}\dfrac{k}{2\omega\mu}|E_0|^2 \end{cases} \qquad (3.1.51)$$

For $\omega < \omega_p$, k is imaginary. The solution (3.1.51) becomes

$$\begin{cases} k = ik_I = i\dfrac{\omega}{c}\sqrt{\dfrac{\omega_p^2}{\omega^2} - 1} \\[2ex] \overline{E} = \hat{x} E_0 e^{-k_I z} \\[2ex] \overline{H} = \hat{y}\dfrac{ik_I}{\omega\mu} E_0 e^{-k_I z} \\[2ex] \overline{S} = \hat{z}\dfrac{-ik_I}{\omega\mu}|E_0|e^{-2k_I z} \\[2ex] <\overline{S}> = 0 \end{cases} \qquad (3.1.52)$$

This result of zero time-average power is significant. The wave that attenuates exponentially in the $\hat{z}$ direction and transmits no time-average power is called an *evanescent wave*.

Phase and Group Velocities

In a dispersive medium, the spatial frequency k is a nonlinear function of the temporal frequency ω. A plasma medium is a dispersive medium with the dispersion relation

$$k(\omega) = \frac{\omega}{c}\sqrt{1 - \frac{\omega_p^2}{\omega^2}}$$

when $\omega > \omega_p$. In a dispersive medium, consider a field composed of two waves with slightly separated temporal frequencies $\omega_1 = \omega_o + \delta\omega$ and $\omega_2 = \omega_o - \delta\omega$. The corresponding spatial frequencies are $k_1 = k_o + \delta k$ and $k_2 = k_o - \delta k$. We write

$$E_x(z,t) = \cos(k_1 z - \omega_1 t) + \cos(k_2 z - \omega_2 t)$$

$$= 2\cos\left(\frac{k_1 + k_2}{2}z - \frac{\omega_1 + \omega_2}{2}t\right)\cos(\delta k z - \delta\omega t)$$

$$= 2\cos(k_o z - \omega_o t)\cos(\delta k z - \delta\omega t)$$
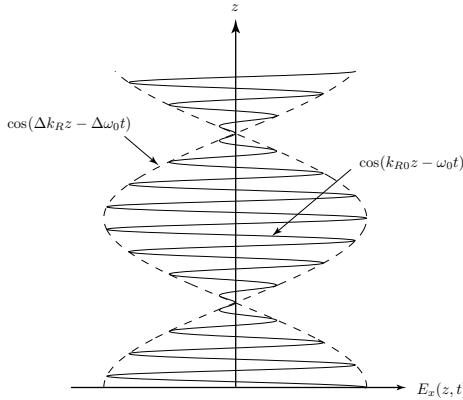
Figure 3.1.3 Wave in dispersive medium at $t = 0$.

where we used the identity $\cos A + \cos B = 2\cos\frac{A+B}{2}\cos\frac{A-B}{2}$. In Fig. 3.1.3, we plot $E_x(z,t)$, which shows a propagating wave $\cos(kz - \omega t)$ with a modulated amplitude $\cos(\delta k z - \delta\omega t)$. The modulated amplitude propagates with the group velocity $v_g = \delta\omega/\delta k$. The carrier $\cos(kz - \omega t)$ propagates with the phase velocity $v_p = \omega/k$. In general, for a narrow-band signal, the group velocity is defined as $v_g = 1/(\partial k/\partial\omega)$.

EXAMPLE 3.1.1

Consider a narrow-band signal propagating in a plasma medium with dispersion relation

$$k(\omega) = \sqrt{\mu_o \epsilon_o (\omega^2 - \omega_p^2)}$$

In Fig. E3.1.1.1, we plot the ω-k diagram for the plasma medium. The phase velocity is found to be

$$v_p = \frac{\omega}{k} = \frac{c}{\sqrt{1 - \omega_p^2/\omega^2}}$$
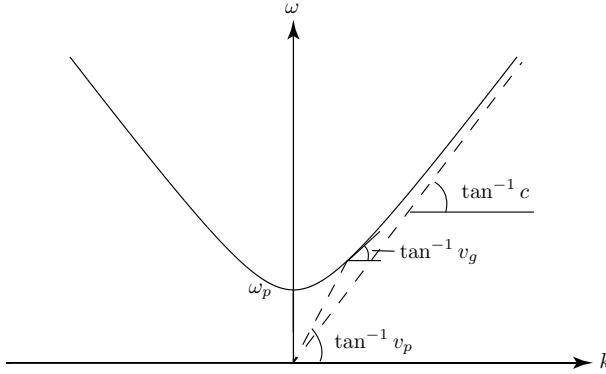
Figure E3.1.1.1 Dispersion relation for plasma media.

which corresponds to the slope of a line from the origin to the dispersion curve. The group velocity is

$$v_g = \frac{1}{\partial k/\partial \omega} = c\sqrt{1 - \omega_p^2/\omega^2}$$

which corresponds to the tangent to the dispersion curve. Notice that $v_g v_p = c^2$. Thus, while the signal propagates with the group velocity which is always smaller than the velocity of light, the phase velocity is larger than the velocity of light.

— END OF EXAMPLE 3.1.1 —

EXAMPLE 3.1.2

The source waveform is a sinusoidally modulated sine wave:

$$E_s(t) = \cos \omega_M t \sin \omega_C t$$

with $\omega_M \ll \omega_C$ at $z = 0$ propagates in the $+\hat{z}$ direction inside a plasma medium with the dispersion relation $k^2 = (\omega^2 - \omega_p^2)/c^2$.

(a) Use the appropriate trigonometric identity to write $E_s(t)$ as a sum of sinusoidally varying signals. What is $E(z, t)$ for $z > 0$? Write the expression for $E(z, t)$ as a product of sinusoids.

(b) If $\omega_M = 0.1\omega_C$, and $\omega_C = \sqrt{2}\omega_0$, sketch the wave form $E(z, t)$ vs. z for several values of the time t. With what speed does the modulation envelope move?

SOLUTION:

(a) $E_s(z = 0, t) = \cos \omega_M t \sin \omega_C t = \frac{1}{2}\left[\sin(\omega_C + \omega_M)t + \sin(\omega_C - \omega_M)t\right]$.

Define $\omega_1 = \omega_C + \omega_M$, $\omega_2 = \omega_C - \omega_M$. Then

$$E(z, t) = \frac{1}{2}\left[\sin(\omega_1 t - k_1 z) + \sin(\omega_2 t - k_2 z)\right]$$

$$= \cos\frac{1}{2}\left[(\omega_1 - \omega_2)t - (k_1 - k_2)z\right] \sin\frac{1}{2}\left[(\omega_1 + \omega_2)t - (k_1 + k_2)z\right]$$

$$= \cos\left[\omega_M t - \frac{(k_1 - k_2)}{2}z\right] \sin\left[\omega_c t - \frac{(k_1 + k_2)}{2}z\right]$$

$$= \cos\omega_M\left[t - \frac{\Delta k}{\Delta\omega}z\right] \sin\omega_c\left[t - \frac{k_o}{\omega_c}z\right]$$

where $\omega_1 - \omega_2 = 2\omega_M \equiv \Delta\omega$, $k_1 - k_2 \equiv \Delta k$, $k_1 + k_2 \equiv 2k_o$, and $\omega_1 + \omega_2 = 2\omega_c$.

(b)

$$\omega_M = 0.1\,\omega_c \qquad\qquad \omega_p = \frac{1}{\sqrt{2}}\,\omega_c$$

$$\omega_1 = \omega_c + \omega_M = 1.1\,\omega_c \qquad \omega_2 = \omega_c - \omega_M = 0.9\,\omega_c$$

$$k_1^2 = \frac{[(1.1)^2 - 0.5]\omega_c^2}{c^2} \cong (0.84)^2\frac{\omega_c^2}{c^2} \qquad k_2^2 = \frac{[(0.9)^2 - 0.5]\omega_c^2}{c^2} \cong (0.56)^2\frac{\omega_c^2}{c^2}$$

$$k_o = \frac{1}{2}(k_1 + k_2) = \frac{1}{2}(0.84 + 0.56)\frac{\omega_c}{c} \cong \frac{1}{\sqrt{2}}\frac{\omega_c}{c}$$

$$\Delta k = k_1 - k_2 = (0.84 - 0.56)\frac{\omega_c}{c} = 0.28\frac{\omega_c}{c}$$

$$\Delta\omega = \omega_1 - \omega_2 = 0.2\omega_c$$

Thus

$$E(z, t) = \cos\left[\omega_M\left(t - \frac{\sqrt{2}}{c}z\right)\right] \sin\left[\omega_c\left(t - \frac{1}{\sqrt{2}c}z\right)\right]$$

$$\text{At} \quad t = 0, \quad E(z,t) = -\cos\left[\frac{\omega_c}{10}(\frac{\sqrt{2}}{c}z)\right]\sin\left[\omega_c\frac{1}{\sqrt{2}c}z\right]$$

$$\text{At} \quad t = \frac{2\pi}{\omega_c}, \quad E(z,t) = -\cos\left[\frac{\omega_c}{10}(t - \frac{\sqrt{2}}{c}z)\right]\sin\left[\omega_c\frac{1}{\sqrt{2}c}z\right]$$

$$\text{At} \quad t = \frac{5\pi}{\omega_c}, \quad E(z,t) = \cos\left[\frac{\omega_c}{10}(t - \frac{\sqrt{2}}{c}z)\right]\sin\left[\omega_c\frac{1}{\sqrt{2}c}z\right]$$
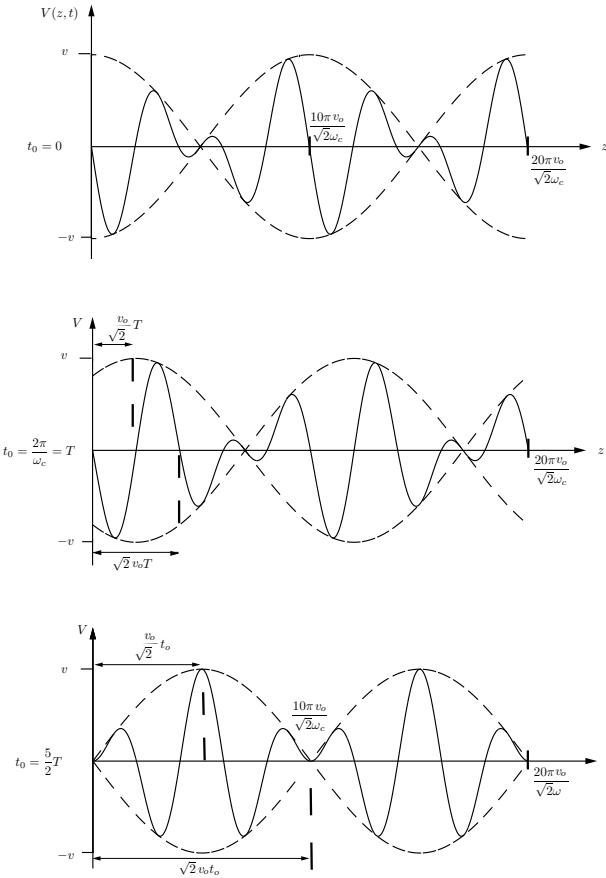
Figure E3.1.2.1

The modulation envelope moves with the speed $v_g \equiv \frac{c}{\sqrt{2}}$ whereas the carrier wave moves with the speed $v_{ph} \equiv \sqrt{2}c$. Thus $v_{ph} = 2v_g$.

<div align="right">— END OF EXAMPLE 3.1.2 —</div>

EXAMPLE 3.1.3

Consider a group of plane waves with different angular frequencies propagating along the $\hat{z}$ direction in a dispersive medium. Assume that all angular frequencies are in the neighborhood of a center frequency ω_0. We can express the wavenumber k around ω_0,

$$k(\omega) = k(\omega_0) + (\omega - \omega_0) \left[\frac{\delta k(\omega)}{\delta \omega} \right]_{\omega = \omega_0}$$

$$+ \frac{1}{2}(\omega - \omega_0)^2 \left[\frac{\delta^2 k(\omega)}{\delta \omega^2} \right]_{\omega = \omega_0} + \cdots \tag{17}$$

For a narrow-band signal, we can retain only the first two terms. The space–time dependence of the group of plane waves becomes

$$e^{ik(\omega)z - i\omega t} = e^{ik(\omega_0)z - i\omega_0 t} e^{-i(\omega - \omega_0)\left\{ t - z \left[\frac{dk(\omega)}{d\omega} \right]_{\omega = \omega_0} \right\}}$$

which can be viewed as a wave propagating with phase delay $T_p = k/\omega_0$ and group delay $T_g = dk(\omega)/d\omega$.

We can construct a $\omega - k$ diagram, plotting ω as a function of k. Figure E3.1.1.1 shows the ω-k diagram for an isotropic plasma medium. The slope of the straight line from the origin to a point on the curve at $\omega = \omega_0$ then represents the phase velocity v_p, and the slope at $\omega = \omega_0$ represents the group velocity v_g. We find

$$v_p = \frac{1}{\sqrt{\mu_o \epsilon_o \left(1 - \omega_p^2/\omega^2 \right)}}$$

and

$$v_g = \frac{\sqrt{1 - \omega_p^2/\omega^2}}{\sqrt{\mu_o \epsilon_o}}$$

It is seen that v_p is larger than the velocity of light $c = (\mu_o \epsilon_o)^{-1/2}$ and that $v_p v_g = c^2$. For a nondispersive medium, the ω-k curves are straight lines starting from the origin, and the phase delay and the group delay are the same, as are the phase velocity and the group velocity.

— END OF EXAMPLE 3.1.3 —

F. Dispersive Media

Time dispersion is a common phenomenon for most media in the presence of time-varying fields. As an example, the permittivity of water drops from $80\epsilon_o$ to approximately $1.8\epsilon_o$ as the frequency increases from static to the optical range. The reason for this decrease is that the alignment of water molecules, which possess permanent dipole moments, is much more ineffective at optical frequencies than in slowly varying fields. In the same fashion, both conducting media and plasma medium are dispersive media as they are described by permittivities which are functions of frequency.

The equation of motion for a bounded electron under the action of an electric field is

$$q\overline{E} = m\left[\frac{d^2\overline{r}}{dt^2} + \gamma\frac{d\overline{r}}{dt} + \omega_o^2\overline{r}\right]$$

where γ is the damping constant which is small compared with the binding or resonant frequency ω_o. The polarization vector is then

$$\overline{P} = Nq\overline{r} = -\frac{Nq^2/m}{\omega^2 - \omega_o^2 + i\omega\gamma}\overline{E}$$

From the source-free Maxwell equation written as

$$\nabla \times \overline{H} = -i\omega(\epsilon_o\overline{E} + \overline{P}) = -i\omega\epsilon_d(\omega)\overline{E}$$

we determine the permittivity

$$\epsilon_d(\omega) = \epsilon_o\left[1 - \frac{\omega_p^2}{\omega^2 - \omega_o^2 + i\omega\gamma}\right] \qquad (3.1.53)$$

where $\omega_p^2 = Nq^2/m\epsilon_o$. In the high frequency limit $\omega \gg \omega_o$, the permittivity reduces to (3.1.47).

For conductors, $\omega_o = 0$, we have

$$\epsilon_d(\omega) = \epsilon_o\left[1 - \frac{\omega_p^2}{\omega^2 + i\omega\gamma}\right] \qquad (3.1.54)$$
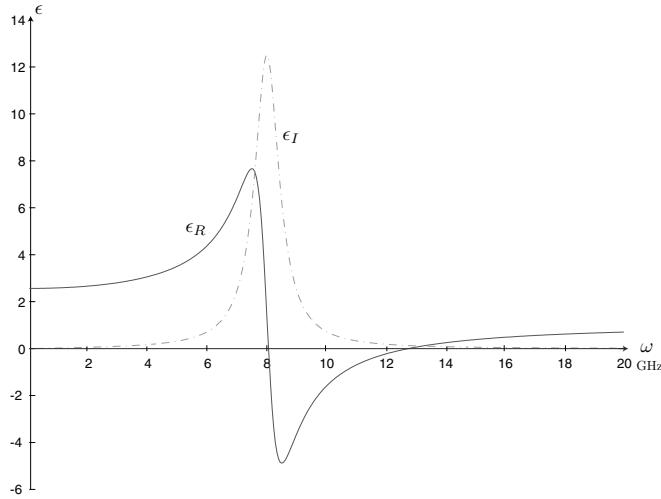
From (3.1.54), let $\epsilon_p = \epsilon_o(1 + i\sigma/\omega)$, we find that in the low frequency limit,

$$\sigma = \epsilon_o\frac{\omega_p^2}{\gamma - i\omega} \approx \epsilon_o\frac{\omega_p^2}{\gamma} = \frac{Nq^2}{m\gamma}$$

For copper, $\sigma \approx 7 \times 10^7$ mho, with $N = 8 \times 10^{28} \, \text{m}^{-3}$, we find $\gamma \approx 3.2 \times 10^{13}$ Hz. For an insulator, $\omega_o \neq 0$, the polarization vector at very low frequency is given by $\overline{P} = \epsilon_o \omega_p^2 \overline{E} / \omega_o^2 = N q^2 \overline{E} / m \omega_o^2$.

Normal dispersion is when $\epsilon_R = \text{Re}\,[\epsilon_d(\omega)]$ increases with ω. In the frequency range when $\epsilon_R = \text{Re}\,[\epsilon_d(\omega)]$ decreases with ω, it is called anomalous dispersion. Anomalous dispersion occurs in the neighborhood of resonant frequency $(\omega = \omega_o)$ when the imaginary part of ϵ_d is appreciable which causes power dissipation known as resonant absorption. From (3.1.53), we find

$$\epsilon_d(\omega) = \epsilon_R + i\epsilon_I$$
$$= \epsilon_o \left[1 - \frac{(\omega^2 - \omega_o^2)\omega_p^2}{(\omega^2 - \omega_o^2)^2 + (\omega\gamma)^2} \right] + i \frac{\omega\gamma\omega_p^2}{(\omega^2 - \omega_o^2)^2 + (\omega\gamma)^2} \quad (3.1.55)$$

Figure 3.1.4 Real and imaginary parts of permittivity,
$\omega_p = 10^{10}, \ \omega_e = 8 \times 10^9, \ \gamma_e = 10^9.$

To determine when $\epsilon_R \leq 0$, we find from (3.1.55)

$$(\omega^2 - \omega_o^2)^2 - (\omega^2 - \omega_o^2)(\omega_p^2 - \gamma^2) + \omega^2\gamma^2 \leq 0 \quad (3.1.56)$$

For $\gamma = 0$, we see that ϵ_R is negative when $\omega_0^2 \leq \omega^2 \leq \omega_0^2 + \omega_p^2$.

EXAMPLE 3.1.4

In studying the negative permeability of artificial metamaterial, O'Brian and Pendry [2002] proposed the model of a split ring resonator (Fig. E3.1.4.1). The fractional area occupied by rings of radius R is f. Let the applied magnetic field be H_0. Consider a two-dimensional configuration, a surface current $J_\phi = H_{ext} - H_{int}$ is induced. The macroscopic average magnetic field intensity $H_{ave} = H_{ext} = H_0 + f J_\phi$. Note that $f H_{int} + (1 - f) H_{ext} = H_0$. The effective permeability is thus

$$\mu_{eff} = \mu_o \frac{H_0}{H_{ext}} = \mu_o \frac{H_{ext} - f J_\phi}{H_{ext}} = \mu_o \left[1 - \frac{f J_\phi}{H_{ext}} \right] \qquad \text{(E3.1.4.1)}$$
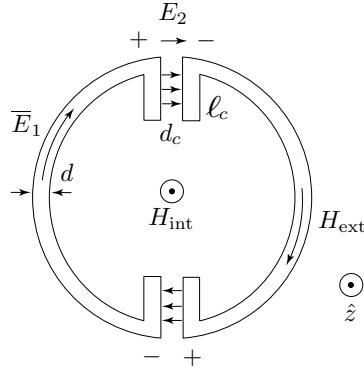
Figure E3.1.4.1 Split ring resonator.

Assuming perfect conduction with $E_1 = 0$, we find

$$2 d_c E_2 = V_\phi = \frac{d}{dt} \iint d\overline{S} \cdot \mu_o \overline{H}_{int} = -i\omega \mu_o \pi R^2 H_{int} = -i\omega L_g H_{int}$$

$$J_\phi = \ell_c \frac{d}{dt} D_{2\phi} = -i\omega \ell_c \epsilon_o E_2 = -i\omega C 2 d_c E_2$$

where $L_g = \mu_o \pi R^2$ and $C = \epsilon_o \ell_c / 2 d_c$. The effective permeability is determined to be

$$\mu_{eff} = \mu_o \left[1 - \frac{f J_\phi}{J_\phi + H_{int}} \right] = \mu_o \left[1 - \frac{f \omega^2}{\omega^2 - \omega_o^2} \right] \qquad \text{(E3.1.4.2)}$$

where $\omega_o^2 = 1/L_g C$. Within the frequency range $\omega_o^2 \le \omega^2 \le \omega_o^2 / (1 - f)$, it is seen that the effective permeability is negative.

— END OF EXAMPLE 3.1.4 —

EXAMPLE 3.1.5

Consider the split ring resonator in [Fig. E3.1.4.1]. When E_1 is not zero inside the metallic wire with very high conductivity whose permittivity is

$$\tilde{\epsilon} = \epsilon_o \left[1 - \frac{\omega_p^2}{\omega(\omega + i\gamma)} \right] \approx -\epsilon_o \left[\frac{\omega_p^2}{\omega(\omega + i\gamma)} \right]$$

We find

$$J_\phi = d\frac{d}{dt}D_{1\phi} = -i\omega d\tilde{\epsilon}E_1 \approx id\epsilon_o \left[\frac{\omega_p^2}{\omega + i\gamma} \right] E_1$$

$$J_\phi = \ell_c \frac{d}{dt}D_{2\phi} = -i\omega\ell_c\epsilon_o E_2$$

$$-i\omega\mu_o\pi R^2 H_{int} = 2\pi R E_1 + 2d_c E_2$$
$$= \left[-i\omega\frac{2\pi R}{d\epsilon_o\omega_p^2} + \gamma\frac{2\pi R}{d\epsilon_o\omega_p^2} + i\frac{2d_c}{\omega\ell_c\epsilon_o} \right] J_\phi = ZJ_\phi \quad \text{(E3.1.5.1)}$$

$$H_{ext} = J_\phi + \frac{i}{\omega L_g} \left[-i\omega L_i + \gamma L_i + \frac{i}{\omega C} \right] J_\phi = (1 + iZ/\omega L_g)J_\phi \quad \text{(E3.1.5.2)}$$

where $L_g = \mu_o\pi R^2$, $L_i = 2\pi R/\omega_p^2\epsilon_o d$, and $C = \epsilon_o\ell_c/2d_c$. The impedance $Z = -i\omega L_i + \gamma L_i + i/\omega C$ represents a series of inductance, resistance, and capacitance.

Eq. (E3.1.4.2) gives

$$\mu_{eff} = \mu_o \left[1 - \frac{f}{1 + iZ/\omega L_g} \right] = \mu_o \left[1 - \frac{f\omega^2 L_g/(L_g + L_i)}{\omega^2 - \omega_o^2 + i\omega\Gamma} \right]$$

where $\Gamma = \gamma L_i/(L_g + L_i)$ and $\omega_o^2 = 1/(L_g + L_i)C$. For perfect conductors, $\Gamma = 0$, and we have

$$\frac{\mu_{eff}}{\mu_o} = 1 - f\frac{\omega^2 L_g/(L_g + L_i)}{\omega^2 - \omega_o^2} = \frac{\omega^2 - \omega_o^2 - f\omega^2 L_g/(L_g + L_i)}{\omega^2 - \omega_o^2}$$

It is seen that within the frequency range $\omega_o^2 \le \omega^2 \le \omega_o^2/[1 - fL_g/(L_g + L_i)]$, the effective permeability is negative.

— END OF EXAMPLE 3.1.5 —

G. Field Energy in Dispersive Media

Poyntings theorem in time-domain as derived from the Maxwell equations gives

$$\nabla \cdot (\overline{E} \times \overline{H}) = -\overline{H} \cdot \frac{\partial \overline{B}}{\partial t} - \overline{E} \cdot \frac{\partial \overline{D}}{\partial t} - \overline{E} \cdot \overline{J} = -\frac{\partial}{\partial t} W - \overline{E} \cdot \overline{J} \qquad (3.1.57)$$

where $-\overline{H} \cdot \frac{\partial \overline{B}}{\partial t} - \overline{E} \cdot \frac{\partial \overline{D}}{\partial t} = -\frac{\partial}{\partial t} W$ in (3.1.57) corresponds to the negative time rate of change of the sum of the magnetic energy and electric energy.

Consider lossless media, where the complex fields $\overline{E}$ and $\overline{D}$ are assumed to have a time dependence. Assuming narrow bandwidth, we express

$$\overline{E}(\overline{r}, t) = \mathrm{Re}\,[\overline{E}(t)e^{-i\omega t}] = \mathrm{Re}\,(\overline{E}_0 e^{-i\omega t} + \overline{E}_\alpha e^{-i(\omega - \alpha)t})$$

with $\overline{E}(t) = \overline{E}_0 + \overline{E}_\alpha e^{i\alpha t}$ and $\frac{d}{dt}\overline{E}(t) = i\alpha \overline{E}_\alpha e^{i\alpha t}$.

$$\overline{D}(\overline{r}, t) = \mathrm{Re}\,[\epsilon(\omega)\overline{E}_0 e^{-i\omega t} + \epsilon(\omega - \alpha)\overline{E}_\alpha e^{-i(\omega - \alpha)t}]$$

$$\begin{aligned}
\frac{\partial}{\partial t}\overline{D}(\overline{r}, t) &= \mathrm{Re}\,[-i\omega\epsilon(\omega)\overline{E}_0 e^{-i\omega t} - i(\omega - \alpha)\epsilon(\omega - \alpha)\overline{E}_\alpha e^{-i(\omega - \alpha)t}] \\
&\approx \mathrm{Re}\,[-i\omega\epsilon(\omega)\overline{E}_0 e^{-i\omega t} - i(\omega - \alpha)\{\epsilon(\omega) - \alpha\frac{d}{d\omega}\epsilon(\omega)\}\overline{E}_\alpha e^{-i(\omega - \alpha)t}] \\
&\approx \mathrm{Re}\,[-i\omega\epsilon(\omega)\overline{E}(t)e^{-i\omega t} + i\alpha\{\epsilon(\omega) + \omega\frac{d}{d\omega}\epsilon(\omega)\}\overline{E}_\alpha e^{-i(\omega - \alpha)t}] \\
&= \mathrm{Re}\,[-i\omega\epsilon(\omega)\overline{E}(t)e^{-i\omega t} + \frac{d}{dt}\{\frac{d}{d\omega}[\omega\epsilon(\omega)]\overline{E}(t)\}e^{-i\omega t}]
\end{aligned}$$

We write the time-average of the term $\overline{E}(\overline{r}, t) \cdot \partial \overline{D}(\overline{r}, t)/\partial t$ as

$$\begin{aligned}
< \overline{E}(\overline{r}, t) \cdot \frac{\partial \overline{D}(\overline{r}, t)}{\partial t} > &= \frac{1}{4}\{\overline{E}^*(t) \cdot [-i\omega\epsilon(\omega)\overline{E}(t) + \frac{d}{dt}\{\frac{d}{d\omega}[\omega\epsilon(\omega)]\overline{E}(t)\}] \\
&\quad + \overline{E}(t) \cdot [i\omega\epsilon(\omega)\overline{E}^*(t) + \frac{d}{dt}\{\frac{d}{d\omega}[\omega\epsilon(\omega)\overline{E}^*(t)\}]\} \\
&= \frac{1}{4}\frac{d}{dt}\{\frac{d}{d\omega}[\omega\epsilon(\omega)]\}|\overline{E}(t)|^2 = < W_E > \qquad (3.1.58)
\end{aligned}$$

which is the time-average electric energy. Similarly we find

$$\begin{aligned}
< W_T > &= < W_E > + < W_M > \\
&= \frac{1}{4}\frac{d}{dt}\{\frac{d}{d\omega}[\omega\epsilon(\omega)]\}|\overline{E}(t)|^2 + \frac{1}{4}\frac{d}{dt}\{\frac{d}{d\omega}[\omega\mu(\omega)]\}|\overline{H}(t)|^2
\end{aligned}$$

which is the total time-average electric and magnetic energy.

EXAMPLE 3.1.6

Consider the permittivity $\epsilon_p(\omega) = \epsilon_0 \left[1 - \frac{\omega_p^2}{\omega^2} \right]$ for a plasma medium. The electric energy is calculated to be

$$< W_E >= \frac{1}{4} \frac{d(\omega \epsilon_p)}{d\omega} |\overline{E}|^2 = \frac{\epsilon_o}{4} \left[1 + \frac{\omega_p^2}{\omega^2} \right] |\overline{E}|^2 \qquad \text{(E3.1.6.1)}$$

— END OF EXAMPLE 3.1.6 —

EXAMPLE 3.1.7 Energy and group velocities.

Consider a lossless medium with the permittivity and permeability

$$\epsilon(\omega) = \epsilon_o \left[1 - \frac{\omega_p^2}{\omega^2 - \omega_e^2} \right]$$

$$\mu(\omega) = \mu_o \left[1 - \frac{F\omega_m^2}{\omega^2 - \omega_m^2} \right]$$

The total stored energy is,

$$< W_T >= \frac{\epsilon_o}{4} \left[1 + \frac{(\omega^2 + \omega_e^2)\omega_p^2}{(\omega^2 - \omega_e^2)^2} \right] |\overline{E}|^2 + \frac{\mu_o}{4} \left[1 + \frac{(\omega^2 + \omega_m^2)F\omega_m^2}{(\omega^2 - \omega_m^2)^2} \right] |\overline{H}|^2$$

$$= \frac{1}{4} \left[\epsilon(\omega) + \epsilon_o \frac{2\omega^2 \omega_p^2}{(\omega^2 - \omega_e^2)^2} \right] |\overline{E}|^2 + \frac{1}{4} \left[\mu(\omega) + \mu_o \frac{2\omega^2 F\omega_m^2}{(\omega^2 - \omega_m^2)^2} \right] |\overline{H}|^2$$

$$= \frac{1}{4} \left[\frac{d[\omega\epsilon(\omega)]}{d\omega} \right] |\overline{E}|^2 + \frac{1}{4} \left[\frac{d[\omega\mu(\omega)]}{d\omega} \right] \frac{\epsilon(\omega)}{\mu(\omega)} |\overline{E}|^2 \qquad \text{(E3.1.7.1)}$$

The time-average Poynting power density for a plane wave in the medium is

$$< S >= \frac{1}{2} |E|^2 \sqrt{\frac{\epsilon(\omega)}{\mu(\omega)}}$$

The energy velocity is

$$v_E = \frac{< S >}{< W_T >} = \frac{2\sqrt{\mu(\omega)\epsilon(\omega)}}{\mu(\omega) \frac{d[\omega\epsilon(\omega)]}{d\omega} + \frac{d[\omega\mu(\omega)]}{d\omega} \epsilon(\omega)}$$

The dispersion relation is $k = \omega\sqrt{\mu(\omega)\epsilon(\omega)}$. The group velocity is

$$v_g = \frac{d\omega}{dk} = \frac{2\sqrt{\mu(\omega)\epsilon(\omega)}}{2\mu(\omega)\epsilon(\omega) + \omega\mu(\omega)\frac{d\epsilon(\omega)}{d\omega} + \omega\epsilon(\omega)\frac{d\mu(\omega)}{d\omega}}$$

$$= \frac{2\sqrt{\mu(\omega)\epsilon(\omega)}}{\mu(\omega) \frac{d[\omega\epsilon(\omega)]}{d\omega} + \frac{d[\omega\mu(\omega)]}{d\omega} \epsilon(\omega)}$$

Thus the energy velocity is equal to the group velocity.

— END OF EXAMPLE 3.1.7 —

EXAMPLE 3.1.8

Consider dispersive media with very small loss and narrow bandwidth. We express

$$\overline{E}(\overline{r}, t) = \text{Re}[\overline{E}e^{-i\omega t}] = \frac{1}{2}(\overline{E}e^{-i\omega t} + \overline{E}^* e^{i\omega t})$$

$$\overline{D}(\overline{r}, t) = \text{Re}[\overline{D}e^{-i\omega t}] = \frac{1}{2}(\overline{D}e^{-i\omega t} + \overline{D}^* e^{i\omega t})$$

where the complex fields $\overline{E}$ and $\overline{D}$ are assumed to have a time dependence. We write the term $\overline{E}(\overline{r}, t) \cdot \partial \overline{D}(\overline{r}, t)/\partial t$ as

$$\overline{E}(\overline{r}, t) \cdot \frac{\partial \overline{D}(\overline{r}, t)}{\partial t} = \frac{1}{4}(\overline{E}e^{-i\omega t} + \overline{E}^* e^{i\omega t}) \cdot \frac{\partial}{\partial t}(\overline{D}e^{-i\omega t} + \overline{D}^* e^{i\omega t})$$

$$= \frac{1}{4}\left(\overline{E}^* \cdot \frac{\partial \overline{D}}{\partial t} + \overline{E} \cdot \frac{\partial \overline{D}^*}{\partial t}\right) + \frac{1}{4}\left(\overline{E} \cdot \frac{\partial \overline{D}}{\partial t}e^{-i2\omega t} + \overline{E}^* \cdot \frac{\partial \overline{D}^*}{\partial t}e^{i2\omega t}\right)$$

$$- i\omega\frac{1}{4}(\overline{E} \cdot \overline{D}e^{-i2\omega t} - \overline{E}^* \cdot \overline{D}^* e^{i2\omega t}) - i\omega\frac{1}{4}(\overline{E}^* \cdot \overline{D} - \overline{E} \cdot \overline{D}^*)$$

$$\text{(E3.1.8.1)}$$

The last term vanishes when $\epsilon_I \approx 0$. The second and third terms are zero upon taking time average. We thus have

$$< \overline{E}(\overline{r}, t) \cdot \frac{\partial \overline{D}(\overline{r}, t)}{\partial t} >=< \frac{1}{4}(\overline{E}^* \cdot \frac{\partial \overline{D}}{\partial t} + \overline{E} \cdot \frac{\partial \overline{D}^*}{\partial t}) > \qquad \text{(E3.1.8.2)}$$

Let the electric field be a slowly varying function of time and spans a narrow frequency range centered at ω. Consider the following:

$$\overline{E}(t) = \overline{E}_0 + \overline{E}_\alpha \cos \alpha t; \qquad \frac{d\overline{E}(t)}{dt} = -\alpha \overline{E}_\alpha \sin \alpha t$$

We write

$$\overline{D} = \epsilon(\omega)\overline{E}_0 + \frac{1}{2}\epsilon(\omega + \alpha)\overline{E}_\alpha e^{-i\alpha t} + \frac{1}{2}\epsilon(\omega - \alpha)\overline{E}_\alpha e^{i\alpha t}$$

It follows that, with $f(\omega) = -i\omega\epsilon(\omega)$,

$$\frac{\partial \overline{D}}{\partial t} = \epsilon(\omega)\overline{E}_0 - i\frac{1}{2}(\omega + \alpha)\epsilon(\omega + \alpha)\overline{E}_\alpha e^{-i\alpha t} - i\frac{1}{2}(\omega - \alpha)\epsilon(\omega - \alpha)\overline{E}_\alpha e^{i\alpha t}$$

$$= f(\omega)\overline{E}_0 + \frac{1}{2}f(\omega + \alpha)\overline{E}_\alpha e^{-i\alpha t} + \frac{1}{2}f(\omega - \alpha)\overline{E}_\alpha e^{i\alpha t}$$

$$\approx f(\omega)\overline{E}(t) + \frac{\alpha}{2}\frac{df(\omega)}{d\omega}\overline{E}_\alpha[e^{-i\alpha t} - e^{i\alpha t}]$$

$$= f(\omega)\overline{E}(t) + \alpha\frac{df(\omega)}{d\omega}E_\alpha[-i \sin \alpha t]$$

$$= f(\omega)E(t) + i\frac{df(\omega)}{d\omega}\frac{d\overline{E}(t)}{dt} = -i\omega\epsilon(\omega)\overline{E} + \frac{d[\omega\epsilon(\omega)]}{d\omega}\frac{d\overline{E}}{dt}$$

From (E3.1.8.1), we find

$$< \frac{1}{4}(\overline{E}^* \cdot \frac{\partial \overline{D}}{\partial t} + \overline{E} \cdot \frac{\partial \overline{D}^*}{\partial t}) >$$

$$=< \frac{1}{4}\left(-i\omega(\epsilon - \epsilon^*)|\overline{E}_0|^2 + [\frac{d(\omega\epsilon)}{d\omega}\overline{E}^* \cdot \frac{d\overline{E}}{dt} + \frac{d(\omega\epsilon^*)}{d\omega}\overline{E} \cdot \frac{d\overline{E}^*}{dt}]\right) >$$

$$\approx < \frac{1}{4}\frac{d(\omega\epsilon)}{d\omega}\frac{d}{dt}(\overline{E} \cdot \overline{E}^*) > = < \frac{1}{4}\frac{d}{dt}\left(\frac{d(\omega\epsilon)}{d\omega}|\overline{E}|^2 \right) > \qquad \text{(E3.1.8.3)}$$

where we have neglected the imaginary part of $\epsilon(\omega)$. Similarly,

$$\frac{1}{4}(\overline{H}^* \cdot \frac{\partial \overline{B}}{\partial t} + \overline{H} \cdot \frac{\partial \overline{B}^*}{\partial t}) = \frac{d}{dt}\left(\frac{d(\omega\mu)}{d\omega}|\overline{H}|^2 \right) \qquad \text{(E3.1.8.4)}$$

Taking time average of (3.1.57) and in the absence of $\overline{J}$, we find

$$\nabla \cdot < \overline{S} > = - < \overline{E} \cdot \frac{\partial \overline{D}}{\partial t} > - < \overline{H} \cdot \frac{\partial \overline{B}}{\partial t} >$$

$$= -\frac{1}{4}(\overline{E}^* \cdot \frac{\partial \overline{D}}{\partial t} + \overline{E} \cdot \frac{\partial \overline{D}^*}{\partial t}) - \frac{1}{4}(\overline{H}^* \cdot \frac{\partial \overline{B}}{\partial t} + \overline{H} \cdot \frac{\partial \overline{B}^*}{\partial t})$$

$$= -\frac{d}{dt}\left(\frac{1}{4}\frac{d(\omega\epsilon)}{d\omega}|\overline{E}|^2 + \frac{1}{4}\frac{d(\omega\mu)}{d\omega}|\overline{H}|^2 \right) \qquad \text{(E3.1.8.5)}$$

We conclude that

$$< W_T > = \frac{1}{4}\frac{d(\omega\epsilon)}{d\omega}|\overline{E}|^2 + \frac{1}{4}\frac{d(\omega\mu)}{d\omega}|\overline{H}|^2 \qquad \text{(E3.1.8.6)}$$

is the electromagnetic field energy for dispersive media.

— END OF EXAMPLE 3.1.8 —

For nondispersive media when ϵ and μ are real constants,

$$\overline{D} = \epsilon\overline{E}$$
$$\overline{B} = \mu\overline{H}$$

(3.1.57) can be written as

$$\nabla \cdot \overline{S} = -\frac{\partial}{\partial t}W_T \qquad \text{(3.1.59)}$$

where

$$W_T = \frac{1}{2}\epsilon|\overline{E}|^2 + \frac{1}{2}\mu|\overline{H}|^2 \qquad \text{(3.1.60)}$$

is the total stored electromagnetic field energy. Thus the divergence of the Poynting power vector density $\overline{S}$ is equal to the time rate of decrease of the stored electromagnetic energy. We identify $\frac{1}{2}\epsilon|\overline{E}|^2 = W_e$ as the electric energy and $\frac{1}{2}\mu|\overline{H}|^2 = W_m$ as the magnetic energy. However, when ϵ and μ are negative, the energy will be negative. It is imperative, the dispersive nature of both ϵ and μ must be considered.

Problems

P3.1.1

Separate the number 10 in two and make their product equal to 125.

P3.1.2

The instruction to a buried treasure site is given as follows: Start from a wood hanger Γ, walking to tree T_1 and turn right at 90 degrees, walk the same distance and mark the ground A. Back to the wood hanger Γ, walking to tree T_2 and turn left at 90 degrees, walk the same distance and mark the ground B. The treasure is buried in between markers A and B. Find its location.

P3.1.3

Consider two real time-harmonic vectors $\overline{E}_1(t)$ and $\overline{E}_2(t)$ represented by complex spatial vectors $\overline{E}_1$ and $\overline{E}_2$ obeying the rule $\overline{E}(t) = \mathrm{Re}\left\{\overline{E}e^{-i\omega t}\right\}$. Let $\overline{E}_1 = \hat{x} + \hat{y}\,i$ and $\overline{E}_2 = i(\hat{x} + \hat{y}\,i)$.

(a) Are both $\overline{E}_1 \times \overline{E}_2$ and $\overline{E}_1(t) \times \overline{E}_2(t)$ zero?

(b) Are both $\overline{E}_1 \cdot \overline{E}_2$ and $\overline{E}_1(t) \cdot \overline{E}_2(t)$ zero?

P3.1.4

For a right-hand circularly polarized wave, the electric field vector in real space time domain is

$$\overline{E}(\overline{r}, t) = \hat{x}\cos(kz - \omega t) - \hat{y}\sin(kz - \omega t)$$

Find the corresponding complex vector.

P3.1.5

An electromagnetic wave with the following electric field

$$\overline{E} = \hat{x}\sin\left[\frac{k}{\sqrt{2}}(y + z) - \omega t\right] + \frac{1}{\sqrt{2}}\left[A\hat{y} + \hat{z}\right]\cos\left[\frac{k}{\sqrt{2}}(y + z) - \omega t\right]$$

is propagating in a plasma medium characterized by the dispersion relation

$$k = \frac{1}{c}\sqrt{\omega^2 - 4\pi^2 \times 10^{12}}$$

where ω is the frequency in rad/sec, and c is the speed of light in free space.

(a) What is the value of A ?
(b) In which direction is the wave propagating and what is wave vector $\overline{k}$?
(c) What is the polarization of the wave?
(d) The permeability of the plasma medium is μ_o of free space, what is the permittivity ϵ of the medium in terms of ω and permittivity of free space ϵ_o ?
(e) What is the magnetic field vector of the wave ?
(f) What is the Poynting power density vector of the wave ?
(g) Show that the plasma frequency is $f_p = 10^6$ Hz.
(h) If $\omega = \sqrt{5}\pi \times 10^6$ rad/sec, what is k and what are the phase velocity v_p and group velocity v_g ?
(i) If $\omega = \sqrt{3}\pi \times 10^6$ rad/sec, what is k and what is the expression for $\overline{E}$?
(j) If $\omega = \sqrt{3}\pi \times 10^6$ rad/sec, what is the group velocity v_g and what is the time-averaged Poynting power density ?

P3.1.6

Consider an $\hat{x}$-polarized uniform electromagnetic plane wave in free space at an angular frequency ω

$$\overline{E}_1(\overline{r}) = \hat{x}E_0 e^{iky}$$

(a) Determine the speed and direction of propagation of this wave.
(b) Find the complex expression for the magnetic field $\overline{H}_1(\overline{r})$.
(c) Determine the complex Poynting vector, $\overline{S}_1 = \overline{E}_1 \times \overline{H}_1^*$, and determine the time average Poynting vector $\langle \overline{S}_1 \rangle$.
(d) A second $\hat{x}$-polarized wave, also of amplitude E_0 and at the same angular frequency ω, is propagating in the $-\hat{y}$ direction. When this wave is added to the first wave, there is a null at $y = 0$ for all t ($\overline{E}_T(y = 0, t) = 0$) where $\overline{E}_T(\overline{r}) = \overline{E}_1(\overline{r}) + \overline{E}_2(\overline{r})$. Determine the complex expression $\overline{E}_2(\overline{r})$ for this second wave.
(e) Let the second $\hat{x}$-polarized wave be $\overline{E}_3 = (\overline{r})\hat{x}E_0 e^{-iky}$. (This may or may not be the answer to (d).) Then the total field is $\overline{E}_1 + \overline{E}_3 = \hat{x}E_x(y)$. Find the positions of the nulls ($ky = ?$) and determine at what speed the nulls move.
(f) For the field in (e), determine the time-average Poynting vector $\langle \overline{S} \rangle$.

P3.1.7

To shield a room from radio interference, the room must be enclosed in a layer of copper five skin-depths thick. Note that this will attenuate fields by a factor of e^5, or about 43 dB. If the frequency to be shielded against is 10 kHz to 1 GHz, what should be the thickness of the copper (in millimeters)? For copper, $\epsilon = \epsilon_0$, $\mu = \mu_0$ and $\sigma = 5.8 \times 10^7$ mho/m.

P3.1.8

(a) At the operating frequency (2.5 GHz) of a microwave oven, the permittivity for bottom round steak is about $\epsilon = 40\epsilon_0$ and the conductivity

$\sigma = 2$ mho/meter. What is the penetration depth? Compare this penetration depth to that of polystyrene foam which has the permittivity $\epsilon = 1.03\epsilon_0$ and conductivity $\sigma = 4 \times 10^{-6}$ mho/meter.

(b) Earth is considered to be a good conductor when $\omega\epsilon/\sigma \ll 1$. Determine the highest frequency for which earth can be considered a good conductor. Assume $\sigma = 5 \times 10^{-3}$ mho/meter and $\epsilon = 10\epsilon_0$.

(c) Aluminum has $\epsilon = \epsilon_0$, $\mu = \mu_0$ and $\sigma = 3.54 \times 10^7$ mho/m. If an antenna for VHF reception is made of wood coated with a layer of aluminum and if its thickness ought to be five times greater than the skin depth of the aluminum at that frequency, determine the thickness of the aluminum layer. Is ordinary aluminum foil thick enough for that purpose? Use $f = 100$ MHz. Ordinary aluminum foil is approximately $1/1000$ inch thick.

(d) Calculate loss tangents and skin depths for sea water at frequencies 100 Hz and 5 MHz. Sea water can be characterized by conductivity $\sigma = 4$ mho/m, permittivity $\epsilon = 80\epsilon_0$, and permeability $\mu = \mu_0$ at those frequencies.

(e) A ship at the ocean surface wishes to communicate electromagnetically with a deeply submerged vehicle 100 meters below the surface. Consider a ULF signal at 1 kHz propagating down into the sea water. What fraction of the incident power density reaches the submerged vehicle?

P3.1.9

(a) An ionized plasma is dispersive; derive its group velocity v_g if $\mu = \mu_0$ and $\epsilon = \epsilon_0(1 - \omega_p^2/\omega^2)$, where $\omega_p = \sqrt{Ne^2/m\epsilon_o}$, N is the number of free electrons per cubic meter, e is the charge of an electron (coulombs), and m is the mass of an electron (kg).

(b) What is the difference in arrival times between a flash of light $(\lambda = 0.5\mu m)$ and a simultaneous radio pulse $(f = 10$ MHz$)$ seen through an idealized homogeneous ionosphere where $\omega_p = 2\pi \times 8$ MHz along a path of 100 km?

P3.1.10

Pulsars are rapidly rotating neutron stars composed primarily of neutrons at nuclear densities. As observed on Earth, these pulsars emit periodic RF pulses each lasting approximately 10 msec. As these sharp pulses propagate through the interstellar medium, the dispersion introduced by the interstellar plasma slows the pulse envelope more at lower RF frequencies than at higher frequencies. The first pulsar to be seen visually is located in the Crab Nebula, and was discovered in 1968 using the data shown in Figure P3.1.10.1. The sloping lines formed by dense dots represent the envelopes of received pulse signals. Optical astronomers estimate that the Crab Nebula is approximately 6×10^{19} m (6,350 light years) from the Earth. In the following analysis, use the permittivity for plasma $\epsilon = \epsilon_0(1 - \omega_p^2/\omega^2)$ and assume $\omega \gg \omega_p$.

(a) For $\omega \gg \omega_p$, find expressions for the phase and group velocities.

(b) As shown in Figure P3.1.10.1, note that there is a 1.5 sec dispersion between frequencies 110 MHz and 115 MHz, i.e., the relative time delay between the 110 MHz and 115 MHz frequency components arriving at

earth is 1.5 sec. Use this fact plus the known distance and the expression for v_g to calculate the interstellar electron density (m^{-3}).
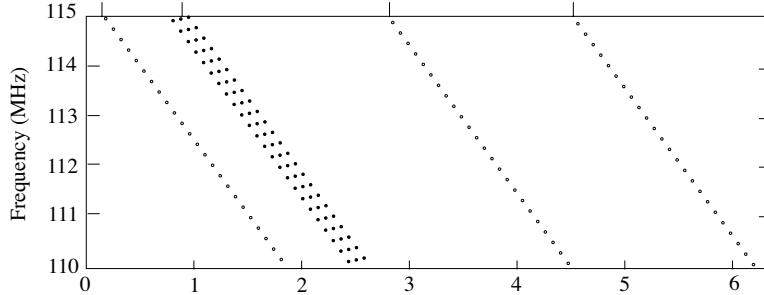
Figure P3.1.10.1

Historical Notes

The pulsar presented in this problem is called Baade's Star and is the remnant of a supernova recorded by the Chinese astronomer Toktagu on July 4, 1054. The star was so bright that, for a time, it was visible in the daytime. The data presented was later used by Taylor, Cocke, and Disney to determine if the star pulsated at optical as well as radio wavelengths. It did.

Pulsars are very dense neutron stars that are the remains of supernovae. Unlike our Earth, whose axis of rotation and magnetic axis are more or less the same, these two axes may be widely separated in a neutron star. The eccentrically rotating magnetic field creates a time varying current density as it exerts a force on charged particles in the vicinity of the pulsar. Hence, radiation!

P3.1.11

The sketch of a simple interferometer is shown in Figure P3.1.11.1. Light from a source is split into two beams by a semi-transparent mirror. The semi-transparent mirror has the property of transmitting $e^{-i\phi_t}/\sqrt{2}$ of the incident electric field and reflecting $e^{-i\phi_r}/\sqrt{2}$ of the incident field. Assume that the two reflecting mirrors are identical and have the same reflection coefficient of $e^{i\phi_0}$.

Consider the light source to be emitting light with field amplitude E_0. The reflected and transmitted fields are as follows

$$\overline{E}_r = E_0 \left(\frac{e^{-i\phi_r}}{\sqrt{2}} \right) e^{i\overline{k}_r \cdot \overline{r}} \hat{e}_r, \quad \overline{H}_r = \frac{E_0}{\eta} \left(\frac{e^{-i\phi_r}}{\sqrt{2}} \right) e^{i\overline{k}_r \cdot \overline{r}} \hat{h}_r$$

$$\overline{E}_t = E_0 \left(\frac{e^{-i\phi_t}}{\sqrt{2}} \right) e^{i\overline{k}_t \cdot \overline{r}} \hat{e}_t, \quad \overline{H}_t = \frac{E_0}{\eta} \left(\frac{e^{-i\phi_t}}{\sqrt{2}} \right) e^{i\overline{k}_t \cdot \overline{r}} \hat{h}_t$$

(a) Show that the semi-transparent mirror transmits and reflects $1/2$ of the incident power.
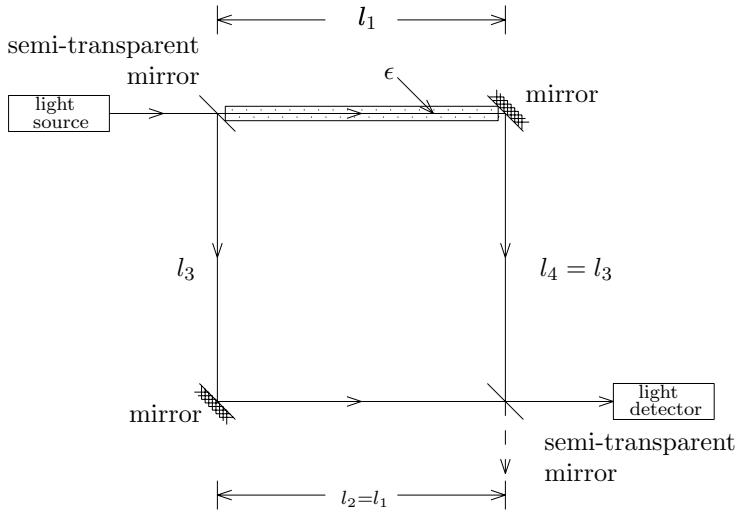
Figure P3.1.11.1

(b) The field goes into the light detector is the sum of the field transversing paths l_1 and l_4 and the field transversing paths l_2 and l_3, each goes through one reflection and one transmission from the semi-transparent mirror and constructively interfere. The field not reaching the detector is the sum of the field transversing paths l_1 and l_4 with two transmission and the field transversing paths l_2 and l_3 with two reflections from the semi-transparent mirror. To determine the relationship between ϕ_r and ϕ_t, assume $\epsilon = \epsilon_o$. The electric field reaching the light detector is

$$\overline{E}_1 = \overline{E}_0 \frac{e^{-i\phi_t}}{\sqrt{2}} e^{ik_0l_1} e^{i\phi_0} e^{ik_0l_3} \frac{e^{-i\phi_r}}{\sqrt{2}} + \overline{E}_0 \frac{e^{-i\phi_r}}{\sqrt{2}} e^{ik_0l_3} e^{i\phi_0} e^{ik_0l_1} \frac{e^{-i\phi_t}}{\sqrt{2}}$$

$$= \overline{E}_0 e^{i(\phi_0 - \phi_r - \phi_t + k_0l_1 + k_0l_3)}$$

The electric field not reaching the detector is

$$\overline{E}_2 = \overline{E}_0 \frac{e^{-i\phi_r}}{\sqrt{2}} e^{ik_0l_3} e^{i\phi_0} e^{ik_0l_1} \frac{e^{-i\phi_r}}{\sqrt{2}} + \overline{E}_0 \frac{e^{-i\phi_t}}{\sqrt{2}} e^{ik_0l_1} e^{i\phi_0} e^{ik_0l_3} \frac{e^{-i\phi_t}}{\sqrt{2}}$$

$$= \overline{E}_0 e^{i\phi_0 + ik_0(l_1+l_3) - i(\phi_r + \phi_t)} \cos(\phi_t - \phi_r)$$

Let the power going to the light detector be equal to the incident power, and the power not going to the light detector be zero. Show that

$$\phi_t - \phi_r = \frac{\pi}{2} + l\pi$$

(c) Suppose the region l_1 is filled with a plasma with electron density N with

$$\epsilon = \epsilon_o \left(1 - \frac{\omega_p^2}{\omega^2}\right)$$

where $\omega_p = \sqrt{Ne^2/m\epsilon_o}$, find the power intensity as a function of N when $\omega_p \ll \omega$. Neglect reflections from the light detector and the plasma boundaries. Show that the sum of the power reaching the light detector plus the power not reaching the detector is equal to the incident power.

P3.1.12

Consider effective permittivity

$$\epsilon_d(\omega) = \epsilon_o \left[1 - \frac{(\omega^2 - \omega_o^2)\omega_p^2}{(\omega^2 - \omega_o^2)^2 + (\omega\gamma)^2} + i\frac{\omega\gamma\omega_p^2}{(\omega^2 - \omega_o^2)^2 + (\omega\gamma)^2} \right]$$

made of conducting rods. We can reinterpret $\omega_p^2 = N_{eff}q^2/m_{eff}\epsilon_o$.
(a) The rods occupy an lattice radius of a. We have

$$N_{eff} = n\frac{\pi r_o^2}{a^2}$$

What are n and r_o?

(b) To calculate the effective mass, use $q\overline{E} = -i\omega m_{eff}\overline{v}r = -i\omega m_{eff}\overline{J}/nq$ and $J = 2\pi rH/\pi r^2$. Show by using Faraday's law that

$$m_{eff} = inq^2 E/\omega J = \pi r^2 nq^2 \frac{\mu_o}{2\pi} \ln\frac{r}{a}$$

3.2   Bianisotropic Media

A. Anisotropic Media

The constitutive relations for anisotropic media are written as

$$\overline{D} = \overline{\overline{\epsilon}} \cdot \overline{E} \tag{3.2.1a}$$
$$\overline{B} = \overline{\overline{\mu}} \cdot \overline{H} \tag{3.2.1b}$$

where $\overline{\overline{\epsilon}}$ is the permittivity tensor and $\overline{\overline{\epsilon}}$ is the permeability tensor.

Crystals are generally described by symmetric permittivity tensors. In the principal coordinate system, called the principal system, a uniaxial crystal with z axis as its optic axis has constitutive relation

$$\overline{\overline{\epsilon}} = \begin{bmatrix} \epsilon & 0 & 0 \\ 0 & \epsilon & 0 \\ 0 & 0 & \epsilon_z \end{bmatrix} \tag{3.2.2}$$

The crystal is positive uniaxial if $\epsilon_z > \epsilon$, and negative uniaxial if $\epsilon_z < \epsilon$.

An electron plasma as described in (3.1.47) becomes anisotropic when an external dc magnetic field $\overline{B}_0$ is applied. Assume that $\overline{B}_0$ is in the $\hat{z}$ direction. The permittivity tensor takes the form

$$\overline{\overline{\epsilon}} = \begin{pmatrix} \epsilon & i\epsilon_g & 0 \\ -i\epsilon_g & \epsilon & 0 \\ 0 & 0 & \epsilon_z \end{pmatrix} \tag{3.2.3}$$

where the magnetic field enters the constitutive parameters via the cyclotron frequency $\omega_c = qB_0/m$.

An anisotropic medium characterized by a hermitian permittivity tensor such as (3.2.3) is called gyroelectric or electrically gyrotropic. An anisotropic medium that is characterized by a hermitian permeability tensor $\overline{\overline{\mu}}$ such as

$$\overline{\overline{\mu}} = \begin{pmatrix} \mu & i\mu_g & 0 \\ -i\mu_g & \mu & 0 \\ 0 & 0 & \mu_z \end{pmatrix} \tag{3.2.4}$$

is called a gyromagnetic medium or a magnetically gyrotropic medium. An example is a ferrite subject to a dc magnetic field in the $\hat{z}$ direction around which the magnetization of the ferrite processes.

EXAMPLE 3.2.1   Gyrotropic media.

An electron plasma becomes anisotropic when an external dc magnetic field $\overline{B}_0$ is applied. Assume that $\overline{B}_0$ is in the $\hat{z}$ direction. Show that the permittivity tensor is

$$\overline{\overline{\epsilon}} = \begin{pmatrix} \epsilon & i\epsilon_g & 0 \\ -i\epsilon_g & \epsilon & 0 \\ 0 & 0 & \epsilon_z \end{pmatrix} \tag{E3.2.1.1}$$

with the constitutive parameters given by

$$\epsilon = \epsilon_0 \left[1 - \frac{\omega_p^2}{(\omega^2 - \omega_c^2)} \right] \tag{E3.2.1.2a}$$

$$\epsilon_g = \epsilon_0 \left[\frac{-\omega_p^2 \omega_c}{\omega(\omega^2 - \omega_c^2)} \right] \tag{E3.2.1.2b}$$

$$\epsilon_z = \epsilon_0 \left[1 - \frac{\omega_p^2}{\omega^2} \right] \tag{E3.2.1.2c}$$

Write the constitutive relation as $\overline{E} = \overline{\overline{\kappa}} \cdot \overline{D}$ with

$$\overline{\overline{\kappa}} = \overline{\overline{\epsilon}}^{-1} = \begin{pmatrix} \kappa & i\kappa_g & 0 \\ -i\kappa_g & \kappa & 0 \\ 0 & 0 & \kappa_z \end{pmatrix}$$

Determine the constitutive parameters κ, κ_g, and κ_z.

SOLUTION:

When the wave frequency is much greater than the electron collision frequency, the collision effect can be neglected and the plasma can be treated as a lossless medium. Using Lorentz Force Law and Newton's Law, we have

$$m \frac{d\overline{v}}{dt} = q(\overline{E} + \overline{v} \times \overline{B})$$

Under the time-harmonic excitation and with $\overline{v}$ much smaller than c, we find

$$-i\omega m \overline{v} = q(\overline{E} + \overline{v} \times \overline{B}_0)$$

Defining a vector $\overline{\omega}_c = q\overline{B}_0/m$, we write

$$-i\omega \overline{v} = \frac{q}{m} \overline{E} + \overline{v} \times \overline{\omega}_c \tag{E3.2.1.3}$$

Dot multiplying (E3.2.1.3) by $\overline{\omega}_c$, we have

$$-i\omega \overline{v} \cdot \overline{\omega}_c = \frac{q}{m} \overline{E} \cdot \overline{\omega}_c \tag{E3.2.1.4}$$

Cross-multiplying (E3.2.1.3) by $\overline{\omega}_c$ and making use of (E3.2.1.4), we have

$$
\begin{aligned}
-i\omega \overline{v} \times \overline{\omega}_c &= \frac{q}{m}\overline{E} \times \overline{\omega}_c + (\overline{v} \times \overline{\omega}_c) \times \overline{\omega}_c \\
&= -\frac{q}{m}\overline{\omega}_c \times \overline{E} + \overline{\omega}_c(\overline{v} \cdot \overline{\omega}_c) - \overline{v}\omega_c^2 \\
&= -\frac{q}{m}\overline{\omega}_c \times \overline{E} + \frac{iq}{\omega m}\overline{\omega}_c(\overline{\omega}_c \cdot \overline{E}) - \omega_c^2 \overline{v} \qquad \text{(E3.2.1.5)}
\end{aligned}
$$

Substituting (E3.2.1.5) into (E3.2.1.3), we obtain

$$
\begin{aligned}
\overline{J} &= Nq\overline{v} \\
&= \frac{Nq}{\omega^2 - \omega_c^2}\left[\frac{q}{m}\overline{\omega}_c \times \overline{E} + \frac{i\omega q}{m}\overline{E} - \frac{iq}{\omega m}\overline{\omega}_c(\overline{\omega}_c \cdot \overline{E})\right] \\
&= \frac{-i\omega\epsilon_o\omega_p^2}{\omega^2 - \omega_c^2}\left[\frac{i}{\omega}\overline{\omega}_c \times \overline{E} - \overline{E} + \frac{1}{\omega^2}\overline{\omega}_c(\overline{\omega}_c \cdot \overline{E})\right] \qquad \text{(E3.2.1.6)}
\end{aligned}
$$

From Ampère's law, we find

$$
\begin{aligned}
\nabla \times \overline{H} &= -i\omega\epsilon_0\overline{E} + \overline{J} = -i\omega\left\{-i\epsilon_g\hat{z} \times \overline{E} + \epsilon\overline{E} + \frac{\omega_p^2\omega_c^2\epsilon_0}{\omega^2(\omega^2 - \omega_c^2)}\hat{z}\hat{z} \cdot \overline{E}\right\} \\
&= -i\omega\overline{\overline{\epsilon}} \cdot \overline{E}
\end{aligned}
$$

where ϵ_g and ϵ are as listed in (E3.2.1.2a) and (E3.2.1.2b). Writing $\overline{\overline{\epsilon}}$ in the matrix form (E3.2.1.1), we find

$$
\epsilon_z = \epsilon_0\left[1 - \frac{\omega_p^2/\omega^2}{1 - \omega_c^2/\omega^2} + \frac{\omega_p^2\omega_c^2/\omega^4}{1 - \omega_c^2/\omega^2}\right] = \epsilon_0\left[1 - \frac{\omega_p^2}{\omega^2}\right]
$$

Carrying on the inverse of $\overline{\overline{\epsilon}}$, we find for $\overline{\overline{\kappa}} = \overline{\overline{\epsilon}}^{-1}$

$$
\kappa = \frac{\epsilon}{\epsilon^2 - \epsilon_g^2} = \frac{1}{\epsilon_0}\left[\frac{1 - \omega_p^2/\omega^2 - \omega_c^2/\omega^2}{(1 - \omega_p^2/\omega^2)^2 - \omega_c^2/\omega^2}\right]
$$

$$
\kappa_g = \frac{-\epsilon_g}{\epsilon^2 - \epsilon_g^2} = \frac{1}{\epsilon_0}\left[\frac{\omega_c\omega_p^2/\omega^3}{(1 - \omega_p^2/\omega^2)^2 - \omega_c^2/\omega^2}\right]
$$

$$
\kappa_z = \frac{1}{\epsilon_z} = \frac{1}{\epsilon_0}\left[\frac{1}{1 - \omega_p^2/\omega^2}\right]
$$

It is easily shown that $\overline{\overline{\epsilon}} \cdot \overline{\overline{\kappa}} = \overline{\overline{I}}$.

In the case of an infinitely strong magnetic field, $\omega_c \to \infty$ and we have

$$
\epsilon = \epsilon_0 \qquad\qquad\qquad \kappa = \frac{1}{\epsilon_0}
$$

$$
\epsilon_g = 0 \qquad\qquad\qquad \kappa_g = 0
$$

$$
\epsilon_z = \epsilon_0\left(1 - \frac{\omega_p^2}{\omega^2}\right) \qquad\qquad \kappa_z = \frac{1}{\epsilon_0}\left[\frac{1}{1 - \omega_p^2/\omega^2}\right]
$$

and the medium becomes a uniaxial plasma.

— END OF EXAMPLE 3.2.1 —

B. Biisotropic Media

Constitutive relations for biisotropic media take the form

$$\overline{D} = \epsilon \overline{E} + \xi \overline{H} \qquad (3.2.5a)$$

$$\overline{B} = \mu \overline{H} + \zeta \overline{E} \qquad (3.2.5b)$$

To realize his new network element, the gyrator, Tellegen in 1948 conceived of a medium possessing constitutive relations of the form

$$\overline{D} = \epsilon \overline{E} + \tau \overline{H} \qquad (3.2.6a)$$

$$\overline{B} = \mu \overline{H} + \tau \overline{E} \qquad (3.2.6b)$$

where $\tau^2/\mu\epsilon$ is nearly equal to 1.

Chiral medium is also biisotropic, which has the constitutive relations

$$\overline{D} = \epsilon \overline{E} + i \chi \overline{H} \qquad (3.2.7a)$$

$$\overline{B} = \mu \overline{H} - i \chi \overline{E} \qquad (3.2.7b)$$

where χ is the chiral parameter.

EXAMPLE 3.2.2

The split ring resonator (SRR) in Figure E3.2.2.1 is bianisotropic as a $\hat{y}$ directed polarization vector is induced by the applied magnetic field in the $\hat{z}$ direction and it is reciprocal. The constitutive relation takes the form:
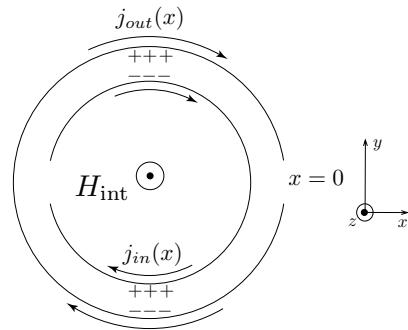
Figure E3.2.2.1   Split ring resonator.

$$
\overline{D} = \begin{pmatrix} \epsilon_x & 0 & 0 \\ 0 & \epsilon_y & 0 \\ 0 & 0 & \epsilon_z \end{pmatrix} \cdot \overline{E} + \begin{pmatrix} 0 & 0 & 0 \\ 0 & 0 & i\xi \\ 0 & 0 & 0 \end{pmatrix} \cdot \overline{H}
$$

$$
\overline{B} = \begin{pmatrix} \mu_x & 0 & 0 \\ 0 & \mu_y & 0 \\ 0 & 0 & \mu_z \end{pmatrix} \cdot \overline{H} + \begin{pmatrix} 0 & 0 & 0 \\ 0 & 0 & 0 \\ 0 & -i\xi & 0 \end{pmatrix} \cdot \overline{E}
$$

— END OF EXAMPLE 3.2.2 —

C. Bianisotropic Media

The constitutive relations for a bianisotropic medium take the form

$$
\overline{D} = \overline{\overline{\epsilon}} \cdot \overline{E} + \overline{\overline{\xi}} \cdot \overline{H} \tag{3.2.8a}
$$

$$
\overline{B} = \overline{\overline{\zeta}} \cdot \overline{E} + \overline{\overline{\mu}} \cdot \overline{H} \tag{3.2.8b}
$$

where $\overline{D}$ depends on both $\overline{E}$ and $\overline{H}$, and so does $\overline{B}$.

The constitutive relations for bianisotropic media (3.2.8) in the $\overline{E}\,\overline{H}$ representation can be written as

$$
\left[\frac{\overline{D}}{\overline{B}} \right] = \overline{\overline{C}}_{EH} \cdot \left[\frac{\overline{E}}{\overline{H}} \right] \tag{3.2.9a}
$$

where

$$
\overline{\overline{C}}_{EH} = \begin{bmatrix} \overline{\overline{\epsilon}} & \overline{\overline{\xi}} \\ \overline{\overline{\zeta}} & \overline{\overline{\mu}} \end{bmatrix} \tag{3.2.9b}
$$

is the constitutive matrix under $\overline{E}\,\overline{H}$ representation. To express $\overline{E}$ and $\overline{H}$ in terms of $\overline{B}$ and $\overline{D}$, we write

$$
\left[\frac{\overline{E}}{\overline{H}} \right] = \overline{\overline{C}}_{DB} \cdot \left[\frac{\overline{D}}{\overline{B}} \right] \tag{3.2.10a}
$$

where

$$
\overline{\overline{C}}_{DB} = \begin{bmatrix} \overline{\overline{\kappa}} & \overline{\overline{\chi}} \\ \overline{\overline{\gamma}} & \overline{\overline{\nu}} \end{bmatrix}
$$

$$
= \begin{bmatrix} (\overline{\overline{\epsilon}} - \overline{\overline{\xi}} \cdot \overline{\overline{\mu}}^{-1} \cdot \overline{\overline{\zeta}})^{-1} & -(\overline{\overline{\epsilon}} - \overline{\overline{\xi}} \cdot \overline{\overline{\mu}}^{-1} \cdot \overline{\overline{\zeta}})^{-1} \cdot \overline{\overline{\xi}} \cdot \overline{\overline{\mu}}^{-1} \\ -(\overline{\overline{\mu}} - \overline{\overline{\zeta}} \cdot \overline{\overline{\epsilon}}^{-1} \cdot \overline{\overline{\zeta}})^{-1} \cdot \overline{\overline{\zeta}} \cdot \overline{\overline{\epsilon}}^{-1} & (\overline{\overline{\mu}} - \overline{\overline{\zeta}} \cdot \overline{\overline{\epsilon}}^{-1} \cdot \overline{\overline{\xi}})^{-1} \end{bmatrix}
$$

$$
\tag{3.2.10b}
$$

is the constitutive matrix under $\overline{D}\,\overline{B}$ representation.

D. Symmetry Conditions for Lossless Media

Consider source-free regions in a medium where $\overline{J} = 0$. The time average of the divergence of Poynting's vector, in view of the complex Poynting's theorem (3.1.16), is

$$<\nabla \cdot \overline{S}> = \frac{1}{2}\text{Re}\left\{i\omega(\overline{H}^* \cdot \overline{B} - \overline{E} \cdot \overline{D}^*)\right\} \qquad (3.2.11)$$

We can classify a medium as lossless if

$$<\nabla \cdot \overline{S}> = 0$$

as passive if $<\nabla \cdot \overline{S}> < 0$, and active if $<\nabla \cdot \overline{S}> > 0$.

The most general representation of constitutive relations is bianisotropic in form. In the $\overline{E}\,\overline{H}$ representation,

$$\overline{D} = \overline{\overline{\epsilon}} \cdot \overline{E} + \overline{\overline{\xi}} \cdot \overline{H}$$
$$\overline{B} = \overline{\overline{\mu}} \cdot \overline{H} + \overline{\overline{\zeta}} \cdot \overline{E}$$

We now apply the complex Poynting's theorem to derive symmetry conditions for *lossless media*. Under time harmonic excitations, the constitutive matrices $\overline{\overline{\epsilon}}, \overline{\overline{\xi}}, \overline{\overline{\mu}},$ and $\overline{\overline{\zeta}}$ are usually complex and frequency-dependent. In general, there are altogether 72 real parameters.

Making use of the relationship $\text{Re}\{C\} = \frac{1}{2}(C + C^*)$ and substituting in the constitutive relation for bianisotropic media, we find from (3.2.11)

$$
\begin{aligned}
<\nabla \cdot \overline{S}> &= \frac{1}{4}\left\{i\omega(\overline{H}^* \cdot \overline{B} - \overline{E} \cdot \overline{D}^*) - i\omega(\overline{H}^* \cdot \overline{B} - \overline{E} \cdot \overline{D}^*)^*\right\} \\
&= \frac{i\omega}{4}\left\{\overline{H}^* \cdot (\overline{\overline{\mu}} \cdot \overline{H} + \overline{\overline{\zeta}} \cdot \overline{E}) - \overline{E} \cdot (\overline{\overline{\epsilon}}^* \cdot \overline{E}^* + \overline{\overline{\xi}}^* \cdot \overline{H}^*) \right. \\
&\qquad \left. - \overline{H} \cdot (\overline{\overline{\mu}}^* \cdot \overline{H}^* + \overline{\overline{\zeta}}^* \cdot \overline{E}^*) + \overline{E}^* \cdot (\overline{\overline{\epsilon}} \cdot \overline{E} + \overline{\overline{\xi}} \cdot \overline{H})\right\} (3.2.12)
\end{aligned}
$$

In matrix manipulation, using superscript t to represent the transpose of a matrix, the scalar quantity $\overline{A} \cdot \overline{\overline{C}} \cdot \overline{B} = \overline{B} \cdot \overline{\overline{C}}^t \cdot \overline{A}$. For the term $\overline{H} \cdot \overline{\overline{\mu}}^* \cdot \overline{H}^*$ in (3.2.12), for instance, we make use of the relation

$$\overline{H} \cdot \overline{\overline{\mu}}^* \cdot \overline{H}^* = \overline{H}^* \cdot \overline{\overline{\mu}}^+ \cdot \overline{H}$$

where the superscript $+$ denotes the transpose and the complex conjugate of the matrix $\overline{\overline{\mu}}$, we find

$$<\nabla \cdot \overline{S}> \; = \frac{i\omega}{4}\left\{\overline{E}^* \cdot (\overline{\overline{\epsilon}} - \overline{\overline{\epsilon}}^+) \cdot \overline{E} + \overline{H}^* \cdot (\overline{\overline{\mu}} - \overline{\overline{\mu}}^+) \cdot \overline{H} \right.$$
$$\left. + \overline{E}^* \cdot (\overline{\overline{\xi}} - \overline{\overline{\zeta}}^+) \cdot \overline{H} + \overline{H}^* \cdot (\overline{\overline{\zeta}} - \overline{\overline{\xi}}^+) \cdot \overline{E} \right\} \quad (3.2.13)$$

For lossless media, (3.2.13) must vanish for all possible $\overline{E}$ and $\overline{H}$ fields, thus we obtain the lossless conditions

$$\overline{\overline{\epsilon}}^+ = \overline{\overline{\epsilon}} \qquad\qquad\qquad (3.2.14a)$$
$$\overline{\overline{\mu}}^+ = \overline{\overline{\mu}} \qquad\qquad\qquad (3.2.14b)$$
$$\overline{\overline{\xi}}^+ = \overline{\overline{\zeta}} \qquad\qquad\qquad (3.2.14c)$$

The lossless conditions $(3.2.14a)$ and $(3.2.14b)$ state that $\overline{\overline{\epsilon}}$ and $\overline{\overline{\mu}}$ are hermitian. Each contains six independent complex elements. Since the diagonal elements must be all real, there are together nine real constitutive parameters. Equation $(3.2.14c)$ relates $\overline{\overline{\xi}}$ and $\overline{\overline{\zeta}}$; both matrices have a total of nine independent elements or 18 real parameters. Thus for a lossless bianisotropic medium, the constitutive relations contain a total of 21 independent complex elements of which six are pure real, or altogether 36 real constitutive parameters.

The lossless conditions for the constitutive parameters in the $\overline{D}\,\overline{B}$ representations as shown in (3.2.10) can be derived to yield

$$\overline{\overline{\kappa}}^+ = \overline{\overline{\kappa}}$$
$$\overline{\overline{\nu}}^+ = \overline{\overline{\nu}}$$
$$\overline{\overline{\chi}}^+ = \overline{\overline{\gamma}}$$

By the same token, we find

$$\overline{\overline{P}}^+ = \overline{\overline{P}}$$
$$\overline{\overline{Q}}^+ = \overline{\overline{Q}}$$
$$\overline{\overline{L}}^+ = -\overline{\overline{M}}$$

for the constitutive parameters in the $\overline{E}\,\overline{B}$ representation.

E. Reciprocity Conditions

We now derive reciprocity conditions for the constitutive parameters of bianisotropic media. Consider a source $\overline{J}_a$ producing electromagnetic field a as follows:

$$\nabla \times \overline{E}_a = i\omega \overline{B}_a \tag{3.2.15}$$
$$\nabla \times \overline{H}_a = -i\omega \overline{D}_a + \overline{J}_a \tag{3.2.16}$$
$$\nabla \cdot \overline{B}_a = 0 \tag{3.2.17}$$
$$\nabla \cdot \overline{D}_a = \rho_a \tag{3.2.18}$$

Another source $\overline{J}_b$ producing electromagnetic field b:

$$\nabla \times \overline{E}_b = i\omega \overline{B}_b \tag{3.2.19}$$
$$\nabla \times \overline{H}_b = -i\omega \overline{D}_b + \overline{J}_b \tag{3.2.20}$$
$$\nabla \cdot \overline{B}_b = 0 \tag{3.2.21}$$
$$\nabla \cdot \overline{D}_b = \rho_b \tag{3.2.22}$$

Form the difference of reactions between source a on field b and source b on field b, we find

$$\nabla \cdot \left[\overline{E}_a \times \overline{H}_b - \overline{E}_b \times \overline{H}_a \right]$$
$$= \overline{H}_b \cdot \nabla \times \overline{E}_a - \overline{E}_a \cdot \nabla \times \overline{H}_b - \overline{H}_a \cdot \nabla \times \overline{E}_b + \overline{E}_b \cdot \nabla \times \overline{H}_a$$
$$= i\omega \left[\overline{H}_b \cdot \overline{B}_a - \overline{H}_a \cdot \overline{B}_b - \overline{E}_a \cdot \overline{D}_b + \overline{E}_b \cdot \overline{D}_a \right] + \overline{J}_a \cdot \overline{E}_b - \overline{J}_b \cdot \overline{E}_a \tag{3.2.23}$$

Integrating over the whole space, we find the left hand side

$$\oiint_S d\overline{S} \cdot \left(\overline{E}_a \times \overline{H}_b - \overline{E}_b \times \overline{H}_a \right) = 0 \tag{3.2.24}$$

because at an infinite distance away from the source, the $\overline{E}$ and $\overline{H}$ fields are related by

$$\overline{H} = \hat{r} \times \overline{E}/\eta$$

and $\hat{r} \cdot \overline{E} = \hat{r} \cdot \overline{H} = 0$. As a consequence, $\overline{E}_a \times \overline{H}_b - \overline{E}_b \times \overline{H}_a = 0$.

Equation (3.2.23) becomes

$$\iiint_V dV \left[\overline{J}_b \cdot \overline{E}_a - \overline{J}_a \cdot \overline{E}_b \right]$$

$$= i\omega \iiint_V dV \left(\overline{E}_b \cdot \overline{D}_a - \overline{E}_a \cdot \overline{D}_b + \overline{H}_a \cdot \overline{B}_b - \overline{H}_b \cdot \overline{B}_a \right)$$

$$= i\omega \iiint_V dV \left[\overline{E}_b \cdot (\overline{\overline{\epsilon}} - \overline{\overline{\epsilon}}^T) \cdot \overline{E}_a + \overline{H}_a \cdot (\overline{\overline{\mu}} - \overline{\overline{\mu}}^T) \cdot \overline{H}_b \right.$$

$$\left. + \overline{E}_b \cdot (\overline{\overline{\xi}} + \overline{\overline{\zeta}}^T) \cdot \overline{H}_a - \overline{H}_b \cdot (\overline{\overline{\zeta}} + \overline{\overline{\xi}}^T) \cdot \overline{E}_a \right]$$

$$(3.2.25)$$

We call the medium reciprocal when the left hand side is zero. Thus the reciprocity condition for the medium is

$$\overline{\overline{\epsilon}}^T = \overline{\overline{\epsilon}} \qquad (3.2.26a)$$

$$\overline{\overline{\mu}}^T = \overline{\overline{\mu}} \qquad (3.2.26b)$$

$$\overline{\overline{\xi}}^T = -\overline{\overline{\zeta}} \qquad (3.2.26c)$$

The reciprocity condition for the constitutive parameters in the $\overline{D}\,\overline{B}$ representations as shown in (3.2.10) can be derived to yield

$$\overline{\overline{\kappa}}^T = \overline{\overline{\kappa}}$$

$$\overline{\overline{\nu}}^T = \overline{\overline{\nu}}$$

$$\overline{\overline{\chi}}^T = -\overline{\overline{\gamma}}$$

By the same token, we find

$$\overline{\overline{P}}^T = \overline{\overline{P}}$$

$$\overline{\overline{Q}}^T = \overline{\overline{Q}}$$

$$\overline{\overline{L}}^T = \overline{\overline{M}}$$

for the constitutive parameters in the $\overline{E}\,\overline{B}$ representation.

F. Causality Relations

We now investigate the relationship between the real and imaginary parts of the complex permittivity of a dispersive medium. The linear relationship between fields $\overline{D}$ and $\overline{E}$ can be written as

$$\overline{D}(t) = \int_{-\infty}^{t} d\tau \, \epsilon(t - \tau)\overline{E}(\tau) = \int_{0}^{\infty} d\tau \, \epsilon(\tau)\overline{E}(t - \tau)$$

The convolution integral signifies that $\overline{D}(t)$ is determined by $\overline{E}$ at all previous times, on account of causality principle. Writing in terms of Fourier transformations, we have

$$\int_{-\infty}^{\infty} d\omega \, \overline{D}(\omega)e^{-i\omega t} = \int_{0}^{\infty} d\tau \, \epsilon(\tau) \int_{-\infty}^{\infty} d\omega \, \overline{E}(\omega)e^{-i\omega(t-\tau)}$$

$$= \int_{-\infty}^{\infty} d\omega \left[\int_{0}^{\infty} d\tau \, \epsilon(\tau)e^{i\omega\tau} \right] \overline{E}(\omega)e^{-i\omega t}$$

with the time dependence $e^{-i\omega t}$ for the fields, the permittivity $\epsilon(\omega)$ is seen to be

$$\epsilon(\omega) = \int_{0}^{\infty} d\tau \, \epsilon(\tau)e^{i\omega\tau} \qquad (3.2.27)$$

Notice that because of causality, the integration range for τ is from 0 to ∞, and $\epsilon(\tau)$ is assumed to be finite throughout the range of integration.

From the defining equation for $\epsilon(\omega)$, we see that

$$\epsilon^*(\omega) = \epsilon(-\omega)$$

For bianisotropic media, we have all constitutive parameters

$$\overline{\overline{\epsilon}}(\omega)^* = \overline{\overline{\epsilon}}(-\omega)$$
$$\overline{\overline{\mu}}(\omega)^* = \overline{\overline{\mu}}(-\omega)$$
$$\overline{\overline{\xi}}(\omega)^* = \overline{\overline{\xi}}(-\omega)$$
$$\overline{\overline{\zeta}}(\omega)^* = \overline{\overline{\zeta}}(-\omega)$$

in $\overline{EH}$ representation and similarly in $\overline{DB}$ and $\overline{EB}$ representations. They are all analytical functions of complex ω on the upper half plane of ω.

EXAMPLE 3.2.3   Anisotropic conducting media.
    Consider an anisotropic conducting medium governed by Ohm's law
$\overline{J}_c = \overline{\overline{\sigma}} \cdot \overline{E}$. From the Maxwell equation

$$\nabla \times \overline{H} = -i\omega \overline{D} + \overline{J}_c + \overline{J}_f \qquad \text{(E3.2.3.1)}$$

where $\overline{J}_f$ represents the source, we can absorb $\overline{J}_c$ in $\overline{D}$ by noting that for
a general bianisotropic medium $\overline{D} = \overline{\overline{\epsilon}} \cdot \overline{E} + \overline{\overline{\xi}} \cdot \overline{H}$. We find

$$\nabla \times \overline{H} = -i\omega \left[\overline{\overline{\epsilon}} + \frac{i}{\omega} \overline{\overline{\sigma}} \right] \cdot \overline{E} - i\omega \overline{\overline{\xi}} \cdot \overline{H} + \overline{J}_f$$

Thus we define a new permittivity tensor

$$\overline{\overline{\epsilon}}_c = \overline{\overline{\epsilon}} + \frac{i}{\omega} \overline{\overline{\sigma}} \qquad \text{(E3.2.3.2)}$$

which is complex and accounts for the anisotropic conductivity of the medium.
— END OF EXAMPLE 3.2.3 —

Problems

P3.2.1
    Estimate the conductivity $\sigma = -\rho_e \mu_e$ for copper with free-electron
charge density $\rho_e \approx -1.8 \times 10^{10}$ Coul/m³ and mobility $\mu_e \approx 3.2 \times 10^3$ m²/Vs.
For semiconductors, the conductivity is a function of both electron and hole
concentrations and mobilities, $\sigma = -\rho_e \mu_e + \rho_h \mu_h$. For silicon, $\rho_h = -\rho_e \approx$
0.011 Coul/m³, $\mu_e \approx 0.12$ m²/Vs, and $\mu_h \approx 0.025$ m²/Vs.

P3.2.2
    Superconductivity was first observed by Kamerlingh Onnes in 1911. In
1933 Meissner and Ochsenfeld discovered that superconducting metals cannot
be penetrated by magnetic fields. Magnetic fields are expelled from a normal
metal when it is cooled to the superconducting state. A macroscopic theory
of superconductivity was developed by London and London in 1935 followed
by the microscopic theory of Bardeen, Cooper, and Schrieffer in 1957.
    A simple model of superconductivity calls for an electron plasma with a
very high electron density N.

 (a) Show that the penetration depth of a plasma with very large N takes
     the form

$$d_p = \sqrt{\frac{m}{Ne^2\mu_o}}$$

 (b) Let $N = 7 \times 10^{28}$ m⁻³ and calculate d_p.

(c) Compare the above result with the skin depth of a good conductor. Explain why a very slowly varying magnetic field can penetrate a good conductor but not a superconductor.

P3.2.3

Consider an electron plasma with collisions, and introduce a collision frequency $\omega_{eff} \approx NT^{-3/2}$ such that a damping term is introduced and the force on the electron in the $\hat{x}$ direction becomes $f_x = d^2(mx)/dt^2 + \omega_{eff}\, d\,(mx)/dt$. Derive the constitutive relation and show that

$$\epsilon = \epsilon_0 \left[1 - \frac{\omega_p^2}{\omega^2 + \omega_{eff}^2} + i\frac{\omega_p^2 \omega_{eff}}{\omega(\omega^2 + \omega_{eff}^2)} \right]$$

What are the limiting cases as $\omega_{eff}/\omega \to \infty$ and $\omega_{eff} = 0$?

P3.2.4

The constitutive relation for superconductors in weak magnetic fields can be macroscopically characterized by London equations proposed by two brothers Fritz and Heinz London in 1935. The first London equation

$$\frac{\partial \overline{J}_{\text{sup}}}{\partial t} = \alpha \overline{E}$$

and the second London equation

$$\left(\nabla \times \overline{J}_{\text{sup}} \right) = -\alpha_1 \overline{B}$$

where $\overline{J}_{\text{sup}}$ stands for the superconducting current, $\alpha = n_s q^2/m$ and $\alpha_1 \simeq \alpha$ with n_s, m and q denoting, respectively, the number density, the effective mass, and the charge of the Cooper pairs responsible for the superconductivity in a charged Boson fluid model.

(a) From the first London equation, derive an equation for $\dot{\overline{B}} = \partial \overline{B}/\partial t$ by using the static Maxwell equation $\nabla \times \overline{H} = \overline{J}_{\text{sup}}$ without the displacement current. Show that

$$\nabla^2 \dot{\overline{B}} = \mu_o \alpha \dot{\overline{B}}$$

and deduce that the penetration depth of the time-varying magnetic field is $(\mu_o \alpha)^{-1/2}$.

(b) From the second London equation, derive an equation for $\overline{B}$ from $\nabla \times \overline{H} = \overline{J}_{\text{sup}}$ and show that the penetration depth of the stationary magnetic field is $(\mu_o \alpha_1)^{-1/2}$. Thus for static fields, both the current and the magnetic field are confined to a thin layer of the order of the penetration depth which is very small. The exclusion of a static magnetic field from a superconductor is known as the Meissner effect experimentally discovered by Walther Meissner in 1933.

P3.2.5

In the macroscopic theory of dielectric dispersion, consider the equilibrium dipolar polarization to be represented by P_s. When an electric field E is applied, a distortion polarization P_1 is immediately established, but the remaining dipolar part of the polarization P_2 takes time to reach its equilibrium state. Letting the macroscopic relaxation time be τ, we have

$$\frac{dP_2}{dt} = \frac{1}{\tau}(P_s - P_1 - P_2)$$

where $P_s = (\epsilon_s - \epsilon_0)E$, $P_1 = (\epsilon_\infty - \epsilon_0)E$, and ϵ_s and ϵ_∞ are both real and representative of the permittivity at static and infinite frequencies respectively. For a time-harmonic field with angular frequency ω, we have $P_2 = (P_s - P_1)/(1 - i\omega\tau)$.

(a) Prove the following formula for the macroscopic permittivity ϵ due to Peter Debye (1884–1966).

$$\epsilon = \epsilon_\infty + \frac{\epsilon_s - \epsilon_\infty}{1 - i\omega\tau} \qquad \text{(Debye Equation)}$$

$$\epsilon = \left\{\epsilon_\infty + \frac{\epsilon_s - \epsilon_\infty}{1 + \omega^2\tau^2}\right\} + i(\epsilon_s - \epsilon_\infty)\frac{\omega\tau}{1 + \omega^2\tau^2}$$
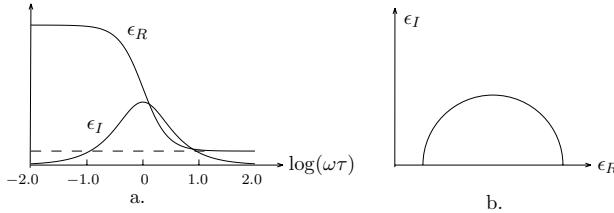

Figure P3.2.5.1

(b) Let $\epsilon = \epsilon_R + i\epsilon_I$ and plot ϵ_R and ϵ_I [Fig. P3.2.5.1a]. Label the values for ϵ_R and ϵ_I including the maximum point for ϵ_I. What are the numerical values for water molecules?

(c) Show that ϵ_I plotted as a function of ϵ_R is a circle. Find the radius of the Debye semicircle [Fig. P3.2.5.1b] and the points of intersection with the ϵ_R axis.

P3.2.6

In this problem we examine dispersion in the vicinity of a resonant frequency. Show that, if an electron is originally bound to an ion as in an atom,

$$\left(\frac{d^2}{dt^2} + g\omega_0\frac{d}{dt} + \omega_0^2\right)\overline{P} = \frac{Ne^2}{m}\overline{E}$$

where $\overline{P} = Nq\overline{r}$ is the total dipole moment per unit volume, g is a damping constant, and ω_0 is the characteristic frequency of the electron and accounts for the restoring force. Derive the complex permittivity

$$\epsilon(\omega) = \epsilon_0 \left(1 + \frac{\omega_p^2}{\omega_0^2 - ig\omega\omega_0 - \omega^2} \right) = \epsilon_R(\omega) + i\epsilon_I(\omega)$$

and plot the real and imaginary parts of $\epsilon(\omega)$. Identify the region of normal dispersion, where ϵ_R increases with frequency, and the region of anomalous dispersion, where ϵ_R decreases with frequency. Show that ϵ_I is highest at the resonant frequency ω_0. Note: use the approximations $\omega \simeq \omega_0$, and $(\omega^2 - \omega_0^2) \simeq 2\omega_0(\omega - \omega_0)$.

3.3 kDB System for Waves in Media

A. Wave Vector $\overline{k}$

In source-free and homogeneous regions in isotropic media, electromagnetic fields are generated by sources outside these regions, and the Maxwell equations are

$$\nabla \times \overline{E} = i\omega\mu\overline{H} \tag{3.3.1}$$

$$\nabla \times \overline{H} = -i\omega\epsilon\overline{E} \tag{3.3.2}$$

$$\nabla \cdot \overline{E} = 0 \tag{3.3.3}$$

$$\nabla \cdot \overline{H} = 0 \tag{3.3.4}$$

A wave equation for $\overline{E}$ can be readily derived by taking the curl of (3.3.1), introducing (3.3.2), and making use of (3.3.3). We obtain

$$\left(\nabla^2 + \omega^2\mu\epsilon\right)\overline{E} = 0 \tag{3.3.5}$$

$$\nabla^2 = \frac{\partial^2}{\partial x^2} + \frac{\partial^2}{\partial y^2} + \frac{\partial^2}{\partial z^2} \tag{3.3.6}$$

as the Laplacian operator ∇^2 in rectangular coordinate system. This is known as the homogeneous Helmholtz wave equation.

An electric field vector representing an electromagnetic wave propagating in a general direction can be written as

$$\overline{E}(\overline{r}) = \overline{E}e^{i(k_x x + k_y y + k_z z)} \tag{3.3.7}$$

which satisfies the homogeneous Helmholtz wave equation.

Substituting (3.3.7) into (3.3.6) yields the dispersion relation

$$k_x^2 + k_y^2 + k_z^2 = \omega^2\mu\epsilon = k^2 \tag{3.3.8}$$

We define a vector [Fig. 3.3.1]

$$\overline{k} = \hat{x}k_x + \hat{y}k_y + \hat{z}k_z \tag{3.3.9}$$

The vector $\overline{k}$ is called the wave vector, the propagation vector, or simply the $\overline{k}$ vector. By virtue of the dispersion relation (3.3.8), we see that the magnitude of the $\overline{k}$ vector is equal to $\omega(\mu\epsilon)^{1/2}$.
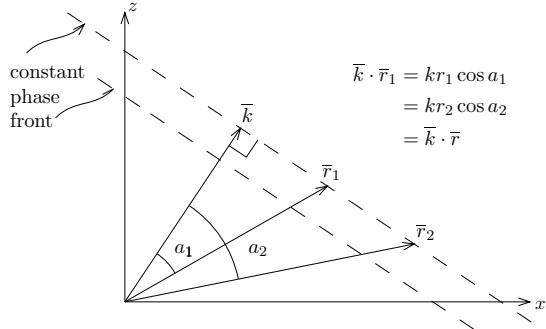
Figure 3.3.1 Constant phase fronts of a plane wave.

The scalar product of the wave vector $\overline{k} = \hat{x}k_x + \hat{y}k_y + \hat{z}k_z$ and the position vector $\overline{r} = \hat{x}x + \hat{y}y + \hat{z}z$ gives

$$\overline{k} \cdot \overline{r} = k_x x + k_y y + k_z z$$

A constant phase front is determined by $\overline{k} \cdot \overline{r} = \text{constant}$, which indicates that the front is a plane perpendicular to the $\overline{k}$ vector [Fig. 3.3.1]. The electromagnetic wave is called a plane wave.

Substituting the plane wave dependence $e^{i(k_x x + k_y y + k_z z)}$ in (3.3.1) -(3.3.4), we find the Maxwell equations become, for the plane wave solution,

$$\overline{k} \times \overline{E} = \omega\mu\overline{H} \tag{3.3.10}$$

$$\overline{k} \times \overline{H} = -\omega\epsilon\overline{E} \tag{3.3.11}$$

$$\overline{k} \cdot \overline{E} = 0 \tag{3.3.12}$$
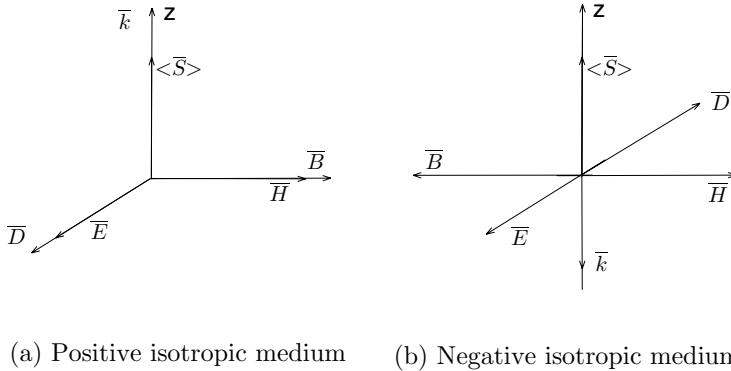
$$\overline{k} \cdot \overline{H} = 0 \tag{3.3.13}$$

The dispersion relation

$$k^2 = \omega^2\mu\epsilon \tag{3.3.14}$$

The time-average vector power density is

$$< \overline{S} > = \frac{1}{2}\text{Re}\left(\overline{E} \times \overline{H}^*\right) = \frac{1}{2}\text{Re}\begin{cases} \dfrac{-1}{\omega\epsilon}\left(\overline{k} \times \overline{H}\right) \times \overline{H}^* = \dfrac{\overline{k}}{\omega\epsilon}|\overline{H}|^2 \\[4mm] \dfrac{1}{\omega\mu^*}\,\overline{E} \times \left(\overline{k}^* \times \overline{E}^*\right) = \dfrac{\overline{k}^*}{\omega\mu^*}|\overline{E}|^2 \end{cases}$$
$$\tag{3.3.15}$$

We see that when μ and ϵ are both positive, Poynting's power vector is in the same direction as $\overline{k}$. From (3.3.10)–(3.3.11), we see that the three vectors $\overline{k}$, $\overline{E}$, and $\overline{H}$ form a right-handed system. If only one of μ or ϵ is negative, the wave is evanescent, which is seen from (3.3.14) as $\overline{k}$ becomes imaginary.

(a) Positive isotropic medium   (b) Negative isotropic medium

Figure 3.3.2 Plane waves in isotropic medium.

In negative isotropic media, μ and ϵ are both negative, Poynting's power vector is in the opposite direction of $\overline{k}$. The three vectors $\overline{k}$, $\overline{E}$, and $\overline{H}$ form a left-handed system. Thus the negative isotropic medium is also called a left-handed medium (LHM). In this medium, the Poynting power vector points in a direction that is opposite to the direction of $\overline{k}$. The plane wave is called a *backward wave*.

EXAMPLE 3.3.1
     In the case of $\sigma/\omega\epsilon \ll 1$, we find

$$k = k_R + ik_I \approx \omega\sqrt{\mu\epsilon}\left[1 + i\frac{\sigma}{2\omega\epsilon}\right]$$
$$= k_R\left[1 + i\frac{\sigma}{2\omega\epsilon}\right]$$

We see that if $\epsilon < 0$, we must also have $k_R < 0$ in order for $k_I = \sigma k_R/2\omega\epsilon > 0$ so that the wave attenuates in the direction of propagation even though the phase propagates in the backward direction.

— END OF EXAMPLE 3.3.1 —

B. The kDB System

We shall now investigate solutions to the Maxwell equations in regions void of source, namely in regions where $\overline{J} = \rho = 0$.

$$\nabla \times \overline{E} = i\omega\overline{B} \tag{3.3.16}$$
$$\nabla \times \overline{H} = -i\omega\overline{D} \tag{3.3.17}$$
$$\nabla \cdot \overline{B} = 0 \tag{3.3.18}$$
$$\nabla \cdot \overline{D} = 0 \tag{3.3.19}$$

We also assume homogeneous media where constitutive relations are independent of spatial coordinates. Plane wave solutions of the form $e^{i\overline{k}\cdot\overline{r}}$ are then admissible. With the wave vector $\overline{k}$

$$\overline{k} = \hat{x}k_x + \hat{y}k_y + \hat{z}k_z \tag{3.3.20}$$

the Maxwell equations (3.3.16)–(3.3.19) become, for the plane wave solutions,

$$\overline{k} \times \overline{E} = \omega\overline{B} \tag{3.3.21}$$
$$\overline{k} \times \overline{H} = -\omega\overline{D} \tag{3.3.22}$$
$$\overline{k} \cdot \overline{B} = 0 \tag{3.3.23}$$
$$\overline{k} \cdot \overline{D} = 0 \tag{3.3.24}$$

We see from (3.3.23) and (3.3.24) that the complex vectors $\overline{D}$ and $\overline{B}$ are always perpendicular to the wave vector $\overline{k}$. Let me call this plane, which is perpendicular to $\overline{k}$ and contains both $\overline{D}$ and $\overline{B}$, the DB plane, and establish a coordinate system formed by the three vectors $\overline{k}$, $\overline{D}$, and $\overline{B}$, the kDB system, noticing that $\overline{D}$ and $\overline{B}$ may not be perpendicular to each other. Since $\overline{E}$ and $\overline{H}$ may not lie on the DB plane, the Poynting vector is in the direction of $\overline{E} \times \overline{H}$ is not necessarily in the same direction of $\overline{k}$ inside an anisotropic medium. Thus the direction of power flow of a plane wave may not always be in the direction of the wave vector $\overline{k}$.

To facilitate the study and understanding of plane waves in homogeneous media whose constitutive relations can be as complicated as bianisotropic in form, I have designed a systematic approach using the kDB system. I shall show in detail the propagation characteristics in several anisotropic and bianisotropic media with the application of the kDB system.

The kDB system has unit vectors $\hat{e}_1$, $\hat{e}_2$, and $\hat{e}_3$. Let $\hat{e}_3$ be in the direction of $\overline{k}$ such that $\overline{k} = \hat{e}_3 k$, and $\hat{e}_3$ is in the $\hat{r}$ direction. In terms of the xyz coordinate system [Fig. 3.3.3], we find

$$\hat{e}_3 = \hat{r} = \hat{x}\sin\theta\cos\phi + \hat{y}\sin\theta\sin\phi + \hat{z}\cos\theta \qquad (3.3.25)$$
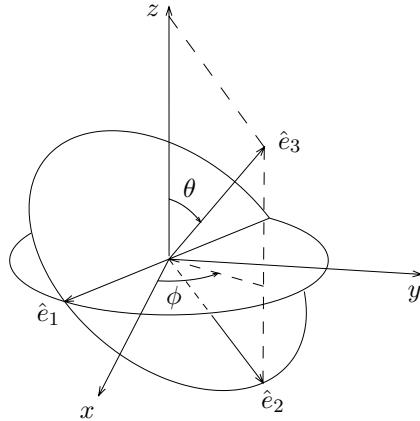

Figure 3.3.3 The kDB system.

The unit vector $\hat{e}_2$ is in the $\hat{\theta}$ direction, we have

$$\hat{e}_2 = \hat{\theta} = \hat{x}\cos\theta\cos\phi + +\hat{y}\cos\theta\sin\phi - \hat{z}\sin\theta \qquad (3.3.26)$$

The unit vector $\hat{e}_1$ is in the $-\hat{\phi}$ direction which is perpendicular to both $\hat{e}_2 = \hat{\theta}$ and $\hat{e}_3 = \hat{r}$. The three unit vectors $\hat{e}_1, \hat{e}_2, \hat{e}_3$ form a right-hand coordinate system.

$$\hat{e}_1 = \hat{e}_2 \times \hat{e}_3 = -\hat{\phi} = \hat{x}\sin\phi - \hat{y}\cos\phi \qquad (3.3.27)$$

which lies in the x-y plane. All three unit vectors are perpendicular to one another as $\hat{e}_1 \cdot \hat{e}_2 = \hat{e}_2 \cdot \hat{e}_3 = \hat{e}_3 \cdot \hat{e}_1 = 0$. The three unit vectors are indicated in Figure 3.3.3. We see that if the x-y plane is rotated counter-clockwise about $\hat{z}$ by $\phi - \pi/2$, and then rotated about the new x-axis by θ, the resulting plane perpendicular to $\overline{k}$ is the DB plane.

We now establish transformation formulas for components of field vectors. Let a vector be called $\overline{A}$ when it is represented by components

projected onto the xyz coordinate system. We write

$$\overline{A} = \begin{pmatrix} A_x \\ A_y \\ A_z \end{pmatrix} \tag{3.3.28}$$

Let the same vector be called $\overline{A}_k$ when it is represented by components projected onto the kDB coordinate system,

$$\overline{A}_k = \begin{pmatrix} A_1 \\ A_2 \\ A_3 \end{pmatrix} \tag{3.3.29}$$

The relation between the components of $\overline{A}$ and the components of $\overline{A}_k$ is governed by

$$\overline{A}_k = \overline{\overline{T}} \cdot \overline{A} \tag{3.3.30}$$

Since $\overline{A}$ and $\overline{A}_k$ denote the same vector, we find

$$\begin{aligned} A_1 &= \hat{e}_1 \cdot \overline{A} = \hat{e}_1 \cdot \hat{x} A_x + \hat{e}_1 \cdot \hat{y} A_y + \hat{e}_1 \cdot \hat{z} A_z \\ &= \sin\phi A_x - \cos\phi A_y \end{aligned} \tag{3.3.31}$$

$$\begin{aligned} A_2 &= \hat{e}_2 \cdot \overline{A} = \hat{e}_2 \cdot \hat{x} A_x + \hat{e}_2 \cdot \hat{y} A_y + \hat{e}_2 \cdot \hat{z} A_z \\ &= \cos\theta \cos\phi A_x + \cos\theta \sin\phi A_y - \sin\theta A_z \end{aligned} \tag{3.3.32}$$

$$\begin{aligned} A_3 &= \hat{e}_3 \cdot \overline{A} = \hat{e}_3 \cdot \hat{x} A_x + \hat{e}_3 \cdot \hat{y} A_y + \hat{e}_3 \cdot \hat{z} A_z \\ &= \sin\theta \cos\phi A_x + \sin\theta \sin\phi A_y + \cos\theta A_z \end{aligned} \tag{3.3.33}$$

where we have made use of (3.3.25)–(3.3.27). Writing (3.3.31)–(3.3.33) in matrix form and comparing with (3.3.30), we obtain

$$\overline{\overline{T}} = \begin{pmatrix} \sin\phi & -\cos\phi & 0 \\ \cos\theta\cos\phi & \cos\theta\sin\phi & -\sin\theta \\ \sin\theta\cos\phi & \sin\theta\sin\phi & \cos\theta \end{pmatrix} \tag{3.3.34}$$

The inverse of $\overline{\overline{T}}$ is simply calculated as

$$\overline{\overline{T}}^{-1} = \begin{pmatrix} \sin\phi & \cos\theta\cos\phi & \sin\theta\cos\phi \\ -\cos\phi & \cos\theta\sin\phi & \sin\theta\sin\phi \\ 0 & -\sin\theta & \cos\theta \end{pmatrix} \tag{3.3.35}$$

which is seen to be the transpose of $\overline{\overline{T}}$. The result (3.3.35) can be obtained in three different ways: (i) by directly calculating the inverse

of $\overline{\overline{T}}$; (ii) by following a procedure similar to (3.3.31)–(3.3.33) and using instead the relations $A_x = \hat{x}\cdot\overline{A}_k$, $A_y = \hat{y}\cdot\overline{A}_k$, and $A_z = \hat{z}\cdot\overline{A}_k$; and (iii) by recognizing that the transformation is orthogonal so that the inverse of $\overline{\overline{T}}$ is equal to the transpose of $\overline{\overline{T}}$. Clearly the product of (3.3.34) and (3.3.35) is a unit matrix.

The transformation formula established in (3.3.30) applies to any field vector $\overline{E}$, $\overline{D}$, $\overline{B}$, or $\overline{H}$. We must now find formulas that transform constitutive relations from xyz to kDB. Notice the fact that vectors $\overline{D}$ and $\overline{B}$ take much simpler forms than $\overline{E}$ and $\overline{H}$ because $D_3 = B_3 = 0$. We express the constitutive relations in xyz by relating $\overline{E}$ and $\overline{H}$ to $\overline{B}$ and $\overline{D}$,

$$\overline{E} = \overline{\overline{\kappa}}\cdot\overline{D} + \overline{\overline{\chi}}\cdot\overline{B} \tag{3.3.36}$$

$$\overline{H} = \overline{\overline{\nu}}\cdot\overline{B} + \overline{\overline{\gamma}}\cdot\overline{D} \tag{3.3.37}$$

We call these the constitutive relations in the $\overline{D}\,\overline{B}$ representation. Making use of the transformation formula (3.3.30) we find $\overline{E} = \overline{\overline{T}}^{-1}\cdot\overline{E}_k$ and similarly for $\overline{H}$, $\overline{D}$ and $\overline{B}$. The result is

$$\overline{E}_k = (\overline{\overline{T}}\cdot\overline{\overline{\kappa}}\cdot\overline{\overline{T}}^{-1})\cdot\overline{D}_k + (\overline{\overline{T}}\cdot\overline{\overline{\chi}}\cdot\overline{\overline{T}}^{-1})\cdot\overline{B}_k \tag{3.3.38}$$

$$\overline{H}_k = (\overline{\overline{T}}\cdot\overline{\overline{\nu}}\cdot\overline{\overline{T}}^{-1})\cdot\overline{B}_k + (\overline{\overline{T}}\cdot\overline{\overline{\gamma}}\cdot\overline{\overline{T}}^{-1})\cdot\overline{D}_k \tag{3.3.39}$$

We thus obtain

$$\overline{\overline{\kappa}}_k = \overline{\overline{T}}\cdot\overline{\overline{\kappa}}\cdot\overline{\overline{T}}^{-1} \tag{3.3.40a}$$

$$\overline{\overline{\chi}}_k = \overline{\overline{T}}\cdot\overline{\overline{\chi}}\cdot\overline{\overline{T}}^{-1} \tag{3.3.40b}$$

$$\overline{\overline{\nu}}_k = \overline{\overline{T}}\cdot\overline{\overline{\nu}}\cdot\overline{\overline{T}}^{-1} \tag{3.3.40c}$$

$$\overline{\overline{\gamma}}_k = \overline{\overline{T}}\cdot\overline{\overline{\gamma}}\cdot\overline{\overline{T}}^{-1} \tag{3.3.40d}$$

such that in the kDB system

$$\overline{E}_k = \overline{\overline{\kappa}}_k\cdot\overline{D}_k + \overline{\overline{\chi}}_k\cdot\overline{B}_k \tag{3.3.41}$$

$$\overline{H}_k = \overline{\overline{\nu}}_k\cdot\overline{B}_k + \overline{\overline{\gamma}}_k\cdot\overline{D}_k \tag{3.3.42}$$

With the transformation formulas (3.3.30) and (3.3.40)–(3.3.40), we can now transform all quantities from the xyz coordinate system to the kDB system.

C. Maxwell Equations in kDB System

Within the frame of the kDB system, the Maxwell equations for plane waves inside source-free homogeneous media take the same form as (3.3.21)–(3.3.24)

$$\overline{k} \times \overline{E}_k = \omega \overline{B}_k \qquad (3.3.43)$$

$$\overline{k} \times \overline{H}_k = -\omega \overline{D}_k \qquad (3.3.44)$$

$$\overline{k} \cdot \overline{B}_k = 0 \qquad (3.3.45)$$

$$\overline{k} \cdot \overline{D}_k = 0 \qquad (3.3.46)$$

but with the $\overline{k}$ vector in the $\hat{e}_3$ direction

$$\overline{k} = \hat{e}_3 k \qquad (3.3.47)$$

From (3.3.45)–(3.3.46), we find $B_3 = D_3 = 0$. From (3.3.43)–(3.3.44), we find

$$\omega \overline{B}_k = k \hat{e}_3 \times (\hat{e}_1 E_1 + \hat{e}_2 E_2 + \hat{e}_3 E_3)$$

$$-\omega \overline{D}_k = k \hat{e}_3 \times (\hat{e}_1 H_1 + \hat{e}_2 H_2 + \hat{e}_3 H_3)$$

Making use of the constitutive relations (3.3.41)–(3.3.42), we obtain

$$\omega B_2 = k E_1 = k(\kappa_{11} D_1 + \kappa_{12} D_2 + \chi_{11} B_1 + \chi_{12} B_2)$$

$$\omega B_1 = -k E_2 = -k(\kappa_{21} D_1 + \kappa_{22} D_2 + \chi_{21} B_1 + \chi_{22} B_2)$$

$$\omega D_2 = -k H_1 = -k(\nu_{11} B_1 + \nu_{12} B_2 + \gamma_{11} D_1 + \gamma_{12} D_2)$$

$$\omega D_1 = k H_2 = k(\nu_{21} B_1 + \nu_{22} B_2 + \gamma_{21} D_1 + \gamma_{22} D_2)$$

We first divide both sides by k and let $u = \omega/k$. Rearranging terms and writing in matrix form, we obtain

$$\begin{pmatrix} \kappa_{11} & \kappa_{12} \\ \kappa_{21} & \kappa_{22} \end{pmatrix} \begin{pmatrix} D_1 \\ D_2 \end{pmatrix} = - \begin{pmatrix} \chi_{11} & \chi_{12} - u \\ \chi_{21} + u & \chi_{22} \end{pmatrix} \begin{pmatrix} B_1 \\ B_2 \end{pmatrix} \qquad (3.3.48)$$

$$\begin{pmatrix} \nu_{11} & \nu_{12} \\ \nu_{21} & \nu_{22} \end{pmatrix} \begin{pmatrix} B_1 \\ B_2 \end{pmatrix} = - \begin{pmatrix} \gamma_{11} & \gamma_{12} + u \\ \gamma_{21} - u & \gamma_{22} \end{pmatrix} \begin{pmatrix} D_1 \\ D_2 \end{pmatrix} \qquad (3.3.49)$$

From the above two equations, we can derive the dispersion relations for the homogeneous media. The procedure is also applicable to dissipative media, where $\overline{k} = \hat{x} k_x + \hat{y} k_y + \hat{z} k_z$ is a complex vector. We first treat k and the angles θ and ϕ as though they were real. After the solution is obtained, we eliminate θ and ϕ by relating them to the rectangular components of $\overline{k}$ in the original xyz coordinate system and allowing the $\overline{k}$ vector to be complex.

D. Waves in Isotropic Media

The constitutive relations for isotropic media in the $\overline{D}\,\overline{B}$ representation can be written as

$$\overline{E} = \kappa \overline{D}$$
$$\overline{H} = \nu \overline{B}$$

where $\kappa = 1/\epsilon$ is called the impermittivity and $\nu = 1/\mu$ is called the impermeability.

In the kDB system, we find that

$$\overline{E}_k = \kappa \overline{D}_k \qquad\qquad (3.3.50a)$$
$$\overline{H}_k = \nu \overline{B}_k \qquad\qquad (3.3.50b)$$

Substituting in (3.3.48)–(3.3.49), we obtain

$$\kappa \begin{pmatrix} D_1 \\ D_2 \end{pmatrix} = \begin{pmatrix} 0 & u \\ -u & 0 \end{pmatrix} \begin{pmatrix} B_1 \\ B_2 \end{pmatrix} \qquad\qquad (3.3.51)$$

$$\nu \begin{pmatrix} B_1 \\ B_2 \end{pmatrix} = \begin{pmatrix} 0 & -u \\ u & 0 \end{pmatrix} \begin{pmatrix} D_1 \\ D_2 \end{pmatrix} \qquad\qquad (3.3.52)$$

Eliminating $\overline{B}_k$ from the above two equations yields

$$\begin{pmatrix} u^2 - \kappa\nu & 0 \\ 0 & u^2 - \kappa\nu \end{pmatrix} \begin{pmatrix} D_1 \\ D_2 \end{pmatrix} = 0 \qquad\qquad (3.3.53)$$

In order to satisfy (3.3.53), we have the following four cases:

    (A) $D_1 = D_2 = 0$
    (B) $D_1 \neq 0$ and $D_2 = 0$, $u^2 - \nu\kappa = 0$
    (C) $D_1 = 0$ and $D_2 \neq 0$, $u^2 - \nu\kappa = 0$
    (D) $D_1 \neq 0$ and $D_2 \neq 0$, $u^2 - \nu\kappa = 0$

In order to have non-zero $\overline{D}_k$, we must have the dispersion relation

$$u^2 - \nu\kappa = 0$$

Case (A) is a trivial case with zero field. Case (B) is a plane wave linearly polarized in the $\hat{e}_1$ direction and Case (C) is a plane wave linearly polarized in the $\hat{e}_2$ direction. Case (D) represents a plane wave of any polarization.

E. Waves in Uniaxial Media

In the principal, xyz, coordinate system of a uniaxial medium the constitutive relations under $\overline{D}\,\overline{B}$ representation are

$$\overline{E} = \overline{\overline{\kappa}} \cdot \overline{D} \qquad (3.3.54)$$

$$\overline{H} = \nu\overline{B} \qquad (3.3.55)$$

where

$$\overline{\overline{\kappa}} = \begin{pmatrix} \kappa & 0 & 0 \\ 0 & \kappa & 0 \\ 0 & 0 & \kappa_z \end{pmatrix} \qquad (3.3.56)$$

is called the impermittivity tensor. The optic axis is in the $\hat{z}$ direction. In terms of the permittivity tensor

$$\overline{\overline{\epsilon}} = \begin{pmatrix} \epsilon & 0 & 0 \\ 0 & \epsilon & 0 \\ 0 & 0 & \epsilon_z \end{pmatrix} \qquad (3.3.57)$$

we find that $\kappa = 1/\epsilon$ and $\kappa_z = 1/\epsilon_z$, since $\overline{\overline{\kappa}} = \overline{\overline{\epsilon}}^{-1}$. The impermeability is related to the permeability μ by $\nu = 1/\mu$. Transforming to the kDB system, we find from (3.3.40), that

$$\overline{\overline{\kappa}}_k = \overline{\overline{T}} \cdot \overline{\overline{\kappa}} \cdot \overline{\overline{T}}^{-1} = \begin{pmatrix} \kappa & 0 & 0 \\ 0 & \kappa\cos^2\theta + \kappa_z\sin^2\theta & (\kappa - \kappa_z)\sin\theta\cos\theta \\ 0 & (\kappa - \kappa_z)\sin\theta\cos\theta & \kappa\sin^2\theta + \kappa_z\cos^2\theta \end{pmatrix}$$
$$(3.3.58)$$

Since the uniaxial medium has cylindrical symmetry around the z-axis, the transformed relation is ϕ-independent as one should expect. Applying (3.3.48)–(3.3.49), we obtain

$$\begin{pmatrix} \kappa_{11} & 0 \\ 0 & \kappa_{22} \end{pmatrix} \begin{pmatrix} D_1 \\ D_2 \end{pmatrix} = \begin{pmatrix} 0 & u \\ -u & 0 \end{pmatrix} \begin{pmatrix} B_1 \\ B_2 \end{pmatrix} \qquad (3.3.59)$$

$$\nu \begin{pmatrix} B_1 \\ B_2 \end{pmatrix} = \begin{pmatrix} 0 & -u \\ u & 0 \end{pmatrix} \begin{pmatrix} D_1 \\ D_2 \end{pmatrix} \qquad (3.3.60)$$

Note that $\overline{\overline{\chi}} = \overline{\overline{\gamma}} = 0$ and, from (3.3.58), $\kappa_{11} = \kappa$ and $\kappa_{22} = \kappa\cos^2\theta + \kappa_z\sin^2\theta$. Note also that although κ_{23} and κ_{33} are both calculated in (3.3.58), they will not be needed either in applying (3.3.59) or in

determining $\overline{E}_k$ from $\overline{D}_k$, as illustrated later. Eliminating $\overline{B}_k$ from (3.3.59) and (3.3.60),

$$\begin{pmatrix} u^2 - \nu\kappa_{11} & 0 \\ 0 & u^2 - \nu\kappa_{22} \end{pmatrix} \begin{pmatrix} D_1 \\ D_2 \end{pmatrix} = 0 \qquad (3.3.61)$$

In order to satisfy (3.3.61), we have the following four cases:

(A) $D_1 = D_2 = 0$
(B) $D_1 \neq 0$ and $D_2 = 0$, $\quad u^2 - \nu\kappa_{11} = 0$
(C) $D_1 = 0$ and $D_2 \neq 0$, $\quad u^2 - \nu\kappa_{22} = 0$
(D) $D_1 \neq 0$ and $D_2 \neq 0$, $\quad u^2 - \nu\kappa_{11} = u^2 - \nu\kappa_{22} = 0$

Case (A) implies that there is no field at all.

a. Ordinary and Extraordinary Waves

Case (B) corresponds to a wave which is linearly polarized in the $\hat{e}_1$ direction. Notice from Figure 3.3.4 that $\hat{e}_1$ is perpendicular to the plane formed by the optic axis and the $\overline{k}$ vector. This linearly polarized plane wave propagates with the phase velocity

$$u = \pm\sqrt{\nu\kappa_{11}} \qquad (3.3.62)$$

The other field components for the wave are determined from (3.3.60) and the constitutive relations (3.3.54) and (3.3.55). We find that
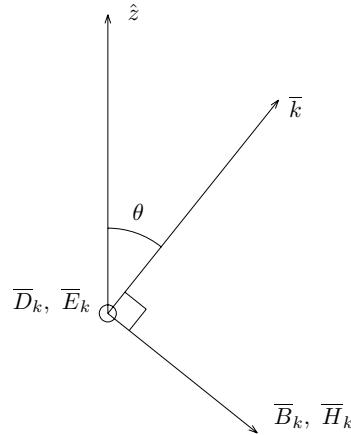
Figure 3.3.4 Ordinary wave in uniaxial medium.

$$\overline{D}_k = \hat{e}_1\, D_1 \qquad\qquad (3.3.63)$$

$$\overline{B}_k = \hat{e}_2\, \frac{u}{\nu} D_1 \qquad\qquad (3.3.64)$$

$$\overline{H}_k = \hat{e}_2\, u D_1 \qquad\qquad (3.3.65)$$

$$\overline{E}_k = \hat{e}_1\, \kappa D_1 \qquad\qquad (3.3.66)$$

Thus $\overline{D}_k$ and $\overline{E}_k$ are in the same direction, as are $\overline{B}_k$ and $\overline{H}_k$ [Fig. 3.3.4]. We call this the ordinary wave in the uniaxial medium.

EXAMPLE 3.3.2

When both ν and κ are negative and u is positive, we see from Fig. E3.3.2.1 that the Poynting power vector is in the opposite direction of the wave vector $\overline{k}$.
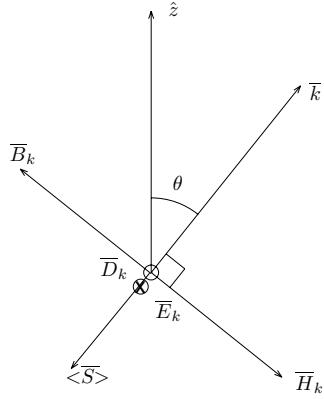
**Figure E3.3.2.1 Ordinary wave in uniaxial medium
with negative constitutive parameters.**

— END OF EXAMPLE 3.3.2 —

For case (C), the wave is linearly polarized in the $\hat{e}_2$ direction. Remember that $\hat{e}_2$ lies in the plane determined by the optic axis and the $\overline{k}$ vector and is perpendicular to the $\overline{k}$ vector. This linearly polarized wave propagates with the phase velocity

$$u = \pm\sqrt{\nu \kappa_{22}} = \pm[\nu(\kappa \cos^2\theta + \kappa_z \sin^2\theta)]^{1/2} \qquad\qquad (3.3.67)$$

which is seen to be dependent upon the direction of propagation. The other field components for the wave are determined from (3.3.60) and

the constitutive relations (3.3.54) and (3.3.55). We find that

$$\overline{D}_k = \hat{e}_2 \, D_2 \tag{3.3.68}$$

$$\overline{B}_k = -\hat{e}_1 \, \frac{u}{\nu} D_2 \tag{3.3.69}$$

$$\overline{H}_k = -\hat{e}_1 \, u D_2 \tag{3.3.70}$$

$$\overline{E}_k = \hat{e}_2 \, \kappa_{22} D_2 + \hat{e}_3 \, (\kappa - \kappa_z) \sin\theta \cos\theta \, D_2 \tag{3.3.71}$$
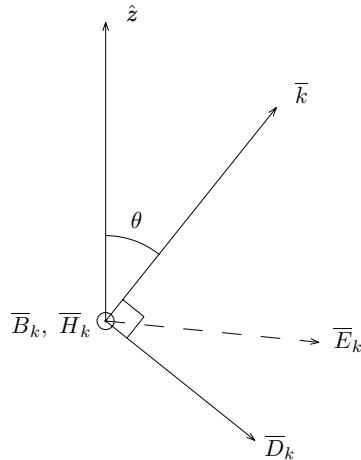
Figure 3.3.5 Extraordinary wave in a positive uniaxial medium.

We see that $\overline{E}_k$ and $\overline{D}_k$ both lie in the plane determined by the optic axis $\hat{z}$ and the wave vector $\overline{k}$ but are no longer in the same direction. For a positive uniaxial medium, $\epsilon_z > \epsilon$, $\overline{E}_k$ lies between the vectors $\overline{k}$ and $\overline{D}_k$ [Fig. 3.3.5]. As a consequence, the direction of the Poynting's vector will not be in the direction parallel to $\overline{k} = \hat{e}_3 k$. This is seen from the cross-product of $\overline{E}_k \times \overline{H}_k^*$. This linearly polarized wave, the phase velocity of which has magnitude dependent on angle and direction different from that of the Poynting's vector, is called an extraordinary wave in the uniaxial medium.

In order for Case (D) to apply, that is, $D_1 \neq 0$ and $D_2 \neq 0$, we must have $\kappa_{11} = \kappa_{22}$, which cannot hold unless (i) the medium is isotropic or (ii) the direction of propagation is along $\hat{z}$. Thus waves with polarizations other than linear can propagate only when the $\overline{k}$ vector is along the direction of the optic axis. In general, plane waves inside a uniaxial medium are either an ordinary wave linearly polarized with the $\overline{D}$ vector perpendicular to the plane determined by the

optic axis and the $\overline{k}$ vector, propagating with the phase velocity in (3.3.62), or an extraordinary wave linearly polarized with the $\overline{D}$ vector lying in the plane of the optic axis and the $\overline{k}$ vector and perpendicular to the $\overline{k}$ vector, propagating with the phase velocity in (3.3.67). The result of these two characteristic waves propagating with different phase velocities in a medium is called birefringence and the medium is called birefringent. When an electromagnetic wave enters a uniaxial medium, it decomposes into the two linearly polarized characteristic waves which propagate with different velocities. This phenomenon is known as double refraction.
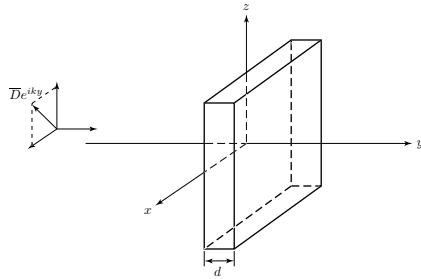
EXAMPLE 3.3.3

Consider a slab of uniaxial medium with optic axis in the $\hat{z}$ direction and with the y axis perpendicular to its front and back surfaces. Let a linearly polarized plane wave with $\overline{D} = (\hat{x}D_o + \hat{z}D_e)e^{iky}$ be normally incident upon the slab in the $\hat{y}$ direction [Fig. E3.3.3.1]. We neglect reflections at the surfaces. Upon entering the medium, the wave is decomposed into an ordinary wave with $\overline{D} = \hat{x}D_o$ and an extraordinary wave with $\overline{D} = \hat{z}D_e$. According to (3.3.62) and (3.3.67), the ordinary and extraordinary waves propagate with the spatial frequencies

$$k^{(o)} = \frac{\omega}{\sqrt{\nu\kappa}}$$

$$k^{(e)} = \frac{\omega}{\sqrt{\nu(\kappa\cos^2\theta + \kappa_z\sin^2\theta)}} = \frac{\omega}{\sqrt{\nu\kappa_z}}$$

Figure E3.3.3.1 Wave incident on a uniaxial slab.

at $\theta = \pi/2$ along the y axis. The spatial dependence of the $\overline{D}$ vector then becomes

$$\overline{D} = \hat{x}D_o\, e^{ik^{(o)}y} + \hat{z}D_e\, e^{ik^{(e)}y}$$

Thus after propagating a distance of y, the polarization of the incoming wave has been changed. If $D_o = D_e$, then at $y = 0$, the wave is linearly polarized in a direction $45°$ with respect to the optic axis. After a distance d such that

$$\left(k^{(o)} - k^{(e)}\right) d = \frac{(2m+1)\pi}{2}$$

where m is an integer, the wave becomes circularly polarized. A slab of such thickness is known as a quarter-wave plate. A polaroid is also a uniaxial medium where ϵ_z has a very large imaginary part such that the extraordinary wave is drastically attenuated after having been transmitted, whereas the ordinary wave component is transmitted with only a little attenuation.

<div align="right">— END OF EXAMPLE 3.3.3 —</div>

b. k Surfaces

The dispersion relations in (3.3.62) and (3.3.67) for the ordinary and extraordinary waves can be converted from their angular dependence to the rectangular components of $\overline{k}$ in a three-dimensional k space with the axes formed by k_x, k_y and k_z. Notice that $u = \omega/k$, $k\cos\theta = k_z$, and $k\sin\theta = k_s$ where k_s is the transverse spatial frequency representing the transverse component of $\overline{k}$. We find that

$$\omega^2 = \nu\kappa k_z^2 + \nu\kappa k_s^2 \tag{3.3.72}$$

for the ordinary wave and

$$\omega^2 = \nu\kappa k_z^2 + \nu\kappa_z k_s^2 \tag{3.3.73}$$

for the extraordinary wave. Equation (3.3.72) describes a circle and (3.3.73) describes an ellipse [Fig. 3.3.6]. Rotating them about k_z, we obtain a sphere for the ordinary wave and an ellipsoid for the extraordinary wave.

We now prove that in general the direction of flow of the time-average Poynting's vector is also normal to the tangent of the k surfaces. Thus the group velocity is in the direction of the energy velocity which is defined as the time-average Poynting's vector divided by the electromagnetic energy density. Mathematically we wish to show that $<\overline{S}>$ is perpendicular to the tangent of the k surface, namely $\delta\overline{k} \cdot <\overline{S}> = 0$. First we take the differential of $\overline{k} \times \overline{E} = \omega\overline{B}$ and $\overline{k} \times \overline{H}^* = -\omega\overline{D}^*$ and obtain

$$\delta\overline{k} \times \overline{E} + \overline{k} \times \delta E = \omega\,\delta\overline{B} \tag{3.3.74}$$

$$\delta\overline{k} \times \overline{H}^* + \overline{k} \times \delta\overline{H}^* = -\omega\,\delta\overline{D}^* \tag{3.3.75}$$
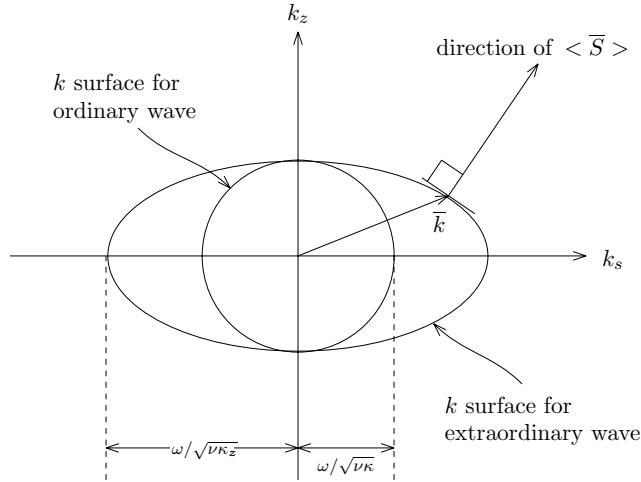
Figure 3.3.6 *k* **surfaces for the ordinary and extraordinary waves inside a positive uniaxial medium with** $\kappa/\kappa_z > 1$.

We dot-multiply (3.3.74) by $\overline{H}^*$ and (3.3.75) by $\overline{E}$ and then subtract. Using the vector identity $\overline{A} \cdot (\overline{B} \times \overline{C}) = \overline{B} \cdot (\overline{C} \times \overline{A}) = \overline{C} \cdot (\overline{A} \times \overline{B})$ we obtain

$$2\delta\overline{k} \cdot (\overline{E} \times \overline{H}^*) = \omega(\overline{H}^* \cdot \delta\overline{B} + \overline{E} \cdot \delta\overline{D}^*) + \delta\overline{E} \cdot (\overline{k} \times \overline{H}^*) - \delta\overline{H}^* \cdot (\overline{k} \times \overline{E})$$
$$= \omega \left\{ \overline{H}^* \cdot \delta\overline{B} + \overline{E} \cdot \delta\overline{D}^* - \overline{D}^* \cdot \delta\overline{E} - \overline{B} \cdot \delta\overline{H}^* \right\} \quad (3.3.76)$$

For the uniaxial medium, we find

$$2\delta\overline{k} \cdot (\overline{E} \times \overline{H}^*) = \omega \left\{ \overline{E} \cdot \overline{\overline{\epsilon}}^* \cdot \delta\overline{E}^* - \delta\overline{E} \cdot \overline{\overline{\epsilon}}^* \cdot \overline{E}^* + \overline{H}^* \cdot \mu\delta\overline{H} - \delta\overline{H}^* \cdot \mu\overline{H} \right\}$$
$$= \omega \left\{ [\overline{E}^* \cdot \overline{\overline{\epsilon}} \cdot \delta\overline{E}]^* - [\overline{E}^* \cdot \overline{\overline{\epsilon}}^+ \cdot \delta\overline{E}] + [\overline{H}^* \cdot \mu\,\delta\overline{H}] - [\overline{H}^* \cdot \mu^*\delta\overline{H}]^* \right\}$$

Using the lossless condition $\overline{\overline{\epsilon}}^+ = \overline{\overline{\epsilon}}$ and $\mu^* = \mu$, we observe that the right-hand side is a pure imaginary quantity. Since the time-average Poynting's vector is equal to one-half times the real part of $\overline{E} \times \overline{H}^*$, we conclude that

$$\delta\overline{k} \cdot < \overline{S} > = 0 \quad\quad\quad (3.3.77)$$

In general we can show that the right-hand side of (3.3.76) is a pure imaginary quantity for lossless bianisotropic media. Thus, at a point on the *k* surface, the direction of the time-average Poynting's vector is normal to the surface at that point.

EXAMPLE 3.3.4

Plotting the the ellipse $\Phi = x^2 + 2y^2$, it can be shown that $\nabla\Phi = \hat{x}2x + \hat{y}4y$ is pointing in the directions of the expanding ellipse.

Now consider the function

$$f(\Phi, x, y) = \Phi(x, y) - x^2 - 2y^2 = 0$$

We find $df = \frac{\partial f}{\partial \Phi}(\frac{\partial \Phi}{\partial x}dx + \frac{\partial \Phi}{\partial y}dy) + \frac{\partial f}{\partial x}dx + \frac{\partial f}{\partial y}dy = 0$ or $\frac{\partial f}{\partial \Phi}\nabla\Phi \cdot d\overline{r} + \nabla f \cdot d\overline{r} = 0$ where $d\overline{r} = \hat{x}dx + \hat{y}dy$. Thus $\nabla\Phi = -\nabla f / \frac{\partial f}{\partial \Phi} = \hat{x}2x + \hat{y}4y$.

— END OF EXAMPLE 3.3.4 —

EXAMPLE 3.3.5

The dispersion relations provide a functional relationship among components of the $\overline{k}$ vector and the angular frequency ω. The equations are usually quadratic in k for each characteristic wave when there are more than one. We write in general

$$f(k_x, k_y, k_z, \omega) = 0$$

In the three-dimensional $\overline{k}$ space, a quadratic equation describes a two-dimensional hypersurface. The surface is called the wave surface or simply the k surface.

We observe that the magnitude of $\overline{k}$, as described by the k surface, may vary as a function of its direction. In a particular direction, the $\overline{k}$ vector intersects the k surface at a point. The magnitude of $\overline{k}$ in this direction is proportional to the length from the origin to this point. The phase velocity of a wave in the media is $u = \omega/k$. The group velocity pertaining to the k surface is

$$\overline{v}_g = \nabla_k \, \omega = -\frac{\nabla_k f}{\partial f/\partial \omega}$$

Since the vector $\nabla_k f$ is normal to the k surface $f(k_x, k_y, k_z, \omega) = 0$, we conclude that, as a wave propagates with phase velocity u along the direction of $\overline{k}$ that intersects the wave surface at a point, the group velocity is in a direction normal to the k surface at that point.

— END OF EXAMPLE 3.3.5 —

F. Waves in Gyrotropic Media

As another example of the application of the kDB system to the solution of characteristic waves inside homogeneous media, consider a gyrotropic medium possessing the following constitutive relations:

$$\overline{H} = \nu \overline{B} \tag{3.3.78}$$

$$\overline{E} = \overline{\overline{\kappa}} \cdot \overline{D} \tag{3.3.79}$$

where

$$\overline{\overline{\kappa}} = \begin{pmatrix} \kappa & i\kappa_g & 0 \\ -i\kappa_g & \kappa & 0 \\ 0 & 0 & \kappa_z \end{pmatrix} \tag{3.3.80}$$

One example of such a gyrotropic medium is an anisotropic plasma with an externally applied dc magnetic field in the $\hat{z}$ direction. The constitutive parameters κ, κ_g and κ_z have been derived and expressed in terms of the plasma frequency and cyclotron frequency as given in Example 3.2.1.

Dispersion Relations and Characteristic Waves

We transform the constitutive matrices to the kDB system by applying (3.3.40)–(3.3.40). We find $\nu_k = \nu$ and

$$\overline{\overline{\kappa}}_k = \overline{\overline{T}} \cdot \overline{\overline{\kappa}} \cdot \overline{\overline{T}}^{-1}$$
$$= \begin{pmatrix} \kappa & i\kappa_g \cos\theta & i\kappa_g \sin\theta \\ -i\kappa_g \cos\theta & \kappa \cos^2\theta + \kappa_z \sin^2\theta & (\kappa - \kappa_z)\sin\theta\cos\theta \\ -i\kappa_g \sin\theta & (\kappa - \kappa_z)\sin\theta\cos\theta & \kappa \sin^2\theta + \kappa_z \cos^2\theta \end{pmatrix} \tag{3.3.81}$$

Substituting the values for the constitutive elements in (3.3.48) and (3.3.49), we obtain

$$\begin{pmatrix} \kappa & i\kappa_g \cos\theta \\ -i\kappa_g \cos\theta & \kappa \cos^2\theta + \kappa_z \sin^2\theta \end{pmatrix} \begin{pmatrix} D_1 \\ D_2 \end{pmatrix} = \begin{pmatrix} 0 & u \\ -u & 0 \end{pmatrix} \begin{pmatrix} B_1 \\ B_2 \end{pmatrix} \tag{3.3.82}$$

$$\nu \begin{pmatrix} B_1 \\ B_2 \end{pmatrix} = \begin{pmatrix} 0 & -u \\ u & 0 \end{pmatrix} \begin{pmatrix} D_1 \\ D_2 \end{pmatrix} \tag{3.3.83}$$

Eliminating $\overline{B}_k$ yields

$$\begin{pmatrix} u^2 - \nu\kappa & -i\nu\kappa_g \cos\theta \\ i\nu\kappa_g \cos\theta & u^2 - \nu(\kappa \cos^2\theta + \kappa_z \sin^2\theta) \end{pmatrix} \begin{pmatrix} D_1 \\ D_2 \end{pmatrix} = 0 \tag{3.3.84}$$

From which we determine the dispersion relations and wave characteristics.

Faraday Rotation

When the wave propagation direction is along $\hat{z}$, we have $\theta = 0$ and (3.3.84) becomes

$$\begin{pmatrix} u^2 - \nu\kappa & -i\nu\kappa_g \\ i\nu\kappa_g & u^2 - \nu\kappa \end{pmatrix} \begin{pmatrix} D_1 \\ D_2 \end{pmatrix} = 0 \qquad (3.3.85)$$

We find

$$\frac{D_2}{D_1} = \frac{u^2 - \nu\kappa}{i\nu\kappa_g} = -\frac{i\nu\kappa_g}{u^2 - \nu\kappa}$$

It follows that

$$u^2 - \nu\kappa = \pm\nu\kappa_g$$

which gives the magnitudes of the phase velocity

$$u = \omega/k = \sqrt{\nu(\kappa \pm \kappa_g)}$$

The two components of the field vector $\overline{D}_k$ are related by

$$\frac{D_2}{D_1} = \mp i$$

Thus, both characteristic waves are circularly polarized.

The type I wave has a velocity $u = (\nu\kappa + \nu\kappa_g)^{1/2}$ with spatial frequency

$$k^I = \omega/\sqrt{\nu(\kappa + \kappa_g)}$$

and

$$\frac{D_2}{D_1} = -i$$

which is left-hand circularly polarized.

The type II wave has a velocity $(\nu\kappa - \nu\kappa_g)^{1/2}$ with spatial frequency

$$k^{II} = \omega/\sqrt{\nu(\kappa - \kappa_g)}$$

and

$$\frac{D_2}{D_1} = i$$

which is right-hand circularly polarized.

Consider a linearly polarized plane wave with $\overline{D} = \hat{e}_1\, 2D_o$ propagating in the $\hat{z}$ direction. Decomposing into superposition of left-hand and right-hand circularly polarized waves $\overline{D} = \hat{e}_1\, 2D_o = D_o(\hat{e}_1 + \hat{e}_2\, i) + D_o(\hat{e}_1 - \hat{e}_2\, i)$, we write

$$\overline{D}(\bar{r}) = D_o(\hat{e}_1 + \hat{e}_2\, i)e^{ik^{II}z} + D_o(\hat{e}_1 - \hat{e}_2\, i)e^{ik^I z}$$

After traveling a distance z_0 inside the medium, the two waves are phase-shifted by different amounts,

$$\begin{aligned}
\overline{D} &= D_o(\hat{e}_1 + \hat{e}_2\, i)e^{i\phi_{II}} + D_o(\hat{e}_1 - \hat{e}_2\, i)e^{i\phi_I} \\
&= \hat{e}_1 D_o(e^{i\phi_{II}} + e^{i\phi_I}) + \hat{e}_2 i D_o(e^{i\phi_{II}} - e^{i\phi_I}) \qquad (3.3.86)
\end{aligned}$$

where

$$\phi_I = k^I z_0 = \frac{\omega z_0}{\sqrt{\nu(\kappa + \kappa_g)}} \qquad (3.3.87)$$

$$\phi_{II} = k^{II} z_0 = \frac{\omega z_0}{\sqrt{\nu(\kappa - \kappa_g)}} \qquad (3.3.88)$$

For the ratio of the two components of $\overline{D}_k$, we find

$$\frac{D_2}{D_1} = i\frac{e^{i\phi_{II}} - e^{i\phi_I}}{e^{i\phi_{II}} + e^{i\phi_I}} = -\tan\frac{(\phi_{II} - \phi_I)}{2}$$
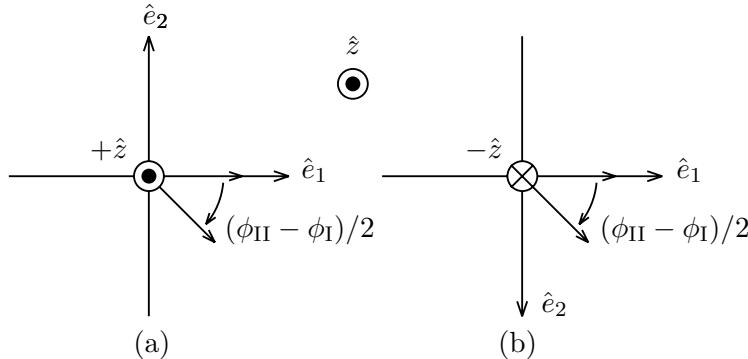
Figure 3.3.7 Faraday rotation.

Both components are in phase and the wave is linearly polarized [Fig. 3.3.7a]. Notice that for an observer viewing into the $-\hat{z}$ direction, the incoming wave is rotated clockwise by an angle $(\phi_{\mathrm{II}} - \phi_{\mathrm{I}})/2$.

Now consider the case when the wave is propagating along the $-\hat{z}$ direction, we have $\theta = \pi$ and (3.3.84) becomes

$$\begin{pmatrix} u^2 - \nu\kappa & i\nu\kappa_g \\ -i\nu\kappa_g & u^2 - \nu\kappa \end{pmatrix} \begin{pmatrix} D_1 \\ D_2 \end{pmatrix} = 0 \qquad (3.3.89)$$

We find

$$\frac{D_2}{D_1} = -\frac{u^2 - \nu\kappa}{i\nu\kappa_g} = \frac{i\nu\kappa_g}{u^2 - \nu\kappa}$$

It follows that

$$u^2 - \nu\kappa = \pm\nu\kappa_g$$

which gives the magnitudes of the phase velocity

$$u = \omega/k = \sqrt{\nu(\kappa \pm \kappa_g)}$$

The two components of the field vector $\overline{D}_k$ are related by

$$\frac{D_2}{D_1} = \pm i$$

Thus, both characteristic waves are circularly polarized.

The type I wave has a velocity $u = (\nu\kappa + \nu\kappa_g)^{1/2}$ with spatial frequency

$$k^I = \omega/\sqrt{\nu(\kappa + \kappa_g)}$$

and

$$\frac{D_2}{D_1} = i$$

which is right-hand circularly polarized.

The type II wave has a velocity $(\nu\kappa - \nu\kappa_g)^{1/2}$ with spatial frequency

$$k^{II} = \omega/\sqrt{\nu(\kappa - \kappa_g)}$$

and

$$\frac{D_2}{D_1} = -i$$

which is left-hand circularly polarized.

Notice that for waves propagating in the $-\hat{z}$ direction, the $\hat{e}_2$ axis in Figure 3.3.7b is now in the opposite direction to that in Figure 3.3.7a as seen from the kDB system shown in Figure 3.3.3. Decomposing a linearly polarized plane wave with $\overline{D} = \hat{e}_1\, 2D_o$ into superposition of left-hand and right-hand circularly polarized waves $\overline{D} = \hat{e}_1\, 2D_o = D_o(\hat{e}_1 + \hat{e}_2\, i) + D_o(\hat{e}_1 - \hat{e}_2\, i)$, we write

$$\overline{D}(\overline{r}) = D_o(\hat{e}_1 + \hat{e}_2\, i)e^{-ik^I z} + D_o(\hat{e}_1 - \hat{e}_2\, i)e^{-ik^{II} z}$$

After traveling a distance $z = -z_0$ inside the medium, the two waves are phase-shifted by different amounts,

$$\begin{aligned}\overline{D} &= D_o(\hat{e}_1 + \hat{e}_2\, i)e^{ik^I z_o} + D_o(\hat{e}_1 - \hat{e}_2\, i)e^{ik^{II} z_o} \\ &= \hat{e}_1 D_o(e^{i\phi_I} + e^{i\phi_{II}}) + \hat{e}_2 i D_o(e^{i\phi_I} - e^{i\phi_{II}})\end{aligned} \qquad (3.3.90)$$

where

$$\phi_I = k^I z_0 = \frac{\omega z_0}{\sqrt{\nu(\kappa + \kappa_g)}} \qquad (3.3.91)$$

$$\phi_{II} = k^{II} z_0 = \frac{\omega z_0}{\sqrt{\nu(\kappa - \kappa_g)}} \qquad (3.3.92)$$

For the ratio of the two components of $\overline{D}_k$, we find

$$\frac{D_2}{D_1} = -i\frac{e^{i\phi_{II}} - e^{i\phi_I}}{e^{i\phi_{II}} + e^{i\phi_I}} = \tan\frac{(\phi_{II} - \phi_I)}{2}$$

Again we see that for an observer viewing into the $-\hat{z}$ direction, the outgoing wave is rotated clockwise by an angle $(\phi_{II} - \phi_I)/2$, as shown in Figure 3.3.7b. Thus, irrespective of whether the wave is propagating in the $+\hat{z}$ or $-\hat{z}$ direction, the wave is rotated in the same direction by the same angle.

The phenomenon of rotation of a linearly polarized field vector when passing through a gyrotropic medium is known as *Faraday rotation*. For a plasma medium, the electrons circulating along the magnetic field lines are responsible for this effect. Faraday rotation also occurs in ferrites in the presence of external magnetic fields; there the effect is caused by precession of spin axes around the magnetic field. A parallel analysis can be carried out for ferrites by using a magnetically anisotropic model with an impermeability tensor $\overline{\overline{\nu}}$.

EXAMPLE 3.3.6

From (3.3.84), we find

$$\frac{D_2}{D_1} = \frac{u^2 - \nu\kappa}{i\nu\kappa_g \cos\theta} = -\frac{i\nu\kappa_g \cos\theta}{u^2 - \nu(\kappa\cos^2\theta + \kappa_z \sin^2\theta)}$$

which gives

$$u^2 - \nu\kappa = \frac{\nu}{2}\left[(\kappa - \kappa_z)\sin^2\theta \pm \sqrt{(\kappa - \kappa_z)^2 \sin^4\theta + 4\kappa_g^2 \cos^2\theta}\right] \quad \text{(E3.3.6.1)}$$

This is the dispersion relation relating ω and $\overline{k}$.

The two components of the field vector $\overline{D}_k$ are related by

$$\frac{D_2}{D_1} = \frac{-2i\kappa_g \cos\theta}{(\kappa - \kappa_z)\sin^2\theta \pm \sqrt{(\kappa - \kappa_z)^2 \sin^4\theta + 4\kappa_g^2 \cos^2\theta}} \quad \text{(E3.3.6.2)}$$

The expression can be greatly simplified if we define an angle ψ such that

$$\tan 2\psi = \frac{2\kappa_g \cos\theta}{(\kappa - \kappa_z)\sin^2\theta} \quad \text{(E3.3.6.3)}$$

We find that for the characteristic wave with the phase velocity u having the plus sign in (E3.3.6.1), (E3.3.6.2) becomes

$$\frac{D_2}{D_1} = -i\tan\psi \quad \text{(E3.3.6.4)}$$

having the spatial frequency

$$k^I = \omega\left\{\nu\kappa + \frac{\nu}{2}\left[(\kappa - \kappa_z)\sin^2\theta + \sqrt{(\kappa - \kappa_z)^2 \sin^4\theta + 4\kappa_g^2 \cos^2\theta}\right]\right\}^{-1/2}$$

We call it the Type I wave in the gyrotropic medium.

For the characteristic wave with the phase velocity u having the minus sign in (E3.3.6.1), we find from (E3.3.6.2)

$$\frac{D_2}{D_1} = i\cot\psi \quad \text{(E3.3.6.5)}$$

having the spatial frequency

$$k^{II} = \omega\left\{\nu\kappa + \frac{\nu}{2}\left[(\kappa - \kappa_z)\sin^2\theta - \sqrt{(\kappa - \kappa_z)^2 \sin^4\theta + 4\kappa_g^2 \cos^2\theta}\right]\right\}^{-1/2}$$

We call it the Type II wave.

Both characteristic waves are elliptically polarized. When κ_g is zero, the medium becomes uniaxial and the characteristic waves become linearly polarized. Both characteristic waves are also linearly polarized when the wave propagation direction is perpendicular to $\hat{z}$ and thus $\theta = \pi/2$. This birefringence is known as the Cotton-Mouton effect.

— END OF EXAMPLE 3.3.6 —

EXAMPLE 3.3.7

The Appleton-Hartree formula for the refractive index, essential to the study of radio waves in ionosphere [Budden, 1985], can be easily derived from the above results. The refractive index is defined to be the ratio $D_1/\epsilon_0 E_1 = D_2/\epsilon_0 E_2$. For instance, from (3.3.81), we find $E_1 = \kappa D_1 + i\kappa_g \cos\theta D_2$. From the first equation of (3.3.84) we also find $u^2 D_1 = \nu(\kappa D_1 + i\kappa_g \cos\theta D_2)$. Thus $u^2 D_1 = \nu E_1$ and $n^2 = D_1/\epsilon_0 E_1 = \epsilon_0/\nu u^2$. A similar derivation can be made for $n^2 = D_2/\epsilon_0 E_2$ which yields the same results.

In order to be consistent with the Appleton-Hartree formula appeared in the literature, we first define $X = \omega_p^2/\omega^2$ and $Y = \omega_c/\omega$. For the constitutive parameters, we find

$$\epsilon_0\kappa = \frac{1 - X - Y^2}{(1 - X)^2 - Y^2}$$

$$\epsilon_0\kappa_z = \frac{1}{1 - X}$$

$$\epsilon_0\kappa_g = \frac{XY}{(1 - X)^2 - Y^2}$$

It follows that the refractive index

$$n^2 = \frac{\epsilon_0}{\nu u^2} = \frac{2(1 - X)\left[(1 - X)^2 - Y^2\right]}{2\left[(1 - X)^2 - Y^2\right] + X\left(Y^2 + Y_L^2\right) \pm \sqrt{Y_T^4 + 4(1 - X)^2 Y_L^2}}$$

where $Y_L = Y\cos\theta$ corresponds to the gyrofrequency along the direction of the $\overline{B}$-field and $Y_T = Y\sin\theta$ corresponds to that transversal to the $\overline{B}$-field direction.

To further cast the result in a form displaying the effects of the plasma media on free space for which $n = 1$, we write

$$n^2 = 1 - \left(1 - \frac{\epsilon_0}{\nu u^2}\right)$$

$$= 1 - X\frac{2\left[(1 - X)^2 - Y^2\right] + \left(Y^2 + Y_L^2\right) \pm \sqrt{Y_T^4 + 4(1 - X)^2 Y_L^2}}{2\left[(1 - X)^2 - Y^2\right] + X\left(Y^2 + Y_L^2\right) \pm X\sqrt{Y_T^4 + 4(1 - X)^2 Y_L^2}}$$

$$= 1 - \frac{2X(1 - X)}{2(1 - X) - Y_T^2 \pm \sqrt{Y_T^4 + 4(1 - X)^2 Y_L^2}} \qquad \text{(E3.3.7.1)}$$

which is in the familiar form for the Appleton-Hartree formula as derived from polarization-current arguments. In the absence of the d.c. magnetic field, $Y_T = Y_L = 0$ and $n^2 = 1 - X$. In the absence of the plasma medium $X = 0$ and $n^2 = 1$ for the free space.

— END OF EXAMPLE 3.3.7 —

G. Waves in Bianisotropic Media

Consider bianisotropic media with the following constitutive relations:

$$\overline{E} = \begin{pmatrix} \kappa & 0 & 0 \\ 0 & \kappa & 0 \\ 0 & 0 & \kappa_z \end{pmatrix} \cdot \overline{D} + \begin{pmatrix} \chi & 0 & 0 \\ 0 & \chi & 0 \\ 0 & 0 & \chi_z \end{pmatrix} \cdot \overline{B} \qquad (3.3.93)$$

$$\overline{H} = \begin{pmatrix} \gamma & 0 & 0 \\ 0 & \gamma & 0 \\ 0 & 0 & \gamma_z \end{pmatrix} \cdot \overline{D} + \begin{pmatrix} \nu & 0 & 0 \\ 0 & \nu & 0 \\ 0 & 0 & \nu_z \end{pmatrix} \cdot \overline{B} \qquad (3.3.94)$$

When $\overline{\overline{\chi}} = \overline{\overline{\gamma}}$, this relation reduces to that used by Dzyaloshinskii in his description of magnetoelectric media.

In the kDB system, the constitutive matrix $\overline{\overline{\kappa}}_k$ becomes

$$\overline{\overline{\kappa}}_k = \begin{pmatrix} \kappa & 0 & 0 \\ 0 & \kappa \cos^2\theta + \kappa_z \sin^2\theta & (\kappa - \kappa_z)\sin\theta\cos\theta \\ 0 & (\kappa - \kappa_z)\sin\theta\cos\theta & \kappa\sin^2\theta + \kappa_z\cos^2\theta \end{pmatrix} \qquad (3.3.95)$$

A similar form holds for the other matrices, $\overline{\overline{\chi}}_k$, $\overline{\overline{\gamma}}_k$ and $\overline{\overline{\nu}}_k$. Inserting the corresponding constitutive parameters in (3.3.48) and (3.3.49) and eliminating $\overline{B}_k$, we obtain

$$\begin{pmatrix} u^2 - \nu_{22}\kappa + \chi\gamma\nu_{22}/\nu & -(\gamma_{22} - \chi\nu_{22}/\nu)u \\ -(\chi_{22} - \gamma\nu_{22}/\nu)u & u^2 - \nu\kappa_{22} + \chi_{22}\gamma_{22} \end{pmatrix} \begin{pmatrix} D_1 \\ D_2 \end{pmatrix} = 0 \quad (3.3.96)$$

where

$$\kappa_{22} = \kappa\cos^2\theta + \kappa_z\sin^2\theta$$

$$\nu_{22} = \nu\cos^2\theta + \nu_z\sin^2\theta$$

$$\chi_{22} = \chi\cos^2\theta + \chi_z\sin^2\theta$$

$$\gamma_{22} = \gamma\cos^2\theta + \gamma_z\sin^2\theta$$

Solving for u and $\overline{D}_k$ from (3.3.96), although tedious, is straightforward. We shall now discuss several special cases.

Consider the case with both χ and γ real and the bianisotropic medium lossless. The lossless condition requires that $\overline{\overline{\gamma}} = \overline{\overline{\chi}}$. Characteristic waves are linearly polarized.

Consider the case with both χ and γ imaginary and the bianisotropic medium lossless. Let $\overline{\overline{\chi}} \to i\overline{\overline{\chi}}$; then the lossless condition requires $\overline{\overline{\gamma}} = -i\overline{\overline{\chi}}$. We see from (3.3.96) that the characteristic waves are elliptically polarized.

Optical Activity in Chiral Media

Chiral media, which characterize many types of polymers, sugar solutions, andbiological substances, possess the following constitutive relations

$$\overline{E} = \kappa\overline{D} - i\chi\overline{B} \qquad\qquad (3.3.97a)$$

$$\overline{H} = i\chi\overline{D} + \nu\overline{B} \qquad\qquad (3.3.97b)$$

Equation (3.3.97) describes a biisotropic medium. Letting $\kappa_z = \kappa$, $\nu_z = \nu$, and $\chi_z = \chi$ in (3.3.96), we find for the biisotropic media

$$\begin{pmatrix} u^2 - \kappa\nu + \chi^2 & -i2\chi u \\ i2\chi u & u^2 - \kappa\nu + \chi^2 \end{pmatrix} \begin{pmatrix} D_1 \\ D_2 \end{pmatrix} = 0 \qquad\qquad (3.3.98)$$

We find

$$\frac{D_2}{D_1} = \frac{u^2 - \nu\kappa + \chi^2}{i2\chi u} = -\frac{i2\chi u}{u^2 - \nu\kappa + \chi^2}$$

It follows that

$$u^2 - \nu\kappa + \chi^2 = \pm 2\chi u$$

which gives the magnitudes of the phase velocity

$$u = \sqrt{\nu\kappa} \pm \chi$$

The two components of the field vector $\overline{D}_k$ are related by

$$\frac{D_2}{D_1} = \mp i$$

Thus, both characteristic waves are circularly polarized.

The type I wave has a velocity $u = \sqrt{\nu\kappa} + \chi$ with spatial frequency

$$k^I = \omega/(\sqrt{\nu\kappa} + \chi)$$

and

$$\frac{D_2}{D_1} = -i$$

which is left-hand circularly polarized.

The type II wave has a velocity $u = \sqrt{\nu\kappa} - \chi$ with spatial frequency

$$k^{II} = \omega/(\sqrt{\nu\kappa} - \chi)$$

and

$$\frac{D_2}{D_1} = i$$

which is right-hand circularly polarized.

Consider a linearly polarized plane wave with $\overline{D} = \hat{e}_1 2 D_o$ propagating in the $\hat{z}$ direction. Decomposing into superposition of left-hand and right-hand circularly polarized waves $\overline{D} = \hat{e}_1 D_o = D_o(\hat{e}_1 + \hat{e}_2 i) + D_o(\hat{e}_1 - \hat{e}_2 i)$, we write

$$\overline{D}(\overline{r}) = D_o(\hat{e}_1 + \hat{e}_2 i)e^{ik^{II}z} + D_o(\hat{e}_1 - \hat{e}_2 i)e^{ik^{I}z}$$

After traveling a distance z_0 inside the medium, the two waves are phase-shifted by different amounts,

$$\overline{D} = D_o(\hat{e}_1 + \hat{e}_2 i)e^{i\phi_{II}} + D_o(\hat{e}_1 - \hat{e}_2 i)e^{i\phi_{I}}$$
$$= \hat{e}_1 D_o(e^{i\phi_{II}} + e^{i\phi_{I}}) + \hat{e}_2 i D_o(e^{i\phi_{II}} - e^{i\phi_{I}}) \qquad (3.3.99)$$

where

$$\phi_I = k^I z_0 = \frac{\omega z_0}{(\sqrt{\nu\kappa + \chi})} \qquad (3.3.100)$$

$$\phi_{II} = k^{II} z_0 = \frac{\omega z_0}{(\sqrt{\nu\kappa - \chi})} \qquad (3.3.101)$$

For the ratio of the two components of $\overline{D}_k$, we find

$$\frac{D_2}{D_1} = i\frac{e^{i\phi_{II}} - e^{i\phi_{I}}}{e^{i\phi_{II}} + e^{i\phi_{I}}} = -\tan\frac{(\phi_{II} - \phi_I)}{2}$$
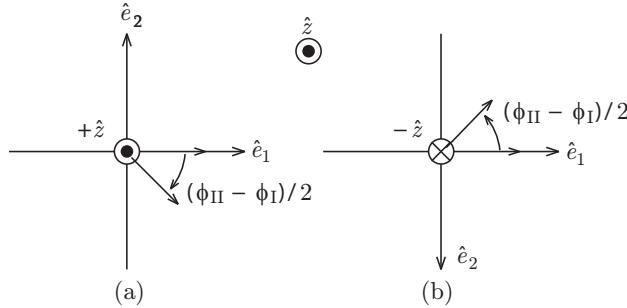
Figure 3.3.8 Optical activity.

Both components are in phase and the wave is linearly polarized [Fig. 3.3.7a]. Notice that for an observer viewing into the $-\hat{z}$ direction, the incoming wave is rotated clockwise by an angle $(\phi_{\text{II}} - \phi_{\text{I}})/2$.

Now consider the case when wave is propagating along the $-\hat{z}$ direction, we have $\theta = \pi$ and (3.3.96) becomes

$$\begin{pmatrix} u^2 - \kappa\nu + \chi^2 & -i2\chi u \\ i2\chi u & u^2 - \kappa\nu + \chi^2 \end{pmatrix} \begin{pmatrix} D_1 \\ D_2 \end{pmatrix} = 0 \qquad (3.3.102)$$

which is identical to (3.3.98). Following same analysis, we find for a linearly polarized plane wave with $\overline{D} = \hat{e}_1 \, 2D_o$, after travelling a distance of $z = -z_0$ in the $\hat{z}$ direction, the ratio of the two components of $\overline{D}_k$, we find

$$\frac{D_2}{D_1} = i\frac{e^{i\phi_{\text{II}}} - e^{i\phi_{\text{I}}}}{e^{i\phi_{\text{II}}} + e^{i\phi_{\text{I}}}} = -\tan\frac{(\phi_{\text{II}} - \phi_{\text{I}})}{2}$$

Notice that for waves propagating in the $-\hat{z}$ direction, the $\hat{e}_2$ axis in Figure 3.3.7b is now in the opposite direction to that in Figure 3.3.7a. Thus for an observer viewing into the $-\hat{z}$ direction, the incoming wave is rotated counterclockwise by an angle $(\phi_{\text{II}} - \phi_{\text{I}})/2$. The phenomenon of rotation of a linearly polarized field vector when passing through a chiral medium is known as *optical activity.*

A profound difference exists, however, between optical rotation and the Faraday rotation. A comparison of (3.3.96) with (3.3.84) reveals that the off-diagonal elements in (3.3.84) change sign when we change θ from 0 to π, while those in (3.3.96) remain unchanged.

The significance of this difference can be demonstrated as follows: consider a linearly polarized wave that propagates through a slab of gyrotropic medium along the $\hat{z}$ direction. Assume that, upon exiting, its polarization vector is rotated $45°$. If the wave is reflected by a mirror and re-enters the slab, the polarization vector is rotated a total of $90°$ after the whole journey. Consider the same experiment with the gyrotropic medium replaced by a biisotropic medium as discussed above. On its return path after being reflected by the mirror, the polarization vector is rotated back to its original position and the net result is no rotation at all. Because of this difference, we call this rotatory power optical activity to distinguish it from the Faraday effect. As we shall see later, the optical activity is reciprocal, whereas the Faraday effect is nonreciprocal.

EXAMPLE 3.3.8
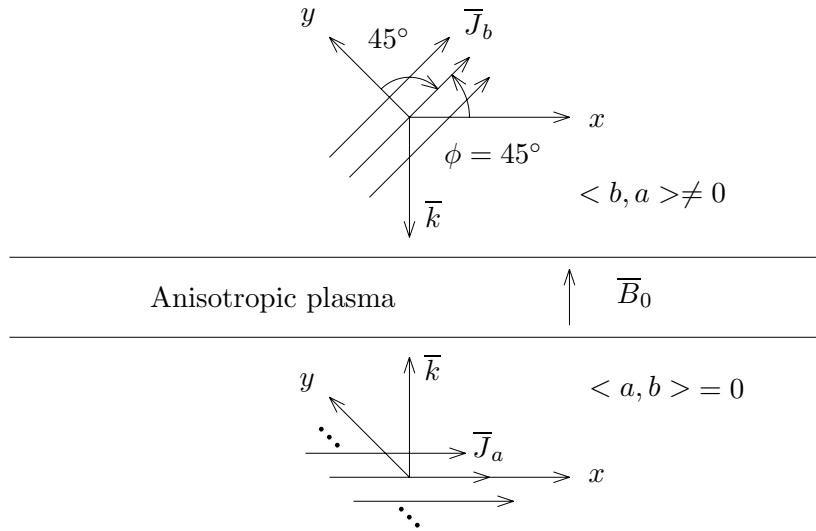
Figure E3.3.8.1 Transmission through an anisotropic plasma slab.

An anisotropic plasma is an example of a nonreciprocal medium. It possesses a permittivity tensor with $\overline{\overline{\epsilon}} = \overline{\overline{\epsilon}}^{+}$, which contradicts (3.2.26a). Consider a slab region filled with the plasma with magnetic field $\overline{B}$ perpendicular to the slab [Fig. E3.3.8.1]. Assume that, when a linearly polarized plane wave is transmitted through the slab, the Faraday rotation causes the field vector to rotate $45°$ in the increasing ϕ direction. Let a current sheet with $\overline{J}_a$ on one side of the slab produce a plane wave polarized in the direction $\phi = 0°$, and a current sheet with $\overline{J}_b$ on the other side of the slab produce a plane wave polarized in the direction $\phi = 45°$. Let $\overline{J}_a$ be source a and $\overline{J}_b$ be source b. The reaction of $< a, b >$ is seen to be zero because the plane wave, as produced by $\overline{J}_b$, is polarized with $\overline{E}_b$ perpendicular to $\overline{J}_a$ after transmitting through the slab, while the reaction of $< b, a >$ is nonzero because $\overline{E}_a$ and $\overline{J}_b$ are in the same direction. Thus $< a, b > \neq < b, a >$ and the Faraday rotation effect is nonreciprocal.

The optical activity also rotates polarization vectors, but the effect is reciprocal. For instance, a quartz crystal exhibits optical rotatory power and can be described as a bianisotropic medium with constitutive relations satisfying (3.2.26). Let the slab region in Figure E3.3.8.1 be filled with an optically active medium such as quartz. The electric field vector will be rotated $45°$ in increasing ϕ when transmitted upward and rotated $45°$ in decreasing ϕ when transmitted downward. Thus we have the reaction $< a, b > = < b, a >$.

— END OF EXAMPLE 3.3.8 —

EXAMPLE 3.3.9

Writing the constitutive relation in EH representation as

$$\overline{D} = \epsilon \overline{E} + i\xi_0 \overline{H} \tag{E3.3.9.1a}$$

$$\overline{B} = -i\xi_0 \overline{E} + \mu \overline{H} \tag{E3.3.9.1b}$$

we find

$$\kappa = 1/\epsilon(1 - \xi_0^2/\mu\epsilon) \tag{E3.3.9.2a}$$

$$\nu = 1/\mu(1 - \xi_0^2/\mu\epsilon) \tag{E3.3.9.2b}$$

$$\chi = \xi_0/\mu\epsilon(1 - \xi_0^2/\mu\epsilon) \tag{E3.3.9.2c}$$

The dispersion relation becomes

$$u = \sqrt{\kappa\nu} \pm \chi = \frac{1 \pm \xi_0/\sqrt{\mu\epsilon}}{\sqrt{\mu\epsilon}(1 - \xi_0^2/\mu\epsilon)}$$

which yields

$$k = \omega(\sqrt{\mu\epsilon} \mp \xi_0)$$

— END OF EXAMPLE 3.3.9 —

EXAMPLE 3.3.10

The split ring resonator can be modelled as a bianisotropic medium with the following constitutive relations:

$$\overline{D} = \overline{\overline{\epsilon}} \cdot \overline{E} + \overline{\overline{\xi}} \cdot \overline{H} = \begin{bmatrix} \epsilon_x & 0 & 0 \\ 0 & \epsilon_y & 0 \\ 0 & 0 & \epsilon_z \end{bmatrix} \cdot \overline{E} + \begin{bmatrix} 0 & 0 & 0 \\ 0 & 0 & 0 \\ 0 & -i\xi_O & 0 \end{bmatrix} \cdot \overline{H} \tag{E3.3.10.1a}$$

$$\overline{B} = \overline{\overline{\zeta}} \cdot \overline{E} + \overline{\overline{\mu}} \cdot \overline{H} = \begin{bmatrix} 0 & 0 & 0 \\ 0 & 0 & i\xi_O \\ 0 & 0 & 0 \end{bmatrix} \cdot \overline{E} + \begin{bmatrix} \mu_x & 0 & 0 \\ 0 & \mu_y & 0 \\ 0 & 0 & \mu_z \end{bmatrix} \cdot \overline{H} \tag{E3.3.10.1b}$$
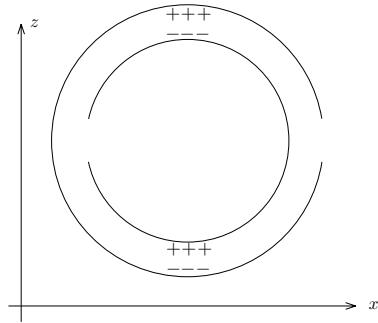
Figure E3.3.10.1 Split ring resonator.

Transforming into DB representation, we have

$$\overline{E} = \overline{\overline{\kappa}} \cdot \overline{D} + \overline{\overline{\chi}} \cdot \overline{B} \qquad (E3.3.10.2a)$$

$$\overline{H} = \overline{\overline{\gamma}} \cdot \overline{D} + \overline{\overline{\nu}} \cdot \overline{B} \qquad (E3.3.10.2b)$$

where

$$\overline{\overline{\kappa}} = \begin{bmatrix} \kappa_x & 0 & 0 \\ 0 & \kappa_y & 0 \\ 0 & 0 & \kappa_z \end{bmatrix} = \begin{bmatrix} 1/\epsilon_x & 0 & 0 \\ 0 & 1/\epsilon_y & 0 \\ 0 & 0 & 1/\epsilon_z D \end{bmatrix} \qquad (E3.3.10.3a)$$

$$\overline{\overline{\nu}} = \begin{bmatrix} \nu_x & 0 & 0 \\ 0 & \nu_y & 0 \\ 0 & 0 & \nu_z \end{bmatrix} = \begin{bmatrix} 1/\mu_x & 0 & 0 \\ 0 & 1/\mu_y D & 0 \\ 0 & 0 & 1/\mu_z \end{bmatrix} \qquad (E3.3.10.3b)$$

$$\overline{\overline{\chi}} = \overline{\overline{\gamma}}^+ = \begin{bmatrix} 0 & 0 & 0 \\ 0 & 0 & 0 \\ 0 & \chi & 0 \end{bmatrix} = \begin{bmatrix} 0 & 0 & 0 \\ 0 & 0 & 0 \\ 0 & i\xi_0/\mu_y\epsilon_z D & 0 \end{bmatrix} \qquad (E3.3.10.3c)$$

where $\kappa_z = 1/\epsilon_z D$, $\nu_y = 1/\mu_y D$, and $D = 1 - \xi_0^2/\mu_y\epsilon_z$ and $\chi = i\xi_0/\mu_y\epsilon_z D$.
Transforming into kDB system, we find

$$\overline{\overline{\kappa}} = \begin{bmatrix} \kappa_{11} & \kappa_{12} & \kappa_{13} \\ \kappa_{21} & \kappa_{22} & \kappa_{23} \\ \kappa_{31} & \kappa_{32} & \kappa_{33} \end{bmatrix} \qquad (E3.3.10.4a)$$

$$\overline{\overline{\nu}} = \begin{bmatrix} \nu_{11} & \nu_{12} & \nu_{13} \\ \nu_{21} & \nu_{22} & \nu_{23} \\ \nu_{31} & \nu_{32} & \nu_{33} \end{bmatrix} \qquad (E3.3.10.4b)$$

$$\overline{\overline{\chi}} = \chi \begin{bmatrix} 0 & 0 & 0 \\ \sin\theta\cos\phi & -\sin\theta\cos\theta\sin\phi & -\sin^2\theta\sin\phi \\ -\cos\theta\cos\phi & \cos^2\theta\sin\phi & \sin\theta\cos\theta\sin\phi \end{bmatrix} \qquad (E3.3.10.4c)$$

$$\overline{\overline{\gamma}} = \chi \begin{bmatrix} 0 & -\sin\theta\cos\phi & \cos\theta\cos\phi \\ 0 & \sin\theta\cos\theta\sin\phi & -\cos^2\theta\sin\phi \\ 0 & \sin^2\theta\sin\phi & -\sin\theta\cos\theta\sin\phi \end{bmatrix} \qquad (E3.3.10.4d)$$

where

$$\kappa_{11} = \kappa_x \sin^2\phi + \kappa_y \cos^2\phi \qquad (E3.3.10.5a)$$

$$\kappa_{12} = \kappa_{21} = (\kappa_x - \kappa_y)\cos\theta\sin\phi\cos\phi \qquad (E3.3.10.5b)$$

$$\kappa_{13} = \kappa_{31} = (\kappa_x - \kappa_y)\sin\theta\sin\phi\cos\phi \qquad (E3.3.10.5c)$$

$$\kappa_{22} = (\kappa_x \cos^2\phi + \kappa_y \sin^2\phi)\cos^2\theta + \kappa_z \sin^2\theta \qquad (E3.3.10.5d)$$

$$\kappa_{23} = \kappa_{32} = (\kappa_x \cos^2\phi + \kappa_y \sin^2\phi - \kappa_z)\sin\theta\cos\theta \qquad (E3.3.10.5e)$$

$$\kappa_{33} = (\kappa_x \cos^2\phi + \kappa_y \sin^2\phi)\sin^2\theta + \kappa_z \cos^2\theta \qquad (E3.3.10.5f)$$

and similar relations for $\overline{\overline{\nu}}$ by replacing κ with ν.

Notice that when either the $\overline{k}$ vector is in the xy-plane with $\theta = \pi/2$ or when the $\overline{k}$ vector is in the xz-plane with $\phi = 0$, $\kappa_{12} = \kappa_{21} = \nu_{12} = \nu_{21} = \chi_{22} = \gamma_{22} = 0$. We now consider such cases by using the kDB system. We obtain

$$\begin{pmatrix} D_1 \\ D_2 \end{pmatrix} = - \begin{pmatrix} 0 & -u/\kappa_{11} \\ (u + \chi_{21})/\kappa_{22} & 0 \end{pmatrix} \begin{pmatrix} B_1 \\ B_2 \end{pmatrix} \qquad \text{(E3.3.10.6)}$$

$$\begin{pmatrix} B_1 \\ B_2 \end{pmatrix} = - \begin{pmatrix} 0 & (u + \gamma_{12})/\nu_{11} \\ -u/\nu_{22} & 0 \end{pmatrix} \begin{pmatrix} D_1 \\ D_2 \end{pmatrix} \qquad \text{(E3.3.10.7)}$$

We obtain, noting that $\gamma_{12} = -\chi_{21} = -\chi \sin\theta \cos\phi$,

$$\begin{pmatrix} u^2 - \kappa_{11}\nu_{22} & 0 \\ 0 & u^2 - \chi_{21}^2 - \kappa_{22}\nu_{11} \end{pmatrix} \begin{pmatrix} D_1 \\ D_2 \end{pmatrix} = 0 \qquad \text{(E3.3.10.8)}$$

When the $\overline{k}$ vector is in the xy-plane with $\theta = \pi/2$, the dispersion relations are

$$\omega^2 = \kappa_y \nu_z k_x^2 + \kappa_x \nu_z k_y^2 \qquad \text{(E3.3.10.9)}$$

$$\omega^2 = \left(\kappa_z \nu_y + \chi^2\right) k_x^2 + \kappa_z \nu_x k_y^2 \qquad \text{(E3.3.10.10)}$$

In terms of constitutive parameters in EH representation, noting that $\kappa_z = /\epsilon_z D$, $\nu_y = 1/\mu_y D$, and $D = 1 - \xi_0^2/\mu_y \epsilon_z = (\mu_y \epsilon_z - \xi_0^2)/\mu_y \epsilon_z$, $\chi = i\xi_0/\mu_y \epsilon_z D$, and $\kappa_z \nu_y + \chi^2 = 1/\epsilon_z \mu_y D^2 - \xi_0^2/\mu_y^2 \epsilon_z^2 D^2 = 1/\epsilon_z \mu_y D$, we find

$$\omega^2 = k_x^2/\epsilon_y \mu_z + k_y^2/\epsilon_x \mu_z \qquad \text{(E3.3.10.11)}$$

$$\omega^2 = k_x^2/\epsilon_z \mu_y D + k_y^2/\epsilon_z \mu_x D \qquad \text{(E3.3.10.12)}$$

$$= k_x^2/(\mu_y \epsilon_z - \xi_0^2) + \mu_y k_y^2/\mu_x(\mu_y \epsilon_z - \xi_0^2) \qquad \text{(E3.3.10.13)}$$

When the $\overline{k}$ vector is in the xz-plane with $\phi = 0$, the dispersion relations are

$$\omega^2 = \kappa_y \nu_z k_x^2 + \kappa_y \nu_x k_z^2 \qquad \text{(E3.3.10.14)}$$

$$\omega^2 = \left(\kappa_z \nu_y + \chi^2\right) k_x^2 + \kappa_x \nu_y k_z^2 \qquad \text{(E3.3.10.15)}$$

$$\omega^2 = k_x^2/\epsilon_y \mu_z + k_z^2/\epsilon_y \mu_x \qquad \text{(E3.3.10.16)}$$

$$\omega^2 = k_x^2/\epsilon_z \mu_y D + k_z^2/\epsilon_x \mu_y D \qquad \text{(E3.3.10.17)}$$

$$= k_x^2/(\mu_y \epsilon_z - \xi_0^2) + \epsilon_z k_z^2/\epsilon_x(\mu_y \epsilon_z - \xi_0^2) \qquad \text{(E3.3.10.18)}$$

The characteristic waves are linearly polarized.

— END OF EXAMPLE 3.3.10 —

EXAMPLE 3.3.11

Wave vector in any direction,

$$\overline{\overline{T}} = \begin{pmatrix} \sin\phi & -\cos\phi & 0 \\ \cos\theta\cos\phi & \cos\theta\sin\phi & -\sin\theta \\ \sin\theta\cos\phi & \sin\theta\sin\phi & \cos\theta \end{pmatrix} ; \overline{\overline{Y}} = \begin{pmatrix} y & y_g & 0 \\ -y_g & y & 0 \\ 0 & 0 & y_z \end{pmatrix}$$

$$\overline{\overline{Y}} = \begin{pmatrix} y & y_g\cos\theta & y_g\sin\theta \\ -y_g\cos\theta & y\cos^2\theta + y_z\sin^2\theta & (y-y_z)\sin\theta\cos\theta \\ -y_g\sin\theta & (y-y_z)\sin\theta\cos\theta & y\sin^2\theta + y_x\cos^2\theta \end{pmatrix}$$

Lossless $\overline{\overline{\kappa}} = \overline{\overline{\kappa}}^+, \overline{\overline{\nu}} = \overline{\overline{\nu}}^+, \overline{\overline{\gamma}} = \overline{\overline{\chi}}^+$. Reciprocal $\overline{\overline{\kappa}} = \overline{\overline{\kappa}}^T, \overline{\overline{\nu}} = \overline{\overline{\nu}}^T, \overline{\overline{\gamma}} = -\overline{\overline{\chi}}^T$

$$\begin{pmatrix} \kappa & \kappa_f & 0 \\ \kappa_f & \kappa & 0 \\ 0 & 0 & \kappa_z \end{pmatrix} ; \begin{pmatrix} \nu & 0 & 0 \\ 0 & \nu & 0 \\ 0 & 0 & \nu_z \end{pmatrix} ; \begin{pmatrix} -i\chi & 0 & 0 \\ 0 & -i\chi & 0 \\ 0 & 0 & -i\chi_z \end{pmatrix} ; \begin{pmatrix} i\chi & 0 & 0 \\ 0 & i\chi & 0 \\ 0 & 0 & i\chi_z \end{pmatrix}$$

$$\begin{pmatrix} \kappa_{11} & \kappa_{12} \\ \kappa_{21} & \kappa_{22} \end{pmatrix} \begin{pmatrix} D_1 \\ D_2 \end{pmatrix} = - \begin{pmatrix} \chi_{11} & \chi_{12} - u \\ \chi_{21} + u & \chi_{22} \end{pmatrix} \begin{pmatrix} B_1 \\ B_2 \end{pmatrix}$$

$$\begin{pmatrix} \nu_{11} & 0 \\ 0 & \nu_{22} \end{pmatrix} \begin{pmatrix} B_1 \\ B_2 \end{pmatrix} = - \begin{pmatrix} \gamma_{11} & \gamma_{12} + u \\ \gamma_{21} - u & \gamma_{22} \end{pmatrix} \begin{pmatrix} D_1 \\ D_2 \end{pmatrix}$$

$$\begin{pmatrix} \kappa_{11} & \kappa_{12} \\ \kappa_{21} & \kappa_{22} \end{pmatrix} \begin{pmatrix} D_1 \\ D_2 \end{pmatrix} = \begin{pmatrix} -i\chi_{11} & -u \\ u & -i\chi_{22} \end{pmatrix} \begin{pmatrix} \frac{1}{\nu_{11}}i\chi_{11} & \frac{1}{\nu_{11}}u \\ -\frac{1}{\nu_{22}}u & \frac{1}{\nu_{22}}i\chi_{22} \end{pmatrix} \begin{pmatrix} D_1 \\ D_2 \end{pmatrix}$$

$$= \begin{pmatrix} \frac{1}{\nu_{22}}u^2 + \frac{1}{\nu_{11}}\chi_{11}^2 & -i(\frac{\chi_{11}}{\nu_{11}} + \frac{\chi_{22}}{\nu_{22}})u \\ i(\frac{\chi_{11}}{\nu_{11}} + \frac{\chi_{22}}{\nu_{22}})u & \frac{1}{\nu_{11}}u^2 + \frac{1}{\nu_{22}}\chi_{22}^2 \end{pmatrix}$$

$$\begin{pmatrix} \frac{1}{\nu_{22}}u^2 + \frac{1}{\nu_{11}}\chi_{11}^2 - \kappa_{11} & -i(\frac{\chi_{11}}{\nu_{11}} + \frac{\chi_{22}}{\nu_{22}})u - \kappa_{12} \\ i(\frac{\chi_{11}}{\nu_{11}} + \frac{\chi_{22}}{\nu_{22}})u - \kappa_{12} & \frac{1}{\nu_{11}}u^2 + \frac{1}{\nu_{22}}\chi_{22}^2 - \kappa_{22} \end{pmatrix} \begin{pmatrix} D_1 \\ D_2 \end{pmatrix} = 0$$

$$(\frac{1}{\nu_{22}}u^2 + \frac{1}{\nu_{11}}\chi_{11}^2 - \kappa_{11})(\frac{1}{\nu_{11}}u^2 + \frac{1}{\nu_{22}}\chi_{22}^2 - \kappa_{22}) - (\frac{\chi_{11}}{\nu_{11}} + \frac{\chi_{22}}{\nu_{22}})^2 u^2 - \kappa_{12}^2 = 0$$

$$\frac{1}{\nu_{11}\nu_{22}}u^4 + -[\frac{\kappa_{11}}{\nu_{11}} + \frac{\kappa_{22}}{\nu_{22}} + 2\frac{\chi_{11}}{\nu_{11}}\frac{\chi_{22}}{\nu_{22}}]u^2 + (\frac{1}{\nu_{11}}\chi_{11}^2 - \kappa_{11})(\frac{1}{\nu_{22}}\chi_{22}^2 - \kappa_{22}) - \kappa_{12}^2 = 0$$

$$u^4 - [\nu_{22}\kappa_{11} + \nu_{11}\kappa_{22} + 2\chi_{11}\chi_{22}]u^2 + (\nu_{11}\kappa_{11} - \chi_{11}^2)(\nu_{22}\kappa_{22} - \chi_{22}^2) - \nu_{11}\nu_{22}\kappa_{12}^2 = 0$$

$$\theta = 0, \kappa_{12} = 0 \Rightarrow \begin{pmatrix} u^2 + \chi^2 - \nu\kappa & -i2\chi u \\ i2\chi u & u^2 + \chi^2 - \nu\kappa \end{pmatrix} \begin{pmatrix} D_1 \\ D_2 \end{pmatrix} = 0$$

$$\theta = \pi, \kappa_{12} = 0 \Rightarrow \begin{pmatrix} u^2 + \chi^2 - \nu\kappa & -i2\chi u \\ i2\chi u & u^2 + \chi^2 - \nu\kappa \end{pmatrix} \begin{pmatrix} D_1 \\ D_2 \end{pmatrix} = 0$$

— END OF EXAMPLE 3.3.11 —

H. Waves in Nonlinear Media

Consider a nonlinear medium characterized by the constitutive relation

$$\overline{D}(\overline{r},t) = \epsilon_0\overline{E}(\overline{r},t) + \overline{P}(\overline{r},t) \qquad (3.3.103a)$$

with the i th component of $\overline{P}$

$$P_i = \chi_{ij}E_j + 2\chi_{ijk}E_jE_k + 4\chi_{ijkl}E_jE_kE_l + \cdots \qquad (3.3.103b)$$

We have studied in previous sections the linear term χ_{ij}. The second-order nonlinear term χ_{ijk} is responsible for the phenomena of second-harmonic generation, and parametric amplification and oscillation. The third-order nonlinear term χ_{ijkl} gives rise to the effects of third-harmonic generation, Raman and Brillouin scattering, self-focusing, and phase conjugation.

The space-time dependent Maxwell equations in source-free regions read

$$\nabla \times \overline{E}(\overline{r},t) = -\frac{\partial}{\partial t}\overline{B}(\overline{r},t) \qquad (3.3.104a)$$

$$\nabla \times \overline{H}(\overline{r},t) = \frac{\partial}{\partial t}\overline{D}(\overline{r},t) \qquad (3.3.104b)$$

Specializing to one dimension by letting $\partial/\partial x = \partial/\partial y = 0$, we obtain the wave equation for the i th component of $\overline{E}$

$$\frac{\partial^2}{\partial z^2}E_i - \mu_0\epsilon_0\frac{\partial^2}{\partial t^2}E_i - \mu_0\frac{\partial^2}{\partial t^2}P_i = 0 \qquad (3.3.105)$$

We assume plane wave solutions of frequency dependence ω_1, ω_2, and ω_3.

$$E_{1i}(z,t) = \frac{1}{2}\left\{E_{1i}(z)e^{i(k_1z-\omega_1 t)} + c.c.\right\} \qquad (3.3.106a)$$

$$E_{2j}(z,t) = \frac{1}{2}\left\{E_{2j}(z)e^{i(k_2z-\omega_2 t)} + c.c.\right\} \qquad (3.3.106b)$$

$$E_{3k}(z,t) = \frac{1}{2}\left\{E_{3k}(z)e^{i(k_3z-\omega_3 t)} + c.c.\right\} \qquad (3.3.106c)$$

where $k_l = \omega_l(\mu_0\epsilon_l)^{1/2}$ with $l = 1,2,3$ and $c.c.$ denotes complex conjugate. When $\overline{P} = 0$, the amplitudes $E_{1i}(z), E_{2j}(z)$, and $E_{3k}(z)$ will be independent of z.

Second-Harmonic Generation (SHG)

Consider only the second-order nonlinear term χ_{ijk}. For the electric fields at ω_3 and ω_2, we have

$$P_i(z,t) = 2\chi_{ijk} \left\{ \frac{1}{2}E_{3j}e^{i(k_3z-\omega_3t)} + \frac{1}{2}E_{2j}e^{i(k_2z-\omega_2t)} + c.c. \right\}$$

$$\cdot \left\{ \frac{1}{2}E_{3k}e^{i(k_3z-\omega_3t)} + \frac{1}{2}E_{2k}e^{i(k_2z-\omega_2t)} + c.c. \right\} \quad (3.3.107)$$

For $\omega_1 = \omega_3 - \omega_2$, the nonlinear polarization is

$$P_{1i}(z,t) = \frac{1}{2}\chi_{ijk} \left\{ (E_{3j}E_{2k}^* + E_{3k}E_{2j}^*)e^{i(k_3-k_2)z-i(\omega_3-\omega_2)t} + c.c. \right\}$$

$$= \chi_{ijk} \left\{ E_{3j}E_{2k}^*e^{i(k_3-k_2)z-i(\omega_3-\omega_2)t} + c.c. \right\} \quad (3.3.108)$$

where use is made of the summation convention and the lossless condition of $\chi_{ijk} = \chi_{ikj}$.

We assume small variation of E_{1i} as a function of z such that $d^2E_{1i}/dz^2 \ll k_1 dE_{1i}/dz$. Letting $k_l = \omega_l(\mu_0\epsilon_l)^{1/2}$ and $\epsilon_{ij} = \epsilon_0 + \chi_{ij} = \epsilon_l\delta_{ij}$ for E_{li} components, we reduce the wave equation in (3.3.105) for $E_{1i}(z,t)$ to the following for the complex $E_{1i}(z)$

$$\frac{d}{dz}E_{1i}(z) - i\omega_1\sqrt{\frac{\mu_0}{\epsilon_1}}\chi_{ijk}E_{3j}(z)E_{2k}^*(z)e^{i(-k_1+k_3-k_2)z} = 0 \quad (3.3.109a)$$

Similarly, we find

$$\frac{d}{dz}E_{3j}(z) - i\omega_3\sqrt{\frac{\mu_0}{\epsilon_3}}\chi_{jkl}E_{1k}(z)E_{2l}(z)e^{i(k_1-k_3+k_2)z} = 0 \quad (3.3.109b)$$

$$\frac{d}{dz}E_{2k}^*(z) + i\omega_2\sqrt{\frac{\mu_0}{\epsilon_2}}\chi_{klm}E_{1l}(z)E_{3m}^*(z)e^{i(k_1-k_3+k_2)z} = 0 \quad (3.3.109c)$$

For second-harmonic generation (SHG), $\omega_1 = \omega_2$ and $\omega_3 = \omega_1 + \omega_2 = 2\omega_1$. Equation (3.3.109c) is merely the complex conjugate of (3.3.109a). Equation (3.3.109b), however, should be rederived from (3.3.107) which now takes the form

$$P_i(z,t) = 2\chi_{ijk} \left\{ \frac{1}{2}E_{1j}\,e^{i(k_1z-\omega_1t)} + c.c. \right\} \left\{ \frac{1}{2}E_{1k}\,e^{i(k_1z-\omega_1t)} + c.c. \right\}$$

which yield for $\omega_3 = 2\omega_1$,

$$P_{3i}(z, t) = \frac{1}{2}\chi_{ijk}\left\{E_{1j}E_{1k}\,e^{i2(k_1 z - \omega_1 t)} + c.c.\right\}$$

Comparison with (3.3.108) shows a factor of $1/2$ difference. The wave equation (3.3.105) that led to (3.3.109b) now becomes

$$\frac{d}{dz}E_{3j}(z) - i\frac{\omega_3}{2}\sqrt{\frac{\mu_0}{\epsilon_3}}\chi_{ikl}E_{1k}(z)E_{1l}(z)e^{-i\Delta kz} = 0 \qquad (3.3.110a)$$

Equation (3.3.109a) can be rewritten as

$$\frac{d}{dz}E_{1i}(z) - i\omega_1\sqrt{\frac{\mu_0}{\epsilon_1}}\chi_{ijk}E_{3j}(z)E_{1k}^*(z)e^{i\Delta kz} = 0 \qquad (3.3.110b)$$

where $\Delta k = k_3 - 2k_1$. Equation (3.3.110) forms the basis for the study of SHG. Notice that $k_3 = \omega_3(\mu_0\epsilon_3)^{1/2}$ and $k_1 = \omega_1(\mu_0\epsilon_1)^{1/2}$, E_{3j} is the jth component of the electric field at frequency ω_3, and E_{1i} is the ith component of the electric field at frequency ω_1.

Assuming weak second-harmonic generation such that the depletion of wave at ω_1 is small. In (3.3.110b) $E_{3j} \approx 0$ and the solution for E_{1i} is a constant. Let there be zero second-harmonic input at $z = 0$ such that $E_{3j}(0) = 0$, we find from (3.3.110a) the approximate solution

$$E_{3j}(z) = \frac{\omega_3}{2}\sqrt{\frac{\mu_0}{\epsilon_3}}\chi_{jkl}E_{1k}E_{1l}\frac{1 - e^{-i\Delta kz}}{\Delta k}$$

It is seen that the power generated at ω_3 contains the interference factor $\sin^2(\Delta kz/2)$. Thus the region of z for generation of second-harmonic wave should be smaller than the coherence length defined by $l_c = 2\pi/\Delta k$.

The coherence length is infinite and the second-harmonic generation is most effective when $\Delta k = 0$, which is known as the phase-matching condition. Notice that the electric field E_{3j} at ω_3 can be polarized differently from E_{1k} at ω_1. It suggests that the phase-matching condition can be met by using dispersive anisotropic media. For instance, E_{1k} can be an extraordinary wave at ω_1 and E_{3j} an ordinary wave at ω_3. The phase-matching condition

$$\Delta k = \omega_3\sqrt{\mu_0\epsilon_3(\omega_3)} - 2\omega_1\sqrt{\mu_0\epsilon_1(\omega_1)} = 0$$
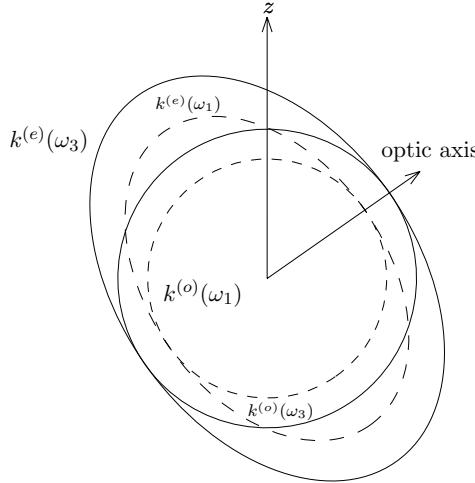
Figure 3.3.9 Phase matching.

with $\omega_3 = 2\omega_1$ gives $n_o(\omega_3) - n_e(\omega_1) = 0$ along the $\hat{z}$ direction, where $n_o(\omega_3) = c\sqrt{\mu\epsilon_3(\omega_3)}$ and $n_e(\omega_1) = c\sqrt{\mu\epsilon_1(\omega_1)}$. Let $k^{(o)}(\omega_3) = \omega\sqrt{\mu\epsilon_3(\omega_3)}$ and $k^{(e)}(\omega_1) = \omega\sqrt{\mu\epsilon_1(\omega_1)}$. We show in Figure 3.3.9 that the k surfaces at ω_1 and ω_3 can be oriented to intersect on the z axis to satisfy the phase-matching condition.

When the phase-matching condition of $\Delta k = 0$ is satisfied, (3.3.110) can be simplified by letting $E_{3j} = i\sqrt{\omega_3/n_o(\omega_3)}\,A_3$, $E_{1k} = \sqrt{\omega_1/n_e(\omega_1)}\,A_1$ and $\kappa = c\mu\chi_{211}\omega_1\sqrt{\omega_3}/n_e\sqrt{n_o}$. We obtain, assuming A_1 to be real,

$$\frac{d}{dz}A_3 = \frac{\kappa}{2}A_1^2 \qquad\qquad (3.3.111a)$$

$$\frac{d}{dz}A_1 = -\kappa A_1 A_3 \qquad\qquad (3.3.111b)$$

Summing (3.3.111a) multiplied by $2A_3$ and (3.3.111b) multiplied by A_1 yields

$$\frac{d}{dz}(A_1^2(z) + 2A_3^2(z)) = 0$$

Since there is no input at ω_3, $A_3(z = 0) = 0$, and we find $A_1^2(z) + 2A_3^2(z) = A_1^2(0)$. Equation (3.3.111a) becomes

$$\frac{d}{dz}A_3(z) = \frac{\kappa}{2}\left[A_1^2(0) - 2A_3^2(z)\right]$$
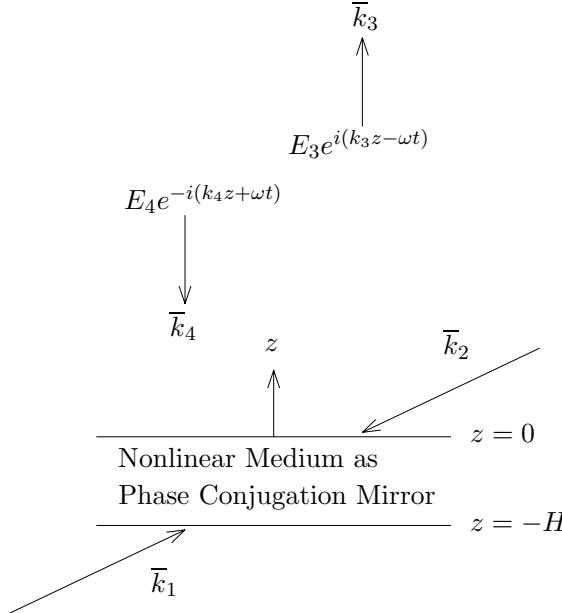
Figure 3.3.10 Generation of phase-conjugated waves.

and the solution is

$$A_3(z) = \frac{A_1(0)}{\sqrt{2}} \tanh \left[\frac{A_1(0)}{\sqrt{2}} \kappa z \right] \qquad (3.3.112)$$

Notice that as $z \to \infty$, $A_3 \to A_1(0)/\sqrt{2}$ and the power generated at the second-harmonic of $\omega_3 = 2\omega_1$ is equal to half of the input power at ω_1 after total conversion is complete. This satisfies energy conservation as the photon energy at ω_3 is $\hbar\omega_3 = 2\hbar\omega_1$.

Phase Conjugation

We now consider phase conjugation caused by four-wave mixing as a result of the third-order nonlinear term χ_{ijkl}. The objective is to generate an output wave at ω_3 which is the phase conjugate of an input wave at ω_4. A nonlinear medium is pumped by waves at ω_1 and ω_2 in opposite directions with $\overline{k}_1 = -\overline{k}_2$ [Fig. 3.3.10]. Assuming plane wave solutions, we find similar to (3.3.107) a nonlinear polarization due

to the electric fields at ω_1, ω_2 and ω_4,

$$P_i(z,t) = \frac{1}{2}\chi_{ijkl}$$
$$\cdot \left\{ E_{1j}e^{i(\overline{k}_1 \cdot \overline{r} - \omega_1 t)} + E_{2j}e^{i(\overline{k}_2 \cdot \overline{r} - \omega_2 t)} + E_{3j}e^{i(\overline{k}_4 \cdot \overline{r} - \omega_4 t)} + c.c. \right\}$$
$$\cdot \left\{ E_{1k}e^{i(\overline{k}_1 \cdot \overline{r} - \omega_1 t)} + E_{2k}e^{i(\overline{k}_2 \cdot \overline{r} - \omega_2 t)} + E_{3k}e^{i(\overline{k}_4 \cdot \overline{r} - \omega_4 t)} + c.c. \right\}$$
$$\cdot \left\{ E_{1l}e^{i(\overline{k}_1 \cdot \overline{r} - \omega_1 t)} + E_{2l}e^{i(\overline{k}_2 \cdot \overline{r} - \omega_2 t)} + E_{3l}e^{i(\overline{k}_4 \cdot \overline{r} - \omega_4 t)} + c.c. \right\}$$

$$(3.3.113)$$

Letting $\omega_1 = \omega_2 = \omega_4 = \omega$, $\overline{k}_1 = -\overline{k}_2$, and $\overline{k}_4 = -\hat{z}k$, we obtain for $\omega_3 = \omega_1 + \omega_2 - \omega_4$,

$$P_{3i}(z,t) = \frac{1}{2}\chi_{ijkl}E_{1j}E_{2k}E_{4l}^* \, e^{i\left[(\overline{k}_1 + \overline{k}_2)\cdot \overline{r} + kz - (\omega_1 + \omega_2)t + \omega_4 t\right]} + c.c.$$

$$= \frac{1}{2}\chi E_1 E_2 E_4^* \, e^{i(kz - \omega t)} + c.c. \qquad (3.3.114)$$

where we ignore the subscripts and set $\chi = 6\chi_{ijkl}$. The nonlinear polarization generates a wave $[\frac{1}{2}E_3(z)e^{i(kz-\omega t)} + c.c.]$ according to the wave equation (3.3.105) which now gives, ignoring the $\partial^2 E_3/\partial z^2$ term

$$ik\frac{d}{dz}E_3(z) = -\frac{1}{2}\omega^2 \mu_0 \chi E_1 E_2 E_4^* \qquad (3.3.115)$$

where $k = \omega(\mu_0\epsilon)^{1/2}$ with $\epsilon_{ij} = \epsilon_0 + \chi_{ij} = \epsilon\delta_{ij}$ and the second-order term $\chi_{ijk} = 0$.

The newly created E_3 wave will mix with E_1 and E_2 to generate the polarization

$$P_4(z,t) = \frac{1}{2}\chi E_1 E_2 E_3^* e^{-i(kz+\omega t)} + c.c. \qquad (3.3.116)$$

which interacts strongly with $E_4 e^{-i(kz+\omega t)}$. The wave equation for $E_4(z)$ gives rise to

$$-ik\frac{d}{dz}E_4(z) = -\frac{1}{2}\omega^2 \mu_0 \chi E_1 E_2 E_3^* \qquad (3.3.117)$$

Equations (3.3.116)–(3.3.117) are obtained by a process similar to (3.3.113)–(3.3.115).

Defining a coupling coefficient

$$\kappa = \frac{\omega}{2}\sqrt{\frac{\mu_0}{\epsilon}}\chi E_1 E_2$$

and noticing that $k = \omega(\mu_0\epsilon)^{1/2}$, we obtain from (3.3.115) and the complex conjugate of (3.3.117) the coupled equations

$$\frac{d}{dz}E_3(z) = i\kappa E_4^*(z) \qquad (3.3.118a)$$

$$\frac{d}{dz}E_4^*(z) = i\kappa^* E_3(z) \qquad (3.3.118b)$$

Given $E_4(0)$ and $E_3(-H)$, the solutions to (3.3.118) take the form

$$E_3(z) = \frac{\cos|\kappa|z}{\cos|\kappa|H}E_3(-H) - i\frac{\kappa\sin|\kappa|(z+H)}{|\kappa|\cos|\kappa|H}E_4^*(0) \quad (3.3.119a)$$

$$E_4^*(z) = i\frac{|\kappa|\sin|\kappa|z}{\kappa\cos|\kappa|H}E_3(-H) - \frac{\cos|\kappa|(z+H)}{\cos|\kappa|H}E_4^*(0) \quad (3.3.119b)$$

Let $E_3(-H) = 0$. The reflected wave $E_3(0)$ at $z = 0$ due to an input wave $E_4(0)$ is

$$E_3(0) = -i\left(\frac{\kappa}{|\kappa|}\tan|\kappa|H\right)E_4^*(0) \qquad (3.3.120)$$

Thus $E_3(0)$ is proportional to $E_4^*(0)$, the complex conjugate of $E_4(0)$.

Notice that the reflected wave is the conjugate of the incident wave in space but not in time. An incident wave with the pulse form $f(z+ct)$ will be of the form $f(z-ct)$ upon reflection from a conjugation mirror. Thus the reflected wave is the time reversal of the incident pulse. Furthermore if the input $E_3(0)$ is not a plane wave but has a complicated wavefront

$$E_4 = Re\left\{E_4(\bar{r})e^{-i(\omega t+kz)}\right\}$$

it follows that

$$E_3 = Re\left\{-i\left(\frac{\kappa}{|\kappa|}\tan|\kappa|H\right)E_4^*(\bar{r})e^{i(kz-\omega t)}\right\}$$

which is easily verified by modifying the above derivations on account of the linearity of the wave equations.

It is interesting to note that $|E_4(-H)| > |E_4(0)|$ and that for $\pi/4 < |\kappa|H < 3\pi/4$, $|E_3(0)| > |E_4(0)|$. The amplification of $E_4(-H)$ and the generation of $E_3(0)$ must be at the expense of the pump waves E_1 and E_2. In fact, as $|\kappa|H = \pi/2$, $|E_4(-H)/E_4(0)| \to \infty$ and $|E_3(0)/E_4(0)| \to \infty$ which gives rise to natural resonance without an input wave.

Exercises

Ex3.3.1

The dispersion relations for plane waves in homogeneous media can be derived in a number of different ways. For instance, making use of the constitutive relations in $\overline{E}\,\overline{H}$ representation

$$\overline{D} = \overline{\overline{\epsilon}} \cdot \overline{E} + \overline{\overline{\xi}} \cdot \overline{H}$$

$$\overline{B} = \overline{\overline{\mu}} \cdot \overline{H} + \overline{\overline{\zeta}} \cdot \overline{E}$$

we can eliminate the field vectors $\overline{D}$, $\overline{B}$ and $\overline{H}$ from the above constitutive relations and (3.3.21)–(3.3.22). Defining an operator $\overline{\overline{k}}$ such that $\overline{\overline{k}}\cdot\overline{A} = \overline{k}\times\overline{A}$ for any vector $\overline{A}$, we obtain

$$\left\{ \omega^2\overline{\overline{\epsilon}} + [\overline{\overline{k}} + \omega\overline{\overline{\xi}}] \cdot \overline{\overline{\mu}}^{-1} \cdot [\overline{\overline{k}} - \omega\overline{\overline{\zeta}}] \right\} \cdot \overline{E} = 0$$

For nontrivial solutions of $\overline{E}$, the determinant of the matrix operating on $\overline{E}$ must be equal to zero. Hence

$$\left| \omega^2\overline{\overline{\epsilon}} + [\overline{\overline{k}} + \omega\overline{\overline{\xi}}] \cdot \overline{\overline{\mu}}^{-1} \cdot [\overline{\overline{k}} - \omega\overline{\overline{\zeta}}] \right| = 0$$

This is the dispersion relation relating the components of $\overline{k}$ and the angular frequency ω. It reduces to the isotropic case in a straightforward manner. However, in the cases of non-isotropic media, the study of the wave behavior becomes extremely involved. It is the kDB system that provides a systematic approach in facilitating the interpretation of the various plane wave characteristics in more general media.

Problems

P3.3.1

In a uniaxial crystal the ray vectors for ordinary and extraordinary rays make an angle α. The extraordinary ray vector $\overline{s}_e$ is normal to the extraordinary wave surface:

$$\overline{s}_e // \frac{1}{2}\nabla_k(\omega^2\mu) = \hat{\rho}\kappa_z k_\rho + \hat{z}\kappa k_z = \hat{\rho}\kappa_z k \sin\theta + \hat{z}\kappa k \cos\theta$$

The ordinary ray vector $\overline{s}_o$ is normal to the k-surface of the ordinary wave, where $\omega^2\mu = \kappa(k_\rho^2 + k_z^2)$:

$$\overline{s}_o // \frac{1}{2}\nabla_k(\omega^2\mu) = \hat{\rho}\kappa k \sin\theta + \hat{z}\kappa k \cos\theta$$

Show that the angle α between $\overline{s}_o$ and $\overline{s}_e$ is determined by

$$\cos\alpha = \frac{\overline{s}_o \cdot \overline{s}_e}{|\overline{s}_o|\ |\overline{s}_e|} = \frac{\kappa_z \sin^2\theta + \kappa\cos^2\theta}{(\kappa_z^2 \sin^2\theta + \kappa^2 \cos^2\theta)^{1/2}}$$

Find θ_0 when the maximum α, $\alpha_{\max}$, occurs and determine $\cos\alpha_{\max}$. When $\sin\theta_0 = \sqrt{\frac{\kappa}{\kappa_z}}\cos\theta_0$, determine $\cos\alpha_{\max}$.

P3.3.2

In a negative uniaxial medium, a wave vector $\overline{k}$ makes an angle θ with the optic axis. Determine whether the direction of the Poynting's vector in the negative uniaxial medium is larger or smaller than θ.

P3.3.3

An electromagnetic wave propagates in a uniaxial medium with

$$\overline{\overline{\varepsilon}} = \begin{bmatrix} \varepsilon_0 & 0 & 0 \\ 0 & \varepsilon_0 & 0 \\ 0 & 0 & \varepsilon_z \end{bmatrix} \quad \text{and} \quad \mu = \mu_0.$$

(a) Let $\varepsilon_z = 4\varepsilon_0$. An electromagnetic wave $\overline{E} = E_0(\hat{x} + \beta\hat{z})$ (at $y = 0$) propagates along $+\hat{y}$ axis.
  (i) If the field $\overline{E}$ is circularly polarized at $y = 0$, find β.
  (ii) At $y = y_0$, $\overline{E}$ is linearly polarized. Find the smallest y_0 when $\omega = 2\pi \times 10^8$ (rad/sec).
(b) The electric field $\overline{E}$ and vector $\overline{k}$ are both in the x-z plane.
  (i) If the angle between vector $\overline{k}$ and axis $\hat{z}$ is θ, what is the complex Poynting vector $\overline{S}$? (Hint: solve this problem in kDB system)
  (ii) What is the angle α between the Poynting vector $\overline{S}$ and vector $\overline{k}$?
  (iii) What is the angle θ when the angle α becomes maximum?

P3.3.4

Consider a conductive uniaxial medium with

$$\bar{\bar{\epsilon}} = \begin{pmatrix} \epsilon & 0 & 0 \\ 0 & \epsilon & 0 \\ 0 & 0 & \epsilon_z \end{pmatrix} ; \qquad \bar{\bar{\sigma}} = \begin{pmatrix} \sigma & 0 & 0 \\ 0 & \sigma & 0 \\ 0 & 0 & \sigma_z \end{pmatrix}$$

Find dispersion relations for this medium. Explain the operation of a polaroid with this model by assuming $\sigma_z/\sigma \ll 1$. Show that a piece of polaroid turns any wave into a linearly polarized wave.

P3.3.5

The *Fresnel ellipsoid* is defined for an anisotropic medium by

$$\epsilon_{ij} x_i x_j = 1$$

where ϵ_{ij} is expressed in the principal coordinates. The inverse of the permittivity tensor $\bar{\bar{\epsilon}}$ is $\bar{\bar{\kappa}}$, which is called the impermittivity tensor. If we define an ellipsoid in terms of $\bar{\bar{\kappa}}$ instead of $\bar{\bar{\epsilon}}$ in the principal coordinate system of the medium and write

$$\kappa_{ij} x_i x_j = 1$$

we have a tensor ellipsoid. Construct the Fresnel ellipsoid and the tensor ellipsoid for a biaxial medium. Expressed in the principal coordinate system, the principal refractive indices are usually used in these definitions by replacing ϵ_{ij} with $n_i^2 \delta_{ij}$ and κ_{ij} with δ_{ij}/n_i^2, in which case the tensor ellipsoid is also called an index ellipsoid or a reciprocal ellipsoid.

P3.3.6

Consider a slab of material of thickness d, as shown in Figure P3.3.6.1, with the following permittivity and conductivity tensors:

$$\bar{\bar{\epsilon}} = \begin{bmatrix} \epsilon_x & 0 & 0 \\ 0 & \epsilon_y & 0 \\ 0 & 0 & \epsilon_z \end{bmatrix} \qquad \bar{\bar{\sigma}} = \begin{bmatrix} 0 & 0 & 0 \\ 0 & 0 & 0 \\ 0 & 0 & \sigma_z \end{bmatrix}$$
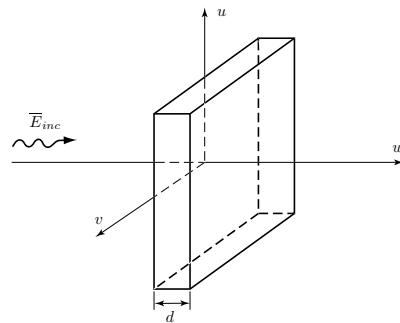
Figure P3.3.6.1

where $\epsilon_x = 12\epsilon_o$, $\epsilon_y = \epsilon_o$, $\epsilon_z = 4\epsilon_o$, and $\mu = \mu_o$. The conductivity for polarized wave in z -direction is $\sigma_z = 0.2\epsilon_o\omega$ mho/meter.

This material can be used to make a polarizer, a quarter-wave plate, and a half-wave plate. Let the incident electric field propagate in the $\hat{w}$ direction.

Polarizer:

(a) Assign x , y , z to u , v , w (not necessarily in that order) so that, for any arbitrarily-polarized incident electric field and sufficiently thick slab, the transmitted field is linearly polarized.

(b) Determine the minimum thickness d in free space wavelength such that the undesirable component of the incident field is attenuated by $1/e$.

Quarter-wave plate:

(c) Assign x , y , z to u , v , w (not necessarily in that order) so that, for a given linearly polarized incident electric field, the transmitted field is circularly polarized. Specify the axes so that there is no power absorption. Give an expression for an incident electric field such that, given the correct thickness, the transmitted electric field is circularly polarized.

(d) For the quarter-wave plate and the incident field of part (c), determine the smallest thickness d in free space wavelength such that the transmitted electric field is left-hand circularly polarized.

Half-wave plate:

(e) Assign x , y , z to u , v , w (not necessarily in that order) so that, for a given linearly polarized incident electric field, the transmitted field may be polarized in a direction orthogonal to the incident wave.

(f) For the half-wave plate of part (e), determine the minimum thickness d in free space wavelength.

P3.3.7

Due to the Earth's magnetic field, the ionosphere becomes a gyrotropic medium. Radio wave propagation through the ionosphere is affected by Faraday rotation. The temporal variations of electron density profile in the ionosphere impose a problem on the antenna design for satellite communications if linearly polarized waves are to be used.

A linearly polarized wave at a microwave frequency f is transmitted down to Earth at an angle θ with respect to nadir, and has a small angular separation ϕ with the direction of the Earth's magnetic field $\overline{H}_e$.

(a) Assuming that the electron density N and the Earth's magnetic field H_e are functions of height h , show that the total amount of the Faraday rotation is approximately

$$\Omega = \frac{\eta e^3 \mu_0}{8\pi^2 m^2 f^2} \int M(h)N(h)\, dh$$

where $\eta = \sqrt{\mu_0/\epsilon_0} = 377\,\Omega$, $M = H_e \sec\theta \cos\phi$, and e and m are the electron charge and mass respectively. In the presence of the magnetic field

$$\kappa = \frac{1}{\epsilon_0}\left[\frac{1 - \omega_p^2/\omega^2 - \omega_c^2/\omega^2}{(1 - \omega_p^2/\omega^2)^2 - \omega_c^2/\omega^2}\right] \qquad \kappa_g = \frac{1}{\epsilon_0}\left[\frac{\omega_c\omega_p^2/\omega^3}{(1 - \omega_p^2/\omega^2)^2 - \omega_c^2/\omega^2}\right]$$

where $\kappa \gg \kappa_g$.

In the above derivation, assume that the operating frequency is much higher than the plasma and cyclotron frequencies and neglect (i) loss due to collisions between particles, (ii) intermediate reflections due to the inhomogeneous nature of the ionosphere, and (iii) splitting of the ordinary and the extraordinary rays.

(b) Assume that the ionosphere has a uniform electron density of $10^{11}/\mathrm{m}^3$, and the Earth's magnetic field makes a $60°$ angle with respect to nadir and has a uniform intensity of $H_e = 50$ amp/m (corresponding to a B field of 0.628 Gauss or 0.628×10^{-4} Tesla). Find the amount of the Faraday rotation for a wave of frequency 1.4 GHz transmitted from 1000 km high down to the Earth along the direction of $\overline{H}_e$.

P3.3.8

A biisotropic medium (Tellegen medium) has the constitutive relation

$$\overline{D} = \epsilon \overline{E} + \xi \overline{H}$$
$$\overline{B} = \xi \overline{E} + \mu \overline{H}$$

Find the constitutive relation in the DB -representation. Use the kDB system to determine the dispersion relations for the biisotropic medium. Discuss your results.

P3.3.9

In biaxial media, the three principal dielectric constants are different. In the principal coordinate system,

$$\overline{\overline{\kappa}} = \begin{pmatrix} \kappa_x & 0 & 0 \\ 0 & \kappa_y & 0 \\ 0 & 0 & \kappa_z \end{pmatrix} \qquad \overline{\overline{\nu}} = \nu \overline{\overline{I}} \qquad \overline{\overline{\chi}} = \overline{\overline{\gamma}} = 0$$

The $\overline{\overline{\kappa}}$ matrix is also called the impermittivity tensor. To relate to the permittivities, we note that $\kappa_x = 1/\epsilon_x$, $\kappa_y = 1/\epsilon_y$, and $\kappa_z = 1/\epsilon_z$. The permeability ν is the reciprocal of μ .

(a) Find the constitutive parameters in the kDB system.

(b) Determine the phase velocities of the characteristic waves and show that

$$\frac{D_2}{D_1} = \tan \psi \quad \text{or} \quad -\cot \psi \qquad \text{with} \qquad \tan 2\psi = \frac{2\kappa_{12}}{\kappa_{11} - \kappa_{22}}$$

The velocities of both waves are functions of θ and ϕ . Show that none of the $\overline{E}$ vectors for the two waves lies on the DB plane and the $\overline{E}$ vector has a component in the $\overline{k}$ direction. Thus, the energy propagation directions are different from the $\overline{k}$ direction and the two characteristic waves are both extraordinary waves.

P3.3.10

The direction of propagation of a wave becomes ambiguous in a complex medium. From Poynting's theorem, we have learned that the energy flow of

an electromagnetic field is governed by Poynting's vector, $\overline{S} = \overline{E} \times \overline{H}$. The Poynting's vector divided by the total electromagnetic energy is referred to as the *energy velocity*. The direction of the energy velocity is thus perpendicular to both $\overline{E}$ and $\overline{H}$. We have also learned that the direction of the phase velocity is along $\overline{k}$, which is perpendicular to both $\overline{D}$ and $\overline{B}$. In a bianisotropic medium, the directions of the energy velocity and the phase velocity $\overline{k}$ do not, in general, coincide.

The Poynting power-flow direction is characterized by the ray vector $\overline{s}$, which is perpendicular to both $\overline{E}$ and $\overline{H}$.

$$\overline{s} \cdot \overline{E} = 0 \qquad \overline{s} \cdot \overline{H} = 0$$

We define the magnitude of $\overline{s}$ by $\overline{s} \cdot \overline{k} = 1$, which has the dimension of length.

(a) Use the vector identity $\overline{s} \times (\overline{k} \times \overline{E}) = \overline{k}(\overline{s} \cdot \overline{E}) - (\overline{k} \cdot \overline{s})\overline{E}$ to show that

$$\overline{s} \times \overline{B} = -\overline{E}/\omega \qquad \overline{s} \times \overline{D} = \overline{H}/\omega$$

(b) For a uniaxial medium, define ray surfaces similar to the wave surfaces. Show that for the extraordinary wave

$$s_x^2 + s_y^2 + \frac{\epsilon}{\epsilon_z} s_z^2 = \frac{1}{\omega^2 \mu \epsilon_z}$$

(c) Since $\overline{s}$ is along the direction of energy velocity, $\overline{s} \cdot \delta\overline{k} = 0$; namely the normal to the wave surface gives the direction of the corresponding ray vector. Prove that the normal to the ray surface gives the direction of the corresponding $\overline{k}$ vector.

(d) The phase of a wave along a ray can be written as

$$\psi = \int \overline{k} \cdot d\overline{l} = \int \overline{k} \cdot \frac{\overline{s}}{s} \, dl = \frac{l}{s}$$

where l denotes the length of the segment along the ray path. In geometrical optics, the dimensionless quantity $\psi/(\omega/c)$ is the eikonal of the wave. Show that the ray surface describes a constant-phase surface.

P3.3.11

A signal wave at frequency ω_1 can be amplified by a nonlinear medium with an intense pump wave at ω_3. This process of parametric amplification by the second-order nonlinearity generates an idler wave at $\omega_2 = \omega_3 - \omega_1$.

(a) Assuming $E_{3j}(z) = E_{3j}(0)$, show that (3.3.109) can be written as

$$\frac{dA_1}{dz} = -i\frac{\alpha}{2} A_2^* e^{-i\Delta k z}$$
$$\frac{dA_2^*}{dz} = i\frac{\alpha}{2} A_1 e^{i\Delta k z}$$

Determine α and Δk.

(b) Let $A_2(0) = 0$ and assume that the phase-matching condition $\Delta k = 0$ is satisfied. Show that

$$A_1(z) = A_1(0)\cosh\frac{\alpha}{2}z$$

$$A_2^*(z) = iA_1(0)\sinh\frac{\alpha}{2}z$$

(c) Derive the Manley-Rowe relation

$$-\frac{\Delta P_3}{\omega_3} = \frac{\Delta P_2}{\omega_2} = \frac{\Delta P_1}{\omega_1}$$

where ΔP_l with $l = 1, 2, 3$ are the change of power between the input and output. For each photon added to the signal wave, there is a photon added to the idler wave, and a photon removed from the pump wave. Is energy conserved?

Answers

P3.1.1

The two numbers are $5 + i10$ and $5 - i10$.

P3.1.2

Set up a complex coordinate with T_1 and T_2 on the real axis, T_1 at the origin and T_2 at a distance a from T_1. Relative to Γ, $A = i\Gamma$, and $B - a = -i(\Gamma - a)$. The treasure is located at $M = (A+B)/2 = a/2 + ia/2$.

P3.1.3

(a) No, $\overline{E}_1 \times \overline{E}_2 = 0$ and $\overline{E}_1(t) \times \overline{E}_2(t) \neq 0$
(b) Yes, $\overline{E}_1 \cdot \overline{E}_2 = 0$ and $\overline{E}_1(t) \cdot \overline{E}_2(t) = 0$.

P3.1.4

$$\overline{E}(\overline{r}) = [\hat{x} + \hat{y}i]\, e^{ikz}$$

P3.1.5

(a) $\overline{E} \cdot \overline{k} = 0 \Rightarrow A = -1$.
(b) $\overline{k} = (\hat{y} + \hat{z})k/\sqrt{2}$.
(c) The wave field is left handed circular polarized (l.h.c.p.).
(d) $k = \sqrt{\omega^2 - 4\pi^2 \times 10^{12}}/c = \omega\sqrt{\mu_o \epsilon} \Rightarrow \epsilon = \epsilon_o \left(1 - 4\pi^2 \times 10^{12}/\omega^2\right)$.
(e) $\overline{H} = \frac{k}{\omega\mu_o}\{\frac{1}{\sqrt{2}}[\hat{y} - \hat{z}]\sin\left[\frac{k}{\sqrt{2}}(y+z) - \omega t\right] + \hat{x}\cos\left[\frac{k}{\sqrt{2}}(y+z) - \omega t\right]\}$
(f) $\overline{S} = \frac{k}{\omega\mu_o\sqrt{2}}(\hat{y} + \hat{z})$
(g) $\epsilon = \epsilon_o\left(1 - \omega_p^2/\omega^2\right) \Rightarrow \omega_p = 2\pi f_p = 2\pi \times 10^6 \Rightarrow f_p = 10^6$ Hz.
(h) $k = \pi/300$, $v_p = 3\sqrt{5} \times 10^8$ m/s, $v_g = 3 \times 10^8/\sqrt{5}$ m/s
(i) $\overline{E} = \left[-\hat{x}\sin\omega t + \frac{1}{\sqrt{2}}(A\hat{y} + \hat{z})\cos\omega t\right] e^{-\frac{k_I}{\sqrt{2}}(y+z)}$, where $k_I = \pi/300$.
(j) $v_g = 0$, $<S> = 0$.

P3.1.6

(a) $\overline{E}_1(\overline{r}) = \hat{x}E_0 e^{iky} \Rightarrow \overline{E}_1(y,t) = \text{Re}\left[\hat{x}e^{iky}e^{-i\omega t}\right] = \hat{x}E_0\cos(\omega t - ky)$
(b) $\overline{H}_1(\overline{r}) = -\hat{z}\frac{E_0}{\eta}e^{iky} \quad \eta = \sqrt{\frac{\mu}{\varepsilon}}$
(c) $\overline{S} = \langle\overline{S}\rangle = \hat{y}\frac{|E_0|^2}{2\eta}$
(d) $\overline{E}_2(\overline{r}) = -\hat{x}E_0 e^{-iky}$
(e) $\overline{E}_1(y) + \overline{E}_3(y) = \hat{x}E_0\left(e^{iky} + e^{-iky}\right) = \hat{x}2E_0\cos ky$
$\overline{E}(y,t) = \hat{x}2E_0\cos ky\cos\omega t$
(f) $\langle\overline{S}\rangle = \frac{1}{2}\text{Re}\left[\hat{x}E_0\left(e^{iky} + e^{-iky}\right) \times -\hat{z}\frac{E_0^*}{\eta}\left(e^{-iky} - e^{iky}\right)\right] = 0$

P3.1.7

Since $\delta_p = \sqrt{2/\omega\mu\sigma} \sim 1/\sqrt{\omega}$, we need to design our enclosure at the lowest frequency of interest - 10 kHz. Here, for copper, $f = 10$ kHz $\rightarrow \omega =$

$2\pi \times 10^4$ rad/s, $\mu = \mu_0 = 4\pi \times 10^{-7}$ H/m, $\sigma = 5.8 \times 10^7$ mho/m so that the skin depth is $\delta_p = 6.6 \times 10^{-4}$ m. Thus, our enclosure (five skin depths thick) must be at least 3.3 mm thick.

P3.1.8

(a) For bottom round steak, $k_I = \frac{2\pi \times 2.5 \times 10^9}{3 \times 10^8}\sqrt{40}\left[\frac{1}{2}\left(\sqrt{1+0.36^2}-1\right)\right]^{1/2} = 58.7(m^{-1})$, $d_p = \frac{1}{k_I} = \frac{1}{58.7}$ m $= 1.7$ cm

For polystyrene foam, $d_p \approx \frac{2}{\sigma\eta} = \frac{2\sqrt{1.03}}{4\times10^{-6}\times377} = 1346.0$ m

(b) $\omega < 0.1 \times \frac{\sigma}{\epsilon} = 5.65$(rad/sec), or $f_{max} = \frac{\omega}{2\pi} = 0.899$(MHz)

(c) $d_p \approx \sqrt{\frac{2}{2\pi \times 10^8 \times 4\pi \times 10^{-7} \times 3.54 \times 10^7}} = 8.46 \times 10^{-6}$(m); $5d_p = 4.24 \times 10^{-5}$(m). Thus ordinary aluminum foil with thickness 10^{-3}(inch) $= 2.54 \times 10^{-5}$(m) is not thick enough.

(d)

   (1) For $f = 100$ Hz, $d_p \approx \sqrt{\frac{2}{\omega\mu_o\sigma}} = \sqrt{\frac{2}{2\pi \times 100 \times 4\pi \times 10^{-7} \times 4}} = 25.2$ m

   (2) For $f = 5$ MHz, $d_p \approx \sqrt{\frac{2}{\omega\mu_o\sigma}} = \sqrt{\frac{2}{2\pi \times 5 \times 10^6 \times 4\pi \times 10^{-7} \times 4}} = 0.11$ m

(e) $d_p \approx \sqrt{2/\omega\mu_o\sigma} = 7.96$(m), $e^{-2k_I z} = e^{-2\times\frac{100}{7.96}} = 1.22 \times 10^{-11} = -109.1$(dB).

P3.1.9

(a) $v_g = \frac{d\omega}{dk} = \frac{k}{\omega\mu_o\epsilon_o} = c\sqrt{1 - \frac{\omega_p^2}{\omega^2}}$

(b) For the flash light, $\omega = 2\pi c/\lambda = \frac{2\pi \times 3 \times 10^8}{0.5 \times 10^{-6}} = 2\pi \times \left(6 \times 10^8 \text{MHz}\right)$

$v_g = c\sqrt{1 - \frac{\omega_p^2}{\omega^2}} = c\sqrt{1 - \frac{8^2}{(6\times10^8)^2}} = c\left(1 - 8.89 \times 10^{-17}\right) \approx 3.0 \times 10^8$m/s

For the radio pulse, $\omega = 2\pi \times (10\text{MHz})$, $v_g = c\sqrt{1 - \frac{8^2}{10^2}} = 0.6c \approx 1.8 \times 10^8$m/s. So the time difference after traveling $100km$ is $\delta t = d\left(\frac{1}{v_{g1}} - \frac{1}{v_{g2}}\right) = 100 \times 10^3\left(\frac{1}{0.6c} - \frac{1}{c}\right) \approx 2.22 \times 10^{-4}$(sec).

P3.1.10

(a) For $\omega \gg \omega_p$, $v_p = \frac{\omega}{k} \approx c\left(1 + \frac{\omega_p^2}{2\omega^2}\right)$, $v_g = \frac{d\omega}{dk} \approx c\left(1 - \frac{\omega_p^2}{2\omega^2}\right)$, where $\omega_p = \sqrt{Ne^2/m_e\epsilon_0}$ is the plasma frequency with $e = 1.6022 \times 10^{-19}$ C and $m_e = 9.1096 \times 10^{-31}$ kg. N is the electron density in m^{-3}. From the above results, we see that $v_g < c$ and $v_p > c$.

(b) The group time delay is

$$t = \frac{1}{v_g} = \frac{dk}{d\omega} = \frac{1}{c}\left(1 - \frac{\omega_p^2}{2\omega^2}\right)^{-1/2} \approx \frac{1}{c}\left(1 + \frac{\omega_p^2}{2\omega^2}\right)$$

The time difference for two RF pulses with different frequencies travelling for a distance L is

$$\Delta t = t_1 - t_2 = L\left(\frac{1}{v_{g1}} - \frac{1}{v_{g2}}\right) = \frac{L}{2c}\omega_p^2\left(\frac{1}{\omega_1^2} - \frac{1}{\omega_2^2}\right)$$

Since $\omega_p^2 = \frac{Ne^2}{m\epsilon_o}$, we have $N = \frac{m\epsilon_o\omega_p^2}{e^2} = 2cm\epsilon_o\Delta t/e^2L\left(\frac{1}{\omega_1^2} - \frac{1}{\omega_2^2}\right)$.

For $\Delta t = 1.5\,\text{sec}$, $m = 9.11 \times 10^{-31}$ kg, $\epsilon_o = 8.85 \times 10^{-12}$ F/m, $c = 3 \times 10^8$ m/s, $L = 6 \times 10^{19}$ m, $\omega_1 = 2\pi \times 110 \times 10^6$ rad/sec, $\omega_2 = 2\pi \times 115 \times 10^6$ rad/sec, and $e = 1.60 \times 10^{-19}$ C, we get $N = 2.65 \times 10^4 m^{-3}$.

P3.1.11

(a) The reflected and transmitted powers are

$$P_r = \frac{1}{2}Re(\overline{E}_r \times \overline{H}_r^*) \cdot \hat{n} = \frac{1}{2\eta}\frac{1}{2}E_0^2 = \frac{1}{2}P_i$$

$$P_t = \frac{1}{2}Re(\overline{E}_t \times \overline{H}_t^*) \cdot \hat{n} = \frac{1}{2\eta}\frac{1}{2}E_0^2 = \frac{1}{2}P_i$$

(b) Assume that the two reflecting mirrors are identical and have the same reflection coefficient of $e^{i\phi_0}$. Let $E_2 = 0$, we find

$$\phi_t - \phi_r = \frac{\pi}{2} + n\pi$$

Since the transmitted and reflected fields acquire a phase difference of $\pi/2$ due to the semi-transparent mirror, the two fields destructively interfere and do not reach the detector.

(c)

$$\overline{E}_1 = \overline{E}_0\frac{e^{-i\phi_t}}{\sqrt{2}}e^{ik_pl_1}e^{i\phi_0}e^{ik_0l_3}\frac{e^{-i\phi_r}}{\sqrt{2}} + \overline{E}_0\frac{e^{-i\phi_r}}{\sqrt{2}}e^{ik_0l_3}e^{i\phi_0}e^{ik_0l_1}\frac{e^{-i\phi_t}}{\sqrt{2}}$$

$$= \overline{E}_0e^{i(\phi_0-\phi_r-\phi_t+k_0l_3)}e^{i\frac{1}{2}(k_0l_1+k_pl_1)}\cos\left(\frac{k_0 - k_p}{2}l_1\right)$$

$$\frac{k_0 - k_p}{2}l_1 = \frac{k_0}{2}(1 - \sqrt{1 - \frac{\omega_p^2}{\omega^2}}) \approx k_0\frac{\omega_p^2}{4\omega^2}l_1 = k_0\frac{Ne^2l_1}{4\omega^2m\epsilon_0} = \phi$$

as $\omega_p \ll \omega$, where $\omega_p^2 = Ne^2/m\epsilon_0$. We find $P_1 = P_i\cos^2\phi$. Using the relation $\phi_t - \phi_r = \frac{\pi}{2} + n\pi$, we have $P_2 = P_i\sin^2\phi$. We thus have $P_1 + P_2 = P_i$, which satisfies energy conservation. The electron density N of the plasma can be determined from ϕ.

P3.1.12

(a) n is the number of rods and r_o is the radius of the rod.

(b) From Faraday's law $\oint d\bar{\ell} \cdot \overline{E} = i\omega\mu_o \iint d\overline{S} \cdot \mu_o \overline{H}$, we have $2\pi r E = i\omega\mu_o 2\pi r \int_a^r dr J/2\pi r = i\omega\mu_o r J \ln(r/a)$. Thus

$$m_{eff} = inq^2 E/\omega J = \pi r^2 n q^2 \frac{\mu_o}{2\pi} \ln \frac{r}{a}$$

P3.2.1

For copper, $\sigma \approx 5.8 \times 10^7$ mho/m. For silicon, $\sigma \approx 1.6 \times 10^{-3}$ mho/m.

P3.2.2

(a) For very large N, $d_p = \frac{1}{k_I} = \sqrt{\frac{m}{Ne^2\mu_o}}$

(b) For electron, $m = 9.1 \times 10^{-31}$ kg, $e = 1.6 \times 10^{-19}$ C, $d_p = 2.0 \times 10^{-8}$ m.

(c) For earth as a good conductor, $d_p = \sqrt{\frac{2}{\omega\mu_o\sigma}}$, for a superconductor, d_p is independent of frequency.

P3.2.3

$\epsilon = \epsilon_0$ as $\omega_{eff}/\omega \to \infty$ and $\epsilon = \epsilon_0(1 - \omega_p^2/\omega^2)$ as $\omega_{eff} = 0$.

P3.2.4

(a) $\nabla \times \overline{H} = \overline{J}_{sup} \Rightarrow \nabla \times \dot{\overline{H}} = \alpha\overline{E} \Rightarrow \nabla \times \nabla \times \dot{\overline{B}} = \mu_0\alpha\nabla \times \overline{E} = -\mu_0\alpha\dot{\overline{B}}$
   $\Rightarrow \nabla(\nabla \cdot \dot{\overline{B}}) - \nabla^2\dot{\overline{B}} = -\mu_0\alpha\dot{\overline{B}} \quad \Rightarrow \quad \nabla^2\dot{\overline{B}} = \mu_0\alpha\dot{\overline{B}}$
   since $\nabla \cdot \overline{B} = 0$. The solution is $\dot{\overline{B}} = \exp(\pm\mu_0\alpha x)$ for $\nabla^2 = \partial/\partial x^2$. The penetration depth $(\mu_0\alpha)^{-1/2}$ is of the order of 10^{-7} m. The first London equation is similar to that for good conductors. The above result suggests that the time varying magnetic field is zero and the static magnetic fields can be frozen in a perfect conductor in the limit $(\mu_0\alpha)^{-1/2} \to 0$.

(b) $\nabla \times \overline{H} = \overline{J}_{sup} \Rightarrow \nabla \times \nabla \times \overline{H} = \nabla \times J_{sup} = -\alpha_1\overline{B} \Rightarrow -\nabla^2\overline{B} = -\mu_0\alpha_1\overline{B}$. The solution is $\overline{B} = \exp(\pm\mu_0\alpha_1 x)$ for $\nabla^2 = \partial^2/\partial x^2$. The small penetration depth $(\mu_0\alpha)^{-1/2}$ suggests that the static magnetic field is zero inside the superconductor. Notice that the second London equation explains the Meissner effect but can not explain why superconductivity disappears in high magnetic fields. One difference between a perfect conductor and a superconductor is that static magnetic fields are frozen in the former but completely excluded from the latter.

P3.2.5

When an electric field E is applied, polarization P_1 occurs immediately. Then the polarization builds up to its steady state P_s with the time constant τ.

$$P(t) = u(t - t_0)\{P_1 + P_2(t)\}$$

$$\frac{d}{dt}P_2(t) = \frac{1}{\tau}[P_s - P_1 - P_2(t)]$$
$$P_s = (\epsilon_s - \epsilon_0)E_1$$
$$P_1 = (\epsilon_\infty - \epsilon_0)E_1$$

(Polar molecules in a viscous fluid take time to align with the applied field, as their motion is dampened.)

(a) For time harmonic excitation

$$-i\omega P_2 = \frac{1}{\tau}(P_s - P_1 - P_2); \quad P_2 = \frac{1}{1 - i\omega\tau}(P_s - P_1) = \frac{\epsilon_s - \epsilon_\infty}{1 - i\omega\tau}E$$

The total polarization is $P_1 + P_2 = \left\{(\epsilon_\infty - \epsilon_0) + \frac{\epsilon_s - \epsilon_\infty}{1 - i\omega\tau}\right\}E$

Permittivity is evaluated from $\epsilon E = \epsilon_0 E + P_1 + P_2$ as

$$\epsilon = \epsilon_\infty + \frac{\epsilon_s - \epsilon_\infty}{1 - i\omega\tau} \quad \text{(Debye Equation)}$$

$$\epsilon = \left\{\epsilon_\infty + \frac{\epsilon_s - \epsilon_\infty}{1 + \omega^2\tau^2}\right\} + i(\epsilon_s - \epsilon_\infty)\frac{\omega\tau}{1 + \omega^2\tau^2}$$

(b) $\epsilon_R = (\epsilon_s + \epsilon_\infty\omega^2\tau^2)/(1 + \omega^2\tau^2)$ $\epsilon_I = (\epsilon_s - \epsilon_\infty)\omega\tau/(1 + \omega^2\tau^2)$

(c) By obvious steps of algebra we obtain

$$\left[\epsilon_R - \left(\frac{\epsilon_s + \epsilon_\infty}{2}\right)\right]^2 + \epsilon_I^2 = \left(\frac{\epsilon_s - \epsilon_\infty}{2}\right)^2$$

It was suggested by K. S. Cole and R. H. Cole [J. Chem. Phys. v. 9,p. 341(1941)] to plot ϵ_I versus ϵ_R (Cole-Cole plot) to determine whether the permittivity of a given material can be described by a single relaxation time. $\epsilon_R - \epsilon_I$ curve is not circular for all material.

P3.2.6

Let $\bar{r}$ be the displacement of an electron from its equilibrium position. The forces impressed on the electron will include

$$\begin{cases} \overline{F}_e = e\overline{E} & \text{electric force} \\ \overline{F}_d = -g\omega_0 m\overline{v} = -g\omega_0 m\,d\bar{r}/dt & \text{damping force} \\ \overline{F}_r = -\omega_0^2 m\bar{r} & \text{restoring force} \end{cases}$$

By Newton's Law

$$m\frac{d^2\bar{r}}{dt^2} = F_e + F_d + F_r = e\overline{E} - g\omega_0 m\frac{d\bar{r}}{dt} - \omega_0^2 m\bar{r}$$

Multiply both sides by Ne/m, and define $\overline{P} = Nq\overline{r}$, use $q = e$ for electron, we find, under time harmonic excitation, $\overline{P} = \epsilon_0 \omega_P^2 \overline{E}/(\omega_0^2 - ig\omega\omega_0 - \omega^2)$ and $\epsilon\overline{E} = \epsilon_0 \overline{E} + \overline{P} = \epsilon(\omega)\overline{E}$. Thus we have

$$\epsilon(\omega) = \epsilon_R(\omega) + i\epsilon_I(\omega) = \epsilon_0 \left(1 + \frac{\omega_P^2}{\omega_0^2 - ig\omega\omega_0 - \omega^2}\right)$$

$$= \epsilon_0 \left[1 + \frac{\omega_P^2(\omega_0^2 - \omega^2)}{(\omega_0^2 - \omega^2)^2 + (g\omega\omega_0)^2} + i\frac{\omega_P^2 g\omega\omega_0}{(\omega_0^2 - \omega^2)^2 + (g\omega\omega_0)^2}\right]$$

$$\frac{\partial\epsilon_R}{\partial\omega} = 2\omega_P^2\omega \frac{(\omega_0^2 - \omega^2)^2 - g^2\omega_0^4}{[(\omega_0^2 - \omega^2)^2 + (g\omega\omega_0)^2]^2}$$

$$\frac{\partial\epsilon_R}{\partial\omega} = 0 \quad \text{when } (\omega_0^2 - \omega^2)^2 = g^2\omega_0^4 \quad \Rightarrow \quad \omega^2 = (1 \pm g)\omega_0^2$$

if $g < 1$
   $0 \le \omega^2 \le (1-g)\omega_0^2$, and $(1+g)\omega_0 \le \omega^2 \le \infty$, $\epsilon(r)$ increases with frequency.
   $(1-g)\omega_0^2 \le \omega^2 \le (1+g)\omega_0^2$, $\epsilon(r)$ decreases with frequency.
if $g > 1$
   $0 \le \omega^2 \le (1+g)\omega_0^2$, then $\epsilon(r)$ decreases with frequency.
   $(1-g)\omega_0^2 \le \omega^2 \le \infty$, then $\epsilon(r)$ increases with frequency.

$$\frac{\partial\epsilon_I}{\partial\omega} = \frac{\omega_P^2 g\omega_0 \left[\omega_0^4 + (2 - g^2)\omega_0^2\omega^2 - 3\omega^4\right]}{\left[(\omega_0^2 - \omega^2)^2 + (g\omega\omega_0)^2\right]^2}$$

$$\frac{\partial\epsilon_I}{\partial\omega} = 0 \quad \Rightarrow \quad \omega_{\max}^2 = \omega_0^2 \frac{(2 - g^2) + \sqrt{(2 - g^2)^2 + 12}}{6}$$

for $g \to 0$, $\omega_{\max} \to \omega_0$.

P3.3.1

Differentiate $\cos\alpha$ with respect to θ and we find $\alpha_{\max}$ occurs when

$$\sin\theta_0 = \sqrt{\frac{\kappa}{\kappa_z}} \quad \cos\theta_0 = \sqrt{\frac{\kappa}{\kappa_z + \kappa}}, \qquad \text{thus} \qquad \cos\alpha_{\max} = \frac{2\sqrt{\kappa/\kappa_z}}{1 + \kappa/\kappa_z}$$

At $\theta = 0$ and $\theta = \pi/2$, $\cos\alpha = 1$ and $\alpha = 0$.

P3.3.2

larger than θ.

P3.3.3

(a) (i) $\beta = \pm i$.

(ii) Since $k_e > k_o$, $(k_e - k_o)y_0 = \frac{1}{2}\pi$ $\Rightarrow$ $y_0 = \frac{3}{4}$ (m).

(b) (i) $\overline{S} = \overline{E} \times \overline{H}^* = [\hat{e}_3 \kappa_{22} - \hat{e}_2(\kappa - \kappa_z)\sin\theta\cos\theta] u |D_2|^2$, where

$$\kappa_{22} = \kappa\cos^2\theta + \kappa_z\sin^2\theta, \qquad u = \sqrt{\nu\kappa_{22}}.$$

(ii) From (i), it follows that $\tan\alpha = |\kappa - \kappa_z|\sin\theta\cos\theta/\kappa_{22}$.

(iii) $\frac{d}{d\theta}\tan\alpha = 0$ $\Rightarrow$ $\theta = \tan^{-1}\sqrt{\varepsilon_z/\varepsilon}$ or $\theta = \pi - \tan^{-1}\sqrt{\varepsilon_z/\varepsilon}$.

P3.3.4

The ordinary wave polarized in $\hat{y}$ direction is not attenuated and the extraordinary wave decays with $\exp(-\sigma_z/2\sqrt{\mu/\epsilon_z}\,x)$. Hence any wave propagating in the $\hat{x}$ passing through the polaroid will become a linearly polarized ordinary wave.

P3.3.5

The Fresnel ellipsoid is $\epsilon_1 x_1^2 + \epsilon_2 x_2^2 + \epsilon_3 x_3^2 = 1$

The tensor ellipsoid is $\frac{x_1^2}{\epsilon_1} + \frac{x_2^2}{\epsilon_2} + \frac{x_3^2}{\epsilon_3} = 1$

P3.3.6

(a) The conductivity is non-zero for the incident electric field in z-direction, we may assign z to u or v axis. There are following possibilities:
   (1) $z \to u$, $x \to v$, $y \to w$; or
   (2) $z \to v$, $x \to w$, $y \to u$. For $z \to u$, the output electric field is linearly polarized horizontally, for $z \to v$, the output electric field is linearly polarized vertically.
(b) For the z component of the incident electric field,

$$\frac{\sigma_z}{\omega\epsilon_z} = \frac{\sigma_z}{\omega 4\epsilon_o} = \frac{0.2}{4} = 0.05,$$

which is small, thus we can use the approximated expression

$$k_{zI} = \left[\frac{1}{2}\omega^2\mu_o\epsilon_z\left(\sqrt{1 + \left(\frac{\sigma_z}{\omega\epsilon_z}\right)^2} - 1\right)\right]^{1/2} \approx \frac{1}{2}\omega\sqrt{\mu_o\epsilon_z}\left(\frac{\sigma_z}{\omega\epsilon_z}\right) = \frac{0.1\pi}{\lambda}$$

The minimum thickness is $d = 1/k_{zI} = \lambda/0.1\pi = 3.18\lambda$.
(c) To make the quarter-wave plate have no power absorption, the incident electric wave must propagate in the z-direction, we assign $z \to w$, $x \to u$, $y \to v$.
(d) Incident wave is $\overline{E}_{inc} = \frac{E_o}{\sqrt{2}}(\hat{x} \pm \hat{y})\cos(k_w z - \omega t)$, where $x, y = u, v$.
(e) For $\overline{E}_{inc} = \frac{E_o}{\sqrt{2}}(\hat{x} - \hat{y})\cos(k_w z - \omega t)$, the x- and y-components of the electric field at $z = d$ are
$E_x = \frac{E_o}{\sqrt{2}}\cos(2\sqrt{3}k_o d - \omega t)$

$E_y = -\frac{E_o}{\sqrt{2}} \cos (k_o d - \omega t) = -\frac{E_o}{\sqrt{2}} \cos \left(2\sqrt{3} k_o d - \omega t - (2\sqrt{3} k_o d - k_o d)\right).$
Thus to get left-hand circularly polarized wave for $z > d$, we need

$$2\sqrt{3} k_o d - k_o d = \frac{(2m+1)\pi}{2}, \quad \text{or} \quad d = \frac{2m+1}{2\sqrt{3}-1} \frac{\lambda}{4}.$$

(f) To make the half-wave plate with no power absorption, the incident electric wave must propagate in the z-direction, we assign $z \to w, \quad x \to u, \quad y \to v$.

(g) Consider the incident electric wave

$$\overline{E}_{inc} = \frac{E_o}{\sqrt{2}} (\hat{x} \pm \hat{y}) \cos (k_w z - \omega t)$$

After passing through the half-wave plate,

$$E_x = \frac{E_o}{\sqrt{2}} \cos \left(2\sqrt{3} k_o d - \omega t\right)$$

$$E_y = \pm \frac{E_o}{\sqrt{2}} \cos \left(2\sqrt{3} k_o d - \omega t - (2\sqrt{3} k_o d - k_o d)\right)$$

Let $2\sqrt{3} k_o d - k_o d = \pi$, so that $E_y = \mp \frac{E_o}{\sqrt{2}} \cos \left(2\sqrt{3} k_o d - \omega t\right)$, and then

$$\overline{E}(z = d) = \frac{E_o}{\sqrt{2}} (\hat{x} \mp \hat{y}) \cos (k_w d - \omega t),$$

which is orthogonal to the incident wave. Therefore $d = \frac{2m+1}{2\sqrt{3}-1} \frac{\lambda}{2}$.

P3.3.7

(a) For E layer $N = 10^{11} /\text{m}^3$, $f_p = 56.4\sqrt{N}/2\pi = 2.84\,\text{MHz}$.
For F layer $N = 6 \times 10^{11} /\text{m}^3$, $f_p = 6.95\,\text{MHz}$.
For microwave frequencies much greater than the electron gyro-frequency and the plasma frequency, the plasma permittivity is approximately equal to that of free space. The splitting of the Type I and the Type II rays is negligible. Also, the plasma collision frequency is typically much smaller than microwave frequencies. In this case, the collision effect can be neglected and the plasma can be considered as lossless.

(b) Now, for one plasma layer, we could decomposed the Earth's magnetic field into two components $\overline{H}_\parallel$ and $\overline{H}_\perp$. Since we assume ϕ to be small, the main effect of $\overline{H}_e$ comes from $\overline{H}_\parallel$. So, we can take the direction of $\overline{k}$ to be $\hat{z}$ and consider an effective external magnetic field to be $\overline{H}_\parallel = H_e \cos \phi$. Under this approximation, the Faraday rotation angle within one layer is given by

$$\Delta\phi = \frac{1}{2}(\phi_r - \phi_\ell) = \frac{\omega dl}{2} \left[\frac{1}{\sqrt{\nu(\kappa - \kappa_g)}} - \frac{1}{\sqrt{\nu(\kappa + \kappa_g)}} \right]$$

$$\approx \frac{\omega dl}{2\sqrt{\nu\kappa}} \left[\left(1 + \frac{1}{2}\frac{\kappa_g}{\kappa}\right) - \left(1 - \frac{1}{2}\frac{\kappa_g}{\kappa}\right) \right] = \frac{\omega dl}{2\sqrt{\nu}} \cdot \frac{\kappa_g}{\kappa^{\frac{3}{2}}}$$

where $dl = dh \sec\theta$. We further simplify $(\kappa_g/\kappa^{\frac{3}{2}})$ by ignoring the second and higher order terms in (ω_p/ω) and (ω_c/ω), i.e.,

$$\frac{\kappa_g}{\kappa^{\frac{3}{2}}} = \sqrt{\epsilon_0}\left[\left(1 - \frac{\omega_p^2}{\omega^2}\right)^2 - \frac{\omega_c^2}{\omega^2}\right]^{\frac{1}{2}}\frac{\omega_c\omega_p^2/\omega^3}{[1 - \omega_p^2/\omega^2 - \omega_c^2/\omega^2]^{\frac{3}{2}}} \approx \sqrt{\epsilon_0}\frac{\omega_c\omega_p^2}{\omega^3}$$

Finally we obtain

$$\Delta\phi \simeq \frac{\omega dl\sqrt{\mu_0\epsilon_0}}{2}\frac{eBNe^2}{m^2\epsilon_0\omega^3} = \frac{\eta e^3\mu_0}{8\pi^2m^2f^2}NH_e\cos\phi\sec\theta dh = \frac{2.97 \times 10^{-2}}{f^2}NMdh$$

The above formula is for one layer only. By dividing the ionosphere into infinitesimal layers, we write the limit of summation as an integral

$$\Omega = \int \Delta\phi dh \cong \frac{\eta e^3\mu_0}{8\pi^2m^2f^2}\int MNdh$$

(c) $N = 10^{11} \text{ /m}^3$, $H_e = 50 \text{ A/m}$, $f = 1.4 \times 10^9 \text{ Hz}$, $\theta = 60°$, $\phi = 0°, h = 10^6 \text{ m}$, the total Faraday rotation angle is

$$\Omega \simeq \frac{2.97 \times 10^{-2} \times 10^{11} \times 50 \times 2 \times 10^6}{(1.4 \times 10^9)^2} = 0.1515 \text{ rad} \sim 8.68°$$

P3.3.8

In the DB-representation, $\kappa = \mu/(\epsilon\mu - \xi^2), \chi = \gamma = \xi/(\xi^2 - \epsilon\mu), \nu = \epsilon/(\epsilon\mu - \xi^2)$.

$$\overline{E} = \kappa\overline{D} + \chi\overline{B}$$
$$\overline{H} = \gamma\overline{D} + \nu\overline{B}$$

In the kDB system the constitutive relation is not changed, so we obtain

$$\begin{bmatrix} \nu\kappa - \chi\gamma - u^2 & (\gamma - \chi)u \\ (\chi - \gamma)u & \nu\kappa - \chi\gamma - u^2 \end{bmatrix}\begin{bmatrix} D_1 \\ D_2 \end{bmatrix} = 0$$

$$u^2 = \left[\nu\kappa - \frac{1}{2}\chi^2 - \frac{1}{2}\gamma^2\right] \pm \sqrt{\left(\nu\kappa - \frac{1}{2}\chi^2 - \frac{1}{2}\gamma^2\right)^2 - (\chi\gamma - \nu\kappa)^2}$$

$$= \left[\nu\kappa - \frac{1}{2}\chi^2 - \frac{1}{2}\gamma^2\right] \pm (\chi - \gamma)\sqrt{\frac{1}{4}(\chi + \gamma)^2 - \nu\kappa}$$

$$\frac{D_1}{D_2} = \frac{(\gamma - \chi)u}{u^2 + \chi\gamma - \nu\kappa}$$

The polarization of the characteristic waves can be one of the following cases:

(i) If $u^2 \geq 0$ then both characteristic waves are linearly polarized.

(ii) If $\nu\kappa > \frac{1}{4}(\chi+\gamma)^2$, or $\nu\kappa < \frac{1}{4}(\chi+\gamma)^2$ with $u^2 < 0$, then the waves are elliptically polarized.

(iii) If $\nu\kappa < \frac{1}{4}(\chi+\gamma)^2$, and u^2 takes different signs, then we have one linearly polarized wave and one elliptically polarized wave.

P3.3.9

(a)

$$\overline{\overline{\kappa}} = \begin{bmatrix} \kappa_x & 0 & 0 \\ 0 & \kappa_y & 0 \\ 0 & 0 & \kappa_z \end{bmatrix}; \qquad \overline{\overline{T}} \cdot \overline{\overline{\kappa}} \cdot \overline{\overline{T}}^{-1} = \begin{bmatrix} \kappa_{11} & \kappa_{12} & \kappa_{13} \\ \kappa_{21} & \kappa_{22} & \kappa_{23} \\ \kappa_{31} & \kappa_{32} & \kappa_{33} \end{bmatrix}$$

$$\kappa_{11} = \kappa_x \sin^2\phi + \kappa_y \cos^2\phi$$
$$\kappa_{12} = \kappa_{21} = (\kappa_x - \kappa_y)\cos\theta\sin\phi\cos\phi$$
$$\kappa_{22} = (\kappa_x \cos^2\phi + \kappa_y \sin^2\phi)\cos^2\theta + \kappa_z \sin^2\theta$$
$$\kappa_{13} = \kappa_{31} = (\kappa_x - \kappa_y)\sin\theta\sin\phi\cos\phi$$
$$\kappa_{23} = \kappa_{32} = (\kappa_x \cos^2\phi + \kappa_y \sin^2\phi - \kappa_z)\sin\theta\cos\theta$$
$$\kappa_{33} = (\kappa_x \cos^2\phi + \kappa_y \sin^2\phi)\sin^2\theta + \kappa_z \cos^2\theta$$

(b)

$$\begin{bmatrix} u^2 - \nu\kappa_{11} & -\nu\kappa_{12} \\ -\nu\kappa_{21} & u^2 - \nu\kappa_{22} \end{bmatrix} \begin{bmatrix} D_1 \\ D_2 \end{bmatrix} = 0$$

$$u^2 = \frac{\nu}{2}\left[(\kappa_{11} + \kappa_{22}) \pm \sqrt{(\kappa_{11} - \kappa_{22})^2 + 4\kappa_{12}^2} \right]$$

The characteristic waves are linearly polarized and

$$\frac{D_2}{D_1} = \frac{\nu\kappa_{21}}{u^2 - \nu\kappa_{22}} = \frac{2\kappa_{12}}{\kappa_{11} - \kappa_{22} \pm \sqrt{(\kappa_{11} - \kappa_{22})^2 + 4\kappa_{12}^2}}$$

$$= \frac{\tan 2\psi}{1 \pm \sqrt{1 + \tan^2 2\psi}} = \frac{\sin 2\psi}{\cos 2\psi \pm 1} = \begin{cases} \frac{2\sin\psi\cos\psi}{2\cos^2\psi} = \tan\psi \\ -\frac{2\sin\psi\cos\psi}{2\sin^2\psi} = -\cot\psi \end{cases}$$

P3.3.10

(a) Cross-multiply Faraday's law by $\overline{s}$: $\overline{s} \times (\overline{k} \times \overline{E}) = \omega\overline{s} \times \overline{B} = (\overline{s} \cdot \overline{E})\overline{k} - (\overline{s} \cdot \overline{k})\overline{E}$ yields

$$\overline{s} \times \overline{B} = -\overline{E}/\omega.$$

Cross-multiply Ampere's law by $\overline{s}$: $\overline{s} \times (\overline{k} \times \overline{H}) = -\omega \overline{s} \times \overline{D} = (\overline{s} \cdot \overline{H})\overline{k} - (\overline{s} \cdot \overline{k})\overline{H}$ yields

$$\overline{s} \times \overline{D} = \overline{H}/\omega.$$

(b) The dispersion relation for the extraordinary wave in a uniaxial medium is

$$\frac{k_x^2}{\epsilon_z} + \frac{k_y^2}{\epsilon_z} + \frac{k_z^2}{\epsilon} = \omega^2 \mu$$

The following vector is normal to this k surface and parallel to $\hat{s}$:

$$\frac{1}{2}\nabla_k(\omega^2\mu) = \hat{x}\frac{k_x}{\epsilon_z} + \hat{y}\frac{k_y}{\epsilon_z} + \hat{z}\frac{k_z}{\epsilon} = c\overline{s}$$

$$\overline{s} \cdot \overline{k} = 1 \quad \Rightarrow \quad c = \omega^2\mu.$$

$$s_x = \frac{k_x}{\omega^2\mu\epsilon_z}; \qquad s_y = \frac{k_y}{\omega^2\mu\epsilon_z}; \qquad s_z = \frac{k_z}{\omega^2\mu\epsilon}$$

$$s_x^2 + s_y^2 + \frac{\epsilon}{\epsilon_z}s_z^2 = \frac{1}{\omega^2\mu\epsilon_z}$$

(c) From $\overline{s} \cdot \overline{k} = 1$, it follows that $0 = (\delta\overline{s} \cdot \overline{k} + \overline{s} \cdot \delta\overline{k})\big|_{\omega \text{ fixed}}$. Since $\overline{s} \cdot \delta\overline{k} = 0$, $\delta\overline{s} \cdot \overline{k} = 0$. Therefore, $\overline{k}$ is normal to the ray-surface.

(d) When l is equal to s multiplied by a constant, the eikonal is equal to c/ω times the constant. The ray surface gives the magnitudes of s in all directions. It follows that the ray surface describes a constant-phase surface.

P3.3.11

(a) $\alpha = -2(\omega_1\omega_2)^{\frac{1}{2}}(\epsilon_1\epsilon_2)^{-\frac{1}{4}}\sqrt{\mu_0}\chi E_{3j}(0); \qquad \Delta k = k_1 + k_2 - k_3$

(b) $\frac{d}{dz}A_1 = -i\frac{\alpha}{2}A_2^* \quad \frac{d}{dz}A_2^* = i\frac{\alpha}{2}A_1 \Rightarrow \frac{d^2 A_2^*}{dz^2} = \left(\frac{\alpha}{2}\right)^2 A_2^* \Rightarrow A_2^*(z) = c_1 \sinh\frac{\alpha}{2}z + c_2\cosh\frac{\alpha}{2}z \Rightarrow c_2 = 0 \Rightarrow A_1(z) = \frac{2}{i\alpha}\frac{dA_2^*}{dz} = \frac{c_1}{i}\cosh\frac{\alpha}{2}z = A_1(0)\cosh\frac{\alpha}{2}z \Rightarrow c_1 = iA_1(0) \Rightarrow A_2^*(z) = iA_1(0)\sinh\frac{\alpha}{2}z$

(c) $E_{1i}(z) = \sqrt{\omega_1/n(\omega_1)}A_1(0)\cosh\frac{\alpha}{2}z$

$$\Rightarrow \Delta P_1 = -\frac{(\omega_1\omega_2)^{\frac{1}{2}}\chi\omega_1}{(\epsilon_1\epsilon_2)^{\frac{1}{4}}\sqrt{\mu_0}c}\Re\left\{E_{3j}(0)|A_1(0)|^2\cosh\frac{\alpha}{2}z\sinh\frac{\alpha}{2}z\Delta z\right\}$$

$$\Delta P_2 = -\frac{(\omega_1\omega_2)^{\frac{1}{2}}\chi\omega_2}{(\epsilon_1\epsilon_2)^{\frac{1}{4}}\sqrt{\mu_0}c}\Re\left\{E_{3j}(0)|A_1(0)|^2\cosh\frac{\alpha}{2}z\sinh\frac{\alpha}{2}z\Delta z\right\}$$

$$\Delta P_3 = \frac{(\omega_1\omega_2)^{\frac{1}{2}}\chi\omega_3}{(\epsilon_1\epsilon_2)^{\frac{1}{4}}\sqrt{\mu_0}c}\Re\left\{E_{3j}(0)|A_1(0)|^2\cosh\frac{\alpha}{2}\sinh\frac{\alpha}{2}\right\}$$

therefore $(\Delta P_1 + \Delta P_2 + \Delta P_3) = c(\omega_1 + \omega_2 - \omega_3) = 0$ because $\omega_1 + \omega_2 = \omega_3$. Thus energy is conserved.

4

REFLECTION AND GUIDANCE

4.1 Reflection and Transmission

A. Reflection and Transmission of TM Waves

B. Reflection and Transmission of TE Waves

C. Phase Matching

D. Total Reflection and Critical Angle

E. Backward Waves and Negative Refraction

F. Double Refraction in Uniaxial Media

G. Total Transmission and Brewster Angle

H. Zenneck Wave

I. Plasma Surface Wave

J. Reflection and Transmission by a Layered Medium

K. Reflection Coefficients for Stratified Medium

L. Propagation Matrices and Transmission Coefficients

4.2 Wave Guidance

A. Guidance by Conducting Parallel Plates

B. Excitation of Modes in Parallel-Plate Waveguides

C. TM Modes in Parallel-Plate Waveguides

D. Attenuation of Guided Waves Due to Wall Loss

E. Guided Waves in Isotropic Medium Coated Conductor

F. Guided Waves in Layered Media

G. Guided Waves in a Symmetric Slab Dielectric Waveguide

H. Cylindrical Waveguides

I. Cylindrical Rectangular Waveguides

J. Cylindrical Circular Waveguides

4.3 Resonance

A. Rectangular Cavity Resonator

B. Circular Cavity Resonator

C. Spherical Cavity Resonator

D. Cavity Perturbation

Answers

4.1   Reflection and Transmission

Maxwell equations for time-harmonic fields are

$$\nabla \times \overline{E} = i\omega\overline{B} \qquad (4.1.1)$$

$$\nabla \times \overline{H} = -i\omega\overline{D} + \overline{J} \qquad (4.1.2)$$

$$\nabla \cdot \overline{B} = 0 \qquad (4.1.3)$$

$$\nabla \cdot \overline{D} = \rho \qquad (4.1.4)$$

where all field quantities are space dependent and complex.

For a boundary surface separating regions 1 and 2, and with a surface normal $\hat{n}$ point from region 2 to region 1. The boundary conditions as developed in Chapter 1 are as follows:

$$\hat{n} \times (\overline{E}_1 - \overline{E}_2) = 0 \qquad (4.1.5)$$

$$\hat{n} \times (\overline{H}_1 - \overline{H}_2) = \overline{J}_s \qquad (4.1.6)$$

$$\hat{n} \cdot (\overline{B}_1 - \overline{B}_2) = 0 \qquad (4.1.7)$$

$$\hat{n} \cdot (\overline{D}_1 - \overline{D}_2) = \rho_s \qquad (4.1.8)$$

where $\overline{J}_s$ is the surface current density and ρ_s is the surface charge density.

In source-free regions of isotropic media, where $\overline{J} = \rho = 0$, $\overline{D} = \epsilon\overline{E}$, and $\overline{B} = \mu\overline{H}$, consider plane wave solutions where all field vectors have spatial dependence

$$e^{i\overline{k}\cdot\overline{r}} = e^{ik_x x + ik_y y + ik_z z} \qquad (4.1.9)$$

characterized by the wave vector

$$\overline{k} = \hat{x}k_x + \hat{y}k_y + \hat{z}k_z \qquad (4.1.10)$$

with the dispersion relation

$$k_x^2 + k_y^2 + k_z^2 = \omega^2\mu\epsilon \qquad (4.1.11)$$

Maxwell equations become

$$\overline{k} \times \overline{E} = \omega\mu\overline{H} \qquad (4.1.12)$$

$$\overline{k} \times \overline{H} = -\omega\epsilon\overline{E} \qquad (4.1.13)$$

$$\overline{k} \cdot \overline{H} = 0 \qquad (4.1.14)$$

$$\overline{k} \cdot \overline{E} = 0 \qquad (4.1.15)$$

We shall assume homogeneous media in each region, and the various regions are separated by boundary surfaces subject to the boundary conditions in (4.1.5)–(4.1.8).

A. Reflection and Transmission of TM Waves

Consider a TM plane wave incident from an isotropic medium with permittivity ϵ and permeability μ upon another isotropic medium with permittivity ϵ_t and permeability μ_t [Fig. 4.1.1]. We assume the plane of incidence to be parallel to the x-z plane, which contains the incident wave vector and the surface normal. An incident wave with any polarization can be decomposed into TE (transverse electric) and TM (transverse magnetic) wave components. The TE wave is linearly polarized with the electric field vector perpendicular to the plane of incidence and is also called perpendicularly polarized, horizontally polarized, or simply an $\overline{E}$ wave or s wave. The TM wave is linearly polarized with the electric vector parallel to the plane of incidence and is also called parallelly polarized, vertically polarized, or simply an $\overline{H}$ wave or p wave.

We write, for an incident TM wave with unit amplitude,

$$\overline{H}_i = \hat{y}\, e^{i\overline{k}_i \cdot \overline{r}} \qquad (4.1.16a)$$

$$\overline{E}_i = -\frac{1}{\omega\epsilon}\overline{k}_i \times \overline{H}_i \qquad (4.1.16b)$$

$$\overline{S}_i = \overline{E} \times \overline{H}^* = \overline{k}_i \frac{1}{\omega\epsilon}|\overline{H}_i|^2 \qquad (4.1.16c)$$
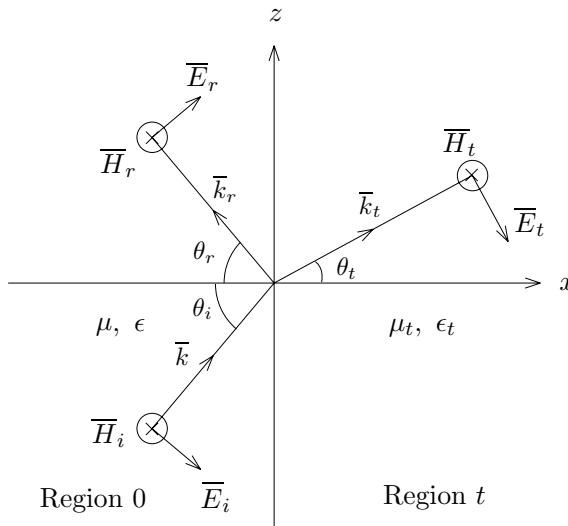
Figure 4.1.1 Reflection and transmission of TM waves.

The reflected field components for the incident TM wave are

$$\overline{H}_r = \hat{y}\, R^{TM} e^{i\overline{k}_r \cdot \overline{r}} \qquad (4.1.17a)$$

$$\overline{E}_r = -\frac{1}{\omega\epsilon}\overline{k}_r \times \overline{H}_r \qquad (4.1.17b)$$

$$\overline{S}_r = \overline{E}_r \times \overline{H}_r^* = \overline{k}_r\, \frac{1}{\omega\epsilon}|\overline{H}_r|^2 \qquad (4.1.17c)$$

where R^{TM} is the reflection coefficient for the magnetic field component H_{iy}.

In region t, the transmitted TM field components are

$$\overline{H}_t = \hat{y}\, T^{TM} e^{i\overline{k}_t \cdot \overline{r}} \qquad (4.1.18a)$$

$$\overline{E}_t = -\frac{1}{\omega\epsilon_t}\overline{k}_t \times \overline{H}_t \qquad (4.1.18b)$$

$$\overline{S}_t = \overline{E}_t \times \overline{H}_t^* = \overline{k}_t\frac{1}{\omega\epsilon_t}|\overline{H}_t|^2 \qquad (4.1.18c)$$

where T^{TM} is the transmission coefficient for the magnetic field component H_{iy}.

The wave vectors and the corresponding dispersions relations are

$$\overline{k}_i = \hat{x}k_x + \hat{z}k_z \qquad (4.1.19)$$
$$\overline{k}_r = \hat{x}k_{rx} + \hat{z}k_{rz} \qquad (4.1.20)$$
$$\overline{k}_t = \hat{x}k_{tx} + \hat{z}k_{tz} \qquad (4.1.21)$$
$$k_x^2 + k_z^2 = \omega^2\mu\epsilon = k^2 \qquad (4.1.22)$$
$$k_{rx}^2 + k_{rz}^2 = \omega^2\mu\epsilon = k^2 \qquad (4.1.23)$$
$$k_{tx}^2 + k_{tz}^2 = \omega^2\mu_t\epsilon_t = k_t^2 \qquad (4.1.24)$$

First we determine the wave vector components by phase matching conditions as derived below.

Let the boundary surface be at $x = 0$ where the tangential components of $\overline{E}$ and $\overline{H}$ are continuous. From continuity of H_y, we obtain

$$e^{ik_z z} + R^{TM} e^{ik_{rz} z} = T^{TM} e^{ik_{tz} z} \qquad (4.1.25)$$

This equation must be true for ALL z, and as a consequence, we obtain the phase matching condition

$$\boxed{k_z = k_{rz} = k_{tz}} \qquad (4.1.26)$$

The boundary conditions of continuity of tangential $\overline{H}$ and $\overline{E}$ give

$$1 + R^{TM} = T^{TM} \tag{4.1.27}$$

$$\frac{k_x}{\epsilon}(1 - R^{TM}) = \frac{k_{tx}}{\epsilon_t}T^{TM} \tag{4.1.28}$$

Note that we did not use the boundary conditions that normal $\overline{D}$ and normal $\overline{B}$ components are continuous at $z = 0$, because these two conditions are not independent of the two tangential $\overline{E}$ and $\overline{H}$ conditions, just as Gauss' two laws are not independent of Faraday's and Ampère's laws. In this case we can see that the condition of continuous normal $\overline{D}$ yields the same equation as (4.1.27) and there is no normal $\overline{B}$ component.

The reflection and transmission coefficients R^{TM} and T^{TM} are determined from (4.1.27) and (4.1.28), as

$$R^{TM} = R_{0t}^{TM} = \frac{1 - p_{0t}^{TM}}{1 + p_{0t}^{TM}} \tag{4.1.29}$$

$$T^{TM} = T_{0t}^{TM} = \frac{2}{1 + p_{0t}^{TM}} \tag{4.1.30}$$

where the parameter

$$p_{0t}^{TM} = \frac{\epsilon k_{tx}}{\epsilon_t k_x} \tag{4.1.31}$$

and R_{0t}^{TM} in (4.1.29) is called the Fresnel reflection coefficient for a TM wave incident from region 0 and reflected at the boundary separating regions 0 and t. In (4.1.30) T_{0t}^{TM} is the transmission coefficient from region 0 to region t. Note that the Fresnel reflection coefficient for TM waves represents the ratio of the reflected and incident *magnetic* fields.

The time-averaged Poynting power vectors for the incident, the reflected, and the transmitted waves are calculated to be

$$< \overline{S}_i > = \frac{1}{2}\text{Re}\left\{\overline{k}\frac{1}{\omega\epsilon}\right\} \tag{4.1.32}$$

$$< \overline{S}_r > = \frac{1}{2}\text{Re}\left\{\frac{\overline{k}_r}{\omega\epsilon}\left|R^{TM}\right|^2\right\} \tag{4.1.33}$$

$$< \overline{S}_t > = \frac{1}{2}\text{Re}\left\{\frac{\overline{k}_t}{\omega\epsilon_t}\left|T^{TM}\right|^2 e^{i(k_{tx}-k_{tx}^*)x}\right\} \tag{4.1.34}$$

where we assume that k_{tx} and ϵ_t may be complex.

B. Reflection and Transmission of TE Waves
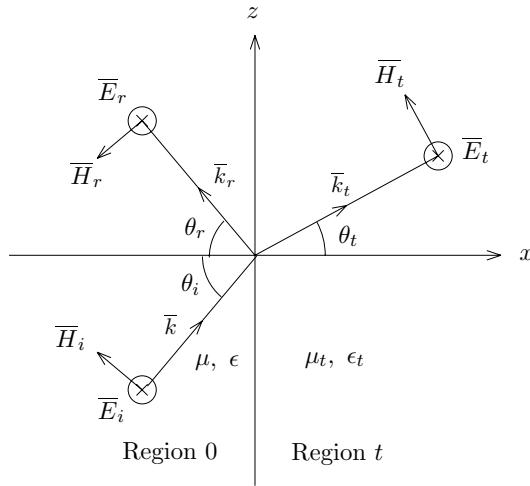
Consider a TE plane wave incidence with [Fig. 4.1.2]

$$\overline{k}_i = \hat{x}\, k_x + \hat{z}\, k_z \qquad (4.1.35a)$$

$$\overline{E}_i = \hat{y}\, e^{i\overline{k}_i \cdot \overline{r}} \qquad (4.1.35b)$$

$$\overline{H}_i = \frac{1}{\omega\mu}\overline{k}_i \times \overline{E}_i \qquad (4.1.35c)$$

$$\overline{S}_i = \overline{E}_i \times \overline{H}_i^* = \overline{k}_i\, \frac{1}{\omega\mu}\, |\overline{E}_i|^2 \qquad (4.1.35d)$$

Figure 4.1.2 Reflection and transmission of TE waves at a plane boundary separating regions 0 and t.

The reflected wave takes the form

$$\overline{k}_r = -\hat{x}\, k_x + \hat{z}\, k_z \qquad (4.1.36a)$$

$$\overline{E}_r = \hat{y}\, R^{TE} e^{i\overline{k}_r \cdot \overline{r}} \qquad (4.1.36b)$$

$$\overline{H}_r = \frac{1}{\omega\mu}\overline{k}_r \times \overline{E}_r \qquad (4.1.36c)$$

$$\overline{S}_r = \overline{E}_r \times \overline{H}_r^* = \overline{k}_r\, \frac{1}{\omega\mu}\, |\overline{E}_r|^2 \qquad (4.1.36d)$$

and in region t,

$$\overline{k}_t = \hat{x}\, k_{tx} + \hat{z}\, k_z \tag{4.1.37a}$$

$$\overline{E}_t = \hat{y}\, T^{TE}\, e^{i\overline{k}_t \cdot \overline{r}} \tag{4.1.37b}$$

$$\overline{H}_t = \frac{1}{\omega\mu_t}\overline{k}_t \times \overline{E}_t \tag{4.1.37c}$$

$$\overline{S}_t = \overline{E}_t \times \overline{H}_t^* = \overline{k}_t^* \frac{1}{\omega\mu_t}|\overline{E}_t|^2 \tag{4.1.37d}$$

The reflection and transmission coefficients R^{TE} and T^{TE} are

$$R^{TE} = \frac{1 - p_{0t}^{TE}}{1 + p_{0t}^{TE}} = R_{0t}^{TE} \tag{4.1.38}$$

$$T^{TE} = \frac{2}{1 + p_{0t}^{TE}} = T_{0t}^{TE} \tag{4.1.39}$$

where

$$p_{0t}^{TE} = \frac{\mu k_{tx}}{\mu_t k_x} \tag{4.1.40}$$

With p_{0t}^{TE} for TE waves defined in (4.1.40), R_{0t}^{TE} in (4.1.38) is the Fresnel reflection coefficient for a TE wave incident from region 0 and reflected at the boundary separating regions 0 and t. In (4.1.39) T_{0t}^{TE} is the transmission coefficient from region 0 to region t.

The time-averaged Poynting power vectors for the incident, the reflected, and the transmitted waves are calculated to be

$$<\overline{S}_i> = \frac{1}{2}\text{Re}\left\{\overline{k}\frac{1}{\omega\mu}\right\} \tag{4.1.41}$$

$$<\overline{S}_r> = \frac{1}{2}\text{Re}\left\{\frac{\overline{k}_r}{\omega\mu}|R^{TE}|^2\right\} \tag{4.1.42}$$

$$<\overline{S}_t> = \frac{1}{2}\text{Re}\left\{\frac{\overline{k}_t^*}{\omega\mu_t^*}|T^{TE}|^2 e^{i(k_{tx}-k_{tx}^*)x}\right\} \tag{4.1.43}$$

where we assume that k_{tx} and ϵ_t may be complex. The above results for the reflection and transmission of TE waves is easily obtained by using the duality property of Maxwell equations with the replacements $\overline{E} \rightarrow -\overline{H}$, $\overline{H} \rightarrow \overline{E}$, and $\mu \rightleftarrows \epsilon$.

C. Phase Matching

According to the phase-matching condition (4.1.26),

$$\boxed{k_z = k_{rz} = k_{tz}} \tag{4.1.44}$$

the incident, reflected and transmitted wave vectors must all lie in the same plane called the *plane of incidence* determined by the incident $\overline{k}_i$ vector and the normal to the boundary surface. Although (4.1.44) is derived for isotropic media, it holds for general homogeneous media with the plane wave solutions (4.1.9).

The phase matching condition in equation (4.1.44) states that the tangential components of the incident, the reflected, and the transmitted wave vectors are continuous. We illustrate the phase-matching condition with Fig. 4.1.3 with x-z plane as the plane of incidence. The phase matching condition states that the tangential components of the wave vectors across the boundary must be continuous as illustrated in Fig. 4.1.3. Let θ_i denote the angle of incidence, θ_r the angle of reflection, and θ_t the angle of transmission, with θ_i, θ_r, and θ_t all less than $\pi/2$, we find from (4.1.44) that $\theta_r = \theta_i$, and

$$\frac{\sin \theta_i}{\sin \theta_t} = \frac{k_t}{k_0} = \frac{n_t}{n_0} \tag{4.1.45}$$

where $n_t = c\sqrt{\mu_t \epsilon_t}$ and $n_0 = c\sqrt{\mu_0 \epsilon_0}$ are the refractive indices. Equation (4.1.45) is known as Snell's law.
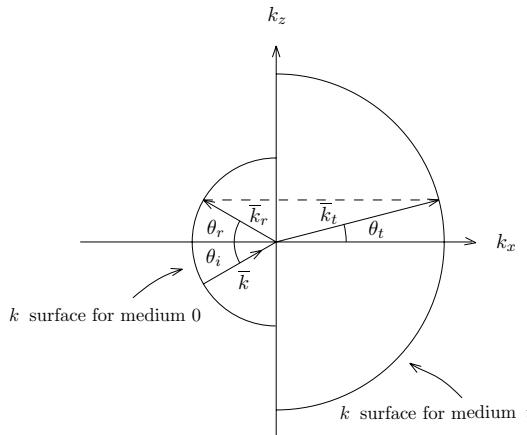
Figure 4.1.3 Phase matching using k surfaces.
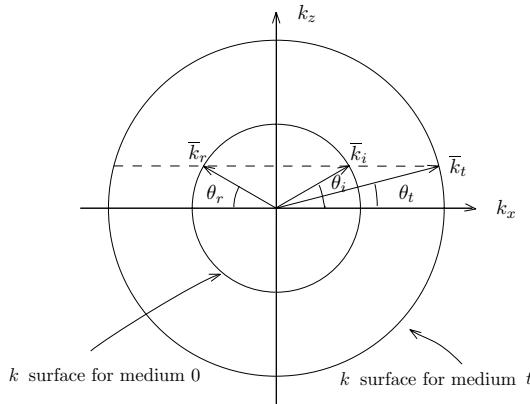
Figure 4.1.4 Phase matching using k surfaces.

In Figure 4.1.4, we let the magnitudes of the wave vectors represented by circles with radii $k_i = k_r = \omega\sqrt{\mu_0 \epsilon_0}$ and $k_t = \omega\sqrt{\mu_t \epsilon_t}$ on the k_x-k_z plane. The circles are called k-surfaces. In three dimensional k-space when $k_y \neq 0$, the k-surfaces are spheres.
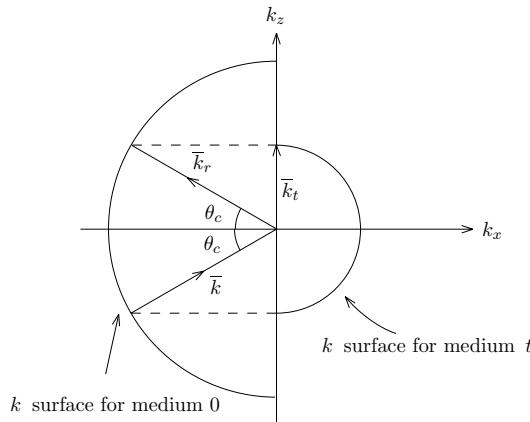
Figure 4.1.5 k surface for medium 0 is larger than that for medium t.

When $n_0 > n_t$, the radius of the k surface in Region t is shorter than that in Region 0 [Fig. 4.1.5]. By the phase-matching condition, we see that as k_z of the incident wave becomes larger than k_t, there is no intersection with the smaller semi-circle. As we shall show in the following that the transmitted wave is evanescent in the $\hat{x}$ direction, a phenomenon known as total reflection.

D. Total Reflection and Critical Angle

Suppose that the medium in region 0 has larger refractive index than the medium does in region t such that $n_0 > n_t$. Then the radius of the k surface in region t is shorter than that in region 0 [Fig. 4.1.6]. By the phase-matching conditions, we see that as k_{iz} of the incident wave becomes larger than k_t, there is no intersection with the small circle because this amounts to requiring that one component of a vector be greater than its magnitude — an impossibility unless the vector is complex.
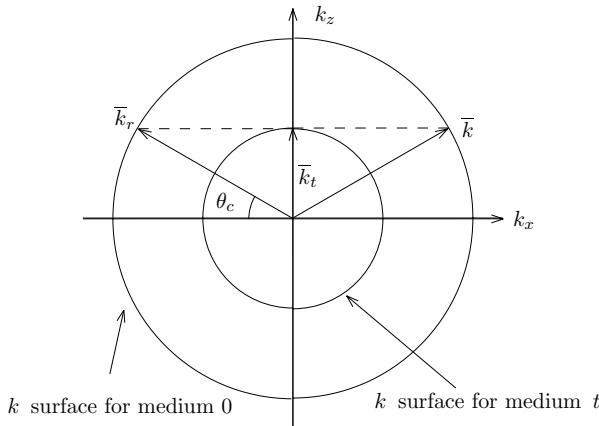
Figure 4.1.6 At critical angle of reflection when the k surface for medium 0 is larger than that for medium t.

The k surface in region t is described by

$$k_{tx}^2 + k_{iz}^2 = k_t^2 \tag{4.1.46}$$

Since $k_{iz} > k_t$, k_{tx} must be purely imaginary,

$$k_{tx} = \sqrt{k_t^2 - k_{iz}^2} = ik_{txI} \tag{4.1.47}$$

Remember that the wave in region t is characterized by $\exp(ik_{tx}x + ik_z z)$. For $k_z > k_t$, it becomes $\exp(-k_{txI}x + ik_z z)$. The transmitted wave thus decays exponentially in the $\hat{x}$ direction. and propagates along the $\hat{z}$ direction with the phase velocity ω/k_z. This can be regarded as a plane wave with constant phase fronts perpendicular to

the boundary surface. Its amplitude is maximum at the surface and decays exponentially away from the surface. The wave is known as a surface wave. The surface wave is evanescent in the $\hat{x}$ direction. Since evanescence in the transmitted wave begins when $k_t = k_z = k \sin \theta_c$, with

$$\theta_c = \sin^{-1} \frac{k_t}{k} = \frac{n_t}{n_0}$$

the angle θ_c is the *critical angle* of incidence. In Fig. 4.1.6, we illustrate phase matching at $k_z = k_t$.

When the incident angle is larger than the critical angle,

$$\overline{k}_t = \hat{x} \, i \, k_{txI} + \hat{z} \, k_z$$

The Fresnel reflection coefficient becomes, as $p_{0t} = i\epsilon k_{txI}/\epsilon_t k_x = i \, p_{0tI}$,

$$R_{0t} = \frac{1 - p_{0t}}{1 + p_{0t}} = \frac{1 - i \, p_{0tI}}{1 + i \, p_{0tI}} = e^{i2\phi_t} \qquad (4.1.48)$$

where

$$\phi_t = -\tan^{-1} p_{0tI} = -\tan^{-1} \frac{\epsilon k_{txI}}{\epsilon_t k_x} \qquad (4.1.49)$$

for TM waves. The transmission coefficient becomes

$$T_{0t} = 1 + R_{0t} = 1 + e^{i2\phi} = 2 \cos \phi_t \, e^{i\phi_t} \qquad (4.1.50)$$

The phase shift 2ϕ of the Fresnel reflection coefficient at total reflection is known as the Goos-Hänchen shift.

The transmitted electromagnetic fields at total reflection are

$$\begin{cases} \overline{k}_t = \hat{x} \, ik_{txI} + \hat{z} \, k_z \\[2mm] \overline{H}_t = \hat{y} \, 2 \cos \phi_t \, e^{i\phi_t} \, e^{-k_{txI}x + ik_z z} \\[2mm] \overline{E}_t = \frac{-1}{\omega \epsilon_t} \overline{k}_t \times \overline{H}_t \\[2mm] <\overline{S}_t> = \frac{1}{2} \text{Re} \left\{ \frac{\overline{k}_t}{\omega \epsilon_t} |\overline{H}_t|^2 \right\} \end{cases} \qquad (4.1.51)$$

The transmitted time-averaged Poynting power vector becomes

$$<\overline{S}_t> = \hat{z} \, k_z \frac{2 \cos^2 \phi}{\omega \epsilon_t} e^{-2k_{txI}x}$$

Thus there is no time-average power transmitted in the $\hat{x}$ direction into region t, and the incident power is totally reflected. At total reflection, the transmitted wave is a surface wave.

E. Backward Waves and Negative Refraction

The phase matching condition was shown in Fig. 4.1.4. Consider another solution as shown in Figure 4.1.7, which can be realized with a negative isotropic medium with $\mu_t = -\mu_n$ and $\epsilon_t = -\epsilon_n$, where μ_n and ϵ_n are positive real.
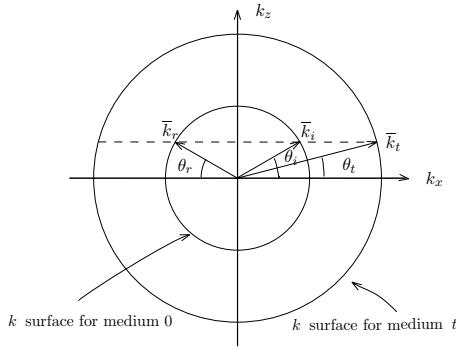
Figure 4.1.7 Phase matching using k surfaces.

Consider the transmitted TM and TE waves as shown in (4.1.18) and (4.1.37). We see that for the transmitted wave vector $\overline{k} = -\hat{x}k_{tx} + \hat{z}k_z$, the Poynting power vector points into the transmitted region. In the negative isotropic media, the backward wave has $\overline{k}$ vector and the tome-averaged Poynting Vector $<\overline{S}>$ point in opposite directions.
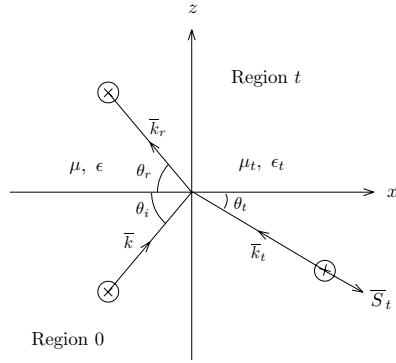
Figure 4.1.8 Reflection and transmission of TM waves from a negative isotropic medium in region t.

F. Double Refraction in Uniaxial Media
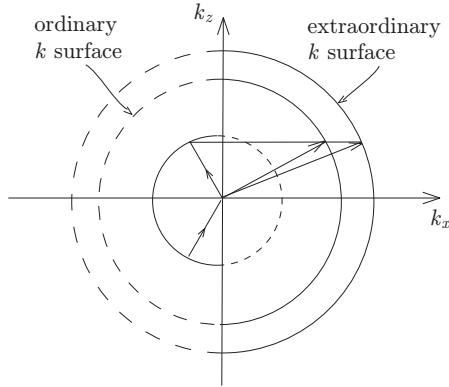
In a uniaxial medium with optical axis in the $\hat{z}$ direction, the wave vectors for extraordinary waves satisfy the dispersion relation

$$k^{(e)} = \frac{\omega}{\sqrt{\nu(\kappa \cos^2 \theta + \kappa_z \sin^2 \theta)}} = \frac{\omega \sqrt{\mu \epsilon_z}}{\sqrt{(\epsilon_z/\epsilon) \cos^2 \theta + \sin^2 \theta}}$$
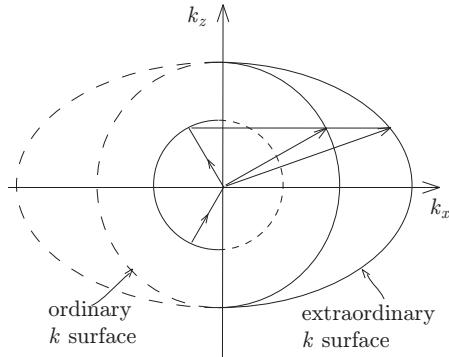
The wave vectors for ordinary waves obey the dispersion relation

$$k^{(o)} = \frac{\omega}{\sqrt{\nu \kappa}} = \omega \sqrt{\mu \epsilon}$$

and the k-surface is a sphere with radius $k = \omega \sqrt{\mu \epsilon}$.

a. Optic axis perpendicular to paper

b. Optic axis along the k_z axis

Figure 4.1.9 Double refraction by uniaxial medium.

Consider the phenomenon of double refraction by a positive uniaxial medium [Fig. 4.1.9]. First, let the optic axis of the medium be

perpendicular to the plane of incidence. The two transmitted wave vectors are shown in Figure 4.1.9a. The power flow directions for the ordinary and extraordinary waves are the same as the directions of the wave vectors. Next, let the optic axis be parallel to the plane of incidence. The two transmitted wave vectors are shown in Figure 4.1.9b. By the nature of the wave surface, the power flow direction of the extraordinary wave is no longer the same as the direction of $\overline{k}$. Note that by proper source excitation we can generate either the ordinary or the extraordinary wave. For instance, if the wave is linearly polarized perpendicular to the plane of incidence only ordinary waves are excited.
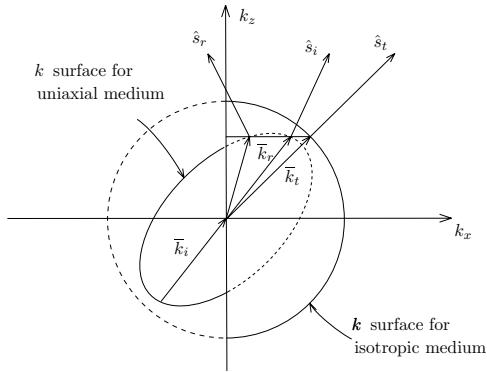
Figure 4.1.10 Wave vector directions and power flow directions.

Consider another wave excited in a uniaxial medium and incident upon the interface of an isotropic medium. Let the optic axis be in the plane of incidence and make an angle with the boundary. The wave surfaces are shown in Figure 4.1.10. In Figures 4.1.4–4.1.9, we have drawn the incident $\overline{k}_i$ vector with arrows pointing toward the origin. Although we use dotted lines for half of the spheres to convey the feeling of a physical boundary, we must realize that the plot is for k space and not physical space. In Figure 4.1.10 we draw the reflected wave vector; instead of pointing in the negative k_x and positive k_z directions, it is now pointing in the positive k_z and k_x directions. The power flow direction for the reflected wave, however, is pointing in the negative k_x and positive k_z directions. Thus the reflected wave, while carrying energy away from the interface, has its phase front propagating toward the interface. This is a *backward wave* with respect to the normal at the interface.

G. Total Transmission and Brewster Angle

Consider total transmission by setting the reflection coefficient equal to zero. For TM waves, $R^{TM} = 0$ yields

$$k_{tx} = \frac{\epsilon_t}{\epsilon} k_x \qquad (4.1.52)$$

From the dispersion relations

$$k^2 = k_x^2 + k_z^2$$
$$k_t^2 = k_{tx}^2 + k_z^2 = \frac{\epsilon_t^2}{\epsilon^2} k_x^2 + k_z^2$$

we find

$$k_x^2 = \frac{k_t^2 - k^2}{(\epsilon_t/\epsilon)^2 - 1} \qquad (4.1.53)$$

$$k_z^2 = \frac{(\epsilon_t/\epsilon)^2 k^2 - k_t^2}{(\epsilon_t/\epsilon)^2 - 1} \qquad (4.1.54)$$

Brewster angle is defined for the case of $\mu_t = \mu$, namely for reflection and transmission at a dielectric interface, which is determined to be

$$\tan \theta_B^{TM} = \frac{k_z}{k_x} = \sqrt{\frac{(\epsilon_t/\epsilon)^2 k^2 - k_t^2}{k_t^2 - k^2}} = \frac{k_t}{k} = \sqrt{\frac{\epsilon_t}{\epsilon}} \qquad (4.1.55)$$
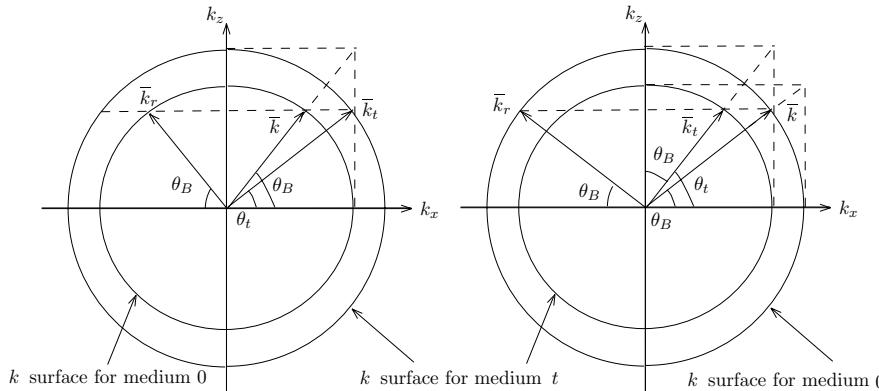
Figure 4.1.11 At Brewster angle of reflection, $\overline{k}$ is perpendicular $\overline{k}_t$.

From the phase matching condition, we find $k_t \sin \theta_t = k \sin \theta_B = k_t \cos \theta_B$. It follows that $\theta_B + \theta_t = \pi/2$.

The reflected and transmitted wave vectors are $\overline{k}_r = -\hat{x}k_x + \hat{z}k_z$ and $\overline{k}_t = \hat{x}k_{tx} + \hat{z}k_z = \hat{x}\frac{\epsilon_t}{\epsilon}k_x + \hat{z}k_z$. We see that

$$\overline{k}_t \cdot \overline{k}_r = -\frac{\epsilon_t}{\epsilon}k_x^2 + k_z^2 = 0$$

Therefore the reflected and transmitted vectors are perpendicular to each other.

For TE waves, when $\mu_t = \mu$, $R^{TE} = 0$ yields $k_{tx} = \frac{\mu_t}{\mu}k_x = k_x$, which gives $k_t = k$. We see that there is no zero reflection unless the two media are identical. When an unpolarized wave is incident upon a dielectric medium at the Brewster angle, the reflected wave becomes linearly polarized perpendicular to the plane of incidence. For this reason, the Brewster angle is also called the polarization angle.

EXAMPLE 4.1.1

For $\epsilon \neq \epsilon_t$ and $\mu \neq \mu_t$, we find from (4.1.53) and (4.1.54),

$$\tan \theta_b^{TM} = \frac{k_z}{k_x} = \sqrt{\frac{(\epsilon_t/\epsilon)^2 k^2 - k_t^2}{k_t^2 - k^2}} = \sqrt{\frac{\left(\frac{\epsilon_t}{\epsilon}\right)^2 - \frac{\mu_t \epsilon_t}{\mu \epsilon}}{\frac{\mu_t \epsilon_t}{\mu \epsilon} - 1}} \qquad (E4.1.1.1)$$

For TE waves, $R^{TE} = 0$ yields

$$k_{tx} = \frac{\mu_t}{\mu}k_x$$

From the dispersion relations

$$k^2 = k_x^2 + k_z^2$$

$$k_t^2 = k_{tx}^2 + k_z^2 = \frac{\mu_t^2}{\mu^2}k_x^2 + k_z^2$$

Brewster angle is defined for the case of $\epsilon_t = \epsilon$, namely for reflection and transmission at a dielectric interface, from which we find

$$k_x^2 = \frac{k_t^2 - k^2}{(\mu_t/\mu)^2 - 1} \qquad (E4.1.1.2)$$

$$k_z^2 = \frac{(\mu_t/\mu)^2 k^2 - k_t^2}{(\mu_t/\mu)^2 - 1} \qquad (E4.1.1.3)$$

$$\tan \theta_b^{TE} = \frac{k_z}{k_x} = \sqrt{\frac{(\mu_t/\mu)^2 k^2 - k_t^2}{k_t^2 - k^2}} = \sqrt{\frac{\left(\frac{\mu_t}{\mu}\right)^2 - \frac{\mu_t \epsilon_t}{\mu \epsilon}}{\frac{\mu_t \epsilon_t}{\mu \epsilon} - 1}} \qquad (E4.1.1.4)$$

— END OF EXAMPLE 4.1.1 —

H. Zenneck Wave

The guidance condition at a plane interface is obtained by letting $R \to \infty$, which amounts to a zero incident wave. For TM waves, we write solutions on both sides of the interface as

$$
\begin{cases}
\overline{H}_0 = \hat{y}\, e^{i\overline{k}\cdot\overline{r}} \\[2mm]
\overline{E}_0 = -\dfrac{1}{\omega\epsilon}\overline{k} \times \overline{H}_0 \\[2mm]
\overline{k} = -\hat{x}k_x + \hat{z}k_z
\end{cases}
\qquad
\begin{cases}
\overline{H}_t = \hat{y}\, e^{i\overline{k}_t\cdot\overline{r}} \\[2mm]
\overline{E}_t = -\dfrac{1}{\omega\epsilon_t}\overline{k}_t \times \overline{H}_t \\[2mm]
\overline{k}_t = \hat{x}k_{tx} + \hat{z}k_z
\end{cases}
$$

The boundary conditions of continuity of tangential electric and magnetic field components yield the guidance condition $k_{tx} = -\frac{\epsilon_t}{\epsilon}k_x$.

Consider a highly conducting medium with permeability $\mu_t = \mu$, and permittivity $\epsilon_t = \epsilon_g + i\sigma/\omega$, with $\sigma/\omega\epsilon_g \gg 1$, where σ is the conductivity. From dispersion relations

$$k^2 = k_x^2 + k_z^2 \tag{4.1.56}$$

$$k_t^2 = k_{tx}^2 + k_z^2 = \frac{\epsilon_t^2}{\epsilon^2}k_x^2 + k_z^2 \tag{4.1.57}$$

and with $k_{tx} = -\frac{\epsilon_t}{\epsilon}k_x$, we find

$$k_x = \left[\frac{k^2}{\epsilon_t/\epsilon + 1}\right]^{1/2} \approx k\left[\frac{\omega\epsilon}{i\sigma}\right]^{1/2} = k\left[\frac{\omega\epsilon}{\sigma}e^{i3\pi/2}\right]^{1/2} = \sqrt{\frac{\omega\epsilon}{2\sigma}}k(-1+i)$$

$$k_z = k\left[\frac{\epsilon_t/\epsilon}{\epsilon_t/\epsilon + 1}\right]^{1/2} = k\left[1 + \frac{\epsilon}{\epsilon_g + i\sigma/\omega}\right]^{-1/2} = k\left[1 - \frac{i\omega\epsilon/\sigma}{1 - i\omega\epsilon_g/\sigma}\right]^{-1/2}$$

$$\approx k\left[1 + \frac{1}{2}\left(\frac{i\omega\epsilon/\sigma}{1 - i\omega\epsilon_g/\sigma}\right) + \frac{3}{8}\left(\frac{i\omega\epsilon/\sigma}{1 - i\omega\epsilon_g/\sigma}\right)^2\right]$$

$$\approx k\left[1 - \frac{3}{8}\left(\frac{\omega\epsilon}{\sigma}\right)^2 - \frac{1}{2}\frac{\omega^2\epsilon\epsilon_g}{\sigma^2} + i\frac{\omega\epsilon}{2\sigma}\right]$$

$$k_{tx} = -\frac{\epsilon_t}{\epsilon}k_x \approx -\frac{i\sigma}{\omega\epsilon}\sqrt{\frac{\omega\epsilon}{2\sigma}}k(-1+i) = \sqrt{\frac{\omega\mu\sigma}{2}}(1+i)$$

Thus, the wave in region 0 has its phase velocity directed towards the interface and exponentially decaying away from the surface. This is known as the Zenneck wave (Jonathan Zenneck, 15 April 1871 – 8 April 1959). Since $k_{zR} < k$, the Zenneck wave is a fast wave along the interface.

I. Plasma Surface Wave

Consider a plane boundary surface at $x = 0$ separating two media μ, ϵ_o for $x < 0$ and $\mu, \epsilon_t = \epsilon_o \left[1 - \omega_p^2/\omega^2\right]$ with $2 < \omega_p^2/\omega^2$, for $x > 0$. From dispersion relations (4.1.56) and (4.1.57), and with guidance condition $k_{tx} = -\frac{\epsilon_t}{\epsilon_o} k_x$, we find

$$k_x = \left[\frac{k^2}{\epsilon_t/\epsilon_o + 1}\right]^{1/2} = k \left[\frac{-1}{\omega_p^2/\omega^2 - 2}\right]^{1/2} = ik \left[\frac{1}{\omega_p^2/\omega^2 - 2}\right]^{1/2} = ik_{xI}$$

$$k_z = k \left[\frac{\epsilon_t/\epsilon_o}{\epsilon_t/\epsilon_o + 1}\right]^{1/2} = k \left[\frac{\omega_p^2/\omega^2 - 1}{\omega_p^2/\omega^2 - 2}\right]^{1/2}$$

$$k_{tx} = -\frac{\epsilon_t}{\epsilon_o} k_x = (\frac{\omega_p^2}{\omega^2} - 1)k_x = ik(\frac{\omega_p^2}{\omega^2} - 1)\sqrt{\frac{1}{\omega_p^2/\omega^2 - 2}} = ik_{txI}$$

We find a surface wave, called the plasma surface wave, that attenuates in the $\hat{x}$ direction inside the plasma media. In region 0 the waves attenuate in the $-\hat{x}$ direction. Here k_z is positive real. Thus plasma waves propagate along the interface and attenuate in both $\hat{x}$ and $-\hat{x}$ directions. As $\omega \to 0$, we have $k_z = k$ and $k_{xI}^2 = k_z^2 - k^2 = 0$ and we have a *uniform* TM plane wave propagating along the surface of a perfect conductor without attenuation.

The Poynting power density vectors in regions 0 and t are

$$\begin{cases} \overline{k} = -\hat{x}\, ik_{xI} + \hat{z}\, k_z \\[2mm] <\overline{S}_0> = \frac{1}{2}\text{Re}\left(\overline{E}_0 \times \overline{H}_0^*\right) = \frac{1}{2}\text{Re}\left(\overline{k}\frac{1}{\omega\epsilon_o}|\overline{H}_0|^2\right) \\[2mm] \qquad\quad = \hat{z}\frac{k_z}{2\,\omega\epsilon_o}e^{2k_{xI}x} \end{cases}$$

$$\begin{cases} \overline{k}_t = \hat{x}\, ik_{txI} + \hat{z}\, k_z \\[2mm] <\overline{S}_t> = \frac{1}{2}\text{Re}\left(\overline{E}_t \times \overline{H}_t^*\right) = \frac{1}{2}\text{Re}\left(\overline{k}_t\frac{1}{\omega\epsilon_t}|\overline{H}_t|^2\right) \\[2mm] \qquad\quad = \hat{z}\frac{k_z}{2\,\omega\epsilon_t}e^{-2k_{txI}x} \end{cases}$$

Notice that $\epsilon_t < 0$. Thus the $\hat{z}$ component of $\overline{S}_t$ is in the opposite direction of $\overline{S}_i$, and the plasma surface wave is a *backward wave*, which occurs when $\epsilon_t < -\epsilon_o$.

J. Reflection and Transmission by a Layered Medium

Consider a plane wave incident on a stratified isotropic medium with boundaries at $x = d_1,\ d_2, \ldots, d_t$ [Fig. 4.1.12]. The $(n+1)$th region is semi-infinite and is labeled region t, $t = n+1$. The permittivity and permeability in each region are denoted by ϵ_l and μ_l. The plane wave is incident from region 0 and has the plane of incidence parallel to the x-z plane. All field vectors are dependent on x and z only and independent of y. Since $\partial/\partial y = 0$, the Maxwell equations in any region l can be separated into TE and TM components governed by E_{ly} and H_{ly}. We obtain

| Region 0 | Region 1 | Region l | Region n | Region $t = n+1$ |

$\mu_0, \epsilon_0 \qquad \mu_1, \epsilon_1 \qquad \mu_l, \epsilon_l \qquad \mu_n, \epsilon_n \qquad \mu_t, \epsilon_t$

$x = d_0 \quad x = d_1 \quad x = d_{l\text{-}1} \quad x = d_l \quad x = d_{n\text{-}1} \quad x = d_n$
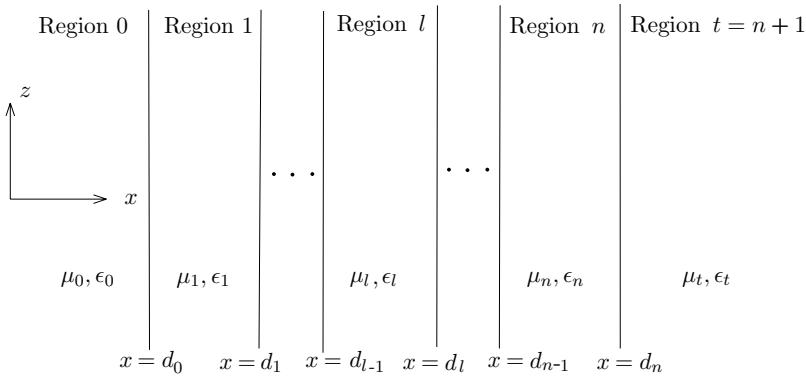
Figure 4.1.12 Layered medium.

$$H_{lx} = \frac{-1}{i\omega\mu_l}\frac{\partial}{\partial z}E_{ly} \tag{4.1.58}$$

$$H_{lz} = \frac{1}{i\omega\mu_l}\frac{\partial}{\partial x}E_{ly} \tag{4.1.59}$$

$$\left(\frac{\partial^2}{\partial x^2} + \frac{\partial^2}{\partial z^2} + \omega^2\mu_l\epsilon_l\right)E_{ly} = 0 \tag{4.1.60}$$

$$E_{lx} = \frac{1}{i\omega\epsilon_l}\frac{\partial}{\partial z}H_{ly} \tag{4.1.61}$$

$$E_{lz} = \frac{-1}{i\omega\epsilon_l}\frac{\partial}{\partial x}H_{ly} \tag{4.1.62}$$

$$\left(\frac{\partial^2}{\partial x^2} + \frac{\partial^2}{\partial z^2} + \omega^2\mu_l\epsilon_l\right)H_{ly} = 0 \tag{4.1.63}$$

The TE waves are completely determined by (4.1.58)–(4.1.60) and the TM waves by (4.1.61)–(4.1.63). The two sets of equations are duals of each other under replacements $\overline{E}_l \to \overline{H}_l$, $\overline{H}_l \to -\overline{E}_l$, and $\mu_l \rightleftarrows \epsilon_l$.

EXAMPLE 4.1.2

The second-order partial differential wave equation (4.1.63) or (4.1.60) can be solved formally with the method of separation of variables. Let

$$H_{ly} = X(x)Y(y)$$

Substituting into the wave equation, we obtain

$$\frac{1}{X(x)} \frac{d^2 X(x)}{dx^2} + \frac{1}{Y(y)} \frac{d^2 Y(y)}{dy^2} + \omega^2 \mu_l \epsilon_l = 0$$

We then let

$$\frac{1}{X(x)} \frac{d^2 X(x)}{dx^2} = -k_x^2$$

$$\frac{1}{Y(y)} \frac{d^2 Y(y)}{dy^2} = k_y^2$$

where k_x and k_y are separation parameters related by

$$k_x^2 + k_y^2 = \omega^2 \mu_l \epsilon_l$$

There are two independent solutions to each of the two ordinary differential equations. Out of the four possible combinations, many are absent owing to the constraints imposed by physical requirements and boundary conditions. For instance, $e^{ik_x x} e^{ik_y y}$ represents a wave propagating with the $\overline{k}$ vector $\overline{k} = \hat{x}k_x + \hat{y}k_y$, and $e^{-k_{xI} x} e^{ik_y y}$ with $k_x = -ik_{xI}$ and $k_z^2 - ik_{xI}^2 = \omega^2 \mu_l \epsilon_l$ propagating in the $\hat{z}$ direction and evanescent in the $\hat{x}$ direction.

— END OF EXAMPLE 4.1.2 —

For a TM plane wave, $H_y = H_0\, e^{ik_x x + ik_z z}$, incident on the stratified medium, the total field in region l can be written as

$$\overline{k}_l = \hat{x}k_{lx} + \hat{z}k_z \tag{4.1.64}$$

$$\overline{H}_l = \hat{y} \left(A_l e^{ik_{lx} x} + B_l e^{-ik_{lx} x} \right) e^{ik_z z} \tag{4.1.65}$$

$$\overline{E}_l = \frac{-1}{\omega \epsilon_l} \overline{k}_l \times \overline{H}_l \tag{4.1.66}$$

and

$$k_{lx}^2 + k_z^2 = \omega^2 \mu_l \epsilon_l$$

is the dispersion relation for region l. We do not write a subscript l for the k_z as a consequence of the phase-matching conditions. Truly, there

are multiple reflections and transmissions in each layer l. The amplitude A_l thus represents all wave components that have a propagating velocity component along the positive $\hat{x}$ direction, and B_l represents those with a velocity component along the negative $\hat{x}$ direction.

We let, in region 0, $\left\{ \begin{array}{l} A_0 = 1 \\ B_0 = R \end{array} \right.$ and in region t $\left\{ \begin{array}{l} A_t = T \\ B_t = 0 \end{array} \right.$ notice that region t is semi-infinite and there is no wave propagating with a velocity component in the positive $\hat{x}$ direction. We denote the transmitted amplitude by T.

The wave amplitudes A_l and B_l are related to wave amplitudes in neighboring regions by the boundary conditions. At $x = d_l$, boundary conditions require that E_z and H_y be continuous. We obtain

$$A_l e^{ik_{lx}d_l} + B_l e^{-ik_{lx}d_l} = A_{l+1}\, e^{ik_{(l+1)x}d_l} + B_{l+1}\, e^{-ik_{(l+1)x}d_l} \tag{4.1.67}$$

$$A_l e^{ik_{lx}d_l} - B_l e^{-ik_{lx}d_l} = p_{l(l+1)} \left[A_{l+1}e^{ik_{(l+1)x}d_l} - B_{l+1}e^{-ik_{(l+1)x}d_l} \right] \tag{4.1.68}$$

where

$$p_{l(l+1)} = \frac{\epsilon_l k_{(l+1)\,x}}{\epsilon_{l+1}\, k_{lx}} = \frac{1}{p_{(l+1)l}} \tag{4.1.69}$$

$$R_{l(l+1)} = \frac{1 - p_{l(l+1)}}{1 + p_{l(l+1)}} = -R_{(l+1)l} \tag{4.1.70}$$

There are $n+1$ boundaries which give rise to $(2n+2)$ equations. In region 0, we have an unknown reflection coefficient R. In region t, we have an unknown transmission coefficient T. There are two unknowns A_l and B_l in each of the regions $l = 1, 2, \ldots, n$. Thus we have a total of $(2n + 2)$ unknowns. To solve for the $(2n + 2)$ unknowns from the $(2n + 2)$ linear equations, we can arrange the equations in matrix form with the unknowns forming a $(2n + 2)$ column matrix and the coefficients forming a $(2n + 2) \times (2n + 2)$ square matrix. The solution is then obtained by inverting the square matrix. This procedure is straightforward but tedious. We shall now describe simpler ways to deal with the problem.

K. Reflection Coefficients for Stratified Media

Since we are interested in finding the reflection coefficient for the stratified medium, let us derive a closed-form formula for R. We first solve (4.1.67) and (4.1.68) for A_l and B_l.

$$A_l e^{ik_{lx}d_l} = \frac{1 + p_{l(l+1)}}{2} \left\{ A_{l+1} e^{ik_{(l+1)x}d_l} + R_{l(l+1)} B_{l+1} e^{-ik_{(l+1)x}d_l} \right\}$$

(4.1.71)

$$B_l e^{-ik_{lx}d_l} = \frac{1 + p_{l(l+1)}}{2} \left\{ R_{l(l+1)} A_{l+1} e^{ik_{(l+1)x}d_l} + B_{l+1} e^{-ik_{(l+1)x}d_l} \right\}$$

(4.1.72)

$$R_{l(l+1)} = \frac{1 - p_{l(l+1)}}{1 + p_{l(l+1)}} = -R_{(l+1)l}$$

(4.1.73)

is the reflection coefficient for waves in region l, caused by the boundary separating regions l and $l+1$, which is equal to the negative of the reflection coefficient $R_{(l+1)l}$ in region $l+1$.

Forming the ratio of (4.1.71) and (4.1.72) we obtain

$$\frac{B_l}{A_l} = \frac{R_{l(l+1)} e^{i2k_{(l+1)x}d_l} + (B_{l+1}/A_{l+1})}{e^{i2k_{(l+1)x}d_l} + R_{l(l+1)}(B_{l+1}/A_{l+1})} e^{i2k_{lx}d_l}$$

(4.1.74)

where B_l/A_l is expressed in terms of B_{l+1}/A_{l+1}.

From (4.1.74) we see that B_l/A_l is the ratio of the amplitude of the wave propagating in the negative $\hat{x}$ direction to that of the wave propagating in the positive $\hat{x}$ direction. Consider a two-layer medium, with $t = 2$ and $n = 1$. From (4.1.74) with $B_2 = 0$, we find

$$\frac{B_1}{A_1} = R_{12} e^{i2k_{1x}d_1}$$

(4.1.75)

Making use again of (4.1.74) and substituting in (4.1.75), we obtain

$$R = \frac{B_0}{A_0} = \frac{R_{01} e^{i2k_{1x}d_0} + (B_1/A_1)}{e^{i2k_{1x}d_0} + R_{01}(B_1/A_1)} e^{i2k_xd_0}$$

$$= \frac{R_{01} + R_{12} e^{i2k_{1x}(d_1-d_0)}}{1 + R_{01}R_{12} e^{i2k_{1x}(d_1-d_0)}} e^{i2k_xd_0}$$

(4.1.76)

For a half-space medium, $B_1 = 0$, we find

$$R = \frac{B_0}{A_0} = R_{01} e^{i2k_xd_0}$$

(4.1.77)

The phase shift is due to the choice of the coordinate system with boundary surface at $x = d_0$ instead of at $x = 0$.

EXAMPLE 4.1.3

We can write (4.1.74) in the following form:

$$
\frac{B_l}{A_l} = \frac{e^{i2k_{lx}d_l}}{R_{l(l+1)}} + \frac{\left[1 - \left(1/R_{l(l+1)}^2\right)\right] e^{i2(k_{(l+1)\,x}+k_{lx})d_l}}{\left[1/R_{l(l+1)}\right] e^{i2k_{(l+1)\,x}d_l} + \left(B_{l+1}/A_{l+1}\right)}
$$

$$
= \frac{e^{i2k_{lx}d_l}}{R_{l(l+1)}} + \frac{\left[1 - \left(1/R_{l(l+1)}^2\right)\right] e^{i2(k_{(l+1)\,x}+k_{lx})d_l}}{\left[1/R_{l(l+1)}\right] e^{i2k_{(l+1)\,x}d_l}} \Bigg| + \frac{B_{l+1}}{A_{l+1}} \qquad \text{(E4.1.3.1)}
$$

With the second equality we introduce a notation for writing a continued fraction. Equation (4.1.74) expresses (B_l/A_l) in terms of B_{l+1}/A_{l+1} and so on, until the transmitted region t, where $B_t/A_t = 0$, is reached.

The reflection coefficient due to the stratified medium is $R = B_0/A_0$. Making use of the continued fractions, we obtain

$$
R = \frac{e^{i2k_x d_0}}{R_{01}} + \frac{\left[1 - (1/R_{01}^2)\right] e^{i2(k_{1x}+k_x)d_0}}{(1/R_{01})e^{i2k_{1x}d_0}} \Bigg| + \frac{e^{i2k_{1x}d_1}}{R_{12}}
$$

$$
+ \frac{\left[1 - (1/R_{12}^2)\right] e^{i2(k_{2x}+k_{1x})d_1}}{(1/R_{12})e^{i2k_{2x}d_1}} \Bigg| + \cdots + \frac{e^{i2k_{(n-1)\,x}d_{n-1}}}{R_{(n-1)\,n}}
$$

$$
+ \frac{\left[1 - (1/R_{(n-1)\,n}^2)\right] e^{i2(k_{nx}+k_{(n-1)\,x})d_{n-1}}}{(1/R_{(n-1)\,n})e^{i2k_{nx}d_{n-1}}} \Bigg| + R_{nt}e^{i2k_{nx}d_n} \quad \text{(E4.1.3.2)}
$$

This is a closed-form solution for the reflection coefficient expressed in continued fractions. Such a solution is very easily programmed for numerical computation.

For a two-layer medium, the result can also be obtained from (E4.1.3.2). Note that when $R_{01} = \pm 1$, the reflection coefficient in (E4.1.3.2) will have magnitude unity, disregarding the composition of the stratified medium below $x = d_1$. This should be the case, as $|R_{01}| = 1$ represents, for instance, a perfectly conducting coating.

— END OF EXAMPLE 4.1.3 —

EXAMPLE 4.1.4

Consider a two-layer medium as shown in Fig. E4.1.4.1. The reflection coefficient for a two-layer medium in (4.1.76) becomes, letting $d_0 = 0$ and $d_1 = d$,

$$R = \frac{R_{01} + R_{12}e^{i2k_{1x}d}}{1 + R_{01}R_{12}e^{i2k_{1x}d}} = \frac{R_{01} + R_{12}e^{i2k_{1x}d}}{1 - R_{10}R_{12}e^{i2k_{1x}d}} \qquad \text{(E4.1.4.1)}$$
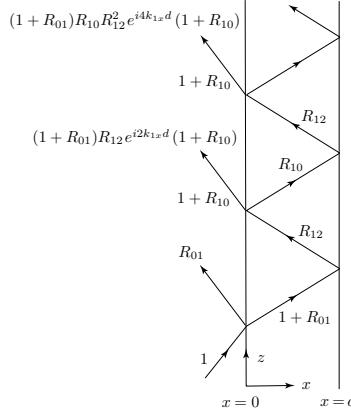
Figure E4.1.4.1 Multiple reflections.

As $R_{01} = -R_{10}$ and the magnitudes of the reflection coefficients R_{01} and R_{12} are smaller than unity, we may expand the denominator of (E4.1.4.1) to obtain

$$R = (R_{01} + R_{12}e^{i2k_{1x}d}) \sum_{m=0}^{\infty} R_{10}^m R_{12}^m e^{i2mk_{1x}d}$$

$$= R_{01} + R_{01}R_{10} \sum_{m=0}^{\infty} R_{10}^m R_{12}^{m+1} e^{i2(m+1)k_{1x}d} + \sum_{m=0}^{\infty} R_{10}^m R_{12}^{m+1} e^{i2(m+1)k_{1x}d}$$

$$= R_{01} + (1 + R_{01}R_{10}) \sum_{m=0}^{\infty} R_{10}^m R_{12}^{m+1} e^{i2(m+1)k_{1x}d}$$

$$= R_{01} + (1 + R_{01}) \left[\sum_{m=0}^{\infty} R_{10}^m R_{12}^{m+1} e^{i2(m+1)k_{1x}d} \right] (1 + R_{10})$$

where we use the relation $1 + R_{01}R_{10} = 1 + R_{01} + R_{10} + R_{01}R_{10} = (1 + R_{01})(1 + R_{10})$. The summation represents the multiply reflected waves from the two-layer medium as illustrated in Fig. E4.1.4.1.

— END OF EXAMPLE 4.1.4 —

L. Propagation Matrices and Transmission Coefficients

We will now show that the transmission coefficient $T = A_t/A_0$ as well as all wave amplitudes in all regions can be obtained by the use of propagation matrices. We solve for A_{l+1} and B_{l+1} in terms of A_l and B_l from (4.1.67)–(4.1.68) and obtain

$$A_{l+1}\, e^{ik_{(l+1)x}d_l} = \frac{1 + p_{(l+1)l}}{2}\left(A_l e^{ik_{lx}d_l} + R_{(l+1)l}B_l e^{-ik_{lx}d_l}\right) \quad (4.1.78)$$

$$B_{l+1}\, e^{-ik_{(l+1)x}d_l} = \frac{1 + p_{(l+1)l}}{2}\left(R_{(l+1)l}A_l e^{ik_{lx}d_l} + B_l e^{-ik_{lx}d_l}\right) \quad (4.1.79)$$

Expressing in the form of matrix multiplication, we have

$$\begin{pmatrix} A_{l+1} \\ B_{l+1} \end{pmatrix} = \overline{\overline{V}}_{(l+1)\,l} \cdot \begin{pmatrix} A_l \\ B_l \end{pmatrix} \quad (4.1.80)$$

$$\overline{\overline{V}}_{(l+1)\,l} = \frac{1 + p_{(l+1)l}}{2}\begin{pmatrix} e^{-i(k_{(l+1)x}-k_{lx})d_l} & R_{(l+1)\,l}e^{-i(k_{(l+1)x}+k_{lx})d_l} \\ R_{(l+1)\,l}e^{i(k_{(l+1)x}+k_{lx})d_l} & e^{i(k_{(l+1)x}-k_{lx})d_l} \end{pmatrix}$$
$$(4.1.81)$$

is called the forward-propagating matrix. It is to be noted for the forward-propagating matrix between layers n and $t = n + 1$,

$$\begin{pmatrix} T \\ 0 \end{pmatrix} = \overline{\overline{V}}_{tn} \cdot \begin{pmatrix} A_n \\ B_n \end{pmatrix}$$

$$\overline{\overline{V}}_{tn} = \frac{1}{2}\left(1 + p_{tn}\right)\begin{pmatrix} e^{-i(k_{tx}-k_{nx})d_n} & R_{tn}e^{-i(k_{tx}+k_{nx})d_n} \\ R_{tn}e^{i(k_{tx}+k_{nx})d_n} & e^{i(k_{tx}-k_{nx})d_n} \end{pmatrix}$$

Similarly, we may express A_l and B_l in terms of A_{l+1} and B_{l+1} using (4.1.71)–(4.1.72) and defining a backward-propagating matrix.

The propagation matrices can be used to determine wave amplitudes in any region in terms of those in any other region. For $m > l$, we make use of the forward propagation matrix to obtain

$$\begin{pmatrix} A_m \\ B_m \end{pmatrix} = \overline{\overline{V}}_{m(m-1)} \cdot \overline{\overline{V}}_{(m-1)(m-2)} \cdots \overline{\overline{V}}_{(l+1)\,l} \cdot \begin{pmatrix} A_l \\ B_l \end{pmatrix}$$

Similarly, backward-propagating matrices can be used to express wave amplitudes in any region j in terms of those in region l for $l > j$.

In particular, the transmission coefficient $T = A_t/A_0$ for a stratified medium with $t = n + 1$ layers can be calculated by the multiplication of $n + 1$ propagation matrices. Using the forward-propagating matrices, we have

$$\begin{pmatrix} T \\ 0 \end{pmatrix} = \overline{\overline{V}}_{tn} \cdot \overline{\overline{V}}_{n(n-1)} \cdots \overline{\overline{V}}_{10} \cdot \begin{pmatrix} 1 \\ R \end{pmatrix}$$

includes all information about the stratified medium. Once $\overline{\overline{V}}_{t0}$ is known, both the reflection and transmission coefficients can be calculated from its matrix elements.

For a one-layer (half-space) medium. From (4.1.81), we find

$$\begin{pmatrix} T \\ 0 \end{pmatrix} = \frac{1}{2}(1 + p_{10}) \begin{pmatrix} e^{-i(k_{tx}-k_x)d_1} & R_{10}e^{-i(k_{tx}+k_x)d_1} \\ R_{10}e^{i(k_{tx}+k_x)d_1} & e^{i(k_{tx}-k_x)d_1} \end{pmatrix} \begin{pmatrix} 1 \\ R \end{pmatrix}$$

With the reflection coefficient

$$R = R_{01}e^{i2k_x d_1} \tag{4.1.82}$$

we obtain the transmission coefficient

$$T = \frac{1}{2}(1 + p_{10})\left(1 - R_{01}^2\right)e^{-i(k_{tx}-k_x)d_1} = \frac{2}{1 + p_{01}}e^{-i(k_{tx}-k_x)d_1} \tag{4.1.83}$$

where we made use of the fact that $p_{10} = 1/p_{01}$ and $R_{10} = -R_{01}$.

For a two-layer medium, we obtain the transmission coefficient from

$$\begin{pmatrix} A_1 \\ B_1 \end{pmatrix} = \frac{1}{2}(1 + p_{10}) \begin{pmatrix} e^{-i(k_{1x}-k_x)d_0} & R_{10}e^{-i(k_{1x}+k_x)d_0} \\ R_{10}e^{i(k_{1x}+k_x)d_{00}} & e^{i(k_{1x}-k_x)d_0} \end{pmatrix} \begin{pmatrix} 1 \\ R \end{pmatrix}$$

$$\begin{pmatrix} T \\ 0 \end{pmatrix} = \frac{1}{2}(1 + p_{t1}) \begin{pmatrix} e^{-i(k_{tx}-k_{1x})d_1} & R_{t1}e^{-i(k_{tx}+k_{1x})d_1} \\ R_{t1}e^{i(k_{tx}+k_{1x})d_1} & e^{i(k_{tx}-k_{1x})d_1} \end{pmatrix} \begin{pmatrix} A_1 \\ B_1 \end{pmatrix}$$

we obtain

$$A_1 = \frac{2e^{-i(k_{1x}-k_x)d_0}}{(1 + p_{01})(1 + R_{01}R_{1t}e^{i2k_{1x}(d_1-d_0)})} = \frac{T_{01}e^{i(k_x-k_{1x})d_0}}{1 + R_{01}R_{1t}e^{i2k_{1x}(d_1-d_0)}}$$

$$B_1 = \frac{2R_{1t}e^{i2k_{1x}d_1}e^{-i(k_{1x}-k_x)d_0}}{(1 + p_{01})(1 + R_{01}R_{1t}e^{i2k_{1x}(d_1-d_0)})} = \frac{T_{01}R_{1t}e^{i(k_x-k_{1x})d_0}e^{i2k_{1x}d_1}}{1 + R_{01}R_{1t}e^{i2k_{1x}(d_1-d_0)}}$$

$$T = \frac{T_{01}T_{1t}e^{i(k_x-k_{1x})d_0}e^{i(k_{1x}-k_{tx})d_1}}{1 + R_{01}R_{1t}e^{i2k_{1x}(d_1-d_0)}} \tag{4.1.84}$$

where we made use of R in (4.1.76).

EXAMPLE 4.1.5

Use the forward-propagation matrix formalism, we can determine the transmission and the reflection coefficients for a periodic medium made of $2N + 2$ isotropic dielectric layers with alternating high and low permittivities ϵ_h and ϵ_l. The thickness of each layer is a quarter-wavelength inside the dielectric. The transmitted region is $t = 2N + 2$ and has permittivity ϵ_t. Consider normal incidence, $k_x = 0$. Using the forward-propagation matrix formalism, we have

$$\begin{pmatrix} 0 \\ T \end{pmatrix} = \overline{\overline{V}}_{th} \cdot \left(\overline{\overline{V}}_{hl} \cdot \overline{\overline{V}}_{lh} \right)^N \cdot \overline{\overline{V}}_{h0} \cdot \begin{pmatrix} R \\ 1 \end{pmatrix}$$

In region $m + 1$, $k_{(m+1)z} = k_{m+1}$ we have $k_{(m+1)z}(d_{m+1} - d_m) = \pi/2$. Note also that $\mu_{m+1} k_{mz}/\mu_m k_{(m+1)z} = (\epsilon_m/\epsilon_{m+1})^{1/2}$. The forward-propagation matrices become

$$\overline{\overline{V}}_{ho} = -\frac{i}{2} \begin{pmatrix} 1 + \sqrt{\epsilon/\epsilon_h} & 1 - \sqrt{\epsilon/\epsilon_h} \\ -1 + \sqrt{\epsilon/\epsilon_h} & -1 - \sqrt{\epsilon/\epsilon_h} \end{pmatrix}$$

$$\overline{\overline{V}}_{hl} \cdot \overline{\overline{V}}_{lh} = -\frac{1}{2} \begin{pmatrix} \sqrt{\epsilon_l/\epsilon_h} + \sqrt{\epsilon_h/\epsilon_l} & \sqrt{\epsilon_l/\epsilon_h} - \sqrt{\epsilon_h/\epsilon_l} \\ \sqrt{\epsilon_l/\epsilon_h} - \sqrt{\epsilon_h/\epsilon_l} & \sqrt{\epsilon_l/\epsilon_h} + \sqrt{\epsilon_h/\epsilon_l} \end{pmatrix}$$

$$\overline{\overline{V}}_{th} = \frac{1}{2} \begin{pmatrix} (1 + \sqrt{\epsilon_h/\epsilon_t})e^{ik_t d} & (1 - \sqrt{\epsilon_h/\epsilon_t})e^{ik_t d} \\ (1 - \sqrt{\epsilon_h/\epsilon_t})e^{-ik_t d} & (1 + \sqrt{\epsilon_h/\epsilon_t})e^{-ik_t d} \end{pmatrix}$$

where d is the total thickness of the periodic medium. The term $(\overline{\overline{V}}_{hl} \cdot \overline{\overline{V}}_{lh})^N$ can be calculated by making use of the matrix identity

$$\begin{pmatrix} a + b & a - b \\ a - b & a + b \end{pmatrix}^N = 2^{N-1} \begin{pmatrix} a^N + b^N & a^N - b^N \\ a^N - b^N & a^N + b^N \end{pmatrix}$$

It follows that

$$R = \frac{(\epsilon_l/\epsilon_h)^N - \sqrt{\epsilon_h^2/\epsilon\epsilon_t}}{(\epsilon_l/\epsilon_h)^N + \sqrt{\epsilon_h^2/\epsilon\epsilon_t}}$$

and

$$T = \frac{2i(-1)^N(\epsilon/\epsilon_t)^{1/2}e^{-ik_t d}}{\sqrt{\epsilon/\epsilon_h}\,(\epsilon_l/\epsilon_h)^{N/2} + \sqrt{\epsilon_h/\epsilon_t}\,(\epsilon_h/\epsilon_l)^{N/2}}$$

We find the reflectivity $r = |R|^2$, and the transmissivity $t = p_{0t} |T|^2$. Note that although both TE and TM waves become TEM at normal incidence, we must use $p_{0t} = k_{tz}/k_z = (\epsilon_t/\epsilon)^{1/2}$ because here R and T are amplitude reflection and transmission coefficients for electric field vectors. It can be shown that $r + t = 1$.

— END OF EXAMPLE 4.1.5 —

EXAMPLE 4.1.6

Define a space-dependent complex reflection coefficient $\Gamma_l(z)$ such that

$$\Gamma_l(z) = \frac{A_l}{B_l} e^{i2k_{lz}z}$$
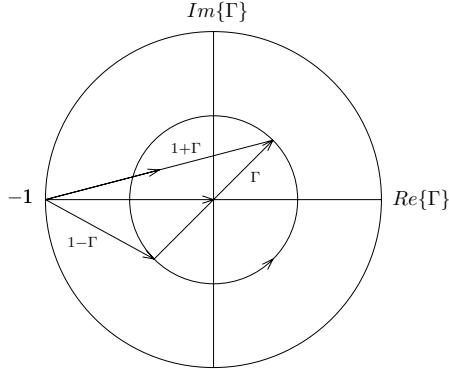
Figure E4.1.6.1 Complex Γ plane.

On the complex $\Gamma_l(z)$ plane [Fig. E4.1.6.1], as the phase $\phi = 2k_{lz}z$ increases with z, $\Gamma_l(z)$ varies in a counterclockwise manner. If k_{lz} is complex, $\Gamma_l(z)$ decreases with increasing z.

Define a wave impedance $Z_l(z)$ in the negative $\hat{z}$ direction:

$$Z_{lz}(z) = \frac{E_{ly}}{H_{lx}} = \frac{\omega\mu_l}{k_{lz}} \frac{1 + \Gamma_l(z)}{1 - \Gamma_l(z)}$$

which is complex. For a plane wave propagating in free space in the absence of any medium, the wave impedance in the direction of wave propagation is $\eta = \omega\mu_o/k = (\mu_o/\epsilon_o)^{1/2} \approx 377\,\Omega$.

With the definition of the complex wave impedance, the ratio of (4.1.67) to (4.1.68) gives $Z_{lz}(z = -d_l) = Z_{(l+1)z}(z = -d_l)$. Thus at each interface the wave impedance is continuous across the boundary.

On the complex Γ plane, $Z_{lz}(z)$ can be interpreted as the ratio of the two lengths as shown in Figure E4.1.6.1. The magnitude of $Z_{lz}(z)$ is maximum when Γ_l is real and positive. We define the dimensionless relative wave impedance as
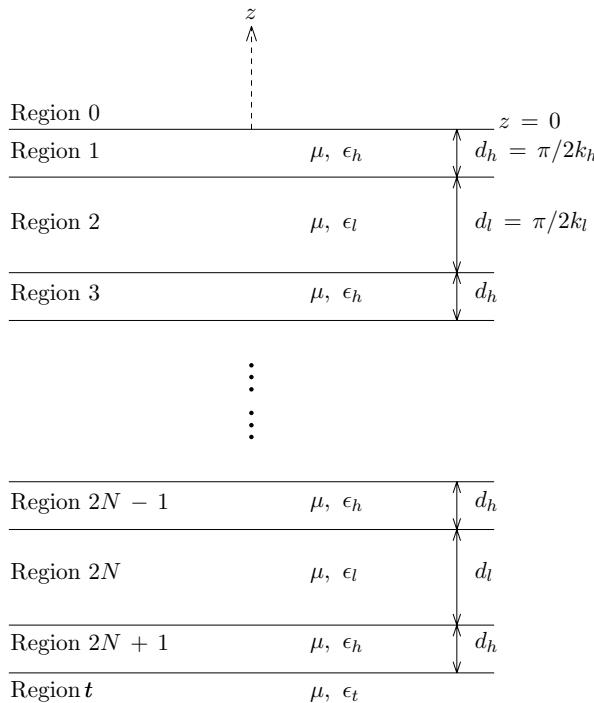
$$z_l = \frac{Z_{lz}}{\omega\mu_l/k_{lz}} = \frac{1 + \Gamma_l}{1 - \Gamma_l}$$

For all possible complex values of $\Gamma_l(z)$, we can map the corresponding $z_l(z)$ values onto the complex $\Gamma_l(z)$ plane. The result is in the form of the Smith chart, which is frequently used in transmission line studies.

— END OF EXAMPLE 4.1.6 —

EXAMPLE 4.1.7

To illustrate the use of the wave impedance concept, consider a stratified medium composed of $2N + 2$ isotropic dielectric layers (corresponding to $2N + 2$ boundaries) with alternating high and low permittivities, ϵ_h and ϵ_l; regions 1, 3, 5, ..., $2N + 1$ are high-permittivity layers, and regions 2, 4, 6, ..., $2N$ are low-permittivity layers. Region 0 has permittivity ϵ and permeability μ. The thickness of each layer is a quarter-wavelength inside the dielectric. The transmitted region is $2N + 2 = t$ and has permittivity ϵ_t. Permeabilities for all layers are equal to μ [Fig. E4.1.7.1].

**Figure E4.1.7.1 Layered medium with alternating high and
low permittivities.**

Consider a wave normally incident upon the stratified medium, $k_x = 0$, $k_{lz} = \omega\sqrt{\mu\epsilon_l}$ for all l. The wave impedance of region t, since there is no reflection, is $Z_t = (\mu/\epsilon_t)^{1/2}$. Because of the continuity of wave impedance across the boundary, the impedance across the interface separating regions $2N + 1$ and t is $Z_{2N+1} = (\mu/\epsilon_t)^{1/2}$. The relative impedance is $z_{2N+1} = (\mu/\epsilon_t)^{1/2}/(\mu/\epsilon_h)^{1/2} = (\epsilon_h/\epsilon_t)^{1/2}$. Making use of the Smith chart concept, and noting the periodicity of the structure, we determine the wave impedance at

$z = 0$:

$$Z_0 = \left(\frac{\epsilon_t}{\epsilon_h}\right)^{1/2} \left(\frac{\epsilon_l}{\epsilon_h}\right)^N \left(\frac{\mu}{\epsilon_h}\right)^{1/2}$$

The reflection coefficient R at $z = 0$ is found to be

$$R_0 = \frac{Z_0/(\mu/\epsilon)^{1/2} - 1}{Z_0/(\mu/\epsilon)^{1/2} + 1} = \frac{(\epsilon_t/\epsilon_h)^{1/2}(\epsilon_l/\epsilon_h)^N(\epsilon/\epsilon_h)^{1/2} - 1}{(\epsilon_t/\epsilon_h)^{1/2}(\epsilon_l/\epsilon_h)^N(\epsilon/\epsilon_h)^{1/2} + 1}$$

We observe that, for a high ϵ_h/ϵ_l ratio and for a larger number of layers, the reflection coefficient R_0 approaches the value -1, and the structure is highly reflective. Such structures are useful at optical frequencies since metallic reflectors are subject to corrosion and tarnishing problems.

— END OF EXAMPLE 4.1.7 —

Problems

P4.1.1
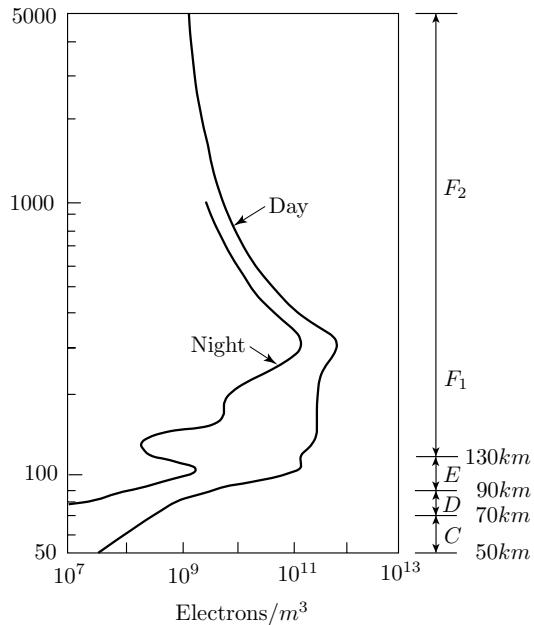
Figure P4.1.1.1 Electron density profile of ionospheric layers.

The ionosphere extends from approximately 50 km above the earth to several earth radii (the mean earth radius is about 6371 km) with the maximum in ionization density at about 300 km [Fig. P4.1.1.1]. The ionization density profile shows ledges where it varies more slowly with altitude. These ledges are the C, D, E, F_1, and F_2 layers as shown in the figure. These maxima arise because both the solar radiation and the composition of the atmosphere change with altitude. The heights and the intensities of ionization of these layers change with the hour of the day, the season of the year, the sunspot cycle, etc. The electron density varies from approximately $10^7 \, \mathrm{m}^{-3}$ to $10^{12} \, \mathrm{m}^{-3}$ in going from the lowest to the highest layer. For simplicity, assume that the ionosphere consists of a 40 km thick E-layer with electron density $N = 10^{11} \, \mathrm{m}^{-3}$ below a 200 km thick F-layer with $N = 6 \times 10^{11} \, \mathrm{m}^{-3}$.

(a) What are the plasma frequencies of the E and F layers ?
(b) Consider a plane wave of 10 MHz incident at an angle θ upon the ionosphere from below the E-layer. What are the transmitted angles θ_t of the ionosphere wave in the E and F layers?
(c) Let $\theta = 30°$. Below what frequency will the wave be totally reflected by the E-layer and below what frequency will it be totally reflected by the F-layer?

P4.1.2

Rainbow arc often appears when sunlight shines on water droplets after a brief shower late in the afternoon. When a sun ray is refracted as it enters the raindrop, total internally reflected from inside the drop, and refracted again as it leaves the drop and passes to the observer.

(a) Consider the ray path with only one internal reflection. Show that the angle between the incident ray and the exit ray is $\phi = 2(2\theta_2 - \theta_1)$, where θ_1 is the incident angle and θ_2 is the refracted angle.
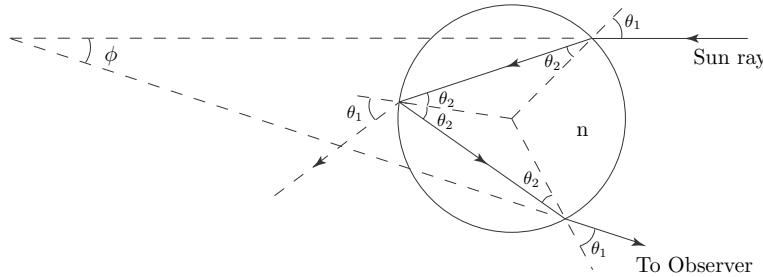
Figure P4.1.2.1   Total internal reflection in a raindrop.

(b) Show that maximum ϕ occurs at $\theta_1 = \sin^{-1} \sqrt{(4 - n^2)/3}$ and $\phi_{\max} \approx 42°$ for $n = 4/3$, with the scattering angle between the incident ray and scattered ray $\theta_s = 138°$.
(c) The refractive index for a raindrop is $n = 1.330$ for red light ($\lambda = 0.7\,\mu$), $n = 4/3 = 1.333$ for orange light, and $n = 1.342$ for violet light

$(\lambda = 0.4\,\mu)$. Determine the scattering angles for the red and violet light rays. What are the relative positions of the different color bands in a rainbow?

P4.1.3
A plane wave is normally incident in $\hat{x}$ direction upon a medium with permeability μ_0 and permittivity ε.
(a) Find the transmitted electric field $\overline{E}_t$.

(b) If the lower half-space is a plasma medium with $\varepsilon = \varepsilon_0\left(1 - \dfrac{\omega_p^2}{\omega^2}\right)$ and $\omega^2 = \dfrac{1}{2}\omega_p^2$, show that the transmitted wave is evanescent and find the exponential attenuation rate. Find the time-average Poynting power density as a function for x for the transmitted wave.

(c) If the half-space is a conducting medium with $\varepsilon = \varepsilon_0\left(1 + i\dfrac{\sigma}{\omega\varepsilon_0}\right)$ and $\sigma \gg \omega\varepsilon_0$. Find the exponential attenuation rate and the time-average Poynting power density as a function of x for the transmitted wave.

P4.1.4
A gas laser is often a tube containing gas, fitted with Brewster-angle windows and external mirrors. The output of the laser beam will be linearly polarized. For what reason and in which direction? Let a solid-state laser be fabricated of rods with ends beveled at the Brewster angle θ_B [Fig. P4.1.4.1]. Calculate all appropriate angles in Figure P4.1.4.1, including the bevel angle of the glass rod, which has a dielectric constant $\epsilon_b = 2.5$.
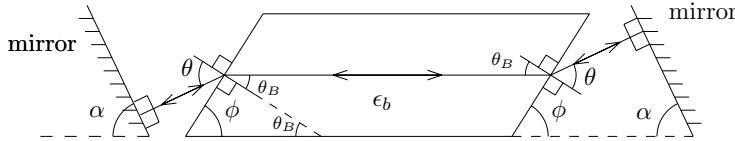
Figure P4.1.4.1 A solid-state laser.

P4.1.5
Let a plane wave be incident on a plane boundary from the inside of a negative uniaxial crystal. Consider the special case in which the optic axis is perpendicular to the plane of incidence. Find the range of θ such that there is only total internal reflection for the ordinary wave and the transmitted waves are extraordinary waves.

P4.1.6
A plane wave is totally reflected when incident upon a glass-air boundary. At this incident angle, another piece of glass is brought very close to the first one so that there is a very small air gap between the two. Calculate the reflection and transmission coefficients as a function of the gap dimension. Show that transmission is now possible.

P4.1.7

Sun light glares caused by reflections from plane surfaces are partially linearly polarized. The reflectivities are functions of incident angle θ.

$$r^{\text{TE}} = |R^{\text{TE}}|^2 = \left| \frac{1 - k_t \cos\theta_t / k \cos\theta}{1 + k_t \cos\theta_t / k \cos\theta} \right|^2$$

$$r^{\text{TM}} = |R^{\text{TM}}|^2 = \left| \frac{1 - \epsilon_0 k_t \cos\theta_t / \epsilon_t k \cos\theta}{1 + \epsilon_0 k_t \cos\theta_t / \epsilon_t k \cos\theta} \right|^2$$

(a) Show that for all incident angles, there are more reflected TE components than TM components $|R^{\text{TE}}|^2 \geq |R^{\text{TM}}|^2$.

(b) Determine the Brewster angle for $\epsilon_t = 3$. The Brewster angle, θ_B, is also called the polarization angle Polarization angle because at θ_B the reflected wave is entirely TE polarized.

(c) Your polaroid glasses absorb one linear component of incident light. To minimize sun glare, what component, TE or TM, reaches your eyes after passing through the glasses? Explain why.

P4.1.8

A plane wave of angular frequency ω is incident on a plasma medium with permeability μ_o and permittivity $\epsilon = \epsilon_o \left(1 - \omega_p^2/\omega^2\right)$, where ω_p is the plasma frequency and $\omega = 2\omega_p$.

(a) Calculate the critical angle θ_C such that the incident wave is totally reflected.

(b) Calculate the Brewster angle θ_B such that TM waves are totally transmitted.

(c) In general for any two isotropic media, can you find an incident angle θ such that $\theta = \theta_B > \theta_C$? If you can, give an example. If you cannot, explain why not.

P4.1.9

When a plane wave is totally internally reflected, nodes of E appear in front of the plane of reflection. Let the incident field, $\overline{E}_i$, be

$$\overline{E}_i = \hat{y} E_0 e^{ik_x x + ik_z z}$$

The reflected field, $\overline{E}_r$, is

$$\overline{E}_r = \hat{y} R^{TE} E_0 e^{-ik_x x + ik_z z + i2\phi}$$

where $\phi = -\tan^{-1}(k_{txI}/k_x) = -\tan^{-1}(\sqrt{\epsilon_r \sin^2\theta - 1}/\cos\theta)$.

(a) Find an expression for the position of the nodal plane nearest to the plane $x = 0$.

(b) The total internal reflection is equivalent to reflection from a perfect conductor located at $x = x_{eff}$ (the medium ϵ being continued into the region $x > 0$). What is the effective position?

(c) Plot the effective position as a function of angle $\theta \geq \theta_c$ with $\epsilon/\epsilon_0 = 2$.
(d) The transmitted wave is damped exponentially in the $-\hat{x}$ direction. Letting δ be the distance over which the field amplitude decreases to $1/e$ of its value at the interface $(x = 0)$, plot δ (penetration depth) as a function of angle $\theta \geq \theta_c$ with $\epsilon/\epsilon_0 = 2$.

P4.1.10

A plane wave is incident from free space on a half-space conducting medium with ϵ_0, μ_0, and conductivity σ. Let the incident wave be

$$\overline{E} = \hat{y} E_0 e^{ik_x x - ik_z z}.$$

(a) Find the incident wave vector.
(b) Show that for $\sigma/\omega\epsilon_0 \gg 1$, the transmitted wave is almost perpendicular to the interface and that the transmitted angle is

$$\theta_t \approx \tan^{-1}\left[\sqrt{2\omega\epsilon_0/\sigma}\, \sin\theta \right].$$

(c) Determine the time average Poynting vector for the power flow in the conducting medium. What is the magnitude of the transmitted electric field compared to E_0?

P4.1.11

A uniform plane wave is incident at an incident angle θ on a plasma characterized by the permittivity ϵ_t and permeability μ_0.

$$\epsilon_t = \epsilon_0 \left[1 - \frac{\omega_p^2}{\omega^2 + \omega_{eff}^2} + i \frac{\omega_p^2 \omega_{eff}}{\omega\left(\omega^2 + \omega_{eff}^2\right)} \right]$$

where ω_p is the plasma frequency and ω_{eff} is the collision frequency.

Let the incident uniform plane wave have the electric field vector

$$\overline{E}_i = \hat{y} E_0 e^{i\frac{k_0}{\sqrt{2}} x - i\frac{k_0}{\sqrt{2}} z}$$

where E_0 is a real constant and $k_0 = \omega\sqrt{\mu_0\epsilon_0}$.

(a) Let $\omega = \sqrt{2}\omega_p$ and $\omega_{eff} = 0$. Give the expression for the transmitted electric field vector and the transmitted time-average Poynting vector $\langle \overline{S}_t \rangle$ in terms of E_0, k_0, ω, ϵ_0, μ_0, and space coordinates.
(b) Let $\omega = \omega_p$ and $\omega_{eff} = 0$. Give the expression for the transmitted electric field vector and the $\hat{z}$ component of the transmitted time-average Poynting vector $\langle S_{tz} \rangle$ in terms of E_0, k_0, ω, ϵ_0, μ_0, and space coordinates.
(c) Let $\omega = \omega_p = \omega_{eff}$. Give the expression for the transmitted electric field vector and the $\hat{z}$ component of the transmitted time-average Poynting vector $\langle S_{tz} \rangle$ in terms of E_0, k_0, ω, ϵ_0, μ_0, and space coordinates.

P4.1.12

Consider a solid-state Fabry-Perot etalon filter made of an eight-layer stratified medium. Regions 1, 3, 5, and 7 are made of magnesium fluoride (refractive index $n = 1.35$) and are a quarter-wavelength thick. Regions 2, 4, and 6 are made of zinc sulfide (refractive index $n = 2.3$). Regions 2 and 6 are a quarter-wavelength thick, but region 4 is a half-wavelength thick. What are the reflectivity and transmissivity for a plane wave normally incident upon this stratified medium? Explain why the structure can be used for filtering purposes.

P4.1.13

In the microwave remote sensing of the Earth from satellite or aircraft, a radiometer is used to measure the emissivity of the area under observation. The emissivity e is related to reflectivity or to the power reflection coefficient by $e = 1 - r$. Theoretically, we should be able to determine, for instance, the ice thickness on a lake. Assume that the lake ice permittivity is $\epsilon = 3.2(1+i0.01)\epsilon_o$ and that the water is a perfect reflector. Discuss the frequency range that you would recommend and the depth that the radiometer can "see" through the ice.

P4.1.14

Show that the difference in relative phase change between TM and TE waves upon total internal reflection from a dielectric medium with refractive index n is

$$\Delta = \phi_{\text{TE}} - \phi_{\text{TM}} = 2\tan^{-1}\left[\frac{\cos\theta\left(\sqrt{\sin^2\theta - n^{-2}}\right)}{\sin^2\theta}\right]$$
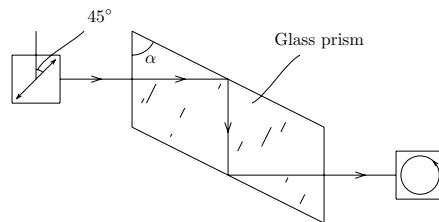
Figure P4.1.14.1

The phase change produced on internal reflection may be utilized to obtain circularly polarized light from linearly polarized light. The scheme, devised by Fresnel, is shown in Figure P4.1.14.1. The essential element is a glass prism with refractive index n made in the form of a rhomb having an apex angle α. Linearly polarized light with a direction of polarization at an angle of $45°$ with respect to the face edge of the rhomb enters normally on one face.

Show that when $\Delta = \pi/4$, the light coming out is circularly polarized. Let $n = 1.6$, calculate the apex angle α.

P4.1.15

A Nicol prism made of calcite is cut diagonally and then joined together with a film of Canada balsam (refractive index $n = 1.53$). Calcite is a negative uniaxial crystal with $\sqrt{\epsilon_z/\epsilon} = 1.49/1.66$. Show that with the arrangement shown in Figure P4.1.15.1 an incident light from the left becomes a linearly polarized light when it leaves the crystal from the right.
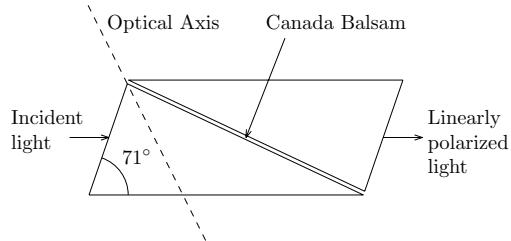
Figure P4.1.15.1

P4.1.16

Compare the phenomena of total reflection for $\theta > \theta_C$ and total transmission for $\theta = \theta_B$ at an isotropic dielectric interface.

(a) Total reflection occurs at a range of incident angles larger than the critical angle θ_C; total transmission of TM waves occurs only at the Brewster angle θ_B.
(b) Total reflection occurs only when the incident medium is denser than the transmitted medium. The Brewster angle occurs for any two media.
(c) When an unpolarized wave is totally reflected, the reflected wave is still unpolarized. When the TM wave components of an unpolarized wave are totally transmitted, the reflected wave contains only TE waves.

Suppose a TM wave is incident at an angle θ such that $\theta = \theta_B > \theta_C$. Then the wave is totally transmitted and at the same time it is totally reflected. Explain.

4.2   Wave Guidance

A. Guidance by Conducting Parallel Plates

Consider the guidance of electromagnetic waves by a pair of perfectly conducting plates at $x = 0$ and $x = d$ [Fig. 4.2.1]. The medium between the plates is homogeneous and isotropic. The width of the waveguide along y is w and we assume $w \gg d$, such that fringing fields can be neglected, and we have $\partial/\partial y = 0$. The Maxwell equations can be decomposed into transverse electric (TE) and transverse magnetic (TM) components. We have

$$H_x = \frac{-1}{i\omega\mu}\frac{\partial}{\partial z}E_y \tag{4.2.1a}$$

$$H_z = \frac{1}{i\omega\mu}\frac{\partial}{\partial x}E_y \tag{4.2.1b}$$

$$\left(\frac{\partial^2}{\partial z^2} + \frac{\partial^2}{\partial x^2} + \omega^2\mu\epsilon\right)E_y = 0 \tag{4.2.1c}$$

for TE waves and

$$E_x = \frac{1}{i\omega\epsilon}\frac{\partial}{\partial z}H_y \tag{4.2.2a}$$

$$E_z = \frac{-1}{i\omega\epsilon}\frac{\partial}{\partial x}H_y \tag{4.2.2b}$$

$$\left(\frac{\partial^2}{\partial z^2} + \frac{\partial^2}{\partial x^2} + \omega^2\mu\epsilon\right)H_y = 0 \tag{4.2.2c}$$

for TM waves. The boundary conditions at the parallel plates require that the tangential electric field be zero at $x = 0$ and $x = d$.

Equations $(4.2.1a)$–$(4.2.1c)$ are duals of $(4.2.2a)$–$(4.2.2c)$. However, the boundary conditions at the parallel plates require a zero tangential electric field for TE waves and also for TM waves. The boundary conditions for TE and TM waves are not duals.

The wave is guided along $\pm\hat{z}$ directions. For waves propagating along the $+\hat{z}$ direction, the solution for TE waves comprises two plane wave components

$$E_y = Ae^{ik_x x + ik_z z} + Be^{-ik_x x + ik_z z} \tag{4.2.3}$$
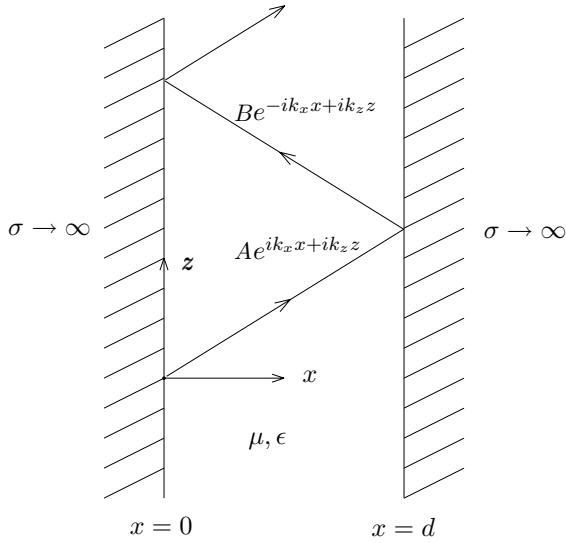
Figure 4.2.1 Parallel-plate waveguide.

Substituting $(4.2.3)$ in $(4.2.1c)$ we find the dispersion relation

$$k_z^2 + k_x^2 = \omega^2\mu\epsilon = k^2 \qquad (4.2.4)$$

The boundary condition at $x = 0$ requires $E_y = 0$, namely,

$$\frac{A}{B} = -1 \qquad (4.2.5a)$$

which is the reflection coefficient at the boundary surface $x = 0$. The boundary conditions at $x = d$ requiring $E_y = 0$ gives

$$\frac{B}{A} = -e^{i2k_x d} \qquad (4.2.5b)$$

which is the reflection coefficient at the boundary surface $x = d$. The factor $e^{i2k_x d}$ is due to the fact that the coordinate origin is at $x = 0$. Multiplying $(4.2.5a)$ and $(4.2.5b)$, we obtain

$$e^{i2k_x d} = 1 = e^{i2m\pi}$$

We thus have

$$2k_x d = 2m\pi$$

which states that the phase of the round trip of the plane wave in $\hat{x}$-direction must add up to integer numbers of 2π. Therefore, as a result of the boundary condition at $x = 0$ and $x = d$, we must have

$$\boxed{k_x = \frac{m\pi}{d} = \frac{m}{2d}\,\mathrm{K}_o}$$

(4.2.6)

where m is any integer. Equation (4.2.6) is called the *guidance condition* which is determined from the boundary conditions. Thus along the $\hat{x}$-direction, the number of periods of the spatial variation of a guided wave must be an integer in a distance of $2d$.

Substituting the guidance condition (4.2.6) in the dispersion relation (4.2.4) we obtain

$$k_z^2 + \left(\frac{m\pi}{d}\right)^2 = k^2$$

(4.2.7)
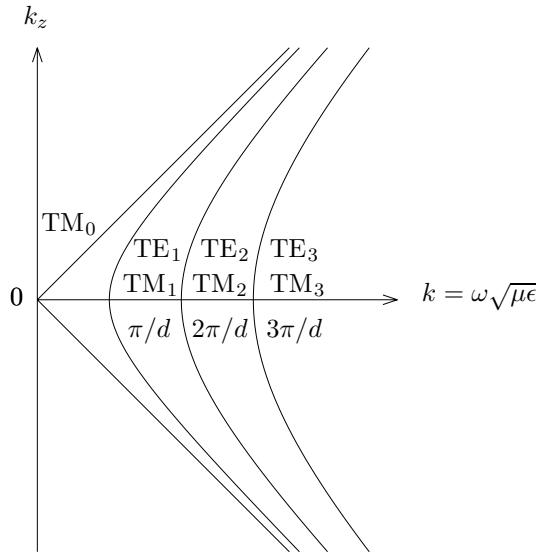
Figure 4.2.2 k_z-k **diagram for guided modes.**

This equation describes a family of hyperbolas for different values of m. In Figure 4.2.2 we plot the k_z-k diagram. We see that for the mth mode k_z will be imaginary if $k < m\pi/d$. The wave then becomes evanescent and attenuates exponentially in the $\hat{z}$ direction.

The spatial frequency at which $k_z = 0$ is called the cutoff spatial frequency k_{cm}

$$k_{cm} = \frac{m\pi}{d} = \frac{m}{2d} \, \text{K}_o \qquad (4.2.8)$$

When $k < k_{cm}$, all modes with order higher than m will be evanescent. In order for the mth order mode to propagate, the spatial frequency k must be larger than k_{cm}. Notice that if the mth mode is propagating, then all lth modes with $l < m$ can also propagate. The cutoff frequency for the TM_0 mode is zero and the TE_0 is zero. Thus for a given spatial frequency k such that $m/2d < k < (m+1)/2d \, \text{K}_o$, there will be m TE modes and $m+1$ TM modes admissible inside the waveguide. The lowest order TE mode is TE_1 whose $k_{c1} = 1/2d \, \text{K}_o$. For $k < 1/2d \, \text{K}_o$, no TE mode can be excited. The single TE_1 mode operation range inside the guide is $1/2d < k < 1/d \, \text{K}_o$.

The corresponding cutoff wavelength is $\lambda_{cm} = 2d/m$ and the corresponding cutoff angular frequency is $\omega_{cm} = m\pi/d(\mu\epsilon)^{1/2}$.

The guidance condition (4.2.6) states that in the $\hat{x}$ direction the bouncing waves must interfere constructively with $2k_x d = 2m\pi$ in order for the wave to be guided. Thus there is only a set of discrete k_x values admissible inside the guide as shown in Figure 4.2.3. The corresponding k_z values are determined from the dispersion relation (4.2.4) and the bouncing place waves are illustrated in Figure 4.2.4.
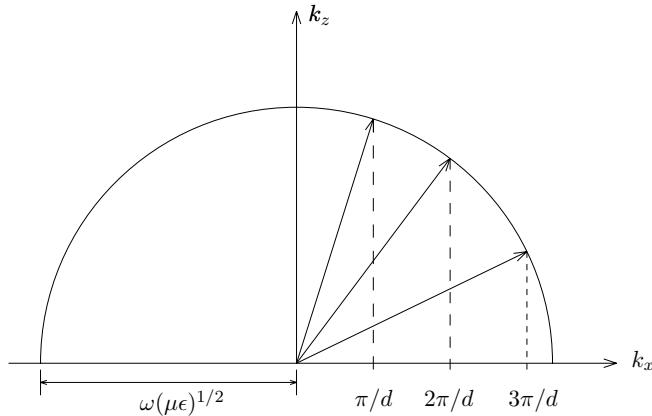
Figure 4.2.3 Interpretation of the guidance condition.
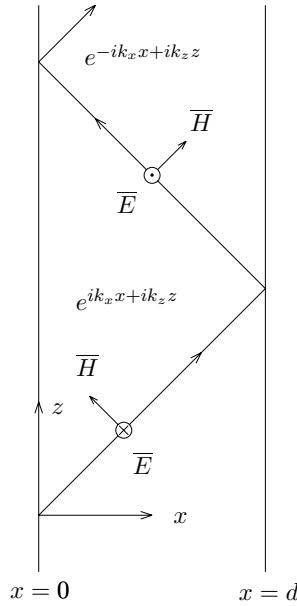
Figure 4.2.4 Plane wave interpretation of guided modes.

Substituting (4.2.5*a*) or (4.2.5*b*) in (4.2.3) we determine the electric field

$$E_y = E_0 \sin k_x x e^{ik_z z} \qquad (4.2.9)$$
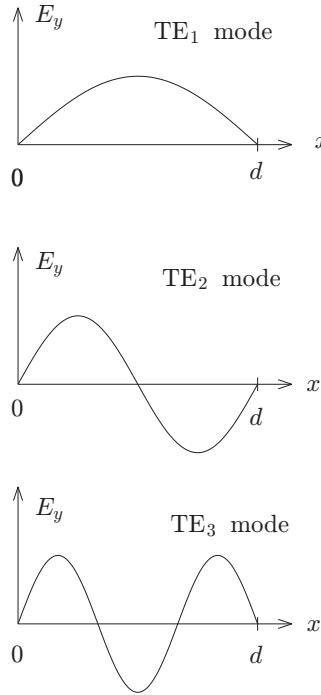
where $E_0 = i2A$. We call the TE wave corresponding to each integer m the TE$_m$ mode. There is no TE$_0$ mode because $E_y = 0$ for $m = 0$. The field patterns for E_y are plotted in Figure 4.2.5 for $m = 1$, 2, and 3.

The magnetic field vector is obtained from (4.2.3) or from (4.2.9) by using Faraday's law

$$
\begin{aligned}
\overline{H} &= \frac{1}{i\omega\mu}\left(-\hat{x}\frac{\partial}{\partial z}E_y + \hat{z}\frac{\partial}{\partial x}E_y\right) \\
&= \frac{A}{\omega\mu}\left[(-\hat{x}k_z + \hat{z}k_x)e^{ik_x x + ik_z z} + (\hat{x}k_z + \hat{z}k_x)e^{-ik_x x + ik_z z}\right] \quad (4.2.10) \\
&= \frac{E_0}{i\omega\mu}\left(-\hat{x}ik_z \sin k_x x + \hat{z}k_x \cos k_x x\right)e^{ik_z z} \qquad (4.2.11)
\end{aligned}
$$

We see that the magnetic field vector is perpendicular to both the electric field vector and the wave vector for the two bouncing plane waves.

Figure 4.2.5 Field amplitudes for TE_1, TE_2, **and** TE_3 **modes.**

We find the complex Poynting power from (4.2.9) and (4.2.11)

$$\overline{S} = \hat{z}\frac{k_z^*}{\omega\mu}|E_0|^2 \sin^2 k_x x e^{i(k_z - k_z^*)z} - \hat{x}\frac{ik_x}{\omega\mu}|E_0|^2 \sin k_x x \cos k_x x e^{i(k_z - k_z^*)z}$$

The time-average Poynting power $< S_x >$ in the transverse direction is always zero. The time-average Poynting power $< S_z >$ in the $\hat{z}$ direction is

$$< S_z > = \frac{1}{2}\text{Re}\left\{\frac{k_z^*}{\omega\mu}|E_0|^2 \sin^2 k_x x e^{i(k_z - k_z^*)z}\right\}$$

When $k_z = \sqrt{k^2 - k_x^2} = \sqrt{k^2 - (m\pi/d)^2}$ is imaginary, $k_z = ik_{zI}$, the time-average Poynting power in the $\hat{z}$ direction $< S_z > = \frac{1}{2}\text{Re}(S_z) = 0$, which happens for higher order modes as $m\pi/d > k$ and those high order modes are evanescent in the $\hat{z}$ direction and carry no time-average power.

B. Excitation of Modes in Parallel-Plate Waveguides

The mode amplitudes of the guided waves are determined by the sources of external excitation. Consider a current sheet located at $z = 0$ which flows in the $\hat{y}$ direction and varies in amplitude in x,

$$\overline{J}_s = \hat{y} J_s(x)$$

This current sheet generates propagating as well as evanescent guided modes in both positive and negative $\hat{z}$ directions. This current sheet can be visualized as composed of closely aligned wires with each wire excited by a different current source. The boundary conditions at $z = 0$ require that (i) E_x and E_y be continuous, (ii) the discontinuity in H_x be equal to a current sheet flowing in the $\hat{y}$ direction, and (iii) the discontinuity in H_y be equal to a current sheet flowing in the $\hat{x}$ direction. The boundary conditions then require that

$$H_x \mid_{z=0_+} - H_x \mid_{z=0_-} = J_s(x)$$

and that all other tangential field components be continuous at $z = 0$.

For a line source located at $x = a$ and flowing in the $\hat{y}$ direction with the dimension ampere per meter, we write

$$\overline{J}_s = \hat{y} I_0 \delta(x - a)$$

According to the boundary conditions, only TE waves will be excited. One can actually assume some amplitudes for the TM modes and find out from the boundary conditions that they are all zero. We write the TE solutions as a superposition of all TE modes

$$E_y = \begin{cases} \displaystyle\sum_{m=1}^{\infty} E_m \sin\frac{m\pi x}{d} e^{ik_z z} & z \geq 0 \\[2em] \displaystyle\sum_{m=1}^{\infty} E_m \sin\frac{m\pi x}{d} e^{-ik_z z} & z \leq 0 \end{cases} \qquad (4.2.12)$$

We see that the boundary condition of E_y continuous at $z = 0$ has been satisfied. The amplitudes E_m in regions $z < 0$ and $z > 0$ are equal as a consequence of symmetry. The x components of the magnetic fields are

$$H_x = \begin{cases} \displaystyle\sum_{n=1}^{\infty} \frac{-k_z}{\omega\mu} E_n \sin\frac{n\pi x}{d} e^{ik_z z} & z \geq 0 \\[2em] \displaystyle\sum_{n=1}^{\infty} \frac{k_z}{\omega\mu} E_n \sin\frac{n\pi x}{d} e^{-ik_z z} & z \leq 0 \end{cases} \qquad (4.2.13)$$

At $z = 0$ the boundary condition gives

$$I_0 \delta(x - a) = \sum_{n=1}^{\infty} \frac{-2k_z}{\omega\mu} E_n \sin \frac{n\pi x}{d} \qquad (4.2.14)$$

Using orthogonality properties of sinusoidal functions, we multiply both sides by $\sin(m\pi x/d)$ and integrate from 0 to d.

$$\int_0^d dx \sin \frac{m\pi x}{d} I_0 \delta(x - a) = \sum_{n=1}^{\infty} \frac{-2k_z}{\omega\mu} \int_0^d dx E_n \sin \frac{m\pi x}{d} \sin \frac{n\pi x}{d}$$

$$= \frac{-k_z d}{\omega\mu} E_m \qquad (4.2.15)$$

The mode amplitude E_m is determined as

$$E_m = -\frac{\omega\mu}{k_z d} I_0 \sin \frac{m\pi a}{d} \qquad (4.2.16)$$

For the TE_1 mode, E_1 is maximum when $a = d/2$. This is because E_y is also maximum at $x = d/2$ and the coupling of source energy into the TE_1 mode is the largest.

The time-average Poynting's power per unit length in y propagating along the waveguide in the $\hat{z}$ direction is given by

$$P = \frac{1}{2} \mathrm{Re} \left\{ \int_0^d dx \left(\sum_{m=1}^{\infty} E_m \sin \frac{m\pi x}{d} e^{ik_z z} \right) \left(\sum_{n=1}^{\infty} \frac{k_z}{\omega\mu} E_n \sin \frac{n\pi x}{d} e^{ik_z z} \right)^* \right\}$$

$$= \frac{1}{2} \mathrm{Re} \left\{ \frac{d}{2} \sum_{m=1}^{\infty} |E_m|^2 \left(\frac{k_z^*}{\omega\mu} \right) e^{i(k_z - k_z^*)z} \right\} \qquad (4.2.17)$$

For spatial frequency k such that $k_{C(N+1)} > k > k_{CN} = N/2d \, K_o$, k_z is real for $m \leq N$ and imaginary for $m > N$. Equation (4.2.17) gives

$$P = \sum_{m=1}^{N} \frac{d}{4\eta} |E_m|^2 \sqrt{1 - \left(\frac{k_{cm}}{k} \right)^2} \qquad (4.2.18)$$

w/m, where $\eta = \sqrt{\mu/\epsilon}$ is the intrinsic impedance of the medium inside the waveguide. The total power inside the guide is a summation of those of all the propagating modes with real k_z. It is important to observe that there is no coupling among the various modes; each individual mode carries its own power.

C. TM Modes in Parallel-Plate Waveguides

For TM waves satisfying the boundary conditions, we find that the solution takes the form

$$
\overline{H} = \hat{y}H_0(e^{ik_x x} + e^{-ik_x x})e^{ik_z z}
$$
$$
= \hat{y}2H_0 \cos k_x x\, e^{ik_z z} \tag{4.2.19a}
$$
$$
\overline{E} = H_0 \frac{1}{\omega\epsilon}\left[(\hat{x}k_z - \hat{z}k_x)e^{ik_x x} + (\hat{x}k_z + \hat{z}k_x)e^{-ik_x x}\right]e^{ik_z z}
$$
$$
= 2H_0 \frac{1}{\omega\epsilon}\left[\hat{x}k_z \cos k_x x - \hat{z}ik_x \sin k_x x\right]e^{ik_z z} \tag{4.2.19b}
$$

The boundary condition of vanishing E_z at $x = 0$ and $x = d$ leads to the guidance condition

$$
k_x = \frac{m\pi}{d} \tag{4.2.20}
$$

which is identical to (4.2.6) and is plotted in Figure 4.2.3.

There is one very important difference between the TM and TE cases. When $m = 0$, the TM field no longer vanishes as in the TE case and we now have the TM_0 mode which is also called the TEM mode. The TM_0 mode has $k_x = 0$ and $k_z = k$ never becomes imaginary and the TEM wave propagates at all frequencies. The time-average Poynting power in the $\hat{z}$ direction is

$$
< S_z > = \frac{1}{2}\text{Re}\left\{\frac{k_z^*}{\omega\epsilon}\,|H_0|^2 \cos^2 k_x x\, e^{i(k_z - k_z^*)z}\right\} = \frac{k}{2\omega\epsilon}\,|H_0|^2
$$

for the TM_0 mode. The TM_0 or TEM mode in a parallel-plate waveguide is termed the fundamental or dominant mode.

Field solutions for the TM_0 mode follows from (4.2.19) when we set $k_x = 0$ and $k_z = k$. We have

$$
\overline{H} = \hat{y}H_0\, e^{ikz} \tag{4.2.21a}
$$
$$
\overline{E} = \hat{x}\eta H_0\, e^{ikz} \tag{4.2.21b}
$$

where $\eta = \sqrt{\mu/\epsilon}$ is the characteristic impedance of the medium. The electric field is seen to be perpendicular to the plates and the magnetic field parallel to the plates.

D. Attenuation of Guided Waves Due to Wall Loss

The flow of power inside the waveguide will not be attenuated if the parallel plates are indeed perfect conductors and the medium is perfectly lossless. Let us now investigate wave attenuation when the conductivity of the plates is large but finite. A perturbation approach will be used.

Due to wall loss, guided waves carrying total time-average power P_f will decrease as a function of z. Assume that the amplitudes of the fields decay exponentially with an attenuation constant α, where α is a small number. When the walls are perfectly conducting, $\alpha = 0$. The total propagating power P will decay exponentially with 2α such that $P \sim e^{-2\alpha z}$. By the power conservation principle, the decrease of P as a function of distance must be equal to the power dissipated per unit length P_d. We have

$$P_d = -\frac{d}{dz}P = 2\alpha P$$

The attenuation constant α is found to be

$$\alpha = \frac{P_d}{2P} \tag{4.2.22}$$

The objective is to calculate α by a perturbation approach.

The starting point of the perturbation process is the exact solution for perfectly conducting waveguides. We calculate the time-average power flow in the $\hat{z}$ direction P by using the unperturbed solutions for the fields

$$P = \frac{1}{2}\text{Re}\left\{ \iint dx\, dy\, \hat{z} \cdot (\overline{E} \times \overline{H}^*) \right\} \tag{4.2.23}$$

The integration is carried over the area perpendicular to the direction of propagation. For the parallel-plate waveguide, the integration is carried out over $x = 0$ to $x = d$, which give the power per unit length along y in the direction of $\hat{z}$.

To estimate the dissipated power per unit length P_d, we first investigate the origin of the dissipation due to imperfect wall conductivity. The surface currents on the plate surfaces are

$$\overline{J}_s = \hat{n} \times \overline{H}_{\text{W}} \quad \text{amp/m} \tag{4.2.24}$$

where $\overline{H}_{\text{W}}$ is the magnetic field at the walls for which $x = 0$ and d.

The electric and magnetic fields at the wall surface are related to each other by the intrinsic impedance of the conductor which is assumed to have a large conductivity σ such that

$$\overline{E}_{\mathrm{W}} = \sqrt{\mu/\epsilon_{\mathrm{W}}}\,\hat{n} \times \overline{H}_{\mathrm{W}} \approx \sqrt{\omega\mu/i\sigma}\,\hat{n} \times \overline{H}_{\mathrm{W}}$$

where we assume the same permeability μ for the conductor as for the guidance medium. Since a guided wave can be viewed as plane waves bouncing at the wall surfaces, a plane wave incident at the surface of a conducting medium results in power dissipation into the conductor. The transmitted plane wave is almost perpendicular to the surface regardless of the angles of incidence. The time-average Poynting power density flow into the two conductors at $x=0$ and $x=d$ is

$$
\begin{aligned}
P_d &= 2 \times \frac{1}{2}\mathrm{Re}\left\{-\hat{n} \cdot (\overline{E}_{\mathrm{W}} \times \overline{H}_{\mathrm{W}}^{*})\right\} \\
&= \mathrm{Re}\left\{-\hat{n} \cdot \sqrt{\frac{\omega\mu}{i\sigma}}\,(\hat{n} \times \overline{H}_{\mathrm{W}}) \times \overline{H}_{\mathrm{W}}^{*}\right\} \\
&= \mathrm{Re}\left\{-\hat{n} \cdot \sqrt{\frac{\omega\mu}{i\sigma}}\,\left[(\hat{n} \cdot \overline{H}_{\mathrm{W}}^{*})\overline{H}_{\mathrm{W}} - \hat{n}\left|\overline{H}_{\mathrm{W}}\right|^{2}\right]\right\} = \sqrt{\frac{\omega\mu}{2\sigma}}\left|\overline{H}_{\mathrm{W}}\right|^{2}
\end{aligned}
$$

$$(4.2.25)$$

where we use the fact that $\hat{n} \cdot \overline{H}_{\mathrm{W}}^{*} = 0$ because $\overline{H}_{\mathrm{W}}$ is perpendicular to the surface normal $\hat{n}$ pointing into the waveguide.

EXAMPLE 4.2.1

From Poynting's theorem, the time-average dissipated power per unit area into the conductors is $<\overline{E}_{\mathrm{W}} \cdot \overline{J}_{s}^{*}>$ watts/m^2. Note that although $\overline{E}_{\mathrm{W}}$ is in the direction of $\overline{J}_s$, $\sigma\overline{E}_{\mathrm{W}}$ is not equal to $\overline{J}_s$ since $\overline{J}_s$ is a surface current, not a volume current. Dimensionally $\sigma\overline{E}_{\mathrm{W}}$ has units amp/m^2 whereas $\overline{J}_s$ has units amp/m. The total dissipated power per unit length P_d is calculated as

$$
\begin{aligned}
P_d &= 2\times <\overline{E}_{\mathrm{W}} \cdot \overline{J}_{s}^{*}> = \mathrm{Re}\left\{\sqrt{\frac{\omega\mu}{i\sigma}}\,(\hat{n} \times \overline{H}_{\mathrm{W}}) \cdot (\hat{n} \times \overline{H}_{\mathrm{W}}^{*})\right\} \\
&= \mathrm{Re}\left\{\sqrt{\frac{\omega\mu}{i\sigma}}\,\hat{n} \cdot \left[\overline{H}_{\mathrm{W}} \times (\hat{n} \times \overline{H}_{\mathrm{W}}^{*})\right]\right\} \\
&= \mathrm{Re}\left\{\sqrt{\frac{\omega\mu}{i\sigma}}\,\hat{n} \cdot \left[\hat{n}\left|\overline{H}_{\mathrm{W}}\right|^{2} - (\hat{n} \cdot \overline{H}_{\mathrm{W}})\overline{H}_{\mathrm{W}}^{*}\right]\right\} = \sqrt{\frac{\omega\mu}{2\sigma}}\left|\overline{H}_{\mathrm{W}}\right|^{2}
\end{aligned}
$$

which is identical to (4.2.25).

— END OF EXAMPLE 4.2.1 —

EXAMPLE 4.2.2   Attenuation of TM$_0$ or TEM mode.

    The electromagnetic field vectors of the TM$_0$ or TEM mode are,

$$\overline{H} = \hat{y}H_0\, e^{ikz} \qquad\qquad (\text{E4.2.2.1}a)$$

$$\overline{E} = \hat{x}\eta H_0\, e^{ikz} \qquad\qquad (\text{E4.2.2.1}b)$$

The propagating Poynting power in the $\hat{z}$ direction is

$$P = \frac{1}{2}\text{Re}\left\{\int_0^d dx\,\hat{z}\cdot(\overline{E}\times\overline{H}^*)\right\} = \frac{\eta d}{2}|H_0|^2 \qquad\qquad (\text{E4.2.2.2})$$
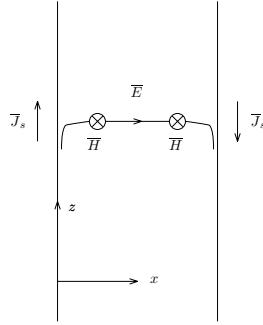
Figure E4.2.2.1 Finitely conducting walls.

When the walls are perfectly conducting, the tangential electric fields are zero and the surface currents flow without the support of any electric field. When the walls are not perfectly conducting, there is a small tangential component of the electric field $\overline{E}_\text{W}$ to support the surface currents [Fig. E4.2.2.1]. Assuming the magnetic field is unperturbed. The small electric field at the wall surface at $x = 0$ is related to the magnetic field H_0 by the intrinsic impedance of the conductor which is assumed to have a large conductivity σ such that

$$\overline{E}_\text{W} = \hat{z}\sqrt{\mu/\epsilon_\text{W}}\,H_0 \approx \hat{z}\sqrt{\omega\mu/i\sigma}\,H_0$$

The time-average Poynting power density flow into the two conductors at $x = 0$ and $x = d$ is

$$P_d = 2\times\frac{1}{2}\text{Re}\left\{\hat{z}\cdot(\overline{E}_\text{W}\times\overline{H}_\text{W}^*)\right\} = \sqrt{\frac{\omega\mu}{2\sigma}}\left|\overline{H}_0\right|^2 \qquad (\text{E4.2.2.3})$$

Thus for TEM mode, or, equivalently, the TM$_0$ mode, the corresponding attenuation constant is

$$\alpha^\text{TEM} = \frac{1}{\eta d}\sqrt{\frac{\omega\mu}{2\sigma}} = \frac{1}{d}\sqrt{\frac{\omega\epsilon}{2\sigma}} \qquad\qquad (\text{E4.2.2.4})$$

— END OF EXAMPLE 4.2.2 —

Consider TE_m modes with the solutions in (4.2.9) and (4.2.11). The time-average power flow P per unit length in y along $\hat{z}$ direction in the waveguide is

$$P = \int_0^d dx \frac{1}{2} \frac{k_z}{\omega\mu} |E_m|^2 \sin^2 \frac{m\pi x}{d} = \frac{d}{4} \frac{k_z}{\omega\mu} |E_m|^2 \qquad (4.2.26)$$

The attenuation constants for TE modes are

$$\alpha^{\text{TE}} = \frac{P_d}{2P} = \sqrt{\frac{\omega\mu}{2\sigma}} |H_\text{W}|^2 \left/ \frac{d}{2} \frac{k_z}{\omega\mu} |E_0|^2 = \frac{1}{d} \sqrt{\frac{\omega\epsilon}{2\sigma}} \frac{2(k_{cm}/k)^2}{\sqrt{1-(k_{cm}/k)^2}} \right. \tag{4.2.27}$$

Notice that $H_\text{W} = k_x E_0/i\omega\mu$ as seen from (4.2.11) with $x = 0$.

We now consider TM_m modes in (4.2.19). The time-average power flow P per unit length in y along $\hat{z}$ direction in the waveguide is

$$P = \int_0^d dx \frac{1}{2} \frac{k_z}{\omega\epsilon} |H_m|^2 \cos^2 \frac{m\pi x}{d} = \frac{d}{4} \frac{k_z}{\omega\epsilon} (1 + \delta_{0m}) |H_m|^2 \quad (4.2.28)$$

where δ_{0m} is the Kronecker delta function with $\delta_{0m} = 0$ for $m \neq 0$ and $\delta_{00} = 1$. The time-average power dissipation per unit length P_d is calculated in (4.2.25). The attenuation constant for TM modes is

$$\alpha^{\text{TM}} = \frac{P_d}{2P} = \frac{1}{d} \sqrt{\frac{\omega\epsilon}{2\sigma}} \frac{2/(1 + \delta_{0m})}{\sqrt{1-(k_{cm}/k)^2}} \qquad (4.2.29)$$
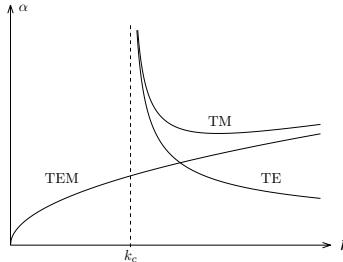
Figure 4.2.6 Attenuation constants.

As $m = 0$, we obtain the attenuation constant α^{TEM} as shown in (E4.2.2.4).

In Figure 4.2.6 the attenuation constants for TEM, TM, and TE modes are plotted. The curve shapes for all TE_m and TM_m modes are the same if we let $k_{cm} = m\pi/d$. We note that for the TEM mode α increases as the square root of k. For TE modes α decreases monotonically with increasing frequency.

E. Guided Waves in Isotropic Medium Coated Conductor

Consider an isotropic-medium-coated conductor in Figure 4.2.7. For the field to be guided in region 0, the field in region 1 must be evanescent in the $\hat{x}$ direction. The field solutions for the TM modes can be written as
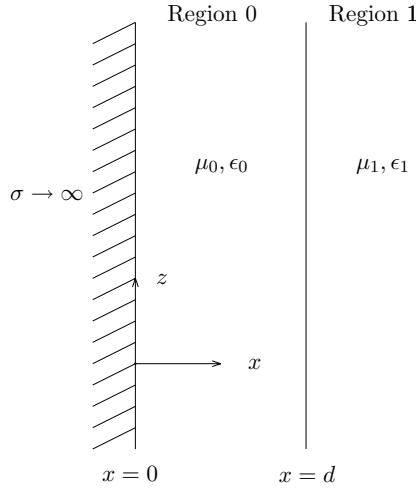
Figure 4.2.7 Guidance by an isotropic-medium-coated conductor.

$$\overline{H}_0 = \hat{y}(A_0 e^{ik_x x} + B_0 e^{-ik_x x})e^{ik_z z} \tag{4.2.29a}$$

$$\overline{E}_0 = \frac{1}{\omega \epsilon} \left[A_0(\hat{x}k_z - \hat{z}k_x)e^{ik_x x} + B_0(\hat{x}k_z + \hat{z}k_x)e^{-ik_x x} \right] e^{ik_z z} \tag{4.2.29b}$$

$$\overline{H}_1 = \hat{y}H_1 e^{-k_{1xI} x} e^{ik_z z} \qquad d \le x \tag{4.2.30a}$$

$$\overline{E}_1 = H_1 \frac{1}{\omega \epsilon_1}(\hat{x}k_z - \hat{z}\, ik_{1xI})e^{-k_{1xI} x} e^{ik_z z} \tag{4.2.30b}$$

The dispersion relations for the two regions are

$$k_z^2 + k_x^2 = \omega^2 \mu \epsilon = k^2 \tag{4.2.31a}$$

$$k_z^2 - k_{1xI}^2 = \omega^2 \mu_1 \epsilon_1 = k_1^2 \tag{4.2.31b}$$

In Figure 4.2.8 we plot two k surfaces with radii k and k_1 for positive k_z as vertical axis and k_x as horizontal axis. For the wave to be guided
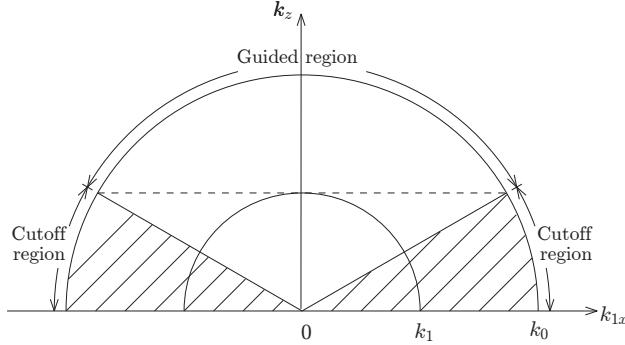
Figure 4.2.8 Guided and cutoff regions.

we must have k_z larger than k. When k_z becomes smaller than k, the wave in region t will no longer be evanescent because k_{1xI} becomes imaginary and the wave begins to propagate. The wave in region 0 is guided only when $k_z > k_1$.

The boundary conditions at $x = 0$ and $x = d$ yields

$$A_0 = B_0 \tag{4.2.32}$$

$$A_0 e^{ik_x d} + B_0 e^{-ik_x d} = H_1 e^{-k_{txI} d} \tag{4.2.33}$$

$$A_0 e^{ik_x d} - B_0 e^{-ik_x d} = p_{01} H_1 e^{-k_{txI} d} \tag{4.2.34}$$

We obtain

$$\frac{A_0}{B_0} = 1 \tag{4.2.35}$$

$$2A_0 \cos k_x d = H_1 e^{-k_{txI} d} \tag{4.2.36}$$

$$\frac{B_0}{A_0} = R_{01} e^{i2k_x d} \tag{4.2.37}$$

Let $B_0/A_0 = R_{0+}$ and $A_0/B_0 = R_{0-}$. The guidance condition is determined by $R_{0+} R_{0-} = 1$, which leads to

$$R_{01} e^{i2k_x d} = 1$$

with $R_{01} = (1 - p_{01})/(1 + p_{01})$, and $p_{01} = i\epsilon k_{1xI}/\epsilon_1 k_x$. We find

$$2k_x d + 2\phi_{01} = 2m\pi \tag{4.2.38}$$
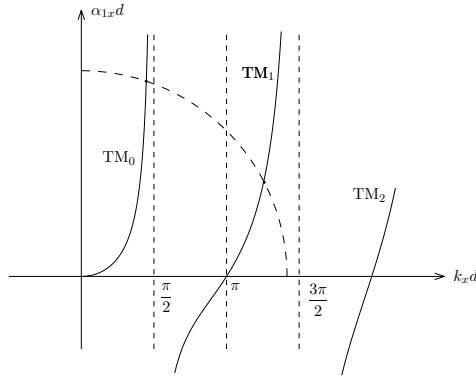
Figure 4.2.9 Interpretation of guidance condition for TM modes.

where $\phi_{01} = -\tan^{-1}(\epsilon k_{1xI}/\epsilon_1 k_x)$. We have

$$k_{1xI}d = \frac{\epsilon_1}{\epsilon}k_x d \tan k_x d \qquad (4.2.39)$$

which is plotted in Figure 4.2.9, where the graphical solution for k_x is illustrated. From (4.2.31), we find

$$k_x^2 + k_{1xI}^2 = k^2 - k_1^2$$

which is the dashed circular arc with radius $\sqrt{k^2 - k_1^2}$.

For the TM_m mode, the magnetic fields in regions 0 and 1 are

$$H_y = H_1 e^{-k_{1xI}d}\frac{\cos k_x x}{\cos k_x d}e^{ik_z z} \qquad (4.2.40)$$

$$H_{1y} = H_1 e^{-k_{1xI}x}e^{ik_z z} \qquad (4.2.41)$$
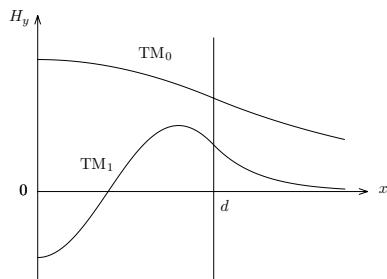
Figure 4.2.10 Magnetic field amplitudes for TM modes.

The field plots for H_y mith $m = 0, 1$ and different amplitudes are illustrated in Figure 4.2.10.

The cutoff frequency k_{cm} for TM_m modes is seen to be

$$k_{cm} = \frac{m\pi}{d\sqrt{1 - \mu_1\epsilon_1/\mu\epsilon}} \qquad m = 0, 1, 2, \ldots \qquad (4.2.42)$$

As in the case of the parallel-plate waveguide, the TM_0 mode has zero cutoff frequency or, equivalently, infinite cutoff wavelength.

EXAMPLE 4.2.3   Guided waves, lateral wave, and leaky waves.

For the TM_m wave shwon in (4.2.40) and (4.2.41), the magnetic and electric fields in regions 0 and 1 are found to be, if we let $k_{1x} = ik_{1xI}$ and the transmitted wave vector take the form $\overline{k}_t = \hat{x}\,k_{1x} + \hat{z}\,k_z$

$$H_y = H_1 e^{ik_{1x}d}\, \frac{\cos k_x x}{\cos k_x d}\, e^{ik_z z} \qquad\qquad (E4.2.3.1a)$$

$$\overline{E} = \frac{H_1}{\omega\epsilon\cos k_x d}\, e^{ik_{1x}d}\, \{\hat{x}k_z \cos k_x x - \hat{z}ik_x \sin k_x x\}\, e^{ik_z z} \quad (E4.2.3.1b)$$

$$H_{1y} = H_1 e^{ik_{1x}x}\, e^{ik_z z} \qquad\qquad (E4.2.3.2a)$$

$$\overline{E}_1 = \frac{-1}{\omega\epsilon_1}\overline{k}_1 \times \overline{H}_1 = \frac{H_1}{\omega\epsilon_1}\, \{\hat{x}k_z - \hat{z}k_{1x}\}\, e^{ik_{1x}x}\, e^{ik_z z} \qquad (E4.2.3.2b)$$

$$< \overline{S}_1 > = \frac{1}{2}\mathrm{Re}\left\{\frac{\overline{k}_1}{\omega\epsilon_1}|\overline{H}_1|^2\right\} \qquad\qquad (E4.2.3.3)$$

The guidance condition in (4.2.39) becomes

$$\tan k_x d = -i\frac{\epsilon k_{1x}}{\epsilon_1 k_x} \qquad\qquad (E4.2.3.4)$$

Together with the dispersiion relations

$$k_{1x}^2 + k_z^2 = k_1^2 \qquad\qquad (E4.2.3.5)$$
$$k_x^2 + k_z^2 = k^2 \qquad\qquad (E4.2.3.6)$$

we see that the solutions for k_z, k_x, k_{1x} from (E4.2.3.4)-(E4.2.3.6) and thus the wave vectors $\overline{k}$ and $\overline{k}_1$ will be complex.

Guided Waves

For guided waves in Region 0, the surface wave in Region 1 has

$$\overline{k}_1 = \hat{x}ik_{1xI} + \hat{z}k_z \qquad\qquad (E4.2.3.7)$$

where k_{1xI} is solved with real k_x and k_z.

Lateral Wave

When $\overline{k}_1 = \hat{z}k_1$, we have $k_z = k_1$, $k_{1x} = 0$, and $k_x = m\pi/d$. The wave in Region 1 propagates in the $\hat{z}$ direction.

$$\overline{H}_1 = \hat{y}\, 2e^{ik_1 z} \tag{E4.2.3.8}$$

$$\overline{E}_1 = \hat{x}\frac{2k_1}{\omega\epsilon_1}e^{ik_1 z} \tag{E4.2.3.9}$$

Interpreting the guided waves in Region 0 as bouncing waves, the waves are incident on the dielectric boundary at $x = 0$ at the critical angle. The wave in Region 1 correspond to a guided wave in Region 0 at cutoff and has uniform amplitudes in the $\hat{x}$ direction and is called a lateral wave.

Leaky Waves

The transmitted wave vector is generally complex, we write

$$\overline{k}_t = \hat{x}k_{tx} + \hat{z}k_z = \overline{k}_R + i\overline{k}_I \tag{E4.2.3.10}$$

From the dispersion relation $\overline{k}_1 \cdot \overline{k}_1 = k_R^2 - k_I^2 + i\overline{k}_R \cdot \overline{k}_I = k_1^2 = \omega^2\mu_1\epsilon_1$. We find

$$\overline{k}_R \cdot \overline{k}_I = 0$$

With α denoting the direction of $\overline{k}_1$ and θ the direction of observation point, we have

$$\begin{aligned}
\overline{k}_1 &= \hat{x}k_1\cos(\alpha_R + i\alpha_I) + \hat{z}k_1\sin(\alpha_R + i\alpha_I) \\
&= k_1(\hat{x}\cos\alpha_R + \hat{z}\sin\alpha_R)\cosh\alpha_I \\
&\quad + ik_1(-\hat{x}\sin\alpha_R + \hat{z}\cos\alpha_R)\sinh\alpha_I
\end{aligned} \tag{E4.2.3.11}$$

$$e^{i\overline{k}_1 \cdot \overline{r}} = e^{ik_1 r\cos(\alpha-\theta)} = e^{ik_1 r\cos(\alpha_R-\theta)\cosh\alpha_I}e^{k_1 r\sin(\alpha_R-\theta)\sinh\alpha_I}$$
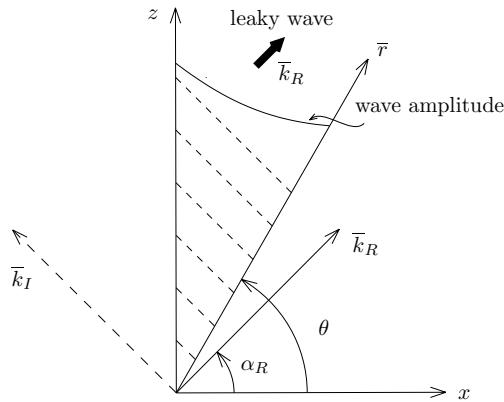
Figure E4.2.3.1 Leaky waves.

For $\alpha_I \geq 0$, the wave grows exponentially in the $\hat{x}$ direction. They are called leaky waves. However the leaky wave mode can be excited only when $\alpha_R - \theta \leq 0$, namely when θ is larger than α_R. As seen from Figure E4.2.3.1, even though the wave amplitude grows exponentially away from the surface, it also attenuates exponentially in the $\hat{z}$-direction. Thus the leaky wave amplitudes will never diverge in the $\hat{r}$ direction.

— End of Example 4.2.3 —

EXAMPLE 4.2.4

We write the field solutions for the TE modes as follows:

$$\overline{E}_0 = \hat{y}\left[A_0 e^{ik_x x} + B_0 e^{-ik_x x}\right]e^{ik_z z} \qquad 0 \leq x \leq d \quad \text{(E4.2.4.0}b)$$

$$\overline{E}_1 = \hat{y}E_1 e^{-k_{1xI}x}e^{ik_z z} \qquad\qquad d \leq x \qquad \text{(E4.2.4.1}a)$$

We find the reflection coefficients $R_{0-} = B_0/A_0 = -1$ and $R_{0+} = A_0/B_0 = R_{01}e^{i2k_x d}$. The guidance condition states that $R_{0+}R_{0-} = 1$ which gives

$$-R_{01}e^{i2k_x d} = 1$$

and thus

$$2k_x d + 2\phi_{01} + \pi = 2m\pi \qquad\qquad \text{(E4.2.4.2)}$$

with $m = 1, 2, \ldots$ It states that the total phase shift in the transverse $\hat{x}$ direction must be integer multiples of 2π to ensure constructive interference.

By using the expression for the Goos-Hänchen shift

$$2\phi_{01} = -2\tan^{-1}(\mu k_{1xI}/\mu_1 k_x)$$

we can express the guidance condition as

$$k_{1xI}d = -\frac{\mu_1}{\mu}k_x d \cot k_x d \qquad\qquad \text{(E4.2.4.3)}$$
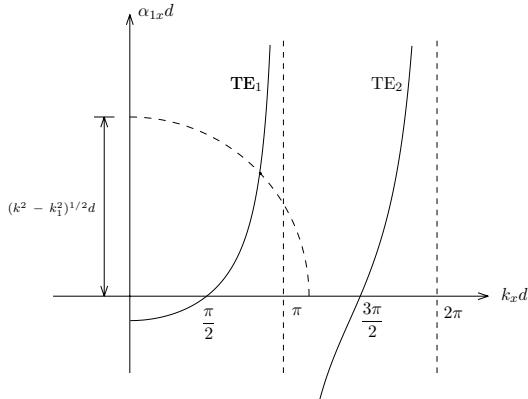
Figure E4.2.4.1 Interpretation of guidance condition for TE modes.

We plot in Figure E4.2.4.1 the guidance condition on the two-dimensional plane with $k_x d$ as the horizontal axis and $k_{1xI} d$ as the vertical axis. The transversal spatial frequency k_x for TE modes can be determined graphically from the dispersion relations (4.2.31a) and (4.2.31b), which give $k_x^2 + k_{1xI}^2 = k^2 - k_1^2$. This is a circle on the $k_{1xI}d$-$k_x d$ plane. We find that for TE_m mode, $(2m-1)\pi/2 < k_x d < m\pi$. The electric field in region 0 is found from (E4.2.4.1) by using the guidance condition of $A_0/B_0 = -1$ and by matching the boundary condition at $x = d$,

$$E_y = E_1 e^{-k_{1xI}d} \frac{\sin k_x x}{\sin k_x d} e^{ik_z z} \qquad (E4.2.4.4)$$

$$E_{1y} = E_1 e^{-k_{1xI}x} e^{ik_z z} \qquad (E4.2.4.5)$$
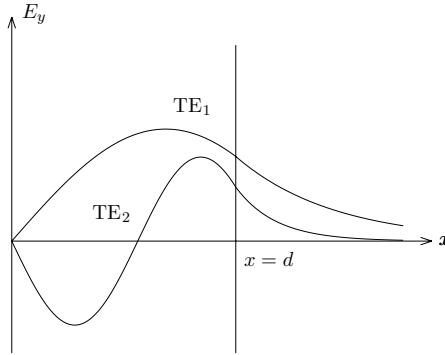
Figure E4.2.4.2 Electric field amplitudes for TE modes.

We show a field plot of E_y for TE_1 and TE_2 mode in Figure E4.2.4.2.

The waves are guided only when $k_z > k$. Cutoff occurs when k_{1xI} becomes imaginary and the wave is no longer evanescent for $x > d$. The cutoff spatial frequency is determined from $\phi_{01} = k_{1xI} = 0$ when $k_z = k_1$. Using the guidance condition (E4.2.4.2) and (4.2.31b) we find $(2m-1)\pi/2 = k_x d = (k^2 - k_1^2)^{1/2} d$. We thus obtain

$$k_{cm} = \frac{(2m-1)\pi}{2d\sqrt{1 - \mu_1 \epsilon_1 / \mu \epsilon}} \qquad m = 1, 2, \ldots \qquad (E4.2.4.6)$$

We see that the TE mode can have a large cutoff frequency k_c when $\mu_1 \epsilon_1$ is very close to $\mu\epsilon$.

— End of Example 4.2.4 —

F. Guided Waves in Layered Media

Consider the stratified isotropic medium with boundaries at $x = d_1, d_2, \ldots, d_t$ shown in Fig. 4.1.12. For a TM plane wave, we write the total field in region l as

$$\overline{k}_l = \hat{x} k_{lx} + \hat{z} k_z \tag{4.2.43}$$

$$\overline{H}_l = \hat{y} \left(A_l e^{ik_{lx}x} + B_l e^{-ik_{lx}x} \right) e^{ik_z z} \tag{4.2.44}$$

$$\overline{E}_l = \frac{1}{\omega \epsilon_l} \overline{k}_l \times \overline{H}_l \tag{4.2.45}$$
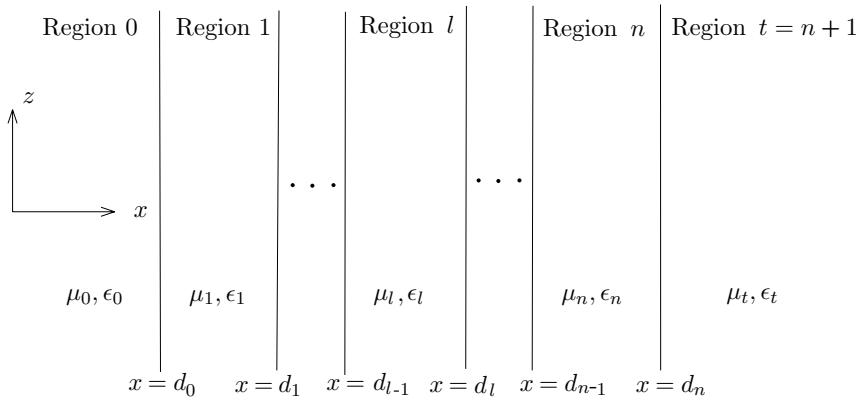
Figure 4.1.12 Layered medium.

For guided waves, $\begin{cases} A_0 = 0 \\ B_0 = R \end{cases}$ in region 0, and $\begin{cases} A_t = T \\ B_t = 0 \end{cases}$ in region t.

The wave amplitudes A_l and B_l are related to wave amplitudes in neighboring regions by the boundary conditions. At $x = d_l$, boundary conditions require that E_y and H_z be continuous. We obtain

$$A_l e^{ik_{lx}d_l} + B_l e^{-ik_{lx}d_l} = A_{l+1} e^{ik_{(l+1)x}d_l} + B_{l+1} e^{-ik_{(l+1)x}d_l} \tag{4.2.46}$$

$$A_l e^{ik_{lx}d_l} - B_l e^{-ik_{lx}d_l} = p_{l(l+1)} \left[A_{l+1} e^{ik_{(l+1)x}d_l} - B_{l+1} e^{-ik_{(l+1)x}d_l} \right] \tag{4.2.47}$$

$$\text{where} \qquad p_{l(l+1)} = \frac{\epsilon_l k_{(l+1)x}}{\epsilon_{l+1} k_{lx}} = \frac{1}{p_{(l+1)l}} \tag{4.2.48}$$

To find the reflection coefficient at the boundary $x = d_l$, we solve (4.2.46) and (4.2.47) for A_l and B_l.

$$A_l e^{ik_{lx}d_l} = \frac{1 + p_{l(l+1)}}{2} \left\{ A_{l+1} e^{ik_{(l+1)x}d_l} + R_{l(l+1)} B_{l+1} e^{-ik_{(l+1)x}d_l} \right\}$$

$$B_l e^{-ik_{lx}d_l} = \frac{1 + p_{l(l+1)}}{2} \left\{ R_{l(l+1)} A_{l+1} e^{ik_{(l+1)x}d_l} + B_{l+1} e^{-ik_{(l+1)x}d_l} \right\}$$

and obtain

$$\frac{B_l}{A_l} = \frac{R_{l(l+1)} e^{i2k_{(l+1)x}d_l} + (B_{l+1}/A_{l+1})}{e^{i2k_{(l+1)x}d_l} + R_{l(l+1)}(B_{l+1}/A_{l+1})} e^{i2k_{lx}d_l} \tag{4.2.49}$$

where B_l/A_l is expressed in terms of B_{l+1}/A_{l+1}.

Similarly, to find the reflection coefficient at the boundary $x = d_{l-1}$, we find from (4.2.46) and (4.2.47), or from (4.1.78) and (4.1.79)

$$A_l e^{ik_{lx}d_{l-1}} = \frac{1 + p_{l(l-1)}}{2} \left\{ A_{l-1} e^{ik_{(l-1)x}d_{l-1}} + R_{l(l-1)} B_{l-1} e^{-ik_{(l-1)x}d_{l-1}} \right\}$$

$$B_l e^{-ik_{lx}d_{l-1}} = \frac{1 + p_{l(l-1)}}{2} \left\{ R_{l(l-1)} A_{l-1} e^{ik_{(l-1)x}d_{l-1}} + B_{l-1} e^{-ik_{(l-1)x}d_{l-1}} \right\}$$

and obtain

$$\frac{A_l}{B_l} = \frac{R_{l(l-1)} e^{-i2k_{(l-1)x}d_{l-1}} + (A_{l-1}/B_{l-1})}{e^{-i2k_{(l-1)x}d_{l-1}} + R_{l(l-1)}(A_{l-1}/B_{l-1})} e^{-i2k_{lx}d_{l-1}} \tag{4.2.50}$$

where A_l/B_l is expressed in terms of A_{l-1}/B_{l-1}.

The guidance condition is obtained by multiplying (4.2.49) and (4.2.50). For a two-layer medium, $n = 1$, we obtain

Region 0   Region 1   Region 2

$\epsilon_0,\ \mu_0$ $\epsilon_1,\ \mu_1$ $\epsilon_2,\ \mu_2$

$x = d_0$ $x = d_1$
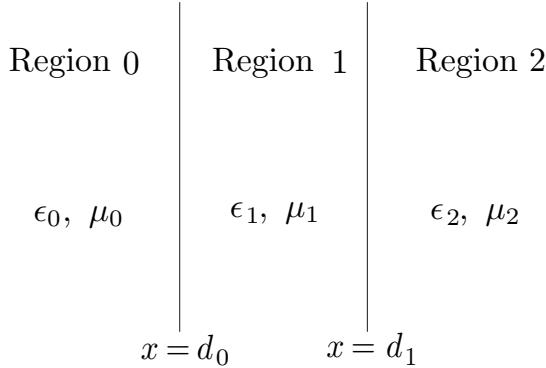
Figure 4.2.11 Two-layer media.

$$\frac{B_1}{A_1} = R_{12}e^{i2k_{1x}d_1} \tag{4.2.51}$$

$$\frac{A_1}{B_1} = R_{10}e^{-i2k_{1x}d_0} \tag{4.2.52}$$

and thus

$$R_{10}R_{12}e^{i2k_{1x}(d_1-d_0)} = 1 = e^{i2m\pi} \tag{4.2.53}$$

The magnetic fields in all regions are

$$\overline{H}_2 = \hat{y}A_1(1 + R_{12})e^{ik_{1x}d_1}e^{ik_{2x}(x-d_1)}e^{ik_zz} \tag{4.2.54}$$

$$\overline{H}_1 = \hat{y}A_1e^{ik_{1x}d_1}\left\{e^{ik_{1x}(x-d_1)} + R_{12}e^{-ik_{1x}(x-d_1)}\right\}e^{ik_zz}$$

$$= \hat{y}A_1e^{ik_{1x}d_0}\left\{e^{ik_{1x}(x-d_0)} + \frac{1}{R_{10}}e^{-ik_{1x}(x-d_0)}\right\}e^{ik_zz} \tag{4.2.55}$$

$$\overline{H}_0 = \hat{y}A_1(1 + \frac{1}{R_{10}})e^{ik_{1x}d_0}e^{-ik_{0x}(x-d_0)}e^{ik_zz} \tag{4.2.56}$$

For guided waves, $k_{0x} = ik_{0xI}$, $k_{0x} = ik_{0xI}$, with $R_{10} = e^{i2\phi_{10}}$ and $R_{12} = e^{i2\phi_{12}}$, where ϕ_{10} and ϕ_{12} are Goos-Hänschen shifts at $x = d_0$ and $x = d_1$. We obtain from (4.2.54) – (4.2.56),

$$\overline{H}_2 = \hat{y}\, 2\cos\phi_{12}A_1e^{-k_{1xI}(x-d_1)}e^{i(k_{1x}d_1+\phi_{1t})}e^{ik_zz} \tag{4.2.57}$$

$$\overline{H}_1 = \hat{y}A_1\left\{e^{ik_{1x}x} + e^{i2(k_{1x}d_1+\phi_{12})}e^{-ik_{1x}x}\right\}e^{ik_zz}$$

$$= \hat{y}A_1\left\{e^{ik_{1x}x} + e^{i2(k_{1x}d_0-\phi_{10})}e^{-ik_{1x}x}\right\}e^{ik_zz} \tag{4.2.58}$$

$$\overline{H}_0 = \hat{y}\, 2\cos\phi_{10}A_1e^{k_{0xI}(x-d_0)}e^{i(k_{1x}d_0-\phi_{10})}e^{ik_zz} \tag{4.2.59}$$

and (4.2.53) gives

$$2\phi_{10} + 2\phi_{12} + 2k_{1x}(d_1 - d_0) = 2m\pi \tag{4.2.60}$$

or that

$$2\phi_{10} + 2\phi_{12} + 2k_{1x}(d_1 - d_0) = 2m\pi \tag{4.2.61}$$

which is the guidance condition stating that the phases gained by the round trip $2k_{1x}d$, plus the phases gained at the boundary surfaces at $x = d_0$ and $x = d_1$ add up to $2m\pi$.

G. Guided Waves in a Symmetric Slab Dielectric Waveguide

Consider a symmetric slab waveguide with boundaries at $x = 0$ and d [Figure 4.2.12]. Equations (4.2.57)–(4.2.59) become

Region 0 | Region 1 | Region 2

$\epsilon_0, \ \mu_0$ $\qquad$ $\epsilon_1, \ \mu_1$ $\qquad$ $\epsilon_0, \ \mu_0$

$x = 0 \qquad\qquad x = d$
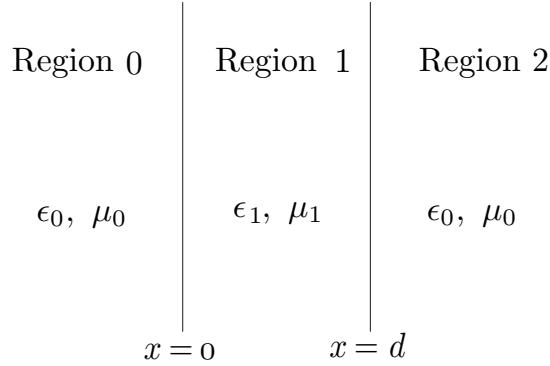
Figure 4.2.12 Symmetric dielectric waveguide.

$$\overline{H}_0 = \hat{y} \ 2\cos\phi_{10} A_1 e^{k_{0xI} x} \ e^{-i\phi_{10}} e^{ik_z z} \tag{4.2.62}$$

$$\overline{H}_1 = \hat{y} A_1 e^{i(\frac{k_{1x}d}{2} + \frac{m\pi}{2})} \cos(k_{1x}x - \frac{k_{1x}d}{2} - \frac{m\pi}{2}) e^{ik_z z} \tag{4.2.63}$$

$$\overline{H}_2 = \hat{y} \ 2\cos\phi_{10} A_1 e^{-k_{1xI}(x-d_1)} \ e^{i(k_{1x}d_1 + \phi_{10})} \ e^{ik_z z} \tag{4.2.64}$$

with the guidance condition as

$$2k_{1x}d + 4\phi_{10} = 2m\pi \tag{4.2.65}$$

The solutions in regions 0 and t are both evanescent; $\overline{H}_0$ decays in $-\hat{x}$ direction and $\overline{H}_t$ decays in $+\hat{x}$ direction. The total transverse phase shift in the $\hat{x}$ direction for a plane wave making a round trip adds to an integer multiple of 2π. Equation (4.2.65) provides a relation between $k_{1x}d$ and $k_{xI}d$.

$$k_{xI}d = \frac{\epsilon_0}{\epsilon_1} k_{1x}d \ \tan\left(\frac{k_{1x}d}{2} - \frac{m\pi}{2}\right) \tag{4.2.66}$$

The dispersion relations in regions 0, 1, and t are,

$$k_z^2 - k_{xI}^2 = \omega^2 \mu_0 \epsilon_0 = k^2 \tag{4.2.67}$$

$$k_z^2 + k_{1x}^2 = \omega^2 \mu_1 \epsilon_1 = k_1^2 \tag{4.2.68}$$
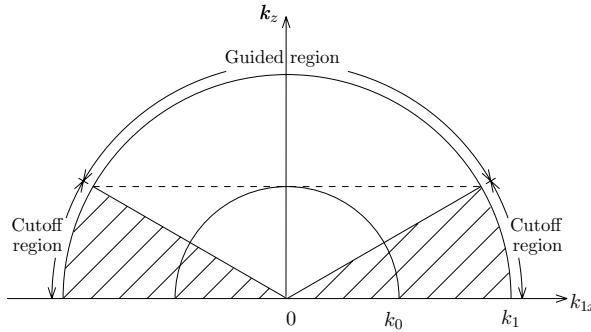
Figure 4.2.13 Guided and cutoff regions.

Eliminating k_z from (4.2.67) and (4.2.68), we obtain

$$k_{xI}^2 + k_{1x}^2 = k_1^2 - k^2 \tag{4.2.69}$$

which provides another equation for $k_{1x}d$ and $k_{xI}d$.

In Figure 4.2.13 we plot two k surfaces with radii k_1 and k for positive k_z as vertical axis and k_x as horizontal axis. For the wave to be guided we must have k_z larger than k. When k_z becomes smaller than k, the wave in regions 0 and t will no longer be evanescent because k_{xI} becomes imaginary and the wave begins to propagate.

Waves are guided inside the slab waveguide when $k \leq k_z \leq k_1$. Cutoff occurs when $k_z = k$ and as a consequence $k_{xI} = 0$. The guidance condition (4.2.66) gives $k_{1x}d = m\pi$ at cutoff. From

$$m\pi = k_{1x}d = \sqrt{k_1^2 - k^2}\, d = k_1\sqrt{1 - \mu_0\epsilon_0/\mu_1\epsilon_1}\ d$$

we find the cutoff spatial frequency for the mth mode
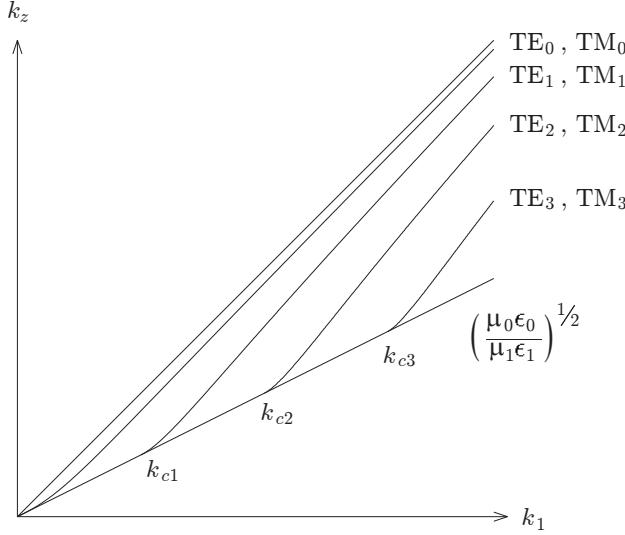
$$k_1 = k_{cm} = \frac{m\pi}{d\sqrt{1 - \mu_0\epsilon_0/\mu_1\epsilon_1}} \tag{4.2.70}$$

At cutoff,

$$k_z = k = k_1\sqrt{\mu_0\epsilon_0/\mu_1\epsilon_1} \tag{4.2.71}$$

It follows that the $0th$ order mode possesses zero cutoff frequency.

We plot k_z as a function of k for the various modes in Figure 4.2.14. The diagram can be generated graphically or numerically from (4.2.66) and (4.2.69). From the k_z-k_1 diagram, the phase and group

4.2.14 Propagation constant k_z as a function of k.

velocities can be determined. The curves for the various modes are shown in Figure 4.2.14.

As $k \to \infty$, we find from (4.2.69) that $k_{0xI} \to \infty$, as k_{1x} is finite, and from (4.2.66), we determine that $k_{1x} = (m+1)\pi/d$, which yields the asymptotic values for k_z as

$$k_z = k_1 \tag{4.2.72}$$

On the k_z-k_1 diagram [Figure 4.2.14], this is a straight line with unit slope. The group velocity of the guided waves as $k \to \infty$ is thus $v_g = (\partial k_z/\partial \omega)^{-1} = (\mu_1 \epsilon_1)^{-1/2}$, which is the velocity of light in the slab region. At cutoff, however,

$$k_z = k_0 = k_1 \sqrt{\mu_0 \epsilon_0 / \mu_1 \epsilon_1} \tag{4.2.73}$$

on the k_z-k diagram [Figure 4.2.14], this is a straight line with slope $(\mu_0 \epsilon_0 / \mu_1 \epsilon_1)^{1/2}$. The group velocity as $k \to k_c$ is $(\mu_0 \epsilon_0)^{-1/2}$, equal to the velocity of light in regions outside the slab.

A graphical approach is useful in determining the propagation constant k_z for a symmetric slab waveguide. The guidance condition (4.2.66) yields, for even m, $k_{0xI}d = (\epsilon_0 k_{1x}d/\epsilon_1)\tan(k_{1x}d/2)$. For odd m, we have $k_{0xI}d = -(\epsilon_0 k_{1x}d/\epsilon_1)\cot(k_{1x}d/2)$ and as $k_{1x}d \to 0$, $k_{0xI}d = -2\epsilon_0/\epsilon_1$. We plot the two sets of curves on a two-dimensional plane determined by $k_{0xI}d$ and $k_{1x}d$ [Fig. 4.2.15].
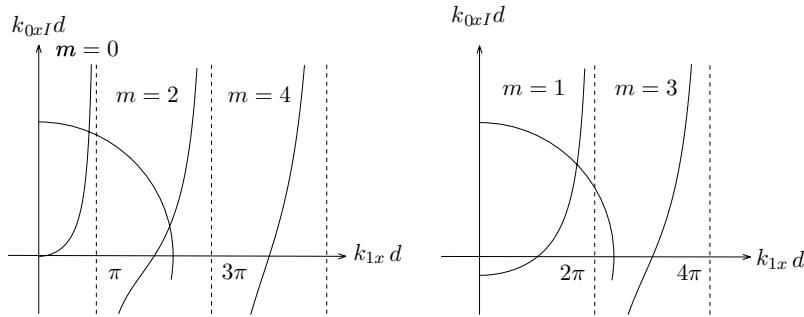
Figure 4.2.15 Graphical determination of $k_x d$.

Draw (4.2.69) as a family of circles on the $k_{0xI}d$ and $k_{1x}d$ plane.

$$(k_{1x}d)^2 + (k_{0xI}d)^2 = (k_1^2 - k_0^2)d^2 \qquad (4.2.74)$$

The intersections with (4.2.66) give rise to values of k_{0xI} and k_{1x}, which in turn determine k_z.
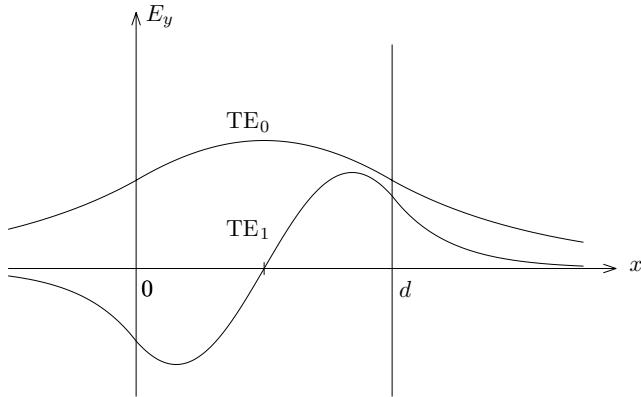
Figure 4.2.16 Field amplitudes for TE_0 and TE_1 modes.

In Figure 4.2.16, we plot the E_y field for the case of $m = 0$ and $m = 1$ for the symmetric slab waveguide. The solutions for H_y are given in (4.2.62), (4.2.63), and (4.2.64). Remember that $k_x d$ can be determined from Figure 4.2.15, where we see that $k_x d$ is larger than $m\pi$ and smaller than $(m+1)\pi$ for the mth mode. Thus, the higher the mode order, the more variations we shall have inside the slab region.

H. Cylindrical Waveguides

In treating guided waves along the $\hat{z}$ direction, the z dependence of all field vectors is written as $e^{\pm ik_z z}$ where k_z is the propagation constant and the $\pm$ signs indicate propagation along positive and negative $\hat{z}$ directions. With this dependence, we can replace $\partial^2/\partial z^2$ by $-k_z^2$. From the Maxwell equations, we can express all field components parallel to the z axis. When all vectors are separated into their transverse and longitudinal components, Maxwell's two curl equations for isotropic media become, in vector notation,

$$\left(\nabla_s + \hat{z}\frac{\partial}{\partial z}\right) \times \left(\overline{E}_s + \overline{E}_z\right) = i\omega\mu\left(\overline{H}_s + \overline{H}_z\right) \qquad (4.2.75)$$

$$\left(\nabla_s + \hat{z}\frac{\partial}{\partial z}\right) \times \left(\overline{H}_s + \overline{H}_z\right) = -i\omega\epsilon\left(\overline{E}_s + \overline{E}_z\right) \qquad (4.2.76)$$

where the subscript s denotes transverse components. Separating into transverse and longitudinal directions, we have

$$i\omega\mu\overline{H}_s = \nabla_s \times \overline{E}_z + \hat{z} \times \partial\overline{E}_s/\partial z \qquad (4.2.77)$$

$$-i\omega\epsilon\overline{E}_s = \nabla_s \times \overline{H}_z + \hat{z} \times \partial\overline{H}_s/\partial z \qquad (4.2.78)$$

$$i\omega\mu\overline{H}_z = \nabla_s \times \overline{E}_s \qquad (4.2.79)$$

$$-i\omega\epsilon\overline{E}_z = \nabla_s \times \overline{H}_s \qquad (4.2.80)$$

From (4.2.77) and (4.2.78) and making use of the identities $\hat{z} \times (\nabla_s \times \overline{E}_z) = \nabla_s E_z$ and $\hat{z} \times (\hat{z} \times \overline{E}_s) = -\overline{E}_s$, we can express $\overline{E}_s$ and $\overline{H}_s$ in terms of E_z and H_z

$$\overline{E}_s = \frac{1}{\omega^2\mu\epsilon - k_z^2}\left[\nabla_s\frac{\partial E_z}{\partial z} + i\omega\mu\nabla_s \times \overline{H}_z\right] \qquad (4.2.81)$$

$$\overline{H}_s = \frac{1}{\omega^2\mu\epsilon - k_z^2}\left[\nabla_s\frac{\partial H_z}{\partial z} - i\omega\epsilon\nabla_s \times \overline{E}_z\right] \qquad (4.2.82)$$

where we make use of the fact that $\partial^2/\partial z^2 = -k_z^2$ and $\overline{E}_z = \hat{z}E_z$ and $\overline{H}_z = \hat{z}H_z$. Substituting (4.2.81) in (4.2.79) and (4.2.82) in (4.2.80) we obtain

$$\left[\nabla_s^2 + \omega^2\mu\epsilon - k_z^2\right]\begin{pmatrix} E_z \\ E_z \end{pmatrix} = 0 \qquad (4.2.83)$$

These are homogeneous Helmholtz equations for E_z and H_z. When the longitudinal components are solved from (4.2.83) and the transverse components determined from (4.2.81)–(4.2.82), we can proceed to match the appropriate boundary conditions imposed by the guiding structures.

I. Cylindrical Rectangular Waveguides

Consider a metallic rectangular waveguide having dimensions a along the x axis and b along the y axis [Fig. 4.2.17]. We first investigate transverse magnetic (TM) fields where all magnetic fields are transverse to the direction of propagation $\hat{z}$. We have $H_z = 0$, and all field components can be derived from a single longitudinal component $E_z = \sin k_x x \sin k_y y \, e^{ik_z z}$. We obtain
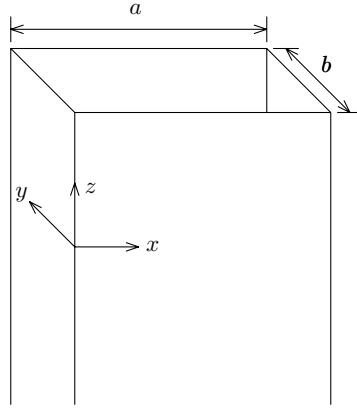
Figure 4.2.17 Metallic rectangular waveguides.

$$E_z = \sin k_x x \sin k_y y \, e^{ik_z z} \tag{4.2.84}$$

$$E_x = \frac{ik_x k_z}{\omega^2 \mu \epsilon - k_z^2} \cos k_x x \sin k_y y \, e^{ik_z z} \tag{4.2.85}$$

$$E_y = \frac{ik_y k_z}{\omega^2 \mu \epsilon - k_z^2} \sin k_x x \cos k_y y \, e^{ik_z z} \tag{4.2.86}$$

$$H_x = \frac{-i\omega\epsilon k_y}{\omega^2 \mu \epsilon - k_z^2} \sin k_x x \cos k_y y \, e^{ik_z z} \tag{4.2.87}$$

$$H_y = \frac{i\omega\epsilon k_x}{\omega^2 \mu \epsilon - k_z^2} \cos k_x x \sin k_y y \, e^{ik_z z} \tag{4.2.88}$$

$$H_z = 0 \tag{4.2.89}$$

We see that at $x = 0$ and a, E_z and E_y vanish, and at $y = 0$ and b, E_z and E_x vanish, provided that

$$k_x a = m\pi \tag{4.2.90a}$$

$$k_y b = n\pi \tag{4.2.90b}$$

where m and n are integer numbers. Equation (4.2.90) gives the guidance conditions. For TM waves neither m nor n can be zero because then E_z will be zero, too. Substituting the guidance conditions (4.2.90) in the field expressions, we see that for larger m there will be more variations for the fields as a function of x, and for larger n there will be more field variations along the $\hat{y}$ direction.

The guidance conditions (4.2.90) and the dispersion relation

$$k_x^2 + k_y^2 + k_z^2 = \omega^2 \mu\epsilon = k^2 \qquad (4.2.91)$$

combine to give the propagation constant

$$k_z = \sqrt{\omega^2 \mu\epsilon - (m\pi/a)^2 - (n\pi/b)^2} \qquad (4.2.92)$$

According to particular values of m and n, the TM waves inside the rectangular waveguide are classified into TM_{mn} modes. The first index m is associated with the number of variations along the $\hat{x}$ direction and the second index with the number of variations along the $\hat{y}$ direction.

Cutoff occurs when k_z becomes imaginary such that the wave attenuates exponentially along the direction of propagation. For a TM_{mn} mode, the cutoff frequency is

$$k_{cmn} = \sqrt{(m\pi/a)^2 + (n\pi/b)^2} \qquad (4.2.93)$$
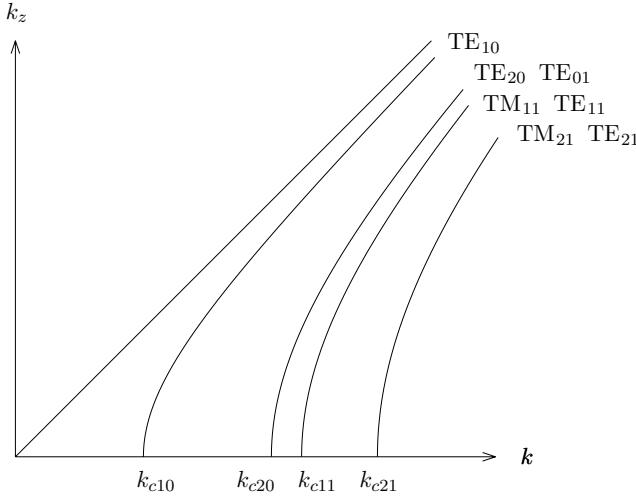
Figure 4.2.18 k_z-k diagram for guided modes.

The lowest order TM mode is seen to be the TM_{11} mode. In Figure 4.2.18 we plot the propagation constant k_z as a function of k for the case $a = 2b$, $k_{cmn} = \sqrt{m^2 + 4n^2}/2a \, \text{K}_o$. As an example, if we let $a = 4$ cm, $b = 2$ cm, we find the cutoff frequency for the TM_{11} mode to be $k_{c11} = \sqrt{5}/2a = 1.12/a = 28\text{K}_o$. Notice that neither m nor n can be zero, thus the smallest cutoff frequency for TM guided waves is the TM_{11} mode.

Next we examine TE fields which are derivable from a single longitudinal component H_z with $E_z = 0$. From (4.2.81) and considering the boundary conditions of vanishing tangential electric fields on the metallic wall surfaces, we obtain

$$H_z = \cos k_x x \cos k_y y \, e^{ik_z z} \tag{4.2.94}$$

$$H_x = \frac{-ik_x k_z}{\omega^2 \mu \epsilon - k_z^2} \sin k_x x \cos k_y y \, e^{ik_z z} \tag{4.2.95}$$

$$H_y = \frac{-ik_y k_z}{\omega^2 \mu \epsilon - k_z^2} \cos k_x x \sin k_y y \, e^{ik_z z} \tag{4.2.96}$$

$$E_x = \frac{-i\omega\mu k_y}{\omega^2 \mu \epsilon - k_z^2} \cos k_x x \sin k_y y \, e^{ik_z z} \tag{4.2.97}$$

$$E_y = \frac{i\omega\mu k_x}{\omega^2 \mu \epsilon - k_z^2} \sin k_x x \cos k_y y \, e^{ik_z z} \tag{4.2.98}$$

$$E_z = 0 \tag{4.2.99}$$

The guidance conditions are obtained from the boundary conditions of $E_x = 0$ at $y = 0$ and b and $E_y = 0$ at $x = 0$ and a. The result is identical to (4.2.90).

$$k_x a = m\pi \tag{4.2.100a}$$

$$k_y b = n\pi \tag{4.2.100b}$$

The propagation constant k_z is again given as (4.2.92) and the cutoff spatial frequencies are found to be (4.2.93).

The time takes for the phase of a wave to travel one meter is the phase delay $T_p = k_z/\omega = \sqrt{\mu\epsilon} \, k_z/k$. The inverse of the phase delay is the phase velocity of the wave. The inverse of the group velocity is the group delay $T_g = \delta k_z/\delta\omega = \sqrt{\mu\epsilon} \, \delta k_z/\delta k = \sqrt{\mu\epsilon} \, k/k_z$.

Notice that while neither m nor n can be zero for TM_{mn} modes, it is possible to have either m or n or both m and n equal to zero for the TE_{mn} modes. For $m = n = 0$, we find $H_z = e^{ikz}$. The equation $\nabla \cdot \overline{H} = 0$ implies $k = \omega(\mu\epsilon)^{1/2} = 0$ and consequently the TE_{00} mode is a static field solution in the waveguide.

EXAMPLE 4.2.5   Parallel plate waveguide.

For parallel plate waveguide with $\partial/\partial y = 0$, (4.2.81)–(4.2.82) become

$$E_x = \frac{1}{\omega^2 \mu \epsilon - k_z^2} \left(\frac{\partial^2}{\partial x \partial z} E_z \right) \qquad (E4.2.5.1a)$$

$$E_y = \frac{1}{\omega^2 \mu \epsilon - k_z^2} \left(-i\omega\mu \frac{\partial}{\partial x} H_z \right) \qquad (E4.2.5.1b)$$

$$H_x = \frac{1}{\omega^2 \mu \epsilon - k_z^2} \left(\frac{\partial^2}{\partial x \partial z} H_z \right) \qquad (E4.2.5.2a)$$

$$H_y = \frac{1}{\omega^2 \mu \epsilon - k_z^2} \left(i\omega\epsilon \frac{\partial}{\partial x} E_z \right) \qquad (E4.2.5.2b)$$

For TM waves, $H_z = 0$, $E_z = \sin k_x x$. For TE waves, $E_z = 0$, $H_z = \cos k_x x$.

For TEM waves, $H_z = E_z = 0$ and (4.2.77)–(4.2.80) become

$$i\omega\mu \overline{H}_s = \hat{z} \times \partial \overline{E}_s / \partial z \qquad (E4.2.5.3)$$

$$-i\omega\epsilon \overline{E}_s = \hat{z} \times \partial \overline{H}_s / \partial z \qquad (E4.2.5.4)$$

$$0 = \nabla_s \times \overline{E}_s \qquad (E4.2.5.5)$$

$$0 = \nabla_s \times \overline{H}_s \qquad (E4.2.5.6)$$

Thus $\overline{E}_s$ and $\overline{H}_s$ are curl free and (E4.2.5.3) and (E4.2.5.4) give

$$\overline{H}_s = \hat{z} \times \sqrt{\frac{\epsilon}{\mu}}\, \overline{E}_s \qquad (E4.2.5.7)$$

$$-\overline{E}_s = \hat{z} \times \sqrt{\frac{\mu}{\epsilon}}\, \overline{H}_s \qquad (E4.2.5.8)$$

The transverse electric and magnetic field vectors and the wave vector follow the right hand rule.

— END OF EXAMPLE 4.2.5 —

We now argue that inside a hollow rectangular waveguide, the TEM mode for which $E_z = H_z = 0$ cannot exist. From $\nabla \cdot \overline{H} = \nabla \cdot \overline{H}_s = 0$ and the boundary condition of vanishing normal $\overline{H}$ field on the wall, we find that the $\overline{H}$ field must form closed loops and $\nabla \times \overline{H}_s = \hat{z} J_z - \hat{z} i\omega\epsilon E_z \neq 0$. Thus either $J_z \neq 0$, which implies the waveguide is not hollow, or $E_z \neq 0$, which implies that the mode cannot be TEM. As a corollary, we have in fact shown that TEM modes do exist when there is another conductor to support the conduction current J_z, as in the case of a coaxial line.

Assuming $a > b$, we see from (4.2.93) that the lowest order TE mode will be TE_{10}, with cutoff frequency

$$k_{c10} = \pi/a = 1/2a \ \mathrm{K}_o \tag{4.2.101}$$

The corresponding cutoff wavelength is $\lambda_c = 2a$. For instance, with $a = 4\,\mathrm{cm}$, $k_{c10} = 12.5\,\mathrm{K}_o$, and $\lambda_c = 8\,\mathrm{cm}$. The field components of the TE_{10} mode are

$$H_z = \cos\frac{\pi x}{a} e^{ik_z z} \tag{4.2.102}$$

$$H_x = \frac{-ik_z a}{\pi}\sin\frac{\pi x}{a} e^{ik_z z} \tag{4.2.103}$$

$$E_y = \frac{i\omega\mu a}{\pi}\sin\frac{\pi x}{a} e^{ik_z z} \tag{4.2.104}$$
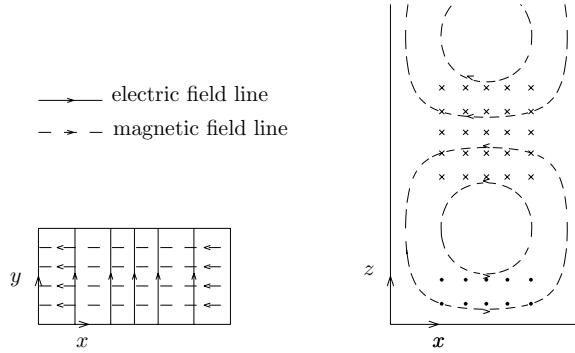
Figure 4.2.19 TE_{10} **mode in a rectangular waveguide.**

The electric field has only a y component. A field plot for the TE_{10} mode is shown in Figure 4.2.19. Written in the form of the superposition of two bouncing plane waves, (4.2.104) becomes

$$E_y = \frac{\omega\mu a}{2\pi}\left[e^{i\frac{\pi x}{a}+ik_z z} - e^{-i\frac{\pi x}{a}+ik_z z}\right] \tag{4.2.105}$$

Higher-order TE and TM modes can also be interpreted as plane waves bouncing around the four walls and propagating along $\hat{z}$ with the propagation constant k_z. The propagation constant k_z for the various modes are plotted in Figure 4.2.18 for the case of $a = 2b$. Since the TE_{10} mode has the lowest cutoff frequency, it is the fundamental mode or the dominant mode of the rectangular waveguide.

J. Cylindrical Circular Waveguides

a. Bessel Functions

In order to study cylindrical waveguides of circular cross-sections, we first consider the wave equation for E_z and H_z in cylindrical coordinates

$$\left[\frac{1}{\rho}\frac{\partial}{\partial\rho}\left(\rho\frac{\partial}{\partial\rho}\right) + \frac{1}{\rho^2}\frac{\partial^2}{\partial\phi^2} + k_\rho^2\right]\left\{\begin{array}{c} E_z \\ H_z \end{array}\right\} = 0 \qquad (4.2.106)$$

where $k_\rho^2 = \omega^2\mu\epsilon - k_z^2$. Solutions to the wave equation are Bessel functions multiplied by sinusoidal functions. The sinusoids can be combinations of $\sin m\phi$, $\cos m\phi$, or $e^{\pm im\phi}$. Substituting in (4.2.106) and making use of the transformation $\xi = k_\rho\rho$, we have the Bessel equation

$$\left[\frac{1}{\xi}\frac{d}{d\xi}\left(\xi\frac{d}{d\xi}\right) + \left(1 - \frac{m^2}{\xi^2}\right)\right]B(\xi) = 0 \qquad (4.2.107)$$

This has solutions in the form of the Bessel function $J_m(\xi)$, Neumann function $N_m(\xi)$, Hankel function of the first kind $H_m^{(1)}(\xi)$, or Hankel function of the second kind $H_m^{(2)}(\xi)$. The two kinds of Hankel functions are related to the Bessel and Neumann functions in the following manner:

$$H_m^{(1)}(\xi) = J_m(\xi) + iN_m(\xi) \qquad (4.2.108)$$
$$H_m^{(2)}(\xi) = J_m(\xi) - iN_m(\xi) \qquad (4.2.109)$$

Let $B_m(\xi)$ represent $J_m(\xi)$, $N_m(\xi)$, $H_m^{(1)}(\xi)$, or $H_m^{(2)}(\xi)$. The recurrence formulas for the Bessel functions $B_m(\xi)$ are as follows:

$$\begin{aligned} B_m'(\xi) &= B_{m-1}(\xi) - \frac{m}{\xi}B_m(\xi) \\ &= -B_{m+1}(\xi) + \frac{m}{\xi}B_m(\xi) \end{aligned} \qquad (4.2.110)$$

where the prime on $B(\xi)$ indicates derivative with respect to its argument. We illustrate $J_m(\xi)$, $J_m'(\xi)$, and $N_m(\xi)$ for $m = 0, 1$, and 2. The asymptotic values of these functions are listed in Table 4.2.1. As $\xi \to \infty$, J_m behaves as cosine, N_m as sine, and H_m as exponents. As $\xi \to 0$, all but J_m become singular.

ξ $B(\xi)$	$\xi \to 0$		$\xi \to \infty$
	$m = 0$	$\mathrm{Re}\,\{m\} > 0$	
$J_m(\xi)$	1	$\frac{(\xi/2)^m}{\Gamma(m+1)}$	$\sqrt{2/\pi\xi}\,\cos(\xi - \frac{m\pi}{2} - \frac{\pi}{4})$
$N_m(\xi)$	$\frac{2}{\pi}\ln\xi$	$-\frac{\Gamma(m)}{\pi}(\frac{2}{\xi})^m$	$\sqrt{2/\pi\xi}\,\sin(\xi - \frac{m\pi}{2} - \frac{\pi}{4})$
$H_m^{(1)}(\xi)$	$i\frac{2}{\pi}\ln\xi$	$-i\frac{\Gamma(m)}{\pi}(\frac{2}{\xi})^m$	$\sqrt{2/\pi\xi}\,\exp[i(\xi - \frac{m\pi}{2} - \frac{\pi}{4})]$
$H_m^{(2)}(\xi)$	$-i\frac{2}{\pi}\ln\xi$	$i\frac{\Gamma(m)}{\pi}(\frac{2}{\xi})^m$	$\sqrt{2/\pi\xi}\,\exp[-i(\xi - \frac{m\pi}{2} - \frac{\pi}{4})]$

Table 4.2.1 Limiting values of J_m, N_m, $H_m^{(1)}$ and $H_m^{(2)}$.

Friedrich Wilhelm Bessel (22 July 1784 – 17 March 1846)

Wilhelm Bessel wrote a paper on Halley's comet in 1804, using observations made in 1607 to calculate its orbit. In 1809 he was appointed director of Frederick William III of Prussia's new Königsberg Observatory and professor of astronomy. At the recommendation of Gauss, a doctorate was awarded to him by the University of Göttingen in 1807. After the completion of the Könisberg Observatory in 1813, Bessel started the task of determining the positions and proper motions of over 50,000 stars and led to the discovery of the parallax of 61 Cygni, a star 10.3 light-years from the earth, in 1838. Bessel functions were introduced in his study of the planetary motion in 1817 and fully developed in 1824.

Franz Ernst Neumann (11 September 1798 – 23 May 1895)

In 1814, Franz Neumann left Berlin Gymnasium and volunteered for the Prussian army, which was defeated by Napoleon on 16 June 1815 at the battle of Ligny. Neumann was seriously wounded and did not take part in the battle at Waterloo two days later. In November 1825 he obtained his doctorate from the University of Berlin and in May 1826, together with Jacob, he was appointed as Privatdozent at the University of Königsberg, where he became Lecturer in 1828 and chair of mineralogy and physics in 1829.

Hermann Hankel (14 February 1839 – 29 August 1873)

Hermann Hankel entered the University of Leipzig in 1857 and became a student of Riemann in Göttingen in 1860 and worked with Weierstrass and Kronecker in Berlin in 1861 and received his doctorate in 1862. He began teaching at Leipzig and became extraordinary professor in the spring of 1867. In the autumn of 1867, he was appointed ordinary professor and in 1869 accepted the chair at Tübingen.
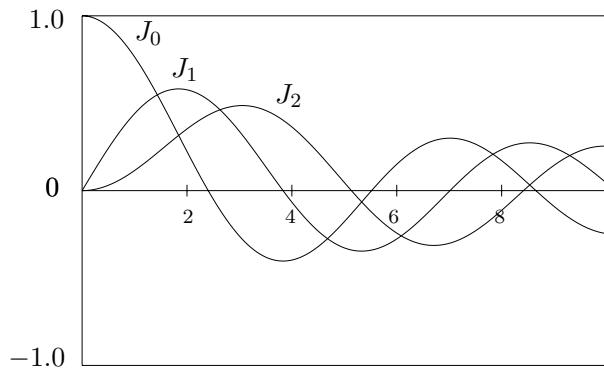
Figure 4.2.20 Bessel functions.
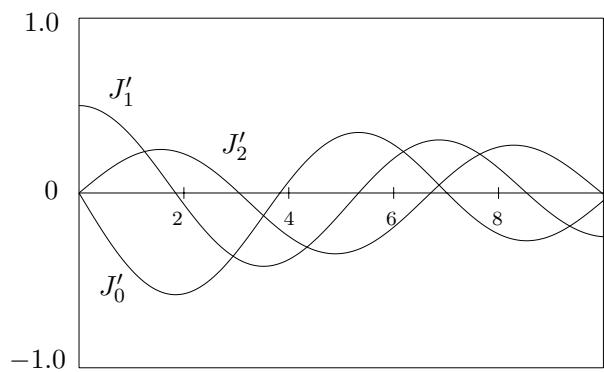
Figure 4.2.21 Derivatives of Bessel functions.
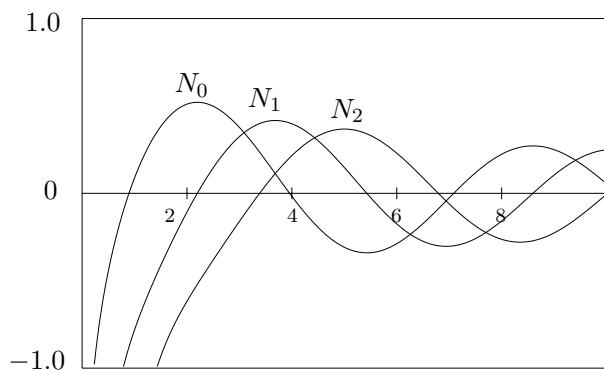
Figure 4.2.22 Neumann functions.

b. Circular Metallic Waveguides

Consider a circular metallic waveguide with radius a [Fig. 4.2.23]. The boundary conditions require that E_z and E_ϕ vanish at $\rho = a$. Since fields must not be singular at $\rho = 0$, the Bessel function J_m is the only logical solution. For TM waves, we have

$$E_z = J_m(k_\rho \rho) \begin{Bmatrix} \sin m\phi \\ \cos m\phi \end{Bmatrix} e^{ik_z z} \qquad (4.2.111)$$
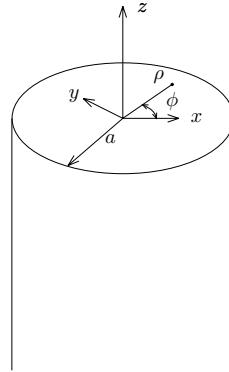
Figure 4.2.23   Circular metallic waveguides.

with the dispersion relation

$$k_z^2 + k_\rho^2 = \omega^2 \mu\epsilon \qquad (4.2.112)$$

Transverse field components are obtained from the guided wave formalism (4.2.81)–(4.2.82),

$$E_\rho = \frac{ik_z k_\rho}{\omega^2 \mu\epsilon - k_z^2} J_m'(k_\rho \rho) \begin{Bmatrix} \sin m\phi \\ \cos m\phi \end{Bmatrix} e^{ik_z z} \qquad (4.2.113)$$

$$E_\phi = \frac{ik_z}{\omega^2 \mu\epsilon - k_z^2} \frac{m}{\rho} J_m(k_\rho \rho) \begin{Bmatrix} \cos m\phi \\ -\sin m\phi \end{Bmatrix} e^{ik_z z} \qquad (4.2.114)$$

$$H_\rho = \frac{-i\omega\epsilon}{\omega^2 \mu\epsilon - k_z^2} \frac{m}{\rho} J_m(k_\rho \rho) \begin{Bmatrix} \cos m\phi \\ -\sin m\phi \end{Bmatrix} e^{ik_z z} \qquad (4.2.115)$$

$$H_\phi = \frac{i\omega\epsilon k_\rho}{\omega^2 \mu\epsilon - k_z^2} J_m'(k_\rho \rho) \begin{Bmatrix} \sin m\phi \\ \cos m\phi \end{Bmatrix} e^{ik_z z} \qquad (4.2.116)$$

where the prime on the Bessel function denotes derivative with respect to its argument. The boundary condition of vanishing E_z and E_ϕ at $\rho = a$ gives the guidance condition

$$J_m(k_\rho a) = 0 \qquad (4.2.117)$$

Let ξ_{mn} denote the n th root of the m th order Bessel function such that $J_m(\xi_{mn}) = 0$. The first three roots of $J_0(\xi_{mn}) = 0$ are $\xi_{01} = 2.405$, $\xi_{02} = 5.52$, $\xi_{03} = 8.65$. For $J_1(\xi_{mn}) = 0$, $\xi_{11} = 3.83$, $\xi_{12} = 7.01$, $\xi_{13} = 10.2$. For $J_2(\xi_{mn}) = 0$, $\xi_{21} = 5.14$, $\xi_{22} = 8.42$, $\xi_{23} = 11.6$. For $J_3(\xi_{mn}) = 0$, $\xi_{31} = 6.38$, $\xi_{32} = 9.76$, $\xi_{33} = 13$. From the guidance condition (4.2.117) and the dispersion relation (4.2.112), we find

$$k_z = \sqrt{\omega^2 \mu \epsilon - (\xi_{mn}/a)^2} \qquad (4.2.118)$$

For each value of ξ_{mn} we label the wave solution TM_{mn} mode, where m is associated with the number of variations in the $\hat{\phi}$ direction and n with the number of variations in the $\hat{\rho}$ direction. The cutoff wavenumbers for the TM_{mn} modes are

$$k_{cmn} = \xi_{mn}/a \qquad (4.2.119)$$
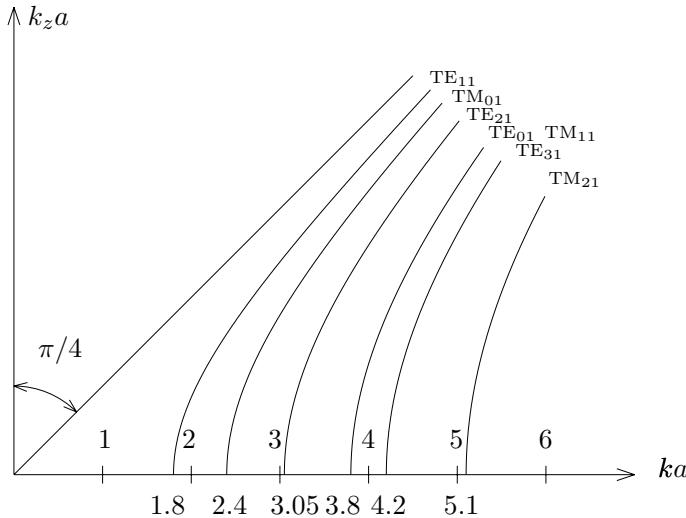
Figure 4.2.24 $k_z a$-ka diagrams for guided modes.

We find from Figure 4.2.20 that for the TM_{01} mode $\xi_{01} = 2.4$ and for the TM_{11} mode $\xi_{11} = 3.8$. The $k_z a$-ka diagram for the guided TM_{mn} modes is plotted in Figure 4.2.24.

For TE wave solutions we have

$$H_z = J_m(k_\rho \rho) \begin{Bmatrix} \sin m\phi \\ \cos m\phi \end{Bmatrix} e^{ik_z z} \tag{4.2.120}$$

with dispersion relation

$$k_z^2 + k_\rho^2 = \omega^2 \mu\epsilon \tag{4.2.121}$$

The transverse field components are

$$H_\rho = \frac{ik_z k_\rho}{\omega^2 \mu\epsilon - k_z^2} J_m'(k_\rho \rho) \begin{Bmatrix} \sin m\phi \\ \cos m\phi \end{Bmatrix} e^{ik_z z} \tag{4.2.122}$$

$$H_\phi = \frac{ik_z}{\omega^2 \mu\epsilon - k_z^2} \frac{m}{\rho} J_m(k_\rho \rho) \begin{Bmatrix} \cos m\phi \\ -\sin m\phi \end{Bmatrix} e^{ik_z z} \tag{4.2.123}$$

$$E_\rho = \frac{i\omega\mu}{\omega^2 \mu\epsilon - k_z^2} \frac{m}{\rho} J_m(k_\rho \rho) \begin{Bmatrix} \cos m\phi \\ -\sin m\phi \end{Bmatrix} e^{ik_z z} \tag{4.2.124}$$

$$E_\phi = \frac{-i\omega\mu k_\rho}{\omega^2 \mu\epsilon - k_z^2} J_m'(k_\rho \rho) \begin{Bmatrix} \sin m\phi \\ \cos m\phi \end{Bmatrix} e^{ik_z z} \tag{4.2.125}$$

The boundary condition of vanishing E_z and E_ϕ at $\rho = a$ gives the guidance condition

$$J_m'(k_\rho a) = 0 \tag{4.2.126}$$

Letting ξ_{mn}' denote the roots of J_m' such that $J_m'(\xi_{mn}') = 0$. The first three roots of $J_0'(\xi_{mn}') = 0$ are $\xi_{01}' = 3.83$, $\xi_{02}' = 7.01$, $\xi_{03}' = 10.2$. For $J_1'(\xi_{mn}') = 0$, $\xi_{11}' = 1.84$, $\xi_{12}' = 5.33$, $\xi_{13}' = 8.54$. For $J_2'(\xi_{mn}') = 0$, $\xi_{21}' = 3.05$, $\xi_{22}' = 6.71$, $\xi_{23} = 9.97$. For $J_3'(\xi_{mn}') = 0$, $\xi_{31}' = 4.2$, $\xi_{32}' = 8.02$, $\xi_{33} = 11.3$. We find from the dispersion relation (4.2.121) and the guidance condition (4.2.126)

$$k_z = \sqrt{\omega^2 \mu\epsilon - (\xi_{mn}'/a)^2} \tag{4.2.127}$$

For each value of ξ_{mn}' we label the wave solution TE_{mn} mode where m is associated with the number of variations in the $\hat{\phi}$ direction and n with the number of variations in the $\hat{\rho}$ direction. The field patterns

TE$_{11}$ mode   TM$_{01}$ mode
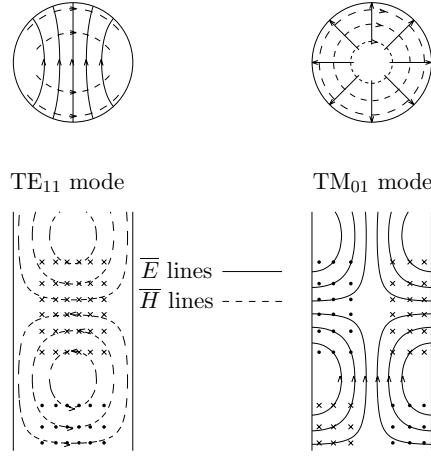
$\overline{E}$ lines ——
$\overline{H}$ lines - - - - -

Figure 4.2.25 Field lines for TE$_{11}$ **and** TM$_{01}$ **modes.**

for the TE$_{11}$ and TM$_{01}$ modes are shown in Figure 4.2.25. The cutoff frequencies for the TE$_{mn}$ modes are

$$k_{cmn} = \xi'_{mn}/a \qquad (4.2.128)$$

We see from Figure 4.2.21 that for the TE$_{11}$ mode $\xi'_{11} = 1.8$, for the TE$_{21}$ mode $\xi'_{21} = 3.05$, and for the TE$_{01}$ mode $\xi'_{01} = 3.8$. The $k_z a$-ka diagram for the guided TE$_{mn}$ modes is shown in Figure 4.2.24.

EXAMPLE 4.2.6   TE$_{11}$ mode.

The transverse electric field for the TE$_{11}$ mode can be expressed in terms of its x and y components. We have

$$E_y = E_\rho \sin\phi + E_\phi \cos\phi = \frac{-i\omega\mu k_\rho}{\omega^2\mu\epsilon - k_z^2}\left[\frac{m}{k_\rho\rho} J_m(k_\rho\rho)\sin^2\phi + J'_m(k_\rho\rho)\cos^2\phi\right]e^{ik_z z}$$

$$= \frac{-i\omega\mu}{2k_\rho}\left[J_{m-1}(k_\rho\rho) + (J_{m-1}(k_\rho\rho) - \frac{2m}{k_\rho\rho}J_m(k_\rho\rho))\cos 2\phi\right]e^{ik_z z}$$

$$E_x = E_\rho\cos\phi - E_\phi\sin\phi = \frac{i\omega\mu\sin 2\phi}{2k_\rho}\left[J'_1(k_\rho\rho) - \frac{1}{k_\rho\rho}J_1(k_\rho\rho)\right]e^{ik_z z}$$

$$= -\frac{i\omega\mu\sin 2\phi}{2k_\rho}\left[J_{m+1}(k_\rho\rho)\right]e^{ik_z z}$$

It is seen that at $\phi = 0$, $E_x = 0$ and $E_y = -i\omega\mu J'_m(k_\rho\rho)/k_\rho$. At $\phi = \pi/2$, $E_x = 0$ and $E_y = -i\omega m\mu J_m(k_\rho\rho)/k_\rho^2\rho$.

— END OF EXAMPLE 4.2.6 —

c. Circular Dielectric Waveguides

Consider a circular waveguide of radius a made of an isotropic medium with constitutive parameters μ and ϵ embedded in another isotropic medium characterized by μ_1 and ϵ_1 [Fig. 4.2.26].
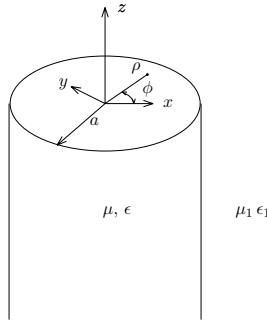
Figure 4.2.26 Circular dielectric waveguides.

Inside the waveguide, solutions for E_z and H_z are Bessel functions,

$$E_z = A J_m(k_\rho \rho) \sin m\phi \, e^{ik_z z} \tag{4.2.129}$$

$$H_z = B J_m(k_\rho \rho) \cos m\phi \, e^{ik_z z} \tag{4.2.130}$$

with the dispersion relation

$$k_z^2 + k_\rho^2 = \omega^2 \mu\epsilon = k^2 \tag{4.2.131}$$

In (4.2.129) and (4.2.130), $\sin m\phi$ and $\cos m\phi$ are chosen for E_z and H_z in anticipation of matching the boundary conditions. They can also be replaced with $\cos m\phi$ and $\sin m\phi$, respectively.

Outside the waveguide, the field associated with the guided waves must be evanescent in the $\hat{\rho}$ direction. The proper choice of the solution will be Hankel functions with imaginary arguments, known as the modified Hankel functions. Letting $k_{1\rho} = ik_{1\rho I}$, we write for $\rho \geq a$

$$E_z = C H_m^{(1)}(ik_{1\rho I}\rho) \sin m\phi \, e^{ik_z z} \tag{4.2.132}$$

$$H_z = D H_m^{(1)}(ik_{1\rho I}\rho) \cos m\phi \, e^{ik_z z} \tag{4.2.133}$$

with the dispersion relation

$$k_z^2 - k_{1\rho I}^2 = \omega^2 \mu_1 \epsilon_1 = k_1^2 \tag{4.2.134}$$

The next step will be to match boundary conditions of tangential electric and magnetic field components at $\rho = a$. The choice of $\sin m\phi$ and $\cos m\phi$ for E_z and H_z in (4.2.132)–(4.2.133) facilitates their equality with (4.2.129)–(4.2.130) at $\rho = a$ for all azimuthal angles ϕ. There are four boundary conditions for the continuity of E_z, H_z, E_ϕ, and H_ϕ at $\rho = a$. We see that separating into TE and TM modes in general will no longer be possible because there will be three equations to be satisfied with two unknown pairs of either A, C or B, D. The guided modes with both E_z and H_z components present are called hybrid modes.

Determining guidance conditions:

Transverse components for the fields are determined from (4.2.81)–(4.2.82). All field components inside and outside the dielectric waveguide are

For $\rho \le a$, and $k_\rho = \sqrt{k^2 - k_z^2}$:

$$E_z = A J_m(k_\rho \rho) \sin m\phi\, e^{ik_z z}$$

$$H_z = B J_m(k_\rho \rho) \cos m\phi\, e^{ik_z z}$$

$$E_\rho = \frac{1}{k_\rho^2} \left[A i k_z k_\rho J_m'(k_\rho \rho) \sin m\phi - B \frac{i\omega\mu m}{\rho} J_m(k_\rho \rho) \sin m\phi \right] e^{ik_z z}$$

$$E_\phi = \frac{1}{k_\rho^2} \left[\frac{A i k_z m}{\rho} J_m(k_\rho \rho) \cos m\phi - B i\omega\mu k_\rho J_m'(k_\rho \rho) \cos m\phi \right] e^{ik_z z}$$

$$H_\rho = \frac{1}{k_\rho^2} \left[B i k_z k_\rho J_m'(k_\rho \rho) \cos m\phi - A \frac{i\omega\epsilon m}{\rho} J_m(k_\rho \rho) \cos m\phi \right] e^{ik_z z}$$

$$H_\phi = \frac{1}{k_\rho^2} \left[-B \frac{i k_z m}{\rho} J_m(k_\rho \rho) \sin m\phi + A i\omega\epsilon k_\rho J_m'(k_\rho \rho) \sin m\phi \right] e^{ik_z z}$$

For $\rho \ge a$, and $k_{1\rho I} = \sqrt{k_z^2 - k_1^2}$:

$$E_z = C H_m^{(1)}(ik_{1\rho I}\rho) \sin m\phi\, e^{ik_z z}$$

$$H_z = D H_m^{(1)}(ik_{1\rho I}\rho) \cos m\phi\, e^{ik_z z}$$

$$E_\rho = \frac{-1}{k_{1\rho I}^2} \left[-C k_z k_{1\rho I} H_m^{(1)\prime}(ik_{1\rho I}\rho) \sin m\phi - D \frac{i\omega\mu_1 m}{\rho} H_m^{(1)}(ik_{1\rho I}\rho) \sin m\phi \right] e^{ik_z z}$$

$$E_\phi = \frac{-1}{k_{1\rho I}^2} \left[C \frac{i k_z m}{\rho} H_m^{(1)}(ik_{1\rho I}\rho) \cos m\phi + D \omega\mu_1 k_{1\rho I} H_m^{(1)\prime}(ik_{1\rho I}\rho) \cos m\phi \right] e^{ik_z z}$$

$$H_\rho = \frac{-1}{k_{1\rho I}^2}\left[-Dk_z k_{1\rho I}H_m^{(1)'}(ik_{1\rho I}\rho)\cos m\phi - C\frac{i\omega\epsilon_1 m}{\rho}H_m^{(1)}(ik_{1\rho I}\rho)\cos m\phi\right]e^{ik_z z}$$

$$H_\phi = \frac{-1}{k_{1\rho I}^2}\left[-D\frac{ik_z m}{\rho}H_m^{(1)}(ik_{1\rho I}\rho)\sin m\phi - C\omega\epsilon_1 k_{1\rho I}H_m^{(1)'}(ik_{1\rho I}\rho)\sin m\phi\right]e^{ik_z z}$$

Matching the z and ϕ components at $\rho = a$ we obtain the following four equations for A, B, C, and D:

$$AJ_m(k_\rho a) = CH_m^{(1)}(ik_{1\rho I}a)$$

$$BJ_m(k_\rho a) = DH_m^{(1)}(ik_{1\rho I}a)$$

$$A\frac{ik_z m}{k_\rho^2 a}J_m(k_\rho a) - B\frac{i\omega\mu}{k_\rho}J'_m(k_\rho a) = -C\frac{ik_z m}{k_{1\rho I}^2 a}H_m^{(1)}(ik_{1\rho I}a) - D\frac{\omega\mu_1}{k_{1\rho I}}H_m^{(1)'}(ik_{1\rho I}a)$$

$$-B\frac{ik_z m}{k_\rho^2 a}J_m(k_\rho a) + A\frac{i\omega\epsilon}{k_\rho}J'_m(k_\rho a) = D\frac{ik_z m}{k_{1\rho I}^2 a}H_m^{(1)}(ik_{1\rho I}a) + C\frac{\omega\epsilon_1}{k_{1\rho I}}H_m^{(1)'}(ik_{1\rho I}a)$$

Eliminating C and D, we have

$$\frac{ik_z m}{a}A\left[\frac{1}{k_\rho^2} + \frac{1}{k_{1\rho I}^2}\right] = i\omega B\left[\frac{\mu}{k_\rho}\frac{J'_m(k_\rho a)}{J_m(k_\rho a)} + i\frac{\mu_1}{k_{1\rho I}}\frac{H_m^{(1)'}(ik_{1\rho I}a)}{H_m^{(1)}(ik_{1\rho I}a)}\right] \quad (4.2.135)$$

$$\frac{ik_z m}{a}B\left[\frac{1}{k_\rho^2} + \frac{1}{k_{1\rho I}^2}\right] = i\omega A\left[\frac{\epsilon}{k_\rho}\frac{J'_m(k_\rho a)}{J_m(k_\rho a)} + i\frac{\epsilon_1}{k_{1\rho I}}\frac{H_m^{(1)'}(ik_{1\rho I}a)}{H_m^{(1)}(ik_{1\rho I}a)}\right] \quad (4.2.136)$$

Eliminating A and B, we determine the guidance condition for the circular dielectric waveguide.

$$\frac{k^2}{k_\rho^2}\left[\frac{J'_m(k_\rho a)}{J_m(k_\rho a)} - p_{10}^{TE}\frac{H_m^{(1)'}(ik_{1\rho I}a)}{H_m^{(1)}(ik_{1\rho I}a)}\right]\left[\frac{J'_m(k_\rho a)}{J_m(k_\rho a)} - p_{10}^{TM}\frac{H_m^{(1)'}(ik_{1\rho I}a)}{H_m^{(1)}(ik_{1\rho I}a)}\right]$$

$$= (mk_z a)^2\left[\frac{1}{k_\rho^2 a^2} + \frac{1}{k_{1\rho I}^2 a^2}\right]^2 \quad (4.2.137)$$

where $p_{10}^{TE} = \mu_1 k_\rho/i\mu k_{1\rho I}$ and $p_{10}^{TM} = \epsilon_1 k_\rho/i\epsilon k_{1\rho I}$. From (4.2.137), we determine

$$\frac{J'^2_m(k_\rho a)}{J_m^2(k_\rho a)} - (p_{10}^{TE} + p_{10}^{TM})\frac{H_m^{(1)'}(ik_{1\rho I}a)}{H_m^{(1)}(ik_{1\rho I}a)}\frac{J'_m(k_\rho a)}{J_m(k_\rho a)} + p_{10}^{TE}p_{10}^{TM}\frac{H_m^{(1)'^2}(ik_{1\rho I}a)}{H_m^{(1)^2}(ik_{1\rho I}a)}$$

$$= \frac{m^2 k_z^2}{k^2 k_\rho^2 a^2}\left(1 + \frac{k_\rho^2}{k_{1\rho I}^2}\right)^2 = m^2\left(\frac{1}{k_\rho^2 a^2} + \frac{1 + k_1^2/k^2}{k_{1\rho I}^2 a^2} + \frac{k_1^2 k_\rho^2}{k^2 k_{1\rho I}^4 a^2}\right) \quad (4.2.138)$$

Solving for $J'_m(k_\rho a)/J_m(k_\rho a)$, we find the guidance conditions for EH modes:

$$\frac{J'_m(k_\rho a)}{J_m(k_\rho a)} = \frac{1}{2}(p_{10}^{TE} + p_{10}^{TM})\frac{H_m^{(1)'}(ik_{1\rho I}a)}{H_m^{(1)}(ik_{1\rho I}a)}$$

$$+ \sqrt{\frac{1}{4}(p_{10}^{TE} - p_{10}^{TM})^2 \frac{H_m^{(1)'2}(ik_{1\rho I}a)}{H_m^{(1)2}(ik_{1\rho I}a)} + m^2\left(\frac{1}{k_\rho^2 a^2} + \frac{1+k_1^2/k^2}{k_{1\rho I}^2 a^2} + \frac{k_1^2 k_\rho^2}{k^2 k_{1\rho I}^4 a^2}\right)}$$

$$(4.2.139)$$

and for HE modes

$$\frac{J'_m(k_\rho a)}{J_m(k_\rho a)} = \frac{1}{2}(p_{10}^{TE} + p_{10}^{TM})\frac{H_m^{(1)'}(ik_{1\rho I}a)}{H_m^{(1)}(ik_{1\rho I}a)}$$

$$- \sqrt{\frac{1}{4}(p_{10}^{TE} - p_{10}^{TM})^2 \frac{H_m^{(1)'2}(ik_{1\rho I}a)}{H_m^{(1)2}(ik_{1\rho I}a)} + m^2\left(\frac{1}{k_\rho^2 a^2} + \frac{1+k_1^2/k^2}{k_{1\rho I}^2 a^2} + \frac{k_1^2 k_\rho^2}{k^2 k_{1\rho I}^4 a^2}\right)}$$

$$(4.2.140)$$

Finding cutoff frequencies for $m = 0$ modes:

When $m = 0$, (4.2.139) becomes

$$\frac{J'_0(k_\rho a)}{J_0(k_\rho a)} = p_{10}^{TE}\frac{H_0^{(1)'}(ik_{1\rho I}a)}{H_0^{(1)}(ik_{1\rho I}a)} \qquad (4.2.141)$$

We see that this corresponds to $A = C = 0$. Consequently, $E_z = 0$, and thus EH_{0p} modes are TE waves. Likewise, (4.2.140) becomes

$$\frac{J'_0(k_\rho a)}{J_0(k_\rho a)} = p_{10}^{TM}\frac{H_0^{(1)'}(ik_{1\rho I}a)}{H_0^{(1)}(ik_{1\rho I}a)} \qquad (4.2.142)$$

and HE_{0p} modes reduce to TM waves. When $m \neq 0$, separation into TE and TM waves is no longer possible and we have hybrid modes.

Cutoff occurs when $k_{1\rho I} \to 0$ as $k_{1\rho I}$ becomes imaginary such that the argument of the first-kind Hankel function becomes real and the field outside is radiating in the radial $\hat{\rho}$ direction. This cutoff criterion is identical to that

used in the case of dielectric slab waveguides. Using the asymptotic values for the Hankel functions as $k_{1\rho I} \to 0$, we have for $m = 0$

$$\frac{J_0'(k_\rho a)}{J_0(k_\rho a)} \sim \frac{\mu_1 k_\rho}{i\mu k_{1\rho I}} \frac{1}{ik_{1\rho I} a \ln(ik_{1\rho I} a)} \qquad \text{for TE modes} \qquad (4.2.143)$$

$$\frac{J_0'(k_\rho a)}{J_0(k_\rho a)} \sim \frac{\epsilon_1 k_\rho}{i\epsilon k_{1\rho I}} \frac{1}{ik_{1\rho I} a \ln(ik_{1\rho I} a)} \qquad \text{for TM modes} \qquad (4.2.144)$$

From the dispersion relations $k_z^2 = k^2 - k_\rho^2 = k_1^2 + k_{1\rho I}^2$, we see that at cutoff, $k_{1\rho I} \to 0$, $k_z \to k_1$, and $k_\rho \to k_c(1 - \mu_1\epsilon_1/\mu\epsilon)^{1/2}$, where k_c is the cutoff frequency.

We see that (4.2.143) and (4.2.144) yield identical equations for TE and TM modes at cutoff,

$$J_0\left(k_{c0p}a\sqrt{1 - \frac{n_1^2}{n^2}}\right) = 0 \qquad (4.2.145)$$

where $n_1 = c(\mu_1\epsilon_1)^{1/2}$ and $n = c(\mu\epsilon)^{1/2}$. We thus have for TE_{0p} and TM_{0p} modes

$$k_{c0p}a(1 - n_1^2/n^2)^{1/2} = \xi_{0p}$$

where ξ_{0p} is the pth root of the zeroth order Bessel function $J_0(\xi)$.

Finding cutoff frequencies for EH modes:

To investigate cutoff conditions for the guided waves when $m \neq 0$, we first approximate the square root term in (4.2.139) and (4.2.140) as $k_{1\rho I} \to 0$. Using the relation $k_z^2 = k^2 - k_\rho^2 = k_1^2 + k_{1\rho I}^2$ and the recurrence formula for Hankel functions, we obtain

$$\frac{H_m^{(1)'}(ik_{1\rho I} a)}{H_m^{(1)}(ik_{1\rho I} a)} = \frac{H_{m-1}^{(1)}(ik_{1\rho I} a)}{H_m^{(1)}(ik_{1\rho I} a)} - \frac{m}{ik_{1\rho I} a} \qquad (4.2.146)$$

where as $k_{1\rho I} \to 0$

$$\frac{H_m^{(1)'}(ik_{1\rho I} a)}{H_m^{(1)}(ik_{1\rho I} a)} \sim iA_m - \frac{m}{ik_{1\rho I} a} \qquad (4.2.147)$$

with $A_1 \sim -k_{1\rho I} a \ln(ik_{1\rho I} a)$ and $A_m \sim \frac{k_{1\rho I} a}{2(m-1)}$ for $m > 1$. The square root term in (4.2.139) and (4.2.140) becomes

$$\sqrt{\frac{1}{4}(p_{10}^{TE} - p_{10}^{TM})^2 \frac{H_m^{(1)'^2}(ik_{1\rho I}a)}{H_m^{(1)^2}(ik_{1\rho I}a)} + m^2 \left(\frac{1}{k_\rho^2 a^2} + \frac{1 + k_1^2/k^2}{k_{1\rho I}^2 a^2} + \frac{k_1^2 k_\rho^2}{k^2 k_{1\rho I}^4 a^2}\right)}$$

$$\approx \sqrt{\frac{1}{4}\left(\frac{\mu_1}{\mu} - \frac{\epsilon_1}{\epsilon}\right)^2 \frac{k_\rho^2}{k_{1\rho I}^2}\left(A_m + \frac{m}{k_{1\rho I}a}\right)^2 + m^2\left(\frac{1}{k_\rho^2 a^2} + \frac{1 + k_1^2/k^2}{k_{1\rho I}^2 a^2} + \frac{k_1^2 k_\rho^2}{k^2 k_{1\rho I}^4 a^2}\right)}$$

$$\approx \sqrt{\frac{1}{4}\left(\frac{\mu_1}{\mu} + \frac{\epsilon_1}{\epsilon}\right)^2 \frac{m^2 k_\rho^2}{k_{1\rho I}^4 a^2} + \frac{1}{2}\left(\frac{\mu_1}{\mu} - \frac{\epsilon_1}{\epsilon}\right)^2 \frac{m k_\rho^2}{k_{1\rho I}^3 a} A_m + m^2\left(\frac{1}{k_\rho^2 a^2} + \frac{1 + k_1^2/k^2}{k_{1\rho I}^2 a^2}\right)}$$

$$\approx \frac{1}{2}\left(\frac{\mu_1}{\mu} + \frac{\epsilon_1}{\epsilon}\right)\frac{m k_\rho}{k_{1\rho I}^2 a}\sqrt{1 + \frac{2(\frac{\mu_1}{\mu} - \frac{\epsilon_1}{\epsilon})^2 \frac{m k_\rho^2}{k_{1\rho I}^3 a} A_m}{(\frac{\mu_1}{\mu} + \frac{\epsilon_1}{\epsilon})^2 \frac{m^2 k_\rho^2}{k_{1\rho I}^4 a^2}} + \frac{4m^2\left(\frac{1}{k_\rho^2 a^2} + \frac{1 + k_1^2/k^2}{k_{1\rho I}^2 a^2}\right)}{(\frac{\mu_1}{\mu} + \frac{\epsilon_1}{\epsilon})^2 \frac{m^2 k_\rho^2}{k_{1\rho I}^4 a^2}}}$$

$$\approx \frac{1}{2}\left(\frac{\mu_1}{\mu} + \frac{\epsilon_1}{\epsilon}\right)\frac{m k_\rho}{k_{1\rho I}^2 a}\sqrt{1 + \frac{2(\frac{\mu_1}{\mu} - \frac{\epsilon_1}{\epsilon})^2 A_m k_{1\rho I} a}{m(\frac{\mu_1}{\mu} + \frac{\epsilon_1}{\epsilon})^2} + \frac{4\left(\frac{k_{1\rho I}^2}{k_\rho^2} + 1 + k_1^2/k^2\right)}{(\frac{\mu_1}{\mu} + \frac{\epsilon_1}{\epsilon})^2}\frac{k_{1\rho I}^2}{k_\rho^2}}$$

$$\approx \frac{1}{2}\left(\frac{\mu_1}{\mu} + \frac{\epsilon_1}{\epsilon}\right)\frac{m k_\rho}{k_{1\rho I}^2 a} + \frac{(\frac{\mu_1}{\mu} - \frac{\epsilon_1}{\epsilon})^2 k_\rho}{2(\frac{\mu_1}{\mu} + \frac{\epsilon_1}{\epsilon})k_{1\rho I}}A_m + \frac{m\left(\frac{k_{1\rho I}^2}{k_\rho^2} + 1 + k_1^2/k^2\right)}{(\frac{\mu_1}{\mu} + \frac{\epsilon_1}{\epsilon})k_\rho a} \quad (4.2.148)$$

Substituting (4.2.148) in (4.2.139), we obtain for EH modes

$$\frac{J_m'(k_\rho a)}{J_m(k_\rho a)} \approx \frac{1}{2}\left(\frac{\mu_1}{\mu} + \frac{\epsilon_1}{\epsilon}\right)\frac{k_\rho}{k_{1\rho I}}\left(A_m + \frac{m}{k_{1\rho I}a}\right)$$

$$+ \frac{1}{2}\left(\frac{\mu_1}{\mu} + \frac{\epsilon_1}{\epsilon}\right)\frac{m k_\rho}{k_{1\rho I}^2 a} + \frac{(\frac{\mu_1}{\mu} - \frac{\epsilon_1}{\epsilon})^2 k_\rho}{2(\frac{\mu_1}{\mu} + \frac{\epsilon_1}{\epsilon})k_{1\rho I}}A_m + \frac{m\left(\frac{k_{1\rho I}^2}{k_\rho^2} + 1 + k_1^2/k^2\right)}{(\frac{\mu_1}{\mu} + \frac{\epsilon_1}{\epsilon})k_\rho a} \quad (4.2.149)$$

Thus we find cutoff frequencies for EH_{mp} modes from

$$J_m\left(k_{cmp}a\sqrt{1 - \frac{n_1^2}{n^2}}\right) = 0 \quad (4.2.150)$$

where $k_{cmp}a(1 - n_1^2/n^2)^{1/2} = \xi_{mp}$, and ξ_{mp} is the p th root of the m th order Bessel function $J_m(\xi)$. However the first root of $\xi = 0$ is excluded since as $k_{1\rho I} \to 0$, we must also have $k_\rho \to 0$. Approximate

$$\frac{J_m'(k_\rho a)}{J_m(k_\rho a)} \approx \frac{m}{k_\rho a}$$

we see that the above equation can not be satisfied with $k_\rho = 0$. Thus the roots of $\xi = 0$ for $J_m(\xi)$, which correspond to zero cutoff frequency, cannot be included. The smallest is the first root of $J_1(\xi)$ with $\xi = 3.832$.

Finding cutoff frequencies for HE modes:

Substituting (4.2.148) in (4.2.140), we obtain for HE modes

$$\frac{J_m'(k_\rho a)}{J_m(k_\rho a)} \approx \frac{1}{2}\left(\frac{\mu_1}{\mu} + \frac{\epsilon_1}{\epsilon}\right)\frac{k_\rho}{k_{1\rho I}}\left(A_m + \frac{m}{k_{1\rho I}a}\right)$$

$$-\frac{1}{2}\left(\frac{\mu_1}{\mu} + \frac{\epsilon_1}{\epsilon}\right)\frac{mk_\rho}{k_{1\rho I}^2 a} - \frac{(\frac{\mu_1}{\mu} - \frac{\epsilon_1}{\epsilon})^2 k_\rho}{2(\frac{\mu_1}{\mu} + \frac{\epsilon_1}{\epsilon})k_{1\rho I}}A_m - \frac{m\left(\frac{k_{1\rho I}^2}{k_\rho^2} + 1 + k_1^2/k^2\right)}{(\frac{\mu_1}{\mu} + \frac{\epsilon_1}{\epsilon})k_\rho a}$$

$$= \frac{2(\frac{\mu_1\epsilon_1}{\mu\epsilon})k_\rho}{(\frac{\mu_1}{\mu} + \frac{\epsilon_1}{\epsilon})k_{1\rho I}}A_m - \frac{m\left(\frac{k_{1\rho I}^2}{k_\rho^2} + 1 + k_1^2/k^2\right)}{(\frac{\mu_1}{\mu} + \frac{\epsilon_1}{\epsilon})k_\rho a} \qquad (4.2.151)$$

For $m > 1$, we determine cutoff frequencies for HE_{mp} modes from

$$\frac{\mu\epsilon_1 + \mu_1\epsilon}{k_\rho a}\frac{J_m'(k_\rho a)}{J_m(k_\rho a)} + m\frac{\mu_1\epsilon_1 + \mu\epsilon}{k_\rho^2 a^2} - \frac{\mu_1\epsilon_1}{m-1} = 0 \quad (4.2.152)$$

$$k_c a\sqrt{1 - n_1^2/n^2}$$
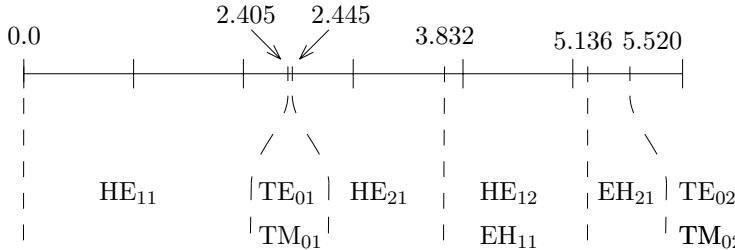
Figure 4.2.27 Cutoff of circular dielectric waveguide modes.

For $\mu = \mu_1$, (4.2.152) gives $(1 + \epsilon/\epsilon_1) = k_\rho a J_m(k_\rho a)/(m-1)J_{m-1}(k_\rho a)$. In Figure 4.2.27, we let $\epsilon_1/\epsilon = 1.1$ and list the cutoff frequencies for the first few modes.

For $m = 1$, we find as $k_{1\rho I}a \to 0$

$$\frac{\mu\epsilon_1 + \mu_1\epsilon}{k_\rho a} \frac{J_1'(k_\rho a)}{J_1(k_\rho a)} + \frac{\mu_1\epsilon_1 + \mu\epsilon}{k_\rho^2 a^2} + 2\mu_1\epsilon_1 \ln(ik_{1\rho I}a) = 0 \quad (4.2.153)$$

Thus the cutoff frequencies are obtained from

$$J_1\left(k_{c1p}a\sqrt{1 - \frac{n_1^2}{n^2}}\right) = 0$$

which gives for HE_{1p} modes

$$k_{c1p}a\sqrt{1 - \frac{n_1^2}{n^2}} = \xi_{1p} \qquad (4.2.154)$$

where ξ_{1p} is the pth root of the first-order Bessel function $J_1(\xi)$. It is important to observe that the first root of J_1 is now zero, which was not the case for EH_{11}. Thus the cutoff frequency for the HE_{11} mode is zero. This is similar to the fundamental TE_0 and TM_0 modes with zero cutoff wavenumbers for symmetric slab waveguides. We can appreciate that as $\mu \to \mu_1$ and $\epsilon \to \epsilon_1$, the HE_{11} mode approaches a TEM wave for which there is no cutoff.

In Figure 4.2.27, we note that (i) TE_{0p} and TM_{0p} are degenerate modes in the sense that they have the same cutoff frequencies determined from (4.2.145); (ii) HE_{1p} and $EH_{1(p-1)}$ modes share the same cutoff frequencies because they are both determined from the roots of the first-order Bessel function $J_1(\xi)$, except that for HE modes the first root is taken to be zero while for EH modes the first root is taken to be 3.832; (iii) the HE_{11} frequency operating range is very wide if the radius a is taken to be small and the refractive index n is only slightly larger than that of its surrounding medium n_1. For instance, in the case of a single-mode fiber waveguide for which $a \approx 1\mu m$, $n \approx 1.05$, and $1 - n_1^2/n^2 \approx 0.09$, the single-mode operating range extends from zero to $8 \times 10^6 \, \text{m}^{-1}$ or $1.3 \times 10^6 \, \text{K}_o$.

EXAMPLE 4.2.7

We can cast (4.2.138) in a symmetric form by using the recurrence formula for Bessel functions $B_m'(\xi) = (B_{m-1}(\xi) - B_{m+1}(\xi))/2$. Making use of the dispersion relations $k_z^2 = k^2 - k_\rho^2 = k_1^2 + k_{1\rho I}^2$, we write (4.2.138) in the following form:

$$\frac{m^2 k_z^2}{k^2 k_\rho^2 a^2}\left(1 + \frac{k_\rho^2}{k_{1\rho I}^2}\right)^2 = \frac{m^2 k_\rho^2}{k^2}\left(\frac{k^2}{k_\rho^2} + \frac{k_1^2}{k_{1\rho I}^2}\right)\left(\frac{1}{k_\rho^2 a^2} + \frac{1}{k_{1\rho I}^2 a^2}\right)$$

$$= \left\{\frac{J_m'(k_\rho a)}{J_m(k_\rho a)} - p_{10}^{TE}\frac{H_m^{(1)'}(ik_{1\rho I}a)}{H_m^{(1)}(ik_{1\rho I}a)}\right\}\left\{\frac{J_m'(k_\rho a)}{J_m(k_\rho a)} - p_{10}^{TM}\frac{H_m^{(1)'}(ik_{1\rho I}a)}{H_m^{(1)}(ik_{1\rho I}a)}\right\}$$

$$= \frac{1}{4}\left\{\left[\frac{J_{m-1}(k_\rho a)}{J_m(k_\rho a)} - \frac{J_{m+1}(k_\rho a)}{J_m(k_\rho a)}\right] - p_{10}^{TE}\left[\frac{H_{m-1}^{(1)}(ik_{1\rho I}a)}{H_m^{(1)}(ik_{1\rho I}a)} - \frac{H_{m+1}^{(1)}(ik_{1\rho I}a)}{H_m^{(1)}(ik_{1\rho I}a)}\right]\right\}$$

$$\left\{\left[\frac{J_{m-1}(k_\rho a)}{J_m(k_\rho a)} - \frac{J_{m+1}(k_\rho a)}{J_m(k_\rho a)}\right] - p_{10}^{TM}\left[\frac{H_{m-1}^{(1)}(ik_{1\rho I}a)}{H_m^{(1)}(ik_{1\rho I}a)} - \frac{H_{m+1}^{(1)}(ik_{1\rho I}a)}{H_m^{(1)}(ik_{1\rho I}a)}\right]\right\}$$

$$= \frac{1}{4}\left\{\left[\frac{J_{m-1}(k_\rho a)}{J_m(k_\rho a)} - p_{10}^{TE}\frac{H_{m-1}^{(1)}(ik_{1\rho I}a)}{H_m^{(1)}(ik_{1\rho I}a)}\right]\left[\frac{J_{m-1}(k_\rho a)}{J_m(k_\rho a)} - p_{10}^{TM}\frac{H_{m-1}^{(1)}(ik_{1\rho I}a)}{H_m^{(1)}(ik_{1\rho I}a)}\right]\right.$$

$$- \left[\frac{J_{m-1}(k_\rho a)}{J_m(k_\rho a)} - p_{10}^{TE}\frac{H_{m-1}^{(1)}(ik_{1\rho I}a)}{H_m^{(1)}(ik_{1\rho I}a)}\right]\left[\frac{J_{m+1}(k_\rho a)}{J_m(k_\rho a)} - p_{10}^{TM}\frac{H_{m+1}^{(1)}(ik_{1\rho I}a)}{H_m^{(1)}(ik_{1\rho I}a)}\right]$$

$$- \left[\frac{J_{m+1}(k_\rho a)}{J_m(k_\rho a)} - p_{10}^{TE}\frac{H_{m+1}^{(1)}(ik_{1\rho I}a)}{H_m^{(1)}(ik_{1\rho I}a)}\right]\left[\frac{J_{m-1}(k_\rho a)}{J_m(k_\rho a)} - p_{10}^{TM}\frac{H_{m-1}^{(1)}(ik_{1\rho I}a)}{H_m^{(1)}(ik_{1\rho I}a)}\right]$$

$$\left. + \left[\frac{J_{m+1}(k_\rho a)}{J_m(k_\rho a)} - p_{10}^{TE}\frac{H_{m+1}^{(1)}(ik_{1\rho I}a)}{H_m^{(1)}(ik_{1\rho I}a)}\right]\left[\frac{J_{m+1}(k_\rho a)}{J_m(k_\rho a)} - p_{10}^{TM}\frac{H_{m+1}^{(1)}(ik_{1\rho I}a)}{H_m^{(1)}(ik_{1\rho I}a)}\right]\right\}$$

On account of the recurrence relation $B_{m-1}(\xi) + B_{m+1}(\xi) = 2mB_m(\xi)/\xi$, the above equation becomes

$$\frac{m^2 k_\rho^2}{k^2}\left(\frac{k^2}{k_\rho^2} + \frac{k_1^2}{k_{1\rho I}^2}\right)\left(\frac{1}{k_\rho^2 a^2} + \frac{1}{k_{1\rho I}^2 a^2}\right)$$

$$= \frac{1}{4}\left\{\left[\frac{J_{m-1}(k_\rho a)}{J_m(k_\rho a)} - p_{10}^{TE}\frac{H_{m-1}^{(1)}(ik_{1\rho I}a)}{H_m^{(1)}(ik_{1\rho I}a)}\right]\left[\frac{2m}{k_\rho a} - p_{10}^{TM}\frac{2m}{ik_{1\rho I}a}\right]\right.$$

$$- 2\left[\frac{J_{m-1}(k_\rho a)}{J_m(k_\rho a)} - p_{10}^{TE}\frac{H_{m-1}^{(1)}(ik_{1\rho I}a)}{H_m^{(1)}(ik_{1\rho I}a)}\right]\left[\frac{J_{m+1}(k_\rho a)}{J_m(k_\rho a)} - p_{10}^{TM}\frac{H_{m+1}^{(1)}(ik_{1\rho I}a)}{H_m^{(1)}(ik_{1\rho I}a)}\right]$$

$$- 2\left[\frac{J_{m+1}(k_\rho a)}{J_m(k_\rho a)} - p_{10}^{TE}\frac{H_{m+1}^{(1)}(ik_{1\rho I}a)}{H_m^{(1)}(ik_{1\rho I}a)}\right]\left[\frac{J_{m-1}(k_\rho a)}{J_m(k_\rho a)} - p_{10}^{TM}\frac{H_{m-1}^{(1)}(ik_{1\rho I}a)}{H_m^{(1)}(ik_{1\rho I}a)}\right]$$

$$\left. + \left[\frac{J_{m+1}(k_\rho a)}{J_m(k_\rho a)} - p_{10}^{TE}\frac{H_{m+1}^{(1)}(ik_{1\rho I}a)}{H_m^{(1)}(ik_{1\rho I}a)}\right]\left[\frac{2m}{k_\rho a} - p_{10}^{TM}\frac{2m}{ik_{1\rho I}a}\right]\right\}$$

$$= \frac{1}{2}\left\{2\left[\frac{m}{k_\rho a} - p_{10}^{TE}\frac{m}{ik_{1\rho I}a}\right]\left[\frac{m}{k_\rho a} - p_{10}^{TM}\frac{m}{ik_{1\rho I}a}\right]\right.$$

$$-\left[\frac{J_{m-1}(k_\rho a)}{J_m(k_\rho a)} - p_{10}^{TE}\frac{H_{m-1}^{(1)}(ik_{1\rho I}a)}{H_m^{(1)}(ik_{1\rho I}a)}\right]\left[\frac{J_{m+1}(k_\rho a)}{J_m(k_\rho a)} - p_{10}^{TM}\frac{H_{m+1}^{(1)}(ik_{1\rho I}a)}{H_m^{(1)}(ik_{1\rho I}a)}\right]$$

$$-\left[\frac{J_{m+1}(k_\rho a)}{J_m(k_\rho a)} - p_{10}^{TE}\frac{H_{m+1}^{(1)}(ik_{1\rho I}a)}{H_m^{(1)}(ik_{1\rho I}a)}\right]\left[\frac{J_{m-1}(k_\rho a)}{J_m(k_\rho a)} - p_{10}^{TM}\frac{H_{m-1}^{(1)}(ik_{1\rho I}a)}{H_m^{(1)}(ik_{1\rho I}a)}\right]\Bigg\}$$

which gives

$$\left[\frac{J_{m-1}(k_\rho a)}{J_m(k_\rho a)} - p_{10}^{TE}\frac{H_{m-1}^{(1)}(ik_{1\rho I}a)}{H_m^{(1)}(ik_{1\rho I}a)}\right]\left[\frac{J_{m+1}(k_\rho a)}{J_m(k_\rho a)} - p_{10}^{TM}\frac{H_{m+1}^{(1)}(ik_{1\rho I}a)}{H_m^{(1)}(ik_{1\rho I}a)}\right]$$

$$+\left[\frac{J_{m+1}(k_\rho a)}{J_m(k_\rho a)} - p_{10}^{TE}\frac{H_{m+1}^{(1)}(ik_{1\rho I}a)}{H_m^{(1)}(ik_{1\rho I}a)}\right]\left[\frac{J_{m-1}(k_\rho a)}{J_m(k_\rho a)} - p_{10}^{TM}\frac{H_{m-1}^{(1)}(ik_{1\rho I}a)}{H_m^{(1)}(ik_{1\rho I}a)}\right]$$

$$+2\left(1 - \frac{\mu_1}{\mu}\right)\left(1 - \frac{\epsilon_1}{\epsilon}\right)\frac{m^2}{k_{1\rho I}^2 a^2} = 0 \qquad\qquad \text{(E4.2.7.1)}$$

As $k_{1\rho I} \to 0$, we make use of the approximations

$$\frac{H_{m+1}^{(1)}(ik_{1\rho I}a)}{H_m^{(1)}(ik_{1\rho I}a)} \sim \frac{2m}{ik_{1\rho I}a}; \quad \frac{H_{m-1}^{(1)}(ik_{1\rho I}a)}{H_m^{(1)}(ik_{1\rho I}a)} \sim A_m$$

where $A_1 = -ik_{1\rho I}a\ln(ik_{1\rho I}a)$ and $A_m = ik_{1\rho I}a/2(m-1)$ for $m > 1$. Under the approximation of $k_{1\rho I} \to 0$, the term $J_{m+1}(k_\rho a)/J_m(k_\rho a)$ can be neglected, and Eq. (E4.2.7.1) becomes

$$(\frac{\mu_1}{\mu} + \frac{\epsilon_1}{\epsilon})k_\rho a\frac{J_{m-1}(k_\rho a)}{J_m(k_\rho a)} - \frac{\mu_1\epsilon_1}{\mu\epsilon}\frac{2A_m}{ik_{1\rho I}a} + m(1-\frac{\mu_1}{\mu})(1-\frac{\epsilon_1}{\epsilon}) = 0$$

$$\text{(E4.2.7.2)}$$

As $k_\rho \to 0$, we make use of the approximation $J_{m-1}(k_\rho a)/J_m(k_\rho a) \sim 2m/k_\rho a$, Eq. (E4.2.7.2) becomes, for $m > 1$

$$\frac{m}{k_{1\rho I}^2 a^2}\left[m(1 + \frac{\mu_1}{\mu})(1 + \frac{\epsilon_1}{\epsilon}) - \frac{\mu_1\epsilon_1}{\mu\epsilon}\frac{k_\rho^2 a^2}{m-1}\right] = 0 \qquad \text{(E4.2.7.3)}$$

It is seen that $k_\rho = 0$ is not an acceptable solution. For $m = 1$, (E4.2.7.2) becomes,

$$\frac{1}{k_{1\rho I}^2 a^2}\left[(1 + \frac{\mu_1}{\mu})(1 + \frac{\epsilon_1}{\epsilon}) + \frac{2\mu_1\epsilon_1}{\mu\epsilon}k_\rho^2 a^2\ln(ik_{1\rho I}a)\right] = 0 \quad \text{(E4.2.7.4)}$$

It is seen that $k_\rho = 0$ is now an acceptable solution as $k_{1\rho I} \to 0$.

For $k_\rho \neq 0$ and as $k_{1\rho I} \to 0$, Eq. (E4.2.7.2) becomes, for $m > 1$,

$$(\frac{\mu_1}{\mu} + \frac{\epsilon_1}{\epsilon})k_\rho a \frac{J_{m-1}(k_\rho a)}{J_m(k_\rho a)} - \frac{\mu_1 \epsilon_1}{\mu \epsilon} \frac{k_\rho^2 a^2}{m-1} + m(1 - \frac{\mu_1}{\mu})(1 - \frac{\epsilon_1}{\epsilon}) = 0$$

which is equivalent to (4.2.152) after making use of recurrence formula $J_{m-1}(\xi) = J_m'(\xi) + mJ_m(\xi)/\xi$. For $m = 1$,

$$(\frac{\mu_1}{\mu} + \frac{\epsilon_1}{\epsilon})k_\rho a \frac{J_0(k_\rho a)}{J_1(k_\rho a)} + 2\frac{\mu_1 \epsilon_1}{\mu \epsilon}k_\rho^2 a^2 \ln(ik_{1\rho I}a) + (1 - \frac{\mu_1}{\mu})(1 - \frac{\epsilon_1}{\epsilon}) = 0$$

which is equivalent to (4.2.153).

$-$ End of Example 4.2.7 $-$

EXAMPLE 4.2.8

Consider an optical fiber with radius a and $\mu = \mu_1$. The cutoff frequencies of EH modes are obtained from (4.2.150). Let $k_{\rho c}a = k_{cmp}a\sqrt{1 - n_1^2/n^2}$. We find, for $m \geq 1$ and $k_{\rho c} \neq 0$,

$$J_m(k_{\rho c}a) = 0$$

The cutoff frequencies of HE modes are obtained, after making use of the recurrence formula $J_m(k_\rho a) = 2(m-1)J_{m-1}(k_\rho a)/k_\rho a - J_{m-2}(k_\rho a)$, we find, for $m > 1$,

$$J_{m-2}(k_{\rho c}a) = 0$$

Assume $\epsilon/\epsilon_1 \approx 1$, we use (E4.2.7.1) to approximate the guidance condition

$$\frac{J_{m+1}(k_\rho a)}{k_\rho J_m(k_\rho a)} \approx \frac{H_{m+1}^{(1)}(ik_{1\rho I}a)}{ik_{1\rho I}H_m^{(1)}(ik_{1\rho I}a)} \quad \text{for EH modes} \quad \text{(E4.2.8.1)}$$

$$\frac{J_{m-1}(k_\rho a)}{k_\rho J_m(k_\rho a)} \approx \frac{H_{m-1}^{(1)}(ik_{1\rho I}a)}{ik_{1\rho I}H_m^{(1)}(ik_{1\rho I}a)} \quad \text{for HE modes} \quad \text{(E4.2.8.2)}$$

As $k_{1\rho I}a \gg 0$,

$$H_m^{(1)}(ik_{1\rho I}a) \approx \sqrt{\frac{2}{i\pi k_{1\rho I}a}}e^{-im\pi/2 - i\pi/4}e^{-k_{1\rho I}a}$$

$$\frac{H_{m+1}^{(1)}(ik_{1\rho I}a)}{ik_{1\rho I}H_m^{(1)}(ik_{1\rho I}a)} \approx \mp i$$

Equations (E4.2.8.1) and (E4.2.8.2) become

$$k_{1\rho I} a J_{m+1}(k_\rho a) \approx -k_\rho a J_m(k_\rho a) \qquad \text{for EH modes} \qquad \text{(E4.2.8.3)}$$
$$k_{1\rho I} a J_{m-1}(k_\rho a) \approx k_\rho a J_m(k_\rho a) \qquad \text{for HE modes} \qquad \text{(E4.2.8.4)}$$

Far away from cutoff, $k_{1\rho I} a \to \infty$ and $k \to \infty$, we find

$$J_{m+1}(k_\rho a) = 0 \qquad \text{for EH modes} \qquad \text{(E4.2.8.5)}$$
$$J_{m-1}(k_\rho a) = 0 \qquad \text{for HE modes} \qquad \text{(E4.2.8.6)}$$

From (4.2.136),

$$\frac{ik_z m}{a} B J_m(k_\rho a) \left[\frac{1}{k_\rho^2} + \frac{1}{k_{1\rho I}^2} \right] = i\omega A \left[\frac{\epsilon}{k_\rho} (J_{m-1}(k_\rho a) - \frac{m}{k_\rho a} J_m(k_\rho a)) \right.$$

$$\left. + i\frac{\epsilon_1}{k_{1\rho I}} \frac{J_m(k_\rho a)}{H_m^{(1)}(ik_{1\rho I} a)} (H_{m-1}^{(1)}(ik_{1\rho I} a) - \frac{m}{ik_{1\rho I} a} H_m^{(1)}(ik_{1\rho I} a)) \right]$$

$$= i\omega A \left[\frac{\epsilon}{k_{1\rho I}} + i\frac{\epsilon_1}{k_{1\rho I}} \frac{H_{m-1}^{(1)}(ik_{1\rho I} a)}{H_m^{(1)}(ik_{1\rho I} a)} - \left(\frac{m\epsilon}{k_\rho^2 a} + \frac{m\epsilon_1}{k_{1\rho I} a} \right) \right] J_m(k_\rho a)$$

$$\approx -i\omega\epsilon A \left[\frac{m}{k_\rho^2 a} + \frac{m}{k_{1\rho I}^2 a} \right] J_m(k_\rho a)$$

$$B \approx \pm\frac{\omega\epsilon}{k_z} \approx \pm\sqrt{\frac{\epsilon}{\mu}} A \qquad \begin{cases} \text{EH} & \text{modes} \\ \text{HE} & \text{modes} \end{cases}$$

The field components inside the fiber are

$$E_z = A J_m(k_\rho \rho) \sin m\phi \, e^{ik_z z}$$

$$H_z = B J_m(k_\rho \rho) \cos m\phi \, e^{ik_z z} \approx \pm\sqrt{\frac{\epsilon}{\mu}} \, A J_m(k_\rho \rho) \cos m\phi \, e^{ik_z z}$$

$$E_\rho = \frac{1}{k_\rho^2} \left[A ik_z k_\rho J_m'(k_\rho \rho) \sin m\phi - B \frac{i\omega\mu m}{\rho} J_m(k_\rho \rho) \sin m\phi \right] e^{ik_z z}$$

$$= \frac{ikA}{k_\rho} \left[J_m'(k_\rho \rho) \mp \frac{m}{k_\rho \rho} J_m(k_\rho \rho) \right] \sin m\phi \, e^{ik_z z}$$

$$= \mp \frac{ikA}{k_\rho} \left[J_{m\pm 1}(k_\rho \rho) \right] \sin m\phi \, e^{ik_z z}$$

$$E_\phi = \frac{1}{k_\rho^2} \left[A ik_z \frac{m}{\rho} J_m(k_\rho \rho) \cos m\phi - B i\omega\mu k_\rho J_m'(k_\rho \rho) \cos m\phi \right] e^{ik_z z}$$

$$= \frac{ikA}{k_\rho} \left[\frac{m}{k_\rho \rho} J_m(k_\rho \rho) \mp J'_m(k_\rho \rho) \right] \cos m\phi e^{ik_z z}$$

$$= \frac{ikA}{k_\rho} \left[J_{m\pm1}(k_\rho \rho) \right] \cos m\phi e^{ik_z z}$$

$$H_\rho = \frac{1}{k_\rho^2} \left[Bik_z k_\rho J'_m(k_\rho \rho) \cos m\phi - A\frac{i\omega\epsilon m}{\rho} J_m(k_\rho \rho) \cos m\phi \right] e^{ik_z z}$$

$$= \frac{ikA}{k_\rho} \sqrt{\frac{\epsilon}{\mu}} \left[\pm J'_m(k_\rho \rho) - \frac{m}{k_\rho \rho} J_m(k_\rho \rho) \right] \cos m\phi e^{ik_z z}$$

$$= -\frac{ikA}{k_\rho} \sqrt{\frac{\epsilon}{\mu}} \left[J_{m\pm1}(k_\rho \rho) \right] \cos m\phi e^{ik_z z}$$

$$H_\phi = \frac{1}{k_\rho^2} \left[-B\frac{ik_z m}{\rho} J_m(k_\rho \rho) \sin m\phi + Ai\omega\epsilon k_\rho J'_m(k_\rho \rho) \sin m\phi \right] e^{ik_z z}$$

$$= \frac{ikA}{k_\rho} \sqrt{\frac{\epsilon}{\mu}} \left[\mp\frac{m}{k_\rho \rho} J_m(k_\rho \rho) + J'_m(k_\rho \rho) \right] \sin m\phi e^{ik_z z}$$

$$= \mp\frac{ikA}{k_\rho} \sqrt{\frac{\epsilon}{\mu}} \left[J_{m\pm1}(k_\rho \rho) \right] \sin m\phi e^{ik_z z}$$

The amplitudes C and D are related to A as

$$C = A\frac{J_m(k_\rho a)}{H_m^{(1)}(ik_{1\rho I}a)}$$

$$D = B\frac{J_m(k_\rho a)}{H_m^{(1)}(ik_{1\rho I}a)} \approx \pm\sqrt{\frac{\epsilon}{\mu}} A\frac{J_m(k_\rho a)}{H_m^{(1)}(ik_{1\rho I}a)}$$

The field components outside the fiber are, after making use of (E4.2.8.3) and (E4.2.8.4) with

$$J_m(k_\rho a) \approx \mp k_{1\rho I}aJ_{m\pm1}(k_\rho a)/k_\rho a \qquad \begin{cases} \text{EH} & \text{modes} \\ \text{HE} & \text{modes} \end{cases}$$

$$E_z = CH_m^{(1)}(ik_{1\rho I}\rho) \sin m\phi e^{ik_z z} \approx AJ_m(k_\rho a)e^{-k_{1\rho I}(\rho-a)} \sin m\phi e^{ik_z z}$$

$$H_z = DH_m^{(1)}(ik_{1\rho I}\rho) \cos m\phi e^{ik_z z} \approx \pm\sqrt{\frac{\epsilon}{\mu}} AJ_m(k_\rho a)e^{-k_{1\rho I}(\rho-a)} \cos m\phi e^{ik_z z}$$

$$E_\rho = \frac{-1}{k_{1\rho I}^2} \left[-Ck_z k_{1\rho I} H_m^{(1)\prime}(ik_{1\rho I}\rho) \sin m\phi - D\frac{i\omega\mu_1 m}{\rho} H_m^{(1)}(ik_{1\rho I}\rho) \sin m\phi \right] e^{ik_z z}$$

$$= \frac{kA}{k_{1\rho I}} \left[H_m^{(1)\prime}(ik_{1\rho I}\rho) \pm \frac{im}{k_{1\rho I}\rho} H_m^{(1)}(ik_{1\rho I}\rho) \right] \frac{J_m(k_\rho a)}{H_m^{(1)}(ik_{1\rho I}a)} \sin m\phi e^{ik_z z}$$

$$= \frac{kA}{k_{1\rho I}} \left[\mp H_{m\pm 1}^{(1)}(ik_{1\rho I}\rho) \right] \frac{J_m(k_\rho a)}{H_m^{(1)}(ik_{1\rho I}a)} \sin m\phi e^{ik_z z}$$

$$= \mp \frac{ikA}{k_\rho} \sqrt{\frac{a}{\rho}} J_{m\pm 1}(k_\rho a) e^{-k_{1\rho I}(\rho - a)} \sin m\phi e^{ik_z z}$$

$$E_\phi = \frac{-1}{k_{1\rho I}^2} \left[C \frac{ik_z m}{\rho} H_m^{(1)}(ik_{1\rho I}\rho) \cos m\phi + D\omega\mu_1 k_{1\rho I} H_m^{(1)\prime}(ik_{1\rho I}\rho) \cos m\phi \right] e^{ik_z z}$$

$$= \frac{-kA}{k_{1\rho I}^2} \left[\frac{im}{\rho} H_m^{(1)}(ik_{1\rho I}\rho) \pm k_{1\rho I} H_m^{(1)\prime}(ik_{1\rho I}\rho) \right] \frac{J_m(k_\rho a)}{H_m^{(1)}(ik_{1\rho I}a)} \cos m\phi e^{ik_z z}$$

$$= \frac{-kA}{k_{1\rho I}} \left[-H_{m\pm 1}^{(1)}(ik_{1\rho I}\rho) \right] \frac{J_m(k_\rho a)}{H_m^{(1)}(ik_{1\rho I}a)} \cos m\phi e^{ik_z z}$$

$$= \frac{ikA}{k_\rho} \sqrt{\frac{a}{\rho}} J_{m\pm 1}(k_\rho a) e^{-k_{1\rho I}(\rho - a)\cos m\phi e^{ik_z z}}$$

$$H_\rho = \frac{-1}{k_{1\rho I}^2} \left[-Dk_z k_{1\rho I} H_m^{(1)\prime}(ik_{1\rho I}\rho) \cos m\phi - C \frac{i\omega\epsilon_1 m}{\rho} H_m^{(1)}(ik_{1\rho I}\rho) \cos m\phi \right] e^{ik_z z}$$

$$= \frac{kA}{k_{1\rho I}^2} \sqrt{\frac{\epsilon}{\mu}} \left[\pm k_{1\rho I} H_m^{(1)\prime}(ik_{1\rho I}\rho) + \frac{im}{\rho} H_m^{(1)}(ik_{1\rho I}\rho) \right] \frac{J_m(k_\rho a)}{H_m^{(1)}(ik_{1\rho I}a)} \cos m\phi e^{ik_z z}$$

$$= \frac{kA}{k_{1\rho I}} \sqrt{\frac{\epsilon}{\mu}} \left[-H_{m\pm 1}^{(1)}(ik_{1\rho I}\rho) \right] \frac{J_m(k_\rho a)}{H_m^{(1)}(ik_{1\rho I}a)} \cos m\phi e^{ik_z z}$$

$$= -\frac{kA}{k_\rho} \sqrt{\frac{\epsilon a}{\mu\rho}} J_{m\pm 1}(k_\rho a) e^{-k_{1\rho I}(\rho - a)} \cos m\phi e^{ik_z z}$$

$$H_\phi = \frac{-1}{k_{1\rho I}^2} \left[-D \frac{ik_z m}{\rho} H_m^{(1)}(ik_{1\rho I}\rho) \sin m\phi - C\omega\epsilon_1 k_{1\rho I} H_m^{(1)\prime}(ik_{1\rho I}\rho) \sin m\phi \right] e^{ik_z z}$$

$$= \frac{kA}{k_{1\rho I}^2} \sqrt{\frac{\epsilon}{\mu}} \left[\pm \frac{im}{\rho} H_m^{(1)}(ik_{1\rho I}\rho) + k_{1\rho I} H_m^{(1)\prime}(ik_{1\rho I}\rho) \right] \frac{J_m(k_\rho a)}{H_m^{(1)}(ik_{1\rho I}a)} \sin m\phi e^{ik_z z}$$

$$= \frac{kA}{k_{1\rho I}} \sqrt{\frac{\epsilon}{\mu}} \left[\mp H_{m\pm 1}^{(1)}(ik_{1\rho I}\rho) \right] \frac{J_m(k_\rho a)}{H_m^{(1)}(ik_{1\rho I}a)} \sin m\phi e^{ik_z z}$$

$$= \mp \frac{ikA}{k_{1\rho I}} \sqrt{\frac{\epsilon a}{\mu\rho}} J_{m\pm 1}(k_\rho a) e^{-k_{1\rho I}(\rho - a)} \sin m\phi e^{ik_z z}$$

In terms of x and y components, we have

for $\rho \le a$,

$$E_y = E_\rho \sin\phi + E_\phi \cos\phi = \frac{ikA}{k_\rho} [J_{m\pm 1}(k_\rho\rho)] [\cos(m\pm 1)\phi] e^{ik_z z}$$

$$E_x = E_\rho \cos\phi - E_\phi \sin\phi = -\frac{ikA}{k_\rho} [J_{m\pm 1}(k_\rho\rho)] [\sin(m\pm 1)\phi] e^{ik_z z}$$

$$H_y = H_\rho \sin\phi + H_\phi \cos\phi = -\frac{ikA}{k_\rho}\sqrt{\frac{\epsilon}{\mu}}\,[J_{m\pm1}(k_\rho\rho)]\,[\sin(m\pm1)\phi]e^{ik_z z}$$

$$H_x = H_\rho \cos\phi - H_\phi \sin\phi = -\frac{ikA}{k_\rho}\sqrt{\frac{\epsilon}{\mu}}\,[J_{m\pm1}(k_\rho\rho)]\,[\cos(m\pm1)\phi]e^{ik_z z}$$

for $\rho \geq a$,

$$E_y = E_\rho \sin\phi + E_\phi \cos\phi = \frac{ikA}{k_\rho}\,[J_{m\pm1}(k_\rho\rho)]\,e^{-k_{1\rho I}(\rho-a)}[\cos(m\pm1)\phi]e^{ik_z z}$$

$$E_x = E_\rho \cos\phi - E_\phi \sin\phi = -\frac{ikA}{k_\rho}\,[J_{m\pm1}(k_\rho\rho)]\,e^{-k_{1\rho I}(\rho-a)}[\sin(m\pm1)\phi]e^{ik_z z}$$

$$H_y = H_\rho \sin\phi + H_\phi \cos\phi = -\frac{ikA}{k_\rho}\sqrt{\frac{\epsilon}{\mu}}\,[J_{m\pm1}(k_\rho\rho)]e^{-k_{1\rho I}(\rho-a)}[\sin(m\pm1)\phi]e^{ik_z z}$$

$$H_x = H_\rho \cos\phi - H_\phi \sin\phi = \frac{ikA}{k_\rho}\sqrt{\frac{\epsilon}{\mu}}[J_{m\pm1}(k_\rho\rho)]e^{-k_{1\rho I}(\rho-a)}[\cos(m\pm1)\phi]e^{ik_z z}$$

It is seen that the x and y components of the electric and magnetic fields are related by the the impedance $\sqrt{\mu/\epsilon}$. The amplitudes of E_z and H_z are vanishingly small as $k_\rho \to 0$.

— END OF EXAMPLE 4.2.8 —

EXAMPLE 4.2.9

To determine the field components of the HE_{11} for the optical fiber studied above, we find

for $\rho \leq a$,

$$E_y = E_\rho \sin\phi + E_\phi \cos\phi = \frac{ikA}{k_\rho}\,[J_0(k_\rho\rho)]\,e^{ik_z z}$$

$$E_x = E_\rho \cos\phi - E_\phi \sin\phi = 0$$

$$H_y = H_\rho \sin\phi + H_\phi \cos\phi = 0$$

$$H_x = H_\rho \cos\phi - H_\phi \sin\phi = -\frac{ikA}{k_\rho}\sqrt{\frac{\epsilon}{\mu}}\,[J_0(k_\rho\rho)]\,e^{ik_z z}$$

for $\rho \geq a$,

$$E_y = E_\rho \sin\phi + E_\phi \cos\phi = \frac{ikA}{k_\rho}\,[J_0(k_\rho\rho)]\,e^{-k_{1\rho I}(\rho-a)}e^{ik_z z}$$

$$E_x = E_\rho \cos\phi - E_\phi \sin\phi = 0$$

$$H_y = H_\rho \sin\phi + H_\phi \cos\phi = 0$$

$$H_x = H_\rho \cos\phi - H_\phi \sin\phi = -\frac{ikA}{k_\rho}\sqrt{\frac{\epsilon}{\mu}}\,[J_0(k_\rho\rho)]\,e^{-k_{1\rho I}(\rho-a)}\phi e^{ik_z z}$$

We see that the field in the fiber approximate a plane wave with $\omega\epsilon/k_z$ relating the electric and magnetic field components. Similar relations can be derived for the field components external to the fiber and characterized by the zeroth order Hankel function of the first kind with imaginary arguments.

— END OF EXAMPLE 4.2.9 —

EXAMPLE 4.2.10

Power series solution of Bessel equation (4.2.107) takes the form

$$B(\xi) = \xi^\alpha \sum_{m=1}^\infty a_m \xi^m = \left(\frac{\xi}{2}\right)^\alpha \sum_{m=1}^\infty a_m \xi^m \frac{(-1)^m}{m!\Gamma(m+\alpha+1)} \left(\frac{\xi}{2}\right)^{2m}$$

(E4.2.10.1)

where $\alpha = \pm\nu$, and the Gamma function

$$\Gamma(p) = \int_0^\infty dx \; x^{p-1} e^{-x}$$

(E4.2.10.2)

When $p = m + 1$ with m an integer, we see that $\Gamma(m+1) = m!$. The two independent solutions of (4.2.107) are the Bessel function $J_\nu(\xi)$ and the Neumann function $N_\nu(\xi)$.

$$J_\nu(\xi) = \sum_{m=0}^\infty \frac{(-1)^m}{m!\Gamma(m+\nu+1)} \left(\frac{\xi}{2}\right)^{2m+\nu}$$

(E4.2.10.3)

$$N_\nu(\xi) = \frac{J_\nu(\xi)\cos\nu\pi - J_{-\nu}(\xi)}{\sin\nu\pi}$$

(E4.2.10.4)

Notice that when $\nu = n$ is an integer, $J_{-n}(\xi) = (-1)^n J_n(\xi)$.

— END OF EXAMPLE 4.2.10 —

EXAMPLE 4.2.11   Phase and group velocity.

Below the cutoff frequency for the mth mode, $k_z = ik_{zI}$ and (4.2.7) give

$$k_{zI}^2 + k^2 = \left(\frac{m\pi}{d}\right)^2$$

Above the cutoff frequency, the phase velocity v_p along the $\hat{z}$ direction is

$$v_p = \frac{\omega}{k_z} = \frac{1}{\sqrt{\mu\epsilon}} \left[1 - \left(\frac{k_{cm}}{k}\right)^2\right]^{-1/2}$$

As the frequency goes to infinity, v_p approaches the velocity of light in the medium. For finite ω, the phase velocity is always larger than $(\mu\epsilon)^{-1/2}$. This is because k_z is always smaller than k. The fact that the phase velocity depends on frequency makes the waveguide a dispersive transmission system. The group velocity of propagation is

$$v_g = \left(\frac{\partial k_z}{\partial \omega}\right)^{-1} = \frac{1}{\sqrt{\mu\epsilon}}\left[1 - \left(\frac{k_{cm}}{k}\right)^2\right]^{1/2}$$

Thus $v_p v_g = 1/\mu\epsilon$. The group velocity is always smaller than the velocity of light inside the medium.

— END OF EXAMPLE 4.2.11 —

Problems

P4.2.1

Consider a perfectly conducting parallel-plate waveguide with the plates (separated by d) parallel to the y-z plane. The waveguide is filled with a plasma medium with the plasma frequency ω_p and permeability μ_o. The permittivity of the plasma medium is $\epsilon = \epsilon_o\left(1 - \omega_p^2/\omega^2\right)$. Let a Hertzian dipole pointing in the $\hat{z}$ direction be placed in the waveguide. Assume that the Hertzian dipole can excite all the modes in the waveguide.
(a) In the absence of the parallel-plate waveguide, sketch the radiation pattern of the Hertzian dipole on the x-y plane in free space.
(b) What is the polarization of the electric field on the x-y plane in the waveguide?
(c) Let $\omega = \sqrt{2}\omega_p$. Find the range of the separation d in terms of the wavelength in free space λ_o, where $\lambda_o = 2\pi/k_o = 2\pi/\omega\sqrt{\mu_o\epsilon_o}$, so that there is ONLY ONE mode propagating in the parallel-plate waveguide. What is this mode (indicate TE or TM, and the mode number m)?

P4.2.2

Consider a perfectly conducting parallel-plate waveguide filled with a dielectric medium for $z > 0$ as shown in Fig. P4.2.2.1. The dielectric medium has permittivity ϵ_1. The operating frequency is $30/2\pi$ GHz. The guided wave propagates in the $\hat{z}$ direction.
(a) Let $d = 2\sqrt{3}\pi$ cm and consider the empty waveguide with $\epsilon_1 = \epsilon_0$ (in the absence of the dielectric). Which TE_m and TM_m modes can propagate in this waveguide.
(b) Find expressions for the $\overline{E}$ and $\overline{H}$ fields for the TM_2 mode in the absence of the dielectric.
(c) What are the phase and group velocities for the TM_2 mode at this operating frequency in the absence of the dielectric?
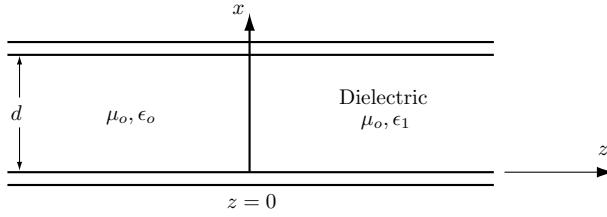
Figure P4.2.2.1 Parallel-plate waveguide.

(d) Let $\epsilon_1 = 3\epsilon_0$ and $d = 2\sqrt{3}\pi$ cm. For waves propagating in the $+\hat{z}$ direction, for which values of m will the TM$_m$ modes be totally reflected at the dielectric boundary? Why?

(e) For which value of m will a propagating TM$_m$ mode be totally transmitted (no reflection) and why?

P4.2.3

Consider a perfectly conducting parallel-plate waveguide, which is filled with air for $z < 0$ and filled with a dielectric medium of permittivity ϵ_1 for $z > 0$. Let $d = 1$ cm and $\epsilon_1 = 4\epsilon_o$. The waveguide is excited at $f = 20$ GHz. Waves are guided in $\pm\hat{z}$ directions.

(a) List all possible propagating modes of TE and TM waves for $z < 0$ and $z > 0$.

(b) If the incident wave comes from $z < 0$, what is the reflection coefficient for TE$_1$ mode at the boundary $z = 0$?

(c) If the dielectric medium (ϵ_1) is replaced by a perfect conducting medium, find the total field $\overline{E}$ for TE$_1$ mode for $z < 0$.

P4.2.4

Consider the excitation of a parallel-plate waveguide by a current sheet

$$\overline{J}_s = \hat{x}J_s \cos\frac{3\pi x}{d}$$

Find the amplitudes of the excited modes.

P4.2.5

Determine the electric field solution for the asymmetric slab waveguide and find its cutoff spatial frequency.

P4.2.6

A parallel-plate waveguide is excited by a line source placed at a distance h from the bottom plate. Write the fields produced by this source inside the waveguide as a superposition of the guided modes, and determine their mode amplitudes.

P4.2.7
A rectangular waveguide is excited by a probe at the position $x = d$, $z = 0$.
Assume that the probe extends from $y = 0$ to $y = b$, and approximate the
current on the probe by

$$J(x, y, z) = I_0 \delta(x - d)\, \delta(z) \cos qy$$

What are the mode amplitudes that are excited by this probe? To achieve
maximum excitation for the TE_{10} mode, where should the probe be placed?

P4.2.8
In an air-filled rectangular waveguide with dimensions $a = 3\sqrt{2}\,\text{cm}$ and
$b = a/2$, the guided wave is given by

$$\overline{E} = \hat{y}E_o \sin\left(\frac{\pi}{a}x\right) \sin\left(\frac{\pi}{a}z - \omega t\right)$$

$$\overline{H} = \hat{x}H_o \sin\left(\frac{\pi}{a}x\right) \sin\left(\frac{\pi}{a}z - \omega t\right) + \hat{z}H_o \cos\left(\frac{\pi}{a}x\right) \cos\left(\frac{\pi}{a}z - \omega t\right)$$

where E_o and H_o are real constants.
(a) What is the mode for this wave? Indicate TE_{mn} or TM_{mn} and the
mode numbers m and n.
(b) Show that the frequency is $f = 5\,\text{GHz}$.
(c) What is the phase velocity in $\hat{z}$ direction in terms of the light speed c?
(d) What is the cutoff frequency of this mode?
(e) If the waveguide is used as a rectangular cavity resonator for frequency
$f = 5\,\text{GHz}$ by closing the ends at $z = 0$ and $z = d$ using perfectly
conducting plates, what is the value of d for the lowest mode? Indicate
this lowest mode (TE_{mnp} or TM_{mnp}) and the mode numbers m, n and
p. (Hint: d can be larger than a and b.)

P4.2.9
Consider a rectangular waveguide with dimensions $1\,\text{cm} \times 0.5\,\text{cm}$.
(a) What are the cutoff frequencies for the first five modes?
(b) If the waveguide is excited at 20 GHz, what are the propagation constants
k_z for the first five modes?
(c) If the waveguide is excited at 50 GHz, how many modes will propagate?

P4.2.10
    Consider a coaxial line with inner radius a and outer radius b. Assume
that $b = a(1 + \delta)$ and $\delta \ll 1$. The fundamental mode in this waveguide
is TEM, which has zero cutoff wavenumber. What are the cutoff wavenum-
bers for the higher-order modes? Rigorously this requires the solution of the
boundary value problem in cylindrical coordinates. The exact solution will
involve Bessel and Neumann functions. However, the question can be an-
swered by observing that, when δ is very small, the guiding space can be
modeled as that between two parallel plates with $x = \rho\phi$ and y from a
to b. Notice that $x = 2\pi a \approx 2\pi b$ and that the fields must be the same at
$x = 0$. Thus there is a periodic variation in the $\hat{x}$ direction. Using this model,

show that the cutoff wavenumber of the next higher order mode is $k_c \approx 1/a$. Note the similarity to the cutoff wavenumber for the TE_{20} mode in a rectangular waveguide with width $2\pi a$ and height δa. Confirm the answer by evaluating the cutoff wavenumber from the guidance condition. Note that the cutoff wavenumber for TE_1 and TM_1 modes in a parallel-plate waveguide is $k_c = \pi/\delta a$, which is much larger than $1/a$.
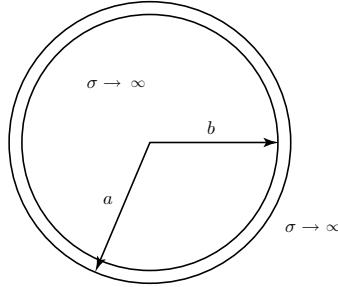
Figure P4.2.10.1 Coaxial cable.

(a) State the first three modes in the increasing cutoff frequencies by using the mode designation convention in rectangular waveguides.
(b) Determine these cutoff frequencies.

P4.2.11

In a fiberglass waveguide having a center core with a radius of the order of $1\,\mu m$ and cladding with a radius of the order of $100\,\mu m$, the HE_{11} mode operating range can be extended to the visible range if the refractive indices $n = c\sqrt{\mu\epsilon}$ and $n_1 = c\sqrt{\mu_1\epsilon_1}$ are also very close. Because the cladding is very thick in comparison to the core, the wave guidance by an optical fiber can be treated with the dielectric waveguide model. Find the value of $(n^2 - n_1^2)^{1/2}$, called the *numerical aperture*, so that the cutoff frequency for the next higher-order mode will be 6×10^{14} Hz. When fiberglass is used as the transmission medium in communications, it provides not only large bandwidth and channel capacity but also physical compactness and flexibility. Compare the result with the slab and with the metallic waveguides.

4.3   Resonance

A. Rectangular Cavity Resonator

A resonator with uniform cross section in the $\hat{z}$ direction can be viewed as a waveguide with both ends closed. Instead of guided waves propagating along the z axis, the waves are standing in the $\hat{z}$ direction. The standing wave can be viewed as a superposition of a guided wave in the $+\hat{z}$ direction and a guided wave in the $-\hat{z}$ direction. The formulation for waveguides is also applicable to resonators. We have

$$\overline{E}_s = \frac{1}{k^2 - k_z^2}\left[\nabla_s\frac{\partial}{\partial z}E_z + i\omega\mu\nabla_s \times \overline{H}_z\right] \qquad (4.3.1a)$$

$$\overline{H}_s = \frac{1}{k^2 - k_z^2}\left[\nabla_s\frac{\partial}{\partial z}H_z - i\omega\epsilon\nabla_s \times \overline{E}_z\right] \qquad (4.3.1b)$$

$$\left(\nabla^2 + k^2\right)E_z = 0 \qquad (4.3.2a)$$

$$\left(\nabla^2 + k^2\right)H_z = 0 \qquad (4.3.2b)$$

where $k^2 = \omega^2\mu\epsilon$ and the Laplacian operation ∇^2 in (4.3.2) is now a three-dimensional operator.

Consider the metallic rectangular cavity as shown in Fig. 4.3.1. It is a waveguide closed with metallic walls at $z = 0$ and $z = d$. We find for TM modes
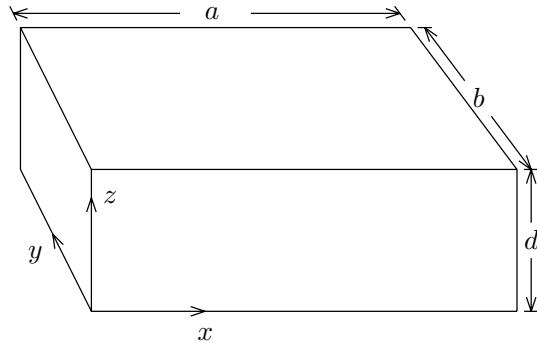
Figure 4.3.1   Rectangular cavity.

$$E_z = E_0 \sin k_x x \sin k_y y \cos k_z z \tag{4.3.3a}$$

$$E_x = \frac{-k_x k_z}{\omega^2 \mu\epsilon - k_z^2} E_0 \cos k_x x \sin k_y y \sin k_z z \tag{4.3.3b}$$

$$E_y = \frac{-k_y k_z}{\omega^2 \mu\epsilon - k_z^2} E_0 \sin k_x x \cos k_y y \sin k_z z \tag{4.3.3c}$$

$$H_x = \frac{-i\omega\epsilon k_y}{\omega^2 \mu\epsilon - k_z^2} E_0 \sin k_x x \cos k_y y \cos k_z z \tag{4.3.3d}$$

$$H_y = \frac{i\omega\epsilon k_x}{\omega^2 \mu\epsilon - k_z^2} E_0 \cos k_x x \sin k_y y \cos k_z z \tag{4.3.3e}$$

$$H_z = 0 \tag{4.3.3f}$$

and for TE modes

$$H_z = H_0 \cos k_x x \cos k_y y \sin k_z z \tag{4.3.4a}$$

$$H_x = \frac{-k_x k_z}{\omega^2 \mu\epsilon - k_z^2} H_0 \sin k_x x \cos k_y y \cos k_z z \tag{4.3.4b}$$

$$H_y = \frac{-k_y k_z}{\omega^2 \mu\epsilon - k_z^2} H_0 \cos k_x x \sin k_y y \cos k_z z \tag{4.3.4c}$$

$$E_x = \frac{-i\omega\mu k_y}{\omega^2 \mu\epsilon - k_z^2} H_0 \cos k_x x \sin k_y y \sin k_z z \tag{4.3.4d}$$

$$E_y = \frac{i\omega\mu k_x}{\omega^2 \mu\epsilon - k_z^2} H_0 \sin k_x x \cos k_y y b \sin k_z z \tag{4.3.4e}$$

$$E_z = 0 \tag{4.3.4f}$$

To satisfy the boundary conditions, we must have

$$k_x a = m\pi \tag{4.3.5a}$$
$$k_y b = n\pi \tag{4.3.5b}$$
$$k_z d = p\pi \tag{4.3.5c}$$

which is the resonance condition for the resonator.

The dispersion relation for both the TM and TE modes is

$$k_r^2 = (m\pi/a)^2 + (n\pi/b)^2 + (p\pi/d)^2$$

This gives the resonant spatial frequency

$$k_r = \sqrt{(m/2a)^2 + (n/2b)^2 + (p/2d)^2} \ \ \mathrm{K}_o \tag{4.3.6}$$

The resonant spatial frequencies for TM_{mnp} modes and TE_{mnp} modes are identical. It is interesting to observe that TM_{mn0} modes correspond to waveguide modes at cutoff, where $k_z = 0$.

EXAMPLE 4.3.1

When the resonator dimensions are such that $a > b > d$, the lowest resonant spatial frequency is found to be

$$k_r = \sqrt{(1/2a)^2 + (1/2b)^2} \ \ \mathrm{K}_o \qquad\qquad (\text{E4.3.1.1})$$

with $m = n = 1$ and $p = 0$. The mode inside the resonator is TM_{110}. The non-zero field components for the TM_{110} mode are

$$E_z = E_0 \sin \frac{\pi x}{a} \sin \frac{\pi y}{b} \qquad\qquad (\text{E4.3.1.2}a)$$

$$H_x = \frac{-i\pi}{\omega\mu b} E_0 \sin \frac{\pi x}{a} \cos \frac{\pi y}{b} \qquad\qquad (\text{E4.3.1.2}b)$$

$$H_y = \frac{i\pi}{\omega\mu a} E_0 \cos \frac{\pi x}{a} \sin \frac{\pi y}{b} \qquad\qquad (\text{E4.3.1.2}c)$$
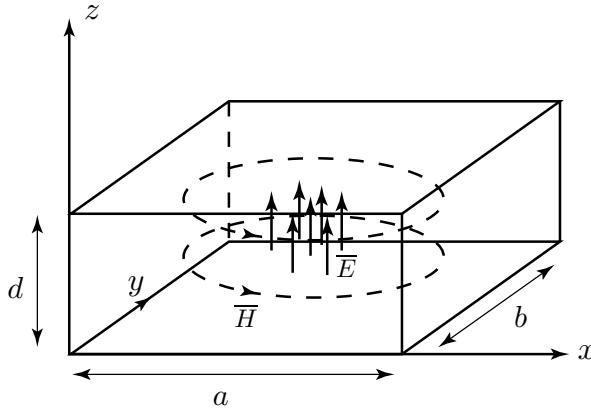
Figure E4.3.1.1 TM_{110} **mode in rectangular cavity.**

The field distribution is illustrated in Fig. E4.3.1.1. We see that the electric fields are perpendicular to the plate boundaries at $z = 0$ and $z = d$ and concentrate at the center of the cavity so that the tangential $\overline{E}$ field vanishes at the boundaries $x = 0, a$ and $y = 0, b$. As an example, if we let $a = 4\,\mathrm{cm}$, $b = 3\,\mathrm{cm}$, and $d = 2\,\mathrm{cm}$, we find the resonant spatial frequency for the TM_{110} mode to be $k_r = 21\,\mathrm{K}_o$.

This field can also be viewed as a dominant waveguide mode propagating in the $\hat{y}$ direction and reflected at the walls $y = 0$ and $y = b$ to form a standing wave. If the labels of the coordinate axes y and z are interchanged, this mode may also be called a TE_{101} mode.

— END OF EXAMPLE 4.3.1 —

The time dependence of electric and magnetic fields is $e^{i\omega_r t}$ with $\omega_r = k_r/\sqrt{\mu\epsilon}$. As time increases, the field amplitudes will decay as $e^{-\alpha_r t}$ with time due to wall loss or material loss. The total energy

$$U(t) = U(0)e^{-2\alpha_r t} \tag{4.3.7}$$

The dissipated power

$$P_d = -\frac{dU}{dt} = 2\alpha_r U \tag{4.3.8}$$

We define a quality factor

$$Q = \omega_r/2\alpha_r = \omega_r U/P_d \tag{4.3.9}$$

which is equal to the total energy divided by average energy loss per angular frequency, and is a measure of the quality of the cavity resonator.

EXAMPLE 4.3.2

In rectangular resonator, we calculate the quality factor $Q = \omega_0 U/rP_d$, where ω_0 is the resonant angular frequency. Under the assumption of a loss-less medium, we find

$$U = \frac{1}{2}\text{Re}\left\{\int_0^d dz \int_0^b dy \int_0^a dx \left[\frac{\epsilon}{2}|E|^2 + \frac{\mu}{2}|H|^2\right]\right\} = \epsilon\frac{abd}{8}E_{110}^2 \tag{E4.3.2.1}$$

for the dominant TM_{110} mode in the rectangular cavity. Integrating over the cavity walls, we obtain

$$P_d = \frac{1}{2}\sqrt{\omega_0\mu/2\sigma}\,\text{Re}\left\{2\int_0^d dz \int_0^a dx\,|H_x|_{y=0}^2\right.$$

$$\left. +2\int_0^d dz \int_0^b dy\,|H_y|_{x=0}^2 + 2\int_0^a dx \int_0^b dy\left(|H_x|^2 + |H_y|^2\right)_{z=0}\right\}$$

$$= \frac{1}{2}\sqrt{\omega_0\mu/2\sigma}\left[\frac{ad}{b^2} + \frac{bd}{a^2} + \frac{1}{2}\left(\frac{b}{a} + \frac{a}{b}\right)\right]\frac{\pi^2\omega_0^2\epsilon^2}{\left(\pi^2/a^2 + \pi^2/b^2\right)^2}E_{110}^2$$

Therefore,

$$Q = \sqrt{\frac{2\sigma}{\omega_0\epsilon}}\,\frac{\pi d(a^2 + b^2)^{3/2}}{2[ab(a^2 + b^2) + 2d(a^3 + b^3)]} \tag{E4.3.2.2}$$

In this derivation, we used the fact that $\omega_0\sqrt{\mu\epsilon} = \sqrt{(\pi^2/a^2) + (\pi^2/b^2)}$. For a cubic cavity with $a = b = d = 2\,\text{cm}$, the resonant frequency, according to (4.3.6), is $10\,\text{GHz}$; and the quality factor is $Q \approx 10^4$ when the cavity is air-filled and is made of copper walls. Other sources of loss, such as the material filling the cavity, surface irregularities of the cavity walls, and coupling with external systems, all contribute toward power dissipation P_d and thereby decrease Q.

<div align="right">— END OF EXAMPLE 4.3.2 —</div>

EXAMPLE 4.3.3

Consider a series R, L, C circuit. The terminal voltage V_s is related to the current I_s in the circuit by

$$V_s = \left(R + sL + \frac{1}{sC}\right) I(s) = \frac{(s - s_+)(s - s_-)}{s/L} I(s)$$

where

$$s_\pm = -\frac{R}{2L} \pm i\sqrt{\frac{1}{LC} - \left(\frac{R}{2L}\right)^2} = -\alpha_r \pm i\sqrt{\omega_0^2 - \alpha_r^2} \approx -\alpha_r \pm i\omega_o$$

$$\alpha_r = \frac{P_d}{2U} = \frac{\frac{1}{2}R|I|^2}{2 \cdot 2 \cdot \frac{1}{4}L|I|^2} = \frac{R}{2L}$$

and $\omega_o = 1/\sqrt{LC}$. The power dissipated at $s = i\omega_o$ is

$$P(\omega_o) = \frac{R}{2}|I(s = i\omega_o)|^2 = \frac{R}{2}\left|\frac{i\omega_o V_s(\omega_o)/L}{\alpha_r(i2\omega_o - \alpha_r)}\right|^2 = \frac{|V_s(\omega_o)|^2}{2R}$$

The power dissipated at $s = i(\omega_o \pm \alpha_r)$ is

$$P(\omega_o \pm \alpha_r) = \frac{R}{2}|I(s = i(\omega_o \pm \alpha_r))|^2 \approx \frac{R}{2}\left|\frac{i\omega_o V_s(\omega_o)/L}{(\alpha_r \pm i\alpha_r)(i2\omega_o \pm \alpha_r - \alpha_r)}\right|^2$$

$$\approx \frac{R}{2}\left|\frac{V_s(\omega_o)/L}{\sqrt{2}2\alpha_r}\right|^2 = \frac{|V_s(\omega_o)|^2}{4R} = \frac{P(\omega_o)}{2}$$

Thus the half-power point bandwidth is $BW = 2\alpha_r$. It is seen that the quality factor

$$Q = \omega_o U/P_d = \omega_o/2\alpha_r = \omega_o/BW = \omega_o L/R = \sqrt{L/C}/R$$

is expressible in terms of inverse attenuation rate, inverse bandwidth, resonator circuit elements, and stored energy over dissipated power.

<div align="right">— END OF EXAMPLE 4.3.3 —</div>

B. Circular Cavity Resonator

Consider a circular cavity of height d and radius a [Fig. 4.3.2]. Under the assumption that $d < a$, the fundamental mode is TM_{010}, which corresponds to the waveguide mode TM_{01} at cutoff. The fields inside the cavity are
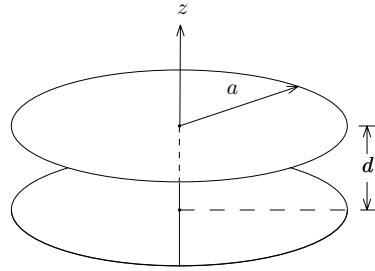
Figure 4.3.2 Circular cavity resonator.

$$E_z = E_0 J_0(k\rho) \tag{4.3.10a}$$

$$H_\phi = -i\sqrt{\epsilon/\mu}\, E_0 J_1(k\rho) \tag{4.3.10b}$$

The resonant wavenumber is

$$k_r a = 2.405 \tag{4.3.10c}$$

The time-average energy stored in the cavity is calculated as

$$U = \frac{1}{2}\int_0^a 2\pi\rho\, d\rho \left[\frac{\epsilon}{2}\,|E_z|^2 + \frac{\mu}{2}\,|H_\phi|^2\right] d = E_0^2\frac{\pi\epsilon d}{2}a^2 J_1^2(ka) \tag{4.3.11}$$

The integral formula for Bessel functions,

$$\int \rho\, d\rho\, B_m^2(k\rho) = \frac{\rho^2}{2}\left[B_m'^2(k\rho) + \left(1 - \frac{m^2}{k^2\rho^2}\right) B_m^2(k\rho)\right] \tag{4.3.12}$$

is used, and so is $J_0(ka) = 0$. The power dissipation caused by wall loss is

$$\begin{aligned}
P_d =\,& \frac{E_0^2}{2}\sqrt{\omega_0\mu/2\sigma}\left[2\pi a d\frac{\epsilon}{\mu}J_1^2(ka) + 2\int_0^a 2\pi\rho\frac{\epsilon}{\mu}J_1^2(k\rho)d\rho\right] \\
=\,& \sqrt{\omega_0\mu/2\sigma}\, E_0^2\frac{\epsilon}{\mu}\pi a(d+a)J_1^2(ka)
\end{aligned} \tag{4.3.13}$$

The first term is due to loss on the side wall and the second term to loss on the walls at $z = 0$ and $z = d$. The quality factor becomes

$$Q = \frac{\omega_0 U}{P_d} = \sqrt{2\sigma/\omega_0\epsilon} \frac{2.405}{2(1 + a/d)} \qquad (4.3.14)$$

where we made use of $(4.3.10c)$. In the mode designation TM_{010} the three subscripts correspond to ϕ, ρ, and z variations, respectively. The TE_{011} mode, for instance, is the waveguide mode TE_{01} forming a standing wave in the $\hat{z}$ direction.

C. Spherical Cavity Resonator

For a spherical cavity, the waveguide formulation breaks down because there is no uniform cross section in any direction. Consider the Maxwell equations in spherical coordinates [Fig. 4.3.3], and treat the case with ϕ symmetry, $\partial/\partial\phi = 0$. Instead of decomposing a general field into TM and TE to $\hat{z}$ components, we decompose into TM and TE to $\hat{r}$ components. For the TM waves, the Maxwell equations give

$$\frac{\partial}{\partial r}(rE_\theta) - \frac{\partial E_r}{\partial \theta} = i\omega\mu r H_\phi \qquad (4.3.15a)$$

$$\frac{1}{r\sin\theta}\frac{\partial}{\partial\theta}(H_\phi \sin\theta) = -i\omega\epsilon E_r \qquad (4.3.15b)$$

$$-\frac{\partial}{\partial r}(rH_\phi) = -i\omega\epsilon r E_\theta \qquad (4.3.15c)$$
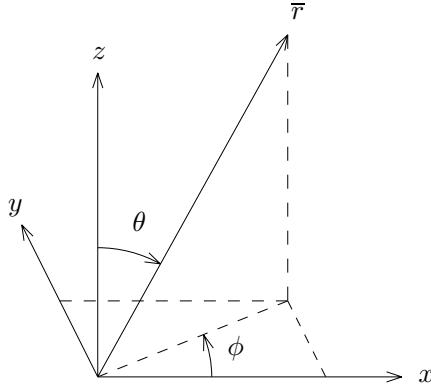
Figure 4.3.3 Spherical coordinate system.

Inserting $(4.3.15b)$ and $(4.3.15c)$ into $(4.3.15a)$ yields an equation for H_ϕ

$$\frac{1}{r}\frac{\partial^2}{\partial r^2}(rH_\phi) + \frac{1}{r^2 \sin\theta}\frac{\partial}{\partial\theta}\left(\sin\theta\frac{\partial H_\phi}{\partial\theta}\right) - \frac{1}{r^2 \sin^2\theta}H_\phi + k^2 H_\phi = 0$$
$$(4.3.16)$$

A similar equation for E_ϕ, which is the dual of $(4.3.16)$, can be obtained for the TE waves.

Before solving for $(4.3.15)$ and $(4.3.16)$, we first study general solutions to Helmholtz wave equations in spherical coordinates. From the source-free Maxwell equations in isotropic media, the wave equation for $\overline{E}$ and $\overline{H}$ is readily derived

$$(\nabla^2 + k^2)\left\{\frac{\overline{E}}{\overline{H}}\right\} = 0$$

Let $W(r, \theta, \phi)$ denote any rectangular component of $\overline{E}$ or $\overline{H}$. The Helmholtz equation takes the form

$$\frac{1}{r}\frac{\partial^2}{\partial r^2}(rW) + \frac{1}{r^2 \sin\theta}\frac{\partial}{\partial\theta}\left(\sin\theta\frac{\partial W}{\partial\theta}\right) + \frac{1}{r^2 \sin^2\theta}\frac{\partial^2 W}{\partial\phi^2} + k^2 W = 0$$
$$(4.3.17)$$

Equation $(4.3.16)$ can be derived directly from $(4.3.17)$ by noting that for $\overline{H} = \hat{\phi}H_\phi$, $\nabla^2\hat{\phi} = -\hat{\phi}\,1/(r^2 \sin^2\theta)$. The solution to the Helmholtz equation $(4.3.17)$ is obtained by separation of variables

$$W = R(r)\Theta(\theta)\Phi(\phi) \tag{4.3.18}$$

The special functions satisfy the following differential equations:

$$r\frac{d^2}{dr^2}(rR) + [(kr)^2 - n(n+1)]R = 0 \quad (4.3.19a)$$

$$\frac{1}{\sin\theta}\frac{d}{d\theta}\left(\sin\theta\frac{d\Theta}{d\theta}\right) + \left[n(n+1) - \frac{m^2}{\sin^2\theta}\right]\Theta = 0 \quad (4.3.19b)$$

$$\frac{d^2\Phi}{d\phi^2} + m^2\Phi = 0 \quad (4.3.19c)$$

Solutions to $(4.3.19a)$, $(4.3.19b)$, and $(4.3.19c)$ are, respectively, the spherical Bessel functions, $b_n(kr)$, the associated Legendre polynomials, $L_n^m(\cos\theta)$, and the harmonic functions, $e^{\pm im\phi}$.

The spherical Bessel functions $b_n(\xi)$ are related to the cylindrical Bessel functions $B_{n+1/2}(\xi)$ which satisfy the Bessel equation

$$\frac{d^2}{d\xi^2}B(\xi) + \frac{1}{\xi}\frac{d}{d\xi}B(\xi) + \left[1 - \frac{(n+1/2)^2}{\xi^2}\right]B(\xi) = 0$$

We can cast (4.3.19a) in the form of the Bessel equation by letting $R(\xi) = (\pi/2\xi)^{1/2}B(\xi)$ with $\xi = kr$. We thus find that

$$b_n(kr) = \sqrt{\pi/2kr}\, B_{n+1/2}(kr) \tag{4.3.20}$$

If n is an integer, $B_{n+1/2}$ reduces to simple sinusoids and powers of r. For the first few orders, for instance

$$j_0(kr) = \frac{\sin kr}{kr} \tag{4.3.21a}$$

$$j_1(kr) = -\frac{\cos kr}{kr} + \frac{\sin kr}{(kr)^2} \tag{4.3.21b}$$

$$j_2(kr) = -\frac{\sin kr}{kr} - \frac{3\cos kr}{(kr)^2} + \frac{3\sin kr}{(kr)^3} \tag{4.3.21c}$$

$$n_0(kr) = -\frac{\cos kr}{kr} \tag{4.3.22a}$$

$$n_1(kr) = -\frac{\sin kr}{kr} - \frac{\cos kr}{(kr)^2} \tag{4.3.22b}$$

$$n_2(kr) = \frac{\sin kr}{kr} - \frac{3\sin kr}{(kr)^2} - \frac{3\cos kr}{(kr)^3} \tag{4.3.22c}$$

The spherical Hankel functions of the first kind take the form

$$h_0^{(1)}(kr) = \frac{e^{ikr}}{ikr} \tag{4.3.23a}$$

$$h_1^{(1)}(kr) = -\frac{e^{ikr}}{kr}\left(1 + \frac{i}{kr}\right) \tag{4.3.23b}$$

$$h_2^{(1)}(kr) = \frac{ie^{ikr}}{kr}\left[1 + \frac{3i}{kr} + 3\left(\frac{i}{kr}\right)^2\right] \tag{4.3.23c}$$

The spherical Hankel function of the second kind is the complex conjugate of $h_n^{(1)}$.

The first few orders of the associated Legendre polynomials of degree 1 take these forms:

$$P_0^1(\cos\theta) = 0 \tag{4.3.24a}$$

$$P_1^1(\cos\theta) = \sin\theta \tag{4.3.24b}$$

$$P_2^1(\cos\theta) = 3\sin\theta\cos\theta \tag{4.3.24c}$$

It is a general property that all of the associated Legendre polynomials $P_n^1(\cos\theta)$ are zero at $\theta = 0$ and π; at $\theta = \pi/2$, they are zero if n is even and maximum if n is odd. For the H_ϕ component,

$$\overline{H} = \hat{\phi}H_\phi = (-\hat{x}\sin\phi + \hat{y}\cos\phi)H_\phi$$

Substituting in (4.3.17) yields

$$\left(\nabla^2 + k^2 - \frac{1}{r^2\sin^2\theta}\right)H_\phi = 0$$

The effect of the last term on the solution is to increase the associated Legendre polynomial by one more degree in m.

In view of (4.3.17) and its solution in (4.3.18), we see that the solutions for H_ϕ in (4.3.16) take the form

$$H_\phi = b_n(kr)P_n^1(\cos\theta) \tag{4.3.25}$$

There is no ϕ dependence. For a spherical cavity with radius a, the spherical Bessel function is used because the origin is included. For the lowest TM mode we let $n = 1$ and use three subscripts on TM to denote the variations around r, ϕ, and θ, respectively. The TM_{101} mode has the field solutions

$$H_\phi = H_0\sin\theta\sqrt{\frac{\pi}{2kr}}J_{3/2}(kr) = H_0\frac{\sin\theta}{kr}\left(\frac{\sin kr}{kr} - \cos kr\right) \tag{4.3.26a}$$

$$E_r = i2H_0\sqrt{\frac{\mu}{\epsilon}}\frac{\cos\theta}{k^2r^2}\left(\frac{\sin kr}{kr} - \cos kr\right) \tag{4.3.26b}$$

$$E_\theta = -iH_0\sqrt{\frac{\mu}{\epsilon}}\frac{\sin\theta}{k^2r^2}\left(\frac{k^2r^2 - 1}{kr}\sin kr + \cos kr\right) \tag{4.3.26c}$$

The boundary condition of vanishing E_θ at $r = a$ gives

$$\tan ka = \frac{ka}{1 - k^2a^2}$$

Solving this transcendental equation yields $ka \approx 2.74$, which gives the resonant wavenumber of the cavity.

D. Cavity Perturbation

The resonant frequency of a cavity changes when a small perturbation is applied to either the cavity wall or the medium inside the cavity. First, we consider an inward perturbation of the cavity wall [Fig. 4.3.4]. The unperturbed fields have resonant frequency ω_0 and satisfy the Maxwell equations:
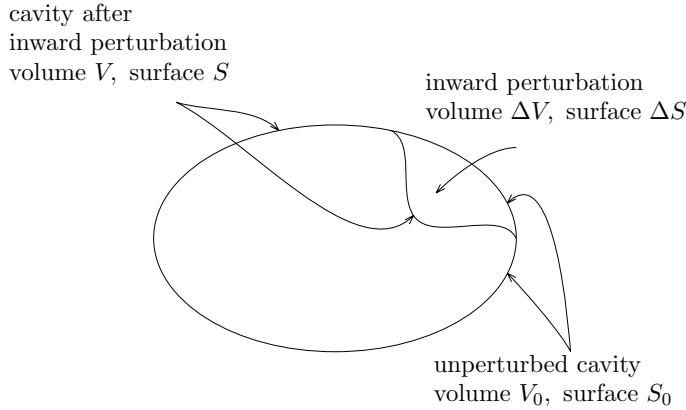
Figure 4.3.4 Cavity perturbation.

$$\nabla \times \overline{E}_0 = i\omega_0\mu\overline{H}_0 \qquad\qquad (4.3.27a)$$

$$\nabla \times \overline{H}_0 = -i\omega_0\epsilon\overline{E}_0 \qquad\qquad (4.3.27b)$$

With the perturbation, the resonant frequency becomes ω and the fields satisfy the Maxwell equations:

$$\nabla \times \overline{E} = i\omega\mu\overline{H} \qquad\qquad (4.3.28a)$$

$$\nabla \times \overline{H} = -i\omega\epsilon\overline{E} \qquad\qquad (4.3.28b)$$

The task is to calculate the deviation of ω from ω_0. We dot-multiply the complex conjugate of $(4.3.27a)$ by $\overline{H}$ and subtract $(4.3.28b)$, dot-multiplied by $\overline{E}_0^*$. The result is

$$\nabla \cdot \left(\overline{E}_0^* \times \overline{H}\right) = -i\omega_0\mu\overline{H} \cdot \overline{H}_0^* + i\omega\epsilon\overline{E} \cdot \overline{E}_0^* \qquad\qquad (4.3.29a)$$

Next, we dot-multiply $(4.3.28a)$ by $\overline{H}_0^*$ and subtract the complex conjugate of $(4.3.27b)$ dot-multiplied by $\overline{E}$. The result is

$$\nabla \cdot \left(\overline{E} \times \overline{H}_0^*\right) = i\omega\mu\overline{H} \cdot \overline{H}_0^* - i\omega_0\epsilon\overline{E} \cdot \overline{E}_0^* \qquad\qquad (4.3.29b)$$

Integrating the sum of $(4.3.29a)$ and $(4.3.29b)$ over the unperturbed volume $V_0 = V + \Delta V$, we find

$$\oiint_{\Delta S} d\overline{S} \cdot \overline{E} \times \overline{H}_0^* = i(\omega - \omega_0) \iiint_{V_0} dV \, (\epsilon \overline{E} \cdot \overline{E}_0^* + \mu \overline{H} \cdot \overline{H}_0^*)$$

In these calculations, we use the fact that tangential $\overline{E}$ vanishes on the perturbed cavity surface and tangential $\overline{E}_0$ vanishes on the unperturbed cavity surface. Note that the surface integration extends over the small perturbed surface ΔS, while the volume integration extends over the unperturbed volume. We obtain the exact equation

$$\omega - \omega_0 = -i \frac{\displaystyle\oiint_{\Delta S} d\overline{S} \cdot \overline{E} \times \overline{H}_0^*}{\displaystyle\iiint_{V_0} dV \, (\epsilon \overline{E} \cdot \overline{E}_0^* + \mu \overline{H} \cdot \overline{H}_0^*)} \qquad (4.3.30)$$

Now we assume that the perturbation is so small that we can replace $\overline{E}$ and $\overline{H}$ on the right-hand side of (4.3.30) by their unperturbed values $\overline{E}_0$ and $\overline{H}_0$ to obtain approximate values for $\omega - \omega_0$:

$$\omega - \omega_0 \approx -i \frac{\displaystyle\oiint_{\Delta S} d\overline{S} \cdot \overline{E}_0 \times \overline{H}_0^*}{\displaystyle\iiint_{V_0} dV \left(\epsilon \left|\overline{E}_0\right|^2 + \mu \left|\overline{H}_0\right|^2 \right)}$$

$$= \omega_0 \frac{\displaystyle\iiint_{\Delta V} dV \left(\mu \left|\overline{H}_0\right|^2 - \epsilon \left|\overline{E}_0\right|^2 \right)}{\displaystyle\iiint_{V_0} dV \left(\mu \left|\overline{H}_0\right|^2 + \epsilon \left|\overline{E}_0\right|^2 \right)}$$

$$= \omega_0 \frac{\Delta W_m - \Delta W_e}{W_m + W_e} \qquad (4.3.31)$$

The denominator is the unperturbed total energy stored in the cavity. The numerator is the difference between the magnetic energy and the electric energy removed by the inward perturbation. Thus, if the inward perturbation is made at a place of large magnetic field, the resonant frequency is raised; if it is made at a place of large electric field, the resonant frequency is lowered. An opposite effect occurs for an outward perturbation.

Next, we investigate the resonant frequency change caused by material perturbation inside the cavity. Let the unperturbed medium be isotropic. To be more general, we include anisotropy in the perturbation. The Maxwell equations before and after perturbation are

$$\nabla \times \overline{E}_0 = i\omega_0\mu\overline{H}_0 \qquad\qquad (4.3.32a)$$

$$\nabla \times \overline{H}_0 = -i\omega_0\epsilon\overline{E}_0 \qquad\qquad (4.3.32b)$$

and

$$\nabla \times \overline{E} = i\omega\mu\overline{H} + i\omega\Delta\overline{\overline{\mu}} \cdot \overline{H} \qquad\qquad (4.3.33a)$$

$$\nabla \times \overline{H} = -i\omega\epsilon\overline{E} - i\omega\Delta\overline{\overline{\epsilon}} \cdot \overline{E} \qquad\qquad (4.3.33b)$$

We dot-multiply the complex conjugate of $(4.3.32a)$ by $\overline{H}$ and subtract $(4.3.33b)$ dot-multiplied by $\overline{E}_0^*$. The result is

$$\nabla \cdot (\overline{E}_0^* \times \overline{H}) = -i\omega_0\mu\overline{H}_0^* \cdot \overline{H} + i\omega\epsilon\overline{E} \cdot \overline{E}_0^* + i\omega(\Delta\overline{\overline{\epsilon}} \cdot \overline{E}) \cdot \overline{E}_0^*$$

A similar operation on $(4.3.32b)$ and $(4.3.33a)$ gives

$$\nabla \cdot (\overline{E} \times \overline{H}_0^*) = i\omega\mu\overline{H} \cdot \overline{H}_0^* + i\omega(\Delta\overline{\overline{\mu}} \cdot \overline{H}) \cdot \overline{H}_0^* - i\omega_0\epsilon\overline{E} \cdot \overline{E}_0^*$$

Integrating the sum of these two equations over the cavity volume and making use of the boundary condition that both $\hat{n} \times \overline{E} = 0$ and $\hat{n} \times \overline{E}_0 = 0$ on the cavity surface, we obtain

$$\frac{\omega - \omega_0}{\omega} = \frac{-\iiint_V dV\left[(\Delta\overline{\overline{\mu}} \cdot \overline{H}) \cdot \overline{H}_0^* + (\Delta\overline{\overline{\epsilon}} \cdot \overline{E}) \cdot \overline{E}_0^*\right]}{\iiint_V dV(\mu\overline{H} \cdot \overline{H}_0^* + \epsilon\overline{E} \cdot \overline{E}_0^*)} \qquad (4.3.34)$$

This is also an exact formula. When the perturbation is so small that we can replace the perturbed fields on the right-hand side by their unperturbed values, we obtain

$$\frac{\omega - \omega_0}{\omega} \approx -\frac{\Delta W_m + \Delta W_e}{W_m + W_e} \qquad\qquad (4.3.35)$$

The denominator expresses the unperturbed total energy inside the cavity, and the numerator corresponds to the increase in magnetic and

electric energies caused by the material perturbation. Thus any in-
crease in the permeability or the permittivity of the material inside the
cavity decreases the resonant frequency. For instance, recall that the
resonant wavenumber for the dominant mode in a circular resonator
is $k_r a = 2.405$. As $k_r = \omega\sqrt{\mu\epsilon}$ increases, the resonant frequency ω_0
decreases. The material, of course, need not be uniformly distributed
throughout the cavity. The calculation of ΔW_m and ΔW_e correspond-
ing to $\Delta\overline{\overline{\mu}}$ and $\Delta\overline{\overline{\epsilon}}$ extends only over the region where perturbation
occurs.

Problems

P4.3.1
    A rectangular cavity $1 \times 2 \times 3$ cm is filled with a dielectric with permit-
tivity $\epsilon = 4\epsilon_o$ and permeability μ_o.
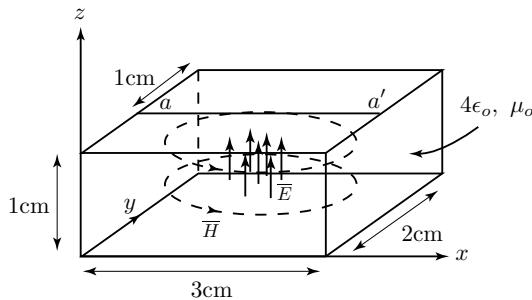
Figure P4.3.1.1 Rectangular cavity.

(a) List the four lowest distinct resonant frequencies of the cavity and their
    corresponding mode designations (TE_{mnp}, TM_{mnp}).
(b) In the above figure, replace the x coordinate with z, y with x, and
    z with y. What is the mode designation now (TE_{mnp}, TM_{mnp}) corre-
    sponding to the fields sketched in Figure P4.3.1.1?
(c) What is the mode designation (TE_{mnp}, TM_{mnp}) and resonant frequency
    ω_0 corresponding to the fields sketched in Figure P4.3.1.1?
(d) What is the internal Q_I of the rectangular cavity operating at its lowest
    order mode if the dielectric material is slightly lossy with conductivity
    $\sigma = 10^{-4}$ mho/meter?
(e) We wish to slightly tune this cavity by appropriately hitting it from the
    outside with a ball-peen hammer. On the diagram indicate the regions
    where hitting the cavity increases the fundamental resonant frequency,

and the region where the resonant frequency decreases. Compute precisely where (if anywhere), along the line aa', the boundary between the two regions is, i.e., where hitting it has no effect on the resonant frequency of the lowest order mode.

P4.3.2

Dissipation occurs when a cavity is filled with conducting media. Since the resonance conditions restrict the values of k_x, k_y, and k_z, the field inside the resonator will attenuate in time. We write the field components for the TM_{110} mode as

$$E_z = \mu_0 A \sin \frac{m\pi x}{a} \sin \frac{n\pi y}{b} (\omega_R \cos \omega_R t - \omega_I \sin \omega_R t) \, e^{-\omega_I t}$$

$$H_x = -\frac{n\pi}{b} A \sin \frac{m\pi x}{a} \cos \frac{n\pi y}{b} \sin \omega_R t \, e^{-\omega_I t}$$

$$H_y = \frac{m\pi}{a} A \cos \frac{m\pi x}{a} \sin \frac{n\pi y}{b} \sin \omega_R t \, e^{-\omega_I t}$$

Determine the rate of attenuation in time and how much ω_R is changed from its value when there is no dissipation due to conductivity.

P4.3.3

Consider a resonator made of a section of coaxial line with length d and short circuited with conducting plates at both ends as shown below.
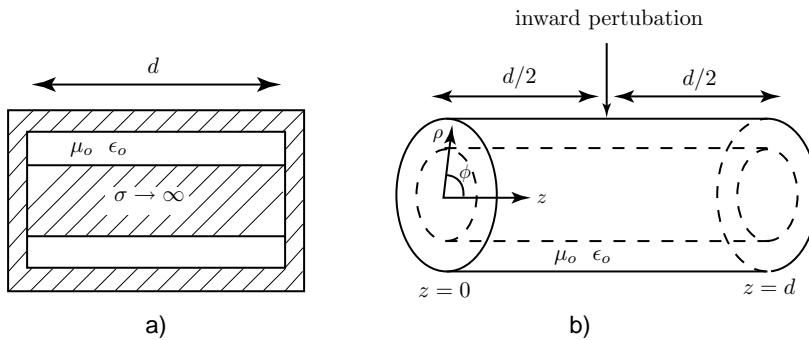
Figure P4.3.3.1 Coaxial resonator.

(a) What are the electric and magnetic fields for the TEM modes?

$$E_\rho = \frac{E_o}{\rho} \cos(kz - \omega t) \qquad H_\phi = \frac{E_o}{\eta\rho} \cos(kz - \omega t)$$

(b) Let $d = 10\,\text{cm}$. What is the lowest nonzero resonant frequency (which is associated with the TEM_1 mode)?
(c) Find the magnitude of the electric field and the magnitude of the magnetic field as functions of z for the TEM_2 mode.

(d) Suppose the TEM_2 mode is excited inside the resonator and an inward perturbation, achieved by using a perfectly conducting screw, is made near the center $(z = d/2)$ of the resonator as shown in Fig. P4.3.3.1b. Will the resonant frequency of that mode be lowered or raised?

Answers

P4.1.1

(a) E layer: $N = 10^{11} m^{-3}$, $\omega_p = 56.349\sqrt{10^{11}} = 1.78 \times 10^7 \, \text{rad/sec}$

F layer: $N = 6 \times 10^{11} m^{-3}$, $\omega_p = 56.349\sqrt{6 \times 10^{11}} = 4.36 \times 10^7 \, \text{rad/sec}$

(b) E layer: $n_E = 0.9590$, $\theta_t^E = \sin^{-1}\left(\frac{n_o}{n_E}\sin\theta\right) = \sin^{-1}(1.0427\sin\theta)$.

F layer: $n_F = 0.7201$, $\theta_t^F = \sin^{-1}\left(\frac{n_o}{n_F}\sin\theta\right) = \sin^{-1}(1.3888\sin\theta)$.

(c) $n_o\sin\theta \geq n_E$, $\frac{\epsilon_E}{\epsilon_o} = 1 - \frac{\omega_p^2}{\omega^2} \leq \sin^2\theta = \sin^2 30° = \frac{1}{4}$,

E layer: $f = \frac{\omega}{2\pi} \leq \frac{1}{\pi\sqrt{3}}\omega_p = \frac{1}{\pi\sqrt{3}} \times 1.78 \times 10^7 \, \text{Hz} = 3.28 \, \text{MHz}$

F layer: $f \leq \frac{1}{\pi\sqrt{3}}\omega_p = \frac{1}{\pi\sqrt{3}} \times 4.36 \times 10^7 \, \text{Hz} = 8.10 \, \text{MHz}$

P4.1.2

(a) $\phi = 2\theta_2 - 2(\theta_1 - \theta_2) = 2(2\theta_2 - \theta_1)$

(b) $\frac{d\phi}{d\theta_1} = \frac{d}{d\theta_1}\left[2\sin^{-1}(\frac{\sin\theta_1}{n}) - \theta_1\right] = 0 \Rightarrow \sin\theta_1 = \sqrt{(4-n^2)/3}$

For $n = 4/3 = 1.33$, $\sin\theta = 0.86 \Rightarrow \phi = 2(2\theta_2 - \theta_1) \simeq 42°$.

(c) For red light, $\theta_1 = 59.58°$, $\theta_2 = 40.42°$, $\phi_{\max} = 42.52°$, and $\theta_s = 137.5°$; for violet light $\theta_1 = 58.89°$, $\theta_2 = 39.64°$, $\phi_{\max} = 40.78°$, and $\theta_s = 139°$. The outer arc of the rainbow will be red, and violet will be on the inner arc of the rainbow.

P4.1.3

(a) $\overline{E}_t = \hat{y}E_0\frac{2}{1+\sqrt{\epsilon/\epsilon_0}}e^{ik_t x}$

(b) $\epsilon = \epsilon_0(1 - 2) = -\epsilon_0$, $\langle\overline{S}\rangle = 0$

(c) $\epsilon \approx i\sigma/\omega$, $\langle\overline{S}\rangle = -\hat{x}\frac{|E_0 T|^2}{2\omega\mu}\sqrt{\frac{\omega\mu\sigma}{2}}e^{2x/\delta}$

P4.1.4

The laser beam is a TM wave linearly polarized in the plane of the paper as the multiple reflections occur at Brewster angle which provides total transmission for TM waves and amplified inside the laser cavity.

For $\epsilon_b = 2.5$, $\tan\theta_B = \sqrt{\epsilon/\epsilon_b} = 1/\sqrt{2.5} = 0.6325$, $\theta_B = 32.3°$

$\theta = 90° - \theta_B = 57.7°$, $\phi = 90° - \theta_B = 57.7°$, $\alpha = 180° - \theta - \phi = 2\theta_B = 64.6°$

P4.1.5

The critical angle for the ordinary wave is $\theta_{oc} = \sin^{-1}\sqrt{\epsilon_0/\epsilon}$.

The critical angle for the extraordinary wave is $\theta_{ec} = \sin^{-1}\sqrt{\epsilon_0/\epsilon_z}$.

Since $\epsilon_z < \epsilon$ for a negative uniaxial crystal, $\theta_{ec} > \theta_{oc}$. For the range of incidence angle θ such that $\theta_{ec} > \theta > \theta_{oc}$, only the extraordinary wave will be transmitted.

P4.1.6

With $R_{01} = R_{ga}$, $R_{1t} = R_{ag} = -R_{ga}$, the reflection coefficient

$$R = \frac{R_{01} + R_{1t}e^{i2k_{1z}d_1}}{1 + R_{01}R_{1t}e^{i2k_{1z}d_1}} = \frac{R_{ga} - R_{ga}\ e^{-2\alpha_{1z}\Delta}}{1 - R_{ga}^2\ e^{-2\alpha_{1z}\Delta}}$$

and the transmission coefficient

$$T = \frac{4e^{-ik_{tz}\Delta}e^{-\alpha_{1z}\Delta}}{(1 + p_{01})(1 + p_{1t})(1 - R_{ga}^2\ e^{-2\alpha_{1z}\Delta})}$$

For θ larger than the critical angle, $|R_{ga}| = 1$, $p_{10} = 1/p_{01} = i\epsilon_g\alpha_{1z}/\epsilon_a k_{tz}$ for TM waves, and $p_{10} = 1/p_{01} = i\alpha_{1z}/k_{tz}$ for TE waves. Note that as $\Delta \to \infty$, $R = R_{ga}$, and $T = 0$; and as $\Delta = 0$, $R = 0$, and $T = 1$. For finite Δ, $T \neq 0$ and is complex, thus transmission is now possible.

P4.1.7

(a) Let $x = k_t \cos\theta_t/k\cos\theta$ and $e = \epsilon_t/\epsilon$. we write

$$r^{TE} - r^{TM} = \frac{(1-x)^2(1+x/e)^2 - (1+x)^2(1-x/e)^2}{(1+x)^2(1+x/e)^2} = 4x\frac{(1-1/e)(x^2/e - 1)}{(1+x)^2(1+x/e)^2}$$

$$x^2/e = \cos^2\theta_t/\cos^2\theta = (1 - \sin^2\theta/e)/(1 - \sin^2\theta)$$

For $e > 1$, $x^2/e > 1$; and for $e > 1$, $x^2/e < 1$. Thus $r^{TE} - r^{TM} > 1$.
(b) $\theta_b = \tan^{-1}\sqrt{3} = 60°$
(c) TM waves reach our eyes.

P4.1.8

(a) $\theta_c = 60°$.
(b) The Brewster angle is $\theta_b = 40.9°$.
(c) It is impossible, $\sin\theta < \tan\theta$ for any θ between $0°$ and $90°$.

P4.1.9

(a) Nulls occur when $\overline{E}_i + \overline{E}_r = 0$, which gives $\cos(k_x x - \phi) = 0$ or $k_x x - \phi = -\frac{\pi}{2}$ nearest to $x = 0$.
Thus

$$x_0 = \left[-\tan^{-1}\frac{\sqrt{\epsilon_r\sin^2\theta - 1}}{\cos\theta} - \frac{\pi}{2}\right]\frac{1}{\sqrt{\epsilon_r}k_0\cos\theta}$$

(b) For perfect conductor at $x = 0$, the nearest null occurs at $\cos(k_x x + \pi/2) = 0$ or $k_x x + \pi/2 = -\frac{\pi}{2}$ or $k_x x = -\pi$. The effective position of the perfect conductor is thus at

$$x_{\text{eff}} = x_o - \pi/k_x = \left[-\tan^{-1} \frac{\sqrt{\epsilon_r \sin^2 \theta - 1}}{\cos \theta} + \frac{\pi}{2} \right] \frac{1}{\sqrt{\epsilon_r} k_0 \cos \theta}$$

(c) With $\epsilon_r = 2$,

θ	$\dfrac{\pi}{4}$	$\dfrac{7\pi}{24}$	$\dfrac{8\pi}{24}$	$\dfrac{9\pi}{24}$	$\dfrac{10\pi}{24}$	$\dfrac{11\pi}{24}$	$\dfrac{\pi}{2}$
$k_0 x_{\text{eff}}$	1.57	1.02	0.87	0.79	0.74	0.72	0.707

(d) The penetration depth, $\delta = 1/k_{txI}$. With $\epsilon_r = 2$, $k_0 \delta = 1/\sqrt{2 \sin^2 \theta - 1}$.

θ	$\dfrac{\pi}{4}$	$\dfrac{7\pi}{24}$	$\dfrac{8\pi}{24}$	$\dfrac{9\pi}{24}$	$\dfrac{10\pi}{24}$	$\dfrac{11\pi}{24}$	$\dfrac{\pi}{2}$
$k_0 \delta$	∞	1.97	1.41	1.19	1.07	1.02	1.00

P4.1.10

(a) The incident wave vector is $\overline{k}_i = \hat{x} k_x - \hat{z} k_z$.

(b) $k_{tz} = \sqrt{k_0^2 (1 + i\sigma/\omega\epsilon_0) - k_0^2 \sin^2 \theta} \approx k_0 \sqrt{i\sigma/(\omega\epsilon_0)} = k_0 \sqrt{\sigma/(2\omega\epsilon_0)}(1+i)$

$$\tan \theta_t = \frac{\text{Re}\{k_{tx}\}}{\text{Re}\{k_{tz}\}} = \sqrt{2\omega\epsilon_0/\sigma} \sin \theta \approx 0$$

(c) $\overline{E}_t = \hat{y} T^{TE} E_0 e^{ik_x x} e^{-ik_{tz} z} = \hat{y} T^{TE} E_0 e^{ik_x x} e^{-ik_R z} e^{k_I z}$

$$T^{TE} = \frac{2k_z}{k_z + k_{tz}} \approx \sqrt{\frac{2\omega\epsilon_0}{\sigma}} \cos \theta (1 - i)$$

Therefore, $|T^{TE}| \approx 2\sqrt{\omega\epsilon_0/\sigma} \cos \theta \ll 1$.

P4.1.11

(a) $\omega = \sqrt{2}\omega_p$, $\omega_{eff} = 0 \quad \Rightarrow \quad \epsilon_t = \epsilon_0 \left[1 - \frac{1}{2} \right] = \frac{\epsilon_0}{2} \quad \Rightarrow \quad k_t^2 = \frac{k_0^2}{2}$

$\overline{k}_i = \dfrac{k_0}{\sqrt{2}} \hat{x} - \dfrac{k_0}{\sqrt{2}} \hat{z} \quad \Rightarrow \quad \overline{k}_t = \hat{x} k_{tx} = \hat{x} \dfrac{k_0}{\sqrt{2}}$

$T^{TE} = \dfrac{2\mu_0 k_z}{\mu_0 k_z + \mu_0 k_{tz}} = 2 \quad \Rightarrow \quad \langle \overline{S}_t \rangle = \hat{x} \dfrac{|E_t|^2}{2\eta_t} = \hat{x}\sqrt{2}\sqrt{\dfrac{\epsilon_0}{\mu_0}} E_0^2$

(b) $\omega = \omega_p$, $\omega_{eff} = 0 \quad \Rightarrow \quad \epsilon_t = 0$

$\quad \Rightarrow \quad \overline{k}_t = \hat{x} \dfrac{k_0}{\sqrt{2}} + \hat{z}\sqrt{\omega^2 \mu_0 \epsilon_t - k_{tx}^2} = \hat{x} \dfrac{k_0}{\sqrt{2}} + \hat{z} i \dfrac{k_0}{\sqrt{2}}$

Since this is an evanescent wave decaying in the z direction, the z component of the transmitted time-average Poynting vector $\langle S_{tz} \rangle = 0$

(c) $\omega = \omega_p = \omega_{eff} \quad \Rightarrow \quad \epsilon_t = \dfrac{\epsilon_0}{2}(1 + i)$

$k_{tz}^2 + k_{tx}^2 = k_{tz}^2 + \dfrac{k_0^2}{2} = \omega^2 \mu_0 \epsilon_t = \dfrac{k_0^2}{2}(1+i) \Rightarrow k_{tz}^2 = i\dfrac{k_0^2}{2} \Rightarrow k_{tz} = \dfrac{k_0}{2}(1+i)$

$$\Rightarrow \overline{k}_t = \hat{x}\frac{k_0}{\sqrt{2}} + \hat{z}\frac{k_0}{2}(1+i)$$

$$T^{TE} = \frac{2\mu_0 k_z}{\mu_0 k_z + \mu_0 k_{tz}} = \frac{2\frac{k_0}{\sqrt{2}}}{\frac{k_0}{\sqrt{2}} + \frac{k_0}{2}(1+i)} = 1 - i\left(\sqrt{2} - 1\right)$$

$$\overline{E}_t = \hat{y}T^{TE}E_0 e^{i\frac{k_0}{\sqrt{2}}x + i\frac{k_0}{2}z} e^{\frac{k_0}{2}z}$$

$$\langle S_{tz}\rangle = \frac{1}{2}\left(4 - 2\sqrt{2}\right)\left(\frac{1}{2}\right)\frac{k_0}{\omega\mu_0}E_0^2 e^{k_0 z} = \left(1 - \frac{1}{\sqrt{2}}\right)\sqrt{\frac{\epsilon_0}{\mu_0}}E_0^2 e^{k_0 z}$$

P4.1.12

The reflectivity is $r = |R|^2 = 0$ and the transmissivity is $t = 1 - r = 1$ which implies that all the energy is transmitted.

The structure works as a filter, because the layers are $\lambda/4$ thick only at the particular frequency. The next lowest frequency that can have total transmission is three times higher. Therefore a signal with spectrum lower than $3f$ (f is the frequency at which the layers are $\lambda/4$-thick), only the component around f can have large transmission.

P4.1.13

For an ice layer on water, water can be approximated by a perfect conductor. Under this assumption, from (3.3.24), with $d_0 = 0$, $d_1 = d$, $R_{12} = \pm 1$, the reflectivity is

$$|R|^2 = \left|\frac{R_{01} \pm R_{01}e^{i\psi}}{1 \pm R_{01}e^{i\psi}}\right|^2$$

where the upper sign applies for TM polarization, and the lower sign for TE polarization. $\psi = 2k_{1z}d$. The operation frequency is limited by two factors:

(1) When the frequency varies over a range smaller than one period of the oscillation, we cannot see two consecutive maxima (or minima). Therefore, the minimum frequency f_{min} has to be such that

$$\text{Re}\left[\psi(f = f_{min}) - \psi(f = 0)\right] = 2\pi \quad \Rightarrow \quad f_{min} = \frac{c}{2d\sqrt{3.2 - \sin^2\theta}}$$

(2) From the expression of $|R|^2$, we see that the oscillation is damped by a factor of $e^{-\text{Im}(\psi)}$. Therefore, if $\text{Im}(\psi)$ is too large, we cannot see the oscillation. Now, suppose that the radiometer can detect the oscillation when $e^{-\text{Im}(\psi)} \geq e^{-\alpha}$. Then, the maximum frequency f_{max} should be such that

$$\text{Im}\left[\psi(f = f_{max})\right] = \alpha = 2d\left(2\pi f_{max}\right)\sqrt{\mu_0\epsilon_0}\left[\frac{0.016}{\sqrt{3.2 - \sin^2\theta}}\right]$$

$$f_{max} = \frac{\alpha c\sqrt{3.2 - \sin^2\theta}}{4\pi d(0.016)} = \frac{5\alpha c}{d}\sqrt{3.2 - \sin^2\theta}$$

Therefore, the frequency range is

$$\frac{c}{2d\sqrt{3.2 - \sin^2\theta}} < f < \frac{5\alpha c}{d}\sqrt{3.2 - \sin^2\theta}$$

P4.1.14

$$\Delta = \phi_{\text{TE}} - \phi_{\text{TM}} = 2\left[\tan^{-1}\frac{\epsilon\alpha_{tz}}{\epsilon_t k_z} - \tan^{-1}\frac{\alpha_{tz}}{k_z}\right] = 2\tan^{-1}\left[\frac{\frac{\epsilon\alpha_{tz}}{\epsilon_t k_z} - \frac{\alpha_{tz}}{k_z}}{1 + \frac{\epsilon\alpha_{tz}^2}{\epsilon_t k_z^2}}\right]$$

$$= 2\tan^{-1}\left[\frac{(n^2 - 1)\frac{\alpha_{tz}}{k_z}}{1 + \frac{\epsilon\alpha_{tz}^2}{\epsilon_t k_z^2}}\right] = 2\tan^{-1}\left[\frac{\sqrt{\sin^2\theta - n^{-2}}}{\frac{\sin^2\theta}{\cos\theta}}\right]$$

For $n = 1.6$, θ is $58.8°$ or $42.5°$. Thus α is either $58.8°$ or $42.5°$.

P4.1.15

Total internal reflection occurs, then in balsam the wave is evanescent, thus the output has very little TE wave, the output wave will be mainly TM polarized.

P4.1.16

The critical angle $\theta_C = \sin^{-1}\sqrt{\frac{\epsilon_t}{\epsilon_o}}$. The Brewster angle $\theta_B = \tan^{-1}\sqrt{\frac{\epsilon_t}{\epsilon_o}}$. The critical angle θ_C is always larger than the Brewster angle θ_B. It is impossible to have total transmission and total reflection at the same time.

P4.2.1

(a) The radiation pattern of the Hertzian dipole on the x-y plane is a circle.
(b) Linearly polarized, perpendicular to the paper, TE wave.
(c) $m = 1$, $\left(\sqrt{2}\pi/\lambda_o\right)^2 - (\pi/d)^2 > 0$. $m = 2$, $\left(\sqrt{2}\pi/\lambda_o\right)^2 - (2\pi/d)^2 < 0$. So $\lambda_o/\sqrt{2} < d < \sqrt{2}\lambda_o$. The propagating mode is TE_1.

P4.2.2

(a) $m < \frac{d\omega\sqrt{\mu_o\epsilon_o}}{\pi} = \frac{d\omega}{\pi c} = \frac{30\times10^9 \times 2\sqrt{3}\pi\times10^{-2}}{3\times10^8\pi} = 3.46$.
   The possible guided modes are TM_m ($m = 0, 1, 2, 3$) and TE_m ($m = 1, 2, 3$).
(b) For TM_2 mode,
$$\overline{E} = \frac{H_o}{\epsilon_o\omega}\left[\hat{x}k_z\cos\frac{2\pi x}{d}\cos(k_z z - \omega t) + \hat{z}\frac{2\pi}{d}\sin\frac{2\pi x}{d}\sin(k_z z - \omega t)\right]$$
(c) $v_p = \frac{\omega}{k_z} = \frac{30\times10^9}{100\sqrt{2/3}} = 3.67 \times 10^8 \text{ (m/s)}$.

$$v_g = \frac{d\omega}{dk_z} = \frac{k_z}{\omega\mu_o\epsilon_o} = \frac{c^2 k_z}{\omega} = \frac{c^2}{v_p} = \frac{(3\times10^8)^2}{3.67\times10^8} = 2.45 \times 10^8 \text{ (m/s)}.$$
(d) Since $\epsilon_1 = 3\epsilon_o > \epsilon_0$, there is no total reflection for any modes.
(e) TM_3 wave can be totally transmitted.

P4.2.3

(a) In region $z < 0$, the possible modes are TE_1, TM_0 TM_1. In region $z > 0$, the possible modes are TE_1 TE_2, TM_0 TM_1 TM_2.

(b) $p_{0t} = \frac{k_{tz}}{k_{0z}} = \sqrt{\frac{55}{7}}$ $R = \frac{1-p_{0t}}{1+p_{0t}} = \frac{\sqrt{7}-\sqrt{55}}{\sqrt{7}+\sqrt{55}} = -0.4741$.

(c) $\overline{E} = \hat{y}E_o \sin\left(\frac{\pi}{d}x\right) \sin\left(k_z z\right)$, where $k_z = \sqrt{\omega^2\mu_o\epsilon_o - \left(\frac{\pi}{d}\right)^2}$.

P4.2.4

$$H_y = \begin{cases} -\frac{J_s}{2}\cos\frac{3\pi x}{d}e^{ik_z z} & z \geq 0 \\ \frac{J_s}{2}\cos\frac{3\pi x}{d}e^{-ik_z z} & z \leq 0 \end{cases}$$

P4.2.5

The electric field solution for the asymmetric slab waveguide is

$$\overline{E}_0 = \hat{y}A_0\left[e^{ik_x x} + R_+^{TE}e^{-ik_x x}\right]e^{ik_z z}$$
$$= \hat{y}A_0 e^{i\phi_{01}+ik_x d}\left[2\cos\left(k_x x - \phi_{01} - k_x d\right)\right]e^{ik_z z}$$

The cutoff spatial frequency is, for $n_{(-1)} < n_1$,

$$k_{cm} = \frac{m\pi + \tan^{-1}\left(\mu\sqrt{1 - \mu_{-1}\epsilon_{-1}/\mu_1\epsilon_1}\Big/\mu_{-1}\sqrt{\mu\epsilon/\mu_1\epsilon_1 - 1}\right)}{d\sqrt{1 - \mu_1\epsilon_1/\mu\epsilon}}$$

P4.2.6

$$\overline{J}_s = \hat{x}\delta(y-h) = \hat{x}\sum_{n=1}^{\infty}\frac{2}{d}\sin\frac{n\pi h}{d}\sin\frac{n\pi y}{d}$$

$$E_x = -\frac{\omega\mu}{d}\sum_{n=1}^{\infty}\left\{\frac{\sin\left(\frac{n\pi h}{d}\right)\sin\left(\frac{n\pi y}{d}\right)}{\left[k^2 - (n\pi/d)^2\right]^{1/2}}e^{k_{zn}|z|}\right\}$$

$$H_z = -i\frac{\pi}{d^2}\sum_{n=1}^{\infty}\left\{\frac{n\sin\left(\frac{n\pi h}{d}\right)\sin\left(\frac{n\pi y}{d}\right)}{\left[k^2 - (n\pi/d)^2\right]^{1/2}}e^{k_{zn}|z|}\right\}$$

$$H_y = \mp(z)\frac{1}{d}\sum_{n=1}^{\infty}\left\{\frac{\sin\left(\frac{n\pi h}{d}\right)\sin\left(\frac{n\pi y}{d}\right)}{\left[k^2 - (n\pi/d)^2\right]^{1/2}}e^{k_{zn}|z|}\right\}$$

P4.2.7

TE_{10} excitation is maximum if $d = a/2$.

P4.2.8

(a) $E_z = 0$, $m = 1$ and $n = 0$, the mode is TE_{10}.

(b) $k_x = k_z = \pi/a$, $k = \sqrt{k_x^2 + k_z^2} = \frac{\sqrt{2}\pi}{a}$, $f = c/\sqrt{2}a = 5\,\mathrm{GHz}$.

(c) $k_z = \pi/a$, $v_p = \omega/k_z = \sqrt{2}c$.

(d) $k_c^2 - (\pi/a)^2 = 0$, $f_c = c/2a = 5/\sqrt{2}\,\mathrm{GHz}$.

(e) $k^2 = \left(\sqrt{2}\pi/a\right)^2 = (m\pi/a)^2 + (n\pi/b)^2 + (p\pi/d)^2$, $m = 1$, $n = 0$, $p = 1$
and $d = a$. The mode is TE_{101}.

P4.2.9

The cutoff wavenumber is $k_c = \sqrt{(m\pi/a)^2 + (n\pi/b)^2}$ and for $a = 2b$,
$f_c = \frac{c}{2a}\sqrt{m^2 + 4n^2}$. Therefore, the first five modes are TE_{10}, TE_{20}, TE_{01},
TE_{11}, and TM_{11} and the cutoff frequencies are 15 GHz, 30 GHz, 30 GHz,
33.5 GHz, and 33.5 GHz respectively.

At a frequency of 20 GHz, $k = \omega/c = 400\pi/3$. Therefore the propaga-
tion constants are

$$\mathrm{TE}_{10}: \quad k_z = 100\pi\sqrt{(4/3)^2 - 1} = 100\pi\sqrt{7/9}$$

$$\left.\begin{array}{ll}
\mathrm{TE}_{20}: & k_z = i100\pi\sqrt{20/9} \\
\mathrm{TE}_{01}: & k_z = i100\pi\sqrt{20/9} \\
\mathrm{TE}_{11}: & k_z = i100\pi\sqrt{29/9} \\
\mathrm{TM}_{11}: & k_z = i100\pi\sqrt{29/9}
\end{array}\right\} \quad \text{evanescent modes}$$

Cutoff frequencies are 43 GHz for TE_{21} and TM_{21} modes, 45 GHz for
TE_{30} modes and 50 GHz for TE_{31} and TM_{31} modes.

At a frequency of 50 GHz, there will be 8 propagating modes TE_{10},
TE_{20}, TE_{01}, TE_{11}, TM_{11}, TE_{21}, TM_{21}, TE_{30}.

P4.2.10

(a) The coaxial cable is modeled as a waveguide with

$$f_{c,mn} = \frac{c}{2\pi}\sqrt{\left(\frac{m\pi}{2\pi a}\right)^2 + \left(\frac{n\pi}{\delta}\right)^2}$$

Since $\delta \ll a$, if $n \neq 0$, $f_{c,mn}$ will be very high, so choose $n = 0$. Since
TM_{m0} mode dose not exist, we consider only TE_{m0} modes. Lowest
three modes: $TE_{20}, TE_{40}, TE_{60}$

(b) $f_{c,20} = \frac{c}{2\pi}\frac{2\pi}{2\pi a} = \frac{c}{2\pi a}$, $f_{c,40} = \frac{c}{2\pi}\frac{4\pi}{2\pi a} = \frac{c}{\pi a}$, $f_{c,60} = \frac{c}{2\pi}\frac{6\pi}{2\pi a} = \frac{3c}{2\pi a}$

P4.2.11

$f_c = 6 \times 10^{14}$ Hz

Comparing with the slab waveguide:

Let $d = 2a = 2 \times 10^{-6}$, $\sqrt{1 - n^2/n_1^2} = 0.191$, $f_c = 1.57 \times 10^{15}$ Hz.
Slab waveguide has wider capacity, but optical fiber has physical compactness.

Comparing with metallic circular waveguide.

The width of capacity is $\Delta f = f_{c2} - f_{c1} = 0.54 \times 10^{14}$ Hz. In contrast
optical fiber has $\Delta f = 6 \times 10^{14}$ Hz and also optical fiber has flexibility.

P4.3.1

(a) $\omega_{mnp} = \frac{c}{2}\sqrt{\left(\frac{m\pi}{a}\right)^2 + \left(\frac{n\pi}{b}\right)^2 + \left(\frac{p\pi}{d}\right)^2}$ and the four lowest order modes:
$TM_{110}, f = 4.5$ GHz; $TM_{210}, f = 6.25$ GHz; $TE_{101}/TM_{120}, f = 7.9$ GHz; $TE_{011}, f = 8.4$ GHz.

(b) For $mnp \rightarrow yzx$, TE_{101}, $f = 4.5$ GHz; TE_{102}, $f = 6.25$ GHz; TE_{011}/TE_{201}, $f = 7.9$ GHz; TM_{110}, $f = 8.4$ GHz.

(c) E field has one peak along x and y direction, but uniform on z direction. As $a > b > d$, $\omega_o = \frac{3\times10^8}{2}\sqrt{(\frac{\pi}{0.03})^2 + (\frac{\pi}{0.02})^2} = 2.83\times10^{10}$rad s^{-1}.

(d) $\omega_0 = \omega_{101}$ $W_T = 2W_E = \frac{1}{8}\epsilon |E_{101}|^2 abd$, $\langle p_d \rangle = \int_V \frac{1}{2}\text{Re}\left\{\sigma\overline{E}\cdot\overline{E}^*\right\}dV$

$$Q_I \triangleq \frac{\omega_0 W_T}{\langle P_d \rangle} = \frac{\sqrt{13}}{6}\frac{\pi c}{2d}\frac{\epsilon}{\sigma} = \frac{\sqrt{13}}{6}\frac{\pi\times3\times10^8}{2\times10^{-2}}\frac{4\cdot(8.9\times10^{-12})}{10^{-4}} = 10,080$$

(e) To increase the resonant frequency, we indent regions where $\overline{H}$ is strong: these are the sides of the cavity and part of the top near the edges. To decrease the resonant frequency, we indent those portions where $\overline{E}$ is strong: these are the top and bottom of the cavity, in the inner circle. Hitting the box for TM$_{110}$ at $y = b/2$ will have no effect where:

$$\mu_0\overline{H}\cdot\overline{H}^* = \epsilon_0\overline{E}\cdot\overline{E}^* \Rightarrow \mu_0\left(\frac{\pi}{a}\right)^2\cos^2\frac{\pi x}{a} = 4\epsilon_0\omega_0^2\mu_0^2\sin^2\frac{\pi x}{a}$$

$\Rightarrow x = 0.483$ cm   and $x = 2.516$ cm.

P4.3.2

It is seen that $\nabla\times\overline{E} = \partial\overline{H}/\partial t$ is satisfied. $\nabla\times\overline{E} = \partial\overline{H}/\partial t$ leads to ω_I and ω_R which yield the rate of attenuation in time $\omega_I = \frac{\sigma}{2\epsilon_0}$ and that $\omega_R^2\mu\epsilon = (m\pi/a)^2 + (n\pi/b)^2 - \mu_0\sigma^2/4\epsilon_0$.

P4.3.3

(a) The total field in the cavity is $E_\rho = \frac{E_1}{\rho}e^{ikz} + \frac{E_2}{\rho}e^{-ikz}$.

$$E_\rho = 2i\frac{E_1}{\rho}\sin\frac{n\pi}{d}z$$

$$\overline{H} = \frac{\nabla\times\overline{E}}{i\omega\mu_0} = \frac{1}{i\omega\mu_0}\hat{\phi}\frac{\partial E_\rho}{\partial z} = \hat{\phi}\frac{2E_1}{\eta\rho}\cos\left(\frac{n\pi}{d}z\right)$$

(b) $d = 0.1m = \frac{\lambda}{2}$, therefore $f = \frac{3\times10^8}{2\times0.1} = 1.5$ GHz.

(c) For TEM_2 mode, $n = 2$, and

$$|E_\rho| = \frac{2E_1}{\rho}\left|\sin\left(\frac{2\pi}{d}z\right)\right|, \quad |H_\phi| = \frac{2E_1}{\eta\rho}\left|\cos\left(\frac{2\pi}{d}z\right)\right|$$

(d) At $z = \frac{d}{2}$, $|E_\rho| = 0$, $|H_\phi| = $ maximum, thus for an inward perturbation at $z = \frac{d}{2}$, the resonant frequency will be raised.

5

RADIATION

5.7 Dipole Antennas in Layered Media

A. Integral Formulation

B. Contour Integration Methods

C. Dipole Antenna on a Two-Layer Medium

Answers

5.1 Čerenkov Radiation

In 1934, P. A. Čerenkov (1904–1990) discovered experimentally that all liquids and solids emit visible radiation when bombarded by fast-moving electron beams. He discovered that (i) in order to achieve radiation, the velocity of the electrons must be very large, (ii) the angles of radiation are related to the velocity of the beam, and (iii) the emitted light has the electric field vector polarized parallel to the plane determined by the direction of the beam and the direction of the radiation. Many unsuccessful attempts were made to explain the discovery with various microscopic approaches. In 1937, I. Frank (1908–1990) and Ig. Tamm (1895–1971) used the macroscopic theory and established that an electron moving uniformly in a medium characterized by a refractive index larger than unity radiates light if the electron velocity is greater than the velocity of light in the medium. Because the discovery of this phenomenon, known as *Čerenkov radiation*, marked a significant triumph for macroscopic electromagnetic theory, we shall devote this section to this subject.

The source of radiation is a particle with charge q moving at a velocity $\overline{v}$ in an isotropic medium. The velocity will decrease as a result of radiation. To simplify discussions, we assume that $\overline{v}$ is a constant in the direction $\hat{z}$. The current density of the moving charge is

$$\overline{J}(\overline{r}, t) = \hat{z} q v \delta(x) \delta(y) \delta(z - vt)$$

In the cylindrical coordinate system, we have ϕ symmetry. Noticing that

$$\int d\rho \, \delta(\rho) = 1 = \iint dx \, dy \, \delta(x) \delta(y) = \int 2\pi \rho d\rho \, \delta(x) \delta(y)$$

We can write $\delta(x)\delta(y) = \delta(\rho)/2\pi\rho$ and therefore

$$\overline{J}(\overline{r}, t) = \hat{z} q v \delta(z - vt) \frac{\delta(\rho)}{2\pi\rho} \tag{5.1.1}$$

This source is not time harmonic. We transform to the frequency domain and obtain

$$\overline{J}(\overline{r}, \omega) = \frac{1}{2\pi} \int dt \, \overline{J}(\overline{r}, t) e^{i\omega t} = \hat{z} \frac{q}{4\pi^2 \rho} e^{i\omega z/v} \, \delta(\rho) \tag{5.1.2}$$

For each spectrum component ω we solve for the electric field

$$\overline{E}(\overline{r}) = \frac{1}{2\pi} \int dt\, \overline{E}(\overline{r}, t) e^{i\omega t}$$

The time-domain values are obtained by the inverse Fourier transform:

$$\overline{E}(\overline{r}, t) = \int d\omega\, \overline{E}(\overline{r}) e^{-i\omega t} \tag{5.1.3}$$

The governing equation for the electric field becomes

$$\nabla \times \nabla \times \overline{E}(\overline{r}) - k^2 \overline{E}(\overline{r}) = \hat{z} \frac{i\omega\mu q}{4\pi^2 \rho} e^{i\omega z/v} \, \delta(\rho) \tag{5.1.4}$$

This equation is conveniently solved by defining a vector Green's function $\overline{g}(\rho, z)$ such that

$$\overline{E}(\overline{r}) = \left[\overline{\overline{I}} + \frac{1}{k^2} \nabla\nabla \right] \cdot \overline{g}(\rho, z) = \overline{g}(\rho, z) + \frac{1}{k^2} \nabla[\nabla \cdot \overline{g}(\rho, z)] \tag{5.1.5}$$

We obtain from (5.1.4) the wave equation for $\overline{g}(\rho, z)$:

$$(\nabla^2 + k^2)\overline{g}(\rho, z) = -\hat{z} \frac{i\omega\mu q}{4\pi^2 \rho} e^{i\omega z/v} \, \delta(\rho) \tag{5.1.6}$$

In view of the z dependence on the right-hand side and the azimuthal symmetry of the problem, we write the wave equation in the cylindrical coordinate system. Let

$$\overline{g}(\rho, z) = \hat{z} g(\rho) \frac{i\omega\mu q}{2\pi} e^{i\omega z/v} \tag{5.1.7}$$

Then we obtain

$$\left[\frac{1}{\rho} \frac{d}{d\rho} \left(\rho \frac{d}{d\rho} \right) - \frac{\omega^2}{v^2} + k^2 \right] g(\rho) = -\frac{\delta(\rho)}{2\pi\rho} \tag{5.1.8}$$

For $\rho \neq 0$, the above equation becomes

$$\left[\frac{1}{\rho} \frac{d}{d\rho} \left(\rho \frac{d}{d\rho} \right) + k_\rho^2 \right] g(\rho) = 0 \tag{5.1.9}$$

where

$$k_\rho = \sqrt{k^2 - \frac{\omega^2}{v^2}} = n\frac{\omega}{c}\sqrt{1 - \frac{1}{(n\beta)^2}} \qquad (5.1.10)$$

$\beta = v/c$, and $n = c\sqrt{\mu\epsilon}$. Eq. (5.1.9) is the Bessel equation of zeroth order. Since (5.1.8) exhibits a singularity at $\rho = 0$ and the solution to the Bessel equation should represent an outgoing wave, we choose

$$g(\rho) = CH_0^{(1)}(k_\rho\rho) \qquad (5.1.11)$$

The constant C is determined by matching the boundary condition at $\rho \to 0$. Integrating (5.1.8) over an infinitesimal area $2\pi\rho d\rho$ and letting $\rho \to 0$, we have

$$\lim_{\rho\to 0} 2\pi\rho \frac{dg(\rho)}{d\rho} = -1$$

Using the asymptotic formula for $H_0^{(1)}(k_\rho\rho) \approx i(2/\pi)\ln(k_\rho\rho)$, we obtain $C = i/4$ and from (5.1.11)

$$g(\rho) = \frac{i}{4}H_0^{(1)}(k_\rho\rho) \qquad (5.1.12)$$

This is the scalar Green's function in cylindrical coordinates. For two-dimensional problems independent of z, the scalar Green's function is simply (5.1.12) with $k_\rho = k$.

The solution for the electric field is determined from (5.1.7) and (5.1.5).

$$\overline{E}(\overline{r}) = \frac{-q}{8\pi\omega\epsilon}\left[\hat{z}k^2 + i\frac{\omega}{v}\nabla\right]H_0^{(1)}(k_\rho\rho)e^{i\omega z/v} \qquad (5.1.13)$$

Since we are interested in radiation from the charge, we use the asymptotic values of $H_0^{(1)}(k_\rho\rho)$ to find the far-field solutions. In the radiation zone, $k_\rho\rho \gg 1$, and $H_0^{(1)}(k_\rho\rho) \approx \sqrt{2/i\pi k_\rho\rho}\,e^{ik_\rho\rho}$. We get

$$\overline{E}(\overline{r}) \approx \frac{q}{8\pi\omega\epsilon}\sqrt{\frac{2k_\rho}{i\pi\rho}}\left[\hat{\rho}\frac{\omega}{v} - \hat{z}k_\rho\right]e^{i(k_\rho\rho + \omega z/v)} \qquad (5.1.14)$$

This represents a plane wave with wave vector $\overline{k} = \hat{\rho}k_\rho + \hat{z}\omega/v$, provided that k_ρ in (5.1.10) is real.

All phenomena observed by Čerenkov can be explained with (5.1.14).

(i) We see that k_ρ is real if $n\beta > 1$, i.e.,

$$v > \frac{c}{n} \tag{5.1.15}$$

Thus, plane waves are radiated if the velocity of the charge is larger than the velocity of light in the medium. When the charge velocity v is smaller than the light velocity, k_ρ is imaginary and the wave is evanescent in the $\hat{\rho}$ direction.

(ii) The constant phase front of the plane waves forms a cone around the $\hat{z}$ direction. The direction θ that $\overline{k}$ makes with $\hat{z}$ [Fig. 5.1.1] is determined from
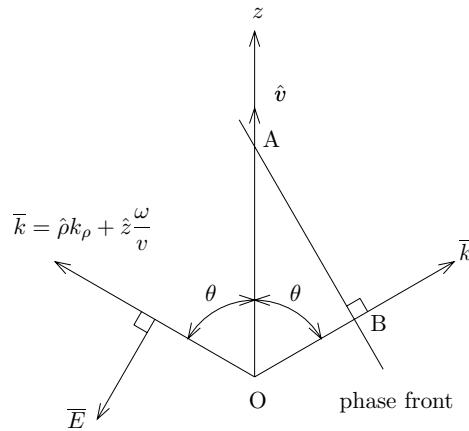
Figure 5.1.1 Čerenkov radiation.

$$\cos\theta = \frac{k_z}{k} = \frac{\omega}{kv} = \frac{1}{n\beta} \tag{5.1.16}$$

where $\beta = v/c$. Note that θ has a real value only if $n\beta > 1$. Notice from Figure 5.1.1 that for the phase front represented by AB, OA is the distance traveled by the charge particle and OB is the distance traveled by the wave originated from point O.

(iii) With regard to the polarization of the emitted electromagnetic wave, we observe from (5.1.14) that $\overline{E}$ lies in the plane determined by $\overline{k}$ and $\hat{z}$ [Fig. 5.1.1]. It is clear that $\overline{E}$ is also perpendicular to the $\overline{k}$ vector because $\overline{k} \cdot \overline{E} = 0$.

EXAMPLE 5.1.1   Čerenkov radiation power.
  To calculate radiated power, we first compute the magnetic field from Faraday's law, which gives, when terms of order $\rho^{-3/2}$ are neglected,

$$\overline{H} = \hat{\phi}\frac{q}{8\pi}\sqrt{\frac{2k_\rho}{i\pi\rho}}\,e^{i(k_\rho\rho+\omega z/v)} \qquad \text{(E5.1.1.1)}$$

The corresponding magnetic field in space-time domain is

$$\overline{H}(\bar{r},t) = \hat{\phi}\frac{q}{4\pi}\sqrt{\frac{2}{\pi\rho}}\int_0^\infty d\omega\,\sqrt{k_\rho}\cos\left(\omega t - k_\rho\rho - \frac{\omega z}{v} + \frac{\pi}{4}\right) \qquad \text{(E5.1.1.2)}$$

where we use the inverse Fourier transform (5.1.3). Noting that k_ρ is proportional to ω because $k_\rho = n\frac{\omega}{c}\sqrt{1-1/n^2\beta^2}$, we change the integration limits from $(-\infty,\infty)$ to $(0,\infty)$. Similarly, the space-time domain electric field is, by taking the inverse Fourier transform of (5.1.14),

$$\overline{E}(\bar{r},t) = -\frac{q}{4\pi}\sqrt{\frac{2}{\pi\rho}}\int_0^\infty d\omega\,\frac{1}{\omega\epsilon}\left(\hat{z}k_\rho - \hat{\rho}\frac{\omega}{v}\right)\sqrt{k_\rho}\cos\left(\omega t - k_\rho\rho - \frac{\omega z}{v} + \frac{\pi}{4}\right)$$
$$\text{(E5.1.1.3)}$$

Consider a cylinder of length l and radius ρ. The total energy radiated through the surface of the cylinder is given by

$$S_\rho = 2\pi\rho l \int_{-\infty}^\infty dt\,[\overline{E}(\bar{r},t)\times\overline{H}(\bar{r},t)]_\rho = 2\pi\rho l\int_{-\infty}^\infty dt\,[E_z(\bar{r},t)\overline{H}_\phi(\bar{r},t)]$$

$$= \frac{q^2 l}{4\pi^2}\int_{-\infty}^\infty dt\int_0^\infty d\omega\int_0^\infty d\omega'\,k_\rho\frac{\sqrt{k_\rho}}{\omega\epsilon}\sqrt{k'_\rho}$$

$$\cos\left(\omega t - k_\rho\rho - \frac{\omega z}{v} + \frac{\pi}{4}\right)\cos\left(\omega' t - k'_\rho\rho - \frac{\omega' z}{v} + \frac{\pi}{4}\right) \quad \text{(E5.1.1.4)}$$

where $k'_\rho = \frac{\omega'}{c}(1-1/n^2\beta^2)^{1/2}$. First we integrate with respect to t. Let $\alpha = k_\rho\rho/\omega + z/v$, we observe that

$$\int_{-\infty}^\infty dt\,\cos\left[\omega'(t+\alpha) + \frac{\pi}{4}\right]\cos\left[\omega(t+\alpha)+\frac{\pi}{4}\right]$$

$$= \frac{1}{2}\int_{-\infty}^\infty dt\,\cos[(\omega-\omega')(t+\alpha)] = \pi\delta(\omega-\omega') \quad \text{(E5.1.1.5)}$$

where we make use of the delta function

$$\delta(\omega-\omega') = \frac{1}{2\pi}\int_{-\infty}^\infty dt\,e^{i(\omega-\omega')t}$$

Thus we obtain

$$S_\rho = \frac{q^2 l}{4\pi} \int_0^\infty d\omega \, \frac{k_\rho^2}{\omega \epsilon} = \frac{\mu q^2 l}{4\pi} \int_0^\infty d\omega \, \omega \left[1 - \frac{1}{n^2 \beta^2} \right] \qquad \text{(E5.1.1.6)}$$

Even though the integration limit is from 0 to ∞, we must remember that the above result is valid only for $n^2 > 1/\beta^2$ in order to achieve Čerenkov radiation. Since all materials are dispersive, the integration limit is actually determined by the frequency range of the refractive index n for which the Čerenkov radiation condition is satisfied. With the use of the above equation, energy radiated per unit length of the electron path can be calculated for materials of various refractive indices. Furthermore, we must note that the above theoretical treatment assumes a constant velocity v. As the charge radiates, the particle slows down and eventually ceases to radiate as $\beta^2 \leq 1/n^2$.

— End of Example 5.1.1 —

Problems

P5.1.1

In the Čerenkov radiation, the total energy radiated out of a cylinder of path l and radius ρ is given by (E5.1.1.6). The energy lost per unit length per unit frequency band is

$$\frac{d^2 S_\rho}{dl \, d\omega} = \frac{\mu q^2}{4\pi} \omega \left(1 - \frac{1}{n^2 \beta^2} \right)$$

(a) By $E_{photon} = \hbar \omega$ and $d\omega/d\lambda = 2\pi c/\lambda^2$, show that the number of photon radiated on unit path at wave length λ is

$$\frac{d^2 N}{dl \, d\lambda} = \frac{q^2 c}{2\lambda^2 \hbar} \mu \left(1 - \frac{1}{n^2 \beta^2} \right)$$

   and show the frequently used formula $\frac{dN}{dl} \propto \frac{d\lambda}{\lambda^2} \sin^2 \theta$, which gives the dependence of N on λ and θ.
(b) Gas Čerenkov detector is widely used in high energy particle experiment. The refractive index of the gas n is typically 1.002. What will be the angle for the Čerenkov radiation in case of $\beta = 1$?
(c) Most energy is radiated by the waves in the band 350 nm $\sim$ 550 nm. How many photons can you get on unit path? In order to get 100 photons for the detector, how long is the path (l)? This is the size the detector should be. Note that the parameters are as follows: $\hbar = 6.63 \times 10^{-34}/(2\pi)$ J·s/rad, $q = 1.6 \times 10^{-19}$ C, $\beta = 1$.

5.2 Green's Functions

A. Dyadic Green's Functions

In antenna and radiation problems, we are interested in finding the solution of electromagnetic fields in the presence of a source distribution $\overline{J}(\overline{r})$ and $\rho(\overline{r})$. The current and charge distributions are related by the conservation law. For time-harmonic fields, $i\omega\rho(\overline{r}) = \nabla \cdot \overline{J}(\overline{r})$. From the Maxwell equations

$$\nabla \times \overline{E}(\overline{r}) = i\omega\mu\overline{H}(\overline{r}) \tag{5.2.1}$$

$$\nabla \times \overline{H}(\overline{r}) = -i\omega\epsilon\overline{E}(\overline{r}) + \overline{J}(\overline{r}) \tag{5.2.2}$$

we can eliminate $\overline{H}(\overline{r})$ and obtain the following equation for $\overline{E}(\overline{r})$:

$$\nabla \times \nabla \times \overline{E}(\overline{r}) - k^2\overline{E}(\overline{r}) = i\omega\mu\overline{J}(\overline{r}) \tag{5.2.3}$$

where $k^2 = \omega^2\mu\epsilon$. To determine $\overline{E}$ in terms of the given source $\overline{J}$, we introduce the use of dyadic Green's functions. A more traditional approach can be taken by making use of a vector potential.

George Green (14 July 1793 – 31 May 1841)

In 1828, George Green published 'An Essay on the Application of Mathematical Analysis to the Theories of Electricity and Magnetism', containing Green's functions and Green's theorem. The paper had only 51 subscribers. In 1833 he enrolled as an undergraduate in Gonville and Caius College, Cambridge University. In 1845 his essay of 1828 was rediscovered by William Thomson (Lord Kelvin) and republished in 1850–1854.

A Green's function characterizes the response due to a point source and is useful in expressing a field in terms of its source. Since $\overline{E}(\overline{r})$ is a vector and so is $\overline{J}(\overline{r})$, we write

$$\overline{E}(\overline{r}) = i\omega\mu \iiint d\overline{r}' \, \overline{\overline{G}}(\overline{r}, \overline{r}') \cdot \overline{J}(\overline{r}') \tag{5.2.4}$$

where $\overline{\overline{G}}(\overline{r}, \overline{r}')$ is the dyadic Green's function that enables one to determine the electric field $\overline{E}$ from a given source $\overline{J}$. The triple integration extends over the volume occupied by $\overline{J}(\overline{r}')$. Since the electric field $\overline{E}$ is a vector and the current source $\overline{J}$ is also a vector, the Green's function $\overline{\overline{G}}$ is called a dyadic operator that operates on a vector giving rise to another vector.

The dot product, or the inner product of two vectors $\overline{A} \cdot \overline{B}$ produces a scalar, and the cross product $\overline{A} \times \overline{B}$ produces a vector. A vector is also a tensor of rank one, or a first rank tensor. The Cartesian components of $\overline{A}$ are A_j. From the identity $\overline{B} \times (\overline{A} \times \overline{C}) = \overline{A}\,\overline{B} \cdot \overline{C} - \overline{B} \cdot \overline{A}\,\overline{C}$, we can identify the direct product $\overline{A}\,\overline{B}$ as a dyad $\overline{\overline{D}} = \overline{A}\,\overline{B}$. A dyad is a tensor of rank two or a second rank tensor, whose Cartesian components are $D_{jk} = A_j B_k$. The operation $\overline{\overline{D}} \cdot \overline{C}$ yields the vector $\overline{A}(\overline{B} \cdot \overline{C})$, which is the vector $\overline{A}$ weighted by the scalar $\overline{B} \cdot \overline{C}$. From $\nabla \times \nabla \times \overline{E} = \nabla\nabla \cdot \overline{E} - \nabla^2\overline{E}$, we see that $\nabla\nabla$ is now a dyadic operator.

The operation of a dyad on a vector may be thought of as a square matrix representing $\overline{\overline{G}}$ multiplying a column matrix representing $\overline{J}$, giving rise to another column matrix representing $\overline{E}$. The right-hand side of (5.2.3) can be cast in a form similar to (5.2.4) by using the three-dimensional delta function $\delta(\overline{r} - \overline{r}')$ such that

$$\overline{J}(\overline{r}) = \iiint d\overline{r}'\, \delta(\overline{r} - \overline{r}')\overline{\overline{I}} \cdot \overline{J}(\overline{r}') \qquad (5.2.5)$$

where $\overline{\overline{I}}$ is a unit dyad which can be represented by a unit diagonal matrix. The operation of $\overline{\overline{I}}$ on any vector yields the vector itself. Substituting (5.2.4) and (5.2.5) into (5.2.3) and noting that the integral holds for arbitrary $\overline{J}(\overline{r}')$, we obtain a differential equation for the dyadic Green's function $\overline{\overline{G}}(\overline{r}, \overline{r}')$

$$\nabla \times \nabla \times \overline{\overline{G}}(\overline{r}, \overline{r}') - k^2\overline{\overline{G}}(\overline{r}, \overline{r}') = \overline{\overline{I}}\delta(\overline{r} - \overline{r}') \qquad (5.2.6)$$

The interchange of the differential operator $\nabla \times \nabla \times$ and the volume integral in (5.2.4) has serious implications when $\overline{r}$ is inside the source region. Here the observation point $\overline{r}$ is always assumed to be outside the source distribution.

The dyadic Green's function can in turn be expressed in terms of a scalar Green's function $g(\overline{r}, \overline{r}')$

$$\overline{\overline{G}}(\overline{r}, \overline{r}') = \left[\overline{\overline{I}} + \frac{1}{k^2}\nabla\nabla\right] g(\overline{r}, \overline{r}') \qquad (5.2.7)$$

Here we make use of the dyadic operator $\nabla\nabla$. We introduce (5.2.7) in (5.2.6) and notice that the operator $\nabla \times \nabla \times$ yields zero when operated

on the second term in (5.2.7). Also $\nabla \times \nabla \times (\bar{\bar{I}}g) = \nabla\nabla g - \bar{\bar{I}}\nabla^2 g$. We obtain the following differential equation for $g(\bar{r},\bar{r}')$:

$$(\nabla^2 + k^2)g(\bar{r},\bar{r}') = -\delta(\bar{r}-\bar{r}') \tag{5.2.8}$$

It is seen that Green's functions are responses to point sources. We now determine the scalar Green's function $g(\bar{r},\bar{r}')$ from (5.2.8) in the spherical coordinate system.

We first translate the coordinate origin such that $\bar{r}' = 0$. We write

$$\nabla \cdot \nabla g(\bar{r}) + k^2 g(\bar{r}) = -\delta(\bar{r}) \tag{5.2.9}$$

We see that (5.2.9) and its solution for $g(\bar{r})$ are spherically symmetric and independent of θ and ϕ.

We write (5.2.9) in the spherical coordinate system

$$\frac{1}{r}\frac{d^2}{dr^2}[rg(\bar{r})] + k^2 g(\bar{r}) = -\delta(\bar{r})$$

For $r \neq 0$ the right-hand side is zero and we have

$$\frac{d^2}{dr^2}[rg(\bar{r})] + k^2 rg(\bar{r}) = 0 \tag{5.2.10}$$

The solution must represent an *outgoing* wave. We find

$$g(r) = C\frac{e^{ikr}}{r} \tag{5.2.11}$$

The constant C is determined by integrating (5.2.9) over a sphere of infinitesimal radius δ centered at the origin. In view of Gauss' theorem in vector calculus, integration of the first term of (5.2.9) yields

$$\iiint dV \, \nabla^2 g = \oiint_{r=\delta} dS \, \hat{r} \cdot \nabla g = \left[4\pi r^2 \frac{dg(\bar{r})}{dr}\right]_{r=\delta} \tag{5.2.12}$$

We obtain from (5.2.9)

$$\left[4\pi r^2 \frac{dg(\bar{r})}{dr}\right]_{r=\delta} + k^2 \int_0^\delta dr \, 4\pi r^2 g(\bar{r}) = -1 \tag{5.2.13}$$

Introducing (5.2.11) we see that in the limit of $\delta \to 0$, the second term is proportional to δ^2 and vanishes. The first term gives $-4\pi C$. Thus we find $C = 1/4\pi$.

Notice that r is the distance between the source and the observation point. Transforming back to the original coordinate system, it is seen that the distance r becomes $|\overline{r} - \overline{r}'|$. We obtain the scalar Green's function

$$g(\overline{r}, \overline{r}') = \frac{e^{ik|\overline{r}-\overline{r}'|}}{4\pi |\overline{r} - \overline{r}'|} \tag{5.2.14}$$

where $|\overline{r} - \overline{r}'|$ is the distance between the field point $\overline{r}$ and the source point $\overline{r}'$ [Fig. 5.2.1].
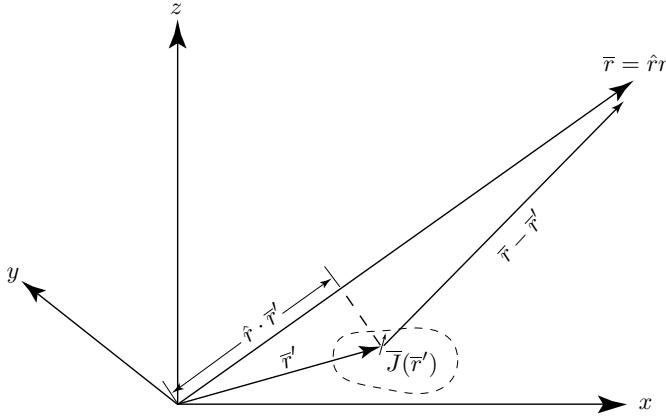
Figure 5.2.1 Observation point $\overline{r}$ is outside the source region.

We assume the observation point is outside of the source region. Substituting (5.2.7) into (5.2.4) and noting that the integration is over the primed quantities while the del operators operate only on the unprimed quantities, we can take the operators out of the integral and write

$$\overline{E}(\overline{r}) = i\omega\mu \left[\overline{\overline{I}} + \frac{1}{k^2}\nabla\nabla \right] \cdot \iiint d\overline{r}'\, g(\overline{r}, \overline{r}')\overline{J}(\overline{r}') \tag{5.2.15}$$

In terms of the scalar Green's function in spherical coordinates as determined in (5.2.14), we find

$$\overline{E}(\overline{r}) = i\omega\mu \left[\overline{\overline{I}} + \frac{1}{k^2}\nabla\nabla \right] \cdot \iiint d\overline{r}' \frac{e^{ik|\overline{r}-\overline{r}'|}}{4\pi |\overline{r} - \overline{r}'|}\overline{J}(\overline{r}') \tag{5.2.16}$$

Thus, for a prescribed source distribution $\overline{J}(\overline{r}')$ in an unbounded isotropic medium, the electric field is determined by evaluating the integral (5.2.16). The magnetic field is then calculated from Faraday's law in (5.2.1).

B. Radiation Field Approximation

When the observation point $\overline{r}$ is very far away from the source, we see from Figure 5.2.1 that the line joining the remote observation point to the origin is almost parallel to the line connecting the observation point to the source points where integration is performed. The radiation field approximation consists of the following two conditions:

$$\left| \overline{r} - \overline{r}' \right| \approx r - \hat{r} \cdot \overline{r}' \tag{5.2.17}$$

$$kr \gg 1 \tag{5.2.18}$$

In the radiation zone, the $\overline{k}$ vector is in the $\hat{r}$ direction, $\overline{k} = \hat{r} k$. We find

$$\overline{E}(\overline{r}) = i \omega \mu \left[\overline{\overline{I}} + \frac{1}{k^2} \nabla \nabla \right] \cdot \iiint d\overline{r}' \, \frac{e^{ik|\overline{r} - \overline{r}'|}}{4\pi \left| \overline{r} - \overline{r}' \right|} \overline{J}(\overline{r}')$$

$$\approx i \omega \mu \left[\overline{\overline{I}} + \frac{1}{k^2} \nabla \nabla \right] \cdot \frac{e^{ikr}}{4\pi r} \iiint d\overline{r}' \, \overline{J}(\overline{r}') e^{-i\overline{k} \cdot \overline{r}'} \tag{5.2.19}$$

In the approximation, we neglect $\hat{r} \cdot \overline{r}'$ in the denominator. The term $k\hat{r} \cdot \overline{r}'$ is kept in the exponent in (5.2.19) because its contribution to the phase variation can be significant when it is of the order of, or larger than, π.

We define a vector current moment

$$\overline{f}(\theta, \phi) = \iiint d\overline{r}' \, \overline{J}(\overline{r}') e^{-i\overline{k} \cdot \overline{r}'} \tag{5.2.20}$$

We see that the current density $\overline{J}(\overline{r}')$, weighted with the phase-retardation factor $e^{-i\overline{k} \cdot \overline{r}'}$, is integrated over the volume. Since the integrand is a function of $\overline{r}'$, the current moment after integration will be a function of θ and ϕ only and independent of the observation distance from the origin r.

The del operator ∇ in (5.2.19) can be replaced by $i\overline{k}$ in the far-field approximation. For instance, consider the gradient

$$\nabla = \hat{r} \frac{\partial}{\partial r} + \hat{\theta} \frac{1}{r} \frac{\partial}{\partial \theta} + \hat{\phi} \frac{1}{r \sin \theta} \frac{\partial}{\partial \phi}$$

The operator $\partial / \partial r$ when operated on e^{ikr} gives ik which yields a term of the order of $1/r$. All other terms of the del operator give

rise to terms of the order of $(1/r)^2$ or higher. Under the far field approximation of $kr \gg 1$, we keep only the term of the order of $1/r$ and replace the del operator by $i\overline{k} = \hat{r}ik$. The radiated electric field becomes

$$\overline{E}(\overline{r}) = i\omega\mu[\overline{\overline{I}} - \hat{r}\hat{r}] \cdot \overline{f} \frac{e^{ikr}}{4\pi r}$$

$$= i\omega\mu\frac{e^{ikr}}{4\pi r}(\hat{\theta}f_\theta + \hat{\phi}f_\phi) \tag{5.2.21}$$

The term $\overline{f}e^{ikr}/4\pi r$ is also referred to as the radiation vector. The magnetic field $\overline{H}(\overline{r})$ is, under the same far-field approximation,

$$\overline{H}(\overline{r}) = \frac{1}{i\omega\mu}\nabla \times \overline{E}(\overline{r}) = \frac{\overline{k}}{\omega\mu} \times \overline{E}(\overline{r})$$

$$= ik\frac{e^{ikr}}{4\pi r}(\hat{\phi}f_\theta - \hat{\theta}f_\phi) \tag{5.2.22}$$

The time-average Poynting's power density is

$$<\overline{S}> = \frac{1}{2}\text{Re}\left\{\overline{E} \times \overline{H}^*\right\}$$

$$= \hat{r}\frac{1}{2}\sqrt{\frac{\mu}{\epsilon}}\left(\frac{k}{4\pi r}\right)^2(|f_\theta|^2 + |f_\phi|^2) \tag{5.2.23}$$

Thus, to calculate the radiation field for a given source $\overline{J}$, the first task is to evaluate the vector current moment $\overline{f}(\theta, \phi)$.

EXAMPLE 5.2.1   Vector potential $\overline{A}$.

An alternate approach to the solution of radiation problems is by means of vector potentials. This approach is especially useful for isotropic media. Difficulties will arise when radiation occurs in non-isotropic media.

For an isotropic medium, Gauss' law $\nabla \cdot \overline{B} = \nabla \cdot \overline{\mu}\overline{H} = 0$, we write

$$\mu\overline{H} = \nabla \times \overline{A}$$

where $\overline{A}$ is the vector potential. This definition does not uniquely determine $\overline{A}$, since letting $\overline{A}' = \overline{A} + \nabla\psi$ with ψ representing any scalar function, we find $\mu\overline{H} = \nabla \times \overline{A}' = \nabla \times \overline{A} + \nabla \times \nabla\psi = \nabla \times \overline{A}$. Thus both $\overline{A}'$ and $\overline{A}$ give rise to the same $\mu\overline{H}$. To uniquely define the vector potential $\overline{A}$, we need to also specify its divergence.

From Faraday's law $\nabla \times \overline{E} = i\omega\overline{B} = \nabla \times (i\omega\overline{A})$, we write

$$\overline{E} = i\omega\overline{A} - \nabla\phi$$

where ϕ is called a scalar potential. We now specify the divergence of $\overline{A}$ by

$$\nabla \cdot \overline{A} - i\omega\mu\epsilon\phi = 0$$

The above equation is known as the Lorenz gauge condition.

From Gauss' law $\nabla \cdot \epsilon\overline{E} = \rho$, we obtain

$$\left(\nabla^2 + \omega^2\mu\epsilon\right)\phi = -\rho/\epsilon.$$

This is Helmholtz equation for the scalar potential ϕ.

From Ampère's law $\nabla \times \overline{H} = -i\omega\epsilon\overline{E} + \overline{J}$, we find $\nabla \times (\nabla \times \overline{A}) = k^2\overline{A} + i\omega\mu\epsilon\nabla\phi + \mu\overline{J} = k^2\overline{A} + \nabla\nabla \cdot \overline{A} + \mu\overline{J}$. It follows that

$$\nabla^2\overline{A} + k^2\overline{A} = -\mu\overline{J}.$$

which is Helmholtz equation for the vector potential $\overline{A}$.

Solution to this equation for the vector potential A is

$$\overline{A} = \iiint dv\, \frac{\mu\overline{J}(\overline{r}')e^{ik|\overline{r}-\overline{r}'|}}{4\pi|\overline{r}-\overline{r}'|}.$$

With this solution, we can calculate the fields

$$\overline{E} = i\omega\overline{A} + \frac{i}{\omega\mu\epsilon}\nabla(\nabla \cdot \overline{A}) = i\omega\mu\left(\overline{\overline{I}} + \frac{\nabla\nabla}{k^2}\right) \cdot \iiint d^3\overline{r}'\, \frac{e^{ik|\overline{r}-\overline{r}'|}}{4\pi|\overline{r}-\overline{r}'|}\overline{J}(\overline{r}')$$

This result is identical to (5.2.16) obtained with the dyadic Green's function approach.

— End of Example 5.2.1 —

EXAMPLE 5.2.2   Radiation condition.

For source distributions of a finite extent radiating in unbounded space, boundary conditions must be imposed at infinity to obtain unique solutions to the radiation problem. Such boundary conditions are called radiation conditions and require that solutions attenuate no slower than the inverse distance far away from the source and that the wave must propagate outward to infinity. In mathematical terms, the radiation conditions for $\overline{E}$ and $\overline{H}$ take the form

$$\lim_{r\to\infty} r[\overline{H} - \hat{r} \times \overline{E}/\eta] = 0$$

$$\lim_{r\to\infty} r[\overline{E} + \hat{r} \times \eta\overline{H}] = 0$$

(a) Show that these conditions are satisfied with the radiation fields

$$\overline{E} = i\omega\mu\frac{e^{ikr}}{4\pi r}(\hat{\theta}f_\theta + \hat{\phi}f_\phi)$$

$$\overline{H} = i\omega\mu\frac{e^{ikr}}{4\pi\eta r}(\hat{\phi}f_\theta - \hat{\theta}f_\phi)$$

where f_θ and f_ϕ are the $\hat{\theta}$ and $\hat{\phi}$ components of the vector current moment.

(b) Applying the Maxwell equations for $\overline{E}$ and $\overline{H}$, show that

$$\lim_{r\to\infty} r[\nabla \times \overline{E} - ik\hat{r} \times \overline{E}] = 0$$

$$\lim_{r\to\infty} r[\nabla \times \overline{H} - ik\hat{r} \times \overline{H}] = 0$$

and show that the radiation condition for the dyadic Green's function is

$$\lim_{r\to\infty} r[\nabla \times \overline{\overline{G}}(\overline{r},\overline{r}') - ik\hat{r} \times \overline{\overline{G}}(\overline{r},\overline{r}')] = 0$$

SOLUTION:
(a) As $r \to \infty$

$$\lim_{r\to\infty} r\left[\overline{H} - \hat{r} \times \overline{E}/\eta\right] = \lim_{r\to\infty} i\omega\mu\frac{e^{ikr}}{4\pi\eta}\left[\hat{\phi}f_\theta - \hat{\theta}f_\phi - \hat{\phi}f_\theta + \hat{\theta}f_\phi\right] = 0$$

$$\lim_{r\to\infty} r\left[\overline{E} + \hat{r} \times \eta\overline{H}\right] = \lim_{r\to\infty} i\omega\mu\frac{e^{ikr}}{4\pi}\left[\hat{\theta}f_\theta + \hat{\phi}f_\phi - \hat{\theta}f_\theta - \hat{\phi}f_\phi\right] = 0$$

(b)

$$\lim_{r\to\infty} r\left[\nabla \times \overline{E} - ik\hat{r} \times \overline{E}\right] = i\omega\mu \lim_{r\to\infty} r\left[\overline{H} - \hat{r} \times \overline{E}/\eta\right] = 0$$

$$\lim_{r\to\infty} r\left[\nabla \times \overline{H} - ik\hat{r} \times \overline{H}\right] = -i\omega\epsilon \lim_{r\to\infty} r\left[\overline{E} + \hat{r} \times \eta\overline{H}\right] = 0$$

$$0 = \lim_{r\to\infty} r\left[\nabla \times \overline{E} - ik\hat{r} \times \overline{E}\right]$$

$$= i\omega\mu \iiint d\overline{r}' \left\{\lim_{r\to\infty} r\left[\nabla \times \overline{\overline{G}}(\overline{r},\overline{r}') - ik\hat{r} \times \overline{\overline{G}}(\overline{r},\overline{r}')\right]\right\} \cdot \overline{J}(\overline{r}')$$

for arbitrary $\overline{J}(\overline{r}')$ of finite extent. Therefore

$$\lim_{r\to\infty} \left[\nabla \times \overline{\overline{G}}(\overline{r},\overline{r}') - ik\hat{r} \times \overline{\overline{G}}(\overline{r},\overline{r}')\right] = 0$$

<div align="right">— END OF EXAMPLE 5.2.2 —</div>

For spherically symmetric $g(r)$, the Laplacian operator

$$\nabla \cdot \nabla g(\bar{r}) = (\frac{\partial^2}{\partial x^2} + \frac{\partial^2}{\partial y^2} + \frac{\partial^2}{\partial z^2})g(r)$$

$$\frac{\partial^2}{\partial x^2}g(r) = \frac{\partial}{\partial x}(\frac{\partial r}{\partial x}\frac{\partial g(r)}{\partial r}) = \frac{\partial}{\partial x}(\frac{x}{r}\frac{\partial g(r)}{\partial r}) = \frac{1}{r}\frac{\partial g(r)}{\partial r} + x\frac{x}{r}\frac{\partial}{\partial r}(\frac{1}{r}\frac{\partial g(r)}{\partial r})$$

$$= \frac{1}{r}\frac{\partial g(r)}{\partial r} + \frac{x^2}{r}(\frac{-1}{r^2}\frac{\partial g(r)}{\partial r} + \frac{1}{r}\frac{\partial^2 g(r)}{\partial r^2})$$

We thus have

$$\nabla \cdot \nabla g(r) = \frac{3}{r}\frac{\partial g(r)}{\partial r} + r(\frac{-1}{r^2}\frac{\partial g(r)}{\partial r} + \frac{1}{r}\frac{\partial^2 g(r)}{\partial r^2}) = \frac{2}{r}\frac{\partial g(r)}{\partial r} + \frac{\partial^2 g(r)}{\partial r^2}$$

$$= \frac{1}{r^2}\frac{\partial}{\partial r}(r^2\frac{\partial g(r)}{\partial r}) \tag{5.2.24}$$

$$= \frac{1}{r}\frac{\partial^2}{\partial r^2}[rg(r)] \tag{5.2.25}$$

The Laplacian operator for spherically symmetric functions can be written either in the form of (5.2.24) or in the form of (5.2.25).

Problems

P5.2.1

What is the differential equation that governs the one-dimensional scalar Green's function in free space $g(x, x')$? Show that Green's function is

$$g(x, x') = \frac{ie^{ik|x-x'|}}{2k}$$

P5.2.2

Show that the two-dimensional Green's function is

$$g(\rho) = \frac{i}{4}H_o^{(1)}(k\rho) = \frac{i}{4\pi}\int_{-\infty}^{\infty}dk_x\frac{e^{ik_x x+ik_y|y|}}{k_y}$$

P5.2.3

Show that the three-dimensional Green's function is

$$g(r) = \frac{e^{ikr}}{4\pi r} = \frac{i}{8\pi^2}\int_{-\infty}^{\infty}\int_{-\infty}^{\infty}dk_x dk_y\frac{e^{ik_x x+ik_y y+ik_z|z|}}{k_z}$$

5.3   Hertzian Dipoles

A. Hertzian Electric Dipole

The most fundamental model for radiating structures is a Hertzian electric dipole which consists of a current-carrying element with an infinitesimal length l. Denoting the current dipole moment with Il, the current density $\overline{J}(\overline{r})$ of a Hertzian dipole pointing in the $\hat{z}$ direction and located at the origin [Fig. 5.3.1] is

$$\overline{J}(\overline{r}') = \hat{z} Il\, \delta(\overline{r}') \tag{5.3.1}$$

A Hertzian dipole can be modeled as two charge reservoirs of equal and opposite charge q and separated by an infinitesimal distance l. One may think of two conducting spheres or a capacitor connected by a constant current source. The dipole has moment $p = ql$ and oscillates in time with angular frequency ω. The current dipole moment is thus $Il = -i\omega p$.

To determine the radiation field of the Hertzian dipole, we insert (5.3.1) into (5.2.20) and find the vector current moment to be

$$\overline{f}(\theta, \phi) = \hat{z} Il = (\hat{r}\cos\theta - \hat{\theta}\sin\theta)\, Il \tag{5.3.2}$$

Noticing that $f_\theta = -Il\sin\theta$, we obtain from (5.2.21)–(5.2.22) the electric and magnetic field vectors
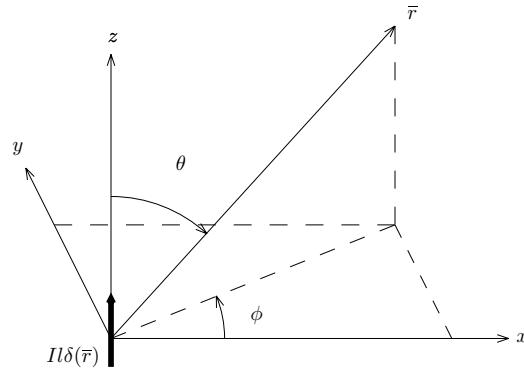
Figure 5.3.1 Hertzian electric dipole.

$$\overline{E}(\overline{r}) = \hat{\theta}\, i\omega\mu\, \frac{e^{ikr}}{4\pi r} f_\theta = -\hat{\theta}\, i\omega\mu Il\, \frac{e^{ikr}}{4\pi r}\sin\theta \qquad (5.3.3)$$

$$\overline{H}(\overline{r}) = \hat{\phi}\, ik\, \frac{e^{ikr}}{4\pi r} f_\theta = -\hat{\phi}\, ikIl\, \frac{e^{ikr}}{4\pi r}\sin\theta \qquad (5.3.4)$$
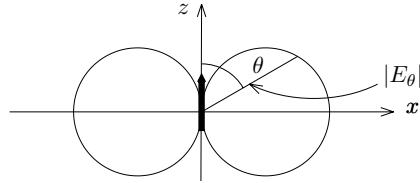
Figure 5.3.2 Radiation field pattern.

and from (5.2.23) the time-average Poynting's power density

$$<\overline{S}> = \hat{r}\frac{1}{2}\sqrt{\frac{\mu}{\epsilon}}\left(\frac{kIl}{4\pi r}\right)^2\sin^2\theta \qquad (5.3.5)$$

The total radiated power P_r is calculated by integrating $\hat{r}\,\cdot<\overline{S}>$ over a sphere of radius r with $r \to \infty$. We obtain

$$P_r = \int_0^{2\pi} d\phi \int_0^{\pi} d\theta\, r^2\sin\theta < S_r > = \frac{4\pi}{3}\eta\left[\frac{kIl}{4\pi}\right]^2 \qquad (5.3.6)$$

The directive gain $G(\theta,\phi)$ is defined as the power density $S_r(\theta,\phi)$ at observation angles (θ,ϕ) divided by the total radiated power averaged over all angles, which gives

$$G(\theta,\phi) = \frac{<S_r(\theta,\phi)>}{P_r/4\pi r^2} = \frac{3}{2}\sin^2\theta \qquad (5.3.7)$$

The directivity D of an antenna is defined to be the gain at the angle where it is maximum. For the Hertzian dipole,

$$D = G(\theta,\phi)_{\max} = \frac{3}{2} \qquad (5.3.8)$$

which occurs at $\theta = \pi/2$, that is perpendicular to the dipole axis.
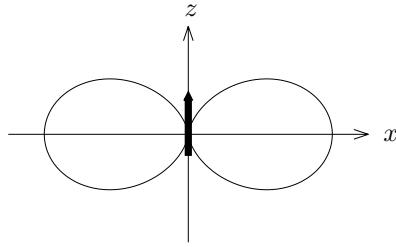
Figure 5.3.3 Radiation power pattern.

A radiation field pattern can be sketched for the magnitude of $|E_\theta|$ at a constant distance r as a function of the angle θ [Fig. 5.3.2]. The pattern consists of two circles describing $\sin\theta$ and is symmetrical about the z axis. The power pattern or the gain pattern is seen to be proportional to $\sin^2\theta$. As shown in Figure 5.3.3, it is in the form of a horizontal "figure eight" in any plane containing the dipole axis.

We now derive the exact expressions for the electric field vector $\overline{E}(\overline{r})$ for an Hertzian dipole with

$$\overline{J}(\overline{r}') = \overline{I}\, l\delta(\overline{r}')$$

We find, noting that $(\overline{I}l \cdot \nabla)\overline{r} = \overline{I}l$,

$$\overline{E}(\overline{r}) = i\omega\mu \left[\overline{\overline{I}} + \frac{1}{k^2}\nabla\nabla\right] \cdot \overline{I}l\frac{e^{ikr}}{4\pi r}$$

$$= i\omega\mu \left[\overline{I}l + \frac{1}{k^2}(\overline{I}l \cdot \nabla)\nabla\right] \frac{e^{ikr}}{4\pi r}$$

$$= i\omega\mu \left[\overline{I}l\frac{e^{ikr}}{4\pi r} + (\overline{I}l \cdot \nabla)\hat{r}[\frac{i}{kr} + (\frac{i}{kr})^2]\frac{e^{ikr}}{4\pi}\right]$$

$$= i\omega\mu \left[\overline{I}l\frac{e^{ikr}}{4\pi r} + \frac{1}{r}[\frac{i}{kr} + (\frac{i}{kr})^2]\frac{e^{ikr}}{4\pi}(\overline{I}l \cdot \nabla)\overline{r}\right.$$

$$\left. +\overline{r}(\overline{I}l \cdot \nabla)\frac{1}{r}[\frac{i}{kr} + (\frac{i}{kr})^2]\frac{e^{ikr}}{4\pi}\right]$$

$$= i\omega\mu \left[\overline{I}l\,[1 + \frac{i}{kr} + (\frac{i}{kr})^2] - \hat{r}(\hat{r} \cdot \overline{I}l)[1 + 3\frac{i}{kr} + 3(\frac{i}{kr})^2]\right] \frac{e^{ikr}}{4\pi r}$$

$$(5.3.9)$$

$$\overline{H}(\overline{r}) = \frac{1}{i\omega\mu}\nabla \times \overline{E} = \nabla \times \overline{I}l\,\frac{e^{ikr}}{4\pi r} = ik\hat{r} \times \overline{I}l\left[1 + \frac{i}{kr}\right]\frac{e^{ikr}}{4\pi r} \quad (5.3.10)$$

$$\overline{S}(\overline{r}) = \overline{E} \times \overline{H}^* = \eta \left[\frac{k}{4\pi r} \right]^2 \left\{ \hat{r}(Il)^2 (1 + \frac{i}{k^3 r^3}) \right.$$

$$\left. - \hat{r}(\hat{r} \cdot \overline{Il})^2 \left[1 + \frac{2i}{kr} + \frac{3i}{k^3 r^3} \right] + (\hat{r} \cdot \overline{Il}) \overline{Il} \left[\frac{2i}{kr} + \frac{2i}{k^3 r^3} \right] \right\} \quad (5.3.11)$$

$$< \overline{S}(\overline{r}) > = \frac{1}{2} \text{Re}\{\overline{E} \times \overline{H}^*\} = \eta \left[\frac{k}{4\pi r} \right]^2 \left\{ \hat{r}(Il)^2 - \hat{r}(\hat{r} \cdot \overline{Il})^2 \right\} \quad (5.3.12)$$

For a Hertzian dipole in the $\hat{z}$ direction, the electric and magnetic fields are

$$\overline{E}(\overline{r}) = \frac{i\omega\mu e^{ikr}}{4\pi r} Il \left\{ \hat{z} \left(1 + \frac{i}{kr} - \frac{1}{k^2 r^2} \right) + \hat{r} \frac{z}{r} \left[-1 - \frac{3i}{kr} + \frac{3}{k^2 r^2} \right] \right\}$$

$$= -\frac{i\omega\mu e^{ikr}}{4\pi r} Il \left\{ \hat{r} \left[\frac{i}{kr} + \left(\frac{i}{kr} \right)^2 \right] 2\cos\theta + \hat{\theta} \left[1 + \frac{i}{kr} + \left(\frac{i}{kr} \right)^2 \right] \sin\theta \right\}$$

$$(5.3.13)$$

$$\overline{H}(\overline{r}) = -\hat{\phi} \, ikIl \frac{e^{ikr}}{4\pi r} \left[1 + \frac{i}{kr} \right] \sin\theta \quad (5.3.14)$$

The magnetic fields are in the $\hat{\phi}$ direction circulating the dipole. The complex Poynting power density is

$$\overline{S} = \overline{E} \times \overline{H}^*$$

$$= \eta \left[\frac{kIl}{4\pi r} \right]^2 \left\{ \hat{r} \left[1 - \left(\frac{i}{kr} \right)^3 \right] \sin^2\theta - \hat{\theta} \left[\left(\frac{i}{kr} \right) - \left(\frac{i}{kr} \right)^3 \right] \sin 2\theta \right\} \quad (5.3.15)$$

The time-average Poynting power density is

$$< \overline{S} > = \frac{1}{2} \text{Re}\{\overline{S}\} = \hat{r} \frac{\eta}{2} \left[\frac{kIl}{4\pi r} \right]^2 \sin^2\theta$$

which is identical to that obtained in (5.3.5).

When the observation point is very far away from the dipole such that $kr \gg 1$, we can neglect the terms of order higher than $1/kr$ as compared with unity. From (5.3.13) and (5.3.14), we find the electric and magnetic field vectors $\overline{E}$ and $\overline{H}$ in the radiation zone reduce to (5.3.3) and (5.3.4).

B. Hertzian Magnetic Dipole and Small Loop Antenna

Consider a small current loop with an infinitesimally small radius a as shown in Figure 5.3.4. Its current density takes the form

$$
\begin{aligned}
\overline{J}(\overline{r}') &= \hat{\phi} I \delta(\rho' - a)\delta(z') \\
&= (-\hat{x}\sin\phi' + \hat{y}\cos\phi')I\delta(\rho' - a)\delta(z')
\end{aligned}
\qquad (5.3.16)
$$
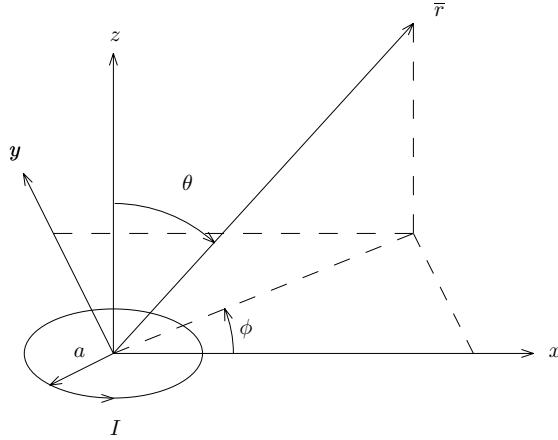
Figure 5.3.4 Small loop antenna.

The electric field vector due to the current loop, is calculated from

$$
\begin{aligned}
\overline{E}(\overline{r}) &= i\omega\mu\left[\overline{\overline{I}} + \frac{1}{k^2}\nabla\nabla\right]\cdot\iiint d\overline{r}'\,\frac{e^{ik|\overline{r}-\overline{r}'|}}{4\pi\,|\overline{r}-\overline{r}'|}\overline{J}(\overline{r}') \\
&= i\omega\mu\left[\overline{\overline{I}} + \frac{1}{k^2}\nabla\nabla\right]\cdot\int_0^{2\pi}d\phi'\int_0^\infty d\rho'\int_{-\infty}^\infty \rho'dz'\,\frac{e^{ik|\overline{r}-\overline{r}'|}}{4\pi\,|\overline{r}-\overline{r}'|}\overline{J}(\overline{r}') \\
&= i\omega\mu\left[\overline{\overline{I}} + \frac{1}{k^2}\nabla\nabla\right]\cdot\int_0^{2\pi}ad\phi'\,\frac{e^{ik|\overline{r}-\overline{r}'|}}{4\pi\,|\overline{r}-\overline{r}'|}\left(-\hat{x}\sin\phi' + \hat{y}\cos\phi'\right)I
\end{aligned}
$$
$$
(5.3.17)
$$

where in terms of their Cartesian components, the radial vectors $\overline{r}$ and $\overline{r}'$ are

$$
\begin{aligned}
\overline{r} &= \hat{x}\,r\sin\theta\cos\phi + \hat{y}\,r\sin\theta\sin\phi + \hat{z}\,r\cos\theta \\
\overline{r}' &= \hat{x}\,a\cos\phi' + \hat{y}\,a\sin\phi'
\end{aligned}
$$

The distance $|\overline{r} - \overline{r}'|$ from observation point $\overline{r}$ to source point $\overline{r}'$ is

$$\left|\overline{r}-\overline{r}'\right| = \left|\hat{x}(r\sin\theta\cos\phi - a\cos\phi') + \hat{y}(r\sin\theta\sin\phi - a\sin\phi') + \hat{z}r\cos\theta\right|$$

$$= r\sqrt{1 + \frac{a^2}{r^2} - \frac{2a}{r}\sin\theta\cos(\phi - \phi')} \tag{5.3.18}$$

We then expand the scalar Green's function in the form of a MacLaurin series for $a/r \to 0$. Taking the first two terms, we have

$$\frac{e^{ik|\overline{r}-\overline{r}'|}}{4\pi\,|\overline{r}-\overline{r}'|} \approx \frac{e^{ikr}}{4\pi r} + \frac{a}{r}\left[\frac{d}{d(\frac{a}{r})}\frac{e^{ik|\overline{r}-\overline{r}'|}}{4\pi\,|\overline{r}-\overline{r}'|}\right]_{a/r\to 0}$$

$$= \frac{e^{ikr}}{4\pi r} + \frac{a}{4\pi r}\left[\frac{(ik\,|\overline{r}-\overline{r}'|-1)e^{ik|\overline{r}-\overline{r}'|}}{|\overline{r}-\overline{r}'|^2}\frac{d}{d(\frac{a}{r})}|\overline{r}-\overline{r}'|\right]_{a/r\to 0}$$

$$= \frac{e^{ikr}}{4\pi r} + \frac{a}{r}(-ikr+1)\sin\theta\cos(\phi - \phi')\frac{e^{ikr}}{4\pi r} \tag{5.3.19}$$

Colin Maclaurin (February 1698 – 14 June 1746)

In 1742 Maclaurin published his 2 volume Treatise of fluxions. The Treatise of fluxions is a major work of 763 pages. It is in the Treatise of fluxions that Maclaurin uses the special case of Taylor's series now named after him. The Maclaurin series was not an idea discovered independently of the more general result of Taylor for Maclaurin acknowledges Taylor's contribution.

The integral in (5.3.17) for the electric field is evaluated using (5.3.19), we find

$$\int_0^{2\pi} a\,d\phi'(-\hat{x}\sin\phi' + \hat{y}\cos\phi')\frac{Ie^{ik|\overline{r}-\overline{r}'|}}{4\pi\,|\overline{r}-\overline{r}'|}$$

$$= (-\hat{x}\sin\phi + \hat{y}\cos\phi)\frac{\pi a^2 Ie^{ikr}}{4\pi r^2}(1-ikr)\sin\theta$$

$$= \hat{\phi}\frac{I\pi a^2 e^{ikr}}{4\pi r^2}(1-ikr)\sin\theta \tag{5.3.20}$$

Substituting the above result back into (5.3.17) and noticing that (5.3.20) is independent of ϕ, we see that the del operator $\nabla\nabla$ does not contribute.

The electric field vector becomes, letting $M = I\pi a^2$,

$$\overline{E} = \hat{\phi}\,\omega\mu k M \frac{e^{ikr}}{4\pi r}\left[1 + \frac{i}{kr}\right]\sin\theta \qquad (5.3.21)$$

The magnetic field vector is

$$\overline{H}(\overline{r}) = \frac{1}{i\omega\mu}\nabla \times \overline{E}(\overline{r})$$

$$= -k^2 M \frac{e^{ikr}}{4\pi r}\left\{\hat{r}\left[\frac{i}{kr} + \left(\frac{i}{kr}\right)^2\right]2\cos\theta + \hat{\theta}\left[1 + \frac{i}{kr} + \left(\frac{i}{kr}\right)^2\right]\sin\theta\right\}$$

$$(5.3.22)$$

We identify $M = I\pi a^2 = IA$ as the magnetic dipole moment of the current loop. The small current loop is also called a Hertzian magnetic dipole.

To summarize the exact expressions of electromagnetic fields produced by both an electric and a magnetic dipole, we let the electric current moment and the magnetic moment be in a general direction.

$$\overline{E}(\overline{r}) = \frac{i\omega\mu e^{ikr}}{4\pi r}\left\{\overline{I}l\left(1 + \frac{i}{kr} - \frac{1}{k^2 r^2}\right) - \hat{r}(\hat{r}\cdot\overline{I}l)\left[1 + \frac{3i}{kr} - \frac{3}{k^2 r^2}\right]\right\}$$

$$(5.3.23)$$

$$\overline{H}(\overline{r}) = \hat{r} \times \overline{I}l\frac{ike^{ikr}}{4\pi r}\left[1 + \frac{i}{kr}\right] \qquad (5.3.24)$$

Applying duality, we find the electric and magnetic fields for a magnetic dipole to be

$$\overline{E}(\overline{r}) = -\hat{r} \times \overline{M}\frac{\omega\mu k e^{ikr}}{4\pi r}\left[1 + \frac{i}{kr}\right] \qquad (5.3.25)$$

$$\overline{H}(\overline{r}) = \frac{k^2 e^{ikr}}{4\pi r}\left\{\overline{M}\left(1 + \frac{i}{kr} - \frac{1}{k^2 r^2}\right) - \hat{r}(\hat{r}\cdot\overline{M})\left[1 + \frac{3i}{kr} - \frac{3}{k^2 r^2}\right]\right\}$$

$$(5.3.26)$$

We observe the duality of electric and magnetic dipoles with the replacement of $\overline{E} \to \overline{H}$, $\overline{H} \to -\overline{E}$, $\mu \to \epsilon$, $\epsilon \to \mu$, $Il = -i\omega\overline{P} \to -i\omega\mu M$, and $i\omega\mu M \to \overline{I}l = -i\omega P$.

This follows from the duality principle $\overline{E} \to \overline{H}$, $\overline{H} \to -\overline{E}, \mu \to \epsilon, \epsilon \to \mu, \overline{D} \to \overline{B}, \overline{B} \to -\overline{D}$ with $\overline{D} = \epsilon\overline{E} + \overline{P}$, $\overline{B} = \mu\overline{H} + \mu\overline{M}$ and $\overline{Il} = -i\omega\overline{P} \to -i\omega\mu\overline{M}$, and $i\omega\mu\overline{M} \to -i\omega\overline{P} = \overline{Il}$.

When the magnetic dipole is in $\hat{z}$-direction, (5.3.25) and (5.3.26) reduce to (5.3.21) and (5.3.22).

Note: The correspondence between the electric and magnetic dipoles can be quantified by letting the Hertzian dipole moment Il to be

$$(Il)_e = (ikIA)_m \tag{5.3.27}$$

where the subscripts e and m are used to denote the electric dipole and the current loop, respectively. The solution for a small current loop in (5.3.21) and (5.3.22) can be obtained from the solutions for electric dipoles by letting

$$\overline{E}_m = \eta\overline{H}_e \tag{5.3.28}$$

$$\overline{H}_m = -\frac{\overline{E}_e}{\eta} \tag{5.3.29}$$

Such relations as illustrated in (5.3.28)–(5.3.29) depict the duality principle. What we have shown is that the complete solution for a small current loop, including both near and far fields, is the dual of that for a Hertzian electric dipole. A small loop can thus be regarded as a magnetic dipole that is the dual of an electric dipole.

Problems

P5.3.1

Derive the instantaneous electric and magnetic fields from the solutions in (5.3.13) and (5.3.14), we multiply (5.3.13) and (5.3.14) by $e^{-i\omega t}$ and take the real part.

P5.3.2

Consider the following two Hertzian dipoles as shown in Fig. P5.3.2.1 driven at an angular frequency ω and with the same dipole moment. The first dipole is located at the origin $(0,0,0)$ and oriented in the $\hat{y}$ direction. The second dipole is located at $(0,0,-3\lambda/4)$ and oriented in the $\hat{x}$ direction.
(a) Give the expression for the vector current moment $\overline{f}(\theta,\phi)$.
(b) Show that in the far field the electric field is given by

$$\overline{E} = \eta_0 \frac{ikI_0\ell}{4\pi r} e^{ikr} \left\{ \hat{\phi}\left[\cos\phi - \sin\phi e^{i\frac{3\pi}{2}\cos\theta}\right] + \hat{\theta}\cos\theta\left[\sin\phi + \cos\phi e^{i\frac{3\pi}{2}\cos\theta}\right] \right\}$$
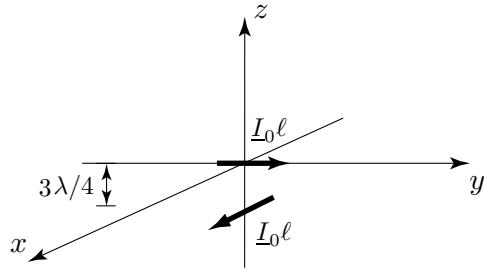
Figure P5.3.2.1

(c) Give all directions (θ, ϕ) for which the wave is right-hand circularly polarized.

(d) Give all directions (θ, ϕ) for which the wave is left-hand circularly polarized.

(e) Give all directions (θ, ϕ) for which the wave is linearly polarized.

P5.3.3

A *turnstile* antenna consists of two Hertzian dipoles positioned at right angles to each other with constant current distributions given by

$$\overline{J}_1 = \hat{x} I l \delta(\overline{r}) \qquad \text{and} \qquad \overline{J}_2 = \hat{y} i I l \delta(\overline{r})$$

respectively.

(a) Show that the electric field produced by this antenna is

$$\overline{E} = -\eta \frac{ik I l e^{ikr}}{4\pi r} e^{i\phi} \left\{ \hat{r} \left[\frac{i}{kr} + \left(\frac{i}{kr} \right)^2 \right] 2\sin\theta \right.$$
$$\left. - \hat{\theta} \left[1 + \frac{i}{kr} + \left(\frac{i}{kr} \right)^2 \right] \cos\theta - \hat{\phi} i \left[1 + \frac{i}{kr} + \left(\frac{i}{kr} \right)^2 \right] \right\}$$

(b) Find the total electric field in the far-field $(k_\rho \gg 1)$ in the x-y plane with $\theta = \pi/2$. Show that the real space-time dependence of the electric field is of the form $\cos(\omega t - \phi - k_\rho \rho)$. Note that

$$\hat{x} = \hat{r} \cos\phi \sin\theta - \hat{\phi} \sin\phi + \hat{\theta} \cos\phi \cos\theta$$
$$\hat{y} = \hat{r} \sin\phi \sin\theta + \hat{\phi} \cos\phi + \hat{\theta} \sin\phi \cos\theta$$

What is the polarization of the radiated wave in the x-y plane?

(c) Find the radiation power pattern in the x-y plane.

(d) Find the total radiated electric field on the z axis. What is the polarization of the radiated wave in the $\hat{z}$ direction?

(e) Calculate the power density radiated in the $+\hat{z}$ direction in the far field and compare it with the radiated power density in the $+\hat{x}$ direction.

P5.3.4

Consider a nucleus with magnetic moment $\overline{M}$ placed in a dc magnetic field $\overline{B}_0$. The classical equation of motion for $\overline{M}$ is

$$\frac{d\overline{M}}{dt} = \gamma \overline{M} \times \overline{B}$$

where γ is the gyromagnetic ratio.

(a) Let $\overline{M} = M_0(-\hat{x}\cos\omega t + \hat{y}\sin\omega t)$. Find the static magnetic field $\overline{B}$ in terms of the frequency ω and the gyromagnetic ratio γ.
(b) Let the nucleus be placed at the origin (at $\overline{r} = 0$). Find the magnetic field produced by $\overline{M}$ on the z-axis at $z = d$.
(c) A pick-up coil with a very small radius R is placed at the z-axis with the center at $z = d$. Let the plane of the coil be parallel to the yz-plane and assume that the magnetic field linking the area $A = \pi R^2$ of the loop is uniform. Find the induced voltage on the pick-up coil.

P5.3.5

In magnetic resonance imaging (MRI) applications, assume the magnetic moment of a nucleus is $\overline{M} = M_0(\hat{x}\cos\omega t + \hat{y}\sin\omega t)$, where the angular Larmor frequency $\omega = \gamma B_0$ and the static magnetic field B_0 is in the $\hat{z}$ direction.

(a) Show that the magnetic field produced by the spinning nucleus in the vicinity of the nucleus is

$$\overline{H}(\overline{r}) = \frac{1}{4\pi r^3}\left\{-\overline{M} + 3\hat{r}(\hat{r}\cdot\overline{M})\right\}$$

(b) Find the x-component of the time-varying magnetic field linking a pickup coil placed on the y-z plane at a distance $x = d$ with its center lined up with the x-axis. The induced voltage (magnetomotive force) on the pick-up coil can be determined using the following formula

$$V = -\frac{\partial}{\partial t}\int_A da\, B_x(\overline{r}, t)$$

Show that the induced voltage on the pick-up coil has the form

$$V = U(\omega)\sin\omega t$$

Find the coefficient $U(\omega)$. Why a large static magnetic field B_0 is needed to obtain large induced voltage on the pick-up coil?
(c) Consider two magnetic dipoles with the same gyromagnetic ratio γ placed on the z-axis with separation δ. Assume that the two magnetic dipoles are close to the origin so that the induced voltage due to each

one can be approximated by $V_i = U(\omega_i) \sin \omega_i t$ $(i = 1, 2)$. Using a radio-frequency (RF) pick-up coil, the Larmor frequency ω_i can be measured accurately. Let $\omega_1 - \omega_2 = \Delta\omega$. Find the difference of the static magnetic field B_0 acting on the two magnetic dipole moments in terms of $\Delta\omega$ and γ.

(d) Let the static magnetic field be $\overline{B}_0 = \hat{z}(b_0 + b_1 z)$ and the difference of the Larmor frequencies be $\omega_1 - \omega_2 = \Delta\omega$. Find the separation δ of the two magnetic dipole moments in terms of $\Delta\omega$, γ, and b_1.

(e) Assume that magnetic dipoles are spinning protons of water at room temperature, and gyromagnetic ratio of proton is $\gamma = 2.7 \times 10^8 \, \text{T}^{-1}\text{s}^{-1}$. Let the two protons locate on the z-axis. The applied static magnetic field is $\overline{B} = \hat{z}(b_0 + b_1 z)$, where $b_0 = 1.0 \, \text{T}$ and $b_1 = 1.0 \, \text{T/m}$. Find the frequency resolution in kHz of the pick-up coil to measure the two protons with separation $\delta = 0.5 \, \text{mm}$ on the z-axis.

P5.3.6

In Magnetic Resonance Imaging (MRI) study, it is very useful to define a rotating frame of reference which rotates about the z axis at the Larmor frequency ($\omega_0 = \gamma B_0$, γ is the gyromagnetic ratio). Consider the bulk magnetic moment $M_0\hat{z}$ placed in a DC magnetic field $B_0\hat{z}$. When a MRI transmitting coil generates a magnetic field of frequency ω_1, effective total magnetic field can be described as

$$\overline{B} = B_0\hat{z} + B_1(\hat{x}\cos\omega_1 t - \hat{y}\sin\omega_1 t)$$

And the rotating coordinate can be defined as

$$\hat{x}' = \hat{x}\cos\omega_1 t - \hat{y}\sin\omega_1 t$$
$$\hat{y}' = \hat{x}\sin\omega_1 t + \hat{y}\cos\omega_1 t$$
$$\hat{z}' = \hat{z}$$

The classical equation of motion for $\overline{M}$ is

$$\frac{d\overline{M}}{dt} = \gamma\overline{M} \times \overline{B}$$

(a) Show that when $\omega_1 \neq \omega_0$ (called "off resonance"), magnetic moment $\overline{M}$ will precess about the ($B_1\hat{x}' + \Delta B_0\hat{z}'$) axis, where $\Delta B_0 = (\omega_0 - \omega_1)/\gamma$.

(b) Show that when $\omega_1 = \omega_0 = \gamma B_0$ (called "on resonance"), magnetic moment $\overline{M}$ will respond to this B_1 field as a rotation about the x' axis in the rotating frame.

P5.3.7

(a) In MRI, the resonance frequency (Larmor frequency) ω_0 of a spin particle is related to the magnetic field B_0 by gyromagnetic ratio, $\omega_0 = \gamma B_0$. [1]H nucleus has two spin states. The energy of the photon needed to cause a transition between the two spin states of ^{1}H nucleus in a 1.5 T magnetic field is 4.2346×10^{-26} J. What is the gyromagnetic ration of [1]H?

(Note that the energy E of a photon at frequency ω is $E = \hbar\omega$, where $\hbar = 6.63 \times 10^{-34}/(2\pi)\,\text{J} \cdot \text{s/rad}$.)

(b) A sample contains two small distinct water locations where there is ^{1}H spin density. In a uniform field, each of the ^{1}H has the same Larmor frequency. However, if a linear gradient G_x is superimposed on the main magnetic filed B_0, the Larmor frequency will depend on position along the x axis. $\omega = \gamma(B_0 + xG_x) = \omega_0 + \gamma xG_x$. The MRI spectrum contains frequencies of $63.8717\,\text{MHz}$ and $63.8666\,\text{MHz}$ when B_0 is 1.5 T and $G_x = 1 \times 10^{-2}\,\text{T/m}$. What are the locations of the water?

P5.3.8

In MRI, it is required to generate a uniform $\overline{B}$ field in the vicinity of a certain point. Helmholtz coil, as shown in Figure P5.3.8.1, can realize this. The two identical circular loops of radius a, separated by distance d, carry the same current I in the same direction.
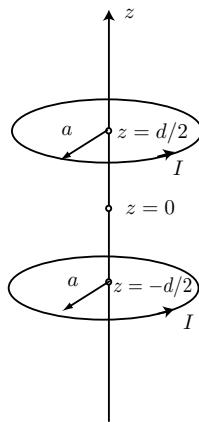
Figure P5.3.8.1

(a) Show the magnetic field along the z-axis is

$$B_z = \frac{\mu_0 I a^2}{2\left[(d/2 - z)^2 + a^2\right]^{\frac{3}{2}}} + \frac{\mu_0 I a^2}{2\left[(d/2 + z)^2 + a^2\right]^{\frac{3}{2}}}$$

(b) Show when $d = a$, the B_z is most uniform in the vicinity of $z = 0$, i.e., $\frac{dB_z}{dz} = 0$ and $\frac{d^2B_z}{d^2z} = 0$ at $z = 0$.

(c) Plot the $B_z(z)$ when $d = a = 5\,\text{cm}$ and $I = 2\,\text{A}$ for $-\frac{d}{2} \le z \le \frac{d}{2}$.

5.4   Linear Dipole Arrays

A. Uniform Array Antenna with Progressive Phase Shift

Consider an array of N elements, pointing in the $\hat{z}$ direction and placed along the x axis with equal spacing d [Fig. 5.4.1]. Each element has a progressive phase shift α relative to its adjacent element. The current density $\overline{J}(\overline{r}')$ takes the form

$$\overline{J}(\overline{r}') = \hat{z}Il \sum_{n=0}^{N-1} e^{in\alpha}\delta(x' - nd)\delta(y')\delta(z') \qquad (5.4.1)$$
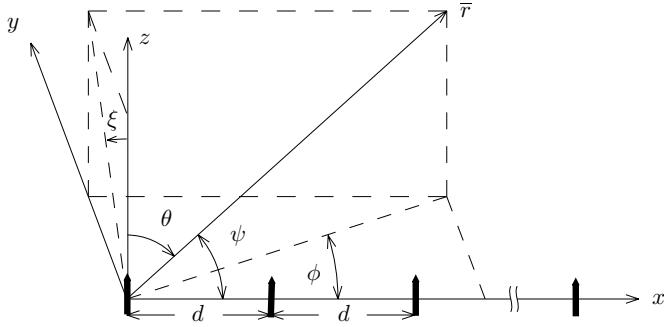
Figure 5.4.1   Linear antenna arrays.

The vector current moment is calculated to be

$$\overline{f}(\theta, \phi) = \int dx' \int dy' \int dz' \, \overline{J}(\overline{r}')e^{-ik(x'\sin\theta\cos\phi+y'\sin\theta\sin\phi+z'\cos\theta)}$$

$$= \hat{z}Il \sum_{n=0}^{N-1} e^{-in(kd\sin\theta\cos\phi-\alpha)} \qquad (5.4.2)$$

The electric field $\overline{E}$ in the radiation zone is, with $\cos\psi = \sin\theta\cos\phi$ and ψ is the angle between the x axis and the position vector $\overline{r}$ [Fig. 5.4.1],

$$E_\theta = -i\omega\mu\frac{Ile^{ikr}}{4\pi r}\sin\theta\left[\sum_{n=0}^{N-1} e^{-in(kd\cos\psi-\alpha)}\right] = -i\omega\mu\frac{Ile^{ikr}}{4\pi r}\sin\theta\, F(u)$$

$$(5.4.3)$$

The factor in front of the square bracket in (5.4.3) is seen to be the radiation field of the individual Hertzian dipoles. The group behavior of the array is governed by the summation term known as the array factor $F(u)$,

$$F(u) = \sum_{n=0}^{N-1} e^{-inu} \qquad (5.4.4)$$

where

$$u = kd\cos\psi - \alpha \qquad (5.4.5)$$

The summation in the array factor is easily carried out and yields the magnitude of $F(u)$

$$|F(u)| = \left| \frac{\sin(Nu/2)}{\sin(u/2)} \right| \qquad (5.4.6)$$

The magnitude of the array factor $|F(u)|$ forms a periodic pattern in u, and is plotted in Figure 5.4.2 for $N = 5$.

The part of the radiation pattern that is physically observed is determined from (5.4.5) for ψ between 0 and π which corresponds to going from the $+\hat{x}$ direction to the $-\hat{x}$ direction. This is called the visible range for which u spans the range kd and $-kd$. We can sketch the radiation pattern for the array factor as a function of the observation angle ψ.

In Figure 5.4.2 we plot the array factor as a function of u for $N = 5$. Letting $\alpha = 0$, the visible range corresponding to $d = \lambda/2$ is illustrated in Figure 5.4.2 together with the radiation pattern. As the observation angles ψ span from 0 to π, the projection $u = kd\cos\psi$ changes from kd to $-kd$ and the corresponding values for the array factor are obtained from the $|F(u)|$ plot. We note that these patterns are physically observed on the x-y plane for which $\theta = \pi/2$. In other planes containing the x axis, the patterns must be modified by multiplication of the unit pattern of the array elements. Because the principal maximum is perpendicular to the array at $\psi = \pi/2$, such a uniform linear array is called *broadside*.

From (5.4.6) we see that the principal maxima $u_{\max}$ occur when the denominator goes to zero, namely $u_{\max}/2 = m\pi$ or

$$u_{\max} = 2m\pi \qquad m = 0, \pm 1, \pm 2, \ldots \qquad (5.4.7)$$

The magnitudes of these principal maxima are all equal to

$$|F(u_{\max})| = N \qquad (5.4.8)$$
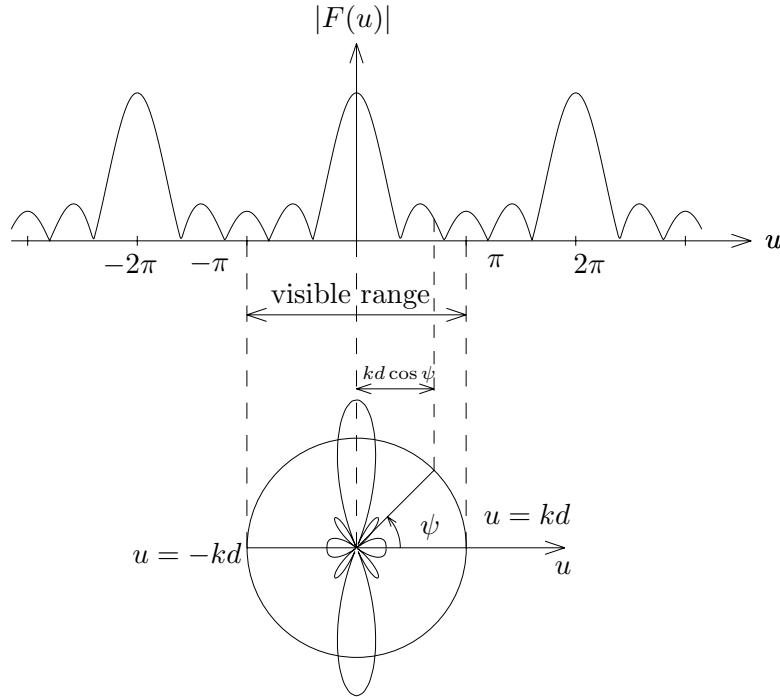
Figure 5.4.2 Array factor and radiation pattern for $N = 5$ and $kd = \pi$.

This is obtained from (5.4.6) by L'Hôpital's rule introduced by Guillaume L'Hôpital (1661–1704) in his book on differential calculus published in 1692.

The location of the nulls u_n occur when the numerator goes to zero, namely $Nu_n/2 = n\pi$ or

$$u_n = \frac{2n\pi}{N} \qquad n = \pm 1, \pm 2, \ldots \qquad (5.4.9)$$

which must be different from $u_{\max}$. For the five-element array shown in Figure 5.4.2, $u_n = \pm 2\pi/5$ and $\pm 4\pi/5$. The magnitude of the sidelobes can be determined from (5.4.6). First locate the positions of the maxima u_m by setting the derivative of $|F(u)|$ equal to zero and then evaluate their magnitudes from (5.4.6).

For broadside arrays, $\alpha = 0$ and the visible range covers $-kd \leq u \leq kd$ as ψ changes from π to 0. For a nonzero phase shift α, the visible range will be shifted to the left of the u coordinate.
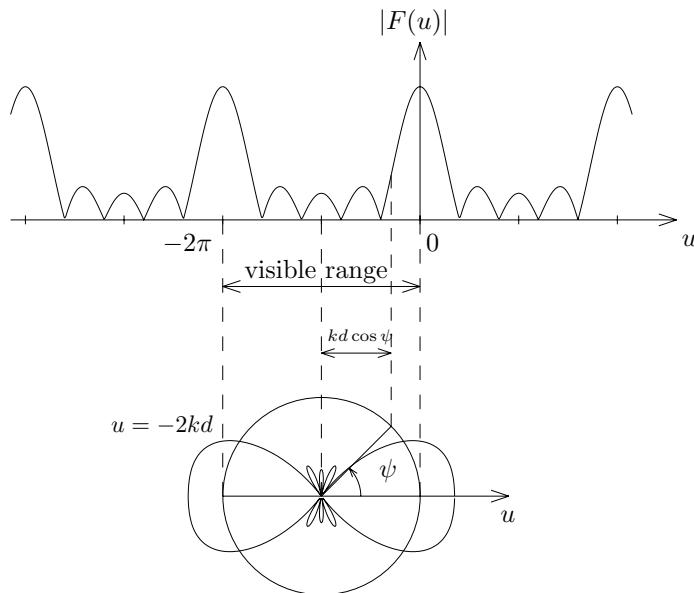
Figure 5.4.3 Visible range for $N = 5$, and $\alpha = kd = \pi$.
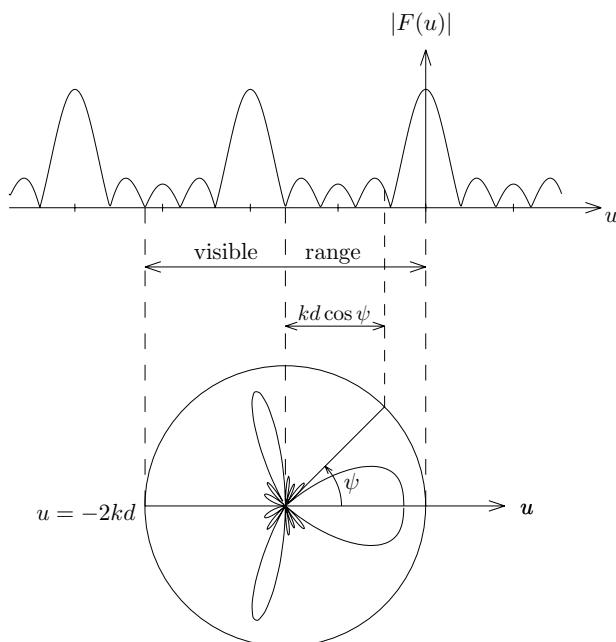
Figure 5.4.4 Visible range for $N = 5$, and $\alpha = kd = 8\pi/5$.

Consider the case of $\alpha = kd$. We have

$$u = kd(\cos\psi - 1) \tag{5.4.10}$$

The visible range covers $-2kd \le u \le 0$. We illustrate the visible range and the radiation patterns in Figure 5.4.3 for $N = 5$ and $d = \lambda/2$, and in Figure 5.4.4 for $N = 5$ and $d = 4\lambda/5$. We see that there may be more than one principal maximum occurring in the visible range for $kd \ge \pi$. A principal maximum always occurs at $\psi = 0$. Thus for $\alpha = kd$, the array is called *endfire*.

EXAMPLE 5.4.1

For a very large array, the sidelobe maxima can be assumed to be located midway between the nulls,

$$u_m \approx \frac{(2m+1)\pi}{N} \qquad m = 1, 2, 3, \ldots$$

The magnitudes are

$$|F(u_m)| = \left| \frac{\sin\left[(2m+1)\pi/2\right]}{\sin\left[(2m+1)\pi/2N\right]} \right| \approx \frac{2N}{(2m+1)\pi} \tag{E5.4.1.1}$$

for large N within the visible range. Since the principal maxima magnitude is N, the relative magnitudes of the sidelobes are

$$\frac{|F(u_m)|}{|F(u_{\max})|} = \frac{2}{(2m+1)\pi}$$

For a large array, the first sidelobe $(m = 1)$ magnitude is $2/3\pi$ or $20\log(2/3\pi) = -13.5\,\text{dB}$ relative to the main lobe.

— END OF EXAMPLE 5.4.1 —

EXAMPLE 5.4.2

It is useful to estimate the beamwidth and directivity for both the broadside and the endfire arrays. There are two kinds of beamwidths we can define. One measures the angular spread of the main lobe in ψ between the first-null positions; the other measures the angular spread between the half-power points of the main lobe. To determine the first-null beamwidth, we find that the first null $u < 0$ occurs at

$$u_1 = kd\cos\psi_1 - \alpha = \frac{-2\pi}{N} \tag{E5.4.2.1}$$

For a broadside array, $\alpha = 0$ and the principal maximum occurs at $\psi = \pi/2$. The beamwidth is $(\text{BW})_b = 2(\psi_1 - \frac{\pi}{2})$. From (E5.4.2.1), we see that for large N,

$$-\frac{2\pi}{Nkd} = \cos\psi_1 = -\sin\left[\psi_1 - \frac{\pi}{2}\right] \approx -\left[\psi_1 - \frac{\pi}{2}\right]$$

Thus,

$$(\text{BW})_b \approx \frac{4\pi}{Nkd} \qquad (\text{E5.4.2.2})$$

For an endfire array, $\alpha = kd$ and the principal maximum occurs at $\psi = 0$. The beamwidth is $(\text{BW})_e = 2\psi_1$. From (E5.4.2.1), we see that for large N,

$$-\frac{2\pi}{Nkd} = \cos\psi_1 - 1 \approx -\frac{\psi_1^2}{2}$$

Thus,

$$(\text{BW})_e = 2\sqrt{\frac{4\pi}{Nkd}} \qquad (\text{E5.4.2.3})$$

The first-null beamwidth for large broadside arrays is inversely proportional to N, whereas that for large endfire arrays is inversely proportional to $\sqrt{N}$. Therefore, large endfire arrays are seen to have a larger first-null beamwidth.

— END OF EXAMPLE 5.4.2 —

EXAMPLE 5.4.3

The directivity D is defined as the ratio of the peak power to the total radiated power distributed over 4π steradians

$$D = G(\theta,\phi)_{\max} = \frac{4\pi\,|E(\theta,\phi)_{\max}|^2}{\displaystyle\int_0^{2\pi} d\phi \int_0^{\pi} d\theta \sin\theta\,|E(\theta,\phi)|^2} \qquad (\text{E5.4.3.1})$$

From (5.4.3), we have

$$E_\theta = E_0 \sin\theta \left[\sum_{n=0}^{N-1} e^{-inu}\right] \qquad (\text{E5.4.3.2})$$

where $u = kd\cos\psi - \alpha$, and $E_0 = -i\omega\mu Ile^{ikr}/4\pi r$. The directivity is

$$D = \frac{4\pi N^2}{\displaystyle\int_0^{2\pi} d\phi \int_0^{\pi} d\theta \sin^3\theta \left[N + 2\sum_{m=1}^{N-1}(N-m)\cos mu\right]} \qquad (\text{E5.4.3.3})$$

To facilitate the integration over 4π steradians, we use the angles ψ and ξ as shown in Figure 5.4.1 and integrate over $d\xi \, d\psi \, \sin\psi$ for ψ from 0 to π and ξ from 0 to 2π. The directivity is calculated as

$$
D = 4\pi N^2 \left\{ \int_0^{2\pi} d\xi \int_0^{\pi} d\psi \, \sin\xi \, (1 - \cos^2\xi \sin^2\psi) \left[N + 2 \sum_{m=1}^{N-1} (N-m) \cos mu \right] \right\}^{-1}
$$

$$
= 4\pi N^2 \left\{ \int_0^{\pi} d\psi \, \sin\psi \, (2\pi - \pi \sin^2\psi) \left[N + 2 \sum_{m=1}^{N-1} (N-m) \cos mu \right] \right\}^{-1}
$$

$$
= 4N^2 \left\{ \int_{-kd-\alpha}^{kd-\alpha} \frac{du}{kd} \left[1 + \frac{1}{(kd)^2}(u+\alpha)^2 \right] \left[N + 2 \sum_{m=1}^{N-1} (N-m) \cos mu \right] \right\}^{-1}
$$

$$
= 4N^2 \left\{ \frac{8}{3}N + \frac{2}{kd} \sum_{m=1}^{N-1} (N-m) \left[\frac{4}{m} \sin(mkd) \cos(m\alpha) \right. \right.
$$

$$
\left. \left. + \frac{4}{m^2 kd} \cos(mkd)\cos(m\alpha) - \frac{4}{m^3(kd)^3} \sin(mkd)\cos(m\alpha) \right] \right\}^{-1}
$$

$$
= N^2 \left\{ \frac{2}{3}N + 2 \sum_{m=1}^{N-1} (N-m) \left[\left(\frac{1}{mkd} - \frac{1}{(mkd)^3} \right) \sin(mkd) \right. \right.
$$

$$
\left. \left. + \frac{1}{(mkd)^2} \cos(mkd) \right] \cos(m\alpha) \right\}^{-1} \tag{E5.4.3.4}
$$

As $kd \to 0$, we have

$$
D = N^2 \left\{ \frac{2N}{3} + \frac{2}{3}(N-m) \cos m\alpha \right\}^{-1}
$$

Letting $\alpha = 0$, we obtain

$$
D = N^2 \left\{ \frac{2N}{3} + \frac{2}{3}N(N-1) \right\}^{-1} = \frac{3}{2} \tag{E5.4.3.5}
$$

which is the directivity for a single Hertzian dipole.

B. Array Antennas with Nonuniform Current Distributions

We see that for uniform linear arrays, whether broadside or endfire, the relative power level of the first sidelobe as compared with the principal maximum is $-13.5\,\mathrm{dB}$ and even higher for modified endfire arrays. With the use of nonuniform current excitations, the sidelobe levels can be reduced. One simple example is a *gabled array* which has an array factor equal to the square of that for a uniform linear array,

$$\tilde{F}(u) = \left[\sum_{n=0}^{N-1} e^{-inu}\right]^2 = 1 + 2e^{-iu} + \cdots + Ne^{-i(N-1)u} + \cdots$$
$$+ 2e^{-i(2N-3)u} + e^{-i2(N-1)u} \qquad (5.4.11)$$

The gabled array consists of $2N - 1$ elements with the center element having current amplitude N relative to the end ones having unit amplitude. The array pattern plotted against u is seen to be the square of the uniform array. The first sidelobe level is now $-27\,\mathrm{dB}$ relative to the main lobe.

A similar construction leads to a *binomial array* which has no sidelobes. Consider a uniform linear array consisting of two elements. The array factor

$$\left|\tilde{F}(u)\right| = \left|\sum_{n=0}^{1} e^{-inu}\right| = \left|\frac{\sin u}{\sin \frac{u}{2}}\right| \qquad (5.4.12)$$
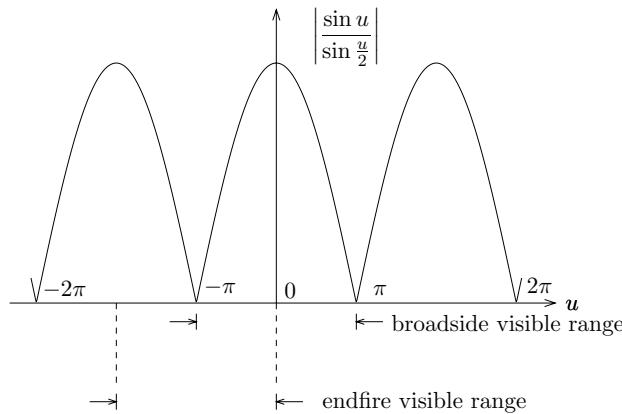
Figure 5.4.5 Array factor for $N = 2$.

If we choose d such that $kd \leq \pi$, we see from the array factor in Figure 5.4.5 (with $kd = \pi$) that neither the broadside nor the endfire pattern has sidelobes. Taking the N th power of $\tilde{F}(u)$, we still do not have any sidelobes,

$$
\left| \tilde{F}(u) \right|^N = \left| 1 + \binom{N}{1} e^{-iu} + \binom{N}{2} e^{-i2u} + \cdots + \binom{N}{N} e^{-iNu} \right|
$$

$$
= \left| \sum_{n=0}^{N} \binom{N}{n} e^{-inu} \right| \tag{5.4.13}
$$

The amplitudes of the current distribution are thus equal to the coefficients of a binomial series $\binom{N}{n}$.

EXAMPLE 5.4.4

In general, linear arrays with nonuniform excitations can be analyzed with the z-transform method if the envelope of the current distribution is describable in functional form. As an example, consider a linear array with the sinusoidal current distribution such that

$$
\overline{J}(\overline{r}') = \hat{z} I_o l \sum_{n=0}^{N-1} \sin(kax')\, \delta(x' - nd)\delta(y')\delta(z') \tag{E5.4.4.1}
$$

For symmetric excitation we also have

$$
(N - 1)kad = \pi \tag{E5.4.4.2}
$$

The array factor becomes

$$
\tilde{F}(u) = \sum_{n=0}^{N-1} \sin(nkad)e^{-inu} \tag{E5.4.4.3}
$$

Notice that the array has only $N - 2$ elements because the two end elements have zero excitation. The array factor can be cast in a standard z-transform format by letting

$$
z = e^{iu} \tag{E5.4.4.4}
$$

$\tilde{F}(u)$ is then in the form of a shifted finite z-transform for the function $\sin(nkad)$. Regarding z as a real quantity, we carry out the summation in (E5.4.4.3) in the following manner

$$\sum_{n=0}^{N-1} \sin(nkad)z^{-n} = -Im\left\{\sum_{n=0}^{N-1} z^{-n}e^{-inkad}\right\} = -Im\left\{\frac{1 - z^{-N}e^{-iNkad}}{1 - z^{-1}e^{-ikad}}\right\}$$

$$= \frac{\left(z^{-1} + z^{-N}\right)\sin\left(\frac{\pi}{N-1}\right)}{1 - 2z^{-1}\cos\left(\frac{\pi}{N-1}\right) + z^{-2}} \tag{E5.4.4.5}$$

where we made use of the symmetry condition in (E5.4.4.2). In fact, once the summation is cast in the z-transform format, standard formulas for many frequently encountered functions are available in tabulated forms.

The magnitude of the array factor is obtained from (E5.4.4.3)–(E5.4.4.5),

$$\left|\tilde{F}(u)\right| = \left|\frac{\cos\left[\frac{(N-1)\,u}{2}\right]\sin\left(\frac{\pi}{N-1}\right)}{\cos u - \cos\left(\frac{\pi}{N-1}\right)}\right| \tag{E5.4.4.6}$$

The principal maximum occurs at $u = 0$ for which

$$\left|\tilde{F}(u_{\max})\right| = \cot\frac{\pi}{2(N-1)} \tag{E5.4.4.7}$$

Nulls occur at $u_n = \pm(2n+1)/(N-1)$ for $n = 1, 2, 3, \ldots$ The value corresponding to $n = 0$ or $u_0 = \pi/(N-1)$ does not yield a null because both the numerator and the denominator of (E5.4.4.6) are zero and in the limit, $\left|\tilde{F}(u_0)\right| = (N-1)/2$.
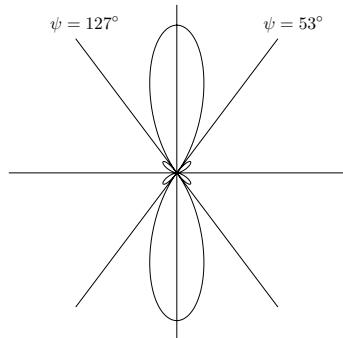
Figure E5.4.4.1 Radiation pattern for $N = 6$ and $d = \lambda/2$.

For $N = 6$ and $d = \lambda/2$, the radiation pattern is shown in Figure E5.4.4.1. The first sidelobe maximum occurs at $u = \pm 2.44$ with $|\tilde{F}(2.44)|/|\tilde{F}(u_{\max})| = 0.12$ or $-18\,\mathrm{dB}$. When $d = \lambda/2$, the directivity is calculated to be $D = 3.79$ for both broadside and endfire arrays.

— END OF EXAMPLE 5.4.4 —

C. Dolph-Chebyshev Arrays

Dolph-Chebyshev arrays have equal sidelobes. The array elements are equally spaced and symmetrically excited, with a uniform progressive phase shift, and with current amplitudes determined by the coefficients of the Chebyshev polynomials. As a result of the properties of Chebyshev polynomials, such arrays provide the minimum beamwidth for a prescribed sidelobe level, and conversely, the minimum sidelobe level for a prescribed beamwidth.
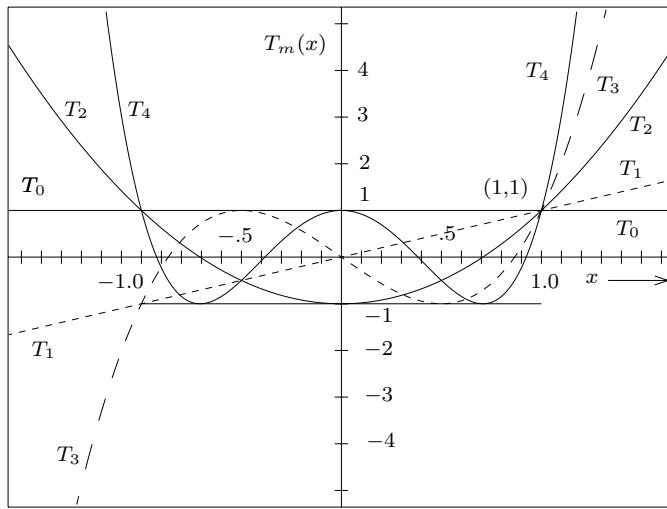
Figure 5.4.6   Chebyshev polynomials T_0, T_1, T_2, T_3 **and** T_4.

The Chebyshev (also spelled Tchebyscheff) polynomials are defined by

$$T_n(x) = \cos\left[n \cos^{-1} x\right] \tag{5.4.14}$$

The first few polynomials are

$$T_0(x) = 1 \tag{5.4.15a}$$
$$T_1(x) = x \tag{5.4.15b}$$
$$T_2(x) = 2x^2 - 1 \tag{5.4.15c}$$
$$T_3(x) = 4x^3 - 3x \tag{5.4.15d}$$
$$T_4(x) = 8x^4 - 8x^2 + 1 \tag{5.4.15e}$$
$$T_5(x) = 16x^5 - 20x^3 + 5x \tag{5.4.15f}$$

Polynomials of higher degree can be obtained from the recurrence relation

$$T_{n+1} = 2x\,T_n(x) - T_{n-1}(x) \tag{5.4.16}$$

which can be obtained from the trigonometric identity $\cos((n+1)\cos^{-1}x) + \cos((n-1)\cos^{-1}x) = 2x\cos(n\cos^{-1}x)$. The polynomials $T_n(x)$ are of degree n in x. For n even, $T_n(x)$ contains only even powers of x; for n odd, $T_n(x)$ contains only odd powers of x. For $|x| > 1$, we let $\cos^{-1}x = \theta = \theta_R + i\theta_I$. It follows that for $x > 1$, $\theta = i\cosh^{-1}x$ and thus $T_n(x) = \cos(n\,\theta) = \cosh[n\cosh^{-1}x]$. For $x < -1$, $\theta = \pi + i\cosh^{-1}x$ and thus $T_n(x) = \cos(n\,\theta) = (-1)^n\cosh[n\cosh^{-1}|x|]$. Within the range $-1 \le x \le 1$, $T_n(x)$ oscillates between ± 1. The polynomial $T_n(x)$ passes 1 at $x = 1$ and $(-1)^n$ at $x = -1$. For $n > 0$ the zeros of $T_n(x)$ occur at

$$x_p = \cos\frac{(2p-1)\pi}{2n} \qquad p = 1, 2, \ldots, n \tag{5.4.17}$$

For $n > 1$ the extrema for $T_n(x)$ within the interval $-1 \le x \le 1$ occur at

$$x_m = \cos\frac{m\pi}{n} \qquad m = 1, 2, \ldots, n-1 \tag{5.4.18}$$

The Chebyshev (Pafnuty Lvovich Chebyshev, 16 May 1821 – 8 December 1894) polynomials of degrees 0 through 4 are shown in Figure 5.4.6.

To determine the excitation amplitudes of an N-element array excited symmetrically, we place the coordinate origin at the midpoint of the array and write the array factor as

$$\tilde{F}(u) = \begin{cases} 2\displaystyle\sum_{m=1}^{N/2} a_m \cos\frac{(2m-1)u}{2} & N = \text{even} & (5.4.19a) \\[2em] a_0 + 2\displaystyle\sum_{m=1}^{(N-1)/2} a_m \cos mu & N = \text{odd} & (5.4.19b) \end{cases}$$

where

$$u = kd\cos\psi - \alpha$$

and α is the phase shift between adjacent array elements, and a_m are the excitation amplitudes.

The excitation amplitudes of an N-element Dolph-Chebyshev array are determined by equating the array factor $\tilde{F}(u)$ with the Chebyshev polynomial $T_{N-1}(x)$. The relationship between u and x is

$$x = b \cos \frac{u}{2} \tag{5.4.20}$$

which was introduced by Charles L. Dolph in 1946, is known as the *Dolph transformation*, where b is a parameter larger than one, $b > 1$.

By the Dolph transformation (5.4.20),

$$u = 2 \cos^{-1} \frac{x}{b} \tag{5.4.21}$$

Equating the array factor to $T_{N-1}(x)$, we find

$$T_{N-1}(x) = \begin{cases} 2 \sum\limits_{m=1}^{N/2} a_m T_{2m-1}(x/b) & N = \text{even} & (5.4.22a) \\ a_0 + 2 \sum\limits_{m=1}^{(N-1)/2} a_m T_{2m}(x/b) & N = \text{odd} & (5.4.22b) \end{cases}$$

The excitation amplitudes a_m are determined by comparing coefficients of like powers on both sides of (5.4.22).

We write the array factor for a five-element Dolph-Chebyshev arrays as

$$\tilde{F}(u) = T_{N-1} \left[b \cos \frac{u}{2} \right] = T_4 [x] \tag{5.4.23}$$

For the five-element Dolph-Chebyshev array,

$$\tilde{F}(u) = a_0 + 2 \sum_{m=1}^{(N-1)/2} a_m \cos mu \qquad N = \text{odd}$$

Thus we have

$$a_0 + 2a_1 T_2(x/b) + 2a_2 T_4(x/b) = T_4(x)$$

The excitation amplitudes a_0, a_1, and a_2 are determined by making use of (5.4.15c) and (5.4.15e)

$$a_0 + 2a_1 \left[2(x/b)^2 - 1 \right] + 2a_2 \left[8(x/b)^4 - 8(x/b)^2 + 1 \right] = 8x^4 - 8x^2 + 1$$

and comparing the coefficients of like powers. We find $a_2 = b^4/2$, $a_1 = 2b^4 - 2b^2$, and $a_0 = 3b^4 - 4b^2 + 1$.

We illustrate the case of a five-element endfire Dolph-Chebyshev array with $d = \lambda/4$ as shown in Figure 5.4.7. We let the visible range cover the Chebyshev polynomial from $x = -1$ to $x = x_0$, where principal maximum occurs. The principal maximum $\tilde{F}(u_{\max}) = R$ occurs at $\psi = 0$, corresponding to

$$x_0 = b \cos \frac{kd - \alpha}{2} \tag{5.4.24}$$

To include all sidelobes in the array pattern and to exclude a main lobe at $\psi = \pi$, we require that $\psi = \pi$ corresponds to $x = -1$. From the Dolph transformation (5.4.20) we have

$$-1 = b \cos \frac{kd + \alpha}{2} \tag{5.4.25}$$
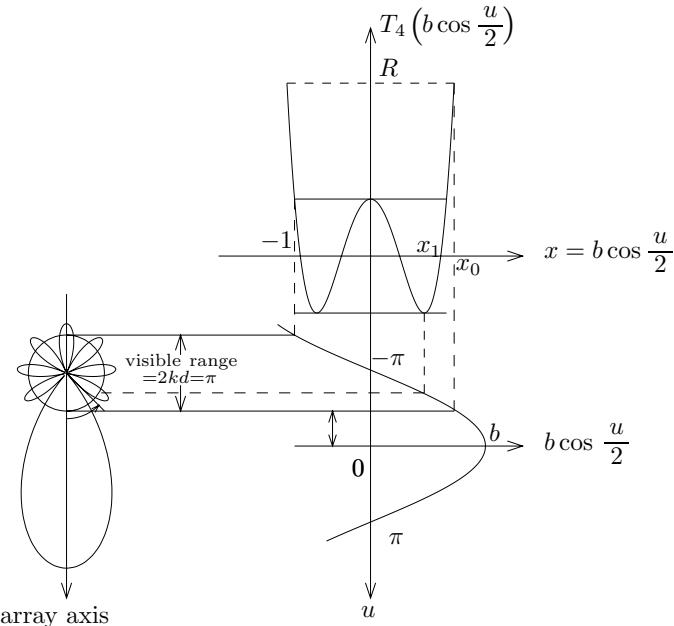
Figure 5.4.7 Endfire Dolph-Chebyshev array with $N = 5$ and $kd = \pi/2$.

which determines the progressive phase shift α. The visible range lies between $u = kd - \alpha$ and $u = -kd - \alpha$. The construction of the radiation pattern when $d = \lambda/4$ is shown in Figure 5.4.7. The variable b is determined by either the main lobe maximum R or the main lobe beamwidth.

For array synthesis suppose the beamwidth $2\psi_1$ is specified, we see that

$$b \cos \frac{kd \cos \psi_1 - \alpha}{2} = \cos \frac{\pi}{2(N-1)} \tag{5.4.26}$$

From (5.4.25) and (5.4.26) α and b can be determined.

If instead the sidelobe level $1/R$ is specified, we find

$$R = T_{N-1}\left[b \cos \frac{kd - \alpha}{2}\right] \tag{5.4.27}$$

Making use of (5.4.14), we obtain the equation

$$b \cos \frac{kd - \alpha}{2} = \cosh\left[\frac{1}{N-1} \cosh^{-1} R\right] \tag{5.4.28}$$

From (5.4.25) and (5.4.28), α and b can be determined.

Notice that the choice of $x = -1$ corresponding to $\psi = \pi$ and the choice of element separation d fix the visible range $2kd$. Main lobes at angles other than $\psi = 0$ will appear if $2kd$ becomes too large, for instance $d = \lambda/2$.

To illustrate the optimum properties of the Chebyshev polynomials, let the largest value of $T_n(x)$ be at x_0, and the first zero be at x_1. For $-1 \le x \le 1$, $T_n(x)$ lies between -1 and 1. Let the visible range cover the Chebyshev polynomial from $x = -1$ to $x = x_0$. We wish to show that for a given beamwidth with first null at x_1, the sidelobe level $1/R$ is the smallest, and conversely for a given sidelobe level, the beamwidth provided by $T_n(x)$ is the smallest.
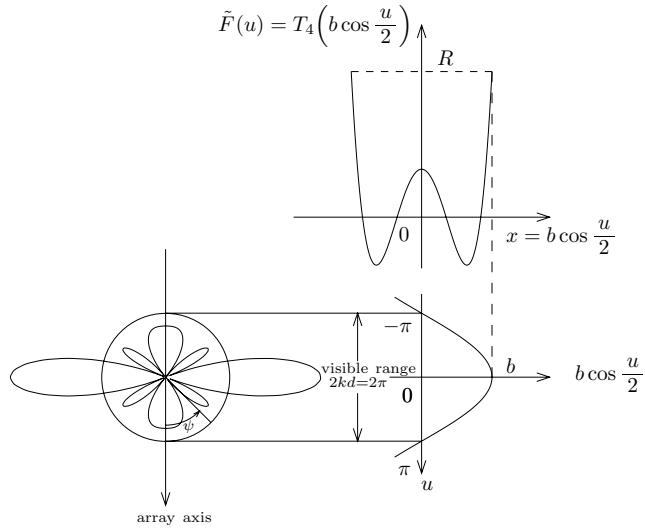
To prove this statement, we let there be another polynomial $P_n(x)$ with the same degree n and the same magnitude $R > 1$ at $x = x_0$. For the case of a given beamwidth, $T_n(x)$ and $P_n(x)$ intersect at values $x = x_0$ and $x = x_1$. If $P_n(x) \le 1$ for $-1 \le x \le x_1$, then $P_n(x)$ intersects $T_n(x)$ at least $n - 1$ more times. However, since specifying $n + 1$ values for a polynomial of degree n uniquely determines all the coefficients of the polynomial, the two polynomials $P_n(x)$ and $T_n(x)$ must be identical.

Conversely, for a given sidelobe level $1/R$, if $P_n(x)$ is to stay within the bounds ± 1 and is to possess the largest zero at x_1', such that $x_1 < x_1' < x_0$, it must intersect $T_n(x)$ at least n more times, and again $P_n(x) = T_n(x)$. This concludes the proof that $T_n(x)$ provides the optimum properties for an array pattern.

EXAMPLE 5.4.5   Broadside Dolph-Chebyshev array.

Consider the construction of the radiation pattern for a five-element broadside Dolph-Chebyshev array with $d = \lambda/2$ and $\alpha = 0$ as shown in Figure E5.4.5.1. The visible range is between $u = -kd = -\pi$ and $u = kd = \pi$.

Figure E5.4.5.1 Broadside Dolph-Chebyshev array with $N = 5$, $kd = \pi$.

Let the first-null beamwidth of the broadside array be $2[(\pi/2) - \psi_1]$. At the first null $x = b\cos[(kd\cos\psi)/2]$, we obtain from (5.4.17) by letting $p = 1$ and $n = N - 1$,

$$b\cos\frac{kd\cos\psi_1}{2} = \cos\frac{\pi}{2(N-1)} \qquad (\text{E5.4.5.1})$$

The principal maximum occurs at $u = 0$ where $\tilde{F}(u) = T_{N-1}(b) = R$. Notice that as $b > 1$, we have

$$R = T_{N-1}(b) = \cosh[(N-1)\cosh^{-1} b] \qquad (\text{E5.4.5.2})$$

Thus with b specified, the beamwidth and sidelobe levels are immediately determined from (E5.4.5.1) and (E5.4.5.2). Conversely, if we specify the sidelobe level $1/R$, b is determined from (E5.4.5.2)

$$b = \cosh\left[\frac{1}{N-1}\cosh^{-1}R\right]$$

and consequently, the beamwidth from (E5.4.5.1).

<div align="right">— End of Example 5.4.5 —</div>

EXAMPLE 5.4.6   Riblet transformation for broadside array.

In the construction of the radiation pattern for broadside arrays, we see that if $d \geq \lambda/2$, the visible range will be larger than that shown in Figure E5.4.5.1, and additional main lobes may be exhibited. However, if $d < \lambda/2$, the visible range will be smaller than that shown in Figure E5.4.5.1, and the whole range of the Chebyshev polynomial will not be used.
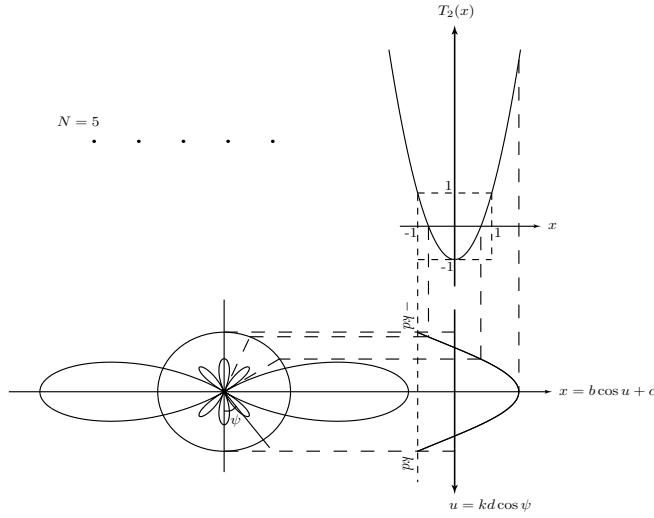
The Dolph-Chebyshev arrays will no longer be the optimum arrays. This can be seen for a broadside array with an odd number of elements by considering another array factor described by, instead of $T_{N-1}(x)$, another symmetric polynomial $P_{N-1}(x)$ which has the property that $P_{N-1}(b) = R$ at the principal maximum and zero at $\cos[\pi/2(N-1)]$ but with $|P_{N-1}(x)| < 1$ for $b\cos(kd/2) < x < \cos[\pi/2(N-1)]$. This is possible because $|P_{N-1}(x)|$ can be larger than unity for $0 < x < b\cos(kd/2)$, which is not in the visible range. The result is an array pattern that has the same beamwidth as a Dolph-Chebyshev array but has a smaller sidelobe level. Thus the optimum characteristic of the broadside Dolph-Chebyshev array is restricted to $d \geq \lambda/2$.

The restriction was removed in 1947 by H. J. Riblet who modified the Dolph transformation (5.4.20) to

$$x = b\cos u + c \tag{E5.4.6.1}$$

for a broadside array with an odd number of elements. R. H. DuHamel in 1953 extended Riblet's method to synthesize broadside arrays, and in 1955 R. L. Pritchard developed the formulation to include arrays of even numbers of elements.

In Figure E5.4.6.1, we employ Riblet transformation (E5.4.6.1) to plot the radiation pattern of a five-element broadside array with separation $d = 0.3\lambda$. Notice that the Riblet transformation is not reducible to the Dolph transformation $x = b\cos\frac{u}{2}$ as $c = 0$. In order to determine uniquely the excitation coefficients for an $(2N+1)$ element array, the array factor is set to equal to the Nth order polynomial $T_N(x)$, which is not the same as that for the Dolph-Chebyshev array where the array factor for $2N+1$ elements is set equal to the $2N$th order polynomial $T_{2N}(x)$. The excitation coefficients are obtained by comparing the coefficients of the equation

Figure E5.4.6.1 Broadside array with Riblet transformation for $N = 5$ and $d = .3\lambda$.

$$T_N(x) = a_0 + 2\sum_{m=1}^{N} a_m T_m \left[\frac{x - c}{b} \right]$$

The whole range of the Chebyshev polynomial can again be used when $d < \lambda/2$ by requiring $x = -1$ for $u = \pm kd$ or $b\cos(kd) + c = -1$. The principal maximum now occurs at $x = b + c$.

— END OF EXAMPLE 5.4.6 —

D. Array Pattern Synthesis

In array synthesis, we are asked to find a set of physically realizable excitation currents for the array elements for a given specification of the array pattern with regard to its beamwidth, sidelobe level, positions of nulls, directivity, and so forth. Consider the synthesis of an array having *symmetric* and nonnegative excitations with maximum possible number of nulls. The array factor takes the form

$$\tilde{F}(u) = 1 + I_1 e^{-iu} + I_2 e^{-i2u} + \ldots + I_{N-2}\, e^{-i(N-2)u} + e^{-i(N-1)u} \quad (5.4.29)$$

where we assume $I_0 = I_{N-1} = 1$ for the two end elements and $I_m = I_{N-1-m}$ for $m = 1, 2, \ldots, N - 2$. The polynomial in $z = e^{-iu}$ is of the

order $N - 1$ roots for z. Note that $\tilde{F}(u)$ has $(N-1)/2$ unknown coefficients when N is odd and $(N-2)/2$ unknown coefficients when N is even. For odd N, we can factor $\tilde{F}(u)$ in the form

$$\tilde{F}_o(u) = \prod_{m=1}^{(N-1)/2} (1 + c_m e^{-iu} + e^{-i2u}) \tag{5.4.30}$$

which gives rise to a polynomial with symmetric coefficients. For even N we factor $\tilde{F}(u)$ in the form

$$\tilde{F}_e(u) = (1 + e^{-iu}) \prod_{m=1}^{(N-2)/2} (1 + c_m e^{-iu} + e^{-i2u}) \tag{5.4.31}$$

Note that the first factor in (5.4.31) is the result of combining the terms from symmetric positions of the polynomial. For instance, the first and last elements yield $1 + e^{-i(N-1)\,u}$, and, since N is an even number, this term possesses the factor $1 + e^{-iu}$.

The power patterns consist of magnitude squares of the elementary factors of $\tilde{F}(u)$. Note that, assuming real c_m,

$$(1 + c_m e^{-iu} + e^{-i2u})(1 + c_m e^{iu} + e^{i2u}) = (\xi + c_m)^2$$

where we let

$$\xi = e^{iu} + e^{-iu} = 2\cos u = 2\cos[kd\cos\psi - \alpha] \tag{5.4.32}$$

The power patterns corresponding to $\tilde{F}_o(u)$ and $\tilde{F}_e(u)$ are, in terms of the new variable ξ,

$$P_o(\xi) = \left|\tilde{F}_o\right|^2 = \prod_{m=1}^{(N-1)/2} (\xi + c_m)^2 \tag{5.4.33}$$

for odd N and

$$P_e(\xi) = \left|\tilde{F}_e\right|^2 = (\xi + 2) \prod_{m=1}^{(N-2)/2} (\xi + c_m)^2 \tag{5.4.34}$$

for even N. We see from (5.4.32) that $-2 \leq \xi \leq 2$; within this interval the power pattern $P(\xi)$ must be real and positive for a physically realizable array. For the maximum possible number of nulls we also have c_m real and $|c_m| < 2$ so that all zeros of the polynomial occur in the range $-2 \leq \xi \leq 2$.

EXAMPLE 5.4.7

As an example, consider the synthesis of a broadside array consisting of five elements with equal spacing of $\lambda/2$ [Ma, 1974]. The power pattern and the corresponding array factor are, respectively,

$$P_o(\xi) = (\xi + c_1)^2(\xi + c_2)^2 \qquad (E5.4.7.1)$$

$$\tilde{F}(u) = (1 + c_1 e^{-iu} + e^{-i2u})(1 + c_2 e^{-iu} e^{-i2u})$$
$$= 1 + (c_1 + c_2)e^{-iu} + (2 + c_1 c_2)e^{-i2u} + (c_1 + c_2)e^{-i3u} + e^{-i4u} \quad (E5.4.7.2)$$

From (E5.4.7.1) we see that nulls occur at $\xi = -c_1$ and $-c_2$. The positions of the sidelobes are determined by setting $dP_o(\xi)/d\xi = 0$ which yields $\xi_1 = -(c_1 + c_2)/2$. The values $\xi = -c_1$ and $-c_2$ are neglected because they are known to be nulls. For non-negative excitation coefficients, we require that $c_1 + c_2 \geq 0$ and $c_1 c_2 \geq -2$ which assures broadside maximum at $\xi = 2$. Substituting back in (E5.4.7.1) we find the corresponding sidelobe level

$$\frac{P[\xi_1 = -(c_1 + c_2)/2]}{P(\xi_m = 2)} = \frac{(c_1 - c_2)^4}{16(c_1 + 2)^2(c_2 + 2)^2} \qquad (E5.4.7.3)$$

we also regard the point $\xi = -2$ as a sidelobe maximum and find

$$\frac{P(\xi_2 = -2)}{P(\xi_m = 2)} = \frac{(c_1 - 2)^2(c_2 - 2)^2}{(c_1 + 2)^2(c_2 + 2)^2} \qquad (E5.4.7.4)$$

The directivity D is defined as the ratio of the peak power to the total radiated power distributed over 4π steradians

$$D = G(\psi, \phi)_{\max} = \frac{4\pi P(\xi)_{\max}}{\displaystyle\int_0^{2\pi} d\phi \int_0^{\pi} d\psi \sin\psi P(\xi)} = \frac{2kdP(\xi)_{\max}}{W} \qquad (E5.4.7.5)$$

where

$$W = \int_0^{\pi} d\psi \sin\psi P(\xi) = 2 \int_{2\cos kd}^2 d\xi \frac{P(\xi)}{\sqrt{4 - \xi^2}}$$

We obtain

$$W = 2\pi \left[6 + 2(c_1^2 + c_2^2) + 8c_1 c_2 + c_1^2 c_2^2 \right]$$

$$D = \frac{(2 + c_1)^2(2 + c_2)^2}{6 + 2(c_1^2 + c_2^2) + 8c_1 c_2 + c_1^2 c_2^2}$$

In the following we discuss several special cases.

Case 1

We require that all excitation amplitudes be equal. From (E5.4.7.2) we set $c_1 + c_2 = 1$ and $c_1 c_2 = -1$ and obtain $c_1 = (1 - \sqrt{5})/2$ and $c_2 = (1 + \sqrt{5})/2$. The array factor is plotted in Figure E5.4.7.1. The first sidelobe level is $(1/4)^2 (\approx -12\,\mathrm{dB})$ and the second sidelobe level $(1/5)^2 (\approx -14\,\mathrm{dB})$. The first-null beamwidth is $47.2°$. The directivity is $D = 5$.
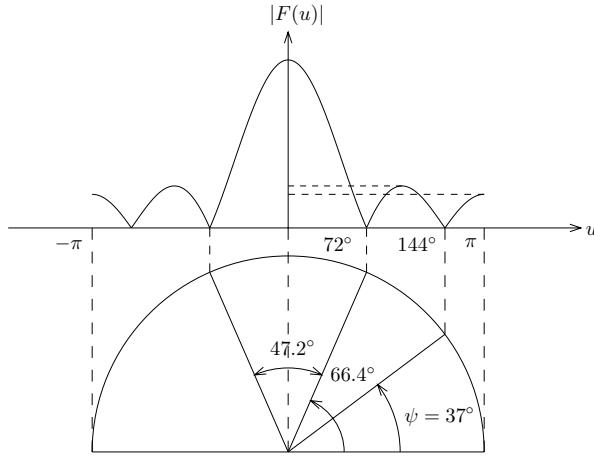
Figure E5.4.7.1 Array factor for Case 1.

Case 2

We require all sidelobe levels be zero $(-\infty\,\mathrm{dB})$. From (E5.4.7.3) and (E5.4.7.4) we find $c_1 = c_2 = 2$. All sidelobe nulls are moved to $\xi = -2$ or $\psi = 0$ and π. Thus no sidelobes occur in the visible range. From (5.4.32) we see that this gives a binomial array with excitation coefficients $1 : 4 : 6 : 4 : 1$. The first-null beamwidth becomes $180°$.

Case 3

We require that both sidelobe levels be maintained at $-20\,\mathrm{dB}$. From (E5.4.7.3) and (E5.4.7.4) we set

$$16(c_1 + 2)^2 (c_2 + 2)^2 = 100(c_1 - c_2)^2$$

and

$$(c_1 + 2)^2 (c_2 + 2)^2 = 100(2 - c_1)^2 (2 - c_2)^2$$
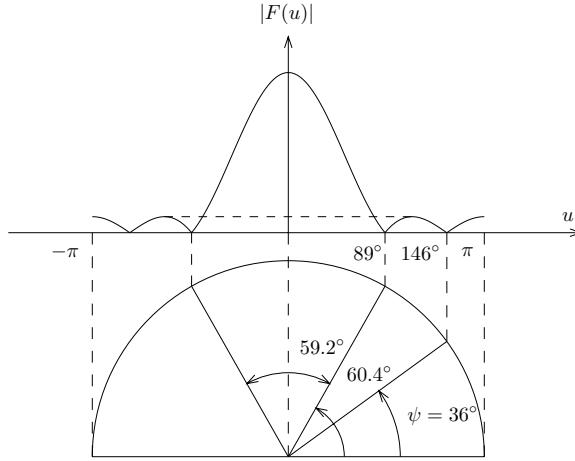
Figure E5.4.7.2 Array factor for Case 3.

which yield $c_1 = -0.0413$ and $c_2 = 1.6498$. From (E5.4.7.2) we find the required excitation coefficients to be $1 : 1.6085 : 1.9318 : 1.6085 : 1$. The array factor is plotted in Figure E5.4.7.2. The first-null beamwidth is $59.2°$. The directivity is $D = 4.686$. Comparing with the uniform excitation, we see that the present case does give a lower sidelobe level of $(1/10)^2 (-20$ dB$)$ but at the expense of a larger first-null beamwidth.

When $d = \lambda/2$, the entire visible range in u is 2π. The prescribed array pattern $\tilde{F}(u)$ can be expanded into a Fourier series and approximated by a sum of the first few terms of the series. For general d including $d = \lambda/2$, we study, in the following, the synthesis of a linear array with a prescribed array pattern by using the method of Lagrange interpolation with Chebyshev polynomials.

$-$ End of Example 5.4.7 $-$

Example 5.4.8

A given array power pattern can be written in the form of $G(\xi)$ with $\xi = 2\cos u$ and $u = kd\cos\psi - \alpha$. As an example consider the synthesis of the array pattern [Ma, 1974]

$$G(\xi) = e^{-(\xi-2)^2/4} \qquad -2 \leq \xi \leq 2 \qquad \text{(E5.4.8.1)}$$
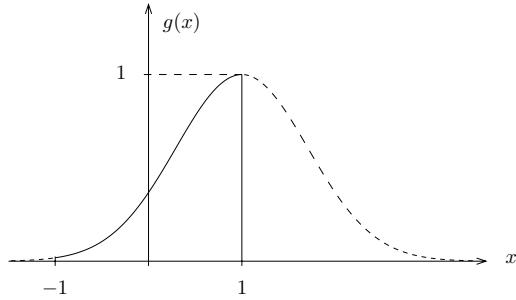
with $N = 4$

We first let $x = \xi/2$ so that

$$g(x) = e^{-(1-x)^2}$$

and the interval is normalized to $-1 \leq x \leq 1$ [Fig. E5.4.8.1]. We wish to match this function with a polynomial of degree 3. To do that, we choose the zeros of the Chebyshev polynomial $T_4(x)$ as the sampling points. We have $x_{N-1-l} = \cos[(2l+1)\pi/2N]$ with $l = 0, 1, 2, \ldots, N-1$ or

$$x_0 = -0.924, \quad x_1 = -0.383, \quad g(x_2) = 0.6840, \quad g(x_3) = 0.9958$$

Figure E5.4.8.1 **Plot of** $g(x) = \exp[-(1-x)^2]$.

To construct the third-degree polynomial, we apply the Lagrange interpolation formula

$$L(x) = \sum_{l=0}^{N-1} \frac{\pi(x)g(x_l)}{(x - x_l)\pi'(x_l)} \tag{E5.4.8.2}$$

where

$$\pi(x) = (x - x_0)(x - x_1)(x - x_2)(x - x_3) \tag{E5.4.8.3}$$

$\pi'(x)$ is the derivative of $\pi(x)$, and $L(x)$ denotes the approximating polynomial of $g(x)$ such that $L(x_i) = g(x_i)$ at $x = x_0$, x_1, x_2, and x_3 over the normalized interval $-1 \leq x \leq 1$.

With the sampling points taken to be the zero of the Chebyshev polynomial $T_4(x)$, we find the Lagrange interpolation formula (E5.4.8.2)

$$\begin{aligned}
L(x) = {} & (x - x_1)(x - x_2)(x - x_3)\frac{g(x_o)}{(x_0 - x_1)(x_0 - x_2)(x_0 - x_3)} \\
& + (x - x_0)(x - x_2)(x - x_3)\frac{g(x_1)}{(x_1 - x_0)(x_1 - x_2)(x_1 - x_3)} \\
& + (x - x_0)(x - x_1)(x - x_3)\frac{g(x_2)}{(x_2 - x_0)(x_2 - x_1)(x_2 - x_3)} \\
& + (x - x_0)(x - x_1)(x - x_2)\frac{g(x_3)}{(x_3 - x_0)(x_3 - x_4)(x_3 - x_2)} \\
= {} & -0.24628x^3 + 0.13343x^2 + 0.73586x + 0.39643 \tag{E5.4.8.4}
\end{aligned}$$

We now estimate the maximum possible error committed by the approximation of $g(x)$ with $L(x)$ as shown in (E5.4.8.2). The accuracy of the approximation is measured by the remainder

$$R = \pi(x)\frac{g^{(N)}(x)}{N!} \qquad x_0 < x < x_{N-1}$$

where the superscript N denotes the N th derivative of $g(x)$. This is similar to the remainder term in a Taylor series expansion where the first N terms are approximated by the $(N-1)$ th order polynomial. The maximum possible error is

$$\epsilon_{max} \leq \frac{|\pi(x)|_{max} \left|g^{(N)}(x)\right|_{max}}{N!}$$

The error size depends on the prescribed function $g(x)$, the number of sampling points, and their locations.

The choice of the sampling points to coincide with the zeros of $T_4(x)$ not only provides a way to determine the otherwise arbitrary sampling point positions but also makes the estimation of $|\pi(x)|_{max}$ simpler. Using the fact that $T_{N-1}(x) = 2^{N-1}(x-x_0)(x-x_1)\dots(x-x_{N-1})$ and that $|g_{N-1}(x)| \leq 1$ for $-1 \leq x \leq 1$, we find

$$|\pi(x)|_{max} = |(x-x_0)(x-x_1)\dots(x-x_{N-1})|_{max}$$

$$= \frac{1}{2^{N-1}}\left|T^{(x)}_{N-1}\right|_{max} = \frac{1}{2^{N-1}}$$

We note that

$$g^{(4)}(x) = (16x^4 - 64x^3 + 48x^2 + 32x - 20)e^{-(1-x)^2}$$

Its maximum occurs at $x = 1$ giving $\left|g^{(4)}(x)\right|_{max} = 12$. We have

$$\epsilon_{max} = \frac{12}{2^3 \cdot 4!} = 0.0625$$

The actual maximum deviation between $g(x)$ and $L(x)$ occurs at $x \approx 0$ which gives an error of $\epsilon(0) = L(0) - G(0) \approx 0.0284$.

Replacing $x = \xi/2$, we find the power pattern

$$P(\xi) = -0.03078\xi^3 + 0.03331\xi^2 + 0.36787\xi + 0.39651$$

Plotted in the region $-2 \leq \xi \leq 2$, we find $P(\xi) > 0$. As $\xi \to \pm\infty$, $P(\xi) \to \mp\infty$.

For arrays with a uniformly progressive phase shift, the power pattern must satisfy the realization condition

$$P(\xi) = \sum_{m=0}^{N-1} A_m\xi^m \geq 0 \qquad \text{for } -2 \leq \xi \leq 2$$

The Weierstrass approximation theorem guarantees the existence of the coefficients A_m and the positive integer N if $g(\xi)$ is continuous for $-2 \leq \xi \leq 2$ such that for a positive quantity ϵ, $|g(\xi) - P(\xi)| < \epsilon$ for $-2 \leq \xi \leq 2$. The polynomial can be plotted for an extended region of ξ values and is found to have a zero at $\xi = 4.4340$. We write

$$P(\xi) = -0.03078(\xi - 4.4340)(\xi^2 + 3.3350\xi + 2.9042) \qquad \text{(E5.4.8.5)}$$

There are no more zeros with real ξ for the second factor.

The power pattern must be inverted to give the array factor in order to determine the excitation coefficients. Note that by definition $\xi = 2\cos u = e^{iu} + e^{-iu}$. If the power pattern has the factor

$$P_l(\xi) = (\xi_l \pm \xi) \qquad \text{(E5.4.8.6a)}$$

then the corresponding array pattern has the factor

$$\tilde{F}_l(u) = \frac{1}{\sqrt{c_l}}(1 \pm c_l e^{-iu}) \qquad \text{(E5.4.8.6b)}$$

with $c_l = [\xi_l \pm (\xi_l^2 - 4)^{1/2}]/2$. When the power pattern has the factor

$$P_l(\xi) = (\xi + \xi_l)^2 \qquad \text{(E5.4.8.7a)}$$

with real ξ_l and $|\xi_l| < 2$, the corresponding array pattern has the factor

$$\tilde{F}(u) = 1 + \xi_l e^{-iu} + e^{-i2u} \qquad \text{(E5.4.8.7b)}$$

If the power pattern has the factor

$$P_l(\xi) = \xi^2 + 2\xi_{l1}\xi + \xi_{l1}^2 + \xi_{l2}^2 \qquad \text{(E5.4.8.8a)}$$

then the corresponding array has the factor

$$\tilde{F}_l(u) = \frac{1}{\sqrt{c_{l1}c_{l2}}}[1 + (c_{l1} + c_{l2})e^{-iu} + c_{l1}c_{l2}e^{-i2u}] \qquad \text{(E5.4.8.8b)}$$

with $c_{l2} = c_{l1}^*$ and $c_{l1} = [\xi_{l1} - i\xi_{l2} \pm ((\xi_{l1} - \xi_{l2})^2 - 4)^{1/2}]/2$ for real ξ_{l1} and ξ_{l2}. In fact we can see that for the realizable $P(\xi)$ such that $P(\xi) \geq 0$ for $-2 \leq \xi \leq 2$, the polynomial only contains those elementary factors as listed in (E5.4.8.5)–(E5.4.8.7).

Returning to (E5.4.7.2), we now find the corresponding array factor to be the multiplication of

$$\tilde{F}_1(u) = \frac{1}{2.0484}(1 - 4.1957 e^{iu})$$

or

$$\frac{1}{0.4882}(1 - 0.2383 e^{-iu})$$

with

$$\tilde{F}_2(u) = \frac{1}{1.3013}(1 + 2.1064e^{iu} + 1.6931e^{-i2u})$$

or

$$\frac{1}{0.7685}(1 + 1.2440e^{-iu} + 0.5906e^{-i2u})$$

Clearly, solutions for the array factor $\tilde{F}(u) = \tilde{F}_1(u)\tilde{F}_2(u)$, and therefore the excitation coefficients are not unique. With the Chebyshev interpolation method as shown above, four sets of excitation coefficients give rise to the same power pattern $P(\xi)$.

<div align="right">— END OF EXAMPLE 5.4.8 —</div>

Problems

P5.4.1

(a) Consider an array of two out-of-phase but equal amplitude $\hat{z}$-directed Hertzian dipoles as shown in Fig. P5.4.1.1.
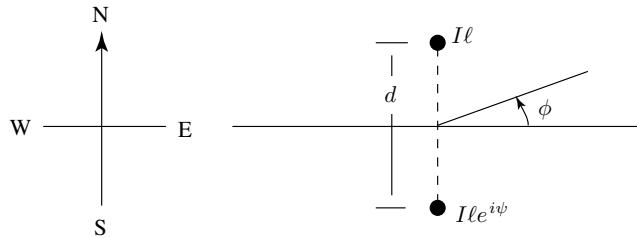
Figure P5.4.1.1

Show that the array factor $|F(\phi)|$ may be expressed as

$$|F(\phi)| = \left| 2\cos\left[\frac{kd}{2}\sin\phi - \frac{\psi}{2}\right]\right|$$

(b) A broadcast array of two vertical towers with equal current amplitude is to have a horizontal plane pattern such that

  (i) maximum field intensity is to the north $(\phi = 90°)$
  (ii) the only nulls are at $\phi = 225°$ and $\phi = 315°$.

  Specify the arrangement of the towers, their spacing and phasing.

P5.4.2

Synthesize a seven-element, equally spaced, broadside Dolph-Chebyshev array with $d = \lambda/2$, which has $-20\,\mathrm{dB}$ sidelobe levels. Determine the excitation coefficients. Find the first-null beamwidth and the directivity if the array elements are isotropic radiators. Now let $d = \lambda/4$. If the above excitation coefficients are used, find the first-null beamwidth and the directivity.

P5.4.3

Consider a linear dipole array with sinusoidal excitation coefficients and $u = kd \cos \psi - \alpha$. The array factor

$$\tilde{F}(u) = \sum_{n=0}^{N-1} \sin \left(\frac{n\pi}{N-1} \right) e^{-inu}$$

$$= \frac{1}{2i} \left[\sum_{n=0}^{N-1} \left\{ \exp in \left[\frac{\pi}{N-1} - u \right] \right\} - \sum_{n=0}^{N-1} \left\{ \exp in \left[-\frac{\pi}{N-1} - u \right] \right\} \right]$$

$$|\tilde{F}(u)| = \left| \frac{\cos \left(\frac{N-1}{2} u \right) \sin \left(\frac{\pi}{N-1} \right)}{\cos u - \cos \frac{\pi}{N-1}} \right|$$

Notice the two end elements of the array have zero excitation.

(a) Determine the global maximum at $u = 0$ and find an asymptotic value as $N \to \infty$.

(b) Show that the global maxima of $|\tilde{F}(u)|$ occurs at $u = 0$ and that $\cos u = \cos \frac{\pi}{N-1}$ is not even a local maxima. Zeros of $\tilde{F}(u)$ occur when

$$u = \frac{(2m+1)\pi}{N-1}$$

where m is any integer but $m/(N-1)$ is not an integer and $m/(N+1)$ is not an integer. Determine the exact sidelobe locations and levels and also obtain asymptotic values as $N \to \infty$. Calculate and compare the results for $N = 6, 10, 15, 50$.

(c) The formula for the directivity of the array $u = kd \cos \psi - \alpha$ and $du = -kd \sin \psi d\psi$ is

$$D = \frac{4\pi |\tilde{F}(u)|_{\mathrm{max}}^2}{\displaystyle\int d\Omega \, |\tilde{F}(u)|^2} = \frac{4\pi \tilde{F}(0)|^2}{\displaystyle\int_0^{2\pi} d\phi \int_0^\pi d\psi \sin \psi |\tilde{F}(u)|^2} = \frac{2kd \cot^2 \left(\frac{\pi}{2(N-1)} \right)}{\displaystyle\int_{-kd-\alpha}^{kd-\alpha} du \, |\tilde{F}(u)|^2}$$

For $N = 6$, and $d = \lambda/2$, calculate D.

P5.4.4

Consider the synthesis of the array pattern [Ma, 1974]

$$G(\xi) = e^{-(\xi-2)^2/4} \qquad\qquad -2 \le \xi \le 2$$

with four elements, where $\xi = 2\cos u = 2\cos[kd\cos\psi - \alpha]$.

(a) Let $x = \xi/2$ and choose the zeros of the Legendre polynomials $P_4(x)$ as the sampling points for $g(x) = \exp[-(1-x)^2]$. The zeros are

$$x_0 = -0.861, \qquad x_1 = -0.340, \qquad x_2 = 0.340, \qquad x_3 = 0.861$$

Making use of the Lagrange interpolation formula, determine $g(x)$, which is positive for $-1 \leq x \leq 1$. Find the power pattern $P(\xi)$, which is positive for $-2 \leq \xi \leq 2$.

(b) Estimate the maximum error, $\epsilon_{\max}$, noting that

$$|\pi(x)|_{\max} = \frac{N!}{(2N-1)(2N-3)\ldots 1}\,|P_N(x)|_{\max}$$

and that $P_N(x) \leq 1$ for $-1 \leq x \leq 1$.

P5.4.5

The method of trigonometric interpolation is very useful when the sampling points are equally spaced [Ma, 1974]. With this method it is more convenient to deal with the power patterns as a function of u, $P(u)$. Remember that $\xi = 2\cos u$. The original visible range can be transformed to give the range of u from 0 to π. The sampling positions are obtained by dividing the u range into $N-1$ intervals.

$$u_l = \frac{l\pi}{N-1} \qquad l = 0, 1, \ldots, N-1$$

For every given function of bounded variation $G(u)$, the trigonometric interpolation method provides $P(u)$ which converges unlimitedly to $G(u)$ as the number of sampling points increases.

Consider Example 4.4.2 and let $kd = \pi$ and $\alpha = 0$ so that the range of u is $[0, \pi]$ without additional transformations. We take

$$u_0 = 0, \qquad u_1 = \pi/3, \qquad u_2 = 2\pi/3, \qquad u_3 = \pi$$
$$G(u_0) = 1, \quad G(u_1) = 0.779, \quad G(u_2) = 0.105, \quad G(u_3) = 0.018$$

Find $P(u)$ and $P(\xi)$. Show that the power pattern satisfies the realization condition $P(\xi) \geq 0$ for $-2 \leq \xi \leq 2$.

P5.4.6

Consider the approximation of a given power pattern by the use of Bernstein polynomials. For a real function $g(x)$ defined in the interval $0 \leq x \leq 1$, the Bernstein polynomial approximation of order n of $g(x)$ is [Ma, 1974]

$$B_n^g(x) = \sum_{l=0}^{n} \frac{n!}{l!(n-l)!}\, g(l/n) x^l (1-x)^{n-l}$$

The convergence of $B_n^g(x)$ to $g(x)$ is also unlimited as n is increased. We see that when $g(x)$ is a constant, $B_n^g(x)$ is equal to the same constant for all n. The most important property of $B_n^g(x)$ in array synthesis is that if $g(x)$ is bounded, $B_n^g(x)$ is bounded with the same upper and lower limits. Thus the resultant approximating polynomial will always satisfy the realization condition while the other interpolation methods provide no such guarantee. For the array pattern as given in Example 4.4.2, find the Bernstein polynomial approximation for $n = 3$ and determine the corresponding array pattern.

5.5　Linear Antennas

From the input terminals of an antenna, the field radiated by the antenna can be viewed as power dissipated in a resistor called the radiation resistance of the antenna. For a wire antenna with a current distribution $\overline{J}(\overline{r}') = \hat{z}I(z')\delta(x')\delta(y')$, the θ component of the vector current moment is

$$f_\theta = -\sin\theta \iiint d^3r' \, J(\overline{r}')e^{-i\overline{k}\cdot\overline{r}'} = -\sin\theta \int dz' \, I(z')e^{-ikz'\cos\theta}$$

(5.5.1)

The electric field is calculated as

$$E_\theta = iw\mu \frac{e^{ikr}}{4\pi r} f_\theta$$

and the magnetic field as

$$H_\phi = ik \frac{e^{ikr}}{4\pi r} f_\theta$$

The total radiated power is

$$P_r = \int_0^{2\pi} d\phi \int_0^\pi d\theta \, r^2 \sin\theta \, \frac{1}{2} E_\theta H_\phi^*$$

$$= \int_0^\pi d\theta \sin\theta \, \pi\eta \left(\frac{k}{4\pi}\right)^2 |f_\theta|^2$$

(5.5.2)

where $\eta = (\mu/\epsilon)^{1/2}$. The radiation resistance is

$$R_r = 2P_r/I_0^2$$

where I_0 is the input current amplitude.

　　Consider a wire antenna with zero radius and length $2l$ excited at the center by a constant current source I_0 [Fig. 5.5.2]. When l is infinitesimally small, we may use the Hertzian dipole model with $I(z') = 2I_0l\delta(z')$. The current moment is found from (5.5.1) to be

$$f_\theta = -2I_0l\sin\theta$$

(5.5.3)

This is the result of the current moment obtained from (5.5.1) by ignoring the contribution from the retardation factor. The total radiated
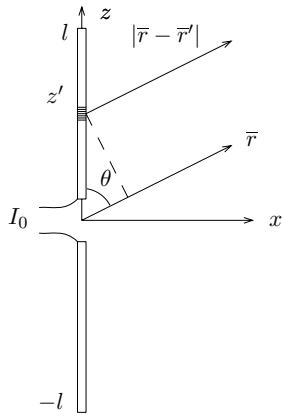
Figure 5.5.1 Wire antenna excited by a current source.
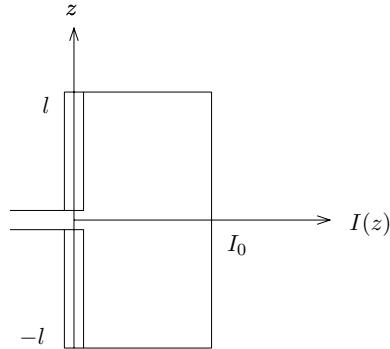
Figure 5.5.2 Uniform current distribution.

power for a wire antenna with the current moment f_θ is calculated
from (5.5.2) to be

$$P_r = \int_0^\pi d\theta \, \sin^3 \theta \, (k/4\pi)^2 4\pi\eta \, I_0^2 l^2 = \frac{(2kI_0 l)^2}{12\pi}\eta$$

Thus the radiation resistance is

$$R_r = \frac{2P_r}{I_0^2} = \frac{(2kl)^2}{6\pi}\eta = 20(2kl)^2 \qquad (5.5.4)$$

where we made use of the fact that $\eta = 120\pi$ ohms. Clearly, the radi-
ation resistance R_r as calculated in (5.5.4) is not applicable to a wire

antenna with any significant length. For instance, when $2l = \lambda/2$, we will find $R_r \approx 200$ ohms where the more accurate value from measurement and from more rigorous calculation is 73 ohms.

In the calculation of R_r in (5.5.4), we assume the current distribution on the wire is uniform [Fig. 5.5.2]. If the wire is made of conductors, boundary conditions at $z = \pm l$ will require $I(z)$ be zero there. A better approximation for the current distribution for a small l takes the form of a triangular shape [Fig. 5.5.3],

$$I(z') = \frac{I_0}{l}(l - |z'|)$$
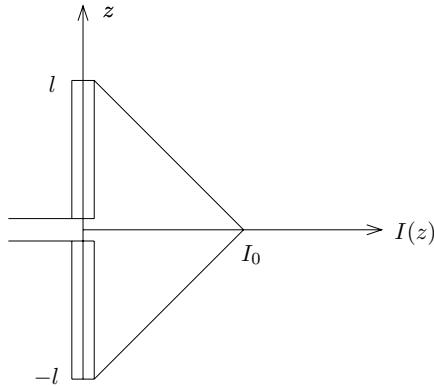
Figure 5.5.3 Triangular current distribution.

In the calculation of the current moment, we neglect the phase retardation factor $e^{-ikz'\cos\theta}$ by assuming the wire length is small,

$$f_\theta \approx -\sin\theta \int_{-l}^{l} dz' \frac{I_0}{l}(l - |z'|) = -I_0 l \sin\theta \qquad (5.5.5)$$

This is equivalent to replacing the current moment $-2I_0 l \sin\theta$ for a Hertzian dipole of uniform current distribution as shown in Figure 5.5.2 with the average current moment $-I_0 l \sin\theta$ of the triangular distributions as shown in Figure 5.5.3. The radiation resistance is calculated to be

$$R_r = \frac{2P_r}{I_0^2} = 5(2kl)^2 \qquad (5.5.6)$$
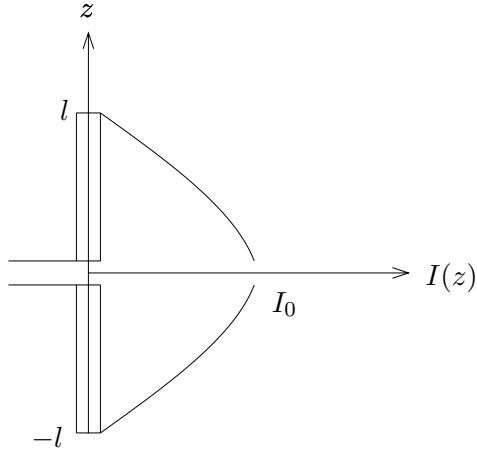
Figure 5.5.4 Sinusoidal current distribution.

which is four times smaller than that in (5.5.4). Stretching the limit
of $2l$ to a half-wavelength, we find $R_r = 50$ ohms. For a wire antenna
with $2l$ smaller than $\lambda/2$, taking into account the phase-retardation
factor will serve to decrease the current moment because the integrand
in (5.5.5) is always positive and the phase-retardation factor causes its
magnitude to decrease. Therefore, the reason for the underestimation
of R_r cannot be attributed to the omission of the phase-retardation
factor. It must be due to the inaccuracy in the assumption of the
current distribution.

For a wire antenna that is not infinitesimally small, the more accu-
rate current distribution is approximated by a sinusoidal distribution.
We assume in [Fig. 5.5.4]

$$I(z') = I_m \sin k(l - \left| z' \right|) \qquad (5.5.7)$$

Notice that I_m is the amplitude of the sinusoid that is related to I_0
by $I_0 = I_m \sin(kl)$. The θ component of the vector current moment
is

$$f_\theta = -\sin\theta \int_{-l}^{l} dz' \, I_m \sin k(l - \left| z' \right|) e^{-ikz'\cos\theta}$$

The integration can be evaluated and gives rise to a closed-form for-
mula.

Before evaluating the integral exactly we again assume that the length $2l$ is small and that the contribution from the phase factor $e^{-ikz'\cos\theta}$ is uniformly close to 1. Evaluating the integral without taking into account the phase factor, we find

$$f_\theta = -\sin\theta\frac{2I_m}{k}(1 - \cos kl) \qquad (5.5.8)$$

Under the limit of $kl \ll 1$, we get the approximate result

$$f_\theta \approx -I_m(kl^2)\sin\theta \qquad (5.5.9)$$

Notice that $I_m \approx I_0/kl$. Thus (5.5.9) is identical to (5.5.5).

Applying the result to a half-wavelength wire, we obtain from (5.5.8),

$$f_\theta = -\sin\theta\left(\frac{2I_m}{k}\right) = -\sin\theta\left(\frac{4}{\pi}\right)I_0l$$

where from $f_\theta = -\sin\theta(2I_m/k)$ we find $I_m = I_0$. Comparing with (5.5.5), it is seen from (5.5.4) that the radiation resistance is

$$R_r = 5(2kl)^2\left(\frac{4}{\pi}\right)^2 = 80 \qquad \text{ohms} \qquad (5.5.10)$$

The reason that the sinusoidal current distribution gives a larger radiation resistance than the triangular assumption is that the area under the sine is larger than the triangle. However, the phase-retardation effect has been neglected. If it is not neglected, the result will be applicable to wire antennas with any length, small or large.

The current moment for a wire antenna of length $2l$ and with the sinusoidal current distribution, taking into account the phase - retardation factor, is calculated as

$$\begin{aligned}
f_\theta &= -\sin\theta\int_{-l}^{l}dz'\, I_m\sin k(l - |z'|)e^{-ikz'\cos\theta} \\
&= -\frac{2I_m}{k}\left[\frac{\cos(kl\cos\theta) - \cos kl}{\sin\theta}\right] \qquad (5.5.11)
\end{aligned}$$

The electric field vector is

$$\overline{E} = \hat{\theta}\,i\omega\mu\frac{e^{ikr}}{4\pi r}f_\theta = -\hat{\theta}\frac{i\eta I_m e^{ikr}}{2\pi r}\left[\frac{\cos(kl\cos\theta) - \cos kl}{\sin\theta}\right]$$

The total radiated power P_r is

$$P_r = \int_0^\pi d\theta\,\sin\theta\,\frac{\eta I_m{}^2}{4\pi}\left[\frac{\cos(kl\cos\theta)-\cos kl}{\sin\theta}\right]^2$$

The radiation resistance is, using I_m as the input current

$$R_r = \frac{2P_r}{I_m{}^2} = \frac{\eta}{2\pi}\int_0^\pi d\theta\,\frac{[\cos(kl\cos\theta)-\cos kl]^2}{\sin\theta} \qquad (5.5.12)$$

Changing variables of integration, we find

$$R_r = \frac{\eta}{2\pi}\int_{-1}^1 du\,\frac{[\cos(klu)-\cos kl]^2}{1-u^2}$$

$$= \frac{\eta}{4\pi}\int_{-1}^1 du\left\{\frac{[\cos(klu)-\cos kl]^2}{1+u}+\frac{[\cos(klu)-\cos kl]^2}{1-u}\right\}$$

$$= \frac{\eta}{2\pi}\int_0^2 dv\left\{\frac{[\cos(klv)-\cos kl]^2}{v}\right\}$$

$$= \frac{\eta}{2\pi}\left\{\left(1+\frac{1}{2}\cos 2kl\right)\int_0^2 dy\,\frac{1}{y}-\int_0^2 dy\,\frac{\cos kly}{y}\right.$$

$$\left.-\int_0^2 dy\,\frac{\cos[kl(y-2)]}{y}+\int_0^2 dy\,\frac{\cos[2kl(y-1)]}{2y}\right\}$$

$$= \frac{\eta}{2\pi}\left\{\int_0^2 \frac{dy}{y}(1-\cos kly)\right.$$

$$+\sin(2kl)\left[\int_0^2 \frac{dy}{2y}\sin 2kly-\int_0^2 \frac{dy}{y}\sin kly\right]$$

$$\left.+\cos(2kl)\left[\int_0^2 \frac{dy}{y}(1-\cos kly)-\int_0^2 \frac{dy}{2y}(1-\cos 2kly)\right]\right\}$$

$$= \frac{\eta}{2\pi}\left\{\gamma+\ln(2kl)-Ci(2kl)+\sin(2kl)\left[\frac{1}{2}Si(4kl)-Si(2kl)\right]\right.$$

$$\left.+\frac{1}{2}\cos(2kl)\left[\gamma+\ln(kl)+Ci(4kl)-2Ci(2kl)\right]\right\} \qquad (5.5.13)$$

where

$$Si(x) = \int_0^x dx'\,\frac{\sin x'}{x'}$$

$$Ci(x) = -\int_x^\infty dx'\,\frac{\cos x'}{x'}$$
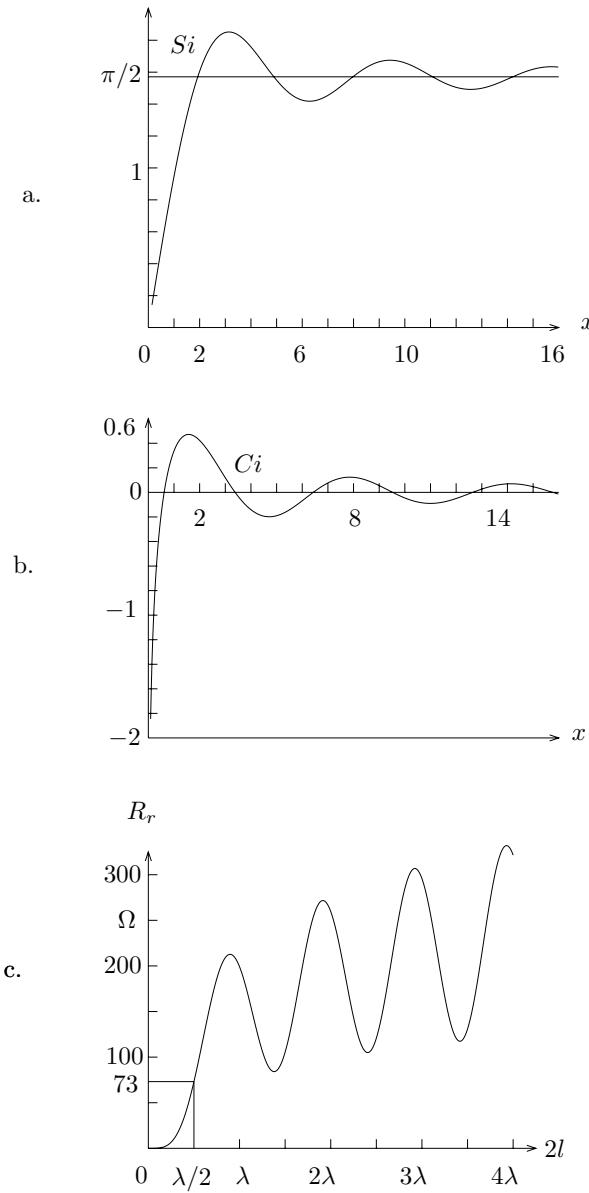
Figure 5.5.5 Functions $Si(x)$ and $Ci(x)$ and radiation resistance R_r.

and $\gamma = 0.5772\ldots$ In the above derivation, we made use of the relation

$$\int_0^x dx' \, \frac{1 - \cos x'}{x'} = \gamma + \ln x - Ci(x)$$

The sine integral $Si(x)$ and the cosine integral $Ci(x)$ are illustrated in Figures 5.5.5a,b. A numerical plot for R_r as a function of $2l$ is shown in Figure 5.5.5c. When $2l = \lambda/2$, we find $R_r = 73$ ohms.

In the above discussions, we have illustrated how an antenna problem is attacked. The results clearly become more accurate as the assumptions become more realistic, which also bring in more complicated mathematical manipulations. Nevertheless, we cannot claim that the wire antenna problem has now acquired a satisfactory answer. Two major problems still remain: (i) The radius of the wire has been tacitly assumed to be infinitesimally small. What if it is not? (ii) How do we know whether the sinusoidal current distribution on the wire is the valid assumption? Why do we not assume other types of current distributions which also satisfy the boundary conditions of zero current at $z = \pm l$? These questions can be answered only with a detailed model of the antenna. With a precise physical structure, the current on the antenna can be *determined* from the Maxwell equations, *not assumed.*

cylindrical   spheroidal   biconical
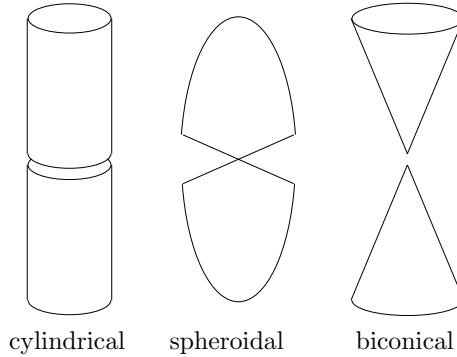
Figure 5.5.6 Models of antenna.

To address the above questions, at least three different models [Fig. 5.5.6] have been used with a rigorous boundary value problem approach. The model by Hällén and King [1969] is a perfectly conducting cylinder with finite radius a and length l with a gap at $z = 0$ where the electric field strength is $-V\delta(z)$. The problem is formulated in the form of integral equations. The second approach is due to Stratton and Chu [1941] who modeled a dipole antenna as a pair of ellipsoids or prolate spheroids. Normal modes associated with the structure are used to match boundary conditions. The third approach is developed by Schelkunoff [1943] with the model of a biconical structure. In the

next section we shall pursue Schelkunoff's approach to the solution of this fundamental problem.

Problems

P5.5.1
(a) Find the far field electric and magnetic vectors due to a line current source with $I(z) = I_0 e^{ik_z z}$, placed along the z axis in free space.
(b) Evaluate the real part of the complex Poynting's vector in the far field. What happens if $k_z > k$?
(c) Determine the equi-phase surfaces (phase fronts) in the far field, both for $k_z < k$ and $k_z > k$. Is the real part of the Poynting's vector normal to the equi-phase surfaces?

P5.5.2
Consider a conducting wire with zero radius and length $2l$ excited by a constant current source I_0. The current density is

$$\overline{J}(\overline{r}') = \hat{z} I_0 \sin(kl - k|z'|)\, \delta(x')\delta(y')$$

which satisfies the boundary condition of zero current at $z' = \pm l$. For the radiation field, show that the vector current moment $\overline{f}(\theta, \phi)$ is

$$\overline{f}(\theta, \phi) = \hat{z}\frac{2I_0}{k\sin^2\theta}[\cos(kl\cos\theta) - \cos(kl)]$$

Find the electric field $\overline{E}$ in the radiation zone. What is $\overline{E}$ at $\theta = 0$ and π? Plot the radiation field pattern for $2l = 3\lambda/2$ and find that the null positions. To help understand these null positions, consider three collinear dipoles separated by $\lambda/2$ in distance with the center element π out of phase with the two end dipoles. Show that the far field is the sum $e^{-i\pi\cos\theta} - 1 + e^{i\pi\cos\theta}$ and determine the null positions.

P5.5.3
(a) Estimate R_r for a half-wavelength dipole.
(b) Calculate the radiation resistance as $kl \to 0$ and compare with that of a Hertzian dipole.

P5.5.4
Find an asymptotic formula for the radiation resistance R_r of a thin, linear dipole antenna, for large l/λ.

5.6   Biconical Antennas

A. Formulation and Wave Solutions

The geometrical configuration of a biconical antenna is shown in Figure 5.6.1. Due to the symmetry, we expect that all field solutions are ϕ-independent. The Maxwell equations can then be reduced to two uncoupled sets of equations; one set relates E_r, E_θ, and H_ϕ and forms the TM modes, and the other set relates H_r, H_θ, and E_ϕ and forms the TE modes. For the biconical antenna problem, the currents are in the $\hat{r}$ direction and we expect TM waves solutions.
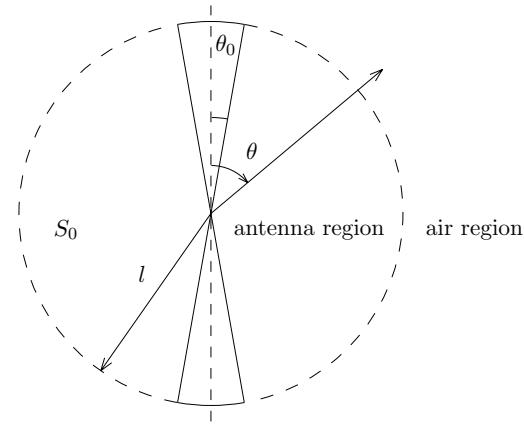
Figure 5.6.1   Biconical antenna.

We deal with the solutions of the Maxwell equations satisfying the following boundary conditions:

(i) In the air region, the electromagnetic field must be an outgoing wave.

(ii) In the antenna region, the tangential electric field vanishes on the surfaces of the cones

$$E_r(\theta_0) = E_r(\pi - \theta_0) = 0 \tag{5.6.1}$$

At the input,

$$V_0 = \lim_{r \to 0} \int_{\theta_0}^{\pi - \theta_0} d\theta \, r E_\theta \tag{5.6.2}$$

where V_0 is the given external excitation voltage.

(iii) On the boundary surface S_0 separating the antenna region and the air region

$$E_\theta(l+0) = 0 \qquad 0 \le \theta \le \theta_0 \text{ and } \pi - \theta_0 \le \theta \le \pi \quad (5.6.3)$$

$$E_\theta(l+0) = E_\theta(l-0) \qquad \theta_0 < \theta < \pi - \theta_0 \qquad (5.6.4)$$

$$E_r(l+0) = E_r(l-0) \qquad \theta_0 < \theta < \pi - \theta_0 \qquad (5.6.5a)$$

$$H_\phi(l+0) = H_\phi(l-0) \qquad \theta_0 < \theta < \pi - \theta_0 \qquad (5.6.5b)$$

Note that boundary conditions $(5.6.5a)$ and $(5.6.5b)$ are not independent of each other because $(5.6.5a)$ is associated with Gauss' law and $(5.6.5b)$ with Ampère's law. They depend on each other as a consequence of the charge-current conservation law. We shall use either $(5.6.5a)$ or $(5.6.5b)$, depending on whichever is more convenient. The governing equations for the TM waves are

$$\frac{1}{r\sin\theta}\frac{\partial}{\partial\theta}(\sin\theta\, H_\phi) = -i\omega\epsilon E_r \qquad (5.6.6a)$$

$$-\frac{1}{r}\frac{\partial}{\partial r}(r\, H_\phi) = -i\omega\epsilon E_\theta \qquad (5.6.6b)$$

$$\frac{1}{r}\frac{\partial}{\partial r}(rE_\theta) - \frac{1}{r}\frac{\partial}{\partial\theta}(E_r) = i\omega\mu H_\phi \qquad (5.6.6c)$$

Substituting $(5.6.6a)$ and $(5.6.6b)$ in $(5.6.6c)$ to eliminate E_r and E_θ, we obtain

$$\frac{\partial^2}{\partial r^2}rH_\phi + \frac{1}{r^2}\frac{\partial}{\partial\theta}\left[\frac{1}{\sin\theta}\frac{\partial}{\partial\theta}(\sin\theta\, r\, H_\phi)\right] + k^2\, r\, H_\phi = 0 \qquad (5.6.7)$$

Equation $(5.6.7)$ is solved by the separation of variables technique. Let

$$H_\phi = R(r)\Theta(\theta) \qquad (5.6.8)$$

We obtain the following two equations

$$\frac{1}{r}\frac{d^2}{dr^2}rR(r) + \left[k^2 - \frac{n(n+1)}{r^2}\right]R(r) = 0 \qquad (5.6.9)$$

$$\frac{d}{d\theta}\left[\frac{1}{\sin\theta}\frac{d}{d\theta}(\sin\theta\Theta(\theta))\right] + n(n+1)\Theta(\theta) = 0 \qquad (5.6.10)$$

with $n(n+1)$ as the separation constant.

Solutions to (5.6.9) are the spherical Hankel functions $h_n^{(1)}(kr)$ and $h_n^{(2)}(kr)$. For the first few orders $n = 0$ to $n = 2$, the spherical Hankel functions of first kind are

$$h_0^{(1)}(kr) = -i\frac{e^{ikr}}{kr} \tag{5.6.11a}$$

$$h_1^{(1)}(kr) = -\left[1 + \frac{i}{kr}\right]\frac{e^{ikr}}{kr} \tag{5.6.11b}$$

$$h_2^{(1)}(kr) = i\left[1 + 3\left(\frac{i}{kr}\right) + 3\left(\frac{i}{kr}\right)^2\right]\frac{e^{ikr}}{kr} \tag{5.6.11c}$$

The second kind spherical Hankel functions $h_n^{(2)}(kr)$ are complex conjugates of $h_n^{(1)}(kr)$. The spherical Bessel functions $b_n(\xi)$ are related to the cylindrical Bessel functions $B_n(\xi)$ by

$$b_n(\xi) = \sqrt{\frac{\pi}{2\xi}}B_{n+\frac{1}{2}}(\xi)$$

with $b_n(\xi)$ representing $h_n^{(1)}$ or $h_n^{(2)}$ and $B_n(\xi)$ representing $H_n^{(1)}$ or $H_n^{(2)}$. The recurrence formulas are

$$B_\nu'(\xi) = B_{\nu-1}(\xi) - \frac{\nu}{\xi}B_\nu(\xi)$$

$$= -B_{\nu+1}(\xi) + \frac{\nu}{\xi}B_\nu(\xi)$$

The spherical Bessel functions $j_n(kr)$ are defined as the real part of either $h_n^{(1)}(kr)$ or $h_n^{(2)}(kr)$. For the first few orders, they are

$$j_0(kr) = \frac{\sin kr}{kr} \tag{5.6.12a}$$

$$j_1(kr) = -\frac{\cos kr}{kr} + \frac{\sin kr}{(kr)^2} \tag{5.6.12b}$$

$$j_2(kr) = -\frac{\sin kr}{kr} - \frac{3\cos kr}{(kr)^2} + \frac{3\sin kr}{(kr)^3} \tag{5.6.12c}$$

Note that the $j_n(kr)$ functions remain finite as $kr \to 0$. The imaginary parts of $h_n^{(1)}(kr)$ are known as the spherical Neumann functions, which become infinite as $kr \to 0$.

Solutions to (5.6.10) are derivatives of the Legendre polynomial $P(\theta)$

$$\Theta(\theta) = \frac{d}{d\theta}P(\theta) \tag{5.6.13}$$

where $P(\theta)$ satisfies the ordinary Legendre equation

$$\frac{1}{\sin\theta}\frac{d}{d\theta}\left[\sin\theta\frac{dP(\theta)}{d\theta}\right] + n(n+1)P(\theta) = 0 \tag{5.6.14}$$

The two independent solutions to (5.6.14) are $P_n(\cos\theta)$ and $Q_n(\cos\theta)$ where

$$P_n(\cos\theta) = \sum_{q=0}^{\infty}\frac{(-1)^q(n+q)!}{(n-q)!(q!)^2}\sin^{2q}(\theta/2) \tag{5.6.15}$$

The other independent solution is $Q_n(\cos\theta) = P_n(-\cos\theta)$ for noninteger values of n. For integer values of n, we have

$$Q_n(\cos\theta) = P_n(\cos\theta)\ln\left(\cot\frac{\theta}{2}\right) - \sum_{s=1}^{n}\frac{P_{n-s}P_{s-1}}{s} \tag{5.6.16}$$

where the summation term contributes when $n \geq 1$. The Rodrigues' formula for generating Legendre polynomials states, for integer values of n,

$$P_n(u) = \frac{1}{2^n n!}\frac{d^n}{du^n}(u^2-1)^n$$

where $u = \cos\theta$. The first few Legendre polynomials $P_n(\cos\theta)$ are

$$P_0(\cos\theta) = 1 \tag{5.6.17a}$$

$$P_1(\cos\theta) = \cos\theta \tag{5.6.17b}$$

$$P_2(\cos\theta) = \frac{1}{2}(3\cos^2\theta - 1) = \frac{1}{4}(3\cos 2\theta + 1) \tag{5.6.17c}$$

Note that the $Q_n(\cos\theta)$ functions for integer values of n become infinite at $\theta = 0$ and $\theta = \pi$. For noninteger values of n the functions $P_n(-\cos\theta)$ become infinite at $\theta = \pi$.

In terms of $R(r)$ and $P(\theta)$, we now find from (5.6.6a), (5.6.6b), and (5.6.8)

$$H_\phi = R(r)\frac{dP(\theta)}{d\theta} \tag{5.6.18a}$$

$$E_r = -\frac{R(r)}{i\omega\epsilon r}\frac{1}{\sin\theta}\frac{d}{d\theta}\left[\sin\theta\frac{dP(\theta)}{d\theta}\right] = \frac{n(n+1)}{i\omega\epsilon r}R(r)P(\theta) \tag{5.6.18b}$$

$$E_\theta = \frac{1}{i\omega\epsilon r}\frac{d[rR(r)]}{dr}\frac{dP(\theta)}{d\theta} \tag{5.6.18c}$$
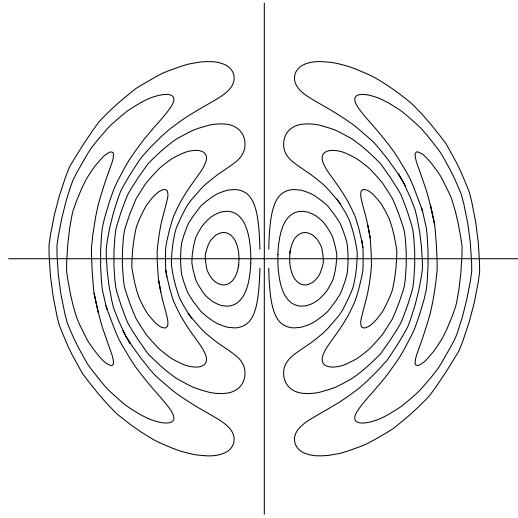
Figure 5.6.2 Electric field lines for TM_1 mode.

B. Solution in the Air Region and Dipole Fields

We first consider solutions in the air region. They take the form, for $n = 0, 1, 2, \ldots$

$$H_\phi = \frac{1}{2\pi} \sum_n b_n h_n^{(1)}(kr) \frac{d}{d\theta} P_n(\cos\theta) \qquad (5.6.19a)$$
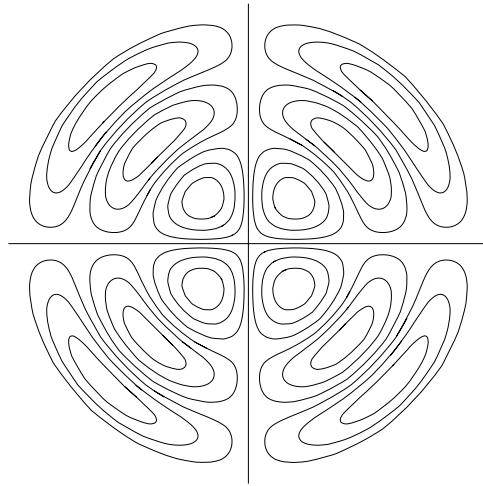
$$E_r = \frac{1}{2\pi i \omega \epsilon r} \sum_n n(n+1) b_n h_n^{(1)}(kr) P_n(\cos\theta) \qquad (5.6.19b)$$

$$E_\theta = \frac{1}{2\pi i \omega \epsilon r} \sum_n b_n \frac{d}{dr}[r h_n^{(1)}(kr)] \frac{d}{d\theta} P_n(\cos\theta) \qquad (5.6.19c)$$

We choose the Hankel functions of the first kind because they represent outgoing waves. The functions with noninteger values of n and the $Q_n(\cos\theta)$ solutions are excluded because they are singular in the directions $\theta = 0$ and $\theta = \pi$. The electric field lines for the TM_1 and TM_2 modes are plotted in Figures 5.6.2–5.6.3.

We note that the TEM (or the TM_0) mode is not present in the air region because $n = 0$ and $P_0(\cos\theta) = 1$. For the TM_1 mode, we find

$$H_\phi = \frac{b_1 e^{ikr}}{2\pi kr} \left[1 + \frac{i}{kr}\right] \sin\theta \qquad (5.6.20a)$$

Figure 5.6.3 Electric field lines for TM_2 **mode.**

$$E_r = \frac{\eta b_1 e^{ikr}}{\pi kr}\left[\frac{i}{kr} + \left(\frac{i}{kr}\right)^2\right]\cos\theta \qquad (5.6.20b)$$

$$E_\theta = \frac{\eta b_1 e^{ikr}}{2\pi kr}\left[1 + \frac{i}{kr} + \left(\frac{i}{kr}\right)^2\right]\sin\theta \qquad (5.6.20c)$$

where $\eta = k/\omega\epsilon = (\mu/\epsilon)^{1/2}$. These are the fields for a Hertzian dipole. We can determine b_1 by using the cylindrical coordinate system and noting that the current dipole moment is

$$I_0 l_{eff} = \int_{-\infty}^{\infty} dz\, I_z \qquad (5.6.21)$$

where

$$I_z = \int_0^{2\pi} \rho\, d\phi\, H_\phi$$

As $r = (z^2 + \rho^2)^{1/2}$ and $\sin\theta = \rho/r$, we obtain from $(5.6.20a)$ as $\rho \to 0$ and $z \to 0$

$$I_z \approx \frac{ib_1\rho^2}{k^2(z^2 + \rho^2)^{3/2}}$$

Notice that $I_z \to 0$ as $\rho \to 0$. At the point $z = 0$, however, $I_z \to \infty$ as $\rho \to 0$. Carrying out the integral (5.6.21), we find

$$I_0 l_{eff} = \frac{i2b_1}{k^2}\int_0^{\infty} dz\frac{\rho^2}{(z^2 + \rho^2)^{3/2}} = \frac{i2b_1}{k^2}$$

which yields

$$b_1 = \frac{k^2}{i2} I_0 l_{eff}$$

The solutions expressed in (5.6.20) are identical to those for an infinitesimal dipole antenna. The electric field lines for the quadrupole field are illustrated in Figure 5.6.3.

C. Solution in the Antenna Region

In the antenna region, we note from (5.6.18b) that the boundary conditions for E_r as expressed in (5.6.1) are satisfied either when $n = 0$ or when

$$P(\theta_0) = P(\pi - \theta_0) = 0 \qquad (5.6.22)$$

When $n = 0$, we have the TEM mode. The solution for $R(r)$ is a linear combination of e^{ikr}/r and e^{-ikr}/r, which represent waves guided by the cones and reflected at the terminals. The $Q_0(\cos\theta)$ function is used since $P_0(\cos\theta) = 1$ and $d[P_0(\cos\theta)]/d\theta = 0$.

For higher-order TM modes, n is determined from (5.6.22) and is in general not an integer. We denote it with u. We choose $P(\theta)$ to be a linear combination of $P_u(\cos\theta)$ and $P_u(-\cos\theta)$:

$$P(\theta) = T_u(\theta) = \frac{1}{2}\left[P_u(\cos\theta) + aP_u(-\cos\theta)\right]$$

Equation (5.6.22) requires that

$$P_u(\cos\theta_0) + aP_u(-\cos\theta_0) = 0$$
$$P_u(-\cos\theta_0) + aP_u(\cos\theta_0) = 0$$

We find that $a = \pm 1$. Therefore we have either

$$T_u(\theta) = \frac{1}{2}\left[P_u(\cos\theta) - P_u(-\cos\theta)\right]$$

which is an odd function in $\cos\theta$, or

$$T_u(\theta) = \frac{1}{2}\left[P_u(\cos\theta) + P_u(-\cos\theta)\right]$$

which is an even function. The derivatives

$$\frac{d}{d\theta}\left\{\frac{1}{2}\left[P_u(\cos\theta) - P_u(-\cos\theta)\right]\right\} = -\frac{1}{2}\left[P_u'(\cos\theta) + P_u'(-\cos\theta)\right]\sin\theta$$

$$\frac{d}{d\theta}\left\{\frac{1}{2}\left[P_u(\cos\theta) + P_u(-\cos\theta)\right]\right\} = -\frac{1}{2}\left[P_u'(\cos\theta) - P_u'(-\cos\theta)\right]\sin\theta$$

are, respectively, even and odd functions. Hence H_ϕ due to odd $T_u(\theta)$ functions are even functions of θ, which means that the currents in the upper and the lower cones are in the same direction. (If current at r_0 in the upper cone is flowing away from the origin, then the current at r_0 in the lower cone is flowing toward the origin.) For the even $T_u(\theta)$ functions, H_ϕ is an odd function of θ, which means the current in the upper and lower cones at some distance r_0 will be flowing in opposite directions. (Both currents will be flowing away from or toward the origin.)

We will only consider the balanced type of feed described by a series of odd $T_u(\theta)$ functions, which is the most important case from the practical point of view. Thus we choose

$$T_u(\theta) = \frac{1}{2}\left[P_u(\cos\theta) - P_u(-\cos\theta)\right] \qquad (5.6.23)$$

The complete solution may be written as a summation over u with u indicating the nearest integer of u,

$$H_\phi = \frac{I_0(r)}{2\pi r \sin\theta} + \frac{1}{2\pi}\sum_u a_u j_u(kr)\frac{d}{d\theta}T_u(\theta) \qquad (5.6.24a)$$

$$E_r = \frac{1}{2\pi r i\omega\epsilon}\sum_u u(u+1)a_u j_u(kr)T_u(\theta) \qquad (5.6.24b)$$

$$E_\theta = \frac{1}{2\pi r i\omega\epsilon \sin\theta}\frac{d}{dr}I_0(r) + \frac{1}{2\pi r i\omega\epsilon}\sum_u a_u \frac{d}{dr}[rj_u(kr)]\frac{d}{d\theta}T_u(\theta) \,(5.6.24c)$$

where $T_u(\theta)$ is given in (5.6.23). The first terms in (5.6.24a) and (5.6.24c) are the TEM solutions obtained from (5.6.9) and (5.6.10) with $n = 0$ and $I_0(r) \sim e^{\pm ikr}$. For higher-order modes, we choose the spherical Bessel functions $j_u(kr)$ only. This is because when the Neumann function $N_u(kr)$ is included, not only would the field quantities H_ϕ and E_θ become infinite as $kr \to 0$, but their integrals, which represent currents and voltages, would become too singular as $kr \to 0$. In the following we shall elaborate on a transmission line model to understand the implications of the above solutions.

D. Transmission Line Model

First we assume the antenna to be infinitely long and we study the outgoing TEM solution. Let $I_0(r) = Ae^{ikr}$ in (5.6.24). A voltage $V(r)$
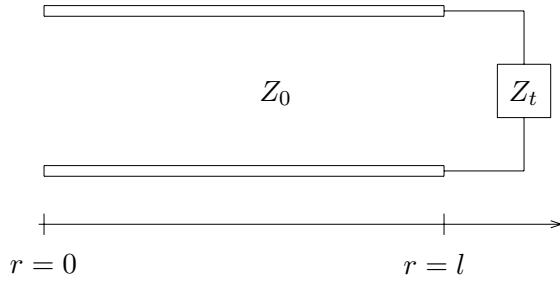
Figure 5.6.4 Transmission line model for the TEM mode.

and current $I(r)$ for the TEM mode can be defined at r as follows:

$$V_0(r) = \int_{\theta_0}^{\pi-\theta_0} d\theta\, r E_\theta = \frac{\eta}{\pi} A \left[\ln\left(\cot\frac{\theta_0}{2}\right)\right] e^{ikr}$$

$$I_0(r) = r\sin\theta_0 H_\phi(\theta = \theta_0) = A e^{ikr}$$

The ratio of $V_0(r)$ and $I_0(r)$ gives the characteristic impedance Z_0

$$Z_0 = \frac{\eta}{\pi} \ln\left(\cot\frac{\theta_0}{2}\right) \tag{5.6.25}$$

which is a constant for all r.

Since the antenna has a finite length l, we can, for the TEM mode, model the antenna as a transmission line [Fig. 5.6.4] with length l, characteristic impedance Z_0, and terminated with an impedance Z_t which is to be determined.

For the TEM mode on a biconical antenna with length l, we write

$$H_\phi = \frac{I_0(r)}{2\pi r \sin\theta} \tag{5.6.26a}$$

$$E_\theta = \frac{\eta}{Z_0} \frac{V_0(r)}{2\pi r \sin\theta} \tag{5.6.26b}$$

where, according to transmission line theory, the voltage along the line can be expressed in terms of the voltage $V_0(l)$ at the terminating impedance Z_t,

$$V_0(r) = V_0(l)\left[\cos k(l-r) - i\frac{Z_0}{Z_t}\sin k(l-r)\right] \tag{5.6.27a}$$

$$I_0(r) = \frac{V_0(l)}{Z_0}\left[-i\sin k(l-r) + \frac{Z_0}{Z_t}\cos k(l-r)\right] \tag{5.6.27b}$$

Thus the voltage at any point r is a superposition of the two independent solutions of sine and cosine functions of kr. Note that

$$E_\theta = \frac{1}{i\omega\epsilon r}\frac{\partial}{\partial r}(rH_\phi)$$

is satisfied and that for $r = l$, $V_0(l)/I_0(l) = Z_t$. The impedance Z_t will be shown to account for all higher-order modes inside the antenna region and the radiation field in the air region.

To include all higher-order modes, we note that along any meridian between the cones, $\nabla \times \overline{E} = 0$. We define a voltage $V(r)$

$$\begin{aligned}
V(r) &= \int_{\theta_0}^{\pi-\theta_0} d\theta\, r E_\theta \\
&= V_0(r) + \frac{1}{2\pi i\omega\epsilon}\sum_u a_u \frac{d}{dr}\left[r\, j_u(kr)\right]\left[P_u(-\cos\theta_0) - P_u(\cos\theta_0)\right] \\
&= V_0(r) \tag{5.6.28}
\end{aligned}$$

The second equality follows from $(5.6.24c)$ and the third equality is due to the boundary condition (5.6.1). The result states that the voltage for all r along the transmission line is none other than that of the TEM mode.

The current along the line $I(r)$ is given by

$$\begin{aligned}
I(r) &= 2\pi r \sin\theta_0 H_\phi(\theta = \theta_0) \\
&= I_0(r) + \sum_u a_u r j_u(kr)\sin\theta_0\left[\frac{d}{d\theta}T_u(\theta)\right]_{\theta=\theta_0} \\
&= I_0(r) + \tilde{I}(r) \tag{5.6.29}
\end{aligned}$$

where we used $\tilde{I}(r)$ to denote complementary currents due to higher-order TM modes. However, at the input end $(r = 0)$

$$I(r = 0) = I_0(r = 0) + \tilde{I}(r = 0) = I_0(r = 0) \tag{5.6.30}$$

because $r j_u(kr) \to 0$ as $r \to 0$. Thus the input current is still the same as that for the TEM modes. As a consequence, the input impedance at the antenna terminal is

$$Z_i = \frac{V(0)}{I(0)} = \frac{V_0(0)}{I_0(0)} \tag{5.6.31}$$

which depends only on the TEM mode. In terms of the terminal impedance Z_t, the input impedance Z_i is immediately determined from (5.6.27) which yields

$$Z_i = \frac{V_0(0)}{I_0(0)} = Z_0 \frac{Z_t - i\, Z_0 \tan kl}{Z_0 - i\, Z_t \tan kl} \tag{5.6.32}$$

The terminal impedance Z_t contains all the information about all the higher-order modes and the antenna configurations. To determine the terminal impedance Z_t, we now turn to the solutions in the air region and match them with those in the antenna region.

In terms of the transmission line model in Figure 5.6.4, the equivalent terminal impedance Z_t is

$$Z_t = \frac{V_0(l)}{I_0(l)} = \frac{V_0(l)}{I(l) - \tilde{I}(l)} \tag{5.6.33}$$

where $I(l)$ denotes the total current on the antenna at $r = l$ and $\tilde{I}(l)$ is the complementary current due to all modes other than TEM.

The equivalent terminal admittance Y_t of the transmission line model as shown in Figure 5.6.4 is the reciprocal of (5.6.33). For very thin antennas

$$Y_t = \frac{I(l)}{V_0(l)} - \frac{\tilde{I}(l)}{V_0(l)} \approx -\frac{\tilde{I}(l)}{V(l)} \tag{5.6.34}$$

This is because the total current at the ends of a thin antenna is vanishingly small. In fact the term $I(l)/V_0(l) = I(l)/V(l)$ is the admittance between the two caps of the antenna and as such is approximately equal to the susceptance of the electrostatic capacitance between the caps.

The complementary current $\tilde{I}(r)$ due to the higher-order TM modes $(n \neq 0)$ is, from (5.6.29)

$$\tilde{I}(r) = \sum_u a_u r j_u(kr) \sin\theta_0 \left[\frac{d}{d\theta} T_u(\theta)\right]_{\theta=\theta_0} \approx \frac{120}{Z_0} \sum_u a_u r j_u(kr) \tag{5.6.35}$$

The second equality is due to the fact that as $\theta_o \to 0$, $u \to 2m+1+\Delta$, and

$$\left[\frac{d}{d\theta} T_u(\theta)\right]_{\theta=\theta_0} \simeq -\frac{1}{2\pi} \sin u\pi \cot\frac{\theta_0}{2} \approx -\frac{\sin u\pi}{\pi\theta_0} \approx \frac{\Delta}{\theta_0} = \frac{120}{Z_0\theta_0} \tag{5.6.36}$$

The complete field solutions in the antenna and air regions are given by (5.6.24) and (5.6.19). At $r = l$, E_r should be continuous, hence

$$\sum_u u(u+1)a_u \, j_u(kl) \, T_u(\theta) = \sum_n n(n+1)b_n \, h_n^{(1)}(kl) \, P_n(\cos\theta)$$

As $\theta_0 \to 0$ and $Z_0 \to \infty$, u approaches $2m+1$ and T_u approaches $P_{2m+1}(\cos\theta)$, the limiting value of a_u is

$$\lim_{\theta_0 \to 0} a_u = \lim_{\theta_0 \to 0} a_{2m+1+\Delta} = b_{2m+1} \frac{h_{2m+1}^{(1)}(kl)}{j_{2m+1}(kl)}$$

Therefore,

$$\tilde{I}(r) = \frac{120}{Z_0} \sum_{m=0}^{\infty} b_{2m+1} \frac{h_{2m+1}^{(1)}(kl)}{j_{2m+1}(kl)} r \, j_{2m+1}(kr)$$

For very thin antennas, the current distribution approaches the sinusoidal distribution of the principal wave

$$I(r) = I_0 \sin k(r - l) \tag{5.6.37}$$

with

$$I_0 = i\frac{V_0(l)}{Z_0}$$

The coefficients b_{2m+1} can be obtained by comparing the expressions of the field due to the current distribution given by (5.6.37) with the field expressions in the air region. For the sinusoidal current distribution of (5.6.37) we have, in the far-field approximation,

$$H_\phi = ik\frac{e^{ikr}}{4\pi r}f_\theta$$

where

$$f_\theta = I_0 \frac{2}{k \sin\theta} \left[\cos(kl \cos\theta) - \cos kl\right]$$

The radial electric field E_r is

$$E_r = \frac{1}{-i\omega\epsilon} \frac{1}{r \sin\theta} \frac{\partial}{\partial\theta}(\sin\theta \, H_\phi) = -\eta I_0 l \frac{e^{ikr}}{2\pi r^2} \sin(kl \cos\theta) \tag{5.6.38}$$

The expansion of $\sin(kl \cos \theta)$ in terms of spherical harmonics is known to be

$$\sin(kl \cos \theta) = \sum_{m=o}^{\infty} (-1)^m (4m + 3) j_{2m+1}(kl) \, P_{2m+1}(\cos \theta) \qquad (5.6.39)$$

Thus (5.6.38) can be written as

$$E_r = -\eta I_o l \frac{e^{ikr}}{2\pi r^2} \sum_{m=0}^{\infty} (-1)^m (4m + 3) j_{2m+1}(kl) P_{2m+1}(\cos \theta) \qquad (5.6.40)$$

On the other hand, in the far-field approximation, $(5.6.19b)$ becomes

$$E_r = \frac{1}{i\omega\epsilon} \frac{e^{ikr}}{2\pi r^2} \frac{1}{k} \sum_{m=0}^{\infty} 2(2m + 1)(m + 1) b_{2m+1} (-1)^{m+1} P_{2m+1}(\cos \theta)$$
$$(5.6.41)$$

due to the fact that for large arguments

$$h_n^{(1)}(kr) \approx (-i)^{n+1} \frac{e^{ikr}}{kr}$$

Equating (5.6.40) and (5.6.41) we obtain

$$b_{2m+1} = -\frac{V_0(l)}{Z_0} \frac{(4m + 3)}{2(2m + 1)(m + 1)} k^2 l \, j_{2m+1}(kl) \qquad (5.6.42)$$

and

$$\tilde{I}(r) = -\frac{60}{Z_0^2} V_0(l) \sum_{m=0}^{\infty} \frac{(4m + 1)}{(2m + 1)(m + 1)} kl \, h_{2m+1}^{(1)}(kl) \, kr \, j_{2m+1}(kr) \qquad (5.6.43)$$

therefore,

$$Y_t = -\frac{\tilde{I}(l)}{V_0(l)} = \frac{Z_a(kl)}{Z_0^2} = \frac{1}{Z_0^2} \left[R_a(kl) - iX_a(kl) \right] \qquad (5.6.44)$$

where

$$R_a(kl) = 60 \sum_{m=0}^{\infty} \frac{(4m + 3)}{(2m + 1)(m + 1)} \left[kl \, j_{2m+1}(kl) \right]^2 \qquad (5.6.45)$$

$$X_a(kl) = -60 \sum_{m=0}^{\infty} \frac{(4m + 3)}{(2m + 1)(m + 1)} kl \, j_{2m+1}(kl) kl \, n_{2m+1}(kl) \qquad (5.6.46)$$
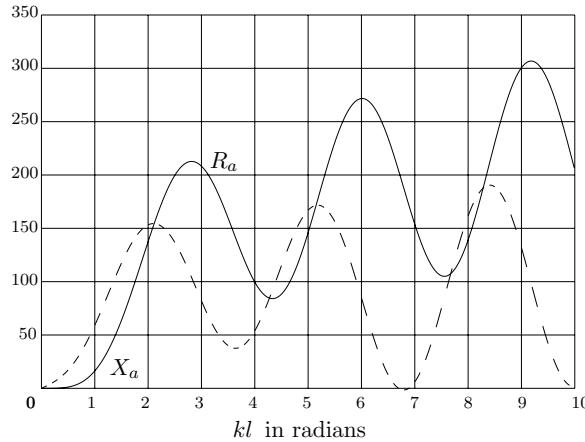
Figure 5.6.5 Resistive and reactive components of $Z_a = R_a - iX_a$.

In terms of cosine and sine integrals

$$R_a(kl) = 60\left[\gamma + \ln(2kl) - Ci(2kl)\right] + 30\left[\gamma + \ln(kl) - 2Ci(2kl)\right.$$
$$\left. + Ci(4kl)\right]\cos(2kl) + 30\left[Si(4kl) - 2Si(2kl)\right]\sin(2kl) \tag{5.6.47}$$

$$X_a(2kl) = 60Si(2kl) + 30\left[Ci(4kl) - \ln(kl) - \gamma\right]\sin 2kl$$
$$- 30Si(4kl)\cos(2kl) \tag{5.6.48}$$

where $\gamma = 0.5772\ldots$ Euler's constant. The values of R_a and X_a are shown in Figure 5.6.5.

We note that although $Z_a = R_a - iX_a$ is not a function of the cone angle θ_0, the characteristic impedance Z_0 is. In view of (5.6.32), the input impedance Z_i of a biconical antenna is thus a function of θ_0, which is assumed to be very small in the above discussions. The characteristic impedance for the $\theta_0 = 2.7°$ antenna is 450 ohms and that for the $\theta_0 = 0.027°$ antenna is 1000 ohms. At $l/\lambda = 0.25$, the input impedance for both antennas is $Z_a(kl = \pi/2) \simeq (73.129 - i153.66)\,\Omega$. For a specific l, the input impedance of the thinner antenna as a function of frequency changes over a much wider range than that of the thicker one. This difference between thick and thin antennas is generally true and not restricted to the conical antenna. Thus, for a fixed length l, the input impedances of thick antennas are less sensitive to frequency changes and thick antennas are therefore more suitable for wide-band applications than thin antennas.

E. Formal Solution of Biconical Antenna Problem

In the general case when θ_0 is not necessarily small, we may obtain the formal solution by making use of the orthogonal properties of the Legendre functions. The expressions for the fields in the antenna and air regions are given by (5.6.24) and (5.6.19). The problem now is to determine the coefficients a_u and b_n by matching the boundary conditions. First we note that H_ϕ in the antenna region (5.6.24a) may be written as

$$H_\phi(r = l) = \frac{Y_t V_0(l)}{2\pi l \sin\theta} + \frac{1}{2\pi}\sum_u a_u \, j_u(kl)\frac{d}{d\theta}T_u(\cos\theta) \qquad (5.6.49)$$

Multiplying both sides by $\sin\theta(dT_{u'}(\theta)/d\theta)$ and integrating from θ_0 to $\pi - \theta_0$, we obtain

$$a_u = \frac{2\pi}{N_u j_u(kl)}\int_{\theta_0}^{\pi-\theta_0} \sin\theta\, d\theta\, H_\phi(r = l)\frac{d}{d\theta}T_u(\theta) \qquad (5.6.50)$$

where we have used the fact that

$$\int_{\theta_0}^{\pi-\theta_0} \sin\theta d\theta\, \left[\frac{d}{d\theta}T_u(\theta)\right]\left[\frac{d}{d\theta}T_{u'}(\theta)\right] = \begin{cases} 0 & \text{if } u \neq u' \\ N_u & \text{if } u = u' \end{cases}$$

However, from (5.6.19a)

$$H_\phi(r = l) = \frac{1}{2\pi}\sum_{n \text{ odd}} b_n \, h_n^{(1)}(kl)\frac{d}{d\theta}P_n(\cos\theta) \qquad (5.6.51)$$

Substituting the above equation into (5.6.50) we obtain an infinite system of linear equations of the form

$$a_u = \sum_{n \text{ odd}} \alpha_{u,n} b_n \qquad (5.6.52)$$

where

$$\alpha_{u,n} = \frac{h_n^{(1)}(kl)}{N_u j_u(kl)}\int_{\theta_0}^{\pi-\theta_0} \sin\theta d\theta\, \left[\frac{d}{d\theta}T_u(\cos\theta)\right]\left[\frac{d}{d\theta}P_n(\cos\theta)\right] \quad (5.6.53)$$

Another system of equations governing the coefficients can be obtained by considering the E_θ components at $r = l$. In the air region $E_\theta(r = l)$ is, from (5.6.19c),

$$l\,E_\theta(r = l) = \frac{1}{2\pi i\omega\epsilon} \sum_{n\ \text{odd}} b_n \left\{ \frac{d}{dr} \left[rh_n^{(1)}(kr) \right] \right\}_{r=l} \frac{d}{d\theta} P_n(\cos\theta)$$

(5.6.54)

Multiplying both sides by $\sin\theta\, d[P_{n'}(\cos\theta)]/d\theta$ and integrating from 0 to π we obtain

$$b_n = \frac{2n(n+1)}{2n+1} \frac{2\pi i\omega\epsilon}{\left\{ d\left[rh_n^{(1)}(kr) \right]/dr \right\}_{r=l}} \int_0^\pi \sin\theta\, d\theta\, lE_\theta(r=l) \frac{d}{d\theta} P_n(\cos\theta)$$

(5.6.55)

where we have used the fact that

$$\int_0^\pi \sin\theta\, d\theta \left[\frac{d}{d\theta} P_n(\cos\theta) \right] \left[\frac{d}{d\theta} P_{n'}(\cos\theta) \right] = \begin{cases} \dfrac{2n+1}{2n(n+1)} & \text{if } n = n' \\ 0 & \text{if } n \neq n' \end{cases}$$

However, according to (5.6.24c)

$$lE_\theta(r = l) = \frac{\eta V_0(l)}{2\pi Z_0 \sin\theta} + \frac{1}{2\pi i\omega\epsilon} \sum_u a_u \left\{ \frac{d}{dr} \left[rj_u(kr) \right] \right\}_{r=l} \frac{d}{d\theta} T_u(\theta)$$

(5.6.56)

for $\theta_0 < \theta < \pi - \theta_0$ and $E_\theta(r = l) = 0$ otherwise.

Therefore, substituting the above equation into (5.6.55) we obtain

$$b_n = \sum_u \beta_{n,u} a_u + K_n \frac{V_0(l)}{Z_0}$$

(5.6.57)

$$\beta_{n,u} = \frac{2n(n+1)}{2n+1} \frac{\left\{ \frac{d[rj_u(kr)]}{dr} \right\}_{r=l}}{\left\{ \frac{d[rh_n^{(1)}(kr)]}{dr} \right\}_{r=l}} \cdot \int_{\theta_0}^{\pi-\theta_0} d\theta \sin\theta \left[\frac{dP_n(\cos\theta)}{d\theta} \right] \left[\frac{dT_u(\theta)}{d\theta} \right]$$

(5.6.58)

$$K_n = i\frac{4n(n+1)}{2n+1} \frac{k}{\left\{ d[rh_n^{(1)}(kr)]/dr \right\}_{r=l}} P_n(\cos\theta_0)$$

(5.6.59)

Therefore, the problem is formally solvable, since the coefficients a_u and b_n may be determined by the linear system of equations given by (5.6.52) and (5.6.57).

Once the coefficients are obtained, the termination admittance Y_t can be easily obtained. First, integrating (5.6.49) from θ_0 to $\pi - \theta_0$ we find

$$Y_t = \frac{\eta l}{Z_0 V_0(l)} \int_{\theta_0}^{\pi-\theta_0} d\theta \, H_\phi(r = l) \qquad (5.6.60)$$

where the characteristic impedance Z_0 is given by (5.6.25). Next, substituting (5.6.51) into the above equation we obtain

$$Y_t = \frac{-\eta}{Z_0 V_0(l)} \frac{l}{\pi} \sum_{n \text{ odd}} b_n \, h_n^{(1)}(kl) P_n(\cos\theta_0)$$

$$= -\frac{120}{Z_0 V_0(l)} l \sum_{n \text{ odd}} b_n \, h_n^{(1)}(kl) P_n(\cos\theta_0) \qquad (5.6.61)$$

The above equation can also be used to calculate Z_a by noting that $Z_a = Z_0^2 Y_t$.

Problems

P5.6.1

Find approximate values for the order of modes (that is, u) in the case of a spherical antenna as a limiting case of the biconical antenna when the cone angle θ_0 approaches $\pi/2$.

P5.6.2

Consider the biconical antenna shown in Figure P5.6.2.1, where the conical boundaries are given by $\theta = \theta_0$ and $\theta = \pi - \theta_1$ and where the antenna region is filled with a dielectric of relative permittivity ϵ.
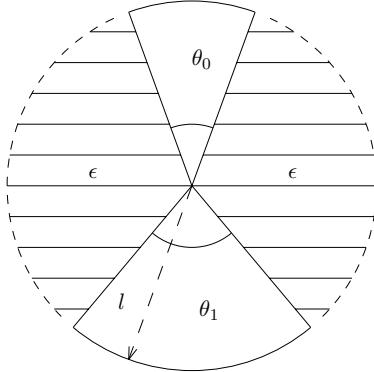
Figure P5.6.2.1

(a) Write the boundary conditions for this biconical antenna.
(b) Find the characteristic impedance and prove that the characteristic impedance of a single cone of angle θ_0 over a perfectly conducting ground plane is half that of a biconical antenna with $\theta_0 = \theta_1$.
(c) Find the capacitance and inductance per unit radial length of this biconical antenna.
(d) Find the approximate values of the orders of modes (that is, u) that can be excited in the antenna region for small cone angles θ_0 and θ_1 . Prove that these are given by, with n an odd integer,

$$u \simeq n + \Delta \simeq n - \frac{1}{2} \frac{\ln(\sin \frac{\theta_0}{2} \sin \frac{\theta_1}{2})}{\ln(\sin \frac{\theta_0}{2}) \ln(\sin \frac{\theta_1}{2})}$$

5.7   Dipole Antennas in Layered Media

A. Integral Formulation

The geometrical configuration of the problem is shown in Figure 5.7.1. The origin of the coordinate system is placed in the location of the dipole which can be a vertical magnetic dipole (VMD), a vertical electric dipole (VED), a horizontal electric dipole (HED), or a horizontal magnetic dipole (HMD). There are M layers above the dipole at $z = d_1, d_2, \ldots d_M$ and N layers below it at $z = d_0, d_{-1}, \ldots, d_{-(N-1)}$. We shall first assume that all regions contain isotropic media. In region l, we denote the permittivity and permeability by ϵ_l and μ_l. Notice that in region 0, ϵ_0 and μ_0 are not necessarily equal to the free space permittivity and permeability which we denote by ϵ_o and μ_o.

Region M

$z = d_M$

Region $M-1$

$z = d_{M-1}$

$z = d_2$

Region 1

$z = d_1$

Region 0 z

dipole
antenna $\longrightarrow \rho$

$z = d_0$

Region -1

$z = d_{-1}$

$z = d_{-(N-2)}$

Region $-(N-1)$

$z = d_{-(N-1)}$

Region $-N$
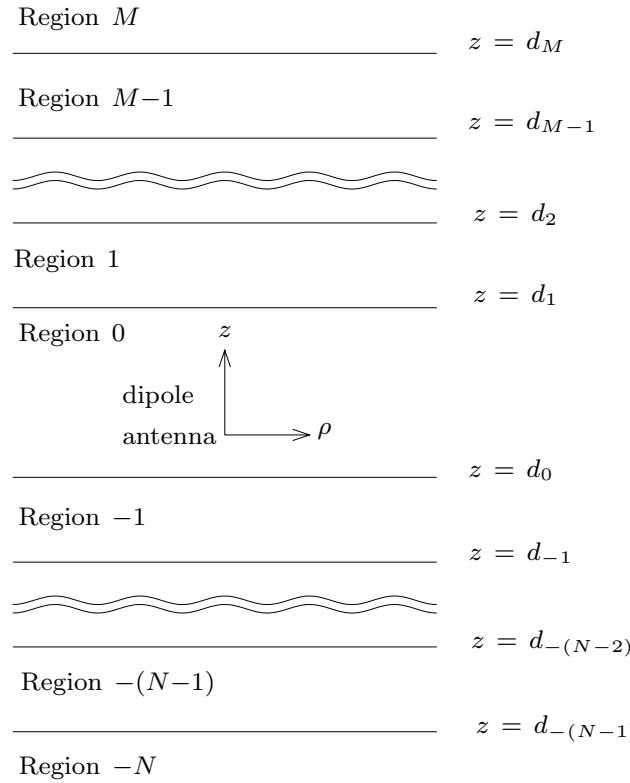
Figure 5.7.1 Dipole in layered medium.

In the absence of the stratified medium, fields of a dipole radiating in unbounded space with permittivity ϵ_0 and μ_0 are well known. The solutions can be transformed from spherical coordinates to cylindrical coordinates by using the Sommerfeld identity

$$\frac{e^{ik_r}}{r} = \frac{i}{2} \int_{-\infty}^{\infty} dk_\rho \, \frac{k_\rho}{k_z} H_0^{(1)}(k_\rho \rho) e^{ik_z|z|} \tag{5.7.1}$$

The electric and magnetic fields of electric dipoles are

$$\overline{E}(\overline{r}) = i\omega\mu \left[\overline{\overline{I}} + \frac{1}{k^2} \nabla\nabla \right] \cdot \overline{I}l \frac{e^{ikr}}{4\pi r} \tag{5.7.2}$$

$$\overline{H}(\overline{r}) = \frac{1}{i\omega\mu} \nabla \times \overline{E} = \nabla \times \overline{I}l \, \frac{e^{ikr}}{4\pi r} \tag{5.7.3}$$

The integrands of transverse field components $\overline{E}_s = \hat{\rho}E_\rho + \hat{\phi}E_\phi$ and $\overline{H}_s = \hat{\rho}H_\rho + \hat{\phi}H_\phi$ are derived from those of the longitudinal components E_z and H_z. Let

$$E_z = \int_{-\infty}^{\infty} dk_\rho \, E_z(k_\rho) \tag{5.7.4}$$

$$H_z = \int_{-\infty}^{\infty} dk_\rho \, H_z(k_\rho) \tag{5.7.5}$$

We have from the Maxwell equations in source-free regions

$$\overline{E}_s(k_\rho) = \frac{1}{k_\rho^2} \left[\nabla_s \frac{\partial}{\partial z} E_z(k_\rho) + i\omega\mu_l \nabla_s \times \overline{H}_z(k_\rho) \right] \tag{5.7.6}$$

$$\overline{H}_s(k_\rho) = \frac{1}{k_\rho^2} \left[\nabla_s \frac{\partial}{\partial z} H_z(k_\rho) - i\omega\epsilon_l \nabla_s \times \overline{E}_z(k_\rho) \right] \tag{5.7.7}$$

In view of the four types of dipole configurations, we find that for

(1) *Vertical electric dipole (VED)*

$$E_z = \int_{-\infty}^{\infty} dk_\rho \, E_{ved} \left\{ \begin{matrix} e^{ik_z z} \\ e^{-ik_z z} \end{matrix} \right\} H_0^{(1)}(k_\rho \rho) \qquad \begin{matrix} z \geq 0 \\ z \leq 0 \end{matrix} \tag{5.7.8a}$$

$$E_{ved} = -\frac{Ilk_\rho^3}{8\pi\omega\epsilon_0 k_z} \tag{5.7.8b}$$

$$H_z = 0 \tag{5.7.9}$$

where Il is the electric dipole moment.

(2) Horizontal electric dipole (HED)

$$E_z = \int_{-\infty}^{\infty} dk_\rho \, E_{hed} \left\{ \begin{array}{c} e^{ik_z z} \\ -e^{-ik_z z} \end{array} \right\} H_1^{(1)}(k_\rho \rho) \cos\phi \qquad \begin{array}{c} z \geq 0 \\ z \leq 0 \end{array} \quad (5.7.10a)$$

$$E_{hed} = i\frac{Il k_\rho^2}{8\pi\omega\epsilon_0} \tag{5.7.10b}$$

$$H_z = \int_{-\infty}^{\infty} dk_\rho \, H_{hed} \left\{ \begin{array}{c} e^{ik_z z} \\ e^{-ik_z z} \end{array} \right\} H_1^{(1)}(k_\rho \rho) \sin\phi \qquad \begin{array}{c} z \geq 0 \\ z \leq 0 \end{array} \quad (5.7.11a)$$

$$H_{hed} = i\frac{Il k_\rho^2}{8\pi k_z} \tag{5.7.11b}$$

(3) Vertical magnetic dipole (VMD)

$$E_z = 0 \tag{5.7.12}$$

$$H_z = \int_{-\infty}^{\infty} dk_\rho \, H_{vmd} \left\{ \begin{array}{c} e^{ik_z z} \\ e^{-ik_z z} \end{array} \right\} H_0^{(1)}(k_\rho \rho) \qquad \begin{array}{c} z \geq 0 \\ z \leq 0 \end{array} \quad (5.7.13a)$$

$$H_{vmd} = -i\frac{IA k_\rho^3}{8\pi k_z} \tag{5.7.13b}$$

where IA is the magnetic dipole moment.

(4) Horizontal magnetic dipole (HMD)

$$E_z = \int_{-\infty}^{\infty} dk_\rho \, E_{hmd} \left\{ \begin{array}{c} e^{ik_z z} \\ e^{-ik_z z} \end{array} \right\} H_1^{(1)}(k_\rho \rho) \sin\phi \qquad \begin{array}{c} z \geq 0 \\ z \leq 0 \end{array} \quad (5.7.14a)$$

$$E_{hmd} = \frac{IA\omega\mu_0 k_\rho^2}{8\pi k_z} \tag{5.7.14b}$$

$$H_z = \int_{-\infty}^{\infty} dk_\rho H_{hmd} \left\{ \begin{array}{c} e^{ik_z z} \\ -e^{-ik_z z} \end{array} \right\} H_1^{(1)}(k_\rho \rho) \cos\phi \qquad \begin{array}{c} z \geq 0 \\ z \leq 0 \end{array} \quad (5.7.15a)$$

$$H_{hmd} = -\frac{IA k_\rho^2}{8\pi} \tag{5.7.15b}$$

Notice that the magnetic dipoles produce fields which are duals of those produced by the corresponding electric dipoles. The results for the magnetic dipoles can be obtained by the replacement $\overline{E} \rightarrow \overline{H}$, $\overline{H} \rightarrow -\overline{E}$, $\mu_0 \rightleftarrows \epsilon_0$, and $Il \rightarrow i\omega\mu_0 IA$.

For the stratified media, the solutions to the wave equations can be written as superpositions of TE and TM wave components. Let A_l and B_l denote amplitudes for the TM waves and C_l and D_l denote amplitudes for the TE waves. We find in region l the following solutions:

$$E_{lz} = \int_{-\infty}^{\infty} dk_\rho \left[A_l e^{ik_{lz}z} + B_l e^{-ik_{lz}z} \right] H_n^{(1)}(k_\rho\rho)C_n(\phi) \tag{5.7.16}$$

$$H_{lz} = \int_{-\infty}^{\infty} dk_\rho \left[C_l e^{ik_{lz}z} + D_l e^{-ik_{lz}z} \right] H_n^{(1)}(k_\rho\rho)S_n(\phi) \tag{5.7.17}$$

$$E_{l\rho} = \int_{-\infty}^{\infty} dk_\rho \frac{ik_{lz}}{k_\rho} \left[A_l e^{ik_{lz}z} - B_l e^{-ik_{lz}z} \right] H_n^{(1)\prime}(k_\rho\rho)C_n(\phi)$$
$$+ \int_{-\infty}^{\infty} dk_\rho \frac{i\omega\mu_l}{k_\rho^2\rho} \left[C_l e^{ik_{lz}z} + D_l e^{-ik_{lz}z} \right] H_n^{(1)}(k_\rho\rho)S_n'(\phi) \tag{5.7.18}$$

$$E_{l\phi} = \int_{-\infty}^{\infty} dk_\rho \frac{ik_{lz}}{k_\rho^2\rho} \left[A_l e^{ik_{lz}z} - B_l e^{-ik_{lz}z} \right] H_n^{(1)}(k_\rho\rho)C_n'(\phi)$$
$$+ \int_{-\infty}^{\infty} dk_\rho \frac{-i\omega\mu_l}{k_\rho} \left[C_l e^{ik_{lz}z} + D_l e^{-ik_{lz}z} \right] H_n^{(1)\prime}(k_\rho\rho)S_n(\phi) \tag{5.7.19}$$

$$H_{l\rho} = \int_{-\infty}^{\infty} dk_\rho \frac{ik_{lz}}{k_\rho} \left[C_l e^{ik_{lz}z} - D_l e^{-ik_{lz}z} \right] H_n^{(1)\prime}(k_\rho\rho)S_n(\phi)$$
$$+ \int_{-\infty}^{\infty} dk_\rho \frac{-i\omega\epsilon_l}{k_\rho^2\rho} \left[A_l e^{ik_{lz}z} + B_l e^{-ik_{lz}z} \right] H_n^{(1)}(k_\rho\rho)C_n'(\phi) \tag{5.7.20}$$

$$H_{l\phi} = \int_{-\infty}^{\infty} dk_\rho \frac{ik_{lz}}{k_\rho^2\rho} \left[C_l e^{ik_{lz}z} - D_l e^{-ik_{lz}z} \right] H_n^{(1)}(k_\rho\rho)S_n'(\phi)$$
$$+ \int_{-\infty}^{\infty} dk_\rho \frac{i\omega\epsilon_l}{k_\rho} \left[A_l e^{ik_{lz}z} + B_l e^{-ik_{lz}z} \right] H_n^{(1)\prime}(k_\rho\rho)C_n(\phi) \tag{5.7.21}$$

In (5.7.16)–(5.7.21), $H_n^{(1)}(k_\rho\rho)$ is the nth order Hankel function of the first kind and $H_n^{(1)\prime}(k_\rho\rho)$ denotes the derivative of $H_n^{(1)}(\xi)$ with respect to its argument ξ. The ϕ-dependent functions $S_n(\phi)$ and $C_n(\phi)$ and the order of the Hankel functions n are all determined by the dipole configurations.

The boundary conditions at the interfaces require that tangential electric and magnetic field components be continuous for all ρ and ϕ.

At $z = d_l$, we obtain

$$k_{lz}\left(A_l e^{ik_{lz}d_l} - B_l e^{-ik_{lz}d_l}\right)$$

$$= k_{(l-1)z}\left(A_{l-1}e^{ik_{(l-1)z}d_l} - B_{l-1}e^{-ik_{(l-1)z}d_l}\right) \quad (5.7.22)$$

$$\epsilon_l\left(A_l e^{ik_{lz}d_l} + B_l e^{-ik_{lz}d_l}\right)$$

$$= \epsilon_{(l-1)}\left(A_{l-1}e^{ik_{(l-1)z}d_l} + B_{l-1}e^{-ik_{(l-1)z}d_l}\right) \quad (5.7.23)$$

$$k_{lz}\left(C_l e^{ik_{lz}d_l} - D_l e^{-ik_{lz}d_l}\right)$$

$$= k_{(l-1)z}\left(C_{l-1}e^{ik_{(l-1)z}d_l} - D_{l-1}e^{-ik_{(l-1)z}d_l}\right) \quad (5.7.24)$$

$$\mu_l\left(C_l e^{ik_{lz}d_l} + D_l e^{-ik_{lz}d_l}\right)$$

$$= \mu_{(l-1)}\left(C_{l-1}e^{ik_{(l-1)z}d_l} + D_{l-1}e^{-ik_{(l-1)z}d_l}\right) \quad (5.7.25)$$

There are altogether $M + N$ boundaries which give rise to $4(M + N)$ equations as shown above. There are altogether $M + N + 1$ regions. In regions M and $-N$ we have $B_M = D_M = 0$ and $A_{-N} = C_{-N} = 0$ because there are no waves originating from infinity. Thus we have a total of $4(M + N + 1) - 4 = 4(M + N)$ unknowns to be solved from the $4(M + N)$ equations. The wave amplitudes are related to the configurations and the excitation amplitudes of the dipole antenna in region 0. The wave solutions in region 0 thus need special attention.

We note in particular that at $z = 0$, the following field components vanish:

(1) VED $\qquad\qquad\qquad\qquad E_\rho = 0 \qquad\qquad\qquad\qquad (5.7.26)$

(2) HED $\qquad\qquad\quad E_z = H_\rho = H_\phi = 0 \qquad\qquad\quad (5.7.27)$

(3) VMD $\qquad\qquad\qquad\qquad H_\rho = 0 \qquad\qquad\qquad\qquad (5.7.28)$

(4) HMD $\qquad\qquad\quad H_z = E_\rho = E_\phi = 0 \qquad\qquad\quad (5.7.29)$

This is seen from (5.7.6)–(5.7.7) and by noting from (5.7.1) that

$$\frac{\partial}{\partial z}\frac{e^{ikr}}{r} = 0 \qquad\qquad \text{at} \quad z = 0 \qquad\qquad (5.7.30)$$

In the presence of the stratified medium, we can write the fields in region 0 by identifying A_0 and B_0 according to the four types of dipoles and whether we have $z > 0$ or $z < 0$. We distinguish the wave amplitudes in region 0 for $z \geq 0$ from those in region 0 for $z < 0$. For $z > 0$ we use A_{0+}, B_{0+}, C_{0+}, and D_{0+}; and for $z < 0$ we use A_{0-}, B_{0-}, C_{0-}, and D_{0-}. It is seen that for

(1) VED

$$\left.\begin{aligned}
A_{0+} &= A_{ved} + E_{ved} & A_{0-} &= A_{ved} \\
B_{0+} &= B_{ved} & B_{0-} &= B_{ved} + E_{ved} \\
C_{0+} &= D_{0+} = C_{0-} = D_{0-} = 0
\end{aligned}\right\} \quad (5.7.31)$$

where A_{ved} and B_{ved} characterize contributions due to the stratified medium and are to be determined by the boundary conditions.

(2) HED

$$\left.\begin{aligned}
A_{0+} &= A_{hed} + E_{hed} & A_{0-} &= A_{hed} \\
B_{0+} &= B_{hed} & B_{0-} &= B_{hed} - E_{hed} \\
C_{0+} &= C_{hed} + H_{hed} & C_{0-} &= C_{hed} \\
D_{0+} &= D_{hed} & D_{0-} &= D_{hed} + H_{hed}
\end{aligned}\right\} \quad (5.7.32)$$

where A_{hed}, B_{hed}, C_{hed}, and D_{hed} characterize contributions due to the stratified medium and are to be determined by the boundary conditions.

(3) VMD

$$\left.\begin{aligned}
A_{0+} &= B_{0+} = A_{0-} = B_{0-} = 0 \\
C_{0+} &= C_{vmd} + H_{vmd} & C_{0-} &= C_{vmd} \\
D_{0+} &= D_{vmd} & D_{0-} &= D_{vmd} + H_{vmd}
\end{aligned}\right\} \quad (5.7.33)$$

where C_{vmd} and D_{vmd} characterize contributions due to the stratified medium and are to be determined by the boundary conditions.

(4) HMD

$$\left.\begin{aligned}
A_{0+} &= A_{hmd} + E_{hmd} & A_{0-} &= A_{hmd} \\
B_{0+} &= B_{hmd} & B_{0-} &= B_{hmd} + E_{hmd} \\
C_{0+} &= C_{hmd} + H_{hmd} & C_{0-} &= C_{hmd} \\
D_{0+} &= D_{hmd} & D_{0-} &= D_{hmd} - H_{hmd}
\end{aligned}\right\} \quad (5.7.34)$$

where A_{hmd}, B_{hmd}, C_{hmd}, and D_{hmd} characterize contributions due to the stratified medium and are to be determined by the boundary conditions. We have expressed the solution in region 0 where the dipoles are located in terms of superpositions of the primary excitations in the absence of the stratified medium and the homogeneous solutions of the stratified medium in the absence of the source. It is easily shown that they satisfy the boundary conditions at $z = 0$ by remembering the vanishing field components as listed in (5.7.26)–(5.7.29) for the primary excitations.

We now determine the wave amplitudes in region 0. For TM waves, (5.7.22)–(5.7.23) can be solved to express A_l and B_l in terms of A_{l-1} and B_{l-1}. We find

$$A_l e^{ik_{lz}d_l} = \frac{1}{2}\left(\frac{\epsilon_{l-1}}{\epsilon_l} + \frac{k_{(l-1)z}}{k_{lz}}\right)\left[A_{l-1}e^{ik_{(l-1)z}d_l} + R^{\mathrm{TM}}_{l(l-1)}B_{l-1}e^{-ik_{(l-1)z}d_l}\right]$$

$$(5.7.35a)$$

$$B_l e^{-ik_{lz}d_l} = \frac{1}{2}\left(\frac{\epsilon_{l-1}}{\epsilon_l} + \frac{k_{(l-1)z}}{k_{lz}}\right)\left[R^{\mathrm{TM}}_{l(l-1)}A_{l-1}e^{ik_{(l-1)z}d_l} + B_{l-1}e^{-ik_{(l-1)z}d_l}\right]$$

$$(5.7.35b)$$

To express A_{l-1} and B_{l-1} in terms of A_l and B_l, we find

$$A_{l-1}e^{ik_{(l-1)z}d_l} = \frac{1}{2}\left(\frac{\epsilon_l}{\epsilon_{l-1}} + \frac{k_{lz}}{k_{(l-1)z}}\right)\left[A_l e^{ik_{lz}d_l} + R^{\mathrm{TM}}_{(l-1)l}B_l e^{-ik_{lz}d_l}\right]$$

$$(5.7.36a)$$

$$B_{l-1}e^{-ik_{(l-1)z}d_l} = \frac{1}{2}\left(\frac{\epsilon_l}{\epsilon_{l-1}} + \frac{k_{lz}}{k_{(l-1)z}}\right)\left[R^{\mathrm{TM}}_{(l-1)l}A_l e^{ik_{lz}d_l} + B_l e^{-ik_{lz}d_l}\right]$$

$$(5.7.36b)$$

In (5.7.35)–(5.7.36),

$$R^{\mathrm{TM}}_{(l-1)l} = -R^{\mathrm{TM}}_{l(l-1)}$$

A similar procedure applies to TE waves. The results are duals of those of (5.7.35)–(5.7.36) with the replacements of A by C, B by D, and ϵ by μ.

For $z \geq 0$, we notice that $B_M = D_M = 0$. Letting $l = 0$, we obtain the reflection coefficients $R^{\mathrm{TM}}_{0+} = B_{0+}/A_{0+}$ and $R^{\mathrm{TE}}_{0+} = D_{0+}/C_{0+}$

in the form of continued fractions. We find

$$R_{0+}^{\text{TM}} = \frac{B_{0+}}{A_{0+}} = \frac{e^{i2k_{0z}d_1}}{R_{01}^{\text{TM}}} + \frac{\left[1 - \left(1/R_{01}^{\text{TM}}\right)^2\right]e^{i2(k_{0z}+k_{1z})d_1}}{(1/R_{01}^{\text{TM}})e^{i2k_{1z}d_1} + (B_1/A_1)} \quad (5.7.37)$$

$$R_{0+}^{\text{TE}} = \frac{D_{0+}}{C_{0+}} = \frac{e^{i2k_{0z}d_1}}{R_{01}^{\text{TE}}} + \frac{\left[1 - \left(1/R_{01}^{\text{TE}}\right)^2\right]e^{i2(k_{0z}+k_{1z})d_1}}{(1/R_{01}^{\text{TE}})e^{i2k_{1z}d_1} + (D_1/C_1)} \quad (5.7.38)$$

where B_1/A_1 and D_1/C_1 can be expressed in terms of B_2/A_2 and D_2/C_2 and so on until region M where $B_M/A_M = 0 = D_M/C_M$.

For $z \leq 0$, we notice that $A_{-N} = C_{-N} = 0$. Letting $l = 0$, we obtain the reflection coefficients $R_{0-}^{\text{TM}} = A_{0-}/B_{0-}$ and $R_{0-}^{\text{TE}} = C_{0-}/D_{0-}$ in the form of continued fractions. We find

$$R_{0-}^{\text{TM}} = \frac{A_{0-}}{B_{0-}} = \frac{e^{-i2k_{0z}d_0}}{R_{0(-1)}^{\text{TM}}} + \frac{\left[1 - \left(1/R_{0(-1)}^{\text{TM}}\right)^2\right]e^{-i2(k_{0z}+k_{-1z})d_0}}{\left(1/R_{0(-1)}^{\text{TM}}\right)e^{-i2k_{-1z}d_0} + (A_{-1}/B_{-1})}$$

$$(5.7.39)$$

$$R_{0-}^{\text{TE}} = \frac{C_{0-}}{D_{0-}} = \frac{e^{-i2k_{0z}d_0}}{R_{0(-1)}^{\text{TE}}} + \frac{\left[1 - \left(1/R_{0(-1)}^{\text{TE}}\right)^2\right]e^{-i2(k_{0z}+k_{-1z})d_0}}{\left(1/R_{0(-1)}^{\text{TE}}\right)e^{-i2k_{-1z}d_0} + (C_{-1}/D_{-1})}$$

$$(5.7.40)$$

where A_{-1}/B_{-1} and C_{-1}/D_{-1} are expressible in terms of A_{-2}/B_{-2} and C_{-2}/D_{-2} and so on until region $-N$, where $A_{-N}/B_{-N} = 0$ and $C_{-N}/D_{-N} = 0$.

Once the wave amplitudes in region 0 are found, wave amplitudes in other regions can be determined by the use of propagation matrices, which are readily determined from (5.7.35) and (5.7.36) and from a set of dual equations for TE waves. We now determine wave amplitudes in region 0.

(1) VED: From (5.7.31), we find

$$R_{0+}^{\text{TM}} = \frac{B_{0+}}{A_{0+}} = \frac{B_{ved}}{A_{ved} + E_{ved}} \quad (5.7.41a)$$

$$R_{0-}^{\text{TM}} = \frac{A_{0-}}{B_{0-}} = \frac{A_{ved}}{B_{ved} + E_{ved}} \quad (5.7.41b)$$

Solving for A_{ved} and B_{ved} and substituting in (5.7.31), we obtain

$$A_{0+} = \frac{1 + R_{0-}^{TM}}{1 - R_{0+}^{TM} R_{0-}^{TM}} E_{ved} \tag{5.7.42a}$$

$$B_{0+} = \frac{R_{0+}^{TM}(1 + R_{0-}^{TM})}{1 - R_{0+}^{TM} R_{0-}^{TM}} E_{ved} \tag{5.7.42b}$$

$$A_{0-} = \frac{R_{0-}^{TM}(1 + R_{0+}^{TM})}{1 - R_{0+}^{TM} R_{0-}^{TM}} E_{ved} \tag{5.7.42c}$$

$$B_{0-} = \frac{1 + R_{0+}^{TM}}{1 - R_{0+}^{TM} R_{0-}^{TM}} E_{ved} \tag{5.7.42d}$$

(2) HED: By the same token, we find from (5.7.32)

$$A_{0+} = \frac{1 - R_{0-}^{TM}}{1 - R_{0+}^{TM} R_{0-}^{TM}} E_{hed} \tag{5.7.43a}$$

$$B_{0+} = \frac{R_{0+}^{TM}(1 - R_{0-}^{TM})}{1 - R_{0+}^{TM} R_{0-}^{TM}} E_{hed} \tag{5.7.43b}$$

$$C_{0+} = \frac{1 + R_{0-}^{TE}}{1 - R_{0+}^{TE} R_{0-}^{TE}} H_{hed} \tag{5.7.43c}$$

$$D_{0+} = \frac{R_{0+}^{TE}(1 + R_{0-}^{TE})}{1 - R_{0+}^{TE} R_{0-}^{TE}} H_{hed} \tag{5.7.43d}$$

$$A_{0-} = -\frac{R_{0-}^{TM}(1 - R_{0+}^{TM})}{1 - R_{0+}^{TM} R_{0-}^{TM}} E_{hed} \tag{5.7.44a}$$

$$B_{0-} = -\frac{1 - R_{0+}^{TM}}{1 - R_{0+}^{TM} R_{0-}^{TM}} E_{hed} \tag{5.7.44b}$$

$$C_{0-} = \frac{R_{0-}^{TE}(1 + R_{0+}^{TE})}{1 - R_{0+}^{TE} R_{0-}^{TE}} H_{hed} \tag{5.7.44c}$$

$$D_{0-} = \frac{1 + R_{0+}^{TE}}{1 - R_{0+}^{TE} R_{0-}^{TE}} H_{hed} \tag{5.7.44d}$$

(3) VMD: From (5.7.33), we find

$$C_{0+} = \frac{1 + R_{0-}^{\text{TE}}}{1 - R_{0+}^{\text{TE}} R_{0-}^{\text{TE}}} H_{vmd} \qquad (5.7.45a)$$

$$D_{0+} = \frac{R_{0+}^{\text{TE}}(1 + R_{0-}^{\text{TE}})}{1 - R_{0+}^{\text{TE}} R_{0-}^{\text{TE}}} H_{vmd} \qquad (5.7.45b)$$

$$C_{0-} = \frac{R_{0-}^{\text{TE}}(1 + R_{0+}^{\text{TE}})}{1 - R_{0+}^{\text{TE}} R_{0-}^{\text{TE}}} H_{vmd} \qquad (5.7.45c)$$

$$D_{0-} = \frac{1 + R_{0+}^{\text{TE}}}{1 - R_{0+}^{\text{TE}} R_{0-}^{\text{TE}}} H_{vmd} \qquad (5.7.45d)$$

(4) HMD: From (5.7.34), we find

$$A_{0+} = \frac{1 + R_{0-}^{\text{TM}}}{1 - R_{0+}^{\text{TM}} R_{0-}^{\text{TM}}} E_{hmd} \qquad (5.7.46a)$$

$$B_{0+} = \frac{R_{0+}^{\text{TM}}(1 + R_{0-}^{\text{TM}})}{1 - R_{0+}^{\text{TM}} R_{0-}^{\text{TM}}} E_{hmd} \qquad (5.7.46b)$$

$$C_{0+} = \frac{1 - R_{0-}^{\text{TE}}}{1 - R_{0+}^{\text{TE}} R_{0-}^{\text{TE}}} H_{hmd} \qquad (5.7.46c)$$

$$D_{0+} = \frac{R_{0+}^{\text{TE}}(1 - R_{0-}^{\text{TE}})}{1 - R_{0+}^{\text{TE}} R_{0-}^{\text{TE}}} H_{hmd} \qquad (5.7.46d)$$

$$A_{0-} = \frac{R_{0-}^{\text{TM}}(1 + R_{0+}^{\text{TM}})}{1 - R_{0+}^{\text{TM}} R_{0-}^{\text{TM}}} E_{hmd} \qquad (5.7.47a)$$

$$B_{0-} = \frac{1 + R_{0+}^{\text{TM}}}{1 - R_{0+}^{\text{TM}} R_{0-}^{\text{TM}}} E_{hmd} \qquad (5.7.47b)$$

$$C_{0-} = -\frac{R_{0-}^{\text{TE}}(1 - R_{0+}^{\text{TE}})}{1 - R_{0+}^{\text{TE}} R_{0-}^{\text{TE}}} H_{hmd} \qquad (5.7.47c)$$

$$D_{0-} = -\frac{1 - R_{0+}^{\text{TE}}}{1 - R_{0+}^{\text{TE}} R_{0-}^{\text{TE}}} H_{hmd} \qquad (5.7.47d)$$

The solutions for the electromagnetic field components are obtained by inserting the values for the wave amplitudes into (5.7.16)–(5.7.21).

EXAMPLE 5.7.1   Vertical magnetic dipole on two-layer media.

   The geometrical configuration of the problem is shown in Figure E5.7.1.1. The origin of the coordinate system is placed in the location of the dipole which is a vertical magnetic dipole (VMD) above a two-layer medium with boundaries at $z = d_0 and d_1$ with $d_0 - d_{-1} = d$.
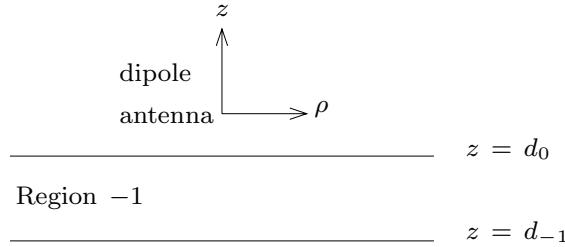
Figure E5.7.1.1 Dipole in layered medium.

   In the presence of the two-layer medium, the vertical magnetic dipole (VMD) has, in Region 0,

$$H_z = \int_{-\infty}^{\infty} dk_\rho \left\{ \begin{array}{l} (H_{vmd} + A_0)e^{ik_z z} \\ A_0 e^{ik_z z} + H_{vmd}e^{-ik_z z} \end{array} \right\} H_0^{(1)}(k_\rho \rho) \qquad \begin{array}{l} z \geq 0 \\ z \leq 0 \end{array} \quad (E5.7.1.1)$$

$$E_\phi = \int_{-\infty}^{\infty} dk_\rho \frac{-i\omega\mu}{k_\rho} \left\{ \begin{array}{l} (H_{vmd} + A_0)e^{ik_z z} \\ A_0 e^{ik_z z} + H_{vmd}e^{-ik_z z} \end{array} \right\} H_0^{(1)}(k_\rho \rho) \quad \begin{array}{l} z \geq 0 \\ z \leq 0 \end{array} \quad (E5.7.1.2)$$

$$H_\rho = \int_{-\infty}^{\infty} dk_\rho \frac{ik_z}{k_\rho} \left\{ \begin{array}{l} (H_{vmd} + A_0)e^{ik_z z} \\ A_0 e^{ik_z z} - H_{vmd}e^{-ik_z z} \end{array} \right\} H_0^{(1)}(k_\rho \rho) \quad \begin{array}{l} z \geq 0 \\ z \leq 0 \end{array} \quad (E5.7.1.3)$$

$$H_{vmd} = -i\frac{IA\, k_\rho^3}{8\pi k_z} \qquad\qquad\qquad\qquad\qquad\qquad (E5.7.1.4)$$

where IA is the magnetic dipole moment. In Region 1,

$$H_{1z} = \int_{-\infty}^{\infty} dk_\rho \left[C_1 e^{ik_{1z} z} + D_1 e^{-ik_{1z} z} \right] H_0^{(1)}(k_\rho \rho) \qquad\qquad (E5.7.1.5)$$

$$E_{1\phi} = \int_{-\infty}^{\infty} dk_\rho \frac{-i\omega\mu_1}{k_\rho} \left[C_1 e^{ik_{1z} z} + D_1 e^{-ik_{1z} z} \right] H_1^{(1)}(k_\rho \rho) \qquad (E5.7.1.6)$$

$$H_{1\rho} = \int_{-\infty}^{\infty} dk_\rho \frac{ik_{1z}}{k_\rho} \left[C_1 e^{ik_{1z} z} - D_1 e^{-ik_{1z} z} \right] H_1^{(1)}(k_\rho \rho) \qquad (E5.7.1.7)$$

At $z = d_{-1}$, $E_\phi = 0$, we find $C_1 = -D_1 e^{-i2k_{1z}d_1}$. At $z = d_0$ which is less than zero, E_ϕ and H_ρ are continuous. We obtain

$$k_z \left(A_0 e^{ik_z d_0} - H_{vmd} e^{-ik_z d_0} \right) = k_{1z} \left(C_1 e^{ik_{1z}d_0} - D_1 e^{-ik_{1z}d_0} \right) \qquad \text{(E5.7.1.8)}$$

$$\mu \left(A_0 e^{ik_z d_0} + H_{vmd} e^{-ik_z d_0} \right) = \mu_1 \left(C_1 e^{ik_{1z}d_0} + D_1 e^{-ik_{1z}d_0} \right) \qquad \text{(E5.7.1.9)}$$

We find

$$A_0 e^{ik_z d_0} = \frac{1}{2} \left(\frac{\mu_1}{\mu} + \frac{k_{1z}}{k_z} \right) \left[C_1 e^{ik_{1z}d_0} + R_{01}^{\text{TE}} D_1 e^{-ik_{1z}d_0} \right] \quad \text{(E5.7.1.10}a\text{)}$$

$$H_{vmd} e^{-ik_z d_0} = \frac{1}{2} \left(\frac{\mu_1}{\mu} + \frac{k_{1z}}{k_z} \right) \left[R_{01}^{\text{TE}} C_1 e^{ik_{1z}d_0} + D_1 e^{-ik_{1z}d_0} \right] \quad \text{(E5.7.1.10}b\text{)}$$

$$\frac{A_0}{H_{vmd}} = e^{-i2k_z d_0} \frac{C_1 e^{ik_{1z}d_0} + R_{01}^{\text{TE}} D_1 e^{-ik_{1z}d_0}}{R_{01}^{\text{TE}} C_1 e^{ik_{1z}d_0} + D_1 e^{-ik_{1z}d_0}}$$

$$= e^{-i2k_z d_0} \frac{R_{01}^{\text{TE}} - e^{i2k_{1z}d}}{1 - R_{01}^{\text{TE}} e^{i2k_{1z}d}} = R_{0+}^{\text{TE}} \qquad \text{(E5.7.1.11)}$$

where $d = d_0 - d_1$, and

$$R_{01}^{\text{TE}} = \frac{1 - \mu k_{1z}/\mu_1 k_z}{1 + \mu k_{1z}/\mu_1 k_z}$$

In Region 0 for $z \geq 0$,

$$H_z = \int_{-\infty}^{\infty} dk_\rho H_{vmd}(1 + R_{0+}^{\text{TE}}) e^{ik_z z} H_0^{(1)}(k_\rho \rho)$$

$$= \int_{-\infty}^{\infty} dk_\rho \frac{-iIA\,k_\rho^3}{8\pi k_z}(1 + R_{0+}^{\text{TE}}) e^{ik_z z} H_0^{(1)}(k_\rho \rho) \qquad \text{(E5.7.1.12)}$$

$$E_\phi = \int_{-\infty}^{\infty} dk_\rho \frac{-i\omega\mu}{k_\rho} H_{vmd}(1 + R_{0+}^{\text{TE}}) e^{ik_z z} H_1^{(1)}(k_\rho \rho)$$

$$= \int_{-\infty}^{\infty} dk_\rho \frac{-\omega\mu IA\,k_\rho^2}{8\pi k_z}(1 + R_{0+}^{\text{TE}}) e^{ik_z z} H_1^{(1)}(k_\rho \rho) \qquad \text{(E5.7.1.13)}$$

$$H_\rho = \int_{-\infty}^{\infty} dk_\rho \frac{ik_z}{k_\rho} H_{vmd}(1 - R_{0+}^{\text{TE}}) e^{ik_z z} H_1^{(1)}(k_\rho \rho)$$

$$= \int_{-\infty}^{\infty} dk_\rho \frac{IA\,k_\rho^2}{8\pi}(1 - R_{0+}^{\text{TE}}) e^{ik_z z} H_1^{(1)}(k_\rho \rho) \qquad \text{(E5.7.1.14)}$$

— End of Example 5.7.1 —

B. Contour Integration Methods

a. Cauchy's Theorem

The most fundamental and useful theorem in functions of complex variables is Cauchy's theorem. Consider a complex function

$$f(\alpha) = f_R + i f_I \tag{5.7.48}$$

of a complex variable

$$\alpha = \alpha_R + i\alpha_I \tag{5.7.49}$$

where f_R, f_I, α_R, and α_I are all real. Assume that $f(\alpha)$ is analytic, namely its derivative exists, over a domain D in the complex α plane as shown in [Fig. 5.7.2]. The boundary line of D forms a closed contour C. Cauchy's theorem states that the line integration of $f(\alpha)$ along C is zero,

$$\oint_C d\alpha\, f(\alpha) = 0 \tag{5.7.50}$$
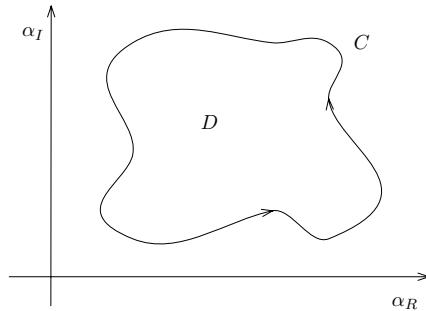
Figure 5.7.2 Contour for Cauchy's theorem.

The direction of integration is such that when one travels along this direction, the domain D is always on his left hand side.

Augustin-Louis Cauchy (21 August 1789 – 23 May 1857)

Cauchy published 789 papers, his works on complex functions and number theory were each over 300 pages long. At the age of twenty-two he became professor at the Ecole Polytechnique. In 1814 he published the memoir on definite integrals that later became the basis of his theory of complex functions. Cauchy also presented a mathematical treatment of optics, hypothesized that ether had the mechanical properties of an elasticity medium.

EXAMPLE 5.7.2

As an example, consider the evaluation of the integral

$$I = \int_0^\infty d\alpha \, \frac{\sin \alpha}{\alpha}$$

Writing $\sin \alpha$ in terms of exponentials, we have

$$I = \frac{1}{2i} \int_0^\infty d\alpha \left[\frac{e^{i\alpha}}{\alpha} - \frac{e^{-i\alpha}}{\alpha} \right] = \lim_{\delta \to 0} \left\{ \int_\delta^\infty d\alpha \, \frac{e^{i\alpha}}{2i\alpha} + \int_{-\infty}^{-\delta} d\alpha \, \frac{e^{i\alpha}}{2i\alpha} \right\}$$
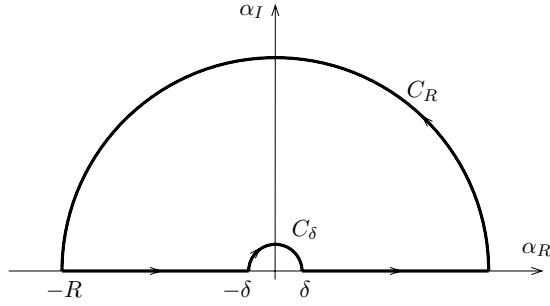
Figure E5.7.2.1 Contour for integration.

We choose a closed contour C composed of C_R, the negative real axis, C_δ, and the positive real axis as shown in Figure E5.7.2.1

$$I = \lim_{\substack{\delta \to 0 \\ R \to \infty}} \left\{ \oint_C - \int_{C_\delta} - \int_{C_R} \right\} d\alpha \, \frac{e^{i\alpha}}{2i\alpha} \qquad \text{(E5.7.2.1)}$$

where $\alpha = \alpha_R + i\alpha_I$. By Cauchy's theorem, the first integral is zero because $e^{i\alpha}/\alpha$ is analytic inside and on contour C. The third integral also vanishes as $R \to \infty$ on account of Jordan's Lemma [Prob. P4.7.4]. The second integral is the only one that contributes. Writing α in polar coordinates, $\alpha = \delta e^{i\phi}$, we therefore obtain

$$I = -\frac{1}{2} \lim_{\delta \to 0} \int_\pi^0 d\phi \, \exp(i\delta e^{i\phi})$$

$$= -\frac{1}{2} \int_\pi^0 d\phi = \frac{\pi}{2} \qquad \text{(E5.7.2.2)}$$

— END OF EXAMPLE 5.7.2 —

Notice that Cauchy's theorem is based on the assumption that the function is analytic on the domain of integration. When there are singularities inside the domain, they must be taken into account separately. Expanding the function $f(\alpha)$ around a singularity α_0, we have

$$f(\alpha) = \sum_{n=0}^{\infty} a_n (\alpha - \alpha_0)^n + \sum_{n=1}^{\infty} \frac{a_{-n}}{(\alpha - \alpha_0)^n} \qquad (5.7.51)$$
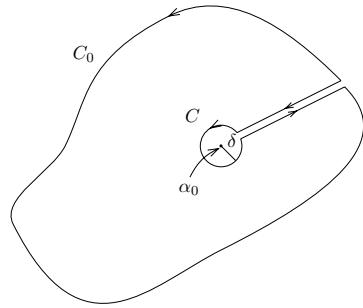
Figure 5.7.3 Contour for proof of Residue theorem.

By Cauchy's theorem no contribution comes from the first summation because it is analytical. To integrate the second summation, we first change the original contour C_0 to a new circular contour C with radius δ surrounding α_0 [Fig. 5.7.3] and let

$$\alpha - \alpha_0 = \delta e^{i\phi}$$

By Cauchy's theorem it is seen that

$$\oint_{C_0} d\alpha \, f(\alpha) - \oint_C d\alpha \, f(\alpha) = 0$$

as the contributions from the two opposite straight lines cancel each other. Thus the integration over the original contour is equal to that over C and we have

$$\oint_C d\alpha \, f(\alpha) = i \sum_{n=1}^{\infty} \frac{a_{-n}}{\delta^{n-1}} \int_0^{2\pi} d\phi \, e^{i(1-n)\phi}$$

Obviously, all terms other than $n = 1$ are zero. Therefore we obtain the Residue theorem:

$$\oint_C d\alpha \, f(\alpha) = 2\pi i a_{-1} \qquad (5.7.52)$$

Since the expansion coefficient a_{-1} is the only one left after the integration, a_{-1} is called the *residue*.

EXAMPLE 5.7.3
   If $f(\alpha)$ has a pole of order m, then all subsequent terms after a_{-m} vanish, namely $a_{-n} = 0$ for $n > m$,

$$f(\alpha) = \sum_{n=0}^{\infty} a_n(\alpha - \alpha_0)^n + \frac{a_{-1}}{(\alpha - \alpha_0)} + \ldots + \frac{a_{-m}}{(\alpha - \alpha_0)^m}$$

and we find

$$a_{-1} = \frac{1}{(m-1)!} \lim_{\alpha \to \alpha_0} \left\{ \frac{d^{m-1}}{d\alpha^{m-1}} (\alpha - \alpha_0)^m f(\alpha) \right\} \qquad (E5.7.3.1)$$

For essential singularities, the residue can be found from known series expansions. For instance, the residue of $\exp(-1/\alpha)$ is -1.
                                                    — END OF EXAMPLE 5.7.3 —

   The residue of a function can be determined in many ways. If $f(\alpha)$ has a single pole, then all a_{-n} but a_{-1} vanish. We have

$$a_{-1} = \lim_{\alpha \to \alpha_o} \left\{ (\alpha - \alpha_0) f(\alpha) \right\} \qquad (5.7.53)$$

If $f(\alpha)$ is analytic over a domain D bounded by contour C, then by the Residue theorem, the function at a regular point α_0 can be represented by the integral

$$f(\alpha_0) = \frac{1}{2\pi i} \oint_C d\alpha \frac{f(\alpha)}{\alpha - \alpha_0} \qquad (5.7.54)$$

which is *Cauchy's integral formula*. Note that we also have

$$f^{(n)}(\alpha_0) = \frac{n!}{2\pi i} \oint_C d\alpha \frac{f(\alpha)}{(\alpha - \alpha_0)^{n+1}} \qquad (5.7.55)$$

This follows from (5.7.54) by using Leibnitz' rule of differentiation.

EXAMPLE 5.7.4

    To illustrate the use of the Residue theorem, consider again the evaluation of

$$I = \int_0^\infty d\alpha \, \frac{\sin \alpha}{\alpha}$$
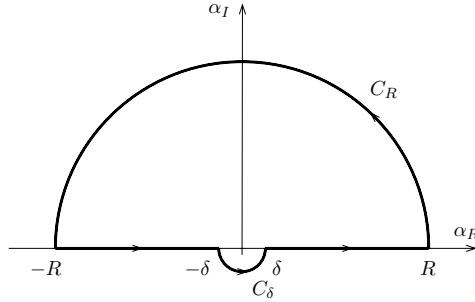
Figure E5.7.4.1   A closed contour including the pole at $\alpha = 0$.

Instead of choosing the contour as shown in Figure E5.7.2.1, we choose to indent around the pole at $\alpha = 0$ from below [Fig. E5.7.4.1]. The contour then encloses the pole which has a residue of $e^{i\alpha}/2i\alpha$ equal to $1/2i$. Thus we have

$$
\begin{aligned}
I &= \lim_{\substack{\delta \to 0 \\ R \to \infty}} \left\{ \oint_C - \int_{C_\delta} - \int_{C_R} \right\} d\alpha \, \frac{e^{i\alpha}}{2i\alpha} \\
&= 2\pi i \left[\frac{1}{2i} \right] - \lim_{\delta \to 0} \int_{C_\delta} d\alpha \, \frac{e^{i\alpha}}{2i\alpha} \\
&= \pi - \frac{1}{2} \int_\pi^{2\pi} d\phi = \frac{\pi}{2}
\end{aligned}
\qquad \text{(E5.7.4.1)}
$$

— END OF EXAMPLE 5.7.4 —

    The residue of a multi-valued function is dependent on the particular Riemann sheet where the singularity lies. To illustrate the concept of a multi-valued function and its associated Riemann sheets, consider the simple function $f(\alpha) = \sqrt{\alpha}$. The function is double-valued since, for example, as $\alpha = 1 = e^{i2m\pi}$, $f(\alpha) = e^{im\pi}$ which is $+1$ or -1 depending on whether m is even or odd. We see that at $\alpha = 0$, it is impossible to define a neighborhood in which the function is single-valued. The point $\alpha = 0$ is called a *branch point* which is another type
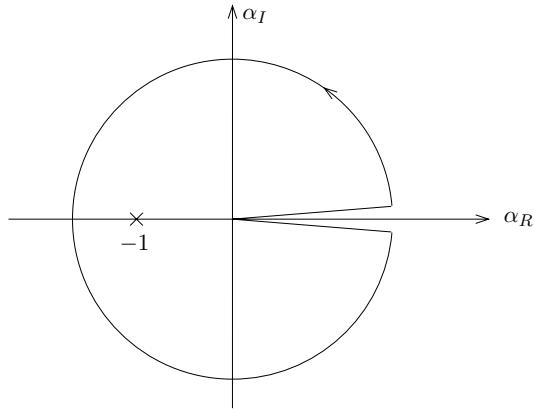
Figure 5.7.4 Contour with a branch cut.

of singularity in addition to the poles and essential singularities where the derivative of the function does not exist.

To make the function single-valued, we define two Riemann sheets such that on the top Riemann sheet $4m\pi \leq \phi \leq 2(2m + 1)\pi$ and on the bottom Riemann sheet $2(2m + 1)\pi \leq \phi \leq 4(m + 1)\pi$ where $m = 0, 1, 2, \ldots$ To separate the two Riemann sheets we choose a branch cut along the positive real α_R axis which can be visualized as creating a wedge-shaped cut [Fig. 5.7.4] such that for $0 < \phi < 2\pi$ we are on the top Riemann sheet; for $2\pi < \phi < 4\pi$, sliding to the bottom Riemann sheet, and, for $4\pi < \phi < 6\pi$, we come up again to the top sheet. It is noted that we could very well choose a different branch cut and define the two Riemann sheets differently. For instance, we may choose a branch cut along the negative α_R axis so that on the top Riemann sheet $(4m - 1)\pi < \phi < (4m + 1)\pi$ and on the bottom Riemann sheet $(4m + 1)\pi < \phi < (4m + 3)\pi$.

Bernhard Riemann (17 September 1826 – 20 July 1866)

In the spring of 1846 Riemann enrolled at the University of Göttingen. From 1847 to 1849 he enrolled at the University of Berlin and worked out his general theory of complex variables that formed the basis of some of his most important work. Riemann defended his dissertation "Foundation of a general function theory of one variable complex number" in December 1851, which was highly commended by Gauss. In 1853 Riemann became the assistant of W. Weber. Riemann in 1859 succeeded Lejeune Dirichlets to become a full professor on the chair that Gauss had occupied only four years ago.

---

b. Kramers-Krönig relations

By the principle of causality, the permittivity $\epsilon(\omega)$ is seen to be an analytical function of complex variable ω on the upper half plane of ω. From the defining equation for $\epsilon(\omega)$, we see that

$$\epsilon^*(\omega) = \epsilon(-\omega)$$

Separating into real and imaginary parts, we have

$$\begin{cases} \epsilon_R(\omega) = \epsilon_R(-\omega) \\ \epsilon_I(\omega) = -\epsilon_I(-\omega) \end{cases}$$

Thus ϵ_R is an even function of ω and ϵ_I is an odd function of ω. Extending to the whole complex $\omega = \omega_R + i\omega_I$ plane, we see that on the imaginary axis ω_I, $\epsilon(i\omega_I) = \epsilon^*(i\omega_I)$. It follows that $\epsilon(\omega)$ is real on the imaginary ω_I axis. On the upper half plane, the integrand includes the exponentially decreasing factor $e^{-\omega_I t}$. Thus $\epsilon(\omega)$ is a single-valued regular function over the upper half of the complex ω plane. The fact that $\epsilon(\omega)$ is an analytical function of complex variable ω on the upper half plane of ω is a direct consequence of the principle of causality.

By Cauchy's theorem, we have

$$\oint_C d\alpha \, \frac{\epsilon(\alpha) - \epsilon_\infty}{\alpha - \omega} = 0 \tag{5.7.56}$$
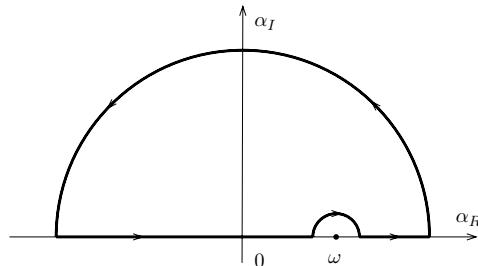
Figure 5.7.5 Contour for Kramers-Krönig's relation.

when integrated over a closed contour consisting of a semicircle of infinite radius with the straight side along the real axis but indented around the point $\alpha = \omega$ [Fig. 5.7.5]. The integral over the semicircle

of infinite radius vanishes in view of Jordan's Lemma. Defining the principal value PV of the integral to be the result of the integration along the real axis except at $\alpha = \omega$, we find

$$\text{PV} \int_{-\infty}^{\infty} d\alpha\, \frac{\epsilon(\alpha) - \epsilon_\infty}{\alpha - \omega} - i\pi[\epsilon(\omega) - \epsilon_\infty] = 0$$

Separating the real and imaginary parts, we find the causality condition

$$\epsilon_R(\omega) - \epsilon_\infty = \frac{1}{\pi}\text{PV} \int_{-\infty}^{\infty} d\alpha\, \frac{\epsilon_I(\alpha)}{\alpha - \omega} \tag{5.7.57a}$$

$$\epsilon_I(\omega) = -\frac{1}{\pi}\text{PV} \int_{-\infty}^{\infty} d\alpha\, \frac{\epsilon_R(\alpha) - \epsilon_\infty}{\alpha - \omega} \tag{5.7.57b}$$

These formulae were first derived by Hendrik Kramers (1894–1952) and Ralph Krönig (1904–1995) in 1927 and are known as the Kramers-Krönig relations. Equation $(5.7.57a)$ is also known mathematically as the Hilbert transform relation that relates the real part of $\epsilon(\omega) - \epsilon_\infty$ to its imaginary part. Equation $(5.7.57b)$ is the inverse Hilbert transform relation.

David Hilbert (23 January 1862 – 14 February 1943)
Hilbert was a member of staff at the University of Königsberg from 1886 to 1895, being a Privatdozent until 1892, then as Extraordinary Professor for one year before being appointed a full professor in 1893. In 1895, Hilbert was appointed to the chair of mathematics at the University of Göttingen, where he continued to teach until he retired in 1930.

Example 5.7.5
From permittivity

$$\epsilon(\omega) = \epsilon_o \left[1 - \frac{\omega_p^2}{\omega^2 - \omega_e^2 + i\omega\gamma}\right] \tag{E5.7.5.1}$$

we find $\epsilon^*(\omega) = \epsilon(-\omega)$. Show that $\epsilon(\omega)$ is analytical on the upper half plane.
Proof:
The poles of the permittivity are found from

$$\omega^2 - \omega_e^2 + i\omega\gamma = 0$$

which gives

$$\omega = \frac{1}{2}\left(-i\gamma \pm \sqrt{4\omega_e^2 - \gamma^2}\right)$$

For $4\omega_e^2 > \gamma^2$, the two poles are on the lower half plane. For $4\omega_e^2 < \gamma^2$, $\sqrt{\gamma^2 - 4\omega_e^2}$ is smaller than γ and the poles are both on the imaginary axis on the lower half plane. Thus the permittivity $\epsilon(\omega)$ in (E5.7.5.1) is analytical on the upper half plane.

— END OF EXAMPLE 5.7.5 —

EXAMPLE 5.7.6

Prove $\frac{\partial \omega \epsilon}{\partial \omega} > 0$ for media with small loss by using the Kramers-Krönig relations

$$\epsilon_R(\omega) - \epsilon_\infty = \frac{1}{\pi}\text{PV}\int_{-\infty}^{\infty} d\alpha \, \frac{\epsilon_I(\alpha)}{\alpha - \omega} \qquad (E5.7.6.1)$$

Proof:

Since $\epsilon_I(\omega)$ is an odd function and with $\epsilon_I \approx 0$, we have

$$\epsilon_R(\omega) - \epsilon_\infty = \frac{1}{\pi}\text{PV}\int_{-\infty}^{\infty} d\alpha \, \frac{\epsilon_I(\alpha)}{\alpha - \omega} = \frac{2}{\pi}\text{PV}\int_0^{\infty} d\alpha \, \frac{\alpha \epsilon_I(\alpha)}{\alpha^2 - \omega^2}$$

$$\approx \frac{2}{\pi}\int_0^{\infty} d\alpha \, \frac{\alpha \epsilon_I(\alpha)}{\alpha^2 - \omega^2} \qquad (E5.7.6.2)$$

Thus

$$\frac{\partial \epsilon_R(\omega)}{\partial \omega} = \frac{4\omega}{\pi}\int_0^{\infty} d\alpha \, \frac{\alpha \epsilon_I(\alpha)}{(\alpha^2 - \omega^2)^2} > 0 \qquad (E5.7.6.3)$$

since the integrand is positive throughout the region of integration.

Another inequality can be derived from

$$\frac{\partial[\omega^2(\epsilon_R(\omega) - \epsilon_\infty)]}{\partial \omega} = \frac{\partial}{\partial \omega}\frac{2}{\pi}\int_0^{\infty} d\alpha \, \frac{\alpha \epsilon_I(\alpha)(\omega^2 - \alpha^2 + \alpha^2)}{\alpha^2 - \omega^2}$$

$$= \frac{4\omega}{\pi}\int_0^{\infty} d\alpha \, \frac{\alpha^3 \epsilon_I(\alpha)}{(\alpha^2 - \omega^2)^2} > 0$$

It follows that

$$\frac{\partial \epsilon_R(\omega)}{\partial \omega} > \frac{2(\epsilon_\infty - \epsilon_R)}{\omega} \qquad (E5.7.6.4)$$

which is a more stringent condition than (E5.7.6.3) when $\epsilon_R < \epsilon_\infty$. Summing over (E5.7.6.3) and (E5.7.6.4), we find

$$\frac{\partial(\omega\epsilon_R)}{\partial \omega} = \omega\frac{\partial(\epsilon_R)}{\partial \omega} + \epsilon_R > \epsilon_\infty > 0 \qquad (E5.7.6.5)$$

— END OF EXAMPLE 5.7.6 —

EXAMPLE 5.7.7

Prove the Kramers-Krönig relations

$$\epsilon_R(\omega) - \epsilon_\infty = \frac{1}{\pi} \text{PV} \int_{-\infty}^{\infty} d\alpha \, \frac{\epsilon_I(\alpha)}{\alpha - \omega} \qquad (E5.7.7.1a)$$

$$\epsilon_I(\omega) = -\frac{1}{\pi} \text{PV} \int_{-\infty}^{\infty} d\alpha \, \frac{\epsilon_R(\alpha) - \epsilon_\infty}{\alpha - \omega} \qquad (E5.7.7.1b)$$

for the permittivity

$$\epsilon(\omega) = \epsilon_o \left[1 - \frac{\omega_p^2}{\omega^2 - \omega_e^2 + i\omega\gamma_e} \right] = \epsilon_R + i\epsilon_I \qquad (E5.7.7.2)$$

$$= \epsilon_e \left[1 - \frac{(\omega^2 - \omega_e^2)\omega_p^2}{(\omega^2 - \omega_e^2)^2 + (\omega\gamma_e)^2} + \frac{i\omega\gamma_e\omega_p^2}{(\omega^2 - \omega_e^2)^2 + (\omega\gamma_e)^2} \right] \qquad (E5.7.7.3)$$

Proof:

The poles of $\epsilon(\omega)$ occur at $(\omega^2 - \omega_e^2)^2 + (\omega\gamma_e)^2 = 0$ which gives $a_1 = \frac{1}{2}(i\gamma_e + \sqrt{\Delta}), a_2 = \frac{1}{2}(i\gamma_e - \sqrt{\Delta}), a_3 = \frac{1}{2}(-i\gamma_e + \sqrt{\Delta}), a_4 = \frac{1}{2}(-i\gamma_e - \sqrt{\Delta})$, where $\Delta = -\gamma_e^2 + 4\omega^4$. Notice that the pole $\alpha = \omega$ is on the real axis, and the two poles $\alpha = \alpha_1$ and $\alpha = \alpha_2$ are included in the upper half-plane. Applying residue theorem, and let $\epsilon_\infty = \epsilon_o$, we find from (E5.7.7.1a)

$$\epsilon_R(\omega) - \epsilon_\infty = \frac{1}{\pi} \text{PV} \int_{-\infty}^{\infty} d\alpha \, \frac{\epsilon_I(\alpha)}{\alpha - \omega}$$

$$= \frac{1}{\pi} \text{PV} \int_{-\infty}^{\infty} d\alpha \, \frac{\alpha\gamma_e\omega_p^2}{(\alpha - \omega)(\alpha - a_1)(\alpha - a_2)(\alpha - a_3)(\alpha - a_4)}$$

$$= \frac{1}{\pi} \left[i\pi \frac{\omega\gamma_e\omega_p^2}{(\omega - a_1)(\omega - a_2)(\omega - a_3)(\omega - a_4)} \right.$$

$$+ i2\pi \frac{a_1\gamma_e\omega_p^2}{(a_1 - \omega)(a_1 - a_2)(a_1 - a_3)(a_1 - a_4)}$$

$$\left. + i2\pi \frac{a_2\gamma_e\omega_p^2}{(a_2 - \omega)(a_2 - a_1)(a_2 - a_3)(a_2 - a_4)} \right]$$

$$= \frac{i\omega\gamma_e\omega_p^2}{(\omega - a_1)(\omega - a_2)(\omega - a_3)(\omega - a_4)}$$

$$+ \frac{\omega_p^2}{(a_1 - \omega)(a_1 - a_2)} + \frac{\omega_p^2}{(a_2 - \omega)(a_2 - a_1)}$$

$$= \frac{i\omega\gamma_e\omega_p^2 - \omega_p^2(\omega - a_3)(\omega - a_4)}{(\omega - a_1)(\omega - a_2)(\omega - a_3)(\omega - a_4)} = -\frac{(\omega^2 - \omega_o^2)\omega_p^2}{(\omega^2 - \omega_e^2)^2 + (\omega\gamma_e)^2}$$

A similar proof applies to (E5.7.7.1b).

<div align="right">— END OF EXAMPLE 5.7.7 —</div>

c. Asymptotic Series for Hankel Functions

The saddle point method is a useful tool in evaluating asymptotic values for an integral when its integrand contains a very large parameter. In the following we illustrate the method by finding the asymptotic values for the Hankel functions. Using wave concepts we argue first that a cylindrical wave can be represented by a superposition of plane waves emerging from all angles, real and complex. Then we define Hankel functions in terms of a contour integration on a complex plane.

The wave equation in cylindrical coordinates takes the form

$$\left[\frac{1}{\rho}\frac{\partial}{\partial\rho}\left(\rho\frac{\partial}{\partial\rho}\right) + \frac{1}{\rho^2}\frac{\partial^2}{\partial\phi^2} + k^2\right] u\left(\rho, \phi\right) = 0 \qquad (5.7.58)$$

The solution to this equation is

$$u(\rho, \phi) = H_n(k\rho)e^{\pm in\phi}$$

where $H_n(k\rho)$ is the Hankel function. The same wave equation in rectangular coordinates takes the form

$$\left[\frac{\partial^2}{\partial x^2} + \frac{\partial^2}{\partial y^2} + k^2\right] \tilde{u}(x, y) = 0$$

The two wave equations are related by a coordinate transformation. The familiar plane wave solution to the above equation is

$$\tilde{u}(x, y) = e^{ik_x x + ik_y y}$$

In cylindrical coordinates, the plane wave becomes

$$e^{ik_x x + ik_y y} = e^{ik\rho\cos(\psi - \phi)}$$

where

$$\overline{k} = \hat{x}k_x + \hat{y}k_y = \hat{x}k\cos\psi + \hat{y}k\sin\psi$$
$$\overline{\rho} = \hat{x}x + \hat{y}y = \hat{x}\rho\cos\phi + \hat{y}\rho\sin\phi$$

The wave vector $\overline{k}$ indicates the plane wave propagation direction, and the position vector $\overline{\rho}$ represents the observation point [Fig. 5.7.6].
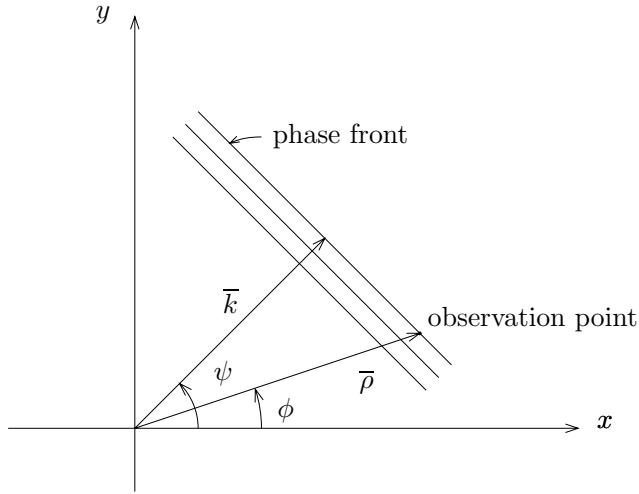
Figure 5.7.6 Cylindrical wave as superposition of plane waves.

We can view a cylindrical wave as a superposition of plane waves, uniform and nonuniform, emerging from all angles ψ, real and complex. Denoting wave amplitudes by $C_n e^{in\psi}$, we write

$$u(\rho, \phi) = \int_\Gamma d\psi \, C_n \, e^{in\psi} e^{ik\rho \cos(\psi - \phi)} \qquad (5.7.59)$$

It is straightforward to show that this integral is indeed a solution to the wave equation (5.7.58) in cylindrical coordinates. The path of integration Γ and the amplitude constant C_n are still to be specified.

The path Γ on the complex ψ plane must be chosen to assure that this integral converges properly. To put the solution into the desired form, we set $\alpha = \psi - \phi$. Thus

$$u(\rho, \phi) = e^{in\phi} \int_\Gamma d\alpha \, C_n e^{ik\rho \cos \alpha + in\alpha} \qquad (5.7.60)$$

We now investigate the convergence of the integral in the neighborhood of infinity. On the complex plane

$$\alpha = \alpha_R + i\alpha_I$$

We let $\xi = k\rho$, the term in the exponent takes the form

$$e^{i\xi \cos \alpha + in\alpha} = e^{\xi \sin \alpha_R \sinh \alpha_I - n\alpha_I} e^{i(\xi \cos \alpha_R \cosh \alpha_I + n\alpha_R)} \qquad (5.7.61)$$

As $\alpha_I \to +\infty$, the real part is positive for $\sin \alpha_R > 0$.
As $\alpha_I \to -\infty$, the real part is positive for $\sin \alpha_R < 0$.
When the real part is positive, the integrand diverges exponentially
as $\alpha_I \to \pm\infty$, and we denote with shaded regions in Figure 5.7.7.
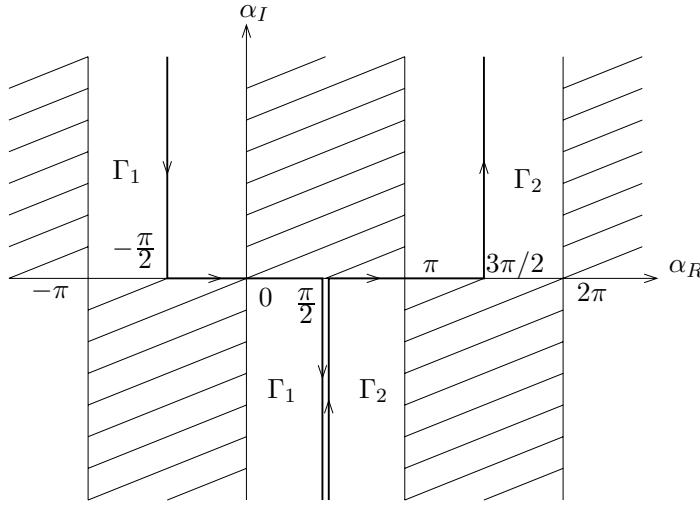
Figure 5.7.7 Integration paths for Hankel functions.

The Hankel function of the first kind is defined as

$$H_\nu^{(1)}(\xi) = \frac{1}{\pi} \int_{\Gamma_1} d\alpha \, e^{i(\xi \cos \alpha + \nu\alpha - \nu\pi/2)} \qquad (5.7.62)$$

where the integration path Γ_1 is shown in Figure 5.7.7. We see that
the real part in (5.7.61) goes to $-\infty$ for $\alpha_R = -\pi/2$ and $\alpha_I \to +\infty$,
and for $\alpha_R = \pi/2$ and $\alpha_I \to -\infty$. Thus the integral converges.

The Hankel function of the second kind is defined by the same
integral but follows a different path Γ_2,

$$H_\nu^{(2)}(\xi) = \frac{1}{\pi} \int_{\Gamma_2} d\alpha \, e^{i(\xi \cos \alpha + \nu\alpha - \nu\pi/2)} \qquad (5.7.63)$$

The path of integration Γ_2 is also shown in Figure 5.7.7.

b. Asymptotic Form of Hankel Functions

We now determine asymptotic values of

$$H_0^{(1)}(\xi) = \frac{1}{\pi} \int_{\Gamma_1} d\alpha \, e^{i\xi \cos \alpha} = \frac{1}{\pi} \int_{\Gamma_1} d\alpha \, e^{i\xi \cos \alpha_R \cosh \alpha_I + \xi \sin \alpha_R \sinh \alpha_I}$$

(5.7.64)

as $\xi \to \infty$ by using the saddle point method. The saddle points are determined from

$$\frac{d}{d\alpha} [\xi \cos \alpha] = 0$$

which gives the saddle point at $\alpha = \alpha_0 = 0$.

We note that away from the saddle point the integrand ascends into the shaded regions and descends into the unshaded regions. Since integration may be viewed as finding the area under a curve, we can search for a new integration path passing the saddle point in such a way that most of the contribution to the integrand comes from a small portion of the new path near the saddle point. By Cauchy's theorem we can deform the original path of integration Γ_1 to the new integration path.
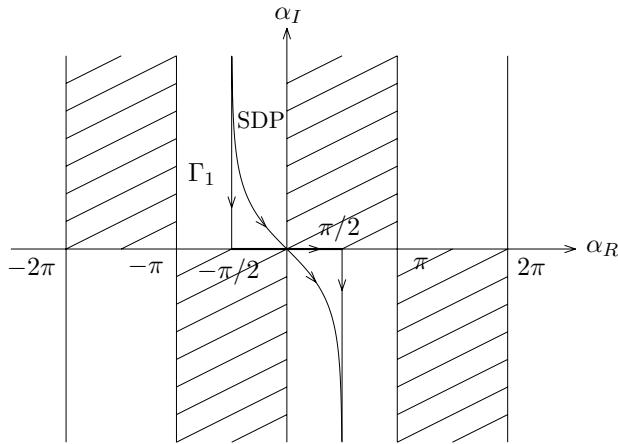
Figure 5.7.8 Integration paths on α plane.

The second step in the saddle point method is to determine the new integration path by requiring that on it the imaginary part of the exponent equal to its value at the saddle point,

$$\cos \alpha_R \cosh \alpha_I = 1$$

(5.7.65)

This choice eliminates the oscillatory behavior caused by the imaginary part in the exponential term $e^{i\xi\cos\alpha}$. The real part of the exponential term has its maximum value at the saddle point and decreases most rapidly along this path. Thus the major contribution to the integral comes from near the saddle point. The new integration path is called the steepest descent path (SDP). We see from (5.7.65) that as $\alpha_I \to \pm\infty$, $\alpha_R \to \mp\pi/2$ so that the ends of SDP meet Γ_1 as shown in Figure 5.7.8. Near the saddle point, we expand (5.7.65) around $\alpha = 0$ to obtain

$$\left(1 - \frac{1}{2}\alpha_R^2 + \ldots\right)\left(1 + \frac{1}{2}\alpha_I^2 + \ldots\right) = 1$$

which gives $\alpha_R \approx \pm\alpha_I$. We choose the negative sign which gives $\alpha_R = -\alpha_I$. Thus the steepest descent path passes through the saddle point at $-\pi/4$ with respect to the α_R axis [Fig. 5.7.8].

The third step is to deform the original path of integration to the steepest descent path. For the Hankel function of the first kind $H_0^{(1)}(\xi)$, no singularity is crossed in the process of deformation. To evaluate the saddle-point contributions of the integral, we let

$$-s^2 = i\cos\alpha - i \approx -i\alpha^2/2 + \ldots .. \tag{5.7.66}$$

which yields $d\alpha = ds\sqrt{2/i}$ where s is a real variable. The integral becomes, near $\alpha \approx \alpha_0 = 0$,

$$H_0^{(1)}(\xi) \approx \frac{1}{\pi}\sqrt{\frac{2}{i}}e^{i\,\xi}\int_{-\delta}^{\delta}ds\,e^{-\xi\,s^2}$$

where δ is a small number. Since away from $\alpha = 0$, $e^{-\xi s^2}$ decays very rapidly, we may replace δ by ∞ and make use of the formula

$$\int_{-\infty}^{\infty}ds\,e^{-\xi s^2} = \sqrt{\frac{\pi}{\xi}}$$

We thus determine the asymptotic value for $H_0^{(1)}(\xi)$ to be, as $\xi \to \infty$,

$$H_0^{(1)}(\xi) \approx \sqrt{\frac{2}{i\pi\xi}}e^{i\,\xi} \tag{5.7.67}$$

This result is to the order of $\xi^{-1/2}$. The saddle-point method can be further used to obtain an asymptotic series for $H_0^{(1)}(\xi)$ in inverse powers of ξ.

EXAMPLE 5.7.8

We now determine asymptotic values of

$$H_\nu^{(1)}(\xi) = \frac{1}{\pi} \int_{\Gamma_1} d\alpha \, e^{i(\xi \cos \alpha + \nu\alpha - \nu\pi/2)} \tag{E5.7.8.1}$$

by using the saddle point method. The saddle points are determined from

$$\frac{d}{d\alpha} \left[\xi \cos \alpha + \nu\alpha\right] = 0$$

There are two saddle points within the interval $-\pi/2$ and $3\pi/2$. For $\nu < \xi$, they are

$$\alpha_0 = \sin^{-1} \frac{\nu}{\xi} \qquad \text{and} \qquad \alpha_0 = \pi - \sin^{-1} \frac{\nu}{\xi} \tag{E5.7.8.2}$$

with $0 \le \sin^{-1}(\nu/\xi) \le \pi/2$. For $\nu > \xi$, they are

$$\alpha_0 = \frac{\pi}{2} - i \cosh^{-1} \frac{\nu}{\xi} \qquad \text{and} \qquad \alpha_0 = \frac{\pi}{2} + i \cosh^{-1} \frac{\nu}{\xi} \tag{E5.7.8.3}$$

In accordance with the original path defined for $H_\nu^{(1)}(\xi)$, the contributing saddle points are $\alpha = \sin^{-1}(\nu/\xi)$ for $\nu < \xi$ and $\alpha = \pi/2 - i \cosh^{-1}(\nu/\xi)$ for $\nu > \xi$.

Since there are no other singularities on the complex α plane, we can deform to the steepest descent path by requiring that on it the imaginary part of the exponent equal to its value at the saddle point, we find,

$$\cos \alpha_R \cosh \alpha_I + \frac{\nu}{\xi} \alpha_R = \text{Re} \left(\cos \alpha_0 + \frac{\nu}{\xi} \alpha_0 \right) \tag{E5.7.8.4}$$

This choice eliminates the oscillatory behavior caused by the imaginary part in the exponential term $e^{i\xi \cos \alpha + i\nu\alpha}$.

The third step is to deform the original path of integration to the steepest descent path. For the Hankel function of the first kind $H_\nu^{(1)}(\xi)$, no singularity is crossed in the process of deformation. To evaluate the saddle-point contributions of the integral, we let

$$-s^2 = i \cos \alpha + i \frac{\nu}{\xi} \alpha - i \cos \alpha_0 - i \frac{\nu}{\xi} \alpha_0 \tag{E5.7.8.5}$$

such that $s = 0$ at $\alpha = \alpha_0 = \sin^{-1}(\nu/\xi)$. Along SDP, the integral (E5.7.8.1) becomes

$$H_\nu^{(1)}(\xi) = \frac{1}{\pi} e^{i(\xi \cos\alpha_0 + \nu\alpha_0 - \nu\pi/2)} \int_{-\infty}^{\infty} ds \, \frac{d\alpha}{ds} \, e^{-\xi s^2}$$

We write (E5.7.8.5) as $-s^2 = f(\alpha)$. Since contributions to the integral come from near the saddle point, we Taylor expand near the saddle point α_0 to obtain $-s^2 = f(\alpha_0) + f'(\alpha_0)(\alpha - \alpha_0) + \frac{1}{2}f''(\alpha_0)(\alpha - \alpha_0)^2 + \ldots$. We find

$$-s^2 \approx -i\frac{1}{2}(\alpha - \alpha_0)^2 \cos\alpha_0$$

which yields

$$d\alpha = ds\sqrt{\frac{2}{i\cos\alpha_0}}$$

where s is a real variable. The integral becomes, near $\alpha = \alpha_0$,

$$H_\nu^{(1)}(\xi) \approx \frac{1}{\pi}\sqrt{\frac{2}{i\cos\alpha_0}}e^{i(\xi\cos\alpha_0 + \nu\alpha_0 - \nu\pi/2)}\int_{-\infty}^{\infty}ds\, e^{-\xi\, s^2}$$

$$\approx \sqrt{\frac{2}{i\pi\xi\cos\alpha_0}}e^{i(\xi\cos\alpha_0 + \nu\alpha_0 - \nu\pi/2)} \qquad \text{(E5.7.8.6)}$$

For $\nu < \xi$, $\alpha_0 = \sin^{-1}(\nu/\xi)$, $\alpha_0 - \pi/2 = -\cos^{-1}(\nu/\xi)$,

$$H_\nu^{(1)}(\xi) \approx \sqrt{\frac{2}{i\pi(\xi^2 - \nu^2)^{1/2}}}\exp\left[i\sqrt{\xi^2 - \nu^2} - i\nu\cos^{-1}\frac{\nu}{\xi}\right] \qquad \text{(E5.7.8.7)}$$

As $\xi \to \infty$, we find

$$H_\nu^{(1)}(\xi) \approx \sqrt{\frac{2}{i\pi\xi}}e^{i\,(\xi + \nu\pi)} \qquad \text{(E5.7.8.8)}$$

This result is to the order of $\xi^{-1/2}$. The saddle-point method can be further used to obtain an asymptotic series for $H_\nu^{(1)}(\xi)$ in inverse powers of ξ.

For $\nu > \xi$, $\alpha_0 = \pi/2 - i\cosh^{-1}(\nu/\xi)$, $\sin\alpha_0 = (\nu/\xi)$, $\xi\cos\alpha_0 = i\sqrt{\nu^2 - \xi^2}$, we find from (E5.7.8.7)

$$H_\nu^{(1)}(\xi) \approx -i\sqrt{\frac{2}{\pi(\nu^2 - \xi^2)^{1/2}}}\exp\left[-\sqrt{\nu^2 - \xi^2} + \nu\cosh^{-1}\frac{\nu}{\xi}\right] \qquad \text{(E5.7.8.9)}$$

For the case $\nu \approx \xi$, the two contributing saddle points begin to merge into one and we need to evaluate the contribution due to both saddle points.

— End of Example 5.7.8 —

d. Saddle-Point Method

The saddle-point method as outlined in the above section for the computation of asymptotic values for $H_\nu^{(1)}(\xi)$ can be generalized to find asymptotic series for integrals of the form

$$I(\xi) = \int_\Gamma d\alpha \, F(\alpha) e^{\xi f(\alpha)} \tag{5.7.68}$$

where ξ is a large real parameter. Let the saddle point be at $\alpha = \alpha_0$ which is determined from $f'(\alpha) = 0$ where we use a prime to denote the derivative of the function. Let Γ be the steepest descent path determined by $f_I(\alpha) = f_I(\alpha_0)$. The contribution to the saddle point is computed with the transformation

$$-s^2 = f(\alpha) - f(\alpha_0) \tag{5.7.69}$$

On the s plane, the integral becomes

$$I(\xi) = e^{\xi f(\alpha_0)} \int_{-\infty}^{\infty} ds \, \Phi(s) e^{-\xi s^2} \tag{5.7.70}$$

where

$$\Phi(s) = \frac{d\alpha}{ds} F\left[\alpha(s)\right] \tag{5.7.71}$$

The idea is to expand $\Phi(s)$ near the saddle point α_0 in a Taylor series,

$$\Phi(s) = \sum_{m=0}^{\infty} A_m s^m \tag{5.7.72}$$

and make use of the formulas

$$\int_{-\infty}^{\infty} ds \, s^{2m+1} e^{-\xi s^2} = 0 \tag{5.7.73a}$$

$$\int_{-\infty}^{\infty} ds \, s^{2m} e^{-\xi s^2} = (-1)^m \frac{d^m}{d\xi^m} \sqrt{\frac{\pi}{\xi}} = \frac{(2m)!}{m! 2^{2m} \xi^m} \sqrt{\frac{\pi}{\xi}} \tag{5.7.73b}$$

to obtain the asymptotic series for $I(\xi)$ in inverse powers of $\xi^{-1/2}$. The result is, by virtue of (5.7.71) and (5.7.73),

$$I(\xi) = e^{\xi f(\alpha_0)} \sum_{m=0}^{\infty} A_{2m} \frac{(2m)!}{m! 2^{2m} \xi^m} \sqrt{\frac{\pi}{\xi}} \tag{5.7.74}$$

The task is to determine the expansion coefficients A_{2m}.

We first expand α and (5.7.69) near the saddle point α_0,

$$\alpha(s) - \alpha_0 = \sum_{n=1}^{\infty} a_n s^n \tag{5.7.75}$$

From Taylor expansion around the saddle point

$$-s^2 = f(\alpha) - f(\alpha_o) = \frac{1}{2!} f''(\alpha_0)(\alpha - \alpha_0)^2 + \frac{1}{3!} f'''(\alpha_0)(\alpha - \alpha_0)^3$$

$$+ \frac{1}{4!} f^{iv}(\alpha_0)(\alpha - \alpha_0)^4 + \cdots$$

$$= \frac{1}{2} f''(\alpha_0) \left[a_1^2 s^2 + 2a_1 a_2 s^3 + (a_2^2 + 2a_1 a_3)s^4 + \cdots \right]$$

$$+ \frac{1}{6} f'''(\alpha_0) \left[a_1^3 s^3 + 3a_1^2 a_2 s^4 + \cdots \right]$$

$$+ \frac{1}{24} f^{iv}(\alpha_0) \left[a_1^4 s^4 + \cdots \right] + \cdots$$

we determine a_n in (5.7.75) by comparing coefficients of s^n

$$a_1 = \sqrt{\frac{-2}{f''}} \tag{5.7.76a}$$

$$a_2 = -\frac{f'''}{6 f''} a_1^2 \tag{5.7.76b}$$

$$a_3 = \frac{1}{24} \left[\frac{5}{3} \left(\frac{f'''}{f''} \right)^2 - \frac{f^{iv}}{f''} \right] a_1^3 \tag{5.7.76c}$$

$$\vdots$$

We now determine the coefficients A_n in (5.7.74) and illustrate the solution to orders of $\xi^{-3/2}$. From (5.7.71) we have

$$\Phi(s) = \frac{d\alpha}{ds} \sum_{k=0}^{\infty} \frac{1}{k!} F^{(k)}(\alpha_0)(\alpha - \alpha_0)^k$$

$$= \left[\sum_{m=1}^{\infty} m a_m s^{m-1} \right] \cdot \sum_{k=0}^{\infty} \frac{1}{k!} F^{(k)}(\alpha_0) \left[\sum_{n=1}^{\infty} a_n s^n \right]^k$$

$$= F(\alpha_0)(a_1 + 2a_2 s + 3a_3 s^2 + \cdots)$$

$$+ F'(\alpha_0)(a_1 s + a_2 s^2 + \cdots)(a_1 + 2a_2 s + \cdots)$$

$$+ \frac{1}{2} F''(\alpha_0)(a_1^2 s^2 + \cdots)(a_1 + \cdots) + \cdots$$

Comparison of coefficients yields

$$A_0 = a_1 F(\alpha_0) \tag{5.7.77a}$$

$$A_2 = 3a_3 F(\alpha_0) + 3a_1 a_2 F'(\alpha_0) + \frac{1}{2} a_1^3 F''(\alpha_0) \tag{5.7.77b}$$

$$\vdots$$

We do not need to evaluate the coefficients A_1, A_3, ... because by virtue of (5.7.73a), they disappear in the final solutions.

Substituting values of a_n from (5.7.76) in (5.7.77) and making use of the formulas (5.7.73), the integral in (5.7.70) gives

$$I(\xi) = F(\alpha_0) e^{\xi f(\alpha_0)} \sqrt{\frac{2\pi}{-\xi f''}} \left\{ 1 + \frac{1}{2\xi f''} \left[\frac{f'''}{f''} \frac{F'}{F} \right. \right.$$
$$\left. \left. + \frac{1}{4} \frac{f^{iv}}{f''} - \frac{5}{12} \frac{(f''')^2}{(f'')^2} - \frac{F''}{F} \right] + \cdots \right\} \tag{5.7.78}$$

Note that the procedure illustrated can be used to determine the coefficients a_n and A_n up to any order and that $I(\xi)$ can be expanded in higher inverse powers of $\xi^{-1/2}$. This series, which is asymptotic, diverges for any fixed ξ. In spite of its divergent behavior, an asymptotic series is very useful. The sum of the first few terms of the series approaches the values of the function that the series represents, and then diverges as more terms are added. The error introduced in representing the function by the first n terms is of the order of the $(n+1)$th term. When the first few terms of the asymptotic series converge to the actual value of the function, the convergence is much faster than a convergent series expansion of the function. The first term of the asymptotic series may be considered as the leading behavior of the integral. The leading behavior of an integral can be evaluated readily by the saddle-point method. When the integral is expressed along either the real or the imaginary axis and can be evaluated without deforming the path of integration, the methods of Laplace and of stationary phase are also very convenient.

Brook Taylor (18 August 1685 – 29 December 1731)

Brook Taylor entered St John's College, Cambridge in 1703. In 1712 he was member of the committee to adjudicate the claim of who invented calculus by Newton and Leibniz. Taylor's expansion appeared in his book published in 1715.

As an example, we find the saddle-point contribution to the integral

$$I(\xi) = \int_{\Gamma} d\alpha \, F(\alpha) e^{i\xi \cos(\alpha - \alpha_0)} \tag{5.7.79}$$

as $\xi \to \infty$. We let

$$f(\alpha) = i \cos(\alpha - \alpha_0)$$

and the saddle point occurs at $\alpha = \alpha_0$. Making use of (5.7.78), we immediately obtain

$$I(\xi) = F(\alpha_0) e^{i\xi} \sqrt{\frac{2\pi}{i\xi}} \left\{ 1 - \frac{i}{2\xi} \left[\frac{1}{4} + \frac{F''}{F} \right] + \cdots \right\} \tag{5.7.80}$$

It is noted that, if the integration path Γ is not the steepest descent path, then in deforming from Γ to the SDP which is determined from $\text{Im}[f(\alpha)] = \text{Im}[f(\alpha_0)]$, there may be singularities lying between the new and the old paths of integration. Contributions attributed to such singularities must be taken into account separately.

Arnold Johannes Wilhelm Sommerfeld (5 December 1868 – 26 April 1951)
   Arnold Sommerfeld attended the Gymnasium in Königsberg and the University of Königsberg where he was awarded his doctorate in 1891. During his emeritus Arnold Sommerfeld compiled his "Lectures into theoretical physics" which were published in six volumes between 1943 and 1953.

EXAMPLE 5.7.9
   Prove the Sommerfeld identity

$$\frac{e^{ik_0 r}}{r} = \frac{i}{2} \int_{-\infty}^{\infty} dk_\rho \, \frac{k_\rho}{k_z} H_0^{(1)}(k_\rho \, \rho) e^{ik_z |z|}$$

   where $k_z = \sqrt{k_0{}^2 - k_\rho{}^2}$.

SOLUTION:
   Write the integral representation for $\frac{e^{ik_0 r}}{r}$ in terms of its Fourier transform as

$$\frac{e^{ik_0 r}}{r} = \frac{1}{(2\pi)^3} \iiint_{-\infty}^{\infty} dk_x dk_y dk_z \, g(k_x, k_y, k_z) e^{ik_x x + ik_y y + ik_z z}$$

Recognizing that $\frac{e^{ik_0 r}}{4\pi r}$ is a solution to the Helmholtz equation

$$\left[\frac{\partial^2}{\partial x^2} + \frac{\partial^2}{\partial x^2} + \frac{\partial^2}{\partial x^2} + k_0^2\right]\frac{e^{ik_0 r}}{4\pi r} = -\delta(x)\delta(y)\delta(z)$$

and using the Fourier integral representation of the delta function, the above equation becomes

$$\frac{1}{(2\pi)^3}\iiint_{-\infty}^{\infty} dk_x dk_y dk_z \; \frac{k_0^2 - k_x^2 - k_y^2 - k_z^2}{4\pi}g(k_x, k_y, k_z)e^{ik_x x + ik_y y + ik_z z}$$

$$= \frac{-1}{(2\pi)^3}\iiint_{-\infty}^{\infty} dk_x dk_y dk_z \; e^{ik_x x + ik_y y + ik_z z}$$

we thus find

$$g(k_x, k_y, k_z) = \frac{-4\pi}{k_0^2 - k_x^2 - k_y^2 - k_z^2}$$

We now continue with the Fourier transform to get

$$\frac{e^{ik_0 r}}{r} = \frac{1}{2\pi^2}\iiint_{-\infty}^{\infty} dk_x dk_y dk_z \frac{-1}{k_0^2 - k_x^2 - k_y^2 - k_z^2}e^{ik_x x + ik_y y + ik_z z}$$

$$= \frac{1}{2\pi^2}\iiint_{-\infty}^{\infty} dk_x dk_y dk_z \frac{e^{ik_x x + ik_y y + ik_z z}}{\left(k_z + \sqrt{k_0^2 + k_x^2 + k_y^2}\right)\left(k_z - \sqrt{k_0^2 - k_x^2 - k_y^2}\right)}$$

$$= \frac{i}{2\pi}\iint_{-\infty}^{\infty} dk_x dk_y \frac{1}{k_z}e^{ik_x x + ik_y y + ik_z |z|}$$

Let

$$k_x = k_\rho \cos\alpha \qquad k_y = k_\rho \sin\alpha$$
$$x = \rho\cos\phi \qquad y = \rho\sin\phi$$

We find

$$\frac{e^{ik_0 r}}{r} = \frac{i}{2\pi}\int_0^{\infty} dk_\rho \int_0^{2\pi} d\alpha \frac{k_\rho}{k_z}e^{ik_\rho \cos(\alpha-\phi) + ik_z |z|} = i\int_0^{\infty} dk_\rho \frac{k_\rho}{k_z}J_0(k_\rho\rho)e^{ik_z |z|}$$

Use $J_0(k_\rho\rho) = \frac{1}{2}[H_0^{(1)}(k_\rho\rho) + H_0^{(2)}(k_\rho\rho)]$. For the integral

$$\frac{i}{2}\int_0^{\infty} dk_\rho \frac{k_\rho}{k_z}H_0^{(2)}(k_\rho\rho)e^{ik_z |z|},$$

we change variables $k_\rho = e^{-i\pi}k_\rho'$ to get

$$\frac{i}{2}\int_{-\infty}^{0} dk_\rho' \frac{k_\rho'}{k_z}H_0^{(1)}(k_\rho'\rho)e^{ik_z |z|}$$

which combines with

$$\frac{i}{2} \int_0^\infty dk_\rho \, \frac{k_\rho}{k_z} H_0^{(1)}(k_\rho \rho) e^{ik_z|z|}$$

resulting in the Sommerfeld identity. We thus have proved

$$\frac{e^{ik_0 r}}{r} = \frac{i}{2\pi} \iint_{-\infty}^{\infty} dk_x dk_y \, \frac{1}{k_z} \, e^{ik_x x + ik_y y + ik_z|z|}$$

$$= \frac{i}{2} \int_{-\infty}^{\infty} dk_\rho \, \frac{k_\rho}{k_z} H_0^{(1)}(k_\rho \rho) e^{ik_z|z|}$$

where $k_z = \sqrt{k_0^2 - k_x^2 - k_y^2}$. Note that the above results state that a spherical wave can be expanded into superpositions of plane waves as well as cylindrical waves.

<div align="right">— END OF EXAMPLE 5.7.9 —</div>

EXAMPLE 5.7.10

We now determine the leading behavior of the Hankel function

$$H_\nu^{(1)}(\xi) = \frac{1}{\pi} \int_{\Gamma_1} d\alpha \, e^{i(\xi \cos \alpha + \nu \alpha - \nu \pi/2)}$$

when both ξ and ν are large. In accordance with the original path defined for $H_\nu^{(1)}(\xi)$, the contributing saddle points are

$$\alpha = \sin^{-1}(\nu/\xi) \qquad\qquad \text{for } \nu < \xi$$

$$\alpha = \pi/2 - i \cosh^{-1}(\nu/\xi) \qquad\qquad \text{for } \nu > \xi$$

We make use of (5.7.78) with the following identifications:

$$F(\alpha) = \frac{1}{\pi} e^{-i\nu\pi/2} \qquad\qquad\qquad (E5.7.10.1)$$

$$\xi f(\alpha) = i\xi \cos \alpha + i\nu\alpha \qquad\qquad (E5.7.10.2)$$

The leading terms in the asymptotic series are

$$H_\nu^{(1)}(\xi) \approx \sqrt{\frac{2}{i\pi(\xi^2 - \nu^2)^{1/2}}} \exp\left[i\left(\sqrt{\xi^2 - \nu^2} - \nu \cos^{-1}\frac{\nu}{\xi}\right)\right] \quad (E5.7.10.3)$$

for $\nu < \xi$ and

$$H_\nu^{(1)}(\xi) \approx -i\sqrt{\frac{2}{\pi(\nu^2 - \xi^2)^{1/2}}} \exp\left[-\sqrt{\nu^2 - \xi^2} + \nu \cosh^{-1}\frac{\nu}{\xi}\right] \quad (E5.7.10.4)$$

for $\nu > \xi$. It is readily seen that (E5.7.8.7) reduces to (E5.7.8.7) for $\nu \ll \xi$.

<div align="right">— END OF EXAMPLE 5.7.10 —</div>

C. Dipole Antenna on a Two-Layer Medium

Consider a vertical magnetic dipole (VMD) placed on the surface of a two-layered medium [Figure 5.7.9]. The electromagnetic field above the surface is TE to $\hat{z}$ and is determined by the H_z component from (5.7.45a) by letting $R_{0+}^{\text{TE}} = 0$.

$$H_z = -i\frac{IA}{8\pi} \int_{-\infty}^{+\infty} dk_\rho \frac{k_\rho^3}{k_z}(1 + R^{TE})H_0^{(1)}(k_\rho\rho)e^{ik_z z} \qquad (5.7.81)$$

When the bottom medium is a perfect conductor,

$$1 + R^{TE} = 1 + \frac{R_{01} - e^{i2k_{1z}d}}{1 - R_{01}e^{i2k_{1z}d}} \qquad (5.7.82)$$

where

$$R_{01} = \frac{1 - k_{1z}/k_z}{1 + k_{1z}/k_z} \qquad (5.7.83)$$

is the reflection coefficient at the surface boundary.

Singularities in the integrand in (5.7.81) contain poles from zeros of the denominator $1 - R_{01}e^{i2k_{1z}d}$ and the branch point at $k_\rho = k$ arising from $k_z = \sqrt{k^2 - k_\rho^2}$. We see that $k_\rho = k_1$ is not a branch point as k_{1z} only appears in R^{TE} and when k_{1z} is replaced by $-k_{1z}$, $R^{TE}(-k_{1z}) = R^{TE}(k_{1z})$.
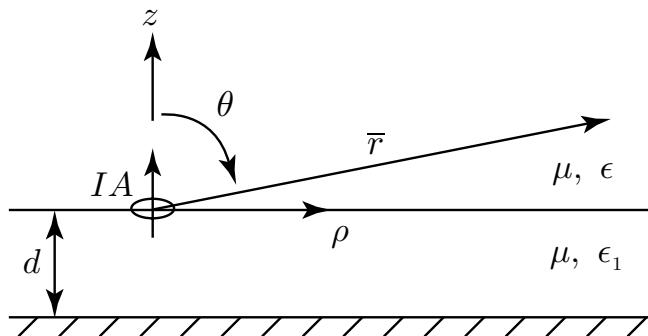
Figure 5.7.9 VMD on two-layer medium.
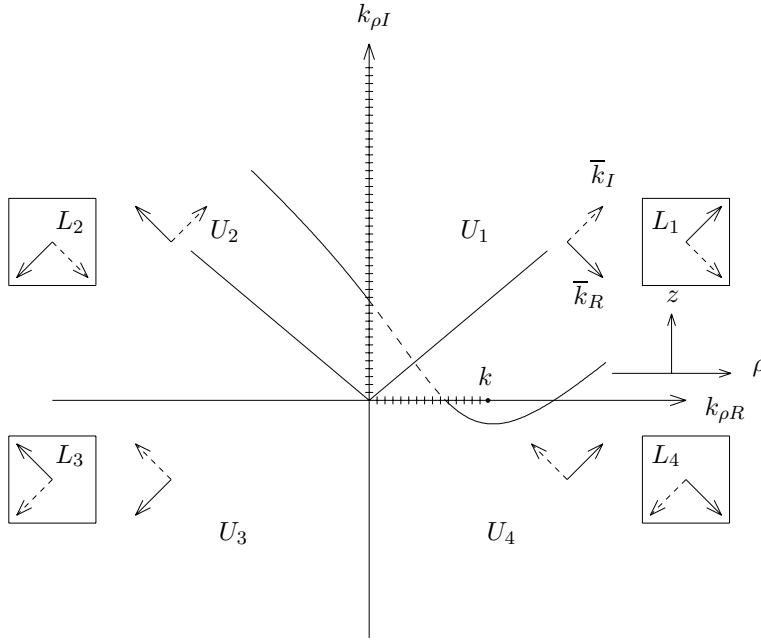
Figure 5.7.10 The complex k_ρ-plane.

To examine the singularities on the complex k_ρ-plane, we first choose a branch cut originated from the branch point $k_\rho = k$. Letting $k_\rho = k_{\rho R} + ik_{\rho I}$ where $k_{\rho R}$ and $k_{\rho I}$ are both real, we write

$$k_z = \sqrt{k^2 - (k_{\rho R} + ik_{\rho I})^2} = \sqrt{k^2 - k_{\rho R}^2 + k_{\rho I}^2 - i2k_{\rho R}k_{\rho I}} \qquad (5.7.84)$$

From (5.7.84), we find that for $\mathrm{Im}(k_z) = k_{zI} = 0$, $k_{\rho R}k_{\rho I} = 0$ and $k^2 - k_{\rho R}^2 + k_{\rho I}^2 \geq 0$. For $k_{\rho I} = 0$, $k_z = \sqrt{k^2 - k_{\rho R}^2 + k_{\rho I}^2}$. For $k_{\rho R} = 0$, $k_z = \sqrt{k^2 + k_{\rho I}^2}$. The Sommerfeld branch cut is defined as

$$\begin{cases} k_{\rho I} = 0, & 0 \leq k_\rho \leq k \\ k_{\rho R} = 0, & k_{\rho I} \geq 0 \end{cases} \qquad (5.7.85)$$

In Figure 5.7.10 we illustrate the Sommerfeld branch cut which originates from k composed of part of the real k_ρ axis $0 \leq k_\rho \leq k$ and the whole positive imaginary k_ρ-axis. On the top Riemann sheet we require that $k_{zI} \geq 0$, and on the bottom Riemann sheet $k_{zI} \leq 0$. This

choice of Riemann sheets guarantees that all singularities on the top sheet will give rise to an exponentially decaying wave for $z > 0$.

To examine the wave behavior associated with the singularities on both the top and bottom Riemann sheets, we let

$$\overline{k} = \hat{\rho}k_\rho + \hat{z}k_z = \overline{k}_R + i\overline{k}_I \tag{5.7.86}$$

where $\overline{k}_R$ and $\overline{k}_I$ are both real vectors while $\overline{k}$ is a complex vector with magnitude $k = \omega(\mu\varepsilon)^{\frac{1}{2}}$ being real. We find $\overline{k} \cdot \overline{k} = k_R^2 - k_I^2 + i2\overline{k}_R \cdot \overline{k}_I = \omega^2\mu\varepsilon$, and consequently

$$\overline{k}_R \cdot \overline{k}_I = 0 \tag{5.7.87}$$

Thus the real and imaginary parts of the complex $\overline{k}$ vector are perpendicular to each other.

In Figure 5.7.10 we use solid arrows to denote $\overline{k}_R$ and dashed arrows to denote $\overline{k}_I$. We first decide the direction of $\overline{k}_I$ and then use (5.7.87) to determine $\overline{k}_R$. For instance, in the first quadrant of the top Riemann sheet, $k_{zI} \geq 0$ and $k_{\rho I} > 0$, the dashed arrow thus points to the upper right signifies the direction where the wave exponentially decays. We also know that $k_{\rho R} > 0$ in the first quadrant. From the fact that $\overline{k}_I \cdot \overline{k}_R = 0$ we determine that $\overline{k}_R$ points to the lower right direction where the wave propagates. For the wave behavior associated with the singularities on the lower Riemann sheet, $k_{zI} \leq 0$, we illustrate in the square box.

a. Direct Wave from Saddle Point Contribution

To evaluate the integral in (5.7.81), we first make the following transformation

$$k_\rho = k \sin\alpha \tag{5.7.88a}$$
$$k_z = k \cos\alpha \tag{5.7.88b}$$
$$\rho = r \sin\theta \tag{5.7.89a}$$
$$z = r \cos\theta \tag{5.7.89b}$$

where $r = (\rho^2 + z^2)^{\frac{1}{2}}$ is the distance from the dipole and θ is the observation angle from the z-axis. The angle α is the angle of the $\overline{k}$ vector with respect to the z-axis. The integral becomes

$$H_z = \int_\Gamma d\alpha \tilde{F}(\alpha)e^{ikr\cos(\alpha-\theta)} \tag{5.7.90}$$

where

$$\tilde{F}(\alpha) = -i\frac{IA}{8\pi} \left[k_\rho^3 (1 + R^{TE}) H_0^{(1)}(k_\rho \rho) e^{-ik_\rho \rho} \right]_{k_\rho = k \sin \alpha} \qquad (5.7.91)$$

noticing that $dk_\rho = k \cos \alpha \, d\alpha = k_z d\alpha$.

The integration path Γ as transformed from the real k_ρ-axis is shown in Figure 5.7.11. The transformation is better illustrated by noting that

$$k_\rho = k_{\rho R} + ik_{\rho I} = k \sin \alpha$$
$$= k \sin \alpha_R \cosh \alpha_I + ik \cos \alpha_R \sinh \alpha_I \qquad (5.7.92)$$

The original integration path Γ along the real k_ρ axis with $k_{\rho I} = 0$ is mapped onto the α plane as shown in Figure 5.7.11.

$$\begin{cases} \alpha_R = -\pi/2, & 0 \le \alpha_I \le \infty \\ \alpha_R = \pi/2, & -\infty \le \alpha_I \le 0 \\ \alpha_I = 0, & -\pi/2 \le \alpha_R \le \pi/2 \end{cases} \qquad (5.7.93)$$

It starts at $\alpha_R = -\pi/2$ and α_I at ∞ corresponding to $k_\rho \to -\infty$, passing through $\alpha_R = \alpha_I = 0$, and ends at $\alpha_R = \pi/2$ and α_I at $-\infty$ corresponding to $k_\rho \to \infty$.
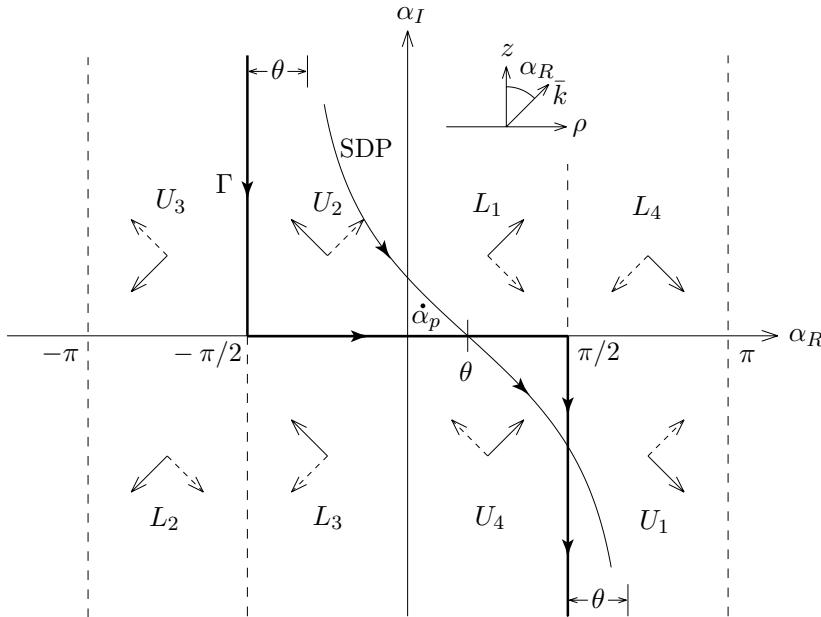
Figure 5.7.11   The complex α-plane.

The saddle point method is applied to distant observation points where $kr \gg 1$. The saddle point is determined from the exponential factor in (5.7.90). We have

$$\frac{d}{d\alpha}\cos(\alpha - \theta) = 0$$

which gives $\alpha = \theta$.

The saddle point contribution to the integral gives

$$
\begin{aligned}
H_z &= e^{ikr}\sqrt{\frac{2\pi}{ikr}}\,\tilde{F}(\theta) \\
&= e^{ikr}\sqrt{\frac{2\pi}{ikr}}\left[-i\frac{IA}{8\pi}k_\rho^3(1+R^{TE})\sqrt{\frac{2}{i\pi k_\rho\rho}}\right]_{k_\rho = k\sin\theta} \\
&= -\frac{IA}{4\pi r}e^{ikr}\left[k_\rho^2(1+R^{TE})\right]_{k_\rho = k\sin\theta} \qquad (5.7.94)
\end{aligned}
$$

where we used the asymptotic form for $H_0^{(1)}(\xi)\,e^{-ik_\rho\rho} \approx (2/i\pi k_\rho\rho)^{\frac{1}{2}}$. The result is seen to represent a direct wave originated from the dipole propagating to the observation point.

The steepest descend path (SDP) is determined by requiring that the imaginary part of the exponent to be a constant equal to that at the saddle point, i.e.,

$$\text{Im}[i\cos(\alpha - \theta)] = \cos(\alpha_R - \theta)\cosh\alpha_I = 1 \qquad (5.7.95)$$

The SDP passes through $\alpha_R = \theta$, $\alpha_I = 0$ and asymptotically as $\alpha_I \to \infty$, $\alpha_R - \theta = -\pi/2$ and as $\alpha_I \to -\infty$, $\alpha_R - \theta = \pi/2$.

$$
\begin{cases}
\alpha_I \to -\infty, & \alpha_R - \theta = -\pi/2 \\
\alpha_I = 0, & \alpha_R = \theta \\
\alpha_I \to \infty, & \alpha_R - \theta = \pi/2
\end{cases}
\qquad (5.7.96)
$$

It is seen from Figure 5.7.11 that all singularities between the original path of integration Γ and the steepest descent path SDP will contribute to the integral. On the k_ρ-plane, the SDP is illustrated in Figure 5.7.10.

b. Normal Mode Approach

The singularities of the integral are determined from

$$1 + R^{TE} = 1 + \frac{R_{01} - e^{i2k_{1z}d}}{1 - R_{01}e^{i2k_{1z}d}} = (1 + R_{01})\frac{1 - e^{i2k_{1z}d}}{1 - R_{01}e^{i2k_{1z}d}} \quad (5.7.97)$$

Setting the denominator equal to zero, we find

$$R_{01}e^{i2k_{1z}d} = 1 = e^{2m\pi} \quad (5.7.98)$$

At total reflection when $k \leq k_{1z}$, (5.7.98) yields the guidance condition for the slab medium.

Remarkably, the transformation (5.7.88) has unfolded the two Riemann sheets in the k_ρ-plane as $k_z = k\cos\alpha$ no longer displays a branch point.

$$k_z = k_{zR} + ik_{zI} = k\cos\alpha$$
$$= k\cos\alpha_R\cosh\alpha_I - ik\sin\alpha_R\sinh\alpha_I \quad (5.7.99)$$

For the upper Riemann sheet on the k_ρ-plane $k_{zI} \geq 0$, we have $\sin\alpha_R \sinh\alpha_I < 0$ which corresponds to (i) $\alpha_I > 0$ and $-\pi < \alpha_R < 0$, and (ii) $\alpha_I < 0$ and $0 < \alpha_R < \pi$. For $k_{zI} \leq 0$, we have (i) $\alpha_I > 0$ and $0 < \alpha_r < \pi$, and (ii) $\alpha_I < 0$ and $-\pi < \alpha_R < 0$. The upper and lower Riemann sheets denoted by U and L are mapped onto the single α-plane, which now contains no branch points.

In Figure 5.7.11 we use solid arrows to denote $\overline{k}_R = \hat{\rho}k_{\rho R} + \hat{z}k_{zR}$ which indicates the direction of wave propagation in the ρ-z plane as shown in Figure 5.7.11. Dashed arrows are used to denote $\overline{k}_I = \hat{\rho}k_{\rho I} + \hat{z}k_{zI}$ which indicates the direction of attenuation of the wave. From the transformations in (5.7.88), we find

$$\overline{k}_R = \hat{\rho}k_{\rho R} + \hat{z}k_{zR} = \hat{\rho}k\sin\alpha_R\cosh\alpha_I + \hat{z}k\cos\alpha_R\cosh\alpha_I \quad (5.7.100a)$$
$$\overline{k}_I = \hat{\rho}k_{\rho I} + \hat{z}k_{zI} = \hat{\rho}k\cos\alpha_R\sinh\alpha_I - \hat{z}k\sin\alpha_R\sinh\alpha_I \quad (5.7.100b)$$

The solid and dashed arrows in Figure 5.7.11 can be determined from the above equations with $\overline{k}_R \cdot \overline{k}_I = 0$.

The singularities enclosed by the original path of integration Γ and the steepest descent path (SDP) represent wave modes that are excited by the dipole antenna. They all have the attenuation direction pointing away from the surface except those in the regions $0 \leq \alpha_R \leq$

$\pi/2$ and $\alpha_I \geq 0$, where the wave is growing exponentially away from the surface. The singularities in this region represent waves that are growing exponentially in the positive $\hat{z}$-direction. These are known as leaky wave modes.

Consider a leaky wave mode at $\alpha = \alpha_p$. The real and imaginary parts of the complex $\overline{k}$ vector are shown in Figure 5.7.12 as $\overline{k}_R$ and $\overline{k}_I$. The leaky wave propagates in the $\overline{k}_R$ direction and attenuates along $\overline{k}_I$ which points in the $-\hat{z}$ and $+\hat{\rho}$ directions. With the transformation (5.7.88) and (5.7.89), we write

$$e^{ikr\cos(\alpha-\theta)} = e^{ikr\cos(\alpha_R-\theta)\cosh\alpha_I} e^{kr\sin(\alpha_R-\theta)\sinh\alpha_I}$$

Since $\alpha_I \geq 0$, the wave grows exponentially in the $\hat{r}$ direction when $\alpha_R - \theta \geq 0$. However the leaky wave mode at α_p can be excited only when θ is larger than α_R of α_p. As seen from Figure 5.7.12, even though the wave amplitude grows exponentially away from the surface, it also attenuates exponentially in the $\hat{\rho}$-direction. Thus the leaky wave amplitudes will never diverge in the $\hat{r}$ direction.
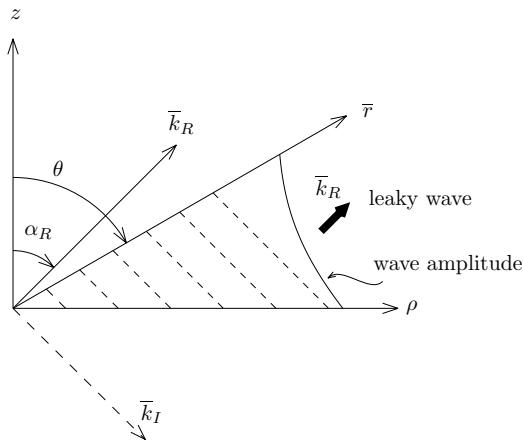
Figure 5.7.12 Leaky wave mode.

The wave modes in the other regions bounded by the original path of integration and the steepest descent path, which are evanescent in the direction pointing away from the surface, are guided wave modes. We call the above procedure in evaluating the integral the normal mode approach as each pole corresponds to a normal wave mode.

c. Geometrical Optics Approach

Another approach of solving the integral in (5.7.81) leads to a geometrical optics interpretation. Since the magnitude R_{01} is less than unity, we may expand the denominator of $(1 + R^{TE})$ to obtain

$$1 + R^{TE} = 1 + \frac{R_{01} - e^{i2k_{1z}d}}{1 - R_{01}e^{i2k_{1z}d}} = 1 + R_{01} - (1 - R_{01}^2)\frac{e^{i2k_{1z}d}}{1 - R_{01}e^{i2k_{1z}d}}$$

$$= (1 + R_{01}) - (1 - R_{01}^2)\sum_{m=1}^{\infty} R_{01}^{m-1}e^{i2mk_{1z}d} \qquad (5.7.101)$$

We substitute (5.7.101) in (5.7.81) and evaluate the first term and the summation terms separately. The first term yields the half-space solution and the summation terms account for contributions from the subsurface layer. The first term yields the result in the upper half-space for a VMD placed at the surface of a dielectric medium with permittivity ϵ_1.

To evaluate the first two terms arising from substituting (5.7.101) in (5.7.81), we find for the radiation field of a vertical magnetic dipole (VMD) placed on the surface of a one-layer (or half-space) medium,

$$H_z = -i\frac{IA}{8\pi} \int_{-\infty}^{+\infty} dk_\rho \frac{k_\rho^3}{k_z}(1 + R_{01})H_0^{(1)}(k_\rho\rho)e^{ik_z z}$$

$$\approx -i\frac{IA}{8\pi} \int_{\text{SIP}} dk_\rho \frac{k_\rho^3}{k_z}\left(\frac{2k_z}{k_z + k_{1z}}\right)\sqrt{\frac{2}{i\pi k_\rho\rho}}e^{ik_\rho\rho + ik_z z} \qquad (5.7.102)$$

The Sommerfeld integration path (SIP) is from $-\infty$ to ∞ in such a way that it is slightly above the negative real $k_{\rho R}$ axis for $-\infty < k_{\rho R} \leq 0$ and slightly below the positive real $k_{\rho R}$ axis for $0 < k_{\rho R} < \infty$.

Applying the saddle-point method and making use of the asymptotic form for the Hankel function we find that, for very large observation distance ρ and z with $\rho = r\sin\theta$ and $z = r\cos\theta$, the saddle point is at $k_\rho = k\sin\theta$ and the leading term of the vertical magnetic field component is

$$H_z = e^{ikr}\sqrt{\frac{2\pi}{ikr}}\left[-i\frac{IA}{8\pi}k_\rho^3\left(\frac{2k_z}{k_z + k_{1z}}\right)\sqrt{\frac{2}{i\pi k_\rho\rho}}\right]_{k_\rho = k\sin\theta}$$

$$= -\frac{IAe^{ikr}}{2\pi r}\frac{k^2\sin^2\theta\cos\theta}{\cos\theta + \sqrt{k_1^2/k^2 - \sin^2\theta}} \qquad (5.7.103)$$

EXAMPLE 5.7.11   VMD on half-space medium.

When the observation point is along the surface where $\theta = \pi/2$ the leading term of the saddle point contribution vanishes. Thus we have to evaluate the integral to second order of $(1/r)^2$ as given by (5.7.80).

$$
\begin{aligned}
I(\xi) &= \int_\Gamma d\alpha \, F(\alpha) e^{i\xi \cos(\alpha - \alpha_0)} \\
&= F(\alpha_0) e^{i\xi} \sqrt{\frac{2\pi}{i\xi}} \left\{ 1 - \frac{i}{2\xi} \left[\frac{1}{4} + \frac{F''}{F} \right] + \cdots \right\}
\end{aligned}
\qquad \text{(E5.7.11.1)}
$$

where

$$
F(\alpha) = -i \frac{IA}{8\pi} k_\rho^3 \left(\frac{2k_z}{k_z + k_{1z}} \right) \sqrt{\frac{2}{i\pi k_\rho \rho}}
\qquad \text{(E5.7.11.2)}
$$

Evaluating the third term in (E5.7.11.1) at $\theta = \pi/2$, we obtain

$$
H_z = i \frac{IA}{2\pi (k_1^2 - k^2)\rho^2} k^3 e^{ik\rho}
$$

At the same time, the leading order contribution from the branch cut originated from the branch point $k_\rho = k_1$ becomes significant. By deforming the integration contour and choosing the branch cuts as that illustrated in Figure E5.7.11.1, the vertical magnetic field is found to be

$$
H_z = i \frac{IA}{2\pi (k_1^2 - k^2)\rho^2} \left\{ k^3 e^{ik\rho} - k_1^3 e^{ik_1\rho} \right\}
$$
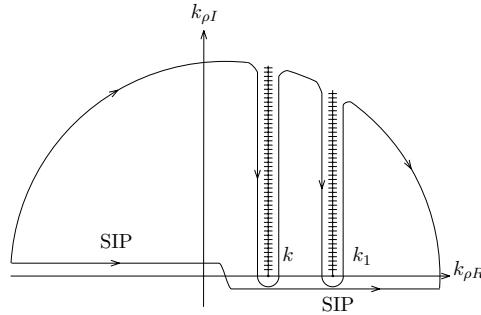
Figure E5.7.11.1

— END OF EXAMPLE 5.7.11 —

To evaluate the summation terms arising from substitution of (5.7.101) into (5.7.81), we consider the case when the observation point is on the surface with $z = 0$. For the mth term in the summation in (5.7.101)

$$H_z^{(m)} = \int_{-\infty}^{\infty} dk_\rho G_m(k_\rho) e^{ik_\rho \rho + ik_{1z}(2md)} \tag{5.7.104}$$

$$G_m(k_\rho) = \frac{iIA}{8\pi} \left[(1 - R_{01}^2) R_{01}^{m-1} \frac{k_\rho^3}{k_z} \sqrt{\frac{2}{i\pi k_\rho \rho}} \right]_{k_\rho = k_1 \sin \alpha} \tag{5.7.105}$$
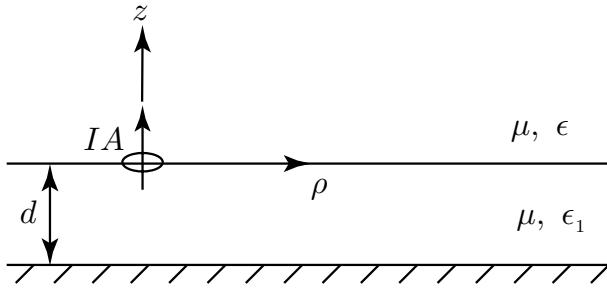
Figure 5.7.9 VMD on two-layer medium.

We make the following transformations:

$$k_\rho = k_1 \sin \alpha \tag{5.7.106a}$$
$$k_{1z} = k_1 \cos \alpha \tag{5.7.106b}$$
$$\rho = R_m \sin \alpha_m \tag{5.7.107a}$$
$$2md = R_m \cos \alpha_m \tag{5.7.107b}$$

where

$$R_m = \sqrt{\rho^2 + (2md)^2} \tag{5.7.107c}$$

Under the transformations (5.7.106) and (5.7.107), we write (5.7.104) as follows:

$$H_z^{(m)} = \int d\alpha \, \tilde{G}_m(\alpha) \, e^{ik_1 R_m \cos(\alpha - \alpha_m)} = e^{ik_1 R_m} \sqrt{\frac{2\pi}{ik_1 R_m}} \, \tilde{G}_m(\alpha_m)$$

$$\tilde{G}_m(\alpha_m) = \frac{iIA}{8\pi} \left[(1 - R_{01}^2) R_{01}^{m-1} \frac{k_\rho^3 k_{1z}}{\sqrt{k^2 - k_1^2 \sin^2 \alpha}} \sqrt{\frac{2}{i\pi k_\rho \rho}} \right]_{\alpha = \alpha_m} \tag{5.7.108}$$

after using the asymptotic form for the Hankel function $H_0^{(1)}(k_\rho \rho)$. The original path of integration runs from $\alpha_I \to \infty$ to $\alpha_I = 0$ at $\alpha_R = -\pi/2$ through $\alpha_R = -\pi/2$ to $\alpha_R = \pi/2$ on the α_R-axis, then at $\alpha_R = \pi/2$ from $\alpha_I = 0$ to end at $\alpha_I \to -\infty$. A saddle point is seen to occur at $\alpha = \alpha_m$. For $k_1 R_m \gg 1$, we calculate the saddle-point contribution by retaining only the first term, which is of the form $e^{ik_1 R_m}/R_m$.

The steepest descent path (SDP) is $\text{Im}[ik_1 \cos(\alpha - \alpha_m)] = k_1$ or

$$\cos(\alpha_R - \alpha_m) \cosh \alpha_I = 1$$

Near $\alpha = \alpha_m$, we have $\alpha_I \approx -(\alpha_R - \alpha_m)$. The SDP makes -45 degree angles from α_R axis. As $\alpha_I \to \pm\infty$, $\alpha_R - \alpha_m = \mp\pi/2$.
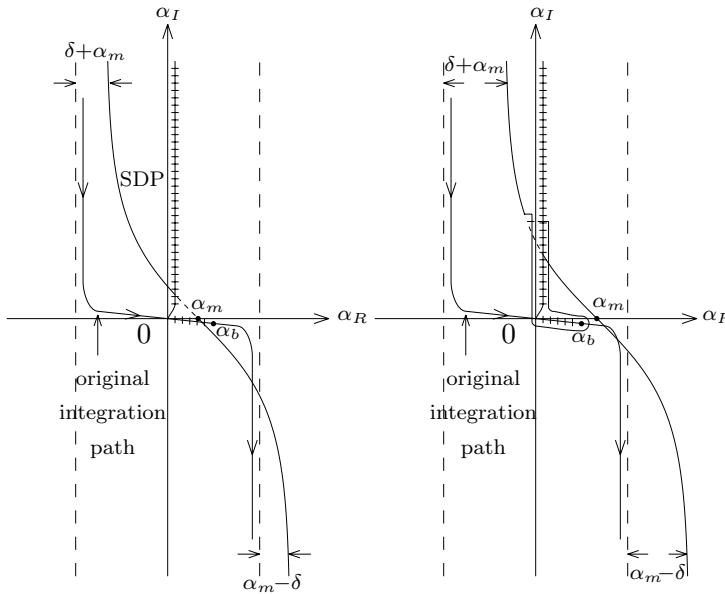
Figure 5.7.13 **(a) The SDP is to the left of the branch point and the saddle point α_m occurs on the lower Riemann sheet where $k_{zI} < 0$. (b) The SDP is to the right of the branch point and the saddle point α_m occurs on the top Riemann sheet where $k_{zI} > 0$.**

It is important to observe that $\sqrt{k^2 - k_1^2 \sin^2 \alpha} = k_z$ gives rise to branch points at

$$\sin \alpha_b = \pm k/k_1$$

which make $G_m(\alpha)$ double valued.

We now assume that k_1 has a small imaginary part, $k_1 = k_{1R} + ik_{1I} = k_{1R}(1 + i\tan\delta)$ with $\delta \ll 1$. The transformation (5.7.106a) is illustrated in Figure 5.7.13.

$$
\begin{aligned}
k_\rho &= k_{1R}(1 + i\tan\delta)(\sin\alpha_R \cosh\alpha_I + i\cos\alpha_R \sinh\alpha_I) \\
&= k_{1R}(\sin\alpha_R \cosh\alpha_I - \tan\delta \cos\alpha_R \sinh\alpha_I) \\
&\qquad\qquad + ik_{1R}(\cos\alpha_R \sinh\alpha_I + \tan\delta \sin\alpha_R \cosh\alpha_I)
\end{aligned}
$$

connects the complex k_ρ-plane with the complex α-plane.

For the real k_ρ-axis, $k_{\rho I} = 0$ gives
$\cos\alpha_R \sinh\alpha_I + \tan\delta \sin\alpha_R \cosh\alpha_I = 0$
As $\alpha_I \to +\infty$, $\tan\delta \tan\alpha_R = -1 \to \alpha_R = \delta - \frac{\pi}{2}$ and $k_{\rho R} \to -\infty$.
As $\alpha_I \to -\infty$, $\tan\delta \tan\alpha_R = 1 \to \alpha_R = -\delta + \frac{\pi}{2}$ and $k_{\rho R} \to +\infty$.
The transformed $k_{\rho R}$ axis is labeled the original integration path.

For the Sommerfeld branch cut, $k_{\rho R}k_{\rho I} = 0$ and $k^2 \geq k_{\rho R}^2 - k_{\rho I}^2$ is mapped onto the α-plane. As $k_{\rho R} = 0$, we have $\tan\alpha_R = \tan\delta \tanh\alpha_I$ which gives $\alpha_R = \delta$ as $\alpha_I \to +\infty$, and $k_{\rho I} \to +\infty$. From origin to α_b, $k_{\rho I} = 0$, the branch cut follows the real axis of $k_{\rho R}$ as shown in Figure 5.7.13.

For the steepest descent path (SDP) $\mathrm{Im}[ik_1\cos(\alpha - \alpha_m)] = k_{1R}$
$\cos(\alpha_R - \alpha_m)\cosh\alpha_I + \tan\delta \sin(\alpha_R - \alpha_m)\sinh\alpha_I = 1$
As $\alpha_I \to \pm\infty$, $\alpha_R - \alpha_m = \pm(\delta - \frac{\pi}{2})$. Near $\alpha = \alpha_m$, we have $1 - (\alpha_R - \alpha_m)^2/2 + \alpha_I^2/2 + \tan\delta(\alpha_R - \alpha_m)\alpha_I \approx 1$, thus $\alpha_I \approx -(k_{1I} \pm |k_1|)(\alpha_R - \alpha_m)/k_{1R}$. The plus sign must be chosen so that it reduces to the case in which $k_{1I} = 0$. Thus the path leans more toward the vertical axis. The SDP is also shown in Figure 5.7.13.

In deforming the original integration path to the SDP, the branch cut originated from the branch point $k_\rho = k$ is crossed. The branch cut is crossed twice when the SDP passing through the saddle point α_m is to the left of the branch point α_b where $k = k_1\sin\alpha_b$ or $\alpha_b = \sin^{-1}(k/k_1)$. In this case, the saddle point is on the lower sheet, corresponding to $k_{zI} < 0$ and giving rise to a leaky wave. When the SDP is to the right of α_b, we have to cross the branch cut in such a manner that both ends of the SDP will be on the top Riemann sheet of $k_{zI} > 0$. The branch-cut contribution needs to be considered and can be shown to be of the order $1/R_m^2$.

Physically, each term in the summation after evaluation by the saddle point method corresponds to a radiation field caused by a dipole
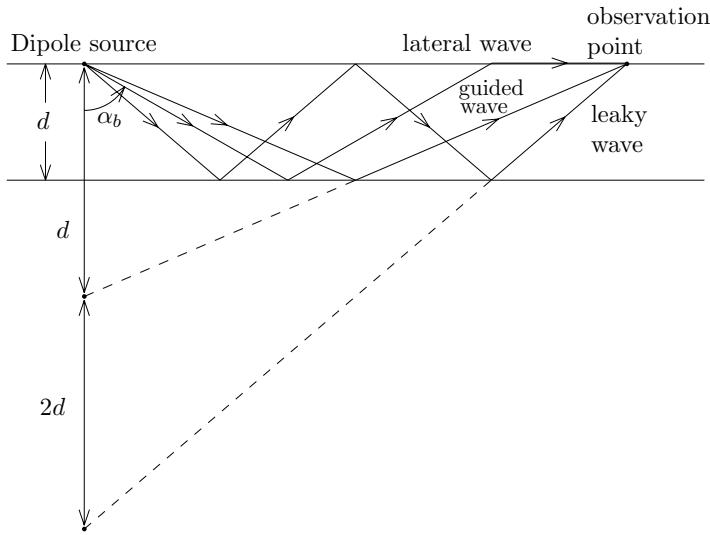
Figure 5.7.14 Total field at the observation point is equal to the half-space solution plus the image contributions shown above.

source at a distance $R_m = [\rho^2 + (2md)^2]^{\frac{1}{2}}$. The dipole source can be viewed as an image of the original dipole, situated at a distance $2md$ below the surface. It may also be viewed as being due to the original dipole field having been reflected at the second boundary m times [Fig. 5.7.14]. The critical angle occurs at $\alpha_b = \sin^{-1}(k/k_1)$, which is the branch point on the α-plane. When the saddle point $\alpha_m = \sin^{-1}(\rho/R_m)$ is at the left of α_b, the angle of reflection is smaller than the critical angle and we find leaky wave behavior. When the saddle point is at the right of α_b, the angle of reflection is larger than α_b and the wave is essentially guided. The wave decays away from the surface because $k_{zI} > 0$. In addition to the saddle point contribution, the branch cut contribution gives rise to a lateral wave. In Figure 5.7.14 we illustrate the various wave components by letting $z = 0$. In this geometrical optics approach the summation series converges faster when the layer is thicker and the medium lossier. As the layer thickness decreases, more terms are needed and it will be more efficient with the normal mode approach by evaluating the residue series.

EXAMPLE 5.7.12   Exact solution of VMD on half-space.
    Using the Sommerfeld identity, show that the exact solution for H_z on

the surface due to a VMD on a half-space is

$$H_z = -\frac{IA}{2\pi(k_t^2 - k^2)} \left\{ \frac{1}{\rho}\frac{\partial}{\partial\rho}\left(\frac{k_t^2}{\rho}e^{ik_t\rho} - \frac{k^2}{\rho}e^{ik\rho} \right) \right.$$
$$\left. + \frac{3}{\rho}\left(\frac{\partial^2}{\partial\rho^2} - \frac{1}{\rho}\frac{\partial}{\partial\rho} \right)\left(\frac{1}{\rho^2}e^{ik_t\rho} - \frac{1}{\rho^2}e^{ik\rho} \right) \right\}$$

This result is due to Van der Pol [Baños, 1966].

SOLUTION:

$$H_z = -i\frac{IA}{4\pi}\int_{-\infty}^{\infty} dk_\rho k_\rho^3 \frac{k_z - k_{tz}}{(k_z + k_{tz})(k_z - k_{tz})}H_0^{(1)}(k_\rho\rho)e^{ik_z z}.$$

Since $k_z^2 - k_{tz}^2 = k^2 - k_t^2$, therefore, at $z = 0$,

$$H_z = \frac{iIA}{4\pi(k_t^2 - k^2)}\int_{-\infty}^{\infty} dk_\rho k_\rho^3(k_z - k_{tz})H_0^{(1)}(k_\rho\rho).$$

Using the Sommerfeld identity and the recurrence formula for Bessel functions, we find that,

$$\left\{ \frac{\partial^4}{\partial z^2 \partial\rho^2}\left(\frac{e^{ikr}}{r} \right) \right\}_{z=0} = \frac{i}{2}\int_{-\infty}^{\infty} H_0^{(1)}(k_\rho\rho)k_\rho^3 k_z dk_\rho$$
$$- \frac{i}{2}\int_{-\infty}^{\infty} \frac{1}{\rho}H_1^{(1)}(k_\rho\rho)k_\rho^2 k_z dk_\rho$$

and

$$\left\{ \frac{\partial^3}{\partial z^2 \partial\rho}\left(\frac{e^{ikr}}{r} \right) \right\}_{z=0} = \frac{i}{2}\int_{-\infty}^{\infty} dk_\rho k_\rho^2 k_z H_1^{(1)}(k_\rho\rho)$$

We conclude that

$$H_z = \frac{IA}{2\pi(k_t^2 - k^2)}\left\{ \left(\frac{\partial^2}{\partial\rho^2} + \frac{1}{\rho}\frac{\partial}{\partial\rho} \right)\frac{\partial^2}{\partial z^2}\left(\frac{e^{ikr}}{r} - \frac{e^{ik_t r}}{r} \right) \right\}_{z=0}$$

carrying the differentiation and setting $z = 0$, we find that

$$H_z = \frac{iIA}{2\pi(k_t^2 - k^2)}\left\{ \frac{e^{ik_t\rho}}{\rho^2}\left(k_t^3 + \frac{4ik_t}{\rho} - \frac{9k_t}{\rho^2} - \frac{9i}{\rho^3} \right) \right.$$
$$\left. - \frac{e^{ik\rho}}{\rho^2}\left(k^3 + \frac{4ik^2}{\rho} - \frac{9k}{\rho^2} - \frac{9i}{\rho^3} \right) \right\}$$
$$= i\frac{IA}{2\pi(k_1^2 - k^2)\rho^2}\left\{ k^3 e^{ik\rho} - k_1^3 e^{ik_1\rho} \right\}$$

— END OF EXAMPLE 5.7.12 —

EXAMPLE 5.7.13   Modified saddle point method.
   The modified saddle-point method deals with poles near the saddle point.
Assume that after transforming to the s plane, the integral

$$I = \int_{-\infty}^{\infty} ds\, F(s) e^{-s^2}$$

has a pair of poles at $s = \pm s_p$. Let

$$F(s) = F_s(s) + \frac{2s_p C}{s^2 - s_p^2}$$

with

$$C = \lim_{s \to s_p} \left[\frac{s^2 - s_p^2}{2s_p} F(s) \right]$$

Since $F_s(s)$ is free of the nearby pole, the integral $\int_{-\infty}^{\infty} ds\, F_s(s)\, e^{-s^2}$ can be
evaluated with the regular saddle-point method.
   Show that

$$I_p = \int_{-\infty}^{\infty} ds\, \frac{2s_p C}{s^2 - s_p^2}\, e^{-s^2} = i2\pi C e^{-s_p^2} \left[1 - \mathrm{erf}(-is_p) \right]$$

where the error function

$$\mathrm{erf}(z) = \frac{2}{\sqrt{\pi}} \int_0^z ds\, e^{-s^2}$$

SOLUTION:
   The integral I_p cannot be simply evaluated by closing the contour at
infinity and applying the Residue theorem because the integrand does not
vanish as $s \to i\infty$.
   We first define a function

$$I(\lambda) = 2s_p C \int_{-\infty}^{\infty} ds\, \frac{e^{-\lambda s^2}}{s^2 - s_p^2}$$

Our integral is $I_p = I(1)$. The function $I(\lambda)$ satisfies the differential equation

$$\frac{dI(\lambda)}{d\lambda} + s_p^2 I(\lambda) = -2s_p C \sqrt{\frac{\pi}{\lambda}}$$

Assume a particular solution of the form

$$I(\lambda) = g(\lambda)e^{-\lambda s_p^2}$$

Substituting into the differential equation yields

$$g'(\lambda) = -2s_p C \sqrt{\frac{\pi}{\lambda}} e^{\lambda s_p^2}$$

By integrating from $\lambda = 0$ to $\lambda = 1$, we obtain

$$g(1) = g(0) - 2s_p C \sqrt{\pi} \int_0^1 d\lambda \, \frac{1}{\sqrt{\lambda}} e^{\lambda s_p^2}$$

Letting $x = -is_p\sqrt{\lambda}$, we have $dx = -is_p d\lambda/2\sqrt{\lambda}$ and

$$g(1) = g(0) - i4C\sqrt{\pi} \int_0^{-is_p} dx \, e^{-x^2} = g(0) - i2\pi C \mathrm{erf}(-is_p)$$

Notice that when s_p is on the upper half of the s plane and possesses a positive imaginary part, we find

$$g(0) = I(0) = 2s_p C \int_{-\infty}^{\infty} ds \, \frac{1}{s^2 - s_p^2} = i2\pi C$$

Since

$$I_p = I(1) = g(1)e^{-s_p^2}$$

we thus find

$$I_p = \int_{-\infty}^{\infty} ds \, \frac{2s_p C}{s^2 - s_p^2} e^{-s^2} = P\left[1 - \mathrm{erf}\left(-is_p\right)\right]$$

where

$$P = i2\pi C e^{-s_p^2}$$

Notably P is precisely the residue of the integrand of I_p at $s = s_p$.

<div align="right">— End of Example 5.7.13 —</div>

EXAMPLE 5.7.14   VED on half-space medium.

Consider the field near the interface for a vertical electric dipole (VED) placed on the surface of a half-space medium with permittivity ϵ_1 and permeability μ. In region 0, the permittivity is ϵ and the permeability is μ. The vertical electric field component E_z is

$$E_z = -\frac{Il}{8\pi\omega\epsilon} \int dk_\rho \frac{k_\rho^3}{k_z} \left(1 + R_{01}^{\text{TM}}\right) H_0^{(1)}(k_\rho\rho) e^{ik_z z}$$

where

$$1 + R_{01}^{\text{TM}} = \frac{2\epsilon_1 k_z}{\epsilon_1 k_z + \epsilon k_{1z}} = \frac{2\epsilon_1 \sqrt{k^2 - k_\rho^2}}{\epsilon_1 \sqrt{k^2 - k_\rho^2} + \epsilon \sqrt{k_1^2 - k_\rho^2}}$$

$k^2 = \omega^2 \mu\epsilon$ and $k_1^2 = \omega^2 \mu\epsilon_1$. Contrary to the case of a vertical magnetic dipole on the half-space medium where no poles exist in the integrand, we now have poles for the VED case.

(a) Setting the denominator of the integrand equal to zero yields

$$k_1^4(k^2 - k_\rho^2) = k^4(k_1^2 - k_\rho^2)$$

Thus two simple poles occur at

$$k_p = \pm\frac{kk_1}{\sqrt{k^2 + k_1^2}}$$

These are known as the Sommerfeld poles. When k and k_1 both have non-negative real and imaginary parts, the pole with the plus sign is in the first quadrant of the k_ρ plane and the one with the minus sign is in the third quadrant.

(b) Inspection of the denominator of the integrand reveals that the poles appear on the Riemann sheet for which k_z and k_{1z} are opposite in sign at $k_\rho = k_p$. At the pole location we find

$$k_z = \pm\sqrt{k^2 - k_p^2} = \pm\frac{k_p k}{k_1}$$

$$k_{1z} = \pm\sqrt{k_1^2 - k_p^2} = \pm\frac{k_p k_1}{k}$$

To determine whether a pole exists on a particular Riemann sheet, we must find the arguments of k_z and k_{1z} to see if the plus sign or the minus sign is needed on that Riemann sheet.

(c) Consider the Sommerfeld pole in the first quadrant. Let both k and k_1 have positive imaginary parts, such that

$$k = |k|\, e^{i\delta}$$

$$k_1 = |k_1|\, e^{i\delta_1}$$

and both δ and δ_1 are positive corresponding to lossy media. We determine the magnitude and phase for k_p to be

$$k_p = \frac{|k|\, e^{i\delta}}{\left[1 + A^2 e^{i2(\delta - \delta_1)}\right]^{1/2}}$$

$$= |k_p| \exp\left\{ i\delta - \frac{i}{2} \tan^{-1} \frac{A^2 \sin 2(\delta - \delta_1)}{1 + A^2 \cos 2(\delta - \delta_1)} \right\}$$

where $A = |k|/|k_1|$ and $|k_p| = |k|\,[1 + 2A^2 \cos 2(\delta - \delta_1) + A^4]^{-1/4}$. The arguments of k_z and k_{1z} are now determined to be

$$k_z(k_p) = \pm \frac{|k_p|\,|k|}{|k_1|} \exp\left\{ i2\delta - i\delta_1 - \frac{i}{2} \tan^{-1} \frac{A^2 \sin 2(\delta - \delta_1)}{1 + A^2 \cos 2(\delta - \delta_1)} \right\}$$

$$k_{1z}(k_p) = \pm \frac{|k_p|\,|k_1|}{|k|} \exp\left\{ i\delta - \frac{i}{2} \tan^{-1} \frac{A^2 \sin 2(\delta - \delta_1)}{1 + A^2 \cos 2(\delta - \delta_1)} \right\}$$

(d) When region 0 is free space and medium 1 is slightly lossy, we let $\delta = 0$, $\delta_1 \ll 1$, and $A^2 \ll 1$ to obtain

$$k_z(k_p) = \pm \frac{|k_p|\,|k|}{|k_1|} \exp\left\{ -i\frac{\delta_1}{1 + A^2} \right\}$$

$$k_{1z}(k_p) = \pm \frac{|k_p|\,|k_1|}{|k|} \exp\left\{ i\delta_1 \frac{1 + 2A^2}{1 + A^2} \right\}$$

(e) When region 0 is free space and medium 1 has a large conductivity such that $k_1 \approx (i\omega\mu\sigma)^{1/2}$, we let $\delta = 0$, $\delta_1 = \pi/4$, and $A^2 \ll 1$ to obtain

$$k_z(k_p) = \pm \frac{|k_p|\,|k|}{|k_1|} \exp\left\{ -i\frac{\pi}{4} + \frac{i}{2} \tan^{-1} A^2 \right\}$$

$$k_{1z}(k_p) = \pm \frac{|k_p|\,|k_1|}{|k|} \exp\left\{ i\frac{\pi}{4} + \frac{i}{2} \tan^{-1} A^2 \right\}$$

To determine $k_z(k_p)$ and $k_{1z}(k_p)$ we have to know their allowed phase values on the particular Riemann sheet which is in turn dependent on how the branch cuts are chosen.
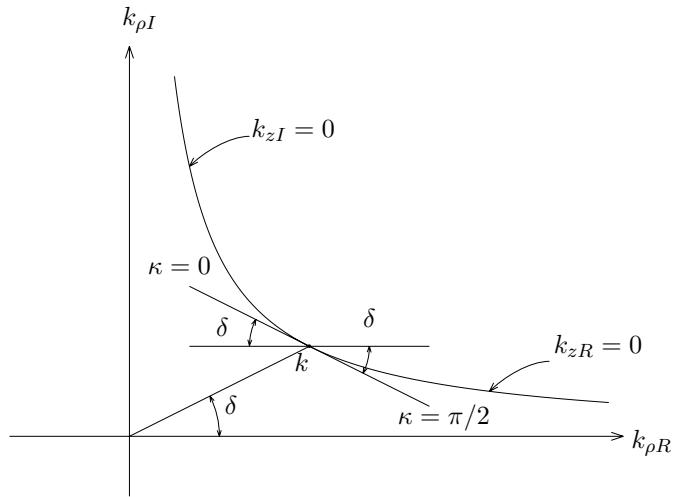
Figure E5.7.14.1
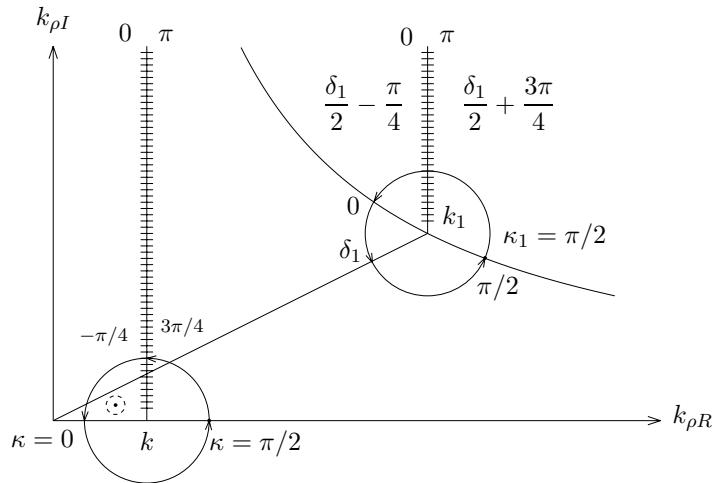
Figure E5.7.14.2

(f) To study the various choices of branch cuts originating from k and k_1, we let k be complex such that

$$k = k_R + ik_I = |k|\, e^{i\delta}$$
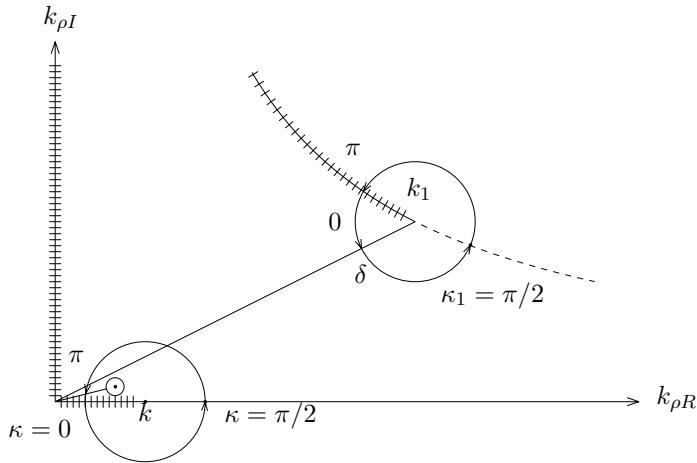
Figure E5.7.14.3
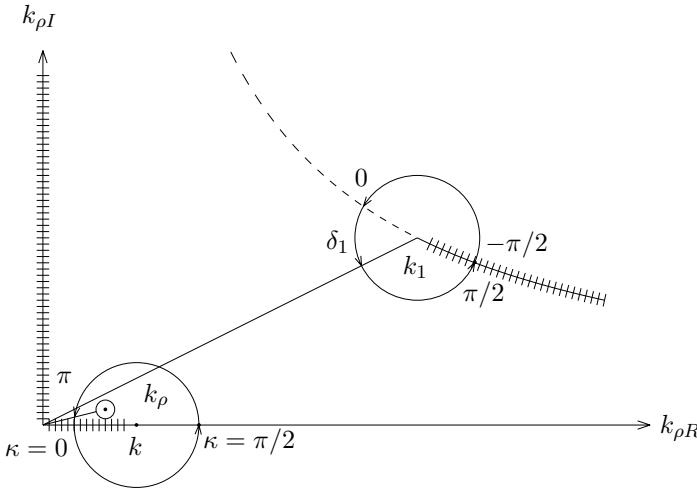
Figure E5.7.14.4

where $k_I \geq 0$ for conductive media. Write

$$k_z = \sqrt{k^2 - k_\rho^2} = |k_z| e^{i\kappa}$$

$$= \sqrt{(k_R^2 - k_{\rho R}^2) - (k_I^2 - k_{\rho I}^2) + i2(k_R k_I - k_{\rho R} k_{\rho I})}$$

Setting the imaginary part inside the square root equal to zero, we find a curve for which k_z is either purely real or purely imaginary. The curve

is a hyperbola determined by

$$k_{\rho R} k_{\rho I} = k_R k_I$$

The slope of the tangent to the hyperbola at $k_\rho = k_1$ is

$$\frac{dk_{\rho I}}{dk_{\rho R}} = -\frac{k_I}{k_R} = -\tan\delta$$

For the part of the hyperbola to the left of k, the curve corresponds to $k_{zI} = 0$. For the part of the hyperbola to the right of k, the curve corresponds to $k_{zR} = 0$ [Fig. E5.7.14.1].

(g) Around the branch point k, let η be a very small number and

$$k_\rho = k + \eta e^{i\beta}$$

Neglecting the η^2 term to obtain

$$k_z = |k_z| e^{i\kappa} \approx \sqrt{2\eta |k|} e^{i[\delta + \beta + (2n+1)\pi]}$$

Thus for $n = 0$ the value of κ increases from 0 to π when β increases from $-\pi - \delta$ to $\pi - \delta$ in the counter-clockwise direction.

Consider the branch cuts originating from the branch points k and k_1 by assuming k real and k_1 complex. Let both branch cuts be vertical as shown in Figure E5.7.14.2. The variation of the phase values for k_z and k_{1z}, denoted by κ and κ_1, on the topmost Riemann sheet, is indicated around the two circles centered at k and k_1. Both $k_z(k_p)$ and $k_{1z}(k_p)$ take the positive sign in order for their phases κ and κ_1 to be less than $\pi/2$ and larger than $-\pi/4$. Thus the pole is absent.

(h) Let both branch cuts follow the constant phase paths as shown in Figure E5.7.14.3. Then $k_z(k_p)$ takes the minus sign in order for $\pi/2 < \kappa < \pi$ and $k_{1z}(k_p)$ takes the plus sign in order for $0 < \kappa_1 < \pi/2$. Thus the pole is present.

(i) Let the branch cut originating from $k_\rho = k$ follows the $k_{zI} = 0$ path and the branch cut originating from $k_\rho = k_1$ follows the $k_{1zR} = 0$ path as shown in Figure E5.7.14.4. Then $k_z(k_p)$ takes the minus sign and $k_{1z}(k_p)$ takes the plus sign. Thus the pole is present.

— END OF EXAMPLE 5.7.14 —

Problems

P5.7.1

(a) Show that if $f(\alpha)$ is analytic in a domain D, then both f_R and f_I satisfy the Cauchy-Riemann equations

$$\frac{\partial f_R}{\partial \alpha_R} = \frac{\partial f_I}{\partial \alpha_I}, \qquad \frac{\partial f_R}{\partial \alpha_I} = -\frac{\partial f_I}{\partial \alpha_R}$$

The converse is true only when these partial derivatives are continuous in D.

(b) Find a differential equation satisfied by both f_R and f_I.

P5.7.2

A function $f(\alpha)$ is analytic in a domain D if its derivative $f'(\alpha)$ exists in D. Prove that $f(\alpha) = \alpha^3$ is analytic everywhere while $f(\alpha) = \alpha^*$, where α^* means complex conjugate of α, is non-analytic. Make use of the definition for derivative

$$f'(\alpha) = \lim_{\Delta\alpha\to 0} \frac{(\alpha + \Delta\alpha)^* - \alpha^*}{\Delta\alpha} = \lim_{\substack{\Delta_R \to 0 \\ \Delta\alpha_I \to 0}} \frac{\Delta\alpha_R - i\Delta\alpha_I}{\Delta\alpha_R + i\Delta\alpha_I}$$

The derivative $f'(\alpha)$ does not exist if the limit depends on how $\Delta\alpha \to 0$. Find the limit for $f'(\alpha)$ by approaching $\alpha = 0$ from the real axis and from the imaginary axis. Does $f'(\alpha)$ exist? Does the function satisfy the Cauchy-Riemann condition for analyticity?

P5.7.3

Making use of the Cauchy-Riemann equations and Green's theorem

$$\oint_C d\bar{l} \cdot \overline{A} = \iint_D d\overline{S} \cdot (\nabla \times \overline{A})$$

prove Cauchy's theorem, which states that if $f(\alpha)$ is analytic in a domain D and on the contour C bounding the domain D, then

$$\oint_C d\alpha\, f(\alpha) = 0$$

P5.7.4

As an example, we find the residues for

$$f(\alpha) = \frac{\sqrt{\alpha}}{\alpha + 1}$$

Notice that there is a pole at $\alpha = -1$ and a branch point at $\alpha = 0$. We choose the branch point as shown in Figure 5.7.4 except now there is a pole at $\alpha = -1$.

On the bottom Riemann sheet $Res. = \lim_{\alpha\to -1} \sqrt{\alpha} = e^{i(4m+3)\pi/2} = -i$.

P5.7.5

Prove Jordan's Lemma which states that

(a) $\lim_{R\to\infty} \int_{C_R} d\alpha\, f(\alpha) = 0$ if $\lim_{R\to\infty} R f(Re^{i\phi}) = 0$

(b) $\lim_{R\to\infty} \int_{C_R} d\alpha\, f(\alpha) e^{ia\alpha} = 0$ if $\lim_{R\to\infty} f(Re^{i\phi}) = 0$

for $a > 0$, where C_R is a semicircle of radius R in the upper half of the α plane.

P5.7.6

Show $\int_0^\infty \sin \alpha^2 \, d\alpha = \int_0^\infty \cos \alpha^2 \, d\alpha = \sqrt{\pi/8}$ by writing

$\int_0^\infty \cos \alpha^2 \, d\alpha + i \int_0^\infty \sin \alpha^2 \, d\alpha = \int_0^\infty e^{i\alpha^2} \, d\alpha$ and choosing a contour C as illustrated in Figure P5.7.6.1. Let $\theta_0 = \pi/4$ and $\alpha = r \, e^{i\pi/4}$ to complete the proof.
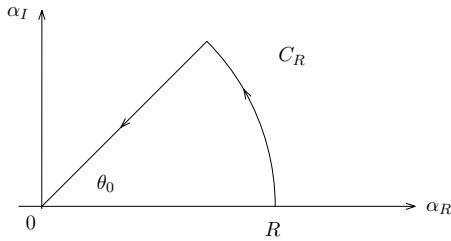
Figure P5.7.6.1

P5.7.7

Show that, by choosing the contour as shown in Figure P5.7.7.1

$$I = \frac{1}{2\pi i} \int_{a-i\infty}^{a+i\infty} d\alpha \, \frac{e^{\alpha t}}{\sqrt{\alpha + 1}} = \sqrt{\frac{1}{\pi t}} e^{-t}$$
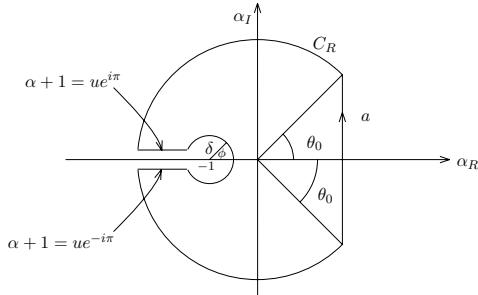
Figure P5.7.7.1

P5.7.8

For a linear, temporally dispersive medium with conductivity σ, we have

$$\epsilon(\omega) = \epsilon_0 \left[1 + \frac{i\sigma}{\omega\epsilon_0} + \int_0^\infty d\tau \, \xi_e(\tau) e^{i\omega\tau} \right]$$

(a) Show that $\epsilon^*(\omega) = \epsilon(-\omega)$.

(b) Integrate $\oint_C d\alpha\, [\epsilon(\alpha) - \epsilon_\infty]/(\alpha - \omega)$ over a semicircle of infinite radius with the straight side along the real axis but indented around the points $\alpha = \omega$ and $\alpha = 0$. Show that the Kramers-Krönig relation is

$$\epsilon_R(\omega) - \epsilon_\infty = \frac{1}{\pi} \mathrm{PV} \int_{-\infty}^{\infty} d\alpha\, \frac{\epsilon_I(\alpha)}{\alpha - \omega}$$

$$\epsilon_I(\omega) = -\frac{1}{\pi} \mathrm{PV} \int_{-\infty}^{\infty} a\alpha\, \frac{\epsilon_R(\alpha) - \epsilon_\infty}{\alpha - \omega} + \frac{\sigma}{\omega}$$

(c) Show that the result in (b) is independent of whether the indentation is made above or below the singularities at $\alpha = \omega$ and $\alpha = 0$.

P5.7.9

From the definition of the second kind Hankel function

$$H_\nu^{(2)}(\xi) = \frac{1}{\pi} \int_{\Gamma_2} d\alpha\, e^{i(\xi \cos \alpha + \nu\alpha - \nu\pi/2)}$$

determine its asymptotic value by using the saddle point method as $\xi \to \infty$.

P5.7.10

Derive Stirling's formula

$$n! \approx (2\pi)^{1/2}\, n^{n+1/2}\, e^{-n}$$

for large n from the defining integral

$$n! = \int_0^\infty dx\, x^n e^{-x}$$

by using the Laplace method.

P5.7.11

The Laplace method is useful in evaluating asymptotic values for an integration along the real axis. Evaluate the integral

$$I(\alpha) = \int_0^\infty dy\, \frac{y^\alpha e^{-y}}{1 + y} \qquad \text{as} \quad \alpha \to \infty$$

P5.7.12

Use the saddle point method to find the asymptotic form of the integral

$$I(\xi) = \int_{-\infty}^\infty d\alpha\, e^{i\xi\alpha - \alpha^2}$$

for $\xi \to \infty$. Show that the leading term in the asymptotic series is also the exact solution to the integral and higher order terms are error terms for the asymptotic series.

P5.7.13

In dealing with Sommerfeld-type integrals, it is often convenient to use an angular variable α such that $k_\rho = k \sin \alpha$. Let k be real and positive, and

$$x = k_{\rho R}/k = \sin \alpha_R \cosh \alpha_I$$
$$y = k_{\rho I}/k = \cos \alpha_R \sinh \alpha_I$$

(a) Show that the vertical lines $(\alpha_R = \text{constant})$ in the complex α plane are mapped to a family of confocal hyperbolas in the complex k_ρ plane with the foci at $x = \pm 1$ and $y = 0$.

(b) Show that the horizontal lines $(\alpha_I = \text{const})$ in the α plane are mapped to a family of confocal ellipses in the k_ρ plane with the foci at $x = \pm 1$ and $y = 0$.

(c) Show that the ellipses and the hyperbolas intersect each other perpendicularly and that the image of the set $\{-\pi/2 \leq \alpha_R \leq \pi/2, -\infty \leq \alpha_I \leq \infty\}$ is the entire k_ρ plane.

(d) With elliptic coordinates defined as

$$x = h \cosh \xi \cos \eta$$
$$y = h \sinh \xi \cos \eta$$

Find the relations between (ξ, η) and (α_R, α_I).

P5.7.14

In the limit when $r \to \infty$, consider the asymptotic behavior of the integral

$$I(r) = \int_{-\infty}^{\infty} dk_\rho \, A(k_\rho) \frac{k_\rho}{k_z} H_0^{(1)}(k_\rho \rho) e^{ik_z z}$$

Noting that $k^2 = k_\rho^2 + k_z^2$ and $r^2 = \rho^2 + z^2$, the following transformations are useful:

$$k_\rho = k \sin \theta, \qquad \rho = r \sin \theta_0$$
$$k_z = k \cos \theta, \qquad z = r \cos \theta_0$$

(a) Show that when calculated to the second order in $1/r$, with the saddle-point method, the asymptotic form for $I(r)$ reads

$$I(r) = \frac{2}{i} \frac{e^{ikr}}{r} \left\{ A(\theta_0) - \frac{i}{2kr} \left[A''(\theta_0) + A'(\theta_0) \cot \theta_0 \right] \right\}$$

(b) In the case when $A(\theta)$ is a constant, deduce the Sommerfeld identity,

$$\frac{e^{ikr}}{r} = \frac{i}{2} \int_{-\infty}^{\infty} dk_\rho \, \frac{k_\rho}{k_z} H_0^{(1)}(k_\rho \rho) e^{ik_z z}$$

(c) Alternatively, consider solving the two differential equations governing the two- and three-dimensional Green's functions by Fourier transforming with respect to z. Show that

$$\frac{e^{ikr}}{r} = \frac{i}{2} \int_{-\infty}^{\infty} dk_z \, H_0^{(1)}(k_\rho \, \rho) e^{ik_z z}$$

and

$$H_0^{(1)}(k\rho) = \frac{1}{i\pi} \int_{-\infty}^{\infty} dz \frac{e^{ikr}}{r}$$

By deforming the contour in the k_z plane, and then changing the integration variable to k_ρ for the first integral, recover the identity in (b).

Answers

P5.1.1

(a)

$$\frac{d^2N}{dl\,d\lambda} = \frac{d^2N}{dl\,d\omega} \cdot \frac{d\omega}{d\lambda} = \frac{d^2S_\rho}{dl\,d\omega} \cdot \frac{1}{E_{photon}} \cdot \frac{d\omega}{d\lambda}$$

$$= \frac{\mu q^2}{4\pi\hbar}\left(1 - \frac{1}{n^2\beta^2}\right) \cdot \frac{2\pi c}{\lambda^2} = \frac{q^2 c\mu}{2\lambda^2\hbar}(1 - \frac{1}{n^2\beta^2})$$

$$\frac{dN}{dl} = d\lambda \cdot \frac{q^2 c\mu}{2\lambda^2\hbar}(1 - \frac{1}{n^2\beta^2}) \propto \frac{d\lambda}{\lambda^2}(1 - \cos^2\theta) = \frac{d\lambda}{\lambda^2}\sin^2\theta$$

(b) $\theta = \cos^{-1}\frac{1}{n\beta} = \cos^{-1}\frac{1}{1.002\times 1} = 0.0632 = 3.62°$

(c) Integrate both sides of the equation in part(a) over λ from 350 nm to 550 nm, we have $\frac{dN}{dl} = 190 \to N = 190l$
When $N = 100$, $l = 100/190 = 0.526\,\mathrm{m}$

P5.2.1

The solution $g(x,x') = Ce^{ik|x-x'|}$ satisfies the homogeneous equation $[\frac{d^2}{dx^2} + k^2]g(x,x') = 0$. Integrating over $x = x'$ of the differential equation

$$[\frac{d^2}{dx^2} + k^2]g(x,x') = -\delta(x - x')$$

yields $C = i/2k$ as $\lim_{x\to x'}[ikCe^{ik(x-x')}] - \lim_{x\to x'}[-ikCe^{-ik(x-x')}] = -1$.

P5.2.2

$g(x,y) = \frac{1}{2\pi}\int_{-\infty}^{\infty} dk_x e^{ik_x x}\tilde{g}(k_x, y)$
make use of the Fourier integral representation of the delta function,
$\frac{1}{2\pi}\int_{-\infty}^{\infty} dk_x e^{ik_x x}[\frac{d^2}{dy^2} + k_y^2]g(k_x, y) = -\frac{1}{2\pi}\int_{-\infty}^{\infty} dk_x e^{ik_x x}\delta(y)$
where $k_y^2 = k^2 - k_x^2$, $[\frac{d^2}{dy^2} + k_y^2]g(k_x, y) = -\delta(y) \Rightarrow g(k_x, y) = \frac{ie^{ik_y|y|}}{2k_y}$,
and $g(\rho) = \frac{i}{4}H_o^1(k\rho) = \frac{i}{4\pi}\int_{-\infty}^{\infty} dk_x \frac{e^{ik_x x + ik_y|y|}}{k_y}$.

P5.2.3

$\frac{e^{ik_0 r}}{r} = \frac{1}{(2\pi)^3}\iiint_{-\infty}^{\infty} dk_x dk_y dk_z\, g(k_x, k_y, k_z)e^{ik_x x + ik_y y + ik_z z}$
Making use of the Fourier integral representation of the delta function
$\left[\frac{\partial^2}{\partial x^2} + \frac{\partial^2}{\partial x^2} + \frac{\partial^2}{\partial x^2} + k_0^2\right]\frac{e^{ik_0 r}}{4\pi r} = -\delta(x)\delta(y)\delta(z)$, we find
$g(k_x, k_y, k_z) = \frac{-4\pi}{k_0^2 - k_x^2 - k_y^2 - k_z^2}$, Thus

$$g(r) = \frac{e^{ik_0 r}}{4\pi r} = \frac{1}{(2\pi)^3}\iiint_{-\infty}^{\infty} dk_x dk_y dk_z \frac{-1}{k_0^2 - k_x^2 - k_y^2 - k_z^2}e^{ik_x x + ik_y y + ik_z z}$$

$$= \frac{1}{(2\pi)^3} \iiint_{-\infty}^{\infty} dk_x dk_y dk_z \frac{e^{ik_x x + ik_y y + ik_z z}}{\left(k_z + \sqrt{k_0^2 + k_x^2 + k_y^2}\right)\left(k_z - \sqrt{k_0^2 - k_x^2 - k_y^2}\right)}$$

$$= \frac{i}{8\pi^2} \iint_{-\infty}^{\infty} dk_x dk_y \frac{1}{k_z} e^{ik_x x + ik_y y + ik_z |z|}$$

P5.3.1

$$\overline{E}(\overline{r}, t) = \frac{\omega \mu I l}{4\pi r} \left\{ \hat{r} 2 \cos\theta \left[\frac{1}{kr} \cos(kr - \omega t) - \frac{1}{k^2 r^2} \sin(kr - wt) \right] \right.$$

$$\left. + \hat{\theta} \sin\theta \left[\left(1 - \frac{1}{k^2 r^2}\right) \sin(kr - \omega t) + \frac{1}{kr} \cos(kr - \omega t) \right] \right\}$$

$$\overline{H}(\overline{r}, t) = \hat{\phi} \frac{kIl}{4\pi r} \sin\theta \left[\sin(kr - \omega t) + \frac{1}{kr} \cos(kr - \omega t) \right]$$

Let $Il = -i\omega ql$, the instantaneous electric and magnetic field vectors become

$$\overline{E}(\overline{r}, t) = \frac{k^2 ql}{4\pi \epsilon_0 r} \left\{ \hat{r} 2 \cos\theta \left[\frac{1}{kr} \sin(kr - \omega t) + \frac{1}{k^2 r^2} \cos(kr - wt) \right] \right.$$

$$\left. + \hat{\theta} \sin\theta \left[\left(-1 + \frac{1}{k^2 r^2}\right) \cos(kr - \omega t) + \frac{1}{kr} \sin(kr - \omega t) \right] \right\}$$

$$\overline{H}(\overline{r}, t) = \hat{\phi} \frac{\omega k ql}{4\pi r} \sin\theta [-\cos(kr - \omega t) + \frac{1}{kr} \sin(kr - \omega t)]$$

which were obtained in Chapter 1.

P5.3.2

(a) $\overline{f} = I_0 \ell \left[\hat{y} + \hat{x} e^{i\frac{3\pi}{2}\cos\theta} \right]$

(b) $\overline{E} = \eta_0 \frac{ik}{4\pi r} e^{ikr} \left[\hat{\theta} f_\theta + \hat{\varphi} f_\varphi \right] \Rightarrow$

   $\overline{E} = \eta_0 \frac{ikI_0\ell}{4\pi r} e^{ikr} \left\{ \hat{\phi} \left[\cos\phi - \sin\phi e^{i\frac{3\pi}{2}\cos\theta} \right] + \hat{\theta} \cos\theta \left[\sin\phi + \cos\phi e^{i\frac{3\pi}{2}\cos\theta} \right] \right\}$

(c) In $+\hat{z}$ direction, $\overline{E} \sim \left[\hat{y} + \hat{x} e^{i\frac{3\pi}{2}} \right] e^{ikz} = [\hat{y} - i\hat{x}] e^{ikz}$ RHCP

   In $-\hat{z}$ direction, $\overline{E} \sim \left[\hat{y} + \hat{x} e^{-i\frac{3\pi}{2}} \right] e^{-ikz} = [\hat{y} + i\hat{x}] e^{-ikz}$ RHCP

   $\theta = 0, \pi$. Waves are RHCP

(d) No directions in which wave is LHCP

(e) Linearly polarized as $\frac{3\pi}{2} \cos\theta = n\pi$ ($\hat{\phi}$ & $\hat{\theta}$ components in phase)

   $\cos\theta = \frac{2n}{3}$ $(n = -1, 0, 1) \to \theta = \cos^{-1}\left(\frac{2}{3}\right)$, $\theta = \frac{\pi}{2}$, $\theta = \cos^{-1}\left(-\frac{2}{3}\right)$

P5.3.3

(a) In spherical coordinates

$$\hat{x} + i\hat{y} = \hat{r}\sin\theta(\cos\phi + i\sin\phi) + \hat{\phi}(i\cos\phi - \sin\phi) + \hat{\theta}(\cos\phi + i\sin\phi)\cos\theta$$

$$= \hat{r} e^{i\phi}\sin\theta + \hat{\theta} e^{i\phi}\cos\theta + \hat{\phi} i e^{i\phi}$$

The electric field $\overline{E}$ is

$$
\begin{aligned}
\overline{E}(\overline{r}) &= i\omega\mu Il \left\{ \hat{r} \left[e^{i\phi} \sin\theta + e^{i\phi} \sin\theta \frac{1}{k^2} \left(-k^2 - \frac{2ik}{r} + \frac{2}{r^2} \right) \right] \right. \\
&\quad \left. + \hat{\theta} \left[1 + \frac{i}{kr} - \frac{1}{k^2 r^2} \right] e^{i\phi} \cos\theta + i\hat{\phi} \left[1 + \frac{ik}{kr} - \frac{1}{k^2 r^2} \right] \right\} \frac{e^{ikr}}{4\pi r} \\
&= -\eta \frac{ikIle^{ikr}}{4\pi r} e^{i\phi} \left\{ \hat{r} \left[\frac{i}{kr} + \left(\frac{i}{kr} \right)^2 \right] 2\sin\theta \right. \\
&\quad \left. - \hat{\theta} \left[1 + \frac{i}{kr} + \left(\frac{i}{kr} \right)^2 \right] \cos\theta - \hat{\phi}i \left[1 + \frac{i}{kr} + \left(\frac{i}{kr} \right)^2 \right] \right\}
\end{aligned}
$$

(b) In the far field on the x-y plane $(\theta = \pi/2)$,

$$
\overline{E}(\overline{r}) = \eta \frac{ikIle^{ikr}}{4\pi r} e^{i\phi}(\hat{\phi}i) = -\hat{\phi}\eta kIl \frac{e^{ikr}}{4\pi r} e^{i\phi}
$$

On the x-y plane $\overline{k} = k_\rho \hat{\rho}$ (radial direction) and $r = \rho$

$$
\overline{E}(\overline{r}, t) = \text{Re} \left\{ -\hat{\phi} \frac{\eta k_\rho Il}{4\pi\rho} e^{ik_\rho\rho} e^{i\phi} e^{-i\omega t} \right\} = -\hat{\phi} \frac{\eta k_\rho Il}{4\pi\rho} \cos(\omega t - \phi - k_\rho\rho)
$$

Thus $\overline{E}$ is linearly polarized.

(c) In the far field on the x-y plane, $\theta = \pi/2$, $< \overline{S} >_\rho = \frac{\eta}{2} \left(\frac{kIl}{4\pi r} \right)^2$. Thus, the radiation pattern in x-y plane is a circle.

(d) For $\theta = 0°$ and in the far field, $\overline{E} = \eta \frac{ikIle^{ikr}}{4\pi r} e^{i\phi} \left\{ \hat{\theta} + i\hat{\phi} \right\}$. Thus, the electric field $\overline{E}$ is right hand circularly polarized.

(e) $< \overline{S} >_z = \hat{z} 2 \frac{\eta}{2} \left(\frac{kIl}{4\pi r} \right)^2$. Thus, the radiated power density in $\hat{z}$ is twice that in $\hat{x}$ direction.

P5.3.4

(a) $\overline{M} = M_o(-\hat{x} + \hat{y}i)$, $\frac{d\overline{M}}{dt} = \omega M_0(\hat{x}i + \hat{y}) = \gamma\overline{M} \times \overline{B}_0$. Thus $\overline{B}_0 = \hat{z}\omega/\gamma$.

(b) The magnetic field due to the precessing $\overline{M}$ is determined from (5.3.26)

$$
\begin{aligned}
\overline{H}(\overline{r}) &= \frac{k^2 e^{ikr}}{4\pi r} \left\{ \overline{M}(1 + \frac{i}{kr} - \frac{1}{k^2 r^2}) - \hat{r}(\hat{r} \cdot \overline{M}) \left[1 + \frac{3i}{kr} - \frac{3}{k^2 r^2} \right] \right\} \\
&= \frac{k^2 e^{ikr}}{4\pi r} \left\{ \overline{M}(1 + \frac{i}{kr} - \frac{1}{k^2 r^2}) \right\}
\end{aligned}
$$

(c) The surface normal of the loop is in the $\hat{x}$- direction. The induced voltage is therefore

$$
V = -\frac{\partial}{\partial t} \int_s d\overline{s} \cdot \overline{B}(z = d, t) = \frac{i\omega k^2 \mu M_0 A e^{ikr}}{4\pi r} (1 + \frac{i}{kr} - \frac{1}{k^2 r^2})
$$

Since $\omega = \gamma B_0$, the induced voltage is directly proportional to the applied dc voltage.

P5.3.5

(a) Keeping terms of the order $\frac{1}{r^3}$, $\overline{H}(\overline{r}) = \frac{1}{4\pi r^3}\left\{-\overline{M} + 3\hat{r}(\hat{r} \cdot \overline{M})\right\}$

(b) Assume a circular loop with radius R. The magnetic field linking the loop with $\rho < R$ in the $\hat{x}$-direction is

$$H_x(\overline{r}, t) = \frac{M_0}{4\pi r^3}\left\{-\cos\omega t + \frac{3}{r^2}\ x(x\cos\omega t + y\sin\omega t)\right\}$$

$$= \frac{M_0}{4\pi(d^2+\rho^2)^{3/2}}\left\{-\cos\omega t + \frac{3}{(d^2+\rho^2)}\ d(d\cos\omega t + \rho\sin\phi\sin\omega t)\right\}$$

$$V = -\frac{\partial}{\partial t}\int_A da B_x(\overline{r}, t) = -\frac{\partial}{\partial t}\int_0^R \rho d\rho \int_0^{2\pi} d\phi B_x(\overline{r}, t)$$

$$= -\frac{\partial}{\partial t}\int_0^R \rho d\rho \frac{\mu M_0}{2(d^2+\rho^2)^{3/2}}\left\{-\cos\omega t + \frac{3}{(d^2+\rho^2)}\ d^2\cos\omega t\right\}$$

$$= \omega\sin\omega t \int_0^R \rho d\rho \frac{\mu M_0}{2(d^2+\rho^2)^{3/2}}\left\{\frac{2d^2-\rho^2}{(d^2+\rho^2)}\right\}$$

$$= \omega\sin\omega t \int_{d^2}^{R^2+d^2} du \frac{\mu M_0(3d^2-u)}{4u^{5/2}}$$

$$= -\frac{\omega\mu M_0\sin\omega t}{4}(2d^2(d^2+R^2)^{-3/2} - 2(d^2+R^2)^{-1/2} - 2d^{-1} + 2d^{-1})$$

$$= \frac{\omega\mu M_0 R^2}{2(d^2+R^2)^{3/2}}\sin\omega t$$

Thus $U(\omega) = \omega\mu M_0 R^2/2(d^2+R^2)^{3/2}$. Since the Larmor frequency $\omega = \gamma B_0$, we need a large B_0 to get large induced voltage V.

(c) $\Delta B_0 = \Delta\omega/\gamma$

(d) Since $\Delta B_0 = b_1\delta$, we find $\delta = \Delta\omega/b_1\gamma$

(e) $\Delta\omega = b_1\delta\gamma = 1.0 \times 0.5 \times 10^{-3} \times 2.7 \times 10^8 = 1.35 \times 10^5(\text{rad/s}) = 21.5\text{kHz}$

P5.3.6

(a) In the rotating coordinate, we can write

$$\overline{B} = B_0\hat{z}' + B_1\hat{x}'$$

$$\overline{M} = \hat{x}'M_x' + \hat{y}'M_y' + \hat{z}'M_z', \quad \overline{M}\times\overline{B} = \hat{x}'B_0 M_y' + \hat{y}'(B_1 M_z' - B_0 M_x') - \hat{z}B_1 M_y'$$

$$\frac{d\overline{M}(t)}{dt} = (\frac{dM_x'}{dt} + \omega_1 M_y')\hat{x}' + (\frac{dM_y'}{dt} - \omega_1 M_x')\hat{y}' + \frac{dM_z'}{dt}\hat{z}'$$

$$= \hat{x}'\omega_0 M_y' + \hat{y}'(\omega_1 M_z' - \omega_0 M_x') - \hat{z}\omega_1 M_y'$$

With $\Delta\omega_0 = \omega_0 - \omega_1$ and the classical equation of motion for $\overline{M}$, we find

$$dM'_x/dt = (\Delta\omega_0)M'_y$$
$$dM'_y/dt = -(\Delta\omega_0)M'_x + \gamma B_1 M'_z$$
$$dM'_z/dt = -\gamma B_1 M'_y$$

Solve this equation system, we will obtain:

$$M'_y = M_0 \sin(\sqrt{(\Delta\omega_0)^2 + (\gamma B_1)^2}\,t)$$
$$M'_x = M_0 \frac{-\Delta\omega_0}{\sqrt{(\Delta\omega_0)^2 + (\gamma B_1)^2}} \cos\,(\sqrt{(\Delta\omega_0)^2 + (\gamma B_1)^2}\,t)$$
$$M'_z = M_0 \frac{\gamma B_1}{\sqrt{(\Delta\omega_0)^2 + (\gamma B_1)^2}} \cos\,(\sqrt{(\Delta\omega_0)^2 + (\gamma B_1)^2}\,t)$$

If we rotate the x', z' axis by an angle $\theta = \tan^{-1}(\frac{\Delta\omega_0}{\gamma B_1})$ (from z' to new z'') while keeping y' axis unchanged, in the new coordinate (x'', y'', z'') the magnetic moments can be written as:

$$M''_x = 0$$
$$M''_y = \sin(\gamma\sqrt{(\Delta B_0)^2 + (B_1)^2}\,t)M_0$$
$$M''_z = \cos(\gamma\sqrt{(\Delta B_0)^2 + (B_1)^2}\,t)M_0$$

It is clear that $\overline{M}$ is precessing about $\hat{x}''$ axis,
where $\hat{x}'' = \frac{1}{\sqrt{(\Delta B_0)^2 + (B_1)^2}}(\Delta B_0 \hat{z}' + B_1 \hat{x}')$ and $\Delta B_0 = (\omega_0 - \omega_1)/\gamma$.

(b) When the coil excitation frequency $\omega_1 = \gamma B_0$ which is also called the Larmor frequency, we can obtain the solution as,

$$M'_x = 0$$
$$M'_y = M_0 \sin(\omega_0 t)$$
$$M'_z = M_0 \cos(\omega_0 t)$$

which is a rotation around x' axis at the Larmor frequency.

P5.3.7
(a) $E = \hbar\omega_0 = \hbar\gamma B_0$
   $\gamma = \frac{E}{\hbar B_0} = \frac{4.2346\times10^{-26}}{6.63/2\pi\times10^{-34}\times1.5} = 42.58 \times 2\pi = 267.538 \,\text{rad MHz/T}$
(b) From $\omega = \gamma(B_0 + xG_x)$, we have
   $x = (\omega/\gamma - B_0)/G_x$
   When $f = 63.8717\,\text{MHz}$, $x = 4\,\text{mm}$
   When $f = 63.8666\,\text{MHz}$, $x = -8\,\text{mm}$

P5.3.8

(a) From Biot-Savart's law, the magnetic field produced by the upper coil is

$$B_u(z) = \frac{\mu_0 I}{4\pi} \int_0^{2\pi} \frac{\hat{z} a^2 \, d\phi'}{\left[(z-\frac{d}{2})^2+a^2\right]^{\frac{3}{2}}} = \hat{z} \frac{\mu_0 I a^2}{2\left[(z-\frac{d}{2})^2+a^2\right]^{\frac{3}{2}}} \, .$$

The magnetic field produced by the lower coil is

$$B_l(z) = \hat{z} \frac{\mu_0 I a^2}{2\left[(z+\frac{d}{2})^2+a^2\right]^{\frac{3}{2}}} \, . \quad \text{The total magnetic is}$$

$$B_z = \frac{\mu_0 I a^2}{2[(d/2-z)^2+a^2]^{\frac{3}{2}}} + \frac{\mu_0 I a^2}{2[(d/2+z)^2+a^2]^{\frac{3}{2}}} \, .$$

(b) $\frac{dB_z}{dz} = \frac{3\mu_0 I a^2}{2} \left\{ \frac{d/2-z}{[(d/2-z)^2+a^2]^{5/2}} - \frac{d/2+z}{[(d/2+z)^2+a^2]^{5/2}} \right\} \, .$

$\frac{d^2 B_z}{dz^2} = \frac{3\mu_0 I a^2}{2} \left\{ \frac{4(d/2-z)^2-a^2}{[(d/2-z)^2+a^2]^{7/2}} + \frac{4(d/2+z)^2-a^2}{[(d/2+z)^2+a^2]^{7/2}} \right\} \, .$

When $d = a$, both of $\frac{dB_z}{dz}$ and $\frac{d^2 B_z}{dz^2}$ will vanish at $z = 0$.

(c)
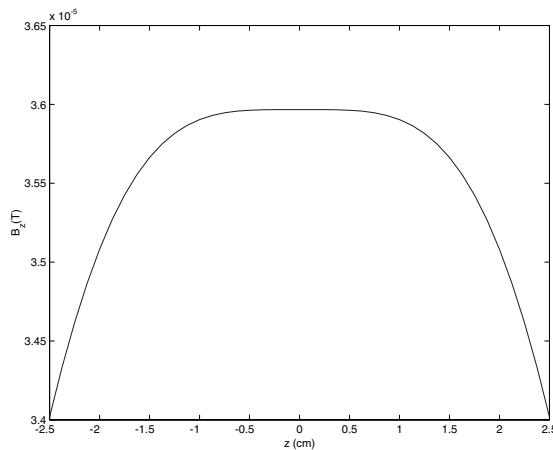
Figure P5.3.8.1

P5.4.1

(a) $F(\phi) = 2 \cos\left(\frac{kd}{2} \sin\phi - \frac{\psi}{2}\right)$

$|F(\phi)| = \left| 2 \cos\left(\frac{kd}{2} \sin\phi - \frac{\psi}{2}\right) \right|$

(b)

(i) max $\quad \phi = 90° = \frac{\pi}{2} \Rightarrow \frac{kd}{2} - \frac{\psi}{2} = m\pi$

(ii) nulls $\phi = 225°, \, 315° \Rightarrow -\dfrac{kd}{2}\dfrac{1}{\sqrt{2}} - \dfrac{\psi}{2} = \left(\dfrac{2n+1}{2}\right)\pi, \, \dfrac{5\pi}{4}, \, \dfrac{7\pi}{4}$

$$d = \frac{\lambda}{2}\frac{1}{\left(1 + \dfrac{1}{\sqrt{2}}\right)} \simeq 0.293\,\lambda \qquad \psi = \pi\left[\frac{1}{1 + \dfrac{1}{\sqrt{2}}} - 2\right] \simeq -1.41\pi$$

Choose $m = 1, \, n = 0$ or $\dfrac{\pi}{1 + \dfrac{1}{\sqrt{2}}} = 0.59\pi$

(Could also do this by visible window, answers come out the same)

P5.4.2

Broadside, $\alpha = 0$, 20 dB sidelobe level, $R = 10$.
$b = \cosh(\frac{1}{6}\cosh^{-1}10)$, excitation coefficients are:
$a_3 = b^6/2$, $a_2 = 3b^4(b^2 - 1)$, $a_1 = (3/2)b^2(5b^2 - 3)(b^2 - 1)$.
The zero of $T_6(x)$ is $x_1 = \cos(\pi/12) = 0.966$.
The first-null beamwidth is BW $= 40.2°$ and the directivity $D = 6.66$.
For $d = \lambda/4$, BW $= 87°$ and $D = 3.3871$.

P5.4.3

(a) $|\tilde{F}(0)| = \left|\cot\dfrac{\pi}{2(N-1)}\right| \sim \dfrac{2}{\pi}(N - 1)$,   as $N \to \infty$.

(b)

N	Sidelobe location (u)		Sidelobe level (dB)	
	exact	asymp.	exact	asymp.
6	2.449	2.374	-18.46	-23.00
10	1.330	1.319	-21.70	-23.00
15	0.851	0.848	-22.47	-23.00
50	0.242	0.242	-22.96	-23.00

(c) $D = 3.789$ for any α.

P5.4.4

(a)

$$\begin{aligned}
P(\xi) &= |\tilde{F}(u)|^2 \\
&= |0.4929990 + 0.448914e^{-iu} + 0.138187e^{-i2u} - 0.0630965e^{-i3u}|^2 \\
&= |-0.0630965 + 0.138187e^{-iu} + 0.448914e^{-i2u} + 0.4929990e^{-i3u}|^2 \\
&= |-0.1152046 + 0.361175e^{-iu} + 0.501022e^{-i2u} + 0.270011e^{-i3u}|^2 \\
&= |0.270011 + 0.501022e^{-iu} + 0.361175e^{-i2u} - 0.1152046e^{-i3u}|^2
\end{aligned}$$

(b) $\epsilon_{\max} \leq \frac{1}{4!} \cdot \frac{4!}{1.3.5.7} \cdot 12 = 0.1143$.

$\epsilon_{\max} = 0.04189$ occurs at the boundary of the visible region $(x = -1)$.
The actual maximum error is $\epsilon(0) = |L(0) - G(0)| \approx 0.0203$.

P5.4.5

$$
\begin{aligned}
P(\xi) &= |\tilde{F}(u)|^2 \\
&= |0.436065 + 0.502108e^{-iu} + 0.1316027e^{-i2u} - 0.0697753e^{-i3u}|^2 \\
&= |-0.0697753 + 0.1316027e^{-iu} + 0.502108e^{-i2u} + 0.436065e^{-i3u}|^2 \\
&= |-0.1077699 + 0.285339e^{-iu} + 0.540102e^{-i2u} + 0.282329e^{-i3u}|^2 \\
&= |0.282329 + 0.540102e^{-iu} + 0.285339e^{-i2u} - 0.1077699e^{-i3u}|^2
\end{aligned}
$$

P5.4.6

$$
G(u) \simeq D(\xi_0 - \xi)(\xi + \xi_1)(\xi + \xi_2) \overset{\Delta}{=} P(\xi)
$$

$$
\begin{aligned}
D &= 0.00679401 \\
\xi_0 &= 8.483269 \\
\xi_1 &= 3.431809 \\
\xi_2 &= 2.179603
\end{aligned}
$$

P5.5.1

(a) $\overline{E}(\overline{r}) \approx \frac{I_0 k_\rho}{4\omega\epsilon}\sqrt{\frac{2}{\pi k_\rho \rho}}[\hat{\rho}k_z - \hat{z}k_\rho]e^{i(k_\rho\rho + k_z z - \frac{\pi}{4})}$

$\overline{H}(\overline{r}) \approx \hat{\phi}\frac{I_0 k_\rho}{4}\sqrt{\frac{2}{\pi k_\rho \rho}}e^{i(k_\rho\rho + k_z z - \frac{\pi}{4})}$

(b) $\overline{S} \approx \overline{E} \times \overline{H}^* = \frac{I_0^2 |k_\rho|^2}{16\omega\epsilon}\left(\frac{2}{\pi k_\rho \rho}\right)(\hat{z}k_z + \hat{\rho}k_\rho)$

$k_\rho^2 = k^2 - k_z^2$, it becomes imaginary when $k_z > k$. No radial power flows.

(c) Equation of constant phase front when $k_z < k$ is

$$
k_\rho\rho + k_z z = \text{const}
$$

When $k_z > k$, the equation of constant phase becomes $k_z z = \text{const}$ or $z = \text{const}$. It is a plane perpendicular to the current.

P5.5.2

$\overline{E} = -\hat{\theta}\frac{i\omega\mu 2I_0 e^{ikr}}{4\pi kr \sin\theta}\left[\cos(kl\cos\theta) - \cos(kl)\right]$.

$\overline{E} = 0$ at $\theta = 0, \pi$ is obtained by L'Hopital's Rule.
For $kl = 3\pi/2$, nulls occur at $\cos\theta = \pm 1/3$.

P5.5.3

(a) $R_r = 73 \; \Omega$.

(b) As $kl \to 0$, $R_r \approx 5(kl)^2$.

P5.5.4

$$R_r \approx 60 \left\{ \gamma + \ln 2 + \tfrac{\gamma}{2} \cos(2kl) - \tfrac{\pi}{4} \sin(2kl) + \left[1 + \tfrac{1}{2} \cos(2kl) \right] \ln(kl) \right\}.$$

P5.6.1

$$u \sim \frac{m\pi}{\dfrac{\pi}{2} - \theta_0} - \frac{1}{2} \text{ as } \theta_0 \to \frac{\pi}{2}.$$

P5.6.2

$$C = \frac{q}{V} = \frac{2\pi\epsilon}{\ln\left(\dfrac{\cot(\theta_0/2)}{\cot \frac{\pi - \theta_1}{2}} \right)} \; ; \; L = \frac{\mu_0}{2\pi} \ln\left(\frac{\cot(\theta_0/2)}{\cot\left(\frac{\pi - \theta_1}{2} \right)} \right).$$

P5.7.1

(a) $f'(\alpha) = \lim_{\substack{\Delta\alpha_R \to 0 \\ \Delta\alpha_I \to 0}} \frac{\Delta f_R + i\Delta f_I}{\Delta\alpha_R + i\Delta\alpha_I}$

Letting $\Delta\alpha_R \to 0$ then $\Delta\alpha_I \to 0$, and equating the real and imaginary parts, we obtain the Cauchy-Riemann equations.

(b) Both f_R and f_I satisfy the Laplace equation

$$\left\{ \frac{\partial^2}{\partial\alpha_R^2} + \frac{\partial^2}{\partial\alpha_I^2} \right\} \begin{bmatrix} f_R(\alpha_R, \alpha_I) \\ f_I(\alpha_R, \alpha_I) \end{bmatrix} = 0$$

P5.7.2

If $\Delta\alpha$ approaches 0 from the real axis, then $\Delta\alpha_I = 0$, and $f'(\alpha) = 1$.
If $\Delta\alpha$ approaches 0 from the imaginary axis, then $\Delta\alpha_R = 0$, and $f'(\alpha) = -1$.

These two results are different, therefore $f'(\alpha)$ does not exist. The Cauchy-Riemann Condition for analytic functions is not satisfied.

P5.7.3

Writing in terms of real variables, and on account of Cauchy-Riemann conditions

$$\oint_C d\alpha \, f(\alpha) = \oint_C (d\alpha_R f_R - d\alpha_I f_I) + i \oint_C (d\alpha_R f_I + d\alpha_I f_R)$$

$$= \oint_C (d\alpha_R, d\alpha_I) \cdot (f_R, -f_I) + i \oint_C (d\alpha_R, d\alpha_I) \cdot (f_I, f_R)$$

$$= \iint_D d\alpha_R d\alpha_I \left\{ \left(-\frac{\partial f_R}{\partial\alpha_I} - \frac{\partial f_I}{\partial\alpha_R} \right) + i \left(\frac{\partial f_R}{\partial\alpha_R} - \frac{\partial f_I}{\partial\alpha_I} \right) \right\} = 0$$

P5.7.5

(a) Let $\alpha = Re^{i\phi}$ and $d\alpha = iRe^{i\phi}d\phi$, we have

$$I_R = \lim_{R\to\infty} \int_{C_R} d\alpha\, f(\alpha) = \int_0^\pi d\phi\, iRe^{i\phi} f(Re^{i\phi})$$

$|I_R| \leq \int_0^\pi d\phi\, |Rf(Re^{i\phi})|$.

Since $\lim_{R\to\infty} Rf(Re^{i\phi}) = 0$, we choose $|Rf(Re^{i\phi})| \leq \delta$.

Thus $|I_R| \leq \delta \int_0^\pi d\phi = \pi\delta \Rightarrow 0$

(b) $I_R = \lim_{R\to\infty} \int_{C_R} d\alpha\, f(\alpha)e^{ia\alpha} = \int_0^\pi d\phi\, iRe^{i\phi} f(Re^{i\phi})e^{iaR\cos\phi - aR\sin\phi}$

$|I_R| \leq R \int_0^\pi d\phi\, |f(Re^{i\phi})|e^{-aR\sin\phi} = 2R \int_0^{\pi/2} d\phi\, |f(Re^{i\phi})|e^{-aR\sin\phi}$

Since $\lim_{R\to\infty} f(Re^{i\phi}) = 0$, we choose $|f(Re^{i\phi})| \leq \delta$.

Also for $0 \leq \phi \leq \pi/2$, we choose $2\phi/\pi \leq \sin\phi$. We thus have

$|I_R| \leq 2R\delta \int_0^{\pi/2} d\phi\, e^{-2aR\phi/\pi} = 2\delta R\frac{1-e^{-aR}}{2aR/\pi} = \delta\frac{\pi}{a}(1-e^{-aR}) \Rightarrow 0$

P5.7.6

$\int_0^\infty e^{i\alpha^2}\, d\alpha = \int_0^\infty e^{-r^2}\, e^{i\pi/4}dr = \frac{\pi}{2}\, e^{i\pi/4} = \sqrt{\pi/8}(1+i)$.

P5.7.7

Using the contour in Figure P5.7.7.1 where $\alpha = -1$ is a branch point,

$$I = \frac{1}{2\pi i} \lim_{\substack{\delta\to 0 \\ R\to\infty}} \left\{ \oint_C - \int_{C_R} - \int_{C_\delta} - \int_{\Gamma_+} - \int_{\Gamma_-} \right\} d\alpha\, \frac{e^{\alpha t}}{\sqrt{\alpha+1}}$$

The first integral vanishes since no poles is inside C. By Jordan's Lemma, the second integral vanishes as $R \to \infty$.

$$\lim_{\delta\to 0} \int_{C_\delta} d\alpha\, \frac{e^{\alpha t}}{\sqrt{\alpha+1}} = e^{-t} \lim_{\delta\to 0} \int_\pi^{-\pi} \frac{e^{\delta e^{i\phi}t}}{\sqrt{\delta e^{i\phi}}} \delta e^{i\phi}id\phi = 0$$

On Γ_+, let $\alpha+1 = ue^{i\pi}$, then $\frac{1}{\sqrt{\alpha+1}} = \frac{1}{\sqrt{u}}e^{-i\frac{\pi}{2}} = -i\frac{1}{\sqrt{u}}$

$$\int_{\Gamma_+} d\alpha\, \frac{e^{\alpha t}}{\sqrt{\alpha+1}} = e^{-t} \int_\infty^0 -i\frac{1}{\sqrt{u}} e^{-ut}du = ie^{-t} \int_0^\infty \frac{1}{\sqrt{u}} e^{-ut}du$$

On Γ_-, let $\alpha+1 = ue^{-i\pi}$, then $\frac{1}{\sqrt{\alpha+1}} = \frac{1}{\sqrt{u}}e^{i\frac{\pi}{2}} = i\frac{1}{\sqrt{u}}$

$$\int_{\Gamma_-} d\alpha\, \frac{e^{\alpha t}}{\sqrt{\alpha+1}} = e^{-t} \int_0^\infty i\frac{1}{\sqrt{u}} e^{-ut}du = ie^{-t} \int_0^\infty \frac{1}{\sqrt{u}} e^{-ut}du$$

Therefore

$$I = \frac{1}{\pi}e^{-t}\int_0^\infty \frac{1}{\sqrt{u}}e^{-ut}du = 2\frac{1}{\pi}e^{-t}\int_0^\infty e^{-y^2 t}dy = \sqrt{\frac{1}{\pi t}}e^{-t}$$

P5.7.4

On the top Riemann sheet, $Res. = \lim_{\alpha \to -1}\sqrt{\alpha} = e^{i(4m+1)\pi/2} = i$.
On the bottom Riemann sheet $Res. = \lim_{\alpha \to -1}\sqrt{\alpha} = e^{i(4m+3)\pi/2} = -i$.

P5.7.8

(a) $\epsilon^*(\omega) = \epsilon(-\omega)$.

(b) $\epsilon_R(\omega) - \epsilon_\infty = \frac{1}{\pi}PV\int_{-\infty}^\infty d\alpha\frac{\epsilon_I(\alpha)}{\alpha - \omega}$ $\epsilon_I(\omega) = -\frac{1}{\pi}PV\int_{-\infty}^\infty d\alpha\frac{\epsilon_R(\alpha)-\epsilon_\infty}{\alpha - \omega} + \frac{\sigma}{\omega}$

(c) Choose the integration path along the real α axis to be indented below $\alpha = 0$ and above $\alpha = \omega$. The residues are calculated in the same way as in part (b). However, the residue at $\alpha = 0$ should be multiplied by πi instead of $-\pi i$. In addition, there will be $2\pi i$ times the residue at $\alpha = 0$ because the contour now encloses the pole $\alpha = 0$. After cancellation, we get the same results. Similarly, if the contour is indented below $\alpha = \omega$ and above $\alpha = 0$ or indented below both $\alpha = 0$ and $\alpha = \omega$, we still get the same results.

P5.7.9

The saddle point is at $\alpha = \pi$. We let $-s^2 = i(\cos\alpha + 1)$ such that $s = 0$ at $\alpha = \pi$. Along the SDP, $-s^2 = \sin\alpha_R\sinh\alpha_I$ is positive real.

$$H_\nu^{(2)}(\xi) = \frac{1}{\pi}e^{-i(\xi+\nu\pi/2)}\int_{-\infty}^\infty ds\frac{d\alpha}{ds}e^{i\nu\alpha}e^{-\xi s^2}$$

Since contributions to the integral come from near the saddle point $\alpha = \pi$ and $\frac{d\alpha}{ds} = \sqrt{2}\,e^{i\pi/4}$, where s is a real variable. The integral becomes, near $\alpha \approx 0$,

$$H_\nu^{(2)}(\xi) \approx \frac{\sqrt{2}}{\pi}e^{-i(\xi-\nu\pi/2)}\int_{-\delta}^\delta ds\, e^{i\pi/4}e^{-\xi s^2} \approx \sqrt{\frac{2}{\pi\xi}}e^{-i(\xi-\nu\pi/2-\pi/4)}$$

P5.7.10

Let $y = x/n$ and $y^n = e^{n\,lny}$,

$$n! = \int_0^\infty dynn^n e^{n(lny-y)}$$

$lny - y \approx -1 + -1/2(y-1)^2$. Let $s = \sqrt{n/2}(y-1)$, we find $n! = n^{n+1/2}e^{-n}\sqrt{2\pi}$.

P5.7.11

We set $y = \alpha x$, and find

$$I(\alpha) = \int_0^\infty \frac{\alpha^{\alpha+1} x^\alpha e^{-\alpha x}}{1 + \alpha x} \, dx = \alpha^{\alpha+1} \int_0^\infty \frac{1}{1 + \alpha x} e^{\alpha(-x + \ln x)} \, dx$$

Obviously, in the interval of integration, the integrand is well behaved; it has value 1 at $x = 0$ and decays to zero at $x \to \infty$. The maximum value of the integrand as $\alpha \to \infty$ occurs at $x = 1$ where the exponential function assumes maximum value. The Laplace method claims that most of the contribution to the integral comes from near this point $x = 1$. Expanding the function in the exponential around $x = 1$, we find

$$I(\alpha) \approx \frac{\alpha^{\alpha+1} e^{-\alpha}}{1 + \alpha} \int_{-\infty}^\infty e^{-\alpha y^2/2} \, dy = \sqrt{2\pi\alpha} \, \frac{\alpha^\alpha}{1 + \alpha} e^{-\alpha}$$

P5.7.12

Let $F(\alpha) = 1$ and $f(\alpha) = i\alpha - \alpha^2/\xi$. The saddle point is at $\alpha_o = i\xi/2$

$$I(\xi) = F(\alpha_o) e^{\xi f(\alpha_o)} \sqrt{\frac{2\pi}{-\xi f''}} = \sqrt{\pi} e^{-\xi^2/4}$$

The exact solution can be obtained by changing integration variable to $u = \alpha - i\xi/2$.

P5.7.13

(a) When α_R is a constant, we find

$$\frac{k_{\rho R}^2}{(k \sin \alpha_R)^2} - \frac{k_{\rho I}^2}{(k \cos \alpha_R)^2} = 1$$

This is a confocal hyperbola with $\sin^2 \alpha_R + \cos^2 \alpha_R = 1$.

(b) When α_I is a constant, we find

$$\frac{k_{\rho R}^2}{(k \cosh \alpha_I)^2} + \frac{k_{\rho I}^2}{(k \sinh \alpha_I)^2} = 1$$

This is a confocal ellipse with $\cosh^2 \alpha_R - \sinh^2 \alpha_R = 1$.

(c) From the tangential equations at any point (x_0, y_0) for the ellipse and the hyperbola, we can easily prove that they are perpendicular, because the set on the α plane can map the entire range of $-\infty < k_{\rho R} < \infty$, and $-\infty < k_{\rho I} < \infty$. Hence, it is the image of the entire k_ρ plane.

P5.7.14

(a)

$$
I(r) \sim \left[A(\theta_0) \sqrt{\frac{2k}{i\pi r}} \left\{ 1 - \frac{i}{8kr\sin^2\theta_0} \right\} + O(r^{-5/2}) \right] e^{ikr} \sqrt{\frac{2\pi}{ikr}}
$$

$$
\cdot \left\{ 1 - \frac{i}{2kr} \left[\frac{A''(\theta_0)}{A(\theta_0)} + \frac{A'(\theta_0)}{A(\theta_0)} \cot\theta_0 - \frac{1}{4\sin^2\theta_0} + O(r^{-1}) \right] \right\}
$$

$$
\sim \sqrt{\frac{2}{i}} \frac{e^{ikr}}{r} \left\{ A(\theta_0) - \frac{i}{2kr} [A''(\theta_0) + A'(\theta_0)\cot\theta_0] \right\} + O(r^{-3})
$$

(b) Let $A(\theta) \equiv 1$ then all the higher-order terms vanish. We have

$$
\frac{e^{ikr}}{r} = \frac{i}{2} \int_{-\infty}^{\infty} dk_\rho \, \frac{k_\rho}{k_z} H_0^{(1)}(k_\rho\rho) e^{ik_z z}
$$

(c) $\frac{e^{ikr}}{r} = \frac{i}{2} \int_{-\infty}^{\infty} dk_z \, H_0^{(1)}(k_\rho\rho) e^{ik_z z}$. On the other hand

$$
\tilde{g}(k_z, \rho) = \frac{i}{4} H_0^{(1)}(k_\rho\rho) = \frac{1}{4\pi} \int_{-\infty}^{\infty} dz \, \frac{e^{ikr}}{r} e^{-ik_z z}
$$

By letting $k_z = 0, \ k_\rho \to k$, we have

$$
H_0^{(1)}(k\rho) = \frac{1}{\pi i} \int_{-\infty}^{\infty} dz \, \frac{e^{ikr}}{r}
$$

To recover the Sommerfeld's identity in part (b), let's deform the integration along the real k_z path of the integral for $g(\overline{r})$ around the Sommerfeld's branch cut of $\text{Im}(k_\rho) = 0$ in the k_z plane. Sommerfeld's branch cut of $\text{Im}(k_\rho) = 0 \ \Rightarrow \ k_{zR}k_{zI} = 0$ and $k^2 - k_{zR}^2 + k_{zI}^2 > 0$. Make the change of variable $k_\rho = \sqrt{k^2 - k_z^2} \ \Rightarrow \ dk_\rho = -\frac{k_z}{k_\rho} dk_z$. We have $k_\rho^2 = (k^2 - k_{zR}^2 + k_{zI}^2) - 2ik_{zR}k_{zI}$. Thus, on the upper Riemann sheet of the k_z plane, the Sommerfeld branch cut corresponds to the real k_ρ axis running from $k_\rho \to -\infty$ to $k_\rho \to -\infty$
• Path L corresponds to the real axis in k_ρ plane
• Point A corresponds to $k_\rho \to +\infty$
• Point B corresponds to $k_\rho \to -\infty$

$$
\frac{e^{ikr}}{r} = \frac{i}{2} \int_{-\infty}^{\infty} dk_z \, H_0^{(1)}(k_\rho\rho) e^{ik_z z}
$$

$$
= \frac{i}{2} \left\{ \int_{R_1} + \int_{R_2} + \int_L \right\} dk_z \, H_0^{(1)}(k_\rho\rho) e^{ik_z z}
$$

Note that the above deformation is for $z > 0$ due to the convergence condition. By Jordan's lemma

$$\left\{\int_{R_1} + \int_{R_2}\right\} dk_z \, H_0^{(1)}(k_\rho\rho)e^{ik_z z} = 0$$

Now, to take care of the integration along path L, let's make the change of variable $k_\rho = \sqrt{k^2 - k_z^2} \Rightarrow dk_\rho = -\frac{k_z}{k_\rho}dk_z$. We have

$$k_\rho^2 = (k^2 - k_{zR}^2 + k_{zI}^2) - 2ik_{zR}k_{zI}$$

Using the above change of variables, we obtain

$$\frac{e^{ikr}}{r} = \frac{i}{2}\int_L dz H_0^{(1)}(k_\rho\rho)e^{ik_z z} = \frac{i}{2}\int_\infty^{-\infty} -\frac{k_\rho}{k_z}dk_\rho H_0^{(1)}(k_\rho\rho)e^{ik_z z)}$$

$$= \frac{i}{2}\int_{-\infty}^{\infty} dk_\rho \frac{k_\rho}{k_z} H_0^{(1)}(k_\rho\rho)e^{ik_z z}$$

For $z < 0$, use similar procedure with appropriate convergence condition to prove the identity.

6

THEOREMS OF WAVES AND MEDIA

6.6 Quantization of Electromagnetic Waves

A. Uncertainty Principle

B. Annihilation and Creation Operators

C. Wave Quantization in Bianisotropic Media

Answers

6.1   Equivalence Principle

When we are interested in a limited region of space, we can replace all
uninteresting regions outside this space by using equivalent sources.
We can place equivalent sources in the uninteresting regions, or we
can place equivalent current sheets on the boundaries of the region of
interest. The equivalent sources are by no means unique, and there
are many different ways of constructing them. We need to make sure
that all boundary conditions are satisfied and that the original fields
and sources in the region of interest are preserved. When two different
specifications of sources give the same solution in the region of inter-
est (they certainly will give different solutions outside the region of
interest), the two problems are called *equivalent*.

 With the various choices of equivalent sources outside and on the
boundaries of interested regions, it must be appreciated that magnetic
sources are useful concepts, although in reality they may not exist. We
add an equivalent magnetic source $\overline{M}$ to Faraday's law:
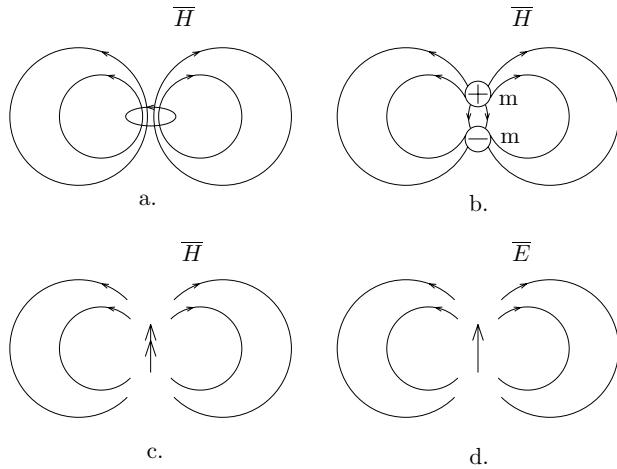
$$\nabla \times \overline{H} = -i\omega\overline{D} + \overline{J} \qquad\qquad (6.1.1)$$
$$\nabla \times \overline{E} = i\omega\overline{B} - \overline{M} \qquad\qquad (6.1.2)$$

The added magnetic source is denoted as $\overline{M}$. Similar to the boundary
condition for tangential magnetic fields of $\hat{n} \times \delta\overline{H} = \overline{J}_s$, the boundary
condition for tangential electric fields becomes $-\hat{n} \times \delta\overline{E} = \overline{M}_s$.

A. Electric and Magnetic Dipole Sources

A small current loop [Fig. 6.1.1a] can be viewed as a magnetic dipole
[Fig. 6.1.1b] if the loop is enclosed by a small volume and we are not
interested in the interior of the volume. A current loop and a mag-
netic dipole yield identical results outside the small volume containing
the loop and the dipole; only when one penetrates the interior of the
sources can one distinguish a current loop from a magnetic dipole. In
the interior the magnetic fields of a loop and a magnetic dipole point
in opposite directions. Just as electric dipoles constitute the build-
ing blocks of electric current sources, the magnetic dipoles constitute
the building blocks of magnetic current sources. We denote a magnetic
dipole with a double arrow [Fig. 6.1.1c] as opposed to an electric dipole
which is denoted with a single arrow [Fig. 6.1.1d].

Figure 6.1.1 The equivalence of a. A small current loop, and b. A magnetic dipole. c. A magnetic dipole denoted with a double arrow. d. An electric dipole denoted with a single arrow.

B. Image Sources

Consider the elementary dipole sources placed in front of a perfect conductor as shown in Figure 6.1.2a. To find solutions in the region of interest, which is the half-space in front of the conductor, we may replace the plane conductor with the images of the dipoles. The image sources thus obtained must satisfy the boundary condition of a zero tangential electric field at the conducting surface. To obtain the image for an electric dipole, we note that the single arrow starts at a negative charge and stops at a positive charge, and that the image of a positive charge is a negative charge and vice versa. To obtain the image for a magnetic dipole, which is representable by a current loop, we note that the image of a moving positive charge is a moving negative charge. The images of the four dipoles shown in Figure 6.1.2a are illustrated in Figure 6.1.2b. Notice that with the aid of the image sources, the solution is valid only in the region of interest and does not hold in the image region where the solution should be zero, because it is occupied by the perfect conductor.

As a dual situation we may define a magnetic conductor on the surface of which the tangential magnetic field vanishes. We use wiggly lines to denote a magnetic conductor [Fig. 6.1.3a]. The images of the elementary dipole sources are shown in Figure 6.1.3b.
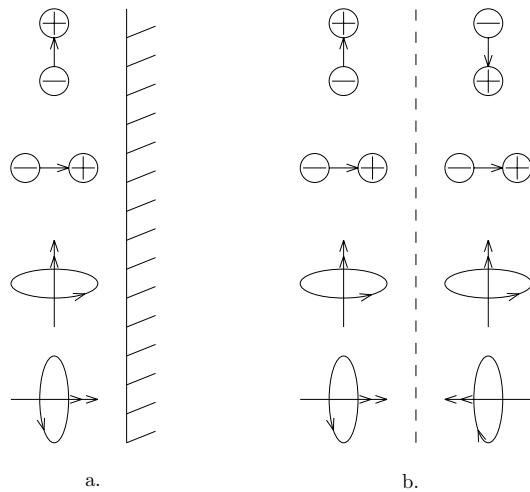
Figure 6.1.2 a. Dipole sources in front of an electric conductor. b. Image sources.
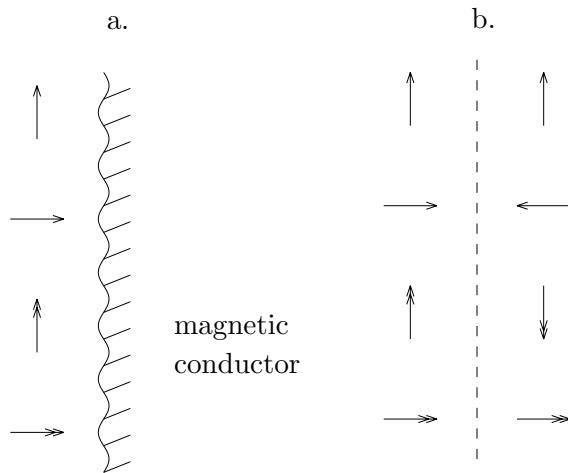
Figure 6.1.3 a. Dipole sources in front of a magnetic conductor. b. Image sources.

As a final example of the image method, consider an electric dipole placed between a pair of parallel conducting plates as shown in Figure 6.1.4a. In order to satisfy the boundary conditions at the surfaces of the two plates, we must have multiple image sources as shown in Figure 6.1.4b. The solutions thus obtained are valid only inside the region between the two plates.

a.

b.
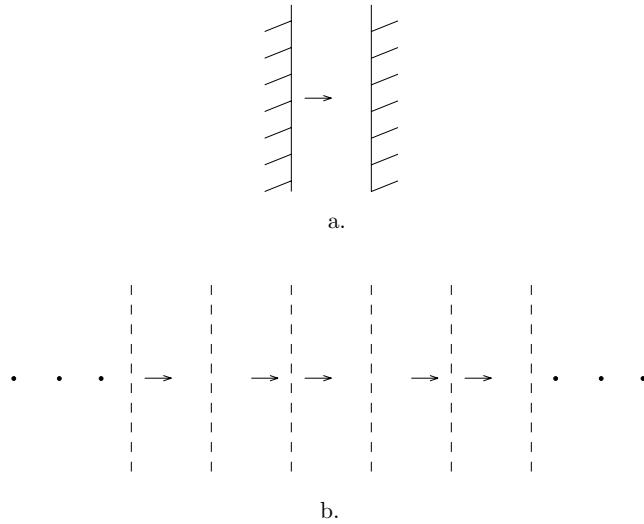
Figure 6.1.4 a. Dipole between two electric conductors. b. Image sources.

C. Electric and Magnetic Current Sheets

When surface boundaries are replaced by equivalent sources, both electric and magnetic current sheets are required. The electric current sheets $\overline{J}_s$ are produced by discontinuities in tangential magnetic field components across the boundary

$$\overline{J}_s = \hat{n} \times \delta\overline{H}$$

where $\hat{n}$ is the surface normal and $\delta\overline{H}$ is the difference between magnetic field components across the boundary. The magnetic surface current sheets are produced by discontinuities in tangential electric field components across the boundary

$$\overline{M}_s = -\hat{n} \times \delta\overline{E}$$

Note that, from the definition for $\overline{M}_s$, the circulation of electric fields around $\overline{M}_s$ follows the left-hand rule while the circulation of magnetic fields around $\overline{J}_s$ follows the right-hand rule.

Consider a surface electric current sheet with surface current density $\overline{J}_s = -\hat{x}J_s$ at $z = 0$ [Fig. 6.1.5a]. This current sheet generates
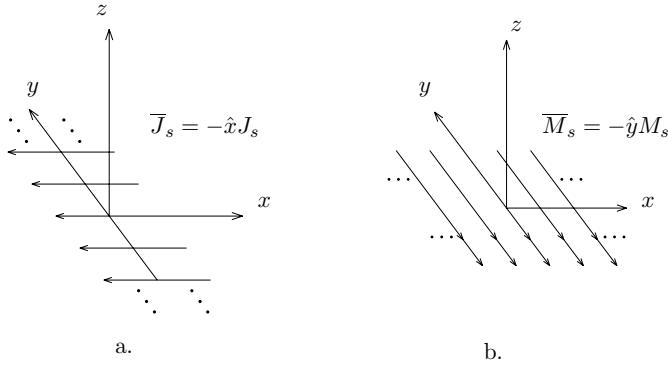
Figure 6.1.5 a. Electric surface currents. b. Magnetic surface currents.

plane waves in both the positive and negative $\hat{z}$ directions

$$\overline{E} = \hat{x}\frac{\eta}{2}J_s e^{ikz}, \qquad \overline{H} = \hat{y}\frac{1}{2}J_s e^{ikz} \qquad z > 0$$

$$\overline{E} = \hat{x}\frac{\eta}{2}J_s e^{-ikz}, \qquad \overline{H} = -\hat{y}\frac{1}{2}J_s e^{-ikz} \qquad z < 0$$

We see that the tangential electric fields are continuous at $z = 0$, and that the discontinuity in tangential magnetic fields on both sides equals the strength of the current sheet, $\hat{n} \times \delta\overline{H} = \overline{J}_s$. Thus, all the boundary conditions are satisfied.

As a dual situation, consider a magnetic surface current sheet $\overline{M}_s = -\hat{y}M_s$ at $z = 0$ [Fig. 6.1.5b]. The boundary condition requires that the tangential magnetic fields be continuous across the boundary and that the discontinuity in tangential electric fields be equal to the strength of the current sheet, $-\hat{n} \times \delta\overline{E} = \overline{M}_s$. The solution is as follows:

$$\overline{E} = \hat{x}\frac{M_s}{2}e^{ikz}, \qquad \overline{H} = \hat{y}\frac{M_s}{2\eta}e^{ikz} \qquad z > 0$$

$$\overline{E} = -\hat{x}\frac{M_s}{2}e^{-ikz}, \qquad \overline{H} = \hat{y}\frac{M_s}{2\eta}e^{-ikz} \qquad z < 0$$

Plane waves are radiated in both positive and negative $\hat{z}$ directions. Note that, by properly choosing the phase of the current sheets, we can generate plane waves in any direction. For instance, let $\overline{J}_s = \hat{x}J_s e^{ik_y y}$; then plane waves with $\overline{k}$ vectors $\overline{k} = \hat{y}k_y + \hat{z}k_z$ and $\overline{k} = \hat{y}k_y - \hat{z}k_z$ are generated. If k_y is larger than k, the waves are evanescent in the $\hat{z}$ directions. Similar arguments apply to magnetic current sheets.

D. Induced and Impressed Current Sheets

It is important to distinguish between the concepts of *induced* and *impressed* current sheets. On the surface of a material body an induced current sheet is physically carried by charged particles attached to the surface of the body, whereas an impressed current sheet is carried by external agents. When a layer of charge or current is impressed along the surface of a body, induced surface charge and current sheets are generated at the surface of the body so that the boundary conditions are satisfied.

EXAMPLE 6.1.1

Consider a plane wave normally incident upon the surface of a perfectly conducting half-space [Fig. E6.1.1.1a]. Let the electric field be $\overline{E} = \hat{x}E_0 e^{ikz}$. An electric current sheet with $\overline{J}_s = \hat{x}2E_0/\eta$ is then induced on the surface of the conductor, and the conductor is replaced by the induced current sheet [Fig. E6.1.1.1b], which radiates into both the $z > 0$ and $z < 0$ half-space. This induced current generates a reflected wave with $\overline{E} = -\hat{x}E_0 e^{-ikz}$, so that at the boundary surface the total electric field is zero. This induced current sheet also generates a plane wave $\overline{E} = -\hat{x}E_0 e^{ikz}$ in the region $z > 0$, which combines with the incident wave to produce zero field inside the conductor.
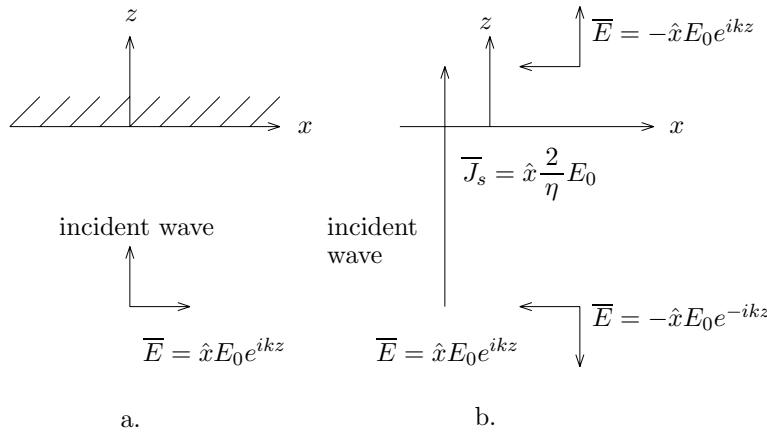
Figure E6.1.1.1 a. Plane wave incident upon a perfect electric conductor. b. Equivalent electric current sheet placed at $z = 0$.

— END OF EXAMPLE 6.1.1 —

EXAMPLE 6.1.2   With the use of equivalent current sheet concepts, we now illustrate several equivalent situations for a plane wave propagating in the $\hat{z}$ direction. Let the electric field be $\hat{x}$ directed:

$$\overline{E} = \hat{x} E_0 e^{ikz}, \qquad \overline{H} = \hat{y} \frac{1}{\eta} E_0 e^{ikz}$$

and let the region of interest be $z > 0$.

Equivalent Problem 1:
    Put an electric current sheet with $\overline{J}_s = -\hat{x} E_0/\eta$ and a magnetic current sheet with $\overline{M}_s = -\hat{y} E_0$; then the same field is preserved for $z > 0$. In the region $z < 0$, there is no field.

Equivalent Problem 2:
    Put an electric current sheet with $\overline{J}_s = -\hat{x} 2 E_0/\eta$; then the same field is preserved for $z > 0$. In the negative $\hat{z}$ direction, a plane wave propagates with $\overline{E} = \hat{x} E_0 e^{-ikz}$.

Equivalent Problem 3:
    Put a magnetic current sheet with $\overline{M}_s = -\hat{y} 2 E_0$; then the same field is preserved for $z > 0$. In the negative $\hat{z}$ direction, a plane wave propagates with $\overline{H} = \hat{y}(E_0/\eta) e^{-ikz}$.

Equivalent Problem 4:
    Replace the region $z < 0$ with a perfect conductor. Place in front of the conductor an electric current sheet with $\overline{J}_s = -\hat{x} E_0/\eta$ and a magnetic current sheet with $\overline{M}_s = -\hat{y} E_0$. The electric current sheet does not generate any field, because an equal and opposite electric current sheet is induced on the surface of the electric conductor and this sheet cancels the impressed $\overline{J}_s$. The magnetic current sheet generates the same field for $z > 0$.

Equivalent Problem 5:
    For a dual situation, we place the same electric and magnetic current sheets as in Equivalent Problem 4 in front of a magnetic conductor. According to a similar argument, the magnetic current sheet does not generate a field in the positive $\hat{z}$ direction. The electric current sheet generates the same field for $z > 0$.

— END OF EXAMPLE 6.1.2 —

From the above discussions on the equivalence principle, we make the following comments: (i) Solutions to the equivalent problems are *not* applicable in the regions of no interest; examples are the $\overline{H}$ field within the small volumes containing a current loop and a magnetic dipole as shown in Figure 6.1.1. (ii) In the case of the image method we turn an unsolved problem of dipoles radiating in the presence of

conductors into another unsolved problem of dipole arrays. In the case of placing current sheets on the boundaries of the regions of interest, the current sheet values $-\hat{n} \times \delta \overline{E}$ and $\hat{n} \times \delta \overline{H}$ are unknown until the original problem is completely solved. So what is the usefulness of the equivalence principle? The equivalence principle is useful in at least two aspects. First, it enables us to reformulate a problem as in the case of the image method. Second, and more importantly, it provides us with the means of obtaining approximate solutions by approximating source distributions on the surfaces of regions of interest. However, we must note that equivalent source specifications are by no means unique. For instance, we may use the image sources as shown in Figures 6.1.2– 6.1.4, or we may place equivalent currents sheets on the surfaces of the conductors. In the following section we discuss the uniqueness theorem which guarantees, at least in the regions of interest, that the solution is unique.

EXAMPLE 6.1.3   Extinction theorem.
    Consider a plane wave normally incident from region 0 with permittivity ϵ_o and permeability μ_o upon a half-space medium with permittivity ϵ and permeability μ. The boundary surface is at $z = 0$ and the incident fields are

$$E_y = E_0 e^{-ikz}$$

$$H_x = \frac{1}{\eta} E_0 e^{-ikz}$$
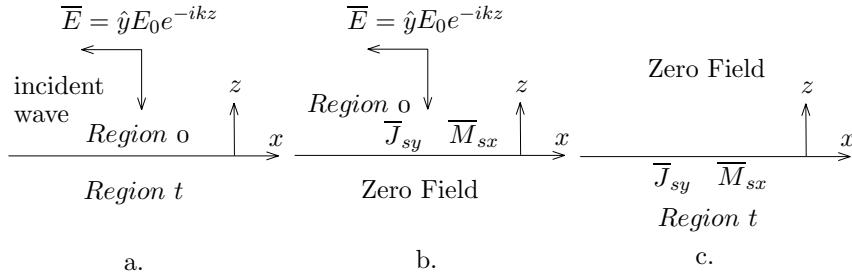
(a) Find the total electric and magnetic fields in both Regions 0 and 1. Determine the values of the induced currents sheets corresponding to the fields at $z = 0^+$ and $z = 0^-$.
(b) Place the obtained surface current sheets at $z = 0^+$. Find the total electric fields in Regions 0. In Region 1, show that the field generated by the surface current sheets together with the incident field added up to zero.
(c) Place the obtained surface current sheets at $z = 0^-$. Find the total electric fields in Regions 0 and 1. Show that the surface current sheet generated field in region 0 is zero.

    The extinction of fields in Region 0 due to the current sheets at $z = 0^+$ and the fields in Region 1 due to the current sheets at $z = 0^-$ is a consequence of the extinction theorem resulted from the current sheets obtained from the so-called extended boundary conditions.

SOLUTION:
 (a) The fields in Region 0 are

$$E_y = E_0(e^{-ikz} + Re^{ikz}) \qquad H_x = \frac{E_0}{\eta}(e^{-ikz} - Re^{ikz})$$

$\overline{E} = \hat{y}E_0 e^{-ikz}$

$\overline{E} = \hat{y}E_0 e^{-ikz}$

incident
wave

Zero Field

Region 0

Region 0 $\overline{J}_{sy}$ $\overline{M}_{sx}$

Region t

Zero Field

$\overline{J}_{sy}$ $\overline{M}_{sx}$

Region t

a.

b.

c.

Figure E6.1.1.1 Extinction Theorem a. Plane wave incident upon a boundary surface. b. Incident wave and equivalent electric and magnetic current sheets placed in Region 0. c. Equivalent electric and magnetic current sheets placed in Region t.

The fields in Region 1 are

$$E_y = E_0(1 + R)e^{-ik_t z} \qquad H_x = \frac{E_0}{\eta_t}(1 + R)e^{-ik_t z}$$

where $R = (\eta_t - \eta)/(\eta_t + \eta)$, $\eta = \sqrt{(\mu/\epsilon)}$, and $\eta_t = \sqrt{(\mu_t/\epsilon_t)}$. The induced surface current sheets at $z = 0^+$ are obtained from the fields in Region 0:

$$J_{sy} = \frac{E_0}{\eta}(1 - R) \qquad M_{sx} = E_0(1 + R)$$

The induced surface current sheets at $z = 0^-$ are obtained from the fields in Region 1:

$$J_{sy} = -\frac{E_0}{\eta_t}(1 + R) \qquad M_{sx} = -E_0(1 + R)$$

(b) In Region 0

$$E_y = E_0 e^{-ikz} + E_0[\frac{1}{2}(1 + R) - \frac{1}{2}(1 - R)]e^{ikz}$$

$$= E_0 e^{-ikz} + RE_0 e^{ikz}$$

$$H_x = \frac{E_0}{\eta}e^{-ikz} + \frac{E_0}{\eta}[-\frac{1}{2}(1 + R) + \frac{1}{2}(1 - R)E_0]e^{ikz}$$

$$= \frac{1}{\eta}E_0 e^{-ikz} - \frac{1}{\eta}RE_0 e^{ikz}$$

In Region 1

$$E_x = E_0 e^{-ikz} + E_0[-\frac{1}{2}(1 + R) - \frac{1}{2}(1 - R)]e^{-ikz} = 0$$

$$H_y = \frac{1}{\eta}E_0 e^{-ikz} + \frac{E_0}{\eta}[-\frac{1}{2}(1 + R) - \frac{1}{2}(1 - R)]e^{-ikz} = 0$$

(c) In Region 0

$$E_y = E_0[\frac{1}{2}(1+R) - \frac{1}{2}(1+R)]e^{ikz} = 0$$

$$H_x = \frac{E_0}{\eta}[-\frac{1}{2}(1+R) + \frac{1}{2}(1+R)E_0]e^{ikz} = 0$$

In Region 1

$$E_x = E_0[\frac{1}{2}(1+R) + \frac{1}{2}(1+R)]e^{-ik_t z} = E_0(1+R)e^{-ik_t z}$$

$$H_y = \frac{E_0}{\eta_t}[\frac{1}{2}(1+R) + \frac{1}{2}(1+R)]e^{-ik_t z} = \frac{E_0}{\eta_t}(1+R)e^{-ik_t z}$$

— END OF EXAMPLE 6.1.3 —

EXAMPLE 6.1.4   Hällén's integral equation.
    In the following, we obtain Hällén's integral equation for a thin linear dipole antenna, and show that the current on the antenna is approximately sinusoidal. First set up an equivalent problem in which $\overline{E} = 0$ and $\overline{H} = 0$ inside the surface S, which is identical to the surface of the conductors of the antenna and $\overline{E}$ and $\overline{H}$ are the same as in the original problem outside S. There are no conducting bodies in the equivalent problem. To accommodate the discontinuity of $\overline{H}_t$ across S, we must impress the surface current $\overline{J}_s$ on the imaginary surface S. This surface current is identical to the induced surface current in the original problem. The electric field along the z axis approaches

$$\overline{E} \to \hat{z}\, V_0 \delta(z) \qquad \text{for} \qquad |a| < l/2$$

as the gap becomes very small. The electric field on the z axis is given by

$$E_z(z)|_{\rho=0} = V_0 \delta(z)$$

$$= i\omega\mu\hat{z} \cdot \left(\overline{\overline{I}} + \frac{\nabla\nabla}{k^2}\right) \int_{-l/2}^{l/2} dz' \cdot \int_0^{2\pi} a\, d\phi' \frac{e^{ik\sqrt{(z-z')^2+a^2}}}{4\pi\sqrt{(z-z')^2+a^2}} \overline{J}_s(z')$$

for $|z| < l/2$. The contribution of the current at the caps of the cylinder is ignored to obtain this last result, which is a good approximation if $a \ll \lambda$ and $a \ll l$. Furthermore, it is reasonable to assume $\overline{J}_s(\overline{r}')$ is along the z axis and $\overline{J}_s$ has no ϕ variation. It follows that $I(z') = 2\pi a J_s(z')$.
    With these simplifications, we find

$$E_z = V_0\, \delta(z) = \frac{i\omega\mu}{k^2}\left(k^2 + \frac{d^2}{dz^2}\right)\int_{-l/2}^{l/2} dz' \frac{e^{ik\sqrt{(z-z')^2+a^2}}}{4\pi\sqrt{(z-z')^2+a^2}} I(z')$$
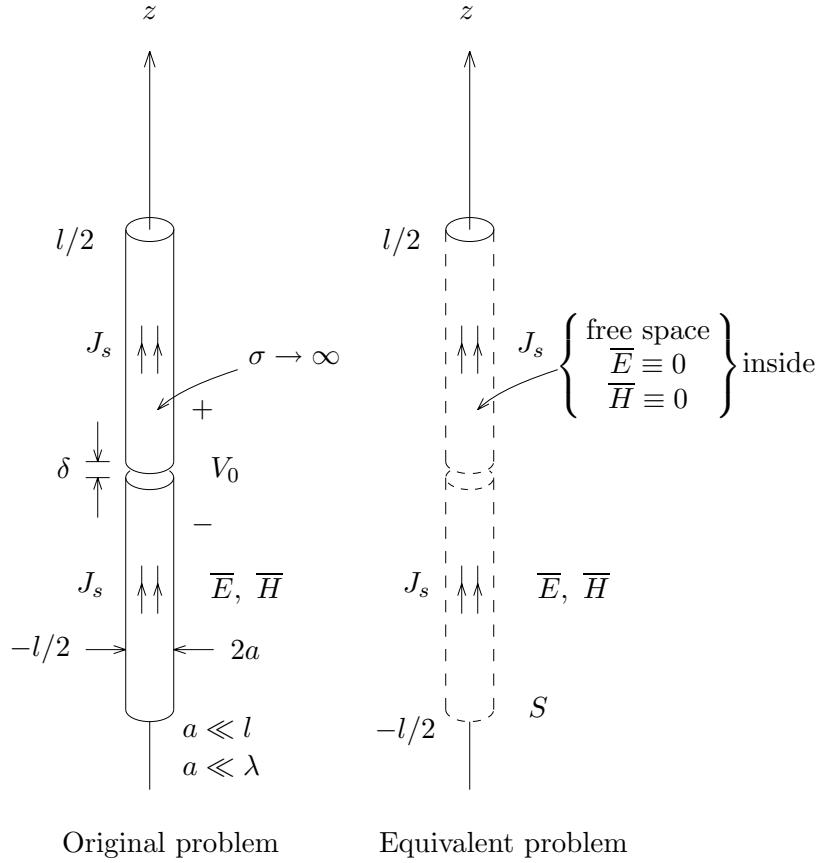
Figure E6.1.4.1

Let

$$A_z(z) = \int_{-\ell/2}^{\ell/2} dz' \, \frac{e^{ik\sqrt{(z-z')^2+a^2}}}{[(z-z')^2+a^2]^{1/2}} I(z')$$

We obtain an ordinary differential equation of the following form:

$$\left(\frac{k^2 V_0}{i\omega\mu}\right)\delta(z) = \left(k^2 + \frac{d^2}{dz^2}\right) A_z(z)$$

Solve this differential equation, we find

$$\frac{i\omega\mu}{k^2} \int_{-l/2}^{l/2} dz' \, \frac{e^{ik\sqrt{(z-z')^2+a^2}}}{4\pi\sqrt{(z-z')^2+a^2}} I(z') = V_0[g(z)+C_1\cos kz + C_2\sin kz]$$

where

$$g(z) = \frac{1}{2ik}e^{ik|z|}$$

is the scalar Green's function of the one-dimensional Helmholtz equation,

$$\left(\frac{d^2}{dz^2} + k^2\right)g(z) = \delta(z)$$

For the case of symmetric excitation, $I(z) = I(-z)$, and $C_2 = 0$. We now obtain the Hällén's integral equation [Hällén, 1938].

$$\int_{-l/2}^{l/2} dz'\ K(z,\, z')I(z') = \frac{4\pi k^2}{i\omega\mu}V_0\left(\frac{e^{ik|z|}}{2ik} + C_1\cos kz\right)$$

where

$$K(z,\, z') = \frac{e^{ik\sqrt{(z-z')^2+a^2}}}{\sqrt{(z-z')^2+a^2}}$$

The kernel $K(z - z')$ is sharply peaked at $z = z'$ (if $a \ll \ell$). The major contribution to the integral comes from the vicinity of the point z on the z' axis. Thus the value of the integral is roughly proportional to $I(z)$.

$$\frac{4\pi k^2}{i\omega\mu}V_0\left(\frac{e^{ik|z|}}{2ik} + C_1\cos kz\right) = I(z)\int_{-\ell/2}^{\ell/2} dz'\ K(z,-z')$$
$$+ \int_{-\ell/2}^{\ell/2} dz'\ K(z-z')[I(z') - I(z)]$$

The second integral on the right hand side can be ignored. So

$$I(z)f(z) \cong \frac{4\pi k^2}{i\omega\mu}V_0\left(\frac{e^{ik|z|}}{2ik} + C_1\cos kz\right)$$

where

$$f(z) \equiv \int_{-\ell/2}^{\ell/2} dz'\ K(z-z') = \int_{-\ell/2}^{\ell/2} dz'\ \frac{e^{ik\sqrt{(z-z')^2+a^2}}}{[(z-z')^2+a^2]^{1/2}}$$

Observe that $|K(z,\, z')|$ is highly peaked at $z = z'$ if $a \ll l$. The function $f(z)$ does not rapidly change, the area under the curves for different z are

close to each other because most of the area is under the peak. As a consequence, $f(z_1) \simeq f(z_2) \simeq f(0)$, a very flat function of z, except at the ends. It is a good approximation to assume that $f(z)$ is constant

$$f(z)I(z) \cong f(0)I(z)$$

Observe that $\lim_{z \to \pm l/2} f(z) \neq 0$, but $f(z)I(z) \to 0$ as $z \to \pm \ell/2$. To evaluate C_1, we impose the condition that $I(\pm l/2) = 0$.

$$I\left(\pm \frac{\ell}{2}\right) = 0 \Rightarrow C_1 = -\frac{e^{ik\ell/2}}{2ik \cos\left(\dfrac{k\ell}{2}\right)}$$

We can now rearrange $I(z)$ into the following form:

$$I(z) \simeq \frac{2kV_0}{i\omega\mu} \frac{\sin(k\,|z| - kl/2)}{f(0)\cos(kl/2)}$$

This is the zero order approximation to the solution of Hällén's integral equation. For more accurate solutions, please refer to [King, 1956].

— End of Example 6.1.4 —

Topic 6.1A Uniqueness Theorem

A given physical situation always leads to one and only one physical solution. However, when formulated in mathematical terms, if not properly done, the problem may lead to many acceptable solutions with underprescribed boundary conditions, or it may permit no solutions at all with overprescribed boundary conditions. The uniqueness theorem indicates how a problem should be properly formulated mathematically so that there is one and only one solution. For electromagnetic field problems, it states that when the sources and the tangential electric *or* magnetic fields are prescribed over the whole boundary surface of a given region, the solution within this region is unique. The uniqueness theorem is thus a most powerful theorem that enables one to find *the* solution via any expedient means. It is the foundation for the equivalence principle, the Huygens' principle, the image theorem, the induction theorem, Babinet's principle, and almost all frequently used methods in electromagnetism.

To prove the uniqueness theorem, we assume that there are two different solutions for a given set of sources. Let the two solutions be

denoted by $\overline{E}_1$ and $\overline{H}_1$, and $\overline{E}_2$ and $\overline{H}_2$. Let the differences be $\delta\overline{E}$ and $\delta\overline{H}$,

$$\delta\overline{E} = \overline{E}_1 - \overline{E}_2$$
$$\delta\overline{H} = \overline{H}_1 - \overline{H}_2$$

Since both field solutions satisfy the Maxwell equations with the same sources, their differences satisfy the source-free Maxwell equations

$$\nabla \times \delta\overline{E} = i\omega\mu\,\delta\overline{H} \tag{6.1A.1a}$$
$$\nabla \times \delta\overline{H} = -i\omega\epsilon\,\delta\overline{E} \tag{6.1A.1b}$$

The proof of the theorem hinges on the assumption that the permittivity ϵ and the permeability μ of the medium have a small imaginary part. Assume the medium is slightly lossy, namely μ and ϵ have a small positive imaginary part,

$$\epsilon = \epsilon_R + i\epsilon_I$$
$$\mu = \mu_R + i\mu_I$$

where ϵ_R, ϵ_I, μ_R and μ_I are real. The proof also holds when the imaginary parts are both negative.

Dot-multiply (6.1A.1a) with $\delta\overline{H}^*$ and (6.1A.1b)* with $\delta\overline{E}$. Subtracting, we obtain

$$\nabla \cdot (\delta\overline{E} \times \delta\overline{H}^*) = i\omega\mu \left|\delta\overline{H}\right|^2 - i\omega\epsilon^* \left|\delta\overline{E}\right|^2 \tag{6.1A.2}$$

The complex conjugate of (6.1A.2) gives

$$\nabla \cdot (\delta\overline{E}^* \times \delta\overline{H}) = -i\omega\mu^* \left|\delta\overline{H}\right|^2 + i\omega\epsilon \left|\delta\overline{E}\right|^2 \tag{6.1A.3}$$

Adding (6.1A.2) and (6.1A.3) and integrating over the volume V enclosed by the surface S, we find

$$\oiint_S d\overline{S} \cdot (\delta\overline{E} \times \delta\overline{H}^* + \delta\overline{E}^* \times \delta\overline{H})$$
$$= -2\omega \iiint_V dV \left(\mu_I \left|\delta\overline{H}\right|^2 + \epsilon_I \left|\delta\overline{E}\right|^2 \right) \tag{6.1A.4}$$

The right-hand side of (6.1A.4) is a negative number. It will be zero if and only if $\delta\overline{H}$ and $\delta\overline{E}$ are identically zero in the region V.

The solution will be unique and $\overline{E}_1 = \overline{E}_2$ and $\overline{H}_1 = \overline{H}_2$ when the left-hand side of (6.1A.4) is zero, which gives

$$\oiint_S d\overline{S} \cdot (\delta\overline{E} \times \delta\overline{H}^* + \delta\overline{E}^* \times \delta\overline{H}) = 0$$

We conclude that the solution will be unique if either $\delta\overline{E}$ *or* $\delta\overline{H}$ is zero on the enclosed surface S. Thus the boundary conditions can be specified in the following manner: (i) tangential electric field over the whole surface of S, or (ii) tangential magnetic field over the whole surface of S, or (iii) tangential electric field over part of the surface S and tangential magnetic field over the rest of S. If both tangential electric and magnetic fields are specified over any part of S, they must be compatible with each other.

Topic 6.1B Duality and Complementarity

Corresponding to the electric current $\overline{J}$ in Ampère's law, a magnetic current $-\overline{M}$ can be added to Faraday's law. The Maxwell equations with both the electric and magnetic current terms read:

$$\nabla \times \overline{H} = -i\omega\epsilon\overline{E} + \overline{J} \qquad (6.1\text{B}.1)$$
$$\nabla \times \overline{E} = i\omega\mu\overline{H} - \overline{M} \qquad (6.1\text{B}.2)$$

The justification of the magnetic current $\overline{M}$ has been carried out with the use of the equivalence principle and is reiterated as follows. First, (6.1B.1) and (6.1B.2) govern *macroscopic* electromagnetic fields under time-harmonic excitations. From the macroscopic point of view, a small current loop acts like a magnetic dipole. As long as one is restricted from penetrating the loop, the fields outside the volume bounding the loop are exactly the dual of those due to a small electric dipole. The fields can be solved in exactly the same manner as in the electric case by neglecting $\overline{J}$ and retaining $\overline{M}$. Second, when (6.1B.1) and (6.1B.2) are applied to a limited region in space, the bounding surfaces of the regions can be viewed as supporting surface electric currents due to discontinuities in tangential magnetic field and surface magnetic currents due to discontinuities in tangential electric field. In fact, in the above discussion of dipole sources, we are limited to the space outside the

volume occupied by the dipoles. If (6.1B.1) and (6.1B.2) are assumed to be valid in all space, then the existence of magnetic monopoles is implied.

Equations (6.1B.1) and (6.1B.2) are now duals of each other. If we make the following replacements:

$$\overline{E} \to \overline{H}$$
$$\overline{H} \to -\overline{E}$$
$$\mu \to \epsilon$$
$$\epsilon \to \mu$$
$$\overline{J} \to \overline{M}$$
$$\overline{M} \to -\overline{J}$$

then (6.1B.1) becomes (6.1B.2) and (6.1B.2) becomes (6.1B.1). The symbolic replacements can further be quantified by equating numerically the left-hand side and the right-hand side of the arrows. When such equalities are established, however, the dual of free space will become a medium with permittivity $4\pi \times 10^{-7}$ f/m and with permeability 8.854×10^{-12} h/m, an undesirable situation for the study of antenna problems.

The duality principle that is suitable for antenna and radiation problems in free space is established by the following equalities:

$$\overline{E} = \eta\overline{H} \qquad\qquad (6.1B.3)$$
$$\overline{H} = -\overline{E}/\eta \qquad\qquad (6.1B.4)$$
$$\overline{J} = \overline{M}/\eta \qquad\qquad (6.1B.5)$$
$$\overline{M} = -\eta\overline{J} \qquad\qquad (6.1B.6)$$

where $\eta = (\mu/\epsilon)^{1/2}$. Clearly under such substitutions, (6.1B.1) becomes (6.1B.2) and (6.1B.2) becomes (6.1B.1). There is no need to replace free space with a different medium. Note that this duality formalism is not applicable to complicated material such as anisotropic and bianisotropic media.

As an example of the application of the duality principle, we shall find a relationship between impedances of complementary metal and aperture antennas. We consider a plane conductor that is cut to make a metal antenna and an aperture antenna complementary to each other
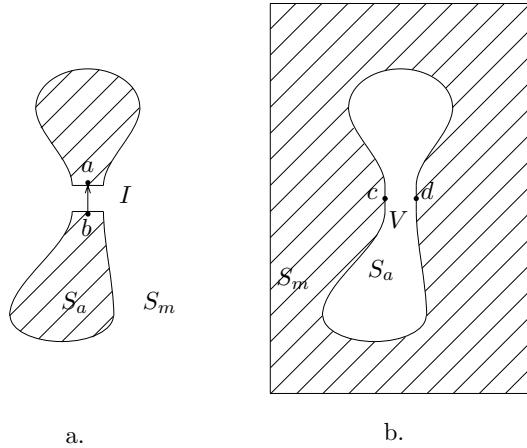
Figure 6.1B.1   a. Metal antenna, and b. Aperture antenna, which are complementary structures.

as shown in Figure 6.1B.1. The input impedance of the metal antenna in Figure 6.1B.1a is

$$Z_m = \frac{-\int_b^a d\bar{l} \cdot \overline{E}_m}{\oint_{cd} d\bar{l} \cdot \overline{H}_m} = \frac{-\int_b^a d\bar{l} \cdot \overline{E}_m}{2 \int_c^d d\bar{l} \cdot \overline{H}_m} \qquad (6.1B.7)$$

where we have assumed that $\overline{E}_m$ is pointing from a to b and $\overline{H}_m$ from c to d. The second equality follows from the fact that tangential magnetic fields are equal and opposite on both sides of the path $c\,d$.

Similarly, the input impedance of the aperture antenna is

$$Z_a = \frac{-\int_c^d d\bar{l} \cdot \overline{E}_a}{\oint_{ab} d\bar{l} \cdot \overline{H}_a} = \frac{\int_c^d d\bar{l} \cdot \overline{E}_a}{2 \int_b^a d\bar{l} \cdot \overline{H}_a} \qquad (6.1B.8)$$

where we assume the dual situation with $\overline{H}_a$ pointing from a to b and $\overline{E}_a$ from d to c.

The two impedances are related by duality properties of the Maxwell equations. The boundary-value problem for the metal antenna is to solve

$$\left(\nabla^2 + \omega^2 \mu \epsilon\right) \overline{E}_m = 0 \qquad (6.1B.9)$$

with boundary conditions

$$\begin{aligned} \hat{n} \times \overline{E}_m = 0 \qquad &\text{on} \quad S_a \\ \hat{n} \times \overline{H}_m = 0 \qquad &\text{on} \quad S_m \end{aligned} \qquad (6.1B.10)$$

where

$$\overline{H}_m = \frac{1}{i\omega\mu}\nabla \times \overline{E}_m \qquad (6.1\text{B}.11)$$

and $\hat{n}$ is the normal to the plane conductor. Note that the second boundary condition in (6.1B.10) can be understood by imagining that the surface currents on the metal are composed of elementary current sources with magnetic field having only components perpendicular to S_m.
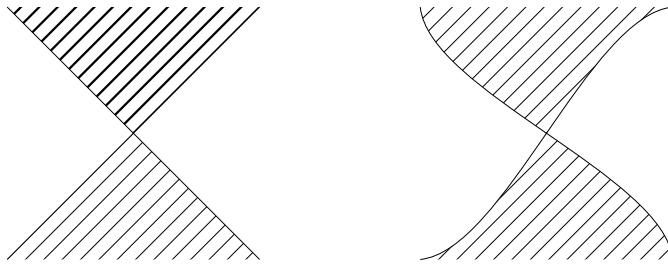
Figure 6.1B.2 Broadband structures.

For the aperture antenna problem, we have to solve

$$\left(\nabla^2 + \omega^2\mu\epsilon\right)\overline{H}_a = 0 \qquad (6.1\text{B}.12)$$

with boundary conditions

$$\begin{aligned}
\hat{n} \times \overline{H}_a &= 0 \qquad \text{on} \quad S_a \\
\hat{n} \times \overline{E}_a &= 0 \qquad \text{on} \quad S_m
\end{aligned} \qquad (6.1\text{B}.13)$$

where

$$\overline{E}_a = -\frac{1}{i\omega\epsilon}\nabla \times \overline{H}_a \qquad (6.1\text{B}.14)$$

The two problems are mathematically dual with the following replacements:

$$\overline{E}_m = \eta\overline{H}_a \qquad (6.1\text{B}.15)$$

$$\overline{H}_m = -\frac{1}{\eta}\overline{E}_a \qquad (6.1\text{B}.16)$$

We find from (6.1B.7) and (6.1B.8)

$$Z_m Z_a = \left(\frac{-\int_b^a \eta\overline{H}_a \cdot d\bar{l}}{-2\int_c^d \frac{1}{\eta}\overline{E}_a \cdot d\bar{l}}\right)\left(\frac{\int_c^d \overline{E}_a \cdot d\bar{l}}{2\int_b^a \overline{H}_a \cdot d\bar{l}}\right) = \frac{\eta^2}{4} \qquad (6.1\text{B}.17)$$
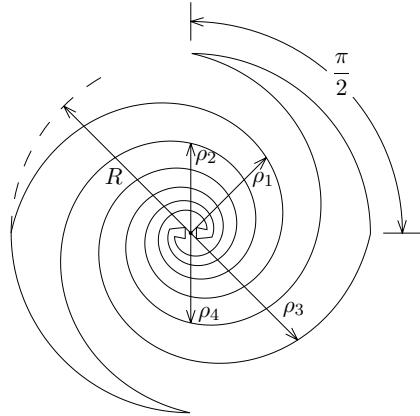
Figure 6.1B.3 Planar equiangular spiral antenna.

Thus, the product of the input impedances of two planar complementary antennas is one-quarter of the square of the characteristic impedance of the free space.

As an example, consider the structures shown in Figures 6.1B.2, where the structure and its complement are identical. It follows that such antennas have input impedance $\eta/2 = 188.5$ ohms. Because the input impedance is independent of frequency, such antennas are ideal broadband antennas. Another self-complementary antenna is shown in Figure 6.1B.3. The four edges of the metal are described by the equations $\rho_1 = \rho_0 e^{a\phi}$, $\rho_2 = \rho_0 e^{a(\phi-\pi/2)}$, $\rho_3 = \rho_0 e^{a(\phi-\pi)}$ and $\rho_4 = \rho_0 e^{a(\phi-3\pi/2)}$, where a is the rate of expansion of the spiral. The structure is known as a planar equiangular spiral antenna.

EXAMPLE 6.1.5 Babinet's principle.

Babinet's principle is another example of duality and complementarity that relates the problem of diffraction by planar apertures to the problem of scattering by its complementary structure. Consider an infinite plane conductor with an aperture as shown in Figure E6.1.5.1a and the complementary structure consisting of the removed plane metal in the formation of the aperture as shown in Figure E6.1.5.1b. Let there be dual sources on the left-hand sides of Figures E6.1.5.1a and E6.1.5.1b. In the absence of the screens, they produce incident fields such that

$$\overline{E}_2^{\,i} = \eta \overline{H}_1^{\,i} \tag{E6.1.5.1a}$$
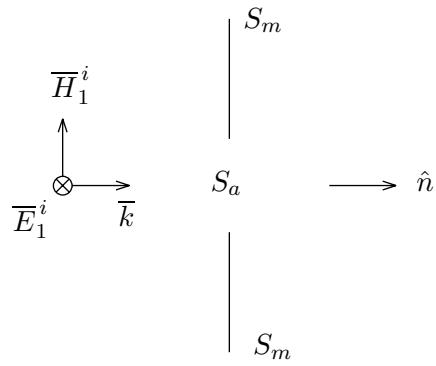
Figure E6.1.5.1a
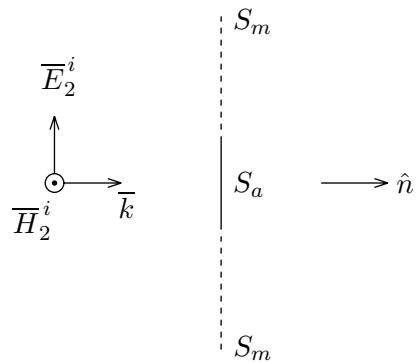
Figure E6.1.5.1b
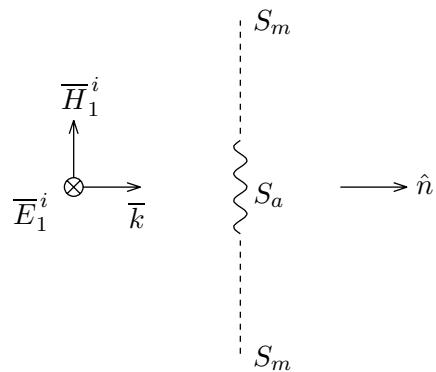
Figure E6.1.5.1c Complementarity and duality for Babinet's principle.

$$\overline{H}_2^i = -\overline{E}_1^i/\eta \qquad\qquad (\text{E6.1.5.1}b)$$

Note that in the presence of the screens the sources are located on the left-hand side.

Now we formulate the problems for the fields on the right-hand sides of the screens. For the problem in Figure E6.1.5.1a, the fields satisfy the Maxwell equations

$$\nabla \times \overline{E}_1 = i\omega\mu\overline{H}_1 \qquad\qquad (\text{E6.1.5.2}a)$$
$$\nabla \times \overline{H}_1 = -i\omega\epsilon\overline{E}_1 \qquad\qquad (\text{E6.1.5.2}b)$$

subject to the boundary conditions

$$\hat{n} \times \overline{E}_1 = 0 \qquad \text{on} \quad S_m \qquad (\text{E6.1.5.3}a)$$
$$\hat{n} \times \overline{H}_1 = \hat{n} \times \overline{H}_1^i \qquad \text{on} \quad S_a \qquad (\text{E6.1.5.3}b)$$

where $\hat{n}$ is the normal to the plane surface. The first boundary condition warrants that tangential electric field vanishes on the conducting surface. The second condition is due to the fact that induced surface currents on the metal surface produce no tangential magnetic field component at the aperture space. The field to the right-hand side of the screen is produced by the equivalent current sheet source on S_a.

For the problem in Figure E6.1.5.1b, the fields on the right-hand side satisfy the Maxwell equations

$$\nabla \times \overline{E}_2 = i\omega\mu\overline{H}_2 \qquad\qquad (\text{E6.1.5.4}a)$$
$$\nabla \times \overline{H}_2 = -i\omega\epsilon\overline{E}_2 \qquad\qquad (\text{E6.1.5.4}b)$$

subject to the boundary conditions

$$\hat{n} \times \overline{H}_2 = \hat{n} \times \overline{H}_2^i \qquad \text{on} \quad S_m \qquad (\text{E6.1.5.5}a)$$
$$\hat{n} \times \overline{E}_2 = 0 \qquad \text{on} \quad S_a \qquad (\text{E6.1.5.5}b)$$

The total fields $\overline{E}_2$ and $\overline{H}_2$ are superpositions of two field solutions:

1. The incident fields $\overline{E}_2^i$ and $\overline{H}_2^i$ in the absence of the screens. They satisfy the source-free Maxwell equations to the right half-space.
2. The scattered fields produced by induced currents on the screens. We denote them by $\overline{E}_2^s$ and $\overline{H}_2^s$.

In terms of the scattered field $\overline{E}_2^s = \overline{E}_2 - \overline{E}_2^i$ and $\overline{H}_2^s = \overline{H}_2 - \overline{H}_2^i$ they satisfy

$$\nabla \times \overline{E}_2^s = i\omega\mu\overline{H}_2^s \qquad\qquad (\text{E6.1.5.6}a)$$
$$\nabla \times \overline{H}_2^s = -i\omega\epsilon\overline{E}_2^s \qquad\qquad (\text{E6.1.5.6}b)$$

subject to the boundary conditions

$$\hat{n} \times \overline{H}_2^s = 0 \qquad\qquad\qquad \text{on} \quad S_m \qquad (\text{E6.1.5.7}a)$$

$$\hat{n} \times \overline{E}_2^s = -\hat{n} \times \overline{E}_2^i = -\hat{n} \times \eta \overline{H}_1^i \qquad \text{on} \quad S_a \qquad (\text{E6.1.5.7}b)$$

Comparing (E6.1.5.6) with (E6.1.5.2) and (E6.1.5.7) with (E6.1.5.3), we see that the two problems are mathematically dual with the following substitutions

$$\overline{H}_2^s = \overline{E}_1 / \eta \qquad\qquad\qquad (\text{E6.1.5.8}a)$$

$$\overline{E}_2^s = -\eta \overline{H}_1 \qquad\qquad\qquad (\text{E6.1.5.8}b)$$

In terms of total fields, we find

$$\overline{E}_2 = \overline{E}_2^s + \overline{E}_2^i = \eta(-\overline{H}_1 + \overline{H}_1^i) \qquad (\text{E6.1.5.9}a)$$

$$\overline{H}_2 = \overline{H}_2^s + \overline{H}_2^i = \frac{1}{\eta}(\overline{E}_1 - \overline{E}_1^i) \qquad (\text{E6.1.5.9}b)$$

This is referred to as Babinet's principle. Note that in the special case of no metallic screens for Figure E6.1.5.1a, $\overline{E}_1 = \overline{E}_1^i$ and $\overline{H}_1 = \overline{H}_1^i$. The complementary case is a complete metallic screen and the result is $\overline{E}_2 = \overline{H}_2 = 0$. Consider the other extreme when Figure E6.1.5.1a is completely metallic with no apertures, $\overline{E}_1 = \overline{H}_1 = 0$. Then the result for Figure E6.1.5.1b becomes $\overline{E}_2 = \eta \overline{H}_1^i$ and $\overline{H}_2 = -\overline{E}_1^i / \eta$, which are just the fields generated by the dual sources.

To examine further the implications of Babinet's principle, consider the dual problem of Figure E6.1.5.1b as illustrated in Figure E6.1.5.1c. The metallic aperture S_a is now replaced by a magnetic conductor and the sources are the dual of Figure E6.1.5.1c and therefore identical to those of Figure E6.1.5.1a. The boundary-value problem for the right-hand side of the magnetic conductor becomes

$$\nabla \times \overline{E}_d = i\omega\mu\overline{H}_d \qquad\qquad (\text{E6.1.5.10}a)$$

$$\nabla \times \overline{H}_d = -i\omega\epsilon\overline{E}_d \qquad\qquad (\text{E6.1.5.10}b)$$

subject to the boundary conditions

$$\hat{n} \times \overline{E}_d = \hat{n} \times \overline{E}_1^i \qquad \text{on} \quad S_m \qquad (\text{E6.1.5.11}a)$$

$$\hat{n} \times \overline{H}_d = 0 \qquad\qquad \text{on} \quad S_a \qquad (\text{E6.1.5.11}b)$$

where $\overline{E}_d$ and $\overline{H}_d$ denote fields of Figure E6.1.5.1c. From (E6.1.5.2) – (E6.1.5.3) and (E6.1.5.10)–(E6.1.5.11) we see that the sums of the fields $\overline{E} = \overline{E}_1 + \overline{E}_d$ and $\overline{H} = \overline{H}_1 + \overline{H}_d$ satisfy the following boundary-value problem

$$\nabla \times (\overline{E}_1 + \overline{E}_d) = i\omega\mu(\overline{H}_1 + \overline{H}_d) \qquad (\text{E6.1.5.12}a)$$

$$\nabla \times (\overline{H}_1 + \overline{H}_d) = -i\omega\epsilon(\overline{E}_1 + \overline{E}_d) \qquad (\text{E6.1.5.12}b)$$

with the boundary conditions

$$\hat{n} \times (\overline{E}_1 + \overline{E}_d) = \hat{n} \times \overline{E}_1^i \qquad \text{on} \quad S_m \qquad (E6.1.5.13a)$$

$$\hat{n} \times (\overline{H}_1 + \overline{H}_d) = \hat{n} \times \overline{H}_1^i \qquad \text{on} \quad S_a \qquad (E6.1.5.13b)$$

Thus the tangential fields on S_m and S_a are identical to those of $\overline{E}_1^i$ and $\overline{H}_1^i$ and by the uniqueness theorem, we conclude that

$$\overline{E}_1 + \overline{E}_d = \overline{E}_1^i \qquad (E6.1.5.14a)$$

$$\overline{H}_1 + \overline{H}_d = \overline{H}_1^i \qquad (E6.1.5.14b)$$

This also follows from Babinet's principle as expressed in (E6.1.5.9) with the substitution of $\overline{E}_2 = \eta \overline{H}_d$ and $\overline{H}_2 = -\overline{E}_d/\eta$ as required by the duality principle.

— END OF EXAMPLE 6.1.5 —

Topic 6.1C Mathematical Formulations of Huygens' Principle

Huygens' principle states that the field solution in a region V' is completely determined by the tangential fields specified over the surface S' enclosing V' [Fig. 6.1C.1]. Formulated in mathematical terms, Huygens' principle expresses fields at an observation point in terms of fields at the boundary surface. Consider a surface S' enclosing a radiating source. The electric and magnetic fields outside the surface will be shown to be of the following forms:

$$\overline{E}(\overline{r}) = \oiint_{S'} dS' \left\{ i\omega\mu \overline{\overline{G}}(\overline{r}, \overline{r}') \cdot [\hat{n} \times \overline{H}(\overline{r}')] \right.$$
$$\left. + \nabla \times \overline{\overline{G}}(\overline{r}, \overline{r}') \cdot [\hat{n} \times \overline{E}(\overline{r}')] \right\} \qquad (6.1C.1)$$

$$\overline{H}(\overline{r}) = \oiint_{S'} dS' \left\{ -i\omega\epsilon \overline{\overline{G}}(\overline{r}, \overline{r}') \cdot [\hat{n} \times \overline{E}(\overline{r}')] \right.$$
$$\left. + \nabla \times \overline{\overline{G}}(\overline{r}, \overline{r}') \cdot [\hat{n} \times \overline{H}(\overline{r}')] \right\} \qquad (6.1C.2)$$

where $\hat{n}$ is the outward normal to the surface S'. The dyadic Green's function $\overline{\overline{G}}(\overline{r}, \overline{r}')$ is given by

$$\overline{\overline{G}}(\overline{r}, \overline{r}') = \left[\overline{\overline{I}} + \frac{1}{k^2} \nabla\nabla \right] g(\overline{r}, \overline{r}') \qquad (6.1C.3)$$
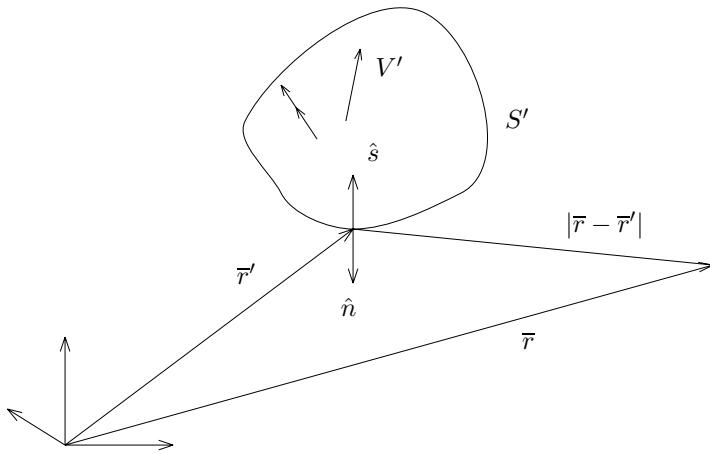
Figure 6.1C.1 Volume V' containing radiation sources.

The scalar Green's function $g(\overline{r},\overline{r}')$ satisfies the Helmholtz equation

$$(\nabla^2 + k^2)g(\overline{r},\overline{r}') = -\delta(\overline{r} - \overline{r}') \qquad (6.1C.4)$$

For three-dimensional problems, the scalar Green's function $g(\overline{r},\overline{r}')$ for isotropic media written in spherical coordinates is of the form

$$g(\overline{r},\overline{r}') = \frac{e^{ik|\overline{r}-\overline{r}'|}}{4\pi\,|\overline{r} - \overline{r}'|} \qquad (6.1C.5)$$

For two-dimensional problems, the scalar Green's function for isotropic media written in cylindrical coordinates is of the form

$$g(\overline{\rho},\overline{\rho}') = \frac{i}{4}H_0^{(1)}(k\,|\overline{\rho} - \overline{\rho}'|) \qquad (6.1C.6)$$

where $H_0^{(1)}$ is the zeroth-order Hankel function of the first kind.

Christiaan Huygens (14 April 1629 – 8 July 1695)

Christiaan Huygens studied law and mathematics at the University of Leiden from 1645–1647. Huygens devised ways of grinding and polishing lenses for telescopes and in 1655 detected the first moon Titan of Saturn. His Traité de la lumiere appeared in 1678, in which Huygens described his wave theory of light, Huygens' principle.

EXAMPLE 6.1.6   Derivation.

From the Maxwell equations, the governing equation for the electric field $\overline{E}(\overline{r})$ with a given current source $\overline{J}(\overline{r})$ is given by

$$\nabla \times \nabla \times \overline{E}(\overline{r}) - k^2\overline{E}(\overline{r}) = i\omega\mu\overline{J}(\overline{r}) \qquad (E6.1.6.1)$$

The solution of $\overline{E}(\overline{r})$ in terms of $\overline{J}(\overline{r})$ can be conveniently expressed in terms of the dyadic Green's function $\overline{\overline{G}}(\overline{r}, \overline{r}')$,

$$\overline{E}(\overline{r}) = i\omega\mu \iiint d^3\overline{r}'\, \overline{\overline{G}}(\overline{r}, \overline{r}') \cdot \overline{J}(\overline{r}') \qquad (E6.1.6.2)$$

Notice that by means of the three-dimensional delta function $\delta(\overline{r} - \overline{r}')$, we can write

$$\overline{J}(\overline{r}) = \iiint d^3\overline{r}'\, \delta(\overline{r} - \overline{r}')\overline{\overline{I}} \cdot \overline{J}(\overline{r}') \qquad (E6.1.6.3)$$

where $\overline{\overline{I}}$ is the unit dyad. Substitution of (E6.1.6.2) and (E6.1.6.3) in (E6.1.6.1) gives the following equation governing the dyadic Green's function $\overline{\overline{G}}(\overline{r}, \overline{r}')$,

$$\nabla \times \nabla \times \overline{\overline{G}}(\overline{r}, \overline{r}') - k^2\overline{\overline{G}}(\overline{r}, \overline{r}') = \overline{\overline{I}}\, \delta(\overline{r} - \overline{r}') \qquad (E6.1.6.4)$$

The derivation of the dyadic form of Huygens' principle calls for the vector identity

$$\overline{E} \cdot [\nabla \times \nabla \times (\overline{\overline{G}} \cdot \overline{a})] - [\nabla \times \nabla \times \overline{E}] \cdot (\overline{\overline{G}} \cdot \overline{a})$$
$$= -\nabla \cdot \left\{ \overline{E} \times \nabla \times \left(\overline{\overline{G}} \cdot \overline{a}\right) + \left(\nabla \times \overline{E}\right) \times \left(\overline{\overline{G}} \cdot \overline{a}\right) \right\}$$

where $\overline{a}$ is an arbitrary constant vector. Integrating over a volume V bounded by the closed surface S' and the surface at infinity, we obtain

$$\iiint_V d^3\overline{r} \left\{ \overline{E}(\overline{r}) \cdot [\nabla \times \nabla \times \overline{\overline{G}}(\overline{r}, \overline{r}') \cdot \overline{a}] \right.$$
$$\left. - [\nabla \times \nabla \times \overline{E}(\overline{r})] \cdot \overline{\overline{G}}(\overline{r}, \overline{r}') \cdot \overline{a} \right\}$$
$$= -\oiint_S dS \left\{ \hat{s} \cdot [\nabla \times \overline{E}(\overline{r})] \times \overline{\overline{G}}(\overline{r}, \overline{r}') \cdot \overline{a} \right.$$
$$\left. + \hat{s} \cdot \overline{E}(\overline{r}) \times \nabla \times \overline{\overline{G}}(\overline{r}, \overline{r}') \cdot \overline{a} \right\}$$

Making use of (E6.1.6.1) and (E6.1.6.4) in the left-hand side of the above equation and assuming that $\overline{J}(\overline{r}) = 0$ in volume V, we find

$$\overline{E}(\overline{r}') \cdot \overline{a} = -\oiint_S dS \left\{ \hat{s} \times [\nabla \times \overline{E}(\overline{r})] \cdot \overline{\overline{G}}(\overline{r}, \overline{r}') \cdot \overline{a} \right.$$
$$\left. + [\hat{s} \times \overline{E}(\overline{r})] \cdot \nabla \times \overline{\overline{G}}(\overline{r}, \overline{r}') \cdot \overline{a} \right\} \quad \text{(E6.1.6.5)}$$

Notice that in the integration of the left-hand side, the points $\overline{r}$ and $\overline{r}'$ are both inside the volume V. We now use $\nabla \times \overline{E}(\overline{r}) = i\omega\mu\overline{H}(\overline{r})$ and interchange the primed and unprimed variables. Since $\overline{a}$ is an arbitrary constant vector, we can delete it from both sides of the equation. Thus

$$\overline{E}(\overline{r}) = -\oiint_{S'} dS' \left\{ i\omega\mu\overline{\overline{G}}(\overline{r}, \overline{r}') \cdot [\hat{s} \times \overline{H}(\overline{r}')] \right.$$
$$\left. + \nabla \times \overline{\overline{G}}(\overline{r}, \overline{r}') \cdot [\hat{s} \times \overline{E}(\overline{r}')] \right\} \quad \text{(E6.1.6.6)}$$

On the right-hand side, the integration of $\overline{r}'$ is over the surface S'. In arriving at (E6.1.6.6) we also make use of the symmetry relations of the dyadic Green's function:

$$\overline{\overline{G}}(\overline{r}, \overline{r}') = \left[\overline{\overline{G}}(\overline{r}', \overline{r}) \right]^{\text{T}} \quad \text{(E6.1.6.7)}$$

and

$$\nabla \times \overline{\overline{G}}(\overline{r}, \overline{r}') = \left[\nabla' \times \overline{\overline{G}}(\overline{r}', \overline{r}) \right]^{\text{T}} \quad \text{(E6.1.6.8)}$$

where superscript T denotes transpose. In view of (6.1C.3) and (6.1C.5) or (6.1C.6), the relation (E6.1.6.7) is evidently true. The relation (E6.1.6.8) is also seen to be true by noting that

$$[\nabla \times \overline{\overline{G}}(\overline{r}, \overline{r}')]_{il} = \epsilon_{ijk}\, \partial_j \left(\delta_{kl} + \frac{1}{k^2}\partial_k\partial_l \right) g(\overline{r} - \overline{r}')$$
$$= -\epsilon_{ijl}\, \partial_j'\, g(\overline{r} - \overline{r}')$$
$$= \epsilon_{ljk}\, \partial_j'\, \delta_{ki}\, g(\overline{r} - \overline{r}')$$
$$= [\nabla' \times \overline{\overline{G}}(\overline{r}, \overline{r}')]_{li} \quad \text{(E6.1.6.9)}$$

where we use the relations $\epsilon_{ijk}\partial_j\partial_k = 0$ and $\partial_j g = -\partial_j' g$. It can also be shown that for general dyadic Green's functions satisfying prescribed boundary conditions, the symmetry relations (E6.1.6.7) and (E6.1.6.8) also hold.

The Huygens' principle is formulated with the identification of the closed surface S comprising a sphere of infinite radius and a surface S' enclosing all sources of radiation [Fig. 6.1C.1]. The surface at infinity gives no contribution

to the surface integral. This follows from the radiation conditions for the electromagnetic fields and the dyadic Green's functions:

$$\lim_{r\to\infty} r[\overline{H} - \hat{r} \times \overline{E}/\eta] = 0 \qquad (E6.1.6.10a)$$

$$\lim_{r\to\infty} \overline{r} \cdot \overline{E} = 0 \qquad (E6.1.6.10b)$$

$$\lim_{r\to\infty} r[\nabla \times \overline{\overline{G}} - ik\hat{r} \times \overline{\overline{G}}] = 0 \qquad (E6.1.6.10c)$$

Note that $\hat{r} = \hat{s}$ in (E6.1.6.6). The term $\hat{s} \times \overline{H}(\overline{r}')$ in (E6.1.6.6) becomes $\hat{r} \times (\hat{r} \times \overline{E}/\eta)$ and the integrand becomes $[-ik\hat{r} \times \overline{\overline{G}} + \nabla \times \overline{\overline{G}}] \cdot [\hat{r} \times \overline{E}]$ which vanishes on the surface at infinity. The contribution to $\overline{E}(\overline{r})$ comes solely from the surface S' [Fig. 6.1C.1]. Thus, noticing that $\hat{s} = -\hat{n}$, we obtain (6.1C.1) and (6.1C.2) which are expressed in terms of the tangential electric and magnetic field components at the boundary surface S'.

— END OF EXAMPLE 6.1.6 —

EXAMPLE 6.1.7   Stratton-Chu formula.

Many different vector forms can be obtained for the Huygens' principle. Making use of (6.1C.3), we obtain from (6.1C.1) and (6.1C.2)

$$\overline{E}(\overline{r}) = \oiint_{S'} dS' \left\{ i\omega\mu g(\overline{r},\overline{r}')[\hat{n} \times \overline{H}(\overline{r}')] + \frac{i\omega\mu}{k^2}\nabla\nabla g(\overline{r},\overline{r}') \cdot [\hat{n} \times \overline{H}(\overline{r}')] \right.$$
$$\left. + \nabla g(\overline{r},\overline{r}') \times [\hat{n} \times \overline{E}(\overline{r}')] \right\} \qquad (E6.1.7.1)$$

$$\overline{H}(\overline{r}) = \oiint_{S'} dS' \left\{ -i\omega\epsilon g(\overline{r},\overline{r}')[\hat{n} \times \overline{E}(\overline{r}')] - \frac{i\omega\epsilon}{k^2}\nabla\nabla g(\overline{r},\overline{r}') \cdot [\hat{n} \times \overline{E}(\overline{r}')] \right.$$
$$\left. + \nabla g(\overline{r},\overline{r}') \times [\hat{n} \times \overline{H}(\overline{r}')] \right\} \qquad (E6.1.7.2)$$

The above formulas are in terms of the tangential field components on S_1 and the scalar Green's function $g(\overline{r},\overline{r}')$.

The Stratton-Chu formula can be derived from (E6.1.6.5) by noting that the first term inside the surface integral is

$$\hat{s} \times (\nabla \times \overline{E}) \cdot \overline{\overline{G}} \cdot \overline{a} = \hat{s} \times (\nabla \times \overline{E}) \cdot [g\overline{a} + \frac{1}{k^2}\nabla\nabla \cdot g\overline{a}] \qquad (E6.1.7.3a)$$

$$= \hat{s} \times (\nabla \times \overline{E}) \cdot g\overline{a} + \frac{1}{k^2}\hat{s} \cdot (\nabla \times \overline{E}) \times \nabla\nabla \cdot g\overline{a} \qquad (E6.1.7.3b)$$

$$= \hat{s} \times (\nabla \times \overline{E}) \cdot g\overline{a} + \frac{1}{k^2}\hat{s} \cdot \left\{ (\nabla \times \nabla \times \overline{E})\nabla \cdot g\overline{a} \right.$$
$$\left. - \nabla \times [(\nabla \cdot g\overline{a})(\nabla \times \overline{E})] \right\} \qquad (E6.1.7.3c)$$

In the above derivations, (E6.1.7.3) is obtained by substitution of (6.1C.3). A vector identity $(\nabla \times \overline{E}) \times \nabla \phi = \phi(\nabla \times \nabla \times \overline{E}) - \nabla \times (\phi \nabla \times \overline{E})$ is used to convert the second term in (E6.1.7.3b) to the second term in (E6.1.7.3c). Substituting (E6.1.7.3c) in (E6.1.6.5) we note that the last term in (E6.1.7.3c) vanishes under the surface integration because by Gauss' theorem it is equivalent to the volume integral of the divergence of a curl. Also note that $\nabla \times \overline{E} = i\omega\mu\overline{H}$ and that for $\overline{J}(\overline{r}) = 0$, $\nabla \times \nabla \times \overline{E}(\overline{r}) = k^2 \overline{E}(\overline{r})$. Thus

$$\overline{E}(\overline{r}') = -\oiint dS' \left\{ i\omega\mu[\hat{s} \times \overline{H}(\overline{r})]g(\overline{r}, \overline{r}') + [\hat{s} \cdot \overline{E}(\overline{r})]\nabla g(\overline{r}, \overline{r}') \right.$$
$$\left. + [\hat{s} \times \overline{E}(\overline{r})] \times \nabla g(\overline{r}, \overline{r}') \right\} \qquad \text{(E6.1.7.4)}$$

Interchanging primed and unprimed quantities, making use of the symmetry properties of $g(\overline{r}, \overline{r}')$, and applying to the surface S' as shown in Fig. 6.1C.1, we obtain the Stratton-Chu formula

$$\overline{E}(\overline{r}) = \oiint_{S'} dS' \left\{ i\omega\mu[\hat{n} \times \overline{H}(\overline{r}')]g(\overline{r}, \overline{r}') + [\hat{n} \cdot \overline{E}(\overline{r}')]\nabla' g(\overline{r}, \overline{r}') \right.$$
$$\left. + [\hat{n} \times \overline{E}(\overline{r}')] \times \nabla' g(\overline{r}, \overline{r}') \right\} \qquad \text{(E6.1.7.5)}$$

$$\overline{H}(\overline{r}) = \oiint_{S'} dS' \left\{ -i\omega\epsilon[\hat{n} \times \overline{E}(\overline{r}')]g(\overline{r}, \overline{r}') + [\hat{n} \cdot \overline{H}(\overline{r}')]\nabla' g(\overline{r}, \overline{r}') \right.$$
$$\left. + [\hat{n} \times \overline{H}(\overline{r}')] \times \nabla' g(\overline{r}, \overline{r}') \right\} \qquad \text{(E6.1.7.6)}$$

Notice that in the Stratton-Chu formula (Julius Adam Stratton, 1901 – 1994; Lan Jen Chu, 1913 – 1973),normal components of $\overline{E}$ and $\overline{H}$ are required on the surface of S'.

<div align="right">— END OF EXAMPLE 6.1.7 —</div>

EXAMPLE 6.1.8   Franz formula.

The Franz formula can be derived from (E6.1.7.5) and (E6.1.7.6) to express $\overline{E}(\overline{r})$ and $\overline{H}(\overline{r})$ in terms of their tangential components on the surface S'. Taking curl of (E6.1.7.6) yields, noting that $\nabla g(\overline{r}, \overline{r}') = -\nabla' g(\overline{r}, \overline{r}')$,

$$\nabla \times \overline{H}(\overline{r}) = -i\omega\epsilon \nabla \times \oiint_{S'} dS' [\hat{n} \times \overline{E}(\overline{r}')]g(\overline{r}, \overline{r}')$$
$$- \nabla \times \oiint_{S'} dS' [\hat{n} \cdot \overline{H}(\overline{r}')]\nabla g(\overline{r}, \overline{r}')$$
$$+ \nabla \times \oiint_{S'} dS' \nabla \times [\hat{n} \times \overline{H}(\overline{r}')]g(\overline{r}, \overline{r}') \qquad \text{(E6.1.8.1)}$$

The second term on the right-hand side of (E6.1.8.1) vanishes and the curl operator inside the integral of the third term can be taken out of the integrand. Making use of the Maxwell equation $\nabla \times \overline{H} = -i\omega\epsilon\overline{E}$, we obtain

$$\overline{E}(\overline{r}) = \nabla \times \oiint_{S'} dS' \, [\hat{n} \times \overline{E}(\overline{r}')]g(\overline{r},\overline{r}')$$

$$+ \frac{i}{\omega\epsilon}\nabla \times \nabla \times \oiint_{S'} dS' \, [\hat{n} \times \overline{H}(\overline{r}')]g(\overline{r},\overline{r}') \quad \text{(E6.1.8.2)}$$

By duality

$$\overline{H}(\overline{r}) = \nabla \times \oiint_{S'} dS' \, [\hat{n} \times \overline{H}(\overline{r}')]g(\overline{r},\overline{r}')$$

$$- \frac{i}{\omega\mu}\nabla \times \nabla \times \oiint_{S'} dS' \, [\hat{n} \times \overline{E}(\overline{r}')]g(\overline{r},\overline{r}') \quad \text{(E6.1.8.3)}$$

The formulas are now dependent only on tangential components of the electric and magnetic fields on the surface S'.

<div align="right">— End of Example 6.1.8 —</div>

Example 6.1.9   Kirchhoff scalar formula for diffraction.

The Kirchhoff scalar formula for diffraction can be conveniently obtained from the Stratton-Chu formula (E6.1.7.5). In view of the fact that $i\omega\mu\overline{H}(\overline{r}') = \nabla' \times \overline{E}(\overline{r}')$ and $(\hat{n} \times \overline{E}) \times \nabla'g = \overline{E}\hat{n} \cdot \nabla'g - \hat{n}\overline{E} \cdot \nabla'g$, (E6.1.7.5) becomes

$$\overline{E}(\overline{r}) = \oiint_{S'} dS' \left\{ [\hat{n} \times (\nabla' \times \overline{E})]g + [\hat{n} \cdot \overline{E}]\nabla'g + \overline{E}\hat{n} \cdot \nabla'g - \hat{n}\overline{E} \cdot \nabla'g \right\}$$

$$= \oiint_{S'} dS' \left\{ \overline{E}\hat{n} \cdot \nabla'g - g(\hat{n} \cdot \nabla')\overline{E} \right\}$$

$$+ \oiint_{S'} dS' \left\{ \nabla'(\hat{n} \cdot g\overline{E}) - \hat{n}\nabla' \cdot (g\overline{E}) \right\} \quad \text{(E6.1.9.1)}$$

In arriving at the last term we use $\nabla' \cdot \overline{E}(\overline{r}') = 0$. The last surface integral in the above equation is zero owing to the fact that the ith component of the two surface integrals can be written as

$$\left[\oiint_{S'} dS' \, \nabla'(\hat{n} \cdot g\overline{E}) \right]_i = \oiint_{S'} dS' \, \partial_i' n_j g E_j = \iiint_{V'} dV' \partial_i' \partial_j' g E_j$$

<div align="right">(E6.1.9.2)</div>

and

$$\left[\oiint_{S'} dS' \, \hat{n}\nabla' \cdot (g\overline{E}) \right]_i = \oiint_{S'} dS' \, n_i \partial_j g E_j = \iiint_{V'} dV' \, \partial_i' \partial_j' g E_j$$

<div align="right">(E6.1.9.3)</div>

The last equality in (E6.1.9.2) and (E6.1.9.3) is the result of the generalized Gauss' theorem in tensor calculus. Thus

$$\overline{E}(\overline{r}) = \oiint_{S'} dS' \left\{ \overline{E}(\overline{r}') \frac{\partial g(\overline{r}, \overline{r}')}{\partial n} - g(\overline{r}, \overline{r}') \frac{\partial \overline{E}(\overline{r}')}{\partial n} \right\} \qquad \text{(E6.1.9.4)}$$

where $\partial/\partial n = \hat{n} \cdot \nabla'$. This is the vector form of the Kirchhoff formula for diffraction.

The scalar form of the Kirchhoff formula for diffraction is obtained by assuming that the electric field has only one cartesian component, say $\overline{E}(\overline{r}) = \hat{y} U(\overline{r})$. It follows that

$$U(\overline{r}) = \oiint_{S'} dS' \left\{ U(\overline{r}') \frac{\partial g(\overline{r}, \overline{r}')}{\partial n} - g(\overline{r}, \overline{r}') \frac{\partial U(\overline{r}')}{\partial n} \right\} \qquad \text{(E6.1.9.5)}$$

This is the most popular formula for diffraction used in physical optics. Clearly, when other components of the electric field become important, the formula breaks down. Thus in the case of diffraction of a linearly polarized plane wave by an aperture, for instance, the formula is valid only along the paraxial direction of observation i.e., near the axis perpendicular to the aperture. Away from the paraxial directions, the diffracted field components will no longer be in the same direction as the linearly polarized aperture field.

Derivation from scalar wave equation

We have seen the limitations of the scalar theory from the point of view of the dyadic and the vector theories. However, the scalar diffraction theory is complete and consistent by itself. Equation (E6.1.9.5) can be derived from the scalar equation

$$(\nabla^2 + k^2) U(r) = 0 \qquad \text{(E6.1.9.6)}$$

by using Green's theorem

$$U \nabla^2 g - g \nabla^2 U = \nabla \cdot [U \nabla g - g \nabla U] \qquad \text{(E6.1.9.7)}$$

Integrating (E6.1.9.7) over the volume V enclosed by the surface S' and the surface at infinity and making use of (6.1C.4) we obtain the Kirchhoff formula (E6.1.9.5). Note that $\hat{n}$ is normal to surface S' and points into the region V and that the surface integral at infinity vanishes owing to the Sommerfeld radiation condition.

The normal derivative of the scalar Green's function in (E6.1.9.5) can be written as

$$\frac{\partial g}{\partial n} = \hat{n} \cdot \nabla' g = -\left(ik - \frac{1}{R} \right) \frac{e^{ikR}}{4\pi R} (\hat{n} \cdot \hat{R})$$

$$U = A \exp(ik_{sx}x + ik_{sz}z)$$
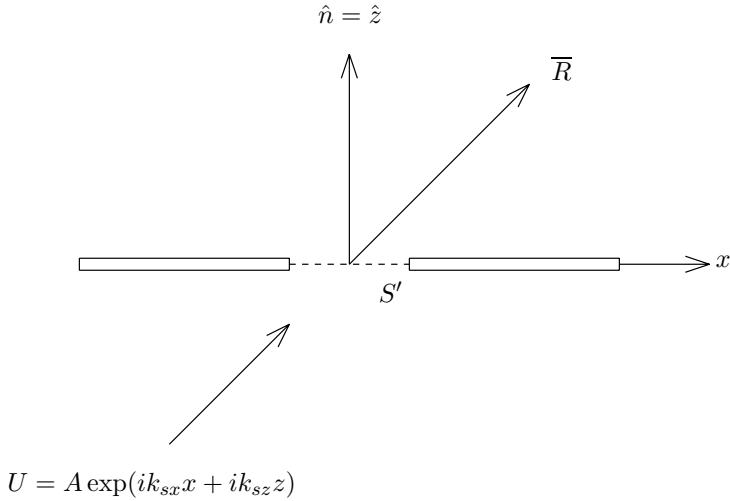
Figure E6.1.9.1 Diffraction by an aperture.

where $\hat{R}$ represents the unit vector in the direction of $\overline{R} = \overline{r} - \overline{r}'$. Substituting in (E6.1.9.5) we find

$$U(\overline{r}) = -\oiint_{S'} dS' \left\{ \left(ik - \frac{1}{R}\right) U(\overline{r}')(\hat{n} \cdot \hat{R}) + \frac{\partial U(\overline{r}')}{\partial n} \right\} \frac{e^{ikR}}{4\pi R} \qquad \text{(E6.1.9.8)}$$

The scalar wave amplitude $U(\overline{r})$ at $\overline{r}$ is thus expressed as a superposition of contributions from the elements of surface dS' with source strength expressed by the term within braces in (E6.1.9.8).

   We now consider the problem of diffraction by an aperture on an infinite plane surface [Fig. E6.1.9.1]. In order to apply (E6.1.9.8), the so-called Kirchhoff approximation (KA) is made: (i) the values of $U(\overline{r}')$ and $\partial U(\overline{r}')/\partial n$ vanish everywhere on S' except at the aperture and (ii) the values of $U(\overline{r}')$ and $\partial U(\overline{r}')/\partial n$ at the aperture are equal to those of the incident wave in the absence of S'. Suppose that the aperture is illuminated by a plane wave

$$U(\overline{r}') = A \exp[ik_{sx}x' + ik_{sz}z'] \qquad \text{(E6.1.9.9)}$$

We have

$$\frac{\partial U}{\partial n} = \hat{n} \cdot \nabla' U(\overline{r}') = i(\hat{n} \cdot \overline{k}_s)U(\overline{r}') \qquad \text{(E6.1.9.10)}$$

where $\overline{k}_s = \hat{x}k_{sx} + \hat{z}k_{sz}$. Furthermore assume that the frequency is high such that the $1/R$ term in (E6.1.9.8) is negligible in comparison with ik. In view of (E6.1.9.10), we obtain from (E6.1.9.8)

$$U(\overline{r}) = -ik \oiint_{aperture} dS' \left\{ (\hat{n} \cdot \hat{R}) + (\hat{n} \cdot \hat{k}_s) \right\} U(\overline{r}') \frac{e^{ikR}}{4\pi R} \qquad \text{(E6.1.9.11)}$$

where $\hat{k}_s = \overline{k}_s/k$. The term $\{(\hat{n} \cdot \hat{R}) + (\hat{n} \cdot \hat{k}_s)\}/2$ is known as the *obliquity factor* which is always positive and less than unity. When the incident wave is normal to the aperture, the obliquity factor simply becomes $(1 + \cos\theta)/2$. If we view the integral as a superposition of contributions from the secondary sources, then the obliquity factor effectively imposes an anisotropic directivity pattern on each element source point. Historically in the construction of the diffraction patterns with Huygens' wavelet concept, Fresnel found that the amplitude factor $ik(\hat{n} \cdot \hat{R} + \hat{n} \cdot \hat{k}_s)$ had to be postulated in order to get accurate results. It was Kirchhoff who showed that the amplitude factor is in fact a direct consequence of the scalar wave theory.

In the Kirchhoff approximation (KA) both $U(\overline{r}')$ and its normal derivative $\partial U(\overline{r}')/\partial n$ are prescribed over the surface S'. Rigorously the uniqueness theorem requires only $U(\overline{r}')$ or $\partial U(\overline{r}')/\partial n$ at every point on S' and not both. Sommerfeld circumvented the difficulty by choosing different scalar Green's functions $g(\overline{r} \cdot \overline{r}')$ such that on the plane surface S', where $g(\overline{r}, \overline{r}')$ or $\partial g(\overline{r}, \overline{r}')/\partial n$ vanishes and we have to specify only $\partial U(\overline{r}')/\partial n$ or $U(\overline{r}')$.

— END OF EXAMPLE 6.1.9 —

EXAMPLE 6.1.10   Extinction theorem and extended boundary conditions.

Consider normal incidence of a plan wave unto a flat half-space medium. Use the vector form of the Kirchhoff formula for diffraction (E6.1.9.4)

$$\overline{E}(\overline{r}) = \oiint_{S'} dS' \left\{ \overline{E}(\overline{r}') \frac{\partial g(\overline{r}, \overline{r}')}{\partial n} - g(\overline{r}, \overline{r}') \frac{\partial \overline{E}(\overline{r}')}{\partial n} \right\} \qquad \text{(E6.1.10.1)}$$

where $\partial/\partial n = \hat{n} \cdot \nabla'$. The total electric field is

$$E_y = E_{yi} + \int_{-\infty}^{\infty} dx' \int_{-\infty}^{\infty} dy' \left[E_y(x', y', 0) \frac{\partial g}{\partial z'} - g \frac{\partial E_y(x', y', z')}{\partial z'} \right]_{z'=0}$$

$$= E_{yi} + \left[E_y(0) \frac{\partial g}{\partial z'} - g \frac{\partial E_y(z')}{\partial z'} \right]_{z'=0}$$

$$= E_{yi} + \left[E_y(0) \frac{\partial g}{\partial z'} - g(-i\omega\mu H_x(0)) \right]_{z'=0}$$

where the Green's function $g(z, z') = ie^{ik|z-z'|}/2k$.

(a) If Region 1 is identical to Region 0, we have $E_y(0) = E_0$ and $H_x(0) = E_0/\eta$. Then in Region 0

$$E_y = E_{yi} + \left\{ E_0 \frac{\partial g}{\partial z'} - g(-ikE_0) \right\} = E_0 e^{-ikz}$$

and in Region 1,

$$E_y = E_{yi} + \left\{ E_0 \frac{\partial g}{\partial z'} - g(-ikE_0) \right\} = E_0 e^{-ikz} - E_0 e^{-ikz} = 0$$

(b) If Region 1 is a perfect conductor, then in Region 0, we have $E_y(0) = 0$ and $H_x(0) = 2E_0/\eta$.

$$E_y = E_{yi} + \left\{ E_0 \frac{\partial g}{\partial z'} - g(-i2kE_0) \right\} = E_0 e^{-ikz} + E_0 e^{ikz}$$

and in Region 1,

$$E_y = E_{yi} + \left\{ E_0 \frac{\partial g}{\partial z'} - g(-i2kE_0) \right\} = 0$$

(c) If Region 1 is a dielectric medium, we have $E_y(z = 0) = (1 + R)E_0$ and $H_x(z = 0) = (1 - R)E_0/\eta$. Then in Region 0

$$E_y = E_{yi} + \left\{ E_0 \frac{\partial g}{\partial z'} - g(-ikE_0) \right\} = E_0 e^{-ikz} + RE_0 e^{ikz}$$

and in Region 1,

$$E_y = E_{yi} + \left\{ E_0 \frac{\partial g}{\partial z'} - g(-ikE_0) \right\} = 0$$

The field produced by the current sheet extinguishes the incident field in Region 0.

<div align="right">— END OF EXAMPLE 6.1.10 —</div>

Topic 6.1D Fresnel and Fraunhofer Diffraction

As an example of the application of Huygens' principle, we consider the diffraction of a plane wave by a two-dimensional aperture. Let the plane wave be linearly polarized in the $\hat{y}$ direction and normally incident upon the aperture in the x-y plane from the region $z < 0$. In the half-space $z > 0$, the wave is diffracted [Fig. 6.1D.1]. To solve for the diffracted field, we use the results derived from the Huygens' principle,

$$\overline{E}(\overline{r}) = \oiint_{S'} dS' \left\{ i\omega\mu \overline{\overline{G}}(\overline{r}, \overline{r}') \cdot \overline{J}_s(\overline{r}') \right.$$

$$\left. - \nabla \times \overline{\overline{G}}(\overline{r}, \overline{r}') \cdot \overline{M}_s(\overline{r}') \right\} \qquad (6.1D.1a)$$

$$\overline{H}(\overline{r}) = \oiint_{S'} dS' \left\{ i\omega\epsilon \overline{\overline{G}}(\overline{r}, \overline{r}') \cdot \overline{M}_s(\overline{r}') \right.$$

$$\left. + \nabla \times \overline{\overline{G}}(\overline{r}, \overline{r}') \cdot \overline{J}_s(\overline{r}') \right\} \qquad (6.1D.1b)$$
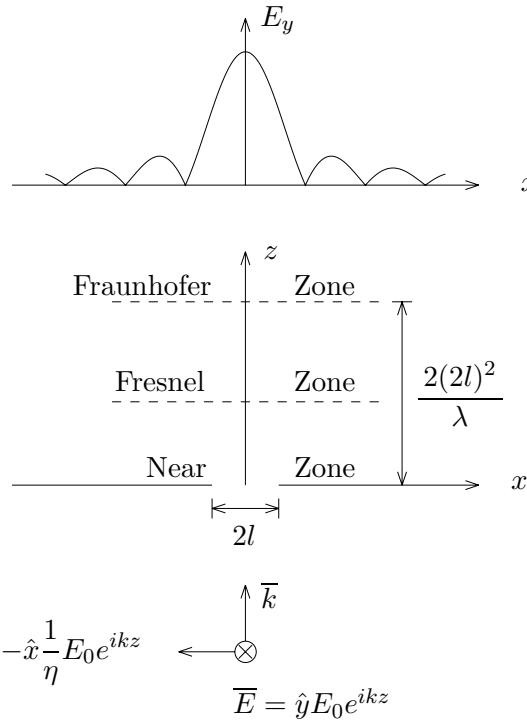
Figure 6.1D.1 Diffraction field in the Fraunhofer zone.

We assume that at the aperture there is an electric current sheet $\overline{J}_s = 2\hat{n} \times \overline{H}$ and no magnetic current sheet:

$$\overline{J}_s = 2\hat{z} \times \overline{H}(\overline{r}') = -\hat{y}\frac{2}{\eta}E(x') \qquad (6.1\text{D}.2)$$

where $E(x')$ describes the aperture field distribution.

With the assumed surface current in (6.1D.2),

$$\overline{E}(\overline{r}) = -\frac{2}{\eta} \oiint_{S'} dS' \, i\omega\mu \overline{\overline{G}}(\overline{r},\overline{r}') \cdot \hat{y}E(x')$$

The problem is two-dimensional, independent of the y coordinate, where $\partial/\partial y = 0$. We use the two-dimensional dyadic Green's function

$$\overline{\overline{G}}(\overline{r},\overline{r}') = \left(\overline{\overline{I}} + \frac{1}{k^2}\nabla\nabla\right)g(\overline{\rho},\overline{\rho}')$$

where

$$g(\overline{\rho}, \overline{\rho}') = \frac{i}{4} H_0^{(1)} \left(k\sqrt{(x - x')^2 + z^2} \right)$$

is the two-dimensional scalar Green's function. We find, recognizing that $\nabla\nabla \cdot \hat{y} = 0$ as $\partial/\partial y = 0$,

$$\overline{E}(x, z) = \hat{y}\frac{k}{2} \int_{-\infty}^{\infty} dx' \, E(x') H_0^{(1)} \left(k\sqrt{(x - x')^2 + z^2} \right) \qquad (6.1\text{D}.3)$$

In the far-field zone, we use the asymptotic form for the Hankel function $H_0^{(1)}(\xi) \approx (2/i\pi\xi)^{1/2} e^{i\xi}$. We also assume $z \gg |x - x'|$ and expand

$$k\sqrt{(x - x')^2 + z^2} \approx kz \left[1 + \frac{1}{2} \left(\frac{x - x'}{z} \right)^2 + \cdots \right] \qquad (6.1\text{D}.4)$$

Equation (6.1D.3) becomes

$$\overline{E}(x, z) = \hat{y}\frac{k}{2} \sqrt{\frac{2}{i\pi kz}} \, e^{ikz} \int_{-\infty}^{\infty} dx' \, E(x') e^{ik(x - x')^2/2z} \qquad (6.1\text{D}.5)$$

where we use the first two terms of expansion (6.1D.4) in the exponent and only the first term in the denominator of the Hankel function expansion.

The expansion (6.1D.4) which gives rise to (6.1D.5) is referred to as the Fresnel approximation. Equation (6.1D.5) is conveniently evaluated in terms of tabulated functions known as Fresnel integrals defined by

$$F(w) = \int_0^w dt \, e^{i\pi t^2/2} = C(w) + iS(w) \qquad (6.1\text{D}.6)$$

We notice the symmetry relation

$$C(w) = \int_0^w dt \, \cos\left(\frac{\pi t^2}{2} \right) = -C(-w) \qquad (6.1\text{D}.7)$$

$$S(w) = \int_0^w dt \, \sin\left(\frac{\pi t^2}{2} \right) = -S(-w) \qquad (6.1\text{D}.8)$$

For small values of w, the integral can be expanded in power series of w to carry out the integration. As $w \to 0$, we have

$$F(w) \approx w$$

For large values of w, the integral can be expanded in series of inverse powers of w. As $w \to \infty$, we have

$$F(\infty) = \int_0^\infty dt\, e^{i\pi t^2/2} = \sqrt{2/\pi}\, e^{i\pi/4} \int_0^\infty dx\, e^{-x^2} = \frac{1}{2} + i\frac{1}{2}$$

The values are shown in Figure 6.1D.2. When they are plotted on the two-dimensional space formed by $C(w)$ and $S(w)$, the trajectory of $C(w) + iS(w)$ forms the Cornu spiral as shown in Figure 6.1D.3.

Note that

$$\frac{dC(w)}{dw} = \cos\left(\frac{\pi}{2}w^2\right)$$

$$\frac{dS(w)}{dw} = \sin\left(\frac{\pi}{2}w^2\right)$$

The slope of the Cornu spiral is seen to be

$$\tan\theta = \frac{dS/dw}{dC/dw} = \tan\left(\frac{\pi}{2}w^2\right) \tag{6.1D.9}$$

The angle θ increases monotonically with w^2. The tangent to the curve is vertical when w^2 is an odd integer and horizontal when w^2 is an even integer.

The incremental length along the curve is

$$(dC)^2 + (dS)^2 = \left[\left(\frac{dC}{dw}\right)^2 + \left(\frac{dS}{dw}\right)^2\right] dw^2 = dw^2 \tag{6.1D.10}$$

Thus w is the length of the curve from the origin.

To illustrate the use of the Cornu spiral, we first consider the diffraction by a half-space aperture. With the integration limit from 0 to ∞, the electric field in (6.1D.6) takes the form

$$\overline{E}(x, z) = \hat{y}\frac{E_0}{\sqrt{2i}}\, e^{ikz} D(x)$$

where

$$D(x) = \sqrt{\frac{k}{\pi z}} \int_0^\infty dx'\, e^{ik(x'-x)^2/2z} = \int_0^\infty dt\, e^{i\pi t^2/2} - \int_0^{-\sqrt{\frac{k}{\pi z}}x} dt\, e^{i\pi t^2/2}$$

$$= F(\infty) - F(-\sqrt{k/\pi z}\, x)$$

$$= \frac{1}{2} - C(-\sqrt{k/\pi z}\, x) + i\left[\frac{1}{2} - S(-\sqrt{k/\pi z}\, x)\right]$$
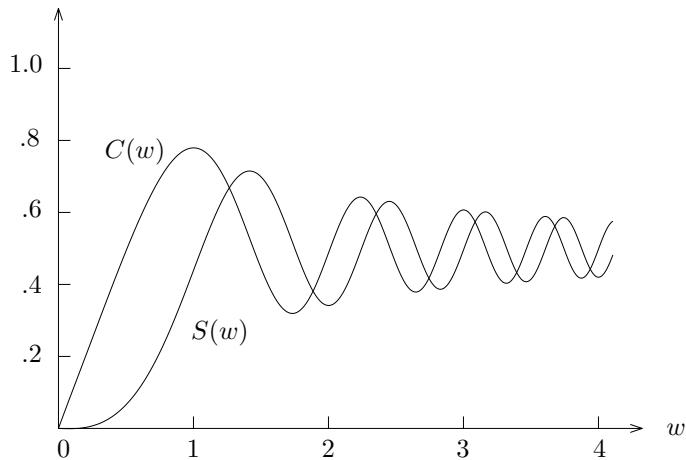
Figure 6.1D.2 Fresnel integrals $C(w)$ and $S(w)$.
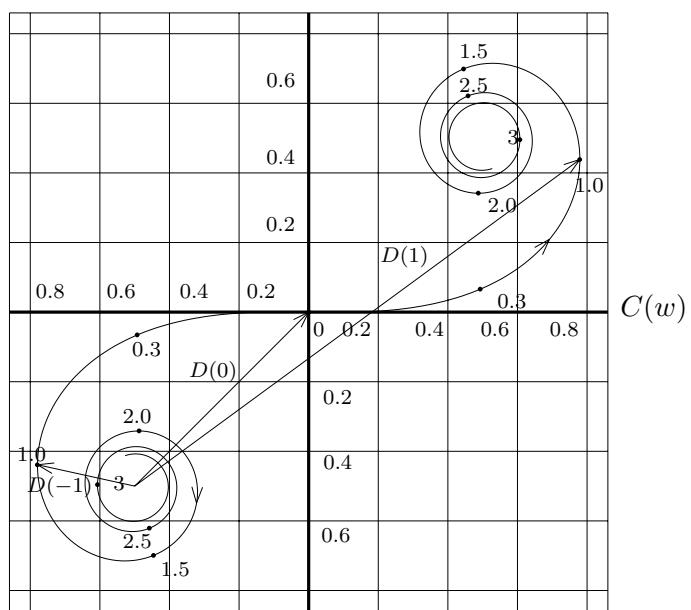
Figure 6.1D.3 Cornu spiral.

The magnitude of $\overline{E}$ is proportional to the magnitude of $D(x)$. We note the following special values for $D(x)$:

$$D(-\infty) = 0$$

$$D(0) = \frac{1}{2} + i\frac{1}{2}$$

$$D(\infty) = 1 + i$$

On the Cornu spiral [Fig. 6.1D.2], we may use the center of the lower left spiral as the reference point for $D(-\infty)$. Then the distance from $D(-\infty)$ to $x = 0$ is the magnitude for $D(0)$. The corresponding point for $D(\infty)$ is at the center of the upper right spiral. The distance from $D(-\infty)$ is the magnitude for $D(\infty)$. When we move from deep in the shadow zone for $x < 0$ towards the illuminated zone for $x > 0$, the magnitude of $D(x)$ is the distance from the reference point $D(-\infty)$ to a point corresponding to the value of x on the spiral. Thus $|D(x)|$ first increases its value monotonically until $x = 0$ and becomes oscillatory and approaches the final value of $\sqrt{2}$. If we normalize the value by $\sqrt{2}$ then the final value is 1 and the value at $x = 0$ is $1/2$ [Fig. 6.1D.4].
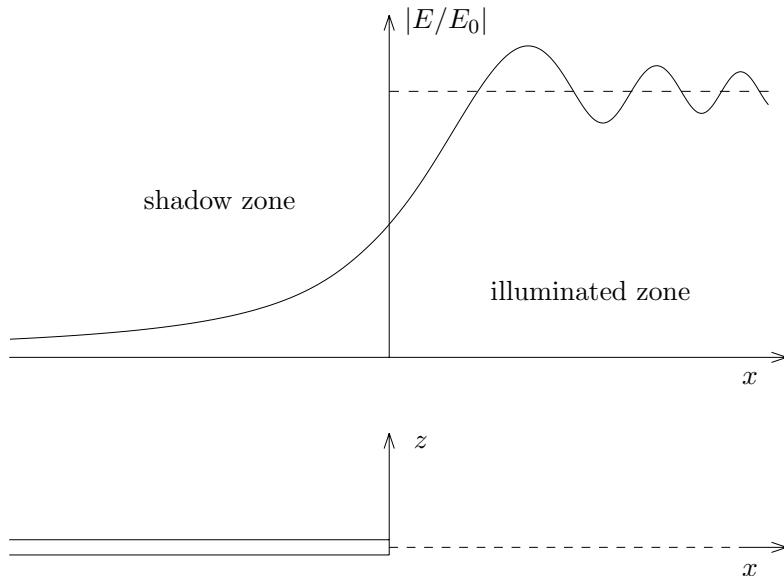
Figure 6.1D.4 Diffraction by a half-plane aperture.

EXAMPLE 6.1D.1   Diffraction by slit.

   We now consider the aperture with width $2l$ in the $\hat{x}$ direction [Fig. 6.1D.1] and infinite in the $\hat{y}$ direction. The aperture surface current is, according to (6.1D.2),

$$\overline{J}_s = -\hat{y}\frac{2E_0}{\eta}U(l - |x'|)$$

where E_0 is the amplitude of the incident wave, $U(l - |x'|)$ is a unit step function that is unity for $|x'| \leq l$ and zero for $|x'| \geq l$. This assumption is justifiable, for instance, in the case of optical diffraction by an opaque screen. In the case of perfectly conducting screens, however, the boundary condition of zero tangential electric field at $x = \pm l$ is not enforced.

   At a distance z in the x-z plane, we have

$$\overline{E}(x, z) = \hat{y}\frac{E_0}{\sqrt{2i}}\, e^{ikz}D(x)$$

with

$$D(x) = F\left[(l - x)\sqrt{k/\pi z}\right] - F\left[-(l + x)\sqrt{k/\pi z}\right]$$
$$= F\left[(l - x)\sqrt{k/\pi z}\right] + F\left[(l + x)\sqrt{k/\pi z}\right]$$

The second equality follows from the symmetry relation for $F(w)$ in (6.1D.8). Clearly $|D(x)|$ is symmetrical with respect to $x = 0$. As seen from (6.1D.10), it corresponds to the distance between the two end points of an arc of constant length proportional to $2l$. At $x = 0$, the magnitude $|D(0)|$ is the greatest. As x increases, $|D(x)|$ first decreases and then becomes oscillatory. For very large z, we move into the Fraunhofer zone where further simplifications can be made.

— END OF EXAMPLE 6.1D.1 —

Fraunhofer Approximation

When the observation point is very far from the finite aperture, the Fresnel approximation for the two-dimensional slit diffraction problem can be further simplified. We have

$$k\sqrt{(x - x')^2 + z^2} \approx kz\left[1 + \frac{1}{2}\left(\frac{x - x'}{z}\right)^2\right]$$
$$\approx kz + \frac{kx^2}{2z} - \frac{kxx'}{z}$$

(6.1D.11)

This is known as the *Fraunhofer approximation*. The electric field in the Fraunhofer zone due to a plane wave normally incident on a slit with width $2l$ becomes

$$\overline{E}(x,z) = \hat{y}\frac{k}{2}\sqrt{\frac{2}{i\pi kz}}\,e^{ikz+ikx^2/2z}\int_{-\infty}^{\infty} dx'\,E_0\,U(l-|x'|)e^{-i(kx/z)x'}$$

$$(6.1D.12)$$

The integral is a Fourier transform of the step function, and

$$\overline{E}(x,z) = \hat{y}klE_0\sqrt{\frac{2}{i\pi kz}}\frac{\sin(kxl/z)}{kxl/z}e^{ikz+ikx^2/2z} \qquad (6.1D.13)$$

Note that in (6.1D.12) the source function $E_0 U[l-|x'|]$ can be replaced by any general aperture field distribution. A general conclusion is that in the Fraunhofer zone, characterized by approximation (6.1D.11), the observed field at a constant z is proportional to the Fourier transform of the aperture field as seen from (6.1D.12). The quadrature phase term $e^{ikx^2/2z}$ in (6.1D.12) accounts for the curvature of the curved phase front. In the Fresnel approximation the inclusion of the quadrature phase correction term $e^{ikx'^2/2z}$ at the aperture leads to the use of Fresnel integrals. In the radiation field approximation, which is not restricted to paraxial directions, the quadrature phase term in Fraunhofer formula is further neglected.

According to the distance from the aperture, the diffracted field can be divided into the near zone, the Fresnel zone, and the Fraunhofer zone [Fig. 6.1D.1]. The separation between the Fresnel zone and the Fraunhofer zone may be taken at $z_F = 2(2l)^2/\lambda$. For an aperture of dimension 1 cm and wavelength $0.63\,\mu$m, the Fraunhofer zone begins at $z_F \approx 320$ m, a rather stringent constraint for Fourier optics experiments. The use of a convergent lens may eliminate this problem. Under paraxial approximation, the effect of a lens amounts to giving a wave transmitting through the lens a phase factor proportional to $e^{-ikx'^2/2f}$, where f is the focal length. If a lens is placed immediately in front of the aperture, we find that at $z = f$ the Fresnel diffraction formula reduces to the Fraunhofer formula under the Fresnel approximation. Thus when a screen is placed a focal length away from the lens, the Fourier transform of the aperture field is observed.

In general, when the observation point is very far from the aperture, the diffracted field is equivalent to the radiation field due to an aperture antenna with a surface current distribution. The radiation

field approximation takes the form

$$\left| \overline{r} - \overline{r}' \right| \approx r - \hat{r} \cdot \overline{r}'$$

where r is the magnitude of $\overline{r}$ and $\hat{r}$ is a unit vector along $\overline{r}$, with $\overline{r} = \hat{r} r$. The radiated field is also in the direction of $\overline{r}$, i.e., $\overline{k} = \hat{r} k$. For three-dimensional problems in free space, the dyadic Green's function is approximated by

$$\overline{\overline{G}}(\overline{r}, \overline{r}') = \left[\overline{\overline{I}} + \frac{1}{k^2} \nabla \nabla \right] \frac{e^{ik|\overline{r} - \overline{r}'|}}{4\pi \left| \overline{r} - \overline{r}' \right|} \approx \frac{e^{ikr}}{4\pi r} \left[\overline{\overline{I}} - \hat{r}\hat{r} \right] e^{-i\overline{k} \cdot \overline{r}'}$$

where the del operator ∇ is replaced by $i\overline{k}$. Huygens' principle can be written in the following form:

$$\overline{E}(\overline{r}) \approx \frac{i\omega\mu e^{ikr}}{4\pi r} \oiint_{S'} dS' \, e^{-i\overline{k} \cdot \overline{r}'}$$

$$\cdot \left\{ \left[\overline{\overline{I}} - \hat{r}\hat{r} \right] \cdot \overline{J}_s(\overline{r}') - \frac{1}{\eta} \hat{r} \times \overline{M}_s(\overline{r}') \right\} \quad (6.1\mathrm{D}.14a)$$

$$\overline{H}(\overline{r}) \approx \frac{ik \, e^{ikr}}{4\pi r} \oiint_{S'} dS' \, e^{-i\overline{k} \cdot \overline{r}'}$$

$$\cdot \left\{ \hat{r} \times \overline{J}_s(\overline{r}') + \frac{1}{\eta} \left[\overline{\overline{I}} - \hat{r}\hat{r} \right] \cdot \overline{M}_s(\overline{r}') \right\} \quad (6.1\mathrm{D}.14b)$$

The two equations are seen to be duals of each other with the replacements $\overline{E} = \eta\overline{H}$, $\overline{H} = -\overline{E}/\eta$, $\overline{J}_s = \overline{M}_s/\eta$ and $\overline{M}_s = -\eta\overline{J}_s$. Observe that the first term in $(6.1\mathrm{D}.14a)$ is identical to the radiation field calculated previously except that instead of volume current densities we are integrating surface current densities over the surface enclosing the source.

As the first example, consider the radiation due to a rectangular aperture antenna with a constant surface current sheet

$$\overline{J}_s = \hat{x} J_s$$

Consider the approximation

$$\left| \overline{r} - \overline{r}' \right| = \left(z^2 + x^2 + y^2 - 2xx' - 2yy' + x'^2 + y'^2 \right)^{1/2}$$

$$= (x^2 + y^2 + z^2)^{1/2} - \frac{xx'}{r} - \frac{yy'}{r} + \delta$$

The error term may be approximated by the quadrature phase

$$\delta \approx \frac{(D_x/2)^2}{2r} + \frac{(D_y/2)^2}{2r}$$

where D_x and D_y are the dimensions of the aperture. Let us apply an arbitrary criterion restricting the phase error due to each dimension to be less than $\pi/8$. Letting D denote either D_x or D_y,

$$\frac{\pi}{8} > \frac{k(D/2)^2}{2r} = \frac{2\pi D^2}{8\lambda r}$$

Thus

$$r > \frac{2D^2}{\lambda}$$

Beyond this distance, we are in the Fraunhofer zone. Making use of the formula in the radiation field, the electric field vector is found to be

$$E_x = \frac{i\omega\mu J_s e^{ikr}}{4\pi r} \int_{-D_x/2}^{D_x/2} dx' \, e^{-ikx' \sin\theta\cos\phi} \int_{-D_y/2}^{D_y/2} dy' \, e^{-iky' \sin\theta\sin\phi}$$

$$= \frac{i\omega\mu J_s e^{ikr}}{4\pi r} D_x D_y \frac{\sin\left(\dfrac{kD_x}{2}\sin\theta\cos\phi\right)}{\dfrac{kD_x}{2}\sin\theta\cos\phi} \frac{\sin\left(\dfrac{kD_y}{2}\sin\theta\sin\phi\right)}{\dfrac{kD_y}{2}\sin\theta\sin\phi}$$

A plot of $(\sin u)/u$ is shown in Figure 6.1D.5. The value at $u = \pm 0.44\pi$ is approximately $1/\sqrt{2}$. The half-power beamwidth (HPBW) is the angle at which the radiated power is half of its value at $u = 0$. The maximum radiation intensity is

$$r^2 \mathrm{Re}\{S\} = \frac{1}{2\eta}\left[\omega\mu\frac{J_s}{4\pi}D_x D_y\right]^2$$

The total radiated power can be calculated by integrating the field over the aperture. As $\overline{E} = -\hat{x}\eta J_s/2$ and $\overline{H} = -\hat{y}J_s/2$, we find

$$P_t = \frac{\eta}{8}J_s^2 D_x D_y$$

and the directivity

$$D = \frac{4\pi r^2 \mathrm{Re}\{S\}}{P_t} = \frac{k^2}{\pi}D_x D_y$$
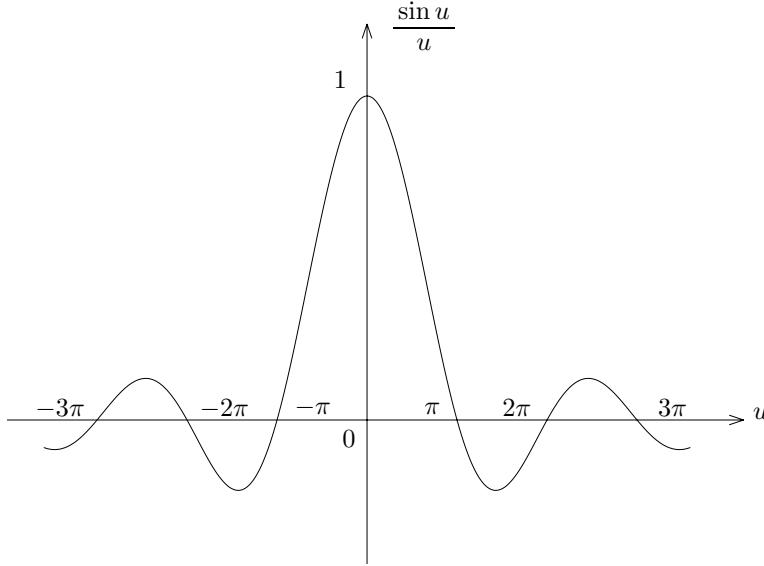
Figure 6.1D.5 Plot of $\sin u/u$.

It is important to note that the radiation characteristics are valid in the far-field zone commonly defined by $r > 2D^2/\lambda$.

As another example, consider the diffraction of a plane wave normally incident on a circular aperture. We shall not restrict observation points to be near the z axis. At the aperture we follow Equivalent Problem 3 for a plane wave by using magnetic current sheets. We assume a magnetic current sheet with $\overline{M}_s = -2\hat{n} \times \overline{E}$ and no electric current sheet. We find from Huygens' principle

$$
\begin{aligned}
\overline{E}(\overline{r}) &= 2 \oiint_{S'} dS' \, \nabla \times \overline{\overline{G}}(\overline{r}, \overline{r}') \cdot [\hat{n} \times \overline{E}(\overline{r}')] \\
&= 2\nabla \times \oiint_{S'} dS' \, \hat{n} \times \overline{E}(\overline{r}') \frac{e^{ik|\overline{r}-\overline{r}'|}}{4\pi \, |\overline{r} - \overline{r}'|}
\end{aligned}
\tag{6.1D.15}
$$

where S' denotes the area of the circular aperture.

In the far-field zone, the observation point is so remote from the aperture that all wave vectors originating from the aperture are essentially parallel and we have $k\,|\overline{r} - \overline{r}'| \approx kr - \overline{k} \cdot \overline{r}'$. The integral in (6.1D.15) becomes

$$
\overline{E}(\overline{r}) \approx \frac{ie^{ikr}}{2\pi r} \overline{k} \times \oiint_{S'} dS' \, \hat{n} \times \overline{E}(\overline{r}') e^{-i\overline{k}\cdot\overline{r}'}
$$

Let the incident plane wave be polarized in the $\hat{x}$ direction, $\overline{k} = \hat{x}k\sin\theta\cos\phi + \hat{y}k\sin\theta\sin\phi + \hat{z}k\cos\theta$. We have

$$\overline{E}(\overline{r}) = \frac{iE_0 e^{ikr}}{2\pi r}(\overline{k}\times\hat{y})\int_0^R d\rho'\int_0^{2\pi}\rho'd\phi'\,e^{-ik\rho'\sin\theta\cos(\phi-\phi')}$$

$$= (\hat{z}\sin\theta\cos\phi - \hat{x}\cos\theta)\frac{ikE_0 e^{ikr}}{r}\int_0^R \rho'd\rho'\,J_0(k\rho'\sin\theta)$$

$$= (\hat{z}\sin\theta\cos\phi - \hat{x}\cos\theta)\frac{ikR^2 E_0 e^{ikr}}{r}\frac{J_1(kR\sin\theta)}{kR\sin\theta}$$

where E_0 is the amplitude of the incident wave and R is the radius of the aperture.

In the previous examples, we assume the aperture to be a hole on an opaque screen and the equivalent source is equal to the part of the surface current sheet due to the original plane wave. We now consider a rectangular waveguide carrying a TE_{10} mode opening into free space. By the equivalence principle, we may approximate the aperture field at the waveguide opening by a current sheet with

$$\overline{J}_s(\overline{r}') = -\hat{y}\frac{2E_0}{\eta}\cos\frac{\pi x'}{a}$$

for $-a/2 < x' < a/2$ and $-b/2 < y' < b/2$. The far field is the Fourier transform of the aperture source

$$\overline{E} = \frac{i\omega\mu e^{ikr}}{4\pi r}\oiint_{S'} dS'e^{-i\overline{k}\cdot\overline{r}'}\,[\overline{\overline{I}} - \hat{r}\hat{r}]\cdot\overline{J}_s(\overline{r}')$$

$$= \frac{-i\omega\mu e^{ikr}}{4\pi r}\frac{2E_0}{\eta}\,[\overline{\overline{I}} - \hat{r}\hat{r}]\cdot(\hat{r}\sin\theta\sin\phi + \hat{\theta}\cos\theta\sin\phi + \hat{\phi}\cos\phi)$$

$$\int_{-b/2}^{b/2} dy'\int_{-a/2}^{a/2} dx'\cos\frac{\pi x'}{a}e^{-ik_x x'-ik_y y'}$$

$$= -(\hat{\theta}\cos\theta\sin\phi + \hat{\phi}\cos\phi)\,i\omega\mu\frac{4E_0}{\eta}\frac{e^{ikr}}{4\pi r}\left(\frac{\sin k_y\frac{b}{2}}{k_y}\right)$$

$$\left\{\frac{\sin\left[\left(k_x + \frac{\pi}{a}\right)\frac{a}{2}\right]}{k_x + \frac{\pi}{a}} + \frac{\sin\left[\left(k_x - \frac{\pi}{a}\right)\frac{a}{2}\right]}{k_x - \frac{\pi}{a}}\right\}$$

where $k_x = k\sin\theta\cos\phi$ and $k_y = k\sin\theta\sin\phi$.

Problems

P6.1.1

Let the tangential $\overline{E}$ field and tangential $\overline{H}$ field on an enclosed surface S be related by an impedance matrix $\overline{\overline{Z}}(\overline{r})$ such that

$$\hat{n} \times \overline{E} = \overline{\overline{Z}}(\overline{r}) \cdot (\hat{n} \times \overline{H})$$

where $\hat{n}$ is inward normal to the surface S bounding the region of interest V

$$Z_{ij}(\overline{r}) = \hat{s}_i \overline{\overline{Z}}(\overline{r}) \hat{s}_j$$

and $\hat{s}_i$ and $\hat{s}_j$ with $i, j = 1, 2$ are unit vectors tangential to the surface S such that $\hat{s}_1, \hat{s}_2$, and $\hat{n}$ form an orthogonal coordinate system. Show that

$$E_1 = -Z_{21}H_2 + Z_{22}H_1$$
$$E_2 = Z_{11}H_2 - Z_{12}H_1$$

Let $\delta\overline{E} = E_1\hat{s}_1 + E_2\hat{s}_2 + E_n\hat{n}$ and $\delta\overline{H} = H_1\hat{s}_1 + H_2\hat{s}_2 + H_n\hat{n}$, then

$$\hat{n} \cdot \delta\overline{E} \times \delta\overline{H}^* = (-Z_{21}H_2H_2^* + Z_{22}H_1H_2^* - Z_{11}H_2H_1^* + Z_{12}H_1H_1^*)$$
$$\hat{n} \cdot \delta\overline{E}^* \times \delta\overline{H} = (-Z_{21}^*H_2^*H_2 + Z_{22}^*H_1^*H_2 - Z_{11}^*H_2^*H_1 + Z_{12}^*H_1^*H_1)$$

Determine the conditions for Z_{ij} such that the uniqueness theorem holds.

P6.1.2

By the image theorem, a vertical monopole antenna on a conducting plane is equivalent to a dipole with the conductor removed. In radio broadcasting stations, the Earth is used as the conducting plane. Calculate the power and the gain for a monopole on a conducting plane.

P6.1.3

Determine the magnetic field $\overline{H}$ for the diffraction pattern in the far field produced by a plane wave with electric field $\overline{E} = \hat{y}E_0 e^{ikz}$ normally incident on a rectangular slit.

P6.1.4

Using the equivalence principle, calculate the field $\overline{H}$ radiated from the open end of a coaxial line. Assume that the field inside the waveguide has only TEM modes with equivalent magnetic surface current

$$\overline{M}_s = -\hat{\phi}' \frac{2E_0 a}{\rho'} = \frac{2E_0 a}{\rho'}(\hat{x}\sin\phi' - \hat{y}\cos\phi') \qquad \text{for } a < \rho' < b$$

where a and b are the inner radius and the outer radius of the coaxial cable respectively.

P6.1.5

Consider a plane wave $\overline{E}_i = \hat{y}E_0 e^{-ikz}$, and $\overline{H}_i = \hat{x}\frac{E_0}{\eta}e^{-ikz}$ incident on a sphere of radius a. The radius of the sphere is much larger than a wavelength. Assume that the following approximate values hold for the scattered fields $\overline{E}_s$ and $\overline{H}_s$ on the surface of the sphere:

(1) in the shadow region $\overline{E}_s \approx -\overline{E}_i$ and $\overline{H}_s \approx -\overline{H}_i$, and

(2) in the illuminated region $\hat{r} \times \overline{E}_s \approx -\hat{r} \times \overline{E}_i$ and $\hat{r} \times \overline{H}_s \approx \hat{r} \times \overline{H}_i$,

where $\overline{E}_i$ and $\overline{H}_i$ are the fields of the incident wave. This assumed source distribution is a result of the physical optics approximation. Solve for the scattered radiation fields and calculate the echo area, defined by

$$A_e = \lim_{r \to \infty} (4\pi r^2 \frac{P_s}{P_i})$$

where P_s is the backscattered power density, and P_i is the incident power density of the plane wave.

P6.1.6

A slot antenna consists of a slot opening in a metallic plane and has an infinitesimally small width w and length $2l$ in the $\hat{z}$ direction. Let the voltage across the slot at $z = 0$ be V and the electric field distribution in the slot region be $(V/w)\sin k(l-|z|)$. Let $l = \lambda/4$, show that the complementary structure is a wire antenna of length $\lambda/2$. Find the input impedance of the slot antenna.

P6.1.7

Calculate the radiated field from an open parallel-plate waveguide. Assume that the field inside is the TE_1 mode with $E_y = E_0 \sin\frac{\pi}{d}\left(x - \frac{d}{2}\right)e^{ik_z z}$.

P6.1.8

For diffraction by a slit of width $w = 2\ell$, the Fraunhofer field is found under the assumptions $dw \gg 1$ and $w/z \ll 1$ with the diffraction pattern proportional to $\sin(kx\ell/z)/(kx\ell/z)$ which peaks at $x = 0$. Let $x/z \approx \theta$ be the angular spread. Show that for the main beam angular spread, $\theta_1 \approx \lambda/2\ell$ where θ_1 is defined to be the first zero of the diffraction pattern. Show also that the maximum number of side lobes $N \leq w/\lambda$.

P6.1.9

The operation of a Synthetic Aperture Radar (SAR) relies on the ability of simulating a large antenna of aperture size L from a moving small antenna with aperture size ℓ by digital signal processing techniques. The synthesized large antenna is based on the precise knowledge of the actual antenna at their spatial positions at different times. The beam width of an actual small antenna is λ/ℓ. Show that the ground resolution of SAR is ℓ, which is a remarkable result as it suggests that the smaller the radiating antenna the finer is the ground resolution. What limits the size of the radiating antenna?

6.2   Reaction and Reciprocity

A. Reaction

Consider a time-harmonic source a, denoted by $\overline{J}_a$ and $\overline{M}_a$, in a field $\overline{E}_b$ and $\overline{H}_b$ produced by source b, denoted by $\overline{J}_b$ and $\overline{M}_b$. The interaction of source a with field b can be characterized by $<a,b>$, defined as

$$<a,b> \equiv \iiint_V dV \left(\overline{J}_a \cdot \overline{E}_b - \overline{M}_a \cdot \overline{H}_b\right) \qquad (6.2.1)$$

Note that in the representation $<a,b>$ the first entry, a, is associated with the source and the second entry, b, with the field; whenever the source is zero, the reaction is zero. The integration extends over the region containing source a, which is composed of volume current densities, as well as surface current densities. In the case of surface current densities, the volume integrals become surface integrals.

The reaction is a complex number and has the dimension of power. It is different from complex power in two respects; first, in the definition of power the current density is complex-conjugated; second, the reaction is defined for a source with respect to the field produced by another source. When the source is reacting to the field produced by itself, we have the self-reaction $<a,a>$.

EXAMPLE 6.2.1

To understand what reaction means physically, consider the case in which source a is a dipole,

$$\overline{J}_a = \overline{I}l\,\delta(\overline{r} - \overline{r}_0)$$

Then the reaction

$$<a,b> = \overline{I}l \cdot \overline{E}_b(\overline{r}_0) \qquad (E6.2.1.1)$$

is proportional to the electric field in the direction of $\overline{I}$ as measured by the dipole. It is equal to the field strength produced by source b at the dipole when the dipole moment Il is unity. For instance, source b can be an antenna located at the origin.

— END OF EXAMPLE 6.2.1 —

Example 6.2.2

   As another example, consider the reactions of a current source and a voltage source in circuits [Fig. E6.2.2.1]. Let V_b and I_b be caused by an unspecified source b. For the current source [Fig. E6.2.2.1a], we have

a.   b.
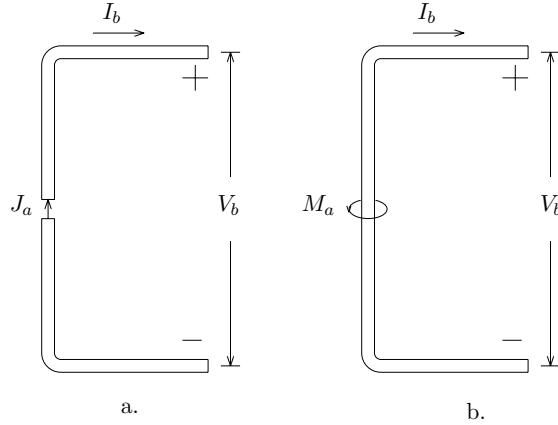
Figure E6.2.2.1 a. Reaction of a current source. b. Reaction of a voltage source.

$$
\begin{aligned}
< a, b > &= \iiint_V dV\, \overline{J}_a \cdot \overline{E}_b \\
&= I_a \int d\bar{l} \cdot \overline{E}_b = -I_a V_b
\end{aligned}
\tag{E6.2.2.1a}
$$

For the voltage source [Fig. E6.2.2.1b], we have

$$
\begin{aligned}
< a, b > &= -\iiint_V dV\, \overline{M}_a \cdot \overline{H}_b \\
&= -V_a \int d\bar{l} \cdot \overline{H}_b = -V_a I_b
\end{aligned}
\tag{E6.2.2.1b}
$$

Thus, if we use a unit current source, the reaction $< a, b >$ is equal to the voltage V_b at source a due to source b. If we use a unit voltage source, the reaction $< a, b >$ is equal to the current I_b at source a due to source b.

                                          — End of Example 6.2.2 —

B. Reciprocity

We define a system as reciprocal if, with respect to two sets of sources a and b,

$$< a, b > = < b, a > \tag{6.2.2}$$

Let the system be an isotropic medium; we shall show that isotropic media are reciprocal. We write the Maxwell equations with source a as

$$\nabla \times \overline{H}_a = -i\omega\epsilon\overline{E}_a + \overline{J}_a \tag{6.2.3a}$$

$$-\nabla \times \overline{E}_a = -i\omega\mu\overline{H}_a + \overline{M}_a \tag{6.2.3b}$$

and the Maxwell equations with source b as

$$\nabla \times \overline{H}_b = -i\omega\epsilon\overline{E}_b + \overline{J}_b \tag{6.2.4a}$$

$$-\nabla \times \overline{E}_b = -i\omega\mu\overline{H}_b + \overline{M}_b \tag{6.2.4b}$$

Forming $\overline{E}_b \cdot (6.2.3a) + \overline{H}_a \cdot (6.2.4b)$ and $\overline{E}_a \cdot (6.2.4a) + \overline{H}_b \cdot (6.2.3b)$, we arrive at

$$-\nabla \cdot \left(\overline{E}_b \times \overline{H}_a\right) = -i\omega\epsilon\overline{E}_a \cdot \overline{E}_b + \overline{J}_a \cdot \overline{E}_b - i\omega\mu\overline{H}_a \cdot \overline{H}_b + \overline{M}_b \cdot \overline{H}_a \tag{6.2.5a}$$

$$-\nabla \cdot \left(\overline{E}_a \times \overline{H}_b\right) = -i\omega\epsilon\overline{E}_a \cdot \overline{E}_b + \overline{J}_b \cdot \overline{E}_a - i\omega\mu\overline{H}_a \cdot \overline{H}_b + \overline{M}_a \cdot \overline{H}_b \tag{6.2.5b}$$

Subtracting $(6.2.5b)$ from $(6.2.5a)$ and integrating, we obtain

$$< a, b > - < b, a > = \oiint_S d\overline{S} \cdot \left(\overline{E}_a \times \overline{H}_b - \overline{E}_b \times \overline{H}_a\right) \tag{6.2.6}$$

By definition, isotropic media are reciprocal provided that

$$\oiint_S d\overline{S} \cdot \left(\overline{E}_a \times \overline{H}_b - \overline{E}_b \times \overline{H}_a\right) = 0 \tag{6.2.7}$$

This statement is referred to as the *Lorentz reciprocity theorem*. When all sources and matter are of finite extent, we can extend the surface of the volume to infinity and the left-hand side of (6.2.6) contains all sources contributing to the reactions. At an infinite distance away

from the source, the $\overline{E}$ and $\overline{H}$ fields are related by $\overline{H} = \hat{r} \times \overline{E}/\eta$ and $\hat{r} \cdot \overline{E} = \hat{r} \cdot \overline{H} = 0$. As a consequence, $\overline{E}_a \times \overline{H}_b - \overline{E}_b \times \overline{H}_a = 0$ and we find that the surface integral in (6.2.7) vanishes.

The reciprocity theorem that we have just proved is useful in many situations. We shall apply it in subsequent sections to derive stationary formulas in variational problems based on reciprocity. We now use it to prove a few simple assertions.
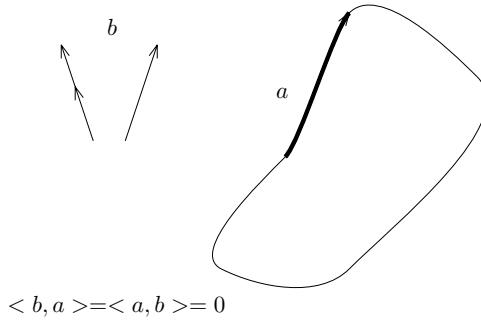
EXAMPLE 6.2.3

Consider an electric current sheet impressed on the surface of a perfect conductor. If the surface of the conductor is a plane, the image theorem assures us that no field is produced by the current. But what if the surface is not a plane? Does it seem reasonable to extend the result and claim that all electric current sheets impressed on the surface of a conductor of any shape do not produce a field? The reciprocity theorem assures us that this is true by a simple argument. Let the impressed source be denoted as source a [Fig. E6.2.3.1]. Let there be a source b that measures the field produced by source a; for instance, source b can be a dipole antenna. Source b produces no tangential electric field along the surface of the conductor, because of the boundary conditions. The reaction of a and b is $< a, b > = 0$. By the reciprocity theorem,

$$< b, a > = < a, b > = 0$$

But $< b, a >$ is the field arising from the impressed source a as measured by source b, and b can be any arbitrary source. Therefore, source b measures no field, and this proves that impressed electric current sheets on the surface of a perfect conductor produce no field.

$$< b, a > = < a, b > = 0$$

Figure E6.2.3.1 Zero field produced by current sheet impressed on perfect conductor.

— END OF EXAMPLE 6.2.3 —

EXAMPLE 6.2.4

For two antennas operating as a transmitter and a receiver, we can regard the terminals of the two antennas as the terminals of a two-port network in circuit theory. We write

$$V_a = Z_{aa}I_a + Z_{ab}I_b \qquad (\text{E6.2.4.1}a)$$
$$V_b = Z_{ba}I_a + Z_{bb}I_b \qquad (\text{E6.2.4.1}b)$$

Suppose both antennas a and b are excited with terminal currents I_a and I_b. Since no magnetic sources are present, $<a,b> = <b,a>$ gives

$$\iiint_{V_a} dV\,\overline{J}_a \cdot \overline{E}_b = \iiint_{V_b} dV\,\overline{J}_b \cdot \overline{E}_a$$

For perfectly conducting antennas, the electric fields are zero over the antennas and we have

$$V_a^{oc}I_a = V_b^{oc}I_b \qquad (\text{E6.2.4.2})$$

where

$$V_a^{oc} = -\int d\bar{l} \cdot \overline{E}_b$$

is the open circuit voltage at the terminal of antenna a due to the field produced by antenna b, and similarly V_b^{oc} is the open circuit voltage at the terminal of antenna b due to the field produced by antenna a. From (E6.2.4.1) we have

$$V_a^{oc} = Z_{ab}I_b$$
$$V_b^{oc} = Z_{ba}I_a$$

It follows from (E6.2.4.2) that

$$Z_{ab} = Z_{ba} \qquad (\text{E6.2.4.3})$$

This is a direct consequence of the reciprocity principle. If a current source I excites antenna a, the open circuit voltage at the terminals of antenna b will be $V_b^{oc} = Z_{ba}I$ which is equal to $V_a^{oc} = Z_{ab}I$ at the terminals of antenna a when the same current source is used to excite antenna b.

— END OF EXAMPLE 6.2.4 —

EXAMPLE 6.2.5

We now prove that the receiving pattern of an antenna is identical to its radiation pattern. Let antenna a be the antenna under consideration, and antenna b be a test antenna, constructed so that it is omnidirectional. For both receiving and radiation patterns we are concerned with far fields. By the reciprocity theorem, we see that, in a direction where a as a transmitter radiates a weaker plane wave to b, a as a receiver also receives a weaker plane wave from b. Thus the radiation pattern and the receiving pattern of antenna a are identical. The gain $G_a(\theta, \phi)$ characterizes the radiation pattern of antenna a when it is acting as a transmitter. When a is acting as a receiver, we can define an effective area $A_a(\theta, \phi)$ to characterize its receiving pattern. From the proof we know that, for any antenna a, the effective area $A(\theta, \phi)$ is related to its gain $G(\theta, \phi)$ by a constant independent of the structure of the antenna. To determine this constant, we consider a dipole antenna with the gain function

$$G(\theta, \phi) = \frac{3}{2} \sin^2 \theta \qquad \text{(E6.2.5.1)}$$
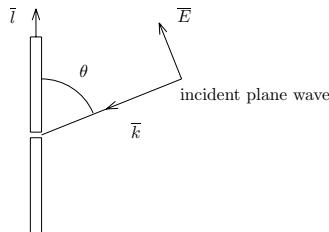
Figure E6.2.5.1 Dipole as receiver.

Let there be a plane wave incident upon the dipole from a direction making angle θ with the dipole axis along $\bar{l}$ [Fig. E6.2.5.1]. The power received by the antenna with a properly matched load Z_L is

$$P = \frac{(\overline{E} \cdot \bar{l})^2}{2(Z_L + Z_L^*)^2} R_r = \frac{E^2 l^2 \sin^2 \theta}{8 R_r} = \left[\frac{\pi}{k^2} \frac{3}{2} \sin^2 \theta \right] S_{inc}$$

The last equality follows on using the dipole radiation resistance $R_r = (\eta/6\pi)k^2 l^2$, and the incident power density $S_{inc} = E^2/2\eta$. Thus we define

$$A(\theta, \phi) = \frac{\pi}{k^2} G(\theta, \phi) \qquad \text{(E6.2.5.2)}$$

The power received by the antenna is equal to the power per unit area of the incident wave times the effective area $A(\theta, \phi)$. Notice that the proportionality factor, π/k^2, even though determined for a dipole antenna, is a universal constant independent of antenna structures.

— END OF EXAMPLE 6.2.5 —

C. Reciprocity Conditions

In the preceding development we proved that isotropic media are reciprocal, and we applied the reciprocity theorem in various situations. We shall now examine the validity of the reciprocity theorem for a bianisotropic medium. Using the same procedure as illustrated in (6.2.3)–(6.2.7), we find

$$
\begin{aligned}
&<a, b> - <b, a> \\
&= i\omega \iiint_V dV \left(\overline{E}_b \cdot \overline{D}_a - \overline{E}_a \cdot \overline{D}_b + \overline{H}_a \cdot \overline{B}_b - \overline{H}_b \cdot \overline{B}_a \right)
\end{aligned}
\tag{6.2.8}
$$

If the right-hand side is zero, the medium is reciprocal. The constitutive relations for bianisotropic media are

$$
\overline{D} = \overline{\overline{\epsilon}} \cdot \overline{E} + \overline{\overline{\xi}} \cdot \overline{H}
\tag{6.2.9a}
$$

$$
\overline{B} = \overline{\overline{\mu}} \cdot \overline{H} + \overline{\overline{\zeta}} \cdot \overline{E}
\tag{6.2.9b}
$$

Inserting (6.2.9) into the right-hand side of (6.2.8), we obtain

$$
\begin{aligned}
&< a, b> - <b, a> \\
&= i\omega \iiint_V dV \left[\overline{E}_b \cdot (\overline{\overline{\epsilon}} - \overline{\overline{\epsilon}}^T) \cdot \overline{E}_a + \overline{H}_a \cdot (\overline{\overline{\mu}} - \overline{\overline{\mu}}^T) \cdot \overline{H}_b \right. \\
&\quad \left. + \overline{E}_b \cdot (\overline{\overline{\xi}} + \overline{\overline{\zeta}}^T) \cdot \overline{H}_a - \overline{H}_b \cdot (\overline{\overline{\zeta}} + \overline{\overline{\xi}}^T) \cdot \overline{E}_a \right]
\end{aligned}
$$

Thus the medium will be reciprocal if

$$
\overline{\overline{\epsilon}} = \overline{\overline{\epsilon}}^T
\tag{6.2.10a}
$$

$$
\overline{\overline{\mu}} = \overline{\overline{\mu}}^T
\tag{6.2.10b}
$$

$$
\overline{\overline{\xi}} = -\overline{\overline{\zeta}}^T
\tag{6.2.10c}
$$

These are the conditions for a medium to be reciprocal. Consequently, isotropic media are reciprocal, and anisotropic media with symmetrical permittivity and permeability tensors are reciprocal. Bianisotropic media that satisfy (6.2.10a), (6.2.10b), and the symmetry condition $\overline{\overline{\xi}} = \overline{\overline{\zeta}}^+$ are reciprocal if $\overline{\overline{\xi}}$ and $\overline{\overline{\zeta}}$ are purely imaginary matrices.

D. Modified Reciprocity Theorem

The reciprocity theorem can be extended as follows. With respect to source a, we write

$$-\nabla \times \overline{E}_a = -i\omega(\overline{\overline{\mu}} \cdot \overline{H}_a + \overline{\overline{\zeta}} \cdot \overline{E}_a) + \overline{M}_a \qquad (6.2.11a)$$

$$\nabla \times \overline{H}_a = -i\omega(\overline{\overline{\epsilon}} \cdot \overline{E}_a + \overline{\overline{\xi}} \cdot \overline{H}_a) + \overline{J}_a \qquad (6.2.11b)$$

The medium is characterized by $\overline{\overline{\mu}}$, $\overline{\overline{\epsilon}}$, $\overline{\overline{\xi}}$, and $\overline{\overline{\zeta}}$. With respect to source b, we use constitutive relations characterized by $\overline{\overline{\mu}}^C, \overline{\overline{\epsilon}}^C, \overline{\overline{\xi}}^C$, and $\overline{\overline{\zeta}}^C$ such that

$$\overline{\overline{\mu}}^C = \overline{\overline{\mu}}^T \qquad (6.2.12a)$$

$$\overline{\overline{\epsilon}}^C = \overline{\overline{\epsilon}}^T \qquad (6.2.12b)$$

$$\overline{\overline{\xi}}^C = -\overline{\overline{\zeta}}^T \qquad (6.2.12c)$$

$$\overline{\overline{\zeta}}^C = -\overline{\overline{\xi}}^T \qquad (6.2.12d)$$

and call this medium the complementary medium. The Maxwell equations for source b in the complementary medium become

$$-\nabla \times \overline{E}_b^C = -i\omega(\overline{\overline{\mu}}^C \cdot \overline{H}_b^C + \overline{\overline{\zeta}}^C \cdot \overline{E}_b^C) + \overline{M}_b \qquad (6.2.13a)$$

$$\nabla \times \overline{H}_b^C = -i\omega(\overline{\overline{\epsilon}}^C \cdot \overline{E}_b^C + \overline{\overline{\xi}}^C \cdot \overline{H}_b^C) + \overline{J}_b \qquad (6.2.13b)$$

where $\overline{E}_b^C$ and $\overline{H}_b^C$ denote the fields produced by $\overline{J}_b$ and $\overline{M}_b$ in the complementary medium. If we define a new reaction

$$< a, b >^C = \iiint_V dV \, (\overline{J}_a \cdot \overline{E}_b^C - \overline{M}_a \cdot \overline{H}_b^C)$$

we find from (6.2.11) and (6.2.13) that

$$< b, a > = < a, b >^C \qquad (6.2.14)$$

This result may be called the modified reciprocity theorem, which states that the reaction $< b, a >$ of source b caused by source a in a bianisotropic medium is equal to the reaction $< a, b >^C$ of source a caused by source b in the complementary medium. The medium is reciprocal if the complementary medium is identical to the original medium.

Topic 6.2A Stationary Formulas and Rayleigh-Ritz Procedure

Consider a cavity at resonance. We want to calculate the resonant frequency, but we do not know the precise field distribution inside the cavity. Nevertheless, we can find a formula that expresses resonant frequencies in terms of field distributions. We can then assume a field distribution and calculate the resonant frequency in terms of the assumed field. If the formula is stationary, we can come closer to the true resonant frequency than is possible by using a nonstationary formula. Consider the formula $y = f(x)$. We want to calculate y at $x = x_0$, but we do not know the precise value of x_0. We assume that $x = x_0 + p$, where p is a parameter characterizing the deviation from x_0. The formula $y = f(x) = f(x_0 + p)$ can be expanded around x_0 in a Taylor series. We call the formula stationary at $p = 0$ if

$$\left.\frac{\partial f}{\partial p}\right|_{p=0} = 0 \tag{6.2A.1}$$

When this condition is satisfied, $f(x) = f(x_0) + (1/2)p^2 f^{(2)}(x_0) + \cdots$ and the deviation of $f(x)$ from $f(x_0)$ is of order p^2. Clearly, the stationary formula has an extremum at $p = 0$. When p is complex, we have a saddle point at $p = 0$.

Stationary Formula for Resonator Wavenumbers

We shall derive a stationary formula for the resonant frequency of a cavity with an assumed electric field. It is appropriate to mention that a stationary formula involving an assumed magnetic field or a mixture of electric and magnetic fields can be similarly derived. In terms of the assumed electric field (with subscript a), the Maxwell equation gives

$$\begin{aligned}\overline{J}_a &= i\omega\epsilon\overline{E}_a + \nabla \times \overline{H}_a \\ &= \frac{1}{i\omega\mu}\left[-k^2\overline{E}_a + \nabla \times (\nabla \times \overline{E}_a)\right]\end{aligned} \tag{6.2A.2}$$

inside the cavity. On the cavity wall, we have

$$\overline{M}_s = \hat{n} \times \overline{E}_a \tag{6.2A.3}$$

where $\hat{n}$ is the unit vector normal to the cavity wall and directed outwards. This magnetic surface current sheet will be zero if the $\overline{E}$

field is the exact electric field, because of the boundary conditions. Since the electric field will be assumed, there is no guarantee that it satisfies the boundary conditions.

Using the definition for reaction, we form a reaction for the cavity,

$$
< a, a > = \iiint_V dV\, \overline{J}_a \cdot \overline{E}_a - \oiint_S dS\, \overline{M}_s \cdot \overline{H}_a
$$

$$
= \frac{1}{i\omega\mu} \left\{ -k^2 \iiint_V dV\, \overline{E}_a^2 + \iiint_V dV\, (\nabla \times \overline{E}_a)^2 \right.
$$

$$
\left. + 2 \oiint_S dS\, \hat{n} \cdot \left[(\nabla \times \overline{E}_a) \times \overline{E}_a \right] \right\} \qquad (6.2\text{A}.4)
$$

In the derivation, we make use of the identities $\hat{n} \times \overline{E}_a \cdot \nabla \times \overline{E}_a = -\hat{n} \cdot \left[(\nabla \times \overline{E}_a) \times \overline{E}_a \right]$ and $\overline{E}_a \cdot \nabla \times (\nabla \times \overline{E}_a) = (\nabla \times \overline{E}_a)^2 + \nabla \cdot [(\nabla \times \overline{E}_a) \times \overline{E}_a]$. We require that reaction $< a, a >$ be equal to the true reaction of the cavity $< c, c >$, with c standing for "correct". What is the true reaction of the cavity? Inside the cavity, where the field is nonzero, the source is zero. On the cavity walls, where the source is nonzero, the field is zero. Thus $< c, c >= 0$. When $< a, a >$ is set equal to $< c, c >$ equal to zero, we obtain from (6.2A.4) a formula for the resonant wavenumber k^2 :

$$
k^2 = \frac{\iiint_V dV\, (\nabla \times \overline{E}_a)^2 + 2 \oiint_S dS\, \hat{n} \cdot (\nabla \times \overline{E}_a) \times \overline{E}_a}{\iiint_V dV\, \overline{E}_a \cdot \overline{E}_a} \qquad (6.2\text{A}.5)
$$

Note that this formula is exact if $\overline{E}_a$ is the exact field. We would like to find out whether this formula is stationary. Let $\overline{E}_a = \overline{E} + p\overline{e}$ and denote (6.2A.5) by $k^2 = N(p)/D(p)$. We wish to examine

$$
\left. \frac{\partial k^2}{\partial p} \right|_{p=0} = \frac{D(0)N'(0) - N(0)D'(0)}{D^2(0)} = \frac{N'(0) - k^2 D'(0)}{D(0)}
$$

since $N(0) = k^2 D(0)$. Differentiating the numerator of (6.2A.5) and setting $p = 0$, we obtain

$$
N'(0) = 2 \iiint_V dV\, (\nabla \times \overline{E}) \cdot (\nabla \times \overline{e}) + 2 \oiint_S dS\, \hat{n} \cdot (\nabla \times \overline{E}) \times \overline{e}
$$

$$
= 2k^2 \iiint_V dV\, \overline{e} \cdot \overline{E} = k^2 D'(0)
$$
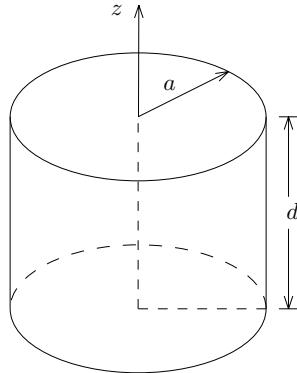
Figure 6.2A.1 Circular cavity resonator.

Here we used the fact that $\hat{n} \times \overline{E} = 0$ on the boundary surface S, the identity $(\nabla \times \overline{E}) \cdot (\nabla \times \overline{e}) = \nabla \cdot (\overline{e} \times \nabla \times \overline{E}) + \overline{e} \cdot \nabla \times \nabla \times \overline{E}$, and the wave equation $\nabla \times \nabla \times \overline{E} = k^2 \overline{E}$. From these results we have proved that $\partial k^2/\partial p\big|_{p=0} = 0$. Therefore, by requiring that the reaction caused by an assumed field be the same as the reaction attributable to the true field, we obtain a stationary formula for the resonant frequency of cavity.

Consider a circular cavity as shown in Figure 6.2A.1. The exact field is known to be, for the fundamental mode, $\overline{E} = \hat{z} E_0 J_0(k\rho)$. The exact resonant wavenumber, which is the first root of $J_0(ka)$,

$$ka = 2.405 \qquad \text{or} \qquad k^2 a^2 = 5.784$$

is also known. We now use (6.2A.5) to estimate the resonant wavenumber. Let us assume a trial field

$$\overline{E}_a = \hat{z} \cos \frac{\pi \rho}{2a}$$

This trial field satisfies the boundary condition at $\rho = a$, and it is not a solution to the wave equation. The curl of $\overline{E}_a$ can be calculated:

$$\nabla \times \overline{E}_a = \hat{\phi} \frac{\pi}{2a} \sin \frac{\pi \rho}{2a}$$

Stationary formula (6.2A.5) becomes

$$k^2 a^2 = \frac{\displaystyle\int_0^d dz \int_0^{2\pi} d\phi \int_0^a \rho d\rho \, (\pi/2)^2 \sin^2(\pi\rho/2a)}{\displaystyle\int_0^d dz \int_0^{2\pi} d\phi \int_0^a \rho d\rho \cos^2(\pi\rho/2a)} = 5.830$$

This is very close to the exact solution.

Next, we assume the trial field

$$\overline{E}_a = \hat{z}\left(1 + A\frac{\rho}{a}\right) \tag{6.2A.6}$$

where A is a constant. We shall determine the constant A by using the Ritz procedure as illustrated below. Applying (6.2A.5), we obtain

$$k^2 a^2 = \frac{\displaystyle\int_0^d dz \int_0^{2\pi} d\phi \int_0^a \rho d\rho\, A^2 - \int_0^d dz \int_0^{2\pi} d\phi\, 2a^2 A(1+A)}{\displaystyle\int_0^d dz \int_0^{2\pi} d\phi \int_0^a \rho d\rho\, [1 + A(\rho/a)]^2}$$

$$= \frac{-2A - (3/2)A^2}{(1/2) + (2/3)A + (1/4)A^2} \tag{6.2A.7}$$

requiring $k^2 a^2$ to be stationary with respect to A. If $\partial(k^2 a^2)/\partial A = 0$, we find $A = -1$ or -2. Inserting $A = -1$ into (6.2A.7) yields $k^2 a^2 = 6$. The value of $A = -1$ also enables the trial field to satisfy the boundary condition at $\rho = a$. The other value of $A = -2$ gives rise to a negative $k^2 a^2$ and is discarded.

The Ritz procedure can then be extended to n parameters A_l, $l = 1, 2, 3, \ldots, n$, which are then determined from the n equations $\partial k^2/\partial A_l = 0$, $l = 1, 2, \ldots n$. As an example, we assume a trial field characterized by parameters A_1 and A_2 and write

$$\overline{E} = \hat{z}(1 + A_1 \frac{\rho}{a} + A_2 \frac{\rho^2}{a^2})$$

Then

$$\nabla \times \overline{E} = -\hat{\phi}(A_1 + 2A_2 \frac{\rho}{a})/a$$

Inserting in the stationary formula and performing the integration, we obtain

$$k^2 a^2 = -\frac{10[18A_2^2 + (28A_1 + 24)A_2 + 9A_1^2 + 12A_1]}{10A_2^2 + (24A_1 + 30)A_2 + 15A_1^2 + 40A_1 + 30}$$

The parameters A_1 and A_2 are determined by requiring that

$$\frac{\partial(k^2 a^2)}{\partial A_1} = 0, \qquad \frac{\partial(k^2 a^2)}{\partial A_2} = 0$$

These yield two equations:

$$38A_2^3 + (90A_1 + 84)A_2^2$$
$$+(51A_1^2 + 45A_1 - 60)A_2 - 45A_1^2 - 135A_1 - 90 = 0$$

$$(76A_1 + 150)A_2^2 + (180A_1^2 + 600A_1 + 540)A_2$$
$$+102A_1^3 + 461A_1^2 + 720A_1 + 360 = 0$$

Solving these equations gives $A_1 = -0.7817$ and $A_2 = -0.1834$. With these values for A_1 and A_2, we obtain

$$k^2 a^2 = 5.934$$

This value is closer to the exact solution than the one we would have obtained by using the trial field (6.2A.6). With these values of A_1 and A_2, we see that the trial field satisfies neither the wave equation nor the boundary condition. Solutions from other values of A_1 and A_2 are not calculated and may correspond to higher resonant wavenumbers. As a final remark, we note that in using the Ritz procedure it is often advisable to choose the trial field components from an orthogonal complete set of functions.

Stationary Formula for Antenna Impedance

We now derive a stationary formula for antenna self-impedance. Consider an antenna made of perfect conductor excited by a current source I. The self-reaction of this antenna is due entirely to the current at the terminal. The reason is that on the conducting surface, where the surface current is not zero, the field is zero. The self-reaction is equal to $-VI$ at the terminal. To calculate the self-impedance, we maintain the same terminal current I and assume a current distribution on the surface of the antenna. The self-reaction $< a, a >$ is then calculated. We require that this reaction be approximately equal to the correct reaction $< c, c >$:

$$< a, a > \approx < c, c > = -VI \qquad (6.2A.8)$$

The input impedance is approximated by

$$Z_{in} = -\frac{< c, c >}{I^2} \approx -\frac{< a, a >}{I^2} \qquad (6.2A.9)$$
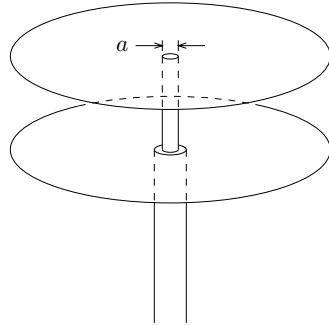
Figure 6.2A.2 Probe excitation of a radial parallel-plate waveguide.

Let $a = c + pe$. We see that

$$\frac{\partial Z_{in}}{\partial p} = -\frac{1}{I^2}(<e,c> + <c,e>) = -\frac{2}{I^2}<e,c> = 0$$

The second equality follows from reciprocity. The last equality is due
to the fact that at the terminal, where the field is not zero, the error
source e is zero; everywhere else the correct field c is zero. Thus the
formula for the input impedance is proved to be stationary.

   We apply the stationary formula for input impedance to a radial
parallel-plate waveguide excited by a probe of diameter a [Fig. 6.2A.2].
The source terminal of the probe is outside the waveguide. For the
TEM mode, we assume that the trial current is uniform along the
probe, $\overline{J}_a = \hat{z}I/\pi a$. The electric field generated by this current is

$$\overline{E}_a = \hat{z}\left[-\frac{k^2 I}{4\omega\epsilon}H_0^{(1)}(k\rho)\right]$$

Letting d denote the distance between the two plates, we find the
input impedance to be

$$Z_{in} = \frac{\eta}{4}kd\,H_0^{(1)}(ka/2)$$

by using the stationary formula (6.2A.9).

Stationary Formula for Scattering

We shall now derive a stationary formula for scattering problems. Con-
sider a transmitter, a receiver, and a conducting scatterer [Fig. 6.2A.3].
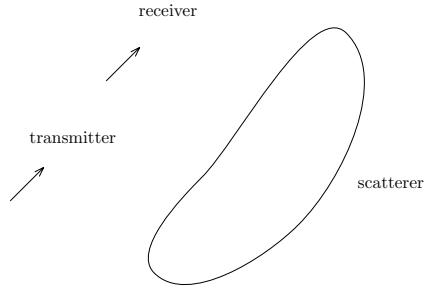
Figure 6.2A.3 A transmitter, a receiver, and a conducting scatterer.

The receiver receives a wave composed of two components; one directly from the transmitter in the absence of the scatterer, and one originating from currents on the scatterer induced by the transmitter alone. Note that the receiver also induces currents on the scatterer. We want to find a stationary formula for the scattered field V_s as received by the receiver, $V_s = - < i, t >$, where i denotes the receiver source current, and t the field produced by the transmitter-induced currents on the scatterer. We anticipate that the stationary formula will comprise of surface integrals over the scatterer surface. By reciprocity, $V_s = - < i, c_t > = - < c_t, i >$, where, in $< c_t, i >$, c_t denotes the current induced by the transmitter on the scatterer, and i the field produced by the receiver in the absence of the scatterer. In the presence of the scatterer, the field on the scatterer is equal and opposite to i because the scatterer is a conducting body. The field on the scatterer combined with the field in the absence of the scatterer gives a zero field at the scatterer. Let this field be denoted by c_r. We then have on the scatterer surface

$$V_s = - < c_t, i > = < c_t, c_r > \qquad (6.2A.10)$$

Thus far, we have established that the signal received by the receiver is equal to the reaction between the current induced on the scatterer by the transmitter and the field generated on the scatterer by the receiver current.

The letter c in (6.2A.10) stands for "correct." To calculate V_s, we approximate $< c_t, c_r >$ and write

$$V_s = < c_t, c_r > \approx < a_t, a_r > \qquad (6.2A.11)$$

where a stands for "assumed." The formula is a stationary formula

provided that the following constraints are met:

$$< a_t, a_r > = < c_t, a_r > = < a_t, c_r > \qquad (6.2\text{A}.12)$$

where c_t is the correct current induced on the scatterer by the trans-
mitter, and c_r is the correct field generated on the scatterer because
of the receiver current.

   To show that the constraints of (6.2A.12) can lead us to a station-
ary formula, let us make a general proposition: a reaction $< a, b >$ is
stationary if it satisfies the constraints

$$< a, b > = < c_a, b > = < a, c_b > \qquad (6.2\text{A}.13)$$

To prove this theorem, let

$$a = c_a + p_a e_a$$
$$b = c_b + p_b e_b$$

where c stands for "correct", and e for "error". By definition, $< a, b >$
is stationary if

$$\left. \frac{\partial < a, b >}{\partial p_a} \right|_{p_a = p_b = 0} = \left. \frac{\partial < a, b >}{\partial p_b} \right|_{p_a = p_b = 0} = 0 \qquad (6.2\text{A}.14)$$

which is seen to be true as the constraint $< a, b > = < c_a, b >$ implies
$< e_a, b > = 0$, and the constraint $< a, b > = < a, c_b >$ implies $< a, e_b >$
$= 0$.

   It is important to note that constraints (6.2A.13) are sufficient
conditions for a formula to be stationary; they are not necessary con-
ditions. Recall that we did not use these constraints in establishing
stationary formulas for the resonant wavenumber of a cavity or for the
input impedance of an antenna. In fact, the constraints may be vio-
lated. For instance, consider the input impedance of an antenna. Here
the constraint $< a, a > = < a, c >$ is violated because, on the antenna
surface, the correct fields are zero, but the assumed fields are not.

Topic 6.2B Method of Moments

The method of moments is a numerical technique useful in the solution of electromagnetic wave scattering and radiation problems. Consider a perfectly conducting scattering body that, when illuminated with an incident field $\overline{E}_i$ and $\overline{H}_i$, produces scattered fields $\overline{E}_s$ and $\overline{H}_s$. The scattered fields $\overline{E}_s$ and $\overline{H}_s$ may be attributed to surface currents induced on the scattering body by the incident field. Letting the surface currents be $\overline{J}_s$, we have

$$\overline{E}_s(\overline{r}) = i\omega\mu \iint dS' \, \overline{\overline{G}}(\overline{r}, \overline{r}') \cdot \overline{J}_s(\overline{r}') \qquad (6.2\text{B}.1)$$

integrating over the surface of the scatterer S. The unknown surface current may be expanded in terms of basis (or expansion) functions $\overline{F}_n(\overline{r}')$ such that

$$\overline{J}_s(\overline{r}') = \sum_n I_n \overline{F}_n(\overline{r}') \qquad (6.2\text{B}.2)$$

Once the expansion coefficients I_n are known, the unknown surface current $\overline{J}_s(\overline{r}')$ will be determined and used to find the desired scattered fields.

The method of moments calls for the use of a set of testing functions $\overline{J}_m(\overline{r})$ with which we form

$$\iint_{S_m} dS_m \, \overline{J}_m(\overline{r}) \cdot \overline{E}_s(\overline{r})$$

$$= \sum_n \left[\iint_{S_m} dS_m \, \overline{J}_m(\overline{r}) \cdot i\omega\mu \iint dS' \overline{\overline{G}} \cdot \overline{F}_n \right] I_n$$

$$= \sum_n Z_{mn} I_n \qquad (6.2\text{B}.3)$$

where

$$Z_{mn} = \iint_{S_m} dS_m \, \overline{J}_m(\overline{r}) \cdot i\omega\mu \iint dS' \overline{\overline{G}} \cdot \overline{F}_n(\overline{r}') \qquad (6.2\text{B}.4)$$

and S_m is part of the surface of the perfectly conducting scatterer. The set of testing functions covers the whole surface S of the scattering body.

On the conducting surface, the boundary condition requires that the total tangential electric field $\overline{E}_s + \overline{E}_i = 0$. From (6.2B.3), we find

$$\iint_{S_m} dS_m \, \overline{J}_m(\overline{r}) \cdot \overline{E}_s(\overline{r}) = - \iint_{S_m} dS_m \, \overline{J}_m(\overline{r}) \cdot \overline{E}_i(\overline{r}) \qquad (6.2\text{B}.5)$$

This should be compared with (6.2A.10) where $< c_t, c_r > = - < c_t, i >$ although c_t is now actually a_t. Defining

$$V_m = - \iint_{S_m} dS_m \, \overline{J}_m(\overline{r}) \cdot \overline{E}_i(\overline{r}) \qquad (6.2\text{B}.6)$$

We find from (6.2B.3)–(6.2B.5)

$$Z_{mn} I_n = V_m \qquad (6.2\text{B}.7)$$

and consequently the unknown expansion coefficients for the surface currents

$$I_n = Z_{mn}^{-1} V_m \qquad (6.2\text{B}.8)$$

Thus the essence of the method of moments lies in the choice of the basis and testing functions, and the numerical inversion of the Z-matrix Z_{mn}. In the point matching technique, we choose the testing functions to be delta functions such that $\overline{J}_m(\overline{r}) = \overline{J}_m \delta(\overline{r} - \overline{r}_m)$ and cover the scattering body with enough points to ensure a convergent result. On those chosen points, the boundary condition of zero tangential $\overline{E}$ field is enforced. When the same function is used for both basis expansion and testing, the technique is called Galerkin's method.

Problems

P6.2.1

Which of the following media are lossless? Which of the following media are reciprocal? For the nonreciprocal ones, what are their complementary media?

(a) A biaxial medium with real constitutive parameters.
(b) A moving biaxial medium.
(c) A chiral medium

$$\overline{D} = \epsilon \overline{E} + i\chi \overline{H}$$
$$\overline{B} = \mu \overline{H} - i\chi \overline{E}$$

(d) A biisotropic medium with a real χ.

$$\overline{D} = \epsilon \overline{E} + \chi \overline{H}$$
$$\overline{B} = \mu \overline{H} - \chi \overline{E}$$

(e) A ferrite in a dc magnetic field.

P6.2.2

Derive a stationary formula for the resonant frequency of a resonator cavity in terms of the magnetic field $\overline{H}$ by assuming a trial field $\overline{H}_a$ to obtain

$$\overline{E}_a = \frac{1}{-i\omega\epsilon}\nabla \times \overline{H}_a, \quad \overline{M}_s = -\frac{1}{i\omega\epsilon}\hat{n} \times (\nabla \times \overline{H}_a)$$

Find the resonant frequency for a circular cavity by assuming approximate magnetic field distributions to be $\overline{H}_a = \hat{\phi}\,(\rho + A\rho^2)$.

P6.2.3

Show that, if the inside of a waveguide is filled with several different isotropic media, the stationary formula for the cutoff frequency in terms of the $\overline{E}$ field is

$$\omega_c^2 = \frac{\displaystyle\iint dS\,\mu^{-1}(\nabla \times \overline{E})^2}{\displaystyle\iint dS\,\epsilon E^2} + \frac{2\displaystyle\int dl\,\hat{n}\cdot\left[\mu^{-1}(\nabla \times \overline{E}) \times \overline{E}\right]}{\displaystyle\iint dS\,\epsilon E^2}$$

where $\hat{n}$ is the outward-pointing unit vector normal to the waveguide walls.

Solve for the cutoff frequency of a rectangular waveguide filled with two different dielectric media. Let the waveguide dimension a be along $\hat{x}$ and b along $\hat{y}$. The dielectric ϵ_1 fills the space from $x = 0$ to $x = a/2$, and the dielectric ϵ_2 fills the space from $x = a/2$ to $x = a$. Assume an electric field of $\overline{E} = \hat{y}\sin(\pi x/a)$.

P6.2.4

Consider backscattering from a linearly polarized wave $\overline{E}^i = \hat{z}E_0\,e^{ikx}$ produced by a current element Il, with $E_0 = -i\omega\mu Il/4\pi r$. For backscattering, transmitter and receiver are the same,

$$V_s = -<c_t, c_t> = -I\int \overline{E}^s \cdot d\ell = -E_\ell^s\,Il$$

where E_ℓ^s signifies the scattered field component along the antenna.

$$E_l^s = \frac{<c_t, c_t>}{(Il)} \simeq \frac{<a_t, a_t>}{(Il)} = \frac{<a_t, c_t>^2}{(Il)<a_t, a_t>} = \frac{\left(\displaystyle\iint \overline{J}^a \cdot \overline{E}^i\,dS\right)^2}{(Il)\displaystyle\iint \overline{J}^a \cdot \overline{E}^a\,dS}$$

Show that the echo area for backscattering resulting from the linearly polar-ized field is

$$
A_e = \lim_{r \to \infty} 4\pi r^2 \left| \frac{E_s}{E^i} \right|^2 = \pi \left| \frac{\eta}{\lambda} \frac{\left(\iint J_z^a e^{+ikx}, dS \right)^2}{\iint \overline{E}^a \cdot \overline{J}_a \, dS} \right|^2 .
$$

$$
A_e = \lim_{r \to \infty} 4\pi r^2 \left| \frac{\overline{E}_s}{\overline{E}^i} \right|^2 = \pi \left| \frac{\eta}{\lambda} \frac{\left(\iint J_z^a \, e^{-ikx} ds \right)^2}{\iint \overline{E}^a \cdot \overline{J}^a ds} \right|^2
$$

Consider a plane wave $\overline{E}^i = \hat{z} E_0 \, e^{ikx}$ is normally incident upon a conducting wire of length $L = \lambda/2$ along the z axis. Assume that the current on the wire is $I^a = \cos kz$. Using the stationary formula and the fact that $< a, a > = 73$, find the echo area for backscattering.

P6.2.5

For a cavity filled with several different isotropic media, show that the stationary formula with an assumed electric field is given by

$$
\omega_r^2 = \frac{\iiint_V dV \mu^{-1} (\nabla \times \overline{E})^2 + 2 \iint_S dS \, \hat{n} \cdot \{ \mu^{-1} (\nabla \times \overline{E}) \times \overline{E} \}}{\iiint_V dV \, \epsilon E^2}
$$

where $\hat{n}$ is the outward-pointing unit vector normal to the cavity walls. Con-sider a microwave oven, which has dimensions $h = 25 \, \text{cm}$, $w = 40 \, \text{cm}$, $d = 40 \, \text{cm}$. Consider a dielectric of rectangular shape with permittivity $\epsilon = 4\epsilon_o$ and dimensions $15 \, \text{cm}(h) \times 30 \, \text{cm}(w) \times 20 \, \text{cm}(d)$. Assume the electric field $\overline{E} = \hat{x} \sin(\pi y/w) \sin(\pi z/d)$ and find the percentage of variation in resonant frequency.

6.3   Quasi-Static Limits

To explore the quasi-static limit, we expand the field vectors in power series of their values around $\omega = 0$. To facilitate the expansion, we separate the field dependence by introducing a new independent variable $\tau = \omega t$. The field quantities $\overline{E}(\overline{r}, \tau, \omega)$, $\overline{H}(\overline{r}, \tau, \omega)$, $\overline{D}(\overline{r}, \tau, \omega)$, $\overline{B}(\overline{r}, \tau, \omega)$, $\overline{J}(\overline{r}, \tau, \omega)$, and $\rho(\overline{r}, \tau, \omega)$ can now be expanded in power series in ω. We write

$$
\overline{E}(\overline{r}, \tau, \omega) = \sum_{m=0}^{\infty} \frac{\omega^m}{m!} \left[\frac{\partial^m}{\partial \omega^m} \overline{E}(\overline{r}, \tau, \omega) \right]_{\omega=0}
$$

$$
= \sum_{m=0}^{\infty} \overline{E}^{(m)}(\overline{r}, \tau, \omega) \tag{6.3.1}
$$

and similarly for other field quantities. From the Maxwell equations, we find

$$
\sum_{m=0}^{\infty} \nabla \times \overline{E}^{(m)} = -\omega \frac{\partial}{\partial \tau} \sum_{m=0}^{\infty} \overline{B}^{(m)}
$$

$$
= -\sum_{m=1}^{\infty} \frac{\partial}{\partial \tau} \frac{\omega^m}{(m-1)!} \left[\frac{\partial^{m-1}}{\partial \omega^{m-1}} \overline{B}(\overline{r}, \tau, \omega) \right]_{\omega=0}
$$

$$
= -\sum_{m=1}^{\infty} \omega \frac{\partial}{\partial \tau} \overline{B}^{(m-1)} \tag{6.3.2}
$$

It follows that

$$
\nabla \times \overline{E}^{(0)} = 0 \tag{6.3.3a}
$$

$$
\nabla \times \overline{E}^{(m)} = -\frac{\partial}{\partial t} \overline{B}^{(m-1)} \qquad m = 1, 2, \dots \tag{6.3.3b}
$$

Similarly,

$$
\nabla \times \overline{H}^{(0)} = \overline{J}^{(0)} \tag{6.3.4a}
$$

$$
\nabla \times \overline{H}^{(m)} = \overline{J}^{(m)} + \frac{\partial}{\partial t} \overline{D}^{(m-1)} \qquad m = 1, 2, \dots \tag{6.3.4b}
$$

$$
\nabla \cdot \overline{D}^{(0)} = \rho^{(0)} \tag{6.3.5a}
$$

$$
\nabla \cdot \overline{D}^{(m)} = \rho^{(m)} \qquad m = 1, 2, \dots \tag{6.3.5b}
$$

$$\nabla \cdot \overline{B}^{(0)} = 0 \tag{6.3.6a}$$

$$\nabla \cdot \overline{B}^{(m)} = 0 \qquad\qquad m = 1, 2, \ldots \tag{6.3.6b}$$

$$\nabla \cdot \overline{J}^{(0)} = 0 \tag{6.3.7a}$$

$$\nabla \cdot \overline{J}^{(m)} = -\frac{\partial}{\partial t} \rho^{(m-1)} \qquad\qquad m = 1, 2, \ldots \tag{6.3.7b}$$

Equations $(6.3.3a)$ and $(6.3.5a)$ are the governing equations for electrostatic fields. Equations $(6.3.4a)$ and $(6.3.6a)$ are the governing equations for magnetostatic fields.

It is important to notice that the m th-order fields are now expressed in terms of the $(m-1)$ th-order fields. Thus, when the zeroth-order fields are obtained for given sources $\overline{J}^{(0)}$ and $\rho^{(0)}$, all higher order fields can be determined in succession. The electrostatic fields are governed by $(6.3.3a)$, $(6.3.5a)$, and $(6.3.7b)$, with $m = 1$. Namely, the zeroth-order electrostatic fields as obtained from $(6.3.3a)$ and $(6.3.5a)$ are now used to find the first-order current $\overline{J}^{(1)}$ from $(6.3.7b)$ and likewise the first-order magnetic field $\overline{H}^{(1)}$ from $(6.3.4b)$. Equations $(6.3.4a)$, $(6.3.6a)$, and $(6.3.3b)$ with $m = 1$ are seen to be the magnetostatic equations. Associated with each differential equation in $(6.3.3)$–$(6.3.7)$, corresponding boundary conditions can be derived.

EXAMPLE 6.3.1   Consider the electromagnetic fields in a parallel-plate waveguide [Fig. E6.3.1.1]. A time-harmonic voltage source is applied at $z = 0$ with

$$V(t) = V_0 \cos \omega t \tag{E6.3.1.1}$$

The zeroth-order electric field is the electrostatic field

$$\overline{E}^{(0)} = -\hat{x}\frac{V_0}{d} \cos \omega t \tag{E6.3.1.2a}$$

$$\overline{H}^{(0)} = 0 \tag{E6.3.1.2b}$$

The first-order magnetic field $\overline{H}^{(1)}$ is found from $(6.3.4b)$, which gives

$$\frac{\partial}{\partial z} H_y^{(1)} = -\omega \frac{\epsilon V_0}{d} \sin \omega t$$
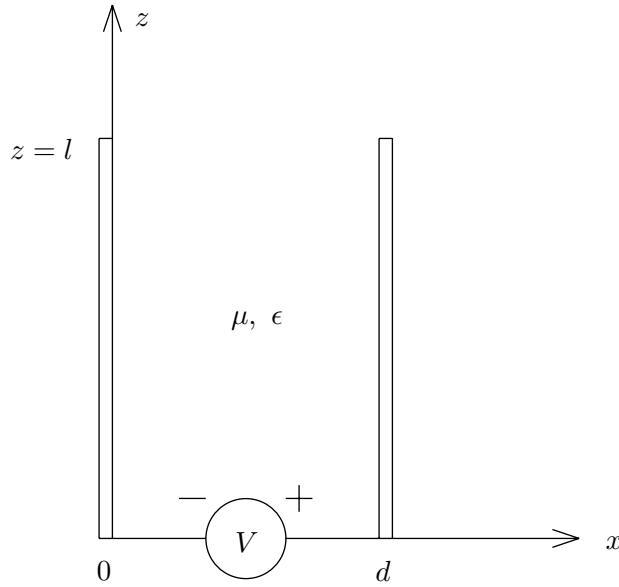
Figure E6.3.1.1 Parallel-plate waveguide.

Thus

$$\overline{H}^{(1)} = -\hat{y}\,\omega\,\frac{\epsilon V_0}{d}\,z\sin\omega t \qquad\qquad (E6.3.1.2c)$$

Since $\overline{H}^{(0)} = 0$, we find that

$$\overline{E}^{(1)} = 0 \qquad\qquad (E6.3.1.2d)$$

for the first-order electric field.

For the second-order field quantities, we find from (6.3.4b) that

$$\overline{H}^{(2)} = 0 \qquad\qquad (E6.3.1.3a)$$

which follows from (E6.3.1.2d). As seen from (6.3.3b),

$$\nabla \times \overline{E}^{(2)} = \hat{y}\,\omega^2\,\frac{\mu\epsilon V_0}{d}\,z\cos\omega t$$

Thus

$$\overline{E}^{(2)} = \hat{x}\,\frac{V_0}{d}\,\frac{k^2 z^2}{2}\cos\omega t \qquad\qquad (E6.3.1.3b)$$

where $k^2 = \omega^2\mu\epsilon$.

Continuing the process, we find that the odd-order terms $\overline{E}^{(m)}$ are all zero and the even-order terms are

$$\overline{E}^{(2n)} = -\hat{x}(-1)^n \frac{V_0}{d} \frac{(kz)^{2n}}{(2n)!} \cos \omega t \qquad n = 0, 1, 2, \ldots \qquad \text{(E6.3.1.4}a\text{)}$$

Similarly, we find that the even-order terms for $\overline{H}^{(m)}$ are all zero and the odd-order terms are

$$\overline{H}^{(2n+1)} = -\hat{y}(-1)^n \frac{V_0}{\eta d} \frac{(kz)^{2n+1}}{(2n+1)!} \sin \omega t \qquad n = 0, 1, 2, \ldots \qquad \text{(E6.3.1.4}b\text{)}$$

Summing over the infinite number of terms, we obtain

$$\overline{E} = \sum_{n=0}^{\infty} \overline{E}^{(2n)} = -\hat{x} \frac{V_0}{d} \cos kz \cos \omega t \qquad \text{(E6.3.1.5}a\text{)}$$

$$\overline{H} = \sum_{n=0}^{\infty} \overline{H}^{(2n+1)} = -\hat{y} \frac{V_0}{\eta d} \sin kz \sin \omega t \qquad \text{(E6.3.1.5}b\text{)}$$

Equation (E6.3.1.5) represents the exact solution for an open-circuited transmission line.

— END OF EXAMPLE 6.3.1 —

EXAMPLE 6.3.2

Consider the electromagnetic fields in between two plates with circular cross-section as shown in [Figure E6.3.2.1]. A time-harmonic voltage source is applied at $z = 0$ with

$$V(t) = V_0 \cos \omega t \qquad \text{(E6.3.2.1)}$$
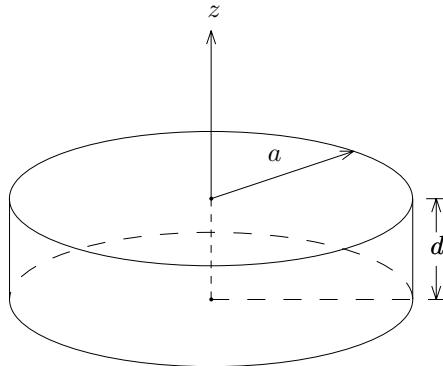
Figure E6.3.2.1 Circular-plate capacitors.

The zeroth-order electric field is the electrostatic field

$$\overline{E}^{(0)} = \hat{z}\frac{V_0}{d}\cos\omega t \qquad (E6.3.2.2a)$$

$$\overline{H}^{(0)} = 0 \qquad (E6.3.2.2b)$$

The m th order fields are derived from the $(m-1)$ th order fields.

$$\frac{\partial}{\partial\rho}E_z^{(m)} = \frac{\partial}{\partial t}\mu H_y^{(m-1)} \qquad (E6.3.2.3a)$$

$$\frac{1}{\rho}\frac{\partial}{\partial\rho}\rho H_\phi^{(m)} = \frac{\partial}{\partial t}\epsilon E_z^{(m-1)} \qquad (E6.3.2.3b)$$

The first-order fields are

$$E_z^{(1)} = 0 \qquad (E6.3.2.4a)$$

$$H_\phi^{(1)} = -\omega\frac{\epsilon V_0}{d}\frac{\rho}{2}\sin\omega t \qquad (E6.3.2.4b)$$

The second-order fields are

$$E_z^{(2)} = -\frac{V_0}{d}(\frac{k\rho}{2})^2\cos\omega t \qquad (E6.3.2.5a)$$

$$H_\phi^{(2)} = 0 \qquad (E6.3.2.5b)$$

The third-order fields are

$$E_x^{(3)} = 0 \qquad (E6.3.2.6a)$$

$$H_y^{(3)} = \frac{V_0}{\eta d}\frac{(kz)^3}{2^24}\sin\omega t \qquad (E6.3.2.6b)$$

Continuing the process, we find

$$\overline{E}^{(2n)} = \hat{z}(-1)^n\frac{V_0}{d}(\frac{(k\rho)^{2n}}{2^2\cdot 4^2\cdot 6^2\cdot\cdots\cdot(2n)^2})\cos\omega t \qquad n = 0,1,2,.\ (E6.3.2.7a)$$

$$\overline{H}^{(2n-1)} = \hat{\phi}(-1)^n\frac{\omega V_0}{\eta d}(\frac{2n\ (k\rho)^{2n-1}}{2^2\cdot 4^2\cdot 6^2\cdot\cdots\cdot(2n)^2})\sin\omega t \qquad n = 1,2,3,.\ (E6.3.2.7b)$$

Summing over the infinite number of terms, we obtain

$$\overline{E} = \sum_{n=0}^{\infty}\overline{E}^{(2n)} = \hat{z}\frac{V_0}{d}\left(1-(\frac{1}{1!})^2(\frac{k\rho}{2})^2+(\frac{1}{2!})^2(\frac{k\rho}{2})^4-(\frac{1}{3!})^2(\frac{k\rho}{2})^6+\cdots\right)\cos\omega t$$

$$= \hat{z}\frac{V_0}{d}J_0(k\rho)\cos\omega t \qquad (E6.3.2.8a)$$

$$\overline{H} = \sum_{n=0}^{\infty}\overline{H}^{(2n+1)} = -\hat{\phi}\frac{\omega V_0}{\eta d}J_1(k\rho)\sin\omega t \qquad (E6.3.2.8b)$$

Equation (E6.3.2.8) represents the exact solution for the fundamental mode inside a cylindrical cavity with circular cross-section.

— END OF EXAMPLE 6.3.2 —

EXAMPLE 6.3.3

The magnetic field $\overline{H}$ for a Hertzian dipole with dipole moment $Il = -i\omega p$ pointing in the $\hat{z}$ direction is

$$\overline{H} = \hat{\phi}\frac{-ikIle^{ikr}}{4\pi r}\left[1 + \frac{i}{kr}\right]\sin\theta \qquad (E6.3.3.1)$$

where $k = \omega/c$. We see from (E6.3.3.1) that the first-order magnetic field for the Hertzian dipole is

$$\overline{H}^{(1)} = \hat{\phi}\frac{Il}{4\pi r^2}\sin\theta$$

which is identical to the magnetic field for an infinitesimal current element pointing in the $\hat{z}$ direction (as obtained from the Biot-Savart law).

— END OF EXAMPLE 6.3.3 —

Problems

P6.3.1

In the electroquasistatic field, the first-order current is obtained from the time derivative of the zeroth-order charge distribution. For a capacitor carrying charge $Q = CV$, the first-order current is

$$I = \frac{dQ}{dt} = C\frac{dV}{dt} + V\frac{dC}{dt}$$

Electroquasistatic transducers are devices that use the second term by mechanically vibrating a capacitor to generate electric current.
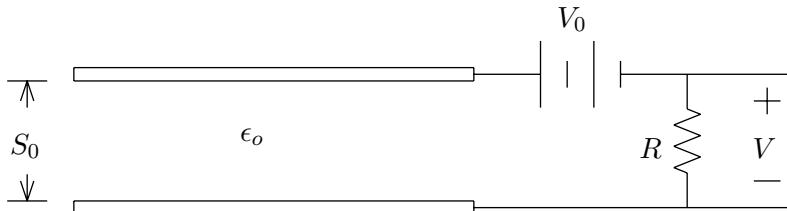
Figure P6.3.1.1

In a condenser microphone, a metal-plate diaphragm is tightly stretched but still capable of movement in response to sound transients. It is often made of a plastic film coated with an extremely fine, thin covering of gold to make it conductive. The diaphragm forms one plate of a capacitor with a dielectric

plastic backing facing the fixed back-plate electrode. The equivalent circuit for a condenser microphone is shown in Figure P6.3.1.1.

For a time-harmonic sound pressure creating a diaphragm movement of $s(t) = S_1 \cos \omega t$, show that the differential equation for $v(t)$ is

$$RC_0 \frac{dv(t)}{dt} + v(t) = RC_0 V_0 \frac{d}{dt} \left[\frac{s(t)}{S_0} \right]$$

where $C_0 = \epsilon_o A/S_0$ and A is the area of the diaphragm. Let $V_0 = 50 \, \text{volts}$, $R = 10^7 \, \text{ohms}$, $A = 8 \, \text{cm}^2$, $f = 1 \, \text{kHz}$, $S_0 = 25 \, \mu\text{m}$, and $S_1 = 1 \, \mu\text{m}$. Find the magnitude of the output voltage. Show that the induced voltage is directly proportional to the diaphragm vibration amplitude S_1 when $\omega RC_0 \gg 1$.

P6.3.2

(a) Consider a surface current sheet with current density given by

$$\overline{J} = \hat{x} J_s \delta(z)$$

Determine the time-average power per unit area generated by the current sheet and the time-average power per unit area carried by the plane wave in the half-space $z > 0$

(b) For a surface current sheet with the current density given by

$$\overline{J} = \hat{x} J_s e^{-j\beta y} \delta(z)$$

determine the amplitudes of the waves generated and the associated time-average power densities. What happens when $\beta = k = \omega \sqrt{\mu_o \epsilon_o}$?

(c) In the quasistatic limit, show that the magnetic field approaches that generated by a sinusoidal current sheet.

6.4   Geometrical Optics Limit

Geometrical optics can be treated as a limiting case of very high frequency approximation in Maxwell's theory. Consider the solution

$$\overline{E}(\overline{r}) = \overline{E}\, e^{ik_0 L(\overline{r})} \tag{6.4.1}$$

$$\overline{H}(\overline{r}) = \overline{H}\, e^{ik_0 L(\overline{r})} \tag{6.4.2}$$

where $k_0 = \omega/c$ and we shall let $k_0 \to \infty$. Substituting in the source-free Maxwell equations and making use of the vector identities $\nabla \times (\overline{A}\phi) = \phi \nabla \times \overline{A} + \nabla\phi \times \overline{A}$, and $\nabla \cdot (\overline{A}\phi) = \nabla\phi \cdot \overline{A} + \phi \nabla \cdot \overline{A}$, we find that in isotropic media,

$$\nabla L(\overline{r}) \times \overline{H} + \frac{n}{\eta}\overline{E} = \frac{i}{k_0}\nabla \times \overline{H} \tag{6.4.3}$$

$$\nabla L(\overline{r}) \times \overline{E} - n\eta\overline{H} = \frac{i}{k_0}\nabla \times \overline{E} \tag{6.4.4}$$

$$\nabla L(\overline{r}) \cdot \overline{E} = \frac{i}{k_0}\nabla \cdot \overline{E} \tag{6.4.5}$$

$$\nabla L(\overline{r}) \cdot \overline{H} = \frac{i}{k_0}\nabla \cdot \overline{H} \tag{6.4.6}$$

where $n = c\sqrt{\mu\epsilon}$ is the refractive index and $\eta = \sqrt{\mu/\epsilon}$ is the characteristic impedance for the isotropic media.

In the high-frequency limit we omit the right-hand sides of (6.4.3)–(6.4.6) and obtain the governing equations for geometrical optics

$$\nabla L \times \overline{H} + \frac{n}{\eta}\overline{E} = 0 \tag{6.4.7}$$

$$\nabla L \times \overline{E} - n\eta\overline{H} = 0 \tag{6.4.8}$$

$$\nabla L \cdot \overline{E} = 0 \tag{6.4.9}$$

$$\nabla L \cdot \overline{H} = 0 \tag{6.4.10}$$

This set of equations is now independent of frequency.

Substituting (6.4.8) in (6.4.7) and making use of (6.4.9) we obtain the eikonal equation in geometrical optics

$$|\nabla L(\overline{r})|^2 = n^2 \tag{6.4.11}$$

The phase function $L(\overline{r})$ is also called the eikonal. The geometrical wavefronts are described by $L(\overline{r}) = constant$. Let the unit normal to a wavefront be $\hat{s}$. We see from (6.4.11) that

$$\nabla L = \hat{s}n \tag{6.4.12}$$

where $\hat{s}n$ is called the ray vector.

We see from (6.4.9) and (6.4.10) that the electric and magnetic fields are perpendicular to the normal of the wavefront. The time-average Poynting's vector is

$$
\begin{aligned}
< \overline{S} > &= \frac{1}{2}\mathrm{Re}\left\{\overline{E} \times \overline{H}^*\right\} = \frac{1}{2n\eta}\mathrm{Re}\left\{\overline{E} \times (\nabla L \times \overline{E})^*\right\} \\
&= \frac{1}{2n\eta}(\overline{E} \cdot \overline{E}^*)\nabla L = \frac{2c}{n^2} < W_e > \nabla L = \hat{s}\frac{2c}{n} < W_e >
\end{aligned}
\tag{6.4.13}
$$

or, in terms of $\overline{H}$,

$$
\begin{aligned}
< \overline{S} > &= -\frac{\eta}{2n}\mathrm{Re}\left\{(\nabla L \times \overline{H}) \times \overline{H}^*\right\} \\
&= \frac{\eta}{2n}(\overline{H} \cdot \overline{H}^*)\nabla L = \frac{2c}{n^2} < W_m > \nabla L = \hat{s}\frac{2c}{n} < W_m >
\end{aligned}
\tag{6.4.14}
$$

where $< W_e > = \epsilon \overline{E} \cdot \overline{E}^*/4$ is the time-average electric energy, and $< W_m > = \mu \overline{H} \cdot \overline{H}^*/4$ is the time-average magnetic energy. We find by equating (6.4.13) and (6.4.14) that $< W_e > = < W_m > = < W > /2$ where $< W >$ is the total time-average stored energy. Thus

$$
< \overline{S} > = \hat{s}\frac{c}{n} < W > = \hat{s}v < W >
\tag{6.4.15}
$$

where $v = c/n$ is the velocity of the electromagnetic wave in the medium. We conclude that the time-average Poynting's power vector is in the direction of the ray vector $\hat{s}n$ and its magnitude is equal to the product of the electromagnetic energy $< W >$ and the velocity v.

The intensity I is defined as the absolute value of the time-average Poynting vector

$$
I = \left|< \overline{S} >\right| = v < W >
$$

Poynting's theorem states that

$$
\nabla \cdot \overline{S} = -i\omega(\epsilon|E|^2 - \mu|H|^2)
$$

Taking time-average of the above equation we obtain

$$
\nabla \cdot (\hat{s}I) = 0
$$
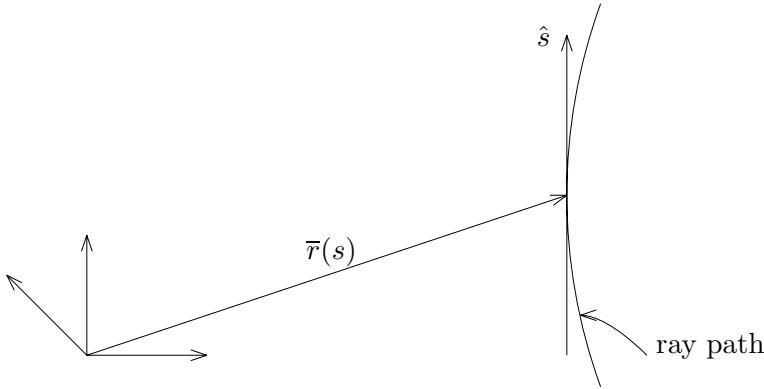
Figure 6.4.1 Ray path in geometrical optics.

This is the conservation equation for the intensity I.

Let the position vector along a ray path [Fig. 6.4.1] be denoted by $\overline{r}(s)$, expressed in terms of the arc length s as the parameter for the path. Since $d\overline{r}/ds = \hat{s}$, we find from (6.4.12)

$$\frac{d^2\overline{r}}{ds^2} = \frac{d\overline{r}}{ds} \cdot \nabla\left(\frac{d\overline{r}}{ds}\right) = \hat{s} \cdot \nabla(\hat{s}) = \frac{\nabla L}{n} \cdot \nabla\left(\frac{\nabla L}{n}\right)$$

For homogeneous media with n being a constant, it is seen that

$$\frac{d^2\overline{r}}{ds^2} = \frac{1}{2}\nabla\left(\frac{|\nabla L|^2}{n^2}\right) = 0$$

in view of (6.4.11). Thus the ray path is a straight line. When n is spatially dependent, we make use of the vector identity

$$\nabla(\overline{A} \cdot \overline{B}) = (\overline{A} \cdot \nabla)\overline{B} + (\overline{B} \cdot \nabla)\overline{A} + \overline{A} \times (\nabla \times \overline{B}) + \overline{B} \times (\nabla \times \overline{A})$$

and find that

$$\frac{d^2\overline{r}}{ds^2} = \frac{1}{2}\nabla\left(\frac{|\nabla L|^2}{n^2}\right) - \frac{\nabla L}{n} \times \left(\nabla\frac{1}{n} \times \nabla L\right)$$

$$= \frac{\nabla L}{n}\left(\nabla L \cdot \nabla\frac{1}{n}\right) - \left(\nabla\frac{1}{n}\right)\frac{|\nabla L|^2}{n} + \frac{1}{2}\nabla\left(\frac{|\nabla L|^2}{n^2}\right)$$

$$= \frac{\nabla L}{n}\left(\nabla L \cdot \nabla\frac{1}{n}\right) - n\nabla\frac{1}{n}$$
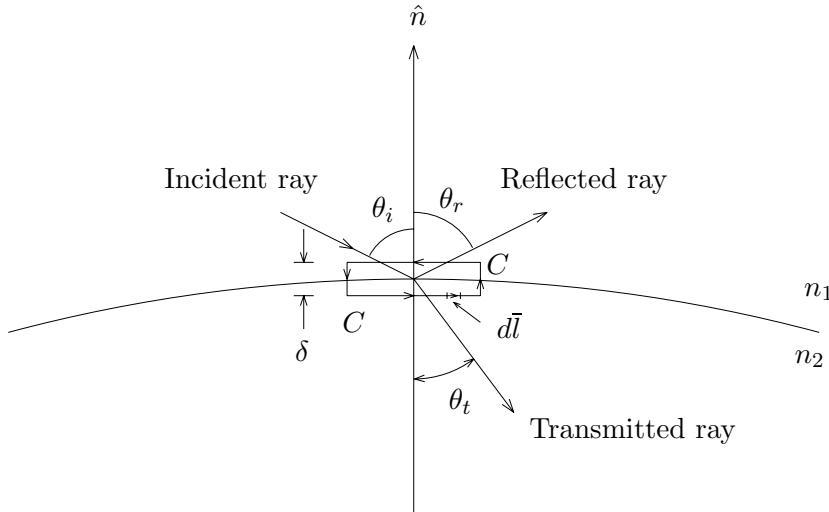
Figure 6.4.2 Derivation of Snell's law.

Thus the ray is curved in inhomogeneous media.

Taking the curl of (6.4.12), we also have

$$\nabla \times (\hat{s}n) = 0 \tag{6.4.16}$$

We now derive Snell's law by integrating (6.4.16) around a ribbon-like contour across the boundary separating two media with refractive indices n_1 and n_2 [Fig. 6.4.2]. Applying Stokes' theorem and letting the ribbon width $\delta \to 0$, we have

$$\iint d\overline{S} \cdot \nabla \times (\hat{s}n) = \oint_C d\overline{l} \cdot \hat{s}n = 0 \tag{6.4.17}$$

where $d\overline{S}$ is the unit vector perpendicular to the ribbon area and $d\overline{l}$ is the differential line element along the closed contour of the ribbon. The contributions from the two sides perpendicular to the surface are neglected because they are proportional to δ. Thus the tangential components of the ray vectors are continuous across the boundary. For the transmitted ray we find from (6.4.17)

$$n_1 \sin \theta_i = n_2 \sin \theta_t \tag{6.4.18}$$

For the reflected ray, we use $\theta_t = \pi - \theta_r$ and $n_2 = n_1$. From (6.4.18), we find $n_1 \sin \theta_i = n_1 \sin \theta_r$. Thus the angle of reflection θ_r is equal to
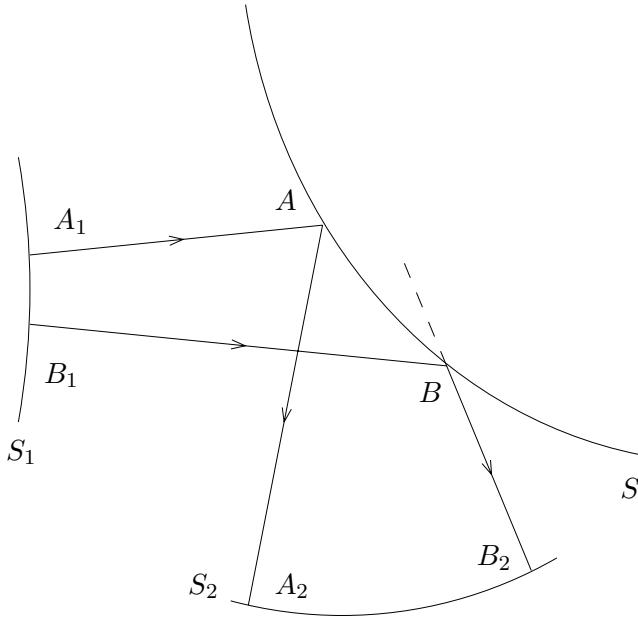
Figure 6.4.3 Reflection of wavefront S_1 by a surface S.

the angle of incidence θ_i. Note that Snell's law has also been derived from phase matching wave vectors for plane waves. The above derivation is valid, provided that the radii of curvature of the incident wave and of the boundary surface are large compared to the wavelength. Due to the curl-free property of the ray vector, we have

$$\oint_C d\overline{r} \cdot \hat{s}n = 0 \qquad (6.4.19)$$

along any closed path C. This equation is true even across the boundary of two different media by virtue of Snell's law.

Consider the problem of reflection of a wavefront S_1 by a surface S and the reflected rays form another wavefront S_2 [Fig. 6.4.3]. Note that A_1AA_2 and B_1BB_2 are the ray paths in the direction of $\hat{s}$ and A_1B_1 and A_2B_2 are wavefronts perpendicular to the ray paths. Applying (6.4.19), we find

$$\left\{ \int_{A_1AA_2} + \int_{A_2B_2} + \int_{B_2BB_1} + \int_{B_1A_1} \right\} d\overline{r} \cdot \hat{s}n = 0$$

The integrals along A_2B_2 and B_1A_1 are zero because $d\overline{r} \cdot \hat{s} = 0$. We
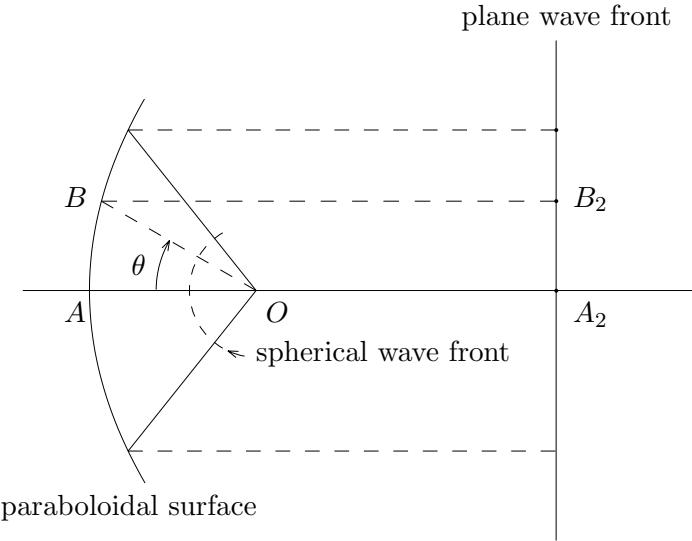
Figure 6.4.4 Converting spherical phase front to plane phase front.

have

$$\int_{A_1 A A_2} d\overline{r} \cdot \hat{s} n - \int_{B_1 B B_2} d\overline{r} \cdot \hat{s} n = 0$$

The vectors $d\overline{r}$ and $\hat{s}n$ are in the same direction on the optical path. The integrals define the optical path lengths along paths $A_1 A A_2$ and $B_1 B B_2$. We conclude

$$\int_{A_1 A A_2} n\, ds = \int_{B_1 B B_2} n\, ds \qquad (6.4.20)$$
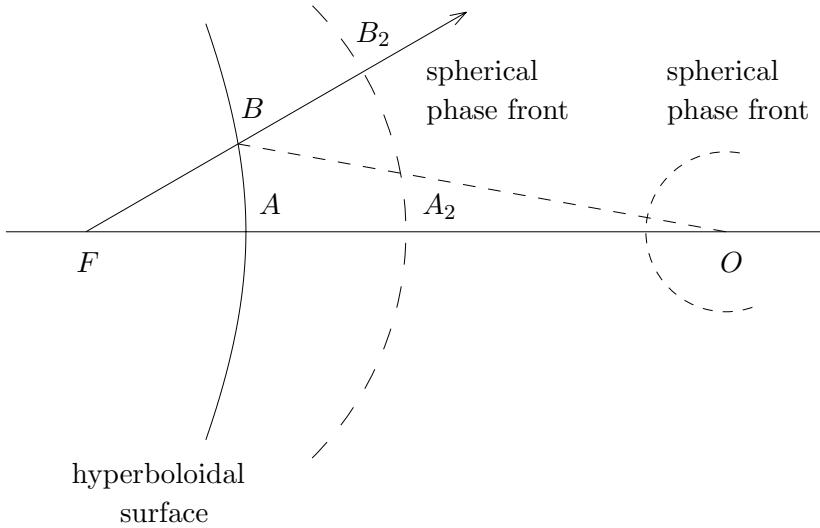
Thus the optical path length between any two wavefronts is the same for all rays. The above theorem is easily generalized to include cases of refraction.

As an example, consider a reflecting surface that converts a spherical phase front to a plane phase front. Consider the ray paths as shown in Figure 6.4.4. In view of (6.4.20), we have

$$\overline{OB} + \overline{BB_2} = \overline{OA} + \overline{AA_2} \qquad (6.4.21)$$

Since all reflected rays are parallel to AOA_2, we have

$$\overline{BB_2} = \overline{OB} \cos \theta + \overline{OA_2} \qquad (6.4.22)$$

Figure 6.4.5   Converting a spherical phase front to another spherical phase front.

Substituting in (6.4.21), we find

$$\overline{OB}(1 + \cos\theta) = \overline{OA} - \overline{OA_2} + \overline{AA_2} = 2\overline{OA}$$
$$r(1 + \cos\theta) = 2f \tag{6.4.23}$$

This equation describes a parabola. Revolving around the axis OA_2 we see that the reflecting surface takes a paraboloidal shape.

A hyperboloidal surface converts one spherical phase front into another spherical phase front. As shown in Figure 6.4.5, we obtain from (6.4.20)

$$\overline{OB} + \overline{BB_2} = \overline{OA} + \overline{AA_2} \tag{6.4.24}$$

The center of the spherical phase front of the reflected rays is at F, since

$$\overline{BB_2} = \overline{FB_2} - \overline{FB} = \overline{FA_2} - \overline{FB}$$

We find from (6.4.24)

$$\overline{OB} - \overline{FB} = \overline{OA} + \overline{AA_2} - \overline{FA_2} = \overline{OA} - \overline{FA} \tag{6.4.25}$$

This equation determines a hyperbola. Revolution around axis FO results in a hyperboloidal surface. Reflectors of this type were originally designed by Cassegrain for optical telescopes.
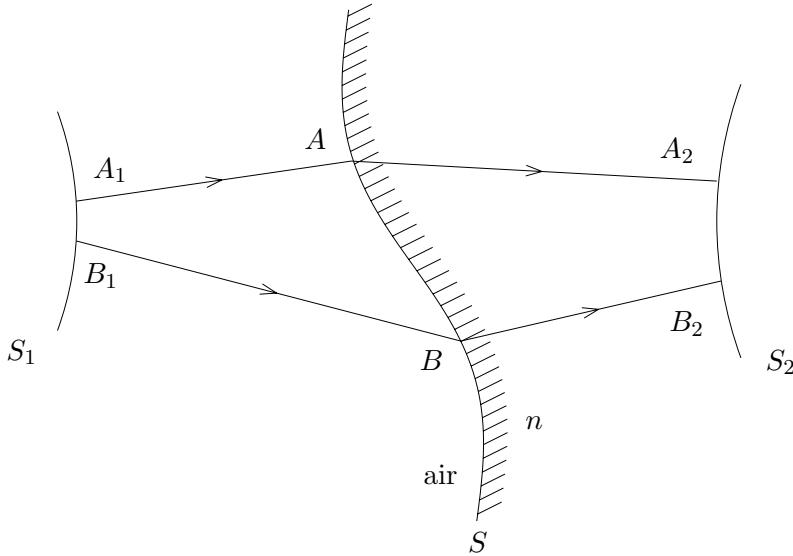
Figure 6.4.6 Establishing optical path-length theorem.

Lens Antennas

We first establish the optical path-length theorem for refraction in geometrical optics. Consider the boundary surface S separating air and a dielectric medium with refractive index n as shown in Figure 6.4.6. The two rays A_1AA_2 and B_1BB_2 emerge from the constant phase front S_1, refracted by the medium and form the new phase front S_2.

The field amplitudes of rays have the dependence $e^{i\omega L(\bar{r})/c}$ and the ray vector $n\hat{s} = \nabla L(\bar{r})$ has the curl-free property

$$\nabla \times n\hat{s} = 0 \qquad (6.4.26)$$

where n is the refractive index of air or the dielectric depending on the ray location. Stokes' theorem yields

$$\int_{A_1A} d\bar{r} \cdot \hat{s} + \int_{AA_2} d\bar{r} \cdot \hat{s}n + \int_{A_2B_2} d\bar{r} \cdot \hat{s}n$$

$$+ \int_{B_2B} d\bar{r} \cdot \hat{s}n + \int_{BB_1} d\bar{r} \cdot \hat{s} + \int_{B_1A_1} d\bar{r} \cdot \hat{s} = 0$$

By the boundary condition of the ray vector at the surface S, the rays A_1A to AA_2 and similarly B_1B to BB_2 satisfy Snell's law.
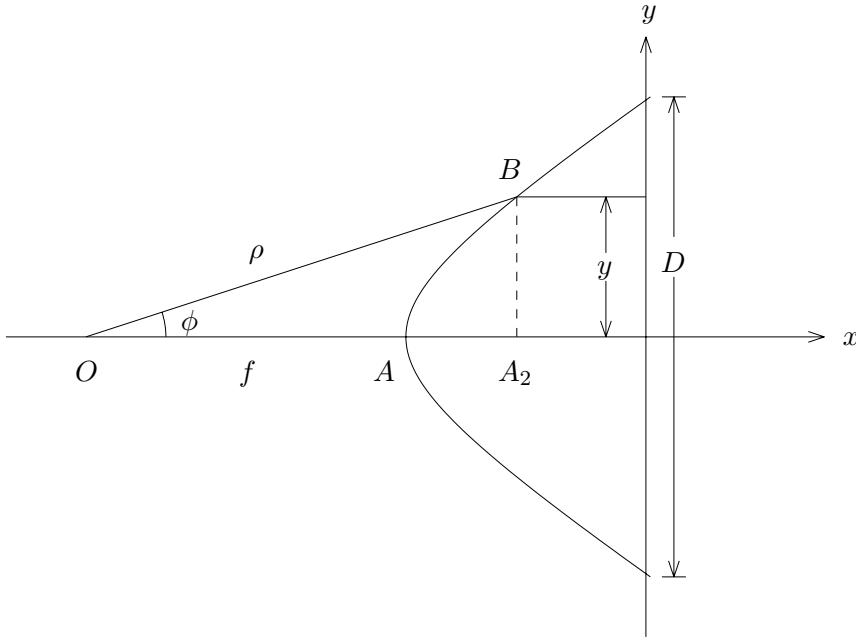
Figure 6.4.7 One-surface lens to convert a spherical phase front to a plane phase front.

The integrals along $A_1 B_1$ and $A_2 B_2$ are zero because $d\overline{r} \cdot \hat{s} = 0$. We thus have

$$\int_{A_1 A} d\overline{r} \cdot \hat{s} + \int_{AA_2} d\overline{r} \cdot \hat{s} n = \int_{B_1 B} d\overline{r} \cdot \hat{s} + \int_{BB_2} d\overline{r} \cdot \hat{s} n \qquad (6.4.27)$$

or simply

$$A_1 A + n\, AA_2 = B_1 B + n\, BB_2 \qquad (6.4.28)$$

This is the optical path length theorem which states that the optical path lengths between two constant phase fronts are equal.

We now construct a one-surface lens that converts a spherical phase front into a plane phase front. By the optical path length theorem, we see from Figure 6.4.7 that

$$\overline{OB} = \overline{OA} + n\,\overline{AA_2} \qquad (6.4.29)$$

Letting the length from the origin O to the refraction surface be ρ, at an angle ϕ with the x axis, we find $\overline{AA_2} = \rho \cos \phi - f$ where

$f = \overline{OA}$. Equation (6.4.29) becomes

$$\rho = \frac{(n-1)f}{n\cos\phi - 1} \qquad (6.4.30)$$

This is the equation for a hyperbola.

Consider a cylindrical lens antenna with the hyperbolic cross-section as described by (6.4.30). The antenna is illuminated with a line source. We shall show that the field amplitude distribution at the aperture with diameter D is tapered. First we note that the total power P_t passing through the strip at y with width dy is

$$P_t = dy\, P(y) \qquad (6.4.31)$$

where $P(y)$ is power per unit length at y. Neglecting reflections, we see that this total power is equal to that radiated by the line source over the angle $d\phi$,

$$P_t = U(\phi)\, d\phi \qquad (6.4.32)$$

where $U(\phi)$ is power per unit angle from the source. Since $y = \rho\sin\phi$, we obtain from (6.4.30)

$$dy = (n-1)f\frac{n-\cos\phi}{(n\cos\phi - 1)^2}d\phi \qquad (6.4.33)$$

Equating (6.4.31) and (6.4.32) and making use of (6.4.33), we obtain

$$P(y) = \frac{(n\cos\phi - 1)^2}{(n-1)f(n-\cos\phi)}\, U(\phi) \qquad (6.4.34)$$

In the aperture plane the ratio of the field amplitude $E(y)$ at y to $E(0)$ at $y = 0$ corresponding to $\phi = 0$ is equal to the square root of their power ratio,

$$\frac{E(y)}{E(0)} = \sqrt{\frac{P(y)}{P(0)}} = \frac{n\cos\phi - 1}{\sqrt{(n-1)(n-\cos\phi)}} \qquad (6.4.35)$$

The amplitude ratio becomes zero when $\phi = \cos^{-1}(1/n)$.

The neglect of reflection at the convex surface increases the transmitted power. Of more importance is the reflection from the plane
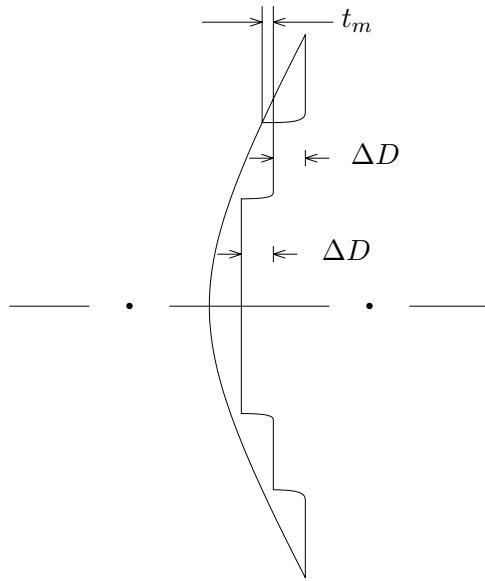
Figure 6.4.8 Zoned dielectric lens.

surface which is focused back into the primary feed and causes a mismatch. The reflections at both surfaces may be reduced with a material of small refractive index. The reflection at the plane surface can also be eliminated by a quarter-wavelength plate with refractive index $\sqrt{n}$. The reason follows from transmission line theory where a quarter-wavelength section with characteristic impedance $\sqrt{(Z_0 Z_1)}$ can be shown to match a line with characteristic impedance Z_0 to another line with Z_1 as its characteristic impedance. The transmission line theory is applicable here because the wave is normally incident at the plane surface.

To reduce the weight of the lens, zoned dielectric lenses are constructed [Fig. 6.4.8]. From the optical path length theorem (6.4.27), we recognize that $d\overline{r} \cdot \hat{s} n = dL$ is the incremental phase change in the field dependence $e^{ik_o L(\overline{r})}$ with $\nabla L(\overline{r}) = \hat{s} n$. Thus we make the zoned step ΔD such that

$$k_o \Delta D\,(n-1) = 2\pi$$

or equivalently

$$\Delta D = \frac{\lambda_o}{n-1}$$

where $\lambda_o = 2\pi/k_o$ is the free-space wavelength. Then the phase dif-
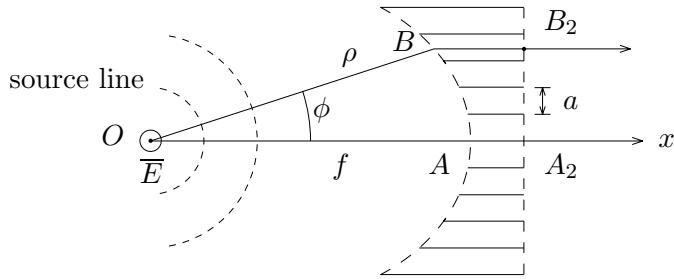
Figure 6.4.9 Metal-plate lens.

ference caused by removal of the dielectric is 2π. When the smallest thickness of the lens is t_m, the maximum thickness of the lens will be $t_m + \lambda_o/(n-1)$.

The conversion of a cylindrical phase front produced by the line source at the focal point to a plane phase front at the aperture plane of the lens can be understood from the point of view of phase retardation due to the dielectric medium. Inside the dielectric the phase velocity is c/n. Close to the x axis, the dielectric is the thickest and the phase retardation is the largest. At the edge of the lens the phase velocity is not slowed down at all. The hyperbolic cross-section provides such distribution in the phase retardation that the resultant phase front is a plane.

The same concept can be used in the understanding of lens antennas made of metal plates. Inside two parallel plates separated by a distance a, the phase velocity of a TE_1 wave is

$$v = c\left[1 - \left(\frac{\pi}{ka}\right)^2\right]^{-\frac{1}{2}} \tag{6.4.36}$$

which is seen to be larger than the velocity of light in free space c. The equivalent index of refraction is

$$n = \frac{c}{v} = \sqrt{1 - \left(\frac{\pi}{ka}\right)^2} \tag{6.4.37}$$

Note that in order to have a TE_1 wave propagating above cutoff inside the plate waveguide, we must have $\pi < ka$.

Consider a metal-plate lens antenna as shown in Figure 6.4.9. The profile of the plates can be determined by the optical path length theorem with the equivalent refractive index concept. We have

$$\overline{OB} + n\,\overline{BB_2} = \overline{OA} + n\,\overline{AA_2} \tag{6.4.38}$$
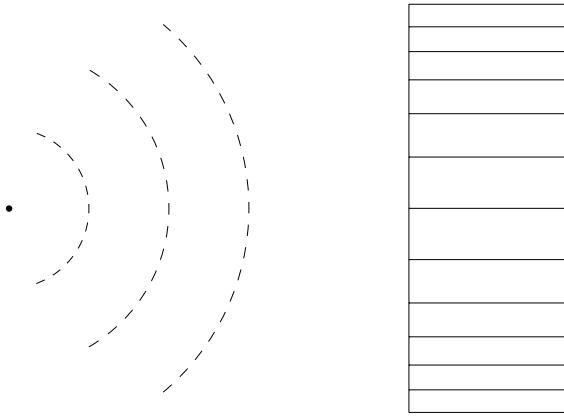
Figure 6.4.10 Metal-plate lens with nonuniform separations.

Letting $\overline{OB} = \rho$ and $\overline{OA} = f$, we find $\overline{BB_2} - \overline{AA_2} = f - \rho \cos \phi$. From (6.4.38) we have

$$\rho = \frac{(1-n)f}{1 - n \cos \phi} \qquad (6.4.39)$$

With $n < 1$, (6.4.39) is the equation for an ellipse.

The effect of the longer metal plate waveguides is to speed up the phase-front propagation to form a plane phase front at the aperture plane. The smaller the separation a the larger the phase velocity inside the plate waveguide; thus, metal-plate lens antennas can be made with uniform length but nonuniform separations. Such an arrangement is shown in Figure 6.4.10.

Paraboloidal Reflector Antenna

For the paraboloidal reflector surface as shown in Figure 6.4.11, it is described by the equation

$$r + r \cos \theta = 2f \qquad (6.4.40)$$

where f is the focal length. Let the plane perpendicular to the z axis at the focal point be called the aperture plane. Equation (6.4.40) states that all path lengths measured from the focal point F to the reflector surface and then to the plane surface perpendicular to the axis at the focal point are equal to the constant $2f$.

It is interesting to find by means of geometrical ray optics that the power distribution on the aperture plane is nonuniform. Consider
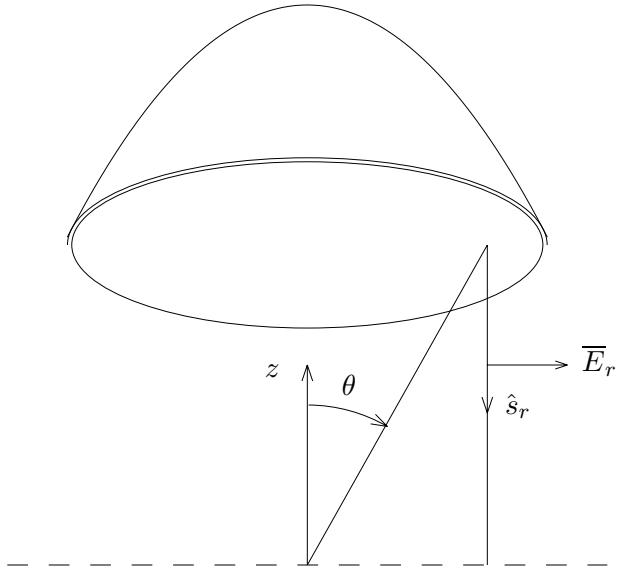
Figure 6.4.11 Paraboloidal reflector.

an omnidirectional source at the focal point; the power radiated in the solid angle $d\theta$ rotating about the z axis is proportional to $2\pi \sin\theta \, d\theta$. We write

$$dp = 2\pi C \sin\theta \, d\theta$$

where C is a constant proportional to the source strength. By the conservation law of geometrical optics, this power appears in the aperture plane through a ring of differential width $d\rho$ with differential area $dA = 2\pi\rho \, d\rho$. Thus

$$\frac{dp}{dA} = \frac{C \sin\theta \, d\theta}{\rho \, d\rho} \tag{6.4.41}$$

From (6.4.40) we have

$$r = f \sec^2\frac{\theta}{2} \tag{6.4.42}$$

and

$$\rho = r \sin\theta = 2f \tan\frac{\theta}{2} \tag{6.4.43}$$

Making use of (6.4.43), we find (6.4.41) becomes

$$\frac{dp}{dA} = \frac{C}{f^2} \cos^4\left(\frac{\theta}{2}\right)$$

On the aperture plane, we have a tapered amplitude distribution. The distribution can be made uniform by making the gain pattern of the feeding source $G(\theta, \phi) = \sec^4(\theta/2)$.

The surface current density at the reflector surface is, under the physical optics approximation,

$$\overline{J}_s = \hat{n} \times (\overline{H}_i + \overline{H}_r) \tag{6.4.44}$$

where $\hat{n}$ is the unit normal to the paraboloidal surface, $\overline{H}_i$ is the incident magnetic field, and $\overline{H}_r$ is the reflected magnetic field. On a perfectly conducting surface, $\hat{n} \times \overline{H}_i = \hat{n} \times \overline{H}_r$. In terms of the incident and reflected electric fields,

$$\overline{H}_i = \frac{1}{\eta} \hat{s}_i \times \overline{E}_i \tag{6.4.45}$$

$$\overline{H}_r = \frac{1}{\eta} \hat{s}_r \times \overline{E}_r \tag{6.4.46}$$

where $\hat{s}_i$ is the unit incident ray vector and $\hat{s}_r$ the unit reflected ray vector. The surface current density becomes

$$\overline{J}_s = \frac{2}{\eta} [\hat{n} \times (\hat{s}_i \times \overline{E}_i)] \tag{6.4.47}$$

or

$$\overline{J}_s = \frac{2}{\eta} [\hat{n} \times (\hat{s}_r \times \overline{E}_r)] \tag{6.4.48}$$

Now assume that at the feed there is a point source generating an incident field vector

$$\overline{E}_i = \hat{e}_i \, E(\theta, \phi) \frac{e^{i\omega r/c}}{r} \tag{6.4.49}$$

on the paraboloidal surface at r where $r \gg \lambda$. The amplitude $E(\theta, \phi)$ is related to the gain factor $G(\theta, \phi)$ of the source by

$$\frac{1}{2\eta} |E(\theta, \phi)|^2 = \frac{P_t}{4\pi} G(\theta, \phi) \tag{6.4.50}$$

where P_t is the total power radiated by the source.

We now study the polarization of the reflected field. The electromagnetic boundary condition requires that tangential electric fields vanish at the reflector surface

$$\hat{n} \times (\overline{E}_r + \overline{E}_i) = 0 \tag{6.4.51}$$

also

$$\hat{n} \cdot \overline{E}_r = \hat{n} \cdot \overline{E}_i \tag{6.4.52}$$

Cross-multiplying (6.4.51) by $\hat{n}$ and making use of (6.4.52), we find

$$\overline{E}_r = 2\hat{n}(\hat{n} \cdot \overline{E}_i) - \overline{E}_i = \hat{e}_r \, E(\theta, \phi) \frac{e^{i\omega r/c}}{r} \tag{6.4.53}$$

The unit vector $\hat{e}_r$ for the reflected wave in (6.4.53) is

$$\hat{e}_r = 2\hat{n} \frac{\left(\hat{n} \cdot \overline{E}_i\right)}{\left|\overline{E}_r\right|} - \frac{\overline{E}_i}{\left|\overline{E}_r\right|} = 2\hat{n}(\hat{n} \cdot \hat{e}_i) - \hat{e}_i \tag{6.4.54}$$

where we use the fact that $\left|\overline{E}_r\right| = \left|\overline{E}_i\right|$ as seen from (6.4.53).

We assume that the point source at the focus is linearly polarized in the $\hat{y}$ direction. The unit vector $\hat{e}_i$ is

$$\hat{e}_i = \frac{\hat{r} \times (\hat{y} \times \hat{r})}{|\hat{r} \times (\hat{y} \times \hat{r})|} = \frac{\hat{y} - (\hat{r} \cdot \hat{y})\hat{r}}{|\hat{y} - (\hat{r} \cdot \hat{y})\hat{r}|} \tag{6.4.55}$$

Since $\hat{r} = \hat{x} \sin\theta \cos\phi + \hat{y} \sin\theta \sin\phi + \hat{z} \cos\theta$, we find

$$\hat{e}_i = \frac{1}{\sqrt{1 - \sin^2\theta \sin^2\phi}} \left\{ -\hat{x} \sin^2\theta \sin\phi \cos\theta \right.$$
$$\left. + \hat{y} \left(1 - \sin^2\theta \sin^2\phi\right) - \hat{z} \sin\theta \cos\theta \sin\phi \right\} \tag{6.4.56}$$

in rectangular coordinates.

The unit normal to the reflector $\hat{n}$ can be found by taking the gradient of (6.4.42),

$$\nabla \left[f - r \cos^2 \frac{\theta}{2} \right] = \left(-\hat{r} \cos \frac{\theta}{2} + \hat{\theta} \sin \frac{\theta}{2} \right) \cos \frac{\theta}{2}$$

Thus

$$\hat{n} = -\hat{r} \cos \frac{\theta}{2} + \hat{\theta} \sin \frac{\theta}{2} \tag{6.4.57}$$

such that $\hat{n} \cdot \hat{n} = 1$. In rectangular coordinates

$$\hat{n} = -\hat{x} \sin \frac{\theta}{2} \cos\phi - \hat{y} \sin \frac{\theta}{2} \sin\phi - \hat{z} \cos \frac{\theta}{2} \tag{6.4.58}$$

We now determine the reflected field polarization $\hat{e}_r$. From (6.4.55) and (6.4.57) we find $\hat{n} \cdot \hat{e}_i = (\hat{\theta} \cdot \hat{y}) \sin(\theta/2) = \sin(\theta/2) \cos\theta \sin\phi$. It follows from (6.4.54), (6.4.56), and (6.4.58), that

$$\hat{e}_r = 2\hat{n}(\hat{n} \cdot \hat{e}_i) - \hat{e}_i = \frac{1}{\sqrt{1 - \sin^2\theta \sin^2\phi}} \left\{ \hat{x}(1 - \cos\theta) \sin\phi \cos\phi \right.$$

$$\left. + \hat{y}(\cos\theta \sin^2\phi + \cos^2\phi) \right\} \quad (6.4.59)$$

As we had expected, $\hat{e}_r$ has no z component because $\hat{s}_r$ is in the $-\hat{z}$ direction and $\overline{E}_r$ is perpendicular to $\hat{s}_r$. The x component of $\hat{e}_r$ gives the newly generated cross-polarized field at the aperture plane. By geometrical optics, the field at the aperture plane acquires an additional phase $(\omega/c)\, r \cos\theta$ as compared with $\overline{E}_r$. We have

$$\overline{E}_{ap} = \hat{e}_r\, E(\theta, \phi) \frac{e^{-i(\omega/c)(r + r\cos\theta)}}{r} \quad (6.4.60)$$

For large f/D ratio, the reflector section is relatively flat. We find $\theta \to 0$ and the x component of $\hat{e}_r$, $e_{rx} \to 0$. It is interesting to note that for an electric dipole at the feed, its incident field is proportional to the sine of the angle γ between $\hat{r}$ and the y axis with $\sin\gamma = \sqrt{1 - \cos^2\gamma} = \sqrt{1 - (\hat{r} \cdot \hat{y})^2} = \sqrt{1 - \sin^2\theta \sin^2\gamma}$. This cancels the angular dependence in the denominator of $\hat{e}_r$.

Having determined the surface current distribution on the reflector surface, we now find the radiation fields from

$$\overline{E}(\overline{r}) = i\omega\mu \frac{e^{ikr}}{4\pi r}(\hat{\theta} f_\theta + \hat{\phi} f_\phi)$$

where the vector current moment

$$\overline{f} = \iint dS\, \overline{J}_s(\overline{r}') \, e^{i\overline{k}\cdot\overline{r}'}$$

The surface current density is derived in (6.4.48)

$$\overline{J}_s(\overline{r}') = \frac{2}{\eta} \left\{ \hat{n} \times [\hat{s}_r \times \overline{E}_r(\overline{r}')] \right\}$$

From (6.4.53), the reflected field

$$\overline{E}_r(\overline{r}') = \hat{e}_r E(\theta', \phi') \frac{e^{ikr'}}{r'}$$

Since $\hat{s}_r = -\hat{z}$ and $-\hat{z} \cdot \hat{n} = \cos(\theta/2)$, we find

$$\overline{J}_s(\overline{r}') = \left[\hat{e}_r \cos\frac{\theta'}{2} - \hat{z}(\hat{n} \cdot \hat{e}_r)\right] \frac{2E(\theta', \phi')}{\eta} \frac{e^{ikr'}}{r'} \tag{6.4.61}$$

where $\hat{e}_r$ is given by (6.4.59) and $\hat{n}$ by (6.4.57).

We see that the vector current moment $\overline{f}(\overline{r})$ has a component along $\hat{e}_r$ which is parallel to the x-y plane and a component along the z axis. The z component makes no contribution to E_ϕ because $\hat{\phi}$ is always perpendicular to z. Its contribution to E_θ is vanishingly small around $\theta = 0$ because $\hat{z} \cdot \hat{\theta} = \sin\theta$. This is similar to the field produced by an electric dipole in the $\hat{z}$ direction. In fact if we use the aperture field distribution to calculate the radiation fields, the equivalent surface current density will have no z component at all.

We therefore consider only the transverse component of $\overline{f}$ and write

$$\overline{f} = \iint dS \, \hat{e}_r \cos\frac{\theta'}{2} \frac{2E(\theta', \phi')}{\eta r'} e^{ikr' - i\overline{k} \cdot \overline{r}'} \tag{6.4.62}$$

The differential area dS on the paraboloidal surface is

$$dS = (r' \sin\theta' \, d\phi')(r' \sec(\frac{\theta'}{2}) \, d\theta')$$

The exponential phase factor inside the integral is

$$-kr' + \overline{k} \cdot \overline{r}' = kr' \left[-1 + \sin\theta \, \sin\theta' \, \cos(\phi' - \phi) + \cos\theta \, \cos\theta'\right]$$

We now examine antenna gain along the z axis where $\theta = \pi$. The radiation vector in (6.4.62) becomes

$$\overline{f} = \int_0^{2\pi} d\phi' \int_0^{\theta_0} d\theta' \, \hat{e}_r r' \sin\theta' \frac{E(\theta', \phi')}{\eta} e^{i2kf} \tag{6.4.63}$$

Neglecting the cross-polarization effect and letting $\hat{e}_r \approx \hat{y}$, we obtain

$$\overline{E}(r, \pi, 0) = \hat{y} \frac{i\omega\mu e^{ik(r+2f)}}{\pi\eta r} \int_0^{2\pi} d\phi' \int_0^{\theta_0} d\theta' \, f \tan\frac{\theta'}{2} E(\theta', \phi') \tag{6.4.64}$$

Suppose the gain of the feed is independent of ϕ'. For instance, a stub-supported dipole-feed [Silver, 1949] satisfies this requirement. Remembering that

$$\frac{1}{2\eta}|E(\theta', \phi')|^2 = \frac{P_t}{4\pi}G(\theta') \tag{6.4.65}$$
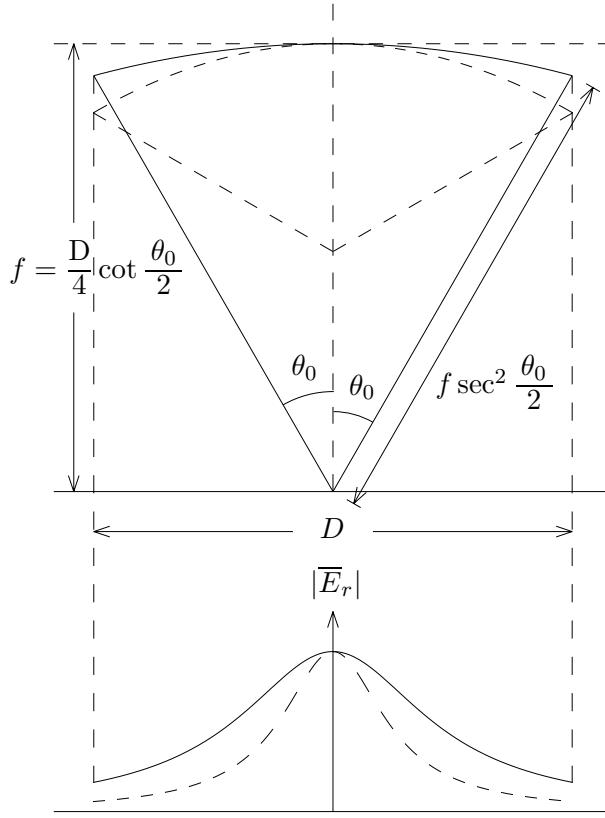
Figure 6.4.12 For a fixed D, gain increases as θ_0 increases.

where P_t is the total radiated power by the feed, we find from (6.4.64) by integrating over ϕ'

$$\overline{E}(r, \pi, 0) = \hat{y} \frac{i2\omega\mu f\, e^{ik(r+2f)}}{\eta r} \int_0^{\theta_0} d\theta' \tan\frac{\theta'}{2} \sqrt{\left[\frac{\eta P_t}{2\pi} G(\theta') \right]} \quad (6.4.66)$$

The antenna gain in the forward direction is

$$g = \frac{4\pi r^2}{P_t} \frac{1}{2\eta} |E(r, \pi, 0)|^2 = 4k^2 f^2 \left[\int_0^{\theta_0} d\theta' \tan\frac{\theta'}{2} \sqrt{[G(\theta')]} \right]^2 \quad (6.4.67)$$

To pursue interpretations of (6.4.67), we define an aperture diameter D as [Fig. 6.4.12]

$$D = 2f \sec^2\frac{\theta_0}{2} \sin\theta_0 = 4f \tan\frac{\theta_0}{2} \quad (6.4.68)$$

We cast (6.4.67) in the form

$$g = \left(\frac{\pi D}{\lambda}\right)^2 \cot^2 \frac{\theta_0}{2} \left[\int_0^{\theta_0} d\theta' \tan \frac{\theta_0}{2} \left[G(\theta')\right]^{1/2}\right]^2 \qquad (6.4.69)$$

The factor $(\pi D/\lambda)^2$ is the gain for a uniformly illuminated circular aperture.

For a fixed D, the gain g increases as θ_0 increases because the available fraction of the total power from the feed is increased. But as θ_0 increases with a fixed D, the aperture efficiency with which the reflector concentrates the available power in the forward direction decreases because the illumination becomes less tapered from the center [Fig. 6.4.12]. As a result, the gain g is decreased. The optimum angle θ_0 is obtained by setting $dg/d\theta_0 = 0$ which gives

$$\sqrt{[G(\theta_0)]} = \frac{1}{2} \csc^2 \left(\frac{\theta_0}{2}\right) \int_0^{\theta_0} d\theta' \tan \frac{\theta'}{2} \sqrt{[G(\theta')]} \qquad (6.4.70)$$

The optimum angular aperture represents the proper compromise between spill-over of the feed energy and the aperture efficiency.

The gain can be modified by a number of factors: (i) phase-error effects due to deviation of the antenna-feed wavefronts from spherical ones, and defocusing effects due to displacement of the feed center from the focus. The maximum tolerable phase deviation is usually set at $\lambda/8$ over the aperture. (ii) The back lobe of the primary antenna feed will interfere with the main lobe of the radiation pattern. This effect may be put into positive use by designing, according to the focal length f, a back lobe that interferes constructively with the main lobe along the axial direction. For a fixed-feed design it may be defocused to achieve constructive interference. (iii) The current at the edge of the reflector acts like a line source and radiates into the backward direction. Such currents can be reduced by making the edges irregular, by placing chokes or impedances on the edge, or by cutting properly spaced loops near the edge. (iv) The blockage of the feed in the path of the reflected ray significantly reduces the gain. This may be remedied by off-axis feeding arrangements but these create other electrical and hardware problems. (v) Cassegrain-fed paraboloidal reflector antennas with a hyperboloidal subreflector are sometimes used with the primary feeding source placed behind the main reflector. The arrangement permits the installation of complex primary feeds, reduces the temperature noise interference in radio astronomical receivers, and shortens

the distance between the two reflectors because the subreflector will be placed before the focal point of the paraboloid. However, the reflector mismatch induced by spurious surface currents on the subreflector due to reflected waves from the main reflector may become serious.

Problems

P6.4.1

Consider a lens formed by rotating a hyperbola around its axis. Assuming that the angular dependence of power density at the source is ϕ-independent, i.e., $u = u(\theta)$, then the power enclosed in the shell formed by revolving $d\theta$ about the z-axis is

$$P_s = u(\theta)2\pi \sin\theta \, d\theta$$

The power transmitted through an annulus of width $d\rho$ and centered on z-axis is

$$P_t = P(\rho)2\pi r \sin\theta d\rho$$

where $P(\rho)$ is the power density of the transmitted beam. By energy conservation, $P_t = P_s$, therefore,

$$\frac{P(\rho)}{u(\theta)} = \frac{1}{r}\frac{d\theta}{d\rho} = \frac{n\cos\theta - 1}{(n-1)f}\frac{d\theta}{d\rho}$$

Find the field amplitude distribution $\frac{E(\rho)}{E(0)}$ at the aperture plane.

P6.4.2

Let the gain function for the feed of a paraboloid reflector antenna be

$$\begin{aligned}
G(\theta') &= 6\cos^2\theta' && 0 \le \theta' \le \pi/2 \\
&= 0 && \pi/2 \le \theta'
\end{aligned}$$

Show that

$$\int G(\theta') \, d\Omega = 4\pi$$

With this gain function what is the optimum aperture angle θ_0?

6.5   Paraxial Limit

In the paraxial limit, solutions to the scalar wave equation

$$(\nabla^2 + k^2)U = 0 \qquad (6.5.1)$$

can be written as

$$U = u(x, y, z)e^{ikz} \qquad (6.5.2)$$

Under the paraxial approximation when we assume that $\partial^2 u/\partial z^2$ is negligible, the wave equation (6.5.1) becomes

$$\frac{\partial^2 u}{\partial x^2} + \frac{\partial^2 u}{\partial y^2} + i2k\frac{\partial u}{\partial z} = 0 \qquad (6.5.3)$$

We substitute into (6.5.3) the trial solution

$$u(x, y, z) = X\left(\frac{\sqrt{2}x}{w}\right)Y\left(\frac{\sqrt{2}y}{w}\right)e^{+i\left[p+\frac{k}{2q}(x^2+y^2)+\Phi(z)\right]} \qquad (6.5.4)$$

where the parameters $w, p,$ and q are all functions of z.

Topic 6.5A Gaussian Beam

For the Gaussian beam solution, we let $X = Y = 1$ and $\Phi(z) = 0$. We find for

$$u(\rho, z) = e^{i\left[p(z)+\frac{k}{2q(z)}\rho^2\right]} \qquad (6.5A.1)$$

where $\rho^2 = x^2 + y^2$, equation (6.5.3) yields

$$2k\left[-p' + \frac{i}{q}\right] + \frac{k^2\rho^2}{q^2}\left[q' - 1\right] = 0 \qquad (6.5A.2)$$

For (6.5A.2) to be valid for all ρ and z, we obtain $p' = i/q$ and $q' = 1$. In the Gaussian beam expression, these conditions are made by choosing

$$q = z - i\frac{kw_o^2}{2} \qquad (6.5A.3)$$

$$p = \tan^{-1}\frac{2z}{kw_o^2} - i\ln\left(\frac{w_o}{w(z)}\right) \qquad (6.5A.4)$$

with

$$w(z) = w_o\sqrt{1 + \left(\frac{2z}{kw_o^2}\right)^2} \tag{6.5A.5}$$

describing the beamwidth as a function of z.

The Gaussian beam solution thus takes the form, by virtue of (6.5.2), (6.5A.1), (6.5A.3) and (6.5A.4)

$$U(\rho, z) = \frac{w_o}{w(z)} \exp\left[-i\tan^{-1}\frac{2z}{kw_o^2}\right] e^{ikz}\, e^{i\frac{2kz\rho^2}{4z^2 + (kw_o^2)^2}}\, e^{-\frac{(kw_o\rho)^2}{4z^2 + (kw_o^2)^2}} \tag{6.5A.6}$$

The ρ-dependent exponentially decaying term $e^{-(kw_o\rho)^2/[4z^2 + (kw_o^2)^2]}$ describes the width of the Gaussian beam as a function of z. At $z = 0$, we define the width to be $\rho = w_o$ for which the term becomes e^{-1}. The ρ-dependent phase term $e^{i2kz\rho^2/[4z^2 + (kw_o^2)^2]}$ describes the phase front curvature. The phase shift at $\rho = \rho_o$ as compared to that at $\rho = 0$ is

$$kb = \frac{2kz\rho_o^2}{4z^2 + (kw_o^2)^2} \tag{6.5A.7}$$

In the paraxial approximation, we have

$$\rho_o^2 + R^2 \approx (R + b)^2 \approx R^2 + 2Rb$$

From (6.5A.7) we find

$$R = \frac{\rho_o^2}{2b} = z\left[1 + \frac{(kw_o^2)^2}{4z^2}\right] \tag{6.5A.8}$$

At $z = 0$, the phase front curvature is infinite. Using (6.5A.5) and (6.5A.8) in (6.5A.6), we obtain

$$U(\rho, z) = \frac{w_o}{w(z)} e^{i\left[kz + \frac{k\rho^2}{2R(z)} - \tan^{-1}\frac{2z}{kw_o^2}\right]} e^{-[\rho/w(z)]^2} \tag{6.5A.9}$$

At $z = 0$, the beam waist is $\rho = w_o$ and the phase front is that of a plane wave. With increasing z, the beam waist increases, and the phase front curves with the curvature equal to R. As $z \to \infty$, the
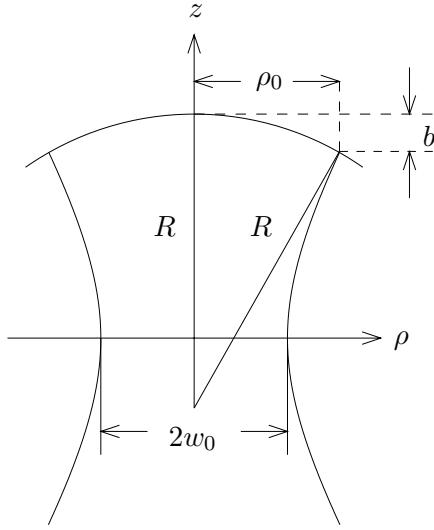
Figure 6.5A.1

phase front curvature vanishes, while the arctangent terms gives $\pi/2$, and the phase front again approaches that of a plane wave.

The scalar wave equation in (6.5.1) can be taken to be the x component of a vector potential $\overline{A} = \hat{x} U(\rho, z)$. The Gaussian beam solution (6.5A.9) is obtained from the paraxially-approximated equation (6.5.2) under the assumption that $|\partial u/\partial z| \ll |ku|$. Corresponding to the paraxial approximation, the magnetic field is

$$\overline{H} = \frac{1}{\mu} \nabla \times \overline{A} = ik \left[\hat{y} U + i\hat{z} \frac{i}{k} \frac{\partial U}{\partial y} \right]$$

and the electric field is

$$\overline{E} = iw \left[\hat{x} U + i\hat{z} \frac{1}{k} \frac{\partial U}{\partial x} \right]$$

and the total power in a Gaussian beam is

$$\int_{-\infty}^{\infty} dx \int_{-\infty}^{\infty} dy \frac{1}{2} \mathrm{Re} \left\{ \overline{E} \times \overline{H}^* \right\} \approx \hat{z} \frac{1}{2\eta}$$

where the amplitude of the Gaussian beam is assumed to be unity.

Gaussian-Hermite Beam Modes

Let the parameters p, q, and w in the trial solution (6.5.4) be given by (6.5A.3)–(6.5A.5). Substituting (6.5.4) into (6.5.3) and making use of (6.5A.2), we find

$$\frac{X''}{X} - i\sqrt{2}\frac{kx}{w}\left(ww' - \frac{w^2}{q}\right)\frac{X'}{X} + \frac{Y''}{Y} - i\sqrt{2}\frac{kx}{w}\left(ww' - \frac{w^2}{q}\right) + kw^2\Phi'(z) = 0$$

$$(6.5A.10)$$

It follows from (6.5A.3) and (6.5A.5) that $ww' - w^2/q = -i2/k$. Separation of variables and setting

$$kw^2\Phi'(z) = 2(m+n) \qquad (6.5A.11)$$

lead to the differential equations for Hermite polynomials

$$X''\left(\frac{\sqrt{2}x}{w}\right) - 2\left(\frac{\sqrt{2}x}{w}\right)X' + 2mX = 0 \qquad (6.5A.12a)$$

$$Y''\left(\frac{\sqrt{2}y}{w}\right) - 2\left(\frac{\sqrt{2}y}{w}\right)Y' + 2nY = 0 \qquad (6.5A.12b)$$

Requiring $\Phi(z = 0) = 0$ and introducing (6.5A.5), we obtain the solution for (6.5A.11)

$$\Phi(z) = (m+n)\tan^{-1}\left(\frac{2z}{kw_o^2}\right) \qquad (6.5A.13)$$

The solution as expressed in (6.5.2) and (6.5.4) now takes the form, after use is made of (6.5A.3), (6.5A.4), and (6.5A.9)

$$U = \frac{w_o}{w(z)}H_m\left(\frac{\sqrt{2}x}{w}\right)H_n\left(\frac{\sqrt{2}y}{w}\right)e^{-[\rho/w(z)]^2}$$

$$\cdot e^{i\left[kz - (m+n+1)\tan^{-1}(2z/kw_o^2) + k\rho^2/2R(z)\right]} \quad (6.5A.14)$$

where $H_m(\sqrt{2}x/w)$ and $H_n(\sqrt{2}y/w)$ are the Hermite polynomials of orders m and n.

Hermite polynomials $H_m(\xi)$ are solutions to the differential equation

$$\frac{d^2}{d\xi^2}H_m(\xi) - 2\xi\frac{d}{d\xi}H_m(\xi) + 2mH_m(\xi) = 0 \qquad (6.5A.15)$$

The first five Hermite polynomials are

$$H_0(\xi) = 1 \qquad (6.5A.16a)$$
$$H_1(\xi) = 2\xi \qquad (6.5A.16b)$$
$$H_2(\xi) = 4\xi^2 - 2 \qquad (6.5A.16c)$$
$$H_3(\xi) = 8\xi^3 - 12\xi \qquad (6.5A.16d)$$
$$H_4(\xi) = 16\xi^4 - 48\xi^2 + 12 \qquad (6.5A.16e)$$

The recurrence formula reads

$$H_{m+1} - 2\xi H_m + 2m H_{m-1} = 0 \qquad (6.5A.17)$$

The Hermite polynomials can be defined by

$$H_m(\xi) = (-1)^m e^{\xi^2} \frac{d^m}{d\xi^m} e^{-\xi^2} \qquad (6.5A.18)$$

There also exist integral relations

$$i^n e^{-\xi^2/2} H_m(\xi) = \frac{1}{\sqrt{2\pi}} \int_{-\infty}^{\infty} d\zeta\, e^{i\xi\zeta} e^{-\zeta^2/2} H_m(\zeta)$$

and the orthogonality conditions

$$\int_{-\infty}^{\infty} d\xi\, H_m(\xi) H_n(\rho) e^{-\xi^2} = 0$$
$$\int_{-\infty}^{\infty} d\xi\, H_m^2(\xi) e^{-\xi^2} = \sqrt{\pi} 2^n n!$$

From (6.5A.14), we observe that all Gaussian-Hermite beam modes have the same beam width parameter $w(z)$, the same phase curvature $R(z)$, and the same q parameter in (6.5A.3). It is to be noted that the Gaussian-Hermite beam modes form a complete system of orthogonal functions and thus paraxial wave fields can be expressed as a superposition of such modes. However the paraxial modes are only approximate solutions to the exact wave equation and the approximation becomes poorer as higher order modes become important.

Transmission of Gaussian Beams

The q parameter as defined in (6.5A.3) has fundamental importance in the description of ray optics with Gaussian beams. In view of (6.5A.5) for the definition of beamwidth w and (6.5A.8) for the definition of curvature R, we can write

$$\frac{1}{q} = \frac{1}{z - ikw_o^2/2} = \frac{1}{R} + i\frac{2}{kw^2} \qquad (6.5\text{A}.19)$$

The q parameter at z becomes

$$q_1 = q + d \qquad (6.5\text{A}.20)$$

at $z + d$. A thin lens can be defined as a device which renders the Gaussian beam in (6.5A.14) a phase shift $e^{-ik\rho^2/2f}$ after the beam passes the lens. We have from (6.5A.14) the new curvature R_e after transmission to be

$$\frac{1}{R_e} = \frac{1}{R} - \frac{1}{f} \qquad (6.5\text{A}.21)$$

where f is the focal length of the lens. A mirror of radius R_o acts like a lens with a focal length of $f = R_o/2$.

Both (6.5A.20) and (6.5A.21) can be expressed as a bilinear transformation with the form

$$q_1 = \frac{A_1 q + B_1}{C_1 q + D_1}$$

For (6.5A.20)

$$\begin{bmatrix} A_1 & B_1 \\ C_1 & D_1 \end{bmatrix} = \begin{bmatrix} 1 & d \\ 0 & 1 \end{bmatrix} \qquad (6.5\text{A}.22)$$

And for (6.5A.21)

$$\frac{1}{q_l} = \frac{1}{q} - \frac{1}{f} \qquad (6.5\text{A}.23)$$

gives

$$q_l = \frac{q}{1 - q/f} = \frac{A_l q + B_l}{C_l q + D_l}$$

The corresponding $ABCD$ matrix is

$$\begin{bmatrix} A_l & B_l \\ C_l & D_l \end{bmatrix} = \begin{bmatrix} 1 & 0 \\ -\frac{1}{f} & 1 \end{bmatrix} \qquad (6.5\text{A}.24)$$
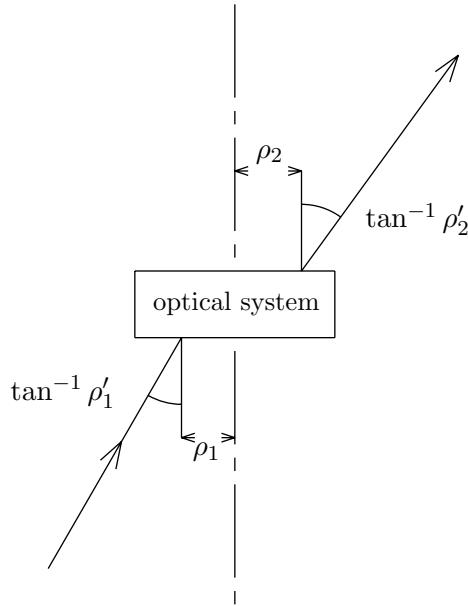
Figure 6.5A.2 Transmission through an optical system.

For a beam with parameter q propagated over a distance d_1, transmitted through a lens of focal length f, and propagated over another distance d_2, we have the last parameter

$$q_2 = q_l + d_2 = \frac{q_1 + d_2 - d_2 q_1/f}{1 - q_1/f}$$
$$= \frac{(1 - d_2/f)q + d_1 + d_2 - d_1 d_2/f}{-q/f + 1 - d_1/f} = \frac{A_2 q + B_2}{C_2 q + D_2}$$

The $A_2 B_2 C_2 D_2$ matrix is easily shown to be a chain multiplication of the following three matrices:

$$\begin{bmatrix} A_2 & B_2 \\ C_2 & D_2 \end{bmatrix} = \begin{bmatrix} 1 & d_2 \\ 0 & 1 \end{bmatrix} \begin{bmatrix} 1 & 0 \\ -1/f & 1 \end{bmatrix} \begin{bmatrix} 1 & d_1 \\ 0 & 1 \end{bmatrix}$$

This chain rule of multiplication is characteristic of bilinear transformations and is extremely useful in the study of Gaussian beam transmission optics.

The $ABCD$ matrix is useful in the description of ray optics. Let a ray have beam position ρ_1 and slope ρ_1'. The ray passes through

an optical system with rotational symmetry and acquires a new beam position ρ_2 and slope ρ_2' [Fig. 6.5A.2]. We can write

$$\begin{bmatrix} \rho_2 \\ \rho_1' \end{bmatrix} = \begin{bmatrix} A & B \\ C & D \end{bmatrix} \begin{bmatrix} \rho_1 \\ \rho_1' \end{bmatrix} \tag{6.5A.25}$$

For propagation in free space, the $ABCD$ matrix is identical to (6.5A.22) and we find $\rho_2 = \rho_1 + d\rho_1'$ and $\rho_2' = \rho_1'$. For transmission through a lens, the $ABCD$ matrix is identical to (6.5A.24) and we have $\rho_2 = \rho_1$ and $\rho_1' = \rho_1' - \rho_1/f$.

Problems

P6.5.1

A Fabry-Perot resonator is composed of two parallel reflectors within which a standing wave is formed. The field inside is a TEM wave standing between the two plates. Show that the resonant wavenumbers are $k_r d = m\pi$. Strictly speaking, because of the finite transverse dimension, a TEM wave is diffracted. Considering diffraction in the cavity, we assume that the transverse field distribution takes a Gaussian form. At $z = 0$, $\overline{E} = \hat{x} E_0\, e^{-y^2/\omega_0^2}$. At $z > 0$, the electric field can be written as a superposition of plane waves with $\overline{k} = \hat{z} k_z + \hat{y} k_y$ and $k_y \ll k_z$:

$$\overline{E} = \hat{x} \int_{-\infty}^{\infty} dk_y\, E_g\, e^{ik_z z + i k_y y}$$

where

$$k_z = \sqrt{k^2 - k_y^2} \approx k\left(1 - \frac{1}{2}\frac{k_y^2}{k^2}\right)$$

The amplitude E_g is determined by the field at $z = 0$. Determine E_g by using an inverse Fourier transformation. Calculate and show that

$$\overline{E} \approx \hat{x}\frac{E_0}{\sqrt{1 + iz/z_F}}\, e^{ikz}\, e^{(i\,z/z_F - 1)y^2/w^2}$$

where $z_F = kw_0^2/2$ and $w(z) = w_0\sqrt{1 + z^2/z_F^2}$. Prove that, for a given ω_0, the locus of w versus z is a hyperbola. The phase front formed by normals to the family of the hyperbolas is curved. Show that the radius of curvature can be determined approximately by $R(z) \approx w(z)/[dw(z)/dz] = z(1 + z_F^2/z^2)$. Draw $w(z)$ and show that the focal points for the right-hand phase front and the left-hand phase front coincide when $z = z_F$. When the mirrors have radius of curvature $R(z_F) = 2z_F$ and are placed at a distance of $d = 2z_F$ apart, the configuration is confocal. Determine modes inside an optical cavity made of confocal mirrors. Are the modes with the confocal configuration stable?

6.6 Quantization of Electromagnetic Waves

In microscopic physics, quantum electrodynamics has become a well-established discipline. In the study of interactions of electromagnetic waves with material media, semi-classical approaches are usually taken, as a full quantum theory is too complicated to carry out. We can either treat electromagnetic waves classically or treat material media classically. In this section we quantize electromagnetic waves with material media characterized by constitutive relations. The Heisenberg representation will be used in the process of quantization. First we give a brief review of this representation.

The state of a physical system is represented by a state vector, which can be viewed either as a column matrix called a *ket* and denoted by $|\psi\!\!>$ or as a row matrix called a *bra* and denoted by $<\!\!\psi|$. The bra $<\!\!\psi|$ is the complex conjugate and transpose of the ket $|\psi\!\!>$. Physical observables are represented by Hermitian operators. An operator can be viewed as a square Hermitian matrix. Any measurement of a physical observable O yields a statistical expectation value for the observable. The average value of a series of measurements made on an ensemble of systems characterized by the same state vector $|\psi>$ is given by

$$< O > = < \psi \,|O|\, \psi >$$

This average value, or expectation value, is a real scalar number.

Each Hermitian operator possesses a set of eigenvectors with associated eigenvalues. The eigenvectors are eigenstates of the corresponding observable. The result of a single measurement for an observable O on a system described by the state vector $|\psi>$ yields an eigenvalue λ_n of the operator O and sends the system into the corresponding eigenstate $|\lambda_n >$. The probability of obtaining this eigenvalue λ_n and resulting in this eigenstate $|\lambda_n >$ is given by $|< \lambda_n \,|\psi >|^2$. As time progresses, the eigenstates of the operator evolve as the operator evolves with time, and the state of the system will no longer be an eigenstate of the operator. The evolution of the operator with time is determined by the equations of the motion. In classical electromagnetic theory the equations of motion for the electromagnetic field vectors are the Maxwell equations. In quantum theory, the field vectors are treated as operators and are governed by the Maxwell equations.

A. Uncertainty Principle

Since operators do not necessarily commute, commutation relations for noncommuting operators must be postulated. The physical interpretation of the commutation relations leads to the uncertainty principle, which states, in essence, that any measurement made on a physical system, no matter how slight, perturbs the system. Thus reality is forever beyond reach; only statistical results show up. This perturbation, induced by a measurement on one observable, may or may not affect the true values of measurements on other observables. When two observables interfere with each other, they are noncommuting operators. When two observables do not interfere with each other, they are simultaneously measurable and the commutation relation is zero. Commutation relations for electromagnetic fields $\overline{D}$ and $\overline{B}$ are postulated as

$$
[D_i(\overline{r}, t), B_j(\overline{r}', t)] = D_i(\overline{r}, t) B_j(\overline{r}', t) - B_j(\overline{r}', t) D_i(\overline{r}, t)
$$

$$
= -i\hbar \, \epsilon_{ijk} \frac{\partial}{\partial x_k} \delta(\overline{r} - \overline{r}') \tag{6.6.1}
$$

where $\hbar = 1.05 \times 10^{-34}$ joule-sec is Planck's constant divided by 2π. The factor $\hbar$ signifies that quantum effects are important whenever $\hbar$ is not numerically negligible. The classical limit is obtained when we let $\hbar \to 0$ and treat operators as classical variables.

In vacuum the commutation relations for other field components follow directly from the constitutive relations for vacuum:

$$
[E_i(\overline{r}, t), B_j(\overline{r}', t)] = -i\hbar \, \epsilon_{ijk} \frac{1}{\epsilon_o} \frac{\partial}{\partial x_k} \delta(\overline{r} - \overline{r}') \tag{6.6.2}
$$

$$
[D_i(\overline{r}, t), H_j(\overline{r}', t)] = -i\hbar \, \epsilon_{ijk} \frac{1}{\mu_o} \frac{\partial}{\partial x_k} \delta(\overline{r} - \overline{r}') \tag{6.6.3}
$$

$$
[E_i(\overline{r}, t), H_j(\overline{r}', t)] = -i\hbar c^2 \, \epsilon_{ijk} \frac{\partial}{\partial x_k} \delta(\overline{r} - \overline{r}') \tag{6.6.4}
$$

The commutation relations state that the perpendicular components of the electric and magnetic fields interfere with each other, whereas parallel components are simultaneously measurable. For instance, to measure an electric field, we may use a test charge and observe its motion along the electric field lines. But when a charge moves, it constitutes a current. The current produces a magnetic field perpendicular

to the electric field. Thus the test charge used in the measurement of the electric fields interferes with a simultaneous measurement on magnetic fields.

Recall that the magnetic field $\overline{B}$ is expressible as the curl of a vector potential $\overline{A}$:

$$\overline{B} = \nabla \times \overline{A} \tag{6.6.5}$$

The commutation relation (6.6.1) can be written as

$$[B_j(\overline{r}, t), D_i(\overline{r}', t)] = -i\hbar\, \epsilon_{ijk} \frac{\partial}{\partial x_k} \delta(\overline{r} - \overline{r}')$$

From (6.6.5), we find

$$[\epsilon_{jkm} \frac{\partial}{\partial x_k} A_m(\overline{r}, t), D_i(\overline{r}', t)] = \epsilon_{jkm} \frac{\partial}{\partial x_k} [A_m(\overline{r}, t), D_i(\overline{r}', t)]$$

$$= -i\hbar\, \epsilon_{ijk} \frac{\partial}{\partial x_k} \delta(\overline{r} - \overline{r}')$$

It follows that in terms of the vector potential $\overline{A}$, the commutation relation can be written as

$$[A_i(\overline{r}, t), D_j(\overline{r}', t)] = -i\hbar\, \delta_{ij}\, \delta(\overline{r} - \overline{r}') \tag{6.6.6}$$

Note that, although all commutation regions are written for equal times, we can also deduce and postulate commutation relations for unequal times.

In our description of a quantized system, the operators evolve with time, as do their associated eigenvectors. The eigenvectors can be viewed as forming base vectors describing a system state vector that is not varying with time. This is known as the Heisenberg picture. The Heisenberg picture is different from the Schrödinger picture, in which the system state vectors are functions of time but the operators and their eigenstates are stationary. In the Schrödinger picture, the equation of motion of a state vector $|\psi(t)>$ is given by the Schrödinger equation. In the Heisenberg picture, the time evolution of an operator O representing a physical observable is governed by the Heisenberg equation of motion. Under the assumption that O is not explicitly dependent on time, the Heisenberg equation of motion for O is

$$i\hbar \frac{dO}{dt} = [O, \mathcal{H}] \qquad (6.6.7)$$

where $\mathcal{H}$ is the Hamiltonian of the system, which corresponds to the total energy of the system. The Hamiltonian of an electromagnetic field in a source-free region is

$$\mathcal{H} = \int d^3\bar{r} \; \frac{1}{2}(\overline{E} \cdot \overline{D} + \overline{H} \cdot \overline{B}) \qquad (6.6.8)$$

The equation of motion of the $\overline{D}$ field is determined from (6.6.7)

$$i\hbar \frac{dD_i}{dt} = [D_i, \mathcal{H}]$$
$$= \int d^3\bar{r}' \left\{ \frac{1}{\epsilon_o}[D_i(\bar{r}), D_j(\bar{r}')]D_j(\bar{r}') + \frac{1}{\mu_o}[D_i(\bar{r}), B_j(\bar{r}')]B_j(\bar{r}')] \right\}$$

Remember that all field observables are now operators. The integral can be evaluated with the use of commutation relations (6.6.1) and (6.6.3). The first two commutators are zero because electric field operators commute. We obtain

$$\frac{dD_i}{dt} = -\epsilon_{ijk} \frac{\partial H_j}{\partial x_k} \qquad (6.6.9)$$

which is Ampère's law in the absence of the source term J_i. If sources are present, the Hamiltonian in (6.6.8) must then include an interaction term $-\overline{J} \cdot \overline{A}$. In view of commutation relation (6.6.6), it is clear that this extra term gives rise to a source term J_i in (6.6.9). Following a similar procedure, we can derive Faraday's law from the Heisenberg equation of motion for $\overline{B}$.

William Rowan Hamilton (4 August 1805 – 2 September 1865)

In 1823, Hamilton entered Trinity College, Dublin and submitted a paper "On Caustics" in 1824. In April 1827 he submitted his paper "Theory of Systems of Rays", and Trinity College elected him to the post of Andrews professor of astronomy and royal astronomer of Ireland while still an undergraduate at age 21. In 1833 Hamilton married Helen Maria Bayley, who bore him two sons and a daughter. In 1835 he published his memoir "On a General Method in Dynamics", and made discovery of quaternions, which freed algebra from the commutative postulate of multiplication. The Elements of Quaternions was published posthumously with a preface by his son William Edwin Hamilton in 1866.

B. Annihilation and Creation Operators

The eigenstates of the Hamiltonian are energy eigenstates because the Hamiltonian $\mathcal{H}$ is an energy operator. To facilitate discussion of the energy states of a quantized wave field, it is useful to transform the operator to $\overline{k}$ space:

$$\overline{A}(\overline{r}) = (2\pi)^{-3/2} \int d^3k \; \overline{A}(\overline{k}) e^{i\overline{k}\cdot\overline{r}} \tag{6.6.10a}$$

$$\overline{D}(\overline{r}) = (2\pi)^{-3/2} \int d^3k \; \overline{D}(\overline{k}) e^{i\overline{k}\cdot\overline{r}} \tag{6.6.10b}$$

The condition that $\overline{D}(\overline{r})$ and $\overline{A}(\overline{r})$ be real operators requires that $\overline{A}^+(\overline{r}) = \overline{A}_i(\overline{r})$ and $\overline{D}^+(\overline{r}) = \overline{D}(\overline{r})$ which yields the reality condition

$$\overline{A}(-\overline{k}) = \overline{A}^+(\overline{k}) \tag{6.6.11a}$$

$$\overline{D}(-\overline{k}) = \overline{D}^+(\overline{k}) \tag{6.6.11b}$$

The reality conditions in (6.6.11) are satisfied with the following representations:

$$\overline{A}(\overline{k}) = \alpha\sqrt{\frac{\hbar}{2}} \, [\overline{a}(\overline{k}) + \overline{a}^+(-\overline{k})] \tag{6.6.12a}$$

$$\overline{D}(\overline{k}) = \frac{i}{\alpha}\sqrt{\frac{\hbar}{2}} \, [\overline{a}(\overline{k}) - \overline{a}^+(-\overline{k})] \tag{6.6.12c}$$

In terms of $\overline{A}(\overline{k})$ and $\overline{D}(\overline{k})$, we have

$$\overline{a}(\overline{k}) = \frac{1}{\sqrt{2\hbar}}[\frac{1}{\alpha}\overline{A}(\overline{k}) - i\alpha\overline{D}(\overline{k})] \tag{6.6.12b}$$

$$\overline{a}^+(\overline{k}) = \frac{1}{\sqrt{2\hbar}}[\frac{1}{\alpha}\overline{A}^+(\overline{k}) + i\alpha\overline{D}^+(\overline{k})] \tag{6.6.13a}$$

As we shall demonstrate in subsequent developments, the operator $\overline{a}(\overline{k})$ is an annihilation operator and the operator $\overline{a}^+(\overline{k})$ is a creation operator. Upon operating on an energy eigenstate $\overline{a}(\overline{k})$ annihilates a photon corresponding to wave vector $\overline{k}$ and polarization $\overline{D}$ in the state, whereas $\overline{a}^+(\overline{k})$ creates such a photon.

The commutation relation (6.6.6)

$$[A_i(\overline{r}, t), D_j(\overline{r}', t)] = -i\hbar \, \delta_{ij} \, \delta(\overline{r} - \overline{r}') \tag{6.6.14}$$

gives rise to, using the integral representation for the delta function,
$\frac{1}{(2\pi)^3}\int d^3 k e^{i\overline{k}\cdot(\overline{r}-\overline{r}')} = \delta(\overline{r}-\overline{r}')$,

$$-i\hbar\delta_{ij}\,\delta(\overline{r}-\overline{r}') = \frac{1}{(2\pi)^3}\int d^3 k \int d^3 k' e^{i\overline{k}\cdot\overline{r}} e^{i\overline{k}'\cdot\overline{r}'}[A_i(\overline{k}),D_j(\overline{k}')]$$

$$= \frac{1}{(2\pi)^3}\int d^3 k \int d^3 k' e^{i\overline{k}\cdot\overline{r}} e^{-i\overline{k}'\cdot\overline{r}'}[A_i(\overline{k}),D_j^+(\overline{k}')]$$

$$= \frac{1}{(2\pi)^3}\int d^3 k \int d^3 k' e^{-i\overline{k}\cdot\overline{r}} e^{i\overline{k}'\cdot\overline{r}'}[A_i^+(\overline{k}),D_j(\overline{k}')]$$

We thus deduce that

$$[A_i(\overline{k}),D_j^+(\overline{k}')] = [A_i^+(\overline{k}),D_j(\overline{k}')] = -i\hbar\delta_{ij}\delta(\overline{k}-\overline{k}') \quad (6.6.15)$$

In terms of $a(\overline{k})$ and $a^+(\overline{k})$, the commutation relation becomes

$$[a_i(\overline{k}),a_j^+(\overline{k}')] = \frac{1}{2\hbar}[(\frac{1}{\alpha}A_i(\overline{k})-i\alpha D_i(\overline{k})),(\frac{1}{\alpha}A_j^+(\overline{k})+i\alpha D_j^+(\overline{k}))]$$

$$= \delta_{ij}\delta(\overline{k}-\overline{k}')$$

$$(6.6.16)$$

Thus perpendicular components commute and only like components are non-commutable.

The Hamiltonian $\mathcal{H}$ becomes, noting that $\overline{B}(\overline{k}) = \overline{k}\times\overline{A}(\overline{k})$,

$$\mathcal{H} = \frac{1}{2(2\pi)^3}\iiint d^3 r d^3 k d^3 k'\left\{\frac{1}{\epsilon_o}\overline{D}(\overline{k})\cdot\overline{D}(\overline{k}')+\frac{1}{\mu_o}\overline{B}(\overline{k})\cdot\overline{B}(\overline{k}')\right\}e^{i(\overline{k}+\overline{k}')\cdot\overline{r}}$$

$$= \frac{1}{2}\int d^3 k\left\{\frac{1}{\epsilon_o}\overline{D}(\overline{k})\cdot\overline{D}^+(\overline{k})+\frac{k^2}{\mu_o}\overline{A}(\overline{k})\cdot\overline{A}^+(\overline{k})\right\}$$

$$= \frac{\hbar}{4}\int d^3 k\left\{\frac{1}{\epsilon_o|\alpha|^2}[\overline{a}^+(\overline{k})-\overline{a}(-\overline{k})]\cdot[\overline{a}(\overline{k})-\overline{a}^+(-\overline{k})]\right.$$

$$\left. +\frac{k^2|\alpha|^2}{\mu_o}[\overline{a}^+(\overline{k})+\overline{a}(-\overline{k})]\cdot[\overline{a}(\overline{k})+\overline{a}^+(-\overline{k})]\right\}$$

$$= \frac{\hbar}{4}\int d^3 k\left\{(\frac{1}{\epsilon_o|\alpha|^2}+\frac{k^2|\alpha|^2}{\mu_o})[\overline{a}^+(\overline{k})\cdot\overline{a}(\overline{k})+\overline{a}(-\overline{k})\cdot\overline{a}^+(-\overline{k})]\right.$$

$$\left. +(\frac{-1}{\epsilon_o|\alpha|^2}+\frac{k^2|\alpha|^2}{\mu_o})[\overline{a}(-\overline{k})\cdot\overline{a}(\overline{k})+\overline{a}^+(\overline{k})\cdot\overline{a}^+(-\overline{k})]\right\}$$

$$= \frac{1}{2}\int d^3 k\ \hbar k c\,[\overline{a}^+(\overline{k})\cdot\overline{a}(\overline{k})+\overline{a}(\overline{k})\cdot\overline{a}^+(\overline{k})] \quad (6.6.17)$$

where we set $k^2|\alpha|^2/\mu_o = 1/\epsilon_o|\alpha|^2$ to obtain $|\alpha|^2 = \sqrt{\mu_o/k^2\epsilon_o} = \eta/k$.

For the case $i = j$ and $\overline{k} = \overline{k}'$, we simply write

$$[a, a^+] = 1 \qquad (6.6.18)$$

The Hamiltonian for the photon with a particular $\overline{k}$ vector becomes

$$\mathcal{H} = \frac{\hbar kc}{2}(a^+a + a^+a) = \hbar\omega(a^+a + \frac{1}{2}) \qquad (6.6.19)$$

where we made the use of commutator (6.6.18) and the vacuum dispersion relation $\omega = kc$. To obtain eigenvalues and eigenvectors for the energy operator $\mathcal{H}$, we write

$$\mathcal{H}|\mathcal{E}> = \mathcal{E}|\mathcal{E}> \qquad (6.6.20)$$

where $|\mathcal{E}>$ denotes the eigenstate, and $\mathcal{E}$ the corresponding eigenvalue. We first show that the eigenvalue $\mathcal{E}$ is always non-negative. Scalar-multiplying (6.6.20) by the eigenbra $<\mathcal{E}|$ and using (6.6.19), we have

$$\hbar\omega <\mathcal{E}|a^+a + \frac{1}{2}|\mathcal{E}> = \mathcal{E} <\mathcal{E}|\mathcal{E}>$$

The scalar $<\mathcal{E}|\mathcal{E}>$ is always non-negative because it is the product of a column matrix $|\mathcal{E}>$ and its complex conjugate and transpose $<\mathcal{E}|$. The term $<\mathcal{E}|a^+a|\mathcal{E}>$ is also non-negative for the same reason. Note that $<\mathcal{E}|a^+$ is the complex conjugate and transpose of $a|\mathcal{E}>$. Consequently, the eigenvalue $\mathcal{E}$ must be non-negative.

We next show that, if $|\mathcal{E}>$ is an eigenstate of $\mathcal{H}$, so are $a|\mathcal{E}>$ and $a^+|\mathcal{E}>$. Consider $\mathcal{H}(a^+|\mathcal{E}>)$. Using commutation relation (6.6.18), we find

$$[\mathcal{H}, a^+] = \hbar\omega[a^+a, a^+] = \hbar\omega a^+$$

Thus

$$\mathcal{H}a^+|\mathcal{E}> = a^+\mathcal{H}|\mathcal{E}> + \hbar\omega a^+|\mathcal{E}> = (\mathcal{E} + \hbar\omega)a^+|\mathcal{E}> \qquad (6.6.21)$$

It is seen that $a^+|\mathcal{E}>$ is an eigenstate of $\mathcal{H}$ with eigenvalue $(\mathcal{E}+\hbar\omega)$. Whenever a^+ is applied to an eigenstate of $\mathcal{H}$ with energy $\mathcal{E}$, the state changes into another eigenstate with energy $\mathcal{E} + \hbar\omega$. Since the

net effect of this operation is to create one more photon with energy $\hbar\omega$, the operator a^+ is called a creation operator.

Following similar reasoning, we can show that

$$\mathcal{H}a \, |\mathcal{E}> = (\mathcal{E} - \hbar\omega)a \, |\mathcal{E}> \qquad (6.6.22)$$

When a is applied to an eigenstate $|\mathcal{E}>$, the result is another eigenstate, $|\mathcal{E} - \hbar\omega>$, with one photon annihilated. The operator a is thus called an annihilation operator.

The separation between energy levels is $\hbar\omega$. When operated on by a, the transition is downward; when operated on by a^+, the transition is upward. The whole energy spectrum can be built up by successively applying a^+ to the ground state, which we denote by ket $|0>$ with 0 indicating no photon in the state. The state of n photons, $|n>$, is then created by operating a^+ on $|0>$ n times.

We have proved that all energy states of $\mathcal{H}$ possess non-negative energy eigenvalues. Suppose that we apply the annihilation operator a to the state $|\mathcal{E}>$ n times and reach the ground state $|0>$. Further operation of a on $|0>$ will then yield a zero:

$$a \, |0> = 0$$

We find the energy of the ground state to be

$$\mathcal{E}_0 = \frac{<0\,|\mathcal{H}|\,0>}{<0\,|\,0>} = \frac{\hbar\omega <0\,|\left(a^+a + \frac{1}{2}\right)|\,0>}{<0\,|\,0>} = \frac{1}{2}\hbar\omega \qquad (6.6.23)$$

Since

$$\mathcal{H} \, |n> = \hbar\omega \left(a^+a + \frac{1}{2}\right) |n> = \hbar\omega \left(n + \frac{1}{2}\right) |n>$$

The energy eigenvalue associated with $|n>$ is thus $(n + 1/2)\hbar\omega$.

The energy eigenstate $|n>$ can be represented by a column matrix with all elements equal to zero except the $(n+1)$th one, which is equal to unity. For instance,

$$|0> = \begin{bmatrix} 1 \\ 0 \\ 0 \\ 0 \\ \vdots \end{bmatrix} \qquad |1> = \begin{bmatrix} 0 \\ 1 \\ 0 \\ 0 \\ \vdots \end{bmatrix} \qquad |2> = \begin{bmatrix} 0 \\ 0 \\ 1 \\ 0 \\ \vdots \end{bmatrix}$$

The Hamiltonian can be represented by a diagonal matrix

$$
\mathcal{H} = \hbar\omega
\begin{bmatrix}
1/2 & 0 & 0 & \cdots \\
0 & 3/2 & 0 & \cdots \\
0 & 0 & 5/2 & \cdots \\
\vdots & \vdots & \vdots & \ddots
\end{bmatrix}
\tag{6.6.24}
$$

The eigenstates of $\mathcal{H}$ are also eigenstates of the number operator $N = a^{+}a$,

$$
N \mid n > = n \mid n >
\tag{6.6.25}
$$

The eigenvalue associated with a particular state of N is equal to the number of photons in that state.

We now find an explicit representation of a and a^{+} in terms of matrices. We write

$$
a \mid n > = C_n \mid n - 1 >
\tag{6.6.26}
$$

The coefficient C_n is determined from normalization. We require that the scalar product of the bra and the ket of an eigenstate be unity. We have

$$
n = < n \left| a^{+}a \right| n > = |C_n|^2
$$

Thus,

$$
a \mid n > = \sqrt{n} \mid n - 1 >
\tag{6.6.27}
$$

The matrix elements of a can be obtained from (6.6.27) by noting that

$$
< n - 1 \left| a \right| n > = \sqrt{n}
\tag{6.6.28}
$$

which is the element in the $(n - 1)$ th row and the n th column. All other elements are zero:

$$
a =
\begin{bmatrix}
0 & 1 & 0 & 0 & \cdots \\
0 & 0 & \sqrt{2} & 0 & \cdots \\
0 & 0 & 0 & \sqrt{3} & \cdots \\
\vdots & \vdots & \vdots & \vdots & \ddots
\end{bmatrix}
\tag{6.6.29}
$$

Following similar reasoning, we let $a^{+} \mid n > = C'_n \mid n + 1 >$ and find

$$
\left| C'_n \right|^2 = < n \left| aa^{+} \right| n > = < n \left| a^{+}a + 1 \right| n > = n + 1
$$

Thus,

$$
a^{+} \mid n > = \sqrt{n + 1} \mid n + 1 >
\tag{6.6.30}
$$

Forming the product

$$< n + 1 \left| a^+ \right| n >= \sqrt{n+1} \qquad (6.6.31)$$

we see that the matrix representation of a^+ takes the following form:

$$a^+ = \begin{bmatrix} 0 & 0 & 0 & 0 & \cdots \\ 1 & 0 & 0 & 0 & \cdots \\ 0 & \sqrt{2} & 0 & 0 & \cdots \\ 0 & 0 & \sqrt{3} & 0 & \cdots \\ \vdots & \vdots & \vdots & \vdots & \ddots \end{bmatrix} \qquad (6.6.32)$$

Obviously, the matrix representation for a^+ is the transpose of that for a. The time evolution of a^+ follows the Heisenberg equation of motion as $\overline{D}$ and $\overline{A}$ do. From matrix multiplication we see that operating a on the state $|n>$ will move the unit element in the nth position to the $(n+1)$th position and form the state $|n-1>$ multiplied by $\sqrt{n}$. Similarly, operating a^+ on $|n-1>$ results in the state $|n>$ multiplied by $\sqrt{n}$. Operating on $|n>$ by a^+a will result in the same state and give the photon number n.

We have discussed energy eigenstates and their associated eigenvalues for the Hamiltonian operator $\mathcal{H}$, and we have seen what results the annihilation operator a and creation operator a^+ have when operating on the eigenstates. It is natural to ask, "What are the eigenstates and eigenvalues for the annihilation and the creation operators?" First we shall prove that a^+ has no nonzero eigenstates. Denote the eigenstates of a^+ as $|e>$ and let the eigenvalues be λ. In view of (6.6.32), we have

$$\lambda \begin{bmatrix} e_0 \\ e_1 \\ e_2 \\ e_3 \\ \vdots \end{bmatrix} = \begin{bmatrix} 0 & 0 & 0 & 0 \\ 1 & 0 & 0 & 0 \\ 0 & \sqrt{2} & 0 & 0 \\ 0 & 0 & \sqrt{3} & 0 \\ \vdots & \vdots & \vdots & \vdots \end{bmatrix} \begin{bmatrix} e_0 \\ e_1 \\ e_2 \\ e_3 \\ \vdots \end{bmatrix} = \begin{bmatrix} 0 \\ e_0 \\ \sqrt{2}e_1 \\ \sqrt{3}e_2 \\ \vdots \end{bmatrix}$$

We see that if $\lambda = 0$, then $e_0 = e_1 = e_2 = \cdots = 0$ and $|e>=|0>$. If $\lambda \neq 0$, then $e_0 = 0$, $e_1 = (1/\lambda)e_0 = 0, \ldots$, $e_n = (1/\lambda)\sqrt{n}e_{n-1} = 0, \ldots$, and the eigenstate is identically zero.

The same procedure can be used to find eigenstates for a. We write, in view of (6.6.29),

$$\lambda \begin{bmatrix} e_0 \\ e_1 \\ e_2 \\ e_3 \\ \vdots \end{bmatrix} = \begin{bmatrix} 0 & 1 & 0 & 0 & \cdots \\ 0 & 0 & \sqrt{2} & 0 & \cdots \\ 0 & 0 & 0 & \sqrt{3} & \cdots \\ \vdots & \vdots & \vdots & \vdots & \\ \vdots & \vdots & \vdots & \vdots & \ddots \end{bmatrix} \begin{bmatrix} e_0 \\ e_1 \\ e_2 \\ e_3 \\ \vdots \end{bmatrix} = \begin{bmatrix} e_1 \\ \sqrt{2}e_2 \\ \sqrt{3}e_3 \\ \sqrt{4}e_4 \\ \vdots \end{bmatrix}$$

$$(6.6.33)$$

We see that $e_1 = \lambda e_0$, $e_2 = (\lambda/\sqrt{2})e_1, \ldots, e_n = (\lambda/\sqrt{n})e_{n-1}, \ldots$ In terms of the energy eigenstates, we obtain

$$|e> = e_0 \left[|0> + \lambda |1> + \frac{\lambda^2}{\sqrt{2!}} |2> + \cdots + \frac{\lambda^n}{\sqrt{n!}} |n> + \cdots \right]$$

$$(6.6.34)$$

Imposing the normalization condition $<e\,|\,e>=1$ yields

$$|e_0|^2 \left[1 + \lambda^2 + \frac{\lambda^4}{2!} + \cdots + \frac{\lambda^{2n}}{n!} + \cdots \right] = 1 \qquad (6.6.35)$$

Thus $e_0 = \exp(-\lambda^2/2)$ and (6.6.34) becomes

$$|e> = e^{-\lambda^2/2} \sum_{n=0}^{\infty} \frac{\lambda^n}{\sqrt{n!}} |n> \qquad (6.6.36)$$

We note that the expectation value for the photon number operator a^+a is determined from

$$\overline{n} = <e\,|a^+a|\,e> = e^{-\lambda^2} \sum_{n=0}^{\infty} n\frac{\lambda^{2n}}{n!} = \lambda^2 \qquad (6.6.37)$$

Consequently, the eigenvalue λ is equal to the square root of the photon number expectation value. Equation (6.6.36) becomes

$$|e> = e^{-\overline{n}/2} \sum_{n=0}^{\infty} \frac{\overline{n}^{n/2}}{\sqrt{n!}} |n> \qquad (6.6.38)$$

This represents the eigenstate of the annihilation operator a. It is also called the coherent state. The probability of finding the average photon number of $\overline{n}$ is

$$|<n\,|\,e>|^2 = \frac{\overline{n}^n e^{-\overline{n}}}{n!} \qquad (6.6.39)$$

This is the Poisson distribution. It is seen that in the energy state representation the precise photon number is given, whereas in the coherent state representation the photon number obeys the Poisson probability distribution.

C. Wave Quantization in Bianisotropic Media

With the use of the annihilation and creation operators a and a^+, we have diagonalized the Hamiltonian for an electromagnetic field in vacuum. The quantized fields have been discussed in terms of the energy states. We now generalize the procedure to carry out wave quantization in bianisotropic media. The commutation relations for $\overline{D}$ and $\overline{B}$ are the same as postulated in (6.6.1), and those for other field operators are derived from (6.6.1) by using the constitutive relations. The annihilation and creation operators are introduced by

$$A_j(\overline{k}) = \alpha_j \sqrt{\frac{\hbar}{2}} \, [a_j(\overline{k}) + a_j^+(-\overline{k})] \tag{6.6.40a}$$

$$D_j(\overline{k}) = \frac{i}{\alpha_j} \sqrt{\frac{\hbar}{2}} \, [a_j(\overline{k}) - a_j^+(-\overline{k})] \tag{6.6.40b}$$

where α_j is a constant to be determined. In view of the reality condition (6.6.11), we must have $\alpha_j(-\overline{k}) = \alpha_j^*(\overline{k})$. Substituting (6.6.40) into (6.6.14), we find that the commutation relations for a and a^+ are identical to (6.6.16) and (6.6.18). Using a and a^+, we shall diagonalize the Hamiltonian by properly choosing α_j.

As an example of bianisotropic media we consider a uniaxial medium moving along the direction of its optic axis. We let the optic axis be along the $\hat{z}$ direction. In the kDB system, $D_3 = B_3 = 0$ and the constitutive relation is

$$\overline{\overline{\kappa}}_k = \begin{bmatrix} \kappa & 0 & 0 \\ 0 & \kappa\cos^2\theta + \kappa_z\sin^2\theta & (\kappa - \kappa_z)\sin\theta\cos\theta \\ 0 & (\kappa - \kappa_z)\sin\theta\cos\theta & \kappa\sin^2\theta + k_z\cos^2\theta \end{bmatrix}$$

$$\overline{\overline{\nu}}_k = \begin{bmatrix} \nu & 0 & 0 \\ 0 & \nu\cos^2\theta + \nu_z\sin^2\theta & (\nu - \nu_z)\sin\theta\cos\theta \\ 0 & (\nu - \nu_z)\sin\theta\cos\theta & \nu\sin^2\theta + \nu_z\cos^2\theta \end{bmatrix}$$

$$\overline{\overline{\chi}}_k = \overline{\overline{\nu}}_k^+ = \begin{bmatrix} 0 & \chi\cos\theta & \chi\sin\theta \\ -\chi\cos\theta & 0 & 0 \\ -\chi\sin\theta & 0 & 0 \end{bmatrix}$$

The Hamiltonian becomes

$$\mathcal{H} = \frac{1}{2} \int d^3\overline{k} \left[\overline{D}^+(\overline{\overline{k}}) \cdot \overline{E}(\overline{k}) + \overline{B}^+(\overline{k}) \cdot \overline{H}(\overline{k}) \right]$$

$$= \frac{1}{2} \int d^3\overline{k} \left\{ \left[\kappa D_1^+(\overline{k})D_1(\overline{k}) + (\kappa\cos^2\theta + \kappa_z\sin^2\theta)D_2^+(\overline{k})D_2(\overline{k}) \right. \right.$$

$$+ k^2\nu A_2^+(\overline{k})A_2(\overline{k}) + k^2(\nu\cos^2\theta + \nu_z\sin^2\theta)A_1^+(\overline{k})A_1(\overline{k}) \right]$$

$$- ik\chi\cos\theta \left[D_1^+(\overline{k})A_1(\overline{k}) - A_1^+(\overline{k})D_1(\overline{k}) \right.$$

$$\left. \left. + D_2^+(\overline{k})A_2(\overline{k}) - A_2^+(\overline{k})D_2(\overline{k}) \right] \right\} \tag{6.6.41}$$

where θ is the angle between the $\overline{k}$ vector and the z axis. To express the Hamiltonian in terms of the annihilation and the creation operators, we note that

$$\int d^3k\, k[D_j^+(\overline{k})A_j(\overline{k}) - A_j^+(\overline{k})D_j(\overline{k})]$$

$$= -i\hbar \int d^3k\, k[a_j(\overline{k})a_j^+(\overline{k}) + a_j^+(\overline{k})a_j(\overline{k})]$$

Introducing (6.6.40) in (6.6.41), we obtain

$$\mathcal{H} = \frac{\hbar}{4} \int d^3k \left\{ \left(\frac{\kappa}{\alpha_1^2} + k^2\alpha_1^2(\nu\cos^2\theta + \nu_z\sin^2\theta) - 2k\chi\cos\theta \right) \right.$$

$$\cdot [a_1(\overline{k})a_1^+(\overline{k}) + a_1^+(\overline{k})a_1(\overline{k})] + \left(\frac{1}{\alpha_2^2}(\kappa\cos^2\theta + \kappa_z\sin^2\theta) \right.$$

$$\left. + \kappa^2\alpha_2^2 - 2k\chi\cos\theta \right) [a_2(\overline{k})a_2^+(\overline{k}) + a_2^+(\overline{k})a_2(\overline{k})]$$

$$+ \left(k^2\alpha_1^2(\nu\cos^2\theta + \nu_z\sin^2\theta) - \frac{\kappa}{\alpha_1^2} \right) \left[a_1(-\overline{k})a_1(\overline{k}) \right.$$

$$\left. + a_1^+(\overline{k})a_1^+(-\overline{k}) \right] + \left(k^2\nu\alpha_2^2 - \frac{1}{\alpha_2^2}(\kappa\cos^2\theta + \kappa_z\sin^2\theta) \right)$$

$$\left. \cdot [a_2(-\overline{k})a_2(\overline{k}) + a_2^+(\overline{k})a_2^+(-\overline{k})] \right\} \tag{6.6.42}$$

We see that the last two terms can be made to vanish by choosing

$$\alpha_1^4 = \frac{\kappa}{k^2(\nu\cos^2\theta + \nu_z\sin^2\theta)} \tag{6.6.43a}$$

$$\alpha_2^4 = \frac{(\kappa\cos^2\theta + \kappa_z\sin^2\theta)}{k^2\nu} \tag{6.6.43b}$$

The Hamiltonian $\mathcal{H}$ is seen to be diagonalized. It can be written as the sum of two Hamiltonians, each corresponding to a characteristic wave in the moving medium:

$$\mathcal{H} = \mathcal{H}_m + \mathcal{H}_e \tag{6.6.44a}$$

$$\mathcal{H}_m = \frac{\hbar}{2} \int d^3\overline{k} \left(\frac{\kappa}{\alpha_1^2} + k\chi\cos\theta \right) [a_1(\overline{k})a_1^+(\overline{k}) + a_1^+(\overline{k})a_1(\overline{k})] \tag{6.6.44b}$$

$$\mathcal{H}_e = \frac{\hbar}{2} \int d^3\overline{k} \left[\frac{(\kappa\cos^2\theta + \kappa_z\sin^2\theta)}{\alpha_2^2} + k\chi\cos\theta \right]$$
$$[a_2(\overline{k})a_2^+(\overline{k}) + a_2^+(\overline{k})a_2(\overline{k})] \tag{6.6.44c}$$

In the case of a stationary uniaxial dielectric medium, $\chi = 0$. We see that the photons associated with $\mathcal{H}_m$ are the ordinary photons and those associated with $\mathcal{H}_e$ are the extraordinary photons. The Hamiltonians in (6.6.44) can be expressed in terms of the number operators. When the Hamiltonian is operated on an energy state, the result is the total photon energy in the state. The photon energies of the two types of photons corresponding to $\mathcal{H}_m$ and $\mathcal{H}_e$ are as follows:

$$E_m = \hbar \left(\frac{\kappa}{\alpha_1^2} + \kappa\chi\cos\theta \right) \tag{6.6.45a}$$

$$E_e = \hbar \left[\frac{(\kappa\cos^2\theta + \kappa_z\sin^2\theta)}{\alpha_2^2} + k\chi\cos\theta \right] \tag{6.6.45b}$$

The photon energies can be negative when the medium velocity is sufficiently high. They correspond to classical slow waves in moving media which can also possess negative energy, and this is a purely kinematic effect when transforming from the moving to the stationary frame.

In general, the energy of a photon with a specified wave vector $\overline{k}$ is equal to $\hbar$ times the angular frequency. Classically, the angular frequency is related to the $\overline{k}$ vector by dispersion relations. The derivation of the dispersion relations is facilitated by the use of the kDB system. Since each characteristic wave has a particular dispersion relation, we expect that for each characteristic wave there will be a corresponding photon after quantization is carried out.

EXAMPLE 6.6.1

To show (6.6.14) gives rise to (6.6.1), we take curl of (6.6.14) with respect to the unprimed coordinate $\overline{r}$.

$$\epsilon_{kli}\frac{\partial}{\partial x_l}[A_i(\overline{r},t),D_j(\overline{r}',t)] = -i\hbar\epsilon_{kli}\frac{\partial}{\partial x_l}\delta_{ij}\,\delta(\overline{r}-\overline{r}') = -i\hbar\epsilon_{klj}\frac{\partial}{\partial x_l}\,\delta(\overline{r}-\overline{r}')$$

We find

$$[B_k(\overline{r},t),D_j(\overline{r}',t)] = -i\hbar\epsilon_{klj}\frac{\partial}{\partial x_l}\,\delta(\overline{r}-\overline{r}')$$

Interchanging B_k and D_j, and $\overline{r}$ and $\overline{r}'$, we obtain (6.6.1).

— END OF EXAMPLE 6.6.1 —

EXAMPLE 6.6.2

The commutation relation for a and a^+ can also be deduced directly from (6.6.14) by substituting (6.6.10) and (6.6.40) into the commutation relation (6.6.14) to yield

$$i\frac{\hbar}{2}\left[\int d^3\overline{k}\ [a_i^+(\overline{k})e^{i\overline{k}\cdot\overline{r}} + a_i(k)e^{-i\overline{k}\cdot\overline{r}}],\right.$$

$$\left.\int d^3\overline{k}'\ [a_j^+(\overline{k}')e^{i\overline{k}'\cdot\overline{r}'} - a_j(\overline{k}')e^{-i\overline{k}'\cdot\overline{r}'}]\right] = -i\hbar\,\delta_{ij}\delta(\overline{r}-\overline{r}')$$

We thus deduce that

$$[a_i(\overline{k}),a_j^+(\overline{k}')] = \delta_{ij}\delta(\overline{k}-\overline{k}')$$

— END OF EXAMPLE 6.6.2 —

Problems

P6.6.1

A simple interferometer is shown in Figure P6.6.1.1. Light from a source is split into two beams by a semi-transparent mirror. The semi-transparent mirror has the property of transmitting $e^{-i\phi_t}/\sqrt{2}$ of the incident electric field and reflecting $e^{-i\phi_r}/\sqrt{2}$ of the incident field with $\phi_t - \phi_r = \pi/2 + l\pi$. In
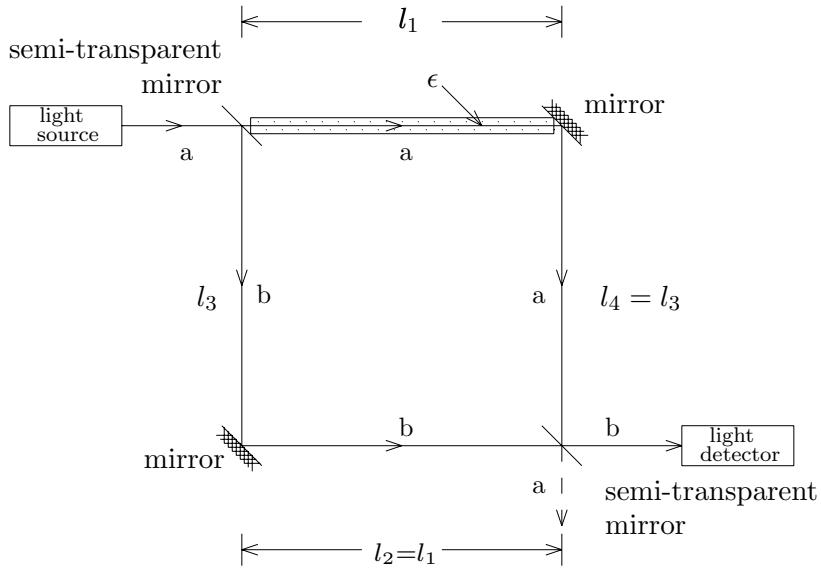
Figure P6.6.1.1   A simple interferometer.

Chapter 3, the interferometry is analyzed with time-harmonic fields at steady state. It is shown that at the light detector, fields constructively interfere.

   Now consider a single photon incident on the system. Define a unitary operator for the semi-transparent mirror as follows:

$$\overline{\overline{U}} = \frac{1}{\sqrt{2}} \begin{bmatrix} 1 & i \\ i & 1 \end{bmatrix}$$

Let the routes of the interferometry be marked as a and b.

(a) Let the state of one photon incident from path a and no photon incident from path b be denoted as $|10> = \begin{bmatrix} 1 \\ 0 \end{bmatrix}$. Find the photon state after the photon passes through the semi-transparent mirror.

(b) Let the dielectric-filled path l_1 render the photon a phase $e^{i\phi}$ and define a unitary operator

$$\overline{\overline{U}}_p = \begin{bmatrix} 1 & 0 \\ 0 & e^{i\phi} \end{bmatrix}$$

Find the photon state after the photon passing through the reflecting mirrors.

(c) Find the final photon state after the second semi-transparent mirror. Where will the photon be when $\phi = 0$?

P6.6.2

For a given energy state $|n>$, what are the expectation values for the field operator $\overline{D}$ and for $\overline{D}^2$?

P6.6.3

Let A, B, and C be Hermitian operators, with $[A, B] = iC$. Let

$$\alpha = A - <A>; \qquad \beta = B - <B>$$
$$\alpha|\psi> = |\phi>; \qquad \beta|\psi> = |\chi>$$
$$(\Delta A)^2 = <\phi|\phi>; \qquad (\Delta B)^2 = <\chi|\chi>$$

With respect to the state function $|\psi>$, define the mean-square deviation by $(\Delta A)^2 = <\psi|(A - <A>)^2|\psi>$ and $(\Delta B)^2 = <\psi|(B - <B>)^2|\psi>$ where $<A> = <\psi|A|\psi>$ and $<B> = <\psi|B|\psi>$ are expectation values of A and B. By Schwartz inequality

$$(\Delta A)^2(\Delta B)^2 = <\phi|\phi><\chi|\chi> \geq |<\phi|\chi>|^2$$

show that

$$(\Delta A)^2(\Delta B)^2 \geq \frac{1}{4}|<\psi|C|\psi>|^2$$

Let $C = \hbar$, find the uncertainty value $\Delta A \, \Delta B$ as implied by the commutation relation for A and B.

P6.6.4

Given $[a, a^+] = 1$, compute $[a, (a^+)^n]$ and $[a, e^{a^+}]$.

Answers

P6.1.1

$$Z_{11} = Z_{22}^*, \ Z_{12} = -Z_{12}^*, \ \text{and} \ Z_{21} = -Z_{21}^*.$$

P6.1.2

$$P_r = 20(kI_0\ell)^2, \qquad G(\theta) = 3\sin^2\theta.$$

P6.1.3

$$\overline{H}(\overline{r}) = i\omega\epsilon 2E_0 \frac{e^{ikr}}{4\pi r}(\hat{\theta}\cos\phi\cos\theta - \hat{\phi}\sin\phi)\frac{4}{k_x k_y}\sin\left(k_x\frac{x_0}{2}\right)\sin\left(k_y\frac{y_0}{2}\right)$$

where $k_x = k\sin\theta\cos\phi; k_y = k\sin\theta\sin\phi.$

P6.1.4

For $a < \lambda$ and $b < \lambda$, $\overline{H}(\overline{r}) = -\hat{\phi}E_0\,\omega\epsilon a\frac{e^{ikr}}{4\pi r}k(b^2 - a^2)\pi\sin\theta.$

P6.1.5

As $\theta_o = 0$, $\overline{E}_s = -\hat{y}\frac{E_0 a}{2r}e^{ikr-2ika}$, and $A_e = \lim_{r\to\infty}\left(4\pi r^2\frac{P_s}{P_i}\right) = \pi a^2$

P6.1.6

$$Z_a = \frac{\eta^2}{4Z_m} = \frac{(377)^2}{4(73)}\ \Omega = 486\ \Omega$$

P6.1.7

$$\overline{E}(\overline{r}) = ik\cos\theta\,\hat{y}2E_0\frac{e^{ikr}}{4\pi r}b\frac{2\frac{\pi}{d}\cos k_x\frac{d}{2}}{\left(\frac{\pi^2}{d^2} - k_x^2\right)}$$

P6.1.8

The first zero of $\sin(kxw/2z)$ occurs at $kxw/2z = \pi$ which yields $2\pi w\theta/2\lambda = \pi$. Consequently $\theta = \lambda/w$.

For the Nth side lobe, $kxw/2z = kw\theta/2 = N\pi$, which yields $\theta_N = N\lambda/w$. Based on the assumption $\theta \approx x/z < 1$, we thus deduce that $N < \lambda/w$.

P6.1.9

Let the size of the ground illuminated by the radiating antenna during the processing time be L. The range from the antenna to ground is R. And the beam width of the small antenna is λ/ℓ. We have $L = R\lambda/\ell$. Since the synthesized antenna of size L have a beamwidth of λ/ℓ, the ground resolution is therefore $R\lambda/L = R\lambda/(R\lambda/\ell) = \ell$. In order to achieve the resolution for a large range R, we must have a large L. This will demand a large processing capability which is inversely proportional to ℓ.

P6.2.1

(a) A biaxial medium is lossless and reciprocal.

(b) A moving biaxial medium is lossless and nonreciprocal. The complementary medium is moving in the opposite direction.

(c) A chiral medium is lossless and reciprocal.

(d) The biisotropic medium with real χ is lossy and reciprocal.

(e) A ferrite in a dc magnetic field is not reciprocal. The complementary medium has its dc magnetic field in the opposite direction.

P6.2.2

$$k^2 = \frac{\iiint dV \, (\nabla \times \overline{H})^2}{\iiint dV \, |\overline{H}|^2}$$

With $Aa = -0.65432929$, $k^2 a^2 = \frac{2 + 4Aa + \frac{9}{4}A^2 a^2}{\frac{1}{4} + \frac{2}{5}Aa + \frac{1}{6}A^2 a^2} = 5.80305$

P6.2.3

$$w_c^2 = \frac{2\pi^2}{a^2 \mu (\epsilon_1 + \epsilon_2)} \, .$$

P6.2.4

$A_e = 0.86\lambda^2$.

P6.2.5

Percentage shift $\frac{\Delta \omega_r}{\omega_{r0}} = \frac{\sqrt{0.410} - 1.0}{1.0} = -0.360 = -36\%$.

36% down in resonant frequency.

P6.3.1

$V(t) \simeq -2 \cos \omega t$

P6.3.2

(a) The time-average power per unit area generated by the sheet per unit area is $<P_g> = -\frac{1}{2} \mathrm{Re} \left\{ E_x \big|_{z=0} J_s^* \right\} = \frac{\eta}{4} |J_s|^2 . .$

The time-average power per unit area carried by the plane wave in $z > 0$ is $<S_{z+}> = \frac{1}{2} \mathrm{Re} \{ \overline{E} \times \overline{H}^* \} = \frac{\eta}{8} |J_s|^2 . .$

An equal amount is carried by the plane wave in $z < 0$.

(b) Evanescent waves are generated. There is no time-average power per unit area generated by the current sheet.

P6.4.1

$$\frac{E(\rho)}{E(0)} = \sqrt{\frac{P(\rho)}{P(0)}} = \frac{1}{n-1} \sqrt{\frac{(n \cos \theta - 1)^3}{n - \cos \theta}}$$

P6.4.2

$\theta_0 \approx 66°.$

P6.6.1

(a) $\dfrac{1}{\sqrt{2}} \begin{bmatrix} 1 & i \\ i & 1 \end{bmatrix} \begin{bmatrix} 1 \\ 0 \end{bmatrix} = \dfrac{1}{\sqrt{2}} \begin{bmatrix} 1 \\ i \end{bmatrix}$

(b) $\dfrac{1}{\sqrt{2}} \begin{bmatrix} 1 & 0 \\ 0 & e^{i\phi} \end{bmatrix} \begin{bmatrix} 1 \\ i \end{bmatrix} = \dfrac{1}{\sqrt{2}} \begin{bmatrix} 1 \\ ie^{i\phi} \end{bmatrix}$

(c) $\dfrac{1}{2} \begin{bmatrix} 1 & i \\ i & 1 \end{bmatrix} \begin{bmatrix} 1 \\ ie^{i\phi} \end{bmatrix} = \dfrac{1}{2} \begin{bmatrix} 1 - e^{i\phi} \\ i + ie^{i\phi} \end{bmatrix} = ie^{i\phi/2} \begin{bmatrix} -\sin\phi/2 \\ \cos\phi/2 \end{bmatrix}$

When $\phi = 0$, the photon reaches the light detector through path b.

P6.6.2

$$< n|D(\overline{k})|n > = \frac{i}{\alpha}\sqrt{\frac{\hbar}{2}}(< n|a(\overline{k})|n > - < n|a^{+}(-\overline{k})|n >) = 0.$$

$$< n|D^{2}(\overline{k})|n > = \frac{\hbar k}{2\eta} < n|a^{+}a + aa^{+}|n > \frac{\hbar k}{2\eta}(2n+1).$$

P6.6.3

The uncertainty relation $\Delta A\, \Delta B \geq \hbar/2$.

P6.6.4

$$[a, (a^{+})^{n}] = n(a^{+})^{n-1}; \qquad\qquad [a, e^{a+}] = e^{a^{+}}$$

7

SCATTERING

7.6 Scattering by Random Media

    A. Dyadic Green's Function for Layered Media

    B. Scattering by a Half-Space Random Medium

7.7 Effective Permittivity for a Volume Scattering Medium

    A. Random Discrete Scatterers

    B. Effective Permittivity for a Continuous Random Medium

Answers

7.1   Scattering by Spheres

A. Rayleigh Scattering

Rayleigh scattering characterizes the scattering of electromagnetic waves by particles much smaller than a wavelength. Consider a spherical particle with permittivity ϵ_s, permeability μ_s, and radius a, at the origin of a coordinate system [Fig. 7.1.1]. A plane wave polarized in the $\hat{z}$ direction is incident upon the particle, $\overline{E} = \hat{z}E_0 e^{ikx}$. Because the particle is very small, the scattered field is essentially that resulting from a point source. The $\hat{z}$ directed electric field induces a dipole moment, and the particle re-radiates as a dipole antenna. The solution takes the form

$$\overline{E} = \frac{-i\omega\mu Il\, e^{ikr}}{4\pi r}\left\{\hat{r}\left[\left(\frac{i}{kr}\right)^2 + \frac{i}{kr}\right]2\cos\theta\right.$$

$$\left. + \hat{\theta}\left[\left(\frac{i}{kr}\right)^2 + \frac{i}{kr} + 1\right]\sin\theta\right\} \quad (7.1.1a)$$

$$\overline{H} = \hat{\phi}\frac{-ikIl\, e^{ikr}}{4\pi r}\left(\frac{i}{kr} + 1\right)\sin\theta \quad (7.1.1b)$$

The dipole moment Il will be determined by E_0 and ϵ_s.
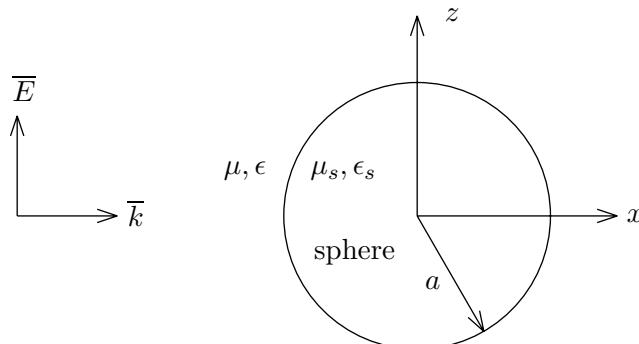
Figure 7.1.1   Rayleigh scattering by a small sphere.

Very close to the origin, $kr \ll 1$. This also corresponds to the static limit when the frequency is very low since $k = \omega/c$. The dipole solution is electric in nature and the magnetic field vanishes in the

limit, since $|\overline{H}| \sim Il$ and $|\overline{E}| \sim Il/k$ while Il is proportional to ω. The electric field in the static limit is

$$
\begin{aligned}
\overline{E} &\approx \frac{i\omega\mu Il}{4\pi r} \frac{1}{(kr)^2} (\hat{r}\, 2\cos\theta + \hat{\theta}\sin\theta) \\
&= (\hat{r}\, 2\cos\theta + \hat{\theta}\sin\theta) \left(\frac{a}{r}\right)^3 E_s
\end{aligned}
\tag{7.1.2a}
$$

where

$$
E_s = \frac{i\eta Il}{4\pi k a^3}
\tag{7.1.2b}
$$

and $\eta = \sqrt{\mu/\epsilon}$. This solution satisfies the Maxwell equations for static fields, that is, $\nabla \times \overline{E} = 0$ and $\nabla \cdot \overline{E} = 0$.

We assume the field inside the sphere to be uniform and is in the same direction as the incident field:

$$
\overline{E} = \hat{z}E_i = (\hat{r}\cos\theta - \hat{\theta}\sin\theta)E_i \qquad r \le a
$$

This solution also satisfies the Maxwell equations for static fields.

On the surface $r = a$, the boundary conditions require that the tangential $\overline{E}$ field and the normal $\overline{D}$ be continuous. We find

$$
-E_0 + E_s = -E_i
\tag{7.1.3a}
$$

$$
\epsilon E_0 + 2\epsilon E_s = \epsilon_s E_i
\tag{7.1.3b}
$$

In terms of the applied field E_0, we find from (7.1.3a) and (7.1.3b)

$$
E_s = \frac{\epsilon_s - \epsilon}{\epsilon_s + 2\epsilon} E_0
\tag{7.1.4a}
$$

$$
E_i = \frac{3\epsilon}{\epsilon_s + 2\epsilon} E_0
\tag{7.1.4b}
$$

From (7.1.2b) and (7.1.4a) we solve for Il and obtain

$$
Il = -i4\pi k a^3 \sqrt{\frac{\epsilon}{\mu}} \left(\frac{\epsilon_s - \epsilon}{\epsilon_s + 2\epsilon}\right) E_0
$$

When this is inserted in (7.1.1), we obtain the electromagnetic fields for Rayleigh scattering.

We shall now study the scattered field as $kr \gg 1$. Equation (7.1.1) gives

$$E_\theta = - \left(\frac{\epsilon_s - \epsilon}{\epsilon_s + 2\epsilon} \right) k^2 a^2 E_0 \frac{a}{r} \, e^{ikr} \sin\theta \qquad (7.1.5a)$$

$$H_\phi = \sqrt{\frac{\epsilon}{\mu}} E_\theta \qquad (7.1.5b)$$

The total scattered power from the sphere is

$$P_s = \frac{1}{2} \int_0^\pi r^2 \sin\theta \, d\theta \int_0^{2\pi} d\phi \, E_\theta H_\phi^* = \frac{4\pi}{3} \sqrt{\frac{\epsilon}{\mu}} \left(\frac{\epsilon_s - \epsilon}{\epsilon_s + 2\epsilon} k^2 a^3 E_0 \right)^2 \qquad (7.1.6)$$

The scattering cross section is calculated as

$$\Sigma_s = \frac{P_s}{\frac{1}{2}\sqrt{\frac{\epsilon}{\mu}} \mid E_0 \mid^2} = \frac{8\pi}{3} \left(\frac{\epsilon_s - \epsilon}{\epsilon_s + 2\epsilon} \right)^2 k^4 a^6 \qquad (7.1.7)$$

Thus the total scattered power is proportional to the fourth power of the wavenumber; high-frequency waves are scattered more than lower ones. The scattered power is also proportional to the sixth power of the radius.

In the case of a perfectly conducting sphere, the electric field inside, $\overline{E}_i$, is identically zero. From (7.1.2b) and (7.1.3a) we find

$$Il = -i4\pi k a^3 \sqrt{\frac{\epsilon}{\mu}} E_0 \qquad (7.1.8)$$

The boundary condition corresponding to (7.1.3b) for the normal $\overline{D}$ field can be used to find the surface charge densities ρ_s. Note that we can obtain (7.1.8) from (7.1.4) by letting $\epsilon_s \to \infty$. Since there are surface charges, their time variation will lead to a surface current, creating magnetic dipoles. The near field $\overline{H}$ for magnetic dipoles is the dual of that for the electric dipole in (7.1.2),

$$\overline{H} \sim \frac{ikKl}{4\pi r} \sqrt{\frac{\epsilon}{\mu}} \frac{1}{(kr)^2} \left(\hat{r} \, 2\cos\theta_y + \hat{\theta}_y \sin\theta_y \right) \qquad (7.1.9)$$

where Kl is the magnetic moment of the dipole. Notice that for the incident $\overline{H}$ field in the $\hat{y}$ direction, the angle θ_y now refers to the

y axis as opposed to the z axis for the electric dipole. The boundary condition requires zero normal $\overline{B}$ field, and the discontinuity of the tangential $\overline{H}$ field gives rise to the surface current densities $\overline{J}_s$. We find

$$Kl = -i2\pi k a^3 \sqrt{\frac{\mu}{\epsilon}} H_0 \tag{7.1.10}$$

where H_0 is the amplitude of the incident plane wave. Thus the scattered field corresponds to that of a magnetic dipole along the y axis.

We shall remember that the above analysis for Rayleigh scattering is valid only when the radius of the sphere is very small. For larger radii, the scattering process is called Mie scattering. In fact, as we shall show in the following, scattering of a plane wave by a sphere of arbitrary size with permittivity ϵ_s and permeability μ_s can be solved exactly in closed form.

B. Mie Scattering

The problem of a plane wave scattered by a sphere can be solved rigorously by matching boundary conditions. To facilitate the solution, we decompose the spherical waves into TM to $\hat{r}$ and TE to $\hat{r}$ components by introducing the Debye potentials π_e and π_m so that

$$\overline{A} = \overline{r}\pi_e \tag{7.1.11a}$$

$$\overline{H} = \nabla \times \overline{A} = \hat{\theta}\frac{1}{\sin\theta}\frac{\partial}{\partial\phi}\pi_e - \hat{\phi}\frac{\partial}{\partial\theta}\pi_e \tag{7.1.11b}$$

for TM to $\hat{r}$ waves, and

$$\overline{Z} = \overline{r}\pi_m \tag{7.1.12a}$$

$$\overline{E} = \nabla \times \overline{Z} = \hat{\theta}\frac{1}{\sin\theta}\frac{\partial}{\partial\phi}\pi_m - \hat{\phi}\frac{\partial}{\partial\theta}\pi_m \tag{7.1.12b}$$

for TE to $\hat{r}$ waves.

The Debye potentials π_e and π_m satisfy the Helmholtz equation in spherical coordinates

$$\left(\nabla^2 + k^2\right)\left\{\begin{array}{c}\pi_e \\ \pi_m\end{array}\right\} = 0 \tag{7.1.13}$$

where

$$\nabla^2 = \frac{1}{r}\frac{\partial^2}{\partial r^2}r + \frac{1}{r^2\sin\theta}\frac{\partial}{\partial\theta}\sin\theta\frac{\partial}{\partial\theta} + \frac{1}{r^2\sin^2\theta}\frac{\partial^2}{\partial\phi^2} \tag{7.1.14}$$

The solution to this equation is composed of superpositions of spherical Bessel functions, associated Legendre polynomials, and sinusoids. Using the Maxwell equations and (7.1.13), we find that the field components in spherical coordinates take the forms

$$E_r = \frac{i}{\omega\epsilon}\left(\frac{\partial^2}{\partial r^2}r\pi_e + k^2 r\pi_e\right) \tag{7.1.15a}$$

$$E_\theta = \frac{i}{\omega\epsilon}\frac{1}{r}\frac{\partial^2}{\partial r\partial\theta}r\pi_e + \frac{1}{\sin\theta}\frac{\partial}{\partial\phi}\pi_m \tag{7.1.15b}$$

$$E_\phi = \frac{i}{\omega\epsilon}\frac{1}{r\sin\theta}\frac{\partial^2}{\partial r\partial\phi}r\pi_e - \frac{\partial}{\partial\theta}\pi_m \tag{7.1.15c}$$

$$H_r = -\frac{i}{\omega\mu}\left(\frac{\partial^2}{\partial r^2}r\pi_m + k^2 r\pi_m\right) \tag{7.1.16a}$$

$$H_\theta = -\frac{i}{\omega\mu}\frac{1}{r}\frac{\partial^2}{\partial r\partial\theta}r\pi_m + \frac{1}{\sin\theta}\frac{\partial}{\partial\phi}\pi_e \tag{7.1.16b}$$

$$H_\phi = -\frac{i}{\omega\mu}\frac{1}{r\sin\theta}\frac{\partial^2}{\partial r\partial\phi}r\pi_m - \frac{\partial}{\partial\theta}\pi_e \tag{7.1.16c}$$

The total electromagnetic fields are now decomposed into TE and TM components and expressed in terms of the Debye potentials π_e and π_m.

Consider a sphere with radius a located at the origin of a coordinate system [Fig. 7.1.2]. The sphere has permittivity ϵ_s and permeability μ_s. A plane wave,

$$\overline{E} = \hat{x}E_0\,e^{ikz} = \hat{x}E_0\,e^{ikr\cos\theta}$$

$$\overline{H} = \hat{y}\sqrt{\frac{\epsilon}{\mu}}E_0\,e^{ikr\cos\theta}$$

is incident upon the sphere. Note that the direction of propagation of the plane wave is along $\hat{z}$. The coordinate system is different from that used for Rayleigh scattering, where the z axis is in the direction of the linearly polarized electric field. Rayleigh scattering

To match boundary conditions at the sphere's surface, we expand the incident wave in terms of spherical harmonics by using the wave transformation:

$$e^{ikr\cos\theta} = \sum_{n=0}^{\infty}(-i)^{-n}(2n+1)j_n(kr)P_n(\cos\theta) \tag{7.1.17}$$
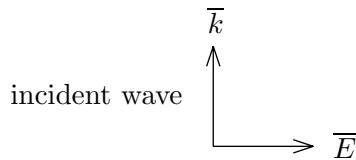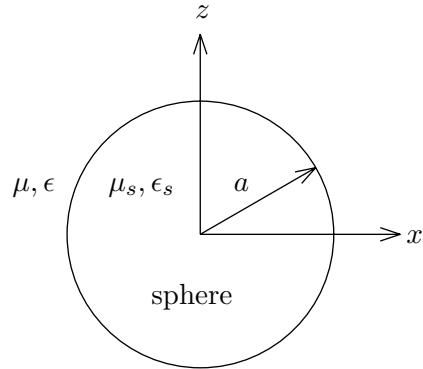
Figure 7.1.2 Mie scattering.

To determine the Debye potentials for the incident wave, we note that

$$E_r = E_0 \sin\theta \cos\phi \, e^{ikr\cos\theta}$$

$$= -\frac{iE_0 \cos\phi}{(kr)^2} \sum_{n=1}^{\infty} (-i)^{-n}(2n+1)\hat{J}_n(kr)P_n^1(\cos\theta)$$

where

$$\hat{J}_n(kr) = krj_n(kr)$$

The summation now starts with $n = 1$ because $P_0^1(\cos\theta) = 0$. The potential π_e satisfies (7.1.15) and can be shown to be

$$\pi_e = -\frac{E_0 \cos\phi}{\omega\mu r} \sum_{n=1}^{\infty} \frac{(-i)^{-n}(2n+1)}{n(n+1)} \hat{J}_n(kr)P_n^1(\cos\theta) \qquad (7.1.18a)$$

By a dual process, the potential π_m is found to be

$$\pi_m = \frac{E_0 \sin\phi}{kr} \sum_{n=1}^{\infty} \frac{(-i)^{-n}(2n+1)}{n(n+1)} \hat{J}_n(kr)P_n^1(\cos\theta) \qquad (7.1.18b)$$

The scattered field can be characterized by Debye potentials:

$$\pi_e^s = -\frac{E_0 \cos\phi}{\omega\mu r} \sum_{n=1}^{\infty} a_n \hat{H}_n^{(1)}(kr) P_n^1(\cos\theta) \qquad (7.1.19a)$$

$$\pi_m^s = \frac{E_0 \sin\phi}{kr} \sum_{n=1}^{\infty} b_n \hat{H}_n^{(1)}(kr) P_n^1(\cos\theta) \qquad (7.1.19b)$$

where

$$\hat{H}_n^{(1)}(kr) = kr h_n^{(1)}(kr)$$

The total field outside the sphere is equal to the sum of the incident and scattered fields.

The field inside the sphere can also be expressed in terms of the Debye potentials:

$$\pi_e^i = -\frac{E_0 \cos\phi}{\omega\mu_s r} \sum_{n=1}^{\infty} c_n \hat{J}_n(k_s r) P_n^1(\cos\theta) \qquad (7.1.20a)$$

$$\pi_m^i = \frac{E_0 \sin\phi}{k_s r} \sum_{n=1}^{\infty} d_n \hat{J}_n(k_s r) P_n^1(\cos\theta) \qquad (7.1.20b)$$

The boundary conditions at $r = a$ require that E_θ, E_ϕ, H_θ, and H_ϕ be continuous, with the result that four equations are solvable for the unknown coefficients a_n, b_n, c_n, and d_n. In view of (7.1.15) and (7.1.16), the coefficients are determined as

$$a_n = \frac{(-i)^{-n}(2n+1)}{n(n+1)} \cdot \frac{-\sqrt{\epsilon_s\mu}\,\hat{J}_n'(ka)\hat{J}_n(k_s a) + \sqrt{\epsilon\mu_s}\,\hat{J}_n(ka)\hat{J}_n'(k_s a)}{\sqrt{\epsilon_s\mu}\,\hat{H}_n^{(1)\prime}(ka)\hat{J}_n(k_s a) - \sqrt{\epsilon\mu_s}\,\hat{H}_n^{(1)}(ka)\hat{J}_n'(k_s a)}$$
$$(7.1.21a)$$

$$b_n = \frac{(-i)^{-n}(2n+1)}{n(n+1)} \cdot \frac{-\sqrt{\epsilon_s\mu}\,\hat{J}_n(ka)\hat{J}_n'(k_s a) + \sqrt{\epsilon\mu_s}\,\hat{J}_n'(ka)\hat{J}_n(k_s a)}{\sqrt{\epsilon_s\mu}\,\hat{H}_n^{(1)}(ka)\hat{J}_n'(k_s a) - \sqrt{\epsilon\mu_s}\,\hat{H}_n^{(1)\prime}(ka)\hat{J}_n(k_s a)}$$
$$(7.1.21b)$$

$$c_n = \frac{(-i)^{-n}(2n+1)}{n(n+1)} \cdot \frac{i\sqrt{\epsilon_s\mu}}{\sqrt{\epsilon_s\mu}\,\hat{H}_n^{(1)\prime}(ka)\hat{J}_n(k_s a) - \sqrt{\epsilon\mu_s}\,\hat{H}_n^{(1)}(ka)\hat{J}_n'(k_s a)}$$
$$(7.1.21c)$$

$$d_n = \frac{(-i)^{-n}(2n+1)}{n(n+1)} \cdot \frac{-i\sqrt{\epsilon\mu_s}}{\sqrt{\epsilon_s\mu}\,\hat{H}_n^{(1)}(ka)\hat{J}_n'(k_s a) - \sqrt{\epsilon\mu_s}\,\hat{H}_n^{(1)\prime}(ka)\hat{J}_n(ka)}$$
$$(7.1.21d)$$

In the case of small spheres, $ka \ll 1$ and $k_s a \ll 1$, only the $n = 1$ terms dominate, with $a_n \to -(ka)^3(\epsilon_s - \epsilon)/(\epsilon_s + 2\epsilon)$, and $b_n \to -(ka)^3(\mu_s - \mu)/(\mu_s + 2\mu)$. The results reduce to those of Rayleigh scattering. Rayleigh scattering For the scattering of electromagnetic waves by spheres of finite radius, where the Rayleigh limit $ka \ll 1$ is not met, the phenomenon is known as *Mie scattering*.

The above results also reduce to the case of a perfectly conducting sphere. In the limit of $\epsilon_s \to \infty$ or $E_i = 0$ for a perfect conductor, the source-free Ampère's law $\nabla \times \overline{H} = -i\omega\epsilon_s\overline{E}$ gives a finite $\overline{H}$. From Faraday's law $\nabla \times \overline{E} = i\omega\overline{B}$, we see that a finite $\overline{B}$ field will give rise to a finite $\overline{E}$ field, violating the definition of a perfect conductor which requires $\overline{E}$ to be zero. Thus, $\overline{B}$ must be zero. However, there are no explicit mathematical requirements that $\overline{H}$ must be zero. If we let the permeability of the perfect conductor be μ_s such that $\overline{B} = \mu_s\overline{H}$, we see that $\mu_s = 0$. We can thus replace the definition of a zero $\overline{E}$ field for a perfect conductor by mathematically letting $\epsilon_s \to \infty$ and $\mu_s = 0$ when the general case of a medium with permittivity ϵ_s and permeability μ_s is solved. As a dual case, we can also define a perfect magnetic conductor by requiring $\overline{H}$ be identically zero, which leads to the mathematical limit of $\mu_s \to \infty$ and $\epsilon_s = 0$.

Problems

P7.1.1
(a) For the electromagnetic field solution of a Hertzian dipole with current moment $Il = -i\omega p$, let $\omega \to 0$ and show that $\overline{H} = 0$. Determine the electric field $\overline{E}$ of a static dipole with moment p.

(b) Consider the Rayleigh scattering of electromagnetic waves by particles of size much smaller than a wavelength, such as sunlight by air molecules. Model the particle as a small sphere of radius a and permittivity ϵ_p. When the particle is illuminated with a light wave with electric field intensity E_0 polarized in the $\hat{z}$ direction, what is the induced dipole moment p?

(c) Find the total power P_s re-radiated by the particle acting as a Hertzian dipole. Find the scattering cross section defined by $2\eta P/E_0^2$. The above result is usually used to explain why the sky is blue (but why isn't it purple?).

(d) Consider an optical fiber with cross section area A. The electromagnetic wave guided inside the fiber is scattered by the atoms and the molecules making up the fiber. Since the size of the scattering particles are much smaller than the guided light wavelength, the process can again be de-

scribed by Rayleigh scattering. Assume the guided light has intensity E_0, wavelength 10^{-6} m, particle radius $a = 10^{-10}$ m, $\mu = \mu_o$, and $\epsilon = 2\epsilon_o$. Find the guided power flow in watts and the total scattered power of a fiber with a length of 1 km. The ratio of the scattered power to the guided power gives the intrinsic loss of the fiber, a lower bound no matter how pure the fiber. Estimate, with the numbers given above, the fiber loss per kilometer (in dB/km) due to the Rayleigh scattering.

(e) The scattering of microwave by rain drops is another example of Rayleigh scattering. Assume a plane wave at a frequency of 10 GHz is incident on a rain drop of radius 1 mm which has a permittivity $\epsilon + i\sigma/\omega$ where $\sigma = \omega\epsilon$ and $\epsilon = 40\epsilon_o$. In addition to the power scattered by the particle, there is also power absorbed due to the imaginary part $i\sigma/\omega$. The absorbed power can be calculated as

$$P_{\text{diss}} = \frac{1}{2} \int dV \sigma |E_o|^2$$

Which is the primary loss of power in the microwave, scattering or absorption?

7.2   Scattering by a Conducting Cylinder

A. Exact Solution

Consider a plane wave incident upon a conducting cylinder [Fig. 7.2.1].
The incident wave is linearly polarized with electric vector $\overline{E}^i$ parallel
to the axis of the cylinder. The incident $\overline{k}$ vector is perpendicular to
the axis of the cylinder. In terms of cylindrical coordinates, we have

$$\overline{E}^i = \hat{z} E_0\, e^{-ikx} = \hat{z} E_0\, e^{-ik\rho\cos\phi} \qquad (7.2.1)$$
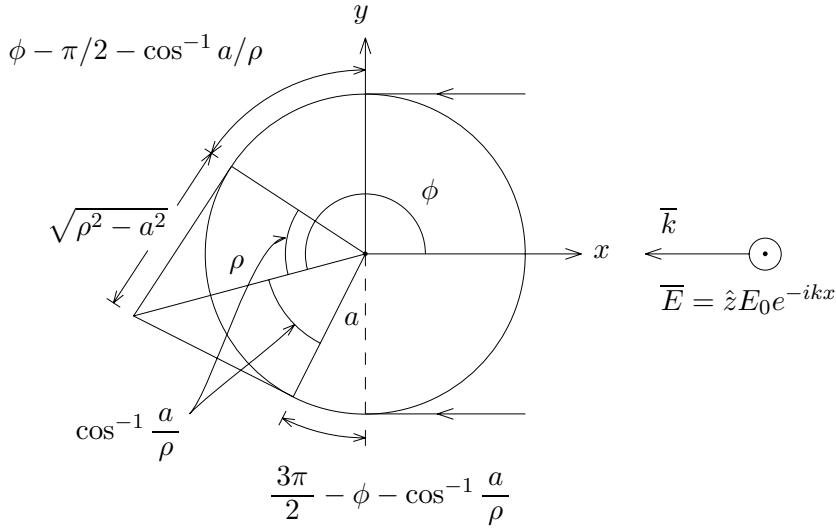
Figure 7.2.1 Scattering by a conducting cylinder.

To match boundary conditions at $\rho = a$, we transform the plane
wave solution into a superposition of cylindrical waves satisfying the
Helmholtz wave equation in cylindrical coordinates:

$$e^{-ik\rho\cos\phi} = \sum_{m=-\infty}^{\infty} a_m J_m(k\rho) e^{im\phi}$$

The constant a_m can be determined by using orthogonality relations
for $e^{im\phi}$. We multiply both sides by $e^{-in\phi}$ and integrate over ϕ from

0 to 2π. In view of the integral representation for the Bessel function,

$$J_n(k\rho) = \frac{1}{2\pi} \int_0^{2\pi} d\phi \, e^{-ik\rho \cos\phi - in\phi + in\pi/2}$$

We obtain $a_n = e^{-in\pi/2}$ and

$$e^{-ik\rho \cos\phi} = \sum_{n=-\infty}^{\infty} J_n(k\rho) e^{in\phi - in\pi/2} \qquad (7.2.2)$$

This expression is referred to as the *wave transformation*, which represents a plane wave in terms of cylindrical waves.

The scattered wave can also be expressed as a superposition of the cylindrical functions satisfying the Helmholtz wave equation. Expecting outgoing waves, we write the solution in terms of Hankel functions of the first kind. The sum of the incident wave and the scattered wave satisfies the boundary condition of a vanishing tangential electric field at $\rho = a$. We find the total solution to be $\overline{E} = \hat{z}E_z$,

$$E_z = E_0 \sum_{n=-\infty}^{\infty} \left[J_n(k\rho) - \frac{J_n(ka)}{H_n^{(1)}(ka)} H_n^{(1)}(k\rho) \right] e^{in\phi - in\pi/2} \qquad (7.2.3)$$

The first summation term represents the incident wave; the second summation term, the scattered wave. At $\rho = a$, we find from (7.2.3) $\overline{E}(\rho = a) = 0$.

In the far-field zone, $k\rho \gg 1$, we make use of the asymptotic formula for $H_n^{(1)}(k\rho)$ and find that the scattered wave takes the form

$$\overline{E}_s \approx -\hat{z}E_0 \sum_{n=-\infty}^{\infty} \sqrt{\frac{2}{i\pi k\rho}} \frac{J_n(ka)}{H_n^{(1)}(ka)} e^{ik\rho + in(\phi - \pi)}$$

We can expand this result with respect to ka:

$$\overline{E}_s = \hat{z}iE_0 \sqrt{\frac{\pi}{i2k\rho}} \left[\frac{1}{\ln ka} + (ka)^2 \cos\phi - \frac{(ka)^4}{8} \cos 2\phi + \cdots \right] e^{ik\rho}$$

$$(7.2.4)$$

Observe that this series converges rapidly when the radius of the cylinder is small compared with the wavelength, $ka \ll 1$. The first term is angle-independent and signifies that the scattered wave caused by a thin wire is isotropic. We can show, however, that for an incident wave with magnetic field $\overline{H}$ parallel to the axis of the cylinder the scattered wave will no longer be isotropic and will be angle-dependent.

B. Watson Transformation

The series in (7.2.4) converges very slowly when the radius of the cylinder is not small compared to the wavelength. In this case, we use the Watson transformation to convert the solution into a rapidly convergent series. The Watson transformation relates a residue series to a contour integration. Let the contour C in the complex ν plane be as depicted in Figure 7.2.2. We find

$$\sum_{n=-\infty}^{\infty} e^{in\phi} E_n = \frac{i}{2} \oint_C d\nu \frac{e^{i\nu(\phi-\pi)}}{\sin \nu\pi} E_\nu \qquad (7.2.5)$$
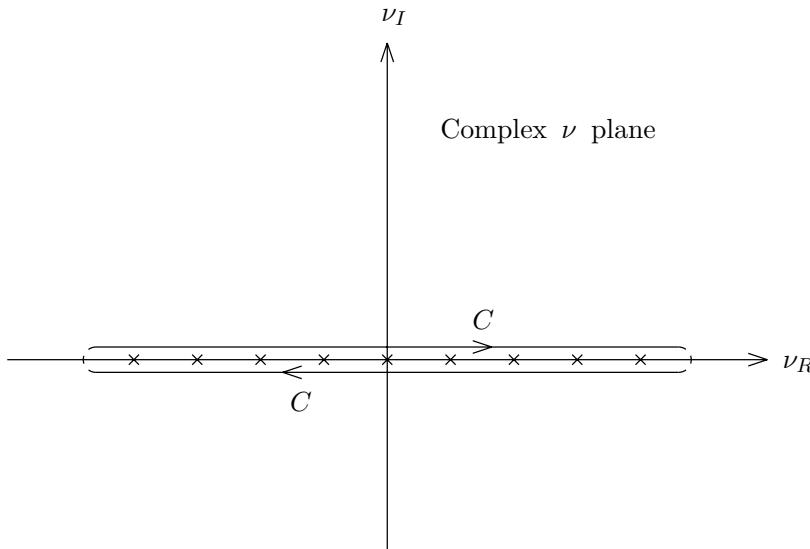
Figure 7.2.2 Watson transformation.

under the assumption that E_ν has no singularities on the real axis. The singularities from $\sin \nu\pi$ are all first-order poles located on the real axis at $\nu = 0, \pm 1, \pm 2, \ldots$ Note that because of the direction of the contour, the contour integral is equal to $-2\pi i$ times the residues of the function $e^{i\nu(\phi-\pi)} E_\nu / \sin \nu\pi$, which are $e^{in\phi} E_n / \pi$ for all integer values of n.
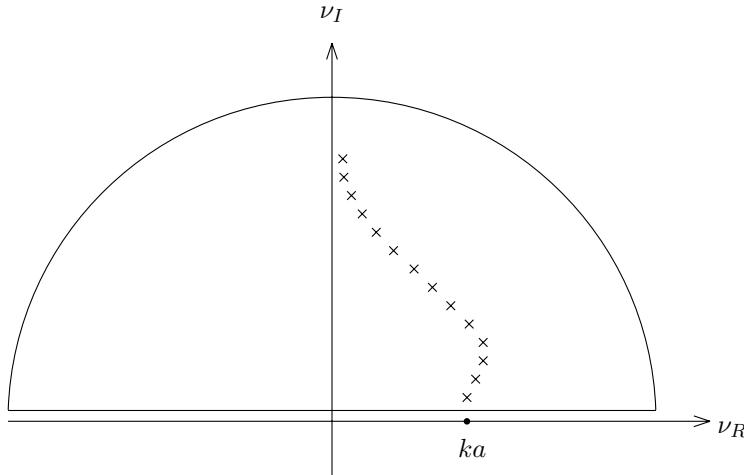
Figure 7.2.3 Integration over complex ν plane.

To make use of the Watson transformation, we identify E_n according to (7.2.3):

$$
\begin{aligned}
E_n &= \frac{E_0}{H_n^{(1)}(ka)} \left[J_n(k\rho)H_n^{(1)}(ka) - J_n(ka)H_n^{(1)}(k\rho) \right] e^{-in\pi/2} \\
&= \frac{E_0}{2H_n^{(1)}(ka)} \left[H_n^{(2)}(k\rho)H_n^{(1)}(ka) - H_n^{(2)}(ka)H_n^{(1)}(k\rho) \right] e^{-in\pi/2}
\end{aligned}
$$

(7.2.6)

The singularities of E_n are caused by the zeros of $H_n^{(1)}(ka)$, which are illustrated in Figure 7.2.3.

Using the relations

$$
\begin{aligned}
H_{-\nu}^{(1)}(\xi) &= e^{i\nu\pi} H_\nu^{(1)}(\xi) \\
H_{-\nu}^{(2)}(\xi) &= e^{-i\nu\pi} H_\nu^{(2)}(\xi)
\end{aligned}
$$

we find $E_{-\nu} = E_\nu$.

The contour integration on the right-hand side of (7.2.5) can be carried out by converting it into an integral from $-\infty$ to $+\infty$ and then closing the contour on the upper half-plane [Fig. 7.2.3]. It can be shown that integration along the large semicircle makes no contribution. The entire contribution comes from the singularities of E_ν. From (7.2.5), we find

$$
\begin{aligned}
E_z &= \sum_{n=-\infty}^{\infty} e^{in\phi} E_n = \hat{z}\frac{i}{2} \oint_C d\nu \frac{e^{i\nu(\phi-\pi)}}{\sin\nu\pi} E_\nu \\
&= \lim_{\delta\to 0}\frac{i}{2}\left\{\int_{-\infty+i\delta}^{\infty+i\delta} + \int_{\infty-i\delta}^{-\infty-i\delta}\right\} d\nu\; \frac{e^{i\nu(\phi-\pi)}}{\sin\nu\pi} E_\nu \\
&= \frac{i}{2}\int_{-\infty}^{\infty} d\nu\,\frac{1}{\sin\nu\pi}\left\{e^{i\nu(\phi-\pi)}E_\nu + e^{-i\nu(\phi-\pi)}E_{-\nu}\right\} \\
&= \frac{i}{2}\int_{-\infty}^{\infty} d\nu\,\frac{1}{\sin\nu\pi}\left\{e^{i\nu(\phi-\pi)} + e^{-i\nu(\phi-\pi)}\right\}E_\nu \\
&= \pi E_0 \sum_{n=1}^{\infty}\frac{H_{\nu_n}^{(2)}(ka)}{[\partial H_\nu^{(1)}(ka)/\partial\nu]_{\nu=\nu_n}}\frac{\cos\nu_n(\phi-\pi)e^{-i\nu_n\pi/2}}{\sin\nu_n\pi}H_{\nu_n}^{(1)}(k\rho)
\end{aligned}
$$

$$(7.2.7)$$

where ν_n denotes zeros of $H_\nu^{(1)}(ka)$. Note that the first term of E_n in (7.2.6) does not contribute because $H_n^{(1)}(ka)$ in the numerator and the denominator cancel each other.

C. Creeping Waves

The series in (7.2.7) converges rapidly when $\pi/2 < \phi < 3\pi/2$. This is due to the fact that

$$
\frac{\cos\nu_n(\phi-\pi)e^{-i\nu_n\pi/2}}{\sin\nu_n\pi} = \frac{-i\left[e^{i\nu_n(\phi-\pi/2)} + e^{i\nu_n(3\pi/2-\phi)}\right]}{1 - e^{i\nu_n 2\pi}} \qquad (7.2.8a)
$$

and ν_n takes positive imaginary values. The convergent range is in the shadow region of the cylinder. An interesting interpretation can be given to the terms involved. We use the asymptotic formula for $H_{\nu_n}^{(1)}(k\rho)$ when $k\rho > \nu_n \gg 1$:

$$
H_{\nu_n}^{(1)}(k\rho) \sim \sqrt{\frac{2}{i\pi(k^2\rho^2 - \nu_n^2)^{1/2}}}\, e^{i\left(\sqrt{k^2\rho^2-\nu_n^2}-\nu_n\cos^{-1}(\nu_n/k\rho)\right)} \qquad (7.2.8b)
$$

Note that the imaginary part of ν_n is positive and increases for increasing n. For the first few dominant terms we may approximate $\nu_n \sim ka$,

$$
\sqrt{k^2\rho^2 - \nu_n^2} \approx k\sqrt{\rho^2 - a^2}
$$

and

$$\cos^{-1}\frac{\nu_n}{k\rho} \approx \cos^{-1}\frac{a}{\rho}$$

In view of (7.2.8), the exponential dependence of (7.2.7) takes the form

$$e^{ik\sqrt{\rho^2-a^2}}\left\{e^{i\nu_n[\phi-(\pi/2)-\cos^{-1}(a/\rho)]} + e^{i\nu_n[3\pi/2-\phi-\cos^{-1}(a/\rho)]}\right\} \quad (7.2.9)$$

Now consider rays or photons incident upon the cylinder at tangent points, traveling along the surface, leaving the cylinder surface, and reaching the observation point at (ρ,ϕ) [Fig. 7.2.1]. The terms $(\phi - \pi/2 - \cos^{-1}a/\rho)$ and $(3\pi/2 - \phi - \cos^{-1}a/\rho)$ correspond to the paths of the two rays along the surface of the cylinder. The attenuation of the two rays is determined by the imaginary part of ν_n. The term $k(\rho^2 - a^2)^{1/2}$ corresponds to the path along which the rays travel after leaving the cylinder surface. The two rays recombine at ρ in the shadow region. Because of this vivid picture, they are called *creeping waves.*

In the illuminated region, $-\pi/2 < \phi < \pi/2$, a useful formula can be obtained by noting that

$$e^{i\nu(\phi-\pi)} + e^{-i\nu(\phi-\pi)} = -i2e^{i\nu\phi}\sin\nu\pi + 2e^{i\nu\pi}\cos\nu\phi$$

When this relation is used, the contour integral in (7.2.5) becomes

$$E_z = \frac{i}{2}\int_{-\infty}^{\infty}d\nu\,\frac{1}{\sin\nu\pi}\left\{e^{i\nu(\phi-\pi)} + e^{-i\nu(\phi-\pi)}\right\}E_\nu$$

$$= \int_{-\infty}^{\infty}d\nu\,e^{i\nu\phi}E_\nu + i\int_{-\infty}^{\infty}d\nu\,\frac{\cos\nu\phi}{\sin\nu\pi}e^{i\nu\pi}E_\nu \quad (7.2.10)$$

instead of (7.2.7). Upon closing the contour in the upper half-plane, the second integral is evaluated in terms of residues from $H_n^{(1)}(ka)$. Because the zeroes of $H_n^{(1)}(ka)$ have positive imaginary parts, this contribution will not be as significant as that of the first integral in the parentheses. The evaluation of the first integral is left as an exercise to the reader. The result is

$$E_z \sim E_0\left[e^{-ik\rho\cos\phi} - \sqrt{\frac{a\cos\phi/2}{2\rho}}\,e^{ik(\rho-2a\cos\phi/2)}\right] \quad (7.2.11)$$

This can be interpreted in terms of geometrical optics. The first term is the incident wave, and the second term corresponds to the ray reflected at the surface of the cylinder. Upon striking the surface at $\rho = a$, the incident ray has a phase factor $e^{-i(ka\cos\phi/2)}$. Upon reflection from the cylinder the ray reaches the observation point and gains another phase factor, $e^{-i(k\rho - ka\cos\phi/2)}$.

Problems

P7.2.1

Consider scattering by a conducting cylinder of radius a of an incident wave with magnetic field $\overline{H}$ parallel to the axis of the cylinder.

$$\overline{H}^i = \hat{z}H_o e^{-ikz} = \hat{z}H_o e^{-ik\rho\cos\phi}$$

Using wave transformation

$$\overline{H}^i = \hat{z}H_o \sum_{n=-\infty}^{\infty} J_n(k\rho)e^{in\phi - in\pi/2}$$

determine the electric field of the incident wave. The scattered wave can be expressed as a superposition of Hankel functions.

$$\overline{H}^s = \hat{z} \sum_{n=-\infty}^{\infty} A_n H_n^{(1)}(k\rho)e^{in\phi - in\pi/2}$$

Determine the electric field of the scattered wave. The tangential component of electric field should vanish at $\rho = a$. Show that

$$\overline{H}^s = -H_o\hat{z} \sum_{n=-\infty}^{\infty} \frac{J_n'(ka)}{H_n^{(1)'}(ka)} H_n^{(1)}(k\rho)e^{in\phi - in\pi/2}$$

For $ka \ll 1$, use small argument approximation of Bessel's function and Hankel's function as $x \to 0$

$$\frac{J_o'(x)}{H_o^{(1)'}(x)} = 0$$

$$\frac{J_n'(x)}{H_n^{(1)'}(x)} = i\frac{\pi x^{2n}}{2^{2n}(n-1)!n!}$$

to find the scattered field in the far field for $ka \ll 1$.

7.3   Scattering by Periodic Rough Surfaces

A. Scattering by Periodic Corrugated Conducting Surfaces

Consider a perfectly conducting surface that is corrugated periodically with rectangular grooves [Fig. 7.3.1] that are infinite in the $\hat{y}$ direction and have width w and depth d. The period of the corrugation is p. A plane wave with incident wave vector $\overline{k} = \hat{x}k_x - \hat{z}k_z$ is scattered by the rough surface. The scattered wave can be expanded in terms of Floquet modes that are characteristic waves for periodic structures. For an incident TM wave,

$$\overline{H} = \hat{y}H_0 \left\{ e^{ik_x x - ik_z z} + \sum_{n=-\infty}^{\infty} R_n\, e^{i(k_x + 2n\pi/p)x + ik_{zn}z} \right\} \qquad (7.3.1a)$$

where

$$k_{zn} = \sqrt{k^2 - (k_x + 2n\pi/p)^2} \qquad (7.3.1b)$$
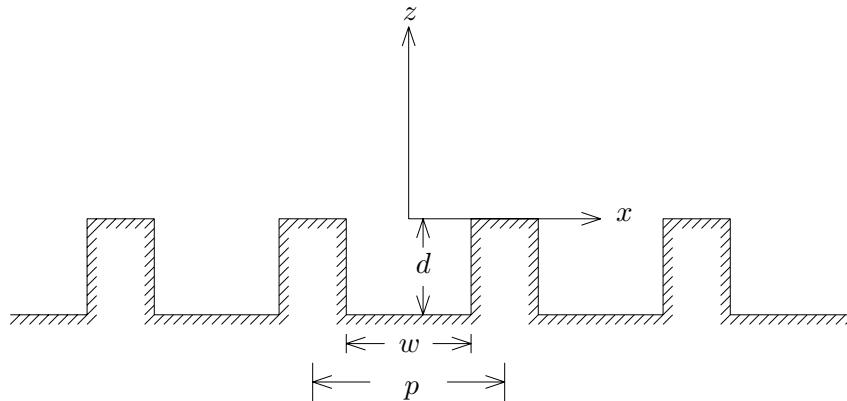
Figure 7.3.1 Scattering by a periodic corrugated surface.

The first term in $(7.3.1a)$ denotes the incident wave. The summation term represents a superposition of the Floquet modes. The electric field follows from the Maxwell equation

$$\overline{E} = \frac{i}{\omega\epsilon}\nabla \times \overline{H} \qquad (7.3.2)$$

We observe that for $k^2 < [k_x + (2n\pi/p)]^2$ the Floquet modes are essentially evanescent waves that decay exponentially in the $\hat{z}$ direction. The $n = 0$ mode corresponds to the specularly reflected wave.

Within the grooves the field can be expanded in terms of waveguide modes:

$$\overline{H} = \hat{y} H_0 \sum_{m=0}^{\infty} G_m \cos \frac{m\pi}{w}(x + w/2) \frac{\cos k_{zm}^{(2)}(z + d)}{\cos k_{zm}^{(2)} d} \quad z < 0 \quad (7.3.3a)$$

where

$$k_{zm}^{(2)} = \sqrt{k^2 - (2m\pi/w)^2} \quad\quad\quad (7.3.3b)$$

The electric field is derived from the magnetic field $\overline{H}$ by using the Maxwell equation

$$\overline{E} = \frac{i}{\omega\epsilon}\nabla \times \overline{H} = \frac{i}{\omega\epsilon}\left\{\hat{z}\frac{\partial}{\partial x}H_y - \hat{x}\frac{\partial}{\partial z}H_y\right\}$$

$$= \hat{x}\frac{ik_{zm}^{(2)}}{\omega\epsilon}H_0 \sum_{m=0}^{\infty} G_m \cos \frac{m\pi}{w}(x + w/2)\frac{\sin k_{zm}^{(2)}(z + d)}{\cos k_{zm}^{(2)} d}$$

$$- \hat{z}\frac{im\pi}{\omega\epsilon w}H_0 \sum_{m=0}^{\infty} G_m \sin \frac{m\pi}{w}(x + w/2)\frac{\cos k_{zm}^{(2)}(z + d)}{\cos k_{zm}^{(2)} d} \quad (7.3.4)$$

It is straightforward to show that the fields in the grooves indeed satisfy the boundary conditions of tangential $\overline{E}$ fields vanishing at the perfectly conducting surfaces.

Consider the special case of normal incidence when $k_x = 0$. At $z = 0$, the boundary conditions require that the tangential magnetic field be continuous for $-w/2 \le x \le w/2$,

$$1 + \sum_{n=-\infty}^{\infty} R_n \, e^{i2n\pi x/p} = \sum_{m=0}^{\infty} G_m \cos \frac{m\pi}{w}(x + w/2) \quad\quad (7.3.5a)$$

The tangential electric field is also continuous for $-w/2 \le x \le w/2$

$$1 - \sum_{n=-\infty}^{\infty} \frac{k_{zn}}{k_z} R_n \, e^{i2n\pi x/p} = -\sum_{m=0}^{\infty} i\frac{k_{zm}^{(2)}}{k_z}G_m \tan\left(k_{zm}^{(2)}d\right)\cos \frac{m\pi(x + w/2)}{w}$$

$$(7.3.5b)$$

The tangential electric field vanishes for $w/2 \leq |x| \leq p/2$,

$$1 - \sum_{n=-\infty}^{\infty} \frac{k_{zn}}{k_z} R_n\, e^{i2n\pi x/p} = 0 \qquad (7.3.5c)$$

The task is to determine R_n and G_m from (7.3.5). We use the orthogonality properties for cosine functions by multiplying both sides of (7.3.5a) by $\cos[m\pi(x + w/2)/w]$ and integrating over the interval $-w/2 \leq x \leq w/2$. We obtain

$$[1 + \delta_{m0}]\frac{w}{2}G_m = \int_{-w/2}^{w/2} dx\, \cos\frac{m\pi(x + w/2)}{w}\left[1 + \sum_{n=-\infty}^{\infty} R_n e^{i2n\pi x/p}\right] \qquad (7.3.6)$$

We multiply (7.3.5b) by $e^{-i2n\pi x/p}$ and integrate over the interval $-p/2 \leq x \leq p/2$. By virtue of (7.3.5c), we know the right-hand side is nonzero only in the interval $-w/2 \leq x \leq w/2$. It follows that

$$p\left[\delta_{n0} - \frac{k_{zn}}{k_z}R_n\right] = -\,i\int_{-w/2}^{w/2} dx\, e^{-2n\pi x/p}$$

$$\cdot \sum_{m=0}^{\infty} \frac{k_{zm}^{(2)}}{k_z}G_m \tan k_{zm}^{(2)}d\,\cos\frac{m\pi(x + w/2)}{w} \qquad (7.3.7)$$

We define

$$P_{mn} = \int_{-w/2}^{w/2} dx\, e^{i2m\pi x/p}\cos\frac{n\pi(x + w/2)}{w}$$

$$= \begin{cases} \dfrac{4m\pi/p}{(2m\pi/p)^2 - (n\pi/w)^2}\sin\dfrac{m\pi w}{p} & n\text{: even} \\[3mm] i\dfrac{4m\pi/p}{(2m\pi/p)^2 - (n\pi/w)^2}\cos\dfrac{m\pi w}{p} & n\text{: odd} \\[3mm] w\delta_{0n} & n = 0 \end{cases} \qquad (7.3.8)$$

Equations (7.3.6) and (7.3.7) can be written as

$$[1 + \delta_{m0}]\frac{w}{2}G_m = P_{0m} + \sum_{n=-\infty}^{\infty} P_{nm}R_n \qquad (7.3.9)$$

$$R_n = \left\{\frac{k_z}{k_{zn}}\delta_{n0} + \sum_{m=0}^{\infty} \frac{ik_{zm}^{(2)}}{pk_{zn}}\tan\left(k_{zm}^{(2)}d\right)P_{nm}^*G_m\right\} \qquad (7.3.10)$$

This represents a set of matrix equations to be solved for R_n. Substituting (7.3.10) into (7.3.9), we find

$$\sum_{l=0}^{\infty} \left[(1 + \delta_{l0}) \frac{w}{2} \delta_{ml} - i \tan \left(k_{zl}^{(2)} d \right) Q_{ml} \right] G_l = 2P_{0m} \qquad (7.3.11)$$

where

$$Q_{ml} = \sum_{n=-\infty}^{\infty} \frac{k_{zl}^{(2)}}{p k_{zn}} P_{nm} P_{nl}^*$$

$$= \begin{cases} \dfrac{1}{p} \left(P_{0m} P_{0l}^* + 2 \sum_{n=1}^{\infty} \dfrac{k_{zl}^{(2)}}{k_{zn}} P_{nm} P_{nl}^* \right) & m + l = \text{even} \\ 0 & m + l = \text{odd} \end{cases} \qquad (7.3.12)$$

The mode amplitudes G_l are solved by straightforward matrix inversion. The number of groove modes needed to calculate the reflection coefficient R_n is determined by the width of the grooves w.

For sufficiently narrow grooves, $kw \ll 1$. We use the lowest mode amplitudes G_0 to calculate R_n. With $m = 0$, (7.3.6) and (7.3.7) become

$$G_0 = 1 + \sum_{n=-\infty}^{\infty} R_n \frac{p}{n\pi w} \sin \frac{n\pi w}{p} \qquad (7.3.13)$$

and

$$R_n = \frac{k_z}{k_{zn}} \delta_{n0} + i \frac{k}{k_{zn}} \frac{\tan kd}{n\pi} \sin \left(\frac{n\pi w}{p} \right) G_0 \qquad (7.3.14)$$

Substituting (7.3.14) into (7.3.13), we obtain

$$G_0 = 2 \left[1 - i \sum_{n=-\infty}^{\infty} \frac{kp \tan kd}{(n\pi)^2 k_{zn} w} \sin^2 \frac{n\pi w}{p} \right]^{-1} \qquad (7.3.15)$$

Substituting back into (7.3.14) we find the reflection coefficients R_n.

This mode-matching technique is often useful in solving problems involving periodic structures. The use of Floquet modes also greatly facilitates the discussions of scattered waves. As another example, consider a similar structure made of parallel conducting plates of widths $(p - w)$ and separated by a distance w. The conducting plane at
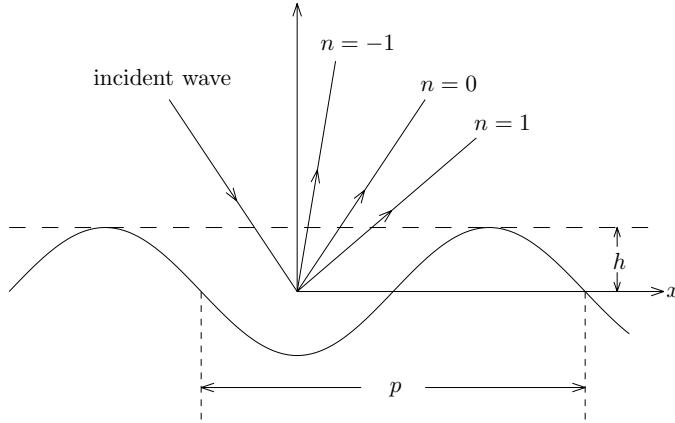
Figure 7.3.2 Scattering by a periodic rough surface.

$z = -d$ in Figure 7.3.1 is now removed. For an incident TM wave with the magnetic field in the $\hat{y}$ direction, the TEM waveguide mode in the parallel-plate regions is excited. The reflectivity is always less than unity. For an incident TE wave with electric field $\overline{E}$ in the $\hat{y}$ direction, the excited guided waves in the plate regions are all TE modes. Thus, if the plate separation is such that $kw < \pi$, all guided-wave modes are evanescent and all the incident power will be scattered.

B. Scattering by Periodic Dielectric Surfaces

Consider a plane wave incident on a periodic surface described by $f(x) = f(x + p)$ where p denotes the period of the surface in the $\hat{x}$ direction [Fig. 7.3.2]. Let the incident field be

$$\overline{E}_i = \hat{y} E_{iy}(\overline{r}) = \hat{y} E_o \, e^{i\overline{k}_i \cdot \overline{r}} \tag{7.3.16}$$

where $\overline{k}_i = \hat{x} k_{ix} - \hat{z} k_{iz}$ is the incident wave vector.

We make use of the scalar formulation of the Huygens' principle to derive the extinction theorem for the solution of the problem. Using the scalar Green's function in region 0, we have the total electric field in regions 0 and 1 as follows:

$$E_{iy}(\overline{r}) + \iint_{-\infty}^{\infty} dS' \left\{ E_y(\overline{r}')\hat{n} \cdot \nabla'_s \, g(\overline{r}, \overline{r}') - g(\overline{r}, \overline{r}')\hat{n} \cdot \nabla'_s E_y(\overline{r}') \right\}$$
$$= \begin{cases} E_y(\overline{r}) & z > f(x) \\ 0 & z < f(x) \end{cases} \tag{7.3.17}$$

where

$$dS' \, \hat{n} = \left[\hat{z} - \hat{x} \frac{d}{dx'} f(x') \right] dx' \qquad (7.3.18)$$

Equation (7.3.17) states that the total field in region 0 is equal to the sum of the incident field and the scattered field produced by the induced surface currents. The sum of the incident field and the scattered field in region 1 is equal to zero on account of Huygens' principle. This is referred to as the *extinction theorem.*

The surface integral in (7.3.17) is over an infinite domain. However, it can be condensed into a single period. First we recognize that the surface fields have periodic properties, e.g.,

$$E_y(\overline{r}' + \hat{x}np) = E_y(\overline{r}')e^{ik_{ix}np} \qquad (7.3.19)$$

From the theory of Fourier series, we can represent a periodic train of Dirac delta functions by an infinite summation of complex exponentials

$$\sum_{m=-\infty}^{\infty} e^{i(k_{ix}-k_x)mp} = \sum_{m=-\infty}^{\infty} \frac{2\pi}{p} \delta\left(k_x - k_{ix} - \frac{2m\pi}{p}\right) \qquad (7.3.20)$$

The Green's function for region 0 is

$$g(\overline{r}, \overline{r}') = \frac{i}{4} H_0^{(1)}(k|\overline{r} - \overline{r}'|) = \frac{i}{4\pi} \int_{-\infty}^{\infty} dk_x \frac{1}{k_z} e^{ik_x(x-x')+ik_z|z-z'|} \qquad (7.3.21)$$

To reduce the surface integral in (7.3.17) to only one period, we use the following identity derived from (7.3.20) and (7.3.21), with the translation phase factor $e^{ik_{ix}mp}$ in (7.3.19) included in the Green's function,

$$\sum_{m=-\infty}^{\infty} g(\overline{r}, \overline{r}' + \hat{x}mp)e^{ik_{ix}mp}$$

$$= \frac{i}{4\pi} \int_{-\infty}^{\infty} dk_x \frac{1}{k_z} e^{ik_x(x-x')+ik_z|z-z'|} \sum_m e^{i(k_{ix}-k_x)mp}$$

$$= g_p(\overline{r}, \overline{r}') = \frac{i}{2p} \sum_n \frac{1}{k_{zn}} e^{ik_{xn}(x-x')+ik_{zn}|z-z'|} \qquad (7.3.22)$$

where

$$k_{xn} = k_{ix} + n\frac{2\pi}{p} \qquad (7.3.23a)$$

$$k_{zn} = (k^2 - k_{xn}^2)^{1/2} \qquad (7.3.23b)$$

When k_{xp}^2 is larger than k^2, we choose $k_{zn} = i(k_{xn}^2 - k^2)^{1/2}$. Making use of (7.3.19) and (7.3.22) in (7.3.17) we obtain

$$E_{iy}(\overline{r}) + \int_p dS' \left\{ E_y(\overline{r}')\hat{n} \cdot \nabla'_s g_p(\overline{r}, \overline{r}') - g_p(\overline{r}, \overline{r}')\hat{n} \cdot \nabla'_s E_y(\overline{r}') \right\}$$

$$= \begin{cases} E_y(\overline{r}) & z > f(x) \\ 0 & z < f(x) \end{cases} \qquad (7.3.24)$$

This integration now only extends over a single period.

In terms of the Green's function (7.3.24) for region 1, we find, similar to (7.3.22) and (7.3.24),

$$\sum_{m=-\infty}^{\infty} g_1(\overline{r}, \overline{r}' + \hat{x}mp)e^{ik_{ix}mp} = g_{1p}(\overline{r}, \overline{r}')$$

$$= \frac{i}{2p} \sum_n \frac{1}{k_{1zn}} e^{ik_{xn}(x-x')+ik_{1zn}|z-z'|} \qquad (7.3.25)$$

where

$$k_{1zn} = (k_1^2 - k_{xn}^2)^{1/2} \qquad (7.3.26)$$
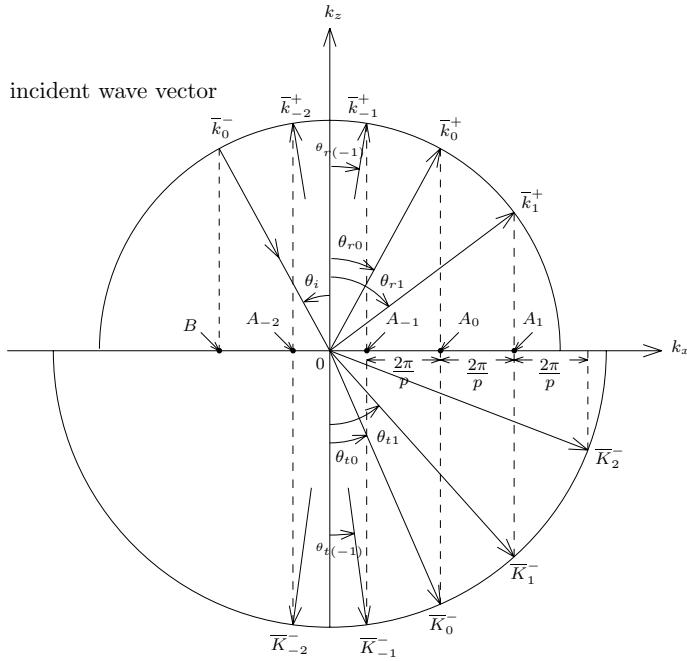
and

$$-\int_p dS' \left\{ E_{1y}(\overline{r}')\hat{n} \cdot \nabla'_s g_{1p}(\overline{r}, \overline{r}') - g_{1p}(\overline{r}, \overline{r}')\hat{n} \cdot \nabla'_s E_{1y}(\overline{r}') \right\}$$

$$= \begin{cases} 0 & z > f(x) \\ E_{1y}(\overline{r}) & z < f(x) \end{cases} \qquad (7.3.27)$$

Notice that the minus sign in front of the integral signifies the fact that the unit vector $\hat{n}$ is the surface normal pointing into region 0 and Huygens' principle requires the surface normal to point outward.

From the representations of the periodic Green's functions in (7.3.22) and (7.3.25), we see that the scattered waves are propagating in discrete Floquet modes, with directions determined by (7.3.23) and (7.3.26). Defining θ_{rn} as the angle of the n th-order reflected Floquet mode and θ_{tn} as the angle of the n th-order transmitted Floquet mode, we find

$$k \sin \theta_{rn} = k_{xn} = k \sin \theta_i + n\frac{2\pi}{p} \qquad (7.3.28a)$$

$$k_1 \sin \theta_{tn} = k_{txn} = k \sin \theta_i + n\frac{2\pi}{p} \qquad (7.3.28b)$$

Figure 7.3.3 k space diagram.

The phase-matching results of (7.3.28) are depicted in Figure 7.3.3. Given the incident wave vector $\overline{k}_0^-$ as shown in the figure, the zeroth order modes of the reflected wave and the transmitted wave are the same as those for a planar surface.

Equation (7.3.24) can be simplified by allowing z to be larger than f_{max} or smaller than f_{min} where f_{max} and f_{min} are respectively the maximum and minimum values of the surface profile $f(x)$. For $z > f_{max}$, $|z - z'|$ becomes $z - z'$ and for $z < f_{min}$, $|z - z'|$ becomes $-(z - z')$. Thus

$$E_y(\overline{r}) = E_{iy}(\overline{r}) + \sum_n b_n \frac{e^{i\overline{k}_n^+ \cdot \overline{r}}}{\sqrt{k_{zn}}} \qquad z > f_{max} \qquad (7.3.29a)$$

$$0 = E_{iy}(\overline{r}) - \sum_n a_n \frac{e^{i\overline{k}_n^- \cdot \overline{r}}}{\sqrt{k_{zn}}} \qquad z < f_{min} \qquad (7.3.29b)$$

where

$$\overline{k}_n^\pm = \hat{x} k_{xn} \pm \hat{z} k_{zn} \qquad (7.3.30)$$

are the wave vectors of the Floquet modes. The coefficients b_n and a_n are related to the surface field by the following integrals:

$$b_n = \frac{i}{2p} \int_p dS' \left\{ E_y(\overline{r}')\hat{n} \cdot \nabla'_s \frac{e^{-i\overline{k}_n^+ \cdot \overline{r}'}}{\sqrt{k_{zn}}} - \frac{e^{-i\overline{k}_n^+ \cdot \overline{r}'}}{\sqrt{k_{zn}}} \hat{n} \cdot \nabla'_s E_y(\overline{r}') \right\} \quad (7.3.31)$$

$$a_n = -\frac{i}{2p} \int_p dS' \left\{ E_y(\overline{r}')\hat{n} \cdot \nabla'_s \frac{e^{-i\overline{k}_n^- \cdot \overline{r}'}}{\sqrt{k_{zn}}} - \frac{e^{-i\overline{k}_n^- \cdot \overline{r}'}}{\sqrt{k_{zn}}} \hat{n} \cdot \nabla'_s E_y(\overline{r}') \right\} \quad (7.3.32)$$

Similarly, making use of (7.3.27) we find

$$0 = -\sum_n B_n \frac{e^{i\overline{k}_{1n}^+ \cdot \overline{r}}}{\sqrt{k_{1zn}}} \qquad\qquad z > f_{max} \qquad (7.3.33a)$$

$$E_{1y}(\overline{r}) = \sum_n A_n \frac{e^{i\overline{k}_{1n}^- \cdot \overline{r}}}{\sqrt{k_{1zn}}} \qquad\qquad z < f_{min} \qquad (7.3.33b)$$

where
$$\overline{k}_{1n}^\pm = \hat{x} k_{1xn} \pm \hat{z} k_{1zn} \qquad\qquad (7.3.34)$$

$$B_n = \frac{i}{2p} \int_p dS' \left\{ E_{1y}(\overline{r}')\hat{n} \cdot \nabla'_s \frac{e^{-i\overline{k}_{1n}^+ \cdot \overline{r}'}}{\sqrt{k_{1zn}}} - \frac{e^{-i\overline{k}_{1n}^+ \cdot \overline{r}'}}{\sqrt{k_{1zn}}} \hat{n} \cdot \nabla'_s E_{1y}(\overline{r}') \right\}$$
$$(7.3.35)$$

$$A_n = -\frac{i}{2p} \int_p dS' \left\{ E_{1y}(\overline{r}')\hat{n} \cdot \nabla'_s \frac{e^{-i\overline{k}_{1n}^- \cdot \overline{r}'}}{\sqrt{k_{1zn}}} - \frac{e^{-i\overline{k}_{1n}^- \cdot \overline{r}'}}{\sqrt{k_{1zn}}} \hat{n} \cdot \nabla'_s E_{1y}(\overline{r}') \right\}$$
$$(7.3.36)$$

Equations (7.3.29b) and (7.3.33a) are referred to as the *extended boundary conditions* (EBC). By letting the observation point be outside the trough regions of the periodic surface, we find from (7.3.29b)

$$E_{iy}(\overline{r}) = \sum_n a_n \frac{e^{i\overline{k}_n^- \cdot \overline{r}}}{\sqrt{k_{zn}}} \qquad\qquad z < f_{min}$$

which gives
$$a_n = \delta_{no}\sqrt{k_z} E_o \qquad\qquad (7.3.37)$$

and from (7.3.33a)
$$B_n = 0 \qquad\qquad (7.3.38)$$

Knowing a_n and B_n, we can solve (7.3.32) and (7.3.35) for the unknown surface fields which can then be used to determine the scattered field amplitudes b_n and A_n from (7.3.31) and (7.3.36).

We now apply the boundary conditions for the tangential fields on the periodic surface S'. The continuity of tangential electric fields requires

$$E_y\left(x, z = f(x)\right) = E_{1y}\left(x, z = f(x)\right) \qquad (7.3.39)$$

and the continuity of tangential magnetic fields requires

$$\hat{n} \times \nabla_s \times \hat{y} E_y = \hat{n} \times \nabla_s \times \hat{y} E_{1y}$$

or equivalently

$$\hat{n} \cdot \nabla_s E_y = \hat{n} \cdot \nabla_s E_{1y} \qquad (7.3.40)$$

where

$$\hat{n} = \frac{\hat{z} - \hat{x}\dfrac{df}{dx}}{\sqrt{1 + (df/dx)^2}}$$

$$\hat{n}dS = dx\left[\hat{z} - \hat{x}\frac{df(x)}{dx}\right]$$

Noting that the surface fields are dependent on x only, we express the unknown fields in terms of Fourier series expansions as follows:

$$E_y(\overline{r}) = \sum_n 2\alpha_n^s\, e^{i(k_{ix}+nK)x} \qquad (7.3.41)$$

$$dS\,\hat{n} \cdot \nabla_s E_y(\overline{r}) = -idx \sum 2\beta_n^s\, e^{i(k_{ix}+nK)x} \qquad (7.3.42)$$

where $K = 2\pi/p$. This choice of basis functions is appropriate because the surface fields when multiplied by the term $\exp(-ik_{ix}x)$ are periodic functions of x [Chuang and Kong, 1983].

Substituting (7.3.41) and (7.3.42) into (7.3.32) and defining $Q_{D1}^{\pm}$ and $Q_{N1}^{\pm}$ as the Dirichlet and Neumann matrices with elements

$$\left[\overline{\overline{Q}}_D^{\pm}\right]_{mn} = \pm\frac{1}{p}\int_p dx\,\frac{e^{-ik_m^{\pm}\cdot\overline{r}}}{\sqrt{k_{zm}}}e^{i[k_{ix}+nK]x}$$

$$= \pm\frac{1}{p\sqrt{k_{zm}}}\int_p dx\, e^{-i[(m-n)Kx\pm k_{zm}f(x)]} \qquad (7.3.43a)$$

$$\left[\overline{\overline{Q}}_N^\pm\right]_{mn} = \pm\frac{(-i)}{p}\int_p dS\,\hat{n}\cdot\left(\nabla_s\frac{e^{-ik_m^\pm\cdot\bar{r}}}{\sqrt{k_{zm}}}\right)e^{i[k_{ix}+nK]x}$$

$$= \pm\frac{(-1)}{p\sqrt{k_{zm}}}\int_p dx\left[k_{xm}\frac{df}{dx}\mp k_{zm}\right]e^{-i[(m-n)Kx\pm k_{zm}f(x)]}$$

$$= \pm\frac{(-1)}{p\sqrt{k_{zm}}}\int_p dx\left[\frac{k_{xm}(m-n)K}{k_{zm}}\mp k_{zm}\right]e^{-i[(m-n)Kx\pm k_{zm}f(x)]}$$

$$= \pm\frac{(-k^2+k_{xm}k_{xn})}{k_{zm}p\sqrt{k_{zm}}}\int_p dx\,e^{-i[(m-n)Kx\pm k_{zm}f(x)]} \qquad (7.3.43b)$$

we obtain the matrix equation

$$\overline{a} = -\overline{\overline{Q}}_D^-\cdot\overline{\beta}^s - \overline{\overline{Q}}_N^-\cdot\overline{\alpha}^s \qquad (7.3.44)$$

Similarly, (7.3.35) leads to the matrix equation

$$-\overline{\overline{Q}}_{D1}^+\cdot\overline{\beta}^s - \overline{\overline{Q}}_{N1}^+\cdot\overline{\alpha}^s = \overline{B} = 0 \qquad (7.3.45)$$

where

$$\left[Q_{D1}^\pm\right]_{mn} = \pm\frac{1}{p\sqrt{k_{1zm}}}\int_p dx\,e^{-i[(m-n)Kx\pm k_{1zm}f(x)]} \qquad (7.3.46a)$$

$$\left[Q_{N1}^\pm\right]_{mn} = \pm\frac{(-k_1^2+k_{1xm}k_{1xn})}{k_{1zm}\sqrt{k_{1zm}}\,p}\int_p dx\,e^{-i[(m-n)Kx\pm k_{1zm}f(x)]} \quad (7.3.46b)$$

Combining (7.3.45) and (7.3.46), we can determine $\overline{\alpha}^s$ and $\overline{\beta}^s$ from the following matrix equation

$$-\begin{bmatrix}\overline{\overline{Q}}_N^- & \overline{\overline{Q}}_D^- \\ \overline{\overline{Q}}_{N1}^+ & \overline{\overline{Q}}_{D1}^+\end{bmatrix}\begin{bmatrix}\overline{\alpha}^s \\ \overline{\beta}^s\end{bmatrix} = \begin{bmatrix}\overline{a} \\ 0\end{bmatrix} \qquad (7.3.47)$$

Notice that $\overline{a}$ on the right-hand side has been calculated and is given by (7.3.37).

After $\overline{\alpha}^s$ and $\overline{\beta}^s$ are determined from (7.3.47), the scattered field amplitudes can be obtained from (7.3.31) and (7.3.36) with the Q matrices defined in (7.3.43) and (7.3.46). The upward-propagating field amplitudes are

$$\overline{b} = -\overline{\overline{Q}}_D^+\cdot\overline{\beta}^s - \overline{\overline{Q}}_N^+\cdot\overline{\alpha}^s \qquad (7.3.48)$$

The downward-propagating field amplitudes are

$$\overline{A} = -\overline{\overline{Q}}_{D1}^{-} \cdot \overline{\beta}^s - \overline{\overline{Q}}_{N1}^{-} \cdot \overline{\alpha}^s \qquad (7.3.49)$$

Thus the problem of the scattering of a TE wave incident upon a periodic dielectric medium is now completely solved. The solution for a TM incident wave can be carried out in a similar manner.

For a sinusoidal rough surface with

$$f(x) = -h \cos\left(\frac{2\pi}{p}x\right) \qquad (7.3.50)$$

the $\overline{\overline{Q}}^{\pm}$ matrices can be calculated by carrying out the integrations in (7.3.43) and (7.3.47). Expressed in terms of Bessel functions, we have

$$\left[\overline{\overline{Q}}_D^{\pm}\right]_{mn} = \pm\frac{1}{\sqrt{k_{zm}}}(\pm i)^{|m-n|} J_{|m-n|}(k_{zm}h) \qquad (7.3.51a)$$

$$\left[\overline{\overline{Q}}_N^{\pm}\right]_{mn} = \left(\frac{-k^2 + k_{xm}k_{xn}}{k_{zm}\sqrt{k_{zm}}}\right)(\pm i)^{|m-n|} J_{|m-n|}(k_{zm}h) \qquad (7.3.51b)$$

$$\left[\overline{\overline{Q}}_{D1}^{\pm}\right]_{mn} = \pm\frac{1}{\sqrt{k_{1zm}}}(\pm i)^{|m-n|} J_{|m-n|}(k_{1zm}h) \qquad (7.3.51c)$$

$$\left[\overline{\overline{Q}}_{N1}^{\pm}\right]_{mn} = \frac{(-k_1^2 + k_{xm}k_{xn})}{k_{1zm}\sqrt{k_{1zm}}}(\pm i)^{|m-n|} J_{|m-n|}(k_{1zm}h) \qquad (7.3.51d)$$

For a general profile of a periodic surface defined by a single-valued function $z = f(x)$, the EBC method can be applied by numerically integrating (7.3.43) and (7.3.46) to calculate the elements of the $\overline{\overline{Q}}^{\pm}$ matrices. In practice, the matrices used may become ill-conditioned when the surface corrugation is deep or when the corrugation depth divided by the period is large.

Problems

P7.3.1

Calculate $\overline{\overline{Q}}_D^{\pm}$, $\overline{\overline{Q}}_N^{\pm}$, $\overline{\overline{Q}}_{D1}^{\pm}$, and $\overline{\overline{Q}}_{N1}^{\pm}$ for the following periodic surface height:

$$f(x) = \begin{cases} h/2 & 0 \le x < p/2 \\ -h/2 & p/2 \le x < p \end{cases}$$

7.4   Scattering by Random Rough Surfaces

Two analytical approaches have been applied to the study of the scattering of electromagnetic waves by random rough surfaces. In the Kirchhoff approximation (KA), the fields at any point on the surface are approximated by the fields that would be present on the tangent plane at that point. Thus the tangent plane approximation requires a large radius of curvature relative to the incident wavelength at every point on the surface. In the small perturbation method (SPM) the surface variations are assumed to be much smaller than the incident wavelength and the slopes of the rough surface are relatively small.
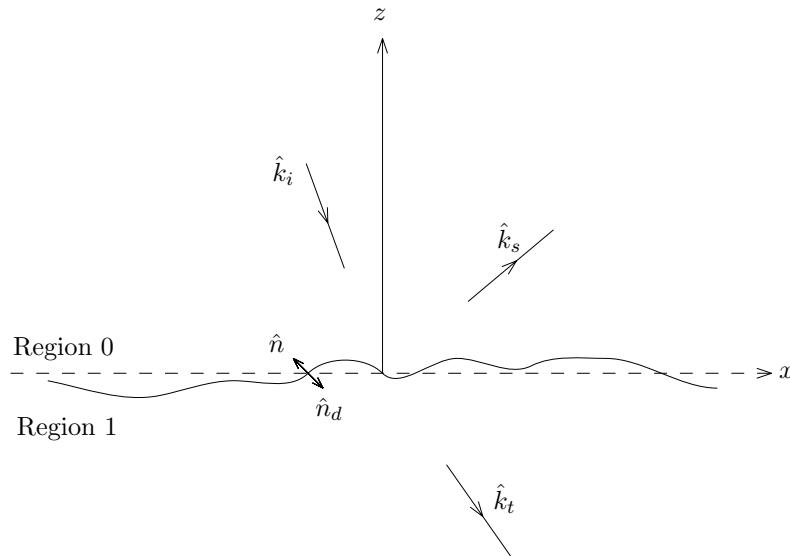
Figure 7.4.1 Scattering by a random rough surface.

Consider a plane wave incident upon a random rough surface [Fig. 7.4.1]. The electric field of the incident wave is given by

$$\overline{E}_i = \hat{e}_i\, E_o\, e^{i\overline{k}_i \cdot \overline{r}}$$

where $\overline{k}_i$ is the incident wave vector and $\hat{e}_i$ the polarization of the electric field vector. The rough surface is characterized by a random height distribution $z = f(\overline{r}_\perp)$ where $f(\overline{r}_\perp)$ is a Gaussian random variable with zero mean, $< f(\overline{r}_\perp) >= 0$. From Huygens' principle,

which expresses the field at an observation point in terms of fields at the boundary surface, the following expressions are obtained for the scattered fields in region 0 and the transmitted fields in region 1:

$$\overline{E}_s(\overline{r}) = \iint_{S'} dS' \left\{ i\omega\mu_o \overline{\overline{G}}(\overline{r},\overline{r}') \cdot [\hat{n} \times \overline{H}(\overline{r}')] \right.$$
$$\left. + \nabla \times \overline{\overline{G}}(\overline{r},\overline{r}') \cdot [\hat{n} \times \overline{E}(\overline{r}')] \right\} \tag{7.4.1a}$$

$$\overline{E}_t(\overline{r}) = \iint_{S'} dS' \left\{ i\omega\mu_o \overline{\overline{G}}_1(\overline{r},\overline{r}') \cdot [\hat{n}_d \times \overline{H}(\overline{r}')] \right.$$
$$\left. + \nabla \times \overline{\overline{G}}_1(\overline{r},\overline{r}') \cdot [\hat{n}_d \times \overline{E}(\overline{r}')] \right\} \tag{7.4.1b}$$

where S' denotes the rough surface on which the surface integration is to be carried out, $\hat{n}$ and $\hat{n}_d$ are the unit vectors normal to the rough surface and pointing into the reflected and transmitted regions [Fig. 7.4.1]. The dyadic Green's function for the homogeneous space of regions 0 and 1, $\overline{\overline{G}}(\overline{r},\overline{r}')$ and $\overline{\overline{G}}_1(\overline{r},\overline{r}')$, are

$$\overline{\overline{G}}(\overline{r},\overline{r}') = \left[\overline{\overline{I}} + \frac{1}{k^2}\nabla\nabla\right] \frac{e^{ik|\overline{r}-\overline{r}'|}}{4\pi |\overline{r} - \overline{r}'|} \tag{7.4.2a}$$

and

$$\overline{\overline{G}}_1(\overline{r},\overline{r}') = \left[\overline{\overline{I}} + \frac{1}{k_1^2}\nabla\nabla\right] \frac{e^{ik_1|\overline{r}-\overline{r}'|}}{4\pi |\overline{r} - \overline{r}'|} \tag{7.4.2b}$$

where $k = \omega\sqrt{\mu_o\epsilon_o}$ and $k_1 = \omega\sqrt{\mu_o\epsilon_1}$. If the observation point is in the far field region, then the dyadic Green's functions can be simplified to

$$\overline{\overline{G}}(\overline{r},\overline{r}') \simeq (\overline{\overline{I}} - \hat{k}_s\hat{k}_s) \frac{e^{ikr}}{4\pi r} \exp(-i\overline{k}_s \cdot \overline{r}') \tag{7.4.3}$$

$$\overline{\overline{G}}_1(\overline{r},\overline{r}') \simeq (\overline{\overline{I}} - \hat{k}_t\hat{k}_t) \frac{e^{ik_1r}}{4\pi r} \exp(-i\overline{k}_t \cdot \overline{r}') \tag{7.4.4}$$

where $\hat{k}_s$ and $\hat{k}_t$ denote the scattered and the transmitted directions in regions 0 and 1.

Substituting (7.4.3) and (7.4.4) into the diffraction integral (7.4.1), we obtain, in the reflected direction $\hat{k}_s$ and the transmitted direction $\hat{k}_t$,

$$\overline{E}_s(\overline{r}) = \frac{ik\, e^{ikr}}{4\pi r}(\overline{\overline{I}} - \hat{k}_s\hat{k}_s)$$
$$\cdot \iint_{S'} dS' \left\{ \hat{k}_s \times [\hat{n} \times \overline{E}(\overline{r}')] + \eta[\hat{n} \times \overline{H}(\overline{r}')] \right\} e^{-i\overline{k}_s \cdot \overline{r}'} \tag{7.4.5a}$$

$$\overline{E}_t(\overline{r}) = \frac{ik_1\,e^{ik_1 r}}{4\pi r}(\overline{\overline{I}} - \hat{k}_t\hat{k}_t)$$

$$\cdot \iint_{S'} dS'\left\{\hat{k}_t \times [\hat{n}_d \times \overline{E}(\overline{r}')] + \eta_1[\hat{n}_d \times \overline{H}(\overline{r}')]\right\} e^{-i\overline{k}_t\cdot\overline{r}'} \quad (7.4.5b)$$

where η and η_1 are the wave impedances in regions 0 and 1.

A. Kirchhoff Approximation

We first form an orthonormal system $(\hat{p}_i, \hat{q}_i, \hat{k}_i)$ at a point $\overline{r}'$, with

$$\hat{q}_i = \frac{\hat{k}_i \times \hat{n}}{|\hat{k}_i \times \hat{n}|} \quad (7.4.6a)$$

$$\hat{p}_i = \hat{q}_i \times \hat{k}_i \quad (7.4.6b)$$

where $\hat{n}(\overline{r}') = -\hat{n}_d(\overline{r}')$ is the normal to the surface at the point $\overline{r}'$ pointing into region 0. The unit vectors are the local perpendicular and parallel polarization vectors at the point $\overline{r}'$. In applying the tangent plane approximation, we solve the boundary value problem for the TE and TM polarization of a wave incident onto an infinite planar interface with the tangent plane as the interface. The incident field is decomposed into locally perpendicular and parallel polarization fields.

The TE component of the incident field is $(\hat{e}_i \cdot \hat{q}_i)\hat{q}_i E_o\,e^{i\overline{k}_i\cdot\overline{r}'}$ and the local reflected field is $R^{\mathrm{TE}}(\hat{e}_i \cdot \hat{q}_i)\hat{q}_i\,E_o\,e^{i\overline{k}_i\cdot\overline{r}'}$ where R^{TE} is the local Fresnel reflection coefficient for the TE component

$$R^{\mathrm{TE}} = \frac{k\cos\theta_{l_i} - \sqrt{k_1^2 - k^2\sin^2\theta_{l_i}}}{k\cos\theta_{l_i} + \sqrt{k_1^2 - k^2\sin^2\theta_{l_i}}}$$

where θ_{l_i} is the local angle of incidence at the point $\overline{r}'$. The magnetic fields associated with the incident and reflected fields are $\hat{k}_i \times (\hat{e}_i \cdot \hat{q}_i)\hat{q}_i\,E_o\,e^{i\overline{k}_i\cdot\overline{r}'}/\eta$ and $R^{\mathrm{TE}}\hat{k}_r \times (\hat{e}_i \cdot \hat{q}_i)\hat{q}_i\,E_o\,e^{i\overline{k}_i\cdot\overline{r}'}/\eta$ where $\hat{k}_r$ is the local reflected direction and is related to the incident direction by

$$\hat{k}_r = \hat{k}_i - 2\hat{n}(\hat{n} \cdot \hat{k}_i) \quad (7.4.7)$$

Hence, the tangential electric field of this perpendicular component at the point $\overline{r}'$ is

$$\hat{n} \times \overline{E} = (\hat{n} \times \hat{q}_i)(\hat{e}_i \cdot \hat{q}_i)(1 + R^{\mathrm{TE}})\,E_o\,e^{i\overline{k}_i\cdot\overline{r}'} \quad (7.4.8a)$$

and the associated magnetic field is

$$
\begin{aligned}
\hat{n} \times \overline{H} &= \frac{1}{\eta}(\hat{e}_i \cdot \hat{q}_i)\hat{n} \times \left[(\hat{k}_i \times \hat{q}_i) + R^{\mathrm{TE}}(\hat{k}_r \times \hat{q}_i) \right] E_o\, e^{i\overline{k}_i \cdot \overline{r}'} \\
&= -(1 - R^{\mathrm{TE}})(\hat{n} \cdot \hat{k}_i)\frac{(\hat{e}_i \cdot \hat{q}_i)}{\eta}\hat{q}_i\, E_o\, e^{i\overline{k}_i \cdot \overline{r}'}
\end{aligned}
\qquad (7.4.8b)
$$

where we have made use of the relations $\hat{n} \cdot \hat{q}_i = 0$ and $\hat{n} \cdot \hat{k}_r = -\hat{n} \cdot \hat{k}_i$. The calculations can be repeated for the local TM component with local reflection coefficient

$$
R^{\mathrm{TM}} = \frac{\epsilon_1 k \cos\theta_{l_i} - \epsilon_o\sqrt{k_1^2 - k^2 \sin^2\theta_{l_i}}}{\epsilon_1 k \cos\theta_{l_i} + \epsilon_o\sqrt{k_1^2 - k^2 \sin^2\theta_{l_i}}}
\qquad (7.4.9)
$$

Summing up the local parallel and perpendicular polarized components, we obtain

$$
\begin{aligned}
\hat{n} \times \overline{E}(\overline{r}') =\, &E_o\Big\{ (\hat{e}_i \cdot \hat{q}_i)(\hat{n} \times \hat{q}_i)(1 + R^{\mathrm{TE}}) \\
&\quad + (\hat{e}_i \cdot \hat{p}_i)(\hat{n} \cdot \hat{k}_i)\hat{q}_i(1 - R^{\mathrm{TM}}) \Big\} e^{i\overline{k}_i \cdot \overline{r}'} \qquad (7.4.10a) \\
\hat{n} \times \overline{H}(\overline{r}') =\, &\frac{E_o}{\eta}\Big\{ -(\hat{e}_i \cdot \hat{q}_i)(\hat{n} \cdot \hat{k}_i)\hat{q}_i(1 - R^{\mathrm{TE}}) \\
&\quad + (\hat{e}_i \cdot \hat{p}_i)(\hat{n} \times \hat{q}_i)(1 + R^{\mathrm{TM}}) \Big\} e^{i\overline{k}_i \cdot \overline{r}'} \qquad (7.4.10b)
\end{aligned}
$$

The local angle of incidence can be calculated from the formula

$$
\cos\theta_{l_i} = -\hat{n} \cdot \hat{k}_i
\qquad (7.4.11)
$$

The normal vector at the point $\overline{r}'$ is given by

$$
\hat{n}(\overline{r}') = \frac{-\hat{x}\alpha - \hat{y}\beta + \hat{z}}{\sqrt{1 + \alpha^2 + \beta^2}}
\qquad (7.4.12)
$$

where α and β are the local slopes in the $\hat{x}$ and $\hat{y}$ directions,

$$
\alpha = \frac{\partial f(x', y')}{\partial x'}
\qquad (7.4.13a)
$$

$$
\beta = \frac{\partial f(x', y')}{\partial y'}
\qquad (7.4.13b)
$$

Substituting (7.4.10) into (7.4.5), we obtain, after some algebraic manipulations,

$$\overline{E}_s(\overline{r}) = \frac{ik\,e^{ikr}}{4\pi r} E_o(\overline{\overline{I}} - \hat{k}_s\hat{k}_s) \cdot \int_{A_o} d\overline{r}'_\perp \, \overline{F}(\alpha,\beta)\, e^{i(\overline{k}_i - \overline{k}_s)\cdot\overline{r}'} \quad (7.4.14a)$$

Similarly, for the transmitted field,

$$\overline{E}_t(\overline{r}) = -\frac{ik_1\,e^{ik_1 r}}{4\pi r} E_o(\overline{\overline{I}} - \hat{k}_t\hat{k}_t) \cdot \int_{A_o} d\overline{r}'_\perp \, \overline{N}(\alpha,\beta)\, e^{i(\overline{k}_i - \overline{k}_t)\cdot\overline{r}'} \quad (7.4.14b)$$

where

$$\overline{F}(\alpha,\beta) = (1 + \alpha^2 + \beta^2)^{1/2}\Big\{ -(\hat{e}_i \cdot \hat{q}_i)(\hat{n} \cdot \hat{k}_i)\hat{q}_i(1 - R^{\mathrm{TE}})$$
$$+ (\hat{e}_i \cdot \hat{p}_i)(\hat{n} \times \hat{q}_i)(1 + R^{\mathrm{TM}})$$
$$+ (\hat{e}_i \cdot \hat{q}_i)(\hat{k}_s \times (\hat{n} \times \hat{q}_i))(1 + R^{\mathrm{TE}})$$
$$+ (\hat{e}_i \cdot \hat{p}_i)(\hat{n} \cdot \hat{k}_i)(\hat{k}_s \times \hat{q}_i)(1 - R^{\mathrm{TM}})\Big\} \quad (7.4.15a)$$

$$\overline{N}(\alpha,\beta) = (1 + \alpha^2 + \beta^2)^{1/2}\Big\{ -\frac{\eta_1}{\eta}(\hat{e}_i \cdot \hat{q}_i)(\hat{n} \cdot \hat{k}_i)\hat{q}_i(1 - R^{\mathrm{TE}})$$
$$+ \frac{\eta_1}{\eta}(\hat{e}_i \cdot \hat{p}_i)(\hat{n} \times \hat{q}_i)(1 + R^{\mathrm{TM}})$$
$$+ (\hat{e}_i \cdot \hat{q}_i)[(\hat{k}_t \times (\hat{n} \times \hat{q}_i)](1 + R^{\mathrm{TE}})$$
$$+ (\hat{e}_i \cdot \hat{p}_i)(\hat{n} \cdot \hat{k}_i)(\hat{k}_t \times \hat{q}_i)(1 - R^{\mathrm{TM}})\Big\} \quad (7.4.15b)$$

We note that except for the phase factors, the expressions in the integrands of the diffraction integral (7.4.14) are not explicit functions of $\overline{r}'$. They are explicit functions of the slopes α and β which are functions of $\overline{r}'$. The tangent-plane-approximated diffraction integrals, as expressed in (7.4.14), do not take into account the effects of shadowing and multiple scattering.

Expanding the integrands $\overline{F}(\alpha,\beta)$ and $\overline{N}(\alpha,\beta)$ about zero slopes, we obtain

$$\overline{F}(\alpha,\beta) = \overline{F}(0,0) + \alpha\, \frac{\partial\overline{F}}{\partial\alpha}\Big|_{\alpha,\beta=0} + \beta\, \frac{\partial\overline{F}}{\partial\beta}\Big|_{\alpha,\beta=0} + \cdots \quad (7.4.16)$$

$$\overline{N}(\alpha,\beta) = \overline{N}(0,0) + \alpha \left.\frac{\partial \overline{N}}{\partial \alpha}\right|_{\alpha,\beta=0} + \beta \left.\frac{\partial \overline{N}}{\partial \beta}\right|_{\alpha,\beta=0} + \cdots \qquad (7.4.17)$$

where $\overline{F}(0,0)$ and $\overline{N}(0,0)$ are evaluated at $\alpha = \beta = 0$, etc. For angles of incidence near normal and for surfaces with small root mean square (rms) slope, the Fresnel reflection coefficients vary only slightly with a change in local angle of incidence. Keeping only the first terms in (7.4.16) and (7.4.17), we obtain from (7.4.14)

$$\overline{E}_s = \frac{ik\,e^{ikr}}{4\pi r}E_o(\overline{\overline{I}} - \hat{k}_s\hat{k}_s)\cdot\overline{F}(0,0)I \qquad (7.4.18a)$$

$$\overline{E}_t = -\frac{ik_1\,e^{ik_1r}}{4\pi r}E_o(\overline{\overline{I}} - \hat{k}_t\hat{k}_t)\cdot\overline{N}(0,0)I_t \qquad (7.4.18b)$$

where the integrals I and I_t are given by

$$I = \iint_{A_o} d\overline{r}'_\perp\, e^{i(\overline{k}_i - \overline{k}_s)\cdot\overline{r}'} \qquad (7.4.19a)$$

$$I_t = \iint_{A_o} d\overline{r}'_\perp\, e^{i(\overline{k}_i - \overline{k}_t)\cdot\overline{r}'} \qquad (7.4.19b)$$

The scattered and transmitted fields are next separated into a mean field and a fluctuating part of the field

$$\overline{E}_s(\overline{r}) = \overline{E}_{sm}(\overline{r}) + \overline{\mathcal{E}}_{sf}(\overline{r}) \qquad (7.4.20a)$$

$$\overline{E}_t(\overline{r}) = \overline{E}_{tm}(\overline{r}) + \overline{\mathcal{E}}_{tf}(\overline{r}) \qquad (7.4.20b)$$

with

$$<\overline{\mathcal{E}}_{sf}(\overline{r})> = <\overline{\mathcal{E}}_{tf}(\overline{r})> = 0$$

where $\overline{E}_{sm}$ and $\overline{E}_{tm}$ denote the mean scattered and transmitted fields respectively. The total scattered intensity is then a sum of coherent and incoherent intensities

$$<|\overline{E}_s(\overline{r})|^2> = |\overline{E}_{sm}|^2 + <|\overline{\mathcal{E}}_{sf}(\overline{r})|^2> \qquad (7.4.21a)$$

$$<|\overline{E}_t(\overline{r})|^2> = |\overline{E}_{tm}|^2 + <|\overline{\mathcal{E}}_{tf}(\overline{r})|^2> \qquad (7.4.21b)$$

In view of (7.4.18) and (7.4.19) and noting that $(\hat{p}_i, \hat{q}_i, \hat{k}_i)$, $(\hat{v}_s, \hat{h}_s, \hat{k}_s)$, and $(\hat{v}_t, \hat{h}_t, \hat{k}_t)$ are the three orthogonal systems for the incident, scattered, and transmitted systems, we find

$$|\overline{E}_{sm}(\overline{r})|^2 = \frac{k^2|E_o|^2}{16\pi^2 r^2} \left\{ \left|\hat{v}_s \cdot \overline{F}(0,0)\right|^2 + \left|\hat{h}_s \cdot \overline{F}(0,0)\right|^2 \right\} |<I>|^2 \quad (7.4.22a)$$

$$<|\overline{\mathcal{E}}_{sf}(\overline{r})|^2> = \frac{k^2|E_o|^2}{16\pi^2 r^2} \left\{ \left|\hat{v}_s \cdot \overline{F}(0,0)\right|^2 + \left|\hat{h}_s \cdot \overline{F}(0,0)\right|^2 \right\} D_I \quad (7.4.22b)$$

$$|\overline{E}_{tm}(\overline{r})|^2 = \frac{k_1^2|E_o|^2}{16\pi^2 r^2} \left\{ \left|\hat{v}_t \cdot \overline{N}(0,0)\right|^2 + \left|\hat{h}_t \cdot \overline{N}(0,0)\right|^2 \right\} |<I_t>|^2 \quad (7.4.23a)$$

$$<|\overline{\mathcal{E}}_{tf}(\overline{r})|^2> = \frac{k_1^2|E_o|^2}{16\pi^2 r^2} \left\{ \left|\hat{v}_t \cdot \overline{N}(0,0)\right|^2 + \left|\hat{h}_t \cdot \overline{N}(0,0)\right|^2 \right\} D_{I_t} \quad (7.4.23b)$$

where

$$D_I = <|I|^2> - |<I>|^2 \quad (7.4.24a)$$
$$D_{I_t} = <|I_t|^2> - |<I_t>|^2 \quad (7.4.24b)$$

We now specify the height distribution function $f(\overline{r}_\perp)$ by assuming a stationary Gaussian process and that the probability for $f(\overline{r}_\perp)$ is independent of the position $\overline{r}_\perp$ on the rough surface and has the Gaussian distribution

$$p(f(\overline{r}_\perp)) = \frac{1}{\sqrt{2\pi}\,\sigma} e^{-f^2/2\sigma^2} \quad (7.4.25)$$

where σ is the standard deviation of the surface height. For two points $\overline{r}_{\perp 1}$ and $\overline{r}_{\perp 2}$ on the surface, the joint probability density is

$$p(f_1(\overline{r}_{\perp 1}), f_2(\overline{r}_{\perp 2})) = \frac{e^{-(f_1^2 - 2Cf_1 f_2 + f_2^2)/2\sigma^2(1-C^2)}}{2\pi\sigma^2\sqrt{1-C^2}} \quad (7.4.26)$$

where C is the correlation coefficient between the two points and is a function of $\overline{r}_{\perp 1}$ and $\overline{r}_{\perp 2}$. For a statistically homogeneous isotropic surface, C is only a function of $\rho = \sqrt{(x_1 - x_2)^2 + (y_1 - y_2)^2}$,

$$<f(\overline{r}_{\perp 1})f(\overline{r}_{\perp 2})> = \sigma^2 C(\rho) \quad (7.4.27)$$

with $C(0) = 1$ and $C(\infty) = 0$. It is easily shown that

$$<e^{i\nu f(\overline{r}_\perp)}> = \int_{-\infty}^{\infty} df\, p(f)e^{i\nu f} = e^{-\sigma^2\nu^2/2} \quad (7.4.28)$$

and

$$< e^{i\nu(f_1(\overline{r}_{\perp 1}) - f_2(\overline{r}_{\perp 2}))} > = \int_{-\infty}^{\infty}\int_{-\infty}^{\infty} df_1\, df_2\; p(f_1, f_2)\, e^{i\nu(f_1 - f_2)}$$

$$= e^{-\sigma^2\nu^2(1 - C(\rho))} \qquad (7.4.29)$$

The expressions for $|<I>|^2$, D_I, $|<I_t>|^2$ and D_{I_t} can now be derived in terms of the statistical moments of the height distribution.

The integral I is given by

$$I = \iint_{A_o} d\overline{r}'_\perp\, e^{i\overline{k}_{d\perp}\cdot\overline{r}'_\perp}\, e^{ik_{dz}f(\overline{r}'_\perp)} \qquad (7.4.30)$$

where

$$\overline{k}_d = \overline{k}_i - \overline{k}_s = \hat{x}k_{dx} + \hat{y}k_{dy} + \hat{z}k_{dz} \qquad (7.4.31)$$

The ensemble average of I is

$$<I> = \iint_{A_o} d\overline{r}'_\perp\, e^{i\overline{k}_{d\perp}\cdot\overline{r}'_\perp} < e^{ik_{dz}f(\overline{r}'_\perp)} >$$

$$= 4L_x L_y\, e^{-k_{dz}^2\sigma^2/2}\, \mathrm{sinc}(k_{dx}L_x)\, \mathrm{sinc}(k_{dy}L_y) \qquad (7.4.32)$$

where $\mathrm{sinc}\, x = \sin x/x$, and $2L_x$ and $2L_y$ are the lengths of the rough surface illuminated in the $\hat{x}$ and $\hat{y}$ directions so that $A_o = 4L_x L_y$. By allowing L_x and L_y to approach infinity in the above expression, we obtain

$$|<I>|^2 = 4\pi^2 A_o e^{-k_{dz}^2\sigma^2}\delta(k_{dx})\delta(k_{dy}) \qquad (7.4.33)$$

where we make use of the identity

$$\lim_{L_x, L_y \to \infty} \frac{L_x L_y}{\pi^2}\, \mathrm{sinc}(k_{dx}L_x)\, \mathrm{sinc}(k_{dy}L_y) = \delta(k_{dx})\, \delta(k_{dy})$$

The integral for $<II^*>$ is given by

$$<II^*> = \iint_{A_o} d\overline{r}_\perp \iint_{A_o} d\overline{r}'_\perp\, e^{i\overline{k}_{d\perp}\cdot(\overline{r}_\perp - \overline{r}'_\perp)} < e^{ik_{dz}(f(\overline{r}_\perp) - f(\overline{r}'_\perp))} >$$

Using (7.4.29) and making the usual change of variables to the difference and half the sum of coordinates, we obtain

$$<II^*> = \int_{-2L_x}^{2L_x} dx \int_{-2L_y}^{2L_y} dy\, (2L_x - |x|)(2L_y - |y|)$$

$$\cdot e^{ik_{dx}x + ik_{dy}y}\, e^{-k_{dz}^2\sigma^2(1 - C(\rho))} \qquad (7.4.34)$$

The correlation function $C(\rho)$ is assumed to have a Gaussian form

$$C(\rho) = e^{-\rho^2/l^2} \qquad (7.4.35)$$

where l is the correlation length for the random variable $f(\overline{r}_\perp)$ in the transverse plane.

The expression for the standard derivation of the integral I can now be evaluated in closed form. First notice that $|<I>|^2$ can also be expressed as

$$|<I>|^2 = \int_{-2L_x}^{2L_x} dx \int_{-2L_y}^{2L_y} dy \, (2L_x - |x|)(2L_y - |y|)e^{ik_{dx}x+ik_{dy}y}e^{-\sigma^2 k_{dz}^2}$$

$$(7.4.36)$$

In view of (7.4.35), we note that the contribution of the integral of $<II^*> - |<I>|^2$ comes from $|x|$ and $|y|$ of the same order of l and the integrand is practically zero for $\rho = (x^2 + y^2)^{1/2}$ larger than a few l's. Assuming that the illuminated rough surface contains many correlation lengths $L_x, L_y \gg l$, we obtain

$$D_I = <II^*> - |<I>|^2$$
$$= A_o \int_{-\infty}^{\infty} dx \int_{-\infty}^{\infty} dy \left\{ e^{-\sigma^2 k_{dz}^2(1-C(\rho))} - e^{-\sigma^2 k_{dz}^2} \right\} e^{ik_{dx}x+ik_{dy}y}$$

$$(7.4.37)$$

Converting the integral in (7.4.37) to cylindrical coordinates and carrying out the integral in $d\phi$ give a Bessel function $J_o(k_\rho \rho)$ where $k_\rho = (k_{dx}^2 + k_{dy}^2)^{1/2}$ in the integrand. We further make a power series expansion

$$e^{-\sigma^2 k_{dz}^2(1-C(\rho))} - e^{-\sigma^2 k_{dz}^2} = e^{-\sigma^2 k_{dz}^2} \sum_{m=1}^{\infty} \frac{(\sigma^2 k_{dz}^2)^m}{m!} e^{-m\rho^2/l^2} \qquad (7.4.38)$$

and make use of the integral identity

$$\int_o^{\infty} d\rho \, \rho \, J_o(k_\rho \rho) \, e^{-m\rho^2/l^2} = \frac{l^2}{2m} e^{-k_\rho^2 l^2/4m} \qquad (7.4.39)$$

Using (7.4.38) and (7.4.39) in (7.4.37), we obtain

$$D_I = <II^*> - |<I>|^2$$
$$= \pi A_o \sum_{m=1}^{\infty} \frac{(k_{dz}^2 \sigma^2)^m}{m!m} l^2 \, e^{-(k_{dx}^2+k_{dy}^2)l^2/4m} \, e^{-\sigma^2 k_{dz}^2} \qquad (7.4.40)$$

In a similar manner, the expressions for $|<I_t>|^2$ and D_{I_t} may be derived. They are

$$|<I_t>|^2 = 4\pi^2 A_o e^{-\sigma^2 k_{tdz}^2} \delta(k_{tdx})\delta(k_{tdy}) \qquad (7.4.41)$$

and

$$D_{I_t} = \pi A_o \sum_{m=1}^{\infty} \frac{(k_{tdz}^2 \sigma^2)^m}{m!m} l^2 \, e^{-(k_{tdx}^2 + k_{tdy}^2)l^2/4m} \, e^{-\sigma^2 k_{tdz}^2} \qquad (7.4.42)$$

where

$$\overline{k}_{td} = \overline{k}_i - \overline{k}_t = \hat{x} k_{tdx} + \hat{y} k_{tdy} + \hat{z} k_{tdz}$$

The bistatic scattering coefficients for the reflected intensities are defined as

$$\gamma_{ab}^r(\hat{k}_s, \hat{k}_i) = \frac{4\pi r^2 (S_r)_a}{A_o \cos\theta_i (S_o)_b} \qquad (a,b = v, h) \qquad (7.4.43)$$

where subscript b represents the polarization of the incident wave, subscript a the polarization of the scattered wave, S_o the Poynting power density of the incident wave, S_r the Poynting density of the scattered wave, A_o the area of the rough surface projected onto the x-y plane, and θ_i the incident angle. From (7.4.18) and (7.4.22), we calculate the vertically and horizontally polarized coherent and incoherent scattered intensities for the cases of vertically and horizontally polarized incident fields. Let

$$\overline{F}_b(0,0) = \overline{F}(0,0)\Big|_{\hat{e}_i = \hat{b}_i}$$

$\overline{F}(0,0)$ can be calculated by setting $\alpha = \beta = 0$ in (7.4.12) and (7.4.15a). Next we take the dot product with $\hat{v}_s$ and $\hat{h}_s$. Thus,

$$\hat{h}_s \cdot \overline{F}_h(0,0) = \left[(1 - R_o^{\text{TE}})\cos\theta_i - (1 + R_o^{\text{TE}})\cos\theta_s\right]\cos(\phi_s - \phi_i)$$
$$(7.4.44a)$$

$$\hat{v}_s \cdot \overline{F}_h(0,0) = \left[(1 - R_o^{\text{TE}})\cos\theta_i \cos\theta_s - (1 + R_o^{\text{TE}})\right]\sin(\phi_s - \phi_i) \quad (7.4.44b)$$

$$\hat{h}_s \cdot \overline{F}_v(0,0) = \left[(1 + R_o^{\text{TM}}) - (1 - R_o^{\text{TM}})\cos\theta_i \cos\theta_s\right]\sin(\phi_s - \phi_i)$$
$$(7.4.44c)$$

$$\hat{v}_s \cdot \overline{F}_v(0,0) = \left[-(1 + R_o^{\mathrm{TM}}) \cos\theta_s + (1 - R_o^{\mathrm{TM}}) \cos\theta_i \right] \cos(\phi_s - \phi_i)$$
$$(7.4.44d)$$

where R_o^{TM} and R_o^{TE} are the Fresnel reflection coefficients of a smooth flat surface for the vertically and horizontally polarized incident waves.

In view of $(7.4.21a)$, the bistatic scattering coefficients γ_{ab}^r can be decomposed into a coherent part and an incoherent part

$$\gamma_{ab}^r(\hat{k}_s, \hat{k}_i) = \frac{k^2}{4\pi A_o \cos\theta_i} \left| \hat{a}_s \cdot \overline{F}_b(0,0) \right|^2 \left\{ |<I>|^2 + D_I \right\} \qquad (7.4.45)$$

The first term is the coherent part. Making use of (7.4.33) and (7.4.44) and the fact that

$$\delta(k_{dx})\delta(k_{dy}) = \frac{\delta(\theta_s - \theta_i)\delta(\phi_s - \phi_i)}{(k^2 \sin\theta_i \cos\theta_i)} \qquad (7.4.46)$$

we find that the coherent part becomes

$$\frac{k^2}{4\pi A_o \cos\theta_i} \left| \hat{a}_s \cdot \overline{F}_b(0,0) \right|^2 |<I>|^2 = \frac{4\pi |R_{bo}|^2}{\sin\theta_i} e^{-4k^2\sigma^2 \cos^2\theta_i}$$
$$\cdot \, \delta(\theta_s - \theta_i)\delta(\phi_s - \phi_i)\delta_{ab} \quad (7.4.47)$$

Thus the coherent wave exists only in the specular directions. Similar derivation and observation follow for the transmitted waves.

B. Geometrical Optics Solution

The diffraction integral in (7.4.14) can also be evaluated with the stationary-phase method which leads to the *geometrical optics* solution. The exponential phase factor in (7.4.14) is

$$\psi = \overline{k}_d \cdot \overline{r}' = k_{dx}x' + k_{dy}y' + k_{dz}f(x', y')$$

Setting $\partial\psi/\partial x' = 0$ and $\partial\psi/\partial y' = 0$, we find the stationary-phase points

$$\alpha_o = -\frac{k_{dx}}{k_{dz}}$$

$$\beta_o = -\frac{k_{dy}}{k_{dz}}$$

The slopes α_o and β_o are such that the incident and scattered wave directions form a specular reflection. This is seen from (7.4.12) which gives

$$\hat{n}(\alpha_o, \beta_o) = (\overline{k}_s - \overline{k}_i)/|\overline{k}_d|$$

Replacing the surface slopes α and β by α_o and β_o, we obtain from (7.4.14)

$$<|\overline{E}_s|^2> = \frac{k^2 \, |E_o|^2}{16\pi^2 r^2} \left| (\overline{\overline{I}} - \hat{k}_s \hat{k}_s) \cdot \overline{F}(\alpha_o, \beta_o) \right|^2 <II^*> \qquad (7.4.48)$$

where

$$<II^*> = < \iint_{A_o} d\overline{r}_\perp \iint_{A_o} d\overline{r}'_\perp \, e^{i\overline{k}_{d\perp} \cdot (\overline{r}_\perp - \overline{r}'_\perp)} \, e^{ik_{dz}(f(\overline{r}_\perp) - f(\overline{r}'_\perp))} >$$

$$(7.4.49)$$

The above integral can be solved by the method of asymptotics. For large k, contributions of the integral come from regions where (x', y') is close to (x, y). Expanding $f(x', y')$ about (x, y),

$$f(x', y') = f(x, y) + \alpha(x' - x) + \beta(y' - y) + \cdots$$

and replacing the integration variables by

$$u = k(x - x')$$
$$v = k(y - y')$$

we obtain

$$<II^*> = \left\langle \frac{1}{k^2} A_o \iint du \, dv \, e^{iu(q_x + \alpha q_z) + iv(q_y + \beta q_z) + O(1/k)} \right\rangle$$

Ignoring the $O(1/k)$ and higher order terms, we have

$$<II^*> = \frac{4\pi^2 A_o}{k^2} <\delta(q_x + \alpha q_z)\delta(q_y + \beta q_z)>$$

Therefore

$$<\lim_{k \to \infty} II^*> = \frac{4\pi^2 A_o}{k^2} \int_{-\infty}^{\infty} \int_{-\infty}^{\infty} d\alpha \, d\beta \, \delta(q_x + \alpha q_z)\delta(q_y + \beta q_z) \, p(\alpha, \beta)$$

where $p(\alpha, \beta)$ is the probability density function for the slopes at the surface. It follows that

$$< \lim_{k \to \infty} II^* > = \frac{4\pi^2 A_o}{k_{dz}^2} p\left(-\frac{k_{dx}}{k_{dz}}, -\frac{k_{dy}}{k_{dz}}\right) \qquad (7.4.50)$$

For the Gaussian random rough surface

$$p(\alpha, \beta) = \frac{1}{2\pi\sigma^2 |C''(0)|} \exp\left[-\frac{\alpha^2 + \beta^2}{2\sigma^2 |C''(0)|}\right] \qquad (7.4.51)$$

where σ is the standard deviation of the height of rough surface and $C''(0)$ is the double derivative of the correlation function at $\rho = 0$. Thus, $\sigma^2 |C''(0)|$ is the mean square surface slope s^2 and for the Gaussian correlation function of $(7.4.35)$ with correlation length l,

$$s^2 = \sigma^2 |C''(0)| = 2\frac{\sigma^2}{l^2}$$

Using $(7.4.51)$ in $(7.4.50)$ gives

$$<II^*> = \frac{2\pi A_o}{k_{dz}^2 \sigma^2 |C''(0)|} e^{-(k_{dx}^2 + k_{dy}^2)/2k_{dz}^2 \sigma^2 |C''(0)|} \qquad (7.4.52)$$

Another way to evaluate $<II^*>$ is to perform the ensemble average first, and then to approximate the integral. From $(7.4.34)$

$$<II^*> = \int_{-2L_x}^{2L_x} dx \int_{-2L_y}^{2L_y} dy\, (2L_x - |x|)(2L_y - |y|) e^{i\overline{k}_{d\perp} \cdot \overline{r}_\perp} e^{-k_{dz}^2 \sigma^2 (1 - C(\rho))}$$

$$(7.4.53)$$

Since $k_{dz}^2 \sigma^2 \gg 1$, most of the contribution comes from around the origin. Thus, expanding the integrand about the origin we have $1 - C(\rho) \approx \rho^2 |C''(0)| /2$, and substituting into $(7.4.53)$ the integral can be evaluated readily by making use of the integral identity of $(7.4.39)$. The final result for $<II^*>$ is the same as $(7.4.52)$.

For an incident field with polarization b, the scattered intensity for polarization a_s is given by

$$< |E_s(\overline{r})|^2 > = \frac{k^2 |E_o|^2}{16\pi^2 r^2} |\hat{a}_s \cdot \overline{F}_b(\alpha_o, \beta_o)|^2 <II^*> \qquad (7.4.54)$$

where

$$\overline{F}_b(\alpha_o, \beta_o) = \overline{F}(\alpha_o, \beta_o)\Big|_{\hat{e}_i = \hat{b}}$$

Using (7.4.15a), we find

$$|\hat{a}_s \cdot \overline{F}_b(\alpha_o, \beta_o)|^2 = \frac{|\overline{k}_d|^4}{k^2 |\hat{k}_i \times \hat{k}_s|^4 k_{dz}^2} f_{ba}$$

where

$$f_{vv} = |(\hat{h}_s \cdot \hat{k}_i)(\hat{h}_i \cdot \hat{k}_s)R^{\text{TE}} + (\hat{v}_s \cdot \hat{k}_i)(\hat{v}_i \cdot \hat{k}_s)R^{\text{TM}}|^2 \qquad (7.4.55a)$$

$$f_{hv} = |(\hat{v}_s \cdot \hat{k}_i)(\hat{h}_i \cdot \hat{k}_s)R^{\text{TE}} - (\hat{h}_s \cdot \hat{k}_i)(\hat{v}_i \cdot \hat{k}_s)R^{\text{TM}}|^2 \qquad (7.4.55b)$$

$$f_{vh} = |(\hat{h}_s \cdot \hat{k}_i)(\hat{v}_i \cdot \hat{k}_s)R^{\text{TE}} - (\hat{v}_s \cdot \hat{k}_i)(\hat{h}_i \cdot \hat{k}_s)R^{\text{TM}}|^2 \qquad (7.4.55c)$$

$$f_{hh} = |(\hat{v}_s \cdot \hat{k}_i)(\hat{v}_i \cdot \hat{k}_s)R^{\text{TE}} + (\hat{h}_s \cdot \hat{k}_i)(\hat{h}_i \cdot \hat{k}_s)R^{\text{TM}}|^2 \qquad (7.4.55d)$$

and R^{TM} and R^{TE} are evaluated at

$$\hat{n} = \frac{\hat{x}\, k_{dx}/k_{dz} + \hat{y}\, k_{dy}/k_{dz} + \hat{z}}{\left(k_{dx}^2/k_{dz}^2 + k_{dy}^2/k_{dz}^2 + 1\right)^{1/2}}$$

In view of (7.4.43) and (7.4.52) the bistatic scattering coefficients for the reflected intensities are

$$\gamma_{ab}^r(\hat{k}_s, \hat{k}_i) = \frac{f_{ab}|\overline{k}_d|^4}{\cos\theta_i |\hat{k}_i \times \hat{k}_s|^4 k_{dz}^4} \frac{e^{-(k_{dx}^2 + k_{dy}^2)/2k_{dz}^2 \sigma^2 |C''(0)|}}{2\sigma^2 |C''(0)|} \qquad (7.4.56)$$

In the backscattering direction $\hat{k}_s = -\hat{k}_i$. The backscattering cross sections are defined to be

$$\sigma_{ab}(\hat{k}_i) = \cos\theta_i\ \gamma_{ab}^r(-\hat{k}_i, \hat{k}_i) \qquad (7.4.57)$$

From (7.4.56), we obtain

$$\sigma_{hh}(\theta_i) = \sigma_{vv}(\theta_i) = \frac{|R|^2\, e^{-\tan^2\theta_i/2\sigma^2 |C''(0)|}}{\cos^4\theta_i\, 2\sigma^2 |C''(0)|} \qquad (7.4.58)$$

$$\sigma_{vh}(\theta_i) = \sigma_{hv}(\theta_i) = 0 \qquad (7.4.59)$$

where R is the reflection coefficient at normal incidence. We note from (7.4.59) that there is no depolarization in the backscattering direction.

C. Small Perturbation Method

In the small perturbation method, use is made of the Huygens' principle in conjunction with the extinction theorem. We have

$$\iint_{S'} dS' \left\{ i\omega\mu_o \overline{\overline{G}}(\overline{r},\overline{r}') \cdot [\hat{n} \times \overline{H}(\overline{r}')] + \nabla \times \overline{\overline{G}}(\overline{r},\overline{r}') \cdot [\hat{n} \times \overline{E}(\overline{r}')] \right\}$$

$$+ \overline{E}_i(\overline{r}) = \begin{cases} \overline{E}(\overline{r}) & z > f(\overline{r}_\perp) & (7.4.60a) \\ 0 & z < f(\overline{r}_\perp) & (7.4.60b) \end{cases}$$

$$\iint_{S'} dS' \left\{ i\omega\mu_1 \overline{\overline{G}}_1(\overline{r},\overline{r}') \cdot [\hat{n}_d \times \overline{H}_1(\overline{r}')] + \nabla \times \overline{\overline{G}}_1(\overline{r},\overline{r}') \cdot [\hat{n}_d \times \overline{E}_1(\overline{r}')] \right\}$$

$$= \begin{cases} 0 & z > f(\overline{r}_\perp) & (7.4.61a) \\ \overline{E}_1(\overline{r}) & z < f(\overline{r}_\perp) & (7.4.61b) \end{cases}$$

Since tangential fields are continuous, we can define surface field unknowns

$$dS' \, \eta \, \hat{n} \times \overline{H}(\overline{r}') = d\overline{r}'_\perp \, \overline{a}(\overline{r}'_\perp) = dS' \, \eta \, \hat{n} \times \overline{H}_1(\overline{r}') \quad (7.4.62a)$$

$$dS' \, \hat{n} \times \overline{E}(\overline{r}') = d\overline{r}'_\perp \, \overline{b}(\overline{r}'_\perp) = dS' \, \hat{n} \times \overline{E}_1(\overline{r}') \quad (7.4.62b)$$

Next we make use of the integral representation of dyadic Green's function (6.6.26) [Zuniga and Kong, 1980]

$$\overline{\overline{G}}(\overline{r},\overline{r}') = -\hat{z}\hat{z}\frac{\delta(\overline{r},\overline{r}')}{k_o^2}$$

$$+ \begin{cases} \dfrac{i}{8\pi^2} \iint d^2\overline{k}_\perp \dfrac{1}{k_z}[\hat{e}(k_z)\hat{e}(k_z) + \hat{h}(k_z)\hat{h}(k_z)]e^{i\overline{k}\cdot(\overline{r}-\overline{r}')} & z > z' \\ \dfrac{i}{8\pi^2} \iint d^2\overline{k}_\perp \dfrac{1}{k_z}[\hat{e}(-k_z)\hat{e}(-k_z) + \hat{h}(-k_z)\hat{h}(-k_z)]e^{i\overline{k}_1\cdot(\overline{r}-\overline{r}')} & z < z' \end{cases}$$

where $\hat{e}(-k_z) = \hat{e}(k_z)$ and $\hat{h}(-k_z) = \hat{e} \times \hat{k}_1/k$. Evaluating (7.4.60b) for $z < f_{min}$ and (7.4.61a) for $z > f_{max}$ we obtain

$$\overline{E}_i(\overline{r}) = \frac{1}{8\pi^2} \int d\overline{k}_\perp \, e^{i\overline{k}_\perp \cdot \overline{r}_\perp} \, e^{-ik_z z} \frac{k}{k_z} \int d\overline{r}'_\perp \, e^{-i\overline{k}_\perp \cdot \overline{r}'_\perp} \, e^{ik_z f(\overline{r}'_\perp)}$$

$$\cdot \left\{ \left[\hat{e}(-k_z)\hat{e}(-k_z) + \hat{h}(-k_z)\hat{h}(-k_z) \right] \cdot \overline{a}(\overline{r}'_\perp) \right.$$

$$\left. + \left[-\hat{h}(-k_z)\hat{e}(-k_z) + \hat{e}(-k_z)\hat{h}(-k_z) \right] \cdot \overline{b}(\overline{r}'_\perp) \right\} \quad (7.4.63a)$$

$$0 = \frac{1}{8\pi^2} \int d\overline{k}_\perp \, e^{i\overline{k}_\perp \cdot \overline{r}_\perp} \, e^{ik_{1z}z} \frac{k_1}{k_{1z}} \int d\overline{r}'_\perp \, e^{-i\overline{k}_\perp \cdot \overline{r}'_\perp} \, e^{-ik_{1z}f(\overline{r}'_\perp)}$$

$$\cdot \left\{ \frac{k}{k_1} \left[\hat{e}_1(k_{1z})\hat{e}_1(k_{1z}) + \hat{h}_1(k_{1z})\hat{h}_1(k_{1z}) \right] \cdot \overline{a}(\overline{r}'_\perp) \right.$$

$$\left. + \left[-\hat{h}_1(k_{1z})\hat{e}_1(k_{1z}) + \hat{e}_1(k_{1z})\hat{h}_1(k_{1z}) \right] \cdot \overline{b}(\overline{r}'_\perp) \right\} \quad (7.4.63b)$$

The above equations are the extended boundary conditions, and can be used to solve for the surface fields along with the following results of (7.4.62)

$$\hat{n}(\overline{r}'_\perp) \cdot \overline{a}(\overline{r}'_\perp) = 0 \qquad\qquad (7.4.64a)$$

$$\hat{n}(\overline{r}'_\perp) \cdot \overline{b}(\overline{r}'_\perp) = 0 \qquad\qquad (7.4.64b)$$

Using (7.4.12), (7.4.64) can be rewritten as

$$a_z(\overline{r}'_\perp) = \left(\hat{x} \frac{\partial f(\overline{r}'_\perp)}{\partial x'} + \hat{y} \frac{\partial f(\overline{r}'_\perp)}{\partial y'} \right) \cdot \overline{a}_\perp(\overline{r}'_\perp) \qquad (7.4.65a)$$

$$b_z(\overline{r}'_\perp) = \left(\hat{x} \frac{\partial f(\overline{r}'_\perp)}{\partial x'} + \hat{y} \frac{\partial f(\overline{r}'_\perp)}{\partial y'} \right) \cdot \overline{b}_\perp(\overline{r}'_\perp) \qquad (7.4.65b)$$

with a_z and b_z as the z components of $\overline{a}$ and $\overline{b}$.

Once the surface fields are obtained, the scattered field in region 0 immediately follows from (7.4.60a)

$$\overline{E}_s(\overline{r}) = -\frac{1}{8\pi^2} \int d\overline{k}_\perp \, e^{i\overline{k}_\perp \cdot \overline{r}_\perp + ik_z z} \frac{k}{k_z} \int d\overline{r}'_\perp \, e^{-i\overline{k}_\perp \cdot \overline{r}'_\perp - ik_z f(\overline{r}'_\perp)}$$

$$\cdot \left\{ \left[\hat{e}(k_z)\hat{e}(k_z) + \hat{h}(k_z)\hat{h}(k_z) \right] \cdot \overline{a}(\overline{r}'_\perp) \right.$$

$$\left. + \left[-\hat{h}(k_z)\hat{e}(k_z) + \hat{e}(k_z)\hat{h}(k_z) \right] \cdot \overline{b}(\overline{r}'_\perp) \right\} \quad (7.4.66)$$

To solve for the surface fields, the perturbation method makes use of series expansions. Let

$$\overline{a}(\overline{r}'_\perp) = \sum_{m=0}^{\infty} \frac{1}{m!} \overline{a}^{(m)}(\overline{r}'_\perp) \qquad\qquad (7.4.67a)$$

$$\overline{b}(\overline{r}'_\perp) = \sum_{m=0}^{\infty} \frac{1}{m!} \overline{b}^{(m)}(\overline{r}'_\perp) \qquad\qquad (7.4.67b)$$

where $\overline{a}^m$ and $\overline{b}^m$ are the mth-order solutions of $\overline{a}$ and $\overline{b}$. We also have

$$e^{\pm ik_z f(\overline{r}'_\perp)} = \sum_{m=0}^{\infty} \frac{1}{m!} [\pm ik_z f(\overline{r}'_\perp)]^m \qquad (7.4.68a)$$

$$e^{\pm ik_{1z} f(\overline{r}'_\perp)} = \sum_{m=0}^{\infty} \frac{1}{m!} [\pm ik_{1z} f(\overline{r}'_\perp)]^m \qquad (7.4.68b)$$

In SPM, f and its derivatives are regarded as small parameters. The expansion of (7.4.67) and (7.4.68) are substituted into (7.4.63) to obtain the set of equations for the different-order solutions. From (7.4.65) and (7.4.67)

$$a_z^{(0)}(\overline{r}'_\perp) = b_z^{(0)}(\overline{r}'_\perp) = 0 \qquad (7.4.69a)$$

$$a_z^{(m)}(\overline{r}'_\perp) = m\left(\hat{x}\frac{\partial f(\overline{r}'_\perp)}{\partial x'} + \hat{y}\frac{\partial f(\overline{r}'_\perp)}{\partial y'}\right) \cdot \overline{a}_\perp^{(m-1)}(\overline{r}'_\perp) \qquad (7.4.69b)$$

$$b_z^{(m)}(\overline{r}'_\perp) = m\left(\hat{x}\frac{\partial f(\overline{r}'_\perp)}{\partial x'} + \hat{y}\frac{\partial f(\overline{r}'_\perp)}{\partial y'}\right) \cdot \overline{b}_\perp^{(m-1)}(\overline{r}'_\perp) \qquad (7.4.69c)$$

In summary, the assumptions for the SPM are

$$k_z f(\overline{r}'_\perp),\ k_{1z} f(\overline{r}'_\perp),\ \frac{\partial f}{\partial x'},\ \frac{\partial f}{\partial y'} \ll 1 \qquad (7.4.70)$$

Substituting (7.4.67)–(7.4.68) into (7.4.63) and (7.4.65) and equating the same-order terms, we shall calculate the scattered fields to the zeroth and first-order in the following.

Zeroth-Order Solution

We first define an orthonormal system $(\hat{q}_i, \hat{p}_i, \hat{z}_i)$, such that

$$\hat{q}_i = \hat{x}\frac{k_{iy}}{k_{i\rho}} - \hat{y}\frac{k_{ix}}{k_{i\rho}} = \hat{e}(k_{iz}) \qquad (7.4.71)$$

$\hat{z}_i = \hat{z}$, $\hat{p}_i = \hat{z}_i \times \hat{q}_i = (\hat{x}k_{ix} + \hat{y}k_{iy})/k_{\rho i}$ where $k_{\rho i}^2 = k_{ix}^2 + k_{iy}^2$ and let

$$\overline{a}(\overline{r}'_\perp) = \hat{q}_i a_q(\overline{r}'_\perp) + \hat{p}_i a_p(\overline{r}'_\perp) + \hat{z}_i a_z(\overline{r}'_\perp) \qquad (7.4.72a)$$

$$\overline{b}(\overline{r}'_\perp) = \hat{q}_i b_q(\overline{r}'_\perp) + \hat{p}_i b_p(\overline{r}'_\perp) + \hat{z}_i b_z(\overline{r}'_\perp) \qquad (7.4.72b)$$

and note that

$$\overline{E}_i(\overline{r}) = \hat{e}_i \, E_o \, e^{i\overline{k}_{i\perp} \cdot \overline{r}_\perp - ik_{iz}z}$$

$$= \frac{\hat{e}_i}{4\pi^2} \int d\overline{k}_\perp \, e^{i\overline{k}_\perp \cdot \overline{r}_\perp - ik_z z} \int d\overline{r}'_\perp \, e^{i\overline{k}_{i\perp} \cdot \overline{r}'_\perp - i\overline{k}_\perp \cdot \overline{r}'_\perp} \quad (7.4.73)$$

Using $(7.4.73)$ in $(7.4.63a)$, we find

$$\hat{e}_i \, e^{i\overline{k}_{i\perp} \cdot \overline{r}'_\perp} = \frac{k}{2k_{iz}} \left\{ \left[\hat{e}(-k_{iz})\hat{e}(-k_{iz}) + \hat{h}(-k_{iz})\hat{h}(-k_{iz}) \right] \cdot \overline{a}^{(0)}_\perp(\overline{r}'_\perp) \right.$$

$$\left. + \left[-\hat{h}(-k_{iz})\hat{e}(-k_{iz}) + \hat{e}(-k_{iz})\hat{h}(-k_{iz}) \right] \cdot \overline{b}^{(0)}_\perp(\overline{r}') \right\}$$

$$(7.4.74a)$$

and from $(7.4.63b)$, we have

$$\left[\hat{e}_1(k_{1iz})\hat{e}_1(k_{1iz}) + \hat{h}_1(k_{1iz})\hat{h}_1(k_{1iz}) \right] \cdot \overline{a}^{(0)}_\perp(\overline{r}'_\perp) \frac{k}{k_1}$$

$$+ \left[-\hat{h}_1(k_{1iz})\hat{e}_1(k_{1iz}) + \hat{e}_1(k_{1iz})\hat{h}_1(k_{1iz}) \right] \cdot \overline{b}^{(0)}_\perp(\overline{r}'_\perp) = 0 \quad (7.4.74b)$$

Using (7.4.69), (7.4.72), and noting that

$$\hat{e}(k_{iz}) = \frac{\hat{k}_i \times \hat{z}}{|\hat{k}_i \times \hat{z}|} = \frac{1}{k_{i\rho}} (\hat{x} k_{iy} - \hat{y} k_{ix})$$

$$\hat{h}(k_{iz}) = \frac{1}{k^2} \hat{e} \times \hat{k}_i = \frac{k_{iz}}{k k_{i\rho}} (\hat{x} k_{ix} + \hat{y} k_{iy}) + \hat{z} \frac{k_{i\rho}}{k}$$

we find from $(7.4.74a)$

$$\hat{e}_i \, e^{i\overline{k}_{i\perp} \cdot \overline{r}'} = \frac{k}{2k_{iz}} \left\{ \hat{e}(-k_{iz}) \left(a^{(0)}_q(\overline{r}') + \frac{k_{iz}}{k} b^{(0)}_p(\overline{r}'_\perp) \right) \right.$$

$$\left. + \hat{h} \, (-k_{iz}) \left(\frac{k_{iz}}{k} a^{(0)}_p(\overline{r}'_\perp) - b^{(0)}_q(\overline{r}'_\perp) \right) \right\} \quad (7.4.75a)$$

Using $(7.4.74b)$, we have

$$k a^{(0)}_q(\overline{r}') - k_{1iz} b^{(0)}_p(\overline{r}') = 0 \qquad\qquad (7.4.75b)$$

$$\frac{k k_{1iz}}{k_1^2} a^{(0)}_p(\overline{r}') + b^{(0)}_q(\overline{r}') = 0 \qquad\qquad (7.4.75c)$$

Since $(7.4.75a)$ contains two scalar equations, $(7.4.75)$ provides four equations for the four unknowns $a_p^{(0)}$, $a_q^{(0)}$, $b_p^{(0)}$, and $b_q^{(0)}$. Solving them and substituting back into $\overline{a}^{(0)}(\overline{r}'_\perp)$ and $\overline{b}^{(0)}(\overline{r}'_\perp)$ give

$$\overline{a}^{(0)}(\overline{r}'_\perp) = \overline{a}^{(0)}(\overline{k}_{i\perp})\, e^{i\overline{k}_{i\perp}\cdot\overline{r}'_\perp} \qquad (7.4.76a)$$

$$\overline{b}^{(0)}(\overline{r}'_\perp) = \overline{b}^{(0)}(\overline{k}_{i\perp})\, e^{i\overline{k}_{i\perp}\cdot\overline{r}'_\perp} \qquad (7.4.76b)$$

where

$$\overline{a}_q^{(0)}(\overline{k}_{i\perp}) = [\hat{e}(-k_{iz})\cdot\hat{e}_i]\frac{k_{iz}}{k}(1 - R_o^{\mathrm{TE}}) \qquad (7.4.77a)$$

$$\overline{a}_p^{(0)}(\overline{k}_{i\perp}) = [\hat{h}(-k_{iz})\cdot\hat{e}_i](1 + R_o^{\mathrm{TM}}) \qquad (7.4.77b)$$

$$\overline{b}_q^{(0)}(\overline{k}_{i\perp}) = -[\hat{h}(-k_{iz})\cdot\hat{e}_i]\frac{k_{iz}}{k}(1 - R_o^{\mathrm{TM}}) \qquad (7.4.77c)$$

$$\overline{b}_p^{(0)}(\overline{k}_{i\perp}) = [\hat{e}(-k_{iz})\cdot\hat{e}_i](1 + R_o^{\mathrm{TE}}) \qquad (7.4.77d)$$

and R_o^{TE} and R_o^{TM} are the Fresnel reflection coefficients for the TE and TM waves

$$R_o^{\mathrm{TE}} = \frac{k_{iz} - k_{1iz}}{k_{iz} + k_{1iz}} \qquad (7.4.78a)$$

$$R_o^{\mathrm{TM}} = \frac{\epsilon_1 k_{iz} - \epsilon_o k_{1iz}}{\epsilon_1 k_{iz} + \epsilon_o k_{1iz}} \qquad (7.4.78b)$$

Using $(7.4.76)$ in $(7.4.66)$, we find the zeroth-order scattered field to be

$$\overline{E}_s^{(0)} = \big\{ R_o^{\mathrm{TE}}[\hat{e}(-k_{iz})\cdot\hat{e}_i]\hat{e}(k_{iz})$$
$$+ R_o^{\mathrm{TM}}[\hat{h}(-k_{iz})\cdot\hat{e}_i]\hat{h}(k_{iz})\big\} E_o e^{i\overline{k}_{i\perp}\cdot\overline{r}_\perp + ik_{iz}z} \quad (7.4.79)$$

which is the reflected field for a flat surface.

First-Order Solution

The first-order solution for the surface fields can be obtained by substituting $(7.4.67)$ and $(7.4.68)$ into $(7.4.63)$, $(7.4.65)$, $(7.4.66)$, and $(7.4.69)$ and equating first-order terms. From $(7.4.69a)$ and $(7.4.76a)$

$$a_z^{(1)}(\overline{r}'_\perp) = \left(\hat{x}\frac{\partial f(\overline{r}'_\perp)}{\partial x'} + \hat{y}\frac{\partial f(\overline{r}'_\perp)}{\partial y'}\right) \cdot \overline{a}_\perp^{(0)}(\overline{k}_{i\perp})\, e^{i\overline{k}_{i\perp}\cdot\overline{r}'_\perp} \qquad (7.4.80)$$

To simplify (7.4.80), we introduce the Fourier transforms

$$F(\overline{k}_\perp) = \frac{1}{(2\pi)^2}\int d\overline{r}'_\perp\, f(\overline{r}'_\perp)\, e^{-i\overline{k}_\perp\cdot\overline{r}'_\perp} \qquad (7.4.81)$$

$$\overline{A}^{(1)}(\overline{k}_\perp) = \frac{1}{(2\pi)^2}\int d\overline{r}'_\perp\, \overline{a}^{(1)}(\overline{r}'_\perp)\, e^{-i\overline{k}_\perp\cdot\overline{r}'_\perp} \qquad (7.4.82a)$$

$$\overline{B}^{(1)}(\overline{k}_\perp) = \frac{1}{(2\pi)^2}\int d\overline{r}'_\perp\, \overline{b}^{(1)}(\overline{r}'_\perp)\, e^{-i\overline{k}_\perp\cdot\overline{r}'_\perp} \qquad (7.4.82b)$$

Strictly speaking, the Fourier transforms do not exist for random functions and stochastic Fourier Stieltjes integral have to be defined [Tatarskii, 1971; Ishimaru, 1978]. However, the final results for scattered intensities are not affected.

Multiply (7.4.80) by $e^{-i\overline{k}_\perp\cdot\overline{r}'_\perp}/(2\pi)^2$ and integrate over $d\overline{r}'_\perp$. We obtain, by expressing $\partial f(\overline{r}'_\perp)/\partial x'$ and $\partial f(\overline{r}'_\perp)/\partial y'$ in terms of $F(\overline{k}_\perp)$,

$$A_z^{(1)}(\overline{k}_\perp) = \left\{\frac{k_x k_{iy} - k_y k_{ix}}{k_{i\rho}}a_q^{(0)}(\overline{k}_{i\perp})\right.$$
$$\left. + \left(\frac{k_x k_{ix} + k_y k_{iy}}{k_{i\rho}} - k_{i\rho}\right)a_p^{(0)}(\overline{k}_{i\perp})\right\}iF(\overline{k}_\perp - \overline{k}_{i\perp})$$
$$(7.4.83a)$$

Similarly from (7.4.69b)

$$B_z^{(1)}(\overline{k}_\perp) = \left\{\frac{k_x k_{iy} - k_y k_{ix}}{k_{i\rho}}b_q^{(0)}(\overline{k}_{i\perp})\right.$$
$$\left. + \left(\frac{k_x k_{ix} + k_y k_{iy}}{k_{i\rho}} - k_{i\rho}\right)b_p^{(0)}(\overline{k}_{i\perp})\right\}iF(\overline{k}_\perp - \overline{k}_{i\perp})$$
$$(7.4.83b)$$

Next we match both sides of equation (7.4.63a) to the first order. We note that

$$\left[\int d\overline{r}'_\perp e^{-i\overline{k}_\perp\cdot\overline{r}'_\perp}\, e^{ik_z f(\overline{r}'_\perp)}\overline{a}(\overline{r}'_\perp)\right]_{\text{first order}}$$
$$= \int d\overline{r}'_\perp e^{-i\overline{k}_\perp\cdot\overline{r}'_\perp}\left[ik_z f(\overline{r}'_\perp)\overline{a}^{(0)}(\overline{k}_{i\perp})e^{i\overline{k}_{i\perp}\cdot\overline{r}'} + \overline{a}^{(1)}(\overline{r}')\right]$$
$$= (2\pi)^2\left[ik_z F(\overline{k}_\perp - \overline{k}_{i\perp})\overline{a}^{(0)}(\overline{k}_{i\perp}) + \overline{A}^{(1)}(\overline{k}_\perp)\right]$$

Hence, the first-order equation from (7.4.63a) is

$$
0 = \left[\hat{e}(-k_z)\hat{e}(-k_z) + \hat{h}(-k_z)\hat{h}(-k_z) \right]
$$
$$
\cdot \left[\overline{A}^{(1)}(\overline{k}_\perp) + ik_z \overline{a}^{(0)}(\overline{k}_{i\perp}) F(\overline{k}_\perp - \overline{k}_{i\perp}) \right]
$$
$$
+ \left[-\hat{h}(-k_z)\hat{e}(-k_z) + \hat{e}(-k_z)\hat{h}(-k_z) \right]
$$
$$
\cdot \left[\overline{B}^{(1)}(\overline{k}_\perp) + ik_z \overline{b}^{(0)}(\overline{k}_{i\perp}) F(\overline{k}_\perp - \overline{k}_{i\perp}) \right] \qquad (7.4.84)
$$

and similarly, from (7.4.63b) we obtain

$$
0 = \frac{k}{k_1} \left[\hat{e}_1(k_{1z})\hat{e}_1(k_{1z}) + \hat{h}_1(k_{1z})\hat{h}_1(k_{1z}) \right]
$$
$$
\cdot \left[\overline{A}^{(1)}(\overline{k}_\perp) - ik_{1z} \overline{a}^{(0)}(\overline{k}_{i\perp}) F(\overline{k}_\perp - \overline{k}_{i\perp}) \right]
$$
$$
+ \left[-\hat{h}_1(k_{1z})\hat{e}_1(k_{1z}) + \hat{e}_1(k_{1z})\hat{h}_1(k_{1z}) \right]
$$
$$
\cdot \left[\overline{B}^{(1)}(\overline{k}_\perp) - ik_{1z} \overline{b}^{(0)}(\overline{k}_{i\perp}) F(\overline{k}_\perp - \overline{k}_{i\perp}) \right] \qquad (7.4.85)
$$

Equations (7.4.84) and (7.4.85) are vector equations so that they comprise four scalar equations for the four unknowns $A_q^{(1)}(\overline{k}_\perp)$, $A_p^{(1)}(\overline{k}_\perp)$, $B_q^{(1)}(\overline{k}_\perp)$, and $B_p^{(1)}(\overline{k}_\perp)$.

The first-order scattered fields can now be obtained from (7.4.66),

$$
\overline{E}_s^{(1)} = -\frac{1}{2} \int d\overline{k}_\perp \, e^{i\overline{k}_\perp \cdot \overline{r}_\perp} \, e^{ik_z z} \frac{k}{k_z} \left\{ \left[\hat{e}(k_z)\hat{e}(k_z) + \hat{h}(k_z)\hat{h}(k_z) \right] \right.
$$
$$
\cdot \left[\overline{A}^{(1)}(\overline{k}_\perp) - ik_z F(\overline{k}_\perp - \overline{k}_{i\perp}) \overline{a}^{(0)}(\overline{k}_{i\perp}) \right]
$$
$$
+ \left[-\hat{h}(k_z)\hat{e}(k_z) + \hat{e}(k_z)\hat{h}(k_z) \right]
$$
$$
\left. \cdot \left[\overline{B}^{(1)}(\overline{k}_\perp) - ik_z F(\overline{k}_\perp - \overline{k}_{i\perp}) \overline{b}^{(0)}(\overline{k}_{i\perp}) \right] \right\} \qquad (7.4.86)
$$

In view of the fact that

$$
< \overline{F}(\overline{k}_\perp) > = \frac{1}{(2\pi)^2} \int d\overline{r}'_\perp \, e^{i\overline{k}_\perp \cdot \overline{r}'_\perp} < f(\overline{r}_\perp) > = 0
$$

we find $< \overline{E}_s^{(1)} > = < \overline{E}_t^{(1)} > = 0$. Thus, the first-order solution does not modify the coherent reflection coefficient and we have to calculate

the second-order solution to see the correction term for the coherent wave due to the rough surface.

The lowest-order incoherent coefficients can be derived from (7.4.86). For an incident field with polarization $\hat{a}_i$, the scattered intensity with polarization $\hat{b}_s$ is given by

$$<|E_s^{(1)}|^2> = \int d\overline{k}_\perp \, f'_{ba} \, W(|\overline{k}_\perp - \overline{k}_{i\perp}|)$$

$$= \int d\Omega_s \, k^2 \cos\theta_s \, f'_{ba} \, W(|\overline{k}_\perp - \overline{k}_{i\perp}|) \qquad (7.4.87)$$

where $W(|\overline{k}_\perp - \overline{k}_{i\perp}|)$ is the spectral density of the rough surface and is the Fourier transform of the correlation function.

The spectral density is

$$W(\overline{k}_\perp) = \frac{\sigma^2}{(2\pi)^2} \int d\overline{r}_\perp \, e^{i\overline{k}_\perp \cdot \overline{r}_\perp} \, C(\overline{r}_\perp)$$

and satisfies the relation

$$<F(\overline{k}'_\perp)F^*(\overline{k}_\perp)> = \delta(\overline{k}'_\perp - \overline{k}_\perp)W(|\overline{k}'_\perp|)$$

For a Gaussian correlation function of (7.4.35), we have the spectral density given by

$$W(|\overline{k}_\perp - \overline{k}_{\perp i}|) = \frac{1}{4\pi}\sigma^2 l^2 \, e^{-(k_{dx}^2 + k_{dy}^2)l^2/4} \qquad (7.4.88)$$

where $\overline{k}_{d\perp} = \overline{k}_\perp - \overline{k}_{i\perp}$, σ is the standard deviation of the surface height and l is the correlation length for $f(\overline{r}_\perp)$ in the transverse plane.

The bistatic scattering coefficients $\gamma^r_{ba}(\hat{k}_s, \hat{k}_i)$ are defined as the ratio of the scattered power of polarization b_s per unit solid angle in the direction $\hat{k}_s$ to the intercepted power of polarization a_i in the direction $\hat{k}_i$ averaged over 4π radians. Thus, from (7.4.87) we have

$$\gamma^r_{ba}(\hat{k}_s, \hat{k}_i) = 4\pi \frac{k^2 \cos\theta_s f'_{ba} W(|\overline{k}_\perp - \overline{k}_{i\perp}|)}{\cos\theta_i |E_o|^2}$$

After carrying out a tedious solution for (7.4.84) and (7.4.85) and making use of (7.4.88), we obtain

$$\gamma_{ba}^r(\hat{k}_s, \hat{k}_i) = \frac{4k^4\sigma^2 l^2 \cos^2\theta_s \cos^2\theta_i}{\cos\theta_i} f_{ba} e^{-k_{d\rho}^2 l^2/4} \tag{7.4.89}$$

where

$$k_{d\rho}^2 = k^2 \left[\sin^2\theta_s + \sin^2\theta_i - 2\sin\theta_s \sin\theta_i \cos(\phi_s - \phi_i) \right]$$

and

$$f_{hh} = \left| \frac{(k_1^2 - k^2)}{(k_z + k_{1z})(k_{iz} + k_{1iz})} \right|^2 \cos^2(\phi_s - \phi_i)$$

$$f_{vh} = \left| \frac{(k_1^2 - k^2)k k_{1z}}{(k_1^2 k_z + k^2 k_{1z})(k_{iz} + k_{1iz})} \right|^2 \sin^2(\phi_s - \phi_i)$$

$$f_{hv} = \left| \frac{(k_1^2 - k^2)k k_{1iz}}{(k_z + k_{1z})(k_1^2 k_{iz} + k^2 k_{1iz})} \right|^2 \sin^2(\phi_s - \phi_i)$$

$$f_{vv} = \left| \frac{(k_1^2 - k^2)}{(k_1^2 k_z + k^2 k_{1z})(k_1^2 k_{iz} + k^2 k_{1iz})} \right.$$
$$\left. \cdot \left[k_1^2 k^2 \sin\theta_s \sin\theta_i - k^2 k_{1z} k_{1iz} \cos(\phi_s - \phi_i) \right] \right|^2$$

In the backscattering direction $\hat{k}_s = -\hat{k}_i$. The backscattering cross sections per unit area are

$$\sigma_{hh} = 4k^4\sigma^2 l^2 \cos^4\theta_i \left| R_o^{\mathrm{TE}} \right|^2 e^{-k^2 l^2 \sin^2\theta_i} \tag{7.4.90a}$$

$$\sigma_{vv} = 4k^8\sigma^2 l^2 \cos^4\theta_i \left| \frac{(k_1^2 - k^2)(k_1^2 \sin^2\theta_i + k_{1z}k_{1zi})}{(k_1^2 k_{zi} + k^2 k_{1zi})^2} \right|^2 e^{-k^2 l^2 \sin^2\theta_i}$$
$$\tag{7.4.90b}$$

$$\sigma_{vh} = \sigma_{hv} = 0 \tag{7.4.90c}$$

It is seen from (7.4.90c) that there is no depolarization in the backscattering direction. In order to calculate for the depolarization returns, we must resort to the solution of second-order fields.

Problems

P7.4.1

Consider the bistatic scattering coefficients for a Gaussian random rough surface $f(x, y)$ under the geometrical optics approximation. Express your answer in terms of the slope probability density function $p(\alpha, \beta)$, where $\alpha = \partial f / \partial x$ and $\beta = \partial f / \partial y$.

P7.4.2

Plot the backscattering coefficients for a random rough surface for $\sigma/L = 0.1$ as a function of incidence angle θ_i using the geometric optics approximation. Let $\epsilon_1 = 80\epsilon_o$.

7.5   Scattering by Periodic Media

In the study of periodic media with applications to holography, to ultrasonic light diffraction, and to various active and passive components in integrated optics, the coupled-mode approach proves to be the simplest method leading to results that can be easily interpreted physically. Consider a periodic medium (Figure 7.5.1 without regions 1 and 3) described by the permittivity

$$\epsilon(x, z) = \epsilon_2(1 + \eta \cos(\overline{K} \cdot \overline{r})) \tag{7.5.1}$$

where $\overline{K} = K(\hat{x} \sin \gamma + \hat{z} \cos \gamma)$, $K = 2\pi/\Lambda$, and Λ is the periodicity. For a TE wave polarized in the $\hat{y}$ direction, the electric field vector $\overline{E}$ satisfies the wave equation

$$\left[\nabla^2 + \omega^2 \mu \epsilon(x, z)\right] E_y(x, z) = 0 \tag{7.5.2}$$

To facilitate the derivation of the coupled-mode equations, we let

$$E_y(x, z) = \sum_{m=-\infty}^{\infty} \phi_m(x) e^{im\pi/2} e^{ik_{mx}x} \tag{7.5.3}$$
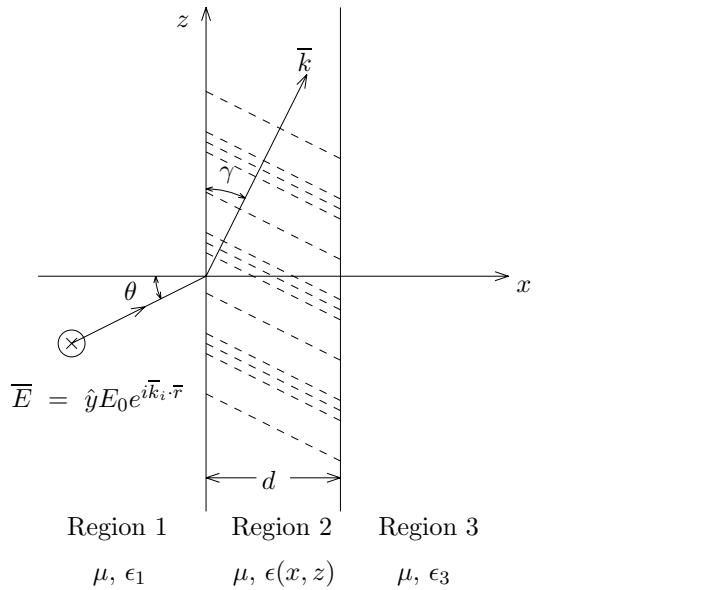
Figure 7.5.1 Geometrical configuration of the problem.

where

$$k_{mx} = k_{0x} + mK\cos\gamma \tag{7.5.4}$$

k_{0x} is the x component of the wave vector for the zeroth-order Floquet mode.

Substituting (7.5.3) in (7.5.2) and letting $\gamma = 0$ yield

$$\frac{d^2\phi_m}{dx^2} + \left(k_2^2 - k_{mx}^2\right)\phi_m + i\frac{\eta}{2}k_2^2\left(\phi_{m+1} - \phi_{m-1}\right) = 0 \tag{7.5.5}$$

where $k_2 = \omega(\mu\epsilon)^{1/2}$. Equation (7.5.5) represents a set of coupled second-order differential equations.

Near the first Bragg angle, the two Floquet modes that couple strongly to each other are of the zeroth order and first order. Keeping only these two modes, (7.5.5) becomes

$$\frac{d^2\phi_0}{dx^2} + \left(k_2^2 - k_{0x}^2\right)\phi_0 = i\frac{\eta k_2^2}{2}\phi_{-1} \tag{7.5.6a}$$

$$\frac{d^2\phi_{-1}}{dx^2} + \left(k_2^2 - k_{-1x}^2\right)\phi_{-1} = -i\frac{\eta k_2^2}{2}\phi_0 \tag{7.5.6b}$$

This set of coupled equations can be converted into two uncoupled Helmholtz equations. We let

$$U_1 = \phi_0 + i\alpha_1\phi_{-1} \tag{7.5.7a}$$

$$U_2 = \phi_0 + i\alpha_2\phi_{-1} \tag{7.5.7b}$$

or, equivalently,

$$\phi_0 = \frac{\alpha_2 U_1 - \alpha_1 U_2}{\alpha_2 - \alpha_1} \tag{7.5.7c}$$

$$\phi_{-1} = i\frac{U_1 - U_2}{\alpha_2 - \alpha_1} \tag{7.5.7d}$$

where α_1 and α_2 are constants to be determined. Adding (7.5.6a) to (7.5.6b) multiplied by α_j, where $j = 1, 2$, we obtain

$$\frac{d^2U_j}{dx^2} + \left(k_2^2 - k_{0x}^2 - \alpha_j\frac{\eta k_2^2}{2}\right)U_j = 0 \tag{7.5.8}$$

and

$$\alpha_j = (1/\eta k_2^2)\left\{k_{-1x}^2 - k_{0x}^2 \pm \left[(k_{-1x}^2 - k_{0x}^2)^2 + \eta^2 k_2^4\right]^{1/2}\right\} \tag{7.5.9}$$

The plus sign in front of the radical is for α_1 and the minus sign for α_2. Clearly, exponential functions are solutions to (7.5.8). The four independent solutions to the two coupled-mode equations in (7.5.6) are therefore

$$\phi_0 = \frac{1}{\alpha_2 - \alpha_1} \left[\alpha_2 \begin{pmatrix} W \exp(ik_{2x}^a x) \\ X \exp(-ik_{2x}^a x) \end{pmatrix} - \alpha_1 \begin{pmatrix} Y \exp(ik_{2x}^b x) \\ Z \exp(-ik_{2x}^b x) \end{pmatrix} \right] \quad (7.5.10a)$$

$$\phi_{-1} = \frac{i}{\alpha_2 - \alpha_1} \left[\begin{pmatrix} W \exp(ik_{2x}^a x) \\ X \exp(-ik_{2x}^a x) \end{pmatrix} - \begin{pmatrix} Y \exp(ik_{2x}^b x) \\ Z \exp(-ik_{2x}^b x) \end{pmatrix} \right] \quad (7.5.10b)$$

where

$$k_{2x}^a = \left[(1 - \alpha_1 \eta/2)k_2^2 - k_{0z}^2 \right]^{1/2} \quad (7.5.11a)$$

$$k_{2x}^b = \left[(1 - \alpha_2 \eta/2)k_2^2 - k_{0z}^2 \right]^{1/2} \quad (7.5.11b)$$

The constants W, X, Y, and Z are to be determined by the appropriate boundary conditions for specific problems.

A. First-Order Coupled-Mode Equations

First-order coupled-mode equations are easily obtained from (7.5.2) and (7.5.3) by letting

$$\phi_m(x) = \psi_m(x)e^{ik_{mx}x} \quad (7.5.12)$$

where

$$k_{mx} = k_{0x} + mK \sin \gamma \quad (7.5.13)$$

and

$$k_{0x}^2 + k_{0z}^2 = k_2^2 \quad (7.5.14)$$

Neglecting the second-order derivative term, we obtain

$$\frac{d\psi_m(x)}{dx} + i\frac{mK}{2k_{mx}} \left[mK + 2(k_{0x} \cos \gamma + k_{0x} \sin \gamma) \right]$$

$$+ \frac{\eta k_2^2}{4k_{mx}} \left[\psi_{m+1}(x) - \psi_{m-1}(x) \right] = 0 \quad (7.5.15)$$

When $\gamma = 0$, it becomes the differential equation used by Klein and Cook [1967] in their numerical solution by converting (7.5.15) to difference equations.

The Raman-Nath regime is characterized by $\gamma = 0$, $k_{0x} = 0$, $k_{mx} \approx k_2$, and neglecting the ψ_m term in (7.5.15). These conditions are met when a wave is normally incident on a periodic medium with periodicity along the $\hat{z}$ direction and with a very small K. Equation (7.5.15) becomes

$$\frac{d\psi_m(x)}{dx} + \frac{\eta k_2}{4}\left[\psi_{m+1}(x) - \psi_{m-1}(x)\right] = 0 \tag{7.5.16}$$

This equation is identical to the recurrence relation for Bessel functions. Thus

$$\psi_m(x) = J_m(\eta k_2 x/2) \tag{7.5.17}$$

Note that $J_0^2(x) + 2\sum_{m=1}^{\infty} J_m^2(x) = 1$, which is a statement of conservation of energy.

We now assume that only two modes exist, $m = 0$ and $m = -1$. Then (7.5.15) becomes

$$\frac{d\psi_0}{dx} - \frac{\eta k_2^2}{4k_{0x}}\psi_{-1} = 0 \tag{7.5.18a}$$

$$\frac{d\psi_{-1}}{dx} + \frac{K}{4k_{-1x}}\left[K - 2(k_{0x}\cos\gamma + k_{0x}\sin\gamma)\right]\psi_{-1}(x) + \frac{\eta k_2^2}{4k_{-1x}}\psi_0 = 0$$
$$\tag{7.5.18b}$$

In Kogelnik's [1969] treatment of thick holograms, he requires that for transmission holograms $\phi_0(x = 0) = 1$ and $\phi_{-1}(x = 0) = 0$, whereas for reflection holograms $\phi_0(x = 0) = 1$ and $\phi_{-1}(x = d) = 0$, where d is the thickness of the hologram. Only two boundary conditions are required because the two governing equations involve only first-order derivatives.

The Phariseau limit is characterized by $\gamma = 0$ and $k_{0x} = K/2$. This condition occurs when a wave propagates at the Bragg angle in a periodic medium with periodicity along the $\hat{z}$ direction. Noting that from $k_{-1x} = k_{0x}$, we obtain from (7.5.18)

$$k_{0x}\frac{d\psi_0(x)}{dx} = \frac{\eta k_2^2}{4}\psi_{-1}(x) \tag{7.5.19a}$$

$$k_{0x}\frac{d\psi_{-1}(x)}{dx} = -\frac{\eta k_2^2}{4}\psi_0(x) \tag{7.5.19b}$$

Imposing the boundary condition $\psi_0(x = 0) = 1$ and $\psi_{-1}(x = 0) = 0$, we have the solution

$$\psi_0(x) = \cos(\eta k_2^2 x/4k_{0x}) \tag{7.5.20a}$$
$$\psi_{-1}(x) = \sin(\eta k_2^2 x/4k_{0x}) \tag{7.5.20b}$$

Conservation of energy holds for all x since $\psi_0^2(x) + \psi_{-1}^2(x) = 1$.

In order to reduce to the first-order coupled-mode equations used by Kogelnik and Shank [1972] in their treatment of distributed feedback devices, we let $\gamma = \pi/2$, $k_{mx} = 0$, and $k_{0x} = k_2$. This occurs when the spatial periodicity is along the $\hat{x}$ direction and the wave is also propagating along the $\hat{x}$ direction. We let

$$E(x, z) = \Psi_0(x)e^{i(K/2)x} + \Psi_{-1}(x)e^{-i(K/2)x} \qquad (7.5.21)$$

Substituting in (7.5.2), and neglecting the second-order derivative term, we have

$$\Psi_0'(x) - (2i/K)(k_2^2 - K^2/4)\Psi_0(x) + (\eta k_2^2/K)\Psi_{-1}(x) = 0 \quad (7.5.22a)$$
$$-\Psi_{-1}'(x) - (2i/K)(k_2^2 - K^2/4)\Psi_{-1}(x) + (\eta k_2^2/K)\Psi_0(x) = 0 \quad (7.5.22b)$$

This set of coupled-mode equations has been extensively studied by Kogelnik and Shank. The wavenumber $k_2 = \omega(\mu\epsilon)^{1/2}$ is made a variable that corresponds to a changing angular frequency ω. Right at the first Bragg frequency, $k_2 = K/2$ and (7.5.22) becomes the coupled equations shown in (7.5.19).

B. Reflection and Transmission by Periodically-Modulated Slab

Consider a periodic slab medium with thickness d [Fig. 7.5.1]. A plane wave is incident at the slab with wave vector $\overline{k} = \hat{x}k_x + \hat{z}k_{0z}$, where $k_{0z} = k_1\sin\theta$, $k_1 = \omega(\mu\epsilon_1)^{1/2}$, and θ is the angle of incidence. The electric field for the reflected wave takes the form

$$E_y = E_0 \exp(ik_{1x}^a x + ik_{0z}z) + R_0 \exp(-ik_{1x}^a x + ik_{0z}z)$$
$$+ R_{-1} \exp(-k_{1x}^b x + ik_{-1x}z) \qquad (7.5.23)$$

where

$$k_{1x}^a = (k_1^2 - k_{0z}^2)^{1/2} \qquad (7.5.24a)$$
$$k_{1x}^b = (k_1^2 - k_{-1z}^2)^{1/2} \qquad (7.5.24b)$$

and R_0 and R_1 are the reflection coefficients for the zeroth- and the first-order modes. The transmitted wave takes the form

$$E_y = T_0 \exp[ik_{3x}^a + ik_{0z}z] + T_{-1} \exp[ik_{3x}^b x + ik_{-1z}z] \qquad (7.5.25)$$

where

$$k_{3x}^a = (k_3^2 - k_{0z}^2)^{1/2} \tag{7.5.26a}$$
$$k_{3x}^b = (k_3^2 - k_{-1x}^2)^{1/2} \tag{7.5.26b}$$

and T_0 and T_{-1} are the transmission coefficients for the zeroth- and the first-order modes.

Inside the slab medium, the electric field E_y takes the form

$$
\begin{aligned}
E_y &= \phi_0 e^{ik_{0z}z} + i\phi_{-1}e^{ik_{-z}z} \\
&= [1/(\alpha_2 - \alpha_1)] \\
&\quad \cdot (\alpha_2 W e^{ik_{2x}^a x} + \alpha_2 X e^{-ik_{2x}^a x} - \alpha_1 Y e^{ik_{2x}^b x} - \alpha_1 Z e^{-ik_{2x}^b x})e^{ik_{0z}z} \\
&\quad - [1/(\alpha_2 - \alpha_1)](W e^{ik_{2x}^a x} + X e^{-ik_{2x}^a x} - Y e^{ik_{2x}^b x} - Z e^{-ik_{2x}^b x})e^{ik_{-1z}z}
\end{aligned}
\tag{7.5.27}
$$

Thus we have a total of eight constants R_0, R_{-1}, T_0, T_{-1}, W, X, Y, and Z to be determined by the boundary conditions, which require that the tangential electric and magnetic fields be continuous at the boundaries $x = 0$ and $x = d$. The tangential magnetic field H_z is determined from E_y by using the Maxwell equation

$$H_z = \frac{1}{i\omega\mu}\frac{\partial}{\partial x}E_y \tag{7.5.28}$$

The four boundary conditions must be met for all z. This results in eight linear simultaneous equations to be solved for the unknown coefficients.

After considerable algebra, we obtain the transmission and reflection coefficients as follows:

$$T_0 = \frac{4(\alpha_2 - \alpha_1)k_{1x}^a(\alpha_1 A_{bb} - \alpha_2 B_{bb})e^{-ik_{3x}^a d}}{(\alpha_2 A_{aa} - \alpha_1 B_{aa})(\alpha_1 A_{bb} - \alpha_2 B_{bb}) - \alpha_1\alpha_2(A_{ab} - B_{ab})(A_{ba} - B_{ba})}$$

$$\tag{7.5.29}$$

$$T_{-1} = \frac{4(\alpha_2 - \alpha_1)k_{1x}^a(A_{ba} - B_{ba})e^{-ik_{3x}^b d}}{(\alpha_2 A_{aa} - \alpha_1 B_{aa})(\alpha_1 A_{bb} - \alpha_2 B_{bb}) - \alpha_1\alpha_2(A_{ab} - B_{ab})(A_{ba} - B_{ba})}$$

$$\tag{7.5.30}$$

$$R_0 = \frac{\alpha_1\alpha_2(\alpha_{ab} - \beta_{ab})(A_{ba} - B_{ba}) - (\alpha_2\alpha_{aa} - \alpha_1\beta_{aa})(\alpha_1 A_{bb} - \alpha_2 B_{bb})}{(\alpha_2 A_{aa} - \alpha_1 B_{aa})(\alpha_1 A_{bb} - \alpha_2 B_{bb}) - \alpha_1\alpha_2(A_{ab} - B_{ab})(A_{ba} - B_{ba})}$$

$$(7.5.31)$$

$$R_{-1} = \frac{(\alpha_2 A_{aa} - \alpha_1 B_{aa})(\alpha_{ab} - \beta_{ab}) - (A_{ab} - B_{ab})(\alpha_2\alpha_{aa} - \alpha_1\beta_{aa})}{(\alpha_2 A_{aa} - \alpha_1 B_{aa})(\alpha_1 A_{bb} - \alpha_2 B_{bb}) - \alpha_1\alpha_2(A_{ab} - B_{ab})(A_{ba} - B_{ba})}$$

$$(7.5.32)$$

where

$$A_{\rho\sigma} = k_{2x}^a\left(1 + \frac{k_{1x}^\rho}{k_{2x}^a}\right)\left(1 + \frac{k_{3x}^\rho}{k_{2x}^a}\right)(e^{-ik_{2x}^a d} - R_{21}^{a\rho}R_{23}^{a\sigma}e^{ik_{2x}^a d}) \qquad (7.5.33)$$

$$B_{\rho\sigma} = k_{2x}^b\left(1 + \frac{k_{1x}^\rho}{k_{2x}^b}\right)\left(1 + \frac{k_{3x}^\rho}{k_{2x}^b}\right)(e^{-ik_{2x}^b d} - R_{21}^{b\rho}R_{23}^{b\sigma}e^{ik_{2x}^b d}) \qquad (7.5.34)$$

$$\alpha_{\rho\sigma} = k_{2x}^a\left(1 + \frac{k_{1x}^\rho}{k_{2x}^a}\right)\left(1 + \frac{k_{3x}^\rho}{k_{2x}^a}\right)(R_{21}^{a\rho}e^{-ik_{2x}^a d} - R_{23}^{a\sigma}e^{ik_{2x}^a d}) \qquad (7.5.35)$$

$$\beta_{\rho\sigma} = k_{2x}^b\left(1 + \frac{k_{1x}^\rho}{k_{2x}^b}\right)\left(1 + \frac{k_{3x}^\rho}{k_{2x}^b}\right)(R_{21}^{b\rho}e^{-ik_{2x}^b d} - R_{23}^{b\sigma}e^{ik_{2x}^b d}) \qquad (7.5.36)$$

$$R_{ij}^{\rho\alpha} = \frac{k_{ix}^\rho - k_{jx}^\sigma}{k_{ix}^\rho + k_{jx}^\sigma} \qquad (7.5.37)$$

The superscripts ρ and σ stand for either a or b and the subscripts i and j for 1, 2, or 3.

The solutions (7.5.29)–(7.5.32) reduce to known results in the absence of modulation, where $A_{\rho\sigma} = B_{\rho\sigma}$, $\alpha_{\rho\sigma} = \beta_{\rho\sigma}$, and

$$R_{ij}^{\rho\sigma} = R_{ij} = \frac{1 - k_{jx}/k_{ix}}{1 + k_{jx}/k_{ix}}$$

we have $R_{-1} = T_{-1} = 0$ and

$$R_0 = \frac{-R_{21} + R_{23}e^{i2k_{2x}d}}{1 - R_{21}R_{23}e^{i2k_{2x}^a d}} \qquad (7.5.38)$$

$$T_0 = \frac{4\exp[i(k_{2x} - k_{3x})d]}{(1 + k_{2x}/k_{1x})(1 + k_{3x}/k_{2x})(1 - R_{21}R_{23}e^{i2k_{2x}^a d})} \qquad (7.5.39)$$

It is easily shown that $|R_0|^2 + k_{3x}|T_0|^2/k_{1x} = 1$, which is the statement for power conservation.

When modulation is present but the wave is incident at exactly the Bragg angle, $K_{0z} = K/2$ and $\alpha_1 = -\alpha_2 = 1$. The expressions for the transmission and reflection coefficients can be simplified to read

$$R_0 = \frac{1}{2}(R_a + R_b) \tag{7.5.40}$$

$$R_{-1} = \frac{1}{2}(R_a - R_b) \tag{7.5.41}$$

$$T_0 = \frac{1}{2}(T_a + T_b) \tag{7.5.42}$$

$$T_{-1} = \frac{1}{2}(T_a + T_b) \tag{7.5.43}$$

where

$$R_a = \frac{-R_{21}^a + R_{23}^a e^{i2k_{2x}^a d}}{1 - R_{21}^a R_{23}^a e^{i2k_{2x}^a d}} \tag{7.5.44}$$

$$R_b = \frac{-R_{21}^b + R_{23}^b e^{i2k_{2x}^b d}}{1 - R_{21}^b R_{23}^b e^{i2k_{2x}^b d}} \tag{7.5.45}$$

$$T_a = \frac{4\exp\left[i(k_{2x}^a - k_{3x})d\right]}{(1 + k_{2x}^a/k_{1x})(1 + k_{3x}/k_{2x}^a)(1 - R_{21}^a R_{23}^a e^{i2k_{2x}^a d})} \tag{7.5.46}$$

$$T_b = \frac{4\exp\left[i(k_{2x}^b - k_{3x})d\right]}{(1 + k_{2x}^b/k_{1x})(1 + k_{3x}/k_{2x}^b)(1 - R_{21}^b R_{23}^b e^{i2k_{2x}^b d})} \tag{7.5.47}$$

$$R_{2j}^\sigma = \frac{k_{2x}^\sigma - k_{jx}}{k_{2x}^\sigma + k_{jx}} \tag{7.5.48}$$

$$k_{2x}^a = \left[(1 - \frac{1}{2}\eta)k_2^2 - \frac{1}{4}K^2\right]^{1/2} \tag{7.5.49}$$

$$k_{2x}^b = \left[(1 + \frac{1}{2}\eta)k_2^2 - \frac{1}{4}K^2\right]^{1/2} \tag{7.5.50}$$

We see that the zeroth-order reflection and transmission coefficients are composed of two terms similar to (7.5.38) and (7.5.39); one term corresponds to the result of reflection and transmission by a slab with equivalent permittivity $(1 - \eta/2)^{1/2}\epsilon_2$ and the other term to a slab with permittivity $(1 + \eta/2)^{1/2}\epsilon_2$, as seen from (7.5.49) and (7.5.50).

Notice that the solutions (7.5.44)–(7.5.47) satisfy conservation of energy, since

$$|R_0|^2 + |R_{-1}|^2 + (k_{3x}/k_{1x})(|T_0|^2 + |T_{-1}|^2)$$
$$= \frac{1}{2} \left[|R_a|^2 + (k_{3x}/k_{1x})|T_a|^2 + |R_b|^2 + (k_{3x}/k_{1x})|T_b|^2 \right] = 1 \qquad (7.5.51)$$

This is also observed from (7.5.3), (7.5.6), and (7.5.28) by requiring that the spatial derivative of the time-average Poynting power density in the $\hat{x}$ direction be zero.

C. Far-Field Diffraction of a Gaussian Beam

The electric field intensity of a transmitted Gaussian beam can be determined from Huygens' principle by using the two-dimensional Green's function

$$\overline{E}_t = \hat{y}\frac{\omega\mu}{2\eta} \int_{-\infty}^{\infty} dz' E_{ap}(z') H_0^{(1)} \left\{ k_3 \left[(z - z')^2 + (x - d)^2 \right] \right\} \qquad (7.5.52)$$

where η is $(\mu/\epsilon_2)^{1/2}$, $E_{ap}(z')$ is the aperture field at $x = d$ representing either E_0 or E_{-1}, $k_3 = \omega(\mu\epsilon_3)^{1/2}$, and $H_0^{(1)}$ is the zeroth-order Hankel function of the first kind. In the radiation zone, the Fraunhofer approximation leads to

$$\overline{E} = \hat{y} \left[\frac{k_3}{i2\pi(x - d)} \right]^{1/2} e^{ik_3 x + ik_3 z^2/2x} \int_{-\infty}^{\infty} dz' E_{ap}(z') e^{ik_3 z' \sin\theta}$$

which is essentially the Fourier transform of the aperture field.

We shall calculate the far-field pattern of the zeroth-order beam as

$$P_0(\theta) = \int_{-z_m}^{z_m} dz \, E_0(d, z) e^{-ik_3 z \sin\theta} \qquad (7.5.53)$$

and the far-field pattern of the Bragg-scattered beam as

$$P_{-1}(\theta) = \int_{-z_m}^{z_m} dz \, E_{-1}(d, z) e^{-ik_3 z \sin\theta} \qquad (7.5.54)$$

where θ is the angle of observation measured from the x axis in the

third medium. The fields E_0 and E_{-1} are

$$E_0(x,z) = \int_{-\infty}^{\infty} dk_{0z}\, G(k_{0z})T_0(k_{0z}) \exp[ik_{3x}^a(x-d) + ik_{0z}z]$$

$$x \geq d$$

$$E_{-1}(x,z) = \int_{-\infty}^{\infty} dk_{0z}\, G(k_{0z})T_{-1}(k_{0z}) \exp[ik_{3x}^b(x-d) - ik_{-1z}z]$$

$$x \geq d$$

In (7.5.53) and (7.5.54), $z_m = d\tan\theta_B + w_0$, where w_0 is the beam width projected along the z axis. This limit is taken because $E_0(d,z;t)$ and $E_{-1}(d,z;t)$ are confined to the region $|z| < d\tan\theta_B + w_0 = z_m$ and the fields are negligibly small for $|z| > z_m$. We have

$$P_0(\theta) = \int_{-z_m}^{z_m} dz \int_{-\infty}^{\infty} dk_{0z}\, G(k_{0z})T_0(k_{0z})e^{ik_{0z}z}\, e^{ik_3 z \sin\theta}$$

$$= \int_{-\infty}^{\infty} G(k_{0z})dk_{0z}\, T_0(k_{0z})2z_m \frac{\sin(k_{0z} - k_3\sin\theta)z_m}{(k_{0z} - k_3\sin\theta)z_m} \quad (7.5.55)$$

$$P_{-1}(\theta) = \int_{-z_m}^{z_m} dz \int_{-\infty}^{\infty} dk_{0z}\, G(k_{0z})T_{-1}(k_{0z})e^{ik_{-1z}z}\, e^{ik_3 z \sin\theta}$$

$$= \int_{-\infty}^{\infty} dk_{0z} G(k_{0z})T_{-1}(k_{0z})2z_m \frac{\sin\left\{(k_3\sin\theta - [k_{0z} - K]\right\}z_m}{\{k_3\sin\theta - [k_{0z} - K]\}z_m}$$

$$(7.5.56)$$

The factor

$$2z_m \frac{\sin(k_{0z} - k_3\sin\theta)z_m}{(k_{0z} - k_3\sin\theta)z_m}$$

effectively confines the far-field pattern $P_0(\theta)$ into a small angular range centered at the first Bragg angle $\theta = \theta_B = \sin^{-1}(\lambda/2\Lambda\sqrt{\epsilon_3})$. Similarly, the factor

$$2z_m \frac{\sin\left\{k_3\sin\theta - [k_{0z} - K]\right\}z_m}{\{k_3\sin\theta - [k_{0z} - K]\}z_m}$$

effectively confines the far-field pattern $P_{-1}(\theta)$ into a small angular range centered at the negative first Bragg angle $\theta = -\theta_B$. It should be noted that both factors reduce to Dirac delta functions as $z_m \to \infty$ and the results in (7.5.55) and (7.5.56) become simply $2\pi GT_0$ and $2\pi GT_{-1}$.

D. Two-Dimensional Photonic Crystals

Consider a photonic crystal with permittivity

$$\epsilon/\epsilon_o = 1 + \Gamma_P \exp(i\overline{P} \cdot \overline{r})$$

where $\overline{P}$ is the periodicity. We write the electric field as

$$\overline{E} = \sum_P E_P e^{i\overline{P} \cdot \overline{r}} e^{i\overline{K} \cdot \overline{r}} e^{-i\omega t} = \sum_P \overline{E}_P e^{i\overline{K}_P \cdot \overline{r}} e^{-i\omega t}$$

and a similar expression for $\overline{D}$ and $\overline{H}$, where $\overline{K}_P = \overline{K} + \overline{P}$. Noting that $\overline{K}_{P'} + \overline{P} = \overline{K}_{P'+P}$, and $\sum_j \sum_k A_j B_k C_{j+k} = \sum_\ell \sum_k A_{\ell-k} B_k C_\ell$, we find

$$\sum_P \overline{D}_P e^{i\overline{K}_P \cdot \overline{r}} = \epsilon_o \left[1 + \sum_{P'} \Gamma_{P'} e^{i\overline{P'} \cdot \overline{r}} \right] \sum_P \overline{E}_P e^{i\overline{K}_P \cdot \overline{r}}$$

$$= \epsilon_o \sum_P \overline{E}_P e^{i\overline{K}_P \cdot \overline{r}} + \epsilon_o \sum_{P'} \sum_N \Gamma_{P'} \overline{E}_N e^{i\overline{K}_{N+P'} \cdot \overline{r}}$$

$$= \epsilon_o \sum_P \overline{E}_P e^{i\overline{K}_P \cdot \overline{r}} + \epsilon_o \sum_P \sum_N \Gamma_{P-N} \overline{E}_N e^{i\overline{K}_P \cdot \overline{r}}$$

which gives

$$\overline{D}_P = \epsilon_o \overline{E}_P + \epsilon_o \sum_N \Gamma_{P-N} \overline{E}_N$$

$$= \epsilon_o (1 + \Gamma_0) \overline{E}_P + \epsilon_o \sum_{N \neq P} \Gamma_{P-N} \overline{E}_N$$

Maxwell equations give

$$\overline{K}_M \times (\overline{K}_M \times \overline{E}_M) = \omega \mu_o (\overline{K}_M \times \overline{H}_M) = -\omega^2 \mu_o \overline{D}_M$$

$$= -\omega^2 \mu_o \epsilon_o [(1 + \Gamma_0) \overline{E}_M + \sum_{N \neq M} \Gamma_{M-N} \overline{E}_N]$$

$$[k^2(1 + \Gamma_0) - \overline{K}_M \cdot \overline{K}_M] \overline{E}_M + \overline{K}_M (\overline{K}_M \cdot \overline{E}_M) = -k^2 \sum_{M \neq N} \Gamma_{M-N} \overline{E}_N$$

Consider TE polarization,

$$[k^2(1 + \Gamma_0) - \overline{K}_0 \cdot \overline{K}_0] \overline{E}_0 = -k^2 \Gamma_{-P} \overline{E}_P \qquad (7.5.57a)$$

$$[k^2(1 + \Gamma_0) - \overline{K}_P \cdot \overline{K}_P] \overline{E}_P = -k^2 \Gamma_P \overline{E}_0 \qquad (7.5.57b)$$

We write the left hand sides of (7.5.57) as

$$[k^2(1+\Gamma_0) - \overline{K}_0 \cdot \overline{K}_0] = [k\sqrt{1+\Gamma_0} + (\overline{K}_0 \cdot \overline{K}_0)^{1/2}]$$
$$[k\sqrt{1+\Gamma_0} - (\overline{K}_0 \cdot \overline{K}_0)^{1/2}] \approx [2k\sqrt{1+\Gamma_0}]\kappa_0$$
$$[k^2(1+\Gamma_0) - \overline{K}_P \cdot \overline{K}_P] = [k\sqrt{1+\Gamma_0} + (\overline{K}_P \cdot \overline{K}_P)^{1/2}]$$
$$[k\sqrt{1+\Gamma_0} - (\overline{K}_P \cdot \overline{K}_P)^{1/2}] \approx [2k\sqrt{1+\Gamma_0}]\kappa_P$$

where

$$[k\sqrt{1+\Gamma_0} + (\overline{K}_0 \cdot \overline{K}_0)^{1/2}] \approx [k\sqrt{1+\Gamma_0} + (\overline{K}_P \cdot \overline{K}_P)^{1/2}]$$
$$\approx [2k\sqrt{1+\Gamma_0}]$$

κ_0 is the difference between $\overline{K}_0$ in the crystal and k corrected by the average value of the dielectric constant $\sqrt{1+\Gamma_0}$. From (7.5.57), we obtain
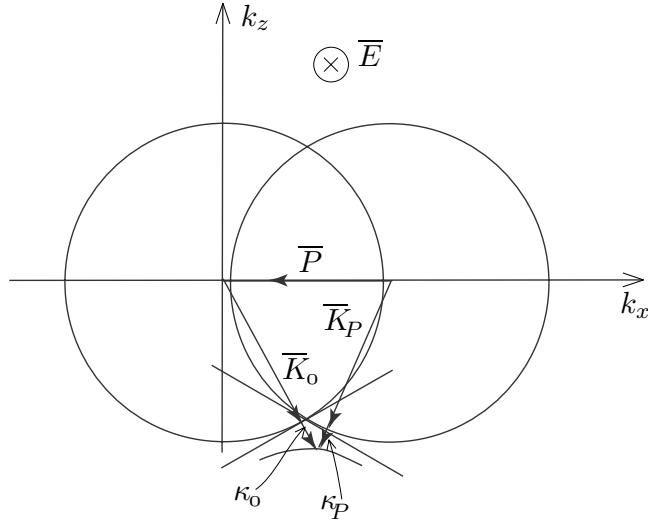
Figure 7.5.2 TE waves.

$$\kappa_0\kappa_P = \frac{k^2}{4}\frac{\Gamma_P\Gamma_{-P}}{1+\Gamma_0} \tag{7.5.58}$$

The product of κ_0 and κ_P is a constant, thus the locus is a hyperbola as shown in Figure 7.5.2.

E. Band Gaps in One-Dimensional Periodical Media

Consider a medium with constitutive relation

$$\epsilon_o \overline{E} = \kappa \overline{D}, \qquad \kappa = \kappa_0 + 2\kappa_1 \cos \frac{2\pi}{a} z$$

From Maxwell Equations

$$\kappa \nabla \times \overline{H} = -i\omega\epsilon_o \overline{E} \qquad (7.5.59)$$

$$\nabla \times \overline{E} = i\omega\mu_o \overline{H} \qquad (7.5.60)$$

we obtain

$$\frac{\omega^2}{c^2}\overline{E} = \kappa \nabla \times \nabla \times \overline{E} \qquad (7.5.61)$$

which yields

$$\frac{\omega^2}{c^2}E_y = -\kappa \frac{\partial^2}{\partial z^2}E_y \qquad (7.5.62)$$

We write E_y in the following form:

$$E_y = \sum_{m=-\infty}^{\infty} E_m \exp\{i(k + \frac{2m\pi}{a})z\} \qquad (7.5.63)$$

Substituting into (7.5.62), we find

$$\frac{\omega^2}{c^2}E_y = \kappa(k + \frac{2m\pi}{a})^2 \sum_{m=-\infty}^{\infty} E_m \exp\{i(k + \frac{2m\pi}{a})z\} \qquad (7.5.64)$$

We thus find

$$\{\frac{\omega^2}{c^2} - \kappa_0(k + \frac{2m\pi}{a})^2\}E_m$$

$$= \kappa_1(k + \frac{2(m-1)\pi}{a})^2 E_{m-1} + \kappa_1(k + \frac{2(m+1)\pi}{a})^2 E_{m+1} \quad (7.5.65)$$

Let $m = -1, 0, 1$, we obtain

$$\{\frac{\omega^2}{c^2} - \kappa_0(k - \frac{2\pi}{a})^2\}E_{-1} = \kappa_1(k - \frac{4\pi}{a})^2 E_{-2} + \kappa_1 k^2 E_0 \qquad (7.5.66)$$

$$\{\frac{\omega^2}{c^2} - \kappa_0 k^2\}E_0 = \kappa_1(k - \frac{2\pi}{a})^2 E_{-1} + \kappa_1(k + \frac{2\pi}{a})^2 E_1 \qquad (7.5.67)$$

$$\{\frac{\omega^2}{c^2} - \kappa_0(k + \frac{2\pi}{a})^2\}E_1 = \kappa_1 k^2 E_0 + \kappa_1(k + \frac{4\pi}{a})^2 E_2 \qquad (7.5.68)$$

Consider the interaction of E_0 and E_{-1} by retaining only two terms:

$$E_y = E_0 e^{ikz} + E_{-1} e^{i(k - \frac{2\pi}{a})z} \tag{7.5.69}$$

From (7.5.66) and (7.5.67), we find

$$\{\frac{\omega^2}{c^2} - \kappa_0(k - \frac{2\pi}{a})^2\}E_{-1} = \kappa_1 k^2 E_0 \tag{7.5.70}$$

$$\{\frac{\omega^2}{c^2} - \kappa_0 k^2\}E_0 = \kappa_1(k - \frac{2\pi}{a})^2 E_{-1} \tag{7.5.71}$$

For $k = \pi/a$

$$[\frac{\omega^2}{c^2} - \kappa_0(\frac{\pi}{a})^2]E_{-1} = \kappa_1(\frac{\pi}{a})^2 E_0$$

$$[\frac{\omega^2}{c^2} - \kappa_0(\frac{\pi}{a})^2]E_0 = \kappa_1(\frac{\pi}{a})^2 E_{-1}$$
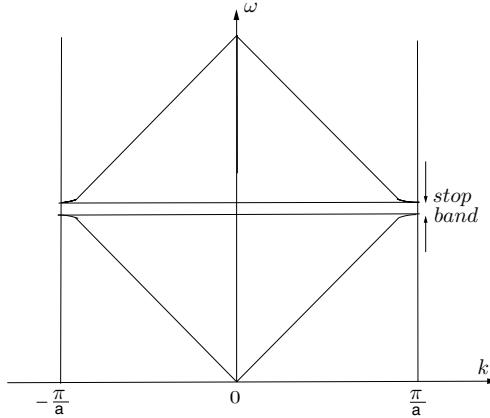
Figure 7.5.3　Bandgap formation.

We find $\omega = \sqrt{\kappa_0 \pm \kappa_1}\, c\pi/a$ and a stop band gap is formed [Fig. 7.5.3]. Thus $E_{-1} = \pm E_0$ and

$$E_y = E_0[e^{i\frac{\pi}{a}z} \pm e^{-i\frac{\pi}{a}z}]e^{-i\sqrt{\kappa_0 \pm \kappa}\,\pi ct/a} \tag{7.5.72}$$

The two standing waves are peaked at $z = 0$ and $z = a/2$.

Problems

P7.5.1

Consider TM wave propagation in a crystal with permittivity

$$\epsilon/\epsilon_o = 1 - \omega_p^2/\omega^2 = 1 - e^2\rho(\overline{r})/m\epsilon_o\omega^2 = 1 - \Gamma\sum_H F_H\exp(-2\pi i\overline{H}\cdot\overline{r})$$

where $\Gamma = e^2/m\epsilon_o\omega^2 V$ and the electron density

$$\rho(\overline{r}) = (1/V)\sum_H F_H\exp(-2\pi i\overline{H}\cdot\overline{r})$$

where

$$F_H = \sum_n f_n\exp(2\pi i\overline{H}\cdot\overline{r}_n)$$

Find an expression similar to (7.5.58).
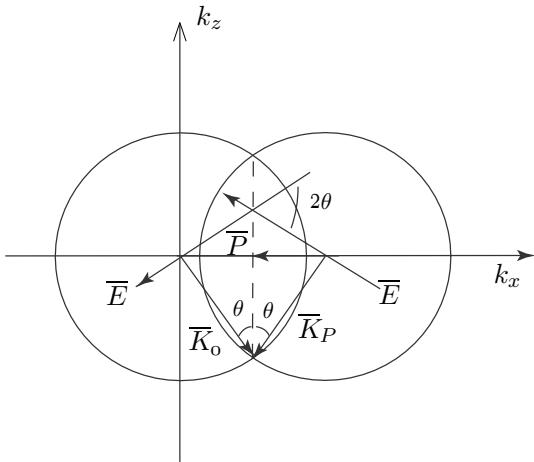
Figure P7.5.1.1 TM waves.

P7.5.2

Consider diffraction by a slab of photonic crystal at the Bragg angle of incidence. The two diffracted rays at the exit plan depends on the thickness of the slab and determined by $\overline{K}_0$ and $\overline{K}_P$. The phenomenon is known as pendellösung. Make use of (7.5.58)

$$\kappa_0\kappa_P = \frac{k^2}{4}\frac{\Gamma_P\Gamma_{-P}}{1+\Gamma_0}$$
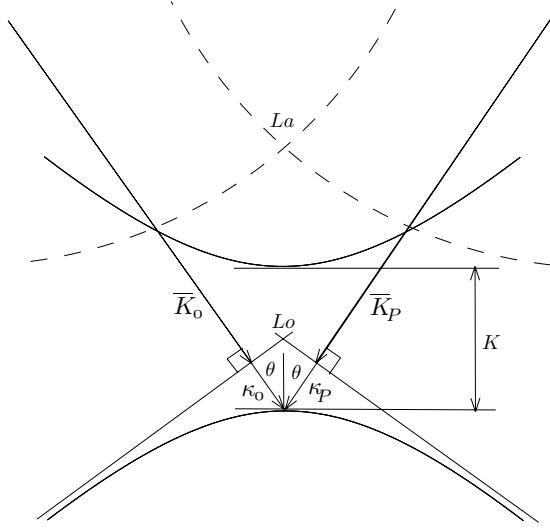
Figure P7.5.2.1 Pendellösung.

and Figure P7.5.2.1, determine the unit of the thickness of the slab such that the ray varies between $\overline{K}_0$ and $\overline{K}_P$.

P7.5.3

Consider a medium with constitutive relation

$$\overline{E} = \kappa \overline{D}, \qquad \kappa = \kappa_0 + 2\kappa \cos \frac{2\pi}{a} z$$

From Maxwell Equations, show that

$$\nabla \times \kappa \nabla \times \overline{H} = \frac{\omega^2}{c^2} \overline{H}$$

Write H_y in the following form:

$$H_y = \sum_{m=-\infty}^{\infty} H_m \exp\{i[(k + \frac{2m\pi}{a})z - \omega t]\}$$

determine wave behavior at $k = \pi/a$.

7.6   Scattering by Random Media

In the remote sensing of earth terrain media such as snow, ice, and vegetation canopy, the model of a layered medium is often used. In order to account for the scattering from such layered media, its volume-scattering effects are characterized by a permittivity with a randomly fluctuating part. We write

$$\epsilon_1(\overline{r}) = \epsilon_1 + \epsilon_{1f}(\overline{r}) \tag{7.6.1}$$

where ϵ_{1f} is the randomly fluctuating part of the permittivity and ϵ_1 is the mean permittivity such that the ensemble average $< \epsilon_1(\overline{r}) > = \epsilon_1$. In region 1, the equation governing $\overline{E}_1$ can be written as

$$\nabla \times \nabla \times \overline{E}_1(\overline{r}) - k_1^2 \overline{E}_1(\overline{r}) = Q(\overline{r})\overline{E}_1(\overline{r}) \tag{7.6.2}$$

where $k_1^2 = \omega^2 \mu \epsilon_1$ and $Q(\overline{r}) = \omega^2 \mu \epsilon_{1f}$. Thus the random variable $Q(\overline{r})\overline{E}_1(\overline{r})$ serves as the distributed volume source.

From (7.6.2), the electric field $\overline{E}_1$ in region 1 can be solved in terms of the dyadic Green's function $\overline{\overline{G}}_{11}(\overline{r}, \overline{r}')$

$$\overline{E}_1 = \overline{E}_1^{(0)} + \iiint_{V_1} d^3\overline{r}_1 \, \overline{\overline{G}}_{11}(\overline{r}, \overline{r}_1) \cdot Q(\overline{r}_1)\overline{E}_1(\overline{r}_1) \tag{7.6.3}$$

where V_1 is the volume for region 1 containing ϵ_{1f}, $\overline{\overline{G}}_{11}(\overline{r}, \overline{r}_1)$ is the dyadic Green's function, and $\overline{E}_1^{(0)}$ the zeroth-order solution in the absence of ϵ_{1f}, namely, $\epsilon_{1f} = 0$.

The solution for the electric field in region 0 is

$$\overline{E}_0 = \overline{E}_0^{(0)} + \iiint_{V_1} d^3\overline{r}_1 \, \overline{\overline{G}}_{01}(\overline{r}, \overline{r}_1) \cdot Q(\overline{r}_1)\overline{E}_1(\overline{r}_1) \tag{7.6.4}$$

The first term in (7.6.4) is the zeroth-order solution $\overline{E}_0$ in the absence of ϵ_{1f}, representing the specularly reflected wave, which is also called the coherent component of the total field. The second term is the scattered field $\overline{E}_s$

$$\overline{E}_s(\overline{r}) = \iiint_{V_1} d^3\overline{r}_1 \, \overline{\overline{G}}_{01}(\overline{r}, \overline{r}_1) \cdot Q(\overline{r}_1)\overline{E}_1(\overline{r}_1) \tag{7.6.5}$$

Equation (7.6.5) can be solved with an iterative approach. We assume that the total field can be expanded in terms of a Born series

$$\overline{E}_l = \sum_{n=0}^{\infty} \overline{E}_l^{(n)} \qquad l = 0, 1 \qquad (7.6.6)$$

Substituting in (7.6.4), we find that the n th-order $\overline{E}$ field is determined by the $(n-1)$ th-order field,

$$\overline{E}_s^{(n)} = \iiint_{V_1} d^3\overline{r}_1 \, \overline{\overline{G}}_{01}(\overline{r},\overline{r}_1) \cdot Q(\overline{r}_1)\overline{E}_1^{(n-1)}(\overline{r}_1) \qquad (7.6.7)$$

Notice that $\overline{E}_l^{(n)}$ with $n \neq 0$ are all randomly fluctuating fields.

Forming the absolute square of $\overline{E}_s^{(1)}$ and taking ensemble average, we obtain the first-order scattered intensity

$$< |\overline{E}_s^{(1)}(\overline{r})|^2 > = \iiint_{V_1} d^3\overline{r}_1 \iiint_{V_1} d^3\overline{r}_2 \, \overline{\overline{G}}_{01}(\overline{r},\overline{r}_1) \cdot \overline{E}_1^{(0)}(\overline{r}_1)$$

$$\cdot \overline{\overline{G}}_{01}^*(\overline{r},\overline{r}_2) \cdot \overline{E}_1^{(0)*}(\overline{r}_2) < Q(\overline{r}_1)Q^*(\overline{r}_2) > \quad (7.6.8)$$

where $< Q(\overline{r}_1)Q^*(\overline{r}_2) >$ is a two-point correlation function. For a statistically homogeneous medium, the correlation function depends only upon the separation of the points $\overline{r}_1$ and $\overline{r}_2$, that is,

$$< Q(\overline{r}_1)Q^*(\overline{r}_2) > = C(\overline{r}_1 - \overline{r}_2) \qquad (7.6.9)$$

Consider the correlation function

$$C(\overline{r}_1 - \overline{r}_2) = \delta |k_1|^4 e^{-|\overline{r}_1 - \overline{r}_2|/r_0} \qquad (7.6.10)$$

where δ is the variance and r_0 the correlation length of the permittivity fluctuations. The variance is related to the strength of fluctuations and the correlation length corresponds roughly to the sizes of the scatterers. We see that major contributions to the scattered-field intensity come from fluctuations separated by no more than a correlation length.

A. Dyadic Green's Function for Layered Media

Consider a layered medium with a source located in region 0. In the absence of the layered medium, the dyadic Green's function is governed by

$$\nabla \times \nabla \times \overline{\overline{G}}(\overline{r}, \overline{r}') - k^2 \overline{\overline{G}}(\overline{r}, \overline{r}') = \overline{\overline{I}} \delta(\overline{r} - \overline{r}') \tag{7.6.11}$$

where we have determined in unbounded space

$$\overline{\overline{G}}(\overline{r}, \overline{r}') = \left[\overline{\overline{I}} + \frac{1}{k^2} \nabla \nabla \right] g(\overline{r}, \overline{r}') \tag{7.6.12}$$

$$g(\overline{r}, \overline{r}') = \frac{e^{ik(\overline{r} - \overline{r}')}}{4\pi |\overline{r} - \overline{r}'|} \tag{7.6.13}$$

Let the source be placed at the origin, $\overline{r}' = 0$. We have

$$(\nabla^2 + k^2) g(\overline{r}) = -\delta(\overline{r}) \tag{7.6.14}$$

Fourier transformation gives

$$\delta(\overline{r}) = \frac{1}{(2\pi)^3} \iiint dk_x \, dk_y \, dk_z \, e^{i\overline{k} \cdot \overline{r}} \tag{7.6.15}$$

$$g(\overline{r}) = \frac{1}{(2\pi)^3} \iiint dk_x \, dk_y \, dk_z \, e^{i\overline{k} \cdot \overline{r}} \, g(\overline{k}) \tag{7.6.16}$$

with

$$g(\overline{k}) = \frac{1}{k_x^2 + k_y^2 + k_z^2 - k^2} \tag{7.6.17}$$

as derived from (7.6.14).

For the triple integral in (7.6.16), we integrate over k_z by noting from (7.6.17) that poles occur at $k_z^2 = k^2 - k_x^2 - k_y^2$. For $z > 0$, we deform the contour upward such that $\text{Im}\{k_z\} > 0$. For $z < 0$, we deform the contour downward. We obtain

$$g(\overline{r}) = \begin{cases} \dfrac{i}{(2\pi)^2} \displaystyle\iint dk_x \, dk_y \, \frac{1}{2k_{0z}} e^{ik_x x + ik_y y + ik_{0z} z} & z > 0 \\[2ex] \dfrac{i}{(2\pi)^2} \displaystyle\iint dk_x \, dk_y \, \frac{1}{2k_{0z}} e^{ik_x x + ik_y y - ik_{0z} z} & z < 0 \end{cases} \tag{7.6.18}$$

where

$$k_{0z} = \sqrt{k^2 - k_x^2 - k_y^2} \tag{7.6.19}$$

To find the expression for $\overline{\overline{G}}(\overline{r})$, we make use of (7.6.12) and notice that there is a discontinuity in $\partial g(\overline{r})/\partial z$ at $z = 0$, which gives

$$\frac{\partial^2}{\partial z^2} g(\overline{r}) = -\delta(\overline{r}) - \begin{cases} \dfrac{i}{(2\pi)^2} \displaystyle\iint dk_x\, dk_y\, \dfrac{k_{0z}}{2} e^{ik_x x + ik_y y + ik_{0z} z} & z > 0 \\[2ex] \dfrac{i}{(2\pi)^2} \displaystyle\iint dk_x\, dk_y\, \dfrac{k_{0z}}{2} e^{ik_x x + ik_y y - ik_{0z} z} & z < 0 \end{cases}$$

$$(7.6.20)$$

We find the expression for $\overline{\overline{G}}(\overline{r})$ to be

$$\overline{\overline{G}}(\overline{r}) = -\hat{z}\hat{z}\frac{1}{k^2}\delta(\overline{r}) + \begin{cases} \dfrac{i}{8\pi^2} \displaystyle\iint dk_x\, dk_y\, \dfrac{1}{k_{0z}} \left[\overline{\overline{I}} - \dfrac{\overline{k}\,\overline{k}}{k^2}\right] e^{i\overline{k}\cdot\overline{r}} & z > 0 \\[2ex] \dfrac{i}{8\pi^2} \displaystyle\iint dk_x\, dk_y\, \dfrac{1}{k_{0z}} \left[\overline{\overline{I}} - \dfrac{\overline{K}\,\overline{K}}{k^2}\right] e^{i\overline{K}\cdot\overline{r}} & z < 0 \end{cases}$$

$$(7.6.21)$$

where

$$\overline{k} = \hat{x}k_x + \hat{y}k_y + \hat{z}k_{0z} \qquad\qquad (7.6.22)$$

$$\overline{K} = \hat{x}k_x + \hat{y}k_y - \hat{z}k_{0z} \qquad\qquad (7.6.23)$$

Recognizing that $\hat{k} = \overline{k}/k$, we form an orthonormal system consisting of unit vectors $\hat{k}$, $\hat{h}(k_{0z})$, and $\hat{e}(k_{0z})$ as follows:

$$\hat{e}(k_{0z}) = \frac{\hat{k} \times \hat{z}}{|\hat{k} \times \hat{z}|} = \frac{(\hat{x}k_y - \hat{y}k_x)}{\sqrt{k_x^2 + k_y^2}} \qquad\qquad (7.6.24)$$

$$\hat{h}(k_{0z}) = \frac{1}{k}\hat{e} \times \overline{k} = \frac{-k_{0z}}{k\sqrt{k_x^2 + k_y^2}}(\hat{x}k_x + \hat{y}k_y) + \hat{z}\frac{\sqrt{k_x^2 + k_y^2}}{k} \qquad (7.6.25)$$

As $\overline{\overline{I}} = \hat{k}\hat{k} + \hat{e}\hat{e} + \hat{h}\hat{h}$, we have $\overline{\overline{I}} - \hat{k}\hat{k} = \hat{e}\hat{e} + \hat{h}\hat{h}$. The dyadic Green's

function $\overline{\overline{G}}(\overline{r}, \overline{r}')$, after translating the origin to $\overline{r}'$, becomes

$$\overline{\overline{G}}(\overline{r}, \overline{r}') = -\hat{z}\hat{z}\frac{1}{k^2}\delta(\overline{r} - \overline{r}')$$

$$+ \begin{cases} \dfrac{i}{8\pi^2} \iint dk_x\, dk_y\, \dfrac{1}{k_{0z}} \left\{ \left[\hat{e}(k_{0z})e^{i\overline{k}\cdot\overline{r}} \right] \hat{e}(k_{0z})e^{-i\overline{k}\cdot\overline{r}'} \right. \\ \qquad\qquad\qquad \left. + \left[\hat{h}(k_{0z})e^{i\overline{k}\cdot r} \right] \hat{h}(k_{0z})e^{-i\overline{k}\cdot\overline{r}'} \right\} \qquad z > z' \\[2em] \dfrac{i}{8\pi^2} \iint dk_x\, dk_y\, \dfrac{1}{k_{0z}} \left\{ \left[\hat{e}(-k_{0z})e^{i\overline{K}\cdot\overline{r}} \right] \hat{e}(-k_{0z})e^{-i\overline{K}\cdot\overline{r}'} \right. \\ \qquad\qquad\qquad \left. + \left[\hat{h}(-k_{0z})e^{i\overline{K}\cdot r} \right] \hat{h}(-k_{0z})e^{-i\overline{K}\cdot\overline{r}'} \right\} \quad z < z' \end{cases}$$

$$(7.6.26)$$

where $\hat{K} = \overline{K}/k$, $\hat{e}(-k_{0z}) = \hat{e}(k_{0z})$, and $\hat{h}(-k_{0z}) = \hat{e} \times \overline{K}/k$ form another orthonormal set of unit vectors about the wave vector $\overline{K}$.

To derive the dyadic Green's function $\overline{\overline{G}}_{l0}(\overline{r}, \overline{r}')$ for a layered medium, we use the first subscript l to denote the region of the observation point and the second subscript 0 to indicate that the source is in region 0. To facilitate the matching of the boundary conditions, we consider, for the Green's function $\overline{\overline{G}}(\overline{r}, \overline{r}')$, only $z < z'$ and thus neglect the delta function term. We write

$$\overline{\overline{G}}_{00}(\overline{r}, \overline{r}') = \frac{i}{8\pi^2} \iint dk_x\, dk_y\, \frac{1}{k_{0z}} \left\{ \left[\hat{e}(-k_{0z})e^{i\overline{K}\cdot\overline{r}} \right. \right.$$

$$+ R^{\text{TE}}\hat{e}(k_{0z})e^{i\overline{k}\cdot\overline{r}} \left] \hat{e}(-k_{0z})e^{-i\overline{K}\cdot\overline{r}'} + \left[R^{\text{TM}}\hat{h}(k_{0z})e^{i\overline{k}\cdot\overline{r}} \right.$$

$$+ \left. \hat{h}(-k_{0z})e^{i\overline{K}\cdot\overline{r}} \right] \hat{h}(-k_{0z})e^{-i\overline{K}\cdot\overline{r}'} \right\} \qquad \text{for } z < z' \qquad (7.6.27)$$

$$\overline{\overline{G}}_{l0}(\overline{r}, \overline{r}') = \frac{i}{8\pi^2} \iint dk_x\, dk_y\, \frac{1}{k_{0z}}$$

$$\left\{ \left[B_l\hat{e}_l(-k_{lz})e^{i\overline{K}_l\cdot\overline{r}} + A_l\hat{e}_l(k_{lz})e^{i\overline{k}_l\cdot\overline{r}} \right] \hat{e}(-k_{0z})e^{-i\overline{K}\cdot\overline{r}'} \right.$$

$$+ \left. \left[C_l\hat{h}_l(k_{lz})e^{i\overline{k}_l\cdot\overline{r}} + D_l\hat{h}_l(-k_{lz})e^{i\overline{K}_l\cdot\overline{r}} \right] \hat{h}(-k_{0z})e^{-i\overline{K}\cdot\overline{r}'} \right\} \quad (7.6.28)$$

$$\overline{\overline{G}}_{t0}(\overline{r}, \overline{r}') = \frac{i}{8\pi^2} \iint dk_x\, dk_y\, \frac{1}{k_{0z}} \left\{ T^{\text{TE}}\, \hat{e}_t(-k_{tz})e^{i\overline{K}_t\cdot\overline{r}}\, \hat{e}(-k_{0z})e^{-i\overline{K}\cdot\overline{r}'} \right.$$

$$+ \left. T^{\text{TM}}\, \hat{h}_t(-k_{tz})e^{i\overline{K}_t\cdot\overline{r}}\, \hat{h}(-k_{0z})e^{-i\overline{K}\cdot\overline{r}'} \right\} \qquad (7.6.29)$$

where

$$k_{lz} = \sqrt{k_l^2 - k_x^2 - k_y^2} \qquad\qquad (7.6.30)$$

$$\overline{k}_l = \hat{x}k_x + \hat{y}k_y + \hat{z}k_{lz} \tag{7.6.31}$$

$$\overline{K}_l = \hat{x}k_x + \hat{y}k_y - \hat{z}k_{lz} \tag{7.6.32}$$

The coefficients A_l, B_l, C_l and D_l are then determined by the boundary conditions.

   To simplify the algebra, we consider a two-layer medium where $t = 2$. The procedure will be easily generalized to that for a general layered medium. With boundaries at $z = 0$ and $z = -d$, we impose the boundary conditions of continuity of $\hat{z} \times \overline{\overline{G}}$ and $\hat{z} \times \nabla \times \overline{\overline{G}}/\mu$ corresponding to continuity of the tangential $\overline{E}$ and $\overline{H}$ fields. We find

$$R^{\text{TE}} + 1 = A_1 + B_1 \tag{7.6.33}$$

$$\frac{k_{0z}}{k}(R^{\text{TM}} - 1) = \frac{k_{1z}}{k_1}(C_1 - D_1) \tag{7.6.34}$$

$$k_{0z}(R^{\text{TE}} - 1) = k_{1z}(A_1 - B_1) \tag{7.6.35}$$

$$k(R^{\text{TM}} + 1) = k_1(C_1 + D_1) \tag{7.6.36}$$

and

$$A_1 e^{-ik_{1z}d} + B_1 e^{ik_{1z}d} = T^{\text{TE}} e^{ik_{2z}d} \tag{7.6.37}$$

$$\frac{k_{1z}}{k_1}(C_1 e^{-ik_{1z}d} - D_1 e^{ik_{1z}d}) = -\frac{k_{2z}}{k_2} T^{\text{TM}} e^{ik_{2z}d} \tag{7.6.38}$$

$$k_{1z}(A_1 e^{-ik_{1z}d} - B_1 e^{ik_{1z}d}) = -k_{2z} T^{\text{TE}} e^{ik_{2z}d} \tag{7.6.39}$$

$$k_1(C_1 e^{-ik_{1z}d} + D_1 e^{ik_{1z}d}) = k_2 T^{\text{TM}} e^{ik_{2z}d} \tag{7.6.40}$$

Solving (7.6.33)–(7.6.40), we obtain all eight unknown wave amplitudes. In particular,

$$\overline{\overline{G}}_{10}(\overline{r}, \overline{r}') = \frac{i}{8\pi} \iint dk_x \, dk_y \, \frac{1}{k_{1z}}$$
$$\left\{ \frac{T_{10}^{\text{TE}}}{D_2(k_\perp)} \left[R_{12}^{\text{TE}} e^{i2k_{1z}d} \hat{e}_1(k_{1z}) e^{i\overline{k}_1 \cdot \overline{r}} + \hat{e}_1(-k_{1z}) e^{i\overline{K}_1 \cdot \overline{r}} \right] \hat{e}(-k_{0z}) e^{-i\overline{K} \cdot \overline{r}'} \right.$$
$$\left. + \frac{k_1}{k} \frac{T_{10}^{\text{TM}}}{F_2(k_\perp)} \left[R_{12}^{\text{TM}} e^{i2k_{1z}d} \hat{h}_1(k_{1z}) e^{i\overline{k}_1 \cdot \overline{r}} + \hat{h}_1(-k_{1z}) e^{i\overline{K}_1 \cdot \overline{r}} \right] \hat{h}(-k_{0z}) e^{-i\overline{K} \cdot \overline{r}'} \right\}$$

$$\tag{7.6.41}$$

where

$$T_{10}^{\text{TE}} = 1 + R_{10}^{\text{TE}} = \frac{2k_{1z}}{k_z + k_{1z}} \tag{7.6.42}$$

$$T_{10}^{\text{TM}} = 1 + R_{10}^{\text{TM}} = \frac{2\epsilon k_{1z}}{\epsilon_1 k_z + \epsilon k_{1z}} \tag{7.6.43}$$

$$D_2(k_\perp) = 1 + R_{01}^{\text{TE}} R_{12}^{\text{TE}} e^{i2k_{1z}d} \tag{7.6.44}$$

$$F_2(k_\perp) = 1 + R_{01}^{\text{TM}} R_{12}^{\text{TM}} e^{i2k_{1z}d} \tag{7.6.45}$$

$$R_{12}^{\text{TE}} = \frac{k_{1z} - k_{2z}}{k_{1z} + k_{2z}} \tag{7.6.46}$$

$$R_{12}^{\text{TM}} = \frac{\epsilon_2 k_{1z} - \epsilon_1 k_{2z}}{\epsilon_2 k_{1z} + \epsilon_1 k_{2z}} \tag{7.6.47}$$

For latter applications we shall be interested in $\overline{\overline{G}}_{01}(\overline{r}, \overline{r}')$ for observation point in region 0 and source in region 1. The symmetric property for dyadic Green's functions calls for [Tai, 1971]

$$\overline{\overline{G}}_{01}(\overline{r}, \overline{r}') = \overline{\overline{G}}_{10}^T(\overline{r}', \overline{r}) \tag{7.6.48}$$

We transpose $\overline{\overline{G}}_{10}$ and change $k_x \to -k_x$, and $k_y = -k_y$. From (7.6.24)–(7.6.25) we also have $\hat{e}(k_{0z}) \to \hat{e}(-k_{0z})$ and $\hat{h}(k_{0z}) \to \hat{h}(-k_{0z})$. Equation (7.6.41) then gives

$$\overline{\overline{G}}_{01}(\overline{r}, \overline{r}') = \iint d\overline{k}_\perp \, \overline{\overline{g}}_{01}(\overline{k}_\perp, z, z') e^{i\overline{k}_\perp \cdot (\overline{r}_\perp - \overline{r}'_\perp)} \tag{7.6.49}$$

where

$$\overline{\overline{g}}_{01}(\overline{k}_\perp, z, z') = \frac{i}{8\pi^2} \frac{e^{ik_z z}}{k_{1z}}$$

$$\left\{ \frac{T_{10}^{\text{TE}}}{D_2(k_\perp)} \hat{e}(k_{0z}) \left[R_{12}^{\text{TE}} e^{i2k_{1z}d} \, \hat{e}_1(-k_{1z}) e^{ik_{1z}z'} + \hat{e}_1(k_{1z}) e^{-ik_{1z}z'} \right] \right.$$

$$\left. + \frac{k_1}{k} \frac{T_{10}^{\text{TM}}}{F_2(k_\perp)} \hat{h}(k_{0z}) \left[R_{12}^{\text{TM}} e^{i2k_{1z}d} \, \hat{h}_1(-k_{1z}) e^{ik_{1z}z'} + \hat{h}_1(k_{1z}) e^{-ik_{1z}z'} \right] \right\} \tag{7.6.50}$$

The integration in (7.6.49) can be evaluated for the radiation field with a two-dimensional stationary-phase method [Born and Wolf, 1970]. As $kr \to \infty$, the dominant term in (7.6.49) is

$$e^{i\overline{k}\cdot\overline{r}} = \exp\left[i(k_x x + k_y y + \sqrt{k^2 - k_x^2 - k_y^2} \, z) \right]$$

With the observation point at $x = r\sin\theta\cos\phi$, $y = r\sin\theta\sin\phi$, and $z = r\cos\theta$, the stationary-phase points are found to be

$$k_x = k\sin\theta\cos\phi$$
$$k_y = k\sin\theta\sin\phi$$

The dyadic Green's function $\overline{\overline{G}}_{01}(\overline{r}, \overline{r}')$ is then determined. We obtain

$$\overline{\overline{G}}_{01}(\overline{r}, \overline{r}') = \frac{e^{ikr}}{4\pi r}\left\{\left[\frac{T_{01}^{\mathrm{TE}}}{D_2}\hat{e}(k_{0z})\hat{e}_1(k_{1z}) + \frac{k}{k_1}\frac{T_{01}^{\mathrm{TM}}}{F_2}\hat{h}(k_{0z})\hat{h}_1(k_{1z})\right]e^{-i\overline{k}_1\cdot\overline{r}'}\right.$$
$$+ \left[\frac{T_{01}^{\mathrm{TE}}}{D_2}R_{12}^{\mathrm{TE}}\hat{e}(k_{0z})\hat{e}_1(-k_{1z}) + \frac{k}{k_1}\frac{T_{01}^{\mathrm{TM}}}{F_2}R_{12}^{\mathrm{TM}}\hat{h}(k_{0z})\hat{h}_1(-k_{1z})\right]$$
$$\left.\cdot\, e^{i2k_{1z}d}e^{-i\overline{K}_1\cdot\overline{r}'}\right\} \qquad (7.6.51)$$

with all k_x and k_y equal to the values at the stationary-phase point.

B. Scattering by a Half-Space Random Medium

To illustrate with a half-space random medium, we consider scattered fields in the far-field zone. Let an incident wave be horizontally polarized with

$$\overline{E}_{0i} = \hat{e}(-k_{0zi})E_0\, e^{-ik_{0zi}z}e^{i\overline{k}_{\perp i}\cdot\overline{r}}$$

where $k_{0zi} = k\cos\theta_i$. The unperturbed field in region 1 is

$$\overline{E}_1^{(0)}(\overline{r}) = E_0\, T_{01i}^{\mathrm{TE}}\,\hat{e}_{1i}(k_{1zi})e^{i\overline{k}_{1i}\cdot\overline{r}}$$

where $k_{1zi} = (k_1^2 - k^2\sin^2\theta_i)^{1/2}$ and $\overline{k}_{1i} = \overline{k}_{\perp i} - \hat{z}k_{1zi}$. The subscript i in T_{01i}^{TE} signifies the fact that the k_z values are those in the incident direction. Making use of the far-field dyadic Green's function derived in the last section and simplify to that for a half-space medium, we have

$$\overline{\overline{G}}_{01}(\overline{r}, \overline{r}') = \frac{e^{ikr}}{4\pi r}\left\{T_{01s}^{\mathrm{TE}}\hat{e}(k_{0zs})\hat{e}_1(k_{1zs}) + \frac{k}{k_1}T_{01s}^{\mathrm{TM}}\hat{h}(k_{0zs})\hat{h}_1(k_{1zs})\right\}e^{-i\overline{k}_{1s}\cdot\overline{r}'}$$

with

$$k_{0zs} = \sqrt{k^2 - k_{xs}^2 - k_{ys}^2}$$
$$k_{1zs} = \sqrt{k_1^2 - k_{xs}^2 - k_{ys}^2}$$
$$\overline{k}_{1s} = \overline{k}_{\perp s} + \hat{z}k_{1zs}$$

The first-order scattered field intensity is obtained as follows:

$$
<|\overline{E}_s^{(1)}(\overline{r})|^2> = \frac{|E_0|^2}{16\pi^2 r^2} \left| \left[T_{01s}^{\text{TE}}\, \hat{e}(k_{0zs})\hat{e}_1(k_{1zs}) \right. \right.
$$

$$
\left. \left. + \frac{k}{k_1}\, T_{01s}^{\text{TM}}\, \hat{h}(k_{0zs})\hat{h}_1(k_{1zs}) \right] \cdot T_{01i}^{\text{TE}}\, \hat{e}_{1i}(k_{1zi}) \right|^2 W \quad (7.6.52)
$$

where

$$
W = \iiint_{V_1} d^3\overline{r}_1 \iiint_{V_1} d^3\overline{r}_2\ C(\overline{r}_1 - \overline{r}_2)e^{i(\overline{k}_{1i}-\overline{k}_{1s})\cdot\overline{r}_1 - i(\overline{k}_{1i}^*-\overline{k}_{1s}^*)\cdot\overline{r}_2}
$$

$$(7.6.53)$$

The correlation function may be expressed as the Fourier transform of a spectral intensity function Φ

$$
C(\overline{r}_1 - \overline{r}_2) = \delta|k_1|^4 \iiint_{-\infty}^{\infty} d\overline{k}\ \Phi(\overline{k})e^{-i\overline{k}\cdot(\overline{r}_1 - \overline{r}_2)} \quad (7.6.54)
$$

For the correlation function in (7.6.10), for instance, we choose the coordinates with the z axis along $\overline{k}$ without loss of generality and find

$$
\Phi(\overline{k}) = \frac{1}{8\pi^3} \iiint d^3\overline{r}\ e^{-r/r_0}e^{i\overline{k}\cdot\overline{r}}
$$

$$
= \frac{1}{4\pi^2} \int_0^{\infty} dr\ r^2 e^{-r/r_0} \int_0^{\pi} d\theta\ \sin\theta\, e^{ikr\cos\theta}
$$

$$
= \frac{r_0^3}{\pi^2(1 + k^2 r_0^2)^2}
$$

Substitution of (7.6.54) into (7.6.53) yields

$$
W = 4\pi^2\delta|k_1|^4 \iiint_{-\infty}^{\infty} d^3\overline{k} \iiint dx_1 dy_1 dz_1\ \exp(i(\overline{k}_{1zi} - \overline{k}_{1zs} - \overline{k}_z)\cdot z_1)
$$

$$
\cdot \exp(i(k_{1zi}^* + k_{1zs}^* + k_z)z_2) \cdot \Phi(\overline{k})\delta(k_{1xi} - k_{1xs} - k_x, k_{1yi} - k_{1ys} - k_y)
$$

$$
= 4\pi^2\delta|k_1|^4 \int_{-\infty}^{\infty} dk_z \int_{-\infty}^{0} dz_1 \int_{-\infty}^{0} dz_2\ \Phi(k_{xi} - k_{xs}, k_{yi} - k_{ys}, k_z)
$$

$$
\cdot \exp(-i(k_{1zi} + k_{1zs} + k_z)z_1)\exp(i(k_{1zi}^* + k_{1zs}^* + k_z)z_2)
$$

$$
= \delta|k_1|^4 A \int_{-\infty}^{\infty} dk_z \frac{\Phi(k_{xi} - k_{xs}, k_{yi} - k_{ys}, k_z)}{(k_{1zi} + k_{1zs} + k_z)(k_{1zi}^* + k_{1zs}^* + k_z)}
$$

where A is the illuminated area resulting from the integration over $dx_1\,dy_1$. Consider low absorption with $k_{1I} \ll k_{1R}$. We apply contour integration and recognize that most of the contribution of the integral comes from the residue of the pole at $k_z = -k_{1zi}^* - k_{1zs}^*$. We find

$$W \approx 4\pi^3 \delta |k_1|^4 A \frac{\Phi(k_{xi} - k_{xs}, k_{yi} - k_{ys}, -k_{1zi}^* - k_{1zs}^*)}{k_{1ziI} + k_{1zsI}}$$

The bistatic scattering coefficients $\gamma_{\mu\nu}(\hat{k}_s, \hat{k}_i)$ are defined as

$$\gamma_{\mu\nu} = \frac{4\pi r^2 < |\overline{E}_s|^2 >_\nu}{A \cos\theta_i |\overline{E}_0|^2_\mu}$$

where μ denotes the incident polarization and ν the scattered polarization. We obtain, for the case $\phi_i = 0$,

$$\begin{Bmatrix} \gamma_{hh} \\ \gamma_{vh} \\ \gamma_{hv} \\ \gamma_{vv} \end{Bmatrix} = \frac{\delta |k_1|^4 \pi^2 \Phi}{\cos\theta_i (k_{1ziI} + k_{1zsI})}$$

$$\cdot \begin{Bmatrix} |T_{01s}^{\mathrm{TE}} T_{01i}^{\mathrm{TE}}|^2 \cos^2\phi_s \\[2mm] |k_{1zs}\dfrac{k}{k_1} T_{01s}^{\mathrm{TM}} T_{01i}^{\mathrm{TE}}|^2 \sin^2\phi_s \\[2mm] |k_{1zi}\dfrac{k}{k_1} T_{01s}^{\mathrm{TE}} T_{01i}^{\mathrm{TM}}|^2 \sin^2\phi_s \\[2mm] |T_{01s}^{\mathrm{TM}} T_{01i}^{\mathrm{TM}}|^2 \dfrac{k^6 \sin^2\theta_s}{k_1^8} |k_{xi} - \dfrac{k_{xs}k_{1zs}k_{1zi}}{k_{xs}^2 + k_{ys}^2}|^2 \end{Bmatrix}$$

For the backscattering coefficient

$$\sigma_{\mu\nu} = \gamma_{\mu\nu}(\theta_s = \theta_i,\, \phi_s = \pi + \phi_i) \cos\theta_i$$

We see that $\sigma_{\mu\nu} = \sigma_{h\nu} = 0$ for the first-order solution from the Born series. To determine the cross-polarized backscattering intensities, we must carry out the Born approximation to the second-order from the iterative procedure.

The above results are obtained with the Born approximation that makes use of the unperturbed field values for the background medium in the absence of the inhomogeneities. In the distorted Born approximation, which often yields better numerical results as compared with

experimental measurements, the unperturbed field values in the background medium with the effective permittivity are used. The Born approximations are valid only for weak permittivity fluctuations. When the variance of the randomly fluctuating part is large, we must resort to the strong fluctuation theory in which the singularities of the dyadic Green's functions are properly taken care of and a new small parameter such as ξ in Section 6.7 can be utilized to affect approximations similar to the Born series.

Problems

P7.6.1

Let $f(x)$ be a stationary Gaussian random process with variance σ^2 and $< f(x) > = 0$. Show that

$$< e^{i\alpha f(x)} > = e^{-\sigma^2 \alpha^2 / 2}$$

7.7 Effective Permittivity for a Volume Scattering Medium

Electromagnetic waves are scattered upon entering a medium containing scatterers or inhomogeneities, which is referred to as a volume scattering medium. A homogeneous dielectric medium is characterized by a permittivity. For a volume scattering medium containing dielectric scatterers, we can account for its scattering effects by characterizing it with an effective permittivity.
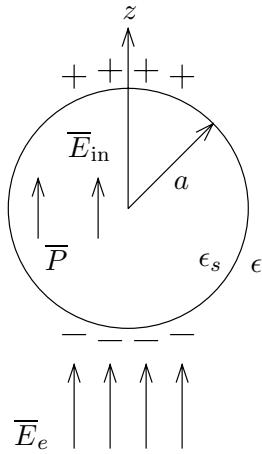
Figure 7.7.1 Sphere of radius a in a field $\overline{E}_e$.

Consider a homogeneous medium with permittivity ϵ containing small spheres of permittivity ϵ_s and radius a [Fig. 7.7.1]. Assume the electric field in the absence of the scatterers to be

$$\overline{E}_e = \hat{z} E_e = E_e(\hat{r}\cos\theta - \hat{\theta}\sin\theta) \tag{7.7.1}$$

In the static limit, the total field inside and outside the sphere is

$$\overline{E} = \begin{cases} \overline{E}_e + E_s(\dfrac{a}{r})^3(\hat{r}2\cos\theta + \hat{\theta}\sin\theta) & z \geq a \\[2mm] E_{\text{in}}\,(\hat{r}\cos\theta - \hat{\theta}\sin\theta) & z \leq a \end{cases} \tag{7.7.2}$$

At $r = a$, the boundary conditions give

$$\begin{cases} -E_e + E_s = -E_{\text{in}} \\ 2\epsilon E_e + \epsilon E_s = \epsilon_s E_{\text{in}} \end{cases} \tag{7.7.3}$$

which yields the solution

$$E_{\text{in}} = \frac{3\epsilon}{\epsilon_s + 2\epsilon} E_e \qquad (7.7.4)$$

$$E_{\text{s}} = \frac{\epsilon_s - \epsilon}{\epsilon_s + 2\epsilon} E_e \qquad (7.7.5)$$

The polarization vector for the sphere is

$$\overline{P} = (\epsilon_s - \epsilon)\overline{E}_{\text{in}} = 3\epsilon \frac{\epsilon_s - \epsilon}{\epsilon_s + 2\epsilon} \overline{E}_e \qquad (7.7.6)$$

The polarizability of the sphere is seen to be

$$\alpha = 3\epsilon \frac{\epsilon_s - \epsilon}{\epsilon_s + 2\epsilon} \left(\frac{4\pi a^3}{3} \right) \qquad (7.7.7)$$

The difference between the total fields inside and outside the sphere can be attributed to the polarization vector $\overline{P}$. From (7.7.4) and (7.7.6) we find

$$\overline{E}_e - \overline{E}_{\text{in}} = \frac{1}{3\epsilon} \overline{P} \qquad (7.7.8)$$

Notice that $\overline{E}_e$ is the field in the absence of the sphere and constitutes only part of the total field outside the sphere as is evident from (7.7.2). We refer to $\overline{E}_e$ as the exciting field.

For a volume scattering medium containing n_0 spheres per unit volume, the polarization vector is related to the exciting field by

$$\overline{P} = n_0 \alpha \overline{E}_e \qquad (7.7.9)$$

We relate the exciting field $\overline{E}_e$ and the macroscopic field $\overline{E}$ in the same manner as (7.7.8)

$$\overline{E} = \overline{E}_e - \frac{1}{3\epsilon} \overline{P} \qquad (7.7.10)$$

In terms of the macroscopic field $\overline{E}$, we find from (7.7.9) and (7.7.10)

$$\overline{P} = \frac{n_0 \alpha}{1 - n_0 \alpha / 3\epsilon} \overline{E} \qquad (7.7.11)$$

The electric displacement vector $\overline{D}$ is

$$\overline{D} = \epsilon\overline{E} + \overline{P} = \frac{1 + 2n_0\alpha/3\epsilon}{1 - n_0\alpha/3\epsilon}\epsilon\overline{E}$$

It follows that the effective permittivity ϵ_{eff} is

$$\epsilon_{eff} = \epsilon\left[\frac{1 + 2n_0\alpha/3\epsilon}{1 - n_0\alpha/3\epsilon}\right] \tag{7.7.12}$$

The fractional volume occupied by the spheres is

$$f_s = n_0\left(\frac{4\pi a^3}{3}\right)$$

which gives

$$n_0\alpha = 3\epsilon\frac{\epsilon_s - \epsilon}{\epsilon_s + 2\epsilon}f_s = 3\epsilon S f_s \tag{7.7.13}$$

where

$$S = \frac{\epsilon_s - \epsilon}{\epsilon_s + 2\epsilon} \tag{7.7.14}$$

In view of (7.7.7), we write (7.7.12) in terms of the fractional volume f_s as follows:

$$\epsilon_{eff} = \epsilon\left[\frac{1 + 2f_sS}{1 - f_sS}\right] \tag{7.7.15}$$

Casting (7.7.12) in a more symmetric form, we obtain

$$\frac{\epsilon_{eff} - \epsilon}{\epsilon_{eff} + 2\epsilon} = f_sS = f_s\frac{\epsilon_s - \epsilon}{\epsilon_s + 2\epsilon} \tag{7.7.16}$$

Equation (7.7.12) is known as the Clausius-Mossotti formula or the Lorenz-Lorentz formula. Equation (7.7.15) is known as the Maxwell-Garnett mixing formula and (7.7.16) as the Rayleigh mixing formula.

It is important to notice from (7.7.15) that as $f_s = 0$, $\epsilon_{eff} = \epsilon$ and as $f_s = 1$, $\epsilon_{eff} = \epsilon_s$. However, if both ϵ_s and ϵ are real, ϵ_{eff} is also real. This is because ϵ_{eff} as calculated above does not account for the scattering effect by the scatterers, which gives rise to an imaginary part for the effective permittivity.

A. Random Discrete Scatterers

In the low frequency limit, the scattered power can be attributed to the scattered power of the induced dipoles of the small spheres. From (7.7.7), (7.7.9), and (7.7.10), we find the relation between the excited field $\overline{E}_e$ and the macroscopic field $\overline{E}$ to be

$$\overline{E} = [1 - f_s S]\,\overline{E}_e \tag{7.7.17}$$

Therefore the induced dipole moment for a small sphere is

$$\overline{p} = \alpha \overline{E}_e = \frac{4\pi a^3 \epsilon S}{1 - f_s S}\overline{E} \tag{7.7.18}$$

Assuming that the attenuation is small on the wavelength scale, we can approximate $\overline{E}$ by

$$\overline{E} = \hat{e} E_0\, e^{i\overline{K}_R \cdot \overline{r}}$$

where K_R is the real part of the wavenumber

$$K = \omega(\mu_o \epsilon_{eff})^{1/2} = K_R + iK_I$$

The complex effective permittivity is related to K_R and K_I as follows:

$$\epsilon_{effR} + i\epsilon_{effI} = \frac{1}{\omega^2 \mu_o}(K_R^2 + i2K_I K_R - K_I^2)$$
$$\approx \frac{1}{\omega^2 \mu_o}(K_R^2 + i2K_I K_R)$$

In order to determine ϵ_{effI}, we now calculate K_I from scattered power by the induced dipoles.

The induced dipole moment $\overline{p}_i$ of the ith scatterer centered at $\overline{r}_i$ is

$$\overline{p}_i = \hat{e}\frac{4\pi a^3 \epsilon S}{1 - f_s S}E_0\, e^{i\overline{K}_R \cdot \overline{r}_i} \tag{7.7.19}$$

The scattered field of the ith dipole is

$$\overline{E}_{si}(\overline{r}) = \frac{\omega^2 \mu_o\, e^{ikR_i}}{4\pi R_i}\left(\hat{R}_i \times \overline{p}_i\right) \times \hat{R}_i \tag{7.7.20}$$

where $\overline{R}_i = \overline{r} - \overline{r}_i$ is the vector pointing from the ith dipole to the observation point. For $r \gg r_i$, we approximate $R_i \approx r - \hat{r} \cdot \overline{r}_i$, $\hat{R}_i = \hat{r}$ and $\hat{r}k = \overline{k}$. Thus (7.7.20) becomes

$$\overline{E}_{si}(\overline{r}) \approx \overline{A} \, e^{i(\overline{K}_R - \overline{k}) \cdot \overline{r}_i}$$

where

$$\overline{A} = \frac{\omega^2 \mu_o e^{ikr}}{4\pi r} (\hat{r} \times \hat{e}) \times \hat{r} \frac{4\pi a^3 \epsilon S}{1 - f_s S} E_0 \qquad (7.7.21)$$

The total scattered field $\overline{E}_s(\overline{r})$ is the sum of that due to all the dipoles,

$$\overline{E}_s(\overline{r}) = \sum_{i=1}^{N} \overline{A} \, e^{i(\overline{K}_R - \overline{k}) \cdot \overline{r}_i} \qquad (7.7.22)$$

where N is the total number of scatterers.

The total scattered intensity is determined to be

$$I_s = \frac{|\overline{E}_s|^2}{2\eta} = \frac{|\overline{A}|^2}{2\eta} \left\{ N + \sum_{i=1}^{N} \sum_{j \neq i} 2\mathrm{Re} \left\{ e^{i\overline{K} \cdot (\overline{r}_i - \overline{r}_j)} \right\} \right\} \qquad (7.7.23)$$

where $\overline{K} = \overline{K}_R - \overline{k}$.

Notice that the position vectors $\overline{r}_i$ and $\overline{r}_j$ are random variables in space. Let $P_N(\overline{r}_1, \ldots, \overline{r}_N)$ be the N-particle probability density function for the scatterers center at $\overline{r}_1, \ldots, \overline{r}_N$. Taking the configuration average of (7.7.23) and assuming that all scatterers are identical, we find

$$<I_s> = \frac{|\overline{A}|^2}{2\eta} \{N + L\} \qquad (7.7.24)$$

where

$$L = \sum_{i=1}^{N} \sum_{j \neq i} 2\,\mathrm{Re} \left\{ \int d\overline{r}_1 \ldots \int d\overline{r}_N \, P_N(\overline{r}_1, \ldots, \overline{r}_N) e^{i\overline{K} \cdot (\overline{r}_i - \overline{r}_j)} \right\}$$

$$= N(N-1)\,\mathrm{Re} \left\{ \int d\overline{r}_i \int d\overline{r}_j \, P_2(\overline{r}_i, \overline{r}_j) e^{i\overline{K} \cdot (\overline{r}_i - \overline{r}_j)} \right\}$$

The two-scatterer probability density function is, by Bayes' rule, $P_2(\overline{r}_i, \overline{r}_j) = P(\overline{r}_i | \overline{r}_j) P(\overline{r}_j)$ where $P(\overline{r}_i | \overline{r}_j)$ is the conditional probability of the ith scatterer at $\overline{r}_i$ given the jth scatterer at $\overline{r}_j$. We assume

uniform distribution with $P(\overline{r}_j) = 1/V$ and $P(\overline{r}_i|\overline{r}_j) = g_2(\overline{r}_i, \overline{r}_j)/V$ where V is the volume containing the scatterers, and $g_2(\overline{r}_i, \overline{r}_j)$ is the two-point distribution function. For radially symmetric problems $g_2(\overline{r}_i, \overline{r}_j) = g(\overline{r}_i - \overline{r}_j)$ where g is called the pair-distribution function. We find

$$L = n_0 N \mathrm{Re} \left\{ \iiint d\overline{r} \; g(\overline{r}) e^{i\overline{K} \cdot \overline{r}} \right\} \tag{7.7.25}$$

where $n_0 = N/V$.

The total scattered power is determined by integrating (7.7.24) over a 4π solid angle. Without loss of generality we let $\hat{e} = \hat{z}$ and obtain

$$P_s = \frac{E_0^2}{2\eta} \frac{8\pi}{3} k^4 a^6 \left| \frac{(\epsilon_s - \epsilon)/(\epsilon_s + 2\epsilon)}{1 - f_s(\epsilon_s - \epsilon)/(\epsilon_s + 2\epsilon)} \right|^2 \{N + L\} \tag{7.7.26}$$

Consider a cylindrical volume of area A and length l containing n_0 scatterers per unit volume. The input power is $P_{\mathrm{in}} = A(E_0^2/2)\sqrt{\epsilon_{eff}/\mu_o} \approx AK_R E_0^2/2\eta k$ with ϵ_{eff} denoting the effective permittivity. The scattered power is given by (7.7.26) with $N = n_0 A l$. The scattering induced attenuation rate is given by

$$2K_I = \frac{P_s}{lP_{\mathrm{in}}} = 2f_s \frac{k^5 a^3}{K_R} \left| \frac{(\epsilon_s - \epsilon)/(\epsilon_s + 2\epsilon)}{1 - f_s(\epsilon_s - \epsilon)/(\epsilon_s + 2\epsilon)} \right|^2 \{1 + L/N\} \tag{7.7.27}$$

For $K_I \ll K_R$, we have $K^2 = \omega^2 \mu_o(\epsilon_{effR} + i\epsilon_{effI}) \approx K_R^2 + i2K_R K_I$. The real part is obtained from (7.7.15) and the imaginary part from (7.7.27). We find the new complex effective permittivity to be

$$\begin{aligned}
\epsilon_{eff} = \epsilon \Bigg\{ & \left[\frac{1 + 2f_s(\epsilon_s - \epsilon)/(\epsilon_s + 2\epsilon)}{1 - f_s(\epsilon_s - \epsilon)/(\epsilon_s + 2\epsilon)} \right] \\
& + i2f_s k^3 a^3 \left| \frac{(\epsilon_s - \epsilon)/(\epsilon_s + 2\epsilon)}{1 - f_s(\epsilon_s - \epsilon)/(\epsilon_s + 2\epsilon)} \right|^2 \{1 + L/N\} \Bigg\}
\end{aligned} \tag{7.7.28}$$

The imaginary part of the complex wavenumber $K = K_R + iK_I$ now accounts for the scattering effects. As $K^2 = \omega^2 \mu_o(\epsilon_{effR} + i\epsilon_{effI})$, the imaginary part of the complex effective permittivity ϵ_{effI} is dependent on the pair distribution function $g(r)$ as seen from (7.7.25).

For independent scattering, the pair distribution function $g(\overline{r}) = 1$ and (7.7.25) can be converted into a surface integral at infinity bounding all the scatterers. As the wave solution satisfies the wave equation

and the radiation condition, the result of the integral is zero,

$$\iiint d\bar{r}\ e^{i\overline{K}\cdot\bar{r}} = 0 \tag{7.7.29}$$

We find from (7.7.28), since $L = 0$,

$$\epsilon_{eff} = \epsilon \left\{ \left[\frac{1 + 2f_s(\epsilon_s - \epsilon)/(\epsilon_s + 2\epsilon)}{1 - f_s(\epsilon_s - \epsilon)/(\epsilon_s + 2\epsilon)} \right] \right.$$

$$\left. + i2f_s k^3 a^3 \left| \frac{(\epsilon_s - \epsilon)/(\epsilon_s + 2\epsilon)}{1 - f_s(\epsilon_s - \epsilon)/(\epsilon_s + 2\epsilon)} \right|^2 \right\} \tag{7.7.30}$$

The real part is the Maxwell-Garnett result and the imaginary part is identical to that obtained from the Rayleigh scattering result.

The hole-correction approximation is often used for impenetrable scatterers that are sparsely distributed (i.e., $f_s \ll 1$). The approximation requires that

$$\begin{array}{lll} g(\bar{r}) = 0 & \text{for} & r < b \\ g(\bar{r}) = 1 & \text{for} & r > b \end{array} \tag{7.7.31}$$

where $b = 2a$ is the distance separating the centers of two spheres, so that when the position of one sphere is given, the probability of another sphere being positioned within the distance b from its center is zero. But outside this exclusion volume of radius b, other spheres can be positioned anywhere else with equal probability as they are sparsely distributed. With this approximation, (7.7.25) becomes

$$L = n_0 N \mathrm{Re} \left\{ \iiint\limits_{r>b} d\bar{r}\ e^{i\overline{K}\cdot\bar{r}} \right\}$$

The integral can be evaluated by converting it into a surface integral and neglecting the surface at infinity bounding the volume containing all the scatterers. We find

$$L = n_0 N\ \mathrm{Re} \left\{ \frac{1}{K^2} \iint d\bar{s} \cdot \nabla(e^{i\overline{K}\cdot\bar{r}}) \right\}$$

$$= -\frac{n_0 N}{K} 2\pi b^2 \int_0^\pi d\theta\ \sin\theta \cos\theta \sin(Kb\cos\theta)$$

$$= -n_0 N \frac{4\pi}{3} b^3 = -8Nf_s \tag{7.7.32}$$

In obtaining the above result, we take the low frequency limit so that $Kb \ll 1$ and that $\sin(Kb\cos\theta) \approx Kb\cos\theta$.

The hole-correction result can also be obtained by making use of (7.7.29) in (7.7.25) which becomes

$$
\begin{aligned}
L &= n_0 N \operatorname{Re} \iiint d\bar{r} \, [g(r) - 1] e^{i\overline{K}\cdot\bar{r}} \\
&\approx n_0 N \operatorname{Re} \iiint d\bar{r} \, [g(r) - 1]
\end{aligned}
\tag{7.7.33}
$$

where we again assume at low frequencies, the exponential term is approximately equal to one since for large distance r, $g(r) \approx 1$. Making use of the hole-correction approximation in (7.7.31), we find $L = -n_0 N(4\pi b^3/3) = -8Nf_s$ which is the result in (7.7.32).

Substituting (7.7.32) into (7.7.28) we find the effective permittivity under the hole-correction (H-C) approximation to be

$$
\begin{aligned}
\epsilon_{eff} = \epsilon \Bigg\{ &\left[\frac{1 + 2f_s(\epsilon_s - \epsilon)/(\epsilon_s + 2\epsilon)}{1 - f_s(\epsilon_s - \epsilon)/(\epsilon_s + 2\epsilon)} \right] \\
&+ i2f_s k^3 a^3 \left| \frac{(\epsilon_s - \epsilon)/(\epsilon_s + 2\epsilon)}{1 - f_s(\epsilon_s - \epsilon)/(\epsilon_s + 2\epsilon)} \right|^2 (1 - 8f_s) \Bigg\}
\end{aligned}
\tag{7.7.34}
$$

Clearly the H-C result is only valid for small fractional volumes. For $f > 1/8$, we observe from (7.7.34) that the imaginary part will be negative, a physically unacceptable result.

The Percus-Yevick pair distribution function [Wertheim, 1963] is a more realistic approximation which, when applied to (7.7.33), gives

$$
L = N \left[\frac{(1 - f_s)^4}{(1 + 2f_s)^2} - 1 \right]
\tag{7.7.35}
$$

Substituting (7.7.35) into (7.7.28) yields

$$
\begin{aligned}
\epsilon_{eff} = \epsilon \Bigg\{ &\left[\frac{1 + 2f_s(\epsilon_s - \epsilon)/(\epsilon_s + 2\epsilon)}{1 - f_s(\epsilon_s - \epsilon)/(\epsilon_s + 2\epsilon)} \right] \\
&+ i2f_s k^3 a^3 \left| \frac{(\epsilon_s - \epsilon)/(\epsilon_s + 2\epsilon)}{1 - f_s(\epsilon_s - \epsilon)/(\epsilon_s + 2\epsilon)} \right|^2 \frac{(1 - f_s)^4}{(1 + 2f_s)^2} \Bigg\}
\end{aligned}
\tag{7.7.36}
$$

Notice that (7.7.36) reduces to (7.7.34) for $f_s \ll 1$. Even more appealingly, we find from (7.7.36), that $\epsilon_{eff} = \epsilon$ as $f_s = 0$ and that $\epsilon_{eff} = \epsilon_s$ as $f_s = 1$.

B. Effective Permittivity for a Continuous Random Medium

Consider a random medium with permittivity $\epsilon(\bar{r})$. Introducing an auxiliary permittivity ϵ_g, we write the vector wave equation as

$$\nabla \times \nabla \times \overline{E} - k_g^2 \overline{E} = k_o^2 \left(\frac{\epsilon(\bar{r}) - \epsilon_g}{\epsilon_o} \right) \overline{E} \qquad (7.7.37)$$

where $k_g^2 = \omega^2 \mu_o \epsilon_g$ and $k_o^2 = \omega^2 \mu_o \epsilon_o$. Let $\overline{\overline{G}}_g(\bar{r}, \bar{r}')$ be the dyadic Green's function that satisfies

$$\nabla \times \nabla \times \overline{\overline{G}}_g(\bar{r}, \bar{r}') - k_g^2 \overline{\overline{G}}_g(\bar{r}, \bar{r}') = \overline{\overline{I}} \delta(\bar{r} - \bar{r}') \qquad (7.7.38)$$

The singularity of the dyadic Green's function depends on the shape of the infinitesimal exclusion volume. We assume the correlation function for the random medium to be spherically symmetric and choose a spherically-shaped exclusion volume. The dyadic Green's function can be decomposed into [Tsang et al., 1985]

$$\overline{\overline{G}}_g(\bar{r}, \bar{r}') = \mathrm{PV}\overline{\overline{G}}_g(\bar{r}, \bar{r}') - \overline{\overline{I}} \frac{1}{3k_g^2} \delta(\bar{r} - \bar{r}') \qquad (7.7.39)$$

where PV stands for principal value.

Let $\overline{E}_0(\bar{r})$ denote the field solution for the homogeneous wave equation with wavenumber k_g in (7.7.37). Notice that the field point $\bar{r}$ and the source point $\bar{r}'$ may coincide and we must account for the singularities of the dyadic Green's functions. It follows that

$$\overline{E}(\bar{r}) = \overline{E}_0(\bar{r}) + k_o^2 \iiint d^3\bar{r}' \, \overline{\overline{G}}_g(\bar{r}, \bar{r}') \frac{\epsilon(\bar{r}') - \epsilon_g}{\epsilon_o} \cdot \overline{E}(\bar{r}') \qquad (7.7.40)$$

$$= \overline{E}_0(\bar{r}) - \frac{\epsilon(\bar{r}) - \epsilon_g}{3\epsilon_g} \overline{E}(\bar{r}) + k_o^2 \iiint d^3\bar{r}' \, \mathrm{PV}\overline{\overline{G}}_g(\bar{r}, \bar{r}') \cdot \xi(\bar{r}')\overline{E}_e(\bar{r}') \qquad (7.7.41)$$

We thus obtain

$$\overline{E}_e(\bar{r}) = \overline{E}_0(\bar{r}) + k_o^2 \iiint d^3\bar{r}' \, \mathrm{PV}\overline{\overline{G}}_g(\bar{r}, \bar{r}') \cdot \xi(\bar{r}')\overline{E}_e(\bar{r}') \qquad (7.7.42)$$

where

$$\overline{E}_e(\bar{r}) = \frac{\epsilon(\bar{r}) + 2\epsilon_g}{3\epsilon_g} \overline{E}(\bar{r}) = \frac{1}{3\epsilon_g} \overline{D}(\bar{r}) + \frac{2}{3}\overline{E}(\bar{r}) \qquad (7.7.43)$$

and

$$\xi(\overline{r}) = 3\frac{\epsilon_g}{\epsilon_o}\left[\frac{\epsilon(\overline{r}) - \epsilon_g}{\epsilon(\overline{r}) + 2\epsilon_g}\right] \tag{7.7.44}$$

Equation (7.7.43) represents the relation for the uniform electric field $\overline{E}$ inside a dielectric sphere when it is placed in an external static field $\overline{E}_e$. Multiplication of (7.7.43) and (7.7.44) yields

$$\xi(\overline{r})\overline{E}_e(\overline{r}) = 3\frac{\epsilon_g}{\epsilon_o}\left[\frac{\epsilon(\overline{r}) - \epsilon_g}{\epsilon(\overline{r}) + 2\epsilon_g}\right]\frac{\epsilon(\overline{r}) + 2\epsilon_g}{3\epsilon_g}\overline{E}(\overline{r}) = \frac{\epsilon(\overline{r}) - \epsilon_g}{\epsilon_o}\overline{E}(\overline{r})$$

which yields
$$\overline{D}(\overline{r}) = \epsilon_g\overline{E}(\overline{r}) + \epsilon_o\xi(\overline{r})\overline{E}_e(\overline{r}) \tag{7.7.45}$$

Applying ensemble averaging to the above equation gives

$$< \overline{D}(\overline{r}) > = \epsilon_g < \overline{E}(\overline{r}) > + \epsilon_o < \xi(\overline{r})\overline{E}_e(\overline{r}) > \tag{7.7.46}$$

Thus $< \xi(\overline{r})\overline{E}_e(\overline{r}) >$ plays the role of a polarization vector in a background medium of ϵ_g.

In the strong fluctuation theory, we impose the condition

$$< \xi(\overline{r}) > = 0 \tag{7.7.47}$$

By virtue of (7.7.44), we require

$$< \frac{\epsilon(\overline{r}) - \epsilon_g}{\epsilon(\overline{r}) + 2\epsilon_g} > = 0 \tag{7.7.48}$$

Suppose there are n constituents in a mixture constituting the random medium with permittivity ϵ_p and fractional volume f_p, where $p = 1, 2, \ldots, n$. We have

$$\sum_{p=1}^{n} f_p = 1 \tag{7.7.49}$$

Equation (7.7.48) gives

$$\sum_{p=1}^{n} \frac{\epsilon_p - \epsilon_g}{\epsilon_p + 2\epsilon_g} f_p = 0 \tag{7.7.50}$$

In light of (7.7.49), algebraic manipulation of (7.7.50) multiplied by $(\epsilon_o + 2\epsilon_g)/3\epsilon_g$ leads directly to the Polder-van Santen mixing formula

$$\sum_{p=1}^{n} \frac{\epsilon_p - \epsilon_o}{\epsilon_p + 2\epsilon_g} f_p = \frac{\epsilon_g - \epsilon_o}{3\epsilon_g} \tag{7.7.51}$$

which was originally derived [Polder and van Santen, 1946] by regarding the inhomogeneities as dipoles. We have thus established that ϵ_g is the effective permittivity in the low-frequency limit.

As frequency increases, the multiple scattering gives rise to an imaginary part in the effective permittivity to account for the wave attenuation. Taking ensemble average of (7.7.42), we obtain by the bilocal approximation

$$<\overline{E}_e(\overline{r})> = \overline{E}_0(\overline{r}) + k_o^2 \iiint d^3\overline{r}' \, \mathrm{PV}\overline{\overline{G}}_g(\overline{r},\overline{r}') \cdot <\xi(\overline{r}')\overline{E}_e(\overline{r}')>$$
$$\approx \overline{E}_0(\overline{r}) + k_o^2 \iiint d^3\overline{r}' \, \mathrm{PV}\overline{\overline{G}}_g(\overline{r},\overline{r}') \cdot \iiint d^3\overline{r}'' \overline{\overline{\xi}}_{eff}(\overline{r}'-\overline{r}'') < \overline{E}_e(\overline{r}'')> \tag{7.7.52}$$

where

$$<\xi(\overline{r}')\overline{E}_e(\overline{r}')> = \iiint d^3\overline{r}'' \, \overline{\overline{\xi}}_{eff}(\overline{r}'-\overline{r}'') \cdot <\overline{E}_e(\overline{r}'')> \tag{7.7.53}$$

$$\overline{\overline{\xi}}_{eff}(\overline{r}'-\overline{r}'') = k_o^2 \, \mathrm{PV}\overline{\overline{G}}_g(\overline{r}',\overline{r}'') R_\xi(|\overline{r}'-\overline{r}''|) \tag{7.7.54}$$

$$R_\xi(|\overline{r}'-\overline{r}''|) = <\xi(\overline{r}')\xi(\overline{r}'')> \tag{7.7.55}$$

We find from (7.7.46), in view of (7.7.53) and (7.7.43)

$$<\overline{D}(\overline{r})> = \epsilon_g <\overline{E}(\overline{r})> + \epsilon_o <\xi(\overline{r})\overline{E}_e(\overline{r})>$$
$$= \epsilon_g <\overline{E}(\overline{r})> + \frac{\epsilon_o}{3\epsilon_g} \iiint d^3\overline{r}' \, \overline{\overline{\xi}}_{eff}(\overline{r}-\overline{r}') \cdot <\overline{D}(\overline{r}')>$$
$$+ \frac{2\epsilon_o}{3} \iiint d^3\overline{r}' \, \overline{\overline{\xi}}_{eff}(\overline{r}-\overline{r}') \cdot <\overline{E}(\overline{r}')> \tag{7.7.56}$$

We define the effective permittivity $\overline{\overline{\epsilon}}_{eff}$ such that

$$<\overline{D}(\overline{r})> = \iiint d^3\overline{r}' \, \overline{\overline{\epsilon}}_{eff}(\overline{r}-\overline{r}') \cdot <\overline{E}(\overline{r}')> \tag{7.7.57}$$

Fourier transforming $\overline{D}$, $\overline{\overline{\epsilon}}_{eff}$, $\overline{E}$, $\overline{\overline{\xi}}_{eff}$, and $\overline{E}_e$, e.g.,

$$\overline{D}(\overline{k}) = \iiint d^3\overline{r} \; \overline{D}(\overline{r})e^{-i\overline{k}\cdot\overline{r}}$$

we find from (7.7.57) and (7.7.56),

$$\left[\overline{\overline{I}} - \frac{\epsilon_o}{3\epsilon_g}\overline{\overline{\xi}}_{eff}(\overline{k})\right] < \overline{D}(\overline{k}) > = \epsilon_g < \overline{E}(\overline{k}) > + \frac{2\epsilon_o}{3}\overline{\overline{\xi}}_{eff}(\overline{k}) < \overline{E}(\overline{k}) >$$

$$(7.7.58)$$

Thus

$$\overline{\overline{\epsilon}}_{eff}(\overline{k}) = \epsilon_g\overline{\overline{I}} + \epsilon_o\left[\overline{\overline{I}} - \frac{\epsilon_o}{3\epsilon_g}\overline{\overline{\xi}}_{eff}(\overline{k})\right]^{-1}\overline{\overline{\xi}}_{eff}(\overline{k}) \qquad (7.7.59)$$

The second term is the correction provided by the bilocal approximation the validity of which is substantiated by

$$|\overline{\overline{\xi}}_{eff}(\overline{k})| \ll 1 \qquad (7.7.60)$$

We obtain from (7.7.59)

$$\overline{\overline{\epsilon}}_{eff} \approx \epsilon_g\overline{\overline{I}} + \epsilon_o\overline{\overline{\xi}}_{eff}^{(0)} \qquad (7.7.61)$$

where

$$\overline{\overline{\xi}}_{eff}^{(0)} = k_o^2 \iiint d^3\overline{r} \; \mathrm{PV}\overline{\overline{G}}_g(\overline{r}) \, R_\xi(|\overline{r}|)$$

follows from the Fourier transform of (7.7.54) in which we let $e^{ikr} \approx 1$, assuming low frequency and small r. For spherical scatterers, we calculate

$$\mathrm{PV}\overline{\overline{G}}_g(\overline{r}) = (\overline{\overline{I}} + \frac{1}{k_g^2}\nabla\nabla)\frac{e^{ik_g r}}{4\pi r} = (\overline{\overline{I}} + \frac{1}{k_g^2}\nabla\hat{r}[ik_g - \frac{1}{r}])\frac{e^{ik_g r}}{4\pi r}$$

$$= (\overline{\overline{I}} + \frac{1}{k_g^2}(\nabla\overline{r})[\frac{ik_g}{r} - \frac{1}{r^2}] + \hat{r}\hat{r}\frac{r}{k_g^2}\frac{\partial}{\partial r}[\frac{ik_g}{r} - \frac{1}{r^2}])\frac{e^{ik_g r}}{4\pi r}$$

$$= \overline{\overline{I}}(-1 + ik_g r + k_g^2 r^2)\frac{e^{ik_g r}}{4\pi k_g^2 r^3} + \hat{r}\hat{r}(3 - i3k_g r - k_g^2 r^2)\frac{e^{ik_g r}}{4\pi k_g^2 r^3}$$

where $\hat{r}\hat{r} = (\hat{x}x/r + \hat{y}y/r + \hat{z}z/r)(\hat{x}x/r + \hat{y}y/r + \hat{z}z/r)$ and $\nabla\overline{r} = \hat{x}\hat{x} + \hat{y}\hat{y} + \hat{z}\hat{z} = \overline{\overline{I}}$. We find

$$
\overline{\overline{\xi}}_{eff}^{(0)} = \overline{\overline{I}} k_o^2 \int dr \, (-1 + ik_g r + k_g^2 r^2) \frac{e^{ik_g r}}{k_g^2 r} R_\xi(|\overline{r}|)
$$

$$
+ k_o^2 \int dr \int_0^\pi d\theta \int_0^{2\pi} d\phi \, r^2 \sin\theta \, \hat{r}\hat{r}(3 - i3k_g r - k_g^2 r^2) \frac{e^{ik_g r}}{4\pi k_g^2 r^3} R_\xi(|\overline{r}|)
$$

$$
= \overline{\overline{I}} k_o^2 \int dr \, (-1 + ik_g r + k_g^2 r^2) \frac{e^{ik_g r}}{k_g^2 r} R_\xi(|\overline{r}|)
$$

$$
+ \overline{\overline{I}} k_o^2 \int dr \, (3 - i3k_g r - k_g^2 r^2) \frac{e^{ik_g r}}{3k_g^2 r} R_\xi(|\overline{r}|)
$$

$$
= \overline{\overline{I}} \frac{2}{3} k_o^2 \int dr \, r \, R_\xi(|\overline{r}|) \, e^{ik_g r}
$$

In the low-frequency limit we approximate $e^{ik_g r} \approx 1 + ik_g r$. Thus we obtain

$$
\overline{\overline{\epsilon}}_{eff}(\overline{k}) = \epsilon_g \overline{\overline{I}} + \epsilon_o \overline{\overline{\xi}}_{eff}^{(0)}(\overline{k}) \approx \epsilon_g + i \frac{2\epsilon_o}{3} k_o^2 k_g \int_0^a dr \, r^2 R_\xi(r)
$$

For two species with fractional volumes f and f_s for permittivities ϵ and ϵ_s, respectively,

$$
R_\xi(r) = <\xi^2> = f_s \left[3\frac{\epsilon_g}{\epsilon_o} \left(\frac{\epsilon_s - \epsilon_g}{\epsilon_s + 2\epsilon_g} \right) \right]^2 + (1 - f_s) \left[3\frac{\epsilon_g}{\epsilon_o} \left(\frac{\epsilon - \epsilon_g}{\epsilon + 2\epsilon_g} \right) \right]^2
$$

In the low-frequency limit, we obtain the effective permittivity

$$
\epsilon_{eff} = \epsilon_g \left\{ 1 + i2k_g^3 a^3 \left[f_s \left(\frac{\epsilon_s - \epsilon_g}{\epsilon_s + 2\epsilon_g} \right)^2 + (1 - f_s) \left(\frac{\epsilon - \epsilon_g}{\epsilon + 2\epsilon_g} \right)^2 \right] \right\}
$$
$$(7.7.62)$$

Remarkably this formula also yields the limiting values of $\epsilon_{eff} = \epsilon_s$ as $f_s = 1$ and $\epsilon_{eff} = \epsilon$ as $f_s = 0$.

For small fractional volume, we let $f_s \ll 1$ and $\epsilon_g \approx \epsilon + \delta$, with δ denoting a small number. The above result reduces to

$$
\epsilon_g \approx \epsilon[1 + 3f_s(\epsilon_s - \epsilon_g)/(\epsilon_s + 2\epsilon_g)]
$$
$$
\epsilon_{eff} \approx \epsilon \left\{ 1 + 3f_s \left(\frac{\epsilon_s - \epsilon_g}{\epsilon_s + 2\epsilon_g} \right) + i2f_s k^3 a^3 \left(\frac{\epsilon_s - \epsilon_g}{\epsilon_s + 2\epsilon_g} \right)^2 \right\}
$$

This is the same as that obtained with the random discrete scatterer model.

Problems

P7.7.1

The constitutive relation $\overline{D} = \overline{\overline{\epsilon}} \cdot \overline{E}$ can also be expressed in terms of a "free-space" part $\epsilon_o \overline{E}$ and a polarization vector $\overline{P}$ characterizing the properties of the material. We write

$$\overline{D} = \epsilon_o \overline{E} + \overline{P}$$

In the case of induced dipole moments, the polarization $\overline{P}$ is proportional to the polarizability per unit volume $N\alpha$, where N is the number of dipoles per unit volume, and α is the polarizability for each dipole

$$\overline{P} = N\alpha \overline{E}_{\text{loc}}$$

The local electric field $\overline{E}_{\text{loc}}$ at the place of the induced dipole comprises the applied field $\overline{E}$ and the field caused by the surrounding dipoles. Under the quasi-static approximation, the local electrical field is shown to be

$$\overline{E}_{\text{loc}} = \overline{E} + \frac{\overline{P}}{3\epsilon_o}$$

Prove that

$$\frac{\epsilon}{\epsilon_o} = \frac{1 + (2N\alpha/3\epsilon_o)}{1 - (N\alpha/3\epsilon_o)}$$

This is the well-known Clausius-Mossotti (or Lorenz-Lorentz formula).

Answers

P7.1.1

(a) $\overline{E} = \frac{p}{4\pi\epsilon r^3} \left(\hat{\theta} \sin\theta + \hat{r}\, 2\cos\theta \right)$

(b) $p = 4\pi\epsilon a^3 \left(\frac{\epsilon_p - \epsilon_o}{\epsilon_p + 2\epsilon_o} \right) E_o$

(c) $P_s = \frac{1}{2} \int_0^\pi r^2 \sin\theta d\theta \int_0^{2\pi} d\phi E_o H_\phi^* = \frac{4\pi}{3\eta} \left(\frac{\epsilon_p - \epsilon_o}{\epsilon_p + 2\epsilon_o} \right)^2 k^4 a^6 E_0^2$

Scattering cross section $2\eta P_s / E_o^2 = \frac{8\pi}{3} \left(\frac{\epsilon_p - \epsilon_o}{\epsilon_p + 2\epsilon_o} \right)^2 k^4 a^6$

(d) The scattered power from each particle is

$$P_{\text{scatt}} = \frac{4\pi}{3\eta} \left[\frac{\epsilon_p - \epsilon_o}{\epsilon_p + 2\epsilon_o} \right]^2 k^4 a^6 E_o^2 = \frac{\pi}{12\eta} k^4 a^6 E_o^2$$

The total power loss of a control-volume with area A and unit length dl is, with particle density approximately $3/4\pi a^3$ per m^3,

$$dP = \frac{\pi}{12\eta} k^4 a^6 E_o^2 \times \frac{3}{4\pi a^3} \times A d\ell$$

The power flow in fiber through a area A is $P = \frac{1}{2\eta} E_o^2 A$. Therefore

$$\frac{1}{P} \frac{dP}{d\ell} = \frac{1}{8} k^4 a^3 \approx 2 \times 10^{-4}\,\text{m}^{-1} = 0.2\,(\text{km})^{-1}$$

which gives rise to a loss of 6.99 dB/km.

(e) $P_{\text{scatt}} = \frac{4\pi}{3\eta} \left| \left(\frac{\epsilon + i\sigma/\omega - \epsilon_o}{\epsilon + i\sigma/\omega + 2\epsilon_o} \right) \right|^2 k^4 a^6 |E_o|^2 \frac{3}{4\pi a^3} A d\ell \approx \frac{1}{\eta} k^4 a^3 |E_o|^2 A d\ell$

$P_{\text{diss}} = \frac{1}{2} \int dV \sigma |E_o|^2 \approx \frac{1}{2} |E_o|^2 \omega \epsilon A d\ell = \frac{1}{2} \omega \epsilon |E_o|^2 A d\ell = \frac{k}{2\eta} |E_o|^2 A d\ell$

$\frac{P_{\text{scatt}}}{P_{\text{diss}}} = 2k^3 a^3 = 2(2\pi)^3 \frac{a^3}{\lambda^3} \ll 1$ as $a \ll \lambda$ so absorption loss is primary.

P7.2.1

The electric field of the incident wave is

$$\overline{E}^i = -\frac{1}{i\omega\epsilon_o} \nabla \times \overline{H}^i = -\frac{H_o}{i\omega\epsilon_o} \sum_{n=-\infty}^{\infty} \left\{ \hat{\rho} i \frac{n}{\rho} J_n(k\rho) - \hat{\phi} k J_n'(k\rho) \right\} e^{in\phi - in\pi/2}$$

The electric field of the scattered wave is

$$\overline{E}^s = -\frac{1}{i\omega\epsilon_o} \sum_{n=-\infty}^{\infty} A_n \left\{ \hat{\rho} i \frac{n}{\rho} H_n^{(1)}(k\rho) - \hat{\phi} k H_n^{(1)'}(k\rho) \right\} e^{in\phi - in\pi/2}$$

In the far field $k\rho \gg 1$

$$\overline{H}^s \approx -\hat{z}H_o \sum_{n=-\infty}^{\infty} \sqrt{\frac{2}{\pi k\rho}} \frac{J_n'(ka)}{H_n^{(1)'}(ka)} e^{ik\rho+in(\phi-\pi)-i\pi/4}$$

$$\approx \hat{z}iH_o\sqrt{\frac{\pi}{2k\rho}} \left[(ka)^2 \cos\phi - \frac{(ka)^4}{8}\cos 2\phi + \cdots \right] e^{ik\rho-i\pi/4}$$

For magnetic field parallel to the axis the scattered wave is no longer isotropic.

P7.3.1

$$[Q_{Di}^{\pm}]_{mn} = \frac{-1}{P\sqrt{k_{izm}}} \int_p dx e^{-i[(m-n)kx \pm k_{izm}f(x)]}$$

$$[Q_{Ni}^{\pm}]_{mn} = \mp \frac{k^2 - k_{izm}k_{izn}}{z_{izm}P\sqrt{k_{izm}}} \int_p dx e^{-i[(m-n)kx \pm k_{izm}f(x)]}$$

$$f(x) = \begin{cases} h/2 & 0 \le x < P/2 \\ -h/2 & P/2 \le x < P \end{cases} \quad k = \frac{2\pi}{P} \quad i = 0,1$$

$$\int_0^P dx e^{-i[(m-n)kx \pm k_{izm}f(x)]}$$

$$= \int_0^{P/2} dx e^{-i\left[(m-n)kx \pm \frac{k_{izm}h}{2}\right]} + \int_{P/2}^P dx e^{-i\left[(m-n)kx \mp \frac{k_{izm}h}{2}\right]}$$

$$= e^{\mp i\frac{k_{izm}h}{2}} \frac{i\left[e^{-i(m-n)\frac{Pk}{2}} - 1\right]}{(m-n)k} + e^{\pm i\frac{k_{izm}h}{2}} \frac{i\left[e^{-i(m-n)Pk} - e^{-i(m-n)\frac{Pk}{2}}\right]}{(m-n)k}$$

$$= e^{\mp i\frac{k_{izm}h}{2}} \frac{i\left[e^{-i(m-n)\pi} - 1\right]}{(m-n)k} + e^{\pm i\frac{k_{izm}h}{2}} \frac{i\left[e^{-i(m-n)2\pi} - e^{-i(m-n)\pi}\right]}{(m-n)k}$$

$$= \frac{i[1-(-1)^{m-n}]}{(m-n)k} 2i\sin\frac{\pm k_{izm}h}{2} = \begin{cases} \frac{\mp 4}{(m-n)k}\sin\frac{k_{izm}h}{2} & m-n: \text{ odd} \\ 0 & m-n: \text{ even} \end{cases}$$

P7.4.1

$$< |\overline{E}|^2 > = \frac{k^2|\overline{E}_0|^2}{16\pi^2 r^2} \left| (\overline{\overline{I}} - \hat{k}_s \cdot \hat{k}_s) \cdot \overline{F}(\alpha_0, \beta_0) \right|^2 < II^* >$$

From equation (7.4.50)

$$< \lim_{k\to\infty} II^* > = \frac{4\pi^2 A_0}{k_{dz}^2} P\left(-\frac{k_{dx}}{k_{dz}}, -\frac{k_{ky}}{k_{dz}} \right)$$

For incident polarization b, the scattered intensity for polarization a is

$$< |E_s(\overline{r})|^2 > = \frac{k^2|E_0|^2}{16\pi^2 r^2} |\hat{a} \cdot \overline{F}_b(\alpha_0, \beta_0)|^2$$

where $\overline{F}_b(\alpha_0, \beta_0) = \overline{F}(\alpha_0, \beta_0)|_{\hat{e}_i = b}$ and

$$\overline{F}(\alpha_0, \beta_0) = (1 + \alpha_0^2 + \beta_0^2)^{1/2} \left\{ \begin{array}{l} -(\hat{e}_i \cdot \hat{q}_i)(\hat{n} \cdot \hat{k}_i)\hat{q}_i(1 - R^{\mathrm{TE}}) \\ +(\hat{e}_i \cdot \hat{p}_i)(\hat{n} \times \hat{q}_i)(1 + R^{\mathrm{TM}}) \\ +(\hat{e}_i \cdot \hat{q}_i)([\hat{k}_s \times (\hat{n} \times \hat{q}_i)](1 + R^{\mathrm{TE}}) \\ +(\hat{e}_i \cdot \hat{p}_i)(\hat{n} \cdot \hat{k}_i)(\hat{k}_s \times \hat{z}_i)(1 - R^{\mathrm{TM}}) \end{array} \right\}$$

Using $\hat{n} = \dfrac{-k_d}{|k_d|} = \dfrac{\overline{k}_s - \overline{k}_i}{|k_d|}$

$\hat{q}_i = \dfrac{\hat{k}_i \times \hat{n}}{|\hat{k}_i \times \hat{n}|} = \dfrac{\hat{k}_i \times \hat{k}_s}{|\hat{k}_i \times \hat{k}_s|}$ $\hat{p}_i = \hat{q}_i \times \hat{h}_i$

$\hat{v} = \hat{h} \times \hat{k}_i$ $\hat{h} = \hat{k} \times \hat{v}$ we can have

$|\hat{a}_s \cdot \overline{F}_b(\alpha_0, \beta_0)|^2 = \dfrac{|k_d|^2}{k^2|\hat{k}_i \times \hat{k}_s|^4 k_{dz}^2} f_{ba}$

$$f_{vv} = |(\hat{h}_s \cdot \hat{k}_i)(\hat{h}_i \cdot \hat{k}_s)R^{\mathrm{TE}} + (\hat{v}_s \cdot \hat{k}_i)(\hat{v}_i \cdot \hat{k}_s)R^{\mathrm{TM}}|^2$$

$$f_{hv} = |(\hat{v}_s \cdot \hat{k}_i)(\hat{h}_i \cdot \hat{k}_s)R^{\mathrm{TE}} - (\hat{h}_s \cdot \hat{k}_i)(\hat{v}_i \cdot \hat{k}_s)R^{\mathrm{TM}}|^2$$

$$f_{vh} = |(\hat{h}_s \cdot \hat{k}_i)(\hat{v}_i \cdot \hat{k}_s)R^{\mathrm{TE}} - (\hat{v}_s \cdot \hat{k}_i)(\hat{h}_i \cdot \hat{k}_s)R^{\mathrm{TM}}|^2$$

$$f_{hh} = |(\hat{v}_s \cdot \hat{k}_i)(\hat{v}_i \cdot \hat{k}_s)R^{\mathrm{TE}} + (\hat{h}_s \cdot \hat{k}_i)(\hat{h}_i \cdot \hat{k}_s)R^{\mathrm{TM}}|^2$$

$$< |E_s|^2 > = \frac{|E_0|^2|k_d|^4 f_{ab}}{16\pi^2 r^2 k^2 |\hat{k}_i \times \hat{k}_s|^4 k_{dz}^2} < II^* >$$

$$= \frac{A_0 |k_d|^4 f_{ab} |E_0|^2}{4\pi r^2 k^2 |\hat{k}_i \times \hat{k}_s|^4 k_{dz}^2} P\left(-\frac{k_{dx}}{k_{dz}} \, , \, -\frac{k_{dy}}{k_{dz}} \right)$$

$$\gamma_{ab} = \frac{4\pi r^2 < |E_s|^2 > a}{A \cos \theta_i |\overline{E}_0|_b^2} = \frac{k^2 |\hat{a} \cdot \overline{F}_b(0,0)|^2| < II^* > |^2}{4\pi A_0 \cos \theta_i}$$

$$\gamma_{ab} = \frac{f_{ab} |k_d|^4}{\cos \theta_i |\hat{k}_i \times \hat{k}_s|^4 k_{dz}^4} P\left(-\frac{k_{dx}}{k_{dz}} \, , \, -\frac{k_{dy}}{k_{dz}} \right)$$

Note: $\int \gamma_{ab} d\Omega = \int \frac{\gamma_{ab}}{k^2} d^2k$.

P7.4.2

From equation (7.4.58)

$$\sigma_{hh}(\theta_i) = \sigma_{vv}(\theta_i) = \frac{|R|^2 e^{-\tan^2 \theta_i / (2\sigma^2 |C''(0)|)}}{\cos^4 \theta_i 2\sigma^2 |C''(0)|}$$

$$\sigma^2 |C''(0)| = 2\frac{\sigma^2}{\rho^2} = 0.02 \, , \, |R|^2 \approx 1$$

$$\sigma_{hh} = \sigma_{vv} = \frac{|R|^2 e^{-\tan^2\theta_i/0.04}}{\cos^4\theta_i(0.04)} = 25\frac{e^{-25\tan^2\theta_i}}{\cos^4\theta_i}$$

at $\theta_i = \pi/2$, $\dfrac{e^{-25\tan^2\theta_i}}{\cos^4\theta_i} = 0$, using L'Hôpital Rule.

P7.5.1

$\overline{D}_P = \epsilon_o\overline{E}_P - \epsilon_o\Gamma\sum_N F_{P-N}\overline{E}_N$, and Maxwell equations give

$$\overline{K}_M\times(\overline{K}_M \times \overline{E}_M) = \omega\mu_o(\overline{K}_M \times \overline{H}_M) = -\omega^2\mu_o\overline{D}_M$$

$$= -\omega^2\mu_o\epsilon_o(\overline{E}_M - \Gamma\sum_N F_{M-N}\overline{E}_N)$$

$$k^2\overline{E}_M - (\overline{K}_M \cdot \overline{K}_M)\overline{E}_M + \overline{K}_M(\overline{K}_M \cdot \overline{E}_M) = k^2\Gamma\sum_N F_{M-N}\overline{E}_N$$

$$[k^2(1 - \Gamma F_0) - \overline{K}_M \cdot \overline{K}_M]\overline{E}_M + \overline{K}_M(\overline{K}_M \cdot \overline{E}_M) = k^2\Gamma\sum_{M\neq N} F_{M-N}\overline{E}_N$$

Consider TM polarization, we find

$$[k^2(1 - \Gamma F_0) - \overline{K}_0 \cdot \overline{K}_0]\overline{E}_0 \approx [2k\sqrt{1-\Gamma_0}]\kappa_0 = k^2\Gamma F_{-P}\overline{E}_P\cos 2\theta$$

$$[k^2(1 - \Gamma F_0) - \overline{K}_P \cdot \overline{K}_P]\overline{E}_P \approx [2k\sqrt{1-\Gamma_0}]\kappa_P = k^2\Gamma F_P\overline{E}_0\cos 2\theta$$

$$\kappa_0\kappa_P = \frac{k^2}{4}\frac{\Gamma^2 F_P F_{-P}}{1-\Gamma_0}\cos^2 2\theta$$

P7.5.2

Referring to Figure P7.5.2.1, we see that $\kappa_0 = \kappa_P$ and $K = 2\kappa_0/\cos\theta = 2\pi/\Lambda_0$, where Λ_0 is the unit of the slab thickness. We thus have $\kappa_p = \kappa_0 = \pi\cos\theta/\Lambda_0$ and $\Lambda_0 = \lambda\cos\theta\sqrt{(1+\Gamma_0)/\Gamma_P\Gamma_{-P}}$ and λ is the wavelength.

P7.5.3

Retain only two terms

$$H_y = H_0 e^{i[kz-\omega t]} + H_{-1}e^{i[(k-\frac{2\pi}{a})z-\omega t]}$$

$$= H_0 e^{i[\frac{\pi}{a}z-\omega t]} + H_{-1}e^{i[-\frac{\pi}{a}z-\omega t]}$$

$$\frac{\omega^2}{c^2}H_y = -i\frac{\pi}{a}\frac{\partial}{\partial z}\kappa\{H_0 e^{i[kz-\omega t]} - H_{-1}e^{i[(k-\frac{2\pi}{a})z-\omega t]}\}$$

$$= -i\frac{\pi}{a}e^{-i\omega t}\frac{\partial}{\partial z}\{H_0[\kappa_0 e^{i[kz]} + \kappa e^{i[(k+\frac{2\pi}{a})z]} + \kappa e^{i[(k-\frac{2\pi}{a})z]}]$$

$$- H_{-1}[\kappa_0 e^{i[(k-\frac{2\pi}{a})z]} + \kappa e^{i[kz]} + \kappa e^{i[(k-\frac{4\pi}{a})z]}]\}$$

$$= (\frac{\pi}{a})^2 e^{-i\omega t}\{H_0[\kappa_0 e^{i[\frac{\pi}{a}z]} + 3\kappa e^{i[\frac{3\pi}{a}z]} - \kappa e^{i[\frac{-\pi}{a}z]}]$$

$$+ H_{-1}[\kappa_0 e^{i[\frac{-\pi}{a}z]} - \kappa e^{i[\frac{\pi}{a}z]} + 3\kappa e^{i[\frac{-3\pi}{a}z]}]\}$$

Comparing coefficients of the same z dependence, we find

$$[\frac{\omega^2}{c^2} - \kappa_0(\frac{\pi}{a})^2]H_0 = -\kappa(\frac{\pi}{a})^2 H_{-1}$$

$$[\frac{\omega^2}{c^2} - \kappa_0(\frac{\pi}{a})^2]H_{-1} = -\kappa(\frac{\pi}{a})^2 H_0$$

We thus find $\omega = \sqrt{\kappa_0 \pm \kappa} \; \pi c/a$ and a stop band gap is formed [Fig. 7.5.3], $H_{-1}/H_0 = \pm 1$. Thus

$$H_y = H_0[e^{i\frac{\pi}{a}z} \pm e^{-i\frac{\pi}{a}z}]e^{-i\sqrt{\kappa_0 \pm \kappa} \; \pi ct/a}$$

P7.6.1

$$P(f(x) = \xi) = \frac{1}{2\sqrt{\sigma\pi}}e^{-\xi^2/2\sigma^2}$$

$$< e^{i\alpha f(x)} > = \frac{1}{2\sqrt{\sigma\pi}} \int_{-\infty}^{\infty} d\xi e^{i\alpha\xi}e^{-\xi^2/2\sigma^2} d\xi$$

$$= \frac{1}{2\sqrt{\sigma\pi}} \int_{-\infty}^{\infty} d\xi e^{-\frac{1}{2\sigma^2}[\xi^2 - i2\sigma^2\alpha\xi - \sigma^4\alpha^2] - \frac{\sigma^2\alpha^2}{2}}$$

$$= \frac{e^{-\frac{\sigma^2\alpha^2}{2}}}{\sqrt{\sigma\pi}} \int_{-\infty}^{\infty} d\xi e^{-\frac{1}{2\sigma^2}[\xi - i\sigma\alpha^{\frac{1}{2}}]} = e^{-\frac{\sigma^2\alpha^2}{2}}$$

P7.7.1

Let $\overline{E}_{SD}$ be the field caused by the surrounding dipoles, we write

$$\overline{E}_{\text{loc}} = \overline{E} + \overline{E}_{SD}$$

Where $\overline{E}$ is the field in the dielectric in the absence of the hole, and $\overline{E}_{SD}$ can be calculated from the polarization charges. Let

$$\sigma_P = \hat{n} \cdot \overline{P} = \text{Polarization surface charge at the spherical surface.}$$

Using spherical coordinates, we have

$$\sigma_P = -\hat{r} \cdot \overline{P} = -P\cos\theta$$

Making electroquasistatic assumptions we write the electric field as

$$\overline{E}_{SD} = \begin{cases} -E_0 \left(\frac{a}{r}\right)^3 \left(\hat{r}2\cos\theta + \hat{\theta}\sin\theta\right) & \text{for } r > a \\ E_0(\hat{r}\cos\theta - \hat{\theta}\sin\theta) & \text{for } r < a \end{cases}$$

The continuity of the tangential $\overline{E}_{SD}$ can be checked by taking the cross product of $\hat{r}$ with $\overline{E}_{SD}$. It is seen that the tangential $\overline{E}_{SD}$ is continues at

$r = a$ and the constant E_0 is evaluated using the discontinuity relation for the normal $\overline{D}$ field:

$$\epsilon_0 \left[\overline{E}_{SD}(r = a^+) - \overline{E}_{SD}(r = a^-) \right] \cdot \hat{r} = \sigma_P = -P \cos \theta$$

We find $E_0 = \dfrac{P}{3\epsilon_0}$ and

$$\overline{E}_{SD} = \begin{cases} -\dfrac{P}{3\epsilon_0} \left(\dfrac{a}{r}\right)^3 (2\hat{r} \cos \theta + \hat{\theta} \sin \theta) & \text{for } r > a \\ +\dfrac{P}{3\epsilon_0} (\hat{r} \cos \theta - \hat{\theta} \sin \theta) = \hat{z}\dfrac{P}{3\epsilon_0} & \text{for } r < a \end{cases}$$

Thus, at the place of the induced dipole, $\overline{E}_{\text{loc}} = \overline{E} + \dfrac{\overline{P}}{3\epsilon_0}$.

$$\overline{P} = N\alpha \overline{E}_{\text{loc}} = N\alpha \left(\overline{E} + \frac{\overline{P}}{3\epsilon_0} \right)$$

$$\overline{P} = \frac{N\alpha}{1 - N\alpha/3\epsilon_0} \overline{E} = (\epsilon - \epsilon_0)\overline{E}$$

$$\frac{\epsilon}{\epsilon_0} = \frac{1 + 2N\alpha/3\epsilon_0}{1 - N\alpha/3\epsilon_0}$$

8

RELATIVITY

8.5 Hamilton's Principle and Noether's Theorem

A. Action Integral

B. Hamilton's Principle and Maxwell Equations

C. Noether's Theorem and Energy Momentum Tensors

Answers

8.1   Maxwell-Minkowski Theory

For the principle of special relativity, we can state the postulate as
follows: physical laws are form-invariant among uniformly moving ob-
servers whose space and time coordinates obey the Lorentz transfor-
mation laws. Thus, the Maxwell equations will have the same form
independent of the frames of reference of all observers, although the
numerical value of all field quantities will be different. On the basis of
this postulate, the constancy of the velocity of light is a direct con-
sequence of the form invariance of the Maxwell equations in vacuum.
The form invariance of physical laws under the Lorentz transforma-
tion of space and time is called Lorentz covariance. In 1908 Minkowski
formally stated that the macroscopic Maxwell equations in material
are Lorentz covariant. With his postulate and the Lorentz transforma-
tion for space and time coordinates, we can obtain the transformation
formulas for electromagnetic field vectors, from which the constitutive
relations for various moving media can be derived.

Suppose that, from the point of view of an observer S, macro-
scopic electrodynamics is described by the Maxwell equations:

$$\nabla \times \overline{E} + \frac{\partial \overline{B}}{\partial t} = 0 \qquad\qquad (8.1.1a)$$

$$\nabla \cdot \overline{B} = 0 \qquad\qquad (8.1.1b)$$

$$\nabla \times \overline{H} - \frac{\partial \overline{D}}{\partial t} = \overline{J} \qquad\qquad (8.1.1c)$$

$$\nabla \cdot \overline{D} = \rho \qquad\qquad (8.1.1d)$$

$$\nabla \cdot \overline{J} + \frac{\partial \rho}{\partial t} = 0 \qquad\qquad (8.1.1e)$$

Then, from the point of view of an observer S' moving with respect
to S, the Maxwell equations take the same form:

$$\nabla' \times \overline{E}' + \frac{\partial \overline{B}'}{\partial t'} = 0 \qquad\qquad (8.1.2a)$$

$$\nabla' \cdot \overline{B}' = 0 \qquad\qquad (8.1.2b)$$

$$\nabla' \times \overline{H}' - \frac{\partial \overline{D}'}{\partial t'} = \overline{J}' \qquad\qquad (8.1.2c)$$

$$\nabla' \cdot \overline{D}' = \rho' \qquad\qquad (8.1.2d)$$

$$\nabla' \cdot \overline{J}' + \frac{\partial \rho'}{\partial t'} = 0 \qquad\qquad (8.1.2e)$$

where primes denote quantities associated with S'. The fundamental field quantities are $\overline{E}$, $\overline{B}$, $\overline{D}$, and $\overline{H}$. If $\overline{E}$ and $\overline{B}$ are regarded as pure field quantities, then $\overline{D}$ and $\overline{H}$ contain information about the material media. Following Sommerfeld, we refer to $\overline{E}$ and $\overline{B}$ as the entity of intensity, and $\overline{D}$ and $\overline{H}$ as the entity of quantity. In four-dimensional Minkowski space the entity of intensity forms a field tensor of second rank, and the entity of quantity forms an excitation tensor of second rank. By Minkowski's postulate, we can find the transformation laws for all field variables from the Lorentz transformation of space and time.

The formulation that we just described is called the *Minkowski formulation*. The concept that all material media can be regarded as source terms in the Maxwell equations and that only two electromagnetic field vectors are fundamental quantities has led to alternative formulations for macroscopic electromagnetic theory.

EXAMPLE 8.1.1   Amperian formulation.

In the *Amperian formulation*, the Maxwell equations take the form

$$\nabla \times \overline{E}_A = -\frac{\partial \overline{B}_A}{\partial t}$$

$$\nabla \times \left[\frac{1}{\mu_o}\overline{B}_A\right] = \frac{\partial}{\partial t}\left(\epsilon_o\overline{E}_A + \overline{P}_A - \frac{1}{c^2}\overline{M}_A \times \overline{v}\right)$$

$$+ \nabla \times \left(\overline{M}_A + \overline{P}_A \times \overline{v}\right) + \overline{J}_A$$

$$\nabla \cdot (\epsilon_o \overline{E}_A) = -\nabla \cdot \left(\overline{P}_A - \frac{1}{c^2}\overline{M}_A \times \overline{v}\right) + \rho_A$$

$$\nabla \cdot \overline{B}_A = 0$$

where the subscript A signifies the Amperian formulation. The two fundamental field vectors are $\overline{E}_A$ and $\overline{B}_A$, while the polarization vector $\overline{P}_A$ and the magnetization $\overline{M}_A$ characterize the material media moving with velocity $\overline{v}$. The variables are related to those in the Minkowski formulation by

$$\overline{E} = \overline{E}_A; \qquad \overline{B} = \overline{B}_A$$

$$\overline{H} = \frac{1}{\mu_o}\overline{B}_A - \overline{M}_A - \overline{P}_A \times \overline{v}$$

$$\overline{D} = \epsilon_o\overline{E}_A + \overline{P}_A - \frac{1}{c^2}\overline{M}_A \times \overline{v}$$

$$\overline{J} = \overline{J}_A; \qquad \rho = \rho_A$$

— END OF EXAMPLE 8.1.1 —

EXAMPLE 8.1.2   Chu formulation.

In the *Chu formulation*, the Maxwell equations take the form

$$\nabla \times \overline{E}_C = -\frac{\partial}{\partial t}\left(\mu_o\overline{H}_C + \mu_o\overline{M}_C\right) - \nabla \times \left(\mu_o\overline{M}_C \times \overline{v}\right)$$

$$\nabla \times \overline{H}_C = \frac{\partial}{\partial t}\left(\epsilon_o\overline{E}_C + \overline{P}_C\right) + \nabla \times \left(\overline{P}_C \times \overline{v}\right) + \overline{J}_C$$

$$\nabla \cdot \epsilon_o\overline{E}_C = -\nabla \cdot \overline{P}_C + \rho_C$$

$$\nabla \cdot \mu_o\overline{H}_C = -\nabla \cdot \mu_o\overline{M}_C$$

where the subscript C signifies the Chu formulation. The variables are related to those in the Minkowski formulation by

$$\overline{E} = \overline{E}_C + \mu_o\overline{M}_C \times \overline{v}$$

$$\overline{B} = \mu_o\overline{H}_C + \mu_o\overline{M}_C$$

$$\overline{H} = \overline{H}_C - \overline{P}_C \times \overline{v}$$

$$\overline{D} = \epsilon_o\overline{E}_C + \overline{P}_C$$

$$\overline{J} = \overline{J}_C; \qquad \rho = \rho_C$$

— END OF EXAMPLE 8.1.2 —

The Maxwell equations as presented in the various formulations are in indefinite form; constitutive relations for material media have to be supplied. Once the constitutive relations are given, it has been shown by Tai [1964] that all formulations are equivalent. In the Amperian and the Chu formulations, models of the constituents of media are elaborated with kinematic approaches. In the Amperian formulation [Panofsky and Phillips, 1962], constituents of a dipolar medium are visualized as two basic elements, an electric dipole and a current loop. The Amperian model is closely related to the atomic structure, where spinning and orbiting electrons act as current loops.

In the Chu formulation [Fano, Chu, and Adler, 1960], a dipolar medium is visualized as containing electric and magnetic dipoles. The Chu formulation is useful because there are no inherently moving parts in a magnetic dipole, as opposed to a current loop. When moments of higher order than the dipole moment are significant in a medium, the task of modeling becomes much more involved. From the point of view of electromagnetic wave theory, we are not interested in the reaction of a medium under the action of a field where a model of the medium constituents may be helpful, but we are interested in the way

the electromagnetic wave behaves. We favor the Maxwell-Minkowski theory not only because of its simplicity and elegance but also because of its practical applicability.

Problems

P8.1.1

In the *Boffi formulation*, the Maxwell equations take the form

$$\nabla \times \overline{E}_B = -\frac{\partial \overline{B}_B}{\partial t}$$

$$\nabla \times \left(\frac{1}{\mu_o} \overline{B}_B \right) = \frac{\partial}{\partial t} \left(\epsilon_o \overline{E}_B + \overline{P}_B \right) + \nabla \times \overline{M}_B + \overline{J}_B$$

$$\nabla \cdot \epsilon_o \overline{E}_B = -\nabla \cdot \overline{P}_B + \rho_B$$

$$\nabla \cdot \overline{B}_B = 0$$

where the subscript B signifies the Boffi formulation. Determine the variables related to those in the Minkowski formulation.

8.2   Lorentz Transformation

A. Lorentz Transformation of Space and Time

The principle of relativity, which requires that all physical laws be form-invariant as described by all observers, is basic in formulating the laws of nature. Space and time constitute the coordinates for descriptions of physical phenomena. The Galilean transformation of space and time was used to provide a basis for deriving transformation laws between observers in relative motion. The principle of relativity that is based on the Galilean transformation is referred to as *Galilean relativity*. Under the Galilean transformation, the laws of Newtonian mechanics are form-invariant, but the laws of electromagnetism change their form. In 1904, Lorentz examined the conditions for form invariance of the Maxwell equations in vacuum between observers moving with constant velocities relative to each other. In 1905, Einstein deduced Lorentz transformation laws from the single postulate that the velocity of light in vacuum is a universal constant, and the assumption that vacuum is linear, isotropic, and homogeneous. Einstein's principle of relativity that is based on the Lorentz transformation is *special relativity*. The laws of Newtonian mechanics, since they were not form-invariant under the Lorentz transformation, have been revised. Physical laws that are form-invariant under the Lorentz transformation are *Lorentz-covariant*.
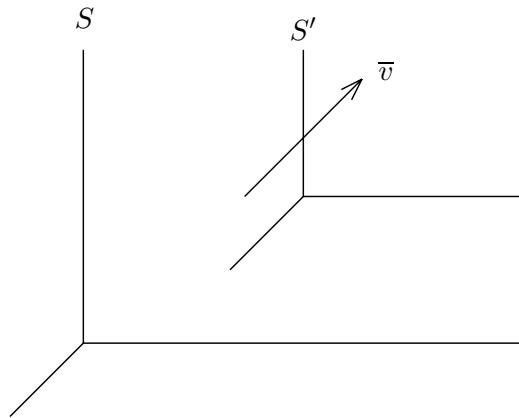
Figure 8.2.1   Observer S' moves with velocity $\overline{v}$ relative to observer S.

Consider the simple case in which the coordinate axes of observers S and S' are parallel, with their origins coinciding at time $t = 0$. Observer S' moves uniformly with velocity $\overline{v}$ relative to S [Fig. 8.2.1]. The Lorentz transformation of space-time coordinates between these two moving observers, with the use of dyadic notation, is given by

$$\text{LT} \begin{cases} ct' = \gamma ct - \gamma \overline{\beta} \cdot \overline{r} & (8.2.1a) \\ \overline{r}' = \overline{\overline{\alpha}} \cdot \overline{r} - \gamma \overline{\beta} ct & (8.2.1b) \end{cases}$$

where

$$\overline{\overline{\alpha}} = \overline{\overline{I}} + (\gamma - 1) \frac{\overline{\beta}\,\overline{\beta}}{\beta^2} \qquad (8.2.2)$$

$$\gamma = \frac{1}{\sqrt{1 - \beta^2}} \qquad (8.2.3)$$

$$\beta^2 = \overline{\beta} \cdot \overline{\beta} \qquad \overline{\beta} = \frac{\overline{v}}{c} \qquad (8.2.4)$$

and $c = 3 \times 10^8\,\text{m/s}$ is the velocity of light in vacuum. In matrix notation, the unit dyad $\overline{\overline{I}}$ is a diagonal matrix

$$\overline{\overline{I}} = \begin{bmatrix} 1 & 0 & 0 \\ 0 & 1 & 0 \\ 0 & 0 & 1 \end{bmatrix} \qquad (8.2.5)$$

and

$$\overline{\overline{\alpha}} = \begin{bmatrix} 1 + (\gamma - 1)\dfrac{\beta_x\,\beta_x}{\beta^2} & (\gamma - 1)\dfrac{\beta_x\,\beta_y}{\beta^2} & (\gamma - 1)\dfrac{\beta_x\,\beta_z}{\beta^2} \\ (\gamma - 1)\dfrac{\beta_y\,\beta_x}{\beta^2} & 1 + (\gamma - 1)\dfrac{\beta_y\,\beta_y}{\beta^2} & (\gamma - 1)\dfrac{\beta_y\,\beta_z}{\beta^2} \\ (\gamma - 1)\dfrac{\beta_z\,\beta_x}{\beta^2} & (\gamma - 1)\dfrac{\beta_z\,\beta_y}{\beta^2} & 1 + (\gamma - 1)\dfrac{\beta_z\,\beta_z}{\beta^2} \end{bmatrix}$$

$$(8.2.6)$$

where β_x, β_y, and β_z are the x, y, and z components of $\overline{\beta}$. Clearly, because $\overline{\overline{\alpha}}$ is symmetrical, the position vector $\overline{r} = \hat{x}x + \hat{y}y + \hat{z}z$ can be viewed as a column matrix operated on by $\overline{\overline{\alpha}}$, giving rise to another column matrix.

EXAMPLE 8.2.1   Velocity along the z axis.

When $\overline{v}$ is along the z axis, $\overline{\beta} = \hat{z}\beta$, $\beta_x = \beta_y = 0$, and $\beta_z = \beta$. The $\overline{\overline{\alpha}}$ matrix is simplified to

$$\overline{\overline{\alpha}} = \begin{bmatrix} 1 & 0 & 0 \\ 0 & 1 & 0 \\ 0 & 0 & \gamma \end{bmatrix}$$

We find from (8.2.1)

$$ct' = \gamma(ct - \beta z) \qquad\qquad (E8.2.1.1a)$$
$$x' = x \qquad\qquad (E8.2.1.1b)$$
$$y' = y \qquad\qquad (E8.2.1.1c)$$
$$z' = \gamma(z - \beta ct) \qquad\qquad (E8.2.1.1d)$$

We observe that the time coordinate is not a universal constant; two physical events that are simultaneous in S' will no longer be simultaneous in S.

— END OF EXAMPLE 8.2.1 —

EXAMPLE 8.2.2   Time dilation.

To consider transformation of time intervals, let a clock be in S', which moves along the $\hat{z}$ direction of S. The time interval of the clock as read by S' is $\Delta t' = t'_2 - t'_1$ and is called the *proper time interval*. The corresponding time interval of the clock as read by S is $t = t_2 = t_1$ and is called the *coordinate time interval*. By Lorentz transformation of space and time,

$$c\Delta t' = \gamma(c\Delta t - \beta\Delta z)$$
$$\Delta z' = \gamma(\Delta z - \beta c\Delta t)$$

The clock is stationary in S', and hence $\Delta z' = 0$. The proper time is $\Delta t'$ and the coordinate time is Δt. We find

$$\Delta t = \gamma\Delta t'$$

Observe that the coordinate time interval is always larger than the proper time interval. This phenomenon is known as time dilation.

— END OF EXAMPLE 8.2.2 —

EXAMPLE 8.2.3   Four-dimensional length.

An important identity can be derived from the LT (8.2.1). Forming the difference of magnitude squares of $\overline{r}'$ and ct', and using (8.2.1), we find

$$|\overline{r}'|^2 - |ct'|^2 = |\overline{r}|^2 - |ct|^2 \qquad\qquad (\text{E8.2.3.1})$$

Equation (E8.2.3.1) is important because it is independent of the relative velocity $\overline{v}$ between S and S'. It is a numerical constant that is invariant under the Lorentz transformation. Its square root can be regarded as expressing the length of a four-dimensional vector representing the space and time coordinates of a physical event. Evidently, in this four-dimensional space, called *Minkowski space*, the length of a vector can be imaginary as well as real.

— END OF EXAMPLE 8.2.3 —

EXAMPLE 8.2.4   First-order Lorentz transformation.

When $\overline{v}$ is so small that only terms of the order of $\overline{v}/c$ are significant, we have $\overline{\overline{\alpha}} = \overline{\overline{I}}$, $\gamma = 1$, and LT (1) becomes

$$\text{FOLT} \begin{cases} ct' = ct - \overline{\beta} \cdot \overline{r} & (\text{E8.2.4.1}a) \\[2mm] \overline{r}' = \overline{r} - \overline{\beta}ct & (\text{E8.2.4.1}b) \end{cases}$$

We call (E8.2.4.1) the *First-Order Lorentz Transformation* (FOLT). As seen from FOLT, the space term $\beta \cdot \overline{r}$ in the time transformation may not be negligible, since $\overline{r}$ and $\overline{r}'$ can be large, while $\overline{\beta}$ is small.

— END OF EXAMPLE 8.2.4 —

EXAMPLE 8.2.5   Galilean transformation.

Before 1905, time was regarded as a universal quantity. For two observers in relative uniform motion, the space coordinate changed because of motion, but the time coordinate remained the same:

$$\text{GT} \begin{cases} t' = t \\ \overline{r}' = \overline{r} - \overline{v}t \end{cases}$$

This transformation law of space and time is the Galilean transformation (GT). We note also that the Galilean transformation is not a limiting case of the LT when velocity $\overline{v}$ is small. Rather, LT reduces to GT when $\overline{v}$ is small and when $\overline{r}$ is small compared with ct/β, as seen from FOLT (E8.2.4.1a). Mathematically, LT reduces to GT when $c \to \infty$.

— END OF EXAMPLE 8.2.5 —

B. Lorentz Transformation of Field Vectors

Transformation formulas for field vectors are direct consequences of the Lorentz transformation for space and time and Minkowski's postulate of the Lorentz covariance of the Maxwell equations. From the LT given in (8.2.1), the following transformation formulas can be derived.

$$\text{LT} \qquad \begin{bmatrix} c\overline{D}' \\ \overline{H}' \end{bmatrix} = \gamma \begin{bmatrix} \overline{\overline{\alpha}}^{-1} & \overline{\overline{\beta}} \\ -\overline{\overline{\beta}} & \overline{\overline{\alpha}}^{-1} \end{bmatrix} \cdot \begin{bmatrix} c\overline{D} \\ \overline{H} \end{bmatrix} \qquad (8.2.7)$$

$$\text{LT} \qquad \begin{bmatrix} \overline{E}' \\ c\overline{B}' \end{bmatrix} = \gamma \begin{bmatrix} \overline{\overline{\alpha}}^{-1} & \overline{\overline{\beta}} \\ -\overline{\overline{\beta}} & \overline{\overline{\alpha}}^{-1} \end{bmatrix} \cdot \begin{bmatrix} \overline{E} \\ c\overline{B} \end{bmatrix} \qquad (8.2.8)$$

where $\overline{\overline{\alpha}}^{-1}$ is the inverse of $\overline{\overline{\alpha}}$

$$\overline{\overline{\alpha}}^{-1} = \overline{\overline{I}} + \left(\frac{1}{\gamma} - 1 \right) \frac{\overline{\beta}\,\overline{\beta}}{\beta^2}$$

$$= \begin{bmatrix} 1 + (\frac{1}{\gamma} - 1)\dfrac{\beta_x\,\beta_x}{\beta^2} & (\frac{1}{\gamma} - 1)\dfrac{\beta_x\,\beta_y}{\beta^2} & (\frac{1}{\gamma} - 1)\dfrac{\beta_x\,\beta_z}{\beta^2} \\ (\frac{1}{\gamma} - 1)\dfrac{\beta_y\,\beta_x}{\beta^2} & 1 + (\frac{1}{\gamma} - 1)\dfrac{\beta_y\,\beta_y}{\beta^2} & (\frac{1}{\gamma} - 1)\dfrac{\beta_y\,\beta_z}{\beta^2} \\ (\frac{1}{\gamma} - 1)\dfrac{\beta_z\,\beta_x}{\beta^2} & (\frac{1}{\gamma} - 1)\dfrac{\beta_z\,\beta_y}{\beta^2} & 1 + (\frac{1}{\gamma} - 1)\dfrac{\beta_z\,\beta_z}{\beta^2} \end{bmatrix}$$

$$= \overline{\overline{\alpha}} - \gamma\overline{\beta}\,\overline{\beta}$$

The 3×3 matrix $\overline{\overline{\beta}}$ is defined such that for any vector $\overline{A}$

$$\overline{\overline{\beta}} \cdot \overline{A} \equiv \overline{\beta} \times \overline{A} \qquad (8.2.9)$$

In explicit matrix form,

$$\overline{\overline{\beta}} = \begin{bmatrix} 0 & -\beta_z & \beta_y \\ \beta_z & 0 & -\beta_x \\ -\beta_y & \beta_x & 0 \end{bmatrix} \qquad (8.2.10)$$

From $(\overline{\overline{\beta}})^2 \cdot \overline{A} = \overline{\beta} \times (\overline{\beta} \times \overline{A}) = \overline{\beta}\,\overline{\beta} \cdot \overline{A} - \beta^2\overline{A}$ it follows that

$$\overline{\overline{\beta}}^2 = \overline{\beta}\,\overline{\beta} - \beta^2\overline{\overline{I}} \qquad (8.2.11)$$

Although both $\overline{\overline{\alpha}}$ and $\overline{\overline{\alpha}}^{-1}$ are symmetric, $\overline{\overline{\beta}}$ is skew-symmetric.

Transformation formulas (8.2.7) and (8.2.8) express the fact that $\overline{H}$ and $\overline{D}$ fields transform as an entity (entity of quantity), and so do $\overline{E}$ and $\overline{B}$ (entity of intensity).

EXAMPLE 8.2.6   Derivation of electromagnetic field transformation.
      From the LT given in (8.2.1) we obtain Lorentz transformation for space-
time derivatives. We make use of the chain rule in differentiation,

$$\frac{\partial}{\partial ct} = \left[\frac{\partial ct'}{\partial ct}\right]\frac{\partial}{\partial ct'} + \left[\frac{\partial x_i'}{\partial ct}\right]\frac{\partial}{\partial x_i'}$$

and

$$\frac{\partial}{\partial x_i} = \left[\frac{\partial ct'}{\partial x_i}\right]\frac{\partial}{\partial ct'} + \left[\frac{\partial x_j'}{\partial x_i}\right]\frac{\partial}{\partial x_j'}$$

Substituting the LT (8.2.1) and noting the fact that $\overline{\overline{\alpha}}$ is symmetrical, we
find

$$\frac{\partial}{\partial ct} = \gamma\frac{\partial}{\partial ct'} - \gamma\overline{\beta}\cdot\nabla' \qquad\qquad (E8.2.6.1a)$$

$$\nabla = \overline{\overline{\alpha}}\cdot\nabla' - \gamma\overline{\beta}\frac{\partial}{\partial ct'} \qquad\qquad (E8.2.6.1b)$$

To derive transformation laws for all field vectors, we substitute (E8.2.6.1)
into the Maxwell equations in the S frame and require them to have the
same forms in the S' frame. First, consider the charge conservation equation.
Transformation from S to S' gives

$$\left[\overline{\overline{\alpha}}\cdot\nabla' - \gamma\overline{\beta}\frac{\partial}{\partial ct'}\right]\cdot\overline{J} + \gamma\left[\frac{\partial}{\partial ct'} - \overline{\beta}\cdot\nabla'\right]c\rho = 0$$

Thus the charge conservation equation is Lorentz-covariant if

$$c\rho' = \gamma(c\rho - \overline{\beta}\cdot\overline{J}) \qquad\qquad (E8.2.6.2a)$$

$$\overline{J}' = \overline{\overline{\alpha}}\cdot\overline{J} - \gamma\overline{\beta}c\rho \qquad\qquad (E8.2.6.2b)$$

Note that a charge distribution stationary in S certainly produces a current
in S', but from (E8.2.6.2b) a uniform current element in S also generates
a charge distribution in S', which is a relativistic effect and cannot be seen
under GT.
      Next, we introduce (E8.2.6.1) into Ampère's law and Gauss' electric field
law:

$$\left[\overline{\overline{\alpha}}\cdot\nabla' - \gamma\frac{\partial}{\partial ct'}\overline{\beta}\right]\times\overline{H} - \left[\gamma\frac{\partial}{\partial ct'} - \gamma\overline{\beta}\cdot\nabla'\right]c\overline{D} = \overline{J} \qquad (E8.2.6.3a)$$

$$\left[\overline{\overline{\alpha}}\cdot\nabla' - \gamma\frac{\partial}{\partial ct'}\overline{\beta}\right]\cdot c\overline{D} = c\rho \qquad\qquad (E8.2.6.3b)$$

To find transformation laws for $\overline{D}'$ and $\overline{H}'$, we wish to cast (E8.2.6.3) into the form

$$\nabla' \cdot \overline{D}' = \rho' \qquad\qquad (E8.2.6.4a)$$

$$\nabla' \times \overline{H}' - \frac{\partial}{\partial t'}\overline{D}' = \overline{J}' \qquad\qquad (E8.2.6.4b)$$

In view of (E8.2.6.2a), we have $\gamma(E8.2.6.3b) - \gamma\overline{\beta} \cdot (E8.2.6.3a) = c\rho'$, which gives

$$\gamma\left[(\overline{\overline{\alpha}} \cdot \nabla') \cdot c\overline{D} - \overline{\beta} \cdot (\overline{\overline{\alpha}} \cdot \nabla') \times \overline{H} - \gamma(\overline{\beta} \cdot \nabla')(\overline{\beta} \cdot cD)\right] = c\rho'$$

Using

$$\overline{\beta} \cdot \left[(\overline{\overline{\alpha}} \cdot \nabla') \times \overline{H}\right] = \overline{\beta} \cdot \left\{\left[\nabla' + (\gamma - 1)\frac{(\overline{\beta} \cdot \nabla')}{\beta^2}\overline{\beta}\right] \times \overline{H}\right\}$$

$$= \overline{\beta} \cdot \nabla' \times \overline{H} = -\nabla' \cdot (\overline{\beta} \times \overline{H})$$

we find

$$\nabla' \cdot \left\{\gamma\left[\overline{\overline{\alpha}} - \gamma\overline{\beta}\,\overline{\beta}\right] \cdot c\overline{D} + \gamma\overline{\beta} \times \overline{H}\right\} = c\rho' \qquad\qquad (E8.2.6.5a)$$

By the same token, we use (E8.2.6.2b) to calculate $\overline{\overline{\alpha}} \cdot (E8.2.6.3a) - \gamma\overline{\beta} \cdot (E8.2.6.3b) = \overline{J}'$ which gives

$$\overline{\overline{\alpha}} \cdot (\overline{\overline{\alpha}} \cdot \nabla') \times \overline{H} + \gamma\overline{\overline{\alpha}} \cdot (\overline{\beta} \cdot \nabla')c\overline{D} - \gamma\overline{\beta}(\overline{\overline{\alpha}} \cdot \nabla')c\overline{D}$$

$$+ \frac{\partial}{\partial ct'}\left[-\gamma\overline{\overline{\alpha}} \cdot (\overline{\beta} \times \overline{H}) - \gamma(\overline{\overline{\alpha}} \cdot c\overline{D}) + \gamma^2\overline{\beta}\,\overline{\beta} \cdot c\overline{D}\right] = \overline{J}'$$

Using the fact that

$$\overline{\overline{\alpha}} \cdot \left[(\overline{\overline{\alpha}} \cdot \nabla') \times \overline{H}\right] = \nabla \times \overline{H} + \frac{\gamma - 1}{\beta^2} \cdot \left[(\overline{\beta} \cdot \nabla')\overline{\beta} \times \overline{H} - \overline{\beta}\nabla' \cdot (\overline{\beta} \times \overline{H})\right]$$

$$= \nabla' \times \left\{\overline{H} - \frac{\gamma - 1}{\beta^2}\left[\overline{\beta} \times (\overline{\beta} \times \overline{H})\right]\right\} = \nabla' \times \left\{\gamma\left[\overline{\overline{I}} + \left(\frac{1}{\gamma} - 1\right)\frac{\overline{\beta}\,\overline{\beta}}{\beta^2}\right] \cdot \overline{H}\right\}$$

and

$$\overline{\overline{\alpha}} \cdot (\overline{\beta} \cdot \nabla')c\overline{D} - \overline{\beta}\left[(\overline{\overline{\alpha}} \cdot \nabla')c\overline{D}\right] = (\overline{\beta} \times \nabla')c\overline{D} - \overline{\beta}(\nabla' \cdot c\overline{D}) = -\nabla' \times (\overline{\beta} \times c\overline{D})$$

We find

$$\nabla' \times \left\{\gamma\left[\overline{\overline{I}} + \left(\frac{1}{\gamma} - 1\right)\frac{\overline{\beta}\,\overline{\beta}}{\beta^2}\right] \cdot \overline{H} - \gamma\overline{\beta} \times c\overline{D}\right\}$$

$$- \frac{\partial}{\partial ct'}\left\{\gamma\left[\overline{\overline{\alpha}} - \gamma\overline{\beta}\,\overline{\beta}\right] \cdot c\overline{D} + \gamma\overline{\beta} \times \overline{H}\right\} = \overline{J}' \qquad (E8.2.6.5b)$$

Comparing (E8.2.6.4) and (E8.2.6.5), we obtain the transformation formulas for $\overline{D}$ and $\overline{H}$:

$$c\overline{D}' = \gamma\left[\overline{\overline{\alpha}} - \gamma\overline{\beta}\,\overline{\beta}\right] \cdot c\overline{D} + \gamma\overline{\beta} \times \overline{H} \qquad\qquad \text{(E8.2.6.6}a\text{)}$$

$$\overline{H}' = \gamma\left[\overline{\overline{I}} + \left(\frac{1}{\gamma} - 1\right)\frac{\overline{\beta}\,\overline{\beta}}{\beta^2}\right] \cdot \overline{H} - \gamma\overline{\beta} \times c\overline{D} \qquad \text{(E8.2.6.6}b\text{)}$$

It is easily shown that the dyadic quantities in the square brackets of (E8.2.6.6a) and (E8.2.6.6b) are equal to the inverse of $\overline{\overline{\alpha}}$

$$\overline{\overline{\alpha}}^{-1} = \overline{\overline{I}} + \left(\frac{1}{\gamma} - 1\right)\frac{\overline{\beta}\,\overline{\beta}}{\beta^2} = \overline{\overline{\alpha}} - \gamma\overline{\beta}\,\overline{\beta} \qquad\qquad \text{(E8.2.6.7)}$$

This is verified by showing that

$$\overline{\overline{\alpha}} \cdot \overline{\overline{\alpha}}^{-1} = \left[\overline{\overline{I}} + (\gamma - 1)\frac{\overline{\beta}\,\overline{\beta}}{\beta^2}\right] \cdot \left[\overline{\overline{I}} + \left(\frac{1}{\gamma} - 1\right)\frac{\overline{\beta}\,\overline{\beta}}{\beta^2}\right] = \overline{\overline{I}}$$

also $\overline{\overline{\alpha}}^{-1} \cdot \overline{\overline{\alpha}} = \overline{\overline{I}}$ and

$$\overline{\overline{\alpha}}^{-1} = \overline{\overline{I}} + \left(\frac{1}{\gamma} - 1\right)\frac{\overline{\beta}\,\overline{\beta}}{\beta^2} = \overline{\overline{\alpha}} - \gamma\overline{\beta}\,\overline{\beta}$$

in view of the fact that $1/\gamma^2 = 1 - \beta^2$. We can further define a 3×3 matrix $\overline{\overline{\beta}}$ such that for any vector $\overline{A}$

$$\overline{\overline{\beta}} \cdot \overline{A} \equiv \overline{\beta} \times \overline{A} \qquad\qquad \text{(E8.2.6.8)}$$

In explicit matrix form,

$$\overline{\overline{\beta}} = \begin{bmatrix} 0 & -\beta_z & \beta_y \\ \beta_z & 0 & -\beta_x \\ -\beta_y & \beta_x & 0 \end{bmatrix} \qquad\qquad \text{(E8.2.6.9)}$$

From $(\overline{\overline{\beta}})^2 \cdot \overline{A} = \overline{\beta} \times (\overline{\beta} \times \overline{A}) = \overline{\beta}\,\overline{\beta} \cdot \overline{A} - \beta^2\overline{A}$ it follows that

$$\overline{\overline{\beta}}^2 = \overline{\beta}\,\overline{\beta} - \beta^2\overline{\overline{I}} \qquad\qquad \text{(E8.2.6.10)}$$

Although both $\overline{\overline{\alpha}}$ and $\overline{\overline{\alpha}}^{-1}$ are symmetric, $\overline{\overline{\beta}}$ is skew-symmetric.

We now write the Lorentz transformation formulas for $c\overline{D}$ and $\overline{H}$ in (8.2.7). In a similar way, we can show that the forms of Faraday's emf law and Gauss' magnetic field law are preserved under LT, provided that $\overline{E}$ and $\overline{B}$ transform as (8.2.8), which is identical in form to (8.2.7).

<div align="right">— E<small>ND OF</small> E<small>XAMPLE</small> 8.2.6 —</div>

For the transformation of $\overline{E}$ and $c\overline{B}$ in (8.2.8), we decompose the field vectors into components parallel and perpendicular to the velocity $\overline{v}$. It is interesting to see that field components parallel to the velocity are left unchanged:

$$\overline{E}'_{\parallel} = \overline{E}_{\parallel} \tag{8.2.12a}$$

$$\overline{B}'_{\parallel} = \overline{B}_{\parallel} \tag{8.2.12b}$$

$$\overline{D}'_{\parallel} = \overline{D}_{\parallel} \tag{8.2.12c}$$

$$\overline{H}'_{\parallel} = \overline{H}_{\parallel} \tag{8.2.12d}$$

and the perpendicular components transform as

$$\overline{E}'_{\perp} = \gamma(\overline{E}_{\perp} + \overline{\beta} \times \overline{c}B_{\perp}) \tag{8.2.13a}$$

$$c\overline{B}'_{\perp} = \gamma(c\overline{B}_{\perp} - \overline{\beta} \times \overline{E}_{\perp}) \tag{8.2.13b}$$

$$c\overline{D}'_{\perp} = \gamma(c\overline{D}_{\perp} + \overline{\beta} \times \overline{H}_{\perp}) \tag{8.2.13c}$$

$$\overline{H}'_{\perp} = \gamma(\overline{H}_{\perp} - \overline{\beta} \times c\overline{D}_{\perp}) \tag{8.2.13d}$$

This is in contrast to the transformation of space coordinates, where the perpendicular components are left unchanged.

EXAMPLE 8.2.7   Galilean transformation.
    For GT, let $c \rightarrow \infty$;

$$\text{GT} \begin{cases} \overline{E}' = \overline{E} + \overline{v} \times \overline{B} & \text{(E8.2.7.1a)} \\[2mm] \overline{B}' = \overline{B} & \text{(E8.2.7.1b)} \\[2mm] \overline{D}' = \overline{D} & \text{(E8.2.7.1c)} \\[2mm] \overline{H}' = \overline{H} - \overline{v} \times \overline{D} & \text{(E8.2.7.1d)} \end{cases}$$

The inverses of all of these transformation formulas can be written with $\overline{\beta}$ replaced by $-\overline{\beta}$.

— END OF EXAMPLE 8.2.7 —

C. Lorentz Invariants

According to both LT $(8.2.13a)$ and GT $(E8.2.7.1a)$, a pure $\overline{B}$ field in S produces an electric field $\overline{E}'$ in S'. Thus a voltage is induced in a moving conductor when its velocity has a component perpendicular to the $\overline{B}$-field lines. According to LT $(8.2.13b)$, for a pure $\overline{E}$ field in S, a magnetic field is witnessed from a moving frame. Thus a stationary electron, when viewed from a moving frame, exhibits a magnetic field. But according to GT $(E8.2.7.1b)$, $\overline{B}'$ is equal to $\overline{B}$ and a stationary electron in S exhibits no magnetic field in S'.

Making use of (8.2.12) and (8.2.13), we find

$$
\begin{aligned}
\overline{E}' \cdot c\overline{B}' &= [\overline{E}_{||} + \gamma(\overline{E}_\perp + \overline{\beta} \times c\overline{B}_\perp)] \cdot [c\overline{B}_{||} + \gamma(c\overline{B}_\perp - \overline{\beta} \times \overline{E}_\perp)] \\
&= \overline{E} \cdot c\overline{B} \tag{8.2.14}
\end{aligned}
$$

$$
\begin{aligned}
|\overline{E}'|^2 - |c\overline{B}'|^2 &= |\overline{E}_{||} + \gamma(\overline{E}_\perp + \overline{\beta} \times \overline{c}B_\perp)|^2 - |c\overline{B}_{||} + \gamma(c\overline{B}_\perp - \overline{\beta} \times \overline{E}_\perp)|^2 \\
&= |\overline{E}|^2 - |c\overline{B}|^2 \tag{8.2.15}
\end{aligned}
$$

The two quantities $\overline{E} \cdot c\overline{B}'$ and $|\overline{E}|^2 - |c\overline{B}|^2$ in (8.2.14) and (8.2.15) are invariant under Lorentz transformation and are called Lorentz invariants.

EXAMPLE 8.2.8

We denote the 6×6 matrix in (8.2.7) and (8.2.8) by $\overline{\overline{L}}_6$:

$$
\overline{\overline{L}}_6(\overline{\beta}) = \gamma \begin{bmatrix} \overline{\overline{\alpha}}^{-1} & \overline{\overline{\beta}} \\ -\overline{\overline{\beta}} & \overline{\overline{\alpha}}^{-1} \end{bmatrix} \tag{E8.2.8.1}
$$

When the velocity is along the z axis, the LT matrix $\overline{\overline{L}}_6$ becomes

$$
\overline{\overline{L}}_6 = \gamma \begin{bmatrix}
1 & 0 & 0 & 0 & -\beta & 0 \\
0 & 1 & 0 & \beta & 0 & 0 \\
0 & 0 & 1/\gamma & 0 & 0 & 0 \\
0 & \beta & 0 & 1 & 0 & 0 \\
-\beta & 0 & 0 & 0 & 1 & 0 \\
0 & 0 & 0 & 0 & 0 & 1/\gamma
\end{bmatrix}. \tag{E8.2.8.2}
$$

The inverse transformation is determined by the inverse of $\overline{\overline{L}}_6(\overline{\beta})$. It can be verified that

$$
\overline{\overline{L}}_6^{-1}(\overline{\beta}) = \overline{\overline{L}}_6(-\beta) = \gamma \begin{bmatrix} \overline{\overline{\alpha}}^{-1} & -\overline{\overline{\beta}} \\ \overline{\overline{\beta}} & \overline{\overline{\alpha}}^{-1} \end{bmatrix} \tag{E8.2.8.3}
$$

By physical reasoning, the inverse of a pure Lorentz transformation is equivalent to changing the direction of velocity.

Let us explore further some properties of the $\overline{\overline{L}}_6$ matrix. Since $\overline{\overline{\alpha}}$ is symmetric and $\overline{\overline{\beta}}$ skew-symmetric, we have

$$\overline{\overline{L}}_6^T = \gamma \begin{bmatrix} (\overline{\overline{\alpha}}^{-1})^T & (-\overline{\overline{\beta}})^T \\ \overline{\overline{\beta}}^T & (\overline{\overline{\alpha}}^{-1})^T \end{bmatrix} = \overline{\overline{L}}_6 \qquad \text{(E8.2.8.4)}$$

where the superscript T denotes the transpose of the matrix. Thus $\overline{\overline{L}}_6$ is a symmetric 6×6 matrix. We can also show that

$$\overline{\overline{L}}_6^T \cdot \begin{bmatrix} \overline{\overline{I}} & \overline{\overline{0}} \\ \overline{\overline{0}} & -\overline{\overline{I}} \end{bmatrix} \cdot \overline{\overline{L}}_6 = \begin{bmatrix} \overline{\overline{I}} & \overline{\overline{0}} \\ \overline{\overline{0}} & -\overline{\overline{I}} \end{bmatrix} \qquad \text{(E8.2.8.5)}$$

$$\overline{\overline{L}}_6^T \cdot \begin{bmatrix} \overline{\overline{0}} & \overline{\overline{I}} \\ \overline{\overline{I}} & \overline{\overline{0}} \end{bmatrix} \cdot \overline{\overline{L}}_6 = \begin{bmatrix} \overline{\overline{0}} & \overline{\overline{I}} \\ \overline{\overline{I}} & \overline{\overline{0}} \end{bmatrix} \qquad \text{(E8.2.8.6)}$$

Numerous other identities can also be derived for the $\overline{\overline{L}}_6$ and $\overline{\overline{\alpha}}$ matrices.

Equation (E8.2.8.5) can be used to find relations that are invariant under the Lorentz transformation. Using LT for the entity of intensity (8.2.8), we have

$$\begin{bmatrix} \overline{E}' , \ c\overline{B}' \end{bmatrix} \cdot \begin{bmatrix} \overline{\overline{I}} & \overline{\overline{0}} \\ \overline{\overline{0}} & -\overline{\overline{I}} \end{bmatrix} \cdot \begin{bmatrix} \overline{E}' \\ c\overline{B}' \end{bmatrix} = \begin{bmatrix} \overline{E} , \ c\overline{B} \end{bmatrix} \cdot \overline{\overline{L}}_6^T \cdot \begin{bmatrix} \overline{\overline{I}} & \overline{\overline{0}} \\ \overline{\overline{0}} & -\overline{\overline{I}} \end{bmatrix} \cdot \overline{\overline{L}}_6 \cdot \begin{bmatrix} \overline{E} \\ c\overline{B} \end{bmatrix}$$
$$\text{(E8.2.8.7)}$$

In view of (E8.2.8.4), (E8.2.8.7) gives

$$\left| \overline{E}' \right|^2 - \left| c\overline{B}' \right|^2 = \left| \overline{E} \right|^2 - \left| c\overline{B} \right|^2 \qquad \text{(E8.2.8.8)}$$

It can be seen that the relative velocity between observers S and S' does not appear in (E8.2.8.8). The difference between the magnitude squared of $\overline{E}$ and the magnitude squared of $c\overline{B}$ is therefore a numerical constant independent of motion. Any quantity that is invariant under LT is called a Lorentz invariant. Note the difference between Lorentz invariance and Lorentz covariance: the former refers to a scalar number, the latter to a physical law. Another Lorentz invariant is obtained by using (8.2.8) and (E8.2.8.6)

$$\begin{bmatrix} \overline{E}' , c\overline{B}' \end{bmatrix} \cdot \begin{bmatrix} \overline{\overline{0}} & \overline{\overline{I}} \\ \overline{\overline{I}} & \overline{\overline{0}} \end{bmatrix} \cdot \begin{bmatrix} \overline{E}' \\ c\overline{B}' \end{bmatrix} = \begin{bmatrix} \overline{E}, c\overline{B} \end{bmatrix} \cdot \overline{\overline{L}}_6^T \cdot \begin{bmatrix} \overline{\overline{0}} & \overline{\overline{I}} \\ \overline{\overline{I}} & \overline{\overline{0}} \end{bmatrix} \cdot \overline{\overline{L}}_6 \cdot \begin{bmatrix} \overline{E} \\ c\overline{B} \end{bmatrix}$$

The result is

$$\overline{E}' \cdot \overline{B}' = \overline{E} \cdot \overline{B} \qquad \text{(E8.2.8.9)}$$

According to (E8.2.8.8) and (E8.2.8.9), the electromagnetic fields can be classified.

<div align="right">— END OF EXAMPLE 8.2.8 —</div>

D. Electromagnetic Field Classification
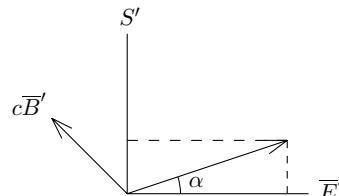
According to (E8.2.8.8) and (E8.2.8.9), the electromagnetic fields can be classified into the following categories:

Free-Space Wave Fields: $\overline{E} \cdot \overline{B} = 0$ *and* $\left|\overline{E}\right| = \left|c\overline{B}\right|$

The field vectors $\overline{E}$ and $c\overline{B}$ are always perpendicular in direction and equal in magnitude. The magnitude changes from observer to observer, as is characteristic of a plane wave in free space. Consider the case $\overline{E} = \hat{x}E$ and $\overline{B} = \hat{y}B$ and assume that an observer S' is moving along the z axis of S. Then by (8.2.13a) and (8.2.13b) we immediately obtain

$$E' = E \left[\frac{1-\beta}{1+\beta}\right]^{1/2}$$

$$B' = B \left[\frac{1-\beta}{1+\beta}\right]^{1/2}$$
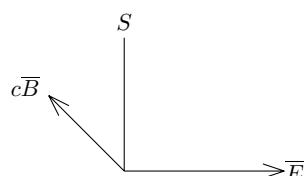
Figure 8.2.2 S' **moves in the direction of** $\overline{E}$.

The amplitude of the wave field decreases as the velocity along the $\hat{z}$ direction increases. When it reaches c, namely, $\beta = 1$, the amplitude is zero. Thus an observer moving in the $\overline{E} \times \overline{B}$ direction

at the velocity of light sees no field at all. An observer moving in a direction opposite to that of $\overline{E} \times \overline{B}$ at the velocity of light sees the amplitude approaching infinity. We can consider another simple case in which S' moves along the $\overline{E}$-field direction; the situation is shown in Figure 8.2.2. As the velocity becomes larger, the $\overline{E}'$-field vector tilts its direction so that $(-\overline{E}' \times c\overline{B}')$ tends to be parallel to $\overline{v}$. We find $c\overline{B} = \hat{y}\gamma E$ and $\overline{E} = \hat{x}E + \hat{z}\gamma\beta E$. The angle of tilt of $\overline{E}'$ is $\alpha = \sin^{-1}\beta$, which increases as β increases.

Electric Fields: $\overline{E} \cdot \overline{B} = 0$ and $\left|\overline{E}\right| > \left|c\overline{B}\right|$

From (8.2.13b) by letting $c\overline{B} - \overline{\beta} \times \overline{E} = 0$, we see that there exists an observer moving in the $\overline{E} \times \overline{B}$ direction who experiences only an electric field and no magnetic field. The velocity of this observer is given by $\beta = \left|c\overline{B}\right| / \left|\overline{E}\right|$. Apparently $|\overline{v}|$ is smaller than c or $\beta < 1$. It is interesting to note that this observer, called S', is not the only one who does not experience a magnetic field. All observers moving along the $\overline{E}'$-field vector relative to S' also do not experience a magnetic field.

Magnetic Fields: $\overline{E} \cdot \overline{B} = 0$ and $\left|\overline{E}\right| < \left|c\overline{B}\right|$

This is the dual of the case above. Observer S' moving with a speed $\beta = |\overline{E}|/|c\overline{B}|$ along the $\overline{E} \times \overline{B}$ direction relative to S, and all other observers moving in the $\overline{B}'$ direction with respect to S' experience only a magnetic field and no electric field.

Wrench Fields: $\overline{E} \cdot \overline{B} \neq 0$

For $\overline{E} \cdot \overline{B} \neq 0$, it is clear that there are frames where $\overline{E}$ and $\overline{B}$ fields are parallel or antiparallel. When they are parallel, $\overline{E} \cdot \overline{B} > 0$, we have a positive wrench field. When they are antiparallel, $\overline{E} \cdot \overline{B} < 0$, we have a negative wrench field. There are six cases in this category:

    i) $\overline{E} \cdot \overline{B} > 0$, $\left|\overline{E}\right| = \left|c\overline{B}\right|$

    ii) $\overline{E} \cdot \overline{B} > 0$, $\left|\overline{E}\right| < \left|c\overline{B}\right|$ which is magnetic

    iii) $\overline{E} \cdot \overline{B} > 0$, $\left|\overline{E}\right| > \left|c\overline{B}\right|$ which is electric

    iv) $\overline{E} \cdot \overline{B} < 0$, $\left|\overline{E}\right| = \left|c\overline{B}\right|$

    v) $\overline{E} \cdot \overline{B} < 0$, $\left|\overline{E}\right| < \left|c\overline{B}\right|$ which is magnetic

    vi) $\overline{E} \cdot \overline{B} < 0$, $\left|\overline{E}\right| > \left|c\overline{B}\right|$ which is electric

E. Transformation of Frequency and Wave Vector

Consider a receiver and a transmitter in relative motion, and assume that the receiver receives a plane wave from the transmitter. According to the transmitter, the plane wave is described by

$$\begin{bmatrix} \overline{E}(\overline{r}, t) \\ c\overline{B}(\overline{r}, t) \end{bmatrix} = \begin{bmatrix} \overline{E}_0 \\ c\overline{B}_0 \end{bmatrix} \cos(\overline{k} \cdot \overline{r} - \omega t) \tag{8.2.16}$$

According to the receiver S', the plane wave is described by

$$\begin{bmatrix} \overline{E}'(\overline{r}', \overline{t}') \\ c\overline{B}'(\overline{r}', \overline{t}') \end{bmatrix} = \begin{bmatrix} \overline{E}'_0 \\ c\overline{B}'_0 \end{bmatrix} \cos(\overline{k}' \cdot \overline{r}' - \omega t') \tag{8.2.17}$$

Let the receiver S' move with uniform velocity $\overline{v}$ with respect to the transmitter S, and let primes denote quantities associated with S'. According to the Lorentz transformation formulas, we have

$$\begin{bmatrix} \overline{E}_0 \\ c\overline{B}_0 \end{bmatrix} = \begin{bmatrix} \overline{\overline{\alpha}}^{-1} & -\overline{\overline{\beta}} \\ \overline{\overline{\beta}} & \overline{\overline{\alpha}}^{-1} \end{bmatrix} \cdot \begin{bmatrix} \overline{E}'_0 \\ c\overline{B}'_0 \end{bmatrix} \tag{8.2.18}$$

and

$$\overline{r} = \overline{\overline{\alpha}} \cdot \overline{r}' + \gamma \overline{\beta} c t' \tag{8.2.19a}$$

$$ct = \gamma(ct' + \overline{\beta} \cdot \overline{r}') \tag{8.2.19b}$$

The phase factor in (8.2.16) becomes

$$\overline{k} \cdot \overline{r} - \frac{\omega}{c} ct = \left(\overline{k} \cdot \overline{\overline{\alpha}} - \gamma \overline{\beta} \frac{\omega}{c} \right) \cdot \overline{r}' - \gamma \left[\frac{\omega}{c} - \overline{\beta} \cdot \overline{k} \right] ct'$$

Comparing with (8.2.17), this is equal to

$$\overline{k}' = \overline{\overline{\alpha}} \cdot \overline{k} - \gamma \overline{\beta} \frac{\omega}{c} \tag{8.2.20a}$$

$$\frac{\omega'}{c} = \gamma \left[\frac{\omega}{c} - \overline{\beta} \cdot \overline{k} \right] \tag{8.2.20b}$$

The transformation formula is identical to that for space and time coordinates with $\overline{r}$ replaced by $\overline{k}$ and ct replaced by ω/c. With transformation formula (8.2.20), the phase of the plane wave in both frames is an invariant quantity. This invariance of phase, which enables us to deduce transformation formula (8.2.20), is referred to as the principle of phase invariance.

Topic 8.2A Aberration Effect

The aberration effect is a consequence of (8.2.20). The perpendicular component of $\overline{k}'$ is equal to that of $\overline{k}$, while the parallel component is changed by the motion. Consider an observer on Earth looking at a star at the zenith. Since the Earth is moving with respect to the star, a $\overline{k}'$ component antiparallel to $\overline{\beta}$ is generated. Thus the observer must tilt his telescope in the direction of the Earth's motion, just as, on a windless rainy day, a bicycle rider always tilts his umbrella in the forward direction. It is straightforward to determine from (8.2.20a) a relation for the angles between $\overline{\beta}$ and $\overline{k}'$ and between $\overline{\beta}$ and $\overline{k}$. Let θ denote the angle between $\overline{k}$ and $\overline{\beta}$, and θ' the angle between $\overline{k}'$ and $\overline{\beta}$. Recall that $\overline{\overline{\alpha}}$ is defined by $\overline{\overline{\alpha}} = \overline{\overline{I}} + (\gamma - 1)(\overline{\beta}\,\overline{\beta}/\beta^2)$. Cross and dot multiplying (8.2.20a) by $\overline{\beta}$, we obtain

$$k' \sin\theta' = k \sin\theta$$

$$k' \cos\theta' = \gamma k \cos\theta - \gamma\beta\frac{\omega}{c}$$

In an isotropic medium, $k = n\omega/c$, elimination of k' and k from these two equations gives

$$\tan\theta' = \frac{\tan\theta}{\gamma[1 - (\beta\sec\theta)/n]} \tag{8.2A.1}$$

This is the relativistic formula for aberration.

Topic 8.2B Doppler Effect

The Doppler effect is a consequence of (8.2.20b). Using the dispersion relation for isotropic media and letting the angle between $\overline{k}$ and $\overline{\beta}$ be θ, we find from (8.2.20b) that

$$\omega' = \gamma\omega(1 - n\beta\cos\theta) \tag{8.2B.1}$$

When the receiver is receiving from the transmitter, $\overline{\beta}$ and $\overline{k}$ are in the same direction. The frequency is shifted downward or red-shifted. When the receiver is approaching the transmitter, the frequency is shifted upward or blue-shifted. When the receiver is moving perpendicularly to $\overline{k}$, we have the transverse Doppler shift $\omega' = \gamma\omega$, which is a purely relativistic effect.

Problems

P8.2.1

In the early stages of special relativity, the sudden disappearance of an absolute time scalar led to the well-known "twin paradox." The paradox as stated was that one of a pair of twins left home, traveled at a uniform (high) speed in some direction for a certain period of time, and then returned home to find himself younger than his brother. By the symmetry argument that motion is relative, it was argued that neither twin should have grown older than the other, and the validity of special relativity was challenged. In the following discussion we show that both of the twins agree that one is older than the other and the problem is not symmetric.

Let both A and B be at the origin in frame S; B starts to move at $t = 0$ with speed v in the positive $\hat{z}$ direction of S. As A reads time t, B moves back with speed v. Consider the following events:

Event 1: Twin B is at $z = vt$ when A reads time t. In frame S, this event is described by (ct, vt) where ct is the time coordinate of the event with the dimension length, and vt is the space coordinate of the event.

Event 2: As A reads time $2t$, both A and B are at $z = 0$. In frame S, this event is described by $(2ct, 0)$.

Consider two other frames of reference, S' and S''. Frame S' moves with velocity v in the positive direction of the z axis, and S'' moves with velocity v in the negative direction of the z axis. All three frames have their origins coincided at $t = 0$. From Lorentz transformation

$$ct' = \gamma(ct - \beta z) \qquad \qquad (P8.2.1.1a)$$
$$z' = \gamma(z - \beta ct) \qquad \qquad (P8.2.1.1b)$$
$$ct'' = \gamma(ct + \beta z) \qquad \qquad (P8.2.1.1c)$$
$$z'' = \gamma(z + \beta ct) \qquad \qquad (P8.2.1.1d)$$

The coordinates for event 1 in S is $ct(1, \beta)$, and, for event 2 is $ct(2, 0)$. Show that the space-time coordinates for the two events in frames S' and S'' are as listed in Table P8.2.1.1.

Event	Observer		
	S	S'	S''
1	$ct(1, \beta)$	$ct(1/\gamma, 0)$	$ct[\gamma(1 + \beta^2), 2\gamma\beta]$
2	$ct(2, 0)$	$ct(2\gamma, -2\gamma\beta)$	$ct(2\gamma, 2\gamma\beta)$

Table P8.2.1.1 Space-time coordinates of the two events in the three frames of reference. The first part in parentheses denotes time coordinates multiplied by c, and the second part denotes space coordinates.

(a) During the initial period before turning around, B is in S', and the elapsed time according to B is t/γ. Show that, according to B, the elapsed time during the final period after turning around is also t/γ by taking the coordinate time difference between events 2 and 1. Thus twin B agrees with twin A that his time space is $2t/\gamma$, while that of A is $2t$.

(b) The problem is inherently asymmetrical; one twin has to turn, and it is this twin that experiences less proper time, $2t/\gamma$. If B does not turn, then, as A reads proper time $2t$, the coordinate time reading for B at two different locations, $z = 0$ and $z = 2vt$, is $2\gamma t$ because of the dilation of time. After turning around and meeting A again at $z = 0$, the proper time reading of B has been shown to be $2t/\gamma$. The effect of turning around causes a time difference of $2t(\gamma - 1/\gamma) = 2\gamma\beta^2 t$. Show that this "lost time" is equal to the time coordinate difference between S' and S'' for Event 1 in Table P8.2.1.1.

(c) All observers moving uniformly relative to A, including A and those in frames S' and S'', must conclude that the proper elapsed time of B is less than that of A by a factor of $1/\gamma$. By time dilation, twin A agrees that the total proper time interval for twin B is $2t/\gamma$, while his own coordinate time interval is $2t$. Consider S', whose space-time coordinate transformation is obtained from (P8.2.1.1),

$$ct'' = \gamma^2((1+\beta^2)ct' + 2\beta z')$$
$$z'' = \gamma^2((1+\beta^2)z' + 2\beta ct')$$

During the initial period before turning around, B is in S', and the elapsed time according to B is t/γ. In the final period, since B is in S'', Δct_B according to S' is

$$\Delta ct_B = \gamma^2(c\Delta t' + \frac{2\beta}{1+\beta^2}\Delta z')$$

From Table P8.2.1.1,

$$\Delta t' = 2\gamma t - t/\gamma$$
$$\Delta z' = -2\gamma\beta ct$$

Therefore,

$$\Delta ct_B = \gamma^2\left(2c\gamma t - \frac{ct}{\gamma} + \frac{2\beta}{1+\beta^2}(-2\gamma\beta ct)\right) = \frac{ct}{\gamma}$$

Thus the total time elapsed for B, according to S', is $2t/\gamma$. Following the same reasoning process, show that the total time elapsed for B, according to S'', is also $2t/\gamma$.

(d) It is interesting to imagine how B experiences the period of losing time during his turning around. Consider a third event, occurring when A

reads time t at $z = 0$ in S. Find the space-time coordinates for Event
3 in S' and S''. Show that, according to S, Events 1 and 3 are simul-
taneous; according to S', Event 1 is earlier than Event 3; and according
to S'', Event 3 is earlier than Event 1. At the turning time, twin B
changes his frame from S' to S''. Show that B loses track of anything
that happens at $z = 0$ during a time period $2\gamma\beta^2 t$.

(e) Suppose that twin B started his journey right after his birth and traveled
with a speed $v = 0.8c$. If he comes back at 30 years of age, how old is
his twin A?

P8.2.2

Assume that S' moves with velocity v_1 relative to S and S'' moves
with velocity v_2 relative to S, both along the z axis of S. The LT between
S'' and S, and between S and S',

$$z'' = \gamma_2(z - \beta^2 ct)$$
$$ct'' = \gamma_2(ct - \beta_2 z)$$
$$z = z' + \gamma_1 \beta_1 ct'$$
$$ct = \gamma_1(ct' + \beta_1 z')$$

Show that in terms of S' coordinate quantities,

$$ct'' = \gamma_2 \gamma_1 (1 - \beta_2 \beta_1) \left\{ ct' - z' \left[\frac{(\beta_2 - \beta_1)}{1 - \beta_1 \beta_2} \right] \right\}.$$

Therefore, the velocity of S'' w.r.t. S' is

$$\beta_{21} = \frac{\beta_2 - \beta_1}{1 - \beta_1 \beta_2}$$

and

$$\gamma_{21} = \gamma_1 \gamma_2 (1 - \beta_1 \beta_2)$$

This is an additive law for two velocities along the same direction. Generalize
this procedure and deduce an additive law for two vector velocities in different
directions.

P8.2.3

The star Alpha Centauri is 4.3 light-years from Earth. Observer B leaves
Earth in a rocket ship that travels toward this star at acceleration g. Halfway
(2.15 light-years from Earth) from α Cen, B turns off the forward accelera-
tion and accelerates backward toward Earth at g, so that the rocket arrives
at α Cen with zero speed and turns back. On the return trip, at the halfway
point, B again changes the direction of acceleration. Observer B arrives at
Earth with zero speed.

Suppose there is an initial frame S' which moves with uniform speed v
with respect to Earth, and suppose at time $t = t_0$, corresponding to $t' = t'_0$,

this inertial frame has its speed coinciding with that of B. Thus, at $t' = t_0'$, $U_B' = 0$ and $dU_B'/dt' = g$, where U_B' is the velocity of B with rest to S'.

By Lorentz transformation, we have

$$\frac{dt}{dt'} = \gamma \left(1 + \frac{v}{c^2} \frac{dz'}{dt'} \right) = \gamma \left(1 + \frac{v U_B'}{c^2} \right)$$

By velocity addition, we have

$$U_B = \frac{U_B' + v}{1 + \frac{U_B' v}{c^2}}$$

where U_B is B's velocity w.r.t. Earth. In the limit $t' \to t_0'$

$$\frac{dU_B'}{dt'} \to g; \qquad U_B' \to 0; \quad v \to U_B; \quad \gamma \to 1/\sqrt{1 - U_B^2/c^2},$$

Show that

$$\frac{dU_B}{dt} = g \left(1 - \frac{U_B^2}{c^2} \right)^{3/2}$$

The above equation is true in general because S' was chosen arbitrarily. (For deceleration, we replace g by $-g$.)

Integrate the above equation and show that for acceleration,

$$U_B = \frac{c(gt + k_1)}{\sqrt{c^2 + (gt + k_1)^2}}$$

and, for deceleration

$$U_B = \frac{c(-gt + k_2)}{\sqrt{c^2 + (-gt + k_2)^2}}$$

where k_1 and k_2 are arbitrary constants. Note that U_B never exceeds c. As $t \to \infty, U_B \to c$. To determine k_1 and k_2, we use our initial conditions. Initially, at $t = 0, U_B = 0$, therefore $k_1 = 0$. Thus,

$$\frac{dz}{dt} = U_B = \frac{gct}{\sqrt{c^2 + (gt)^2}}$$

Since at $t = 0, z = 0$, show that

$$z = \frac{c^2}{g} \left\{ \sqrt{1 + \left(\frac{gt}{c} \right)^2} - 1 \right\}$$

The distance from Alpha Centauri to earth is $0.452c^2$ meters. Determine the total time elapsed for the entire journey according to twin A on Earth.

For the traveling twin B, use proper time $c^2 d\tau^2 = c^2 dt^2 - dz^2$ to show that

$$\tau = \int_0^{0.31c} \frac{dt}{\sqrt{1 + \left(\frac{gt}{c}\right)^2}} + \int_{0.31c}^{0.62c} \frac{dt}{\sqrt{1 + \left(\frac{k_2 - gt}{c}\right)^2}}$$

Calculate the total time elapsed for the entire journey according to twin B. The star Vega is 26 light-years from Earth, calculate the time elapsed according to twins A and B.

P8.2.4

Show that a rigid rod moving along its longitudinal direction with velocity v appears to be shortened. This phenomenon is known as the *Lorentz contraction*. Let the rod be at rest in S'. Its two end points are $z' = 0$ and $z' = l'$. In the laboratory frame S, the rod is moving along z with velocity v. Its length is measured by recording the positions of its end points simultaneously, $t_2 = t_1 = 0$.

Show that the time-space coordinates of the two end points at the measurement time in frame S are

Event	Observer	
	S	S'
1	$[0, 0]$	$[0, 0]$
2	$[0, l'/\gamma]$	$[-\beta l', l')]$

Table P8.2.4.1   Space-time coordinates of two end points.

What is the rod length l as measured in S. Note that from the point of view of observer S', who moves with the rod, the laboratory observer is not measuring the two end points simultaneously. For the rod moving from left to right, while S measures the two ends at the same time $t = 0$, show that, according to S', S measures the right end first at $ct' = -\beta l'$ before measuring the left end at $ct' = 0$. Thus S' expects that S will claim a shorter length.

P8.2.5

Consider the transformation from observer S' to observer S of the length of a rod that may or may not be rigid. From the point of view of S, the length of the rod at time t_0 is defined as the difference between space positions of the two end points as measured simultaneously at t_0 in his frame of reference

$$\bar{l}(t_0) = \overline{Q}(t_0) - \overline{P}(t_0)$$

where $\overline{Q}(t_0)$ and $\overline{P}(t_0)$ denote position readings of the two end points. But a simultaneous measurement at two space points in S is not simultaneous in S'. Consider the general case when the length of the rod is time-variant, and let the measurement performed be represented by two events. Their space-time coordinates are listed in Table P8.2.5.1.

By using the space-time Lorentz transformation formulas,

$$ct' = \gamma(ct_0 - \overline{\beta} \cdot \overline{Q}(t_0))$$
$$ct'_0 = \gamma(ct_0 - \overline{\beta} \cdot \overline{P}(t_0))$$
$$\overline{Q}'(t') = \overline{\overline{\alpha}} \cdot \overline{Q}(t_0) - \gamma\overline{\beta}ct_0$$
$$\overline{P}'(t'_0) = \overline{\overline{\alpha}} \cdot \overline{P}(t_0) - \gamma\overline{\beta}ct_0$$

show that

$$\overline{X} = \overline{Q}'(t') - \overline{P}'(t'_0)$$
$$t' - t'_0 = -\overline{\beta} \cdot \overline{X}$$
$$\overline{l} = Q(t_0) - \overline{P}(t_0) = \overline{\overline{\alpha}}^{-1} \cdot \overline{X}$$

Note that, when the rod is not rigid and stationary in S', $\overline{X}$ is not the result of a length measurement performed in S' because the two end points are not measured simultaneously and hence do not conform to the definition of length.

Event	Observer	
	S	S'
1	$[t_0, \overline{P}(t_0)]$	$[t'_0, \overline{P}'(t'_0)]$
2	$[t_0, \overline{Q}(t_0)]$	$[t', \overline{Q}'(t')]$

Table P8.2.5.1 Space-time coordinates of two end points.

(a) Show that, when the rod is rigid and stationary in S', $\overline{l}' = \overline{Q}'(t') - \overline{P}'(t'_0) = \overline{X}$ the rod as viewed from S has length

$$\overline{l} = \overline{\overline{\alpha}}^{-1} \cdot \overline{l}' = \frac{1}{\gamma}\overline{l}_{||} + \overline{l}'_{\perp}$$

where subscripts $||$ and $\perp$ denote components of a vector parallel and perpendicular, respectively, to the velocity. Thus the parallel component is unchanged. The rod appears to be shortened and rotated by an angle.

(b) When the rod is rigid and is moving uniformly with velocity $\overline{v}'$ in S', the length of the rod in S' at t'_0 is

$$\overline{l}'(t'_0) = \overline{Q}'(t'_0) - \overline{P}(t'_0)$$

We can write $\overline{X}$ in terms of $\vec{l}'$ and $\vec{v}'$:

$$\overline{X} = \vec{v}'(t' - t_0') + \vec{l}'$$

Show that, in terms of $\vec{l}'$,

$$\overline{l} = \overline{\overline{\alpha}}^{-1} \cdot \left[\vec{l}' - \overline{\beta}' \frac{\overline{\beta} \cdot \vec{l}'}{1 + \overline{\beta} \cdot \overline{\beta}} \right]$$

where $\overline{\beta}' = \vec{v}'/c$. Thus, together with the Lorentz contraction, there is another change of length in the rigid rod because of its motion in S'.

(c) The rod is short and is time-variant. Since it is short, we can expand $t' - t_0$ to

$$t' - t_0' = \sum_{l=1}^{n} A_l \delta^l$$

where $\delta = \overline{\beta} \cdot \vec{l}'$ denotes a small quantity. Expand $\overline{X}$ to the n th order in δ, and show that

$$\overline{X} = \vec{l}' + \sum_{k=1}^{\infty} \frac{\overline{Q}'^{(k)}(t_0')}{k!}(t' - t_0')^k = \vec{l}' + \sum_{k=1}^{N} \frac{\overline{Q}'^{(k)}}{k!} \left[\sum_{l=1}^{n} A_l \delta^l \right]^k$$

where $\overline{Q}'^{(k)}(t_0)$ is the k th derivative of $\overline{Q}'(t')$ relative to t' at $t' = t_0'$. Comparing coefficients for δ^k, $k = 1, 2, \ldots, n$, determine the coefficients A_1, A_2, and A_3.

Show that, to the second order in δ, $\overline{l}$ reads as

$$\overline{l} = \overline{\overline{\alpha}}^{-1} \cdot \left(\overline{\overline{I}} + A_1 \overline{D}'^{-} \right) \left[\overline{\overline{I}} + \frac{1}{2} A_1^2 \delta \left(1 - A_1^2 \delta \overline{\beta} \cdot \overline{Q}'^{(2)} \right) \overline{Q}'^{(2)} \overline{\beta} \right] \cdot \vec{l}^{-1}$$

and, to the third order in δ,

$$\overline{l} = \overline{\overline{\alpha}}^{-1} \cdot \left(\overline{\overline{I}} + A_1 \overline{D}'^{-} \overline{\beta} \right)$$

$$\cdot \left[\overline{\overline{I}} + \frac{1}{2} A_1^2 \delta \left(1 - A_1^2 \delta \overline{\beta} \cdot \overline{Q}'^{(2)} + \frac{1}{3} A_1^3 \delta^2 \overline{\beta} \cdot \overline{Q}' \right) \overline{Q}'^{(2)} \overline{\beta} \right] \cdot \vec{l}^{-1}$$

P8.2.6

Show that a moving current loop generates an electric dipole moment. For simplicity, consider a square loop with corners labeled as A, B, C, and D. Current J_0' flows from A to B to C to D. The square moves with velocity

parallel to the current direction along side AB in the $\hat{z}$ direction. In which direction is the electric dipole moment?

P8.2.7

In a certain reference frame, a static uniform electric field E_0 is parallel to the z axis and a static uniform magnetic field $cB_0 = 2E_0$ forms a $30°$ angle with respect to $\hat{z}$. Determine the relative velocity of a reference frame in which the electric and magnetic fields are parallel.

P8.2.8

An observer S observes a uniform electric field in the $\hat{x}$ direction, $\overline{E} = \hat{x}E_0$, and a uniform magnetic field in the $\hat{y}$ direction, $\overline{B} = \hat{y}B_0$. Let $E_0 > cB_0$. Find an observer S' moving relative to S with velocity v in the $\hat{z}$ direction, so that he observes only an electric field. Determine the electric field strength and the velocity v. Can you find an observer moving with a velocity less than c, who observes only a magnetic field?

P8.2.9

(a) Show that the electric and magnetic fields of a charge q_1 moving along $\hat{z}$ direction with the velocity $\overline{v}_1 = \hat{z}v_1$ are

$$\overline{E} = \frac{q_1}{4\pi\epsilon_o} \cdot \frac{(1 - \beta_1^2)\overline{r}}{\left[(1 - \beta_1^2)r^2 + (\overline{\beta}_1 \cdot \overline{r})^2\right]^{3/2}}$$

$$\overline{B} = \frac{1}{c}\overline{\beta}_1 \times \overline{E} = \frac{q_1}{4\pi c\epsilon_o} \cdot \frac{(1 - \beta_1^2)\overline{\beta}_1 \times \overline{r}}{\left[(1 - \beta_1^2)r^2 + (\overline{\beta}_1 \cdot \overline{r})^2\right]^{3/2}}$$

(b) Determine the force acting on a charge q_2 moving with velocity $\overline{v}_2$.
(c) When charge q_2 is moving with $\overline{v}_2 = \overline{v}_1 = \overline{v}$ and situated at $x = z = 0$ and $y = d$, the force is

$$\overline{F}_{12} = \frac{(1 - \beta^2)q^2}{4\pi\epsilon_o d^2}\hat{y}$$

P8.2.10

Consider two negative line charges moving with same velocity $\overline{v} = \hat{z}v$. Let line b situated at $x = y = 0$ and line a at $x = 0$ and $y = -d$.

(a) Regard the moving charge as the combination of a static charge and a current source, then calculate $\overline{F}_e$ produced by the static charge and $\overline{F}_c$ produced by the current source. The sum of $\overline{F}_e$ and $\overline{F}_c$ is the total force the line a acts on the segment of line b.

(b) Find the force in frame S by using relativistic transformation of force $\gamma F_\perp = F'_\perp$. Here we define the frame in the problem to be S and the frame moving along $\hat{x}$ in which the line charge is static to be S'. (Hint: Total charge is conserved and the relativistic transformation of length is $l_\parallel = l'_\parallel/\gamma$).

(c) Find the force by using relativistic transformation of electromagnetic fields. Calculate $\overline{E}'$ and $\overline{H}'$ in frame S', then get $\overline{E}$ and $\overline{H}$ in frame S. Finally, Lorentz force law gives the total force.

P8.2.11

This problem shows that two parallel current-carrying wires attract each other. Consider two negative line charges moving with same velocity $\overline{v} = \hat{z}v$. Let line b situated at $x = y = 0$ and line a at $x = 0$ and $y = -d$. We now calculate the force wire a acts on a segment of wire b. The wire is modeled as a combination of a static positive line charge and a moving negative line charge with velocity $\overline{v} = \hat{z}v$, the charge density of both lines being λ. The segment is modeled as a combination of a static positive charge $(+q)$ and a moving negative charge $(-q)$ with the velocity v, where $q = \lambda l$. The force on the segment is $\overline{F}_{seg} = \overline{F}_{(+\lambda)(+q)} + \overline{F}_{(-\lambda)(+q)} + \overline{F}_{(+\lambda)(-q)} + \overline{F}_{(-\lambda)(-q)}$. Calculate $\overline{F}_{seg}$ in the following way:

Discretize the infinite line charge into point charges, calculate the force each point charge acts on the segment of the other wire, and integrate each force to obtain the total force the line charge acts on the segment. Write the expression for $\overline{F}_{(+\lambda)(+q)}$, $\overline{F}_{(-\lambda)(+q)}$, $\overline{F}_{(+\lambda)(-q)}$ and $\overline{F}_{(-\lambda)(-q)}$, and show the sum of them is equal to $\overline{J} \times (\mu_o \overline{H})$, where $\overline{J} = -(-qv)\hat{z}$ and $\overline{H} = \left(-\frac{\lambda v}{2\pi d_o}\right)\hat{x}$.

P8.2.12

Two parallel wires with current in the same direction will attract each other according to Lorentz force law. Think in the following way: if the current is regarded as the flow of negative charges, the two negative charges moving with the same velocity, thus being static to each other, will repel each other. How to explain the above discrepancy?
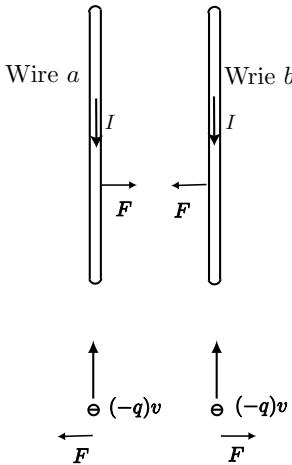
Figure P8.2.12.1 Observer S' moves with $\overline{v}$ relative to observer S.

8.3   Waves in Moving Media

A. Transformation of Constitutive Relations

We have seen that, in the transformation of electromagnetic field vectors, $\overline{E}$ and $c\overline{B}$ transform together, forming the entity of quantity, which is a four-dimensional second-rank tensor in the Minkowski space. The electromagnetic field vectors $\overline{H}$ and $c\overline{D}$ transform together and form the entity of excitation, which is also a four-dimensional second-rank tensor. Thus we write the constitutive relations in the $\overline{E}\,\overline{B}$ representation:

$$\left[\begin{array}{c} c\overline{D} \\ \overline{H} \end{array} \right] = \overline{\overline{C}} \cdot \left[\begin{array}{c} \overline{E} \\ c\overline{B} \end{array} \right] \tag{8.3.1}$$

where

$$\overline{\overline{C}} = \left[\begin{array}{cc} \overline{\overline{P}} & \overline{\overline{L}} \\ \overline{\overline{M}} & \overline{\overline{Q}} \end{array} \right] \tag{8.3.2}$$

is the constitutive matrix the elements of which are constitutive parameters. This representation provides a Lorentz covariant description of the constitutive relations.

The Lorentz transformation formulas for the electromagnetic field vectors can now be used to derive transformation laws for the constitutive relations. A medium at rest in one frame becomes a medium in motion when viewed from another frame. The derivation of equivalent constitutive relations for a moving medium in the laboratory frame is useful conceptually and practically. It is indeed true that a problem involving one moving medium can always be solved in its rest frame and the results can be transformed back to the laboratory frame. In practice, the Lorentz transformation method cannot be applied when more than two relatively moving media are involved because, in the rest frame of one medium, all others are in motion. Thus constitutive relations for moving media have to be determined.

Moving Isotropic Media

Consider two reference frames in relative uniform motion. In the reference frame S' there is an isotropic medium with permittivity ϵ' and permeability μ'. The constitutive matrix takes the form

$$\overline{\overline{C}}' = \left[\begin{array}{cc} c\epsilon'\overline{\overline{I}} & \overline{\overline{0}} \\ \overline{\overline{0}} & \dfrac{1}{c\mu'}\overline{\overline{I}} \end{array} \right] \tag{8.3.3}$$

In the laboratory frame S we obtain the constitutive matrix for the moving isotropic medium

$$\overline{\overline{C}} = \overline{\overline{L}}_6^{-1} \cdot \overline{\overline{C}}' \cdot \overline{\overline{L}}_6$$

$$= \frac{\gamma^2}{c\mu'} \left[\begin{array}{cc} (n^2 - \beta^2)\overline{\overline{I}} - (n^2 - 1)\overline{\beta}\,\overline{\beta} & (n^2 - 1)\overline{\overline{\beta}} \\ (n^2 - 1)\overline{\overline{\beta}} & (1 - n^2\beta^2)\overline{\overline{I}} + (n^2 - 1)\overline{\beta}\,\overline{\beta} \end{array} \right]$$

$$(8.3.4)$$

where $n^2 = c^2\mu'\epsilon'$ is the squared refractive index of the moving medium in its rest frame of reference. Clearly (8.3.4) reduces to (8.3.3) when $\beta = 0$. In vacuum when $n = 1$, $\overline{\overline{C}}$ reduces to (8.3.3) with $\mu = \mu_o$. For an isotropic medium in motion, it becomes bianisotropic.

When the velocity is along the $\hat{z}$ direction, (8.3.1) becomes

$$\overline{\overline{C}} = \frac{\gamma^2}{c\mu'} \begin{bmatrix} n^2 - \beta^2 & 0 & 0 & 0 & -(n^2-1)\beta & 0 \\ 0 & n^2 - \beta^2 & 0 & (n^2-1)\beta & 0 & 0 \\ 0 & 0 & n^2(1-\beta^2) & 0 & 0 & 0 \\ 0 & -(n^2-1)\beta & 0 & 1 - n^2\beta^2 & 0 & 0 \\ (n^2-1)\beta & 0 & 0 & 0 & 1 - n^2\beta^2 & 0 \\ 0 & 0 & 0 & 0 & 0 & 1/\gamma^2 \end{bmatrix}$$

$$(8.3.5)$$

Note that, although we assume μ' and ϵ' to be scalar numbers, the derivation remains valid even if they are not scalar. We have to remember that μ' and ϵ' are measured in the rest frame of the medium. If they are dependent on parameters pertaining to their rest frame, these parameters must be properly transformed. For instance, when the medium in its rest frame is a plasma we need to transform the plasma frequency to the laboratory frame.

The constitutive relations for a moving isotropic medium can be written in the form of $\overline{B}$ and $\overline{D}$ expressed in terms of $\overline{E}$ and $\overline{H}$. The result is

$$\overline{B} = \mu'\overline{\overline{A}} \cdot \overline{H} - \overline{\Omega} \times \overline{E} \qquad\qquad (8.3.6a)$$

$$\overline{D} = \epsilon'\overline{\overline{A}} \cdot \overline{E} + \overline{\Omega} \times \overline{H} \qquad\qquad (8.3.6b)$$

where

$$\overline{\overline{A}} = \frac{1 - \beta^2}{1 - n^2\beta^2} \left[\overline{\overline{I}} - \frac{n^2 - 1}{1 - \beta^2}\overline{\beta}\,\overline{\beta} \right] \qquad\qquad (8.3.7)$$

$$\overline{\Omega} = \frac{n^2 - 1}{1 - n^2\beta^2}\overline{\beta}/c \qquad\qquad (8.3.8)$$

When $\overline{v}$ is in the $\hat{z}$ direction, $\overline{\overline{A}}$ becomes a diagonal matrix.

Moving Bianisotropic Media

We now consider the general case in which a bianisotropic medium with constitutive relations (8.3.1) is in motion. We assume that the velocity is in the $\hat{z}$ direction. By application of the Lorentz transformation laws for electromagnetic field vectors, the constitutive matrix is determined to be

$$
\overline{\overline{P}} = \begin{bmatrix} \gamma^2 \left[p_{xx} - \beta(l_{xy} - m_{yx}) - \beta^2 q_{yy} \right] \\ \gamma^2 \left[p_{yx} + \beta(l_{yy} + m_{xx}) + \beta^2 q_{xy} \right] \\ \gamma(p_{zx} - \beta l_{zy}) \end{bmatrix}
$$

$$
\begin{matrix} \gamma^2 \left[p_{xy} - \beta(l_{xx} + m_{yy}) + \beta^2 q_{yx} \right] & \gamma(p_{xz} + \beta m_{yz}) \\ \gamma^2 \left[p_{yy} + \beta(l_{yx} - m_{yx}) - \beta^2 q_{xx} \right] & \gamma(p_{yz} - \beta m_{xz}) \\ \gamma(p_{zy} + \beta l_{zx}) & p_{zz} \end{matrix} \Bigg] \quad (8.3.9a)
$$

$$
\overline{\overline{Q}} = \begin{bmatrix} \gamma^2 \left[q_{xx} + \beta(m_{xy} - l_{yx}) - \beta^2 p_{yy} \right] \\ \gamma^2 \left[q_{yx} + \beta(m_{yy} + l_{xx}) + \beta^2 p_{xy} \right] \\ \gamma(q_{zx} + \beta m_{zy}) \end{bmatrix}
$$

$$
\begin{matrix} \gamma^2 \left[q_{xy} - \beta(m_{xx} + l_{yy}) + \beta^2 p_{yx} \right] & \gamma(q_{xz} - \beta l_{yz}) \\ \gamma^2 \left[q_{yy} - \beta(m_{yx} - l_{xy}) - \beta^2 p_{xx} \right] & \gamma(q_{yz} + \beta l_{xz}) \\ \gamma(q_{zy} - \beta m_{zx}) & q_{zz} \end{matrix} \Bigg] \quad (8.3.9b)
$$

$$
\overline{\overline{L}} = \begin{bmatrix} \gamma^2 \left[l_{xx} + \beta(p_{xy} + q_{yx}) + \beta^2 m_{yy} \right] \\ \gamma^2 \left[l_{yx} + \beta(p_{yy} - q_{xx}) - \beta^2 m_{xy} \right] \\ \gamma(l_{zx} + \beta p_{zy}) \end{bmatrix}
$$

$$
\begin{matrix} \gamma^2 \left[l_{xy} - \beta(p_{xx} - q_{yy}) - \beta^2 m_{yx} \right] & \gamma(l_{xz} + \beta q_{yz}) \\ \gamma^2 \left[l_{yy} - \beta(p_{yx} + q_{yx}) + \beta^2 q_{xx} \right] & \gamma(l_{yz} - \beta q_{xz}) \\ \gamma(l_{zy} - \beta p_{zx}) & l_{zz} \end{matrix} \Bigg] \quad (8.3.9c)
$$

$$
\overline{\overline{M}} = \begin{bmatrix} \gamma^2 \left[m_{xx} - \beta(q_{xy} + p_{yx}) + \beta^2 l_{yy} \right] \\ \gamma^2 \left[m_{yx} - \beta(q_{yy} - p_{xx}) - \beta^2 l_{xy} \right] \\ \gamma(m_{zx} - \beta q_{zy}) \end{bmatrix}
$$

$$
\begin{matrix} \gamma^2 \left[m_{xy} + \beta(q_{xx} - p_{yy}) - \beta^2 l_{yx} \right] & \gamma(m_{xz} - \beta p_{yz}) \\ \gamma^2 \left[m_{yy} + \beta(q_{yx} + p_{xy}) + \beta^2 l_{xx} \right] & \gamma(m_{yz} + \beta p_{xz}) \\ \gamma(m_{zy} + \beta q_{zx}) & m_{zz} \end{matrix} \Bigg] \quad (8.3.9d)
$$

It is noted that if a bianisotropic medium satisfies the symmetry conditions in its rest frame, then the moving bianisotropic medium also satisfies the symmetry conditions. We conclude that for moving non-absorbing bianisotropic media, the 6×6 constitutive matrix $\overline{\overline{C}}$ can contain only up to 21 independent complex elements.

Moving Uniaxial Media

Constitutive relations for a moving uniaxial medium are also derived from the general formulas (8.3.9). We assume that in the rest frame of the moving medium the constitutive relations are as follows:

$$\overline{\overline{\epsilon}} = \begin{bmatrix} \epsilon' & 0 & 0 \\ 0 & \epsilon' & 0 \\ 0 & 0 & \epsilon'_z \end{bmatrix} \tag{8.3.10a}$$

$$\overline{\overline{\mu}} = \begin{bmatrix} \mu' & 0 & 0 \\ 0 & \mu' & 0 \\ 0 & 0 & \mu'_z \end{bmatrix} \tag{8.3.10b}$$

where the z axis coincides with the optic axis. Note that isotropic media and electric or magnetic uniaxial media are all special cases of (8.3.10). The primes indicate that these quantities are associated with the rest frame of the medium. In the laboratory frame, where the media appear to be moving uniformly with the velocity $\overline{v}$ along the $\hat{z}$ direction, the constitutive matrix of the medium is determined to be

$$\overline{\overline{C}} = \begin{bmatrix} p & 0 & 0 & 0 & -l & 0 \\ 0 & p & 0 & l & 0 & 0 \\ 0 & 0 & p_z & 0 & 0 & 0 \\ 0 & -l & 0 & q & 0 & 0 \\ l & 0 & 0 & 0 & q & 0 \\ 0 & 0 & 0 & 0 & 0 & q_z \end{bmatrix} \tag{8.3.11}$$

The constitutive matrix can be transformed into the $\overline{E}\,\overline{H}$ and the $\overline{D}\,\overline{B}$ representations. We obtain

$$\overline{\overline{C}}_{EH} = \begin{bmatrix} \epsilon & 0 & 0 & 0 & \xi & 0 \\ 0 & \epsilon & 0 & -\xi & 0 & 0 \\ 0 & 0 & \epsilon_z & 0 & 0 & 0 \\ 0 & -\xi & 0 & \mu & 0 & 0 \\ \xi & 0 & 0 & 0 & \mu & 0 \\ 0 & 0 & 0 & 0 & 0 & \mu_z \end{bmatrix} \tag{8.3.12}$$

$$\overline{\overline{C}}_{DB} = \begin{bmatrix} \kappa & 0 & 0 & 0 & \chi & 0 \\ 0 & \kappa & 0 & -\chi & 0 & 0 \\ 0 & 0 & \kappa_z & 0 & 0 & 0 \\ 0 & -\chi & 0 & \nu & 0 & 0 \\ \chi & 0 & 0 & 0 & \nu & 0 \\ 0 & 0 & 0 & 0 & 0 & \nu_z \end{bmatrix} \tag{8.3.13}$$

$\overline{E}\,\overline{B}$ Representation

$$p = \frac{n^2 - \beta^2}{c\mu'(1 - \beta^2)}, \qquad p_z = c\epsilon_z',$$

$$q = \frac{1 - n^2\beta^2}{c\mu'(1 - \beta^2)}, \qquad q_z = \frac{1}{c\mu_z'},$$

$$l = \frac{\beta(n^2 - 1)}{c\mu'(1 - \beta^2)}$$

$\overline{E}\,\overline{H}$ Representation

$$\epsilon = \frac{(qp + l^2)}{q} = \frac{\epsilon'(1 - \beta^2)}{(1 - n^2\beta^2)}, \quad \epsilon_z = \epsilon_z'$$

$$\mu = \frac{1}{cq} = \frac{\mu'(1 - \beta^2)}{(1 - n^2\beta^2)}, \qquad \mu_z = \mu_z'$$

$$\xi = \frac{-l}{cq} = \frac{-\beta(n^2 - 1)}{c(1 - n^2\beta^2)}$$

$\overline{D}\,\overline{B}$ Representation

$$\kappa = \frac{c}{p} = \frac{c^2\mu'(1 - \beta^2)}{(n^2 - \beta^2)}, \qquad \kappa_z = \frac{1}{\epsilon_z'}$$

$$\nu = \frac{c\mu'(qp + l^2)}{p} = \frac{c^2\epsilon'(1 - \beta^2)}{(n^2 - \beta^2)}, \quad \nu_z = \frac{1}{\mu_z'}$$

$$\chi = \frac{cl}{p} = \frac{c\beta(n^2 - 1)}{(n^2 - \beta^2)}$$

Table 8.3.1 Constitutive parameters for moving media.

The element values of the constitutive matrices in different representations are summarized in Table 8.3.1. The primed quantities are measured in the rest frame of the media. From Table 8.3.1 we see that the constitutive matrices will become diagonal if $\mu'\epsilon' = 1/c^2 \, (n = 1)$, which can be achieved for an anisotropic plasma subject to a strong magnetic field in the $\hat{z}$ direction, and for a Veselago [1968] medium with $\epsilon' = -\epsilon_o$ and $\mu' = -\mu_o$. These are examples of moving me-

dia that are not bianisotropic. Constitutive relations of other moving media take the forms (8.3.11)–(8.3.13).

Moving Gyrotropic Media

Formulas (8.3.9) enable an observer to characterize a bianisotropic medium moving along the $\hat{z}$ direction. We observe that when a medium is in motion, it becomes bianisotropic. For a moving electrically gyrotropic medium with scalar permeability μ and permittivity tensor

$$
\bar{\bar{\epsilon}} = \begin{bmatrix} \epsilon & i\epsilon_g & 0 \\ -i\epsilon_g & \epsilon & 0 \\ 0 & 0 & \epsilon_z \end{bmatrix}
\tag{8.3.14}
$$

we obtain

$$
\bar{\bar{C}} = \frac{\gamma^2}{c\mu} \begin{bmatrix}
n^2-\beta^2 & in_g^2 & 0 & i\beta n_g^2 & -(n^2-1)\beta & 0 \\
-in_g^2 & n^2-\beta^2 & 0 & (n^2-1)\beta & i\beta n_g^2 & 0 \\
0 & 0 & n_z^2/\gamma^2 & 0 & 0 & 0 \\
i\beta n_g^2 & -(n^2-1)\beta & 0 & 1-n^2\beta^2 & -i\beta n_g^2 & 0 \\
(n^2-1)\beta & i\beta n_g^2 & 0 & i\beta n_g^2 & 1-n^2\beta^2 & 0 \\
0 & 0 & 0 & 0 & 0 & 1/\gamma^2
\end{bmatrix}
\tag{8.3.15}
$$

where $n_g^2 = c^2\mu\epsilon_g$ and $n_z^2 = c^2\mu\epsilon_z$. The parameters that govern the gyrotropic nature of the medium must be carefully transformed. For example [Chawla and Unz, 1971], the plasma frequency is a Lorentz-invariant $\omega_p' = \omega_p$, while the cyclotron frequency transforms as $\omega_c' = \gamma\omega_c$. Remember that the static magnetic field is in the direction of motion. If the magnetic field were perpendicular to the direction of motion, we would have $\omega_c' = \gamma^2\omega_c$ instead. The applied frequency ω must also be properly transformed.

Accelerated Media

The constitutive relations of an accelerated medium are also bianisotropic in form. They are space dependent and can be viewed as inhomogeneous. General formulations in arbitrary accelerating frames have been considered by some authors, and explicit forms for the constitutive relations have been proposed for rotating and linearly accelerated media. Not only relative motion but also absolute motion of both observer and medium plays a crucial role in determining the constitutive relations.

B. Waves in Moving Uniaxial Media

We make use of the kDB system to study propagation of plane waves in unbounded moving uniaxial media. The constitutive relations in the $\overline{D}\,\overline{B}$ representation take the form

$$\overline{E} = \overline{\overline{\kappa}} \cdot \overline{D} + \overline{\overline{\chi}} \cdot \overline{B} \qquad (8.3.16a)$$

$$\overline{H} = \overline{\overline{\gamma}} \cdot \overline{D} + \overline{\overline{\nu}} \cdot \overline{B} \qquad (8.3.16b)$$

where

$$\overline{\overline{\kappa}} = \begin{bmatrix} \kappa & 0 & 0 \\ 0 & \kappa & 0 \\ 0 & 0 & \kappa_z \end{bmatrix} \qquad (8.3.17a)$$

$$\overline{\overline{\nu}} = \begin{bmatrix} \nu & 0 & 0 \\ 0 & \nu & 0 \\ 0 & 0 & \nu_z \end{bmatrix} \qquad (8.3.17b)$$

$$\overline{\overline{\chi}} = \overline{\overline{\gamma}}^{+} = \begin{bmatrix} 0 & \chi & 0 \\ -\chi & 0 & 0 \\ 0 & 0 & 0 \end{bmatrix} \qquad (8.3.17c)$$

With constitutive parameters $\kappa,\ \kappa_z, \nu,\ \nu_z$ and χ listed in Table 8.3.1.

In the kDB system, the constitutive matrices become

$$\overline{\overline{\kappa}}_k = \begin{bmatrix} \kappa & 0 & 0 \\ 0 & \kappa\cos^2\theta + \kappa_z\sin^2\theta & (\kappa - \kappa_z)\sin\theta\cos\theta \\ 0 & (\kappa - \kappa_z)\sin\theta\cos\theta & \kappa\sin^2\theta + \kappa_z\cos^2\theta \end{bmatrix} \quad (8.3.18a)$$

$$\overline{\overline{\nu}}_k = \begin{bmatrix} \nu & 0 & 0 \\ 0 & \nu\cos^2\theta + \nu_z\sin^2\theta & (\nu - \nu_z)\sin\theta\cos\theta \\ 0 & (\nu - \nu_z)\sin\theta\cos\theta & \nu\sin^2\theta + \nu_z\cos^2\theta \end{bmatrix} \quad (8.3.18b)$$

$$\overline{\overline{\chi}}_k = \overline{\overline{\gamma}}_k^{+} = \begin{bmatrix} 0 & \chi\cos\theta & \chi\sin\theta \\ -\chi\cos\theta & 0 & 0 \\ -\chi\sin\theta & 0 & 0 \end{bmatrix} \qquad (8.3.18c)$$

Substituting into Maxwell Equations the kDB system

$$\begin{pmatrix} \kappa_{11} & \kappa_{12} \\ \kappa_{21} & \kappa_{22} \end{pmatrix} \begin{pmatrix} D_1 \\ D_2 \end{pmatrix} = - \begin{pmatrix} \chi_{11} & \chi_{12} - u \\ \chi_{21} + u & \chi_{22} \end{pmatrix} \begin{pmatrix} B_1 \\ B_2 \end{pmatrix} \qquad (8.3.19a)$$

modes wave character	Type I wave	Type II wave
$\overline{D}_k$	$\begin{pmatrix} 1 \\ 0 \\ 0 \end{pmatrix}$	$\begin{pmatrix} 0 \\ 1 \\ 0 \end{pmatrix}$
$\overline{B}_k$	$\begin{pmatrix} 0 \\ \kappa/(u-\chi\cos\theta) \\ 0 \end{pmatrix}$	$\begin{pmatrix} -(u-\chi\cos\theta)/\nu \\ 0 \\ 0 \end{pmatrix}$
$\overline{E}_k$	$\begin{pmatrix} \kappa u/(\nu-\chi\cos\theta) \\ 0 \\ 0 \end{pmatrix}$	$\begin{pmatrix} 0 \\ (u-\chi\cos\theta)/\nu \\ \left[\frac{\chi}{\nu}(u-\chi\cos\theta)+(\kappa_z-\kappa)\cos\theta\right]\sin\theta \end{pmatrix}$
$\overline{H}_k$	$\begin{pmatrix} 0 \\ u \\ -\chi+\frac{\kappa(\nu_z-\nu)\cos\theta}{u-\chi\cos\theta}\sin\theta \end{pmatrix}$	$\begin{pmatrix} -u \\ 0 \\ 0 \end{pmatrix}$
u	$\chi\cos\theta\pm\sqrt{\kappa(\nu\cos^2\theta+\nu_z\sin^2\theta)}$	$\chi\cos\theta\pm\sqrt{\nu(\kappa\cos^2\theta+\kappa_z\sin^2\theta)}$
Dispersion Relation	$k_x^2+k_y^2+\frac{\nu}{\nu_z}k_z^2-\frac{1}{\kappa\nu_z}(\omega-\chi k_z)^2=0$	$k_x^2+k_y^2+\frac{\kappa}{\kappa_z}k_z^2-\frac{1}{\nu\kappa_z}(\omega-\chi k_z)^2=0$

Table 8.3.2 Characteristic waves in moving uniaxial medium.

$$\begin{pmatrix} \nu_{11} & \nu_{12} \\ \nu_{21} & \nu_{22} \end{pmatrix} \begin{pmatrix} B_1 \\ B_2 \end{pmatrix} = - \begin{pmatrix} \gamma_{11} & \gamma_{12}+u \\ \gamma_{21}-u & \gamma_{22} \end{pmatrix} \begin{pmatrix} D_1 \\ D_2 \end{pmatrix} \quad (8.3.19b)$$

and eliminating $\overline{B}$, we obtain the following equation for $\overline{D}$:

$$\begin{bmatrix} 1-(u-\chi\cos\theta)^2/[\kappa(\nu\cos^2\theta+\nu_z\sin^2\theta)] & 0 \\ 0 & 1-(u-\chi\cos\theta)^2/[\nu(\kappa\cos^2\theta+\kappa_z\sin^2\theta)] \end{bmatrix} \begin{bmatrix} D_1 \\ D_2 \end{bmatrix} = 0 \quad (8.3.20)$$

The phase velocities of the two characteristic waves are easily obtained. Other field components are found from (8.3.18b) and the constitutive relations. The results are listed in Table 8.3.2. Writing explicitly in terms of components of the $\overline{k}$ vector and noting that $k_z^2 = k^2\cos^2\theta$ and $k_x^2+k_y^2 = k^2\sin^2\theta$, we find the dispersion relation for Type I wave

$$k_x^2 + k_y^2 + \frac{\nu k_z^2}{\nu_z} - \frac{(\omega-\chi k_z)^2}{\kappa\nu_z} = 0 \quad (8.3.21)$$

which propagates with velocity

$$u = \chi \cos\theta \pm \sqrt{\kappa(\nu\cos^2\theta + \nu_z\sin^2\theta)} \qquad (8.3.22)$$

The dispersion relation for Type II wave is

$$k_x^2 + k_y^2 + \frac{\kappa k_z^2}{\kappa_z} - \frac{(\omega - \chi k_z)^2}{\nu\kappa_z} = 0 \qquad (8.3.23)$$

which propagates with velocity

$$u = \chi \cos\theta \pm \sqrt{\nu(\kappa\cos^2\theta + \kappa_z\sin^2\theta)} \qquad (8.3.24)$$
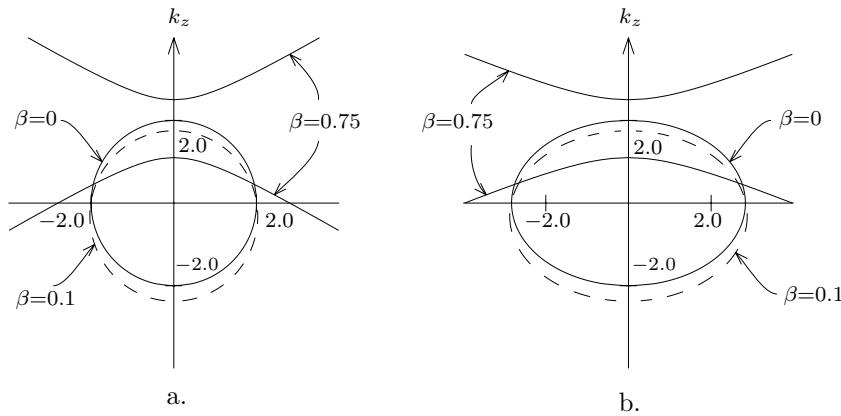
The plus sign in (8.3.22) and (8.3.24) corresponds to waves propagating in the direction of medium motion, and the negative sign to waves propagating opposite to the direction of medium motion.

It is interesting to note the $\pm$ signs in (8.3.22) and (8.3.24). The plus sign corresponds to waves propagating in the direction of medium motion; the negative sign, to waves propagating opposite to the direction of medium motion. For the same type of wave, the magnitude of the velocity in opposite directions are now different, as opposed to all previous cases, in which they are the same. In Figure 8.3.1, we plot the k surfaces for a moving isotropic medium with $n = 2$ in its rest frame and for a moving uniaxial medium with $n = 2$ and $a = b = 2$. For $1 - n^2\beta^2 > 0$, the surface is an ellipse rotated about the k_z axis; this is the non-relativistic case. For $1 - n^2\beta^2 < 0$, the k surface becomes a hyperbola rotated about the k_z axis; this is the relativistic case. We call this high-velocity region the Čerenkov zone. The velocity that separates the non-relativistic zone and the Čerenkov zone is $\beta = \pm 1/n$, which is equal to the velocity of light in the rest frame of the moving medium.

To facilitate further discussion, we make use of Table 8.3.2 and write (8.3.21) and (8.3.23) explicitly in terms of β dependence. After some manipulations, we obtain

$$k_x^2 + k_y^2 + b\frac{1 - n^2\beta^2}{1 - \beta^2}\left[k_z - \frac{n + \beta}{n\beta + 1}\frac{\omega}{c}\right] \cdot \left[k_z - \frac{n - \beta}{n\beta - 1}\frac{\omega}{c}\right] = 0 \quad (8.3.25)$$

$$k_x^2 + k_y^2 + a\frac{1 - n^2\beta^2}{1 - \beta^2}\left[k_z - \frac{n + \beta}{n\beta + 1}\frac{\omega}{c}\right] \cdot \left[k_z - \frac{n - \beta}{n\beta - 1}\frac{\omega}{c}\right] = 0 \quad (8.3.26)$$

Figure 8.3.1 k **surfaces for moving medium.**

where $b = \mu_z'/\mu'$ and $a = \epsilon_z'/\epsilon'$. As $1 - n^2\beta^2 > 0$ or $\beta < 1/n$, the dispersion relations are ellipsoids and they become hyperboloids when $\beta > 1/n$.

We examine two cases. First, consider a wave propagating in the $\hat{x}$ direction perpendicular to the medium velocity, $k_z = 0$. The $\overline{k}$ vectors become

$$\overline{k} = \hat{x}k_x = \pm\hat{x}\frac{\omega}{c}\left[b\frac{n^2 - \beta^2}{1 - \beta^2}\right]^{1/2} \tag{8.3.27}$$

$$\overline{k} = \hat{x}k_x = \pm\hat{x}\frac{\omega}{c}\left[a\frac{n^2 - \beta^2}{1 - \beta^2}\right]^{1/2} \tag{8.3.28}$$

The $\pm$ sign distinguishes waves propagating in the positive and the negative $\hat{x}$ directions. As β increase from 0 to 1, k increases from $an\omega/c$ or from $bn\omega/c$ to infinity. Thus the velocity along the $\hat{z}$ direction is zero when the medium velocity approaches the velocity of light in vacuum.

Second, consider a wave propagating in the direction of medium motion, $k_x = k_y = 0$. The two types of waves degenerate into one, and the k vectors become

$$\overline{k} = \hat{z}\frac{n + \beta}{n\beta + 1}\frac{\omega}{c} \tag{8.3.29}$$

$$\overline{k} = \hat{z}\frac{n - \beta}{n\beta - 1}\frac{\omega}{c} \tag{8.3.30}$$

Equation (8.3.29) corresponds to waves propagating in the positive $\hat{z}$ direction, and (8.3.30) to waves propagating in the negative $\hat{z}$ direction. For the wave propagating in the positive $\hat{z}$ direction, we observe that, as β increases from 0 to 1, k decreases from $n\omega/c$ to ω/c. The corresponding velocity of the wave increases from c/n to c. For the wave propagating in the negative $\hat{z}$ direction, we observe that, as β increases from 0 to $1/n$, k changes from $-n\omega/c$ to $-\infty$, and the velocity changes from $-c/n$ to 0. As β further increases from $1/n$ to 1, k reverses sign and decreases from infinity to ω/c. In the Čerenkov zone the negatively propagating wave now propagates in the positive $\hat{z}$ direction. As β approaches 1, the velocity approaches c. In all cases, the wave appears to be dragged by the motion of the medium. This phenomenon is referred to as the *Fizeau-Fresnel drag*.

C. Moving Boundary Conditions

Consider an interface separating regions 1 and 2 [Fig. 8.3.2]. Assume a small pillbox volume across the interface. Integrating Maxwell equations over the volume, we obtain

$$\oiint dS\,\hat{s} \times \overline{E} = -\iiint dV \frac{\partial}{\partial t}\overline{B} \tag{8.3.31}$$

$$\oiint dS\,\hat{s} \times \overline{H} = \iiint dV \frac{\partial}{\partial t}\overline{D} + \iiint dV\,\overline{J} \tag{8.3.32}$$

$$\oiint dS\,\hat{s} \cdot \overline{B} = 0 \tag{8.3.33}$$

$$\oiint dS\,\hat{s} \cdot \overline{D} = \iiint dV\,\rho \tag{8.3.34}$$

To derive the boundary conditions at moving boundaries, we let the pillbox move with the boundary surface. In accordance with kinematic theory, for a moving volume with velocity $\overline{v}$,

$$\frac{d}{dt}\iiint dV\,\overline{A} = \lim_{\Delta t \to 0} \frac{1}{\Delta t}\left\{ \iiint_{t+\Delta t} dV\,\overline{A}(t+\Delta t) - \iiint_t dV\,\overline{A}(t) \right\}$$

$$= \lim_{\Delta t \to 0} \frac{1}{\Delta t}\left\{ \left[\iiint_t dV + \oiint dS(\hat{s}\cdot\overline{v}\Delta t)\right]\left[\overline{A}(t) + \frac{\partial\overline{A}}{\partial t}\Delta t\right] - \iiint_t dV\,\overline{A}(t) \right\}$$

$$= \iiint dV \frac{\partial}{\partial t}\overline{A} + \oiint dS\,(\hat{s}\cdot\overline{v})\,\overline{A} \tag{8.3.35}$$
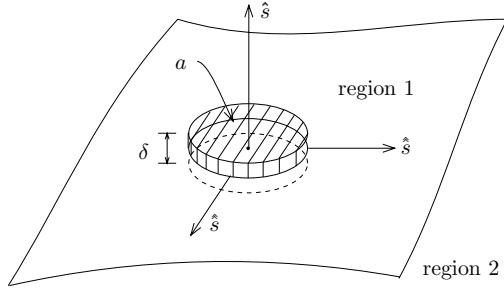
Figure 8.3.2 Pillbox for derivation of boundary conditions.

where $\overline{A}$ denotes any vector field. The surface integration term accounts for the motion of the boundary. We see that for moving boundaries, the Maxwell equations in integral form (8.3.31)–(8.3.34) become

$$\oiint dS \left[\hat{s} \times \overline{E} - (\hat{s} \cdot \overline{v})\overline{B} \right] = -\frac{d}{dt} \iiint_V dV \, \overline{B} \qquad (8.3.36)$$

$$\oiint dS \left[\hat{s} \times \overline{H} + (\hat{s} \cdot \overline{v})\overline{D} \right] = \frac{d}{dt} \iiint_V dV \, \overline{D} + \iiint_V dV \, \overline{J} \quad (8.3.37)$$

$$\oiint dS \left(\hat{s} \cdot \overline{B} \right) = 0 \qquad (8.3.38)$$

$$\oiint dS \left(\hat{s} \cdot \overline{D} \right) = \iiint dV \, \rho \qquad (8.3.39)$$

We shrink the pillbox in the same manner as before such that terms of the order of δ are disposed of. The boundary conditions now become

$$\hat{n} \times \left(\overline{E}_1 - \overline{E}_2 \right) - (\hat{n} \cdot \overline{v}) \left(\overline{B}_1 - \overline{B}_2 \right) = 0 \qquad (8.3.40)$$

$$\hat{n} \times \left(\overline{H}_1 - \overline{H}_2 \right) + (\hat{n} \cdot \overline{v}) \left(\overline{D}_1 - \overline{D}_2 \right) = \overline{J}_s \qquad (8.3.41)$$

$$\hat{n} \cdot \left(\overline{B}_1 - \overline{B}_2 \right) = 0 \qquad (8.3.42)$$

$$\hat{n} \cdot \left(\overline{D}_1 - \overline{D}_2 \right) = \rho_s \qquad (8.3.43)$$

Notice that $(\hat{n} \cdot \overline{v})(\overline{D}_1 - \overline{D}_2) = -\hat{n} \times \overline{v} \times (\overline{D}_1 - \overline{D}_2) + \overline{v}\hat{n} \cdot (\overline{D}_1 - \overline{D}_2)$, thus (8.3.41) can be written as

$$\hat{n} \times \left[(H_1 - H_2) - \overline{v} \times (\overline{D}_1 - \overline{D}_2) \right] = \overline{J}_s - \overline{v}\rho_s$$

When the velocity is parallel to the interface, $\hat{n} \cdot \hat{v} = 0$, the boundary conditions of such a moving boundary are identical to those of a stationary boundary.

EXAMPLE 8.3.1

Consider at time t a surface S_1 bounded by the contour C_1 [Fig. E8.3.1.1]. Let $\overline{v}$ be the instantaneous velocity of the element $d\overline{S}$ of the surface. The surface S_1 together with the contour C_1 may change shape with time, as $\overline{v}$ need not be a constant for all elements of S_1. At time $t + \Delta t$, S_1 and C_1 become S_2 and C_2 [Fig. E8.3.1.1].
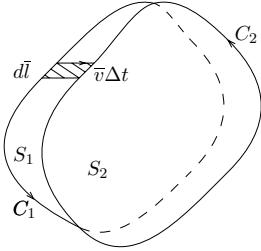
Figure E8.3.1.1

(a) Applying the divergence theorem to the volume bounded by $\overline{S}_1$, $\overline{S}_2$, and the differential ribbon area $d\overline{l} \times \overline{v}\Delta t$ between C_1 and C_2

$$\iint_S (d\overline{S} \cdot \overline{v}\Delta t)(\nabla \cdot \overline{A}) = \iint_{S_2} d\overline{S}_2 \cdot \overline{A} - \iint_{S_1} d\overline{S}_1 \cdot \overline{A} + \oint_C (d\overline{l} \times \overline{v}\Delta t) \cdot \overline{A}$$

show that the total time derivative of a vector field $\overline{A}$ integrated over the surface is

$$\frac{d}{dt} \iint_S d\overline{S} \cdot \overline{A} = \iint_S d\overline{S} \cdot \left[\frac{\partial \overline{A}}{\partial t} + \nabla \times (\overline{A} \times \overline{v}) + \overline{v} \nabla \cdot \overline{A} \right]$$

The rate at which the flux of $\overline{A}$ through S changes is seen to depend on three processes. The first term is due to the time rate of change of $\overline{A}$ for a stationary contour. The second term accounts for the contribution due to the flux crossing the surface generated by the motion of the contour C. The last term arises when the surface moves through the regions of the sources for the flux $\overline{A}$. When $\overline{A}$ is identified as the magnetic induction $\overline{B}$, the last term will be zero.

(b) Identifying $\overline{A}$ with $\overline{B}$ and $\overline{D}$ field vectors and employing Faraday's law and Ampère's law to obtain

$$\oint d\overline{l} \cdot (\overline{E} + \overline{v} \times \overline{B}) = -\frac{d}{dt} \iint dS\,\hat{s} \cdot \overline{B}$$

$$\oint d\overline{l} \cdot (\overline{H} - \overline{v} \times \overline{D}) = \frac{d}{dt} \iint dS\,\hat{s} \cdot \overline{D} + \iint dS\,\hat{s} \cdot (\overline{J} - \overline{v}\rho)$$

Applying the integrals to a ribbon-like area , which is now moving with the boundary surface, determine the relationship between $\overline{E}_1, \overline{H}_1$ in region 1 and $\overline{E}_2, \overline{H}_2$ in region 2.

SOLUTION:

(a)

$$\frac{d}{dt} \iint_S d\overline{S} \cdot \overline{A}$$

$$= \lim_{\Delta t \to 0} \frac{1}{\Delta t} \left\{ \iint_{S_2} d\overline{S}_2 \cdot \overline{A}(\overline{r}, t + \Delta t) - \iint_{S_1} d\overline{S}_1 \cdot \overline{A}(\overline{r}, t) \right\}$$

$$= \lim_{\Delta t \to 0} \frac{1}{\Delta t} \left\{ \iint_{S_2} d\overline{S}_2 \cdot \left[\overline{A}(\overline{r}, t) + \Delta t \frac{\partial}{\partial t} \overline{A}(\overline{r}, t) \right] - \iint_{S_1} d\overline{S}_1 \cdot \overline{A}(\overline{r}, t) \right\}$$

$$= \iint_S d\overline{S} \cdot \frac{\partial}{\partial t} \overline{A}(\overline{r}, t) + \iint_S d\overline{S} \cdot \overline{v} \nabla \cdot \overline{A} - \oint_C (d\overline{l} \times \overline{v}) \cdot \overline{A}$$

$$= \iint_S d\overline{S} \cdot \frac{\partial}{\partial t} \overline{A} + \oint_C d\overline{l} \cdot \overline{A} \times \overline{v} + \iint_S d\overline{S} \cdot \overline{v} \nabla \cdot \overline{A}$$

$$= \iint d\overline{S} \cdot \left[\frac{\partial \overline{A}}{\partial t} + \nabla \times (\overline{A} \times \overline{v}) + \overline{v} \nabla \cdot \overline{A} \right]$$

The last equality is obtained by using Stokes' Theorem.

(b) Identifying $\overline{B}$ with $\overline{A}$ and using the identity in (a)

$$\iint_S d\overline{S} \cdot \frac{\partial \overline{B}}{\partial t} = \frac{d}{dt} \iint_S d\overline{S} \cdot \overline{B} + \oint_C d\overline{l} \cdot \overline{v} \times \overline{B} - \iint_S d\overline{S} \cdot \overline{v} \nabla \cdot \overline{B}$$

Since $\nabla \cdot \overline{B} = 0$, the last integral vanishes. From $\nabla \times E = -\dfrac{\partial B}{\partial t}$ we obtain

$$\oint_C d\overline{l} \cdot (\overline{E} + \overline{v} \times \overline{B}) = -\frac{d}{dt} \iint_S d\overline{S} \cdot \overline{B}$$

Taking the integral over the shaded region which moves together with the boundary and letting $\delta \to 0$, we obtain

$$\left(\overline{E}_1 + \overline{v} \times \overline{B}_1 \right) \cdot d\overline{l} - \left(\overline{E}_2 + \overline{v} \times \overline{B}_2 \right) \cdot d\overline{l} = 0$$

since $d\overline{l}$ is tangential to the surface but otherwise arbitrary,

$$\left\{ \left(\overline{E}_1 + \overline{v} \times \overline{B}_1 \right) - \left(\overline{E}_2 + \overline{v} \times \overline{B}_2 \right) \right\} \underset{\substack{\text{Tangential} \\ \text{Components}}}{} = 0$$

or equivalently,

$$\hat{n} \times \left\{ \left(\overline{E}_1 + \overline{v} \times \overline{B}_1 \right) - \left(\overline{E}_2 + \overline{v} \times \overline{B}_2 \right) \right\} = 0 \,.$$

This boundary condition is equivalent to (8.3.40), because

$$0 = \hat{n} \times (\overline{E}_1 - \overline{E}_2) + \hat{n} \times \left\{ \overline{v} \times (\overline{B}_1 - \overline{B}_2) \right\}$$

$$= \hat{n} \times (\overline{E}_1 - \overline{E}_2) - (\hat{n} \cdot \overline{v})(\overline{B}_1 - \overline{B}_2) + \overline{v}\hat{n} \cdot (\overline{B}_1 - \overline{B}_2)$$

$$0 = \hat{n} \times (\overline{E}_1 - \overline{E}_2) - (\hat{n} \cdot \overline{v})(\overline{B}_1 - \overline{B}_2)$$

Identifying $\overline{D}$ with $\overline{A}$ and using the identity in (a), we have

$$\iint_S d\overline{S} \cdot \frac{\partial \overline{D}}{\partial t} = \frac{d}{dt} \iint_S d\overline{S} \cdot \overline{D} + \oint_C d\overline{l} \cdot \overline{v} \times \overline{D} - \iint_S d\overline{S} \cdot \overline{v} \nabla \cdot \overline{D}$$

$$= \frac{d}{dt} \iint_S d\overline{S} \cdot \overline{D} + \oint_C d\overline{l} \cdot \overline{v} \times \overline{D} - \iint_S d\overline{S} \cdot \overline{v}\rho$$

Applying Ampère's law $\nabla \times \overline{H} = \frac{\partial \overline{D}}{\partial t} + \overline{J}$, we obtain

$$\oint_C dl \cdot (\overline{H} - \overline{v} \times \overline{D}) = \frac{d}{dt} \iint_S d\overline{s} \cdot \overline{D} + \iint_S d\overline{s} \cdot (\overline{J} - \overline{v}\rho)$$

By a similar argument,

$$\left\{ (\overline{H}_1 - \overline{v} \times \overline{D}_1) - (\overline{H}_2 - \overline{v} \times \overline{D}_2) + \hat{n} \times (\overline{J}_s - \overline{v}\rho_s) \right\}_{\substack{\text{Tangential} \\ \text{Components}}} = 0$$

or equivalently,

$$n \times (H_1 - H_2) - \hat{n} \times \left[\overline{v} \times (\overline{D}_1 - \overline{D}_2) \right] = \overline{J}_s - \overline{v}\rho_s$$

— End of Example 8.3.1 —

Example 8.3.2

The jump conditions for moving boundaries have been derived by assuming that the pillbox moves with the boundary. If the pillbox is stationary while the boundary is moving, then $v = 0$ in (8.3.36) and (8.3.37) as v refers to the velocity of the pillbox:

$$\oiint dS\hat{s} \times \overline{E} = -\frac{d}{dt} \iiint_V dV \, \overline{B}$$

$$\oiint dS\hat{s} \times \overline{H} = \frac{d}{dt} \iiint_V dV \, \overline{D} + \iiint_V dV \, \overline{J}$$
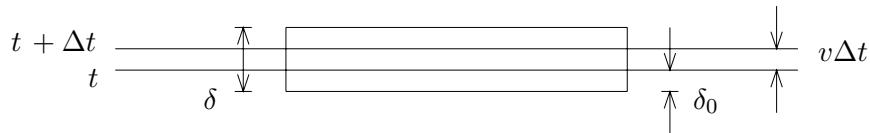
Figure E8.3.2.1

Refer to Fig. E8.3.2.1. The boundary surface has been moved a distance $v\Delta t$ from time t to time $t + \Delta t$. Show that for a vector field $\overline{A}$

$$\iiint_t dV \, \overline{A} = a \int_0^{\delta_0} dz \, A + a \int_{\delta_0}^{\delta} dz \, \overline{A} = \overline{A}_2 a \delta_0 + \overline{A}_1 a(\delta - \delta_0)$$

and that

$$\iiint_{t+\Delta t} dV \, \overline{A} = a \int_0^{\delta_0 + v\Delta t} dz \, \overline{A} + a \int_{\delta_0 + v\Delta t}^{\delta} dz \, \overline{A}$$
$$= \overline{A}_2 a(\delta_0 + v\Delta t) + \overline{A}_1 a(\delta - \delta_0 - v\Delta t)$$

$$\iiint_{t+\Delta t} dV \, \overline{A} - \iiint_t dV \, \overline{A} = \overline{A}_2 \, av\Delta t - \overline{A}_1 av\Delta t$$

where a is the area of the top side or the bottom side of the pillbox and $\overline{A}_1$ and $\overline{A}_2$ denote the $\overline{A}$ field in medium 1 and medium 2, respectively. Identifying $\overline{A}$ with $\overline{B}$ and $\overline{D}$, determine the relationship between $\overline{E}_1, \overline{H}_1$ in region 1 and $\overline{E}_2, \overline{H}_2$ in region 2.

— END OF EXAMPLE 8.3.2 —

EXAMPLE 8.3.3

Derive the boundary conditions associated with Maxwell's two curl equations by using a) a pillbox, and b) a ribbon contour. When the boundary is moving, determine the boundary conditions and discuss the difference from the stationary ones.

SOLUTION:

Integrating Maxwell equations over a volume, we get (for $\overline{V} = 0$)

$$\oiint_\Sigma dS \left(\hat{s} \times \overline{E} \right) = - \iiint_V \frac{\partial B}{\partial t} dv \qquad \text{(E8.3.3.1)}$$

$$\oiint_\Sigma dS \left(\hat{s} \times \overline{H} \right) = \iiint_V J dv + \iiint_V \frac{\partial D}{\partial t} dv \qquad \text{(E8.3.3.2)}$$

To find the boundary conditions we apply these equations to a pillbox with area A and thickness δ. First we let $\delta \to 0$. Since B and D and their time derivatives are finite and the volume of the volume integral goes to zero. So we get

$$\iiint_V \frac{\partial B}{\partial t} dv = \iiint_V \frac{\partial D}{\partial t} dv = 0$$

From the definition of surface current, we also have

$$\lim_{\delta \to 0} \iiint_V \overline{J}\,dv = \iint_A \overline{J}_s\,da$$

By letting $\delta \to 0$ our total surface integral (over Σ) reduces to integral over the circular contours at A_+ and A_- (i.e., from both sides). So we now have

$$\left(\iint_{A+} + \iint_{A-} \right) \hat{s} \times \overline{E}\,ds = 0 \qquad\qquad (\text{E8.3.3.3})$$

$$\left(\iint_{A+} + \iint_{A-} \right) \left(\hat{s} \times \overline{H} \right) ds = \iint_A \overline{J}_s\,da \qquad (\text{E8.3.3.4})$$

Now as we let $\delta \to 0$, take $A \to 0$ in such a way that $\delta/A \to 0$. This ensures that the pillbox will always enclose the boundary. When $A \to 0$, we get $\hat{s} \to \hat{n}$ over A_+ and $\hat{s} \to -\hat{n}$ over A_-. (We also have $A = A_+ = A_-$ for a cylinder.) So the boundary conditions become

$$\hat{n} \times \left(\overline{E}_1 - \overline{E}_2 \right) = 0$$
$$\hat{n} \times \left(\overline{H}_1 - \overline{H}_2 \right) = J_s$$

If the boundary is moving we would have

$$\frac{d}{dt} \iiint_V B\,dv = \iiint_V \frac{\partial B}{\partial t}\,dv + \iint_\Sigma \left(\hat{s} \cdot \overline{V} \right) \overline{B}$$

and

$$\frac{d}{dt} \iiint_V D\,dv = \iiint_V \frac{\partial D}{\partial t}\,dv + \iint_\Sigma \left(\hat{s} \cdot \overline{V} \right) \overline{D}\,ds$$

Taking $\delta \to 0$, the volume integral terms are treated as before and the surface integral terms may be grouped together with the surface integral terms on the RHS (of say, Eqs. (E8.3.3.1) and (E8.3.3.2)). We then have, analogous to Eqs. (E8.3.3.3) and (E8.3.3.4)

$$\left(\iint_{A+} + \iint_{A-} \right) \left[\hat{s} \times \overline{E} - \left(\hat{s} \cdot \overline{V} \right) B \right] ds = 0$$

$$\left(\iint_{A+} + \iint_{A-} \right) \left[\hat{s} \times \overline{H} + \left(\hat{s} \cdot \overline{V} \right) D \right] ds = \iint J_s\,da$$

And as $A \to 0$ we get in the same fashion

$$\hat{n} \times (E_1 - E_2) - \left(\hat{n} \cdot \overline{V}\right)\left(\overline{B}_1 - \overline{B}_2\right) = 0$$
$$\hat{n} \times (H_1 - H_2) + \left(\hat{n} \cdot \overline{V}\right)\left(\overline{D}_1 - \overline{D}_2\right) = J_s$$

We integrated Maxwell's equations over a volume in order to use the pillbox geometry. If we wish to use the ribbon contour geometry, we will find it useful to integrate Maxwell's equations over a surface and (using Stoke's theorem) we get Maxwell's equations in the form (for $V = 0$).

$$\oint_c \overline{E} \cdot d\overline{\ell} = -\frac{d}{dt}\int_s \overline{B} \cdot \overline{n}da \qquad\qquad (\text{E8.3.3.5})$$

$$\oint_c \overline{H} \cdot d\overline{\ell} = \frac{d}{dt}\int_s \overline{D} \cdot \overline{n}da + \int_s \overline{J} \cdot nda \qquad (\text{E8.3.3.6})$$

We now apply a rectangular "ribbon" to the boundary in such a way that the normal to the plane of the ribbon is tangential to the boundary at the point that we are interested in.
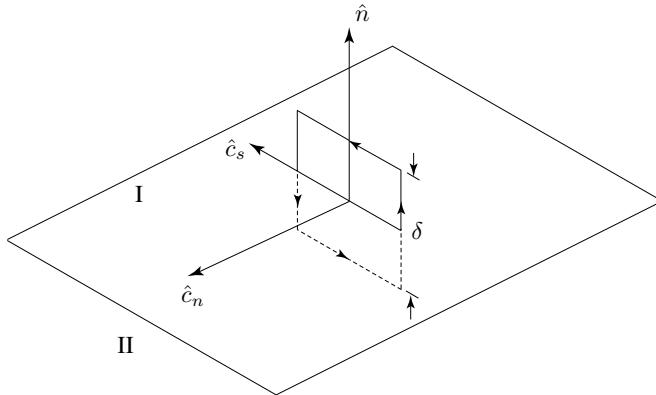
Figure E8.3.3.1

As $\delta \to 0$, the area enclosed by the ribbon goes to zero and so all the surface integrals over $\frac{\partial B}{\partial t}$ or $\frac{\partial D}{\partial t}$ vanish since these quantities are finite. The integral over $\overline{J}$ becomes a surface current as before. We then have as the length of the ribbon goes to zero

$$\left(\overline{E}_1 - \overline{E}_2\right) \cdot \hat{c}_s = 0$$
$$\left(\overline{H}_1 - \overline{H}_2\right) \cdot \hat{c}_s = \overline{J}_s \cdot \hat{c}_n$$

where $\hat{c}_s$ is the unit vector defining the intersection of the plane of the ribbon and the plane of the boundary and $\hat{c}_n$ is the unit normal to the plane of the ribbon.

Now note that the orientation of the ribbon plane is arbitrary. Since $\hat{c}_s$ is arbitrary on the plane parallel to the boundary, we have

$$\hat{n} \times \left(\overline{E}_1 - \overline{E}_2\right) = 0$$

where n is the unit vector perpendicular to the boundary, also by orienting, $\hat{c}_n$ such that $\hat{c}_n \| \overline{J}_s$, we get

$$\overline{J}_s = \hat{c}_n \left(\overline{J}_s \cdot \hat{c}_n\right) = \hat{c}_n \left(\overline{H}_1 - \overline{H}_2\right) \cdot \hat{c}_s = (\hat{c}_s \times \hat{c}_n) \times (H_1 - H_2) - [(H_1 - H_2) \cdot \hat{c}_n] \hat{c}_s$$

where we used the vector identity $A(B \cdot C) = -B \times (A \times C) \times (A \cdot B)C$. We know that $(H_1 - H_2) \cdot \hat{c}_n = 0$ since $\hat{c}_n \perp \hat{c}_s$ (in other words we would then have from above $(H_1 - H_2) \cdot \hat{c}_n = \overline{J}_s \cdot \hat{c}_s$ but since $J_s \| \hat{c}_n \perp \hat{c}_s$ our results follow). Note also that

$$\hat{c}_s \times \hat{c}_n = \hat{n}$$

So we can write

$$n \times (H_1 - H_2) = J_s$$

Now to solve for the moving boundary conditions, let us transform to a reference frame stationary in the boundary frame. We then have

$$\overline{E}' = \overline{E} + \overline{V} \times \overline{B}$$
$$\overline{H}' = \overline{H} - \overline{V} \times \overline{B}$$
$$\overline{J}' = \overline{J} - \rho\overline{V}$$

Now we can apply the stationary boundary conditions

$$[n \times E']_2^1 = 0$$
$$[n \times H']_2^1 = \overline{J}_s$$

where $[A]_2^1$ means $A_1 - A_2$. We find

$$[n \times E + n \times (V \times B)]_2^1 = 0$$
$$[n \times H - n \times (V \times D)]_2^1 = J_s - \sigma V$$

Now use vector identity

$$n \times (V \times B) \equiv V(n \cdot B) - (n \cdot V)B$$
$$n \times (V \times D) \equiv V(n \cdot D) - (n \cdot V)D$$

So we get

$$n \times (E_1 - E_2) - (\hat{n} \cdot \overline{V})(B_1 - B_2) + \overline{V}\hat{n} \cdot (\overline{B}_1 - \overline{B}_2) = 0$$

$$n \times (H_1 - H_2) + (\hat{n} \cdot \overline{V})(D_1 - D_2) - V\hat{n} \cdot (\overline{D}_1 - \overline{D}_2) = J_s - \sigma V$$

Now from the 1st set of boundary conditions we had

$$n \cdot (B_1 - B_2) = 0$$

$$n \cdot (D_1 - D_2) = \sigma$$

So we get

$$n \times (E_1 - E_2) - (\hat{n} \cdot \overline{V})(\overline{B}_1 - \overline{B}_2) = 0$$

$$n \times (H_1 - H_2) + (n \cdot V)(\overline{D}_1 - \overline{D}_2) = J_s$$

The important thing to notice is now tangential E, H discontinuous because surface moves in a direction normal to its surface.

<div align="right">— END OF EXAMPLE 8.3.3 —</div>

D. Phase Matching at Moving Boundaries

Previously, we have studied phase-matching conditions for a stationary boundary surface. When the boundary is moving, we let its velocity be

$$\overline{v} = \hat{x}v_x + \hat{y}v_y + \hat{z}v_z \tag{8.3.44}$$

At $t = 0$, the surface is at $x = 0$. At other times, the boundary surface is at $x = v_x t$. The incident, the reflected, and the transmitted waves now have space-time dependence as follows:

$$\text{incident}: \quad e^{ik_x x + ik_y y + ik_z z - i\omega t}$$

$$\text{reflected}: \quad e^{ik_{rx} x + ik_{ry} y + ik_{rz} z - i\omega_r t}$$

$$\text{transmitted}: \quad e^{ik_{tx} x + ik_{ty} y + ik_{tz} z - i\omega_t t}$$

where we distinguish between the angular frequencies ω, ω_r and ω_t. We require that the moving boundary conditions (8.3.40)–(8.3.43) be satisfied, which gives

$$k_x(v_x t) + k_y(y + v_y t) + k_z(z - v_z t) - \omega t$$

$$= k_x(v_x t) + k_{ry}(t + v_y t) + k_{rz}(z + v_z t) - \omega_r t$$

$$= k_{tz}(v_x t) + k_{ty}(y + v_y t) + k_{tz}(z + v_z t) - \omega_t t \tag{8.3.45}$$

Since these equalities must hold for all y, z and t, we conclude that

$$k_y = k_{ry} = k_{ty} \tag{8.3.46}$$

$$k_z = k_{rz} = k_{tz} \tag{8.3.47}$$

$$k_x v_x - \omega = k_{rx} v_x - \omega_r = k_{tx} v_x - \omega_t \tag{8.3.48}$$

Thus the phase-matching conditions are the same as for the case of a stationary boundary; tangential components of the wave vectors are continuous. The frequencies of the three waves are now different; they are determined only by the normal component of the velocity.

Consider the simple case of a wave normally incident from an isotropic medium upon another isotropic medium moving in the $\hat{x}$ direction toward the wave. The incident wave vector is

$$\overline{k} = \hat{x} k_x = -\hat{x} n \frac{\omega}{c} \tag{8.3.49}$$

and the reflected vector is

$$\overline{k}_r = \hat{x} k_{rx} = \hat{x} n \frac{\omega_r}{c} \tag{8.3.50}$$

Substituting (8.3.49)–(8.3.50) into (8.3.48) we find

$$\omega_r = \omega \frac{1 + n\beta}{1 - n\beta} \tag{8.3.51}$$

$$k_r = -k \frac{1 + n\beta}{1 - n\beta} = n \frac{\omega}{c} \frac{1 + n\beta}{1 - n\beta} \tag{8.3.52}$$

where $\beta = v_x/c$. The reflected wave is seen to be Doppler-shifted toward the high-frequency side. Its wavenumber is also increased by the same amount. In order to determine the transmitted wavenumber and angular frequencies, we must know the dispersion relations for a moving medium.

E. Force on a Moving Dielectric Half-Space

Consider a plane wave normally incident upon a dielectric medium ($\mu' = \mu_o$) moving toward the wave. Let the boundary be moving in the $\hat{z}$ direction with velocity v, and the electric field be linearly polarized in the $\hat{x}$ direction. Write

$$\overline{E}_i = \hat{x} E_0 e^{ikz - i\omega t}, \qquad k = -\frac{\omega}{c}$$

The fields for the reflected and transmitted waves are

$$\overline{E}_r = \hat{x} R E_0 e^{ik_r z - i\omega_r t}, \qquad k_r = \frac{\omega_r}{c}$$

$$\overline{E}_t = \hat{x} T E_0 e^{ik_t z - i\omega_t t}, \qquad k_t = -\frac{n - \beta}{1 - n\beta}\frac{\omega_t}{c}$$

$$c\overline{B}_r = \hat{y}\frac{ck_r}{\omega_r} E_r = \hat{y} E_r$$

$$c\overline{B}_t = \hat{y}\frac{ck_t}{\omega_t} E_t = -\hat{y}\frac{n - \beta}{1 - n\beta} E_t$$

$$c\overline{D}_r = \hat{x} c\epsilon_o E_r$$

$$c\overline{D}_t = \hat{x}\frac{1}{c\mu_o}\left[p - l\frac{ck_t}{\omega_t}\right] E_t = \hat{x}\frac{1}{c\mu_o}\frac{n(n - \beta)}{1 - n\beta} E_t$$

$$\overline{H}_r = \hat{y}\frac{1}{c\mu_o} E_r$$

$$\overline{H}_t = \hat{y}\frac{1}{c\mu_o}\left[l + q\frac{ck_t}{\omega_t}\right] E_t = -\hat{y}\frac{1}{c\mu_o} n E_t$$

where $n = c\sqrt{\mu_o \epsilon_t}$ and $\beta = \nu/c$.

    To calculate amplitudes for the reflected and transmitted waves, we apply the moving boundary conditions (8.3.40) and (8.3.41), which require that $E_x - \beta c B_y$ and $H_y - \beta c D_x$ be continuous across the boundary. We find

$$1 + R - \beta(-1 + R) = T + \beta\frac{n - \beta}{1 - n\beta} T$$

$$-1 + R - \beta(1 + R) = -nT - \beta\frac{n(n - \beta)}{1 - n\beta} T$$

The reflection and transmission coefficients are found to be

$$R = -\frac{1 + \beta}{1 - \beta}\frac{n - 1}{n + 1}$$

$$T = \frac{1 - n\beta}{1 - \beta}\frac{2}{n + 1}$$

The reflectivity and transmissivity are

$$r = \frac{\hat{z} \cdot (\overline{E}_r \times \overline{H}_r)}{-\hat{z} \cdot (\overline{E}_i \times \overline{H}_i)} = |R|^2$$

$$t = \frac{-\hat{z} \cdot (\overline{E}_t \times \overline{H}_t)}{-\hat{z} \cdot (\overline{E}_i \times \overline{H}_i)} = n\,|T|^2$$

It is seen that $r + t \neq 1$ when $\beta \neq 0$. Is power conservation being violated?

To answer this question [Daly and Gruenberg, 1967], conceive a cylinder of unit cross-section erected across the boundary with its axis parallel to the z axis and containing a portion of the interface. The sum of the incident, reflected, and transmitted waves gives the total time-average electromagnetic power flow into the cylinder:

$$< P_{elec} >= \frac{1}{2c\mu_o}(E_i^2 - E_r^2 - nE_t^2) = 4cU_0\beta\frac{(n-1)(1-n\beta)}{(n+1)(1-\beta)^2}$$

where

$$U_0 = \frac{1}{2c^2\mu_o}\,|E_0|^2$$

Inside the cylinder, there is an increase in the time-average electromagnetic energy, $Re(\overline{E}\cdot\overline{D}^* + \overline{H}\cdot\overline{B}^*)/4$ as the moving dielectric occupies more free space. The rate of this increase in the stored energy is given by the velocity times the difference between the electromagnetic energy in the dielectric and that in the vacuum. We find

$$< P_{stored} >= \frac{c\beta}{2}\{\overline{E}_t\cdot\overline{D}_t^* - \overline{E}_r\cdot\overline{D}_i^* - \overline{E}_t\cdot\overline{D}_i^*\}$$

$$= \frac{\beta}{2c\mu_o}\left\{n\left[\frac{n-\beta}{1-n\beta}\right]E_t^2 - E_r^2 - E_i^2\right\} = 2cU_0\beta\frac{(n-1)(1-2n\beta+\beta^2)}{(n+1)(1-\beta)^2}$$

When the medium is stationary, $< P_{elec} >=< P_{stored} >= 0$. When the medium is in motion, this equality does not hold because mechanical power is required to keep the dielectric moving at constant velocity. The rate at which mechanical work has to be supplied to the system is given by the difference between $< P_{stored} >$ and $< P_{elec} >$. We find

$$< P_{mech} >=< P_{stored} > - < P_{elec} >= -\frac{2cU_0\beta(n-1)(1+\beta)}{(n+1)(1-\beta)}$$

The negative sign indicates that mechanical work has been done to the system. The force per unit area acting on the dielectric medium is obtained from $\overline{F} \cdot \overline{v} = < P_{mech} >$. Thus

$$\overline{F}_{mech} = -\frac{\hat{z} 2 U_0 (n - 1)(1 + \beta)}{(n + 1)(1 - \beta)}$$

This mechanical force is needed to maintain the medium at constant velocity. We note that the force is in the negative $\hat{z}$ direction; this means that mechanical force must be applied to stop the medium from accelerating toward the wave. The electromagnetic force $\overline{F}_{elec}$ exerted on the medium by the wave is equal to the negative of $\overline{F}_{mech}$, as required by the basic laws of mechanics.

We double-check this assertion by using the conservation theorem to calculate the electromagnetic force $\overline{F}_{elec}$. When the force density is integrated over the volume of the cylinder, the force per unit area acting on the surface is

$$\overline{F}_{elec} = \hat{z} \left(< T_{zz} >_i + < T_{zz} >_r - < T_{zz} >_t \right)$$
$$+ v \left(< \overline{G} >_i + < \overline{G} >_r - < \overline{G} >_t \right)$$
$$= \frac{\hat{z} 2 U_0 (n - 1)(1 + \beta)}{(n + 1)(1 - \beta)}$$

Clearly, $\overline{F}_{elec}$ and $\overline{F}_{mech}$ are indeed in opposite directions. Thus the radiation pressure exerted on a dielectric half-space by a plane wave at normal incidence results in a force attracting the medium toward the wave. This force is there whether the dielectric is stationary or in motion. A mechanical force counterbalancing $\overline{F}_{elec}$ is needed either to keep the dielectric medium stationary or to maintain its constant velocity when it is in motion.

For a perfect conductor,

$$< P_{mech} > = \frac{1}{2 c \mu_o} \left[-(E_i^2 + E_r^2) - (E_i^2 - E_r^2) \right]$$
$$= \frac{2 c U_0 \beta (1 + \beta)}{(1 - \beta)}$$

It follows that $\overline{F}_{mech} = \hat{z} 2 U_0 (1 + \beta)/(1 - \beta)$. Note in particular the sign of $\overline{F}_{mech}$ which is now in the positive $\hat{z}$ direction, demonstrating that the wave is exerting a force to push the conductor away. Thus the electromagnetic force is attractive when the medium is a dielectric, and repulsive when the medium is a perfect conductor.

F. Guided Waves in a Moving Dielectric Slab

Consider TE modes guided by a slab medium moving between two identical stationary isotropic media. Let the guidance direction be parallel to the direction of motion of the slab. We follow the graphical approach to determine the cutoff wavenumbers and the propagation constant k_z.

The constitutive parameters for a moving medium have been determined. We use subscript 1 to denote the parameters pertaining to the moving dielectric slab waveguide. The transverse wavenumber k_{1x} inside the waveguide, by making use of the dispersion relations, may be cast into the form:

$$k_{1x}^2 = p_1 k_o^2 - 2l_1 k_z k_o - q_1 k_z^2 \qquad (8.3.53)$$

where $k_o = \omega/c$ and $k_z = k_o(n^2 + \alpha_x^2/k_o^2)^{1/2}$. The guidance condition becomes

$$(\alpha_x d)^2 + (k_{1x} d)^2 = (k_x^2 - k^2)d^2 + (pk_o^2 - 2lk_o k_z - qk_z^2)d^2$$

$$= (k_o d)^2 \left\{ \frac{n_1^2 - \beta^2}{1 - \beta^2} - n^2 - 2\beta \frac{n_1^2 - 1}{1 - \beta^2} \sqrt{n^2 + \left(\frac{\alpha_x}{k_o}\right)^2} \right.$$

$$\left. + \beta^2 \frac{n_1^2 - 1}{1 - \beta^2} \left[n^2 + \left(\frac{\alpha_x}{k_o}\right)^2\right] \right\} \qquad (8.3.54)$$

The shape of the curve described by this equation is a function of the slab velocity. At $\beta = 0$, the curve is a circular arc, the expected result for a stationary slab. When the isotropic medium surrounding the slab is free space, $n = 1$ and this equation becomes

$$(\alpha_x d)^2 + (k_{1x} d)^2 = (k_o d)^2 \left[\frac{n_1^2 - 1}{1 - \beta^2}\right] \left[1 - \beta\sqrt{1 + \left(\frac{\alpha_x}{k_o}\right)^2}\right]^2 \qquad (8.3.55)$$

a result that can be derived by applying the Lorentz transformation directly. We observe that at cutoff

$$k_o d = \sqrt{(1 + \beta)/(1 - \beta)} \, m\pi \sqrt{n_1^2 - 1}$$

the cutoff wavenumber increases as β increases. In general, we see that as β increases, α_x decreases, and so does k_x. Thus the guided

waves possess higher cutoff frequencies and propagate at larger phase velocities. A parallel analysis results in similar conclusions for the TM waves.

Next, we consider an isotropic medium moving between two perfectly conducting parallel plates. The guidance condition for both TE and TM modes is

$$\frac{m\pi}{d} = k_{1x} = \gamma\sqrt{(n_1^2 - \beta^2)k_o^2 - 2\beta(n_1^2 - 1)k_o k_z - (1 - n_1^2\beta^2)k_x^2} \quad (8.3.56)$$

Note that $m\pi/d$ is the cutoff wavenumber for the mth mode when the medium is stationary. Solving for k_z, we obtain from this equation

$$k_z = \frac{k_o}{1 - n_1^2\beta^2}\left\{-\beta(n_1^2 - 1) \pm (1 - \beta^2)\sqrt{n_1^2 - \left(\frac{1 - n_1^2\beta^2}{1 - \beta^2}\right)\left(\frac{m\pi}{k_o d}\right)^2}\right\}$$

$$(8.3.57)$$

Observe that cutoff occurs when k_z becomes imaginary. When the velocity of the medium exceeds the Čerenkov velocity so that $n_1\beta > 1$, k_z will always be real for real n_1 and no cutoff will occur. The propagation constant k_z is always positive when

$$\beta(n_1^2 - 1) \geq \left[n_1^2(1 - \beta^2)^2 - (1 - \beta^2)^2(1 - n_1^2\beta^2)(m\pi/k_o d)\right]^{1/2}$$

or, equivalently, $k_o d \geq m\pi\left[m\pi(1 - \beta^2)/(n_1^2 - \beta^2)\right]^{1/2}$.

In the low-velocity regime when $n_1\beta < 1$, cutoff occurs for $k_o d \leq m\pi(1 - n_1^2\beta^2)/(1 - \beta^2)n_1^2$. Comparing this with the stationary case in which $k_c d = m\pi/n_1^2$, we see that motion of the medium always lowers the cutoff wavenumber. For frequencies above cutoff but with the square-root term smaller than the first term in the equation, the phase velocities of the guided waves are all in the negative $\hat{z}$ direction. Phase velocities in both directions become possible when $k_o d \geq m\pi\left[(1 - \beta^2)/(n_1^2 - \beta^2)\right]^{1/2}$.

It is of interest to investigate the power flow carried by each mode in the waveguide. Consider the TE modes with

$$E_y = E_m \sin\frac{m\pi x}{d}e^{ik_z z}$$

The magnetic field components are determined from the Maxwell equations and the constitutive relations for the moving medium:

$$\overline{B} = \frac{1}{i\omega}\nabla \times \overline{E}$$
$$= \left[-\hat{x}\frac{k_z}{\omega}E_m \sin\frac{m\pi x}{d} - \hat{z}i\frac{m\pi}{\omega d}E_m \cos\frac{m\pi x}{d}\right]e^{ik_z z}$$

$$\overline{H} = \frac{1}{c\mu'}\left[\hat{x}(-lE_y + qc\beta_x) + \hat{z}(c\beta_z)\right]$$
$$= \hat{x}\frac{1}{c\mu'}\left[-l - \frac{qck_z}{\omega}\right]E_y - \hat{z}i\frac{m\pi}{\omega\mu'd}E_m \cos\frac{m\pi x}{d}e^{ik_z z}$$

The power flow in the $\hat{z}$ direction after integrating over the waveguide cross section is found to be

$$P_z = -\int_0^d dx \frac{1}{2}\mathrm{Re}(E_y H_x^*) = \mathrm{Re}\sum_{m=1}^{\infty}\frac{d}{2c\mu'}\left[l + \frac{qk_z}{k_o}\right]^* |E_m|^2$$
$$= \mathrm{Re}\sum_{m=1}^{\infty}\frac{d}{2c\mu'}\left[\pm\sqrt{n_1^2 - \left[\frac{1 - n_1^2\beta^2}{1 - \beta^2}\right]\left[\frac{m\pi}{k_o d}\right]^2}\right]^* |E_m|^2$$

Thus each individual mode carries its own power; the total power is the sum of all individual components. At $\beta = 0$ this result reduces to the case of a stationary medium. Above the Čerenkov velocity, the square root always gives real values and all modes carry time-average power. Below the Čerenkov velocity, modes below cutoff will not carry time-average power. In all cases, the $\pm$ sign in front of the square root indicates that power can propagate in both positive and negative $\hat{z}$ directions, as opposed to the phase velocities, which in some cases can be in only one direction. In this velocity range, guided backward waves can be generated in the moving medium.

G. Guided Waves in Moving Gyrotropic Media

For guided waves in anisotropic and bianisotropic media the wave equations for E_z and H_z are usually coupled. We illustrate this with the general case of a bianisotropic medium realized by a moving gyrotropic

medium. The gyrotropic medium in its rest frame has the tensor permittivity

$$\overline{\overline{\epsilon}}' = \begin{bmatrix} \epsilon' & -i\epsilon'_g & 0 \\ i\epsilon'_g & \epsilon' & 0 \\ 0 & 0 & \epsilon'_z \end{bmatrix} \tag{8.3.58}$$

In the laboratory frame the constitutive matrix is given by (8.3.14). We transform to $\overline{E}\,\overline{H}$ representation and obtain the following constitutive relations:

$$\overline{D} = \overline{\overline{\epsilon}}_s \cdot \overline{E}_s + \epsilon'_z \overline{E}_z + \overline{\overline{\xi}}_s \cdot \overline{H}_s \tag{8.3.59a}$$

$$\overline{B} = \overline{\overline{\mu}}_s \cdot \overline{E}_s + \mu'_z \overline{E}_z - \overline{\overline{\xi}}_s \cdot \overline{H}_s \tag{8.3.59b}$$

where

$$\overline{\overline{\epsilon}}_s = \epsilon' \begin{bmatrix} a & -ia_g \\ ia_g & a \end{bmatrix}$$

$$= \frac{(1-\beta^2)\epsilon^2}{n^2\left[(1-n^2\beta^2)^2 - n_g^4\beta^4\right]}$$

$$\cdot \begin{bmatrix} n^2(1-n^2\beta^2) + n_g^4\beta^2 & -in_g^2 \\ in_g^2 & n^2(1-n^2\beta^2) + n_g^4\beta^2 \end{bmatrix} \tag{8.3.60}$$

$$\overline{\overline{\mu}}_s = \mu' \begin{bmatrix} b & -ib_g \\ ib_g & b \end{bmatrix}$$

$$= \frac{(1-\beta^2)\mu'}{(1-n^2\beta^2)^2 - n_g^4\beta^4} \begin{bmatrix} 1-n^2\beta^2 & -in_g^2\beta^2 \\ in_g^2\beta^2 & 1-n^2\beta^2 \end{bmatrix} \tag{8.3.61}$$

$$\overline{\overline{\xi}}_s = \frac{1}{c} \begin{bmatrix} -i\xi_g & -\xi \\ \xi & -i\xi_g \end{bmatrix}$$

$$= \frac{(1-\beta^2)/c}{(1-n^2\beta^2)^2 - n_g^4\beta^4}$$

$$\cdot \begin{bmatrix} -n_g^2\beta & -\gamma^2\beta\left[(n^2-1)(1-n^2\beta^2)+n_g^4\beta^2\right] \\ \gamma^2\beta\left[(n^2-1)(1-n^2\beta^2)+n_g^4\beta^2\right] & -in_g^2\beta \end{bmatrix} \tag{8.3.62}$$

At $\beta = 0$, (8.3.60) reduces to (8.3.58), $\overline{\overline{\mu}}_s = \mu'\overline{\overline{I}}$, $\overline{\overline{\xi}}_s = 0$, and we have the gyrotropic medium at rest.

We can express the transverse components in terms of the longitudinal components E_z and H_z and derive wave equations for E_z and

H_z . We find

$$\nabla_s \times \overline{E}_z = i\omega \overline{\overline{\mu}}_s \cdot \overline{H}_s \cdot \overline{\overline{d}} \cdot \overline{E}_s \tag{8.3.63a}$$

$$\nabla_s \times \overline{H}_z = -i\omega \overline{\overline{\epsilon}}_s \cdot \overline{H}_s - \overline{\overline{d}} \cdot \overline{H}_s \tag{8.3.63b}$$

$$\nabla_s \times \overline{E}_s = i\omega \mu'_z \overline{H}_z \tag{8.3.64a}$$

$$\nabla_s \times \overline{H}_s = -i\omega \epsilon'_z \overline{E}_z \tag{8.3.64b}$$

where

$$\overline{\overline{d}} = \begin{bmatrix} d_g & -id \\ id & d_g \end{bmatrix} = \begin{bmatrix} \omega\xi_g/c & -i(k_z + \omega\xi/c) \\ i(k_z + \omega\xi/c) & \omega\xi_g/c \end{bmatrix} \tag{8.3.65}$$

In terms of E_z and H_z , the transverse components are

$$\overline{E}_s = (\overline{\overline{I}} - \omega^2 \overline{\overline{d}}^{-1} \cdot \overline{\overline{\mu}}_s \cdot \overline{\overline{d}}^{-1} \cdot \overline{\overline{\epsilon}}_s)^{-1} \cdot \left[-\overline{\overline{d}}^{-1} \cdot (\nabla_s \times \overline{E}_z) \right.$$
$$\left. - i\omega \overline{\overline{d}}^{-1} \cdot \overline{\overline{\mu}}_s \cdot \overline{\overline{d}}^{-1} (\nabla \times \overline{H}_z) \right] \tag{8.3.66a}$$

$$\overline{H}_s = (\overline{\overline{I}} - \omega^2 \overline{\overline{d}}^{-1} \cdot \overline{\overline{\epsilon}}_s \cdot \overline{\overline{d}}^{-1} \cdot \overline{\overline{\mu}}_s)^{-1} \cdot \left[-\overline{\overline{d}}^{-1} \cdot (\nabla_s \times \overline{H}_z) \right.$$
$$\left. - i\omega \overline{\overline{d}}^{-1} \cdot \overline{\overline{\epsilon}}_s \cdot \overline{\overline{d}}^{-1} (\nabla \times \overline{E}_z) \right] \tag{8.3.66b}$$

after considerable algebraic manipulations, the wave equations for the longitudinal field components are determined to be

$$\left[\nabla_s^2 + \frac{\epsilon'_z}{\epsilon'} k^2 e \right] E_z = i\omega \mu' h_g H_z \tag{8.3.67a}$$

$$\left[\nabla_s^2 + k^2 h \right] H_z = -i\omega \epsilon'_z e_g E_z \tag{8.3.67b}$$

where

$$e = \frac{1}{b} \left[b^2 - b_g^2 + \frac{(bd - b_g d_g)^2}{d_g^2 - k^2 ab} \right] \tag{8.3.68a}$$

$$h = \frac{1}{a} \left[a^2 - a_g^2 + \frac{(ad - a_g d_g)^2}{d_g^2 - k^2 ab} \right] \tag{8.3.68b}$$

$$e_g = \frac{1}{a} \left[ab_g - a_g d - \frac{(ad - a_g d_g)(dd_g - kab_g)}{d_g^2 - k^2 ab} \right] \qquad (8.3.68c)$$

$$h_g = \frac{1}{b} \left[bb_g - b_g d - \frac{(bd - b_g d_g)(dd_g - ka_g b)}{d_g^2 - k^2 ab} \right] \qquad (8.3.68d)$$

The two equations in (8.3.67) for E_z and H_z are coupled. Thus the guided wave modes are hybrid because the wave equations are coupled. In the stationary case when $\beta = 0$, the wave equations are decoupled and the hybrid modes are consequences of boundary conditions.

Obtaining solutions to the coupled equations in (8.3.67) can be facilitated by transforming them into decoupled homogeneous Helmholtz equations. We define

$$\psi_j = E_z - i\alpha_j H_z \qquad j = 1, \ 2 \qquad (8.3.69)$$

then multiply (8.3.67b) by $i\alpha_j$, and subtract the result from (8.3.67a). Using (8.3.69) to eliminate E_z and requiring that the coefficient for H_z be zero, we obtain the following second-order equation for α_j:

$$\omega \epsilon_z e_j \alpha_j^2 - k^2 \left[h - \frac{\epsilon_z'}{\epsilon'} e \right] \alpha_j - \omega \mu h_g = 0 \qquad (8.3.70)$$

The two roots for α_j from (8.3.70) are the values for α_1 and α_2. With (8.3.70) satisfied, (8.3.67a) and (8.3.67b) combine to yield a single second-order, two-dimensional, scalar, homogeneous Helmholtz equation:

$$\nabla_s^2 \psi_j + q_j^2 \psi_j = 0 \qquad (8.3.71)$$

where

$$\begin{aligned} q_j &= \frac{\epsilon_z'}{\epsilon'} k^2 e + \alpha_j \omega \epsilon_z' e_g \\ &= k^2 h + \frac{1}{\alpha_j} \omega \mu h_g \end{aligned} \qquad (8.3.72)$$

For waveguides of conventional cross section (rectangular or circular), ψ_j can be determined from (8.3.71) in an appropriate coordinate system. With ψ_1 and ψ_2 known, we have from (8.3.69),

$$E_z = \frac{1}{\alpha_1 - \alpha_2} (\alpha_2 \psi_1 - \alpha_1 \psi_2) \qquad (8.3.73a)$$

$$H_z = -\frac{1}{\alpha_1 - \alpha_2} (\psi_1 - \psi_2) \qquad (8.3.73b)$$

The transverse field components can then be derived from (8.3.66) and be made to satisfy the boundary conditions. It is obvious that for guided waves in a moving gyrotropic medium the modes are hybrid. Even when the gyrotropic medium is stationary, the two wave equations for E_z and H_z are still coupled and the modes are hybrid. The two wave equations will be decoupled if the medium is uniaxial, regardless of whether it is stationary or in motion, for then $\epsilon_g = 0$ and all parameters with subscript g will vanish.

Problems

P8.3.1
(a) Determine the constitutive relations for a moving biisotropic medium which has the constitutive relations

$$\begin{bmatrix} cD' \\ H' \end{bmatrix} = \begin{bmatrix} p'\overline{\overline{I}} & \ell'\overline{\overline{I}} \\ -\ell'\overline{\overline{I}} & q'\overline{\overline{I}} \end{bmatrix} \begin{bmatrix} \overline{E}' \\ c\overline{B}' \end{bmatrix}.$$

in the rest frame of reference.
(b) Find the constitutive relations a biaxial medium moving along one of its principal axes.

8.4   Maxwell Equations in Tensor Form

In tensor notation, Maxwell equations read as

$$F_{\alpha\beta,\gamma} + F_{\beta\gamma,\alpha} + F_{\gamma\alpha,\beta} = 0 \qquad (8.4.1a)$$

$$G^{\alpha\mu}_{,\alpha} = J^{\mu} \qquad (8.4.1b)$$

We summarize the rules for using the indices associated with the tensor notation as follows:

(i) When an index is denoted by a Greek letter, it ranges from 0 to 3. When an index is denoted by a Roman letter, it ranges from 1 to 3.

(ii) When the index of a tensor is raised or lowered, the zeroth component of the vector changes sign, while the other components remain unchanged.

(iii) When an index is repeated on the same side of an equation, a summation over the index is implied. Summation is always carried out over a contravariant index and its corresponding covariant index.

(iv) Free (nonrepeated) indices on one side of an equation must be balanced by the same indices on the other side of the equation.

(v) Contravariant components of a tensor are denoted by superscripts; covariant components, by subscripts.

The electromagnetic field tensor $F_{\alpha\beta}$ and an excitation tensor $G^{\mu\nu}$ are defined in terms of matrix representation as follows:

$$F_{\mu\nu} = \begin{bmatrix} 0 & E_x & E_y & E_z \\ -E_x & 0 & -cB_z & cB_y \\ -E_y & cB_z & 0 & -cB_x \\ -E_z & -cB_y & cB_x & 0 \end{bmatrix} \qquad (8.4.2)$$

$$G^{\mu\nu} = \begin{bmatrix} 0 & -cD_x & -cD_y & -cD_z \\ cD_x & 0 & -H_z & H_y \\ cD_y & H_z & 0 & -H_x \\ cD_z & -H_y & H_x & 0 \end{bmatrix} \qquad (8.4.3)$$

The three-dimensional field vectors are related to the field tensor

and the excitation tensor in the following manner:

$$E_i = F_{0i}$$

$$cB_i = -\frac{1}{2}\epsilon_{ijk}F_{jk}$$

$$cD_i = -G^{0i}$$

$$H_i = -\frac{1}{2}\epsilon_{ijk}G^{jk}$$

We now demonstrate that (8.4.1) is equivalent to the full set of the Maxwell equations. If none of the three indices α, β, γ in (8.4.1a) is zero, we find Gauss' law of magnetism:

$$\nabla \cdot \overline{B} = 0$$

If one of α, β, γ is zero, (8.4.1a) gives Faraday's law:

$$\nabla \times \overline{E} + \frac{\partial \overline{B}}{\partial t} = 0$$

If $\mu = 0$ in (8.4.1b), we obtain Gauss' law of electricity:

$$\nabla \cdot \overline{D} = \rho$$

For $\mu \neq 0$, (8.4.1b) gives

$$\nabla \times \overline{H} - \frac{\partial \overline{D}}{\partial t} = \overline{J}$$

which is Ampère's law with the Maxwell's displacement current term $\partial \overline{D}/\partial t$.

The charge current conservation law states that

$$J^\alpha{}_{,\alpha} = 0 \tag{8.4.4}$$

The charge current density is

$$J^\alpha = (c\rho, \overline{J}) \tag{8.4.5}$$

The space-time derivative of J^α

$$J^\alpha{}_{,\alpha} = \frac{\partial \rho}{\partial t} + \nabla \cdot \overline{J} \tag{8.4.6}$$

becomes a scalar.

The conventional exercise of expressing field vectors in terms of vector and scalar potentials is observed from (8.4.1a). It is quite easy to show that (8.4.1a) is satisfied if

$$F_{\alpha\beta} = A_{\alpha,\beta} - A_{\beta,\alpha} \tag{8.4.7}$$

where A_α is a covariant four-vector, its zeroth contravariant compo-
nent is the scalar potential ϕ, and its space components are the vector
potential $\overline{A}$ times c:

$$A_\alpha = \begin{bmatrix} -\phi \\ c\overline{A} \end{bmatrix}, \qquad A^\alpha = \begin{bmatrix} \phi \\ c\overline{A} \end{bmatrix} \tag{8.4.8}$$

Writing (8.4.7) in three-dimensional notation, we have the familiar
expressions

$$\overline{E} = -\frac{\partial \overline{A}}{\partial t} - \nabla \phi$$
$$\overline{B} = \nabla \times \overline{A}$$

If we make a gauge transformation from A_α to A'_α so that

$$A_\alpha = A'_\alpha + \psi_{,\alpha} \tag{8.4.9}$$

where ψ is any scalar function of space-time by introducing (8.4.9) in
(8.4.1a), we have

$$F_{\alpha\beta} = A_{\alpha,\beta} - A_{\beta,\alpha} = A'_{\alpha,\beta} - A'_{\beta,\alpha} \tag{8.4.10}$$

This shows that both A_α and A'_α give rise to the same field tensor.
This arbitrariness is fixed by the gauge condition. The Lorenz gauge
is

$$A^\mu_{,\mu} = 0 \tag{8.4.11}$$

which takes the same form as the continuity equation for charge current
densities. Unlike the Coulomb gauge, the Lorenz gauge is relativisti-
cally covariant.

A. Contravariant and Covariant Vectors

One can imagine a four-dimensional (4D) space composed of coordi-
nates formed by time and three-dimensional space. Space-time coor-
dinates of a physical event possess properties of a vector in 4D space.
Let us denote the four components of an event by

$$x^0 = ct, \quad x^1 = x, \quad x^2 = y, \quad x^3 = z, \tag{8.4.12}$$

where we use the superscript 0 to denote the time component, and
1, 2, 3 to denote the space components. A popular convention in spe-
cial relativity is to write the time component with the subscript 4 and

designate it as imaginary. This should be carefully distinguished from the imaginary notations used in quantum theory and in wave theory. The notation that we use does not require an imaginary signature, but we must distinguish between superscripts and subscripts. This notation is readily generalized when general relativity is considered.

The transformation of the space-time coordinate vector from one observer to another is given by the Lorentz transformations. Under the Lorentz transformation,

$$x^2 + y^2 + z^2 - c^2t^2 = x'^2 + y'^2 + z'^2 - c^2t'^2 \tag{8.4.13}$$

is an invariant quantity independent of velocity. The square root of (8.4.13) expresses the magnitude of a 4D vector and in effect defines the transformation. As numerical values of other physical quantities change from one frame to another, this number stays unchanged in all frames. We note that in 4D space the magnitude of a vector can now be imaginary as well as real. A 4D vector is called a *spacelike* vector, a *null* vector, or a *timelike* vector, according to whether its magnitude is real, zero, or imaginary, respectively. The space-time coordinates of two physical events (ct_1, x_1, y_1, z_1) and (ct_2, x_2, y_2, z_2) form a four-vector with magnitude squared

$$(X_1 - X_2)^2 = -c^2(t_1 - t_2)^2 + (x_1 - x_2)^2 + (y_1 - y_2)^2 + (z_1 - z_2)^2$$

which is a Lorentz invariant. When the vector is timelike, $(X_1 - X_2)^2$ is negative. We can always find a moving observer such that, in his rest frame, the two events occur at the same location but at different times. He therefore observes the two events in person at times t'_1 and t'_2 :

$$-c(t'_1 - t'_2)^2 = (X_1 - X_2)^2$$

When the vector is a null vector, $|r_1 - r_2|^2 - c^2(t_1 - t_2)^2 = 0$ and an observer has to move at velocity c in order to see the two events in person. When the vector is spacelike, there exists an observer in whose frame the two events occur at different locations but simultaneously. The 4D space with coordinates governed by the Lorentz transformation laws is called *Minkowski space.*

To visualize the fourth dimension, imagine that this 4D space is spanned by four unit base vectors,

$$\hat{e}_\alpha = (\hat{e}_0, \hat{e}_1, \hat{e}_2, \hat{e}_3) \tag{8.4.14}$$

Any 4D vector X can thus be expressed in terms of $\hat{e}_\alpha$:

$$X = x^\alpha \hat{e}_\alpha = x^0 \hat{e}_0 + x^1 \hat{e}_1 + x^2 \hat{e}_2 + x^3 \hat{e}_3 \qquad (8.4.15)$$

In (8.4.15) we use the Einstein summation convention: the repeated Greek index α implies summation from 0 to 3. We shall use Greek letters to indicate 0 to 3, and Roman letters to denote 1 to 3. The square of the length of X is defined as the scalar product of X with itself:

$$X^2 = \hat{e}_\alpha \cdot \hat{e}_\beta \, x^\alpha x^\beta \qquad (8.4.16)$$

In view of (8.4.13),

$$X^2 = x^2 + y^2 + z^2 - c^2 t^2 \qquad (8.4.17)$$

Thus we must have

$$\hat{e}_\alpha \cdot \hat{e}_\beta = 0 \qquad \text{for} \quad \alpha \neq \beta \qquad (8.4.18a)$$
$$\hat{e}_0 \cdot \hat{e}_0 = -1 \qquad (8.4.18b)$$
$$\hat{e}_1 \cdot \hat{e}_1 = \hat{e}_2 \cdot \hat{e}_2 = \hat{e}_3 \cdot \hat{e}_3 = 1 \qquad (8.4.18c)$$

By (8.4.18a), all four base vectors are orthogonal to one another; by (8.4.18b), the three-space base vectors have unit magnitude as usual; and, by (8.4.18c), the zeroth (or fourth) base vector describing the fourth dimension possesses a magnitude squared of -1. It follows that the length of the zeroth base vector is imaginary. These four base vectors may be called *contravariant base vectors* which span a contravariant 4D space. A vector expressed in terms of the contravariant base vectors is called a *contravariant* vector.

We can define a set of *covariant base vectors* $\hat{e}^0$, $\hat{e}^1$, $\hat{e}^2$, and $\hat{e}^3$ such that

$$\hat{e}^0 = -\hat{e}_0 \qquad (8.4.19a)$$
$$\hat{e}^i = \hat{e}_i \qquad i = 1, 2, 3 \qquad (8.4.19b)$$

The product of $\hat{e}^0 \cdot \hat{e}_0 = -\hat{e}_0 \cdot \hat{e}_0 = 1$ in view of (8.4.18c). The vector $\hat{e}^0$ also has a magnitude squared of -1 as $\hat{e}^0 \cdot \hat{e}^0 = \hat{e}_0 \cdot \hat{e}_0$ by definitions of (8.4.19a) and (8.4.18c). These four base vectors $\hat{e}^\alpha$ may be called covariant base vectors which describe a covariant 4D space. A vector

expressed in terms of the covariant base vectors is called a *covariant* vector. We write

$$X = x_\alpha \hat{e}^\alpha \tag{8.4.20}$$

Components of X in the new base are now denoted as x_α, which, in view of (8.4.19), are related to x^α by

$$x^0 = -x_0 \tag{8.4.21a}$$
$$x^i = x_i \tag{8.4.21b}$$

The contravariant components of X are denoted by superscripts, and its covariant components by subscripts. We define

$$\eta_{\alpha\beta} = \hat{e}_\alpha \hat{e}_\beta = \begin{bmatrix} -1 & 0 & 0 & 0 \\ 0 & 1 & 0 & 0 \\ 0 & 0 & 1 & 0 \\ 0 & 0 & 0 & 1 \end{bmatrix} \tag{8.4.22a}$$

and

$$\eta^{\alpha\beta} = \hat{e}^\alpha \hat{e}^\beta = \begin{bmatrix} -1 & 0 & 0 & 0 \\ 0 & 1 & 0 & 0 \\ 0 & 0 & 1 & 0 \\ 0 & 0 & 0 & 1 \end{bmatrix} \tag{8.4.22b}$$

to express the transformation between the two sets of base vectors and the contravariant and covariant components of a vector:

$$\hat{e}^\alpha = \eta^{\alpha\beta}\hat{e}_\beta, \qquad \hat{e}_\alpha = \eta_{\alpha\beta}\hat{e}^\beta \tag{8.4.23a}$$
$$\hat{x}^\alpha = \eta^{\alpha\beta}\hat{x}_\beta, \qquad \hat{x}_\alpha = \eta_{\alpha\beta}\hat{x}^\beta \tag{8.4.23b}$$

Equation (8.4.23) is equivalent to (8.4.19) and (8.4.21). The scalar product of two vectors is defined to be the summation over the contravariant components of one vector and the corresponding covariant components of another. Thus the magnitude squared of x^α is

$$x^2 = x^\alpha x_\alpha = \eta_{\alpha\beta} x^\alpha x^\beta \tag{8.4.24}$$

in view of (8.4.23b). Notice that contravariant components of a vector are denoted by superscripts; covariant components, by subscripts. The notation for the base vectors is just the opposite; subscripts denote contravariant base vectors, and superscripts denote covariant base vectors.

We have discussed the transformation between contravariant and covariant representations. We shall now consider the transformation of a contravariant or a covariant vector from one frame of reference to another. When two frames are in relative uniform motion, the transformation is determined by the Lorentz transformation laws. We can express the space-time coordinates of a physical event by either a contravariant or a covariant vector. The transformation from an unprimed frame to a primed frame is

$$x'^{\alpha} = P^{\alpha}_{\beta} x^{\beta} \qquad (8.4.25a)$$

or

$$x'_{\alpha} = Q^{\beta}_{\alpha} x_{\beta} \qquad (8.4.25b)$$

We can view P^{α}_{β} as a matrix, denoted by $\overline{\overline{P}}$, operating on column matrix x^{β} and giving column matrix x'^{α}. A similar view is applied to Q^{β}_{α}. In view of (8.2.1), the transformation matrices $\overline{\overline{P}}$ and $\overline{\overline{Q}}$ are as follows:

$$\overline{\overline{P}} = \begin{bmatrix} \gamma & -\gamma\beta_x & -\gamma\beta_y & -\gamma\beta_z \\ -\gamma\beta_x & 1+(\gamma-1)\beta_x^2/\beta^2 & (\gamma-1)\beta_x\beta_y/\beta^2 & (\gamma-1)\beta_x\beta_z/\beta^2 \\ -\gamma\beta_y & (\gamma-1)\beta_y\beta_x/\beta^2 & 1+(\gamma-1)\beta_y^2/\beta^2 & (\gamma-1)\beta_y\beta_z/\beta^2 \\ -\gamma\beta_z & (\gamma-1)\beta_z\beta_x/\beta^2 & (\gamma-1)\beta_z\beta_y/\beta^2 & 1+(\gamma-1)\beta_z^2/\beta^2 \end{bmatrix} \qquad (8.4.26a)$$

$$\overline{\overline{Q}} = \begin{bmatrix} \gamma & \gamma\beta_x & \gamma\beta_y & \gamma\beta_z \\ \gamma\beta_x & 1+(\gamma-1)\beta_x^2/\beta^2 & (\gamma-1)\beta_x\beta_y/\beta^2 & (\gamma-1)\beta_x\beta_z/\beta^2 \\ \gamma\beta_y & (\gamma-1)\beta_y\beta_x/\beta^2 & 1+(\gamma-1)\beta_y^2/\beta^2 & (\gamma-1)\beta_y\beta_z/\beta^2 \\ \gamma\beta_z & (\gamma-1)\beta_z\beta_x/\beta^2 & (\gamma-1)\beta_z\beta_y/\beta^2 & 1+(\gamma-1)\beta_z^2/\beta^2 \end{bmatrix} \qquad (8.4.26b)$$

A few properties of $\overline{\overline{P}}$ and $\overline{\overline{Q}}$ follow from (8.4.25). The magnitude squared of x^{α} is a Lorentz invariant. From

$$x'^{\mu} x'_{\mu} = P^{\mu}_{\alpha} Q^{\beta}_{\mu} x^{\alpha} x_{\beta}$$

we learn that

$$P^{\mu}_{\alpha} Q^{\beta}_{\mu} = \delta^{\beta}_{\alpha}$$

The summation is over μ. In matrix form, we have

$$\overline{\overline{P}}^{t} \cdot \overline{\overline{Q}} = \overline{\overline{I}}$$

where $\overline{\overline{I}}$ is the 4×4 unit matrix. Obviously, $\overline{\overline{P}}^t$ is the inverse of $\overline{\overline{Q}}$:

$$\overline{\overline{P}}^t = \overline{\overline{Q}}^{-1} \qquad\qquad (8.4.27a)$$

The inverse of $\overline{\overline{P}}$ is then the transpose of $\overline{\overline{Q}}$:

$$\overline{\overline{P}}^{-1} = \overline{\overline{Q}}^t \qquad\qquad (8.4.27b)$$

With these last two relations, the inverse transformation from primed to unprimed coordinates is as follows:

$$x^\alpha = Q^\alpha_\beta x'^\beta \qquad\qquad (8.4.28a)$$

$$x_\alpha = P^\beta_\alpha x'_\beta \qquad\qquad (8.4.28b)$$

When (8.4.28) is compared with (8.4.25), it can be verified that the two are equivalent by using (8.4.27).

Conventionally, a contravariant vector is defined as one that transforms with the transformation matrix $\overline{\overline{P}}$ as (8.4.25a); a covariant vector transforms with the matrix $\overline{\overline{Q}}$ as (8.4.25b). Extending the definition, an nth-rank contravariant tensor transforms from one Lorentz frame to another by using the transformation matrix $\overline{\overline{P}}$ n times. An nth-rank covariant tensor transforms from one Lorentz frame to another by using $\overline{\overline{Q}}$ n times. The scalar product of an nth-rank contravariant tensor with an nth-rank covariant tensor is Lorentz-invariant. For instance, the space-time derivatives $(\partial/\partial ct, \nabla)$ form a covariant four-vector because, according to (8.4.25), the transformation is like (8.4.25b) and (8.4.28b). If we denote the derivatives of a scalar function $\chi(x)$ by

$$\chi_{,\alpha} = (\partial\chi/\partial ct, \nabla\chi)$$

we find

$$\chi'_{,\alpha} = Q^\beta_\alpha \chi_{,\beta}$$

The charge current density, written as

$$J^\alpha = (c\rho, \overline{J}) \qquad\qquad (8.4.29)$$

is seen to be a contravariant vector because it transforms as (8.4.25a) and (8.4.28a). The space-time derivative of J^α

$$J^\alpha{}_{,\alpha} = \frac{\partial\rho}{\partial t} + \nabla \cdot \overline{J} \qquad\qquad (8.4.30)$$

becomes a scalar. The charge current conservation law states that

$$J^{\alpha}{}_{,\alpha} = 0 \qquad\qquad (8.4.31)$$

From (8.4.22), we can show that $\eta_{\alpha\beta}$ is a second-rank covariant tensor and $\eta^{\alpha\beta}$ is a second-rank contravariant tensor. They are known as metric tensors.

The transformation matrices P^{α}_{β} and Q^{β}_{α} are pure Lorentz transformations. A pure Lorentz transformation satisfies two assumptions: (i) the coordinate axes of S and S' are parallel, and (ii) the origins of the two coordinate systems coincide at $t = 0$. A Lorentz transformation (LT) that satisfies (ii) but does not satisfy (i) is called a homogeneous LT (HLT). A HLT is a combination of a pure LT plus a spatial rotation. Mathematically, the whole class of HLTs satisfies the postulates of a group and is called an HLT group. It is important to note that the group multiplication of two pure LTs results not in a pure LT, but in a pure LT plus a spatial rotation. The matrices P^{α}_{β} and Q^{β}_{α} in (8.4.25) can be used to represent the HLT group. Although as represented in (8.4.26) they appear to be symmetrical, symmetry is not a general property of all elements in the HLT group. For instance, the transformation matrix for a spatial rotation is not symmetrical. When assumption (ii) is violated, the LT is inhomogeneous. An inhomogeneous LT can be made homogeneous by re-choosing the time-space origins. The whole class of inhomogeneous LTs also forms a group called an inhomogeneous Lorentz group or simply the Poincaré group. The HLT group is a subgroup of the Poincaré group because the identity element is there. Any element in a Poincaré group can be joined to the identity element continuously by successive LTs. For completeness, we mention the LTs in which a spatial or space-time inversion is involved. This group of LTs is called an improper Lorentz group in which an element cannot continuously join to the identity. In our treatment, we confine ourselves to pure LTs in the HLT group.

B. Field Tensor and Excitation Tensor

To write the Maxwell equations in compact tensor form, we define a field tensor $F_{\alpha\beta}$ and an excitation tensor $G_{\alpha\beta}$. Explicitly in terms of

matrix representation, we have

$$F_{\mu\nu} = \begin{bmatrix} 0 & E_x & E_y & E_z \\ -E_x & 0 & -cB_z & cB_y \\ -E_y & cB_z & 0 & -cB_x \\ -E_z & -cB_y & cB_x & 0 \end{bmatrix} \tag{8.4.32}$$

$$G_{\mu\nu} = \begin{bmatrix} 0 & cD_x & cD_y & cD_z \\ -cD_x & 0 & -H_z & H_y \\ -cD_y & H_z & 0 & -H_x \\ -cD_z & -H_y & H_x & 0 \end{bmatrix} \tag{8.4.33}$$

The contravariant tensors corresponding to $F_{\alpha\beta}$ and $G_{\alpha\beta}$ can be obtained by using the matrix tensor $\eta^{\alpha\beta}$. For instance,

$$G^{\mu\nu} = \eta^{\mu\alpha}\eta^{\nu\beta}G_{\alpha\beta} = \begin{bmatrix} 0 & -cD_x & -cD_y & -cD_z \\ cD_x & 0 & -H_z & H_y \\ cD_y & H_z & 0 & -H_x \\ cD_z & -H_y & H_x & 0 \end{bmatrix} \tag{8.4.34}$$

The three-dimensional field vectors are related to the field tensor and the excitation tensor in the following manner:

$$E_i = F_{0i} = -F^{0i} \tag{8.4.35a}$$

$$cB_i = -\frac{1}{2}\epsilon_{ijk}F_{jk} = -\frac{1}{2}\epsilon_{ijk}F^{jk} \tag{8.4.35b}$$

$$cD_i = G_{0i} = -G^{0i} \tag{8.4.35c}$$

$$H_i = -\frac{1}{2}\epsilon_{ijk}G_{jk} = -\frac{1}{2}\epsilon_{ijk}G^{jk} \tag{8.4.35d}$$

This result can be obtained by the convention of raising and lowering indices. The contravariant components G^{0i} are negatives of their corresponding covariant components because an index 0 is raised.

Both the field and excitation tensors are skew-symmetric:

$$F_{\alpha\beta} = -F_{\beta\alpha}$$
$$G_{\alpha\beta} = -G_{\beta\alpha}$$

They are second-rank covariant tensors and transform as

$$F'_{\mu\nu} = Q_\mu^\alpha Q_\nu^\beta F_{\alpha\beta} \tag{8.4.36a}$$

$$G'_{\mu\nu} = Q_\mu^\alpha Q_\nu^\beta G_{\alpha\beta} \tag{8.4.36b}$$

Using matrix notation, we write

$$\overline{\overline{F}}' = \overline{\overline{Q}} \cdot \overline{\overline{F}} \cdot \overline{\overline{Q}}^t$$

$$\overline{\overline{G}}' = \overline{\overline{Q}} \cdot \overline{\overline{G}} \cdot \overline{\overline{Q}}^t$$

Written in explicit matrix form for an observer S' moving with velocity $\overline{\beta} = \hat{z}\beta$ along the $\hat{z}$ direction with respect to the observer S, we find

$$
\begin{bmatrix}
0 & E'_x & E'_y & E'_z \\
-E'_x & 0 & -cB'_z & cB'_y \\
-E'_y & cB'_z & 0 & -cB'_x \\
-E'_z & -cB'_y & cB'_x & 0
\end{bmatrix}
= \overline{\overline{Q}} \cdot \overline{\overline{F}} \cdot \overline{\overline{Q}}^t
$$

$$
=
\begin{bmatrix}
\gamma & 0 & 0 & \beta\gamma \\
0 & 1 & 0 & 0 \\
0 & 0 & 1 & 0 \\
\beta\gamma & 0 & 0 & \gamma
\end{bmatrix}
\begin{bmatrix}
0 & E_x & E_y & E_z \\
-E_x & 0 & -cB_z & cB_y \\
-E_y & cB_z & 0 & -cB_x \\
-E_z & -cB_y & cB_x & 0
\end{bmatrix}
\begin{bmatrix}
\gamma & 0 & 0 & \beta\gamma \\
0 & 1 & 0 & 0 \\
0 & 0 & 1 & 0 \\
\beta\gamma & 0 & 0 & \gamma
\end{bmatrix}
$$

$$
=
\begin{bmatrix}
0 & \gamma(E_x - \beta c B_y) & \gamma(E_y + \beta c B_x) & E_z \\
-\gamma(E_x - \beta c B_y) & 0 & -cB_z & \gamma(cB_y - \beta E_x) \\
-\gamma(E_y + \beta c B_x) & cB_z & 0 & -\gamma(cB_x + \beta E_y) \\
-E_z & -\gamma(cB_y - \beta E_x) & \gamma(cB_x + \beta E_y) & 0
\end{bmatrix}
$$

$$\text{(8.4.37)}$$

The result of this transformation is seen to be identical to the Lorentz transformation which is obtained with three-dimensional notation.

EXAMPLE 8.4.1   Lorentz invariants of the field tensor.
    The covariant field tensor is

$$
F_{\alpha\beta} =
\begin{bmatrix}
0 & E_x & E_y & E_z \\
-E_x & 0 & -cB_z & cB_y \\
-E_y & cB_z & 0 & -cB_x \\
-E_z & -cB_y & cB_x & 0
\end{bmatrix}
\tag{E8.4.1.1}
$$

The contravariant field tensor is

$$F^{\alpha\beta} = \eta^{\alpha\mu}\eta^{\beta\nu}F_{\mu\nu} = \begin{bmatrix} 0 & -E_x & -E_y & -E_z \\ E_x & 0 & -cB_z & cB_y \\ E_y & cB_z & 0 & -cB_x \\ E_z & -cB_y & cB_x & 0 \end{bmatrix} \qquad \text{(E8.4.1.2)}$$

A contravariant dual tensor is defined as

$$F^{*\alpha\beta} = \frac{1}{2}\eta^{\alpha\beta\rho\sigma}F_{\rho\sigma} = \begin{bmatrix} 0 & cB_x & cB_y & cB_z \\ -cB_x & 0 & -E_z & E_y \\ -cB_y & E_z & 0 & -E_x \\ -cB_z & -E_y & E_x & 0 \end{bmatrix} \qquad \text{(E8.4.1.3)}$$

where $\eta^{\alpha\beta\rho\sigma} = 1$ when α, β, ρ, σ is even permutation of 0, 1, 2, 3, $\eta^{\alpha\beta\rho\sigma} = -1$ when α, β, ρ, σ is odd permutation of 0, 1, 2, 3, and $\eta^{\alpha\beta\rho\sigma} = 0$ when any two of α, β, ρ, σ is equal. The covariant dual tensor is seen to be obtained from $F_{\alpha\beta}$ by replacing $\overline{E}$ with $c\overline{B}$ and $c\overline{B}$ with $-\overline{E}$.

$$F^*_{\mu\nu} = \begin{bmatrix} 0 & cB_x & cB_y & cB_z \\ -cB_x & 0 & E_z & -E_y \\ -cB_y & -E_z & 0 & E_x \\ -cB_z & E_y & -E_x & 0 \end{bmatrix} \qquad \text{(E8.4.1.4)}$$

There are two Lorentz invariants of the second rank tensor $F_{\alpha\beta}$. They are determined from

$$F_{\alpha\beta}F^{\alpha\beta} = 2(|c\overline{B}|^2 - |\overline{E}|^2)$$

$$F^*_{\alpha\beta}F^{\alpha\beta} = -4c\overline{B}\cdot\overline{E}$$

The electromagnetic fields have been classified according to the above two Lorentz invariants.

<div align="right">— END OF EXAMPLE 8.4.1 —</div>

EXAMPLE 8.4.2   Eigenvectors and eigenvalues of the field tensor $F_{\alpha\beta}$.
Write

$$F_{\alpha\beta}\,\xi^\beta = \lambda\,\eta_{\alpha\beta}\,\xi^\beta$$

in matrix form, we have

$$\begin{bmatrix} \lambda & E_1 & E_2 & E_3 \\ -E_1 & -\lambda & -cB_3 & cB_2 \\ -E_2 & cB_3 & -\lambda & -cB_1 \\ -E_3 & -cB_2 & cB_1 & -\lambda \end{bmatrix} \cdot \begin{bmatrix} \xi^0 \\ \xi^1 \\ \xi^2 \\ \xi^3 \end{bmatrix} = 0 \qquad \text{(E8.4.2.1)}$$

Write out the linear equations in (E8.4.2.1) explicitly, we have

$$\lambda \xi^0 + E_1 \xi^1 + E_2 \xi^2 + E_3 \xi^3 = 0$$
$$-E_1 \xi^0 - \lambda \xi^1 - cB_3 \xi^2 + cB_2 \xi^3 = 0$$
$$-E_2 \xi^0 + cB_3 \xi^1 - \lambda \xi^2 - cB_1 \xi^3 = 0$$
$$-E_3 \xi^0 - cB_2 \xi^1 + cB_1 \xi^2 - \lambda \xi^3 = 0$$

The determinant equal to zero yields

$$\lambda \Delta_0 + E_1 \Delta_1 + E_2 \Delta_2 + E_3 \Delta_3 = 0$$

where

$$\Delta_0 = \begin{vmatrix} -\lambda & -cB_3 & cB_2 \\ cB_3 & -\lambda & -cB_1 \\ -cB_2 & cB_1 & -\lambda \end{vmatrix} = -\lambda(\lambda^2 + |c\overline{B}|^2)$$

$$\Delta_1 = -\begin{vmatrix} -E_1 & -cB_3 & cB_2 \\ -E_2 & -\lambda & -cB_1 \\ -E_3 & cB_1 & -\lambda \end{vmatrix} = \lambda^2 E_1 - \lambda(E_2 cB_3 - E_3 cB_2) + (\overline{E} \cdot c\overline{B})cB_1$$

$$\Delta_2 = \begin{vmatrix} -E_1 & -\lambda & -cB_2 \\ -E_2 & -cB_3 & -cB_1 \\ -E_3 & -cB_2 & -\lambda \end{vmatrix} = \lambda^2 E_2 - \lambda(E_3 cB_1 - E_1 cB_3) + (\overline{E} \cdot c\overline{B})cB_2$$

$$\Delta_3 = -\begin{vmatrix} -E_1 & -\lambda & -cB_3 \\ -E_2 & cB_3 & -\lambda \\ -E_3 & -cB_2 & cB_1 \end{vmatrix} = \lambda^2 E_3 - \lambda(E_1 cB_2 - E_2 cB_1) + (\overline{E} \cdot c\overline{B})cB_3$$

which gives an equation for eigenvalues λ

$$\lambda^4 - \lambda^2(E^2 - c^2 B^2) - c^2(\overline{E} \cdot \overline{B})^2 = 0$$

Thus

$$\lambda = \pm \frac{1}{\sqrt{2}} \sqrt{\pm \sqrt{(E^2 - c^2 B^2)^2 + 4c^2(\overline{E} \cdot \overline{B})^2} + (E^2 - c^2 B^2)}$$

$$= \pm \frac{1}{2} \sqrt{\pm \sqrt{(F_{\alpha\beta} F^{\alpha\beta})^2 + (F^*_{\alpha\beta} F^{\alpha\beta})^2} - F_{\alpha\beta} F^{\alpha\beta}}$$

$$= \lambda_R, \lambda_I$$

$$\lambda_R = \pm \frac{1}{\sqrt{2}} \sqrt{\sqrt{(E^2 - c^2 B^2)^2 + 4c^2(\overline{E} \cdot \overline{B})^2} + (E^2 - c^2 B^2)}$$

$$\lambda_I = \pm i \frac{1}{\sqrt{2}} \sqrt{\sqrt{(E^2 - c^2 B^2)^2 + 4c^2(\overline{E} \cdot \overline{B})^2} - (E^2 - c^2 B^2)}$$

The components of the eigenvectors can be written as

$$\xi^1 = \frac{\Delta_1}{\Delta_0}\xi^0; \quad \xi^2 = \frac{\Delta_2}{\Delta_0}\xi^0; \quad \xi^3 = \frac{\Delta_3}{\Delta_0}\xi^0$$

We see that for imaginary λ, ξ^μ is complex; for real λ, ξ^μ is real; and for a complex conjugated imaginary λ_I pair, the eigenvectors are also a complex conjugate pair. It can also be shown that for $\lambda \neq 0$, $-(\xi^0)^2 + (\xi^1)^2 + (\xi^2)^2 + (\xi^3)^2 = 0$ and thus the eigenvectors are null vectors.

— END OF EXAMPLE 8.4.2 —

EXAMPLE 8.4.3

We now classify the electromagnetic fields by their eigenvalues and eigenvectors.

(1) Wrench field: $\lambda \neq 0$

(a) $E^2 - c^2 B^2 \neq 0$, $\overline{E} \cdot c\overline{B} \neq 0$; $\lambda_R \neq 0$, $\lambda_I \neq 0$.

$E^2 - c^2 B^2 = 0$, $\overline{E} \cdot c\overline{B} \neq 0$; $\lambda_R = \lambda_I = (\overline{E} \cdot c\overline{B})^{1/4}$.

(b) $E^2 - c^2 B^2 > 0$, $\overline{E} \cdot c\overline{B} = 0$; $\lambda_R \neq 0$, $\lambda_I = 0$.

(c) $E^2 - c^2 B^2 < 0$, $\overline{E} \cdot c\overline{B} = 0$; $\lambda_R = 0$, $\lambda_I \neq 0$.

For $\overline{E} \cdot \overline{B} \neq 0$ and $|\overline{E}| \neq |c\overline{B}|$. If $|\overline{E}| > |c\overline{B}|$, we let $\overline{E} = \hat{x}E_1$ and $c\overline{B} = \hat{x}cB_1 + \hat{y}cB_2$. Eq. (E8.4.2.1) becomes

$$\begin{bmatrix} \lambda & E_1 & 0 & 0 \\ -E_1 & -\lambda & 0 & cB_2 \\ 0 & 0 & -\lambda & -cB_1 \\ 0 & -cB_2 & cB_1 & -\lambda \end{bmatrix} \cdot \begin{bmatrix} \xi^0 \\ \xi^1 \\ \xi^2 \\ \xi^3 \end{bmatrix} = 0 \qquad \text{(E8.4.3.1)}$$

From (8.4.37), we find that for an observer S moving with velocity $\overline{v} = \hat{z}cB_2/E_1$, the magnetic field in y direction is zero. We call this observer a canonical observer and

$$F_{\mu\nu} = \begin{bmatrix} 0 & E_1 & 0 & 0 \\ -E_1 & 0 & 0 & 0 \\ 0 & 0 & 0 & -cB_1 \\ 0 & 0 & cB_1 & 0 \end{bmatrix} \qquad \text{(E8.4.3.2)}$$

the canonical form of the field tensor. All observers moving along the $\hat{x}$ direction of coordinate system (ct, x, y, z), in which $\overline{E} = \hat{x}E$ and $\overline{B} = \hat{x}B_1$, are canonical observers.

The eigenequation takes the form

$$
\begin{bmatrix}
\lambda & E_1 & 0 & 0 \\
-E_1 & -\lambda & 0 & 0 \\
0 & 0 & -\lambda & -cB_1 \\
0 & 0 & cB_1 & -\lambda
\end{bmatrix}
\cdot
\begin{bmatrix}
\xi^0 \\
\xi^1 \\
\xi^2 \\
\xi^3
\end{bmatrix}
= 0
\qquad (E8.4.3.3)
$$

The eigenvectors and eigenvalues are determined from $\lambda = \pm E_1$, $\xi^1 = \pm \xi^0$ and $\lambda = \pm icB_1$, $\xi^3 = \mp i\xi^2$. This is invariant for all observers moving along the $\hat{x}$ direction.

For $\overline{E} \cdot \overline{B} = 0$ and $\left| \overline{E} \right| > \left| c\overline{B} \right|$, $\lambda = \pm\sqrt{E^2 - c^2B^2}$. Let $\overline{E} = \hat{x}E$ and $c\overline{B} = \hat{y}cB$. Eq. (E8.4.3.3) becomes

$$
\begin{bmatrix}
-\lambda & E & 0 & 0 \\
-E & \lambda & 0 & cB \\
0 & 0 & \lambda & 0 \\
0 & -cB & 0 & \lambda
\end{bmatrix}
\cdot
\begin{bmatrix}
\xi^0 \\
\xi^1 \\
\xi^2 \\
\xi^3
\end{bmatrix}
= 0
\qquad (E8.4.3.4)
$$

From (8.4.37), we find that for an observer S moving with velocity in the $\overline{v} = \hat{z}cB/E$, the magnetic field is zero. This yields the canonical form of the field tensor

$$
F_{\mu\nu} =
\begin{bmatrix}
0 & E & 0 & 0 \\
-E & 0 & 0 & 0 \\
0 & 0 & 0 & 0 \\
0 & 0 & 0 & 0
\end{bmatrix}
\qquad (E8.4.3.5)
$$

and the eigenequation becomes

$$
\begin{bmatrix}
-\lambda & E & 0 & 0 \\
-E & \lambda & 0 & 0 \\
0 & 0 & \lambda & 0 \\
0 & 0 & 0 & \lambda
\end{bmatrix}
\cdot
\begin{bmatrix}
\xi^0 \\
\xi^1 \\
\xi^2 \\
\xi^3
\end{bmatrix}
= 0
\qquad (E8.4.3.6)
$$

This gives $\xi^1 = \pm\xi^0$ and $\xi^1 = \xi^2 = 0$. All canonical observers moving along the $\hat{x}$ axis of this canonical system only observe an electric field.

(2) Wave field: $\lambda = 0$, $E^2 - c^2B^2 = 0$, $\overline{E} \cdot c\overline{B} = 0$.

(a) Free-space wave fields: $\overline{E} \cdot \overline{B} = 0$ and $\left| \overline{E} \right| = \left| c\overline{B} \right|$, $\lambda = 0$. Let $\overline{E} = \hat{x}E$ and $c\overline{B} = \hat{y}E$. The canonical form of the field tensor is

$$
F_{\mu\nu} =
\begin{bmatrix}
0 & E & 0 & 0 \\
-E & 0 & 0 & E \\
0 & 0 & 0 & 0 \\
0 & -E & 0 & 0
\end{bmatrix}
\qquad (E8.4.3.7)
$$

Eq. (E8.4.3.4) becomes

$$
\begin{bmatrix}
0 & E & 0 & 0 \\
-E & 0 & 0 & E \\
0 & 0 & 0 & 0 \\
0 & -E & 0 & 0
\end{bmatrix}
\cdot
\begin{bmatrix}
\xi^0 \\ \xi^1 \\ \xi^2 \\ \xi^3
\end{bmatrix}
= 0
\qquad \text{(E8.4.3.8)}
$$

We have the solution $\xi^0 = \xi^3$ and $\xi^1 = 0$ while ξ^2 is left arbitrary. This defines a two-dimensional subsurface containing the y-axis and the eigenvector $(\xi^0, 0, \xi^2, \xi^0)$. Kinematically, it corresponds to the motion, with the speed of light, of a linear element having the same direction as the magnetic field in the $\hat{y}$ direction.

— END OF EXAMPLE 8.4.3 —

EXERCISE 8.4.1
   For the free-space wave fields, if we let $\overline{E} = \hat{y}E$ and $c\overline{B} = -\hat{x}E$, the canonical form of the field tensor is

$$
F_{\mu\nu} =
\begin{bmatrix}
0 & 0 & E & 0 \\
0 & 0 & 0 & 0 \\
-E & 0 & 0 & E \\
0 & 0 & -E & 0
\end{bmatrix}
\qquad \text{(Ex8.4.1.1)}
$$

Eq. (E8.4.3.4) becomes

$$
\begin{bmatrix}
0 & 0 & E & 0 \\
0 & 0 & 0 & 0 \\
-E & 0 & 0 & E \\
0 & 0 & -E & 0
\end{bmatrix}
\cdot
\begin{bmatrix}
\xi^0 \\ \xi^1 \\ \xi^2 \\ \xi^3
\end{bmatrix}
= 0
\qquad \text{(Ex8.4.1.2)}
$$

We have the solution $\xi^0 = \xi^3$ and $\xi^2 = 0$ while ξ^1 is left arbitrary. This defines a two-dimensional subsurface containing the x-axis and the eigenvector $(\xi^0, \xi^1, 0, \xi^0)$. Kinematically, it corresponds to the motion, with the speed of light, of a linear element having the same direction as the magnetic field in the $\hat{x}$ direction.

— END OF EXERCISE 8.4.1 —

EXERCISE 8.4.2
   Consider the dual field tensor

$$
F^*_{\mu\nu} =
\begin{bmatrix}
0 & cB_x & cB_y & cB_z \\
-cB_x & 0 & E_z & -E_y \\
-cB_y & -E_z & 0 & E_x \\
-cB_z & E_y & -E_x & 0
\end{bmatrix}
\qquad \text{(Ex8.4.2.1)}
$$

For free space fields, $\overline{E} \cdot \overline{B} = 0$ and $\left| \overline{E} \right| = \left| c\overline{B} \right|$, $\lambda = 0$. Let $\overline{E} = \hat{x}E$ and $c\overline{B} = \hat{y}E$. The canonical form of the field tensor is

$$F^*_{\mu\nu} = \begin{bmatrix} 0 & 0 & E & 0 \\ 0 & 0 & 0 & 0 \\ -E & 0 & 0 & E \\ 0 & 0 & -E & 0 \end{bmatrix} \qquad \text{(Ex8.4.2.2)}$$

Eq. (E8.4.3.4) becomes

$$\begin{bmatrix} 0 & 0 & E & 0 \\ 0 & 0 & 0 & 0 \\ -E & 0 & 0 & E \\ 0 & 0 & -E & 0 \end{bmatrix} \cdot \begin{bmatrix} \xi^0 \\ \xi^1 \\ \xi^2 \\ \xi^3 \end{bmatrix} = 0 \qquad \text{(Ex8.4.2.3)}$$

We have the solution $\xi^0 = \xi^3$ and $\xi^2 = 0$ while ξ^1 is left arbitrary. This defines a two-dimensional subsurface containing the x-axis and the eigenvector $(\xi^0, \xi^1, 0, \xi^0)$. Kinematically, it corresponds to the motion, with the speed of light, of a linear element having the same direction as the electric field in the $\hat{x}$ direction.

<div align="right">— END OF EXERCISE 8.4.2 —</div>

EXAMPLE 8.4.4

Let the two real eigenvectors corresponding to the real eigenvalues be denoted by p^μ and q^μ, and the complex conjugated eigenvectors corresponding to the imaginary eigenvalues be denoted by m^μ and $\overline{m}^\mu$. The field tensor can be written as

$$F^{\mu\nu} = \lambda_R(p^\mu q^\nu - p^\nu q^\mu) + \lambda_I(m^\mu \overline{m}^\nu - m^\nu \overline{m}^\mu)$$
$$p^\mu p_\mu = q^\mu q_\mu = m^\mu m_\mu = \overline{m}^\mu \overline{m}_\mu = 0$$
$$p^\mu q_\mu = -m^\mu \overline{m}_\mu = 1$$
$$p^\mu m_\mu = p^\mu \overline{m}_\mu = q^\mu m_\mu = q^\mu \overline{m}_\mu = 0$$

for then

$$F^{\mu\nu} = -F^{\nu\mu}$$
$$\xi^\mu \xi_\mu = 0$$
$$F^{\mu\nu} p_\nu = \lambda_R p^\mu, \quad F^{\mu\nu} q_\nu = -\lambda_R q^\mu$$
$$F^{\mu\nu} m_\nu = i\lambda_I m^\mu \quad F^{\mu\nu} \overline{m}_\nu = -i\lambda_I \overline{m}^\mu$$

Now the subclasses of the wrench field tensor can be represented as:

(a) $\lambda_R \neq 0$, $\lambda_I \neq 0$, $F^{\mu\nu} = \lambda_R(p^\mu q^\nu - p^\nu q^\mu) + i\lambda_I(m^\mu \overline{m}^\nu - \overline{m}^\nu m^\mu)$

(b) $\lambda_R \neq 0$, $\lambda_I = 0$, $F^{\mu\nu} = \lambda_R(p^\mu q^\nu - p^\nu q^\mu)$

(c) $\lambda_R = 0$, $\lambda_I \neq 0$, $F^{\mu\nu} = i\lambda_I(m^\mu \overline{m}^\nu - \overline{m}^\nu m^\mu)$

With the canonical forms of the field tensor, the normalized eigenvectors take the following forms:

$$p^\mu = \begin{bmatrix} 1/\sqrt{2} \\ 1/\sqrt{2} \\ 0 \\ 0 \end{bmatrix} ; \quad q^\mu = \begin{bmatrix} 1/\sqrt{2} \\ -1/\sqrt{2} \\ 0 \\ 0 \end{bmatrix} ; \quad m^\mu = \begin{bmatrix} 0 \\ 0 \\ 1/\sqrt{2} \\ -i/\sqrt{2} \end{bmatrix} ; \quad \overline{m}^\mu = \begin{bmatrix} 0 \\ 0 \\ 1/\sqrt{2} \\ i/\sqrt{2} \end{bmatrix}$$

For the wave field, $F^{\mu\nu}$ is completely degenerated, since $\lambda_R = \lambda_I = 0$. With the eigenequation in (Ex8.4.2.3), we write in the canonical coordinate system the eigenvectors as follows:

$$p^\mu = \begin{bmatrix} 1/\sqrt{2} \\ 0 \\ 0 \\ 1/\sqrt{2} \end{bmatrix} ; \quad x^\mu = \begin{bmatrix} 0 \\ 1 \\ 0 \\ 0 \end{bmatrix}$$

The field tensor can be represented by

$$F^{\mu\nu} = A(p^\mu x^\nu - p^\nu x^\mu))$$
$$x^\mu x_\mu = 1$$

We see that the real null vector p^μ points into the future, and x is a space-like vector.

— END OF EXAMPLE 8.4.4 —

C. Constitutive Relations in Tensor Form

The constitutive relations in tensor notation provide a relation for the excitation tensor $G^{\alpha\beta}$ and the field tensor $F_{\alpha\beta}$. We write

$$G^{\alpha\beta} = \frac{1}{2}C^{\alpha\beta\rho\sigma}F_{\rho\sigma} \tag{8.4.38}$$

We call the fourth-rank tensor $C^{\alpha\beta\rho\sigma}$ the constitutive tensor. Because of the skew-symmetric properties of $F_{\rho\sigma}$ and $G^{\alpha\beta}$, we see that

$$C^{\alpha\beta\rho\sigma} = -C^{\beta\alpha\rho\sigma} = -C^{\alpha\beta\sigma\rho} = C^{\beta\alpha\sigma\rho} \tag{8.4.39}$$

The constitutive tensor is skew-symmetric with respect to the first pair, as well as the second pair, of indices. In general, a fourth-rank tensor in a four-dimensional space possesses 256 elements. Because of this skew

symmetry, the first pair of indices has six independent elements and so does the second pair, giving rise to a total of 36 independent elements. Thus the 6×6 constitutive matrix $\overline{\overline{C}}$ is a faithful representation of the constitutive tensor.

We shall establish relations between the tensor elements of $C^{\alpha\beta\rho\sigma}$ and the matrix elements of $\overline{\overline{C}}$ in (8.3.2) by making use of (8.4.32) – (8.4.35). It follows that $cD_i = -G^{0i} = -C^{0i0j}F_{0j} - \frac{1}{2}C^{0ilm}F_{lm} = -C^{0i0j}E_{0j} + \frac{1}{2}C^{0ilm}\epsilon_{jlm}cB_j = p_{ij}E_j + l_{ij}cB_j$ and $H_i = -\frac{1}{2}\epsilon_{ijk}G^{jk} = -\frac{1}{2}\epsilon_{ilk}C^{lk0j}F_{0j} - \frac{1}{4}\epsilon_{ijk}C^{jklm}F_{lm} = -\frac{1}{2}\epsilon_{ilk}C^{lk0j}E_j + \frac{1}{4}\epsilon_{ilk}C^{lkpq}\epsilon_{jpq}cB_j = m_{ij}E_j + q_{ij}cB_j$. We find

$$p_{ij} = -C^{0i0j} \tag{8.4.40a}$$

$$l_{ij} = \frac{1}{2}\epsilon_{jkl}C^{0ikl} \tag{8.4.40b}$$

$$m_{ij} = -\frac{1}{2}\epsilon_{ikl}C^{kl0j} \tag{8.4.40c}$$

$$q_{ij} = \frac{1}{4}\epsilon_{ilk}C^{lkpq}\epsilon_{jpq} \tag{8.4.40d}$$

Likewise, $G^{0i} = C^{0i0j}F_{0j} + \frac{1}{2}C^{0ipq}F_{pq} = -cD_i = -p_{ij}E_j - l_{ij}cB_j = -p_{ij}E_j + \frac{1}{2}l_{ij}\epsilon_{jpq}F_{pq}$ and $G^{kl} = C^{kl0j}F_{0j} + \frac{1}{2}C^{klpq}F_{pq} = -\epsilon_{ikl}H_i = -\epsilon_{ikl}m_{ij}E_j - \epsilon_{ikl}q_{ij}cB_j = -\epsilon_{ikl}m_{ij}F_{0j} + \frac{1}{2}\epsilon_{ikl}q_{ij}\epsilon_{jpq}F_{pq}$. We find

$$C^{0i0j} = -p_{ij} \tag{8.4.41a}$$

$$C^{0ipq} = l_{ij}\epsilon_{jpq} \tag{8.4.41c}$$

$$C^{kl0j} = -m_{ij}\epsilon_{ikl} \tag{8.4.41d}$$

$$C^{klpq} = q_{ij}\epsilon_{ikl}\epsilon_{jpq} \tag{8.4.41b}$$

The symmetric conditions for lossless media can be written as

$$C^{\alpha\beta\rho\sigma} = (C^{\rho\sigma\alpha\beta})^* \tag{8.4.42}$$

which yields $p_{ij} = p_{ji}^*$, $q_{mn} = q_{nm}^*$, and $l_{kn} = -m_{nk}^*$ as discussed in Chapter 3.

At this point it is appropriate to mention the work of von Tischer and Hess [1969] on a covariant description of a conducting medium. Ohm's law relates the conduction current to the electric field by conductivity, which can be isotropic as well as anisotropic. For moving

anisotropic conducting media, von Tischer and Hess introduced a new three-dimensional vector, together with the conducting current, to form a four-dimensional skew-symmetric tensor just like $F_{\mu\nu}$ and $G_{\mu\nu}$. They thus obtained a covariant description of what we may call bian-isotropic conducting media. The implications of the new vector have not been explored.

Other covariant descriptions of moving isotropic media exist, such as

$$(\delta_\rho^\alpha + u^\alpha u_\rho)J_c^\rho = \sigma u_\beta F^{\alpha\beta}$$

for Ohm's law and

$$G_{\lambda\mu} = F_{\lambda\mu} + (n^2 - 1)(F_{\mu\sigma}u^\sigma u_\lambda - F_{\lambda\sigma}u^\sigma u_\mu)$$

for isotropic nonconducting media. The velocity four-vector $u^\alpha = (1, \overline{\beta})$. Thus the manifestly covariant descriptions explicitly display the velocity dependence. When reference is made to the rest frame of the medium, $u^\alpha = (1, 0, 0, 0)$ and the two equations yield $\overline{J} = \sigma\overline{E}$, $\overline{D} = \epsilon\overline{E}$, and $\overline{H} = \overline{B}/\mu$.

Problems

P8.4.1

Show that $\eta_{\alpha\beta\rho\sigma} = -1$ when α, β, ρ, σ is even permutation of $0, 1, 2, 3$, $\eta_{\alpha\beta\rho\sigma} = 1$ when α, β, ρ, σ is odd permutation of $0, 1, 2, 3$, and $\eta^{\alpha\beta\rho\sigma} = 0$ when any two of α, β, ρ, σ is equal.

P8.4.2

Show that the eigenvector of an antisymmetric tensor corresponding to a non-zero eigenvalue is null.

P8.4.3

In general, there are two real null eigenvectors for the electromagnetic field tensor $F^{\mu\nu}$, and when $F^{\mu\nu}$ is degenerate, there is only one real null eigenvector. Show that

$$p_{[\alpha}F_{\mu]\nu}p^\nu = 0$$
$$F^{\mu\nu}p_\nu = 0$$

8.5   Hamilton's Principle and Noether's Theorem

A. Action Integral

Starting from a postulated Lagrangian density, the variational princi-
ple provides an elegant and systematic way of deriving the equations
of motion and the conservation laws of a physical system. In the case
of macroscopic electromagnetic fields the Lagrangian density is postu-
lated as

$$
\begin{aligned}
L[x_\alpha, A_\alpha(x_\mu),\, A_{\alpha,\beta}(x_\mu)] &= -\frac{1}{4}F^{\alpha\beta}G_{\alpha\beta} + J^\alpha A_\alpha \\
&= -\frac{1}{8}C^{\alpha\beta\rho\sigma}(A_{\alpha,\beta} - A_{\beta,\alpha})(A_{\rho,\sigma} - A_{\sigma,\rho}) + J^\alpha A_\alpha
\end{aligned}
\tag{8.5.1}
$$

The Lagrangian density $L(x, A_\alpha, A_{\alpha,\beta})$ is a function of the space-time
coordinates x_α, the potential functions A_α, and the space-time deriva-
tives of the potential functions $A_{\alpha,\beta}$. The potential functions A_α are
also called state functions. The charge current four-vector J_α is an
externally given state function.

   The variational principle applies to an action integral I, defined
by integration of the Lagrangian density over a four-dimensional space
R :

$$
I = \int_R d^4x \; L[x_\alpha, A_\alpha(x_\mu),\, A_{\alpha,\beta}(x_\mu)]
\tag{8.5.2}
$$

The variation of the action integral is caused by either a variation of the
state functions A_α or a variation of the domain of integration R which
induces variations on the space-time-dependent state functions A_α,
and on the externally given J_α because both are space-time dependent.

Joseph-Louis Lagrange (25 January 1736 – 10 April 1813) was born in Turin,
Sardinia-Piedmont (Italy) and died in Paris, France. In 1755, he impressed
Euler with his method of maxima and minima on the tautochrone problem,
and was appointed professor of mathematics at the Royal Artillery School
in Turin on 28 September. In 1756, he applied the calculus of variations to
mechanics and advocated for the principle of least action. On 6 November
1766 Lagrange succeeded Euler as Director of Mathematics at the Berlin
Academy of Science. On 18 May 1787 he left Berlin to become a member of
the Académie des Sciences in Paris, where he remained for the rest of his life.
In 1788 he published mécanique analytique in which Lagrange transformed
mechanics into a branch of mathematical analysis.

B. Hamilton's Principle and Maxwell Equations

In Hamilton's principle, the domain of integration R is not varied. The state function A_α inside the domain R is varied by an arbitrary and infinitesimally small amount δA_α :

$$A'_\alpha(x_\mu) = A_\alpha(x_\mu) + \delta A_\alpha(x_\mu) \qquad (8.5.3)$$

where A'_α are new state functions. The state functions on the boundary of R are not varied, where $\delta A_\alpha = 0$. The principle requires that the action integral be stationary under such variations:

$$\delta I = \int_R d^4x \left[L'(x_\alpha, A'_\alpha, A'_{\alpha,\beta}) - L(x_\alpha, A_\alpha, A_{\alpha,\beta}) \right] = 0 \qquad (8.5.4)$$

The new Lagrangian density $L'(x_\alpha, A'_\alpha, A'_{\alpha,\beta})$ is related to the old Lagrangian density L as follows:

$$L'(x_\alpha, A'_\alpha, A'_{\alpha,\beta}) = L(x_\alpha, A_\alpha, A_{\alpha,\beta}) + \frac{\partial L}{\partial A_\alpha}\delta A_\alpha + \frac{\partial L}{\partial A_{\alpha,\beta}}\delta A_{\alpha,\beta}$$

$$= L(x_\alpha, A_\alpha, A_{\alpha,\beta}) + \frac{\partial L}{\partial A_\alpha}\delta A_\alpha$$

$$- \frac{d}{dx^\beta}\left(\frac{\partial L}{\partial A_{\alpha,\beta}}\right)\delta A_\alpha + \frac{d}{dx^\beta}\left(\frac{\partial L}{\partial A_{\alpha,\beta}}\delta A_\alpha\right)$$

Substituting in (8.5.4) yields

$$\int_R d^4x \left\{ \left[\frac{\partial L}{\partial A_\alpha} - \frac{d}{dx^\beta}\left(\frac{\partial L}{\partial A_{\alpha,\beta}}\right) \right]\delta A_\alpha + \frac{d}{dx^\beta}\left(\frac{\partial L}{\partial A_{\alpha,\beta}}\delta A_\alpha\right) \right\} = 0$$
$$(8.5.5)$$

The last term vanishes after integration because of the condition that δA_α vanishes on the boundary of R. Since δI vanishes for all variations of the state function δA_α, we have

$$\frac{\partial L}{\partial A_\alpha} - \frac{d}{dx^\beta}\left(\frac{\partial L}{\partial A_{\alpha,\beta}}\right) = 0 \qquad (8.5.6)$$

which is known as the *Euler-Lagrangian equation.*

   The Maxwell equation

$$F_{\alpha\beta,\gamma} + F_{\beta\gamma,\alpha} + F_{\gamma\alpha,\beta} = 0 \qquad (8.5.7)$$

is a direct consequence of the definition

$$F_{\alpha\beta} = A_{\alpha,\beta} - A_{\beta,\alpha} \qquad (8.5.8)$$

The other Maxwell equation,

$$G^{\beta\alpha}_{,\beta} = J^{\alpha} \qquad (8.5.9)$$

can be derived from the Euler-Lagrangian equation by using the equations $\partial L/\partial A_{\alpha} = J^{\alpha}$ and $\partial L/\partial A_{\alpha,\beta} = -G^{\alpha\beta}$.

C. Noether's Theorem and Energy Momentum Tensors

In Noether's theorem the domain of integration R is rendered an infinitesimal transformation, which induces variations on both state functions A_{α} and J_{α}. Suppose that the domain R is mapped onto a new domain R' such that

$$x'_{\alpha} = x_{\alpha} + \delta x_{\alpha} \qquad (8.5.10)$$

This mapping transplants a state function from x_{α} to x'_{α} :

$$A'_{\alpha}(x') = A_{\alpha}(x) + \delta A_{\alpha} \qquad (8.5.11)$$

Note that δA_{α} gives the difference between the new state function $A'_{\alpha}(x')$ at the new location x'_{α} and the old state function $A_{\alpha}(x)$ at the old location x_{α} before it is transplanted. Usually the state functions are not explicit functions of space-time coordinates. Consider an infinitesimal translation of the domain R :

$$x'_{\alpha} = x_{\alpha} + \epsilon_{\alpha} \qquad (8.5.12)$$

From the active viewpoint of a coordinate transformation, all state functions are transplanted by an infinitesimal amount. The new and the old state functions are equal in magnitude, and there is no change in the orientation. From the passive viewpoint of coordinate transformation, the coordinate axes are translated by an infinitesimal amount and the state functions are left unchanged. We have

$$\delta A_\alpha = 0 \tag{8.5.13}$$

Next, consider an infinitesimal rotation of the coordinate axes:

$$x'_\alpha = x_\alpha - \omega_\alpha^\beta x_\beta \tag{8.5.14}$$

The induced variations on the state functions are

$$\delta A_\alpha = \omega_\alpha^\beta A_\beta \tag{8.5.15}$$

From the active viewpoint, the state functions are rotated by an infinitesimal amount. From the passive viewpoint, the amount is equal to the change of the component projections on the new and the old coordinate axes.

The variation denoted by δA_α is rather awkward because it compares two state functions at different locations. We define instead

$$\overline{\delta} A_\alpha = A'_\alpha(x') - A_\alpha(x') = A'_\alpha(x) - A_\alpha(x) \tag{8.5.16}$$

to denote the difference between the new and the old state functions at the same location. The second equality is valid up to the first order, as shown here:

$$\begin{aligned} \overline{\delta} A_\alpha &= A'_\alpha(x') - A_\alpha(x') \\ &= A'_\alpha(x) - A_\alpha(x) + (A'_{\alpha,\beta} - A_{\alpha,\beta})\delta x^\beta + \cdots \\ &\approx A'_\alpha(x) - A_\alpha(x) \end{aligned} \tag{8.5.17}$$

As a matter of fact, all first-order quantities with infinitesimal space-time separation can be shown to be equal. The relation between δA_α and $\overline{\delta} A_\alpha$ is easily established:

$$\begin{aligned} \overline{\delta} A_\alpha &= A'_\alpha(x') - A_\alpha(x') \\ &= A'_\alpha(x') - A_\alpha(x) - [A_\alpha(x') - A_\alpha(x)] \\ &= \delta A_\alpha - A_{\alpha,\beta}\delta x^\beta \end{aligned} \tag{8.5.18}$$

Note that, when the domain variation is a translation, $\delta A_\alpha = 0$ because the new state function is the same as the old one. But $\overline{\delta} A_\alpha \neq 0$ because the new state function at x'_α is transplanted from a neighboring location and is certainly different from the old state function at x'_α, which has been transplanted to another location.

Under the infinitesimal domain variations, variations are induced on both the state functions A_α, $A_{\alpha,\beta}$ and the externally given J_α. The new Lagrangian density is related to the old one by

$$
\begin{aligned}
L'(x'_\alpha, A'_\alpha, A'_{\alpha,\beta}) &= L + L_{,\alpha}\delta x^\alpha + \frac{\partial L}{\partial A_\alpha}\delta A_\alpha + \frac{\partial L}{\partial A_{\alpha,\beta}}\delta A_{\alpha,\beta} + \frac{\partial L}{\partial J_\alpha}\delta J_\alpha \\
&= L + \frac{dL}{dx^\rho}\delta x^\rho + \frac{\partial L}{\partial A_\alpha}\overline{\delta} A_\alpha + \frac{\partial L}{\partial A_{\alpha,\beta}}\overline{\delta} A_{\alpha,\beta} + \frac{\partial L}{\partial J_\alpha}\overline{\delta} J_\alpha
\end{aligned}
$$

where

$$
\frac{dL}{dx^\rho} = L_{,\rho} + \frac{\partial L}{\partial A_\alpha}A_{\alpha,\rho} + \frac{\partial L}{\partial A_{\alpha,\beta}}A_{\alpha,\beta\rho} + \frac{\partial L}{\partial J_\alpha}J_{\alpha,\rho}
$$

The new domain of integration R' is related to the old domain of integration by the Jacobian, which is

$$
\det\left|\frac{\partial x'^\alpha}{\partial x^\beta}\right| = 1 + (\delta x^\alpha)_{,\alpha} \tag{8.5.19}
$$

The variation of the action integral under this domain variation becomes, to the first order,

$$
\begin{aligned}
\delta I &= \int_{R'} d^4x'\, L'(x'_\alpha, A'_\alpha, A'_{\alpha\beta}) - \int_R d^4x\, L(x_\alpha, A_\alpha, A_{\alpha,\beta}) \\
&= \int_R d^4x \left\{ [1 + (\delta x^\alpha)_{,\alpha}] \left(L + \frac{dL}{dx^\rho}\delta x^\rho + \frac{\partial L}{\partial A_\alpha}\overline{\delta} A_\alpha + \frac{\partial L}{\partial J_\alpha}\overline{\delta} J_\alpha \right. \right. \\
&\qquad\qquad\qquad\qquad\qquad \left.\left. + \frac{\partial L}{\partial A_{\alpha,\beta}}\overline{\delta} A_{\alpha,\beta} \right) - L \right\} \\
&= \int_R d^4x \left\{ \left[\frac{\partial L}{\partial A_\alpha} - \frac{d}{dx^\beta}\left(\frac{\partial L}{\partial A_{\alpha,\beta}}\right) \right] \overline{\delta} A_\alpha \right. \\
&\qquad\qquad\qquad \left. + \frac{d}{dx^\rho}\left[L\delta x^\rho + \frac{\partial L}{\partial A_{\alpha,\rho}}\overline{\delta} A_\alpha \right] + \frac{\partial L}{\partial J_\alpha}\overline{\delta} J_\alpha \right\}
\end{aligned}
$$

Note that, although this variation of the action integral is derived from induced variations caused by infinitesimal domain changes, the result is fairly general and includes Hamilton's principle as a special case. Let us keep the domain unchanged; we then have $\delta x^\rho = 0$, $\overline{\delta} A_\alpha = \delta A_\alpha$. The externally given J_α is also not varied: $\delta J_\alpha = 0$. This result is seen to reduce to (8.5.5).

Noether's theorem requires that the action integral be stationary, and that the Euler-Lagrangian equations be satisfied for the state functions A_α under the domain variations. As a result, we obtain

$$\frac{d}{dx^\rho} \left[L\delta x^\rho + \frac{\partial L}{\partial A_{\alpha,\rho}} \overline{\delta} A_\alpha \right] + \frac{\partial L}{\partial J_\alpha} \overline{\delta} J_\alpha = 0 \qquad (8.5.20)$$

This equation gives all of the conservation laws.

Emmy Noether (23 March 1882 – 14 April 1935)

Emmy Noether obtained her doctorate degree in 1907 from the University of Erlangen, where her father Max Noether was a professor. During the next ten years she worked with her father at the Mathematics Institute in Erlangen. In 1915 Noether started teaching at the University of Göttingen and in 1919 officially became a member of its faculty. Noether's theorem was her first piece of work at Göttengen in 1915. In 1933, she became a visiting professor at Bryn Mawr College in US and also lectured at the Institute for Advanced Study in Princeton.

We shall first consider the case of translation, which yields energy momentum tensors for macroscopic electromagnetic fields. The case of four-dimensional rotation is then considered, and the angular momentum conservation laws are derived. Under an infinitesimal translation, we have

$$\overline{\delta} A_\alpha = -A_{\alpha,\beta} \epsilon^\beta \qquad (8.5.21a)$$

$$\overline{\delta} J_\alpha = -J_{\alpha,\beta} \epsilon^\beta \qquad (8.5.21b)$$

Equation (8.5.20) gives

$$\epsilon^\beta \left[\frac{d}{dx^\rho} \left(-\frac{1}{4} F^{\mu\nu} G_{\mu\nu} \delta_\beta^\rho + J^\alpha A_\alpha \delta_\beta^\rho + G^{\alpha\rho} A_{\alpha,\beta} \right) - A^\alpha J_{\alpha,\beta} \right] = 0$$

This equation can be expressed in terms of field variables alone. After some manipulation and by use of the fact that $G^{\alpha\rho} A_{\beta,\alpha\rho} = 0$, we eliminate the potentials and obtain

$$T^{\alpha\beta}_{,\alpha} = -f^\beta \qquad (8.5.22)$$

where

$$T^{\alpha\beta} = -\frac{1}{4}\eta^{\alpha\beta}F_{\rho\sigma}G^{\rho\sigma} + \eta^{\mu\beta}G^{\rho\alpha}F_{\rho\mu}$$
$$= -\frac{1}{2}\eta^{\alpha\beta}[\overline{H}\cdot c\overline{B} - \overline{E}\cdot c\overline{D}] + \eta^{\mu\beta}G^{\rho\alpha}F_{\rho\mu} \qquad (8.5.23)$$

is the four-dimensional energy momentum tensor, and

$$f^{\beta} = J_{\alpha}F^{\alpha\beta} \qquad (8.5.24)$$

In three-dimensional vector notation, we find that

$$f^{\beta} = \begin{bmatrix} \overline{J}\cdot\overline{E} \\ c\rho\overline{E} + \overline{J}\times c\overline{B} \end{bmatrix} \qquad (8.5.25)$$

$$T^{\alpha\beta} = \begin{bmatrix} cW & c^2\overline{G} \\ \overline{S} & c\overline{\overline{T}} \end{bmatrix} \qquad (8.5.26)$$

where

Electromagnetic energy $W = \dfrac{1}{2}(\overline{D}\cdot\overline{E} + \overline{B}\cdot\overline{H})$

Energy flow density $\overline{S} = \overline{E}\times\overline{H}$

Momentum density $\overline{G} = \overline{D}\times\overline{B}$

Maxwell stress tensor $\overline{\overline{T}} = \dfrac{1}{2}(\overline{D}\cdot\overline{E} + \overline{B}\cdot\overline{H})\overline{\overline{I}} - \overline{D}\,\overline{E} - \overline{B}\,\overline{H}$

The conservation law (8.5.22), written in vector notation, takes the form

$$\nabla\cdot\overline{S} + \frac{\partial W}{\partial t} = -\overline{J}\cdot\overline{E} \qquad (8.5.27a)$$

$$\nabla\cdot\overline{\overline{T}} + \frac{\partial\overline{G}}{\partial t} = -(\rho\overline{E} + \overline{J}\times\overline{B}) \qquad (8.5.27b)$$

Under an infinitesimal rotation, we have

$$\overline{\delta}A_{\alpha} = \delta A_{\alpha} - A_{\alpha,\beta}\delta x^{\beta} = \omega_{\alpha}^{\beta}A_{\beta} - A_{\alpha,\beta}\omega_{\rho}^{\beta}x^{\rho} \qquad (8.5.28a)$$

$$\overline{\delta}J_{\alpha} = \omega_{\alpha}^{\beta}J_{\beta} - J_{\alpha,\beta}\omega_{\rho}^{\beta}x^{\rho} \qquad (8.5.28b)$$

After some manipulations, (8.5.20) gives

$$\omega_{\alpha\beta}\left[\frac{d}{dx^\rho}(T^{\rho\alpha}x^\beta + G^{\alpha\rho}A^\beta + G^{\beta\rho}A^\alpha) + J_\rho F^{\rho\alpha}x^\beta + \eta^{\alpha\beta}J^\rho A_\rho\right] = 0$$

(8.5.29)

Interchanging α and β, we have

$$\omega_{\beta\alpha}\left[\frac{d}{dx^\rho}(T^{\rho\beta}x^\alpha + G^{\alpha\rho}A^\alpha + G^{\beta\rho}A^\beta) + J_\rho F^{\rho\beta}x^\alpha + \eta^{\beta\alpha}J^\rho A_\rho\right] = 0$$

(8.5.30)

We add the two equations above and note that $\omega_{\beta\alpha} = -\omega_{\alpha\beta}$, obtaining

$$\frac{d}{dx^\rho}M^{\rho\alpha\beta} = x^\alpha J_\rho F^{\rho\beta} - x^\beta J_\rho F^{\rho\alpha}$$

(8.5.31)

where

$$M^{\rho\alpha\beta} = T^{\rho\alpha}x^\beta - T^{\rho\beta}x^\alpha$$

(8.5.32)

is the four-dimensional angular momentum tensor for electromagnetic fields.

Problems

P8.5.1

To determine eigenvectors and eigenvalues of the energy tensor, we write

$$T^{\alpha\beta}\xi_\beta = \eta^{\alpha\beta}\lambda\xi_\beta$$

The determinant of the above equation must be zero. Let z axis be perpendicular to both $\overline{E}$ and $\overline{H}$, determine $T_{\alpha\beta}$ and show that eigenvalue

$$\lambda^2 = \frac{1}{16}\frac{\epsilon}{\mu}[(F_{\alpha\beta}F^{\alpha\beta})^2 + (F^*_{\alpha\beta}F^{\alpha\beta})^2]$$

Answers

P8.1.1

$$\overline{E} = \overline{E}_B; \qquad\qquad \overline{B} = \overline{B}_B$$
$$\overline{H} = \frac{1}{\mu_o}\overline{B}_B - \overline{M}_B; \qquad \overline{D} = \epsilon_o\overline{E}_B + \overline{P}_B$$
$$\overline{J} = \overline{J}_B; \qquad\qquad \rho = \rho_B$$

P8.2.1

(e) $\gamma = 1/0.6$, twin A will be $30/0.6 = 50$ years old.

P8.2.2

The velocity of S'' w.r.t. S' is $\overline{\beta}_{21} = \dfrac{\overline{\overline{a}}_1 \cdot \overline{\beta}_2/\gamma_1 - \overline{\beta}_1}{1 - \overline{\beta}_1 \cdot \overline{\beta}_2}$.

P8.2.3

B takes 7 years to complete the round trip, while the elapsed time on Earth is 12 years.

P8.2.4

$l = l'/\gamma$.

P8.2.5

(c)

$$k = 1: \quad (1 + \overline{\beta} \cdot \overline{Q}')A_1 = -1$$
$$k = 2: \quad (1 + \overline{\beta} \cdot \overline{D}')A_2 = -\frac{1}{2}(\overline{\beta} \cdot \overline{Q}'^{(2)})A_1^2$$
$$k = 3: \quad (1 + \overline{\beta} \cdot \overline{D}')A_3 = 1(\overline{\beta} \cdot \overline{Q}'^{(2)})A_1\, A_2 - \frac{1}{3!}(\overline{\beta} \cdot \overline{Q}'^{(3)})A_1^3$$

P8.2.6

On side AB, $c\rho = \gamma\overline{\beta} \cdot \overline{J}' = \gamma\beta J_0'$. On side CD, $c\rho = \gamma\overline{\beta} \cdot \overline{J}' = -\gamma\beta J_0'$. On sides BC and DA, since $\overline{\beta} \cdot \overline{J}' = 0$, $\rho = 0$. Thus there is negative charges on CD and positive charges on AB. A net electric dipole moment exists along CB and DA direction.

P8.2.7

Suppose that in S frame

$$\overline{E} = \hat{z}E_0$$
$$c\overline{B} = \hat{x}E_0 + \hat{z}\sqrt{3}E_0$$

Consider a S' frame moving in $\hat{y}$ direction with velocity β. In S' frame, we have

$$\overline{E}' = \hat{x}\sqrt{3}\gamma\beta E_0 + \hat{z}\gamma(E_0 - \beta E_0)$$
$$c\overline{B} = \hat{x}\gamma(E_0 - \beta E_0) + \hat{z}\sqrt{3}\gamma E_0.$$

We want $\overline{E}$ and $\overline{B}$ fields to be parallel. Let a be the constant of proportionality, then

$$\sqrt{3}\gamma\beta E_0 = a\gamma(E_0 - \beta E_0)$$
$$\gamma(E_0 - \beta E_0) = a\sqrt{3}\gamma E_0.$$

Eliminating E_0 and a from the above equation, we get $\beta^2 - 5\beta + 1 = 0$ which gives $\beta = \dfrac{5 - \sqrt{25 - 4}}{2} = 0.21$.

P8.2.8

$\beta = cB_0/E_0$, and $E'_x = \gamma(E_0 - \beta cB_0) = E_0\sqrt{1 - c^2 B_0^2/E_0^2}$.

Since $|\overline{E}'|^2 - |c\overline{B}'|^2 = |\overline{E}|^2 - |c\overline{B}|^2$ is an invariant quantity, it is impossible to find an observer moving with velocity less than c who observes only a magnetic field.

P8.2.9

(a) In the frame of reference of S' where q_1 is stationary at the origin of reference frame S,

$$\overline{E}' = \frac{q_1}{4\pi\epsilon_o} \cdot \frac{\overline{r}'}{r'^3}, \qquad B' = 0$$

In the frame of reference of S:

$$\overline{E} = \hat{x}\gamma\, E'_x + \hat{y}\gamma\, E'_y + \hat{z}E'_z = \frac{q_1}{4\pi\epsilon_o}\left(\hat{x}\gamma\frac{x'}{r'^3} + \hat{y}\gamma\frac{y'}{r'^3} + \hat{z}\frac{z'}{r'^3}\right)$$

where $\gamma = 1/\sqrt{1 - \beta_1^2}$ and $\beta_1 = v_1/c$. By Lorentz Transformation, $x' = x,\ y' = y,\ z' = \gamma z$

$$r'^2 = x'^2 + y'^2 + z'^2 = \gamma^2\left(\frac{x^2 + y^2}{\gamma^2} + z\right) = \gamma^2\left[(1 - \beta_1^2)r^2 + \left(\overline{\beta}_1 \cdot \overline{r}\right)^2\right]$$

which yields

$$\overline{E} = \frac{q_1}{4\pi\epsilon_o} \cdot \frac{(1 - \beta_1^2)\overline{r}}{\left[(1 - \beta_1^2)r^2 + (\overline{\beta}_1 \cdot \overline{r})^2\right]^{3/2}}$$

Since $B_z = 0$, $\overline{B}_\perp = \frac{\gamma}{c}\overline{\beta}_1 \times \overline{E}'_\perp = \frac{1}{c}\overline{\beta}_1 \times \overline{E}_\perp$, we have

$$\overline{B} = \frac{1}{c}\overline{\beta}_1 \times \overline{E} = \frac{q_1}{4\pi c\epsilon_o} \cdot \frac{(1 - \beta_1^2)\overline{\beta}_1 \times \overline{r}}{\left[(1 - \beta_1^2)r^2 + (\overline{\beta}_1 \cdot \overline{r})^2\right]^{3/2}}$$

(b) $\overline{F}_{12} = q_2(\overline{E} + \overline{v}_2 \times \overline{B}) = q_2(1 - \overline{\beta}_2 \cdot \overline{\beta}_1)\overline{E} + q_2(\overline{\beta}_2 \cdot \overline{E})\overline{\beta}_1$

(c) For the case $\overline{r} = d\hat{y}$, $\overline{v}_1 = \overline{v}_2 = \hat{z}v$, and $q_1 = q_2 = -q$, we have

$$\overline{E} = \frac{(-q)}{4\pi\epsilon_o d^2}\hat{y} ; \quad \overline{F}_{12} = \frac{(1 - \beta^2)q^2}{4\pi\epsilon_o d^2}\hat{y}$$

They repel each other.

P8.2.10

(a) The electric field generated by an infinite line source is $\overline{E} = \hat{y}\frac{(-\lambda)}{2\pi\epsilon_0 d}$. The electric force for length l is $\overline{F}_e = \hat{y}(-\lambda l)\frac{(-\lambda)}{2\pi\epsilon_0 d} = \hat{y}\frac{\lambda^2 l}{2\pi\epsilon_0 d}$. The magnetic field generated by infinite current source is $\overline{B} = -\hat{x}\frac{\mu_0 v(-\lambda)}{2\pi d}$. The magnetic force for length l is $\overline{F}_c = -\hat{y}\frac{\mu_0 v^2 \lambda^2 \, l}{2\pi d}$. Total force for length l in frame S is $\overline{F} = \overline{F}_e + \overline{F}_c = \hat{y}\frac{\lambda^2 l}{2\pi\epsilon_0 d}(1 - \frac{v^2}{c^2}) > 0$.
The force is repulsion.

(b) In frame S' , the current $I' = 0$. Total force acted by one line on length l' on the other line in S' frame (only electrostatic force exists between two relatively static infinite line charge) is $\overline{F}' = \overline{F}'_e = \hat{y}'\frac{\lambda'^2 l'}{2\pi\epsilon_0 d}$, where $\hat{y}' = \hat{y}$ due to the velocity of frame is along $\hat{z}$. The relativistic transformation of length is $l' = \gamma \, l$. Based on charge conservation $Q = l\lambda = l'\lambda'$, we get line charge density $\lambda' = \lambda/\gamma$. Transform the force in S' to frame S (only y component is not zero):

$$F_y = \frac{1}{\gamma}F'_y = \hat{y}\frac{\lambda^2 l}{2\pi\epsilon_0 d}\frac{1}{\gamma^2} = \hat{y}\frac{\lambda^2 \, l}{2\pi\epsilon_0 d}(1 - \frac{v^2}{c^2}) > 0$$

The force is repulsion in lab frame S .

(c) Fields in frame S' : Only electrostatic field exists between two relatively static infinite line charges: $\overline{E}' = \hat{y}\frac{(-\lambda')}{2\pi\epsilon_0 d} = \hat{y}\frac{-\lambda/\gamma}{2\pi\epsilon_0 d}$. Fields in frame S :
Frame S moves with $\overline{v}_s = -v\hat{z}$ with respect to S'

$$\overline{E} = \hat{y}E_y = \hat{y}\gamma E'_y = \hat{y}\frac{(-\lambda)}{2\pi\epsilon_0 d}$$

$$\overline{B} = -\hat{x}B_z = \frac{\gamma}{c}\left(-\frac{\overline{v}}{c} \times \overline{E}'\right) = -\hat{x}\frac{v}{c^2}\frac{(-\lambda)}{2\pi\epsilon_0 d}$$

Finally, we get the same fields as method 1, which give the same force.

P8.2.11

(a) $\overline{F}_{(+\lambda)(+q)} = q\overline{E} = q\frac{\lambda}{2\pi\epsilon_o d_o}\hat{y}$
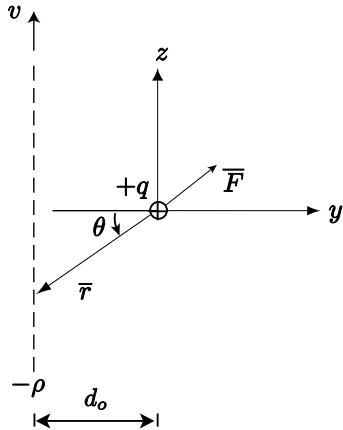
Figure A8.2.11.1 Observer S' **moves with velocity** $\overline{v}$ **relative to observer** S.

The static positive line charge will repel the static positive point charge.

(b) $\overline{F}_{(+\lambda)(-q)} = -\overline{F}_{(+\lambda)(+q)} = -q\frac{\lambda}{2\pi\epsilon_o d_o}\hat{y}$

The static positive line charge will attract the moving negative point charge.

(c) Calculate $\overline{F}_{(-\lambda)(+q)}$. In this case, $\overline{v}_1 = v\hat{x}$, $\overline{v}_2 = 0$.

$$\overline{F}_{(-\lambda)}(+q) = q \int_{\theta=-\frac{\pi}{2}}^{\theta=\frac{\pi}{2}} d\overline{E}(\theta)$$

$$= q \int_{\theta=\frac{-\pi}{2}}^{\theta=\frac{\pi}{2}} \frac{1}{4\pi\epsilon_o} \cdot \frac{(1-\beta^2)(-\overline{r})}{\left[(1-\beta^2)r^2 + (\frac{\overline{v}\cdot(-\overline{r})}{c})^2\right]^{\frac{3}{2}}} \cdot d(-\lambda d_o\tan\theta)$$

$$= q \int_{\frac{-\pi}{2}}^{\frac{\pi}{2}} \frac{1}{4\pi\epsilon_o} \cdot \frac{(1-\beta^2)r(\sin\theta\hat{x} + \cos\theta\hat{y})}{\left[(1-\beta^2)(\frac{d_o}{\cos\theta})^2 + (\frac{vr\sin\theta}{c})^2\right]^{\frac{3}{2}}} \cdot (-\lambda d_o)\sec^2\theta d\theta$$

$$= (-q) \int_{\frac{-\pi}{2}}^{\frac{\pi}{2}} \frac{\lambda(1-\beta^2)}{4\pi\epsilon_o d_o} \frac{\cos\theta}{(1-\beta^2 + \beta^2\sin^2\theta)^{\frac{3}{2}}}\hat{y}d\theta$$

$$= -\frac{q\lambda}{2\pi\epsilon_o d_o}\hat{y}$$

The moving negative line charge will attract the static positive point charge.

(d) Using similar derivation, we have

$$\overline{F}_{(-\lambda)(-q)} = -(1-\beta^2)\overline{F}_{(-\lambda)(+q)} = (1-\beta^2)\frac{q\lambda}{2\pi\epsilon_o d_o}\hat{y}$$

The moving negative line charge will repel the moving negative point charge.

(e) $\overline{F}_{seg} = \overline{F}_{(+\lambda)(+q)} + \overline{F}_{(-\lambda)(+q)} + \overline{F}_{(+\lambda)(-q)} + \overline{F}_{(-\lambda)(-q)} = -\beta^2 \frac{q\lambda}{2\pi\epsilon_o d_o}\hat{y}$
The wire will attract the segment! Also

$$\overline{F}_{seg} = -\beta^2 \frac{q\lambda}{2\pi\epsilon_o d_o}\hat{y} = \frac{v^2}{c^2}\frac{q\lambda}{2\pi\epsilon_o d_o}(-\hat{y}) = qv\mu_o\frac{\lambda v}{2\pi d_o}(-\hat{y})$$

$$= (-qv\hat{x}) \times \mu_o \left(-\frac{\lambda v}{2\pi d_o}\hat{z}\right) = \overline{J} \times \mu_o\overline{H} = \overline{J} \times \overline{B}$$

P8.2.12

The discrepancy lies in the wrong assumption that the current-carrying wire can be regarded as moving negative charges alone. In fact, the current-carrying wire is electrically neutral. It consists of static positive charges and moving negative charges. See Problem 8.2.11.

P8.3.1

(a) In the laboratory frame,

$$\overline{\overline{C}}_{EB} = \overline{\overline{L}}_6^{-1}\overline{\overline{C}}_{EB}\overline{\overline{L}}_6$$

$$= \gamma^2 \begin{bmatrix} p'-\beta^2 q' & 0 & 0 & \ell'(1-\beta^2) & \beta(-p'+q') & 0 \\ 0 & (p'-q'\beta^2) & 0 & \beta(p'-q') & \ell'(1-\beta^2) & 0 \\ 0 & 0 & \frac{p'}{\gamma^2} & 0 & 0 & \frac{\ell}{\gamma^2} \\ -\ell'(1-\beta^2) & -\beta(p'-q') & 0 & (-p'\beta^2+q') & 0 & 0 \\ \beta(p'-q') & -\ell'(1-\beta^2) & 0 & 0 & (-p'\beta^2+q') & 0 \\ 0 & 0 & \frac{-\ell}{\gamma^2} & 0 & 0 & \frac{q}{\gamma^2} \end{bmatrix}$$

(b) For a biaxial medium in its rest frame S'

$$\overline{\overline{\epsilon}}' = \begin{bmatrix} \epsilon'_x & & \\ & \epsilon'_y & \\ & & \epsilon'_z \end{bmatrix}$$

$$\overline{\overline{C}}'_{EB} = \begin{bmatrix} c\overline{\overline{\epsilon}}' & 0 \\ 0 & \frac{1}{c\mu'}\overline{\overline{I}} \end{bmatrix}.$$

By brute force matrix multiplication, in ways exactly the same as done previously for the moving biisotropic medium, we obtain

$$\overline{\overline{C}}_{EB} = \gamma^2 \cdot$$

$$\begin{bmatrix} c\epsilon'_x - \frac{\beta^2}{c\mu'} & 0 & 0 & 0 & \beta(-c\epsilon'_x + \frac{1}{c\mu'}) & 0 \\ 0 & c\epsilon'_y - \frac{\beta^2}{c\mu'} & 0 & \beta(c\epsilon'_y - \frac{1}{c\mu'}) & 0 & 0 \\ 0 & 0 & \frac{c\epsilon'_z}{\gamma^2} & 0 & 0 & 0 \\ 0 & \beta(-c\epsilon'_y + \frac{1}{c\mu'}) & 0 & -c\epsilon'_y\beta^2 + \frac{1}{c\mu'} & 0 & 0 \\ \beta(c\epsilon'_x - \frac{1}{c\mu'}) & 0 & 0 & 0 & -\beta^2 c\epsilon'_x + \frac{1}{c\mu'} & 0 \\ 0 & 0 & 0 & 0 & 0 & \frac{1}{\gamma^2 c\mu'} \end{bmatrix}$$

We notice that both moving biisotropic medium and moving biaxial medium are bianisotropic.

P8.4.1

$\eta_{\alpha\beta\rho\sigma} = \eta_{\alpha\mu}\eta_{\beta\nu}\eta_{\rho\gamma}\eta_{\sigma\omega}\eta^{\mu\nu\gamma\omega}$. For instance, let $\alpha = 0$, $\beta = 1$, $\rho = 2$, $\sigma = 3$. We find that $\eta_{0123} = \eta_{00}\eta_{11}\eta_{22}\eta_{33} = -\eta^{0123} = -1$.

P8.4.2

The eigenequation is $F_{\mu\nu}\xi^\nu = \lambda\eta_{\mu\nu}\xi^\nu$

Contracting by ξ^μ, we obtain $\lambda\eta_{\mu\nu}\xi^\mu\xi^\nu = F_{\mu\nu}\xi^\mu\xi^\nu = 0$

Therefore for $\lambda \neq 0$, $\xi^\mu\xi^\nu = 0$.

P8.4.3

For the wrench field

$$F^{\mu\nu} = \lambda_R(p^\mu q^\nu - p^\nu q^\mu) + i\lambda_I(m^\mu\overline{m}^\nu - m^\nu\overline{m}^\mu)$$
$$p^\mu p_\mu = q^\mu q_\mu = m^\mu m_\mu = \overline{m}^\mu\overline{m}_\mu = 0$$
$$p^\mu q_\mu = -m^\mu\overline{m}_\mu = 1$$
$$p^\mu m_\mu = p^\mu\overline{m}_\mu = q^\mu m_\mu = q^\mu\overline{m}_\mu = 0$$

we find $p_{[\alpha}F_{\mu]\nu}p^\nu = p_\alpha F_{\mu\nu}p^\nu - p_\mu F_{\alpha\nu}p^\nu = p_\alpha p_\mu - p_\mu p_\alpha = 0$.

For the wave field

$$F^{\mu\nu} = A(p^\mu y^\nu - p^\nu y^\mu))$$
$$y^\mu y_\mu = 1$$

we find $F^{\mu\nu}p_\nu = A(p^\mu y^\nu - p^\nu y^\mu))p_\nu = 0$.

P8.5.1

$$T_{00} = \frac{c}{2}(\overline{D}\cdot\overline{E} + \overline{B}\cdot\overline{H})$$

$$T_{11} = \frac{c}{2}[(D_1 E_1 + B_1 H_1) - (D_2 E_2 + B_2 H_2)]$$

$$T_{22} = -\frac{c}{2}[(D_1 E_1 + B_1 H_1) - (D_2 E_2 + B_2 H_2)] = -T_{11}$$

$$T_{33} = \frac{c}{2}(\overline{D}\cdot\overline{E} + \overline{B}\cdot\overline{H}) = T_{00}$$

$$T_{12} = -c(D_1 E_2 + B_1 H_2)$$

$$T_{21} = -c(D_2 E_1 + B_2 H_1) = T_{12}$$

$$T_{03} = c^2(D_1 B_2 - D_2 B_1)$$

$$T_{30} = (E_1 H_2 - E_2 H_1) = T_{03}$$

and we have

$$\begin{bmatrix} T_{00} + \lambda & 0 & 0 & T_{03} \\ 0 & T_{11} - \lambda & T_{12} & 0 \\ 0 & T_{21} & T_{22} - \lambda & 0 \\ T_{30} & 0 & 0 & T_{33} - \lambda \end{bmatrix} \cdot \begin{bmatrix} \xi^0 \\ \xi^1 \\ \xi^2 \\ \xi^3 \end{bmatrix} = 0$$

The eigenvalues are determined by setting

$$
\begin{vmatrix}
T_{00} + \lambda & 0 & 0 & T_{03} \\
0 & T_{11} - \lambda & T_{12} & 0 \\
0 & T_{12} & -T_{11} - \lambda & 0 \\
T_{03} & 0 & 0 & T_{00} - \lambda
\end{vmatrix} = 0
$$

which yields

$$
\lambda^2 = T_{00}^2 - T_{03}^2 = \frac{c^2}{4}(\overline{D} \cdot \overline{E} + \overline{B} \cdot \overline{H})^2 - c^4(D_1 B_2 - D_2 B_1)^2
$$

$$
= \frac{1}{4}[c^2(\overline{D} \cdot \overline{E} + \overline{B} \cdot \overline{H})^2 - 4c^4(D_1 B_2 - D_2 B_1)^2]
$$

$$
= \frac{1}{4}[c^2(D_1 E_1 + D_2 E_2 + B_1 H_1 + B_2 H_2)^2 - 4c^4(D_1 B_2 - D_2 B_1)^2]
$$

$$
= \frac{1}{4}[c^2(\epsilon E_1^2 + \epsilon E_2^2 + \epsilon c^2 B_1^2 + \epsilon c^2 B_2^2)^2 - 4(\frac{1}{c\mu}E_1 c B_2 - \frac{1}{c\mu}E_2 c B_1)^2]
$$

$$
= \frac{1}{16}\frac{\epsilon}{\mu}[4(2E_1^2 + 2E_2^2 + c^2 B_1^2 + c^2 B_2^2 - E_1^2 - E_2^2)^2 - 16(E_1 c B_2 - E_2 c B_1)^2]
$$

$$
= \frac{1}{16}\frac{\epsilon}{\mu}[(F_{\alpha\beta}F^{\alpha\beta})^2 + 16(E_1^2 + E_2^2)^2 + 16(E_1^2 + E_2^2)(c^2 B_1^2 + c^2 B_2^2 - E_1^2 - E_2^2)
$$

$$
- 16(E_1 c B_2 - E_2 c B_1)^2]
$$

$$
= \frac{1}{16}\frac{\epsilon}{\mu}[(F_{\alpha\beta}F^{\alpha\beta})^2 + 16(E_1^2 + E_2^2)(c^2 B_1^2 + c^2 B_2^2) - 16(E_1 c B_2 - E_2 c B_1)^2]
$$

$$
= \frac{1}{16}\frac{\epsilon}{\mu}[(F_{\alpha\beta}F^{\alpha\beta})^2 + (F_{\alpha\beta}^* F^{\alpha\beta})^2]
$$

where

$$
F_{\alpha\beta}F^{\alpha\beta} = 2(|c\overline{B}|^2 - |\overline{E}|^2) = 2(c^2 B_1^2 + c^2 B_2^2 - E_1^2 - E_2^2)
$$

$$
F_{\alpha\beta}^* F^{\alpha\beta} = -4c\overline{B} \cdot \overline{E} = -4c(B_1 E_1 + B_2 E_2)
$$

REFERENCES

Abramowitz, M. and I. A. Stegun, *Handbook of Mathematical Functions,* Dover Publications, New York, 1965.

Adams, A. T., *Electromagnetics for Engineers,* Renold Press, New York, 1971.

Agarwal, G. S., "Interaction of electromagnetic waves at rough dielectric surfaces," *Phys. Rev. B,* **15**, 2371–2383, 1977.

Anderson, J. L., *Principles of Relativity Physics,* Academic Press, New York, 1967.

Anderson, J. L. and J. W. Ryon, "Electromagnetic radiation in accelerated system," *Phys. Rev.,* **181**, 1765–1775, 1969.

Appel-Hansen, J., "The loop antenna with director arrays of loops and rods," *IEEE Trans. Antennas Propagat.,* **AP-20**, 516–517, 1972.

Arnaud, J. A. and A. A. M. Saleh, "Guidance of surface waves by multilayer coatings," *Appl. Optics,* **13**, 2343–2345, 1974.

Asrar, G., *Theory and Application of Optical Remote Sensing,* John Wiley & Sons, New York, 1989.

Astrov, D. N., "The magnetoelectric effect in antiferromagnetics," *Zh. Eksp. Teor. Fiz.,* **38**, 984–985, 1960.

Bach, H. and J. E. Hansen, "Uniformly spaced arrays," *Antenna Theory,* R. E. Collin and F. J. Zucker (eds.), Chapter 5, McGraw-Hill, New York, 1969.

Balanis, C. A., *Antenna Theory: Analysis and Design,* Harper & Row, New York, 1982.

Bannister, P. R., "The image theory for electromagnetic fields of a horizontal electric dipole in the presence of a conducting half space," *Radio Sci.,* **17**, 1095–1102, 1982.

Baños, A., Jr., *Dipole Radiation in the Presence of a Conducting Half-Space,* Pergamon Press, New York, 1966.

Barabanenkov, Y. N., Y. A. Kravtsov, S. M. Rytov, and V. I. Tatarskii, "Status of the theory of propagation of wave in a randomly inhomogeneous medium," *Soviet Phys. Usp.,* **13**, 551–580, 1971.

Barrick, D. E. and W. H. Peake, "A review of scattering from surfaces with different roughness scales," *Radio Sci.,* **3**, 865–868, 1968.

Barut, A. O., *Electrodynamics and Classical Theory of Fields and Particles,* MacMillan, New York, 1964.

Batterman, B. W. and H. Cole, "Dynamical diffraction of X rays by perfect crystals," *Rew. Modern Physics,* **36**, 681–717, 1964.

Beckmann, P. and A. Spizzichino, *The Scattering of Electromagnetic Waves from Rough Surfaces,* Pergamon Press, New York, 1963.

Bennett, C. L. and G. F. Ross, "Time-domain electromagnetics and its applications," *Proc. IEEE,* **66**, 299–318, 1978.

Bergmann, P. G., *Introduction to the Theory of Relativity,* Prentice-Hall, Englewood Cliffs, NJ, 1942.

Birss, R. R., "Macroscopic symmetry in space-time," *Rep. Prog. Phys.,* **26**, 307–310, 1963.

Birss, R. R. and R. G. Shrubsall, "The propagation of EM waves in magnetoelectric crystals," *Phil. Mag.,* **15**, 687–700, 1967.

Bjorken, J. D. and S. D. Drell, *Relativistic Quantum Fields,* McGraw-Hill, New York, 1965.

Blanchard, A. J. and J. W. Rouse, Jr., "Depolarization of electromagnetic waves scattered from an inhomogeneous half space bounded by a rough surface," *Radio Sci.,* **15**, 773–780, 1980.

Boerner, W. M., M. B. El-Arini, C. Y. Chan, and P. M. Mastoris, "Polarization dependence in electromagnetic inverse problems," *IEEE Trans. Antennas Propagat.,* **AP-29**, 262–271, 1981.

Bolotovskii, B. M. and A. N. Lebedev, "On threshold phenomena in classical electrodynamics," *Soviet Phys. JETP,* **26**, 784, 1968.

Booker, H. G., *Energy in Electromagnetism,* Peter Peregrinus, New York, 1982.

Borgeaud, M., S. V. Nghiem, R. T. Shin, and J. A. Kong, "Theoretical models for polarimetric microwave remote sensing of earth terrain," *J. Electromagnetic Waves and Applications,* **3**, 61–81, 1989.

Born, M. and E. Wolf, *Principles of Optics,* Pergamon Press, New York, 1970.

Botros, A. Z. and S. F. Mahmoud, "The transient fields of simple radiators from the point of view of remote sensing of the ground subsurface," *Radio Sci.,* **13**, 379–389, 1978.

Bouwkamp, C. J. and H. B. G. Casimir, "On multipole expansions in the theory of electromagnetic radiation," *Physica,* **20**, 539–554, 1954.

Bowman, J. J., T. B. A. Senior, and P. L. E. Uslenghi, *Electromagnetic and Acoustic Scattering by Simple Shapes,* North Holland, Amsterdam, 1969.

Boyd, G. D. and J. P. Gordon, "Confocal multimode resonator for millimeter through optical wavelength masers," *Bell System Tech. J.,* **40**, 489–508, 1961.

Brekhovskikh, L. M., *Waves in Layered Media,* Academic Press, New York, 1960.

Brevik, I. and B. Lautrap, "Quantum electrodynamics in material media," *K. Dan Vidensk, Selsk, Mat. Fys. Medd.,* **38**, 3–36, 1970.

Brown, G. S., "The validity of shadowing corrections in rough surface scattering," *Radio Sci.,* **19**, 1461–1468, 1984.

Budden, K. G., *The Propagation of Radio Waves,* Cambridge Univ. Press, 1985.

Burke, H.-H. K. and T. J. Schmugge, "Effects of varying soil moisture contents and vegetation canopies on microwave emissions," *IEEE Trans. Geosci. Remote Sensing,* **GE-20**, 268–274, 1982.

Campbell, L. and W. Garnett, *The Life of James Clerk Maxwell,* MacMillan, London, 1882.

Carniglia, C. D. and L. Mandel, "Quantization of evanescent electromagnetic waves," *Phys. Rev. D,* **3**, 280–296, 1971.

Čerenkov, P. A., "Visible radiation produced by electrons moving in a medium with velocities exceeding that of light," *Phys. Rev.,* **52**, 378–379, 1937.

Chang, D. C., E. F. Kuester, and A. R. Mahmad, "Geometrical theory of a one-dimensional microstrip resonator: the effect of topside charges and currents," *Radio Sci.,* **20**, 819–826, 1985.

Chang, S. K. and K. K. Mei, "Application of the unimoment method to electromagnetic scattering of dielectric cylinders," *IEEE Trans. Antennas Propagat.,* **AP-24**, 35–42, 1976.

Chari, M. V. K. and P. P. Silvester, *Finite Elements in Electric and Magnetic Field Problems,* John Wiley & Sons, New York, 1980.

Chawla, B. R. and H. Unz, *Electromagnetic Waves in Moving Magneto-Plasmas,* University Press, Lawrence, Kansas, 1971.

Chen, Y., K. Sun, B. Beker, and R. Mittra, "Unified matrix presentation of Maxwell's and wave equations using generalized differential matrix operators," *IEEE Trans. on Education,* **41**, 61–69, 1998.

Cheng, D. K., *Field and Wave Electromagnetics,* Addison-Wesley, MA, 1983.

Cheng, D. K. and B. J. Strait, "An unusually simple method for sidelobe reduction," *IEEE Trans. Antennas Propagat.,* **AP-11**, 375–376, 1963.

Chu, L. J. and J. A. Stratton, "Forced oscillations of a prolate spheroid," *J. Appl. Phys.,* **12**, 241–248, 1941.

Chu, R. S. and J. A. Kong, "Diffraction of optical beams with arbitrary profiles by a periodically-modulated layer," *J. Opt. Soc. Am.,* **70**, 1–6, 1980.

Chu, R. S., J. A. Kong, and T. Tamir, "Diffraction of Gaussian beams by a periodically-modulated layer," *J. Opt. Soc. Am.,* **67**, 1555–1561, 1977.

Chu, T. S. and D. C. Hogg, "Effects of precipitation on propagation at 0.63, 3.5 and 10.6 microns," *Bell System Tech. J.,* **47**, 723–759, 1968.

Chuang, S. L. and J. A. Kong, "Wave scattering and guidance by dielectric waveguides with periodic surface," *J. Opt. Soc. Am.,* **73**, 669–679, 1983.

Chuang, S. L., L. Tsang, J. A. Kong, and W. C. Chew, "The equivalence of the electric and magnetic surface current approaches in microstrip antenna studies," *IEEE Trans. Antennas Propagat.,* **AP-28**, 569–571, 1980.

Clemmow, P. C., *The Plane Wave Spectrum Representation of Electromagnetic Fields,* Pergamon Press, New York, 1966.

Colbeck, S., "The geometry and permittivity of snow at high frequencies," *J. Appl. Phys.,* **53**, 4495–4500, 1982.

Cole, J. D., *Perturbation Methods in Applied Mathematics,* Blaisdell, Waltham, Mass., 1968.

Collier, J. R. and C. T. Tai, "Guided waves in moving media," *IEEE Trans. Microwave Theory Tech.,* **MTT-13**, 441–445, 1965.

Collin, R. E., *Field Theory of Guided Waves,* McGraw-Hill, New York, 1960.

Collin, R. E. and F. J. Zucker, *Antenna Theory,* McGraw-Hill, New York, 1969.

Compton, R. T., Jr., "The time-dependent Green's function for electromagnetic waves in moving simple media," *J. Math. Phys.,* **7**, 2145–2152, 1966.

Condon, E. U., "Theories of optical rotatory power," *Rev. of Modern Phys.,* **9**, 432–457, 1937.

Corson, D. and P. Lorrain, *Electromagnetic Waves and Fields,* Freeman, San Francisco, 1962.

Costen, R. C. and D. Adamson, "Three-dimensional derivation of the electrodynamic jump conditions and momentum-energy laws at a moving boundary," *Proc. IEEE,* **53**, 1181–1196, 1965.

Cox, D. C., "Depolarization of radio waves by atmospheric hydrometers in earth-space paths: A review," *Radio Sci.,* **16**, 781–812, 1981.

Crane, R. K., "Propagation phenomena affecting satellite communication systems operating in the centimeter and millimeter wavelength bands," *Proc. IEEE,* **59**, 173–188, 1971.

Daly, P. and H. Gruenberg, "Energy relations for plane waves reflected from moving media," *J. Appl. Phys.,* **38**, 4486–4489, 1967.

Dashen, R., "Path integrals for waves in random media," *J. Math. Phys.,* **20**, 894–920, 1979.

de Hoop, A. T. and H. J. Erankena, "Radiation of pulses generated by a vertical electric dipole above a plane non-conducting earth," *Appl. Sci. Res.,* **B8**, 369–377, 1960.

DeGroot, S. R. and L. G. Suttorp, *Foundations of Electrodynamics,* North-Holland, Amsterdam, 1972.

Deirmendjian, D., *Electromagnetic Scattering on Spherical Polydispersions,* Elsevier, New York, 1969.

Deringin, L. N., "The reflection of a longitudinally polarized plane wave from a surface of rectangular corrugations," *Radio Technol.,* **15**, 9–16, 1960.

DeSanto, J. A., "Green's function for electromagnetic scattering from a random rough surface," *J. Math. Phys.,* **15**, 283–288, 1974.

DeVries, H., "Rotatory power and other properties of certain liquid crystals," *Acta Crystallogs.,* **4**, 219–226, 1951.

Dirac, P. A. M., *Principles of Quantum Mechanics,* 4th ed., Oxford University Press, London, 1958.

Dirac, P. A. M., *Lectures on Quantum Field Theory,* Yeshiva University, New York, 1966.

Djermakoye, B. and J. A. Kong, "Radiative transfer theory for the remote sensing of layered media," *J. Appl. Phys.,* **50**, 6600–6604, 1979.

Dolph, C. L., "A current distribution for broadside arrays which optimizes the relationships between beam width and side-lobe level," *Proc. IRE and Waves and Electrons,* **34**, 337–348, 1946.

Du, L. J. and R. T. Compton, "Cutoff phenomena for guided waves in moving media," *IEEE Trans. Microwave Theory Tech.,* **MTT-14**, 358–363, 1966.

DuHamel, R. H., "Optimum patterns for endfire arrays," *Proc. IRE,* **41**, 652–659, 1953.

Dzyaloshinskii, I. E., "On the magnetoelectrical effect in antiferromagnets," *Soviet Phys. JETP,* **10**, 628–629, 1960.

Elachi, C., *Introduction to the Physics and Techniques of Remote Sensing,* Wiley-Interscience, New York, 1987.

Elliott, R. S., *Antenna Theory and Design,* Prentice-Hall, New York, 1981.

Elliott, R. S., *An Introduction to Guided Waves and Microwave Circuits,* Prentice-Hall, New York, 1993.

El'yashevich, M. A., N. G. Kembrovskaya, and L. M. Tomil'chik, "Walter Ritz as a theoretical physicist and his research on the theory of atomic spectra," *Physics - Uspekhi,* **38**(4), 435–456, 1995.

England, A. W., "Thermal microwave emission from a scattering layer," *J. Geophys. Res.,* **80**, 4484–4496, 1975.

Evans, S., "Dielectric properties of ice and snow — A review," *J. Glaciology,* 773–792, 1965.

Fano, F. M., L. J. Chu, and R. B. Adler, *Electromagnetic Fields, Energy, and Forces,* Wiley, New York and M.I.T. Press, Cambridge, Mass., 1960.

Fante, R. L., "Relationship between radiative-transport theory and Maxwell's equations in dielectric media," *J. Opt. Soc. Am.,* **71**, 460–468, 1981.

Felsen, L. B. and N. Marcuwitz, *Radiation and Scattering of Electromagnetic Waves,* Prentice-Hall, Englewood Cliffs, New Jersey, 1973.

Feynman, R. P. and A. R. Hibbs, *Quantum Mechanics and Path Integrals,* McGraw-Hill, New York, 1965.

Fikioris, J. G. and P. C. Waterman, "Multiple scattering of waves: II. Hole corrections in the scalar case," *J. Math. Phys.,* **5**, 1413–1420, 1964

Foldy, L. L., "The multiple scattering of waves," *Phys. Rev.,* **67**, 107–119, 1945.

Frank, I. and Ig. Tamm, "Coherent visible radiation of fast electrons passing through matter," *Compt. Rend. (Dokl.),* **14**, 109–114, 1937.

Frankl, D. R., *Electromagnetic Theory,* Prentice-Hall, N.J., 1986.

Franz, W., "Zur Formulierung des Huygenschen Prinzips," *Z. Naturforchung,* **3a**, 500–506, 1948.

Frisch, V., "Wave propagation in random medium," *Probabilistic Methods in Applied Mathematics,* **1**, A. T. Bharuch-Reid (ed.), Academic Press, 1968.

Fuchs, R., "Wave propagation in a magnetoelectric medium," *Phil. Mag.,* **11**, 647, 1965.

Fulton, R. L., "Macroscopic quantum electrodynamics," *Jour. Chem. Phys.,* **50**, 3355–3377, 1969.

Fung, A. K. and R. K. Moore, "The correlation function in Kirchhoff's method of solution of scattering of waves from statistically rough surfaces," *J. Geophys. Res.,* **71**, 2939–2943, 1966.

Furutsu, K., "Statistical theory of scattering and propagation over a random surface," *Proc. IEE,* **130**, 601–622, 1983.

Garcia, N., V. Celli, N. R. Hill, and N. Cabrera, "Ill-conditioned matrices in the scattering of waves from hard corrugated surfaces," *Phys. Rev. B,* **18**, 5184–5189, 1978.

Ginzburg, V. L., "Radiation of an electron moving in a crystal with a constant velocity exceeding that of light," *J. Phys.,* **3**, 101–106, 1940.

Ginzburg, V. L., *Propagation of Electromagnetic Waves in Plasma,* Addison-Wesley, Reading, Mass., 1964.

Goldman, M., *The Demon in the Aether,* Paul Harris Publishing, Edinburgh, 1983.

Goldstein, H., *Classical Mechanics,* Addison-Wesley, Reading, Mass., 1950.

Goodman, J. W., *Introduction to Fourier Optics,* McGraw-Hill, New York, 1968.

Goos, Von F. and H. Hänchen, "Ein neuer und fundamentaler Versuch zur Totalreflexion," *Ann. der Phys.,* **6**, 333–346, 1947.

Gradshteyn, I. S. and I. M. Ryzhik, *Table of Integrals, Series and Products,* Academic Press, New York, 1965.

Grant, I. S. and W. R. Phillips, *Electromagnetism,* John Wiley & Sons, New York, 1975.

Gray, E. P., R. W. Hart, and R. A. Farrell, "An application of a variational principle for scattering by random rough surfaces," *Radio Sci.,* **13**, 333–343, 1978.

Gray, K. G. and S. A. Bowhill, "Transient response of stratified media: multiple scattering integral and differential equation for an impulsive incident plane wave," *Radio Sci.,* **9**, 57–62, 1974.

Gruodis, A. J. and C. S. Chang, "Coupled lossy transmission line characterization and simulation," *IBM J. Res. Develop.,* **25**, 1981.

Gurvich, A. S., V. L. Kalinin, and D. T. Matveyer, "Influence of the internal structure of glaciers on their thermal radio emission," *Atm. Oceanic Phys. USSR,* **9**, 713–717, 1973.

Habashy, T. M., J. A. Kong, and W. C. Chew, "Scalar and vector Mathieu transform pairs," *J. Appl. Phys.,* **60**, 3395–3400, 1986.

Hällén, E., "Theoretical investigations into the transmitting and receiving qualities of antennae," *Nova Acta Regiae Soc, Sci. Upsaliensis,* **4**, 1938.

Hansen, W. W. and J. R. Woodyard, "A new principle in directional antenna design," *Proc. IRE,* **26**, 333–345, 1938.

Harman, P. M. (ed.), *The Scientific Letters and Papers of James Clerk Maxwell,* Cambridge University Press, New York, 1990.

Harrington, R. F., *Time-Harmonic Electromagnetic Fields,* McGraw-Hill, New York, 1961.

Harrington, R. F., *Field Computation by Moment Methods,* MacMillan, New York, 1968.

Harrington, R. F. and A. T. Villeneuve, "Reciprocity relationships for gyrotropic media," *IRE Trans. Microwave Theory Tech.,* **MTT-6**, 308–310, 1958.

Heitler, W., *The Quantum Theory of Radiation,* 3rd ed., Oxford University Press, London, 1966.

Hertz, H. R., *Electric Waves,* MacMillan and Co., New York, 1893.

Hill, D. A. and J. R. Wait, "Excitation of the Zenneck surface wave by a vertical aperture," *Radio Sci.,* **13**, 969–977, 1978.

Hill, E. L., "Hamilton's principle and the conservation theorems of mathematical physics," *Rev. Mod. Phys.,* **23**, 253–260, 1951.

Hu, C. and J. R. Whinnery, "Field-realigned nematic-liquid-crystal optical waveguides," *IEEE J. Quantum Electron.,* **QE-10**, 556–562, 1974.

Huang, H. C., *Coupled Mode Theory,* VNU Science Press, The Netherlands, 1984.

Hutley, M. C. and V. M. Bird, "A detailed experimental study of the anomalies of a sinusoidal diffraction grating," *Opt. Acta.,* **20**, 771–782, 1973.

Indenbom, V. L., "Irreducible representations of the magnetic groups and allowance for magnetic symmetry," *Soviet Phys. Crystallogr.,* **5**, 493, 1960.

Ishimaru, A., *Wave Propagation and Scattering in Random Media,* Academic Press, New York, 1978.

Ishimaru, A., D. Lesselier, and C. Yeh, "Multiple scattering calculations for nonspherical particles based on the vector radiative transfer theory," *Radio Sci.,* **19**, 1356–1366, 1984.

Ishimaru, A., R. Woo, J. W. Armstrong, and D. C. Backman, "Multiple scattering calculation of rain effects," *Radio Sci.,* **17**, 1425–1433, 1982.

Ito, S. and S. Adachi, "Multiple scattering effect on backscattering from a random medium," *IEEE Trans. Antennas Propagat.,* **AP-25**, 205–208, 1977.

Itoh, T., "Generalized spectral domain method for multiconductor printed lines and its application to tunable suspended microstrips," *IEEE Trans. Microwave Theory Tech.,* **MTT-26**, 983–987, 1978.

Jackson, J. D., *Classical Electrodynamics,* Wiley, New York, 1962.

Jaggard, D. L., X. Sun, and N. Engheta, "Canonical sources and duality in chiral media," *IEEE Trans. Antennas and Propagat.,* **AP-35**, 1007–1013, 1988.

James, G. L., *Geometrical Theory of Diffraction for Electromagnetic Waves,* Peter Peregrinus, England, 1976.

James, J. R., P. S. Hall, and C. Wood, *Microstrip Antenna,* Peter Peregrinus, New York, 1981.

Jauch, J. M. and K. M. Watson, "Phenomenological quantum electrodynamics," *Phys. Rev.,* **74**, 950–957, 1948.

Jauch, J. M. and K. M. Watson, "Phenomenological quantum electrodynamics. Part II: Interaction of the field with charges," *Phys. Rev.,* **75**, 1485–1493, 1948.

Jauch, J. M. and K. M. Watson, "Phenomenological quantum electrodynamics. Part III: Dispersion," *Phys. Rev.,* **75**, 1249–1261, 1949.

Jordan, A. K. and R. H. Lang, "Electromagnetic scattering patterns from sinusoidal surface," *Radio Sci.,* **14**, 1077–1088, 1979.

Jordan, E. C. and K. G. Balmain, *Electromagnetic Waves and Radiating Systems,* Prentice-Hall, Englewood Cliffs, NJ, 1968.

Kapany, N. S. and J. J. Burke, *Optical Waveguides,* Academic Press, New York, 1972.

Katehi, P. B. and N. G. Alexopoulos, "On the modeling of electromagnetically coupled microstrip antennas — the printed strip dipole," *IEEE Trans. Antennas Propagat.,* **AP-32**, 1179–1186, 1984.

King, R. W. P., *The Theory of Linear Antennas,* Harvard University Press, Cambridge, Mass., 1956.

King, R. W. P. and C. W. H. Harrison, Jr., *Antennas and Waves,* MIT Press, Cambridge, Mass., 1969.

King, R. W. P., R. B. Mack, and S. S. Sandler, *Arrays of Cylindrical Dipoles,* Cambridge Univ. Press, New York, 1968.

Klauder, J. R. and E. C. G. Sudarshan, *Fundamentals of Quantum Optics,* Benjamin, New York, 1968.

Klein, W. R. and B. D. Cook, "Unified approach to ultrasonic light diffraction," *IEEE Trans. Sonics Ultrason.,* **SU-14**, 123–134, 1967.

Kogelnik, H., "Coupled wave theory for thick hologram gratings," *Bell System Tech. J.,* **48**, 2909–2947, 1969.

Kogelnik, H. and C. V. Shank, "Coupled-wave theory of distributed feedback lasers," *J. Appl. Phys.,* **43**, 2327–2335, 1972.

Kohler, W. E. and G. C. Papanicolaou, "Some applications of the coherent potential approximation," *Multiple Scattering and Waves in Random Media,* P. L. Chow, W. E. Kohler, and G. C. Papanicolaou (eds.), 199–223, North-Holland Publishing Company, New York, 1981.

Kong, J. A., "Electromagnetic waves in moving media," *Ph.D. Thesis*, Syracuse University, Syracuse, New York, 1968.

Kong, J. A., "Theorems of bianisotropic media," *Proc. IEEE,* **60**, 1036–1046, 1972.

Kong, J. A., "Dispersion analysis of reflection and transmission by a plane boundary — a graphical approach," *Am. J. Phys.,* **43**, 73–76, 1975.

Kong, J. A., *Theory of Electromagnetic Waves,* Wiley-Interscience, New York, 1975.

Kong, J. A., "Second-order coupled mode equations for spatially periodic media," *J. Opt. Soc. Am.,* **67**, 825–829, 1977.

Kong, J. A., *Research Topics in Electromagnetic Wave Theory,* Wiley-Interscience, New York, 1981.

Kong, J. A., *Electromagnetic Waves Theory,* Wiley-Interscience, New York, 1986, 1990 (2nd ed.).

Kraus, J. D., *Electromagnetics,* McGraw-Hill, New York, 1984.

Lanczos, C., *Applied Analysis,* Prentice-Hall, NJ, 1956.

Landau, L. D. and E. M. Lifshitz, *Quantum Mechanics: Non-Relativistic Theory,* Addison-Wesley, Reading, Mass., 1958.

Landau, L. D. and E. M. Lifshitz, *Electrodynamics of Continuous Media,* Addison-Wesley, Reading, Mass., 1960.

Landau, L. D. and E. M. Lifshitz, *Mechanics,* 2nd ed., Addison-Wesley, Reading, Mass., 1960.

Landau, L. D. and E. M. Lifshitz, *Classical Theory of Fields,* 3rd ed., Addison-Wesley, Reading, Mass., 1971.

Lax, M., "Wave propagation and conductivity in random media," *Proc. SIAM-AMS,* **VI**, 35–95, 1973.

Leader, J. C., "Bidirectional scattering of electromagnetic waves from rough surfaces," *J. Appl. Phys.,* **42**, 4808–4816, 1971.

Lee, J. K. and J. A. Kong, "Dyadic Green's functions for layered anisotropic medium," *Electromagnetics,* **3**, 111–130, 1983.

Lee, K. F., *Principles of Antenna Theory,* John Wiley & Sons, New York, 1984.

Lee, K. S. H. and C. H. Papas, "Electromagnetic radiation in the presence of moving simple media," *J. Math. Phys.,* **5**, 1668–1672, 1964.

Lee, S. W. and Y. T. Lo, "Reflection and transmission of electromagnetic waves by a moving uniaxially anisotropic medium," *J. Appl. Phys.,* **38**, 870–875, 1967.

Lindell, I. V., E. Alanen, and K. Mannersalo, "Exact image method for impedance computation of antennas above the ground," *IEEE Trans. Antennas Propagat.,* **AP-33**, 937–945, 1985.

Lindell, I. V. and A. H. Sihvola, "Dielectrically loaded corrugated waveguide: variational analysis of a nonstandard eigenproblem," *IEEE Trans. Microwave Theory Tech.,* **MTT-31**, 552–556, 1983.

Lorentz, G., *Bernstein Polynomials,* Toronto University Press, Can., 1953.

Louisell, W., *Radiation and Noise in Quantum Electronics,* McGraw-Hill, New York, 1964.

Lynch, P. J. and R. J. Wagner, "Rough-surface scattering: shadowing, multiple scatter, and energy conservation," *J. Math. Phys.,* **11**, 3032–3042, 1970.

Ma, M. T., *Theory and Application of Antenna Arrays,* Wiley-Interscience, New York, 1974.

MacDonald, D. K. C., *Faraday, Maxwell, and Kelvin,* Anchor Books, Garden City, New York, 1964.

Marcuse, D., *Light Transmission Optics,* Van Nostrand-Reinhold, New York, 1972.

Marion, J. B. and M. A. Heald, *Classical Electromagnetic Radiation,* 2nd ed., Academic Press, New York, 1980.

Mason, W. P., *Crystal Physics and Interaction Processes,* Academic Press, New York, 1966.

Maxwell, J. C., *A Treatise on Electricity and Magnetism,* Dover Publications, New York, 1954.

Maxwell-Garnett, J. C., "Colours in metal glasses and in metallic films," *Trans. Roy. Soc. London,* **203**, 385–420, 1904.

McKenzie, J. F., "Electromagnetic waves in uniformly moving media," *Proc. Phys. Soc.,* **91**, 532–536, 1967.

Mergelyan, O. S., "A point charge in a gyrotropic dielectric," *Soviet Phys. Tech. Phys.,* **12**, 594–597, 1967.

Mittra, R. and S. W. Lee, *Analytical Techniques in the Theory of Guided Waves,* Macmillan, New York, 1971.

Mo, T. C., "Theory of electrodynamics in media in noninertial frames and applications," *J. Math. Phys.,* **11**, 2589–2610, 1970.

Mocella, V., "Negative refraction in photonic crystals: thickness dependence and pendellösung phenomenon," *Optics Express,* **13**, 2005.

Møller, C., *The Theory of Relativity,* Oxford University Press, London, 1966.

Morse, P. M. and H. Feshbach, *Methods of Theoretical Physics,* McGraw-Hill, New York, 1953.

Nahin, P. J., *Oliver Heaviside: Sage in Solitude,* IEEE Press, New York, 1988.

Niven, W. D. (ed.), *The Scientific Papers of James Clerk Maxwell,* Dover Publications, New York, 1965.

O'Brian, S. and J. B. Pendry, "Magnetic activity at infrared frequencies in structured metallic photonic crystals," *J. Phys. Condens. Matter,* **14**, 6383–6394, 2002.

O'Connor, J. J. and E. F. Robertson, *http://www-groups.dcs.st-and.ac.uk/~history/,* 1999.

O'Dell, T. H., "Magnetoelectricsa new class of materials," *Electron. Power,* **11**, 266–267, 1965.

O'Dell, T. H., *The Electrodynamics of Magneto-Electric Media, 11: Selected Topics in Solid State Physics,* E. P. Wohlforth (ed.), North-Holland, Amsterdam, 1970.

Oguchi, T., "Electromagnetic wave propagation and scattering in rain and other hydrometeors," *Proc. IEEE,* **71**, 1029–1078, 1983.

Ogura, H., "Theory of waves in a homogeneous random medium," *Phys. Rev. A,* **11**, 942–956, 1975.

Oliner, A. A. and A. Hessel, "Guided waves on sinusoidally-modulated reactance surfaces," *IRE Trans. Antenna Propagat.,* S201–S208, 1959.

Onstott, R. G., R. K. Moore, and W. F. Weeks, "Surface-based scatterometer results of Arctic sea ice," *IEEE Trans. Geosci. Electron.,* **GE-17**, 78–85, 1979.

Pampaloni, P., *Microwave Radiometry and Remote Sensing Applications,* VSP, Utrecht, Netherlands, 1989.

Panofsky, W. K. H. and M. Phillips, *Classical Electricity and Magnetism,* 2nd ed., Addison-Wesley, Reading, Mass., 1962.

Papanicolaou, G. C. and J. B. Keller, "Stochastic differential equations with applications to random harmonic oscillators and wave propagation in random media," *SIAM J. Appl. Math.,* **21**, 287–305, 1971.

Papas, C. H., *Theory of Electromagnetic Wave Propagation,* McGraw-Hill, New York, 1965.

Paris, D. T. and G. K. Hurd, *Basic Electromagnetic Theory,* McGraw-Hill, New York, 1969.

Peake, W. H., "Interaction of electromagnetic waves with some natural surfaces," *IEEE Trans. Antennas Propagat.,* **AP-7**, Special Supplement, S324–S329, 1959.

Peake, W. H., D. E. Barrick, A. K. Fung, and H. L. Chan, "Comments on 'Backscattering of waves by composite rough surfaces'," *IEEE Trans. Antennas Propagat.,* **AP-18**, 716–726, 1970.

Pendry, J. B., A. J. Holden, D. J. Robbin, and W. J. Stewart, "Magnetism from conductors and enhanced nonlinear phenomena," *IEEE*

Trans. Microwave Theory and Tech., **47**, 2075–2084, 1999.

Peng, S. T. and T. Tamir, "Directional blazing of waves guided by asymmetrical dielectric gratings," *Opt. Comm.,* **11**, 405–409, 1974.

Percus, J. K. and G. J. Yevick, "Analysis of classical statistical mechanics by means of collective coordinates," *Phys. Rev.,* **110**, 1–13, 1958.

Peterson, B. and S. Strom, "T matrix for electromagnetic scattering from an arbitrary number of scatterers and representation of E(3)," *Phy. Rev. D,* **8**, 3661–3678, 1973.

Plonus, M. A., *Applied Electromagnetics,* McGraw-Hill, New York, 1978.

Poh, S. Y. and J. A. Kong, "Transient response of a vertical electric dipole on a two-layer medium," *J. Electromagnetic Waves and Applications,* **1**, 135–158, 1987.

Polder, D. and J. H. van Santen, "The effective permeability of mixtures of solids," *Physica,* **12**, 257–271, 1946.

Popovic, B. D., *Introductory Engineering Electromagnetic,* Addison-Wesley, Reading, Mass., 1971.

Post, E. J., "Electromagnetism and the principle of equivalence," *Ann. Phys.,* **70**, 507–515, 1972.

Pritchard, R. L., "Discussion of DuHamel's paper," *IRE Transactions on Antennas and Propagation,* **43**, 40–43, 1955.

Purcell, E. M., *Electricity and Magnetism,* McGraw-Hill, New York, 1963.

Rado, G. T., "Observation and possible mechanisms of magnetoelectric effects in a ferromagnet," *Phys. Rev. Lett.,* **13**, 355, 1964.

Raman, C. V. and N. S. N. Nath, "The diffraction of light by high frequency sound waves; I-V," *Proc. Ind. Acad. Sci.,* **2-3**, 1935-36.

Ramo, S., J. R. Whinnery, and T. Van Duzer,*Fields and Waves in Communication Electronics,* Pergamon Press, New York, 1970.

Rao, B. R. and T. T. Wu, "On the applicability of image theory in anisotropic media," *IEEE Trans. Antennas Propagat.,* **AP-13**, 814–815, 1965.

Rao, N. N., *Basic Electromagnetism with Applications,* Prentice-Hall, New Jersey, 1972.

Rao, S. M., D. R. Wilton, and A. W. Glisson, "Electromagnetic scattering by surfaces of arbitrary shape," *IEEE Trans. Antennas Propagat.,* **AP-30**, 409–418, 1982.

Read, F. H., *Electromagnetic Radiation,* John Wiley & Sons, New York, 1980.

Riblet, H. J., "Discussion of Dolph's paper," *Proc. IRE,* **35**, 489–492, 1947.

Rice, S. O., "Reflection of EM waves by slightly rough surfaces," in *The Theory of Electromagnetic Waves,* M. Kline (ed.), Interscience, New York, 1963.

Richards, W. F., S. E. Davidson, and S. A. Long, "Dual-band reactively loaded microstrip antenna," *IEEE Trans. Antennas Propagat.,* **AP-23**, 556–561, 1985.

Riley, J., W. A. Davis, and I. M. Besieris, "The singularity expansion method and multiple scattering," *Radio Sci.,* **20**, 20–24, 1985.

Roberts, W. K., "A new wide-band Balun," *Proc. IRE,* **45**, 1628–1631, 1957.

Röentgen, W. C., "Ueber die durch Bewegung eines in homogenenen

Rohrlich, F., *Classical Charged Particles,* Addison-Wesley, Reading, Mass., 1965.

Rosenbaum, S., "The mean Green's function: a nonlinear approximation," *Radio Sci.,* **6**, 379–386, 1971.

Rumsey, V. H., "Reaction concept in electromagnetic theory," *Phys. Rev.,* **94**, 1483–1491; **95**, 1706, 1954.

Ruppin, R., "Electromagnetic energy density in a dispersive and absorptive material," *Physics Letters A,* **299**, 309–312, 2002.

Ryzhov, Y. A., V. V. Tamoikin, and V. I. Tatarskii, "Spatial dispersion of inhomogeneous media," *Soviet Phys. JETP,* **21**, 433–438, 1965.

Sakoda, K., *Optical Properties of Photonic Crystals,* Springer, Berlin, 2001.

Sarkar, T. K., M. F. Costa, I. Chi-Lin, and R. F. Harrington, "Electromagnetic transmission through mesh covered apertures and arrays of apertures in a conducting screen," *IEEE Trans. Antennas Propagat.,* **AP-32**, 908–913, 1984.

Saxton, J. A. and J. A. Lane, "Electrical properties of sea water," *Wireless Engineer,* 269–275, 1952.

Schelkunoff, S. A., *Electromagnetic Waves,* D. Van Nostrand, 1943.

Schelkunoff, S. A., *Advanced Antenna Theory,* Wiley, New York, 1952.

Schiff, L. I., *Quantum Mechanics,* McGraw-Hill, New York, 1968.

Schlomka, V. T., "Das Ohmsche Gesetz bei Bewegten Körpern," *Ann. Phys.,* **6**, 246–252, 1951.

Scott, A. C. and F. Y. F. Chu, "Pulse saturation in a traveling wave parametric amplifier," *Proc. IEEE,* **62**, 1720–1721, 1974.

Sen, P. N., C. Scala, and M. H. Cohen, "A self-similar model for sedimentary rocks with applications to the dielectric constant of fused glass beads," *Geophysics,* **46**, 781–795, 1981.

Senior, T. B. A. and R. F. Goodrich, "Scattering by a sphere," *Proc. IEEE,* **111**, 907–916, 1964.

Seshadri, S. R., *Fundamentals of Transmission Line and Electromagnetic Fields,* Addison-Wesley, Reading, Mass., 1971.

Sezginer, A. and J. A. Kong, "Transient response of line source excitation in cylindrical geometry," *Electromagnetics,* **4**, 35–54, 1984.

Shen, L. C. and J. A. Kong, *Applied Electromagnetism,* Brooks/Cole, California, 1983.

Shin, R. T. and J. A. Kong, "Scattering of electromagnetic waves from a randomly perturbed quasiperiodic surface," *J. Appl. Phys.,* **56**, 10–21, 1984.

Shiozawa, T. and N. Kumagai, "Total reflection at the interface between relatively moving media," *Proc. IEEE,* **55**, 1243–1244, 1967.

Silver, S., *Microwave Antenna Theory and Design,* Dover Publications, New York, 1949.

Skolnik, M. I., *Introduction to Radar Systems,* McGraw-Hill, New York, 1980.

Snitzer, E., "Cylindrical dielectric waveguides," *J. Opt. Soc. Am.,* **51**, 491, 1961.

Snyder, A. W., "Understanding monomode optical fibers," *Proc. IEEE,* **69**, 6–13, 1981.

Sommerfeld, A., *Electrodynamics,* Academic Press, New York, 1949.

Sommerfeld, A., *Optics,* Academic Press, New York, 1949.

Sommerfeld, A., *Partial Differential Equations,* Academic Press, New York, 1962.

Staelin, D. H., "Passive remote sensing at microwave wavelengths," *Proc. IEEE,* **57**, 427–459, 1969.

Stogryn, A., "Electromagnetic scattering by random dielectric constant fluctuations in a bounded medium," *Radio Sci.,* **9**, 509–518, 1974.

Stratton, J. A., *Electromagnetic Theory,* McGraw-Hill, N.Y., 1941.

Stutzman, W. L. and G. A. Thiele, *Antenna Theory and Design,* John Wiley & Sons, New York, 1981.

Synge, J. L., *Relativity: The Special Theory,* North-Holland, Amsterdam, 1965.

Szekielda, K., *Satellite Monitoring of the Earth,* Wiley-Interscience, New York, 1989.

Tai, C. T., "A study of electrodynamics of moving media," *Proc. IEEE,* **52**, 685–689, 1964.

Tai, C. T., *Dyadic Green's Function in Electromagnetic Theory,* Intext Publishers, New York, 1971.

Tai, C. T., "On the eigenfunction expansion of dyadic Green's functions," *Proc. IEEE,* **61**, 480–481, 1973.

Tan, H. S., A. K. Fung, and H. Eom, "A second order renormalization theory for cross-polarized backscatter from a half space random medium," *Radio Sci.,* **15**, 1059–1065, 1980.

Tatarskii, V. I., *Wave Propagation in a Turbulent Medium,* McGraw-Hill, New York, 1961.

Tatarskii, V. I., "Propagation of electromagnetic waves in a medium with strong dielectric constant fluctuations," *Soviet Phys. JETP,* **19**, 946–953, 1964.

Tatarskii, V. I., *The Effects of Turbulent Atmosphere on Wave Propagation,* National Tech. Information Service, 472, Springfield, VA, 1971.

Tellegen, B. D. H., "The Gyrator, a new electric network element," *Phillips Res. Rept.,* **3**, 81–101, 1948.

Tijhuis, A. G., *Electromagnetic Inverse Profiling: Theory and Numerical implementation,* VNU Science Press, Netherlands, 1987.

Tolman, R. C., *Relativity, Thermodynamics, and Cosmology,* Oxford University Press, London, 1966.

Tsang, L., A. J. Blanchard, R. W. Newton, and J. A. Kong, "A simple relation between active and passive microwave remote sensing measurements of earth terrain," *IEEE Trans. Geosci. Remote Sensing,* **GE-20**, 482–485, 1982.

Tsang, L. and J. A. Kong, "Microwave remote sensing of a two-layer random medium," *IEEE Tans. Antennas Propagat.,* **AP-24**, 283–287, 1976.

Tsang, L., J. A. Kong, and R. T. Shin, *Theory of Microwave Remote Sensing,* Wiley-Interscience, New York, 1985.

Tseng, F. I. and D. K. Cheng, "A synthesis technique for linear arrays with wide-band elements," *Proc. IEEE,* **51**, 1679–1681, 1963.

Twersky, V., "Coherent electromagnetic waves in pair-correlated random distributions of aligned scatterers," *J. Math. Phys.,* **19**, 215–230, 1978.

Tyras, G., *Radiation and Propagation of Electromagnetic Waves,* Academic Press, New York, 1969.

Van Bladel, J., *Electromagnetic Fields,* McGraw-Hill, New York, 1964.

Van de Hulst, H. C., *Light Scattering by Small Particles,* John Wiley & Sons, New York, 1957.

Van den Berg, P. M., "Diffraction theory of a reflection grating," *Appl. Sci. Res.,* **24**, 261–293, 1971.

Van Duzer, T. and C. W. Turner, *Principles of Superconductive Devices and Circuits,* Elsevier, 1981.

Vant, M. R., R. O. Ramseier, and V. Makios, "The complex dielectric constant of sea ice at frequencies in the range 0.1–40 GHz," *J. Appl. Phys.,* 1264–1280, 1978.

Veselago, V., "The electrodynamics of substances with simultaneously negative values of ϵ and μ," *Sov. Phys. Usp.,* **10**, 509–514, 1968.

Vezzetti, D. J. and J. B. Keller, "Refractive index, attenuation, dielectric constant and permeability of waves in a polarizable medium," *J. Math. Phys.,* **8**, 1861–1870, 1967.

von Schmutzer, E., "Zur Relativistischer Elektrodynamik in Beliebigen Medien," *Ann. Phys. (Liepzig),* **6**, 171–180, 1956.

von Tischer, M. and S. Hess, "Die Materialgleichungen in Beliebigen Medien," *Ann . Phys. (Leipzig),* **3**, 113–121, 1969.

Wait, J. R., *Electromagnetic Waves in Stratified Media,* 2nd ed., Pergamon Press, New York, 1970.

Waterman, P. C. and R. Truell, "Multiple scattering of waves," *J. Math. Phys.,* **2**, 512–537, 1961.

Watson, G. N., *A Treatise on the Theory of Bessel Functions,* 2nd ed., Pergamon Press, New York, 1944.

Watson, J. G. and J. B. Keller, "Reflection, scattering, and absorption of acoustic waves by rough surfaces," *J. Acoust. Soc. Am.,* **74**, 1887–1894, 1983.

Wei, C., R. F. Harrington, J. R. Mautz, and T. K. Sarkar, "Multiconductor transmission lines in multilayered dielectric media," *IEEE Trans. Microwave Theory Tech.,* **32**, 439–449, 1984.

Weil, H. and C. M. Chu, "Scattering and absorption of electromagnetic radiation by thin dielectric discs," *Appl. Optics,* **15**, 1832–1836, 1976.

Wertheim, M. S., "Exact solution of the Percus-Yevick integral equation for hard spheres," *Phys. Rev. Lett.,* **20**, 321–323, 1963.

Whitman, G. M. and F. Schwering, "Scattering by periodic metal surfaces with sinusoidal height profilesa theoretical approach," *IEEE Trans. Antennas Propagat.,* **AP-25**, 869–876, 1977.

Wilson, H. A., "On the electric effect of a rotating dielectric in a magnetic field," *Phil. Trans. Roy. Soc. London,* **204A**, 121–137, 1905.

Wolff, E. A., *Antenna Analysis,* Wiley, New York, 1966.

Wu, T. T. and H. Lehmann, "Spreading of electromagnetic pulses," *J. Appl. Phys.,* **55**, 2064–2065, 1985.

Yaghjian, A. D., "Electric dyadic Green's functions in the source region," *Proc. IEEE,* **68**, 248–263, 1980.

Yang, Y. E., J. A. Kong, and Q. Gu, "Time domain perturbational analysis of nonuniformly coupled transmission lines," *IEEE Trans. Microwave Theory Tech.,* **MTT-33**, 1120–1130, 1985.

Yariv, A., *Optical Electronics,* Holt, Rinehart, and Winston, New York, 1985.

Yariv, A. and P. Yeh, *Optical Waves in Crystals,* Wiley-Interscience, New York, 1984.

Yeh, C. and K. F. Casey, "Reflection and transmission of electromagnetic waves by a moving dielectric slab," *Phys. Rev.,* **144**, 665–669, 1966.

Yeh, K. C. and C. H. Liu, *Theory of Ionospheric Waves,* Academic Press, New York, 1972.

Yueh, H. A., R. T. Shin, and J. A. Kong, "Scattering of electromagnetic waves from a periodic surface with random roughness," *J. Appl. Phys.,* **64**, 1657–1670, 1988.

Zernike, F. and J. E. Midwinter, *Applied Nonlinear Optics,* Wiley-Inter-science, New York, 1973.

Ziman, J. M., *Elements of Advanced Quantum Theory,* Cambridge University Press, London, 1969.

Zuniga, M. and J. A. Kong, "Modified radiative transfer theory for a two-layer random medium," *J. Appl. Phys.,* **51**, 5228–5244, 1980.

INDEX